

Oncology: Peptide

OS-1

I. Mathieu, F. Jamar, S. Walrand, D. Labar, J. De Camps, M. Lonnew, E. Zang*, T. Chen*, M.C.Smith*, S. Pauwels. Nuclear Medicine and Laboratory of Positron Emission Tomography, University of Louvain, Brussels and Louvain-la-Neuve, Belgium; *Novartis Pharma Corp., NJ 07936, USA.

BIODISTRIBUTION OF Y-86-DOTA-TYR3-OCTREOTIDE (SMT487) AND RENAL PROTECTIVE EFFECT OF AMINO ACID INFUSION: A PHASE I STUDY.

This study was aimed to evaluate the biodistribution and pharmacokinetics (PK) of Y-86-SMT487 (β^*) in order to predict the behaviour of the Y-90-labelled peptide (β), developed for therapy of somatostatin-receptor rich tumours and to assess the renal protective effect of amino acid (aa) infusion.

Six patients with metastatic carcinoid tumours underwent two PET studies which included measurement of urine and blood PK and 3 whole-body scans (4, 24 and 48h). Studies were performed after injection of 3.3 mCi Y-86-SMT487 (250 μ g), one study was performed with aa infusion (26.4 g) over 4h, started 30min before tracer injection. Uptake measurements of Y-86-SMT487 were input into the MIRDOSE program to estimate Y-90-SMT487 dosimetry.

Tumours were clearly shown and uptake was stable over time. Among normal organs, kidneys and to a lesser extent spleen, showed significant uptake of Y-86-SMT487. Amino acid infusion induced a 15-55% reduction of renal dosimetry ($p < 0.05$; t test, one-tailed) with no significant effect on tumour dosimetry (Table). PK analysis revealed a biphasic disposition of Y-86-SMT487 in plasma (T1/2 β : 7-8h) with >60% activity in urine by 24h.

Parameter	Unit	amino acids (-)	amino acids (+)
Renal uptake 4h*	% ID	2.41 \pm 0.61	1.48 \pm 0.36
Renal uptake 24h*	% ID	2.35 \pm 0.63	1.85 \pm 0.51
Renal uptake 48h*	% ID	1.61 \pm 0.43	1.25 \pm 0.52
Tumour uptake 4h	% ID	0.49 \pm 0.73	0.50 \pm 0.68
Tumour uptake 24h	% ID	0.63 \pm 0.97	0.66 \pm 0.96
Tumour uptake 48h	% ID	0.55 \pm 0.95	0.57 \pm 0.97
Dosimetry kidneys (Y-90)*	mGy/MBq	4.08 \pm 1.42	2.67 \pm 1.01
Dosimetry tumours (Y-90)	mGy/MBq	1.76 \pm 1.07	1.78 \pm 0.97

*: n=4; 1pt with no evaluable kidney uptake, 1 unstable between PET studies.

In conclusion, Y-90-SMT487, given along with aa infusion, is a promising compound for therapy of somatostatin-receptor positive tumours. It is worth noting that the uptake of Y-86-SMT487 by tumours was stable over 48 hours and was not influenced by aa infusion which reduced renal doses. A comparison with In-111-pentetreotide will also be presented.

OS-2

M. Bangard, M. Behe*, H. Bender, S. Guhlke, J. Risse, F. Grünwald, H. Mäcke*, H.-J. Biersack. Departments of Nuclear Medicine, University of Bonn, Germany and University Hospital Basel*, Switzerland.

TECHNETIUM-99M-OCTREOTIDE FOR THE DETECTION OF SOMATOSTATIN RECEPTOR POSITIV (SSTR+) TUMORS: PRELIMINARY RESULTS

Aim: The aim of the study was to determine (1.) the biodistribution of a new Tc-99m labeled HYNIC-octreotide-conjugate in patients with SSTR+ tumors and (2.) compare the Tc-99m-octreotide versus In-111-octreotide.

Methods: 7 patients (mean age 41 yrs., range 20-54 yrs., m:f = 5:2) with somatostatin receptor positive tumors (3 carcinoids, 2 c-cell thyroid-carcinomas and 2 pancreas-carcinoma) were examined. All patients were found to be SSTR+ as shown by a positive In-111 scan one week prior to the Tc-99m scan. All patients underwent the following acquisition protocols: Bolus injection of (a) 370 MBq Tc-99m-octreotide and (b) 111 MBq In-111-octreotide (Octreo-scan®, Mallinckrodt Medical). (a) Whole-body-scan, planar images and SPECT images 1, 4 and 24 hrs. p.i. (b) planar images and SPECT images 4 and 24 hrs. p.i.. In both protocols a double head camera (ADAC Vertex) with appropriate collimators was used.

Results: Tc-99m-octreotide showed a biodistribution comparable to the In-111 labeled analogue: high uptake and excretion by the kidneys and minimal uptake in the liver. Known tumor sites were visualized by both labels. Overall, the following tumor sites were detected by both compounds: 15 liver, 7 mediastinal, 6 abdominal, 2 lung and 1 axillary lymph node metastases. Image quality was better with the Tc-99m labeled compound.

Conclusion: Our preliminary data demonstrate that Tc-99m-octreotide show (1.) biodistribution characteristics similar to the well established In-111-octreotide and (2.) these data show rather identical SSTR+ tumor targeting capabilities. However, it should be noted that Tc-99m-octreotide had better image qualities. Further studies are necessary in order to substantiate these findings.

OS-3

J. Valencak, M. Raderer, A. Kurtaran, J. Drach, T. Pangerl, M. Hejna, F. Pfeffel, A. Chott and I. Virgolini. University of Vienna SOMATOSTATIN RECEPTOR EXPRESSION IN LYMPHOMA OF MUCOSA ASSOCIATED LYMPHOID TISSUE (MALT).

Extranodal lymphoma of the MALT-type is a distinct pathologic entity with a usually indolent clinical course, which has been classified as marginal zone lymphoma according to the REAL-classification. The majority of cases arise in the stomach and are thought to be related to the presence of Helicobacter pylori, but also extragastric locations are frequently encountered. While the optimal treatment of such patients remains a matter of debate at the moment, there is widespread consensus that exact staging including endosonography, CT-scanning, endoscopy and bone marrow biopsy is mandatory. We report the results of a study evaluating the role of somatostatin receptor (SSTR) imaging using 111In-DTPA-D-Phe1-octreotide (111In-OCT) in 22 patients with MALT lymphoma, which displays a high affinity to SSTR-subtypes 2 and 5. In addition, we have investigated the SSTR-subtype expression in 4 human MALT-lymphoma specimens (5 gastric and 2 extragastric). All patients included in the study had histologically verified MALT-lymphoma: 7 had low-grade extragastric manifestations (1 lymphoma of the lung, 3 conjunctival lymphomas, 1 breast and 2 cases with supraclavicular lesions), 4 had stage I and 3 had stage II disease. 15 patients presented with gastric lymphoma (8 high-grade and 7 low-grade), 6 had stage II and 9 stage I tumours. All patients were injected 111In-OCT before initiation of therapy, and results of gamma camera imaging were compared to conventional imaging including CT and endosonography. 20 patients were considered evaluable, 1 patient with gastric lymphoma was excluded due to the additional presence of CLL and 1 due to additional lung cancer. All 7 patients with extragastric lymphoma had positive scans, while only 1 patient with gastric lymphoma had slight focal tracer uptake in the epigastric area, which was rated as unspecific. The remaining patients had negative scans irrespective of low- or high-grade histology. In vitro results also revealed a different pattern of SSTR-subtype expression in extragastric (expression of SSTR2) and gastric MALT-lymphomas (expression of SSTR4). These results indicate that extragastric MALT-lymphomas can be readily visualized by SSTR-imaging using 111In-OCT and might be potential targets for therapy with SSTR-analogues. In contrast, gastric MALT-lymphomas do not appear to express relevant amounts of respective SSTR. Our findings suggest a difference between extragastric and gastric MALT-lymphomas on the cellular level despite a well established morphologic and immunohistochemical uniformity.

OS-4

M. Raderer, M. Leimer, A. Kurtaran, B. Niederle, F. Vorbeck, H. Vierhapper, S. Li, P. Angelberger, J. Pidlich and I. Virgolini. University of Vienna, Austria. VALUE OF PEPTIDE RECEPTOR IMAGING USING 111IN-OCTREOTIDE AND 123I-VASOACTIVE INTESTINAL PEPTIDE IN PATIENTS WITH CARCINOID TUMOURS: VIENNA UNIVERSITY EXPERIENCE 1993-1997

Radiolabeled peptide analogs (111In-OCT, 123I-VIP) are being used to identify primary and metastatic tumor sites in patients with neuroendocrine tumours. We report our experience with both 123I-VIP and 111In-OCT for imaging of carcinoid patients. 132 patients (102 with a verified and 30 with a clinically suspected diagnosis of a carcinoid tumor) were referred to our department between 1993 and 1996. A total of 96 patients underwent scanning with both 123I-VIP and 111In-OCT in random order, while 36 were injected 111In-OCT only. Imaging results were compared to CT scans not older than 4 weeks, results of conventional ultrasound and endosonography as well as endoscopy, and results of surgical exploration in case of inconclusive conventional imaging. In total, 84% primary or recurrent carcinoids could be visualized by means of 123I-VIP, while metastatic sites were identified in 82% of patients. In 25% of patients with carcinoid syndrome, focal tracer uptake detected the carcinoid tumor. In patients scanned with OCT 91% primary or recurrent carcinoid tumors could be identified, and 95% of patients demonstrated metastatic disease. 45% of tumor localizations in patients with carcinoid syndrome were identified. In a direct comparison in the 96 patients undergoing both imaging modalities, 111In-OCT was found to be superior to 123I-VIP, with 93% vs 84% scans being positive in primary or recurrent tumors, and 90% vs 82% being positive in metastatic sites, and 45% vs 25% in patients with carcinoid syndrome. Overall, peptide receptor scanning proved to be more sensitive than conventional imaging modalities, which located tumor lesions in 71% patients, while receptor scintigraphy detected neoplastic lesions in a total of 117 patients during long term follow-up and repeated scanning. Our results indicate a high sensitivity for both peptide tracers for localizing tumor sites in patients with ascertained or suspected carcinoid tumors, with 111In-OCT scintigraphy being more sensitive than 123I-VIP receptor scanning. Both 123I-VIP and 111In-OCT had a higher diagnostic yield than conventional imaging, as verified by surgical intervention or long term follow-up. We conclude that 111In-OCT scintigraphy represents the more sensitive method for diagnosis and staging of patients suffering from carcinoid tumors, while the combination of both peptide scans does not appear to further enhance diagnostic information.

OS-5

A.Chiti, S.Fanti, G.Savelli, A.Romeo, M. Rodari, B.J. van Graafeiland, N.Monetti, E.Bombardieri
Istituto Nazionale Tumori, Milano and Policlinico S.Orsola Malpighi, Bologna - ITALY

SOMATOSTATIN RECEPTOR IMAGING (SRI) IN GASTRO-ENTERO-PANCREATIC (GEP) NEUROENDOCRINE TUMORS

Introduction: Somatostatin receptor imaging has been assessed as an accurate tool for imaging somatostatin receptor bearing tumors. However, its role may vary depending on the clinical setting. **Methods:** We studied 131 patients (pts) (61 female, 70 male, mean age 52.7 y) affected by GEP tumors. A pathological diagnosis was obtained in 116 pts, instrumental in 11, clinical in 4. 51 pts were in staging, 80 in follow-up. Images were acquired 4, 24 and 48 hours after the injection of 150-220 Mbq of 111-In-pentetreotide. Whole body and SPECT images were recorded in all pts. Pts were also studied with computed tomography (CT), ultrasound (US), and other procedures (Other). Tumors were classified according to Capella et al. (Virchows Archiv 425:547-560,1991): pancreas=39, upper intestine=42, biliary tract=2, stomach=16, lower intestine=15, liver metastases (mts) from unknown primary (UP)=15, diffuse mts from UP=2. **Results:**

Primary tumor localization sensitivity:

SRI (55 pts): 62%	CT (49 pts): 43%	US (44 pts): 36%	Other (29 pts): 4%
-------------------	------------------	------------------	--------------------

Liver mts:	SRI (131 pts)	CT (109 pts)	US (102 pts)
sensitivity	90%	78%	88%
specificity	97%	93%	95%
accuracy	93%	83%	91%
Other soft tissue lesions:	SRI (131 pts)	CT (75 pts)	Other (48 pts)
sensitivity	90%	66%	61%
specificity	98%	98%	97%
accuracy	95%	83%	83%

Bone lesions sensitivity: SRI (38 pts): 24%, bone scan (10 pts): 60%.

In 28% of the pts SRI revealed previously unknown lesions, in 21% SRI determined a significant modification of therapy.

Conclusions: Although this study confirms the important role of SRI in GEP tumors management, it is our opinion that a critical investigation should address its role in localizing primary tumors, in particular in patients with mts from UP.

OS-6

O.Schillaci*, F.Scopinaro, R.Danieli, P.Cannas, S.Angeletti, V.Picardi, V.Corleto, F.Montealeone, G.DelleFave, A.CentiColella Dept. Exp.Med.Path.and Gastroent., Univ. "La Sapienza", Rome and *Nucl.Med., Univ.L'Aquila, Italy

THE ADDITIVE VALUE OF SPECT IMAGING IN THE DETECTION OF GASTROENTEROPANCREATIC NEUROENDOCRINE (GEP) TUMOURS (T) WITH SOMATOSTATIN RECEPTOR SCINTIGRAPHY (SRS).

The accurate localizations of all the neoplastic lesions (le), whether primary or metastatic, has important therapeutic implications in patients (pts) with GEP T. SRS using In-111 pentetreotide (In-pe) has proved to be useful in the detection of GEP T; however, the role of abdominal (ab) SPECT imaging is still controversial. The aim of this study was to evaluate if In-pe ab SPECT can provide more informations than planar images (PI) in evaluating GEP T. 87 pts (including 41 carcinoids, 25 gastrinomas, 10 nonfunctioning islet cell carcinomas, 5 insulinomas, 3 somatostatinomas, 2 vipomas and 1 glucagonoma) underwent total body PI (at 4 and 24 hrs) and ab SPECT (at 4 hrs) after In-pe injection. MRI and CT were performed within one month. Only ab localizations were considered, and 5 or more liver sites were counted as 5. In-pe PI detected 36 ab extrahepatic (eh) le in 29 pts and 62 liver sites in 26 pts. SPECT visualized a total of 58 ab eh le and 113 liver metastases in 50 and 42 pts, respectively. MRI and CT detected 26 eh le in 22 pts and 94 liver le in 34 pts. In-pe SPECT was the only method able to detect le in 25 pts; these le were then histologically proven. In particular, in pts with insulinoma SPECT was positive in 5/5, whereas PI and MRI only in 1/5. The scintigraphic visualization of tumor tissues did not depend on the site of the le or on the presence of hormonal hypersecretions. In conclusion, our results demonstrate that In-pe SPECT is the single most accurate method to detect GEP T and their metastases: it is more sensitive than PI and CT/MRI not only in localizing primary le, but also in assessing liver and ab eh involvement. So SPECT is mandatory when ab le are to be detected; it should be the first imaging modality in pts with GEP T, and its initial use will result in more informations which allow proper management of the disease.

Oncology: Breast

OS-7

G.Paganelli, C.De Cicco, M.Cremonesi, A.Luini*, M.Bartolomei, C.Grana, G.Prisco, V.Galimberti, P.Calza, G.Viale***, U.Veronesi* Divisions of Nuclear Medicine, Senology* and Pathology*** European Institute of Oncology, Milan, Italy

LYMPHOSCINTIGRAPHY AND RADIOGUIDED BIOPSY OF THE SENTINEL AXILLARY NODE IN BREAST CANCER

Lymphoscintigraphy (LS) associated with radioguided biopsy of the sentinel node (SN) is well-established in clinical practice for melanoma. In breast cancer the sentinel node concept is similarly valid and lymphoscintigraphy is a useful method for localizing the axillary sentinel node. The aim of the present study was to optimize the LS technique in association with a gamma detecting probe (GDP) for identifying and removing the SN in breast cancer patients.

Methods: Two hundred fifty patients with operable breast tumor underwent LS before surgery. Three different size ranges of ^{99m}Tc-labelled colloid particles (<50, <80, and 200-1000 nm) were used, with either subdermal (above tumor) or peritumoral injection. Early and late scintigraphic images were obtained in anterior and oblique projections, and the skin projection of the detected SN was marked. SNs were identified and removed with the aid of the GDP during breast surgery; they were tagged separately. Complete axillary dissection followed. In 40 patients a blue dye was also administered in addition to subdermal radiolabeled colloid to compare blue dye mapping with LS localization.

Results: LS successfully revealed lymphatic drainage in 245/250 patients (98%). The axillary SN was identified in 240 patients (96%). SN biopsy correctly predicted axillary node status in 234/240 patients (97.5%). LS and GDP detected the SN most easily and consistently when 200-1000 nm colloid was administered subdermally in an injection volume of 0.4 mL. Blue dye mapping was successful in 30/40 patients (75%), in 26 of whom the dye and LS identified the same node; in four cases different nodes were identified. None of these four patients had axillary disease.

Conclusions: LS is a simple procedure that is well-tolerated by patients. SN identification is more reliable when large-size radiolabeled colloids are injected in a relatively small injection volume (0.4ml). Use of a GDP greatly facilitates precise pin-pointing and rapid removal of the SN.

Work supported by grants of the Italian Association for Cancer Research (AIRC)

OS-8

P.L.Jager, M.H.E.Doting, L.Jansen, O.E.Nieweg, C.Hoefnagel, R.Valdés Olmos, E.J.Th.Rutgers, B.B.R.Kroon, H.Schraffordt Koops, J. de Vries, D.A.Piers. University Hospital Groningen and The Netherlands Cancer Institute, Amsterdam, the Netherlands.

SENTINEL NODE LOCALISATION IN BREAST CANCER

Purpose: to determine the ability to identify a sentinel node (SN), its predictive value and the impact on operation logistics.

Methods: A total of 90 patients with palpable breast cancer were enrolled. Lymphoscintigraphy was performed up to 6 hr after injection of 50 MBq ^{99m}Tc-nanocolloid (0.2 ml) in the tumor, followed by surgery the next day. Immediately before surgery 1 ml of patent blue was injected in the tumor. SNs were retrieved guided by skinmarks, a handheld gammadetection probe (Neoprobe 1000) and the blue dye. In addition, a full axillary lymph node dissection was performed and surgery for the primary tumor.

Results: Scintigraphy revealed one or more SNs (mean 1.5, max 3) in 74 patients (82%). All but four of these radioactive SNs could be localized the next day at surgery: 13% only by the blue dye, 22% only by the probe, 65% by both methods. In 18 of these 74 patients scattered radiation from the injection site prevented probe localisation of the SN, and therefore the primary tumor had to be removed before the axilla was searched.

In the 16 cases where the gammacamera showed no SN, 8 SN (one per case) were still identified because of blue color, 4 of which contained micrometastatic disease. In the remaining 8 cases no SN could be identified. Possible reasons for these scintigraphic failures are impaired drainage from the center of the tumor, old age, extensive nodal metastatic disease or leakage of colloid to the circulation.

In 45% of the patients where a SN was identified, this SN was tumor-positive and in 24% this SN was the only positive node in the entire axilla specimen. Never were other nodes found to contain metastatic disease when the SN was tumor-free except in one patient, but this patient had a multicentric tumor.

Conclusion: a SN could be identified in 82% pre-operatively and in 91% intra-operatively with our combined approach using intra-tumoral injection, scintigraphy, patent blue and intra-operative gammadetection. Discrepancies between individual methods were present in ~20% of cases. The primary tumor had to be removed before opening the axilla in 24%. Despite these difficulties the sensitivity of this combined approach for the determination of the axillary tumor status was 100%.

OS-9

G. Villa, F. Schenone, M. Gipponi, P. Bianchi, F. Buffoni, S. Bertoglio, C. Vecchio, A. Peressini, G. Agnese, G.F. Conzi, G. Canavese, G. Nicolò, and G. Mariani.
Nuclear Medicine Service, DIMI, University of Genoa; and Nuclear Medicine, Surgical Oncology and Pathology Divisions, IST; Genoa (Italy)

COMBINED LYMPHOSCINTIGRAPHY, PATENT-BLUE-V AND INTRASURGICAL GAMMA-PROBE FOR THE IDENTIFICATION OF SENTINEL LYMPH NODE IN BREAST CANCER

Identification of the sentinel node (sN), the first draining lymph node of primary tumors, is crucial for the surgical approach as well as for staging and long-term prognosis of patients (pts). Aims of this study: 1) to evaluate the potential of combined lymphoscintigraphy and intrasurgical gamma-probe for identifying sN in breast cancer pts; 2) to optimize the scintigraphic technique; 3) to predict axillary-node status by the sN.

49 pts with N0/N1 breast cancer underwent lymphoscintigraphy 18 hr before surgery: 300 µCi in 150 µl of HSA ^{99m}Tc-microcolloids or nanocolloids (Amersham-Sorin) was injected peritumorally, or intradermally over the tumor mass. Images were acquired at 10 min, then every 30 min until scintigraphic identification of the sN. Just before surgery, 1-2 ml of Patent-Blue-V (PB-V) was injected peritumorally. Before axillary dissection, the sN was searched by using in all patients two hand-held collimated gamma-probes (Neoprobe and Scintiprobe-Pol.hi.tech), and by the dye method. When possible, the sN was surgically isolated.

No significant difference in the sN-localizing properties was found between the two probes, although higher target/background ratios were observed with Scintiprobe. The sN was not identified in 4/49 pts (8%), while combined gamma-probe and PB-V identified 45/49 sNs (92%). PB-V identified fewer sNs than gamma-probe (51% versus 74%), while the success rate for PBV alone was 6% versus 29% for gamma-probe alone. At scintigraphy, peritumoral injection visualized the sN in only 3/15 pts (27%), while intradermal injection visualized 36/38 sNs (95%). 14/45 identified sNs were metastatic, the sN alone being involved in 7 pts; skip metastasis was found in only 1/45 pts (2.2%).

Intradermal rather than peritumoral injection was the optimal technique for identifying the sN, and combining gamma-probe guidance with PB-V significantly improved the intrasurgical identification of sNs. There was a high correlation between negative sN and negative axilla.

OS-10

J.B. Cwikla, J.R. Buscombe*, S.P. Parbhoo*, D.S. Thakrar*, J.Hinton*, A.J.W. Hilson*.

PSK2; Department of Radiology and Nuclear Medicine. Otwock; Poland Royal Free Hospital and School of Medicine*, Departments of Nuclear Medicine, Breast Surgery and Radiology. London; UK.

EVALUATION OF AXILLARY NODE INVOLVEMENT IN PATIENTS WITH BREAST CANCER

The most important prognostic factor in primary and recurrent breast cancer is the presence of axillary node involvement. A prospective trial was performed to assess the accuracy of Tc-99m MIBI scintimammography (SMM) in patients with breast cancer and suspected axillary disease. Study was performed in 95 patients (mean age 53.3, SD 12; range 28-84 years). In each case X-ray mammography (XM) and Tc-99m MIBI (SMM) was performed. All patients had histological confirmation of the lesions both the breast and axilla.

SMM was done by intravenous injection of 740 MBq of Tc99m MIBI in the foot. Standard prone lateral and anterior images were performed at 10 min. post injection. Planar images were performed with 256x256 matrix, imaging with 10% windows around a 140keV photopeak.

There were 91 patients with cancer, 8 different histological types. Axillary disease was noted in 40 patients. SMM diagnosed 22 patients correctly as a true positive. There were 18 false negative cases. XM identified correctly 13 of these cancers in 27 cases was false negative. There were 55 cases without axillary involvement. 41 of them were correctly assessed by SMM (14 false positives) and 50 patients were correctly diagnosed by XM (5 false positives). Overall diagnostic accuracy of SMM for assessing axillary node involvement in these patients was as follows: sensitivity, specificity, PPV and NPV, 55%, 75%, 61% and 69% and for XM was as follows: 33%, 91%, 20%, 65%. This difference was significant (Fisher's two tailed exact test p<0.05).

Tc99m MIBI SMM may provide unique information on the presence of axillary node involvement in breast cancer. The accuracy of the technique is not sufficient to replace biopsy. However if axillary uptake is found as part of a standard SMM the axilla should be explored.

OS-11

V.Briganti*, F.Meucci*, P.Ferri*, C.Gallini*, E.Costanzo*, L.Vaggelli*, R.Masi*, V.Distante#, L.Cataliotti# and A.Castagnoli*
U.O. Medicina Nucleare, Az. Ospedaliera Careggi, # Cl. Chirurgica I, Università degli Studi di Firenze.

^{99m}Tc-TETROFOSMIN SPET SCAN QUANTITATIVE EVALUATION IN DETECTING BREAST CANCER LYMPH NODE INVOLVEMENT: CAN IT SAVE AXILLARY LIMP NODE DISSECTION ?

All patients with breast cancer virtually undergo an axillary lymph node dissection (ALND) in order to evaluate lymph node involvement. A sensitive tool is needed to select patients in order to save ALND, a procedure not without cost and morbidity. The aim of the study was to evaluate ^{99m}Tc-Tetrofosmin (Tfos) in the assessment of lymph node involvement in patients with proven breast cancer with the possible saving of ALND. Twenty females were studied by means of Tfos SPET scan quantitative TNT-ROIs evaluation of axillae. All patients underwent surgery within two days from SPET study, axillary nodes were excised and histology obtained. All TNT-ROIs > 1.2 was considered positive, being high sensitivity the goal of the study. All patients had breast carcinoma. Ten patients had not axillary lymph node metastases. Quantitative Tfos SPET was positive in 13/20 (65%) of axillae. Sensitivity, specificity, PPV and NPV for axillary node involvement were 100%, 70%, 64%, 100%, respectively. Using this technique 7/11 (64%) ALND should have been spared. In our opinion quantitative Tfos SPET scan appears a valuable tool in selecting patients not to be explored by ALND in breast cancer.

OS-12

E. Bombardieri, F. Crippa, R. Agresti, M. Leutner, V. Delledonne, M. Greco, B. Salvadori

Istituto Nazionale per lo Studio e la Cura dei Tumori di Milano (Italy), Divisione Medicina Nucleare

FDG-PET IN THE DETECTION OF AXILLARY METASTASES IN BREAST CANCER PATIENTS: ECONOMIC IMPLICATIONS

Introduction: This study analyzes the accuracy of FDG-PET in preoperative detection of axillary metastases. A cost-effectiveness of FDG-PET in the management of patients was retrospectively evaluated. **Methods:** 134 patients with palpable breast lesions scheduled for surgery and, if indicated, ALND, were studied. Preoperative FDG-PET was compared with postoperative histopathology. The clinical stage was: N0 (58pts), N1a (47 pts), N1b-2 (29 pts). The results of histopathology were as follows: 117 carcinomas (80 pure ductal carcinoma) and 17 dysplasias. The 117 patients underwent ALND; the mean number of dissected nodes was 23 (range 9-49). Histology diagnosed 56 cases as being pN+ and 61 as pN-. **Results:** The performance of FDG-PET in the axillary staging is shown in the following table.

FDG-PET	No (n = 58)	N1a (n = 47)	N1b-2 (n = 29)	Overall (n = 134)
Sensitivity	84% (16/19)	87.5% (14/16)	95% (20/21)	89% (50/56)
Specificity	92% (36/39)	87% (27/31)	62.5% (5/8)	87% (68/78)
Accuracy	90% (52/58)	87% (41/47)	86% (25/29)	88% (118/134)
Positive PV	84% (16/19)	78% (14/18)	87% (20/23)	83% (50/60)
Negative PV	92% (36/39)	93% (27/29)	85% (5/6)	92% (68/74)

Considering that surgeons are not likely to give up ALND in N1b-2 patients, FDG-PET could be used for surgical planning in N0-1 patients. In our patients FDG-PET could have avoided unnecessary ALND in 90% (63/70) of patients without axillary metastases and would have correctly referred to ALND 86% (30/35) of patients with axillary metastases. As regards the cost savings resulting from omission of unnecessary ALND, taking into consideration the mean cost in Italy of ALND (\$ 3,310) and Italian reimbursement rate for FDG-PET (\$ 1,185), the total savings amounted to \$ 995 per patient, without considering additional cost due to the morbidity of ALND. **Conclusions** FDG-PET showed good overall diagnostic accuracy in the detection of axillary metastases. The very high accuracy in N0 (90%) patients is of particular importance. Considering the economic costs this evaluation was performed only on the crude economic costs, without considering other factors such as side effects of ALND, quality of life, and survival. However, it is clear that the application of FDG-PET may contribute to the avoidance of a certain number of surgical dissections, thus involves some economic benefits (partially supported by AIRC Project and by Italian Ministry of Public Health)

■ Cardiovascular: Prognosis

Cardiovascular: Prognosis

OS-13

P. Zanco, A. Desideri*, F. Chierichetti, D. Rubello, S. Bissoi, C. Cernetti*, A. Fini, L. Celegon*, G. Ferlin.
Nuclear Medicine-PET Center and *Cardiology, Castelfranco Veneto, Italy.

LONG TERM PROGNOSTIC ROLE OF 13N-AMMONIA (13NH3)/18F-FLUORODEOXYGLUCOSE (18FDG) PET IN THE FOLLOW UP OF CAD PATIENTS.

13NH3-18FDG PET is the gold standard in myocardial viability searching, but the real impact of this technique in the long-term prognosis of CAD patients is unknown.

To this aim, among the CAD patients examined by 13NH3(basal)-18FDG(glucose load-insulin) PET in our center searching for viable myocardium, 59 patients (52M, 7F, age 59 ± 9 y, mean ejection fraction 34 ± 12 %) with a follow-up superior to 3 years were enrolled. For the PET analysis the left ventricle wall was divided into 16 segments and a perfusion/metabolism mismatch (MM) was considered present when the 18FDG uptake was superior to 13NH3 in at least 2 segments.

After PET 26 patients were submitted to surgical therapy (24 revascularizations and 2 cardiac transplants). During the follow-up, no revascularized patient suffered from cardiac events. Among the 33 patients maintained in medical therapy, 9 patients were affected by a hard cardiac event (8 deaths and 1 MI). The percentages of events in patients with and without MM are reported in table:

	medical therapy
MM	62%*
no MM	16%*

* p < 0.05

In conclusion our experience suggests a strong prognostic impact of 13NH3-18FDG PET in long term follow-up of CAD patients, with a significant higher risk for hard cardiac events in patients with perfusion/metabolism mismatch maintained in medical therapy.

OS-14

M. De Groof, F. Eerens, A. Maes, J. Nuyts, V. Van den Maegdenbergh, P. Michiels, W. Flameng, P. Sergeant, F. Van de Werf, L. Mortelmans.

University Hospital Gasthuisberg, Leuven, Belgium, Department of nuclear medicine

LONG TERM (FOUR YEAR) FUNCTIONAL FOLLOW UP OF POSITRON EMISSION TOMOGRAPHY VIABILITY STUDIES.

Purpose: the present study was performed to determine whether positron emission tomography could predict long term (4 year) functional improvement in patients with chronic coronary artery disease after revascularization.

Methods: the study population consists of 52 chronic CAD patients who underwent combined nitrogen-13-ammonia/fluorine-18-fluorodeoxyglucose PET imaging to assess myocardial viability. Overall resting LV function was determined with radionuclide angiography using technetium-99m labelled red blood cells. The patients were reinvestigated 4.2 ± 0.8 years after the PET imaging procedure with a follow-up resting radionuclide angiography. An increase of 5 % in ejection fraction was considered as the cut off for functional improvement. Shortly after the PET scan 37 of these 52 patients had a successful revascularization in one or more vascular territories. Myocardium was classified using a polar map approach in 3 categories as PET mismatch (metabolism/flow ratio > 1.2), match ($0.8 < \text{metabolism/flow ratio} < 1.2$) and reverse mismatch (metabolism/flow ratio < 0.8). The relative amount of myocardial tissue belonging to each of these 3 categories was determined semiquantitatively for the whole heart. Statistical analysis was performed using one way analysis of variance and Scheffé analysis for multiple comparisons.

Results: in the successfully revascularised patients the only significant ($p < 0.05$) difference that could be detected between the group of patients with improved ejection fraction ($n=13$; EF $49 \pm 9\%$ -> $59 \pm 11\%$) and the group without improvement ($n=24$; EF $52 \pm 15\%$ -> $48 \pm 16\%$) is the relative amount of "mismatched" myocardium: mean value 29 % versus 15 % (standard errors 3 % and 7 %). In the patients without intervention ($n=15$) no significant functional improvement was observed (EF $43 \pm 12\%$ -> $42 \pm 14\%$).

Conclusion: myocardial viability characterized by the relative amount of "PET mismatched" myocardium is a prognostic factor for long term functional improvement in patients with chronic coronary artery disease after revascularization.

OS-15

J.J. Bax*, J.H. Cornel**, F.C. Visser#, A. van Lingen#, P.M. Fioretti##, C.A. Visser##.

University Hospital Leiden*, Medical Center Alkmaar**, Free University Hospital Amsterdam#, Netherlands and Istituto di Cardiologia##, Udine, Italy.

PREDICTION OF IMPROVEMENT OF HEART FAILURE SYMPTOMS BY FDG SPECT.

F18-fluorodeoxyglucose (FDG) SPECT can predict improvement of LV function after revascularization. It is uncertain whether viability on SPECT is also predictive for improvement of heart failure (HF) symptoms. In the current study, the predictive value of FDG SPECT for improvement of HF symptoms was assessed. Patients ($n=32$) with chronic coronary artery disease (mean LVEF $28 \pm 6\%$) were studied. Glucose utilization was assessed by FDG SPECT during hyperinsulinemic glucose clamp. Regional perfusion was assessed by early TI-201 SPECT. The data were analyzed semi-quantitatively and displayed in polar map format (13 segment-model). Regional contraction was assessed by echo (13-segment model). Dysfunctional segments with normal perfusion or perfusion-FDG mismatch were considered viable. A patient was considered viable when ≥ 3 dysfunctional segments were viable on SPECT. HF status was assessed before and 3 months after revascularization using the New York Heart Association (NYHA) criteria.

Of the 18 patients with ≥ 3 viable segments on SPECT, 13 improved their NYHA status by 1 grade or more; the NYHA score improved from 2.9 ± 0.3 to 1.5 ± 0.7 ($P < 0.01$). Conversely, 3 of the 14 patients with < 3 viable segments improved their NYHA status by 1 grade or more ($P < 0.05$). The mean NYHA score did not change after revascularization: 2.6 ± 0.5 vs 2.4 ± 0.7 , NS. SPECT had a positive predictive value of 87% and a negative predictive value of 70% to predict improvement of HF symptoms. In conclusion, patients with substantial viability on FDG SPECT frequently improve in HF symptoms after revascularization.

OS-16

*H J Neethling, B B van Heerden, A Ellmann, J F Klopper

Departments of Internal Medicine* and Nuclear Medicine, Tygerberg Hospital, Tygerberg, South Africa

THE PROGNOSTIC SIGNIFICANCE OF NORMAL TECHNETIUM-99m SESTAMIBI MYOCARDIAL PERFUSION SPECT IMAGING OVER A FOUR YEAR FOLLOW-UP PERIOD.

The benign long term outcome in patients with a normal TI-201 myocardial perfusion study has been well documented. In the case of Tc-99m sestamibi, a normal study has been shown to indicate a favourable prognosis over the short and medium term. Our aim was to determine the longer term prognostic significance of a normal Tc-99m sestamibi myocardial perfusion SPECT study.

A retrospective analysis of the data obtained from 209 consecutive patients with a normal Tc-99m sestamibi stress-rest myocardial perfusion SPECT study, was performed. Follow-up data could be obtained in 157 (complete in 121 and partial in 36) of these patients. Patients were evaluated for the occurrence of primary (cardiac death or non-fatal myocardial infarction) or secondary (recurring chest pain requiring revascularisation) cardiac events following the sestamibi study.

The mean follow-up period was 50.3 ± 15.5 months. The study group had a moderate mean pre-test probability ($48 \pm 30.7\%$) for coronary artery disease (CAD). Two probable cardiac deaths were recorded (cardiac death rate of 0.95%). No other primary cardiac events were recorded, but 6 secondary events were observed in the group with complete follow-up information (cardiac event rate of 4.9% over the whole follow-up period). The yearly event rate in this group was 1.1%. No primary or secondary events were recorded in the group with partial follow-up, during the period for which follow-up information was available (32.3 ± 14.6 months). The incidence of secondary or non-fatal primary events could not be determined in the latter group for the period after they got lost for follow-up, or in the group with no follow-up information. There was, however no statistically significant difference between the various groups (complete, partial and no follow-up information) with regard to age, pre-test probability for CAD or exercise parameters, which makes it unlikely that the incidence of cardiac events would differ between these groups.

The results of this study indicate a benign longer term prognosis, comparable to the data obtained with TI-201, in patients with a normal stress-rest Tc-99m sestamibi myocardial perfusion SPECT study.

OS-17

IY Hyun, J Kwan*, KS Park*, W Choe, WH Lee*.

Inha University Hospital, Incheon, Korea:
Department of Nuclear Medicine, and Internal Medicine*,

REST TI-201 UPTAKE OF EARLY REST/DELAY TI-201 SPECT PREDICTS WALL MOTION IMPROVEMENT IN PATIENTS WITH ACUTE MYOCARDIAL INFARCTION(AMI) AFTER REPERFUSION

Purpose: We studied to compare the criterias of early TI-201 SPECT for prediction of wall motion(WM) improvement in patients(pts.) with AMI after reperfusion. **Methods:** Among 17 pts.(M:F=11:6, age 59 ± 13) with AMI, 13 pts. were treated with PTCA(direct 2, delay 11), 2 pts. were treated with IV. urokinase. Spontaneous resolution was occurred in infarct-related artery(IRA) of 2 pts. We confirmed TIMI 3 flow of IRA in all pts. with coronary angiogram. We performed rest TI-201 SPECT less than 12 hrs. after reperfusion and delay SPECT next day. TI-201 uptake was visually graded as 4 point score from normal(0) to absent(3). The criterias for predicting WM improvement with TI-201 SPECT were classified to 1)rest TI-201 uptake<3, 2)rest TI-201 uptake<3, or late reversibility. Myocardial WM was graded as 5 point score from normal(1) to dyskinesia(5). WM was considered to be improved when a segment(seg.) showed an improvement ≥ 1 grade in follow-up echo compared with the baseline values. A 16-seg. model was used for TI-201 SPECT, and echocardiography. **Results:** Among 98 seg. with abnormal WM, the severity of myocardial WM decrease was as follows: mild hypokinesia: 18/98(18%), severe hypokinesia: 28/98(29%), akinesia: 51/98(52%), dyskinesia: 1/98(1%). WM improved in 85%. Redistribution(13%), and reverse redistribution(4%) were observed in delay SPECT. Positive predictive value(PPV) of rest TI-201 uptake was 100%, and negative predictive value(NPV) was 52%. PPV/NPV of combination of late reversibility and rest TI-201 uptake were 99%/54%. There was no significant difference of predictive values between rest TI-201 uptake and combination of late reversibility and rest TI-201 uptake. **Conclusions:** We concluded that early TI-201 SPECT predicted myocardial WM improvement with excellent PPV in pts. with AMI after reperfusion. Using the criteria of rest TI-201 uptake had equal diagnostic accuracy to combination of late reversibility and rest TI-201 uptake, and advantage in that only one image acquisition was enough.

OS-18

B.Dokumaci, S.Atalay, C.Kirdar, E.Entok*, I.Ak*, A. Ünalır, E.Varderehi*, Y.Çavuşoğlu, B.Timuralp
Hospital : Osmangazi University Faculty of Medicine, Department of Cardiology,
*Department of Nuclear Medicine

THE CLINICAL IMPORTANCE OF THE T WAVE INVERSION AND ITS' RELATION WITH THE RESIDUAL ISCHEMIA AFTER RECANALISATION IN ACUTE MYOCARDIAL INFARCTION.

We studied, the clinical importance of the T wave inversion and its' relation with the residual ischemia after recanalisation in acute myocardial infarction.

Methods: The study group consisted of 36 patients, 26 of which were reperfused with thrombolytic therapy and 10 patients with spontaneous reperfusion. Twentysix of the patients were male and the mean age was 56 ± 2 years (±SEM). To determine the defect area before reperfusion, IV tetrafosmine was injected to all the patients, just before the reperfusion procedure. Myocardial perfusion scintigraphies were repeated in the days 12 - 26 (mean 17±1 day) with symptom limited exercise testing. Coronary angiographies were performed before and 32 ± 3 hours following the thrombolytic therapies. ECGs taken after 24 hours of the reperfusion were compared with the initial ECGs. In the 24th hour ECGs, we investigated the presence of the T wave inversions in at least half of the derivations with ST segment elevations which were seen in the first ECGs. T wave was accepted to be inverted if it was monophasic negative with at least 1 mm of amplitude. **Results:**The results are shown in the table.

	Patients without residual isch area	Patients with residual isch. area	Total
Patients with Early T wave Inversion	18	2	20
Patients without Early T wave Inversion	2	14	16
Total	20	16	36

The sensitivity and the specificity of the T wave inversion, in determining the absence of the residual ischemic area were 90 % and 88 %, respectively. Sensitivity and specificity in spontaneously reperfused patients were 100 %, whereas in patients with reperfused by means of thrombolytic therapy, sensitivity was 86% and specificity was 88%. As a result, early T wave inversion is an important determinant of the absence of residual ischemia, following reperfusion in acute myocardial infarction.

Neurology/Psychiatry: Epilepsy

OS-19

I.Podreka¹, F. Leutmezer, S. Asenbaum, E. Punz¹, W. Serles, E. Pataraja, T. Heller¹, C. Baumgartner

Neurologische Universitätsklinik Wien, ¹Neurologische Abteilung der KA-Rudolfstiftung Wien

TEMPORAL LOBE EPILEPSY (TLE): WHAT IS DEACTIVATED DURING THE SEIZURE ?

Ictal hyperperfusion in the epileptogenic zone visualized by SPECT is a well known phenomenon, which is used besides other techniques for seizure focus lateralisation. However, deactivation of brain areas, which may account for impaired consciousness during the seizure was not investigated until now. Our goal was to identify brain areas with decreased ictal regional cerebral blood flow (rCBF), when compared to the interictal state.

A group of 25 (13f, 12m;18-24 yrs) patients suffering from TLE was investigated. 740MBq of HMPAO were injected 12-56 sec after seizure onset, which was documented by video-EEG. Interictal SPECT-studies and MRI were also performed in each patient. After coregistration of the interictal and ictal SPECT study 107 ROIS were drawn on 9 adjacent transversal cross-sections of the interictal SPECT study and then transferred to the correspondent ictal SPECT-sections. Normalized rCBF values were calculated (regional index=RI= mean cts in ROI/mean cts of all ROIS). Paired t-test was applied for comparison of interictal and ictal RI-values. Normalized rCBF decreased significantly (p<0.04 to p<0.0001) during the seizure in 21 ROIS, located in the right (10 ROIS) and left lateral frontal cortex (4 ROIS), in the right (2 ROIS) and left (1 ROI) occipital cortex, in the right parietal cortex (2 ROIS) and in 2 ROIS located in the SMA region. After correction for multiple comparisons (Bonferroni: level of significance p<0.05) significant RI values persisted in 4 laterofrontal ROIS.

We conclude that a significant decrease of normalized rCBF in the lateral frontal cortex is a common rCBF pattern, which is observed during TL-seizures. This frontal lobe deactivation may contribute, besides other unknown factors, to the ictal impairment of consciousness. This hypothesis is supported by the observation in patients with epileptogenic psychosis, who show an increase of normalized rCBF in temporal ROIS. This increase is slightly less pronounced when compared to the ictal state. However, frontal "deactivation" and loss of consciousness are not present during epileptogenic psychosis.

OS-20

S.Asenbaum, I.Podreka, F.Leutmezer, E.Pataraja, W.Serles, W.Pirker, A.Becherer and C.Baumgartner

Departments of Neurology and Nuclear Medicine, University of Vienna, and Krankenanstalt Rudolfstiftung, Vienna, Austria

CHANGES OF CEREBRAL BLOOD FLOW AFTER SELECTIVE AMYGDALO-HIPPOCAMPECTOMY IN PATIENTS WITH TEMPORAL LOBE EPILEPSY

The aim of the present study was to evaluate cerebral blood flow (CBF) before and after selective amygdalo-hippocampctomy (AH) in patients with medically intractable mesiotemporal lobe epilepsy (MTLE) using 99mTc-HMPAO and the SPECT technique. **Methods:** 14 pts (6male, 17-49y) with MTLE (defined by typical clinical seizure semiology, interictal and ictal EEG-findings and hippocampal atrophy/sclerosis on MRI) were investigated under antiepileptic therapy during the interictal state before and 3 months (n=12), 1 year (n=4) and 2 years (n=5) after AH. Postoperatively, 11 patients were seizure-free. For evaluation of SPECT studies 107 regions of interest (ROI) were drawn manually on 9 slices after image reorientation, applying the same set of ROI on the individual follow-up studies. Regional indices (RI) of 107 and 38 ROI (gained after summing values of corresponding regions in different slices), normalized to individual brain values, were calculated and comparisons between pre- and individual postoperative data were performed by using a paired Student's t-test. **Results:** In comparison to preoperative values not only RI of the mesiotemporal regions corresponding to the resected tissue were significantly reduced at every time point, but also RI of all ipsilateral laterotemporal regions and of the inferior frontal/frontobasal cortex. Furthermore, the investigation 3 months after AH revealed a significantly higher RI in supra- and laterotemporal regions and the basal ganglia contralaterally to the resection. (see table, values for 38 ROI).

ipsilat.	3 months	1 year	2 years	contralat.	3 months	1 year	2 years
lat.temp.	t=4.4, p<.001	t=3.3, p<.04	t=2.8, p<.04	lat.temp.	t=-3.2, p<.008	n.s.	n.s.
mes.temp.	t=4.2, p<.001	t=6.5, p<.007	t=2.8, p<.04	supratemp.	t=-3.0, p<.01	n.s.	n.s.
inf.front.	t=3.05, p<.01	n.s.	t=2.6, p<.05	basal gangl.	t=-3.1, p<.01	n.s.	n.s.

Conclusion: The permanent relative hypoperfusion of ipsilateral laterotemporal and inferior frontal/frontobasal regions may indicate persistent neuronal deafferentation of these regions after AH. Findings contralateral to the resection, mainly in the temporal lobe, could be explained by temporary compensatory activation due to functional interhemispheric connections.

OS-21

D.S. Lee, S.K. Kim, S.K. Lee, D-W. Kang, J-K Chung, M.C. Lee.

Seoul National University College of Medicine, Seoul, Korea

BETTER DIFFERENTIATION OF FRONTAL FROM TEMPORAL LOBE EPILEPSY USING CHARACTERISTIC PROPAGATION PATTERN OF HYPERPERFUSION WITH Tc-99m-HMPAO ICTAL SPECT

Ictal propagation of hyperperfusion could confound the localizing power of ictal perfusion SPECT. Frontal or temporal lobe epilepsy could be mistaken with each other if we regarded the most hyperperfused area as epileptogenic zones. We investigated that diagnostic performance increased if we considered propagation pattern of hyperperfusion to localize frontal or temporal lobe epilepsy.

Sixty-five patients were studied, who were proven (Engel class I or II) frontal lobe epilepsy (FLE, n=19: 12 lesional and 7 cryptogenic) and temporal lobe epilepsy (TLE, n=46; medial TLE (32): all hippocampal sclerosis or lateral TLE (14): 8 lesional and 6 cryptogenic).

Using ictal Tc-99m-HMPAO SPECT, we graded hyperperfusion as 0 (normal) to 2 (the most hyperperfused) and classified the propagation pattern blinded to the final diagnosis. While 10 out of 19 FLE and 8 out of 46 TLE patients did not show any area of hyperperfusion, we found ictal hyperperfusion in 9 (47%) FLE and in 38 (83%) TLE patients, respectively. In only 4 (21%) of 19 FLE patients, frontal lobes were found as the most hyperperfused areas, however, all these patients did not show anterior temporal lobe hyperperfusion. In 7 TLE patients propagation of ictal hyperperfusion was so prominent from temporal to frontal lobe that we recognize frontal lobe as the most hyperperfused area. Temporal lobe was the most hyperperfused area in 20 (63%) of 32 medial TLE patients and in 9 (64%) of 14 lateral TLE patients. In 5 FLE patients with possible lateralization, characteristic fronto-temporo-parietal lobe hyperperfusion was found in 4. If we considered that temporal to frontal propagation was found only in temporal lobe epilepsy though the most hyperperfused area was frontal lobe, we could differentiate correctly TLE from FLE in 11 more patients among 14 possibly misclassified patients.

We conclude that propagation pattern of hyperperfusion helped correct localization with ictal SPECT and that 78% of TLE and 42% of FLE patients were localized correctly in our surgically proven series of patients.

OS-22

S.K. Kim, D.S. Lee, J.-Y. Kim, S.-K. Lee, J.-K. Chung, M.C. Lee.

Seoul National University College of Medicine, Seoul, Korea

DIAGNOSTIC PERFORMANCE OF ICTAL Tc-99m-HMPAO SPECT AND F-18-FDG PET IN OCCIPITAL LOBE EPILEPSY

Ictal perfusion SPECT and FDG PET proved to be useful in localizing epileptogenic zones in neocortical lateral temporal or frontal lobe epilepsy as well as in medial temporal lobe epilepsy. We investigated if ictal SPECT or FDG PET was also useful to find epileptogenic zones in occipital lobe epilepsy (OLE).

We reviewed pattern of hyperperfusion in ictal perfusion SPECT, ictal semiology and ictal EEG in 15 OLE patients (28±7 year old, M:F=10:5 injection time=41±23 sec) and also looked for area of hypometabolism in F-18-FDG PET in 13 out of 15 patients. OLE was diagnosed by surgical outcome (Engel class I or II in 9 patients) or invasive EEG (in 6 patients).

On ictal Tc-99m-HMPAO SPECT, epileptogenic hemisphere was correctly lateralized in 12 patients (80%) but 3 were normal. We found localized occipital hyperperfusion only in 1 patient and temporo-occipital-lobe hyperperfusion in another. We observed temporal-lobe-only hyperperfusion in 4 patients: they could be mistaken as temporal lobe epilepsy. Two patients showed temporo-parietal, one fronto-temporo-parietal, and another fronto-temporal lobe hyperperfusion. One patient experienced complex partial status epilepticus and showed frontal hyperperfusion. We could not relate hyperperfusion of adjacent lobes with complex or simple types of partial seizures. There was no difference in injection time between well-localized cases and lateralized-only ones. On F-18-FDG PET, lateralization was successful in 10 out of 13 patients (69%) while in 9 patients localization was also correct. The other 3 did not have any hypometabolic area. There was found no false lateralization on ictal SPECT and PET.

Occipital lobe epilepsy was less well localized by ictal SPECT than other neocortical epilepsy, though lateralization was successful in 73%. We suggest that we should be cautious not to mistake occipital lobe epilepsy as temporal lobe epilepsy referring only to ictal SPECT and that F-18-FDG PET could be very helpful for differentiation.

OS-23

D.Y. Kang, D.H. Moon, J.W. Shin, J.S. Ryu, J.K. Kang, M.J. Lee, and H.K. Lee.

Asan Medical Center, University of Ulsan, Seoul, Korea.

CROSSED CEREBELLAR HYPERPERFUSION (CCH) ON Tc-99m ECD ICTAL BRAIN SPECT IN TEMPORAL LOBE EPILEPSY: DIAGNOSTIC VALUE IN THE LATERALIZATION OF SEIZURE FOCI AND CORRELATION WITH ASSOCIATED PERFUSION ABNORMALITIES.

Although CCH on ictal brain SPECT has been described in epilepsy, its significance in temporal lobe epilepsy is still uncertain. We compared CCH with ictal temporal hyperperfusion to evaluate the additional diagnostic value for the lateralization of seizure foci. Ictal hyperperfusion of basal ganglia (BGH) was also correlated, because CCH and BGH may involve the activation of common pathway.

The study population consists of consecutive 29 patients with temporal lobe epilepsy who underwent ictal brain SPECT and their seizure foci were confirmed by surgery (n=24) or other noninvasive studies (n=5). Injection of Tc-99m ECD was done during ictal phase in all patients with the mean delay of 37±16 sec (mean seizure duration: 104±83 sec). Ictal Tc-99m brain SPECT was visually analyzed by three blinded observers.

Ipsilateral ictal hyperperfusion of temporal lobe was observed in 28 (sensitivity: 97%) patients, whereas ipsilateral BGH was found in 14 (48%), and CCH in 10 (35%) patients. In one patient with false lateralization of contralateral temporal lobe, BGH or CCH was not observed. However, in 2 patients, CCH is more prominent than temporal hyperperfusion, and it helped to lateralize temporal hyperperfusion. In 10 patients with CCH, BGH was observed in 8 (80%) patients. On the other hand, among 19 patients without CCH, 13 (68%) showed normal BG perfusion. CCH and BGH were significantly correlated (p < 0.05).

In conclusion, CCH is less frequently observed than temporal hyperperfusion in temporal lobe epilepsy, and it may be helpful in patients with equivocal hyperperfusion of the temporal lobe. The significant correlation between BGH and CCH suggests they may result from the same mechanism of seizure propagation involving common neural pathway.

OS-24

*K. Borbely, ^A. Balogh, ^V. Juhas, **P. Bazso, *A. Solyom, *J. Vajda

*National Institute of Neurosurgery, ^Szent-István Hospital, **International Medical Center, Budapest, Hungary

PROVOKED ICTAL SPECT STUDIES BY USING PENTETRAZOL

Epilepsy surgery requires high accuracy in localization of the offending focus. Hyperperfusion detected ictally shows a good correlation with surgical findings. Ictal studies are of high importance in presurgical evaluation of epileptogenic areas, particularly in patients with normal MRI findings. However, the execution of ictal examinations is not always possible. The reduction of drugs or deprivation of sleep is not always effective. The administration of the tracer has to be performed under a habitual form of seizure.

PURPOSE: In order to assess the perfusion patterns in brain tissue within, adjacent to, and remote from the epileptogenic foci baseline, ictal and/or provoked ictal studies were performed in six patients with temporal complex partial seizures.

Methods: Baseline, ictal and/or provoked SPECT studies were carried out with a standard technique for each patient and compared with clinical, electrophysiological, and MRI data. The MRI was positive in five cases and in one patient there was no abnormality. The provoked ictal examinations were performed using 6mg/kg of Pentetrazol under EEG recording. SPECT examinations were started 20 minutes following intravenous (iv) administration of 740 MBq of ^{99m}Tc-HMPAO. The duration of time between the beginning of seizures and the application of tracer was a maximum of 15 seconds. The results of perfusion patterns were compared to surgical findings and three-year patient follow-ups.

Results: The MRI correlated well in 5/6 cases. The baseline studies demonstrated a temporal hypoperfusion in 3/6 cases, 1/6 bitemporal, and 2/6 normal. 2/6 of the ictal studies showed a marked hyperperfusion in the epileptogenic area, while in four cases the execution of ictal studies was impossible due to the occurrence of seizures exclusively during nighttime. In the case of slow iv injection of Pentetrazol generalized seizures occurred which were recorded by EEG. In six cases of fast iv injection of Pentetrazol, habitual seizures occurred and were recorded by EEG. In the provoked ictal studies focal hypoperfusion was detected on SPECT images (n=6, p<0.0001), which is contradictory to perfusion patterns of spontaneous ictal studies. The results of the spontaneous as well as provoked ictal studies correlated well with electrophysiological, clinical, MRI data, and with three-year patient follow-ups.

Conclusion: The fast iv administration of Pentetrazol results in habitual seizures both clinically and electrophysiologically. The perfusion patterns of provoked ictal SPECT examinations in brain tissue within, adjacent to, and remote from the epileptogenic area are contradictory to spontaneous ictal studies. In the absence of spontaneous seizures the use of provoking methods is recommended. Pharmacological provocation might be useful in execution of ictal studies, which improves the sensitivity and reliability of SPECT studies, among the multimodal techniques used for the assessment of epileptogenic foci.

Radiopharmacy and radiochemistry: HALOGENS

OS-25

D. W. McPherson, H. Luo, A. L. Beets and F. F. (Russ) Knapp, Jr.

Nuclear Medicine Group, Oak Ridge National Laboratory, Oak Ridge, TN

A NOVEL *IN VIVO* METHOD FOR THE DETERMINATION OF MUSCARINIC LIGAND SUBTYPE SELECTIVITY.

Subtypes alterations of muscarinic acetylcholinergic receptors (mAChR) have been implicated to play an important role in various dementias and spurred interest in the development of new subtype specific drugs, but the evaluation of *in vivo* subtype selectivity of new agents has proven difficult. The E-isomer of R-1-azabicyclo[2.2.2]oct-3-yl R- α -hydroxy- α -(1-iodo-1-propen-3-yl)- α -phenylacetate (IQNP,1) has high *in vitro* binding affinity to m1, m4 mAChR subtypes and the Z-isomer subtype is non-selective. *In vivo* the E isomer binds to cerebral regions containing high concentrations of the m1, m4 subtype while the Z isomer binds to all cerebral regions studied and the heart. Utilizing a dual label study in the same animals, differences between the uptake of these two isomers after 6 hours was observed to reflect the density of the m2 subtype. We report the potential use of this technique for the evaluation of subtype selectivity in a series of established mAChR antagonists. Utilizing female rats, 50 nmol of the cold ligand [(E-(R,R)-IQNP, scopolamine (SCOP), (R)-QNB, R,S-4IQNB, Z-(S)-IPIP, methoctramine (MET)] were preinjected 1 to 3 h prior to the injection of I-125-Z/I-131-E-(R,R)IQNP. The animals were killed 3 h post-injection and the radioactivity in the various brain regions determined. E-(R,R)-IQNP demonstrated the highest subtype selectivity by blocking uptake of radioactivity in cerebral regions containing a high concentrations of m1 and m4 subtypes with respect to controls. SCOP, R-QNB, R,S-4IQNB and Z-(S)-IPIP were able to block uptake of both I-131-E-1 and I-125-Z-1 in all regions of the brain and were therefore determined to be mAChR subtype non-selective. Met, reported to be m2 selective *in vivo*, did not demonstrate binding to cerebral or heart mAChR receptors. This novel method of utilizing a "dual label cocktail" of E and Z -RR-1 demonstrates potential for a routine cost effective tool in the development of new subtype selective mAChR ligands for both SPECT imaging and pharmaceutical drug development. ORNL is managed by Lockheed Martin Energy Research Corporation for the U.S. DOE under contract DE-AC05-96OR22464.

OS-26

Ulrika Berndtsson, Mikael Nilsson, Eva Forsell-Aronsson

University of Göteborg, Sahlgrenska University Hospital, Sweden, Departments of Radiation Physics and Anatomy and Cell Biology.

COMPARISON BETWEEN 211AT AND 125I ION UPTAKE AND TRANSPORT IN PRIMARY CULTURED THYROID FOLLICLE CELLS

Today there is no method for curative treatment of low differentiated thyroid cancer. These tumours do not accumulate 131I but 211At, according to preliminary studies. The properties of the alpha emitter 211At (T1/2=7.21 h) would give rise to a highly localised energy deposition in cancerous cells with minimal irradiation of surrounding normal tissue if it is specifically taken up by tumour tissue. The differences between 211At and 125I are of great importance in the investigation of 211At for future treatment of thyroid cancer.

In the present study the uptake and transport of 211At (astatide) and 125I (iodide) was investigated in porcine thyroid follicle cells cultured in bicameral chambers. For a correct comparison, the number of atoms of 211At and 125I was equal in each experiment.

The results indicate both similarities and differences between the two radionuclides. Both 211At and 125I were transported from the basal medium through the cells in a thyroid-stimulating hormone (TSH) dose dependent manner. As for 125I, the 211At transport was sensitive to perchlorate which inhibited the transport in the basal to apical direction. However 211At transport rate was only reduced by about 50% while the 125I transport was almost blocked. Ouabain, an inhibitor of the Na+/K+-ATPase and pump, reduced the basal to apical transport of 211At less than for 125I. However the cellular content of 211At was similar independent of treatment with perchlorate or ouabain, while perchlorate reduced the cellular content of 125I with 95% and for ouabain with 60%. In the apical to basal direction, 125I was totally inhibited while 211At seemed to be transported in this direction, however, at a lower extent compared to basal to apical direction.

This indicates that at least one part of the transport mechanism differ between astatide and iodide and a possibility for 211At to be accumulated in tumour cells which do not take up 125I.

OS-27

K. Schomäcker, T. Fischer, B. Meller*, D. Moka, H. Schicha, Clinic of Nuclear Medicine), University of Cologne, *Clinic of Radiation Therapy and Nuclear Medicine, Medical University, Lübeck, Germany

PREPARATION AND CHARACTERIZATION OF IODINE LABELLED DIETHYSTIBESTROL

Purpose: Diethylstilbestrol (DES) is a nonsteroidal estrogen with favourable affinity and specificity for estrogen receptor. After first successful animal experiments with radioiodine labelled Diethylstilbestrol-phosphate (DESP) we wanted to develop a fast labelling procedure with reproducible results. Another intention was to determine the labelling position of the iodinated product. We used the DES itself for this purpose because the radioiodination of DESP was time-consuming, very sensitive against variations of pH and temperature and had non-reproducible yields.

Methods: The DES was labelled in methanolic solution on neutral pH by ¹²⁵I, ¹²³I and stable iodine using a modified Chloramine-T-method at room temperature within 10 min. The separation and quality control of the iodinated products was carried out by preparative or analytical HPLC (gradient, eluent: water/methanol, Hypersil C-18 columns). ¹H- and ¹³C-NMR-studies (BRUKER, 300 MHz) were carried out to determine the position of iodine in the molecule. The receptor- and tumour-affinity was investigated on MCF-7 tumour cells and tumour bearing mice.

Results: The labelling of DES succeeded with reproducible yields > 80%, radiochemical and chemical purities > 95 % and specific activities of 80 TBq/mmol for ¹²⁵I-DES and 810³ TBq/mmol for ¹²³I-DES. The iodine is bound in ortho-position related to the OH-group. The binding of ¹²³I-DES to the estrogen-receptor-positive MCF-7 cells could be blocked by excess of cold DES. The compound showed a tumour affinity (10-15 % ID).

Conclusion: We developed a reliable method for labelling of DES with radioactive iodine with a definite labelling position and clear receptor affinity. The substance can be used for *in vivo*-receptor detection and receptor mediated tumour therapy.

OS-28

E. Mennicke, H. Henneken, M. Holschbach, H. H. Coenen

Institut für Nuklearchemie, Forschungszentrum Jülich GmbH, D-52425 Jülich

THALLIUM-TRIS(TRIFLUOROACETATE): A POWERFUL REAGENT FOR THE N.C.A. RADIOIODINATION OF WEAKLY ACTIVATED ARENES

Since its first application in radiochemistry in the early eighties, the thallium-tris(trifluoroacetate) (TTFA)/trifluoroacetic acid (TFA) system has rarely been used for the radioiodination of arenes, despite its handling is simple for direct labelling of aromatic compounds. Although the TTFA/TFA system can be used on the n.c.a. level, radioiodinations by this method were performed with the addition of carrier iodide. Since this method lends itself to the direct and regioselective iodination of aromatic compounds which are weakly activated towards electrophilic substitution, the potential of the TTFA/TFA method was investigated for the n.c.a. radioiodination in detail using toluene as a model compound.

The n.c.a. radioiodination of toluene proceeded with good radiochemical yield (RCY) if optimized reaction parameters were used. A modest RCY of 40% could be obtained using the „classical“ arylthallium precursor and n.c.a. radioiodide. Using TTFA as an oxidant, analogous to the known TFA/oxidant-method (*Appl. Radiat. Isot.* **45**, 929-935 [1994]), n.c.a. radioiodotoluene was obtained with a RCY of >70%. The dependence of the RCY on added carrier iodide for both methods was examined. Using a preformed arylthallium precursor, the RCY reaches a maximum with added carrier and, additionally, shows a high preference for the formation of the para-isomer (o/p = 4). In contrast, using TTFA as an oxidant, the radioiodination reaction is carrier independent over a wide range of added iodide and exhibits only a weak regioselectivity (o/p = 1.2).

The TTFA/TFA system has already been applied to improve the n.c.a. radiosynthesis of OM*IMT (*J. Lab. Compds. Radiopharm.* **40**, 107-108 [1997]). Moreover 4-methoxy-N-methylbenzamide, the basic structure of melanoma seeking tracers, was radiolabelled using the TTFA/TFA method. It could be shown that, using TTFA as an oxidant at elevated temperatures, n.c.a. radioiodination of 4-methoxy-N-methylbenzamide was possible and, as postulated in an earlier publication (*J. Nucl. Med.* **38**, 127-132 [1997]), yielded exclusively the meta-radioiodo isomer in a RCY of 30%. Using the arylthallium precursor in combination with carrier bromide at room temperature a RCY of 60% could be obtained.

OS-29

A. Mohammed, W. Mier, U. Haberkorn, M. Eisenhut

Department of Nuclear Medicine, University of Heidelberg, Germany

INVESTIGATION OF MYOCARDIAL AFFINE RADIOLABELLED PYRIDINIUM COMPOUNDS

The heterobifunctional bis(aminoethanethiol) ligand (BAT), carrying pyridinium (PYR) in the side chain, has been shown to exhibit myocardial affinity in mice (A Mohammed et al. J.Labeled.Comp.Radioph. 35:59,1994). In order to receive structural informations in relation to this effect two radiiodinated pyridinium derivatives PYR2 and PYR3 have been synthesized and tested in NMRI mice. Both compounds showed high initial myocardial uptake. Release of myocardial activity was most pronounced with PYR2. In order to get an idea about the binding site of these compounds we injected atropin (25 µmole/kg) 15 min. before tracer injection. After tracer injection the heart values (15 min. p.i.) showed 19% reduction for ^{99m}Tc-BAT-Pyr⁺ and 25% for PYR2, indicating competitive influence at the M2 binding sites. Acetylcholine esterase, an alternative binding site, was blocked using edrophonium chloride at 25-33 µmole/kg 15 min prior tracer injection. For ^{99m}Tc-BAT-Pyr⁺ and ¹³¹I-PYR2 divergent results were obtained: 15% decrease for ^{99m}Tc-BAT-Pyr⁺ and 60% (!) increase for PYR2. The increase may be the result of an allosteric effect of edrophonium at the M2 binding site (NH Lee et al. Biochem. Pharmacol. 42:199,1991). Competitive binding of ³H-NMS with atropine and PYR3 at rat-heart membranes showed 87% and 44% reduction, respectively, indicating M2-receptor binding.

	^{99m} Tc-BAT-PYR		I-PYR2		I-PYR3	
Time	Blood	Heart	Blood	Heart	Blood	Heart
5'	1.49	3.60	2.11	25.1	-	-
15'	-	-	0.86	17.4	1.57	22.9
60'	0.16	3.35	1.00	3.66	1.25	11.3

OS-30

K.A. Bergström^{1,2}, C. Halldin¹, A. Savonen³, Y. Okubo¹, J Hiltunen³, C-G Swahn¹, D. McPherson⁴, F.F. Knapp Jr.⁴, S. Larsson¹, P.O. Schnell¹, L. Farde¹. ¹Karolinska Inst., Sweden; ²Kuopio Univ. Hosp., ³MAP Medical Technol., Finland; ⁴Oak Ridge Natl. Laboratory, USA

IODINE-123 LABELLED Z-(R,R)-IQNP: A POTENTIAL RADIOLIGAND FOR VISUALIZATION OF M2 MUSCARINIC ACETYLCHOLINE RECEPTORS IN BRAIN WITH SPECT

Z-(R)-1-Azabicyclo[2.2.2]oct-3-yl (R)-α-hydroxy-α-(1-iodo-1-propen-3-yl)-α-phenylacetate, (Z-(R,R)-IQNP) has a high affinity to M2 muscarinic acetylcholine receptor (mAChR) subtype according to previous *in vitro* and *in vivo* studies in rats. In the present study I-123 labelled Z-(R,R)-IQNP was prepared for *in vivo* SPECT studies in Cynomolgus monkeys.

The tributylstannyl derivative of Z-(R,R)-IQNP was labelled with no-carrier-added I-123 by the chloramine-T method with a radiochemical purity higher than 98%. The SPECT imaging was performed with Trionix gamma camera with low-energy collimators. The metabolite pattern of Z-(R,R)-[I-123]IQNP in monkey plasma was determined with a gradient HPLC method.

SPECT studies with Z-(R,R)-[I-123]IQNP in the Cynomolgus monkey demonstrated a high accumulation brain (>5% of injected dose at 60 min p.i.) in brain regions such as the midbrain, the neocortex, the striatum and the cerebellum. Pretreatment with the non-selective mAChR compound scopolamin (0.2 mg/kg) inhibited Z-(R,R)-[I-123]IQNP binding in all these regions. The percentage of unchanged Z-(R,R)-[I-123]IQNP measured in plasma was less than 10% at 10 min after injection which may be due to rapid hydrolysis as has been demonstrated previously with E-isomer of IQNP.

In conclusion, the radioactivity distribution from Z-(R,R)-[I-123]IQNP in monkey brain indicates that Z-(R,R)-[I-123]IQNP is a potential ligand for mAChR imaging with SPECT. Future pretreatment experiment with subtype selective mAChR compounds is needed to prove M2 subtype selectivity. (Research supported at ORNL by U.S. Department of Energy for OBER under contract DE-AC05-96OR22464.)

General nuclear medicine: Renal hypertension

OS-31

K.Kumaresan, J.Venkateshwarlu & BVR.Murthy
Medwin Hospital, Hyderabad, India.

CAPTOPRIL Tc99m-DTPA SCINTIGRAPHY IN THE ASSESSMENT OF RENO-VASCULAR INTERVENTIONS AND PREDICTION OF THEIR OUTCOME.

Aim: To assess the ability of Captopril effect in Tc99m DTPA Scan to predict the outcome of Renovascular intervention in patients with Renal Artery Stenosis[RAS].

Material & Method: 24 hypertensive patients with RAS in 27 kidneys were included in this study (Age 18-66Yrs, Males 9 & Females 15, LK 6, RK 15 & Bilateral RAS in 3). Renovascular intervention was carried out in these patients : ballon angioplasty in 16, auto-transplantation in 6, saphenous vein graft in 1 and lienorenal arterial anastomosis in 1. Among the 3 bilateral RAS patients one had bilateral angioplasty, one had both angioplasty and auto transplantation and one died after angioplasty on one side.Tc99m DTPA scan was performed (Baseline/Post Captopril/Both) before and after intervention.The renogram curves were scored form 0 to 3 based on working party diagnostic criteria.

Results: In pre intervention scans characteristic captopril changes were seen in 50%(8/16). Post-intervention scans were mostly single, either baseline or captopril. Following intervention baseline scan showed improvement in 10/13 (77% with a mean score difference of 1.8) whereas captopril scan showed improvement in 11/13 (84% with a mean score difference of 2.3). Clinically hypertension was cured in 13 and controlled well in 5. Improvement in kidney function alone was noted in 3. Scintigraphic improvement correlated well with technical success of intervention and the clinical outcome.

Conclusion: Whenever captopril effect could be demonstrated before intervention it predicted potentially curable hypertension with very high accuracy ; however severe baseline abnormality and inability to produce captopril effect on scan does not always indicate adverse outcome by intervention.

OS-32

G.Piccioletto, A.Sargiotto, C.Rabbia, B.Elia, P.G.DeFilippi

Dipartimento di Radiodiagnostica e di Medicina Nucleare,

Azienda Ospedaliera S.Giovanni Battista,Torino

MAG 3 RENOGRAPHIC APPEARANCES IN CAPTOPRIL ERA

There are few data about the usefulness and renographic appearances of MAG 3 Captopril Renography (CR) in Patients with renovascular hypertension secondary to accessory renal artery stenosis or segmental artery stenosis. We compared the results of Captopril-Baseline Renography and Doppler US examination in 16 Patients (aged 23-68 years) with subsequent angiographic evidence of > 70% unilateral renal artery stenosis in an accessory renal artery (7) or stenosis in a segmental artery (9), undergone revascularization (13 angioplasty, 2 vascular stenting and 1 surgical repair). Using 'two-day protocol', CR was performed with 111 MBq of MAG 3 1h after Captopril 50 mg orally and hydration with 0.5 l water. On the basis of visual and quantitative detection of asymmetrical or focal parenchymal retention in the CR, MAG 3 renography was repeated under baseline condition, with evidence in all Pts of significant improvement of the Retention Index (20 min activity/peak activity). Based on the early blood pressure outcome after revascularization, 14/16 subjects were classified as renovascular hypertensive (87.5 % Specificity) and in 13 Pts improvement of the Retention Index perdured on CR at 6-month follow-up (one early restenosis in a superior polar artery). Of interest, Doppler US failed to detect stenosis in 6 out of 16 Pts (62.5% Sensitivity); moreover, in 8 stenosed kidney (57%) from hilar branch or hilar accessory artery stenosis, pre-intervention CR showed a gradual increase in the renogram curve after normal/near-normal Peak. In conclusion, we found that Captopril-Baseline MAG 3 renography was a more useful diagnostic tool than Doppler US in this group of Pts; taking care to exclude the presence of urinostasis in the pelvi-calyceal system by visual inspection, the most suggestive pattern was the appearance of unilateral rising renogram curve after normal/near-normal Peak, suggesting the coexistence in the same kidney of ischemic and non-ischemic nephrons.

OS-33

L. Kerenyi, Z. Szabo, U. Scheffel, K. Szabo, R. Brown, W.B. Mathews, H.T. Ravert, R.F. Dannals
The Johns Hopkins Medical Institutions, Baltimore, Maryland, U.S.A.
Division of Nuclear Medicine (Department of Radiology) and
Department of Comparative Medicine

EFFECT OF RADIOLIGAND METABOLISM ON THE ESTIMATED KINETIC PARAMETERS OF [C-11]L-159,884

The radioligand, [carbon-11] N-[[4'-[(2-ethyl-5,7-dimethyl-3H-imidazo[4,5-B]pyridin-3-yl)methyl] [1,1'-biphenyl]-2-yl]sulfonyl]-4-methoxybenzamide (L-159,884) has been introduced for positron emission tomography investigations of renal angiotensin II subtype 1 receptors. Accumulation of metabolites of the radioligand in plasma and kidneys may interfere with the estimated kinetic parameters. The purpose of this study was to investigate the potential effect of radioligand metabolism on tracer kinetic parameter estimates.

Dynamic PET studies were performed in four beagle dogs with 18±2 mCi [C-11]L-159,884. Arterial blood metabolites were identified by HPLC (method I) and by a simplified SEP-PAK technique (method II). Comparing method I with method II, parameters k_4 (receptor release), and DV (distribution volume) were slightly higher (ratio 1.12-1.16) while k_3 (receptor binding) was lower (ratio 0.88). There was a high correlation between the parameters estimated with the two methods ($r = 0.94-0.99$). Accumulation of metabolites in the kidneys was assessed in 8 rats. In these animals the kidney to blood radioactivity ratio was 8.1 at 60 minutes. The extraction efficiency of radioactivity from the kidney was 80 % of which as much as 90 % was unmetabolized radioligand.

In conclusion, most of the radioactivity in the kidneys is in form of unmetabolized radioligand. Differences between the kinetic parameters estimated by applying different techniques for metabolite determination are small and systematic. Thus, this radioligand is expected to provide reproducible estimates of Angiotensin II subtype 1 receptor densities in the kidneys (Supported by Grant # DK50183).

OS-34

J.Kostadinova, A. Simeonova

Medical Faculty, Clinical Center of Nuclear Medicine, Sofia, Bulgaria

THE POSSIBILITY OF CAPTOPRIL AND ASPIRIN TEST FOR THE DIAGNOSIS OF PATIENTS WITH RENOVASCULAR HYPERTENTION / RVH /

The aim of the study was to compare the diagnostic value of Captopril and Aspirin test in patients for the diagnosis of RVH. A dynamic renal scintigraphy with ^{99m}Tc -MAG3 /Firm "Mallinkrodt"/ was done in 23 patients, proven angiographically and in 10 controls as a basal test, with application of Captopril / 50mg / and Aspirin/ 20mg/kg /. The results were evaluated with qualitative / visual analysis/ and quantitative criteria - T_{max} , $T_{1/2}$, divided renal function and retention index. In 30,4% of the patients the Captopril test was conclusive for making diagnosis, in 56,6% - Aspirin test, in 8,7% - the both tests and in 4,3% - neither test. As a whole, the sensitivity of Captopril test was 73,9% and of Aspirin test - 86,9%. We consider that Aspirin test has to be the method of choice for the diagnosis of patients with RVH. Test with captopril is suitable when there are some contraindications for the application of aspirin.

OS-35

Rakesh Kumar, AK Padhy, M Sriram, C Patel, A Malhotra.

All India Institute of Medical Sciences, New Delhi-29, INDIA
Department of Nuclear Medicine.

EFFECT OF CAPTOPRIL ON NORMAL KIDNEY IN PATIENTS WITH UNILATERAL RENAL ARTERY STENOSIS

The use of captopril scintigraphy for the non-invasive diagnosis of renovascular hypertension is well established. Some patients of long standing hypertension due to renal artery stenosis(RAS) may remain hypertensive even after surgical correction of the condition. Preoperative prediction of this group can spare patients a major procedure.

Thirty patients of angiographically proven unilateral RAS were evaluated by baseline and captopril (45min after 50mg of captopril orally) renal dynamic study after injecting 5mCi of Tc 99m-DTPA intravenously. Out of 30 abnormal renal units, captopril scintigraphy was positive in 10 renal units only. The remaining 20 renal units were either non-functioning (6 units) or very poorly functioning (14 units), therefore no comment was possible in these renal units.

Surprisingly, captopril scintigraphy was also positive in 14 out of 30 contralateral angiographically normal renal units. This finding was mostly confined to those patients whose abnormal kidney had less than 20% function. This may be attributed to the long standing hypertension leading to a renal microvascular disorder. The results of angioplasty and surgical interventions are mentioned below.

Captopril scan of 'normal' kidney	C/L kidney function	Total	Intervention	Impr-oved	No impr-ovement
Positive	Poor	14	05	01	04
Negative	Poor	06	-	-	-
Negative	Good	10	02	02	-

In conclusion, captopril scintigraphy in patients with unilateral RAS can be used to predict the patients who are unlikely to have a good outcome after therapeutic intervention.

OS-36

Roland Müller-Suur, Tidgren B, Lundberg H.J.

Karolinska Institute Danderyds Hospital , Dep of Clinical Physiology and Hospital Physics, Danderyd, Sweden

EFFECT OF CAPTOPRIL ON MAG-3 CLEARANCE IN PATIENTS WITH AND WITHOUT RENAL ARTERIAL STENOSIS AND AFTER PTR A

Angiotensin converting enzyme inhibition by captopril decrease renal hippuran or thalamate extraction in patients with renal artery stenosis, RAS (BritMedJ288:886,1984).The present study investigates the effect of captopril on MAG-3 clearance. Three groups of patients were studied: Group 1(no RAS): 19 patients with low likelihood of RAS (negative captopril renography, confirmed by angiography in 5) . group 2 (RAS): 21 patients with documented RAS and hypertension (angio positive, captopril renography and plasma renin response positive) , and group 3 (postPTR A): 8 patients after successful angioplasty(PTR A) with negative captopril renography results. The 44 or 60 minutes single sample MAG-3 clearance (Müller-Suur et al Eur J Nucl Med 18:28,1990) was measured during baseline and captopril renography (70 MBq ^{99m}Tc -MAG3 each , 50 mg captopril).**Results:** Mean values ±SEM of MAG-3 clearance (C MAG3) and P values using paired t-test were the following:

C MAG3 (ml/min1.73 sqm)	no RAS		RAS		post PTR A	
	baseline	captopril	baseline	captopril	baseline	captopril
	218±22	235±25	231±22	190±19	257±24	269±27
(P)	n= 19 (<0.02)		n=21 (<0.01)		n=8 (ns)	

In 15/19 (79%) patients without RAS the MAG-3 clearance increased during captopril compared with baseline conditions, whereas in 16/21 (76%) in the RAS group the MAG-3 clearance decreased during captopril. In the 8 patients with successful PTR A the MAG-3 clearance did not change significantly after captopril. The decrease of clearance was not correlated to the blood pressure fall or plasma renin response after captopril. **Conclusions:** In most hypertensive patients with renal artery stenoses ACE inhibition decreases renal function assessed by MAG-3 plasma clearance in contrast to a rise observed in most patients without RAS. Thus measurements of MAG-3 clearance at baseline and during captopril renography may give additional diagnostic information.

Cardiovascular: Viability

OS-37

J. F. Batista, O. Perezto, J. A. Valdés, E. Sánchez, R. Stusser, L. M. Rochela, D. López.

Center for Clinical Research.

NITROGLICERYN Tc-99m-MIBI VERSUS TI-201 REINJECTION ON DETECTION OF MYOCARDIAL REVERSIBILITY

Background. Several studies, have suggested that, rest Tc-99m-MIBI underestimate the extent of viable myocardium compared with Positron Emission Tomography and TI-201 reinjection imaging. The role of Tc-99m-MIBI with the addition of nitroglycerin and comparison its with TI-201 reinjection in the identification of reversible myocardium in patients with coronary artery disease has not yet been completely clarified. This study aimed to test whether sublingual administration of nitroglycerin (NTG) could increase the capability of Tc-99m-MIBI to detect reversibility in exercise-induced perfusion defects and to compare it with the TI-201 stress-redistribution-reinjection protocol, in the same sample. **Methods and Results.** Thirty eight patients (33 men, 5 women, mean age 49.3±8.2 years) with previous myocardial infarction (mean evolution 7.1±3.9 months) were submitted to exercise, redistribution and reinjection TI-201 imaging. Patients also underwent exercise, rest and rest-NTG Tc-99m-MIBI myocardial scintigraphy (3-days protocol). A total of 494 myocardial segments were analyzed, of which 136 (28%) had irreversible Tc-99m-MIBI defects on rest images before rest-NTG. Of the 136 irreversible defects on standard stress-rest Tc-99m-MIBI, 109 (80%) appeared as fixed defects and 27 (20%) were reversible on NTG rest Tc-99m-MIBI. In 210 abnormal uptake segments, rest Tc-99m-MIBI had 65% and rest-NTG Tc-99m-MIBI 52% of non reversible segments. (P<.009, McNemar's test). Of the 140 myocardial segments with irreversible defects on standard stress-redistribution thallium cardiac imaging, 112 (80%) did not change at reinjection and 28 (20%) demonstrated enhanced uptake of TI-201 after reinjection. In the 210 concordant segments on both studies with perfusion defects, rest-NTG Tc-99m-MIBI had 51.9% versus TI-201 reinjection 51.4% of irreversible segments, with 0.5% of non-coincident segments (P>.05, McNemar's test). The observed concordance was 78%, with a significant kappa=.55±.07 standard error, 95% confidence interval from .41 to .69 (P=.00005). **Conclusion.** Our data suggest that the study of rest-NTG Tc-99m-MIBI shows an incremental detection capability of myocardial reversibility, in comparison with standard Tc-99m-MIBI exercise-rest study and achieves similar results that TI-201 reinjection protocol.

Key words: nitroglycerin; Tc-99m-MIBI; TI-201reinjection.

OS-38

A. Hubalewska-Hola, J. Pach, D.Pach, Z.Szybiński, S.Kroch

Jagiellonian University, Collegium Medicum Chair and Department of Endocrinology, Department of Toxicology, Kraków - Poland.

USEFULNESS OF MYOCARDIAL PERFUSION SCINTIGRAPHY WITH Tc99mMIBI SPECT IN EVALUATION OF EARLY AND REMOTE EFFECTS OF CARBONE MONOXIDE CARDIOTOXICITY

Using myocardial perfusion scintigraphy with Tc99mMIBI SPECT in toxicology seems necessary for the evaluation of the clinical state and permits assess next of the injury organ with better sensitivity. It is important in treatment and prognosing remote effects. Acute carbon monoxide /CO/ poisoning causes ischemia- and hypoxia-related myocardial damage to the heart with subsequent lactic acidosis. CO affects on mitochondrial cytochrome oxidase, mitochondria appear to be a source of oxygen-based free radicals within the first several hours after CO poisoning. An alternative mechanism for mitochondrial dysfunction is, that CO exposure causes a several hundred-fold increase in the release of free radicals and nitric oxide from platelets. NO, and NO-derived oxidants may inactivate mitochondrial enzymes release mitochondrial enzymes, neurotransmitters and physiological cytotoxic mediators. Blood viscosity and aggregation of platelets are increased by CO. CO accelerates atherosclerosis in animal experiments. **Material and methods:** 29 patients, aged from 14 to 46, acutely poisoned with CO at home were examined. Measurement of COHb, blood lactate level /LA/, duration of exposure and ECG were performed on admission to the Clinic of Toxicology. Enzymes activity /ALT,AST,CPK/ was evaluated after 24hours. Tc99mMIBI SPECT was performed in all patients on day 2-5 after intoxication, 16 patients performed stress and rest Tc99mMIBI SPECT 6 months later. The changes in myocardial scan were graded: as I⁰-diminished and non-homogenic uptake, II¹- diminished uptake and small foci of tracer absence, III⁰- visibly diminished uptake of tracer + one bigger „cold spot”, IV⁰-large and numerous „cold spots”. **Results:** The mean level of COHb was 35,0±7,22%, LA- 4,4±3,71mmol/l, duration of exposure was 123±201min, the level of ALS and AST was normal, CPK was slightly elevated. All patients showed various grades of changes in Tc99m MIBI scan: I⁰-17%, II⁰-24%, III⁰-55%, IV⁰-4% of patients. ECG was normal in 48,3%, abnormalities of depolarisation were noted in 40%,arrhythmia and conduction disorders in 10%. One patient had subendocardial myocardial infarction. CPK activity was higher in patients with III⁰ and IV⁰changes in scintigraphic scans. 9 patients had COHb level higher than 40% and LA concentration over 3mmol/l- in this group 7 patients had III⁰scintigraphic changes. After 6 months an improvement in rest scintigraphic scans was seen in 80% of patients, 20% of patients had similar scans. Effort related disturbances in myocardial perfusion were noted in 5 patients /slight changes/. **Conclusions:** The changes in Tc99mMIBI SPECT were observed in all acutely CO poisoned patients. Pathological changes in scintigraphic scans were dependent on poisoning severity. Myocardial perfusion imaging, ECG, and measurement of enzyme activity performed simultaneously appear to be well fitted methods for morphological and functional evaluation of the myocardium in acutely CO poisoning. The patients require further observation.

OS-39

P Dougall, C. Patel, R Sharma, S Srivastav

Sitaram Bhartia Institute, N. Delhi, Department of Nuclear Medicine

COMPARISON OF THALLIUM-201 AND Tc99m-TETROFOSMIN FOR DETECTION OF REVERSIBLE ISCHAEMIA / MYOCARDIAL VIABILITY

Tc99m-labelled myocardial perfusion agents provide good quality images due to better imaging characteristics but the role as a myocardial viability marker remains to be confirmed. This study was undertaken to compare Thallium-201 & Tc99m-Tetrofosmin for the detection of reversible ischaemia/myocardial viability.

18 patients , 16 males & 2 females, with a mean age of 50 years , were included in the group. 8 patients had a history of prior myocardial infarction, 1 had single vessel disease, 3 double vessel disease, 5 triple vessel disease and 3 were normal on angiography. The mean left ventricular ejection fraction was 39.4%. Planar thallium and tetrofosmin studies were performed, using the same day protocol, on an Elscint Apex-SP4 system, in the anterior, LAO-BS and LAO70 views ,within 3 weeks of each other. Each image was divided into 5 segments, with a total of 15 myocardial segments per patient. Corresponding segments of stress / redistribution studies were compared and graded by two experienced observers, using a scoring system (0-3), for both thallium and tetrofosmin. Out of a total of 270 segments, 248 showed concordance between Thallium and Tetrofosmin (91.9%) and 22 segments were discordant (8.1%). Of the 248 concordant segments 62 showed fixed defects (25%) and 186 had reversible defects (75%). Of the 22 discordant segments, the stress : rest score decreased from 33 to 26 for tetrofosmin and 39 to 12 for thallium.

Tetrofosmin underestimates reversible ischaemia / viability in only 8% of segments and hence appears to be comparable to Thallium-201 for the assessment of reversible ischaemia / viability.

OS-40

G. A. Hurwitz, P.J. Slomka

London Health Sciences Centre, Department of Nuclear Medicine, London, Ontario, Canada

THE "CLEAVAGE SIGN" ON PLANAR MYOCARDIAL PERFUSION IMAGING: RE-EMERGENCE ON EARLY POST-STRESS Tc-99m SESTAMIBI IMAGING.

Breast attenuation artifacts present an important pitfall in interpretation of myocardial perfusion imaging. Such artifacts are more prominent with low energy TI-201 and with planar imaging than with Tc-99m-based agents. In 1988, we described the "cleavage sign", a potentially misleading appearance of transient lateral wall and septal TI-201 defects in obese females. Recently, a similar pattern suggesting artifact has been frequently observed in performing early post-stress images with Tc-99m sestamibi (to assess lung uptake and wall motion).

Planar ECG-gated left anterior oblique images obtained at 4 minutes after stress sestamibi injection were reviewed in a consecutive series of 750 women; diagnostic stress tomography was acquired 1 hour later. The full-fledged artifactual appearance, i.e. a severe defect in the lateral wall, and a mild defect in the mid-septum, was observed in 25 cases. Each of the following features was found in more than 75 % of such cases: (i) weight over 80 Kg, (ii) low attained exercise workload, (iii) normal wall motion on cine-images, (iv) normal lung uptake of sestamibi, and (v) normal stress tomography as confirmed by a quantitative program. A partial cleavage sign was seen in another 62 patients.

With changing radiotracers and imaging protocols, planar imaging with Tc-based agents may be initiated relatively early after stress injection; awareness of the cleavage sign with Tc99m may prevent inaccurate diagnosis in these situations.

OS-41

P.Zanco, A.Desideri*, G.Mobilis*, F.Chierichetti, S.Cargnel, D.Rubello, B. Saitta, G.Ferlin.
Nuclear Medicine-PET Center and Cardiology*, Castelfranco V. and Montebelluna, Italy.

EFFECTS OF LEFT BUNDLE BRANCH BLOCK ON MYOCARDIAL 18F-FLUORODEOXYGLUCOSE UPTAKE EVALUATED BY POSITRON EMISSION TOMOGRAPHY.

To evaluate the effects of left bundle branch block (LBBB) on perfusion and metabolic cardiac PET imaging, 38 patients (28M, 10F, aged 37-82 yrs, mean 63) affected by permanent, complete LBBB were enrolled and submitted to: 1) glucose load 18F-fluorodeoxyglucose PET (FDG-PET); 2) rest 13N-ammonia PET (NH3-PET); 3) coronary angiography; 4) echocardiography. Nineteen patients presented a history of a previous myocardial infarction, anterior in localization in 7 and infero-posterior in the other 12 at the echocardiography. The other 19 patients presented a left ventricular dilatation, without signs of previous necrosis. The mean ejection fraction was 33±9. At the coronary angiography 19 patients presented a significant stenosis of LAD, 15 of these with involvement of other coronaries, while 4 patients presented only stenoses in RCA and LCx and in the other 15 patients no significant coronary stenosis was found.

At the FDG-PET all the LBBB patients presented a severe uptake defect in the septum, with a "reverse mismatch" with respect to NH3-PET, extending to nearby regions of the anterior and inferior left ventricular wall in 23 patients. At the semiquantitative analysis, performed by ROIs, the mean septum/lateral ratio was 0.58±0.18 for FDG (range 0.27-1.09) and 1.11±0.25 for NH3 (range 0.72-1.92), with a p value < 0.0001 at the Student's t test. At the echocardiography the wall motion segmental analysis revealed no significant correlation between the dysfunctional area and the site of the FDG uptake defect.

In conclusion our study could suggest that: 1) in LBBB a change in 18F-FDG uptake in the septum occurs without correlated damage in perfusion; 2) this is evident also in the patients without LAD stenosis; 3) this could lead to an overestimation of necrosis using FDG-PET or FDG-SPECT in LBBB patients.

OS-42

J.J. Bax*, J.H. Cornel**, F.C. Visser#, A. van Lingen#, P.M. Fioretti##, C.A. Visser##.
University Hospital Leiden*, Medical Center Alkmaar**, Free University Hospital Amsterdam#, Netherlands and Istituto di Cardiologia##, Udine, Italy.

HOW MUCH VIABLE TISSUE IS NEEDED TO RESULT IN IMPROVEMENT OF LEFT VENTRICULAR EJECTION FRACTION AFTER REVAS-CULARIZATION?

Assessment of viable myocardium before coronary revascularization allows prediction of improvement of regional left ventricular (LV) function after revascularization. It is unknown how much viable myocardium is needed to result in improvement of global LV function. Hence, the aim of the present study was to assess the relation between the extent of viable tissue and the magnitude of improvement of LV ejection fraction (EF) after revascularization. Also, the optimal cutoff level (in terms of number of viable segments) to establish improvement of LVEF post-revascularization was determined by ROC analysis. Patients (n=32) were studied with FDG SPECT before revascularization. Early thallium-201 SPECT was used to assess perfusion. The SPECT studies were analyzed using polar maps (divided in 13 segments). Regional contractile function was assessed by resting echocardiography (13-segment model). Dysfunctional segments showing either normal perfusion or hypoperfusion with increased FDG uptake were considered viable. LVEF was assessed before and 3 months after revascularization by echocardiography or radionuclide ventriculography. Improvement of LVEF >5% was considered significant. A significant relation existed between the number of viable segments on FDG SPECT and the improvement of LVEF after revascularization:

$y = 1.5 \cdot x - 0.98$ ($r = 0.70$, $P < 0.01$). ROC analysis results:

viable segments	sensitivity (%)	specificity (%)
≥1	100	19
≥2	100	63
≥3	94	81
≥4	75	88
≥5	44	94

In 18 patients with ≥3 viable segments the LVEF improved from 27±8% to 34±9% ($P < 0.05$). In 14 patients with <3 viable segments the LVEF remained unchanged (31±8% versus 31±8%, NS). In conclusion, FDG SPECT can adequately predict improvement of LVEF after revascularization when substantial (23% of the LV) viability is present.

Oncology: Single photon

OS-43

H.WU,ZY.PENG, YF.ZHOU

Department of Nuclear Medicine and Cardiology, Tongji Hospital, Tongji Medical University, Wuhan, China

DIFFERENTIAL DIAGNOSIS WITH ^{99m}Tc-MIBI SPECT IN PATIENTS WITH PULMONARY NODULAR LESIONS

In order to evaluate the value of ^{99m}Tc-MIBI SPECT in differentiating pulmonary nodular lesions, 40 patients with radiologically demonstrated pulmonary nodules underwent ^{99m}Tc-MIBI SPECT studies. Of the 40 cases, 23 were pathologically proved with malignant tumors and 17 with benign lesions. An biphasic imaging with semiquantitative and quantitative analyses was performed on all subjects. Semiquantitative diagnosis was based on comparing the activity uptake of thoracic vertebrae and lesions. Results: (1) There were significant differences between benign and malignant lesions in such parameters as early uptake ratio (1.12±0.15 vs 1.28±0.23, $p < 0.05$), delayed uptake ratio (UR_d) (1.55±0.40 vs 2.31±0.76, $p < 0.01$) or retention index (RI) (39.5±27.8 vs. 83.8±57.2, $p < 0.01$). (2) The quantitative diagnostic thresholds were defined based on ROC curves. The diagnostic sensitivity and specificity were 78.3% and 76.4% with UR_d (≥1.8); 65.6% and 76.4% with RI (±60%) respectively. When the above two thresholds combined, the specificity may be improved as 92.3%. (3) There was no significant difference between semiquantitative and quantitative parameters in diagnostic sensitivity and specificity. (4) The sensitivity and specificity of detecting mediastinal metastasis in the cancer cases were 85.7% and 88.2%. Conclusion: ^{99m}Tc-MIBI SPECT appears to be helpful in differential diagnosis of pulmonary nodular lesions. It may be more valuable in detecting mediastinal metastatic foci in patients with lung cancer.

OS-44

M.Mubashar, KS Chaudhary, K Harrington, D Bradley, EN Lalani, GW Stamp, P Desai, HD Sinnet, AM Peters
HammerSmith Hospitals NHS Trust, Imperial College School of Medicine
Department of Breast Surgery, Histopathology and Imaging

IN VITRO AND IN VIVO STUDIES WITH Tc-99m-SESTAMIBI FOR THE EVALUATION AND REVERSAL OF MULTIDRUG RESISTANCE (MDR) IN CANCER

MDR to a range of chemotherapeutic agents is a cause of anti-cancer treatment failure. It is attributed to the expression of P-glycoprotein (Pgp) which acts as an energy-dependent efflux transporter. Tc-99m-sestamibi is a substrate for Pgp. MDR can be reversed *in vitro* with several modulators including toremifene which is an analogue of tamoxifen. We tested toremifene for *in vitro* reversal of MDR in (a) sensitive and adriamycin-resistant breast cancer and (b) sensitive and vinblastine-resistant epidermoid cancer cell lines. Toremifene showed 2-3 and 10-13 fold decrease in the EC 50 of adriamycin in sensitive and resistant cell lines respectively. Toremifene also modulated vinblastine resistance by 1.5 and 5 fold decrease in EC 50 of sensitive and resistant cell lines respectively. The role of toremifene on the uptake of Tc-99m-sestamibi was also investigated in the above cell lines. In contrast to the reversal of drug resistance, Tc-99m-sestamibi uptake significantly decreased (4-10 fold) in the resistant cell lines when toremifene was added to the growth medium. Similar findings were obtained *in vivo* in 15 biopsy-proven breast cancer patients. A baseline Tc-99m-sestamibi study was followed by 3 days of toremifene administration (720-780 mg/day) and a second scan. Breast images were acquired 20 and 120 min after 440 MBq of iv Tc-99m-sestamibi. 3/15 tumours were not visualised in either pre or post-toremifene scans. In pre-toremifene scans, 7 of the remaining 12 showed a significant decrease in tumour to background ratio (T/B) between 20 and 120 minutes as a result of MDR while 5/12 showed no significant change or increase. Toremifene did not improve the T/B ratio in 7 patients with MDR; instead it further decreased the uptake in 5 of them. It also decreased the uptake in 2/5 without MDR. Interaction of toremifene with sestamibi or changes in the cell membrane could be mechanisms inhibiting sestamibi entry into the tumour cells.

OS-45

R.M. Aigner, G.F.Fueger, *H.Cerwenka, *HJ.Mischinger
Karl- Franzens University Graz, Department of Radiology, Division of
Nuclear Medicine, *Department of General Surgery, Austria
DETECTION OF HEPATOCELLULAR CARCINOMA IN CIRRHOSIS
WITH Tc-99m-FURIFOSMIN

The recognition of hepatocellular carcinoma in patients suffering from liver cirrhosis still remains an unresolved diagnostic problem, even for the newest radiological imaging modalities. Recent in vitro studies suggest that Tc-99m-furifosmin (Q12) may have tumour-seeking properties. This prospective study concerns eight patients, seven male, one female, aged between 64 and 74 years, in whom cirrhosis with associated hepatocellular carcinoma was proven surgically and histologically. Ga-67-citrate- and Tc-99m-Q12 scintigraphy (planar and SPECT) was used pre-operatively to detect hepatocellular carcinoma in these patients. Assessment also included ultrasonography, helical computed tomography and angiography in all patients. Pathologically increased Tc-99m-Q12- and Ga-67- uptake in the tumour was seen in 7/8 patients. The Tc-99m-Q12 scintigraphy demonstrated correctly more sites of involvement than the Ga-67-scintigraphy. Tc-99m-Q12 and Ga-67-citrate both failed to visualize the carcinoma in 1/8 patients. The present study suggests Tc-99m-Q12 scintigraphy as a most promising method for the detection of hepatocellular carcinoma (in the presence of cirrhosis). Tc-99m-Q12 may be made readily available and permits imaging within 30 min. after injection; it provides a better photon flux rate, lower radiation burden and perhaps lower cost than Ga-67-citrate. Obviously further studies are necessary to confirm our first experiences.

OS-46

H. Wang, J.X.Zhang, M.Li,W.J.Tian,M.F.Bo,G.W.Feng,C.M.Zhu
Nuclear Medicine, Rui Jin Hospital, Shanghai, China

EVALUATION OF MEDIASTINAL METASTASES IN PATIENTS WITH LUNG CANCERS USING ^{99m}Tc-TETROFOSMIN (TF) SPECT:COMPARISON WITH CT SCAN

^{99m}Tc- Tetrofosmin(TF) as a tumor imaging agent has been used to study on lung cancer. However, a few dates can be available in evaluation of mediastinal metastases in patents with lung cancer, its role has not been definitely established.In this study,the results of ^{99m}Tc-TF SPECT and CT were directly compared with surgical findings for evaluating the mediastinal metastases in 27 patients (21 M,6 F,age=53±12) with lung cancers(15 epidermoid, 8 adenocarcinoma,4 small cell carcinoma).Before surgical operation,all patients underwent the ^{99m}Tc-TF SPECT (740 MBq,iv) and CT chest scan,TF SPECT and CT images were qualitatively analyzed,then their results were compared with pathological findings.The results were listed in the table.

	CT			TF SPECT		
	TP	FP	TN FN	TP	FP	TN FN
Patients	10	5	8 4	13	1	11 2

(TP: true positive, FP: false positive,TN:true negative,FN:false negative).The results showed the TF SPECT has better specificity and sensitivity(92% and 87%) than CT scan (62% and 71%).

This study demonstrated that TF SPECT is an accurate and effective tool in evaluating the mediastinal metastases in patients with lung cancer.In particular,the TF SPECT seems to be obviously better than CT scan,but the further study is needed.

OS-47

M.Mubashar, KS Chaudhary, EN Lalani, GW Stamp, D Glass, HD Sinnet, AM Peters
Hammersmith Hospitals NHS Trust, Imperial College School of Medicine
Department of Histopathology and Imaging

PRESENCE OF P-GLYCOPROTEIN LOWERS THE SENSITIVITY OF Tc-99m-SESTAMBI IMAGING IN BREAST CANCER

Tc-99m-sestamibi has been used successfully for imaging tumours especially malignant tumours of the breast with a reasonably high rate of success. Tc-99m-sestamibi also acts as a P-glycoprotein (Pgp) substrate and like anticancer drugs is thereby extruded from Pgp-positive tumour cells, which share a common mechanism of multidrug resistance. We studied 14 patients with histologically proven palpable breast cancer to test the hypothesis that the presence of Pgp may lower the sensitivity of Tc-99m-sestamibi for breast imaging. Prone lateral and anterior images were acquired 20 and 120 minutes post 440 MBq of Tc-99m-sestamibi given intravenously in the contralateral arm. Tumour samples were tested immunohistochemically *in vitro* using monoclonal antibodies C494 and C219 for the presence of Pgp. 4/14 tumours were not visualised: 3 of them were positive for Pgp with C219 and all 4 were positive with C494. Six out of the remaining 10 showed significant reduction in tumour to background ratio between 20 and 120 minutes (≥0.10) and 5 out of these were positive for Pgp. 4/10 showed no significant change between 20 and 120 minutes: all 4 were negative for Pgp with C219 and 3 with C494. This study suggests that the presence of Pgp in a breast tumour is an important marker which decreases the sensitivity of Tc-99m-sestamibi imaging but may predict the presence of resistance to anticancer treatment.

OS-48

Q.Schillaci**, V. Picardi, R. Massa, F. Monteleone, P. Volpino*, N. D'Andrea*, V. Cangemi*, O. Bagni, F. Scopinaro
Nucl.Med.Sect.,Dept Exp.Med.Pathol.,*I Surgery, Univ. " La Sapienza", Rome and **Nucl.Med, Univ. " L'Aquila, Italy

EVALUATION OF MEDIASTINAL LYMPH NODE (MLN) METASTASES (MET) IN NON SMALL CELL LUNG CANCER (NSCLC) WITH Tc-99m TETROFOSMIN (TF) IMAGING: COMPARISON WITH CT.

In patients (pts) with NSCLC, surgical resection offers the best chance of cure. The preoperative (pre) assessment of MLN involvement is crucial to select pts in whom surgery is really indicated. To evaluate the role of TF imaging in the pre detection of MLN met from NSCLC, we performed a prospective comparative study with CT in 35 pts (23 males, age range: 39-75 years) with primary NSCLC (18 adenocarcinomas, 15 squamous cell cancers and 2 large cell carcinomas). They were submitted to 360° chest SPECT and to anterior and posterior thoracic planar images 10-20 min after TF injection (740 MBq i.v.). The metastatic involvement of MLNs was assessed by histology after mediastinoscopy (med) or thoracotomy (tho). Both CT and TF scintigraphy were performed 1-8 days before med and/or tho. MLN met were present in 15 pts (42.8%). Results:

	TF SPECT	TF planar	CT
Sensitivity	86.6%	53.3%	66.7%
Specificity	90%	90%	70%
Pos.pred.val.	86.7%	80%	62.5%
Neg.pred.val.	90%	72%	73.7%
Accuracy	88.6%	74.3%	68.5%

TF SPECT was significantly more accurate than CT (p<0.05). However, a precise anatomic localizations of TF uptake in the mediastinum could not always be determined on SPECT, and imaging fusion (SPECT and CT) should be performed to this end. In the 16 pts with positive CT results (enlarged MLNs with a short axis ≥1 cm), accuracy of TF SPECT was 93.8%. The false negative SPECT results were in Ns sized less than 1 cm. In conclusion, our results indicate that TF SPECT is an useful pre noninvasive method to assess MLN involvement in NSCLC, and it can play a clinical role in reducing the number of invasive staging procedures, especially in pts with enlarged Ns at CT.

Oncology: Miscellaneous

OS-49

P J Julian¹, S R Hessewood², L W Seymour³, D R Ferry³, S Daryani³, C M Boivin¹, J Doran³, M David³, D Anderson³, C Christodoulou³, A M Young³, D J Kerr³
 Department Nuclear Medicine, Queen Elizabeth Hospital¹, City Hospital NHS Trust², and CRC Institute for Cancer Studies³, Birmingham, UK

IMAGING OF A 123I-LABELLED HPMA COPOLYMER BEARING DOXORUBICIN AND GALACTOSAMINE IN A PHASE I DOSE ESCALATION TRIAL OF PATIENTS WITH HEPATOMA AND COLORECTAL LIVER METASTASES

Galactose-targeted delivery of macromolecules and drug conjugates to asialoglycoprotein receptor positive cells has been documented in animals. Here we demonstrate for the first time the pharmacokinetics and imaging of patients enrolled in a phase I clinical study of the poly-N-(2-hydroxypropyl) methacrylamide (HPMA) copolymer bearing doxorubicin and galactosamine, known as PK2.

Imaging was achieved by 123I labelling of the tyrosinamide derivative of PK2 using an Iodogen technique. Of 16 patients recruited to the trial to date, 13 have undergone imaging with 27-170 MBq (mean 115 MBq) administered simultaneously with the therapeutic dose of PK2 of between 20 and 160 mg/m² doxorubicin equivalent.

Gradient HPLC and gamma counting of plasma showed similar biphasic clearances of the labelled and unlabelled drug with half-lives of 1.7±0.7 and 18±8 hours (1 SD).

Planar whole body imaging at 24 hours showed 26±10 % (1 SD) delivery of the drug to the hepatic region. This fraction is approximately independent of the total therapeutic PK2 dose administered.

SPECT analysis with image registration to CT, performed to show more precisely the uptake into tumour tissue compared to normal liver, gave a ratio of approximately 1:3 at 24 hours.

Radiolabelled drug imaging has demonstrated effective hepatic targeting of PK2 linearly up to a dose of 160 mg/m². This study highlights the potential value of nuclear medicine imaging in phase I/II drug development trials.

OS-50

PF Rambaldi*, GL Cascini*, F Casale, A Murano, F Fallanca*, P Indolfi, MT Di Tullio, L Mansi*.
 *Institute of Radiological Sciences, Department of Paediatrics - II University of Naples

In-111 OCT AND Tl-201 SCINTIGRAPHY IN THYMIC REBOUND AFTER CHEMOTHERAPY IN CHILDREN WITH LYMPHOMA.

Ga-67 scintigraphy in children with lymphoma can be affected by false positive results due to thymic rebound after chemotherapy.

Aim of the study was to evaluate the role of In-111 pentetreotide (OCT) and Tl-201, that have already been proposed in diagnosis of lymphoma, to differentiate relapse and thymic hyperplasia in patients presenting Ga-67 mediastinal uptake at follow up studies.

Twenty pts, 12 males and 8 females (age range 3-16 years), with a diagnosis of lymphoma, were evaluated at stop therapy. In 6 pts presenting intense mediastinal Ga-67 uptake, In-111 OCT scintigraphy at 4 and 24 hrs and Tl-201 scintigraphy, 10 min after i.v. injection, were performed.

Using OCT, a mild 4 hour mediastinal uptake decreasing at 24 hours was observed. Tl-201 scan was negative. A thymic rebound has been confirmed by CT and clinical data in follow up. Our results suggest that Tl-201 scan is a useful tool to exclude tumour recurrence in children with lymphoma.

Concerning OCT, even though a 4 hour scan can not differentiate between thymic hyperplasia and neoplasm, tracer washout at 24 hours may suggest a thymic rebound.

OS-51

Z. Yao, M. Zhang, H. Sakahara, Y. Arano and J. Konishi.
 Kyoto University Hospital, Department of Nuclear Medicine

RAPID INTERNALIZATION OF AVIDIN AFTER BINDING TO TUMOR CELLS.

We have discovered the high targeting efficiency of avidin in intraperitoneal (i.p.) tumors. This study was undertaken to verify the internalization of avidin after binding to tumor cells both in vitro and in vivo. Avidin was labeled with In-111 and I-125 through DTPA-biotin and N-succinimidyl 3-(tri-n-butylstannyl) benzoate (ATE), respectively. Three cultured human tumor cell lines, including an ovarian cancer, SHIN-3, a colon cancer, LS180, and a gastric cancer, MKN45, were used for in vitro study. Two tumor models were established by i.p. injections of 5x10⁶ SHIN-3 or MKN45 cells in nude mice. In-111-avidin was incubated with 1-3x10⁶ tumor cells at 4°C or 37°C and, 0.5, 2, 4 or 6 hours later, the cells were washed with PBS or an acid solution. Then, radioactivity associated with the cells was counted. Biodistribution of radioactivity was examined at 0.5, 2, 24, and 48 hours after i.p. injections of In-111 and I-125 dual labeled avidin into the tumor-bearing mice. In vitro study revealed that the radioactivity associated with tumor cells after acid treatment increased with time at 37°C but not at 4°C. More than 40% and 90% of radioactivity were acid-resistant after 0.5 and 6 hour incubation, respectively, at 37°C, whereas less than 30% of radioactivity was acid-resistant at 4°C throughout. In vivo study showed that the radioactivities of both In-111 and I-125 in xenografted tumors at 0.5 hour postinjection were almost the same, more than 30% ID/g. However, the radioactivity of I-125 in the tumors decreased rapidly, less than 2% ID/g at 48 hours, while that of In-111 in the tumors remained constant. Results from this study suggest that avidin is rapidly internalized after binding to tumor cells, therefore, it would be a useful carrier of beta emitters, drugs, toxins, or therapeutic genes for the treatment of malignant ascites.

OS-52

OC Boerman¹, MHGC Kranenborg¹, GL Griffiths², JC Oosterwijk¹, MCA de Weijert¹, B McBride², HJ Hansen², E Oosterwijk¹, FHM Corstens¹.
 University Hospital Nijmegen¹, The Netherlands, Immunomedics² Inc., Morris Plains, NJ.

PRETARGETING OF RCC TUMORS IN NUDE MICE: IMPROVED TUMOR UPTAKE AND RETENTION WITH A BIVALENT CHELATE
 Radiolabeled antibodies (MAbs) can target tumors selectively. Sustained activity levels in non-target tissues limit their application. Pretargeting protocols using bispecific MAbs fundamentally change the pharmacokinetics of the radiolabeled targeting vehicle. In previous studies we have shown successful radioimmunotargeting of ¹¹¹In-DTPA to renal cell carcinoma (RCC) after pretargeting with a bispecific antibody (bsAb) anti-RCC x anti-DTPA (G250xDTIn1) in nude mice. Here we report on the further optimization of this two-step approach.

In our two-step protocol relatively high ¹¹¹In-DTPA blood activity was observed at early time points. We have blocked the binding of ¹¹¹In-DTPA to circulating G250xDTIn1 by injection of IgM-DTPA-In. One hour postinjection tumor-to-blood ratios increased 24-fold using a 1-fold molar excess IgM-DTPA-In. However, ¹¹¹In-DTPA was less well retained in the tumor in this three-step protocol. Therefore, further studies were performed using the two-step method. Subsequently, multiple injections of ¹¹¹In-DTPA were given following pretargeting. The amount of ¹¹¹In-DTPA targeted to the tumor with a second or third injection was as high as the amount of ¹¹¹In-DTPA that localized in the tumor after a first injection. Finally, we studied whether the use of a bivalent chelate (¹¹¹In-diDTPA-FKYK) could improve radioimmunotargeting. The bsAb:diDTPA molar ratio greatly affected the tumor uptake. At low bsAb:diDTPA ratios (< 1), tumor uptake of diDTPA-¹¹¹In was extremely high (80 %ID/g, 1 hr p.i.) as compared to the tumor uptake of monovalent DTPA-¹¹¹In (9 %ID/g, 1 hr p.i.). More importantly, the bivalent chelate was better retained in the tumor (55 %ID/g, 48 hr p.i.). Tumor-to-blood ratios reached values of 1400 (48 h p.i.).

In conclusion, the efficacy of two-step radioimmunotargeting could be enhanced very effectively using ¹¹¹In-diDTPA-FKYK instead of ¹¹¹In-DTPA. Very high tumor uptake and excellent tumor retention were obtained. Our studies indicate that the use of bivalent chelates can very effectively optimize two-step targeting of tumors with bsAbs.

OS-53

M.G. Steffens, O.C. Boerman, E. Oosterwijk, M.H.G.C. Kranenborg, J.M.B. Manders, F.M.J. Debruyne and F.H.M. Corstens.
Departments of Nuclear Medicine and Urology, University Hospital Nijmegen, The Netherlands.

IN VIVO AND IN VITRO CHARACTERIZATION OF THREE ^{99m}Tc LABELED MONOCLONAL ANTIBODY G250 PREPARATIONS.

In previous clinical studies excellent visualisation of tumor lesions was observed with I-131 labeled monoclonal antibody (mAb) G250 in patients with renal cell carcinoma (RCC). In several cases ¹³¹I-cG250 immunoscintigraphy disclosed tumor lesions which were not visualized by X-ray or CT. We now aim to develop a ^{99m}Tc-labeled mAb G250 preparation for radioimmunodetection (RAID) of RCC. Here we studied the stability, the biodistribution and the imaging potential of three ^{99m}Tc-labeled G250 preparations in nude mice with s.c. RCC xenografts. ¹²⁵I-G250 and the non-specific mAb ¹³¹I were used as control antibodies.

Labeling of mAb G250 with ^{99m}Tc was done according to three methods: (I) using hydrazinonicotinamide (HYNIC), (II) using S-benzoylmercaptoacetyltriglycerine (MAG3), and (III) directly labeled (Schwarz method). The stability of all preparations was tested in serum at 37 °C during 48 hours (h) and analyzed by ITLC and HPLC. In addition DTPA, Cysteine and Glutathione challenge assays were performed. Mice were imaged at 1, 8 and 24 h p.i. Biodistribution was determined 24 h and 48 h p.i.

All preparations were stable (≤ 15 % loss of radiolabel) in serum during the 48 h incubation period. ^{99m}Tc-G250 (Schwarz) showed instability at a 1000-fold molar excess of DTPA, ^{99m}Tc-MAG3-G250 showed instability at a 10,000-fold molar excess of cysteine. ^{99m}Tc-HYNIC-G250 was stable under all conditions. Tumors were clearly visualized with all preparations. ^{99m}Tc-G250 (Schwarz) showed enhanced blood clearance (3.75 % ID/g) as compared to all other preparations (13.4, 10.4, and 13.4 %ID/g for MAG3, HYNIC and ¹²⁵I-G250 respectively, 48 h p.i.). At 24 h p.i. mean tumor uptake was high with all mAb G250 preparations: 63.4 (MAG3), 76.7 (HYNIC), 31.1 (Schwarz) and 70.7 (¹²⁵I-G250) %ID/g. Uptake of the non-specific ¹³¹I-MN14 mAb was 7.9 % ID/g. At 48 h p.i. mean tumor uptake was even higher: 126 (MAG3), 84.9 (HYNIC), 29.4 (Schwarz), 75.4 (¹²⁵I-G250) and 6.6 % ID/g (¹³¹I-MN14). Uptake in normal organs was low (< 8 % ID/g) except for HYNIC liver uptake (8.6 % ID/g).

In this study ^{99m}Tc-HYNIC-G250 showed good stability and excellent tumor targeting. Moreover, this preparation can be labeled with high efficiency (> 95%) at room temperature within 15 min. Therefore, ^{99m}Tc-HYNIC-G250 seems to be an ideal candidate for RID of renal cell carcinoma.

OS-54

SM Lim, HC Kang, SH Lee, CW Choi, KS Woo, WS Chung, SJ Lim, SB Kahl.
Korea Cancer Center Hospital, Oxy Co. Ltd., Seoul Korea, University of California, San Francisco, U.S.A.

BIODISTRIBUTION OF THE ⁵⁷CO-BOPP(BORONATED PORPHYRIN) IN 9L GLIOMA BEARING MICE AS A NEW CANCER IMAGING AGENT.

Boronated porphyrin(BOPP) showed high tumor uptake, and can be used for photodynamic therapy(PDT) or boron neutron capture therapy(BNCT). Radiolabeled BOPP can be used as a tumor imaging agent and noninvasive tracer for the tissue BOPP content. BOPP (250µg/250µl) was labeled with ⁵⁷CoCl₂ (25 µCi/5 µl) in 70°C for 10 minutes. The labeling yield was over 90% with TLC. Cultured 9L glioma cells were injected subcutaneously in right thigh of the mouse, and 14 days later tumor uptake and biodistribution study was done. Biodistribution study was performed at 2hr, 4hr, 24hr, 48hr, 72hr and 96hr after injection of ⁵⁷Co-BOPP(n=3 group). Tissue ⁵⁷Co-BOPP was measured with gamma counter. Tumor uptake was increased until 48 hours after injection. Scintigraphy at 48 hours showed hot uptake in tumor. Tumor to blood and tumor to muscle ratio was 2.76 and 7.45 respectively in 48 hours after injection. Liver, spleen and kidney showed persistent hot uptake. ⁵⁷Co-BOPP could be a promising radiopharmaceutical for tumor imaging or tracer of the BOPP in PDT/BNCT.

Cardiovascular: Prognosis

OS-55

O.Schiliaci*, C.Moroni^, R.Danieli, A.D'Agostino, G.Neri, N.S.Tiberio, V.Fiore, R.Cassone^, F.Scopinaro
Nucl.Med.Sect., Dept.Exp.Med.Pathol., ^Intern.Med, Univ. "La Sapienza", Rome and *Nucl.Med., Univ. L'Aquila, Italy

LONG TERM PROGNOSTIC VALUE OF NORMAL Tc-99m SESTAMIBI (SM) MYOCARDIAL (MYO) TOMOGRAPHY AFTER HIGH DOSE DIPYRIDAMOLE (DIP) ECHOCARDIOGRAPHY (ECHO).

The benign prognosis of patients (pts) with stable, proven or suspected CAD and normal dip Tl-201 imaging is well known. Nevertheless, the prognostic implications of a normal SM SPECT after high-dose dip echo test have not been specifically assessed. To this aim, 63 pts (39 males, mean age 56±7 years) with normal studies were followed-up >3 years (49±12 months) for the occurrence of subsequent cardiac events. They had been referred to our institution because of chest pain and clinical suspicion of CAD; none had a previous myo infarction. Pre-scan Bayesian likelihood (lk) of CAD was calculated from clinical and ECG exercise data, and pts were stratified into 3 lk groups: low (n=27), intermediate (int, n=24) and high (n=12). SM (740 MBq) was injected 2-4 min after the end of dip (up to 0.84 mg/kg over 10 min) echo; SPECT were acquired 1 hour later, divided in 22 segments and quantitatively analyzed using a 4 point scoring system (0=normal to 3=absent uptake). The sum of the scores of the myo segments was calculated for each patient, resulted <3 in all cases, so scintigraphies were considered as demonstrating normal perfusion. Follow-up data were obtained over a 37 to 63 month period by clinic visits, communication with the pts'physician and patient telephon interview. No hard cardiac event, including nonfatal myocardial infarction or death caused by a primary cardiac cause, were observed. Soft events occurred only in 1 case (1.6% of pts) of the int lk group: hospitalization for unstable angina followed by coronary angioplasty. These findings indicate that pts with chest pain and clinical suspicion of CAD with a normal dip SM SPECT after echo testing have an excellent long-term prognosis with respect to hard and soft cardiac events. The benign prognosis extends even to pts with a high pre-test lk of CAD.

OS-56

S.Fukuzawa, S.Ozawa, M.Inagaki, J.Sugioka, M.Daimon, S.Kusida

Hospital: Funabashi Municipal Medical Center, Division of Cardiology

PREDICTION OF REGIONAL AND GLOBAL FUNCTIONAL RECOVERY AFTER ACUTE MYOCARDIAL INFARCTION TREATED WITH PRIMARY PTCA BY EARLY Tl-201/I-123 BMIPP DUAL SPECT

To assess whether Tl-201/I-123 BMIPP dual SPECT performed in the early stage of acute myocardial infarction (AMI) treated with successful primary PTCA (TIMI flow grade 3, residual stenosis < 30%) can predict late regional and global functional recovery, 48 pts (39 male, mean age 62±12, 32 anterior AMI) underwent Tl/BMIPP dual SPECT within 5 days of index AMI. The short axis and vertical long axis of dual SPECT were divided into 18 segments for each patient. These segments were assigned in 8 evenly spaced regions in the mid and basal short-axis views, and 2 apical segments were in mid-ventricular long-axis slice. Segments were scored using 4 point system (normal=0 to severe reduction of radioisotope uptake=3). Defect score (DS) of Tl/BMIPP image was provided from summated serial slices. Echocardiography were performed at admission and at 1 month after AMI. Regional wall motion was scored from 1 (normal) to 4 (dyskinesis) according to a 16 segment model. Anterior and inferior infarct zone (IZ) were constructed and IZ wall motion score index (WMSI) was derived. Reversible dysfunction at follow-up was defined as a reduction of IZ WMSI of >0.2. All pts were classified into 2 groups based on reduction of WMSI.

	Tl DS	BMIPP DS	
Gp 1 (Reduction of WMSI>0.2)	12.8±5.2	18.4±4.9	p<0.05
Gp 2 (Reduction of WMSI<0.2)	13.9±6.8	14.2±5.8	n.s

In Gp 1 pts, LVEF significantly increase from 43±9 at baseline to 52±6 at 1 month (p<0.05), while only a small, not significant improvement was found in Gp 2 (42±8 vs. 46±6).

Conclusion: our data indicate that in pts with AMI in whom antegrade flow is fully restored without residual stenosis, early Tl-201/I-123 BMIPP dual SPECT can predict not only the recovery of left ventricular segmental function but also whether a relevant change in global LVEF will occur at follow-up.

OS-57

R. Sciagrà, M. Pellegrini, G.M. Santoro*, S. Sestini, F. Zerauscheck, P. F. Fazzini*.

Nuclear Medicine, University of Florence; *Division of Cardiology, Careggi Hospital; Florence, Italy.

PROGNOSTIC IMPLICATIONS OF VIABILITY DETECTION WITH BASELINE-NITRATE Tc-99m-SESTAMIBI SPECT IN PATIENTS WITH LV DYSFUNCTION

The detection of viable myocardium in patients (pts.) with coronary artery disease (CAD) and left ventricular (LV) dysfunction is important to identify those who will functionally improve after revascularization. PET and TI-201 studies suggest that viability in pts. not submitted to revascularization might have an adverse prognostic meaning. This study aimed to investigate the relationship between viability recognition using baseline-nitrate Tc-99m-sestamibi SPECT and outcome of CAD pts. with LV dysfunction, taking into account the sort of treatment and the achievement of complete revascularization.

We enrolled 89 CAD pts. with LV dysfunction, who underwent Tc-99m-sestamibi SPECT using a baseline-nitrate imaging protocol for viability detection. SPECT was quantitatively analyzed using a 13-segment model: viable myocardium was defined considering either baseline or nitrate activity or nitrate activity plus nitrate-induced activity changes. Decisions concerning treatment were made by the referring physician. Follow up data were obtained from hospital records and telephonic interviews.

The mean follow up period was 33.2 ± 21.8 months and data were obtained for 81 pts.. Revascularization was performed in 63 pts., and was complete in 45; 18 pts were kept on medical therapy. According to SPECT and revascularization completeness, 4 groups were defined: A (11 pts.) = no viability, no (or incomplete) revascularization; B (15 pts.) = no viability, complete revascularization; C (25 pts.) = viability, no (or incomplete) revascularization; D (30 pts.) = viability, complete revascularization. Both hard (cardiac death, myocardial infarction) and soft (unstable angina or heart failure with or without late revascularization) events were considered, and were significantly ($\chi^2 = 15.6, p < 0.002$) more frequent in C (= 60%) as compared to the other groups (A = 27%, B = 27%, D = 17%). In a Cox regression model, the number of segments that were defined viable using nitrate activity plus nitrate-induced changes and lay in non-revascularized coronary territories was the best predictor of future events ($\chi^2 = 17.7, p < 0.00005$).

In conclusion, these data confirm that viable myocardium has an adverse prognostic meaning in CAD patients with LV dysfunction who do not undergo (complete) revascularization. Tc-99m-sestamibi SPECT using a baseline-nitrate protocol is effective for viability detection also in terms of prognostic stratification.

OS-58

D. Colombana, P. Jean, N. David, N. Hassan, M. Angioi, P. Olivier, C. Mercenier, P.Y. Marie, N. Danchin, G. Karcher, A. Bertrand. Departments of Nuclear Medicine and of Cardiology, CHU-Nancy, France.

PROGNOSTIC VALUE OF TI-201 SPECT IN DIABETICS WITH MULTIPLE RISK FACTORS

The identification of diabetic patients at high risk of cardiac events remains a challenge for the clinician. The aim of the present study was to assess the prognostic value of TI-201 SPECT performed on a routine basis in a consecutive population of diabetic patients who had ≥ 3 risk factors for coronary artery disease.

The population comprised 116 patients, of whom 27 (23 %) had a history of coronary artery disease and 8 (7 %) had angina. TI-201 SPECT was performed after exercise test (n = 32), dipyridamole infusion (n = 21) or both (n = 63) ; 24 patients (21 %) had abnormal scans. Over a 2-year follow-up period, 14 patients had a cardiac event (3 major events: 2 death and 1 infarction ; 6 revascularization procedures ; 5 hospital admission for angina).

In patients with normal SPECT, the annual event rate was low (3 %) (major event rate: 0.5 %) ; and in patients with abnormal SPECT the annual event rate was markedly higher (28 %, p < 0.001).

Using Cox multivariate analysis, the 2 best independent predictors of events were: [1] presence of abnormal SPECT (p = 0.001) and [2], previous history of coronary artery disease (p = 0.005). In patients with abnormal SPECT, the annual event rate was 44% in patients with and 7% in those without history of coronary artery disease. In patients with normal SPECT, the respective figures were 9% and 2%.

In diabetic patients with multiple coronary risk factors, TI-201 SPECT yields important prognostic informations. In patients with a history of coronary disease, however, the incidence of cardiac events remain unexpectedly high, bearing witness of the potential rapid evolution of the disease specific to diabetic patients.

OS-59

A. Cuocolo, M. Petretta, E. Nicolai, W. Acampa, A. Varrone, D. Bonaduce, M. Salvatore.

Nuclear Medicine Center of the National Council of Research (CNR), Department of Biomorphological and Functional Sciences, University Federico II, Napoli, Italy.

COMBINED ASSESSMENT OF LEFT VENTRICULAR FUNCTION AND REGIONAL MYOCARDIAL THALLIUM-201 ACTIVITY FOR PROGNOSTIC EVALUATION OF PATIENTS WITH CHRONIC ISCHEMIC LEFT VENTRICULAR DYSFUNCTION.

This study evaluated the prognostic value of combined assessment of left ventricular (LV) function and regional myocardial thallium activity in patients with non recent myocardial infarction and LV dysfunction. Eighty-two patients with previous myocardial infarction (>8 weeks) and echocardiographic evidence of LV dysfunction underwent thallium-201 rest-redistribution tomography and cardiac catheterization. During the follow-up (mean 25 months) there were 18 cardiac events (14 deaths and 4 nonfatal myocardial infarctions). Multivariate Cox regression analysis on clinical, angiographic and thallium variables showed that the number of echocardiographic dysfunctional segments with preserved thallium uptake (≥50% of peak activity) (chi-square 11.03, p<0.005) and age (chi-square 8.12, p<0.01) were predictive of poor outcome. The threshold of 6 dysfunctional viable segments (46% of the total LV myocardium) was the cutoff point that maximized the predictive power for the occurrence of subsequent events. Survival rate was 28% in patients above and 94% in patients below this cutoff point (p<0.001). At incremental analysis, combined echocardiographic and thallium data provided significant additional information to clinical, thallium and LV functional data (global chi-square from 22.4 to 31.5, p<0.01). Similarly, combined data gave additional information after considering clinical, echocardiographic and LV functional data (global chi-square from 17.8 to 22.3, p<0.05). The number of diseased vessels at coronary angiography did not add further prognostic information. These results demonstrate that in patients with previous myocardial infarction and chronic ischemic LV dysfunction the combination of echocardiographic and thallium rest-redistribution imaging data gives prognostic information incremental to those of clinical and LV functional data and to those of each technique considered separately.

OS-60

MS Jiang

Shanghai HuaDong Hospital, Department of Nuclear Medicine

PROGNOSTIC VALUE OF DIPYRIDAMOL TECHNETIUM-99MSESTAMIBI TOMOGRAPHY IN ELDERLY PATIENTS WITH CORONARY ARTERY DISEASE

In This study, the prognostic value of dipyridamole Tc-99m MIBI tomography (same day rest-stress protocol) was assessed in 362 elderly patients hospitalized with a diagnosis of CAD. Patients were followed for 12 to 60 months (mean 37 ± 12 months). 32 patients had a cardiac event --cardiac death(n=12) or nonfatal myocardial infarction(n=20). Clinical variable associated with increased cardiac risk included a history of diabetes mellitus, congestive heart failure or prior myocardial infarction. Only 2% patients with normal scan had a later cardiac event compared with 10% of those with abnormal perfusion studies. Relative risks (univariate cox analysis) associated with multiple perfusion defects, increased lung uptake and a dilatation of LV were 8.7(95% confidence interval(CI) 3.5to21.9), 11.5(95%CI 2.5-26.1) and 13.5(95%CI 5.5-33.1) respectively. 5 years cardiac event free survival was significantly decreased in patients with multiple perfusion myocardial defects(73%) , increased lung uptake (64%) and LV dilatation (43%), compared with those with normal scans(97%).

The results showed that dipyridamole MIBI SPECT findings of multiple perfusion defects accompanied with increased lung uptake and/or dilated LV are strong prognostic indication of diminished survival at 5 years, identified patients at increased risk. Dipyridamol Tc-99m MIBI myocardial tomography provides long term prognostic information.

Neurology/Psychiatry: Cerevascular

OS-61

I. Odano, and M. Ohkubo.

Niigata University School of Medicine, Niigata, Japan.

QUANTIFYING CEREBRAL BLOOD FLOW WITH ^{99m}Tc ECD AND SPECT BY A SINGLE VENOUS SAMPLE

The aim of this study was to develop a new simple and non-invasive method for quantifying regional cerebral blood flow (rCBF) with ^{99m}Tc ECD (ECD) SPECT and a single venous sample based on a 3-compartment model. We performed dynamic SPECT scans and both serial sampling of arterial and venous blood in 12 subjects. Using Patlak plot analysis, time T for the steady-state was determined. Regional CBF is assumed to be obtained from the following composite function. $F = \Omega(k)$ and $k = Cb(t) / \int Ca(t)$, where $Ca(t)$ and $Cb(t)$ are the respective concentrations of ECD in arterial blood and brain tissue. At the steady-state ($t=T$), k is constant. When F is obtained by the ¹³³Xe inhalation method, and k is obtained by a SPECT scan at time T and integral of arterial input, the relation between F and k is approximated by the following exponential function using non-linear least squares analysis. $k = \Omega^{-1}(F) = a \cdot \{1 - \exp(-F/b)\}$, a, b=constant, then $F = -b \cdot \ln(1 - k/a)$. When a and b can be experimentally determined, F (=rCBF) is calculated from k obtained. Moreover, the relationship between arterial input and venous activity was analyzed, and optimum sampling time for estimating integral of arterial input by a single venous sample was determined. The time T was 28.3 ± 1.4 min (≈ 30 min), and the values, a=0.521, b=0.875. The optimum sampling time of venous blood was 6 min after tracer injection. To validate the present method requiring a SPECT scan at 30 min and single venous sampling at 6 min post-injection, we examined other 10 patients with cerebrovascular diseases. By comparing with rCBF obtained by the ¹³³Xe inhalation technique, rCBF values obtained were in good agreement ($r=0.854$, slope ≈ 1). The underestimation of rCBF in high flow range was corrected completely. This method was accurate, simple, non-invasive and useful in the clinical SPECT studies.

OS-62

G. Demonceau, M. Bister, H. Colaert, C. Monte.

Hospital: St Elisabeth, Dpt of Nuclear Medicine, Zottegem, Belgium

EVALUATION OF THE CLINICAL USEFULNESS OF DATABASE COMPARISON IN UNILATERAL CEREBRAL LESIONS.

In case of diffuse or bilateral cerebral pathology, comparison with a database may be diagnostically worthwhile. With unilateral lesions, where a straightforward comparison with the contralateral hemisphere is possible, it is not necessarily obvious which of both methods is the most efficient: individual variations as are built into a database, may well mask an existing lesion, whereas physiologic asymmetries within one and the same brain may, contrariwise, be considered as pathologic. The efficiency of the two methods was compared, using the clinical data and the CT-scanner as a reference.

In this study, 206 patients suffering from CVA or TIA were included. A SPECT and a CT-scan were obtained within 3 days after the attack. Acquisition started 10 minutes after injection of 500 Mbq of Tc-HMPAO. Images were obtained on a 3-head camera in a 128x128 matrix, 25 sec/step, 90 steps over 360°. After backprojection with adaptive filters, the images were fully automatically processed by both methods. In the semiquantitative method, after detecting the mid-sagittal plane and assuming left-right symmetry along this plane, lower and upper percentiles were defined, allowing the classification of the cortex in zones of low, normal and high flow. The database method compares the SPECT images, after geometric and gray value transformation into a standard coordinate system, with a normal database depending on age. Voxels deviating more than two standard deviations were classified as low or high perfusion areas.

Agreement between both methods occurred in 155 cases (75%). In 36 of the remaining 51 patients, the localisation of the lesion based on clinical history and CT-scan was not possible, resulting from equivocal symptoms and the absence of a clear lesion on CT. For the other 15 cases, 9 were correctly diagnosed by database comparison against 6 by the percentile method.

In conclusion, the database comparison seems to be the preferred method for the automatic detection of an unilateral brain lesion: the risk of mispositioning and distortion of the tomographies was lower, compared to the false detection occurring from physiological variations and the underestimation of zones of high flow (only about 20% of our zones of high flow had an activity higher than these of the cerebellum). Nevertheless, this slight advantage should be balanced against the requirement of a database taking into account the patients age as well as the data acquisition and processing methods.

OS-63

J.Karonen, E.Vanninen, P.Vainio, R.Vanninen, K.Partanen, J.Nuutinen, J.Sivenius, R.Roivainen, J.Onatsu, K.Korhonen, Y.Liu, M.Könönen, J.Kuikka, H.J.Aronen
Kuopio University Hospital, Departments of Clinical Radiology, Clinical Physiology and Neurology, Kuopio, Finland

THE ECD-SPET AND DIFFUSION WEIGHTED MRI IN THE DIAGNOSIS OF ACUTE STROKE

Purpose of the study: To compare findings in diffusion weighted magnetic resonance imaging (DWI) and single photon emission tomography (SPET) of brain during the evolution of acute ischemic stroke.

Patients and methods: Sixteen patients (9 women, 7 men, age range 48-89, mean 73 yrs) with suspected acute stroke were studied. CT was performed in order to exclude hemorrhage. DWI and SPET were performed in the acute phase (3-31 hrs after onset of symptoms) and one week later. DWI was performed by using echo-planar spin echo sequence that produced 19 axial slices (slice thickness 5 mm, interslice gap 1.5 mm) of the brain. Diffusion gradients were applied in three orthogonal directions (b-value 1000 s/mm²) in order to overcome the effects of diffusion anisotropy. SPET was performed with 3-headed system with fanbeam collimators. Tc-99m-ECD (550 MBq) was injected about 1 h before SPET imaging and within one hour from DWI except in one patient, for whom it was given 4.5 hours before DWI. Comparison of DWI and color-coded SPET images (slice thickness 7.0 mm) was done visually.

Results: In the acute phase, DWI detected areas of decreased diffusion in all 16 cases, whereas SPET detected hypoperfused areas in 14 cases. Small volumes (< 1.0 cc) of abnormal diffusion were not detected by SPET. In the acute phase, most areas with very low perfusion (< 20 % maximum) were well comparable with diffusion abnormalities. In general, the milder hypoperfusion area on SPET was considerably larger than the corresponding diffusion abnormality. The ischemic penumbra was identified by using the combination of DWI and SPET.

Conclusion: In acute stroke, early SPET imaging can detect larger areas of decreased perfusion than permanently injured areas detected by DWI. This hypoperfused area around the diffusion defect may represent the area of ischemic penumbra. The combination of DWI and SPET seems to be useful in the evaluation of the time course of ischemic stroke.

OS-64

H. Barthel, J. Berrouschot*, S. Hesse, C. Dannenberg, R. von Kummer***, D. Schneider*, J. Dietrich**, P. Georgi

Departments of Nuclear Medicine and *Neurology, **Department of Radiology, University Leipzig and ***Department of Neuroradiology, University Dresden, Germany

PROSPECTIVE VALUE OF CT AND Tc-99m-ECD-SPECT WITHIN 6 HOURS AFTER CEREBRAL ISCHEMIA

Adequate treatment of cerebral infarction, e.g. thrombolysis, should be started within 6 hours after onset of symptoms. However, within this time-window, detection of cerebral infarction is difficult using morphological imaging (CT). This present study was carried out to test the hypothesis that additional brain perfusion SPECT can improve prognosis early after stroke.

Patients: n = 108, 44 f, 64 m, age: 65 ± 13 y, acute ischemia in the territory of the medial cerebri artery (MCA), scandinavian stroke scale (SSS) < 40 points. Imaging: CT (Somatom Plus S, Siemens) and SPECT (400 - 600 MBq Tc-99m-ECD, high-resolution Ceraspect camera, DSI) within 6h after onset of stroke symptoms. Image analysis: (1) CT and SPECT separately, (2) SPECT together with CT; visual analysis; each 3 independent experts: signs of infarction (CT), extend and severity of activity deficits (SPECT). Patient groups (according to findings of CT after 5d): gr. A (n = 21): no hypodensities, gr. B (n = 76): hypodensities in subtotal MCA territory, gr. C (n = 11): hypodensities in total MCA territory.

Results of differentiation between gr.A and gr.B:

Method	Sensitivity (%)	Specificity (%)	Positive predictive value (%)	Negative predictive value (%)
CT	66.1	80.0	91.5	42.1
SPECT	96.0	85.0	96.0	85.0
SPECT + CT	96.0	90.5	97.3	86.4

SPECT evaluation together with CT resulted in lower number of false positive results compared to separate SPECT analysis, since some activity deficits in SPECT were assigned to local atrophy. Whereas no significant differences between gr.B and gr.C were found analysing CT (hypodensity or focal swelling > 66% of MCA territory: 2.6% vs. 18.2%, n.s.), SPECT analysis revealed high significant group differences (activity deficit 100% of MCA territory: 1.3% vs. 81.9%, p < 0.001).

It is concluded, that brain perfusion SPECT (additional to CT) within 6 hours after onset of stroke symptoms considerable improves prognostication of outcome, especially in case of reversible cerebral ischemia and total MCA infarctions. Thus early SPECT has the potential to gain an important tool for therapeutic decisions after stroke.

OS-65

Y. Hyun, JH Na*, IG Lee*, CG Ha*, W Choe

Inha University Hospital, Incheon, Korea
Department of Nuclear Medicine, and Neurology*

DOSE Tc-99m ECD UPTAKE SUGGEST TISSUE VIABILITY IN SUBACUTE STROKE?

Purpose: The redistribution pattern of I-123 IMP correlates closely with cerebral metabolic rate of oxygen (CMRO₂) and with clinical outcome. Tc-99m ECD (ECD) is metabolic tracer related with cell viability, similar to I-123 IMP, whereas Tc-99m HMPAO (HMPAO) suggests tissue perfusion. We studied to assess efficacy of ECD for prediction of cell viability during subacute stroke. **Methods:** Twenty patients (M/F: 11/9, range: 39-88 yrs.) showed mismatched uptake of ECD and HMPAO with sequential HMPAO/ECD SPECT at same position during the subacute phase (less than 11 days). We could perform follow-up sequential HMPAO/ECD SPECT in 8 patients during chronic phase (range: 32-125 days). **Results:** ECD uptake was always less than HMPAO in all lesions with mismatched uptake. During chronic phase, we observed diverse change of ECD and HMPAO uptake. HMPAO uptake was changed two directions of aggravation (6), or no change (2). However, ECD uptake was changed three directions of improvement (2), aggravation (2), or no change (4). During chronic phase, we still observed mismatched uptake of ECD and HMPAO in 6 patients. It meant mismatch of flow/metabolism might prolong. **Conclusion:** The change of ECD and HMPAO uptake in patients with stroke from subacute to chronic phase showed that the degree of ECD uptake linked to cell viability. However, improvement of ECD uptake during chronic phase compared with subacute phase suggests ECD uptake overestimate tissue damage in some patients with stroke during subacute phase.

OS-66

O. Sabri, D. Hellwig, M. Schreckenberger, H.J. Kaiser, G. Wagenknecht, U. Büll.
Dept. of Nuclear Medicine, RWTH Aachen, Germany

DO LACUNAR INFARCTIONS (LI) AND DEEP WHITE MATTER LESIONS (DWML) JUSTIFY A DIAGNOSIS OF VASCULAR DEMENTIA?

Purpose: Magnetic resonance imaging (MRI) of cerebral microangiopathy (CMA) shows LI, DWML and atrophy (ATR). LI/DWML are diagnostic criteria for the so-called vascular dementia. First results from statistical single-case comparisons of 57 CMA patients showed only ATR and neuropsychological deficits (NPS), but not LI/DWML, as cause of lowered rCBF/rMRGlu. Since we assumed multivariate correlations, we sought to determine whether an LI/DWML-based diagnosis of vascular dementia still is permissible when considering multivariate correlations. 57 patients were examined using a neuropsychological test battery (7 cognitive, 3 mnemonic, 4 attention tests). **Methods:** Using a special head holder system for exact repositioning, rCBF (SPECT with 99mTc-HMPAO) and rMRGlu (PET with 18-FDG) were imaged and measured in slices, followed by MRI. The white matter (periventricular, centrum semiovale) and cortex (frontal, parietal, temporal, occipital) were defined in ROIs taken topographically from the MRI (overlay). rMRGlu was calculated according to Sokoloff, rCBF normalised to cerebellum. **Results:** Univariate Spearman correlations were done for all rCBF (r > 0.70), rMRGlu (r > 0.74) and NPS (r > 0.55) scores to atrophy (r = -0.66, all p < 0.0005) and to LI/DWML (r < 0.22, all p > 0.1), then the variables reduced by factor analysis (principal component, varimax rotation) to yield global rCBF (rCBFall), global rMRGlu (rMRGluall) and 2 neuropsychological factors NPSsum1, NPSsum2. Next, a factor analysis was done with atrophy, microangiopathy, rCBFall, rMRGluall, NPSsum1, NPSsum2.

	Factor 1	Factor 2
NPSsum1	0.79	-0.09
NPSsum2	0.79	-0.13
rCBFall	0.76	0.05
rMRGluall	0.65	-0.04
Atrophy	-0.75	0.19
LI/DWML	-0.09	0.98
% explained variance	48.70	25.90

Factor loadings > 0.6 in bold (quality criteria: KMO=0.85, MSA>0.75 [good fit])

The uni- and multivariate analyses clearly show that the LI/DWML which define Factor 2 have no bearing on the other variables, while NPS correlates highly positively to rCBF/rMRGlu and highly negatively to atrophy. **Conclusion:** A diagnosis of "vascular dementia" can not be made on the basis of LI/DWML.

Radiopharmacy and radiochemistry: PET

OS-67

C. Halldin¹, P. Emond², J. Sandell¹, Y.-H. Chou¹, J. Helfenbein², P. Karlsson¹, S. Chalon², C.-G. Swahn¹, D. Guilloteau² and L. Farde¹.
¹Karolinska Institutet, Department of Clinical Neuroscience, Stockholm, Sweden. ²INSERM U316 Université François Rabelais, Tours, France.

THE FIRST SELECTIVE SEROTONIN TRANSPORTER RADIOLIGAND SUITABLE FOR BOTH PET AND SPECT

The dopamine transporter (DAT) ligands β-CIT and nor-β-CIT have been used for imaging the serotonin transporter (5HTt) with PET and SPECT. However, their poor selectivity for the 5HTt limit their use in quantitation. Recently, SAR studies have shown that several non iodinated nortropane derivatives bearing an alkyl or alkenyl moiety at the 4' position of the aromatic ring have increased affinity and specificity properties for the 5HTt compared to nor-β-CIT (Blough et al., J. Med. Chem., 1996). Moreover, the same authors have reported the synthesis of 2β-carbomethoxy-3β-(4'-ethyl-3'-iodophenyl)nortropane that presented high in vitro affinity and specificity for the 5HTt (Blough et al., J. Med. Chem., 1997). In order to develop a tracer suitable for both PET and SPECT, we report the synthesis of a new selective tropane analog for the 5HTt: 2β-carbomethoxy-3β-(4'-isopropyl-3'-iodophenyl)-nortropane (LBT44) that can be labelled both for PET and SPECT. The aim of this work was to label LBT44 with carbon-11 and examine the binding of [¹¹C]LBT44 *in vivo* with PET in Cynomolgus monkeys. LBT44 was synthesized according to earliest published procedures (Emond et al., J. Med. Chem., 1997). The acid precursor for ¹¹C radiolabelling was obtained in 90% yield by treating at reflux LBT44 with HCl 0.1N. [¹¹C]LBT44 was labelled from [¹¹C]methyl triflate and LBT44 acid and injected into two Cynomolgus monkeys. There was a rapid accumulation of radioactivity in the brain after i.v. injection of [¹¹C]LBT44 (4.2% after 4 min). There was a high accumulation of radioactivity in 5HTt rich brain regions such like the thalamus and the brain stem with only minor accumulation in striatum. The ratio of thalamus to cerebellum was about 1.7 at a transient equilibrium which was obtained at 30-40 minutes. Metabolite studies measured in plasma demonstrated only polar labelled metabolites (42% unchanged radioligand at 45 minutes). In conclusion, LBT44 is the first selective 5HTt radioligand suitable for quantitation with both PET and SPECT.

OS-68

C. Lundkvist¹, C. Loch², C. Halldin¹, M. Bottlaender², C. Fuseau², M. Ottaviani², J. Mertens³, L. Farde¹, B. Mazière².
¹Department of Clinical Neuroscience, Karolinska Institutet, Stockholm, Sweden, ²Service Hospitalier Frédéric Joliot, CEA, Orsay, France, ³VUB-Cyclotron, Brussel, Belgium.

DEVELOPMENT OF BR-76 R88504 AS A PET LIGAND FOR IMAGING OF 5-HT_{2A} RECEPTORS.

Dysfunctions of the serotonergic (5-HT) system are believed to be involved in depression and other psychiatric disorders. R93274 (4-amino-N-[1-[3-(4-fluorophenoxy)propyl]-4-methyl-4-piperidinyl]-5-iodomethoxybenzamide) is a iodinated 5-HT_{2A} antagonist with high affinity and selectivity for 5-HT_{2A} receptors (5-HT_{2A}Rs). In the search for tracers which would allow *in vivo* quantification of 5-HT_{2A}R concentration by SPECT, R93274 has previously been labelled with I-123. In order to study by PET, the *in vivo* behaviour of the bromo analogue, R88504 and to characterise its pharmacological properties, we have labelled R88504 with Br-76 (T_{1/2} = 16 h).

[Br-76]R88504 was prepared by electrophilic substitution of the trimethyltin precursor using nca Br-76 and peracetic acid. The tracer was purified by RP-HPLC and obtained in 40% radiochemical yield with a specific radioactivity of 20 GBq/μmol.

In vivo autoradiographic studies in rats, the regional distribution of [Br-76]R88504 paralleled the neuroanatomical localisation of 5-HT_{2A} receptors in the brain but a weak signal was observed.

PET imaging of [Br-76]R88504 in baboon demonstrated a rapid and high uptake in the brain (2%ID). Peak uptake in cortical area reached a maximum (20% ID/L) at 15 min p.i. One hour later, the radioactivity concentration in the cortical regions, in the striatum and in the cerebellum were 15, 12, 10% ID/L, respectively. Due to the constant washout in the cerebellum, the cortex to cerebellum ratio was 1.7 at 1.5 h p.i. At that time, IV injection of ketanserin (1 mg/kg) reduced the radioactivity concentration in cortex to the level of cerebellum in 1 h. These preliminary results suggest that [Br-76]R88504 has the potential to be developed as a useful PET radiotracer for imaging 5-HT_{2A}Rs in the brain.

This work was performed within a COST-B3 action from EEC.

OS-69

ILJ Dearing^a, GED Mullen^a, JS Lewis^a, MT Rae^a, J Zweib^b, PJ Blower^{a,c}

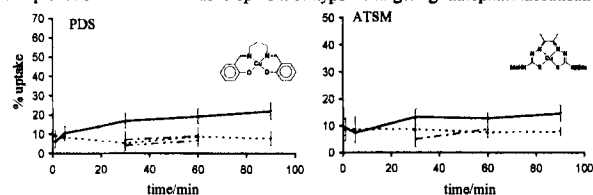
^aBiosciences Dept, University of Kent, Canterbury, UK

^bJoint Dept of Physics, Institute of Cancer Research, Sutton, UK

^cNuclear Medicine Dept, Kent and Canterbury Hospital, Canterbury, UK

HYPOXIA-TARGETING RADIOPHARMACEUTICALS: SELECTIVE UPTAKE OF COPPER-64 COMPLEXES BY HYPOXIC CELLS IN VITRO

Radiopharmaceuticals selective for hypoxic tissue would offer a non-invasive means of measuring localised hypoxia in tumours and heart disease. The well-known blood flow tracer CuPTSM, labelled with ⁶²Cu or ⁶⁴Cu, is believed to be trapped in cells non-selectively by a bioreductive mechanism. It is proposed that by modifying the ligand to increase its electron donor strength, for example by adding alkyl groups or replacing sulfur donors with oxygen, the copper complexes will become less easily reduced and tracers with selectivity for hypoxic tissues could thus be developed. **Aim:** to prepare ⁶⁴Cu-labelled complexes of two series of ligands designed according to these principles, based on the bis(thiosemicarbazone) (13 ligands) and bis(salicylaldimine) (three ligands) skeletons, and to evaluate the hypoxia-dependence of their uptake in cells. **Methods:** The complexes were incubated with suspensions of Chinese hamster ovary cells under normoxic and hypoxic conditions, and the cells isolated by centrifugation to determine radioactivity uptake at various time points up to 2 h. **Results:** Several members of both series demonstrated significant ($p < 0.05$) or highly significant ($p < 0.01$) hypoxia selectivity by 30 minutes of incubation. Two examples of a highly hypoxia-selective complex, CuPDS and CuATSM, are shown below (solid line: hypoxic; broken line, normoxic; the hypoxic and normoxic cell-free controls, showing binding of tracer to the tubes, are also shown). **Conclusion:** these complexes offer a basis for development of hypoxia-targeting radiopharmaceuticals.

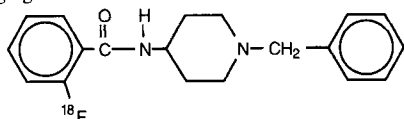


OS-70

C.-Y. Shiuie, G.G. Shiuie, F. Benard, A. Cesano and A.A. Alavi, Department of Radiology, University of Pennsylvania and The Wistar Institute, Philadelphia, PA., U. S. A.

N-(N-BENZYLPIPERIDIN-4-YL)-2-[F-18]FLUOROBENZAMIDE (2-FBP) : A POTENTIAL RADIOLIGAND FOR PET IMAGING OF HUMAN BREAST TUMORS IN HUMANS.

Sigma (σ) receptors have been implicated in psychoses, movement disorders, neuroprotection and schizophrenia. In addition, it has been found that σ receptor subtypes are also expressed in a variety of human and rodent tumor cell lines including human breast tumor tissue. Therefore, a σ receptors specific ligand may also be a potential breast tumors imaging agent. We recently reported that 2-FBP is a potent σ receptors specific ligand (Nucl. Med. Biol. 24:671-676, 1997). The purpose of this study is to evaluate whether 2-[F-18]FBP is a radioligand for PET imaging of human breast tumors. 2-[F-18]FBP was synthesized in one step by nucleophilic substitution of the 2-nitro precursor with [F-18]fluoride in DMSO at 140°C for 20 min followed by purification with HPLC in 4-10% yield. Following i.v. injection into Severe Combined Immunodeficiency (SCID) mice bearing primary tumor explants from a human breast cancer patient, the uptake of 2-[F-18]FBP in the brain, heart, liver, lungs, spleen, kidneys, small intestine and tumor are high. The ratio of tumor/muscle is 6.3/1 and 3.3/1, respectively, at 1 hr and 2 hr post-injection. Pretreatment of mice with haldol (a non-selective, high-affinity σ receptor ligand, 2.5 mg/kg i.p. 30 min prior) reduced the ratio of tumor/muscle to 1.3 and 0.9, respectively, at 1 hr and 2 hr post-injection. These results suggest that the human breast tumor uptake of 2-[F-18]FBP is probably sigma receptors-mediated, and that 2-[F-18]FBP may be a useful ligand for PET imaging of human breast tumors in humans.



OS-71

Jörg T. Patt, Jörg E. Spang, Gerrit Westera, P. August Schubiger

Center for Radiopharmaceutical Science, Swiss Federal Institute of Technology, Paul Scherrer Institute and Clinic of Nuclear Medicine, University Hospital Zürich, Zürich, Switzerland.

[C-11]N-METHYLEPIBATIDINE AND [C-11]N-METHYLHOMOEPIBATIDINE: COMPARISON OF THE STEREOISOMERS IN VIVO

Epibatidine (2 β -(2-Chloro-5-pyridinyl)-7-azabicyclo[2.2.1]heptane) and homoepibatidine (6 β -(2-Chloro-5-pyridinyl)-8-azabicyclo[3.2.1]octane) and their methylated derivatives show high affinity and selectivity for α 4 β 2 nAChRs (nicotinic acetylcholine receptor) in the brain. The C-11-methylated compounds are possible PET-tracers for this receptor. Homoepibatidine is less toxic than the natural occurring epibatidine.

The stereoisomers of epibatidine and homoepibatidine are well separated by semipreparative HPLC on a Chirobiotic T column (250 x 10) (epibatidine: flow 9 ml/min, eluent MeOH/AcOH/TEA (99.8/0.1/0.1, v/v/v), (-)-isomer 16.9 min, (+)-isomer 26.4 min); homoepibatidine: flow 9 ml/min, eluent MeOH/AcOH/TEA (99.4/0.3/0.3, v/v/v), (-)-isomer 7 min, (+)-isomer 8.3 min). Enantiomeric purity was >97 % ee. Radiolabelling of 0.05 to 0.1 mg of precursor with [C-11]methyl iodide in MeCN (100 °C, 10 min) yielded 50 to 150 MBq of radiochemical pure product in high specific activity (200 to 500 GBq/ μ mol EOS). The in vivo behaviour was evaluated in female ICR-mice and male Sprague Dawley rats. Biodistribution of the tracer was determined by dissection and measuring in a γ -counter and by PET. The amount of carrier injected was in the range of 0.01 to 0.001 μ g/kg. For both compounds, epibatidine and homoepibatidine, the stereoisomers showed characteristic differences in biodistribution, especially in the brain uptake curve. [C-11]N-methyl-(+)-epibatidine showed a very fast uptake, a very sharp maximum and rapid washout from the brain. [C-11]N-methyl-(-)-epibatidine showed a slow uptake to the brain and does not reach maximum during 60 min. A similar difference was found for the [C-11]N-methyl-homoepibatidine enantiomers. [C-11]N-methyl-(+)-homoepibatidine showed a very fast uptake and washout from the brain. [C-11]N-methyl-(-)-homoepibatidine showed a slower brain uptake than its enantiomer. The brain uptake curve reached its maximum after 10 to 20 minutes followed by slow washout. In conclusion the methylated epibatidine and homoepibatidine enantiomers showed a characteristically different behaviour in vivo. [C-11]N-methyl-(-)-homoepibatidine is the most promising candidate for C-11 imaging of neuronal nAChRs due to the result, that an equilibrium is reached after 10 to 20 minutes. Lower toxicity of the homoepibatidine is a further good argument for this class of receptor ligands.

OS-72

U. Scheffel¹, J.L. Musachio¹, A.G. Horti², M. Kassiou², P.A. Finley¹, Y. Zhan¹, H.T. Ravert¹, W.B. Mathews¹, E.D. London², and R.F. Dannals¹. Department of Radiology, Johns Hopkins University¹ and Brain Imaging Center, Div. of Intramural Research, National Institute on Drug Abuse², Baltimore, MD. U.S.A.

IN VIVO EVALUATION OF NEW, HIGH AFFINITY RADIOLIGANDS FOR IMAGING CENTRAL NICOTINIC ACETYLCHOLINE RECEPTORS.

Tomographic imaging of nicotinic acetylcholine receptors (nAChRs) has, until recently, been difficult because of the lack of high affinity radiotracers binding to nAChRs. In vivo quantitation of central nAChRs might become important as a diagnostic tool in neurodegenerative diseases, such as Alzheimer's disease, in the development of therapeutic drugs targeted to bind to nAChRs, and in studies of the effects of nicotine in the brains of smokers. During the past few years new nAChR radiotracers have been developed which are based either on the highly potent ligand epibatidine or on 3-pyridyl ethers. The [18F]-labeled norchloro-epibatidine analog [18F] FPH ((+)-2-(2-[18F]fluoro-5-pyridyl)7-azabicyclo [2.2.1] heptane) and the [125I]-labeled analog IPH have previously been shown in animals to be excellent agents for the visualization of nAChRs by PET or SPECT, respectively. However, these epibatidine derived analogs are highly toxic which may preclude their use for studies in humans.

We, therefore synthesized three new radiotracers, i.e. [11C]-A-84543, 2-[18F]fluoro-A-85380, and 5-[125I]-iodo-A-85380, which are less toxic, and tested them in vivo in mice. After intravenous injection, all three radiotracers showed appropriate regional distribution (thalamus>superior colliculus>striatum, cortex>cerebellum), their binding was saturable and was blocked by various nAChR agonists, such as (-)-nicotine and cytisine, but not by the non-nicotinic cholinergic drug scopolamine or by mecamylamine (a non-competitive nAChR antagonist). In contrast to [18F]- and [125I]-A-85380, [11C]-A-84543 displayed high nonspecific in vivo binding. [18F]- and [125I]-A-85380 were found to be considerably less toxic than the [18F]- and [125I]-labeled epibatidine analogs.

The results of our studies indicate that 2-[18F] and 5-[125I]-A-85380 bind specifically and selectively to nAChRs in vivo and are safer than the epibatidine based tracers. These new radioligands should be excellent agents for in vivo imaging of nAChRs.

General nuclear medicine: Renal function

OS-73

K. Melis, M. Tondeur, C. De Sadeleer, J. Verhelst, M.B. Van Espen, H. Ham, A. Piepsz
Free Universities of Brussels (ULB-VUB)

INTEROBSERVER REPRODUCIBILITY OF THE RELATIVE ^{99m}Tc DMSA LEFT TO RIGHT UPTAKE RATIO.

Relative left and right ^{99m}Tc DMSA uptake can be used to determine and to follow the relative renal function. In the framework of a wide Belgian study on reproducibility on reporting on DMSA images, the present work was designed to evaluate the robustness of the calculation of the relative DMSA uptake. Planar ^{99m}Tc DMSA images from 49 randomly selected patients (10 adults, 39 children) were sent to 15 Belgian centers. They were asked to calculate, using their own routine program, the relative uptake (in %) of each kidney. The data were sent on disks formatted in order to be readable by each participant, using his own computer system. For each scan, interobserver variability was expressed by the maximum difference and the standard deviation (SD) of the left renal uptake. Left renal uptake measured by the 15 observers in the 49 patients was comprised between 29% and 72% (mean: 49.8, SD: 6.4). Maximum differences in left renal uptake ranged between 1.7% and 12% (mean: 4.5, SD: 2.6); however, the maximum difference did not exceed 8% in about 90% of the patients. The standard deviations of the individual left renal uptake were comprised between 0.6 and 3.9 (mean: 1.3, sd: 0.8). The standard deviations were significantly higher in adults (mean SD: 2.05) than in children (mean SD: 1.12) (p < 0.001); this could be related to high background which was observed in 3 adult cases with severe renal impairment. The analysis of the results obtained by each of the 15 observers revealed that the differences between right and left renal uptake were systematically lower for some observers, suggesting the effect of the calculation method. While theoretically the calculation of the relative left and right uptake in DMSA scintigraphy does not seem to present any difficulty, these results are surprisingly disappointing. Therefore standardisation of the calculation method is mandatory.

OS-74

C. De Sadeleer, M. Tondeur, K. Melis, M.B. Van Espen, J. Verhelst, H. Ham, and A. Piepsz.

Free Universities of Brussels (VUB – ULB)

A BELGIAN STUDY ON THE REPRODUCIBILITY IN REPORTING ON Tc-^{99m} DMSA PLANAR SCINTIGRAPHY.

Conflicting results regarding reproducibility in Tc-^{99m} DMSA renal images interpretation have been published. Therefore, all Belgian nuclear medicine centers were invited to participate into a large study. To those who were willing to join the study (79%), a series of computer disks containing 49 DMSA studies were sent. To avoid potential problems related to unfamiliar display, the disks were formatted in order to be readable using the participants' own computer systems. Each participant was then free to use his usual display (hard copies, contrast enhancement, color scale, grey scale, ...). DMSA scans obtained in 10 adults and 39 children were randomly selected from the databases of 2 hospitals. For each kidney, the observers had to choose between the following answers: normal, abnormal, equivocal, and lack of quality. Additionally, they had to localize the abnormality. A total of 42 responses were obtained, issued from a wide variety of institutions and from observers with different levels of experience in reporting on DMSA scintigraphy. Altogether, the following reports were obtained: 60.8% normals, 25.2% abnormal, 7.0% equivocal, and 3.2% lack of quality. The median percentage agreement (overall reproducibility) for the 42 observers was 92%. Two groups of kidneys were identified: a large majority with a very good reproducibility and a small number (n = 4) of kidneys with reproducibility ranging from 51% to 70%. Reproducibility was significantly higher in evaluating the medial (94.8%) and lateral (94.7%) parts compared to the upper (91.1%) and lower (89.9%) poles. Except 2 observers who behave like outliers, all others had the same level of performance. In conclusion, in a large number of Belgian nuclear medicine physicians, on a large randomly selected sample of Tc-^{99m} DMSA studies, an excellent interobserver agreement was observed.

OS-75

D. Djokic, D. Jankovic, T. Maksin*, E. Jaksic, S. Beatovic, R. Han**

*VINCA Institute of Nuclear Sciences, P.Box 522, 11001 Belgrade
**Institute of Nuclear Medicine-CCS, Belgrade, Yugoslavia

^{99m}Tc-PAH AS A NEW RENAL REAGENS

This paper presents the results of investigation of chemical, biological and pharmacokinetic studies of ^{99m}Tc-PAH, as well as its clinical evaluation in two human volunteers. PAH is labelled with ^{99m}Tc in presence of calcium trisodium salt of DTPA by use of Sn(II)-reduction method. Radiochemical purity was determined by ITLC-SA (acetone, saline) and gel chromatography (Sephadex G-25, saline and H₂O₂). The protein binding was determined by TCA-precipitation method. Biological studies included the animal biodistribution, rat probenecid studies, rat clearance studies and scintigraphic renal studies (white Wistar rats). The preliminary clinical studies in two human volunteers include dynamic images in the supine position, the analysis of the scintigraphic images and calculation of split renal function, T_{max}, T_{1/2} and percentage of residual activity in each kidney.

Results of this studies showed that obtained radiopharmaceutical is at high radiochemical purity (>95% 15min and 99% 240min after labelling). The percentage of protein binding is 32.3%, and the percentage of activity of administered dose in kidneys are: 10.7% and 2.2% 2min and 60min postinjection. Renal excretion of ^{99m}Tc-PAH was reduced from 85.5% to 50.8%, i.e. 40% 30min postinjection in presence of renal tubular transport inhibitor probenecid. The pharmacokinetic parameters are: t_{1/2}(α)=2.5min, t_{1/2}(β)=41.7min, Cl= 5.22 ml/min, K_{el}= 0.0511/min. Scintigrams from rat revealed that ^{99m}Tc-PAH was rapidly excreted in urine and provide satisfactory renal images with no significant extrarenal background. Significant accumulation of renal activity 2min after injection was followed by rapid excretion phase: time to fall peak activity to its half value was 1min. Evaluation in human beings has shown that no extrarenal activity was noted during the period of study. Maximum of radiotracer in kidney was between 2 and 3 min. with rapid decrease in time and low residual activity at the end of study. The percentage relative function of kidneys varied between 45 % and 55%. Peak activity is reached 2.5-3.5min, and fall to its half value between 1.5 and 6.25min.

The results of ^{99m}Tc-PAH-studies confirmed favourable radiochemical and biological characteristics. This complex seems to be a suitable tracer for routine renal scintigraphy, and due to its very fast kinetics, short half-life, and faster renal excretion characteristics, could be useful substitute for ^{99m}Tc-DTPA.

OS-76

M. Rehling, C. Stadeager, JH. Henriksen, O. Siemsen, JJ. Krintel, A. Malchow-Møller, H. Ring-Larsen.

Dept's of Clinical Physiology, Gastroenterology, Hvidovre Hospital, Copenhagen and Nuclear Medicine, Skejby Hospital, Aarhus, Denmark.

MEASUREMENT OF GLOMERULAR FILTRATION RATE IN PATIENTS WITH ASCITES

In clinical practice the glomerular filtration rate (GFR) is assessed from serum creatinine or more reliable from plasma clearance of ⁵¹Cr-EDTA after a single injection.

The aim of the study was to determine the accuracy of these methods in patients with ascites.

In 88 patients with ascites due to cirrhosis of the liver GFR was assessed by 1) plasma clearance of ⁵¹Cr-EDTA (Cl_p) from 14 blood samples 5-300 min post injection (p.i.), 2) estimated endogenous creatinine clearance (EECC) from serum creatinine, sex, age and weight of the patient (Kampmann et al. 1974, 3) renal plasma clearance of ⁵¹Cr-EDTA (Cl_r) from the excreted amount of activity and the area under the time/activity curve 0-300 min p.i.

Cl_p overestimated Cl_r by 15.8 ± 1.4 ml/(min x 1.73 m₂)(mean ± SEM)

EECC overestimated Cl_r by 23.1 ± 2.0 ml/(min x 1.73 m₂)

EECC overestimated Cl_p by 7.3 ± 1.4 ml/(min x 1.73 m₂).

Earlier studies in patients without ascites have shown a difference in Cl_p and Cl_r of approximately 4 ml/min. In this study in patients with ascites the difference was significantly higher indicating extrarenal clearance and non-equilibrated distribution to transcellular fluids. The overestimation of Cl_r by EECC may be due to a low muscle mass relative to the body weight of the patients.

Taking Cl_r as reference of GFR Cl_p overestimated GFR substantially but EECC overestimated GFR even more. Thus, these methods are inaccurate in patients with ascites. In these patients GFR has to be assessed by a direct renal clearance technique.

OS-77

M. Rehling, LE. Nielsen and J. Marqvorsen.

Hospital: Department of Clinical Physiology and Nuclear Medicine, Aarhus University Hospital, Skejby Hospital, Aarhus, Denmark.

IN VITRO AND IN VIVO PROTEIN BINDING OF ^{99m}Tc-DTPA.

^{99m}Tc-DTPA, ⁵¹Cr-EDTA and ¹²⁵I-iothalamate are widely used for measurement of the glomerular filtration rate (GFR). It has been emphasized, however, that commercial DTPA-preparations sometimes contain impurities that bind to plasma protein causing errors in GFR measurement. We therefore decided to study the protein binding (Pb) of the ^{99m}Tc-DTPA preparation we use in daily routine (DTPA from Amersham).

Using an in vitro technique, in which the radiopharmaceutical was incubated in donor plasma, we compared the Pb of the ^{99m}Tc-DTPA preparation, 1) with the other five DTPA-kits available on the European market, 2) with ⁵¹Cr-EDTA and ¹²⁵I-iothalamate (both Amersham). Finally, we studied the in vivo Pb of the ^{99m}Tc-DTPA preparation 5 and 40 min after a single injection. Pb was determined by ultrafiltration (Centrisart 1, Sartorius, Germany).

The in vitro Pb of the six DTPA-kits was, mean of six and (range): 0.67% (-0.04-1.64%). The Pb varied significantly but only two were significantly different from zero (IFE, Norway and SORIN, Italy).

The average in vitro Pb of ^{99m}Tc-DTPA (Amersham) (1.47%) was significantly lower than that of ⁵¹Cr-EDTA (4.45%) and ¹²⁵I-iothalamate (3.96%) (n=16).

In eight patients the average in vivo Pb of ^{99m}Tc-DTPA (Amersham) was 3.45% without difference 5 and 40 min after the injection.

In conclusion:

There were only small differences in the in vitro Pb of the six commercially available DTPA-kits.

The in vitro Pb of ^{99m}Tc-DTPA was significantly lower than the Pb of ⁵¹Cr-EDTA and ¹²⁵I-iothalamate.

The in vitro Pb underestimated the in vivo Pb of ^{99m}Tc-DTPA but the in vivo Pb was low.

OS-78

I. CIFTCI and B. ERBAS.

Hacettepe University, Department of Nuclear Medicine, Ankara-TURKEY

ESTIMATION OF ^{99m}Tc-ETHYLENEDICYSSTEINE CLEARANCE USING SINGLE SAMPLE TECHNIQUE.

Technetium-^{99m}-ethylenedicysteine (^{99m}Tc-EC) has been introduced as an alternative tubular agent to ¹³¹I-IOH and ^{99m}Tc-MAG3. Although several simplified methods for calculating ¹³¹I-OIH and ^{99m}Tc-MAG3 clearance from single plasma sample have been reported, there are very few reports on the measurement of ^{99m}Tc-EC clearance. Optimal sampling time was reported to be 80 minute and 54 minute in two different studies (Stoffel et al., Kabasakal et al.). Therefore, this study was designed to develop a simplified single sample formula for the estimation of ^{99m}Tc-EC clearance.

Following i.v. injection of 5 mCi ^{99m}Tc-EC, multiple plasma samples were obtained from 83 subjects (19 normals, 64 patients, age range=15-73 years). Plasma clearance values of ^{99m}Tc-EC were measured using bi-exponential analysis of plasma disappearance curves and corrected for body surface area. The mean value was 316±103 mL/min/1.73 m² (range=93-518 mL/min/1.73 m²). The theoretical volumes of distribution at various times were calculated and plotted against reference clearance values. An exponential fit was carried out as suggested by Tauxe.

time (min)	F max (mL/min)	α (liter-1)	V lag (liter)	Correlation (r)	see (mL/min)
40	675.1	0.0172	8.08	0.962	27.80
50	727.5	0.0110	5.30	0.971	24.96
53	730.0	0.0099	4.41	0.972	24.54
54	728.3	0.0097	4.15	0.972	24.19
55	723.8	0.0095	3.93	0.972	24.60
60	682.5	0.0091	3.26	0.970	25.31
65	628.6	0.0093	3.4	0.967	26.68

The optimal time for plasma sampling was found to be 54. min. being in agreement with the report published by Kabasakal et al. Our data provided a lower error of estimation compared to their results, but higher values than the results of Stoffel et al. The equation best fitting our data was: **Clearance (^{99m}Tc-EC)=728x [1-e^{-0.0097(ID/C₅₄ - 4.15)}] In conclusion, using our simplified formula plasma clearance of ^{99m}Tc-EC can be estimated with an acceptable error.**

Cardiovascular: Viability

OS-79

J.Knuutila, U Ruotsalainen, M Mäki, M Haaparanta, J Bergman, L-M Voipio-Pukki, P Nuutila, H Iida.

Turku PET Centre, Turku University Central Hospital, Finland and Research Institute for Brain and Blood Vessels-Akita, Akita City, Japan

WATER-PERFUSABLE TISSUE FRACTION AND F-18-FDG UPTAKE IN THE ASSESSMENT OF MYOCARDIAL VIABILITY BY PET

The water perfusable tissue fraction (PTF) has been proposed as an alternative approach to assess myocardial viability since it is obtained routinely together with myocardial flow (MBF) measurement. PTF has been shown to have high sensitivity in distinguishing reversibly from irreversibly injured myocardium in both the acute and chronic setting. However, there are no direct comparison between FDG and PTF in the assessment of myocardial viability in a clinical patient population.

Methods: Head-to-head comparison between MBF, PTF and FDG uptake in 16 patients with previous myocardial infarction who underwent revascularization was performed. Predictive values of the wall motion recovery after the successful revascularization therapy were compared between the measures. Both qualitative and quantitative values of MBF, PTF and glucose uptake were calculated for each segment (7 seg/pts).

	Images	PPV	NPV	Accuracy
Glucose (Relative)		86 %	88 %	87 %
Glucose (Absolute)		90 %	68 %	80 %
MBF		92 %	62 %	76 %
PTF		91 %	85 %	89 %
Glucose (Relative) + MBF		92 %	94 %	93 %

Conclusions: The present study is the first to directly compare FDG and PTF approaches in the assessment of myocardial viability in a clinical patient population. The results demonstrate that both PTF and the relative FDG uptake well predict the wall motion recovery after the successful revascularization in the hypocontractile segments. However, absolute quantitation of glucose consumption and MBF are limited in terms of assessing myocardial viability.

OS-80

L.Ö.Kapucu, T. Atasever, M. Cemri, S. Atavcı, A. Çengel, H. Dörtmeç, M. Ünü

Gazi University, Faculty of Medicine Departments of Nuclear Medicine and Cardiology

ASSESSMENT OF MYOCARDIAL VIABILITY BY REST-REDISTRIBUTION-NITRATE TI-201 SPECT IN PATIENTS WITH ACUTE MYOCARDIAL INFARCTION: COMPARISON WITH NITRATE ECHOCARDIOGRAPHY

The aim of the study was to evaluate Rest-Redistribution-Nitrate TI-201(RRNTI) SPECT with nitrate echocardiography (NE) for the identification of viable myocardium. Thirteen patients were studied with RRNTI and NE 11±3 days following acute myocardial infarction. All of the patients underwent coronary artery bypass surgery after 28±10 days of acute myocardial infarction(MI) and postoperative echocardiographies(PE) were also obtained following 45±14 days of revascularisation. In RRNTI SPECT, following rest-redistribution TI-201(RRTI) study, dinitrate isosorbide (p.o:5mg) was administered and SPECT study was repeated after 20 minutes. NE was performed after basal echocardiography(BE) by administering i.v nitroglycerine starting at 0.4 ucg/kg/min with equal increments every 5 minutes up to 2 ucg/kg/min. Left ventricular wall motion analysed by dividing the left ventricle(LV) into 16 segments and a wall motion score index(WMSI) was calculated. Semiquantitative visual analysis was performed by assigning regional TI-201 tracer activities on a four grade scoring system, ranging from 0 to 3. Perfusion defects that improved at least one grade on the subsequent redistribution and/or nitrate images were considered to represent viable myocardium. Basal echocardiography (BE) demonstrated 75 dysynergic segments; 42 of these 75 segments (56%;8pts) showed improved contractility on NE. While 53 segments(70%;10pts)were viable on RRTI study and 68 segments revealed improved perfusion on RRNTI study(90% 11pts). Postoperative echocardiography(PE) showed improvement in 57 segments (76%;11pts) WMSI of BE showed significant improvement in both NE and PE (1.73±0.4 vs 1.51±0.2 and 1.44±0.3). In our study, RRNTI was found to be the most sensitive method in detecting viable myocardium in comparison to RRTI and NE(sensitivity;RRNTI:100%,RR:92%,NE:72%). Addition of nitrate TI-201 to routine RRTI viability study can be an effective and easy test in selecting patients who can get benefit from coronary revascularisation.

OS-81

A.W.Kedra, M.Duet, D.Vilain, S.Benelhadj, O.Bailliar, O.Mundler :

Hôpital Lariboisière, Paris France Departments of Nuclear Medicine and Fonctionnal Exploration

EFFICACY OF THALLIUM 201 REDISTRIBUTION AFTER NITROGLYCERIN ADMINISTRATION TO DETECT ISCHAEMIC BUT VIABLE MYOCARDIUM : COMPARISON WITH 24 HOURS REDISTRIBUTION.

The improvement of initial stress ²⁰¹Tl defects is usually evaluated 4 hours after stress test and reinjection in the evaluation of coronary artery disease (CAD) by SPECT. Some authors also have demonstrated the interest of delayed 24 hours ²⁰¹Tl acquisition. Nitrates (NTG) act at the myocardium level by a vasodilatory effect on the large coronary artery and they are the most potent stenotic site vasodilators. So the aim of this study was to evaluate if NTG administration after ST just before 4 hours redistribution ²⁰¹Tl images is able to give the same results than late redistribution which is constraining for the patient.

Twenty four patients with angiographically documented CAD (12 with prior myocardial infarction) had 3 SPECT ²⁰¹Tl (S) : the first one immediately after stress (S1), the second one 4 hours later 30 minutes after sublingual administration of 0.4 mg NTG and ²⁰¹Tl reinjection (S2), and the third one at rest, 24 hours after stress (S3). Images were evaluated using left ventricular segmentation (LV) and ²⁰¹Tl distribution as proposed by A.R Shehata.

Four hundred and eighty LV segments were analyzed ; 240 (50%) showed ²⁰¹Tl defect after S1, 62 were unchanged at S2 and S3, 161 were improved at S2 and 178 at S3 (NS). Although the 24 hours images showed a slightly better ²⁰¹Tl uptake in 17 cases (versus 11 at 4 hours.), it does not influence any clinical decision (no evidence of wide regional defects at 4 hours NTG SPECT which be improved at 24 hours images).

In conclusion sublingual administration of 0.4 mg NTG, 30 minutes before ²⁰¹Tl SPECT realized 4 hours after stress test lets the same evaluation of reversible myocardial ischemia as 24 hours rest images.

OS-82

R.Bangsgaard, K.F.Kofoed, H.Kelbæk, A.Rabøl, B.Hesse Rigshospitalet, Dpts.Cardiology and Clin.Physiol.Nucl:Med., Copenhagen University, Denmark.

EARLY POSTOPERATIVE MYOCARDIAL TETROFOSMIN SPECT PREDICTS IMPROVED LONGTERM, RESTING MYOCARDIAL PERFUSION AFTER CABG IN HIBERNATION

Background and purpose: The time course of changes in myocardial function and perfusion after CABG for hibernating myocardium is not known. The purpose of this investigation was to study if early myocardial SPECT reflects permanent changes .Patients and methods: Of the 49 revascularised pts. with LVEF below .45, entering the study, 27 pts. (mean age 64 y, SD 7.3; 26 m, 1 f) underwent all 3 planned resting SPECT studies with tetrofosmin: Just before operation (I) and 1-2wks (II) and 6 mths(III) after CABG. The SPECT data were scored visually (no uptake:0; normal: 4) in a blinded fashion and with quantitative severity scores according to the Cequal program: >10% reduction in severity score in II or III vs.I was considered a significant change.

Results: Changes in visual and quantitative scores were correlated (r =.71) and early changes (II vs I) and late changes (III vs. I) were correlated both at visual and quantitative analyses (r= .8 and .6, resp.). Both evaluations showed that ca. half of the pts.had improved SPECT at II, 9-10 of them maintaining this change, while 1/3 lost it again. A few pts. deteriorated at II and were rather stable from II to III. Finally some pts.had nearly unchanged perfusion, both at II and III. No pt. showed only late improvement (i.e. only from II to III), whereas two pts. with improvement from I to II had some continued improvement II to III.. Comment and conclusion: Improved myocardial perfusion after revascularisation in hibernating myocardium is present and can be demonstrated by tetrofosmin SPECT early after revascularisation. However, some of the pts. with early improvement return to preoperative flow distribution, probably due to re-occlusion after CABG.

OS-83

T.Kajiya, H. Kurogane, A.Takarada, T. Hayashi, J. Shite, A. Yoshida, T. Itagaki, Y. Yoshida.

Hospital: Division of cardiology, Himeji Cardiovascular Center, Japan

RELATION OF VIABILITY AND UPTAKE AND KINETICS OF TC-99M TETROFOSMIN IN POST-REPERFUSION MYOCARDIUM.

Ability of viability detection by Tc-99m tetrofosmin (TF) is thought to be inferior to Tl-201 due to its lack of redistribution. The myocardial uptake and retention mechanism of TF which depend on electrical potential of both plasma and mitochondrial membrane are different from those of Tl-201 which depends on Na-K ATPase activity. To date, relation of TF and myocardial viability is poorly clarified in the post-perfusion myocardium. We studied the uptake and retention kinetics of TF in 30 patients (pts) with 1st acute LAD myocardial infarction treated by direct PTCA. During subacute phase (2-4 weeks), blood-pool scan and TF SPECT were performed. SPECT was performed at 15 minutes (initial) and 3 hours (delayed) after TF administration at rest. SPECT images were quantitatively analyzed and mean LAD %activity was obtained. Blood-pool scan was repeated at 3 months. On TF initial image, mean LAD activity of all pts was 61.4 ± 19.6%, while it decreased to 47.0 ± 17.0% (P<0.001) on delayed image. In 11pts with good viability indicated as subacute LVEF=>50%, high initial LAD activity significantly decreased on delayed image (from 73.8 ± 12.4 to 59.5 ± 16.2%, P<0.01). Among 19 pts with impaired subacute LV function (EF<50%), 10 pts showed subsequent improvement in LV function considered to have substantial viability. Their initial LAD activity dramatically decreased on delayed image (from 63.0 ± 15.7 to 45.9 ± 10.2%). Nine pts without viability indicated as persistent LV dysfunction had low initial LAD activity (42.7 ± 17.8%) and lower delayed activity (33.1 ± 12.95). Pts with reversible LV dysfunction revealed greater washout of LAD activity (difference between initial and delayed activity) than those with persistent LV dysfunction (17.6 ± 8.3 vs. 9.6 ± 6.7%, P=0.02). In conclusion, post-perfusion myocardium shows disturbance in TF retention. Viability assessment by TF should be made not only from myocardial uptake but also its retention kinetics. Delay in SPECT acquisition after TF injection may underestimate myocardial viability.

OS-84

R.Moncayo, E.Kowald, N. Schauer, O. Pachinger, M. Schmutz, P. Fritsch, G. Riccabona, N. Sepp University of Innsbruck, Depts. of Nuclear Medicine, Dermatology and Cardiology

DETECTION OF MYOCARDIAL INVOLVEMENT IN SYSTEMIC LUPUS ERYTHEMATOSUS: MISMATCH BETWEEN NORMAL PERFUSION SCANS AND PATHOLOGICAL ¹⁸FDG UPTAKE

Metabolic studies of the heart using ¹⁸F-deoxy-glucose (¹⁸FDG) were done in a series of 15 SLE patients (13 females, 2 males; age 18-64 years; duration of disease 1-21 years) who presented symptoms of cardiac disease. The clinical complaints included chest pain, fatigue, dyspnea, or recurrent palpitations. Furthermore, cardiologic parameters including echocardiography, blood pressure, and chest X-ray were also altered. The SLE patients were compared with 3 female patients presenting also cardiac symptoms and having dermatomyositis, ocular mitochondrial myopathy, and the so-called anti-phospholipid syndrome. Twenty three patients with suspicion of coronary heart disease were taken as controls. Heart scintigraphy was carried out with 296 to 333 MBq of ¹⁸FDG using 511 keV collimators on a 2-head hybrid camera system (ADAC Vertex). In addition a ²⁰¹thallium perfusion SPECT was done with 111 MBq using the same camera system with appropriate collimators. Further cardiologic studies included resting ECG, echocardiography, and stress ECG with ergometry. Laboratory studies included immunological activity parameters, antibody analyses (ANA, ENA, anti-cardiolipin antibodies), as well as enzymatic tests including CPK, troponin-T, and lipid profiles. Echocardiography revealed signs of pericardial involvement in 11 cases, the ECG was abnormal in 10 patients. Diastolic blood pressure was elevated in 10 cases. Anti-cardiolipin antibodies were detected in 10/15 patients, ENA were positive in 9/15, and ANA in 14/15. Elevated CPK levels were seen only in one case. None of these changes were associated with parameters of immune activation. The ¹⁸FDG scan showed a homogeneous normal distribution pattern only in 2 patients and in one patient who did not present cardiac disease. In 2 SLE cases, with known coronary heart disease, both the ¹⁸FDG and the ²⁰¹Tl scan showed corresponding defects. In the remaining 11 patients the ¹⁸FDG scan revealed a speckled, inhomogeneous pattern of distribution, which contrasted sharply with a normal ²⁰¹Tl scan. Similar speckled distribution patterns for ¹⁸FDG were observed in the patients with ocular mitochondrial myopathy, the anti-phospholipid syndrome as well as in dermatomyositis. Our preliminary results suggest that SLE patients with cardiac symptoms can present an abnormal glucose metabolism of the myocardium as shown by a pathological ¹⁸FDG scan, whereas the ²⁰¹Tl perfusion scan was normal, so that perfusion defects can be ruled out. The lack of correlation with acute elevation of cardiac enzymes or with ECG changes suggest a chronic process.

■ General topics: Radiation protection quality control/other

General topics: Radiation protection/quality control/other OS-85

J.C. Hung, A.D. Amundson, T.L. Mays, R.J. Vetter

Nuclear Medicine, Department of Diagnostic Radiology; and Safety,
Department of Human Resources, Mayo Clinic, Rochester, Minnesota, USA

EVALUATION OF A REMOTE ASSAY DEVICE TO MEASURE Mo-99 AND Tc-99m ACTIVITY FROM A NEW Mo-99/Tc-99m GENERATOR

With introduction of the new UTK[®]-DTE Tc-99m generator (Mallinckrodt, Inc., St. Louis, MO, USA), a 145-kg auxiliary shield is used to increase whole-body radiation protection. A heavy elution shield (~2.3 kg) is also provided to reduce hand dose during the elution process. However, Mo-99 and Tc-99m measurements with the new elution shield still require manual transfer of the unshielded radioactive vial. The purpose of this study was to evaluate the performance of a modified auxiliary shield along with a redesigned CAP-MAC canister (Capintec, Inc., Ramsey, NJ, USA) which can remotely measure Mo-99 and Tc-99m activities without the need to handle unshielded eluate vials. The plug and lid on the auxiliary shield were modified to make a larger opening (6-cm diameter) to accommodate the thicker CAP-MAC device. To facilitate retrieval of the CAP-MAC canister after elution, the device was constructed with a thicker base (2.2 cm). Due to the new design of the CAP-MAC canister, the dial settings and conversion factor for Mo-99 and Tc-99m measurements must be reestablished. Two types of the CAP-MAC device (i.e., lead and tungsten canisters) were evaluated in our study. A standard Mo-99 source (22.2 MBq, 5-ml ampule) from the National Institute of Standards and Technology (NIST, Gaithersburg, MD, USA) was used to adjust dose calibrator (Capintec's CRC-5R or CRC-12R) dial settings for the Mo-99 measurement. We found that for the lead and tungsten CAP-MAC devices, dial settings of 026 (023-029) and 023 (022-025), respectively, with a conversion factor of 4.0, can be used to accurately measure Mo-99 activity. For measurement of Tc-99m activity, eluate samples (2-10 ml) with radioactivities ranging from 14.1-160.5 GBq were used to compare use of an unshielded vial to both the body-retrieved lead and tungsten CAP-MAC canisters. Our results demonstrated that a dial setting of 042 (CRC-5R) can be used for both types of the CAP-MAC device without the need to apply a conversion factor to the Tc-99m activity reading (% difference=0.69±0.62%, n=34). In conclusion, with slight modification of the auxiliary shield, the newly designed lead and tungsten CAP-MAC canisters can be used effectively to assay Mo-99 breakthrough and bulk Tc-99m activity with no personnel exposure to the unshielded eluate vial.

OS-86

T.V. Bogsrud, T.J. Herold, D.W. Mahoney, J.C. Hung

Nuclear Medicine, Department of Diagnostic Radiology; and Section of Biostatistics, Department of Health Sciences Research, Mayo Clinic Rochester, MN, USA.

COMPARISON OF THREE KIT RECONSTITUTION TECHNIQUES FOR THE REDUCTION OF EXTREMITY RADIATION DOSE

Nuclear medicine staff usually receive the highest radiation dose to their fingers, especially during the reconstitution of radiopharmaceuticals. This study was conducted to compare the extremity radiation doses incurred during the preparation of Tc-99m MDP with using three different reconstitution techniques: (1) standard procedure (i.e., withdrawing Tc-99m activity and saline into the same syringe before adding to the cold kit), (2) use of two separate syringes, adding saline before Tc-99m pertechnetate to the cold MDP kit, and (3) standard reconstitution procedure, but utilizing a robotic system (Americare Syringe Fill Station, model NuMed SFS 3a, Americare Ltd., Oxon, UK). Radiation doses were monitored by thermoluminescent dosimeters (Landauer, Inc., Glenwood, IL, USA) on the base of the 4th finger of left hand (non-dominant hand) and on the mid portion of the 2nd finger of right hand (dominant hand). Three sets of ring badges were measured for each procedure, with 10 simulated reconstitutions for each set. Mean activities in the Tc-99m eluate vials/Tc-99m MDP kits for the three different methods were 104.4±3.6/20.6±1.2 GBq, 103.8±0.7/20.9±0.9 GBq, and 99.6±6.3/20.5±0.6 GBq, respectively. Average hand doses for the 10 simulated preparations employing the three techniques are listed as follows:

Procedure	Left hand (mSv)	Right hand (mSv)
Standard	14.2±0.9	2.8±0.8
Two syringes	10.0±0.6	2.7±0.2
Robot	0.6±0.1	1.3±0.1

Compared to the standard reconstitution procedure, our results show that the 2-syringe technique slightly reduced the hand dose to personnel reconstituting Tc-99m MDP kits. However, the robotic system is the most effective method to considerably reduce the extremity dose. Additionally, the robotic system should be a useful ALARA tool to prepare other high-activity Tc-99m kits as well.

OS-87

E Prvulovich, PH Jarritt, GC Vivian, SEM Clarke, DJ Pennell, SR Underwood

British Nuclear Cardiology Society (BNCS) and British Nuclear Medicine Society (BNMS)

QUALITY ASSURANCE IN MYOCARDIAL PERFUSION TOMOGRAPHY

The BNCS and BNMS began a collaborative Nuclear Cardiology Audit Programme in 1995. The aim of this study was to assess the status of acquisition and reporting of myocardial perfusion tomography in the UK. Centres were asked to provide an "expert" panel with information about clinical history, cardiac stress and data acquisition, digital and hard copy of raw data and reconstructed tomograms as well as their report (optional) for five randomly selected studies. 52 of the 220 invited centres wanted to participate, 40 proved able to electronically transmit digital data and 18 of these ultimately submitted studies for audit. A total of 88 studies were received and digital data were reviewed on a Nuclear Diagnostic Hermes workstation at a single site. Six parameters (stress technique, radiopharmaceutical usage, image acquisition and processing, report images and text) were scored as good (2.0), adequate (1.0) or poor (0) by consensus. Centres received the quality scores for each study and a mean score for their centre, a graph showing the distribution of quality scores across participating centres against which to judge their performance, a consensus clinical report and the specific comments and recommendations of the panel. Stress technique was scored as inadequate in 10 (11%) studies, radiopharmaceutical usage and image acquisition as inadequate in 5 (6%) studies, image processing as inadequate in 9 (10%) studies and report images as inadequate in 3 (3%) studies. Report text was felt to be inadequate in 21 (23%) studies; in eleven of these (52%) the report text was judged to be incorrect and in ten (48%) it was essentially correct but misleading because of poor phraseology. The mean quality score per study was 1.3 (range 0.5 to 2.0). Seventeen of 88 (19%) studies scored less than 1.0 and were considered to be of poor quality. The mean quality score per centre was 1.3 (range 0.8 to 2.0) and 4 of 18 (22%) centres scored below 1.0. The mean quality score across participating centres was 1.5 (range 0.7 to 2.0) for stress technique, 1.5 (range 0 to 2.0) for radiopharmaceutical usage, 1.3 (range 0.5 to 2.0) for image acquisition, 1.2 (range 0.25 to 2.0) for image processing, 1.6 (range 0.5 to 2.0) for report images and 0.9 (range 0.2 to 1.8) for report text. **A large variation in standards of myocardial perfusion tomography was seen across participating centres. Data acquisition was generally satisfactory but problems were seen with report text in over 20% of studies. Quality of service may be improved by allowing centres to compare their own assessment of cases with that of an expert panel.**

OS-88

M.Laßmann, L.Schelper, H.Hänscheid, C.Körber, Chr.Reiners

Department of Nuclear Medicine, University of Würzburg, Germany

I-131 INTAKE OF PERSONS LIVING IN CLOSE CONTACT TO PATIENTS WHO HAD RADIOIODINE THERAPY

Aim of the study: After administration of radioiodine patients exhale radioactive I-131. The aim of the present study is to determine the intake of I-131 and the resulting dose to the thyroid of persons in close contact to patients after therapy.

Material and Methods: For 31 persons living in close contact with 25 patients treated with I-131 due to benign thyroid diseases we determined the radioactivity level of the thyroid. Among these 31 persons there were 8 children. The remaining thyroid activity of the patients was measured after their dismissal from the therapy ward with a calibrated sodium iodide detector. The mean activity value of I-131 in the thyroid after discharge from the ward was 158 MBq.

For measuring the relatives a collimated and calibrated Germanium detector was used. The detector is installed in the shielded chamber of a whole body counter in order to reduce the background radiation level. The measurements of the I-131 thyroid intake were carried after a mean of six days after dismissal of the patients from the therapy ward.

Results: 12 of the 31 relatives showed values equal or less than the minimal detectable activity of 13 Bq. The mean value of the remaining 19 people (among them 3 children at the age of 4,6, and 16) was 104 Bq (minimum: 39 Bq, maximum: 203 Bq). Using these data as input data for dose calculations we determined the intake for adults and children according to the biokinetic data of recent ICRP reports. The thyroid doses and effective doses were determined from the intake values using the age-dependant dose factors given by the ICRP. As a conservative estimate the intake of gaseous elemental iodine was assumed.

The mean value of the thyroid dose was 0.2 mSv (maximum: 2.0 mSv for one child, 0.4 mSv for adults). This corresponds to a maximal effective dose of 0.01 mSv.

Conclusion: The I-131 intake of persons living in close contact to patients treated with radioiodine is small. If patients are treated in a therapy ward until their activity level has dropped to 250 MBq or less no internal doses of more than 1 mSv should be expected.

OS-89

M. Cremonesi, M. Ferrari, E. Sacco, A. Rossi, L. Leonardi^o, S. Monti*, G. Paganelli^o, G. Tosi.
Medical Physics, ^oNuclear Medicine, *Surgical Senology Departments, European Institute of Oncology, Milan, Italy

RADIATION PROTECTION ISSUES IN RADIOGUIDED SURGERY OF BREAST CANCER

Aim: Recent techniques in nuclear medicine permitted to implement new methodologies useful in surgery. Among these, the techniques of localization of the sentinel lymph node (SN) and of the non-palpable breast lesions (Radioguided Occult Lesion Localization - ROLL) are of great interest. The protocols for SN and ROLL developed at the European Institute of Oncology (IEO, Milan, Italy) are based on the injection of radiopharmaceuticals labeled with ^{99m}Tc. Aim of this work is to collect and present the dosimetric data related to patients and hospital personnel and to evaluate the possible need and the specific kind of radiation protection procedures. **Materials and methods:** 50 patients with non-palpable breast lesions (ROLL) and 50 patients with suspect lymph node involment (SN) have been included in the study. All the patients underwent surgery the day after the *in loco* injection of the radiopharmaceutical (~ 11 MBq of ^{99m}Tc). As for radiation protection evaluations for patients and hospital personnel, absorbed dose (by thermoluminescent dosimeters -TLD) and air kerma rate (by ionization chamber) measurements were carried out. In the operating theatre, activity measurements were obtained (by NaI detector) on excised tissues (lymph nodes and tumour lesions) and surgical objects. **Results:** After 100 cases, the mean absorbed dose to the hands of the surgeon resulted 450±20 µGy and the mean effective dose to the surgeon was 90±25 µSv; in patients, the mean absorbed dose to abdomen was 450 µGy (range: 50-3000 µGy). **Conclusions:** The data support the validity of the planned protocols. Absorbed doses to hospital personnel -compared to recommended annual limits for the population (hands: 50 mSv; effective dose: 1 mSv - ICRP Publication 60, 1991)- are very low, as well as absorbed doses to patients-compared to other diagnostic examinations (ICRP Publication 53, 1987).

OS-90

B. Meller, M. Baehre, E. Richter
Clinic of Radiotherapy and Nuclear Medicine, Medical University of Luebeck, Germany

SYNTHESIS OF [¹⁸F]FDG FOR CLINICAL PET WITHOUT CYCLOTRON: EXPERIENCES AND RESULTS OF AN MODIFIED AND ECONOMICAL SATELLITE MODEL.

Limiting factors for clinical PET are the number of imaging devices as well as the availability of PET tracers. In conventional satellite models, [¹⁸F]FDG is distributed by PET centers. However, there is only a small selection of distribution centers in Europe, and they have limited capacity for the synthesis of PET tracers. Therefore, we investigated the possibilities for the synthesis of PET radiopharmaceuticals in our department without a cyclotron nearby. Syntheses were carried out by a module for nucleophilic substitution (nuclear interface). The integrated radio-HPLC can be used for automatic quality control of [¹⁸F]FDG or separation of other radiopharmaceuticals. Other quality control procedures were performed by gas chromatography and a second HPLC. During the last 15 months, we carried out 122 [¹⁸F]FDG-syntheses. In the beginning, we performed 10 test syntheses in order to establish the method. The results of the remaining 112 productions were as follows: In the mean (m) 9.3 GBq ¹⁸F in H₂¹⁸O arrived at our clinic from a cyclotron 80 km away. During 47.5 min (standard deviation σ=0.9 min) we achieved a yield of m=49.8 % (uncorrected, σ=4.2 %). Radiochemical purity was m=99.1 % (σ=0.5 %). All syntheses fulfilled quality criteria (chemical purity, solvent content) and microbiologic tests without problems. Only in one case the yielded activity (18 %) was too poor for all planned PET scintiscans. Additionally, we investigated the synthesis of other ¹⁸F-tracers, like [¹⁸F]Fluoromisonidazole in the meantime. Primary results are promising (yield 40 %), so that the clinical evaluation is at the planning stage.

Conclusions: Our modified satellite concept facilitated reliable synthesis of [¹⁸F]FDG at high quality. Because of the purposeful choice of equipment we have the opportunity to synthesize other ¹⁸F-radiopharmaceuticals for routine and research. This model can contribute to overcome the problems of limited availability of PET tracers in Europe.

Oncology: Breast

OS-91

D.M.Howarth, R.Sillar*, L.Lan, D.Clark*
Departments of Nuclear Medicine and Surgery(*), John Hunter Hospital Newcastle, NSW Australia.

THE ROLE OF SCINTIMAMMOGRAPHY IN THE MANAGEMENT OF PATIENTS WITH BREAST CANCER INCLUDING THOSE WHO HAVE UNDERGONE PREVIOUS BREAST SURGERY OR RADIOTHERAPY.

Using standard radiological means, the diagnosis of breast cancer can be problematic in patients who have undergone previous breast surgery or external beam radiotherapy. Tc-99m sestamibi scintimammography (BrMIBI) has the potential to discriminate between scar tissue/ reactive changes and breast carcinoma (ca). The aim of this descriptive outcome study was to compare the diagnostic accuracies of scintimammography and mammography in patients presenting de novo to those who had previous breast surgery or radiotherapy. A total of 107 female patients investigated by mammography and BrMIBI prior to surgical excision biopsy were consecutively enrolled. All but 8 patients had a palpable breast lump. The median age of the patients was 50 years (range 23-87 years). The median size of excised ductal or lobular carcinomas was 20 mm (range 0.8-80 mm). Thirty seven of the 107 patients had undergone previous breast surgery, including 7 who had bilateral silicone breast prostheses. Sixteen of these patients had also been treated with local radiotherapy to the breast. The overall (n=107) sensitivity for the detection of breast cancer with BrMIBI was 80% compared to 65% for mammography (p=0.025) and the respective specificities were 83% and 70% (p=0.47).

	Previous Surgery		No Previous Surgery	
	BrMIBI	MAMMOGRAM	BrMIBI	MAMMOGRAM
Sensitivity	65%	33% (p=0.02)	85%	74% (p=0.13)
Specificity	86%	71% (p=0.24)	75%	75%

BrMIBI imaging of patients with breast prostheses detected one true positive, one false positive, 4 true negatives and one false negative. All patients with ductal *in situ* (DCIS) (n=4), ductal ca and DCIS (n=10), lobular ca + DCIS (n=1) and Paget's disease + DCIS (n=2) had positive BrMIBI studies. DCIS was not detected by mammogram. BrMIBI sensitivities for the detection of ductal and lobular ca were 77% and 64% respectively (p=0.34). BrMIBI offers a significant diagnostic advantage in the detection of breast cancer in patients who have had previous breast surgery or local radiotherapy. BrMIBI may also play an important role in the detection of DCIS, allowing curative treatment before invasive carcinoma develops.

OS-92

W.Yu.Ussov, E.M.Slonimskaya, V.A.Dmitrichenko S.D.Kalashnikov, Ju.E.Riannel, S.A.Velichko. Tomsk Institute of Oncology and Moscow Institute of Medical Devices, Russia

QUANTIFICATION OF BREAST CANCER BLOOD FLOW IN ABSOLUTE UNITS USING RUTLAND - PATLAK ANALYSIS OF ^{99m}Tc-MIBI UPTAKE

Scintimammography with ^{99m}Tc-MIBI has been proven as highly sensitive and specific technique of diagnosis of breast cancer. Nevertheless, quantification of breast carcinoma blood flow (BCBF) in absolute units from ^{99m}Tc-MIBI accumulation is not yet developed.

To compensate this, we analysed kinetics of ^{99m}Tc-MIBI uptake in breast cancer using Rutland-Patlak approach. If BC is radioactivity in breast cancer quantified by dynamic scintigraphic study, C_b-blood concentration of ^{99m}Tc-MIBI obtained by counting of blood samples and K - transport constant, then, assuming ^{99m}Tc-MIBI uptake to breast carcinoma unidirectional for early few minutes after injection and hencefore subjected to equation d(BC)/dt = K * C_b, classic Rutland-Patlak plot can be obtained from this by integration, as BC/C_b=K * (∫ C_b dt)/C_b + V₀ and placing {(∫ C_b dt)/C_b} as X, and (A/C_b) as Y. The K can be then obtained as slope. K is breast cancer clearance constant equal to product (retention fraction) * (blood flow) : K=E * BCBF. E can be calculated from A(t) and C_b(t) as asymptote of ^{99m}Tc-MIBI impulse retention function h(t)=F⁻¹{F[A(t)]/F[C_b(t)]}, where F depicts Fourier transforms. The BCBF can be then obtained as ratio K/E.

We employed the technique in 24 patients with breast carcinoma of stages T₁₋₃N₀₋₃M₀₋₁ injecting ^{99m}Tc-MIBI (370-510 MBq) as i.v. bolus. In five scintigraphy with ^{99m}Tc-MAA (370 MBq) injected via catheter into aortic root was performed as validation study. E values were essentially uniform over the population with overall mean 0.58 sd 0.06. Blood clearance curves did not differ between various stages also and were subjected to biexponential approximation. K was in all cases obtained from the slope of initial 3 min part of Rutland-Patlak plot, strongly linear (>0.95, p<0.001) in all cases. ^{99m}Tc-MAA validation study revealed significant correlation with ^{99m}Tc-MIBI blood flow values (r=0.82, p<0.05). The BCBF(as ml/min/100cm³) was 11.8 sd 3.7 in T1, 14.9 sd 5.1 in T2, and 21.4 sd 6.2 in T3, expressing tendency to increase with stage. Higher BCBF was significantly (r = 0.57, p<0.01) associated with metastatic spread and in patients with BCBF over 23 ml/min/100cm³ distant mets were revealed in all cases.

Hence we conclude analysis of early kinetics of ^{99m}Tc-MIBI in breast carcinoma provides correct estimates of blood flow in the neoplasm and can be applied in clinical studies and for calculation of cytostatic delivery to BC.

OS-93

H. Sinzinger, R. Obwegeser, M. Rodrigues, S. Granegger, P. Berghammer, E. Kubista
University Hospital, Departments of Nuclear Medicine, Gynecology and Oncology, Vienna, Austria

HEAD-TO-HEAD COMPARISON OF ^{99m}Tc-TETROFOSMIN- AND ^{99m}Tc-SESTAMIBI SCINTIGRAPHY IN BREAST CANCER.

Physical breast examination and mammography remain the most routinely used procedures for screening women for primary breast cancer. Nevertheless, mammography shows low specificity and low positive predictive value for breast cancer. The purpose of this blinded ongoing, prospective study is to evaluate and compare the value of ^{99m}Tc-tetrofosmin- (TS) and ^{99m}Tc-sestamibi scintigraphy (SS) for detecting primary and metastatic lesions in a randomized group of patients with histologically confirmed breast cancer.

50 female patients, aged from 23 to 77 years (mean age: 54.7 years), were so far evaluated, 3 to 27 days prior to breast surgery. TS was performed within 4 to 10 days before or after SS.

Breast lesions of less than 1 cm in size could be visualized. SPECT studies were significantly improving the sensitivity for detecting primary as well as metastatic lesions by an additional 25% as compared to planar images. SPECT allows an easier axillary lymph node evaluation as well with respect to planar images. Present data indicate a higher sensitivity of TS as compared to SS for detection of primary and secondary lesions. There is preliminary evidence that breast cancer can be detected by TS or SS before a positive mammographic result. The preliminary results indicate, that these tracers are of utmost value for detecting malignant disease at a very early clinical stage and that these techniques might eventually become a screening test for both primary and metastatic disease of breast cancer patients.

OS-94

T. Home, I. Pappo*, M. Cohenpour, R. Orda*
Hospital: Assaf Harofeh Medical Center, Zerifin, Israel, Institute of Nuclear Medicine & Department of Surgery "A".

TC-99M-SESTAMIBI SCINTIMAMMOGRAPHY FOR EVALUATION OF BREAST MALIGNANCIES: THE CONTRIBUTION OF THE COUNT RATIO FOR INCREASING THE SPECIFICITY

We evaluated the efficacy of Tc-99-m sestamibi (MIBI) scintimammography for the detection of breast cancer in 351 patients. 226 scans were confirmed by histological or cytological results, while the other patients were examined because they belong to high risk groups, or had dense fibroglandular breast.

The mean age of the patients was: 49.8 yrs (range 17-84 yrs). The results demonstrated among the patients with pathological results, positive scan in 125 women: 86 scans were true positive (TP), while 39 were false positive (FP). In 101 patients scintimammography was negative: 94 were true negative, while in 7 cases the result was false negative and the patients suffered from malignant breast tumor. 6 of 7 false negative results were obtained in patients with non-palpable tumor.

Among those patients with pathological results, the sensitivity, specificity, positive and negative predictive values were: 92.3%, 70.7%, 68.8% and 93.1%, respectively. Total accuracy was 81.3%.

In order to reduce FP results, the count ratio of the lesion to the contralateral normal area in 38 TP and 29 FP examinations, was calculated from the ROI drawn on the Tc-99-m MIBI scan (L/N ratio). Significantly higher ratio was found in the TP scans: 1.583 ± 0.501 vs 1.246 ± 0.213 ($p=0.012$).

In our study only 4 out of 38 cases of TP had these values and could have been missed, while 10 out of 28 FP fitted this criteria and could have been interpreted as FP.

Our conclusion is that MIBI scan is a sensitive and accurate method of detecting breast cancer and L/N ratio increased the specificity and the positive predictive value.

OS-95

C. Corone, D. Stevens, J.P. Muratet, O. Switsers, A. Boneu, P. Carpentier, J.C. Liehn, D. Mestas, F. Bonichon, V. Edeline, C. Soler, J. Fonroget, P. Chereil, V. Becette, A. Pecking, S. Petras, J. Hermans, J. Maublant.
Rene Huguenin CLCC, Department of Nuclear Medecine. Saint Cloud, France.

SCINTIMAMMOGRAPHY (SMM) WITH Tc ^{99m} MIBI FOR BREAST CANCER RECURRENCE: RESULTS OF A PROSPECTIVE FRENCH MULTICENTER TRIAL.

Tc ^{99m} MIBI SMM has emerged as a new imaging technique for primary breast carcinomas. The aim of this study was to assess the performances of SMM to detect breast recurrent tumors and to compare it to MRI or CT enhancement imaging. Twelve centers included 61 patients with clinical and/or radiological suspicious of recurrence. 51 patients are evaluable. To date, the raw data of 44 SMM have been blindly reviewed by 3 independent readers. The median delay between initial treatment and suspicious recurrence was 4 years (1 - 25). 23 lesions were palpable. All patients had 10 min bilateral prone and anterior images after IV injection of 740 - 1100 MBq Tc ^{99m} MIBI. Enhancement radiological imaging of the suspicious breast was done with MRI for 30 patients and with CT for 13. Final diagnosis confirmed by histology demonstrated 29 recurrences and 15 benign lesions.

Results per patients show :

	TP	TN	FP	FN	D	Sens°	Spe°
MRI + CT* (43)	18	11	3	4	7	81.8 %	78.6 %
SMM* (44)	13	12	0	12	7	52 %	-
SMM** (44)	15	12	3	14	-	51.7 %	80 %

* institutional reading ** blinded reviewing

° calculated without D = doubtful results

The major finding of this study is that the sensitivity of SMM seems to be much lower for the detection of recurrent than for primary tumors (which is generally around 80 - 90 %, as in the preliminary results of our multicenter trial unpublished data). This lack of sensitivity is not only related to the size since the FN lesions ranged from 2 to 30 mm. A weak uptake might be due to scar modifications by previous treatments. Another hypothesis might be that these FN recurrent tumors have chemoresistant characteristics with expression of the MDR1 - Pgp which extrudes MIBI as cytotoxic agents. If this could be demonstrated, Tc ^{99m} SMM might become an interesting tool to predict chemoresistance in breast loco regional cancer recurrences and to monitor therapy.

OS-96

(1)S.Koukouraki,(2)I. Askoxilakis,(3)E. Vagios,(4)I. Manousakas,(2)D. Tsiftsis,(1)N. Karkavitsas
(1,2)Department of Nuclear Medicine and Surgery Oncology-University Hospital of Heraklion-Crete,Greece.(3)Diagnostic Center "Pagritia Ygia",(4)Diagnostic "Medical Center of Crete"

THE ROLE OF ^{99m}Tc-SESTAMIBI AND COLOR DOPPLER IMAGING IN THE EVALUATION OF BREAST CANCER AS A COMPLEMENT TO CONVENTIONAL MAMMOGRAPHY

Purpose: The aim of this study is the comparison and evaluation of MIBI scintimammography and color Doppler ultrasonography concerning sensitivity and specificity in the diagnosis of breast cancer.

Patients and Methods: This prospective study is still in progress. We have studied 31 patients with palpable and non palpable breast lesions. Mammography, scintimammography, color doppler and postsurgery biopsy were evaluated. Each patient received 25-30 mCi(925-1100MBq)^{99m}Tc-sestamibi intravenously. Ten minutes and two hours after the injection, multiple planar views and SPECT images were obtained using a single head γ -camera GE Millenim equipped with a LEGP collimator. A special designed bed was used in a part of these cases allowing the patient to be in a prone position with the breast in a dependent position. Color Doppler was performed with an Accuson128XP/10C using linear transducer of 5MHz.

Results: The calculated sensitivity, specificity, accuracy, positive predictive value and negative predictive values of scintimammography was 91,3%,100%, 93,9%, 100% and 83,3% respectively. Doppler revealed sensitivity91,3%, specificity,accuracy, positive and negative predictive values 91%, 90%, 91%, 95,5%and81,8% respectively.

Conclusion: On the basis of these results, the use of scintimammography in conjunction with Doppler ultrasonography provides high accuracy so that it may reduce significantly the number of biopsies in patients with breast lumps.

Keywords: ^{99m}Tc MIBI scintimammography, Color Doppler ultrasound, Breast lumps.

Oncology: Therapy

OS-97

K. Liepe¹, J. Kropp¹, F. Jr. Knapp², R. Hliscs¹, A. Kühne¹, WG Franke¹
¹University Hospital Dresden, Departments of Nuclear Medicine, Germany
²Nuclear Medicine Group, Oak Ridge National Laboratory, Tennessee

RHENIUM-188 IN COMPARISON TO RHENIUM-186 AND STRONTIUM-89 IN THE TREATMENT OF BONE METASTASES
 In recent years radionuclide therapy played an increasing role in treatment of bone pain due to metastases. Rhenium-188 (Re-188), as a generator product, is very cost effective. In 33 patients (pts) we investigated the influence of Re-188 (4 pts) Re-186 (17 pts) or Strontium-89 (Sr-89) (12 pts) on pain relief, reduction of analgesic consumption, and impairment of bone marrow function. We used a dose from 1600 to 3244 MBq for Re-188, from 1050 to 1538 MBq for Re-186 and from 100 to 167 MBq for Sr-89. Bone metastases originated from prostate-, breast-, lung-, bladder-carcinoma and B-cell-lymphoma. We calculated the blood clearance, excretion rate in the urine and accumulation in the bone. 5 pts. received a second treatment with the same radionuclide. Blood samples were drawn weekly for 6 weeks or 12 weeks (pts with Re-188) and counted. **Results:** All pts with Re-188 showed an improvement of life quality (raise of Karnovsky-index of 14% [10-19%]) and reduced their analgesic intake, as well as pts with Re-186 or Sr-89. From pts with Re-186 or Sr-89 66% had a significant, 17% a minor improvement of life quality (avg. raise of Karnovsky-index of 7% [4-12%]). The analgesic intake was reduced in 69% of the pts. No difference was observed between Sr-89 and Re-186-therapy. Platelets decreased to $134 \pm 68 /\text{mm}^3$ (max. to $72/\text{mm}^3$) and leucocytes to $4,1 \pm 2,0 /\text{mm}^3$ (max. to $2,4/\text{mm}^3$). The nadir occurred between the fourth and the sixth week. The bone accumulation of Re-188 4 hour p.i. was 42% in the whole body and with 24% in the metastases [avg.]. The bone accumulation of Re-186 4 hours p.i. was lower with 36% in the whole body and with 17% in the metastases [avg.]. In one pt the Re-188 was administrated in two doses in a period of two days. The Re-188-scan showed in both times the same good accumulation of the radionuclide. **Conclusion:** The results of therapy with Re-188 were encouraging. All pts with Re-188 experienced an improvement of life quality without induction of serious bone marrow reduction. The bone accumulation of Re-188 4 hours p.i. is higher than in Re-186. Re-188 product as a generator is a convenient tool for clinical use.

OS-98

S.C. Srivastava, G.E. Meinken, L.F. Mausner, and H.L. Atkins.

Brookhaven National Laboratory, Upton, NY.

TIN-117m STANNIC CITRATE: A NEW RADIOTHERAPEUTIC AGENT.

Purpose: In preliminary clinical trials (n=47), 370-740MBq/70 kg tin-117m stannic DTPA (molar ratio DTPA/tin=20; sp. act. of Sn-117m=100-350MBq/mg) has been found to be effective for palliation of metastatic bone pain with much less myelosuppression compared to other existing agents. To allow administration of higher doses of Sn-117m for other therapies including primary osteosarcoma and bone metastases from this and other primaries, which will require use of a chelating agent less toxic than DTPA, we have developed and tested tin-117m stannic citrate. **Methods and Results:** We evaluated a number of chelating agents including polyhydroxycarboxylic acids and found that citrate (mole ratio 5-20 over tin) is effective in quantitatively chelating stannic tin under appropriate reaction conditions. Tin-117m stannic citrate is stable at room temperature for at least 30 d, and gives a biodistribution in mice which is unaltered after storage. It clears rapidly from blood and other organs and, like the DTPA chelate, is taken up almost exclusively into bone. In mice, the 24 h bone uptake (% ID per g) of tin-117m stannic citrate, tin-117m stannic DTPA, and Tc-99m MDP, respectively, was 19.8 ± 1.7 , 18.4 ± 0.5 , and 11.0 ± 1.7 . The bone to tissue ratios, respectively, were as follows: blood, 1595, 1352, 157; liver, 92, 84, 18; spleen: 230, 242, 7; kidney, 33, 28, 21; and muscle, 347, 109, 367. **Conclusions:** We conclude that: (1) tin-117m stannic citrate is simple to prepare and its chemical and in-vivo properties are essentially similar to those of tin-117m stannic DTPA; (2) Due to less in-vivo toxicity, citrate will allow (i) the administration of higher, more effective, doses of tin-117m for various therapies; and (ii) the use of tin-117m of a wide range of specific activities, including low specific activity tin-117m from the more commonly available low-flux reactors.

This work was supported by the U.S. Dept. of Energy, under Contract No. DE-AC02-98CH10886, and in part by Diatide, Inc.

OS-99

P.G. Gopinathan Nair, A.K.Padhy, J.Fettich, J.Stare, N.Nair, R.Morales, M.Tanumihardja, G.Riccabona

IAEA co-ordinated study, IAEA, P.O.Box 100, A-1400 Vienna, Austria

EFFICACY AND TOXICITY OF BONE PAIN PALIATION USING 89-SR AND 32-P

Paliative treatment of bone pain due to bony metastases using 89-Sr become widely accepted. 32-P can be used for the same purpose. As it is several times less expensive as Sr it is more accessible, especially in poorer, developing countries. The goal of the study was to compare efficacy and toxicity of both radiopharmaceuticals in the framework of an IAEA co-ordinated multicentric randomised study. A very strict protocol for unified patient inclusion and follow up was used. 92 patients with osteoblastic bony metastases due to different forms of cancer were included into the study, 46 were treated by 89-Sr (150 MBq) and 46 by 32-P (450 MBq). Pain score, analgesic consumption, quality of life, and indices of bone marrow depression were monitored 2 weeks pre- and up to 4 months post treatment. Favourable response to treatment was recorded in 75 % of patients treated with 89-Sr and in 72 % of those treated with 32-P. "Survival analysis" was used to assess the duration of pain paliation, which was the same in both groups. There was moderate but insignificant drop in haemoglobin levels in both groups, and in the levels of platelets and granulocytes in 89-Sr treated group, as compared with pretreatment data. Granulocytes and platelets decreased significantly in 32-P treated patients, but no toxic effects requiring specific treatment were seen in either group. No statistically significant differences between the two groups were found in efficacy indices. Statistically significant haematologic toxicity was detected in 32-P treated patients, which was not important enough to require any treatment. According to our results it may be concluded that 32-P is slightly but not significantly more toxic and as effective as 89-Sr for paliation of bone pain due to bony metastases.

OS-100

S.K.Shukla^{1,2}, C.Cipriani¹, G.Atzei¹, S.Boemi¹, G.S.Limouris³, C.Desiderio², M.Cristalli², L.Ossicini²
 1. Servizio di Medicina Nucleare, Ospedale S.Eugenio, Roma, Italy; 2. Istituto di Cromatografia, C.N.R., Area della Ricerca di Roma, Roma, Italy; 3. Nuclear Medicine Section, Areteion University Hospital, Athens, Greece

STRONTIUM-89 RADIOPHARMACEUTICALS FOR THE TREATMENT OF ADVANCED PROSTATE CANCER PATIENTS. I. IMPROVING THE THERAPEUTIC ACTION OF Sr-89 CHLORIDE (METASTRON)

The object of our research has been to improve the therapeutic action of Sr-89 chloride and find more effective Sr-89 radiopharmaceuticals for the cure of advanced prostate cancer patients. The nature and stability of Sr-89 species in metastron solution were studied in different usual drinks (distilled water, tap water, black tea, black coffee, red wine, white wine, lemon juice, clementin juice, mandarin juice, orange juice, coca cola, pepsi cola) chromatographically and electrophoretically. Only lemon, clementin, mandarin and orange juices stabilized the cationic Sr-89 species in metastron. In water, tea, coffee it is intensely hydrolysed while in wine, coca cola and pepsi cola the radionuclide forms insoluble species concentrating in liver and spleen. During the past three years 104 advanced prostate cancer patients with intense bone metastasis pain were treated with 4mCi metastron. Only 3 patients strictly followed our recommendations to avoid wine, smoking and pure water, coffee, tea and colas at least one week before and during whole period of observation after the i.v. injection of metastron. In these patients pain paliation was observed within 3 days p.i., and they are free of pain and well for 7 months. In other patients the pain relief started after 3 to 4 weeks Sr-89 p.i. and lasted for nearly 3 months. The pain free patients were only 20% while nearly 50% experienced some pain relief. The effect of Sr-89 stabilizing drinks on the therapeutic action of metastron is being continued in other prostate cancer patients. Strontium-89 radiopharmaceuticals more stable than Sr-89 chloride are being also studied by their total-body distribution by Bremsstrahlung scintigraphy and therapeutic results.

OS-101

D. Kendler, E. Donnemiller, G. Riccabona, M. Oberladstätter

Hospital: Dept. of Nuclear Medicine, University of Innsbruck, Austria

POSSIBLE IMPROVEMENTS IN DOSIMETRY FOR ¹⁵³Sm EDTMP THERAPY

¹⁵³Sm EDTMP is used for pain therapy in patients with disseminated bone metastases since years and was applied recently also for treatment of rheumatoid arthritis. Standardized amounts of activity applied (e. g. 37 MBq/ kg BW), however, are unlikely to give optimal results as ¹⁵³Sm EDTMP concentration in lesions and tumor volume can vary widely. We tried therefore to improve dosimetry of ¹⁵³Sm EDTMP considering the parameters mentioned above. Twenty four hours whole body retention (WBR) and effective half-life data, whole body scans with ^{99m}Tc DPD including SPECT scans were analyzed in 7 patients from overall 22 cases who had ¹⁵³Sm EDTMP-therapy. The validity of tumor volume assessment by SPECT was tested with a Jaszczak phantom. Relative uptake of ^{99m}Tc DPD and ¹⁵³Sm EDTMP in normal bone and metastases was calculated by evaluation of conjugated whole body images with ROI's over whole body, skeleton contour and metastases sparing bladder and soft tissue. The values of ^{99m}Tc DPD regional uptake in metastases and of tumor volumes were used to estimate radiation dose to tumor using self-dose S-values supplied by RIDIC/ Oak Ridge, USA after application of standard amounts of activity (1 pat. 37 MBq/ kg BW, 6 pats. 55 MBq/ kg).

Results: WBR of ¹⁵³Sm EDTMP ($x = 69,2\%$) and ^{99m}Tc DPD were similar ($x = 71,01\%$), tumor volume varied from 226 - 652 ml ($x = 339$ ml), count ratio tumor/ normal bone also (1,72 - 2,41), uptake in tumor was 17 - 57 %. Derived radiation doses to tumors were 4 - 13,7 Gy. While the overall response rate was 65 %, it was only 43 % in the 7 analyzed cases. Therefore trials with higher doses applying the described dosimetric approach seem to be justified if increased myelotoxicity can be controlled.

OS-102

C. Pizzocaro, G. Maira, R. Pagliani, MB. Panarotto, R. Giubbini.

Spedali Civili, Brescia, ITALY- Nuclear Medicine Department -

EFFECTS OF A SECOND SR-89 TREATMENT IN PATIENTS WITH METASTATIC PROSTATIC CANCER AND DISEASE PROGRESSION.

Several studies have documented that Sr-89 systemic radiotherapy is an effective tool for the treatment of pain in patients (pts) with metastatic prostatic carcinoma. Less data are at present time available concerning the use of a 2nd administration of Sr-89 in pts with recurrence of pain after a 1st treatment. We have treated 72 pts with a first dose of 145 MBq of Sr-89. All pts were under continuous analgesic medication and had evidence of multiple metastatic lesions (n.50) or superscan pattern (n.22) at Tc^{99m}-MDP bone scintigraphy. The response to the treatment were graded according to a standard four grade scale: 1) excellent: complete pain relief or marked reduction of intensity and frequency of symptoms and of analgesic regimen, 2) good: incomplete pain relief with significant reduction of analgesic medication 3) mild: fair effects on pain control with no change of analgesic treatment, 4) no effects were observed. Pt follow up was monitored by physical examination at three months and by physical examination or telephone interview every next three months. Excellent response was observed in 41% of treated pts, good in 28%, fair in 14% and no response in 17%, respectively. The treatment was effective over a period of 2 to 18 months (median value=4 months). Twenty one pts (16 with excellent and 5 with good response after the 1st treatment) had recurrence of pain and general conditions and sufficient life expectancy to be considered candidate for a 2nd treatment with same activity. In this sub-group the average of Karnofsky index was 59±9 before the 1st and 53±3 before the 2nd treatment (p<.01). The average bone scan index was 53±21 before the 1st and 67±15 before the 2nd treatment (p<.001). After the 2nd treatment excellent response was observed in 2 pts (11%), good in 3 (16.6%), fair in 3 (16.6%), no response in 10 pts (55.5%), respectively. 3 pts were lost at follow up because of death within 30 days from the treatment. The 2nd treatment was effective over a period of 3 to 8 months (median value=3.5 months). Side effects were negligible after both 1st and 2nd therapy. **In conclusion** our results are in agreement with previously reported studies and demonstrate that Sr-89 is an effective tool for palliative pain relief in nearly 70% of pts with symptomatic prostatic cancer after the 1st treatment; despite the disease progression Sr-89 systemic radiotherapy is still effective in 28% of pts after a 2nd treatment. Taking into account the optimal pt. tolerability and the minimal incidence of side effects, a 2nd treatment is justifiable in pts with severe symptoms.

Paediatrics**OS-103**

L. Burrioni, A. Orsi*, Y. Hayek*, D. Volterrani, P. Bertelli, A. Vella, M. Zappella* and A. Vattimo. Depts. of Nuclear Medicine and Infantile Neuropsychiatry*, University of Siena, Policlinico "Le Scotte", Viale Bracci, 53100 Siena, Italy.

QUANTITATIVE EVALUATION OF BRAIN PERFUSION WITH ECD-Tc^{99m} SPET IN AUTISTIC DISORDER OF CHILDHOOD

Childhood autism is an early and severe developmental disorder of unknown origin characterized by deficits in verbal and non-verbal language and social and cognitive functioning. In addition, the children present an abnormal repertoire of behaviours. Morphological investigations (CT and MRI) have revealed several brain abnormalities without demonstrating any concordance in dysfunctions. The aim of this study was to establish a link between rCBF assessed with Tc^{99m}-ECD SPET and the clinical manifestation of the disease. We performed the study on 15 right-handed children (6 F and 9 M; mean age 9.5 yrs) displaying autistic behaviour and we compared their data with that of an age-matched reference group of 8 normal children. All the patients had been diagnosed as having child autism according to DMS-IV criteria and presented normal brain MRI. A quantitative analysis of rCBF was performed calculating a perfusion index (PI=cortex/cerebellum) and an asymmetry index (AI=[r-l]/{(r+l)/2}x100) in each lobe. A statistically significant (p=.003) global reduction of CBF was found in the group of autistic children (PI=1.07±.07) when compared with the reference group (PI=1.25±.12). Moreover, a significant difference was also observed between the right-to-left asymmetry of emispheric perfusion of the control group and autistic patients (p=.0085) with a right prevalence greater in autistic (2.90±1.68) than in normal children (1.12±0.49). The area with greatest CBF asymmetry was the temporo-parietal region, in concordance with previous studies. Our data show a significant decrease of global cerebral perfusion in autistic children in comparison with normal ones. In addition our results confirm the existence of left-hemispheric dysfunction in childhood autism, especially in the temporo-parietal areas devoted to language. Tc^{99m}-ECD SPET seems to be sensitive in revealing diffuse brain blood flow reductions and left to right asymmetries, even when neuroanatomical patterns are normal. Moreover, brain blood flow abnormalities are related to the clinical manifestation of the disease.

OS-104

L.Ö. Kapucu, A. Serdaroglu, G. Köse, N. Gökçora, S. Atavcı, K. Gücüyener.

Gazi University, Faculty of Medicine, Depart. of Nuclear Medicine and Pediatric Neurology, Ankara-Turkey

BRAIN SPECT EVALUATION OF CHILDREN WITH ABSENCE EPILEPSY

The aim of this study was to evaluate cerebral blood flow alterations using baseline and activation ^{99m}Tc-HMPAO brain SPECT method in children with absence epilepsy.

Twenty-three right-handed children (13 f, 10 m; mean age: 10 ± 2.4 yr) with suspected absence epilepsy underwent serial neurologic examinations, interictal and ictal EEGs and SPECT imaging. All patients were free of medication before SPECT studies. Baseline SPECT study was performed during the interictal period with the dose of 297-370 MBq ^{99m}Tc-HMPAO. On a separate day, activation study was performed while the patients were having seizures provoked by hyperventilation. Immediately after clinical observation of seizures that occurred simultaneously with generalized spike and wave discharges on EEG, 297-370 MBq ^{99m}Tc-HMPAO was injected through an i.v. catheter. Transaxial, sagittal and coronal slices were obtained were obtained for both studies. The mean counts per pixel were calculated on 11 regions of interest (ROIs) on three representative transaxial slices. Count density was calculated for each region. Region/occipital ratios were obtained. For each region normalized ratios were used to obtain side to side % asymmetry index between baseline and activation studies.

Visual interpretation of the baseline study showed that 10 of the 23 patients had a detectable abnormality in rCBF during the interictal period. These abnormalities consisted of relative hypoperfusion in the frontal lobes that could involve neighbouring parietal and temporal regions. The activation study revealed that 13 of 23 patients had relative hyperperfusion in these brain regions that were relatively hypoperfused in the baseline study. However, quantitative evaluation of these visually detected abnormalities was not statistically significant.

This relatively consistent pattern of frontal rCBF alterations in visual interpretation suggests that frontal lobe functions were implicated in the evolution of generalized seizures in patients with absence epilepsy.

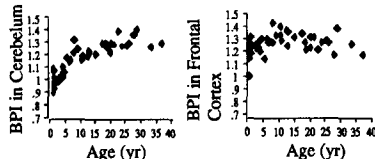
OS-105

H. Sumiya, I. Kuji, Y. Niida, T. Michigishi, N. Tonami.

Departments of Nuclear Medicine and Pediatrics, Kanazawa University, Kanazawa, Japan

AGE-RELATED BRAIN DISTRIBUTION OF TECHNETIUM-99m-ETHYL CYSTEINATE DIMER

The purpose of this study was to clarify the change of Tc-99m-ethyl cysteinate dimer (ECD) distribution, especially in children and infants compared to adults. Forty-two patients (age range, 3 months to 36 years; average age, 11.7± 10.1 years) suspected epilepsy were studied. Because normal children and infants are hard to be allowed to perform radionuclide studies, subjects in this study were all patients without brain operation. Tc-99m-ECD (200-740MBq) was injected interictally before sedation to avoid the effect of sedatives. SPECT data were acquired using a triple-head gamma camera and reconstructed with a triple-energy window scatter correction. Mean whole-brain counts were obtained from whole-brain counts of ten sequential axial SPECT images above the lower base of basal ganglia. Regions of interest (ROIs) were bilaterally set on five cortices, basal ganglia, thalamus and cerebellar cortex. A brain perfusion index (BPI) was obtained as a ratio of the mean counts of each ROI compared to the mean whole-brain counts. An evidence of positive correlation between age and BPI in cerebellum, markedly increasing under ten years, was demonstrated, although BPIs in cerebral cortices were almost constant in all ages. BPI in thalamus and basal ganglia also increased age-dependently beyond ten years. Because cerebellar and cerebral perfusions were reported to show similar changes, the age-related change of BPI with ECD in cerebellum may show normal maturation process of esterase density in cerebellum. In conclusion, we confirmed the age-related change of ECD uptake in cerebellum, thalamus and basal ganglia compared to the uptake in cerebral cortices. The ECD uptake in children is different from that of blood flow by PET, especially in cerebellum.



OS-106

T. Martins, A. Daniel, G. Cantinho, A. Levy Gomes, F. Godinho

Instituto Medicina Nuclear, Faculdade Medicina Lisboa
Unidade Neurologia, S.Pediatria, H.Sta Maria, Lisboa, Portugal

EXPERIENCE WITH INTERICTAL 99mTc-HMPAO BRAIN SPECT IN THE MANAGEMENT OF CHILDREN WITH MEDICALLY REFRACTORY EPILEPSY

The aim of this prospective study was to evaluate the importance of 99mTc-HMPAO brain SPECT (SPECT) as a functional noninvasive method, in the management of children (ch) with medically refractory epilepsy, MRE (≥3 episodes of seizures /month for >18 months, in spite of adequate treatment), for whom surgery is becoming the method of choice. We studied 30 ch (16 males, 14 females), aged between 18m and 20y (11±4.6 y), mostly suffering from partial motor or complex seizures, with age of onset before 5y. All ch were submitted to interictal EEG, ictal VIDEOEEG monitoring (VIDEOEEG), radiological imaging (CT, NMR) and interictal SPECT. SPECT was performed 15-30 min after e.v administration of body area adjusted activity (370-550 MBq) of 99mTc-HMPAO, in a 90° fixed angle two headed gammacamera (GE-Optima), with LEHR collimators (circular orbit, 360°, 128 views, 20 s/view, 128x128 matrix) and analysed visually by two independent observers. Seizures were classified according to VIDEOEEG in partial - frontal (F) 15, temporal (T) 8, fronto-temporal (FT) 3, occipital (O) 1 - continuous spikewave during sleep (CSWS) 1 and undetermined (U) 1. SPECT was concordant with this classification in 18 ch (8/15 F, 7/8 T, 1/3 F-T, 1/1 O e 1/1 CSWS), discordant in 5 (F), normal in 3 (2 F) and inconclusive in 4. CT/RMN was concordant in 11 ch (3/15 F, 6/8 T, 1/1 O e 1/1 POCS), discordant in 2 (1 T e 1 F), normal in 13 (10 F) and inconclusive in 4. VIDEOEEG, CT/RMN and SPECT agreed in 10 ch (3 F, 5 T, 1 O, 1 POCS). SPECT was the method which agreed more often with VIDEOEEG (60%), although the hypoperfused area frequently surpassed the EEG focus or radiological lesion. While both SPECT and NMR had better results in T seizures, accurate focus identification remained difficult in F epilepsy; nevertheless, SPECT was correct in ≥ half of these ch. Based on these results 7 ch were operated (4 T, 3 F, 1 O), with cure in 5 (3 T, 1 F, 1 O), reduction of seizures in 1 (T) and relapse in 2 (F, with partial removal of focus). A match between morphological lesion and impaired perfusion was strictly required for surgery. We consider interictal SPECT an easy to perform and important diagnostic tool in the management of these children.

OS-107

I.Roca, M.Simó, M.Soler, S.Aguadé, F.Porta, X.Bruna, G.Enríquez, E. Vilaplana, F.Castelló.
Servei de Medicina Nuclear
Servei de Lactants, Servei de Radiologia Infantil
Hospitals Vall d'Hebron. Barcelona

Follow-up of Acute Pyelonephritis (APN) in children under 2 year.

This study presents the incidence of parenchymal sequelae in a group of 52 children under the age of 2 year, who suffered a first episode of APN. All children were admitted during the acute phase of APN, and evaluated clinically and by means of ultrasonography (US), DMSA scintigraphy and voiding cystourethrography (VCUG). Follow-up included clinical evaluation, US and DMSA scan. The diagnosis of APN was based on clinical findings, US and DMSA images. US assessed renal size, dilation of the excretory system and parenchymal echogenicity. In DMSA scan, we analyze absolute tubular uptake, differential function, and parenchymal uptake (presence or absence of rounded, hypoactive areas, single or multiple, unilateral or bilateral). DMSA scintigraphy performed during the acute phase (2-7 days after onset of symptoms) showed rounded, focal hypoactive areas in 25/58 kidneys and multifocal parenchymal hypoactivities in 33/58, with associated kidney enlargement or not. Follow-up DMSA scintigraphies were performed 3 to 5 months later, and repeated when abnormal. Abnormal US findings were present in 8/58: 6 dilated excretory systems, 2 kidneys with increased size and hyperechogenicity. Among 58 abnormal kidneys (6 bilateral APN), 24 (41 %) presented vesicoureteral reflux (VUR)(14 grade II, 10 grade III or higher). In babies under 3 months, the incidence of VUR was lower (8/29, 27 %).

Follow-up	DMSA		VUR		
	unifocal	multifocal	no VUR	II	> = III
Normalization	16	15	19	9	3
Improvement	1	5	5	-	1
Sequelae	4	8	6	1	5

In DMSA scans performed X = 8 months after the acute phase, parenchymal scars improved or resolved in 75 %. Cortical scars were more severe in cases of VUR grade III or higher, but significant differences were not found in lesion severity between patients with VUR grade II and those without reflux.

OS-108

G.Cantinho, S.Kaku, MA Nunes, MJ Sousa, S Ramos, M Ferreira, M Magalhães, F Pinto, R Ferreira

Atomedical Lab. Medicina Nuclear Lisboa
Serviço Cardiologia Pediátrica- H. Santa Marta - Lisboa, Portugal

PERFUSION MYOCARDIAL SPECT AFTER ARTERIAL SWITCH PROCEDURE

Myocardial ischemia or sudden death in children after arterial switch operation for transposition (TGA) of the great arteries has been reported. The cause however remains unknown. To evaluate the continuous patence of coronary arteries we conducted a prospective study on 20 children with TGA a mean of 43.7 months after switch operation. 15 children had intact ventricular septum and 5 had ventricular septal defect. Perfusion Myocardial SPECT with 2 mCi (74 Mbq) of Thallium after Dipyridamol stress and at rest redistribution has been performed in a two head gamma camera in 180° orbit, 64x64 matrix, 40 sec/view, 64 views. SPECT studies were analysed visually and in cases of doubt, relative quantification was performed. All the children had performed also dobutamine stress echocardiography and cardiac catheterism. Left ventricular and aortic root angiograms were performed in all cases. In five children selective coronariography were obtained. SPECT perfusion defects were identified in three patients. One of them had a mammary artery to anterior descending artery bypass during switch and suffered from supravalar end-diastole pressure. Echo studies were normal in all cases. Cardiac catheterism and angiogram reveled a normal LV function in all cases. In four patients supravalar pulmonary stenosis and in one patient moderate aortic insufficiency was found. Coronary arteries were patent with no stenosis in all cases. In our study we concluded that myocardial perfusion was preserved at four years post SWITCH in almost all cases. Small discrepancies between the three methods, remain unexplained in 2 patients obligated a careful follow-up to find an explanation. For children, myocard SPECT perfusion was the least invasive method and the best tolerated.

Neurology/Psychiatry: Cerevascular

OS-109

D.S. Lee, K.M. Kim, Y. So, B.W. Yoon, J.-K. Chung, M.C. Lee.

Seoul National University and Hanyang University, Seoul, Korea

PRESERVED CEREBRAL PERFUSION RESERVE EXAMINED BY QUANTITATIVE REST/ACETAZOLAMIDE Tc-99m-HMPAO SPECT IN TAKAYASU'S ARTERITIS WITH NEAR-TOTAL ARTERIAL OCCLUSION.

Though patients with Takayasu's arteritis suffered near-total occlusion of carotid or vertebral arteries, few patients experienced neurologic deficits. We investigated whether quantitative evaluation using rest/acetazolamide Tc-99m-HMPAO SPECT and Lassen's correction could reveal preserved perfusion reserve despite near-total occlusion of arteries in these patients.

Six patients with Takayasu's arteritis (all women, 34±1.9 year old, 5 type I, 1 type III) who had near-total occlusion of arteries were studied. Sequential acquisition (555 and 1110 MBq HMPAO, 1 g acetazolamide) and subtraction technique (triple head, fan-beam) was used for rest/acetazolamide SPECT. Cerebral perfusion at basal state and acetazolamide stress was calculated by Lassen's algorithm using two fixed values of basal cerebellar perfusion (=55 ml/100g/min) and K2/k3 ratio (=1.5).

Three patients experienced transient ischemic attack and had near-total occlusion of carotid and vertebral arteries. MR was normal and rest/stress SPECT was also normal. Basal perfusion and stress perfusion were 39±/-5.2 and 52±/-8.7 ml/100g/min. One of 3 having evidence of infarction on MR and severe stenosis had normal perfusion and reserve. Another patient showed mildly decreased reserve visually; however, he had preserved reserve of 38.5% on quantitation. The other patient who had large infarction in left middle cerebral artery territory lost perfusion reserve beyond the area of infarction. This patient showed decreased stress perfusion than the rest on the whole cerebrum.

We found that cerebral perfusion and perfusion reserve were preserved well in patients with Takayasu's arteritis though they had severely stenosed or occluded carotid and vertebral arteries probably because stenosis progressed very slowly only on the proximal arteries. Quantitative evaluation of rest perfusion and reserve using quantitative rest/acetazolamide SPECT differentiated preserved reserve or rarely decreased reserve though they were similar on visual assessment in Takayasu's arteritis.

OS-110

D.S. Lee, S.K. KIM, K.M. Kim, B. W. Yoon, J.-K. Chung, M.C. Lee.

Seoul National University, Seoul, Korea.

SIGNIFICANCE OF CROSSED CEREBELLAR DIASCHISIS DEVELOPED AT STRESS EXAMINED BY QUANTITATIVE REST/ACETAZOLAMIDE SPECT

As cerebellar perfusion is influenced by the status of contralateral hemispheric perfusion and reserve, we observed, not infrequently, development or aggravation of crossed cerebellar diaschisis (CCD) after acetazolamide challenge (at stress). We investigated if this acetazolamide-induced CCD was a sign of the development of cerebral steal and so the evidence of poorer reserve of hemispheric perfusion at stress.

We studied in-situ sequential-subtraction basal/acetazolamide SPECT in 60 patients having cerebrovascular disease (cerebral infarction: 32, moyamoya disease: 14, transient ischemic attack: 4, dizziness/vertigo: 4, aneurysm: 2 and others: 3, M:F=34:26, age 2-69). We graded perfusion decrease visually using 4 point scores both at rest and at stress (normal: 0 to defect: 3). We found CCD in 20 patients at rest. We used Lassen's method to quantify hemispheric and cerebellar perfusion (ml/min/g) both at rest and at stress. Normal hemispheric perfusion increased by 44% on average after acetazolamide using this method. Visual examination and quantitative method was well correlated, as difference (Δ ASI) of cerebellar asymmetric index ($ASI=200 \times (\text{contralateral perfusion} - \text{ipsilateral perfusion}) / (\text{contralateral perfusion} + \text{ipsilateral perfusion})$) between stress and rest was correlated with Δ difference of visual scores of cerebellar difference between stress and rest ($r=0.73$).

Visually, cerebellar perfusion contralateral to lesional hemisphere did either improve ($n=12$), or aggravate ($n=10$) at stress. Three of the latter 10 patients developed CCD only at stress. The other 38 did not change. Upon quantitation, acetazolamide-induced increase of perfusion (Δ perfusion) of cerebellum was well correlated with Δ perfusion of contralateral hemisphere ($r=0.96$). Cerebellar Δ ASI between rest and stress was related with Δ perfusion of contralateral hemisphere ($r=0.35$) and not with rest perfusion ($r=0.19$). Area of lower perfusion visually at stress was not found to be actually lower than at rest on quantitation, which did not suggest cerebral steal in these patients.

We concluded that increase of cerebellar perfusion at stress reflected honestly the increase of perfusion of contralateral hemisphere. Though acetazolamide-induced CCD was not the evidence of cerebral steal, newly-developed or aggravated cerebellar diaschisis at stress implied that the contralateral hemisphere suffered severe loss of perfusion reserve.

OS-111

Y.Xiu, XG Sun, SL Chen

Hospital: Zhongshan Hospital, Department of Nuclear Medicine.

DETECTING SLE BRAIN INVOLVEMENT USING SPECT CEREBRAL BLOOD FLOW PERFUSION IMAGING

Purpose: Involvement of the central nervous system (CNS) is one of the most important complications of systemic lupus erythematosus (SLE), it may lead to death and deformity. SPECT cerebral blood flow perfusion imaging was performed for these patients to evaluate CNS conditions in SLE patients. **METHODS:** Sixteen patients who fulfilled the criteria for SLE were enrolled in this study, all are female, age rang 37.73±14.49, disease course was between on month and 20 years. Four of 16 have some headache, sickness, vomit. CT was done for these four patients within one week. Nine healthy volunteers were selected as controls. ^{99m}Tc -ECD was prepared for imaging with radiochemical purity above 90 percent. Image was performed 30min later after intravenous administration of 1110 MBq ^{99m}Tc -ECD. Patients were positioned supine on the image table with head unmoved. Scanning equipment was Elscint Apex SP-6 SPECT with low energy general collimator. Visual interpretation and semiquantitation were carried out to detect rCBF abnormality. Eighteen ROIs were symmetrically on inferior frontal, middle frontal, temporal parietal, temporal, occipital, vision cross, basal ganglia, superior frontal and parietal on 3 transverse slices using software edited by ourselves, selecting contralateral region as the reference region. Counts per pixel in each ROI were divided by that of corresponding region to obtain the uptake ratio. It was regarded abnormality rCBF if the ratio was above 1.1 or below 0.9. **RESULTS:** rCBF was decreased in 11 of 16 patients, one has diffused abnormality for visual interpretation, the sensitivity was 75%, specificity was 100%, accuracy was 94%, CT scan was normal for all four patients. Sensitivity was 87.5% for semiquantitation. The results indicate that rCBF in SLE patients was generally diffused abnormal, but more often in frontal, temporal and parietal. **CONCLUSION:** SPECT cerebral perfusion imaging was an invasive method to evaluate rCBF in SLE patients, it may interpret some neuropsychiatry syndrome. It can provide early rCBF abnormalities than CT with high sensitivity, specificity and accuracy.

OS-112

V.A. Holthoff, B. Beuthien-Baumann, J. Pinkert, L.Oehme, U.Pietrzyk*, W.-G. Franke and O. Bach

Dresden Technology University and *Max-Planck-Institute for Neurological Research, Cologne, Germany

FOLLOW-UP STUDIES WITH TC-99M HMPAO SPECT BEFORE AND AFTER SLEEP DEPRIVATION - A POSSIBILITY FOR MONITORING OF TREATMENT RESPONSE IN PATIENTS SUFFERING FROM DEPRESSION.

Some PET and SPECT studies were carried out until now to assess perfusion and metabolism in depressive disorders. Although functional deviations from the normal activity pattern were seen in such patients (pts.) direct comparisons between different pts. as well as the situations before and after therapy are hardly studied until now. Therefore the objective of this follow-up study was to investigate by SPECT the relationship between the effect of sleep deprivation (sp.), recovery and regional brain perfusion in pts. with major depression (d). Fourteen pts. (9 females, 5 males, mean age 52.4 ± 13.62 years) treated by antidepressant medication underwent a total sleep deprivation lasting 40 hours. Tc-99m HMPAO-SPECT was assessed at noon each before and after the sleep deprivation for all pts. Apart from that 3 pts. were studied during the clinical remission too. Following regions were evaluated: Prefrontal cortex, anterior cingulum, hippocampus, parahippocampus and amygdala. Statistical calculations took place for dependent as well as independent samplings by the tests of Wilcoxon and Mann-Whitney resp. There were 8 responders and 6 non-responders. At baseline all pts. revealed hypoperfusion in the left prefrontal cortex when compared to the right side (prefrontal cortex right: 0.93±0.08, left: 0.76±0.08), which was not affected by sd., whereas prefrontal hypoperfusion was reversible upon remission. The responding pts. had a significantly higher anterior cingulate perfusion than the nonresponding pts., that normalized after sd. (before sd: right (r) 1.18±0.04, left (l) 1.24±0.09 after sd (r): 0.96±0.11, (l) 0.96±0.10, significance level < 0.05). The results obtained by SPECT correspond with the few ones obtained by PET until now. They showed a significant increase of metabolism in the cingulum of pts. before sd. which was normalized after sd. The cingulate functionality seems to be suited for identification of subgroups of depressive pts. Therefore SPECT studies provide additionally to PET studies also evidence for cingulate and prefrontal dysfunction associated with depression that are reversible by successful treatment and may represent a state marker.

OS-113

F.M. Fringuelli, R. Campini, R. Giubbini*, A. Braghiroli, C. Sacco

*Salvatore Maugeri Foundation", IRCCS, Medical Center of Rehabilitation Veruno; *Spedali Civili Brescia

BRAIN PERFUSION IN OBSTRUCTIVE SLEEP APNEA SYNDROME (OSAS) EVALUATED BY ECD BRAIN SPET BEFORE AND AFTER CONTINUOUS POSITIVE AIRWAY PRESSURE (CPAP) THERAPY

The association between OSAS and cerebrovascular disorders has been investigated mainly by retrospective studies. We prospectively studied the incidence of cerebral regional blood flow (RBF) defects in OSAS pts with nocturnal desaturation (SaO₂<90%) and without clinical signs of neurological disorders. Forty consecutive OSAS pts, (55±11 years, BMI 34±6Kg/m², with apnea-hypopnea index (AHI)=61± 32 and sleep time with <90% SaO₂ =168±161 minutes) performed a ^{99m}Tc ECD-SPET in the morning after polysomnography. Twenty-three pts repeated the study after 6 months of treatment with nasal CPAP, able to prevent most of apneas (AHI 8±8) and desaturations (minutes < 90% SaO₂ 10±12). Both at baseline and 6 months later, cerebral RBF imaging was performed 90 minutes after injection of the tracer, avoiding visual, acoustic or mental provocation in the 15 min before ECD injection, by a dual-headed γ-camera equipped with a fan-beam collimator. Three blind experienced observers evaluated the scintigrams for presence/absence of perfusion defects. Extent and severity of SPET perfusion defects were also graded according to a standard score (0=normal, 1=mild, 2=moderate, 3=severe). Cerebral perfusion defects at baseline study were detected in 21/40 (52%) patients; they involved the right frontal lobe (9 pts), left frontal lobe(12 pts), right temporal lobe (6 pts), left temporal lobe (6 pts), right occipital lobe(1 pt), left basal nuclei (1 pt). In 23 pts that repeated the SPET after 6 months, the perfusion was unmodified in 10/11 pts with normal pattern. In the group of pts with abnormal SPET at baseline (12 pts), RBF worsened in 5, improved in 3 and unchanged in 4. In conclusion, an impairment of cerebral perfusion pattern is frequently present in asymptomatic OSAS patients; RBF after 6 months nasal CPAP treatment improves in only 25% of pts.

OS-114

D. Salvo, A. Versari, D. Guidetti, F. Fallanca, D. Serafini, E. Vecchiati, G. Casali.

Hospital: S. Maria Nuova, Dept of Nuclear Medicine-Reggio Emilia

EVALUATION OF CEREBRAL BLOOD FLOW RESERVE WITH DIPYRIDAMOLE STRESS BRAIN SPECT.

In this study dipyridamole (DIP) was tested as a stress agent evaluating the brain blood flow reserve (BFR) in pts with carotid artery (CA) disease. 29 pts (m/f 22/7, mean age 72.4 yrs, range 53-87 yrs), 25 affected by bilateral CA stenosis, 4 unilateral, were included in the study. 7 pts had severe stenosis (>70%; 6 asymptomatic) and 22 moderate (30-70% ; 8 asymptomatic). All of them was investigated with brain CT, TSA doppler and/or arteriography. Then, brain SPECT with and without DIP stress was performed. For the stress study a dose of 0.57 mg/kg over 4 min. of DIP was given 3 min. before administration of 740 MBq ^{99m}Tc-ECD. Both SPECT studies were evaluated by a qualitative and semiquantitative method (square ROIs symmetrically drawn on the frontal, parietal and temporal lobes and, as reference, on cerebellar hemispheres). A baseline/dipyridamole perfusion ratio (B/DIP) was calculated. BFR was considered significantly reduced for B/DIP < 0.9 (perfusional worsening > 10% on DIP study) **Results:** all pts with severe stenosis had an abnormal baseline study, 4 (57%) with a reduced BFR. Pts with moderate stenosis had 16 (73%) abnormal baseline study (13 - 81% - with reduced BFR) and 6 (27%) normal baseline study (4 - 66% - with reduced BFR). 9 pts (43%) with reduced BFR were asymptomatic. During DIP test 2 pts was found affected by unknown myocardial ischemia. **Conclusions:** These data suggest that DIP stress SPECT is an useful and safe method to identify pts, also asymptomatic, with potential risk of brain ischemia who might benefit from carotid endarterectomy.

Radiopharmacy and radiochemistry: Technetium

OS-115

R. Bergmann, P. Brust, H.-J. Pietzsch, M. Scheunemann, B. Johannsen Forschungszentrum Rossendorf, Institut für Bioorganische und Radiopharmazeutische Chemie POB 51 01 19, D-01314 Dresden

Evaluation of the *in vitro* and *in vivo* properties of a potential Tc-labelled inhibitor of the MDR gene product P-glycoprotein.

Human multiple drug resistance (MDR) gene transfer and expression in bone marrow cells followed by autologous bone marrow transplantation in patients with advanced cancer is seen as a strategy to minimize the risks of high dose chemotherapy. Monitoring of the successful gene transfer may be a prerequisite for the therapy, i.e. it is required to study the expression of the MDR genes products, P-glycoprotein (Pgp) and the multidrug resistance-related protein (MRP) after gene transfer. Up to now the available clinical radiopharmaceuticals to study the expression of the Pgp and MRP the lipophilic ^{99m}Tc-cations (sestamibi, tetrofosmin) as well as ^{99m}Tc-Q57, ^{99m}Tc-Q58, and ^{99m}Tc-Q63. All these complexes are transported by the Pgp. Here we describe the *in vitro* and *in vivo* properties of the structurally different (3-thiapentane-1,5-dithiolato)[N-(3-phenylpropyl)-N-2(3-chinazoline-2,4-dionyl)-ethyl]amino-ethylthiolato)-oxotechnetium(V) (P398) complex as a potential inhibitor of the Pgp. P398 and its rhenium congener enhance the net cell accumulation of the Pgp substrates 3H-vinblastine, 3H-vincristine, 3H-colchicine, ^{99m}Tc-sestamibi, ^{99m}Tc-tetrafosmine in RBE4 cells, an immortalized endothelial cell line which expresses Pgp and MRP. However, the cell accumulation of the n.c.a. P398 could not be influenced by quinidine and reserpine as known Pgp inhibitors. A multitracer approach was used to study also the side effects of P398 on cell metabolism. The cells were simultaneously incubated with ^{99m}Tc-sestamibi, ^{18F}-FDG and various 3H-labelled tracers. Two-dimensional scatter plots of ^{99m}Tc-Sestamibi uptake / ^{18F}-FDG uptake show typical changes of known Pgp inhibitors including the P398. Also the effects of the P398 on the *in vivo* distribution of ^{99m}Tc-sestamibi and ^{18F}-FDG in rats are comparable with the effects of verapamil, an established Pgp inhibitor and Ca-channel blocker. Taken together, our data show that the multitracer approach can be used *in vitro* and *in vivo* to measure the functional characteristics of the Pgp and to study the interaction of potential radioligands with the Pgp. We conclude that P398 is not a transport substrate but a potential inhibitor of the Pgp and/or verapamil-sensitive Ca-channel. Our approach may be useful in the design of new radiotracers with specificity to the Pgp.

OS-116

P. Laverman, E.T.M. Dams, W.J.G. Oyen, G. Storm, E.B. Koenders, R. Prevost, J.W.M. van der Meer, F.H.M. Corstens and O.C. Boerman. Departments of Nuclear Medicine and Internal Medicine, University Hospital Nijmegen, Nijmegen and Department of Pharmaceutics, Utrecht University, Utrecht, The Netherlands.

AN IMPROVED Tc-99m LABELING METHOD TO LABEL LIPOSOMES VIA THE HYDRAZINO NICOTINYL DERIVATIVE

Stealth[®]-liposomes labeled with Tc-99m have shown to be good vehicles to image infection and inflammation. We developed a new labeling method for polyethyleneglycol-coated (PEG) liposomes, based on the bifunctional chelator hydrazino nicotinamide (HYNIC).

Succinimid-HYNIC was conjugated to distearyl phosphatidyl-ethanolamine (DSPE). The conjugate was incorporated into the lipid bilayer of the liposome. Liposomes were sized by extrusion to a size of approximately 90 nm. In the newly developed HYNIC-liposomes 230 hydrazine groups per liposome were incorporated. Radiolabeling was performed by incubating 0.1 ml of liposomes (100 mmol phospholipid/l) with stannousulphate in the presence of tricine as a coligand at room temperature for 15 min. The *in vitro* as well as the *in vivo* characteristics were compared to Tc-99m-HMPAO labeled glutathione containing PEG-liposomes.

Labeling efficiency of the HYNIC-liposomes was always higher than 95%, thus no postlabeling purification was required. Transchelation assays showed greater stability of the Tc-99m-HYNIC-liposomes as compared to the Tc-99m-HMPAO-liposomes. Twenty-four hours after induction of a *Staphylococcus aureus* abscess in the left calf muscle, rats were *i.v.* injected with liposomes (15 MBq/rat, 1 μmol phospholipid). The abscess uptake of HYNIC-liposomes was significantly higher (1.74 ± 0.38 vs. 1.26 ± 0.29 %ID/g, 24 hr *p.i.*). Furthermore, kidney uptake of the HYNIC-liposomes was three-fold lower as compared to the glutathione-liposomes (0.79 ± 0.07 vs. 2.47 ± 0.35 %ID/g, 24 hr *p.i.*) suggesting reduced release of the radiolabel from the liposomes *in vivo*.

In conclusion, the HYNIC-based labeling method for PEG-liposomes improved the *in vitro* stability and *in vivo* behavior for application as an infection imaging agent. This rapid, one-step labeling procedure, is a step forward towards a liposome-based radiopharmaceutical that can be applied in routine clinical practice.

OS-117

F. Wüst, J. A. Katzenellenbogen*, H. Spies, B. Johannsen

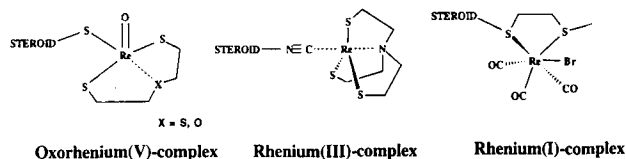
Institute for Bioinorganic and Radiopharmaceutical Chemistry, Research Center Rossendorf, Inc., Germany

*Department of Chemistry, University of Illinois at Urbana-Champaign, USA

RHENIUM COMPLEXES OF 17 α -SUBSTITUTED ESTRADIOL CAPABLE OF BINDING TO THE ESTROGEN RECEPTOR

The gonadal steroids are implicated in hormone-dependent cancers of the breast and prostate.

In order to image estrogen receptor positive tumors by using ^{99m}Tc based radiopharmaceuticals, we have synthesized novel rhenium(V), (III) and (I) complexes of 17 α -substituted estradiol. In our first investigations we used rhenium as a model for the radioactive technetium.



These complexes represent new classes of estrogen receptor-binding rhenium complexes.

The binding affinities (lambda-cytosol) at 0°C reveal RBA values of about 23 % for the oxorhenium(V) complexes when X = O and 8 % when X = S. The RBA values at 25°C are 10 % for the oxorhenium(V) complexes when X = O and 15 % when X = S. For the rhenium(III) and rhenium(I) complexes the RBA values are significantly lower for 0°C and 25°C, ranging from 0.6 % to 2.5 %.

Further studies will investigate the stability of these complexes under in-vivo conditions using the corresponding ^{99m}Tc-complexes.

OS-118

C. Decristoforo, S.J. Mather.

Nuclear Medicine Research Laboratory, St. Bartholomews Hospital, London, UK

TC-99M LABELLED SOMATOSTATIN ANALOGUE RC160: INFLUENCE OF BIFUNCTIONAL CHELATORS ON IN VITRO AND IN VIVO PROPERTIES

The diagnostic use of radiolabelled neuropeptides in-vivo is a new and exciting development in nuclear medicine and is exemplified by the use of the ¹¹¹In labelled somatostatin (SST) analogue octreotide for imaging neuroendocrine tumours. For routine applications the radiolabel of choice would be ^{99m}Tc, but radiolabelling procedures for peptides are yet not well established. The aim of this project was the labelling of RC-160, a somatostatin analogue with additional binding affinity for the SST receptor subtype 4, with ^{99m}Tc comparing the influence of different attached bifunctional chelators (BFC) on the properties of the ^{99m}Tc-labelled peptide.

Three different BFC were conjugated to protected RC-160: Hydrazino-nicotinamide (HYNIC), Benzoyl-MAG3 and a N3S-Adipate derivative. The deprotected conjugates were purified by HPLC and Solid Phase extraction and characterized by HPLC and MS. Radiolabelling was performed using tricine and ethylenediamine diacetic acid (EDDA) as coligands for the HYNIC conjugate and a ligand exchange method for the N3S- and MAG3 conjugates. The stability in plasma as well as to Cystein challenge and plasma protein binding was determined. Radioligand binding assays were performed on rat cortex membranes and rat pituitary cell lines. The biodistribution was studied in normal rats.

^{99m}Tc-labelling yields were > 90% for HYNIC conjugates using Tricine and 40-80% using EDDA as coligand, > 90% for the N3S and MAG3 conjugates, each with specific activities >1Ci/μmol. HPLC analysis of the radiolabelled peptides showed >90% single species for all conjugates except for the MAG3 derivative which had lipophilic impurities. All ^{99m}Tc-complexes were stable to proteases in human plasma and to cystein challenge for > 24hrs. Plasma protein binding was significantly lower for HYNIC- compared to MAG3- and N3S-compounds. A high binding affinity to SST receptors (IC50=1,5-9nM) was found for all derivatives. The HYNIC derivative using EDDA as coligand had the most favourable biodistribution in rats showing rapid renal clearance whereas N3S and MAG3 derivatives were mainly excreted via the liver.

Our results show that the kind of bifunctional chelator used for radiolabelling of a highly specific peptide with ^{99m}Tc had no substantial influence on the in vitro properties but had a major effect on the biodistribution. Results of tumour uptake in vivo and a comparison with Tyr³-Octreotide will be presented.

OS-119

Monica Santimaria¹, Hans Feitsma², Dik Blok², Ulderico Mazzi¹, Ernest Pauwels².

²Dept. of Nuclear Medicine, AZL, Leiden, The Netherlands

¹Dept. of Pharmaceutical Sciences, University of Padova, Padova, Italy.

EVALUATION OF A BIFUNCTIONAL PN₂S CHELATING SYSTEM FOR THE PREPARATION OF Tc-99m LABELLED BIOMOLECULES.

By linking a chelator for Tc-99m to a biologically active molecule, it is possible to prepare selective Tc-99m labelled imaging agents. Recently, our efforts were aimed to use phosphine containing compounds presented as a novel class of ligands able to give stable complexes with technetium as well as amenable to be derivatized for coupling with biologically active compounds. By incorporating tertiary phosphines into small receptor-binding peptides it is possible to create a chelating system into the peptides. The prototype of these ligands is the newly developed diphenylphosphinepropionyl-glycyl-(S-benzyl)cysteine. It is a tetradentate ligand generating a cage of PN₂S-nucleophiles which forms hexa-coordinated oxotechnetium(V) complexes and has the ability to conjugate to H₂N-groups of a biomolecule by means its carboxyl moiety.

This study deals with the development of a Tc-99m-PN₂S labelling protocol for conjugation with the tetrapeptide cholecystokinin (CCK-4) as a model peptide using HPLC techniques to assess the integrity of the Tc-99m-labelled species and labelling yield. Complexation of the diphenylphosphinepropionyl-glycyl-(S-benzyl)cysteine methyl ester with Tc-99m (by Sn(II)pyrophosphate reduction of TcO₄⁻ in alkaline media) yielded a single stable complex after 1 h heating at 60°C. By using a large excess of 2,3,5,6-tetrafluorophenol (TFP) and 1-ethyl-3-(3-dimethylaminopropyl)carbodiimide (EDAC) the formation of two derivatives of the labelled ligand can be detected within 10 minutes reaction. They have been attributed to two isomers of the TFP-active ester complex. Conjugation to CCK-4 fragment was carried out by addition of a 10 mg/mL solution of the peptide in bicarbonate buffer 0.1 M and resulted in two main peaks revealed by HPLC. These results indicated the diphenylphosphinepropionyl-glycyl-(S-benzyl)cysteine chelator to be promising for labelling of biologically active molecules.

OS-120

A. K. Mishra, P. Mishra, K. Chuttani, R. Kashyap, V. Jain

Depts of Radiopharmaceuticals, Nuclear Medicine, Biocybernetics Institute of Nuclear Medicine and Allied Sciences, Delhi-54, India

A NEW BIFUNCTIONAL Tc-99m BASED RADIOPHARMACEUTICAL FOR BONE IMAGING; ISOTHIOCYANATO-BENZYL-ETHYLENE DIAMINE TETRAMETHYLENE PHOSPHONIC ACID

Background: The development of new bifunctional chelating agents for the labeling of small specific peptides with radiometals is a desirable goal in the area of radioimmunodetection and radioimmunotherapy of cancer. The authors have developed a new phosphonate ligand, Isothiocyanato-Benzyl-Ethylene Diamine Tetramethylene Phosphonic Acid (IBz-EDTPA) for technetium-99m (^{99m}Tc) labeling of specific small peptides for two step targeting.

Methods: Synthesis of bifunctional chelating agent, IBz-EDTPA was accomplished by total synthesis starting from L-phenylalanine in nine steps. The conversion from carboxylic acid to phosphonic acid was performed by known procedure with slight modification in high yield. Each step is characterized by spectral studies and purity was checked on HPLC, using C18 RP column. The compound IBz-EDTPA was labeled with technetium at pH range 5.5 to 6.0 after reducing technetium in acidic condition using stannous chloride dihydrate at 25°C. IBz-EDTPA forms stable complex with technetium with a radiochemical yield above 98%. The ratio of metal to ligand is 1:1 for the complex.

Results: Serum stability studies showed that the metal is intact under physiological conditions. The images in normal mice, rat and rabbit showed the complex to be an excellent bone agent. Biodistribution in normal mice show skeleton uptake at 1hr to be significantly higher with Tc-99m-IBz-EDTPA than with Tc-99m-MDP (4.93 ± 0.22 Vs 1.10 ± 0.03, expressed as % ID/g). The complex cleared rapidly from blood circulation and showed low soft tissue uptake. Among the various organs, significant accumulation of the radiopharmaceutical IBz-EDTPA was found in the lungs (1.13% ± 0.15% mean ± s. d.), liver (0.43% ± 0.04%), and kidney (2.03% ± 0.15% mean ± s. d.) at 1 hr postadministration. These values were reduced to 0.46% ± 0.06%, 0.29% ± 0.04% and 1.10% ± 0.21% respectively, at 24 hr.

Conclusion: This new radiopharmaceutical showed promising results with technetium-99m for early bone imaging (30 minutes post injection). It may be concluded that IBz-EDTPA is more favorable for labeling with technetium for bone imaging. Clinical evaluations on a group of patients are promising. It is possible to label with rhenium-188 for the development of Re-188-IBz-EDTPA as a therapeutic bone agent.

General nuclear medicine: Lung

OS-121

Grahek D¹, Montravers F¹, Kerrou K¹, Younsi N¹, Wartski M², Zerbib E², Talbot JN¹.
Services de médecine nucléaire, hôpital Tenon¹, centre chirurgical Marie Lannelongue², Paris-Ile de France, FRANCE.

DETECTION OF MALIGNANCY IN PULMONARY NODULES BY [18F]-FDG SCAN ON A DUAL-HEADED GAMMACAMERA WITH COINCIDENCE DETECTION (CDET).

The clinical value of [18F]-FDG with positron emission tomography (PET) has been recognized in the characterisation of pulmonary nodules. More recently, dual headed gamma-cameras were equipped with coincidence detection (CDET) and thick crystals, to be able to detect FDG by means of coincidence emission of two 511 keV X photons, just as PET scanners do. Our aim was therefore to evaluate FDG-CDET in this indication, in a clinical trial (coordinator : JL Moretti).

Methods : Between July 1997 and March 1998, 24 patients (pts) were referred for an isolated nodule with a diameter less than 4 cm at CT and no histologic proof of malignancy (biopsy was negative in 14 pts, equivocal in 1 pt or not done, bronchoscopy was normal in 10 pts or just showed inflammatory lesions). 150-250 MBq of [18F]-FDG were injected intravenously via an infusion catheter to the patient fasting for 6h or more. 45 min after, FDG-CDET was performed using a PICKER Prism XP 2000, consisting of a whole-body scan and at least one tomoscintigram. The nodules which were either not visible or with a counting rate ratio to contralateral parenchyma less than 3 were considered FDG negative.

Results : Post surgical histology was until now obtained in 13 pts and an abscess found in 2 pts :

- 6 benign nodules were FDG negative (6 TN), consisting of 2 abscess, 1 granuloma, 1 aspergilloma, 1 Wegener disease, 1 histiocytosis.
- 9 malignant nodules were FDG positive (9 TP).

Conclusion : These excellent preliminary results (Se=Sp=100%) suggest that FDG-CDET with a semi quantification is an effective tool for characterisation of pulmonary nodule which will permit avoidance of invasive procedures, and also allows staging in FDG positive nodules. The diagnostic accuracy of FDG-CDET appears to be identical to that of FDG-PET (e.g. Se=100%, Sp=89% in 30 pts reported by Bury et al. in 1996) for the characterisation of the solitary pulmonary nodule.

OS-122

S. Koukouraki¹, M. Koukourakis², K. Perisinakis³, A. Giatromanolaki⁴, I. Manousakas⁵, N. Karkavitsas¹.
Departments of ¹Nuclear Medicine, ²Radiotherapy and ³Medical Physics of University Hospital of Iraklion, Department of ⁴Isotopathology of University Hospital of Alexandroupoli, ⁵Diagnostic Medical Center of Crete, Greece.

FUNCTIONAL IMAGING OF NON-SMALL CELL LUNG CANCER WITH ^{99m}Tc SESTAMIBI PREDICT RESPONSE TO CHEMOTHERAPY AND RADIOTHERAPY

Purpose: Application of a test that reliably evaluates the P-glycoprotein activity in vivo would be useful as a predictor for responses to chemo/radiotherapy. Tc-99m radiolabelled hexakis-2-methoxyisobutyl-isonitrile (sestamibi) has been recently shown to be extruded from cell through P-glycoprotein activity. The purpose of this study is to evaluate the uptake of Tc-99m sestamibi and its extrusion rate in patients with NSCLC undergoing chest radiotherapy/chemotherapy.

Methods: In the present study we prospectively examined the uptake and extrusion rate of Tc-99m sestamibi in 55 patients with NSCLC. Each patient received 20 mCi (740 MBq) of Tc-99m sestamibi in an antecubital vein. Multiple planar views of the chest were acquired in the anterior projection on a gamma camera GE Millenium equipped with a LEGP collimator and a PHILIPS Tomo gamma camera equipped with pinhole collimator, 10 and 120 min after the injection. A single head rotating camera (GE Millenium) was used to obtain early and late SPECT images. Regions of interest were drawn around tumor mass and normal lung. The efflux rate was evaluated using the formula:

$$E = \frac{(U/n1)_{10min} - (U/n1)_{120min}}{(U/n1)_{10min}}$$

Results: Thirteen out of 55 (23%) tumors showed a 1.3-1.8 times higher extrusion rate as compared to that of normal lung tissue. Data from SPECT, planar and pinhole images is highly correlated to each other (p<0.001, r=0.84). Increased tumor clearance of Tc-99m sestamibi is significantly correlated with resistance to radiotherapy (p<0.001). Patients with known resistance to chemotherapy had a higher extrusion rate as compared to those who had not received chemotherapy in the past.

Conclusions: We conclude that SPECT, planar and pinhole functional images of NSCLC using Tc-99m sestamibi are predictive of disease resistance to chemo/radiotherapy. Clinicopathological trials are now conducted to investigate possible association of P-glycoprotein expression or angiogenesis with 99mTc-sestamibi kinetics.

OS-123

G. Boni,*A. Chella, M. Grosso,*G.F. Menconi, G. Manca,* F.M.A. Melfi, C.R. Bellina,^oR. Cioni, C.A. Angeletti* and R. Bianchi. Division of Nuclear Medicine and ^oRadiology (Dept. Oncology); *Service of Thoracic Surgery (Dept. Surgery), University of Pisa, Italy.

USEFULNESS OF GAMMA PROBE GUIDED LOCALIZATION OF PULMONARY NODULES FOR THE VIDEO ASSISTED THORACOSCOPIC SURGERY

Video-assisted thoracic surgery (VATS) is a safe procedure for the diagnosis and treatment of peripheral pulmonary nodules. One limitation of the thoracoscopic technique is the loss of the manual palpation to identify the nodule that is either too deep beneath the pleural surface. Several methods, including methylene blue injection and introduction of hooked-wire, are used to localize occult lesions prior to excision. However, all methods suffer from limitations. Recent advancements in intraoperative radio-localization of nonpalpable breast lesions prompt us to develop a new technique for detection pulmonary nodules by VATS. For this reason, we started to perform two hours before surgery a CT-scan guided perilesional injection of 0.5-1 ml of a solution containing 99mTc labeled human serum albumin microspheres (5-10 Mbq) and contrast media. Then, a gamma ray detector (ScintiProbe MR 100 - pol.hi.tech. s.r.l, Aquila, Italy), equipped with a 11 mm diameter collimated thoracoscopic probe, was used during VATS to localize the pulmonary. The total excision of the lesion was confirmed by the presence of radioactivity in the removed specimen and its absence in the resection margins of the lung.

From June 1997 to January 1998 we treated 15 consecutive patients (10 men and 5 woman, age range 13-80 years) with subcentimeter pulmonary nodules. Nine patients were affected by a synchronous and metachronous malignant neoplasm in other sites. Histological examination showed 8 benign lesions and 7 malignant lesions (4 metastases and 3 lung cancer). Subsequently, all patients with lung cancer underwent to lobectomy.

In our preliminary experience this technique proves safe and accurate, allowing easy detection of the pleural surface projection and fast removal of the lesion, with the advantage that the resection margins can be detected during the operation. This technique offers a simple and reliable method for localization of primary and metastatic tumors by VATS.

OS-124

F. P. Xue (1), Z. H. Zhang (2), X. T. Lin (1), Y. Z. Guo (3), Q. F. Kuang (3), X. D. Liu (1), Y. Q. Yang (2), Z. Y. Zhang (3)
1. Dept. of Nucl. Med. Hua Shan Hospital. Shanghai 200040, China
2. Shanghai Tumor Research Institute. Shanghai 200032, China
3. Shanghai Syncor Pharmaceutical Co. Ltd. Shanghai 201103, China

EXPERIMENTAL STUDY ON RADIOIMMUNOIMAGING AND BIODISTRIBUTION OF ^{99m}Tc LABELED ANTI-HUMAN SMALL CELL LUNG CANCER McAb (2F7) F(ab')₂ FRAGMENTS

PURPOSE The biodistribution and radioimmunoinaging of ^{99m}Tc-2F7 in tumor bearing SCID mice were studied in order to provide some basis for clinical applications. **METHODS** 2F7 F(ab')₂, anti-human small cell lung cancer McAb fragments, was labeled with ^{99m}Tc and injected into normal mice and SCID mice bearing human small cell lung cancer. The blood samples were obtained for the study of plasma clearance. The biodistribution of ^{99m}Tc-2F7 F(ab')₂ and whole body imaging were studied at different intervals after injection. **RESULTS** The blood clearance of ^{99m}Tc-2F7 F(ab')₂ was a biexponential curve (C = 14.5e^{-0.06t} + 2.5e^{-0.007t}). T_{1/2 α} = 0.04min and T_{1/2 β} = 16.5h, CL = 0.03ml/min. The plasma clearance of the radiolabeled F(ab')₂ was quick. ^{99m}Tc-2F7 F(ab')₂ was eliminated mainly via renal excretion. It suggested the radiolabeled F(ab')₂ is stable in vivo. The T/NT ratios were good and the imaging showed accumulation of ^{99m}Tc-2F7 F(ab')₂ in the tumor but there was very little uptake in the inflammatory foci. **CONCLUSIONS** The McAb 2F7 bind to the tissue of small cell lung cancer specifically and suggested that ^{99m}Tc-2F7 may have potential clinical application value in tumor localization.

OS-125

S.Raja, O.A.Minai, A.Duggal, D.Neumann, A.Dasgupta, A. Arroliga, A.C.Mehta, G.Saha, K.Amin, S.Khandekar, R.Go.
The Cleveland Clinic Foundation, Department of Nuclear Medicine
Cleveland, OH. USA

UTILITY OF Tc-99m-METHOXYISOBUTYL ISONITRILE (MIBI) IN DIFFERENTIATING MALIGNANT FROM BENIGN SOLITARY PULMONARY NODULES (SPN)?

Currently, apart from F-18 FDG PET, there is no reliable non-invasive imaging modality that differentiates malignant from benign SPN. MIBI is known to accumulate in neoplastic tissue including lung Ca. We conducted a double blind prospective study to evaluate the utility of MIBI in differentiating SPN.

Twenty-five patients with recently detected SPN on chest radiographs and/or CT scans and also scheduled for biopsy, were recruited into the study. SPECT and planar imaging of the chest were obtained in all patients, 10 minutes after the injection of 20 - 30 mCi of Tc-99m MIBI intravenously. The images were interpreted by a nuclear medicine physician blinded to the histopathology results.

Histopathology was available in 18 patients (M=7, F=11; age 46-81 years, mean 51.6 years), the following analysis is based on these 18 patients. The sizes of the nodules were 1.3 to 5 cm. (mean 2.75 cm). Four nodules were benign and 14 were malignant (8 adenoma Ca, 2 non-small cell Ca, 1 each bronchoalveolar cell Ca, anaplastic Ca, spindle cell Ca and metastatic Ca). All four benign nodules were true negative, 12/14 of malignant nodules were true positive, while 2/14 were false negative. The results are tabulated below.

True Positive 12	True Negative 4	Sensitivity 87%	PPV* 100%
False Positive 0	False Negative 2	Specificity 100%	NPV* 67%

* PPV: Positive Predictive Value, NPV: Negative Predictive Value

The preliminary results of our study suggest that Tc-99m MIBI would be useful in the differentiation of benign vs. malignant SPN.

OS-126

Rakesh Kumar, Srikant Sharma*, M Sriram, S Dilip, A Malhotra, S Sharma

All India Institute of Medical Sciences, New Delhi-110029.
Departments of Nuclear Medicine & Medicine.

COMPARISON OF 99m Tc-TETROFOSMIN AND 201 TI IN THE DETECTION OF LUNG TUMORS.

Thallium 201 and 99mTc-Tetrofosmin(TFN) are widely used for myocardial perfusion studies. Both these agents also show good tracer uptake in various tumors. This study was designed to assess the usefulness of TFN in detecting mediastinal and lung tumours. The results were compared with those of 201TI studies.

A total of 22 patients were included in this study. All tumours were histologically proven. All these patients underwent 99mTc-TFN and 201TI scintigraphy. The planar static images were acquired at 30 minutes and 2 hours, after intravenous injection of 370-555 Mbq of 99mTc-TFN and 74-111 MBq of 201TI on different days. Semiquantitative analysis was done by drawing a region of interest on the lesion and normal lung. Early uptake ratio, delayed uptake ratio, retention index and wash out ratio were calculated and results of the two agents were compared. All the lesions were detected by both the tracers. No significant difference was observed between the indices except for wash out ratio.

In conclusion, TFN may be a useful tracer for the detection of lung tumours as the uptake ratio of TFN is same as that of 201TI and image quality is much better.

Cardiovascular: Innervation

OS-127

D. Agostini¹, Y. Darlas¹, O. Citerne², JE Filmont¹, Gilles Grollier², JC Potier², G. Bouvard².

Departements of Nuclear Medecine¹ and Cardiology², CHU Côte de Nacre, Caen, France.

REVERSIBILITY OF CARDIAC NEURONAL FUNCTION AFTER REMOVAL OF PHEOCHROMOCYTOMA : A ¹²³I-MIBG SCINTIGRAPHIC STUDY.

Decreased cardiac metaiodobenzylguanidine (MIBG) uptake has been found to reflect impairment in adrenergic nerve function involved on the cardiac outcome of patients with pheochromocytoma. However, the assessment of cardiac neuronal function after removal of tumor has not yet been done. We prospectively studied 15 consecutive patients with proven pheochromocytoma (clinical status, CT scan, biological data) patients (age 40±9 years). Before tumoral removal, LVEF assessed by echocardiography, was within the normal range (70±7%). Urinary normetanephrine (NMNE), metanephrine (MN) and vanilylmandelic acid (VMA) rates were significantly increased (6541±4354 µg/day, 4087±3266 µg/day, 41±25 mg/day) respectively. Cardiac MIBG uptake was measured as the heart to mediastinum activity ratio (HMR) on the planar image (10-min acquisition in the chest anterior view) obtained 4h after a 185 MBq IV injection of I-123 MIBG (HMR = 141±18%). After tumoral removal, HRM increased significantly to 197±19% (p<.05), NMNE, MNE and VMA decreased significantly in order to return within the normal range (<100 µg/day, <100 µg/day, <8 mg/day, p<.001) respectively. LVEF did not change significantly (72±9%, NS). No significant correlation was found between cardiac MIBG uptake and urinary metabolic rates. In conclusion, adrenergic nerve function has been restored without adverse effect on myocardial contractility and 2/ norepinephrine-MIBG competition is not the main biochemical mechanism after removal of pheochromocytoma.

OS-128

N. Delahaye, J. Delforge, S. Dinanian, D. Samuel, M. Slama, A. Syrota, P. Merlet, D. Le Guludec.

Bichat and Bécélère Hospitals, S.H.F.J. DSV-CEA, Paris and Orsay, France.

MYOCARDIAL POSTSYNAPTIC PARASYMPATHETIC MODIFICATION AND SYMPATHETIC DENERVATION IN FAMILIAL AMYLOID POLYNEUROPATHY.

Familial amyloid polyneuropathy (FAP) is a rare hereditary form of amyloidosis including a progressive autonomic neuropathy. These patients usually do not present heart failure, but sudden death, arrhythmias and conduction disturbances have been reported. Impairment of cardiac autonomic nervous system was studied in 8 FAP pts (46 ± 14 years), all with normal coronary arteries and left ventricular function (LVEF: 69 ± 7%, cardiac index: 3.4 ± 1.2 l/mn/m²).

Presynaptic sympathetic myocardial denervation was assessed by 123 I MIBG scintigraphy (heart to mediastinum activity ratio measured on the chest anterior image 20 mn and 4 hrs after intravenous injection of 300 MBq). The postsynaptic parasympathetic modification was evaluated by positron emission tomography with 11 C MQNB (methylquinuclidinyl benzilate), a specific antagonist of muscarinic receptors. PET data were corrected for losses in count recovery. All results were compared with 12 age-matched control subjects.

MIBG uptake was extremely decreased in FAP pts compared to the control group (at 4 hrs: 1.35 ± 0.23 versus 1.98 ± 0.35, p<0.001), without difference in washout rates. The mean muscarinic receptor concentration was higher in FAP pts compared to the control group (β' max: 46 ± 19 versus 25 ± 8 pmol/mL, p<0.005), with no change in the fraction of extravascular fluid in which MQNB can interact with the receptors. The change in heart rate after injection of 0.6 mg of cold MQNB (an equivalent of atropine) was lower in pts compared to the control group (12 ± 19% versus 55 ± 36%, p<0.01), and the maximal heart rate achieved after MQNB injection inversely correlated with β' max (r=-0.77, p=0.003).

This study confirms the impairment of cardiac autonomic nervous system in FAP patients, resulting in pre- and postsynaptic abnormalities.

OS-129

Ch. Maunoury, D. Agostini*, P. Acar, G. Bouvard*, L. Barrिताult

Hôpital Necker-Enfants Malades, Paris, *CHU Caen, France

IMPAIRMENT OF CARDIAC NEURONAL FUNCTION IN CHILDREN WITH DILATED CARDIOMYOPATHY: A 123I MIBG SCINTIGRAPHIC STUDY

Decreased cardiac neuronal function has been reported in adults with heart failure using 123I MIBG scintigraphy. However, no data are available in children with heart failure. The purpose of the study was to assess the cardiac neuronal function in children with dilated cardiomyopathy. **Methods:** We studied 25 consecutive children (9 male, 16 female, aged 51±54 months) who had dilated cardiomyopathy with left ventricular dysfunction (LVEF=25±12%). As a group control, we studied 10 children (7 male, 3 female, aged 55±69 months) referred for suspected neuroblastoma and/or pheochromocytoma with normal left ventricular function (LVEF=73±5%). All subjects underwent a planar scintigraphy performed 4 hrs after IV injection of 20-75 MBq of 123I MIBG. The static acquisition was performed in anterior view for 10 minutes. The ROI's average size was 4x4 pixels (matrix size 64x64). Cardiac 123I MIBG uptake was calculated as heart to mediastinum count ratio. **Results:** There was a significant decrease of 123I MIBG cardiac uptake (172±30%, range 121-230) in children with cardiomyopathy when compared to controls (276±15%, range 256-298, P=0.0001). **Conclusion:** The 123I MIBG cardiac scintigraphy is a useful tool for assessing cardiac neuronal function, which is dramatically impaired in children with dilated cardiomyopathy. It might be a striking functional index to list children for heart transplantation.

OS-130

M.J. Reinhardt, S. Braune, I. Brink, F. Jüngling, T. Krause, C.H. Lücking, E. Moser
Departments of Nuclear Medicine and Neurology, Hospital of the Albert-Ludwigs-University, Freiburg i.Br., Germany

INVOLVEMENT OF CARDIAC SYMPATHETIC EFFERENTS IN PATIENTS WITH PARKINSON'S DISEASE AND AUTONOMIC FAILURE - DETECTION BY 123I-MIBG SCINTIGRAPHY

The purpose of this study is to assess involvement of cardiac sympathetic efferents in patients with Parkinson's disease (PD) and autonomic failure (AF). There is accumulating evidence that postganglionic neurons could be predominantly affected in PD with AF, whereas in patients with multiple system atrophy (MSA), who frequently present with Parkinson's syndrome, preganglionic sympathetic neurons are affected. 123I-Metaiodobenzylguanidine (MIBG) accumulates selectively in postganglionic sympathetic neurons.

A total of 20 subjects was investigated. Autonomic failure was diagnosed in 10 patients with PD by standardized autonomic function tests. Six patients were clinically symptomatic and four patients were clinically asymptomatic. Ten age and sex matched subjects, in whom suspected pheochromocytoma could be excluded, served as controls. Thoracic planar and SPECT images were performed 4 hours after i.v. injection of 185 MBq 123I-MIBG. Semiquantitative evaluation was done by forming a heart/mediastinum ratio (H/M ratio). In case of decreased cardiac MIBG uptake, 99mTc-MIBI scintigraphy was performed to rule out a cardiovascular origin. In patients with PD and AF, the H/M ratio was significantly lower compared to controls (1.05±0.05 versus 2.02±0.16, p<0.001). There was no difference between clinically symptomatic and clinically asymptomatic patients. 99mTc-MIBI scintigraphy showed no perfusion defects in all patients.

123I-MIBG scintigraphy enables detection of involvement of the autonomous nervous system in patients with PD before clinical symptoms become apparent. Thus, there might be a possible role for 123I-MIBG scintigraphy in the early differentiation of patients with autonomic failure.

OS-131

H. Takatsu, H. Nishida, H. Matsuo, T. Aoyama, S. Watanabe, M. Shimizu, H. Fujiwara
Gifu University School of Medicine, Second Depart. of Int. Med. Gifu Prefectural Hospital, Neurology.

REMARKABLE REDUCTION OF CARDIAC I-123 MIBG ACCUMULATION IN PARKINSON DISEASE

I-123 metaiodobenzylguanidine (MIBG) is known to accumulate in the sympathetic nerve endings, and its significant reduction has been reported in the heart with myocardial infarction or cardiac myopathies. Since heart is richly innervated by sympathetic nerves, the loss of its accumulation is thought to be a good index for the cardiac sympathetic denervation or dysfunction. We found that I-123 MIBG accumulation was remarkably reduced in the whole heart with Parkinson disease, in spite of they had no obvious cardiac disease. Therefore, we examined the cardiac I-123 MIBG accumulation in correlation with the clinical stages and sympathetic disorder in the 18 patients with Parkinson disease. Diagnosis was confirmed by two neurologists, and the patients with secondary Parkinsonism were excluded. Patients were injected with 111 MBq of I-123 MIBG at rest, and imaged 15 min and 4 hours after the tracer injection. Their clinical stages were determined according to the Hoehn-Yahr classification. Overnight ambulatory blood pressure monitoring was also performed. In the patients at the stage III or IV, almost null accumulation was visually detected in both initial and delayed images. Heart to mediastinum (H/M) ratio in the delayed images ranged from 1.1 to 1.5, which were significantly decreased compared with the normal controls (1.8±0.2). At the stage II, the I-123 MIBG accumulation also decreased in the delayed image although cardiac accumulation was visible in the initial images. In the patients with severely decreased MIBG accumulation, all of them were found to be non-dippers in the blood pressure monitorings, except for one patient. In conclusion, remarkable reduction of I-123 MIBG was observed in the patients with Parkinson disease, associated with non-dipper pattern in the overnight blood pressure monitoring.

OS-132

S. Tsuchimochi, M. Nakajo, A. Tani and Y. Nakabeppu

Hospital: Kagoshima University, Department of Radiology

AGE-RELATED CHANGES OF NORMAL HUMAN REGIONAL MYOCARDIAL DISTRIBUTION AND WASHOUT RATES OF I-123 METAIODOBENZYLGUANIDINE (MIBG)

This study was undertaken to reveal the age-related changes of normal regional myocardial distribution and washout rates (WRs) of I-123 MIBG. In a total of 65 patients (33 males; age 9 - 76 yrs, and 32 females; age 13 - 86 yrs) with no significant cardiac disorders, early (30 min) and late (4 hr) SPECT images were obtained after i.v. injection of 111 MBq of I-123 MIBG. The left ventricular myocardium was divided into 5 regions using the bull's eye map display to calculate the % mean count ratios of each region, each region to anterior wall count ratios and WRs from 30 min to 4 hr. 1) Early regional myocardial distribution: The activity was higher in the lateral and inferior walls and relatively homogenous in the other regions in the younger age group (less than 20 yrs). However, with aging, the activity became higher in the anterior and lateral walls and septum and lower in the inferior wall and apex. Decrease of the activity in the inferior wall began earlier in the males than in the females. 2) Late regional myocardial distribution: The points different from the early distribution were as follow; (1) The relative activity in the lateral wall compared to the anterior wall and septum was lower in the late imaging than in the early imaging. (2) The activity in the inferior wall decreased rapidly in the male group of 21 to 40 yrs and in the female group of 41 to 60 yrs. 3) WRs: (1) The WRs in all regions had significant positive correlations with aging. (2) Negative WRs were observed in the male and female group of less than 20 yrs and in the female group of 21 to 40 yrs. Then the WRs showed positive values with aging. (3) The WR was more rapid in the inferior wall, apex and lateral wall than in the anterior wall and septum. 4) There was a significant correlation of WRs with the late myocardial distribution but not with the early myocardial distribution. These results suggest that 1) the functional amount of myocardial sympathetic neurons is higher in the inferior and lateral walls in younger persons and decreases in the inferior wall with aging, and 2) the adrenergic nerve activity accelerates with aging.

Dosimetry and radiobiology: Biokinetics/dosimetry

OS-133

E. Th. M. Dams¹, W. J. G. Oyen¹, O. C. Boerman¹, P. Laverman¹, G. Storm², J. W. M. van der Meer¹, F. H. M. Corstens¹.

University Hospital Nijmegen¹, Nijmegen and Utrecht University², Utrecht, The Netherlands.

EFFECT OF MULTIPLE INJECTIONS ON PHARMACOKINETICS AND BIODISTRIBUTION OF PEG-LIPOSOMES.

Surface coating of liposomes with hydrophilic polymers such as polyethyleneglycol (PEG) extends their circulation time by decreasing opsonization and subsequent uptake by cells of the reticuloendothelial system. These PEG-liposomes are considered to be nonimmunogenic, and are viewed as promising carriers of therapeutic agents as they can increase efficacy while reducing drug-related toxicity. In addition, they appear to be attractive vehicles for infection/inflammation imaging. Here, we studied the effect of repeated injections with radiolabeled PEG-liposomes on pharmacokinetics and biodistribution in normal rats. **Methods.** Tc-99m-labeled PEG-liposomes were administered intravenously to rats with fixed intervals. Length of the interval was varied from 1 to 4 weeks. The *in vivo* distribution of the radiolabel was monitored by gamma camera imaging up to 4 hr p.i. After acquiring the last image, rats were killed to determine *ex vivo* biodistribution of the radiolabel by counting dissected tissues. The effect of repeated injections was also studied in mice and a baboon. In a separate experiment, Tc-99m-PEG-liposomes were administered to rats after transfusion with serum derived from either liposome-injected or control rats. **Results.** Weekly injections of Tc-99m-PEG-liposomes dramatically influenced the circulation life in rats. Biodistribution 4 hr after the second dose showed a significant fall in blood level (from 52.6 ± 3.7 %ID to 0.6 ± 0.1 %ID) and highly increased uptake in the liver (from 8.1 ± 0.8 %ID to 37.6 ± 9.8 %ID) and -to a lesser extent- the spleen (from 2.2 ± 0.2 %ID to 5.3 ± 0.7 %ID). Subsequent injections attenuated this effect: after the 4th dose, biodistribution had almost returned to normal. Increasing the length of interval also diminished the observed effect. The same phenomenon was noted in a baboon, but not in mice. The enhanced blood clearance of the PEG-liposomes was also observed in rats after transfusion of serum from pretreated rats. **Conclusion.** Intravenous administration of sterically stabilized PEG-liposomes significantly alters pharmacokinetic behaviour on subsequent exposure to PEG-liposomes in a time and frequency dependent manner. This seems to be mediated by a serum factor. The observed phenomenon may have important implications for the clinical use of sterically stabilized liposomes as radiopharmaceuticals, as well as for targeted drug delivery.

OS-134

M. Cremonesi, M. Chinol, M. Ferrari, *H.R. Macke, *E. Jermann, M. Fiorenza and G. Paganelli. Division of Nuclear Medicine. European Institute of Oncology, Milan, Italy and *University Hospital Basel, Switzerland

BIOKINETICS AND DOSIMETRIC CALCULATIONS IN PATIENTS WITH SOMATOSTATIN RECEPTOR EXPRESSING TUMORS ADMINISTERED WITH INDIUM-111 LABELED DOTA-TYR³-OCTREOTIDE (DOTATOC).

Recent advancements in receptor mediated tumor imaging led to the development of a new octreotide analog which can be labeled with the therapeutic radionuclide Y-90 via the macrocyclic chelating agent DOTA coupled to octreotide via the exocyclic D-Phe residue. The new analog, named DOTATOC, has shown high affinity for somatostatin receptors ($K_D \sim 2$ nM), ease of labeling with Y-90 and favorable biodistribution in animal models. The aim of this work was to evaluate the biodistribution and dosimetry of DOTATOC, radiolabeled with In-111, in view of therapy trials with Y-90-DOTATOC. A group of 20 patients affected with neuroendocrine tumors were injected with DOTATOC (10 µg) labeled with 185-222 MBq of In-111. Blood samples were obtained every 5 min in the first hour after injection and less frequently thereafter (up to 50h). The patients were hospitalized and urine was collected throughout the duration of the study (0-2d). Planar and Spect images were acquired using a medium energy collimator at 1, 3, 24, 48h. Regions of interest were drawn over the organs and the tumor area to obtain time activity curves. Two methods were used to calculate the cumulated activities and residence times for each organ: the numerical fit and the compartmental model. Dosimetric calculations were performed according to the MIRD formalism (MIRD3 software). Patients showed no acute or delayed adverse reactions. The residence time in blood was 1.1 ± 0.7 h. The % of the injected dose excreted in the urine in the first 24h was 60 ± 20 %. The agent localized primarily in spleen (S), kidneys (K) and liver (L). The residence times in S, K, L, bladder (B) and remainder of the body (RB) resulted as follows: 2.6 ± 1.9 (S), 1.9 ± 1.1 (K), 2.3 ± 1.8 (L), 4.3 ± 0.2 (B) and 9.7 ± 4.6 h (RB) by numerical fit and 2.2 ± 1.7 (S), 1.8 ± 1.1 (K), 2.2 ± 1.8 (L), 2.4 ± 0.3 (B) and 9.5 ± 4.6 h (RB) by compartmental model. The mean residence time in tumor (T) with both methods was 0.25h (range 0.03-1.1h). In conclusion, the compartmental model seems more appropriate, giving a more accurate analysis of biodistribution and exchange of the radiolabel between organs. Based on this method, the predicted absorbed doses with Y-90-DOTATOC would be 28.0 ± 10.6 (S), 12.3 ± 8.2 (K), 2.7 ± 2.4 (L), 12.3 ± 3.4 (B), 0.3 ± 0.2 (red marrow) and 50 (range 7-350) (T) cGy/37 MBq. These results indicate that high activities can be administered without risk of myelotoxicity although the high radiation doses to the spleen and kidneys impose careful consideration.

OS-135

M. Ricard^{1,2}, I. Clairand¹, B. Collot¹, B. Aubert^{1,2}, M. Schlumberger¹.

¹Institut Gustave-Roussy & ²INSERM U494, Villejuif, France.

RESIDENCE TIME ESTIMATES OF 131I IN HYPOTHYROID CANCER PATIENTS.

Internal dosimetry is needed to evaluate both the mean dose absorbed by a tumor and the risk related to the use of radiopharmaceuticals. Such calculations are generally based on the MIRD method, which assumes a previously determined cumulated activity (\bar{A}). In hypothyroid patients after thyroidectomy standard parameters (e.g. ICRP) may be unreliable.

Thirteen hypothyroid patients after total thyroid ablation for thyroid carcinoma and oral administration of 131I (150 MBq - 4 mCi) underwent whole body external probe counting at day 0 and day 2 and gamma camera examination at day 2. The external probe consisted of a NaI(Tl) scintillator connected to a multi channel analyzer (Nucleus - USA) fitted with a dedicated collimator. Whole body examinations were performed at 6 cm.min⁻¹ using a dual head gamma camera (DHD SMV - France) equipped with a high energy collimator. Total body retention was obtained from the external probe measurements. The activity in stomach, large intestine, bladder contents and pathological foci when exist, was determined on the gamma camera conjugate opposite views (geometrical mean) using ROI.

In the 13 patients, the mean residence times (\bar{A}/A_0) for stomach, large intestine, remaining tissues and total body (as defined in ICRP 53) were respectively equal to 11.9 (sd = 2.3), 14.9 (sd = 3.2), 16.6 (sd = 6.3) and 22.6 (sd = 8.8) hours assuming a monoexponential effective decay. Concerning the total body, the only organ specified in ICRP 53 (thyroid blocked, uptake 0%), the residence time is more two times longer than the data previously published by the ICRP (11.1 hr). Concerning stomach, large intestine and remaining tissues our data are complementary to those of ICRP.

In conclusion this study provides original dosimetric data when the model deviates from the standard one. For instance, regarding the contribution to the total body dose due to the total body retention our data lead to an absorbed dose two times greater when compared to the ICRP data.

OS-136

A.M. Palmer, M. Saunders, S.Whittle and A.W. Preece.

Bristol Fetal Dosimetry Group, Radiopharmacy Unit, Bristol General Hospital, Bristol, BS1 6SY, United Kingdom.

TRANSFER OF RADIONUCLIDES ACROSS THE HUMAN PLACENTA *IN VITRO*.

Purpose: Human data on the transfer of radiopharmaceutical is sparse and therefore extrapolation from experimental animal studies is difficult. This investigation was undertaken to quantify the potential human placental transfer of radionuclides used in medicine or present in the environment in order to provide comparison with data obtained from animal models and to assess the value of this experimental model as an adjunct or potential replacement for animal studies in fetal dosimetry. **Method:** Human placentas were obtained immediately after normal term spontaneous delivery or elective caesarean from women with no identified pathology and where there has been no fetal distress or meconium staining of liquor or placenta. Placentas were transferred to a purpose-built perfusion cabinet maintained at 37°C and maternal and fetal circulation of an isolated cotyledon perfused at physiological pressure with oxygenated heparinised Earls Balanced Salt Solution. This preparation represents the closest *in vitro* approximation to the dynamics of the placenta *in vivo* and has been assessed and validated in physiological terms. The transfer of antipyrine was used as an internal control to provide an index of the efficiency of perfusion. The transfer of 99m-Sodium pertechnetate, 99mTc-MAA, 131-Iodide, 45-Calcium Chloride, 57-Cobalt Chloride and 59-Iron III Chloride were measured by sampling both maternal and fetal perfusion circuits. **Results:** 99mTc, 131-I, 45-Ca and 57-Co all crossed the placenta readily with activity in the fetal circulation steadily increasing as that in the maternal circulation decreased. 99mTc-MAA and 59-Fe did not cross the placenta in significant quantities. After one hour perfusion the transfer of radionuclides was ranked as $131-I > 45-Ca > 57-Co > 99mTc > 59-Fe > 99mTc-MAA$. **Conclusion:** Relative transfer across the placenta in this model did not always correspond with *in vivo* animal data, where Fe-59 readily transfers to the fetus, although the rapid transfer of the other radionuclides is similar to that seen *in vivo*. However, the model appears to have value in screening various chemical forms of a radionuclide, either those used in medicine or present in the environment, in order to target experimental effort in animal models to determine fetal dosimetry.

OS-137

D. Sandrock, U. Dopichaj-Menge, B. Kettner, and D.L. Munz

Clinic for Nuclear Medicine, Charité, Humboldt University Berlin, Germany

HYDRATION DOES NOT IMPROVE IMAGE QUALITY OF BONE SCANS

The incidental observation of good image quality bone scans in those patients who had not taken the recommended 1 liter of fluid between tracer injection and image acquisition inspired us to perform this prospective study on the effect of hydration on the quality of bone scans.

Overall, 3 x 20 patients entered the study, randomized for age and sex (mean age +/- SD, 50.2 +/- 12.2 years; 38 women, 22 men) fulfilling the following criteria: i) no history of kidney disease; ii) normal serum creatinine; iii) no bladder dysfunction/voiding problems; iv) faint uptake in normally shaped kidneys on bone scan. Whole body scintigraphy was performed 180 (+/- 15) min after i.v. injection of 600 MBq Tc-99m MDP. Three groups of 20 patients each were studied: In group 1 they were requested to drink 1 l of water between 1 and 2 hrs p.i.; group 2 had to drink > 1.5 l beginning 1 hr p.i.; group 3 had to drink < 0.25 l, also beginning 1 hr p.i. All patients were requested to void before the beginning of the scintigraphic procedure. The whole body retention of Tc-99m was measured (% injected dose, geometric mean of counts in anterior and posterior view, subtracted for urine activity, corrected for physical decay) and a ratio bone / soft tissue (prox. thigh) was calculated using ROI technique.

To our surprise there was no significant difference in the whole body retention values between the 3 groups (group 1, 50.7 %; group 2, 51.9 %; group 3, 52.0 %; p > 0.1). Group 3 (< 0.25 l fluid intake) had the highest bone / soft tissue ratio (2.75 +/- 0.34) as compared to group 1 (1 l; 2.47 +/- 0.34; p < 0.05) and group 2 (> 1.5 l; 2.24 +/- 0.49; p < 0.01), respectively. There was no dependence of the ratio upon age, sex or serum creatinine (comparable mean value of creatinine in all 3 groups).

Conclusion: According to our data there is at least no benefit to the image quality of bone scans and - due to comparable whole body uptake values in all 3 groups - also no lower radiation burden by forcing hydration.

OS-138

J.A.A. Verwey, A. Hogenbirk, W.F.A.R. Verbakel

ECN - The Netherlands Energy Research Foundation (Petten)

A NEW, FAST 3D MONTE CARLO TREATMENT PLANNING MODEL FOR NUCLEAR MEDICINE

Treatment planning software which is based on interpolation and convolution of dose measurements in a phantom has several limitations. When there is no electron equilibrium (e.g. at material transitions) the calculated dose of such non-physical methods deviates from the actual absorbed dose. Furthermore, these planning programs are generally only 2 or 2* dimensional. Therefore several attempts have been made to build a treatment planning program based on the physical simulation of particle transport using Monte Carlo methods. However, standard Monte Carlo programs are not suited for detailed dose-distribution calculations in a clinical environment due to the vast amount of computation time required. At ECN a software package has been developed which greatly reduces this time of calculation.

A commonly used software package which incorporates the physical aspects of particle transport (photo-electric effect, Compton scattering, pair production, Bremsstrahlung, energy loss etc.) is MCNP. MCNP is a general purpose, coupled photon/electron /neutron 3D Monte Carlo transport program. In MCNP a three dimensional model of a patient can be constructed based on CT-scans.

At ECN MCNP has been substantially modified. Currently ECN-MCNP is capable of calculating detailed 3D dose distributions over a 3D lattice of arbitrary dimensions (voxels of less than 1 mm³ if so required) due to electrons, photons and/or neutrons, for both internal source and external beam geometries.

A case study is presented in which a 3D dose distribution is calculated due to a distributed I-131 source in the mathematical Cristy and Eckerman liver phantom. The separate contributions to the absorbed dose by electrons and photons are obtained concurrently. The case study demonstrates that ECN-MCNP, with its greatly reduced calculation time, is suitable for clinical treatment planning.

Oncology: Breast

OS-139

P. Lind, W. Umschaden, J. Oman, E. Forsthuber, H.J. Gallowitsch, O. Unterweger, H.P. Dinges

Department of Nuclear Medicine & Endocrinology, LKH Klagenfurt, AUSTRIA

COMPARISON OF Tc-99m HYDROXYMETHYLENE DIPHOSPHONAT AND Tc-99m TETROFOSMIN SCINTIMAMMOGRAPHY WITH CONTRAST ENHANCED MRI IN PATIENTS WITH SUSPICIOUS BREAST LESIONS

Mammography (MM) and high frequency ultrasonography (US) are well established methods to screen women for breast cancer. However, the problems of mammography in patients with dense breast and the low specificity make further methods desirable. Aim: The purpose of this study was to compare scintimammography using Tc-99m hydroxymethylene diphosphonate (HDP) and Tc-99m tetrofosmin (TETRO) with Gd-DTPA enhanced MRI in patients with mammographically suspicious breast lesions. Patients and Methods: In 35 women with suspicious MM and/or US further diagnostic work up (MRI, HDP and TETRO) was done within one week. Those 29 patients, who underwent surgery for histological clarification of the lesions were considered for further evaluation of MRI, HDP and TETRO. MRI imaging was performed using T2 TSE (TE 4000, TR 180), dynamic Gd-DTPA enhanced 3D FFE (TR15, TE 6.9, flip 30°) with subtraction. Planar scintimammography in prone position, using a special wedge-shaped device to allow the breasts freely pendent, was performed five minutes after i.v. injection of 555 MBq Tc-99m TETRO and Tc-99m HDP respectively followed by supine SPECT imaging 20 minutes p.i. for Tc-99m TETRO (Elscent Helix HR, LEHR collimator). Results: Histological evaluation of the 29 patients revealed breast cancer in 19 cases (8 pT1, 6 pT2, 5 pT4) and benign disease in 10 of them (7 FCM, 3 FA). The following table shows the results of TETRO (planar and SPECT), HDP and MRI.

	t.p.	f.n.	t.n.	f.p.	SENS	SPEC	NPV	PPV
TETRO SPECT SM	17	2	8	2	89	80	80	89
TETRO PLANAR SM	16	3	9	1	84	86	80	94
HDP SM	13	6	8	2	68	80	57	87
GD-DTPA MRI	17	2	9	1	89	90	82	95

Conclusion: This study shows that both Tc-99m tetrofosmin scintimammography and Gd-DTPA MRI are of additional value in evaluating mammographic suspicious breast lesions. Because of the inferior image quality and the bad overall results of early soft tissue imaging using Tc-99m HDP before bone scanning, this tracer can not be recommended for scintimammography.

OS-140

T.A. El-Magraby¹, H.M. Moustafa¹, S. Galal², A. Selium³, S. Wagih¹.

Departments of Nuclear Medicine¹, Surgery² and Radiology³. Faculty of Medicine, Cairo University, Egypt.

COMPARISON BETWEEN TL-201, 99mTC-MIBI AND MAMMOGRAPHY IN EVALUATION OF BENIGN VERSUS MALIGNANT BREAST LESIONS.

Forty two females with mean age of 44.9 ± 11 years with different breast lesions were all subjected to clinical examination, mammography, radionuclide scanning and biopsy for histopathologic confirmation to evaluate the role of radionuclides in breast lesions. Mammograms were initially routinely interpreted in the radiology department and there reports were considered as a non expert interpretation. The mammograms were then re-interpreted by another radiologist expert in mammography. Radionuclide scanning with TL-201 was performed in 20 patients using a dose of 111 MBq, while 22 patients were studied with 99mTC-MIBI using a dose of 550 MBq. Both qualitative and quantitative evaluation using uptake ratio were done with cut-off level of 1.6 to differentiate between benign and malignant lesions. Mammograms interpreted by the non-expert radiologist had a sensitivity, specificity and accuracy of 73.9%, 63.2%, 69% versus 95.7%, 94.7% and 95.2% by the expert radiologist with significant difference (P < 0.01). TL-201 had a sensitivity, specificity and accuracy of 90.9%, 88.9% and 90.9% versus 100%, 80% and 85.7% in 99mTC-MIBI with no significant difference (P > 0.05). Comparison of both radionuclide scanning with sensitivity, specificity, +ve and -ve predictive values of 95.7%, 84.3%, 88% and 94% respectively versus 73.9%, 63.2%, 70.8% and 66% by non-expert radiologist revealed significant difference while they were comparable with the expert radiologist with a sensitivity, specificity +ve and -ve predictive values of 95.7%, 94.7%, 95% and 94.7% respectively (P > 0.05).

Our preliminary data suggest that the results of both TL-201 and TC-99m MIBI were comparable. Both radionuclides can be very helpful in differentiation between benign and malignant breast lesions and as a complementary method for mammography.

OS-141

L. Mansi*, PF Rambaldi*, V Cuccurullo*, A Laprovitera°, M Scarano* , E Procaccini°
 *Institute of Radiological Sciences, °Institute of Experimental Surgery - II University, Naples

100 BREAST LESIONS EVALUATED WITH Tc-99m TETROFOSMIN SCINTIMAMMOGRAPHY.

We evaluated the role of Tc-99m Tetrofosmin (TF) scintimammography (SMM) in diagnosis of primary breast cancer, local recurrence and axillary lymph node metastases in 90 pts (age range 16-74) with 100 breast lesions (0.4 - 10 cm) or clinical suspicion of recurrence. Static planar images in supine anterior, lateral and prone position were acquired 10 and 120 minutes after i.v. injection of 555 - 740 MBq of TF. SMM detected 63 out of 67 malignant lesions , including 4 recurrences, in 58 out of 62 pts with cancer. The smallest detected tumor was a 0.6 cm infiltrating ductal carcinoma. No clear focal uptake was observed in benign lesions, in the contralateral normal breast or after surgery in absence of relapse. In the same group of pts mammography did not provide a final diagnosis in 20 out of 90 pts. Lymph node uptake was observed in 28 out of 32 pts with axillary and in 2 pts with internal mammary chain metastases. No diagnostic information was added by delayed scans. At a semiquantitative analysis T/Bkg ratios were significantly higher in lateral and prone projections than in anterior views and slightly higher in lateral vs prone. Furthermore, malignant lesions behaved differently with regard to wash-out, suggesting a possible role of TF SMM in functional imaging of chemoresistance, as already demonstrated for MIBI.

OS-142

O.Schillaci*, F.Scopinaro,R.Danieli,M.Ierardi,V.Picardi,P.Cannas,N.S.Tiberio,E.DiLuzio,F.MonteLeone,A.CentiColella Nucl.Med.Sect.,Dept.Exp.Med.Path.,Univ." LaSapienza" ,Rome and *Nucl.Med.,Univ.L'Aquila,Italy

Tc-99m MIBI (M) AND Tc-99m TETROFOSMIN (TF) IMAGING IN PRESURGICAL STAGING OF THE AXILLA IN BREAST CANCER (BC).

M and TF are lipophilic cationic complexes which proved to be useful tumour-seeking agents and showed good accuracy in detecting primary BC. In this study we investigated the presurgical staging of axillary lymph node (ALN) for metastases (met) using M and TF before surgery in 103 female pts (age range: 31-81 years) with BC. Four pts had bilateral Cs, so a total of 107 cases were considered. 57 pts were injected with M and 56 with TF (19 with both tracers in different days). The scintigraphic protocol included 3 planar images, 2 prone lateral and 1 supine anterior views, and 360° chest SPECT with pts in supine position. The clinical stages of the primary Bcs were T1 (n=52), T2 (n=54) and T3 (n=1), those of the axilla were N0 (n=43), N1 (n=58) and N2 (n=6). All pts underwent quadrantectomy (n=39) or mastectomy (n=68) with ALN dissection; ALN status was finally evaluated by histology. The average number of dissected Ns was 19 (range: 12-37); 44/107 cases had met. Results (%):

	PLANAR				SPECT			
	N0	N1	N2	TOTAL	N0	N1	N2	TOT.
SENS.	43.8	73.9	80	63.6	68.8	91.3	100	84.1
SPEC.	100	94.3	100	96.8	96.3	94.3	100	95.2
ACC.	79.1	86.2	83.3	83.1	80.4	93.1	100	90.7

Our findings indicate that SPECT is mandatory for assessing ALN met in BC using M or TF, and show a clear relationship between SPECT results and clinical A stage: sensitivity rose from 68.8% in N0 pts to 92.9% in N1-2 pts. Nevertheless, the high specificity also in pts with palpable Ns is of particular clinical relevance. In pts submitted to both M and TF imaging, the same results were observed. In conclusion, this study suggests that M and TF SPECT might be useful in the noninvasive presurgical evaluation of ALN status in BC; however, false-negative findings in nonpalpable Ns have to be taken into account.

OS-143

E.Scopinaro,*O.Schillaci,R.Danieli,P.Cannas,V.Picardi,E.DiLuzio,F.Capocchetti,M.Di Loreto,A.Centi Colella Nucl.Med.Sect.,Dept.Exp.Med.Path.,Univ." La Sapienza" , Rome and *Nucl.Med.,Univ.L'Aquila,Italy

In-111 OCTREOTIDE AND Tc-99m ANTI-EGFR MoAb UPTAKE IN BREAST CANCER.

The presence of somatostatin receptors in breast cancer has been reported by some authors, whereas the role of epithelial growth factor receptors (EGFR) is still debated.

We have performed double radioisotope scan with In-111 pentatreotide and Tc-99m anti-EGFR MoAb in 6 pts with breast cancer. Written informed consent was always obtained. 3 cancers were N0, 2 N1 and one N2. Scintigraphies were performed at 4 and 24 hrs after i.v. administration of 74 MBq of In-111 octreotide and 900 MBq of Tc-99m MoAb. All the primary tumors, including a very small T1a cancer, showed positive octreotide scan, whereas only one axillary node (N2) was octreotide +. Only N+ pts showed MoAb uptake on primary tumours, with positive scans in 2 out of 3 axillas. As a collateral finding, all the pts aged less than 50 showed In-11 octreotide uptake in the nipples (well distinct from tumour uptake); one woman (35 years old) in premenstrual phase showed diffuse breast uptake of In-111 octreotide. The presence of EGF receptors on breast cancers seems to be related to cancer invasiveness. It can be theorized that In-111 octreotide uptake is related to angiogenesis, regardless its nature (neoplastic or physiologic).

OS-144

H.A. Nabi¹, D.M. Goldenberg², L. Lamki³, B. Barron³, and the Immunomedics Study Group.

State University of New York at Buffalo, NY,¹ Garden State Cancer Center, Belleville, NJ² and University of Texas Medical Center, Houston, TX, USA³

THE ROLE OF CARCINOEMBRYONIC ANTIGEN (CEA) IMAGING IN THE DIAGNOSIS OF BREAST CARCINOMA

Numerous methods have demonstrated the expression of CEA in breast cancers, despite only modest or no elevations in the serum of patients with limited disease. The current prospective, multicenter trial assessed the diagnostic role of CEA immunoscintigraphy (IS) with Arcitumomab (CEA-Scan® Immunomedics, Morris Plains, NJ, USA), a ⁹⁹Tc-conjugated anti-CEA Fab¹. Both patients with proven (N=78) or suspected (N=80) breast cancer were given a 1mg, 20 mCi, dose of Arcitumomab, and supine planar images of the anterior and lateral chest views were made at ca. 4 h. Prior to IS, all patients had a mammography (MM), followed by biopsy after IS. In the confirmed breast cancer group, a sensitivity of 82% was found; lesions > 1 cm were more detectable than smaller ones. In 80 patients presenting with non-palpable lesions and suspicious MM, tumor/nontumor ratios (compared to the contralateral breast) discriminated benign from premalignant and malignant pathology. In this difficult population, IS had a sensitivity and PPV in 16 T1 breast cancers of 44% and 78%, whereas MM was 62% and 40% respectively. Among 64 patients with proven benign breast disease, IS showed a significantly higher specificity (P=0.002) than MM (97% vs. 77%) IS with Arcitumomab showed a lower FP rate than MM (2.5% vs. 19%), and a lower FN rate than MM (5.4% vs. 10.3%) in 55 patients with indeterminate or suspicious MM. Thus, Arcitumomab provides the high specificity needed as a secondary test complementing the high sensitivity of MM. (Supported in part by NIH grant CA 39841 and by Immunomedics, Inc.)

Oncology: Therapy
OS-145

D.ia Goldenbere¹, M. Juweid¹, R.M. Sharkey¹, J. Burton¹, A. Bhatnagar², and A. Alavi²

Garden State Cancer Center, Belleville, NJ¹ and the Hospital of the University of Pennsylvania, Philadelphia, PA, USA²

RADIOIMMUNOTHERAPY OF B-CELL LYMPHATIC TUMORS WITH A RADIOIODINATED, HUMANIZED, ANTI-CD22 MONOCLONAL ANTIBODY, hLL2.

Escalating doses of hLL2 labeled with ¹³¹I (LymphoCide™, Immunomedics, Morris Plains, NJ, USA) are being given I.V. to patients with non-Hodgkin's lymphoma (NHL) and B-CLL who failed prior chemotherapy. The dose given was based on red marrow radiation dose (RMD) estimates, as determined by a trace study with 6 mCi ¹³¹I-hLL2 (0.75 mg/kg) 1 wk prior to therapy (0.75 mg/kg protein). The RMD was obtained by sacral scintigraphy, and showed a good agreement between the tracer and therapy studies (r=0.75). Human anti-hLL2 Mabs did not develop in any of the patients treated. Marrow doses up to 100 cGy (30-44 mCi injections) did not result in dose-limiting toxicity, so the escalation is continuing. Of the 13 patients (1 high-, 8 intermediate-, 3 low-, and 1 unknown grade) treated to date, 1 had a CR for 9+ mos, 1 a PR for 3 mos, 2 a mixed response for 4 mos, and 2 stable disease for 1.5 and 3 mos. Of the 9 who failed prior high-dose chemotherapy, 3 showed an objective response, including the CR. Hence, radioimmunotherapy with ¹³¹I-hLL2 can be implemented in NHL and CLL with marrow suppression being the only limiting toxicity, and can result in objective responses in patients with chemoresistant, aggressive forms of NHL, as well as the indolent type. Since hLL2 is an internalizing antibody, studies with ⁹⁰Y-hLL2 are beginning. (Supported in part by NIH grants CA67026 and CA39841.)

OS-146

J. Tennvall, O Lindén, E Cavallin-Ståhl, L Darte, M Garkavij, KJ Lindner, M Ljungberg, T Ohlsson, K Sjögreen, K Wingårdh, S-E Strand. Depts. of Oncology, Radiophysics, Hospital Pharmacy, University Hospital, Lund, Sweden.

RADIOIMMUNOTHERAPY USING ¹³¹I-IODINE ANTI-CD22 (LL2) IN PATIENTS WITH PREVIOUSLY TREATED B-CELL LYMPHOMAS. PRELIMINARY RESULTS.

The CD 22 B-lymphocyte surface antigen expressed by B-cell lymphomas has been previously described as a target for radioimmunotherapy (RIT) using radiolabelled antibodies. Here we report our preliminary results of a phase I-II trial of nonmyeloablative doses of a ¹³¹I-labelled mouse anti-CD 22 antibody (LL2, Immunomedics, Morris Plains N.J.).

Patients and Methods: Patients with B-cell lymphomas, who had failed at least one, but not more than two chemotherapy regimens and had measurable disease stage I-IV with less than 25% B-cells in unseparated bone marrow and targeted at least one lesion on immunoscintigram with ^{99m}Tc LL2Fab were eligible for RIT. Five of 6 patients examined with immunoscintigraphy did unequivocally target and were given trace labelled doses of ¹³¹I anti-CD22 for dosimetric studies. One week later treatment with labelled antibody 36mCi/m² (1330MBq/m²) preceded by 20mg of cold antibody was administered.

Results: Response. All 5 treated patients are evaluable for response. There are 2 partial remissions, one stable disease (duration 6+, 3+, 13+ months) and two patients with progressive disease. Of the responders one has a diffuse large cell lymphoma, and the other a follicle center lymphoma grade II. **Toxicity.** Four of 5 patients are evaluable for haematological toxicity. One patient died of progressive disease four weeks after RIT. Of evaluable patients two had subnormal blood counts on enrolment and they suffered a grade 3 and a grade 4 toxicity respectively, that did not return to baseline. The other two patients had only transient grade 3 and grade 2 toxicity, respectively. Two patients have developed HAMA. Non-haematological toxicity was mild.

Conclusions: Nonmyeloablative RIT in B-cell lymphomas with ¹³¹I labelled mouse anti-CD22 can induce objective remissions in patients with aggressive as well as indolent lymphomas, who had failed prior chemotherapy. The toxicity is mainly haematological and patients with subnormal blood counts on enrolment seem to be more at risk for haematological side-effects.

OS-147

YM Zhang, JL Deng, Y Peng

German Cancer Research Center, Heidelberg, Germany.

ENDOSCOPIC TUMOR INTRASTITIAL INJECTION RADIOIMMUNOTHERAPY OF GASTRIC CARCINOMA: BIODISTRIBUTION, PHARMACOKINETICS AND DOSE ESTIMATIONS

To increase the therapeutic ratio of radioimmunotherapy, 370-555 MBq I-131-labeled anti-gastric carcinoma monoclonal antibody MG7 (I-131-MG7) was administered to 10 patient with gastric carcinoma using endoscopic tumor intrastitial injection(TISI). Two typical patients were taken for pharmacokinetics and dosimetric study. Serial whole body and static images were taken; blood, urine and feces samples were collected until 144 h post TISI. AT 72 h, 10 mCi Tc-99m pertechnetate was iv injected for orientation the ROIs of the normal gastric tissue and other organs. Tumor and organs radiation absorbed doses were calculated according to MIRD Schema. The findings were as follows: Higher activity and prolonged retention in tumor were observed with a cumulated activity reaching up to 5.6 (case 1) and 7.2 (case 2) MBq-h /MBq, respectively. There were two different distribution and pharmacokinetics patterns. One was feces excretion dominant (case 1), substantial activity in the gastrointestinal tract was visualized and 31 % injected dose excreted into feces within 48 h post TISI, and less than 10% injected dose was found in urine until the end of the study (144h). The other pattern was urine excretion dominant (case 2), in which 36 % injected dose was excreted into urine and no detectable activity in feces until the end of study. The absorbed doses (mGy/MBq) were:

	Tumor	Gastric	Liver	Kidney	Gut	WB	BM
Case 1	20,68	1,08	0,27	0,32	0,89	0,05	0,05
Case 2	29,14	1,27	0,49	0,59	1,41	0,14	0,68

The effective dose equivalent was 1.74 cSv with 555 MBq I-131-MG7. In conclusion, the method we used could deliver much higher radiation doses to the tumor and lower radiation burdens on the normal tissues that the conventional RIT and TISI with free- I-131 sodium iodine we used in the previous study.

OS-148

P.Riva*, G.Franceschi*, M.Casi*, R.Gentile*, G.Moscatelli*, A.M.Cremonini*, M.Frattarelli*,G.Guiducci*,N.Riva* and H.Make^.

*Nuclear Med. Dept. and Ist.Oncologico Romagnolo, ^Neurosurgery Dept. "M.Bufalini" H.-Cesena ITALY; ^Inst.of Nuclear Med. Kantonsspital-Basel (SWITZERLAND).

LOCO-REGIONAL RADIOIMMUNOTHERAPY WITH Y-90 LABELED MONOCLONAL ANTIBODIES IN THE TREATMENT OF HIGH GRADE MALIGNANT GLIOMA: A PHASE I AND PHASE II TRIAL.

A previous pilot study regarding the loco-regional radioimmunotherapy of 81 evaluable glioblastoma patients by means of antitenascin Mabs labelled with I-131 (mean dose 2035 MBq) was carried out on the course of seven years. The outcomes were as follows: the median survival was prolonged up to 25 months and the response rate (PR+CR+NED:No Evidence of Disease in cases treated with minimal lesions after previous regimens) was 44%. Following this promising experience the protocol was modified by using Y-90 instead of I-131. The benzyl-DTPA-BC2 or BC-4-Y-90 complexes were utilised: they showed a very good stability both in vitro and in vivo. Firstly a phase I study was carried out in 15 patients, already submitted to all conventional treatments, but with progressive disease. They were intralesionally given escalating Y-90 doses (185-370-555-740-925 MBq), 3 cases were included in each incremental level. This treatment did not produce any change in blood cells as well as in liver and kidney parameters. The normal brain was spared in most cases. Only in few patients a local transient cerebral oedema was recorded. The radiopharmaceutical concentrated only in the tumoral bed and did not spread in healthy cerebral tissue or in distant normal organs. The radiation dose delivered to the tumour was, on mean, 0.54 Gy per MBq of Y-90 administered and resulted about 4 times higher with respect to I-131. Then a phase II study has been started including, so far, 26 evaluable patients (19 glioblastoma and 7 anaplastic astrocytoma; 7 newly diagnosed and 19 recurrent tumour) who previously received all customary regimens. The mean dose of Y-90 was 740 MBq; in many cases the cycles were repeated: 14 patients had two infusions, 7 three infusions and 2 four courses. The tolerance, the biodistribution and the dosimetry resulted identical with the values recorded during the Phase I. The objective response consisted in 6 PD, 4 SD, 7 PR, 3 CR and 6 NED. The global response rate (PR+CR+NED) was 61.5% (57.8% in glioblastomas and 85.7% in anaplastic astrocytoma group). In 6 cases (3 glioblastoma and 3 anaplastic astrocytoma) a complete tumour disappearance was radiologically (MRI) observed. These data are preliminary but indicate the possibility to improve the clinical effects by employing this novel isotope with respect to I-131, to better control these otherwise intractable tumours.(Work supported by AIRC: Italian Association on Cancer Research and by Cassa di Risparmio Cesena).

OS-149

AC PERKINS, ODM HUGHES, M FRIER, MC BISHOP, MR PRICE, G DENTON, ML WASTIE, PA SHUBIGER. University Hospital and City Hospital, Nottingham, UK and Paul Scherrer Institute, Switzerland.

DIAGNOSIS AND THERAPY OF BLADDER CANCER USING RADIOLABELLED ANTI-MUC1 MUCIN ANTIBODY (C595)

Introduction: C595 antibody recognises the protein core of MUC1 mucin which is upregulated in bladder cancer. We have evaluated the diagnostic and therapeutic potential of this antibody using In-111 and Cu-67 respectively.

Materials & Methods: 8 patients with superficial, locally invasive or metastatic disease were given of 80MBq (1mg) In-111-C595 i.v. and whole body imaging performed after 48 hours. 14 patients with superficial tumours identified by preoperative radiology underwent intravesical administration of 20MBq (500mg) Cu-67-595 antibody. Activity was drained after 1 hr and the bladder washed out. Uptake was assessed by imaging and assay of activity in resected tissues.

Results: Locally invasive disease (n=3) and distant metastases (n=3) were identified following i.v. administration of In-111-C595. Superficial tumours (n=2) were not seen using the systemic approach. Following intravesical administration, 11 of 13 patients with superficial tumour confirmed by cystoscopy were correctly identified. No uptake was seen in 1 patient with cystitis and no tumour. The mean % dose/gram was 0.056%±0.048% in tumour and 0.0082%±0.0086% in normal tissue (p<0.001) giving a T:NT ratio of 14:1.

Conclusions: These studies indicate the potential of anti-mucin antibody in the staging and therapy of bladder cancer. A Tc-99m conjugate is currently being evaluated for staging. The intravesical administration of a therapeutic conjugate such as Cu-67-C595 provides an attractive approach for the therapy of superficial bladder tumours.

OS-150

T.M. Behr¹, T. Liersch², S. Gratz¹, F. Schmidt³, R. Canelo³, T. Lor³, S. Post², B. Wörmann⁴, W. Hiddemann⁵, H. Becker², B. Ringe³, and W. Becker¹.

Departments of Nuclear Medicine¹, General² and Transplantation³ Surgery, and Hematology-Oncology⁴ of the Georg-August-University of Göttingen, Germany.

RADIOIMMUNOTHERAPY OF COLORECTAL CANCER PATIENTS WITH SMALL VOLUME DISEASE: RESULTS OF A CLINICAL PHASE-I/II TRIAL.

The five-year survival of colorectal cancer patients with surgically unresectable metastases is close to zero, despite the development of several new chemotherapeutic agents. Therefore, novel therapeutic strategies are warranted. Whereas radioimmunotherapy (RIT) has shown disappointing results in "bulky disease" of solid tumors, preclinical results in small volume disease are promising. The aim of this ongoing study is to evaluate, in a phase-I/II trial, the therapeutic efficacy and dose-limiting toxicity of RIT in colorectal cancer patients with small volume disease.

So far, 40 colorectal cancer patients with small volume disease (all lesions ≤ 2.5 cm) have been entered in the ongoing mCi/m²-based dose escalation study with the ¹³¹I-labeled murine anti-CEA MAb, F023C5, which belongs to the IgG₁ subtype. The patients were given single injections, starting at 50 mCi/m², and escalating in 10 mCi/m² increments (3 patients/dose level; 6 patients, if one of these three patients develops a grade-4 toxicity). The maximum tolerated dose (MTD) is defined as the very dose level where ≤ 1/6 patients develop a grade-4 myelotoxicity.

Thirty-one of the 40 patients had lesions known from radiological procedures (CT, MRI), 9 patients suffered from occult disease, as indicated by elevated and/or rising tumor markers (CEA, CA19-9) without radiological correlate. At mean red marrow doses of 0.45 cGy/mCi, myelotoxicity was dose-limiting, and a fairly good correlation between the red marrow doses and resulting toxicities was found. At 110 mCi/m² (i.e., the MTD), patients regularly developed grade-3, at 120 mCi/m² 2/6 patients had a grade-4 leuco- or thrombopenia. Tumor doses increased exponentially with decreasing tumor sizes (up to 185 cGy/mCi in a 0.5-cm lung lesion). In the 31 patients with radiologically documented lesions, one had a complete, 7 had partial remissions (corresponding to an objective response rate of 26%); twelve patients (i.e., 39%) experienced stabilization of their previously rapidly progressing disease, lasting for up to 18+ months. The majority of patients showed a significant (i.e., > 50%) decrease of tumor marker levels in blood.

Myelotoxicity is the only dose-limiting toxicity of the ¹³¹I-labeled monoclonal anti-CEA antibody F023C5. The MTD has been reached at 110 mCi/m², which is, therefore, the very dose level of the ongoing phase-II arm. Although many patients have been treated below this dose level, the observed anti-tumor effects are encouraging. Further studies are ongoing. (Supported in part by DFG grant Be 1689/4-1).

Infection/inflammation/hematology: Imaging infections

OS-151

R Binnink, M Peeters, F Van Acker, G D'Haens, P Rutgeerts, L Mortelmans.

Dept. Nuclear Medicine UZ Leuven Belgium.

Tc99m-HMPAO WBC SCINTIGRAPHY IN THE ASSESSMENT OF THE EXTENT AND SEVERITY OF AN ACUTE EXACERBATION OF ULCERATIVE COLITIS.

Introduction: Ulcerative colitis (UC) is an inflammatory bowel disease with frequent acute exacerbations with risk of toxic megacolon and severe complications. In severe disease, it is contraindicated to perform a colonoscopy to assess the severity and the extent of the disease. The aim of the present study was to assess if Tc99m-HMPAO labeled white blood cell (WBC) scintigraphy can replace colonoscopy to determine the extent and the severity of the disease in these critically ill patients.

Methods: 20 consecutive patients (7F, 13M, age 38.1 ± 13.1 yr.), with a severe attack of UC, underwent scintigraphy the day of admission. WBC's were labeled with 200 MBq Tc99m-HMPAO. Planar anterior and posterior imaging of the abdomen was performed 45 and 120 min. after WBC reinjection. The tracer uptake in the different colon segments was scored in comparison with the normal bone marrow uptake¹ on a scale from 0 to 3. Rectosigmoidoscopy with biopsy was performed within 24 hours after scintigraphy. Sign test for matched pairs was used for statistical analysis.

Results: The mean symptom score (Lichtiger) and CRP were respectively 12.7 (±0.7) and 6.8 (±1.3) mg/dl. No significant difference was found between the scintigraphic score¹ of the rectum and respectively the endoscopic (Loefberg, NS), the symptoms (NS) and the histologic (Gomez, NS) score. The best correlation was found with the latter score (r=0.98). Based on scintigraphy, disease was found to involve the left side of the colon up to the splenic flexure in 10 patients. The other patients had a pancolitis.

In conclusion: Disease severity can adequately be determined by planar white blood cell scintigraphy in patients with a severe attack of ulcerative colitis. Since presence and severity of disease correlates well with endoscopic and histologic findings, WBC scintigraphy can assess disease extent without need for colonoscopy. This reduces morbidity in already critically ill patients.

¹Papos et al. Dig Dis Sci 1996;41:412-420.

OS-152

K.E. Britton, V. Soroa, H. Amaral, J. Malamitsi, H. Kartamihardja, F. Sundrum, H. Mustafa, A. Bhatnagar, G. Nair, St. Barts, London; CNEA, Buenos Aires; Alemana, Santiago; Hippokraton, Athens; Sadikin, Bandung; General Hospital, Singapore; Nemrock, Cairo; INMAS, Delhi; IAEA, Vienna.

Tc-99m "INFECTON", PRELIMINARY EVALUATION IN OVER 500 PATIENTS THROUGH AN IAEA CO-ORDINATED RESEARCH PROGRAMME

The aim of the study was to evaluate a 4-fluoroquinolone antibiotic ciprofloxacin, labelled by reduction with Tc-99m, called Infecton, in patients with a range of acute or chronic inflammation, infection or fever in eight centres around the world. The new formulation takes 10 minutes to prepare. After i.v. injection 400 MBq Tc-99m Infecton whole body and or local images were taken at 1 and 4 hours (and 24 hours for joints) using a conventionally set up gamma camera. Findings were evaluated against microbiology, an alternate imaging agent (labelled white cells, immune globulin, dextran colloid as appropriate to the country), a radiological technique and clinical outcome.

Results show 333 true positive, 28 false positive, 165 true negative, 27 false negative, giving a sensitivity of 93%, specificity 86%, and predictive values: positive 92%, negative 86%, accuracy 90%. No side effects were seen in these 553 studies. Tc-99m Infecton has been shown to be a bacterial specific imaging agent. It was particularly effective in evaluating painful joint prostheses for infection.

OS-153

MM. Wellington¹, PH. Nibbering², A. Paulusma-Annema², PS. Hiemstra³, W. Calame^{1,4}, EKJ. Pauwels¹

¹ Departments of Radiology, Division of Nuclear Medicine, ² Infectious Diseases, and ³ Pulmonology, Leiden University Medical Center, Hercules European Research Center, Barneveld, The Netherlands

IMAGING OF EXPERIMENTAL BACTERIAL INFECTIONS WITH A 99mTECHNETIUM LABELED ANTIBACTERIAL PEPTIDE

This study was designed to evaluate whether 99mTc-labeled human neutrophil peptide (HNP)-1 can be employed as tracer for rapid localization of experimental bacterial infections.

Methods: Thigh muscle infections were induced in mice by injection of 1 x 10⁸ viable *Klebsiella pneumoniae* (KP) or *Staphylococcus aureus* (SA). Five minutes (acute phase infections) or 18 h (established infections) thereafter, 0.4 µg of 99mTc-labeled HNP-1 was administered intravenously and high resolution whole body scintigraphy was performed. To obtain data about its clearance by organ uptake, and accumulation at sites of infection, regions of interest were drawn over the heart, major organs, and both thighs at various time intervals. Accumulation of 99mTc-HNP-1 is expressed as the ratio between the target (infected) and non-target (non-infected) thigh. For reasons of comparison the behaviour of 99mTc-IgG was studied. At 4 h or 24 h after injection, the binding of 99mTc-HNP-1 to blood leucocytes was determined and a possible relationship between the binding to blood leucocytes and the ratio of accumulation of 99mTc-HNP-1 in infected areas was estimated using the Pearson correlation coefficient. Also, a peritoneal infection model was used to investigate whether accumulation of 99mTc-HNP-1 was related with binding to bacteria and leucocytes at the site of infection.

Results: In this study we observed a significant (p<0.05) faster accumulation of 99mTc-HNP-1 at the site of KP and SA infections than with 99mTc-IgG. Calculations revealed a relationship (r=0.867, P<0.005) between binding of 99mTc-HNP-1 to blood monocytes and its accumulation in infected areas. At early time-intervals, we observed a relationship between the binding to granulocytes (r=0.639, P<0.05), macrophages (r=0.697, P<0.05), and bacteria (r=0.597, P<0.05), and the accumulation of 99mTc-HNP-1 in the infected peritoneum.

Conclusions: 99mTc-HNP-1 is a potential marker for fast detection of bacterial infections. Binding of HNP-1 occurs to bacteria as well as to phagocytes at the site of infection appears to be related to the early accumulation of 99mTc-HNP-1 in infected areas.

OS-154

W.J.G. Oyen, O.C. Boerman, J.A. Barrett^{*}, F.W.A. Verheugt, D.J. Ruiters, J.W.M. van der Meer, F.H.M. Corstens.

University Hospital Nijmegen, Dpts. of Nuclear Medicine, Cardiology, Pathology and Internal Medicine, The Netherlands and ^{*} The DuPont Merck Pharmaceutical Company, Radiopharmaceutical Division, North Billerica MA, USA.

Tc-99m-LABELED GLYCOPROTEIN IIb/IIIa RECEPTOR ANTAGONIST DMP444 FOR EVALUATION OF EXPERIMENTAL BACTERIAL ENDOCARDITIS.

Bacterial endocarditis is an important clinical problem, that may result in persisting bacteremia and irreversible cardiac damage. Since endocarditis is characterized by aggregation of activated platelets, fibrin and bacteria, we studied the potential of DMP444, a technetium-99m-labeled high-affinity antagonist of the glycoprotein (GP) IIb/IIIa receptor, expressed on activated platelets.

In five Beagle dogs (11-15 kg), the left ventricle was catheterized via the right carotid artery. One hour later, 5x10⁷ colony forming units of *S. aureus* were injected intracardially via the catheter. Half an hour later, the catheter was removed. Two extra dogs underwent a complete sham procedure, only omitting injection of bacteria. One day after the intervention, the dogs were injected with 37 MBq/kg DMP444 and imaged up to 4 hours after injection. Subsequently, the dogs were killed and samples were obtained for tissue counting, microbiology and histology.

All infected dogs developed endocarditis, as proven by cultures and histology. The control dogs showed no growth of bacteria and normal histology. From 1 to 2 hour post injection onward, the images showed clear focal and with time increasing DMP444 accumulation at the aortic valve region when endocarditis was present. The controls only showed persisting blood pool activity without any focal abnormality, indicating that the procedure itself did not cause detectable platelet aggregation. At 4 hours post injection, image analysis showed *in-vivo* valve-to-blood-pool ratios of 1.87 ± 0.18 in endocarditis and 1.01 ± 0.05 in controls (p<0.05). *Ex-vivo*, the valve region to blood ratios were 1.75 ± 0.45 and 0.10 ± 0.01, respectively (p<0.05).

Targeting activated platelets with the Tc-99m-labeled GP-IIb/IIIa antagonist DMP444 allows a final diagnosis of experimental bacterial endocarditis within a 4 hour time span, due to high, specific and fast *in-vivo* uptake.

OS-155

Matteucci E.^{*}, Corbelli C.^{*}, Calandra G.[^], Morisi C.[°], Zabberoni W.[#]

^{*}Nuclear Medicine Dpt, Faenza (Ra), [^]Urgency Dpt, [°]Pathology Dpt and [#]Infective Disease Division, Ravenna (Italy).

RELEVANCE OF NUCLEAR MEDICINE METHODS IN THE DIAGNOSIS OF OSTEOMYELITIS (OM) IN DIABETIC FOOT.

Early and accurate diagnosis of infection of the diabetic foot is the key to successful management; diagnosis is difficult because the clinical likelihood of OM often does not appear through radiographic imaging.

The aim of our study was to evaluate the diagnostic value of 99mTc-HMPAO-leukocyte scan (WBS) in combination with 99mTc-MDP bone scintigraphy (BS) for detection of OM in diabetic patients.

We have studied 35 patients (pts), (14 male and 21 female) with mean-age 59 (range 22-74 yr.) with insulin dependent-diabetes, foot ulceration and suspicion of OM; all patients were submitted to clinical examination, radiography, ultrasonography and bacterial culture. All pts underwent BS with 740 Mbq Tc-99m-MDP while injected, five minutes and three hours after being injected; a week later they were submitted to WBS, 4 and 24 hours after the administration. BS and WBS images were compared and defined as positive or negative for OM. The final diagnosis was established by clinical follow-up and histological findings.

OM was confirmed in 18 cases with WBS and BS; in 9 patients WBS and BS were negative for OM, confirmed by clinical follow-up; in 3 patients who resulted affected by OM, BS was negative while WBS was positive. In 3 patients giving negative results, BS showed a false-positive pattern, while in 2 patient with OM and BS positives, WBS was false negative.

The estimated diagnostic value of the methods was reported in the table

	WBS	BS
SENSITIVITY %	91	87
SPECIFICITY %	100	75
ACCURACY %	94	83

Our study confirms the importance of the nuclear-medicine procedures in the diagnosis of OM; compared with BS, WBS proved to be more sensitive, specific and accurate.

OS-156

V. Ivančević, S. Sen Gupta, D.L. Munz

Clinics for Nuclear Medicine and Bone and Joint Surgery, Charité, Humboldt University Berlin, Germany

IMAGING OF LOW-GRADE OSTEOMYELITIS WITH Tc-99m LABELLED MONOCLONAL ANTI-NCA 90 Fab' FRAGMENT

Low-grade osteomyelitis represents a serious clinical problem, since diagnostic options are often insufficient, yet therapeutic implications of proven disease important, especially in patients with prosthetic joint replacement. Tc-99m labelled monoclonal anti-NCA 90 granulocyte antibody Fab' fragment (AGFab) has been shown to be useful in bone and joint infection, but there is no data specifically referring to low-grade osteomyelitis.

We prospectively analyzed 22 scans in 17 consecutive patients (age range, 30-85 years; median age, 63 years) referred for suspected low-grade osteomyelitis. There were 11 patients (13 scans) with prosthetic hip replacement, one with knee replacement, two patients (3 scans) with resected hips and no endoprosthesis (Girdlestone) and 3 (5 scans) without prior surgery. Low-grade osteomyelitis was proven clinically, serologically and/or by surgery in 7 patients and excluded in 8, among the latter being a patient from the infectious group after successful therapy. Another patient turned out to have a synovialitis and in two patients final diagnosis could not be established.

One, 5 and 24 h after intravenous injection of up to 1.1 GBq of AGFab whole-body and planar scans were performed using a dual-head gamma camera. There were 8 true positive scans in the 7 patients with verified osteomyelitis and 5 true negative scans in 5 patients. However, 4 scans in 3 patients were judged as false positive, whereas 4 scans were positive in the two patients without final diagnosis. The patient with synovialitis showed a positive scan which therefore had to be considered as false positive regarding low-grade osteomyelitis. Interestingly, 6/7 true positive and all the 5 true negative patients had hip endoprostheses. Of the 3 patients with false positive scans, two (3 scans) had Girdlestone hips and the third a loosened hip endoprosthesis.

In conclusion, AGFab imaging proved to be accurate in detecting and excluding low-grade osteomyelitis in our group of patients with hip endoprostheses. The results in patients with Girdlestone hips and loosening of hip endoprosthesis, respectively, indicate that there is reactive inflammation, probably due to mechanical irritation caused by the bone fragments, which cannot be differentiated from low-grade osteomyelitis.

Neurology/Psychiatry: PET

OS-157

O. Sabri, D. Hellwig, M. Schreckenberger, H.J. Kaiser, G. Wagenknecht, U. Büll.

Dept. of Nuclear Medicine, RWTH Aachen, Germany

INFLUENCE OF DIABETES MELLITUS (DM) ON REGIONAL CEREBRAL GLUCOSE METABOLISM (rMRGlu) AND REGIONAL CEREBRAL BLOOD FLOW (rCBF)

Aim: Different studies show both increased and decreased cerebral rMRGlu/rCBF values in DM. We sought to elucidate the influence of DM on rMRGlu/rCBF in 57 patients with cerebral microangiopathy (CMA).

Methods: 16 patients showed a DM requiring therapy (11 oral antidiabetics [ODM], 5 insulin-dependent DM [IDDM]). Using a special head holder for exact repositioning, rMRGlu (PET with 18-FDG) and rCBF (SPECT with 99mTc-HMPAO) were imaged and measured in slices, followed by MRI. White matter (periventricular, centrum semiovale) and cortex (frontal, parietal, temporal, occipital) were defined within ROIs taken topographically from the MRI (overlay). rMRGlu was calculated after Sokoloff, rCBF normalised to the cerebellum. Diabetic and non-diabetic CMA patients were compared to age-matched controls (n=19).

Results: DM patients showed significantly lower rMRGlu/rCBF values in all cortical and subcortical ROIs ($p < 0.05$) than did controls, while non-diabetic patients did not show different rMRGlu/rCBF values ($p > 0.05$). There were no significant ODM-IDDM differences ($p > 0.70$). The rMRGlu/rCBF values did not depend on the venous blood glucose levels at the time of the PET examination. However, analyses of variance (ANOVAs) with the factors DM, atrophy, and morphological severity of microangiopathy (as determined by the number of lacunar infarctions [LI] and severity of deep white matter lesions [DWML] on MRI) showed that lowered rMRGlu/rCBF values in the DM group were due only to the concomitant atrophy ($F > 7.5$, $p < 0.01$) while neither DM nor LI/DWML had any influence on rMRGlu/rCBF ($F < 1.5$, all $p > 0.2$). No 2-way or higher interactions were found for any of the factors. **Conclusion:** It can thus be seen that a supposed decrease of rMRGlu/rCBF in DM is in fact only mimicked by the concomitant atrophy. All earlier studies failed to correct for atrophy, and a critical reappraisal of these findings is in order.

OS-158

F. Chierichetti, P. Zanco, D. Rubello, S. Cargnel, A. Fini, B. Saitta, L. Vettorato, G. Ferlin.

General Hospital: Nuclear Medicine - PET Center, Castelfranco Veneto ITALY

18F-FLUORODEOXYGLUCOSE (18F-FDG) POSITRON EMISSION TOMOGRAPHY (PET) IN THE FOLLOW UP OF PRIMARY BRAIN TUMORS: ANYTHING NEW?

AIM OF THE STUDY: many studies have been performed by 18F-FDG PET in brain tumors. The aim of our report is to assess, considering retrospectively a large group of patients (pts), if 18F-FDG PET may add something, respect to previous experiences, in the clinical follow up of primary brain tumors.

PATIENTS AND METHODS: we studied by 18F-FDG PET 211 pts who underwent surgery, radio- and/or chemotherapy for primary brain tumors (190 gliomas grade I-IV, 17 lymphomas and 4 primary neuroectodermal tumors). All pts were evaluated over a 3 years period and serial (up to 7) PET and MRI studies were performed. Brain biopsy and late clinical evidence were taken as gold standards. PET scans were examined both visually and by semi-quantitative analysis (lesion/controlateral white matter FDG uptake, according to the method proposed by Di Chiro).

RESULTS: considering the first imaging, both PET and MRI correctly diagnosed tumor recurrence in 96 and radionecrosis in 68 cases out of 211. Among these pts there was a miscellaneous for kind of tumor and initial grading. In other 43 pts PET but not MRI was positive for tumor relapse. In most pts (70%) of this group, with low grade gliomas, the FDG uptake in the lesion was greater than expected for the initial grading and histology showed a shift to a higher one. In some cases, pts were not immediately treated but further studied by MRI which became positive for recurrence later. Finally, in 4 pts with low grade gliomas MRI but not PET proved the relapse.

CONCLUSIONS: in our experience, 18F-FDG PET was a significantly more sensitive (97.2%) tool than MRI (69.9%) (χ^2 -square, $p < 0.001$) in the diagnosis of tumor recurrence, thus confirming previous reports. However, in our pts, PET was much more usefull in presence of grading shift suggesting that, especially for low grade tumors, PET scan in the follow up represents a substantial gain in the timing of diagnosis and treatment.

OS-159

L. Bick, B. Baument, S. Kneifel, U.M. Lütolf, G.K. von Schulthess

University of Zürich, Clinical Center, Department of Radiology, Division of Nuclear Medicine and Division of Radio-Oncology, Zürich, Switzerland

SERIAL FDG-PET STUDIES OF HIGH GRADE GLIOMAS AFTER RT: PATTERNS OF RECURRENCE AND PREDICTION OF SURVIVAL

The aim of this study was to evaluate changes in FDG-uptake after radiation therapy (RT). We were interested in the accuracy of FDG-PET in predicting patient survival and the response to RT. Furthermore, patterns of recurrence should be determined.

Methods: From March 1996 until January 1998, 121 serial FDG-PET studies were performed on 18 patients (16 male, 2 female, age 30-74 ys). All patients had histologically confirmed high grade glioma (glioblastoma multiforme, n=16, grade III anaplastic astrocytoma, n=1, oligo-astrocytoma grade III, n=1). Repeated PET scans were performed before and immediately after surgery, during RT and in monthly intervals for 6 months and finally one 12 months after RT. FDG-PET studies of the brain were carried out with the patients n.p.o. for at least 4 hours. PET data were interpreted visually and semi-quantitatively. The images were normalized to the ipsilateral cerebellar cortex and ROIs were drawn in the region of the tumor. All sequential studies were plotted against time with the first postoperative study as starting point (=uptake slope). Correlation with patient survival and FDG uptake changes over time was performed.

Results: In the first postoperative FDG-PET study, 10 patients showed residual elevated FDG uptake in the tumoral bed. In 6 of these patients, PET demonstrated a decrease of regional FDG uptake during RT, whereas in 4 patients, there was no response to RT. In 2 of them, an increase and extension of the tumor could be observed under RT. In 8 patients without detectable postoperative residual tumor, 2 patients were diagnosed with focal tumor recurrence 6 and 12 months after RT by PET. In 2 patients, tumor recurrence presented as „filling-in“ of the postoperative cavity, which could be reliably confirmed by quantitative data analysis as an increase in FDG uptake over time. Furthermore, reappearance of diaschisis cerebellaris could be observed even before definite diagnosis of tumor recurrence could be established by FDG-PET.

Conclusion: Tumor recurrence presents either as focal region of elevated FDG uptake or as „filling-in“ of the postoperative cavity. This „filling-in“ usually appears as intermediate FDG uptake, visually not distinguishable from normal cortical activity. However, these recurrences can be reliably detected by use of time-activity-curve plots. Therefore, „filling-in“, as well as reappearance of diaschisis cerebellaris have to be considered as parameters for tumor recurrence. The increase in FDG uptake over time seems to be a predictor of patient survival.

OS-160

CYO Wong, MG Luciano, J Tsao, WJ MacIntyre, S Raja, GB Saha, EQ Chen, RT Go. Departments of Nuclear Medicine, Neurosurgery, and Neurology. The Cleveland Clinic Foundation, Cleveland, Ohio 44195, USA.

PREDICTIVE VALUES OF PRE-OPERATIVE CEREBRAL PERFUSION SPET (CP) AND CEREBRAL METABOLISM PET (CM) IN ASSESSING RESPONSE TO SHUNTING OF HYDROCEPHALUS.

About 40-80% of hydrocephalic (H) patients (pts) will improve after shunting. But the relatively high complication rate (including mortality) of up to 30% has prompted continued investigations for a pre-operative (op) positive predictor of shunt outcome. We performed pre-op CP with SPET (20-25 mCi Tc-99m ECD) using a triple detector gamma camera equipped with high resolution collimators and CM with PET (5-10 mCi F-18 FDG) using uniform attenuation coefficients of 0.11 and 0.096 cm⁻¹ respectively in 9 consecutive H pts (age=66±16 yrs, M:F=5:4). All pts were followed up with CM PET 3-6 months after shunting. Pre-op CM, CP and post-op CM images in each pt were co-registered with one another and multiple ROIs (16 in total) were placed in cortical and subcortical regions in identical positions for quantitation. The pre-operative CP and CM values in each ROI [counts/pixel (c/p)] were normalized to average c/p of cerebella. These indices were used to predict the response after shunting according to the groups categorized below.

To define an objective criteria for improvement after shunting, the mean (μ) and standard deviations (σ) of the percentage change in CM [$\Delta\text{CM} = \frac{\text{post-op CM} - \text{pre-op CM}}{\text{pre-op CM}} \times 100\%$] from an identical set of ROIs in a non-H control (who received shunting for arachnoid cyst) were first determined as 1.8±2.3%. The global μ from non-cerebellar ROIs in all pts was calculated similarly and compared to that of the control. Group B was defined as those who showed clinical improvement of symptoms together with μ greater than 2 σ above the control (otherwise, group A). The age, ΔCM range, and pre-op values of non-cerebellar CP and CM are:

Group	ΔCM range	Age (yrs)	No.	Pre-op CP	Pre-op CM
A	-13.5 to 3.99%	72±5	4	0.799±0.077	0.856±0.144
B	10.7 to 37.2%	62±22	5	0.899±0.096	1.126±0.141

The μ from cerebellar ROIs of all pts were within 2 σ that of the control, justifying the use of cerebella as the reference. Pre-op CM in group B was significantly higher than that in group A ($p < 0.03$). There were no significant differences in age ($p = \text{ns}$) or in pre-op CP ($p = \text{ns}$). We conclude that pre-op CM but not pre-op CP may be a positive predictor in pre-shunting evaluation of H pts.

OS-161

K.Tatsch, P.A.Winkler, W.Stummer, M.Holtmannspoetter, K.Stein, K.Hahn

Depts. of Nuclear Medicine and Neurosurgery, Klinikum Grosshadern, University of Munich, Munich, Germany

FDG-PET FOR ASSESSING THE EFFECTS OF CRANIOPLASTY FOLLOWING DECOMPRESSIVE CRANIECTOMY

In particular situations decompressive craniectomy is regarded as an effective tool to relief the live-threatening increase of intracranial pressure. After recovery from the acute event usually cranioplasty is performed, which has been repeatedly associated with improvement of the neurological and neuropsychological deficits in those patients even though the pathophysiological background therefore is not yet fully understood. Aim of the present study was to investigate, whether cranioplasty causes noticeable changes of regional cerebral glucose metabolism as compared to the clinically stable condition after decompressive craniectomy.

So far 11 pts with extensive craniectomy following subdural and intracerebral hematoma or cerebral infarction were studied with FDG-PET before and within 2-16 weeks after cranioplasty (Siemens HR+; cold transmission scan; 2D acquisition). For further evaluation PET data before and after cranioplasty were intra-individually compared using a standardized region map covering cortical and subcortical structures (frontal, central, parietal, temporal, occipital cortex, basal ganglia, cerebellum) and related to the results of transcranial doppler investigations and neuropsychological tests.

In the study after decompressive craniectomy all pts presented with moderately to extensively reduced regional cerebral glucose metabolism. Gyri adjacent to the craniectomy had lost their normal convex surface structure impressing flattened and hypometabolic. Crossed cerebellar diaschisis was present in 9/11 cases at baseline (mean: 12±10%), remaining unchanged in 2/9 and improving in 7/9 after cranioplasty (mean: 8±9%). As compared to baseline metabolic improvement after cranioplasty ranged from 9% to max. 39% (mean: 23±11%) in the most severely affected structures, from 1.5% to max. 26% (mean: 13±6%) in the entire affected hemisphere, and from 0% to 8% (mean 5±3%) in the primary non affected hemisphere, respectively. FDG PET data were related to changes in flow velocity assessed with TCD as well as neuropsychological test results.

Our data indicate that cranioplasty following decompressive craniectomy may markedly improve cerebral glucose metabolism as assessed with FDG-PET. Therefore, this surgical procedure does not only restore cerebral protection and ensures cosmetic repair but is also associated with partial functional recovery of non-irreversibly damaged cortical and subcortical structures of the primarily affected and also the non-affected hemisphere.

OS-162

M. Schreckenberger¹, E. Gouzoulis-Mayfrank², O. Sabri¹, Ch. Arning¹, G. Schulz¹, M. Zimny¹, H.-J. Kaiser¹, G. Wagenknecht¹, Th. Tuttass¹, H. Sass², and U. Büll¹

Departments of Nuclear Medicine¹ and Psychiatry²
Aachen University of Technology, Aachen, Germany

The Psilocybin Psychosis As A Model Psychosis Paradigm For Acute Schizophrenias: A PET Study with 18-FDG

Background: The indolehallucinogen psilocybin (o-phosphoryl-4-hydroxy-N,N-dimethyltryptamine) is able to induce a psychosis-like syndrome that is very similar to acute schizophrenias (model psychosis paradigm). Little is known about the neuro-metabolic basis of the psilocybin psychosis compared to schizophrenias. It was the aim of this study to investigate the acute effects of psilocybin on cerebral regional glucose metabolism (rMRGlu), and to survey the associations between rMRGlu and the psychopathology.

Methods: In this randomized double-blind study, 16 healthy volunteers received orally either 0.2 mg/kg psilocybin (n=8) or placebo (n=8) 90 - 120 min before 18-FDG injection. Subjects had to perform a constant cognitive stimulation task (word repetition) during 30 min after 18-FDG injection until PET scan started. After absolute quantification of MRGlu (Sokoloff), 39 regions-of-interest were defined on individual 3D-flash MRI data for regional quantification, and were superimposed on the PET data (PET/MRI overlay). Acute psychopathology was assessed by the PANSS score (Positive And Negative Syndrome Scale). Statistical analysis by U-test and by the Spearman correlation coefficient (correlations between rMRGlu and PANSS).

Results: Comparison psilocybin versus placebo showed significant increases of rMRGlu in the right operculum (+7.7%) and the anterior cingulum (+9.8%). Decreased rMRGlu was found in the left precentral cortex (-6.1%) and in the right thalamus (-8.7%); all p<0.05. Positive correlations were found between left inferior temporal and delusions (r=0.73), left occipital and excitement (r=0.9), left occipital and distrust (r=0.87), left operculum and difficulties in abstract thinking (r=0.87), anterior cingulum and stereotyped ideas (r=0.76), left thalamus and stereotyped ideas (r=0.76)

Conclusion: The psilocybin psychosis shows functional alterations of the cortico-striato-thalamic feedback loop as postulated for acute schizophrenias. However, there are high correlations between rMRGlu and PANSS being totally different from the correlations in untreated acute schizophrenias. It has to be discussed, why a very similar psychopathology may be associated with quite different neurometabolic processes. *Approved by the local ethical committee and the German Federal Pharmaceutical Commission. Supported by Deutsche Forschungsgemeinschaft (GO 717/1-1)*

Radiopharmacy and radiochemistry: Ria/Others

OS-163

L.Jin, B.C Wang, P Fang, R.J Zhang, Y.H Tao, M.D Zhang

National Laboratory of Nuclear Medicine, P.R.China, Department of Biochemistry and Molecular Biology

STUDIES ON THE FUNCTION REGULATION OF PROTEIN C SYSTEM AND NOVEL HIGH RISK OF VENOUS THROMBOSIS

Protein C system is an anticoagulation pathway which consists of protein C(PC), protein S(PS), thrombomodulin(TM) and protein C inhibitor(PCI). The procedures for isolation and purification of PC, PS, PCI and antithrombin III(AT III) from human plasma, and TM from human urine were developed. Five RIAs were also developed, on the equilibrium method, by raising the antisera in rabbits. 125I-PC, 125I-PS and 125I-AT III were prepared using the chloramine-T method, 125I-PCI by Iodogen method and 125I-TM by Bolton-Hunter method. All of their sensitivities were below 10ug/L, and the ranges of recovery rates were 94.30% to 105.22%. The antisera provided a linear response from 6.25 to 1024ug/L for PC, 21 to 700ug/L for PS, 4 to 800ug/L for AT III, 4.8 to 1024ug/L for PCI and 8.1 to 560ug/L for TM. The intra- and inter- assay CV were 4.4% and 9.68% for PC RIA, 4.99% and 13.14% for PS RIA, 3.56% and 8.01% for AT III RIA, 2.73% and 8.62% for PCI RIA, 5.10% and 10.94% for TM RIA. The cross reactivities of these methods with factor II and thrombin(Th) were negligible. These methods can be used as effective tools especially for diagnosis of thrombosis and basic or clinical studies of protein C system.

We investigated the functional regulation of protein C system with flow cytometry and the five RIAs. We found: (1)There are very high affinity and saturable specific binding sites for PC on cultured human umbilical vein endothelial cells. It is speculated that may be a way for protecting PC against digested-enzymes or storage form or favorable rapid reaction as soon as Th appears. (2)PCI inhibited activated PC(APC) appeared to be dependent on membrane or phospholipid. (3)AT III regulates the production of APC with a rapid regulation manner by the Th- AT III complex dissociates rapidly from TM.

On the basis of the five RIAs, we developed the technique of APC-APTT, which is a simple and reliable method to detect APC-resistance. We also developed a PCR for identification and verification of G1691A transition or point mutation of factor V on homozygotes and heterozygotes. Even though the diagnostic level of APC-APTT were the same as, we have observed that factor V G1691A mutation incidence on Chinese is much lower than on North European. There may be other factors about APC-resistance, such as factor VIII mutation or factor V mutation but not on G1691A in Chinese.

OS-164

V.Prassopoulos, K. Vonorta, V. Kontopoulos, E. Mitrou, G. Alexandrakis, P. Kostamis

Dept of Nuclear Medicine «IASO» Hospital, Athens, Greece

COMPARISON OF IGF-1 (INSULIN LIKE GROWTH FACTOR) IGFBP-1 (INSULIN LIKE GROWTH FACTOR BINDING PROTEIN) AND E2 (ESTRADIOL) LEVELS IN SERUM AND FOLLICULAR FLUID FROM WOMEN UNDERGOING IN VITRO FERTILIZATION

Insulin-like growth factor (IGF-1) is an anabolic polypeptide structurally and functionally similar to insulin that mediates the actions of growth hormone. Insulin-like growth factor binding protein-1 (IGFBP-1) is a specific carrier protein that regulates the actions of IGF and is growth hormone-independent. In this study the levels of IGF-1, IGFBP-1 and E2 in serum and follicular fluid from women undergoing in vitro fertilization (IVF) were compared and their role in controlled stimulation of the ovaries was studied.

Materials-Methods: Participants were 12 women (36±5,5 years old) undergoing controlled ovarian hyperstimulation with hormone therapy(FSH, LH). Blood samples were collected on the last day the hormones were administered (A) and on the day of the ovum pick-up (B). The levels of E2, IGF-1 (RIA method) and IGFBP-1 (IRMA method) were determined in serum samples A and B and in follicular fluid (FF).

Results: Pregnancy was succeeded in 2 out of 12 women. The levels of E2 (A), E2 (B) and E2 (FF) were 1095±789, 541±445 and 104582±49043 pg/ml respectively, the levels of IGF-1 (A), (B) and (FF) 251±101, 193±93 and 139±69 ng/ml respectively and of the IGFBP-1 (A), (B) and (FF) 59±35, 30±23 and 105±38 ng/ml respectively. The mean number of collected oocytes during ovum pick-up was 10±8 (range 2-31). There was a statistical correlation between the levels of E2 (A, FF) and IGF-1 (p<0,05), as well as between the levels of E2 and IGFBP-1 (p<0,01). There was also correlation between IGFBP-1 (A), the age of the women and the levels of hormone therapy (p<0,05). There was a statistically significant difference between the levels of IGF-1 in women with «positive» fertilization and the rest, p<0,05. The levels of IGFBP-1 (FF) were greater than the IGFBP-1 (A), (B) (p<0,001). The levels of IGF-1 (FF) were lower than the IGF-1 (A), (p<0,01).

Conclusion: Growth factors have a role in IVF. IGFBP-1 may determine the level of controlled ovarian stimulation. The levels of IGF-1 may be a prognostic factor for successful implantation. The role of growth factors in ovum quality and the implantation rate of the process during controlled ovarian stimulation needs to be investigated further.

OS-165

V.R. Pallela, R. Patti, J. Li, M.L. Thakur. Thomas Jefferson University Hospital, Philadelphia, PA 19107
 INTERFERON- α -2b IMMUNOCONJUGATE ENHANCES TUMOR TARGETING OF ^{99m}Tc LABELED MONOCLONAL ANTIBODIES (MABs)

Enhanced tumor uptake and reduced liver uptake will improve results of diagnostic and therapeutic applications of radiolabeled MABs. We have (Thakur, et al, J Immunotherapy 20, 194-201, 1997) shown that recombinant interferon- α -2b (IFN- α -2b) when conjugated (1:1) with MAB and administered i.v. to tumor bearing mice followed by the administration of ^{99m}Tc labeled F(ab')₂ of the same MAB significantly enhanced tumor uptake (P<0.01) and reduced liver uptake (P<0.01). Results were attributed to enhanced tumor blood flow and to increased cell surface antigen expression by IFN- α -2b and to blockage of hepatic non-specific Fc receptors by the MAB injected. In this investigation we studied the influence of time between the administration of two agents on the uptake in the tumor and liver.

IFN- α -2b (Schering-Plough Corp, NJ) and anti-CEA F-6 (IgG 2a) MAb (ImmunoTech, France) were conjugated and F(ab')₂ fragments of the MAB were labeled with ^{99m}Tc as described previously (Op.Cit). Tumors were grown in nude mice by implanting 5×10^5 human colorectal carcinoma cells (LS174T) grown in culture. Control group of animals (n=5) received (300 $\mu\text{Ci}/20 \mu\text{g}$) ^{99m}Tc -F-6-F(ab')₂ alone. The study groups also received the agent but at 1.5 hr, 3 hr, 6 hr, and 24 hr after i.v. administration of (20x10³ i.u.30 μg) IFN:MAB conjugate. Twenty-four hrs later animals were sacrificed, tissues dissected, and radioactivity was determined. The *in vitro* antigen expression studies were performed using 2x10⁵ confluent LS174T cells incubated with 10³ i.u. IFN in a 24 well plate for predetermined periods up to 24 hrs. DMEM medium was then removed, cells resuspended, and incubated with ^{99m}Tc -F-6-F(ab')₂ (2 $\mu\text{Ci}/0.05 \mu\text{g}$) at 37°C for 30 min. Cells were then dissolved in 0.5M NaOH and radioactivity was determined.

As compared to the control group, radioactivity in tumors increased in all study groups and was maximum (x3.5) at 0.5 hrs. It then slowly declined (x1.5) in the 24 hrs. This suggests that the early enhancement of radioactivity in the tumor may have been due to modulation of blood flow and then due to enhanced antigenic expression (Li et al, J Immunotherapy 16, 175-180, 1994). The subsequent decrease in tumor uptake may be attributed to antigen shedding (Murray et al, J Biol Response Modifiers 9, 556-563, 1990). These data were consistent with the results of antigen expression studies *in vitro*. The liver uptake decreased in all study groups.

Results indicate that IFN:MAB conjugate may improve diagnostic and therapeutic applications of MABs and is worthy of further study.

OS-166

J. Baranowska-Kortylewicz, D. Hoffman, J. Lai, D. Stark, G.V. Dalrymple

University of Nebraska Medical Center, Departments of Radiation Oncology and Radiology, J. Bruce Henriksen Laboratories, Omaha, NE

NOVEL RED BLOOD CELL-BASED IMAGING AGENTS

Red blood cells labeled with chromium-51 or technetium-99m have been used in nuclear medicine for almost 40 years. The mode of binding involves a direct chemical reaction of a non-chelated radioisotope with cell structures. Similar approach for indium-111 or paramagnetic metals, e.g. Gd, is not possible. Coordination of these metal ions to appropriate ligands is necessary to successfully apply them in the clinic. The purpose of our studies was to develop a new class of intravascular imaging agents based on RBC labeled with chelated gadolinium as a paramagnetic contrast agent for MRI (Gd-RBC) and with chelated indium-111 (In-111-RBC) for scintigraphy.

To achieve this goal we have synthesized high affinity peptides specific to RBC conjugated to chemically altered p-Lys and labeled then with Gd-153 and In-111. In a typical synthesis, p-Lys (M.W. 19,000; 37,000, 65,000) was first reacted with 5 molar equivalents of either SPDP or the Traut's reagent, purified on a Sephadex G10 column and further modified with DTPA, typically at 50 : 1 and 100 : 1 molar ratios. On average 10 - 25 DTPA molecules were incorporated into the p-Lys at these ratios. The RBC-binding peptides contain a terminal cysteine residue and this was used to conjugate modified p-Lys.

For the binding assays RBC obtained from anticoagulated fresh blood were washed with 1% BSA-PBS. RB cells resuspended in this same buffer at 1×10^8 cells/mL were reacted with peptides or peptide-p-Lys conjugates labeled with either In-111 or Gd-153. The stability of RBC complexes was tested at 37°C in serum with and without excess of unlabeled peptides. The *in vitro* studies of Gd-153-RBC and In-111-RBC indicate virtually unchanged affinity constants of Gd-153 and In-111-p-Lys-peptide complexes with RBC as compared to unmodified peptides. The binding assay with the excess of unmodified RBC peptides indicates less than 5% loss of the conjugate from its RBC complex after 120 min incubation at 37°C. The stability studies of the radiolabeled conjugates in mouse serum indicate only marginal losses of the radiolabel after 24 h incubation at 37°C. The analysis of the conjugates in the presence of hepatocytes and whole liver homogenates indicate partial degradation of the peptide without any detectable release of the free radiometal.

OS-167

A. Ramirez, *D. Barajas, JP. Diaz, T. Arroyo, *J. Pedrero, *B. Bravo, JM. López, JM. Llamas. Nuclear Medicine Department and *Child Nephrology Unit, Virgen de las Nieves University Hospital, Granada.

ASSESSMENT OF URINARY ENDOTHELIN-1 AND MICROALBUMINURIA IN CHILDREN WITH REFLUX NEPHROPATHY

Objectives: To evaluate the utility of urinary endothelin-1 (ET-1) and microalbuminuria (MA) in the diagnosis and assessment of reflux nephropathy (RN) in children.

Patients and methods: 222 children were studied, composing a control group (n=96) and a problem group of children with primary vesicoureteral reflux (n=126). Both groups were subdivided into children ≤ 2 yr. and > 2 yr. The ET1/creatinine and MA/creatinine ratios were determined in urine samples from all the children and renal scintigraphy with ^{99m}Tc -DMSA was performed on the problem group, following the Goldraich method and scoring each patient with the sum of the lesions of both kidneys. A total score of ≤ 2 denoted a mild lesion and of > 2 a moderate/severe lesion. Analysis with two-way ANOVA and the Bonferroni t test gave these results:

	≤ 2 years			> 2 years		
	Control (n=37)	DMSA ≤ 2 (n=22)	DMSA > 2 (n=9)	Control (n=59)	DMSA ≤ 2 (n=49)	DMSA > 2 (n=46)
ET-1/Cr (ng/g)	500 SD=345	681 SD=379	1108 ^{a,b} SD=765	388 SD=174	461 SD=197	437 ^c SD=399
MA/Cr (mg/g)	23.8 SD=22	26.3 SD=20.5	26.4 ^d SD=18.4	13.6 SD=19	11.6 SD=16.1	14.4 ^d SD=32.9

a) p<0,01 DMSA >2 vs Control; (b) p<0,05 vs DMSA ≤ 2 ; (c) NS DMSA > 2 vs Control and DMSA ≤ 2 ; (d) NS DMSA > 2 vs control and DMSA ≤ 2 in both age groups.

Conclusions: Fibrogenesis of the RN onset in the renal medullary tissue, the origin of ET-1, so that the increase in ET-1 secretion may serve as a marker in its initial stages. With respect to the MA, no significant differences were detected between the lesion groups and the controls.

OS-168

S. Nuvoli, A. Mocci, A. Spanu, A. Scanu, C. Pala, A. Masia, G. Spano, A. Marrosu, C. Bagella, M.E. Solinas, E. Bercovich and G. Madeddu. Depts. of Nuclear Medicine and Urology. University and General Hospital, Sassari, Italy.

FREE/TOTAL PSA RATIO (F/T) AND TOTAL (T) PSA COMBINED USE IN MONITORING FINASTERIDE (F) TREATED BENIGN PROSTATIC HYPERPLASIA(BPH).

To evaluate whether combined F/T and T-PSA may provide more information than T-PSA alone in monitoring the response to F in BPH pts, we studied 58 male pts, aged 44-90 yrs, diagnosed by biopsy. At first observation, 31 pts had had no therapy (Group A), while 27 had been on F treatment for 8-22 mths (Group B). In all pts and in 61 sex-age matched controls (C), both T and F-PSA were assayed by IRMA (cut-off: 4.0 and 2.1 ng/ml, respectively) and F/T was also calculated (cut-off: 0.18). In Group A, T-PSA was above cut-off in 15/31 cases, with values > 10 ng/ml in 5 and within the gray area (4-10 ng/ml) in 10. F-PSA was high in 7/31 pts, while F/T was ≥ 0.18 in 26/31 cases. In Group B, T-PSA was above cut-off in 10/27 pts, 9 in the gray area. F-PSA was high in 3/27 cases, while F/T was under cut-off in 2 pts with T-PSA in the gray area. Mean T and F-PSA values were higher and F/T lower in groups A and B in respect of C. When groups A and B were mutually compared, T and F-PSA were significantly higher in Group A (5.56 \pm 4.87 and 1.52 \pm 1.46 ng/ml vs 6.82 \pm 9.15 and 1.40 \pm 1.31 ng/ml, respectively), but no difference was found in F/T values. Both T and F-PSA initial mean values had a significant (p<0.007 and p<0.0008, respectively) decrease (3.23 \pm 2.66 and 0.73 \pm 0.59 ng/ml, respectively), while F/T showed no statistical variation. Group A pts all had reduced prostate volume and improved clinical signs after 8-15 mths of F therapy. Both T and F-PSA initial mean values had a significant (p<0.007 and p<0.0008, respectively) decrease (3.23 \pm 2.66 and 0.73 \pm 0.59 ng/ml, respectively), while F/T showed no statistical variation. During follow-up, one Group B pt developed prostate cancer, while an intraepithelial neoplasia pattern was ascertained in another at histology; both pts, who at first observation had T-PSA in the gray area and F/T under cut-off, presented a further F/T decrease. Our data indicate that F therapy in BPH pts may improve clinical symptoms and reduce T and F-PSA levels without modifying F/T. This seems to confirm that F/T may distinguish between BPH and cancer during F treatment, particularly when T-PSA is within the gray area.

General nuclear medicine: Lung

OS-169

M. Lemb, T.H. Oei, B. Wenz, B. Haubold-Reuter

Röntgeninstitut, Bürger166, D-27568 Bremerhaven/Germany

PULMONARY THROMBOEMBOLISM: HOW TO GET RID OF THE INTERMEDIATE SCAN BY V/P-SPECT USING TECHNEGAS

Purpose: In the PIOPED-study, performed with a conventional planar technique using Xc133, a high degree of 39% intermediate scans resulted. It is the purpose of our retrospective study, whether the consequent use of ventilation/perfusion (V/P) SPECT can reduce this rate.

Methods: On 458 patients (277 female, 181 male, age 18-85), referred to our laboratory because of suspected pulmonary thromboembolism (PTE), the following investigation was performed: patients inhaled 37MBq of Technegas in supine position. Afterwards a SPECT-acquisition was started (64 angles, 25sec per view). After SPECT-completion 185MBq 99mTc-MAA are injected intravenously. SPECT-acquisition then is started again (5sec per view). Coronal and transversal ventilation and perfusion SPECT-slices are reconstructed by filtered back projection and compared slice by slice.

Results: Evaluation of the SPECT-images according to the revised PIOPED criteria (Original PIOPED-results in parenthesis):
 normal/near normal: 241 pat = 53% (PIOPED: 14%)
 low probability: 91 pat = 20% (PIOPED: 33%)
 intermediate prob.: 76 pat = 17% (PIOPED: 39%)
 high probability: 50 pat = 11% (PIOPED: 13%)
 Proceeding on the assumption, that PTE is primarily a disturbance of pulmonal parenchymal perfusion we subcategorized the group of intermediate and low probability scans as embolic (PTE+), if there was at least one matching defect, and as non embolic (PTE-), if there were none. Our results then are in good accordance with the final PIOPED PTE status:
 PTE+: 92 pat = 20% (PIOPED: 27%),
 PTE-: 363 pat = 79% (PIOPED: 65%),
 uncertain: 3 pat = 1% (PIOPED: 9%)
 37 pat., categorized as PTE+ underwent a control V/P scan after anticoagulant therapy. 34 of these pat. showed a better or normalized perfusion scan.
 In a control group of 14 PTE- pat., control scans were unchanged in 12 cases.

Conclusion: We conclude, that the results of the PIOPED-study can be improved dramatically by using a consequent perfvent SPECT-technique using Technegas.

OS-170

P.E. Christian, S Valdivia, MR Banish, H Ranganath

University of Utah School of Medicine, Salt Lake City, UT, SY Technology, Inc., Huntsville, AL, and University of Alabama, Huntsville, AL

FULLY AUTOMATED COMPUTERIZED ANALYSIS OF LUNG IMAGES TO DIAGNOSE PULMONARY EMBOLISM

Purpose: Accurate interpretation of lung images to diagnose pulmonary embolism (PE) is highly variable between physicians which results in a low sensitivity and specificity.

Methods: We studied 103 consecutive VQ scans for acute PE. Clinical interpretation by three nuclear medicine physicians, using PIOPED criteria, was compared to interpretation by a fully automated computer algorithm. The final patient diagnosis was determined at six month follow up of all patients medical record review for results of pulmonary angiography, chest CT, extremity doppler US, and repeat lung scans. Pattern recognition software was developed to analyze both ventilation and perfusion lung images. The signal processing module analyzes each image using a smart region growth algorithm to identify the lung shape. The margins of the lung region are then examined by shape analysis to determine areas of diminished radionuclide concentration. Segments are analyzed and correlated between image views. A diagnostic classification module correlates regional ventilatory and perfusion defects and analyzes them according to the PIOPED criteria that physicians use in visual interpretation.

Results: Several upgrades in the computer algorithm were made during the study. These included improved defect detection, better separation of the right and left lungs on the anterior oblique views, and improved recognition of the normal heart defect on the anterior view and diaphragms on the lateral views. These modifications decreased the number of false negative and false positive studies from six to one and eighteen to zero, respectively for the fully automated computer interpretation. In comparison, the physician had only one false negative study. However, the physician interpreted 33% of the studies intermediate while the computer interpreted only 5% as intermediate.

Conclusion: We have developed a computer program which assists the nuclear medicine physician to accurately interpret VQ scans with a marked decrease in the number of intermediate studies. This algorithm has the potential to assist physicians by improving the accuracy of diagnosis and reducing intermediate results.

OS-171

CH. Nair¹, R.J. Browitt¹, EA. Shats¹, T.J. Senden², L. Maxwell³, WM. Burch¹

1, John Curtin School of Medical Research; 2, Research School of Physical Sciences and Engineering; Australian National University, and 3, The Canberra Hospital; 1,2&3, Canberra, Australia.

THROMBOTRACE® , A NEW DIAGNOSTIC AGENT WITH HIGH SPECIFICITY TO BIND FIBRIN *IN VIVO*.

We have discovered that if Technegas particles are rendered hydrophilic and taken up in about 2.5mL of water they have a very high affinity for Fibrin, the structural matrix of blood clots. Experiments *in vitro* have demonstrated a strong binding for the matrix itself, also for the precursor "soluble fibrin" moiety, but a much lower affinity (<25%) for fibrinogen. In addition, the strength of the bond was tested by crushing and multiple washing of the clot which retained 87% of the activity originally present in the plasma.

A well-known experimental model of PE in which rabbits are injected via the jugular vein with small clots (~ 1mmx1.5mm) of human blood grown on a cotton thread, was then used to test the action of the new agent *in vivo*. Anaesthetised rabbits were placed supine on the upturned collimator of a gamma camera and, after inoculation with the clot, which generally fragmented into 3 or more PE in the lung, were injected in a peripheral ear artery with approximately 1mL of the agent containing approximately 20MBq activity.

Both the main and satellite PE were visualised maximally after about 4 minutes when most of the agent had cleared from the lungs to the RE system. Basic image processing enabled a standard initial "perfusion" image containing the defect to be overlaid with the relevant proximal "hot spot" image to add weight to the visualisation of the PE. Emboli retrieved from the lungs under gamma camera localisation *post mortem*, were found to have the activity concentrated in them.

A preliminary phase 1 clinical trial is being evaluated for ethics approval following acute animal toxicity studies. It is hoped to be able to include clinical images with this derivative of Technegas we have named ThromboTrace® by the time of the meeting.

OS-172

PR VandeStreek, FL Weiland, P Bosco, GT Obranovich, RF Carretta
 Sutter Roseville Medical Center, Department of Nuclear Medicine

TECHNETIUM-99m P-280 (AcuTec) LABELED PEPTIDE IN THE DETECTION OF ACTIVE THROMBUS FORMATION: A PROSPECTIVE STUDY WITH ANALYSIS OF A TRAUMA PATIENT POPULATION SUBSET.

Hospitalized trauma patients are at increased risk for deep vein thrombosis (DVT) with an incidence of 20% to 90%. Duplex ultrasound and venography are utilized in the diagnosis of DVT. A recently completed trial demonstrated the safety and efficacy of 99mTc P-280 in identifying active thrombus formation. Tc99m P-280, a synthetic cyclic peptide, binds to the GPIIb/GPIIIa receptors expressed on activated platelets which incorporate inactive thrombus. This study prospectively evaluated the use of Tc-99m P-280 in the detection of thrombus in a population with suspected DVT. In addition, analysis of a subset of hospitalized trauma patients was performed.

Twenty-six patients were evaluated with doppler ultrasound for suspected thrombus. A subset of 15 trauma patients were identified. Tc-99m P-280, 20 mCi (740 MBq) / 70 kg of body weight, was injected intravenously and flow images obtained. Appropriate images were performed at 10 min. and 60 min. post-injection. Whole body images were performed as possible. Results of the imaging sessions were compared to ultrasound.

	TruePos	True Neg	False Pos	False Neg
Overall	20	5	0	1
Trauma	9	4	0	0
	Sens	Spec	PosPredValue	NegPredValue
Overall	95.2%	100%	100%	83%
Trauma	100%	100%	100%	100%

We conclude that Tc-99m P-280 may be an effective agent in the detection of thrombus particularly in the high risk subset of trauma patients in whom ultrasound or venography may be difficult for clinical reasons.

OS-173

G. Barghouth¹, B. Yersin², F. Doenz³, A. Bischof Delaloye¹

Services de Médecine Nucléaire¹, de Médecine Interne², de Radiodiagnostic et Radiologie interventionnelle³ - CHUV - CH 1011 Lausanne

CLINICAL PRE-TEST PROBABILITY AND LUNG SCAN IN THE DIAGNOSTIC APPROACH OF PULMONARY EMBOLISM: 2 YEAR PATIENT OUTCOME.

The aim of this study was to evaluate the combined assessment of the probability of pulmonary embolism (PE) based on the clinical impression and the ventilation/perfusion lung scan (V/Q) in unselected patients addressed to the emergency room with the suspicion of pulmonary embolism (PE).

We included 134 consecutive patients (60 males aged 28-87y and 74 females aged 18-90 y) who could be followed up for 2 years. The lung scans were performed in 8 incidences each for ventilation (Tc-99m-Technegas) and perfusion (Tc-99m-MAA). Initial diagnosis was made on the basis of clinical and V/Q probability, completed if necessary by pulmonary angiography (n=27, 20%). Final diagnosis was established 2 years later after having contacted patients and/or their physician by phone.

Probability of PE was considered high, intermediate or low according to clinical and V/Q evaluation (modified PLOPED criteria). In order to facilitate comparison, we included in the low V/Q probability group (n=76) 15 patients with normal scans. Clinical and V/Q probabilities were high in 22.5% and 14%, intermediate in 23.5% and 18%, and low in 54% and 68%, respectively. Incidence of PE was 25%. Clinicians considered all 19 patients with high V/Q probability as having pulmonary embolism regardless of the pretest clinical probability (no angiogram) whereas PE was excluded (1 angiogram) in all patients with a normal scan (n=15). PE was diagnosed in 10/24 (42%) patients with intermediate (15 angiograms) and in 4/76 (5%) with low V/Q probability (11 angiograms). At 2 y follow-up the mortality rate was 9% (12/134), 8 patients died from cancer, 3 from cardiac failure, one committed suicide. No death was related to PE or anticoagulation. None of the patients with low clinical and scintigraphic probability presented PE during follow-up.

In 107/134 (80%) patients the combined evaluation of clinical and V/Q probability allowed to confirm or exclude PE. angiography was required in only 20%. This approach appears to be safe, as shown by the absence of major events related to PE at 2 y follow-up, and cost-efficient.

OS-174

V. Podio, A. Francini, G. Bertuccio, C. Carbonero, C. Baiocco, I. Masaneo, G. Bisi

Nuclear Medicine Dpt., University of Turin (I)

D-dimer test in patients with deep venous thrombosis: is it predictive of pulmonary embolism?

Aim of our study is the evaluation of positive and negative predictive values of D-dimer test for pulmonary embolism (PE), as assessed by pulmonary perfusion scintigraphy in a prospective series of 189 consecutive patients referred to our Emergency Department and affected by deep venous thrombosis (DVT), as demonstrated by ultrasonography; 177 patients had D-dimer higher than 0,5 µg/ml (positive) while 12 patients had D-dimer lower than 0,5 µg/ml (negative).

Lung scintigraphies were classified according to Biello's criteria: normal (N), low probability (LP), intermediate (IP) and high probability (HP) (see table).

	N	LP	IP	HP	Total
D-dimer -	3	4	1	4	12
D-dimer +	10	28	29	110	177
Total	13	32	30	114	189

We excluded from further analysis the group of patients with IP. D-dimer positive predictive value was 74% and negative predictive value 64% (specificity 16% and sensitivity 96%). Chi² test was shown to be highly significant with p<0,05. The number of patients with normal scans is very small: this reduces the relevance of statistics. D-Dimer value, which is generally high due to the underlying disease (DVT), is unreliable to predict PE; asymptomatic PE in patients with DVT is highly prevalent so that it seems to be necessary to proceed routinely to perfusion scintigraphy in patients with DVT regardless of D-Dimer value.

Cardiovascular: Innervation

OS-175

P. Zanco, L. D'Alento*, F. Chierichetti, M.C. Baratella*, L. Menti*, G. Rizzoli°, D. Rubello, G. Ferlin.

Nuclear Medicine, Castelfranco Veneto, *Cardiology Dept. and °Institute of Cardiovascular Surgery, Padua University, Italy.

RISK STRATIFICATION OF VENTRICULAR ARRHYTHMIAS (VA) IN PATIENTS OPERATED FOR TETRALOGY OF FALLOT (TOF) : AN ANALYSIS BY PET AND SPECT.

To evaluate the significance of abnormalities in myocardial adrenergic activity, perfusion and metabolism in arrhythmogenesis after surgical correction of TOF, 15 patients (mean age at operation 11±10 yrs, mean follow-up 18±6 yrs) underwent I123-MIBG SPECT (MS) and planar LAO 45° (MPI) at 30' and 5 h, rest N13-NH3 perfusion PET (PP) and glucose load F18-FDG PET (MP). With regard to MPI, a wash-out index (WI=30/5h myocardial uptake ratio) and a heart/mediastinum ratio at 5 h (HMR) were calculated both for the right and the left ventricle wall. Regarding the SPECT and PET studies a severity index (SI), concerning the extension and the severity of the uptake defects, was calculated.

Twelve patients presented VA (group A), while the other 3 had no history of VA (group B). Comparing the two groups, group A presented: 1) higher WI of MIBG both in the right and in the left ventricle (respectively 1.58±0.2 vs 1.19±0.46, p=0.04; 1.63±0.16 vs 1.13±0.39, p=0.004); 2) increased HMR of the right ventricle (1.48±0.24 vs 1.07±0.5, p=0.05); 3) higher MIBG-SI (9.58±5.48 vs 1.33±2.30, p=0.03). No significant difference was found in PP- and MP-SI.

In conclusion our study suggests that TOF operated patients at risk of VA presented abnormalities in the myocardial sympathetic nervous system, not correlated to perfusion and metabolism damage. Moreover I123-MIBG scan may be considered a useful marker of VA in these patients.

OS-176

T. Kajiya, H. Kurogane, A.Takarada, T. Hayashi, J. Shite, A. Yoshida, T. Itagaki, Y. Yoshida.

Hospital: Division of cardiology, Himeji Cardiovascular Center, Japan

REVERSIBLE LV DYSFUNCTION AFTER β -BLOCKER IS PREDICTED BY I-123 METAIODOBENZILGUANIDINE (MIBG) IMAGING IN PATIENTS WITH DILATED CARDIOMYOPATHY.

Dilated cardiomyopathy (DCM) has poor prognosis due to its progressive nature of LV dysfunction. But recent advances in medical therapy including β -blocker therapy promise functional improvement in selected DCM patients (pts). Response to β -blocker therapy has been thought to be unpredictable. In this study we tested the hypothesis that response to β -blocker therapy could be predicted by assessment of cardiac sympathetic nerve activity with MIBG. We performed planar MIBG imaging at 15 min. and 3 hours after the drug injection in consecutive 74 pts with DCM (echo-data at entry: LVDD=67.1 ± 7.5mm, %FS=17.0 ± 4.7). MIBG indices were obtained as heart to mediastinum counts ratio (H/M) at 3 hours and normalized wash-out rate. Pts were assigned to conventional therapy with digitalis, diuretics and ACEI (group C, n=36) or β -blocker therapy (group B, n=38). Echocardiography was repeated at 6 months or later and functional improvement was defined by decrease in Dd<5mm or/and increase in %FS>5%. In group C, 19 pts demonstrated functional improvement but did not correlate with H/M (1.81 ± 0.3 vs 1.83 ± 0.4, NS), wash-out rate (0.89 ± 0.08 vs 0.91 ± 0.08, NS) or echo data at entry (Dd: 63.5 ± 6.3 vs 64.8 ± 6.9, %FS:17.3 ± 5.2 vs 17.8 ± 4.1, NS). On the contrary, in group B, 19 pts revealed subsequent improvement in LV function and associated with significant higher wash-out rate (0.87 ± 0.08 vs 0.95 ± 0.07, P<0.01), but did not correlate with other MIBG or echo indices (H/M:1.74 ± 0.3 vs 1.91 ± 0.4, Dd:68.9 ± 6.8 vs 70.8 ± 7.8, %FS:15.9 ± 5.2 vs 16.9 ± 4.0, NS). Conclusion: Response to conventional medical therapy still remains unpredictable. But increased cardiac sympathetic nerve activity demonstrated by higher MIBG wash-out rate may be a required condition for favorable response to β -blocker therapy in pts with DCM. Candidates for β -blocker therapy can be selected by MIBG imaging.

OS-177

J. Ermert, K. Hamacher, H.H. Coenen

Institut für Nuklearchemie, Forschungszentrum Jülich GmbH, D-52425 Jülich

4-[¹⁸F]FLUOROMETARAMINOL: A N.C.A. LABELLED SYMPATHOMIMETIC FOR PET-IMAGING OF HEART INNERVATION

A general strategy to synthesize complex 18F-labelled aromatic compounds is based on the nucleophilic 18F-fluorination of carbonyl activated arenes. With regard to a stereoselective reduction of the carbonyl compound, a new pathway of the no-carrier added 18F-labelling of biogenic arylalkylamines such as the [¹⁸F]fluorophedrine derivative 4-[¹⁸F]fluorometaraminol (FMR) has been developed. In difference to norepinephrine, metaraminol is characterized by one aromatic hydroxy function in the meta-position and an additional α -methyl group which metabolically stabilize the tracer against mono amine oxidase and catechol O-methyl transferase.

Until now, the no-carrier added tracer was attempted via an inconvenient four step reaction (J. Lab. Compds. Radiopharm., 37: 66 (1995)). An alternative electrophilic 18F-fluorination led to an intolerable amount of unlabelled FMR in the range of pharmacological levels (J. Med. Chem. 31: 362 (1988)).

The n.c.a. labelling of 4-[¹⁸F]fluorometaraminol was performed via 18F-for-N(CH₃)₂ substitution on 4-(2-N,N-dibenzylaminopropionyl)-2-benzyloxyphenyl-1-N,N,N-trimethylammonium triflate which has been synthesized in an eleven step reaction sequence. The diastereomerically pure 18F-labelled erythro isomer (radiochemical yield: 20...30 %), which is of interest for pharmacological studies, was obtained within about 90 min by stereoselective reduction of the corresponding 18F-labelled ketone with borane in THF followed by debenzoylation via hydrogenolysis.

Biochemical evaluation of the enantiomerically pure erythro isomers in mice has shown that both isomers accumulate very rapidly in heart tissue; however, only the R,S-isomer remains in the heart tissue on a level of 20...25% ID/g whereas the S,R-enantiomer is washed out to about 3 % ID/g at 60 min p.i. indicating stereoselective accumulation. According to a rapid blood clearance and metabolic stability, the high heart-to-blood and heart-to-lung ratio of >10 and 3, respectively, of the R,S-isomer is advantageous for further PET-investigation.

OS-178

A. Giordano, M.L. Calcagni, F. Rulli*, M. Muzi*, G. Martino, G. Meduri, G. D'Andrea, E. Zanella*, G. Galli.

Dpt of Nuclear Medicine, Università Cattolica del Sacro Cuore, Rome, and *Dpt of Surgery, Università «Tor Vergata», Rome. Italy.

HIGH DIAGNOSTIC VALUE OF ^{99m}Tc-RED BLOOD CELL PHLEBOSCINTIGRAPHY IN CHRONIC VENOUS INSUFFICIENCY.

Phleboscintigraphy (PS) of the lower limbs has been mainly utilized for the diagnosis of deep venous thrombosis and, despite its theoretical potential, has never been employed in chronic venous insufficiency of the lower limbs (CVI). The aim of this study was to verify the diagnostic value of PS in pts with CVI and to correlate the scintigraphic assessment of CVI with the clinical grading of the severity of the disease. Equilibrium ^{99m}Tc red blood cell PS was performed in 27 pts with CVI. Scintigraphic images of 52/54 limbs (excluding 2 limbs previously safenectomized) were classified according to a four class qualitative grading of the severity of the venous insufficiency (according to SVS/ISCVS criteria published in 1988), and a quantitative scintigraphic index (saphena/ femoral ratio) was assigned to each limb. Results: the scintigraphic qualitative grading showed a highly significant correlation with the clinical grading (Rs= 0.81, p<0.01), a good inter- and intra-observer agreement (86.5% and 92.3%, respectively), 96% sensitivity and 88% specificity to identify the presence or absence of significant CVI; the diagnostic value of the quantitative assessment was not as good. Conclusion: on the basis of the close correlation of the scintigraphic assessment of CVI with the clinical grading of disease severity and of the remarkable values of sensitivity and specificity, we believe that PS of the lower limbs has the potential to become a valuable diagnostic tool for the non-invasive assessment of CVI, since other diagnostic modalities (air- and photoplethysmography as well as duplex scan) are limited and showed lower reproducibility and much weaker correlation with the clinical severity of disease (J Vasc Surg 1994;19:1001-1997).

OS-179

E. Vanoli, C. Rossetti, A. Carpinelli, A. Savi, A. D'Angelo, R. Crippa, M.A. Schmidt, A. Srinivasan, E. Deutsch, F. Fazio, CNR-INB, H. S. Raffaele, University of Milan, Milan, Italy, Mallinckrodt Medical, St. Louis, Missouri, USA.

COMPARISON OF ACTIVATED PLATELETS IMAGING WITH MP2026 (THROMBOSCAN) WITH ECHODOPPLER AND FIBRIN DEGRADATION PRODUCTS: THREE MONTHS FOLLOW UP.

In humans the peptide MP2026 (Thromboscan) labeled with Tc99m has been shown to be a promising radiotracer for imaging activated platelets in vivo. Aim of this study was to evaluate this tracer in monitoring the functional activity of fresh thrombi in patients affected by deep venous thrombosis (DVT) up to three months from symptom onset. With this purpose 10 patients presenting with subacute or acute DVT as assessed by echo at the inferior limbs without clear signs of oedema and positive plasmatic fibrin degradation products (xdp) were selected. Patients were intravenously injected with 20 mCi (> 90% of radiochemical purity) of the tracer within 2 hrs from hospital admission. Whole body scans were performed 30 min and 60 min after tracer administration. Patients underwent the same sequence of exams for the 3 months follow up. The activity ratios between affected and contralateral limb were calculated and the difference between acute phase and 3 month follow up were statistically evaluated by T Student test. The difference was also calculated for the plasmatic xdp values. The results indicate a significative decrease of limb ratio activity (P< 0.0058) three months after the acute phase. No significative differences were found between the 30 min and 60 min studies (P>). In parallel, also xdp values exhibit a significative decrease (P<0.0038). Echo findings were not significantly changed. These results indicate the capability of Thromboscan of monitoring simultaneously the localization and the functional activity of the fresh thrombi. The imaging study can be conveniently performed at 30 min after injection making possible the diagnosis within short time from hospital admission. This approach can be particularly helpful in individual tailoring of therapy and in patients with suspected DVT recurrency where echo is often doubtful.

OS-180

A. Cuocolo, P. Mainenti, E. Nicolai, F. Menna, W. Acampa, G. Florimonte, G. Storto, P. Gisonni, M. Salvatore. Nuclear Medicine Center of the National Council of Research (CNR), Department of Biomorphological and Functional Sciences, University Federico II, Napoli, Italy.

TECHNETIUM-99m FURIFOSMIN MYOCARDIAL UPTAKE IN PATIENTS WITH CORONARY ARTERY DISEASE AND LEFT VENTRICULAR DYSFUNCTION: RELATION TO THALLIUM-201 ACTIVITY.

The role of technetium-99m (Tc-99m) furifosmin in the identification of dysfunctional but viable myocardium has been not yet defined. This study was designed to compare the results of Tc-99m furifosmin cardiac tomography with those of thallium-201 imaging in the same patients with chronic coronary artery disease and left ventricular (LV) dysfunction. Twenty patients with angiographically documented coronary artery disease and chronic ischemic LV dysfunction (ejection fraction 36±7%) underwent on the same day rest-redistribution thallium imaging and resting technetium-99m (Tc-99m) furifosmin cardiac tomography. In each patient thallium and Tc-99m furifosmin myocardial uptake was quantitatively measured in 22 segments. LV systolic function was assessed by echocardiography in corresponding myocardial segments. In all segments, a significant relationship between Tc-99m furifosmin uptake and rest-redistribution thallium activity was observed (r=0.81 and r=0.86, respectively, both p<0.001). Of the 440 total segments, 106 (24%) had normal function, 154 (35%) were hypokinetic, and 180 (41%) a-dyskinetic. No difference between Tc-99m furifosmin and rest-redistribution thallium uptake was observed in normal, hypokinetic, and a-dyskinetic segments. Of the 180 a-dyskinetic segments, 148 (82%) showed moderate reduction (≥50% of peak activity) and 32 (18%) severe reduction (<50%) of thallium uptake. Tc-99m furifosmin uptake was significantly lower in a-dyskinetic segments with severe reduction of thallium activity as compared to those with moderate reduction of thallium activity (41±10% vs 71±14%, p<0.001). In conclusion, these results suggest that Tc-99m furifosmin cardiac tomography may be useful in the identification of dysfunctional but still viable myocardium in patients with chronic coronary artery disease.

Dosimetry and radiobiology: radiobiology/dosimetry

OS-181

T.M. Behr, P. Hötte, E. Weber, S. Yücekent, S. Gratz, M. Conrad, J. Meller, M. Hüfner*, and W. Becker.

Dept. of Nuclear Medicine and Endocrinology* of the Georg-August-University of Göttingen, Germany.

RADIATION ABSORBED DOSES AND THEIR BIOLOGICAL EFFECTS IN THE RADIOIODINE THERAPY OF DIFFERENTIATED THYROID CANCER: A RE-INVESTIGATION OF FACTORS THAT MAY INFLUENCE THE DOSIMETRY AND THE THERAPEUTIC OUTCOME.

Almost 15 years ago, Maxon et al. published (*N. Engl. J. Med.* 1983; 309: 937) and updated (*J. Nucl. Med.* 1992; 33: 1132) a detailed analysis of factors that influence the radiation dosimetry, as well as the therapeutic efficacy in the ^{131}I therapy of differentiated thyroid cancer (DTC). The aim of this study was to investigate whether these factors hold true in a different patient population (Europe vs. US) with a significantly lower alimentary iodine intake ($\leq 100 \mu\text{g/day}$) than in these earlier studies.

A total of 67 patients with DTC (23 papillary, 39 follicular, 3 Hürthle cell, and 2 anaplastic cancers) were given 65-350 mCi Na^{131}I for thyroid remnant ablation ($n=37$) or therapy of metastases ($n=30$). All patients had stopped thyroid hormone replacement for ≥ 4 weeks, with the intention to obtain TSH levels $\geq 40 \mu\text{U/ml}$. Quantitative conjugate view whole-body scans were performed daily over at least 96 h after ^{131}I administration. Activities of various tissues were calculated at each time point by using the build-up factor methodology by a PC software developed for this purpose. Resulting residence times were entered into the MIRDOSE3 program (Stabin M., *J. Nucl. Med.* 1996; 37: 538) which yields the radiation dosimetry according to the MIRD scheme. Clinical follow-up was obtained from all patients.

The mean radiation doses to the thyroid remnants were 23.5 Gy / administered mCi of ^{131}I (range 0.4-62.5 Gy/mCi), with a mean effective $t_{1/2}$ of 39.3 ± 27.0 h (range 11.9-109.3 h). Doses needed for successful remnant ablation were ≥ 300 Gy. Mean doses to metastases were 4.7 Gy/mCi (range 0.1-42 Gy/mCi), with mean effective $t_{1/2}$ s of 34.0 ± 44.1 h (9.6-192 h). The biological $t_{1/2}$ s in remnants and metastases were strongly dependent upon the TSH values (the higher the TSH, the shorter the $t_{1/2}$), whereas no significant correlation was found between TSH and absolute radioiodine uptake values (range in thyroid remnants: 1.4-70 $\mu\text{Ci/mCi} \times \text{g}$ tissue; in metastases: 0.1-25.8 $\mu\text{Ci/mCi} \times \text{g}$) or resulting doses.

Radioiodine uptake, thus, radiation doses per administered mCi were significantly higher in the present study in patients from iodine-deficient areas as compared to those published earlier. Although threshold doses for successful tissue ablation are similar between this and earlier studies, uptake values, and not effective $t_{1/2}$ s seem to be the most important parameters determining the radiation dose to the tissues.

OS-182

J. Lampinen*†, A. Kuronen†, P. Välimäki*, J. Stepanek§ and S. Savolainen‡, *Dept of Physics, Helsinki University (POB 9, FIN-00014 Helsinki University), †Helsinki University Central Hospital, ‡Helsinki University of Technology, §Paul Scherrer Institut

CLUSTER MODELS IN CELLULAR LEVEL DOSE CALCULATIONS

The dosimetry protocols of the systemic radiation therapy (SRT) are still under construction. One aspect of the problem is the cellular level energy deposition in tumour and healthy cells. The therapeutic effect of radionuclides used in radioimmunotherapy (RIT) depends e.g. on the microscopic activity distribution. A program for modelling absorbed electron dose in different cell cluster models was used to determine the difference in the therapeutic effect when calculated using a close-packed cubic geometry and our cell cluster model. Our cluster model piles the cells individually as close to the origin as possible. Using both cell cluster models we generated clusters with spherical tumours of variable diameters inside healthy tissue. The cells were modelled as spheres of diameters of 12 (tumour) and 30 (normal cell) μm . Activity was assumed to be homogeneously distributed in the tumour cells or on the surface of them. The program uses dose kernels calculated with the Monte Carlo code. Small energy Auger and Coster-Kronig electrons ($E < 1\text{keV}$) were assumed to deposit their energy at their creation point. Calculation of the electron radiation spectra was based on the Auger and X-ray transition strengths and fluorescence yields of the isotopes. The program uses the dose kernels to calculate dose from one cell (source) to another (target) in any distance. The therapeutic effects of ^{111}In , ^{113}In and ^{114m}In were calculated for both cell cluster models with different geometries. In case of ^{111}In and a small tumour cluster (60 μm of diameter), the ratio of the therapeutic effects calculated with different cluster models may at the vicinity of the tumour be as high as 200. This indicates that the choice of cluster model is important in cellular level dose calculations. Especially near the tumour/healthy tissue interface, the doses are different due to geometrical differences.

OS-183

T.M. Behr¹, S. Memtsoudis¹, R.M. Sharkey², S. Gratz¹, M. Béhé¹, R.D. Blumenthal², R.M. Dunn², D.M. Goldenberg², W. Becker¹.

Department of Nuclear Medicine¹ of the University of Göttingen, Germany, and Garden State Cancer Center², Belleville, NJ, USA.

THE ROLE OF THE RADIATION DOSE AND DOSE RATE ON MYELOTOXICITY AND ANTI-TUMOR EFFICACY IN RADIOIMMUNOTHERAPY (RIT) WITH MONOCLONAL ANTIBODY FRAGMENTS.

Whereas bivalent fragments (e.g., F(ab)_2) have been widely used for RIT, no systematic study has been published on the therapeutic performance of monovalent Fab *in vivo*. Therefore, the aim of this study was to determine, in an animal model, the therapeutic performance of ^{131}I -labeled Fab as compared to F(ab)_2 or IgG, and to analyze factors that influence their dose-limiting toxicities and anti-tumor efficacy.

The maximum tolerated doses (MTD), as well as dose-limiting organ toxicities, of the ^{131}I -labeled anti-CEA antibody, MN-14 (IgG, F(ab)_2 , and Fab), were determined in nude mice bearing s.c. xenografts of the human colon cancer line, GW-39. The mice were treated with or without bone marrow transplantation (BMT), or inhibition of the renal accretion of antibody fragments by D-lysine, or combinations thereof. Blood counts, kidney and liver function parameters, as well as tumor growth, were monitored. Radiation dosimetry was calculated from the biodistribution data.

With all three ^{131}I -labeled immunoconjugates (IgG, F(ab)_2 , and Fab), the red marrow was the only dose-limiting organ; maximum tolerated activities were 260 μCi for IgG, 1200 μCi for F(ab)_2 , and 3 mCi for Fab, corresponding to blood doses of 17 Gy, 9 Gy, and 4 Gy, respectively. Initial dose rates were ten times higher with Fab as compared to IgG, and still three times higher as compared to F(ab)_2 . The MTD of all three conjugates could be increased by BMT by approximately 30%. In accordance with renal doses < 10 Gy, no sign of nephrotoxicity was observed with any of the conjugates. In accordance to dose rates never exceeding those occurring at the single injection MTD, two subsequent injections of 2400 μCi ^{131}I -Fab (i.e., $2 \times 80\%$ of the single shot MTD) were tolerated without increased lethality, if administered 48 h apart. In contrast, re-injection of bivalent conjugates was not possible within 6 weeks. Despite lower tumor doses (e.g., 9 vs. 18 Gy for ^{131}I -Fab vs. -IgG or - F(ab)_2), but 7-times higher initial dose rates at equitoxic dosing, Fab was more effective in controlling tumor growth than the respective bivalent fragment or IgG.

These data show an improved anti-tumor efficacy of antibody fragments, as compared to intact IgG. The improved anti-tumor efficacy, but also the higher myelotoxicity at lower marrow doses, are most likely due to the substantially higher initial dose rates observed with antibody fragments. (Supported in part by grant Be 1689/4-1 from the Deutsche Forschungsgemeinschaft DFG).

OS-184

T.M. Behr, M. Löhr, E. Wehrmann, M. Béhé, S. Memtsoudis, V. Vougioukas, S. Yücekent, S. Gratz, K. Nebendahl, and W. Becker.

Department of Nuclear Medicine of the Georg-August-University of Göttingen, Germany.

THERAPEUTIC EFFICACY AND DOSE-LIMITING TOXICITY OF AUGER ELECTRON (^{125}I , ^{111}In) VERSUS CONVENTIONAL BETA EMITTERS (^{131}I , ^{90}Y) IN RADIOIMMUNOTHERAPY (RIT) OF COLORECTAL CANCER WITH INTERNALIZING ANTIBODIES.

Recent studies suggest a higher anti-tumor efficacy of internalizing monoclonal MAbs, when labeled with Auger-electron-, as compared to β -emitters. The aim of this study was to compare the anti-tumor efficacy and toxicity of the internalizing Mab, CO17-1A, labeled with Auger emitters (^{125}I , ^{111}In) versus β -emitters (^{131}I , ^{90}Y) in a colon cancer model, and to assess whether the residualizing radiometals may have therapeutic advantages over the conventionally iodinated conjugates.

Biodistribution studies of ^{125}I -, ^{111}In -, or ^{88}Y -labeled CO17-1A were performed in nude mice, bearing subcutaneous human colon cancer xenografts. For therapy, the mice were injected either with 200 μg of unlabeled, ^{125}I - or ^{131}I -, ^{111}In - or ^{90}Y -labeled CO17-1A IgG_{2a}, whereas control groups were left untreated. The maximum tolerated dose (MTD) of each agent was determined. Myelo- (leukocyte and platelet counts) and potential second-organ toxicities (e.g., liver, kidney, as indicated by GOT, GPT, BUN, creatinine levels in serum), as well as tumor growth were monitored. Bone marrow transplantation (BMT) was performed in order to enable dose-intensification.

Radiometals showed significantly better tumor-to-blood ratios than the respective iodinated conjugates. The MTDs of ^{131}I - and ^{125}I -CO17-1A without artificial support were 300 μCi and 3 mCi, respectively; the MTD of the metals was reached at 100 μCi for ^{90}Y -, and at 2.5 mCi for ^{111}In -CO17-1A. Myelotoxicity was dose-limiting in all cases. BMT enabled an increase of the MTD to 400 μCi of ^{131}I -labeled, to 120 μCi of ^{90}Y -, and to 3.2 mCi of the ^{111}In -labeled CO17-1A, whereas the MTD of ^{125}I -17-1A has not been reached at 5 mCi with BMT. The therapeutic results were significantly ($p < 0.001$) better with both Auger electron- (^{125}I and ^{111}In) than with the β -emitters, and, in accordance to the biodistribution data, a trend versus better therapeutic results with radiometals was found as compared to radioiodine ($p < 0.05$).

These data suggest the superiority of Auger-electron emitters, such as ^{125}I or ^{111}In , at equitoxic doses as compared to therapy with internalizing MAbs labeled with conventional β -emitters. The lower toxicity of Auger emitters may be due to the short path length of their low-energy electrons, which can reach the nuclear DNA only if the antibody is internalized (as is the case in antigen-expressing tumor tissue, but not in the stem cells of the red marrow). (Supported in part by DFG grant Be 1689/4-1).

OS-185

J. Kotzerke¹, R. Gertler², R. Baur², O. Ickrath³, A. Both³, V. Hombach², S.N. Reske¹, R. Voisard². Department of Nuclear Medicine¹ and Department of Cardiology², University of Ulm, Katharinen Hospital Stuttgart³, Germany

INHIBITION OF PROLIFERATIVE ACTIVITY OF HUMAN CORONARY VASCULAR CELLS AFTER RADIATION FROM A BALLOON CATHETER FILLED WITH LIQUIDE RHENIUM-188

A new concept uses irradiation to overcome the problem of restenosis after angioplasty (PTCA). Rhenium-188 is a high energy beta-emitter which is routinely available from the tungsten-188/rhenium-188 generator in liquide form. Using a specific activity of 2 GBq/ml in a PTCA catheter, 30 Gy at the vessel surface can be achieved within 10 mins. The biologic effect of this procedure on the predominant cells of the coronary artery was investigated.

Smooth muscle cells from human coronary plaque material (HCPSMC, plaque material of 52 patients), smooth muscle cells from the human coronary media (HCMSMC, Clonetics), human coronary endothelial cells (HCAEC, Clonetics) and human umbilical endothelial cells (HUVEC) were successfully isolated (HCPSMC and HUVEC), identified and cultured (HCPSMC, HCMSMC, HCAEC, HUVEC).

Cells were seeded, cultured in normal growth medium and irradiated after 24 hrs in a density of 3,000-5,000 cells/cm². The radioactive balloon catheter was fixed in a specially designed device with a minimal distance to the cell monolayer (<100 µm) and 10-50 Gy were applied to the cells (radiation time: 5-30 min). 18 hrs before fixation, bromodeoxyuridine (BrdU) was added to the cultures. After 18 hrs the number of BrdU-positive cells was analysed in a strictly limited field opposite to the radioactive catheter (sample size: 500 cells) and compared to non-irradiated controls. Dose depending inhibition of the proliferation could be observed. After irradiation with 30 Gy, there was an inhibition of proliferative activity of HCPSMC (minus 66%, p<0.05), HCMSMC (minus 55%, p<0.05), HCAEC (minus 50%, p<0.05), and HUVEC (minus 64%, p<0.05).

In conclusion, proliferation of the predominant cells of the coronary artery could be inhibited by irradiation using a Re-188 filled balloon catheter. An effective dose of 30 Gy could be achieved in 10 mins which might be a tolerable interval in patients (if necessary with interruption).

OS-186

¹F. F. (Russ) Knapp, Jr., ¹A. L. Beets, ^{1,2}S. Guhlke, ²H.-J. Biersack, ³M. Stabin and ³R. E. Spencer. ¹Nucl. Med. Group, Oak Ridge Nat. Lab. (ORNL), TN; ²Clinic Nucl. Med., Univ. Bonn, Germany; ³Oak Ridge Associated Univ. (ORAU), TN; ⁴Knoxville Carr. Group, Knoxville, TN.

LIQUID-FILLED BALLOONS FOR CORONARY RESTENOSIS THERAPY - STRATEGY AND DOSIMETRY FOR USE OF RHENIUM-188 (Re-188).

Use of radioisotopes for vascular irradiation is an effective method to inhibit coronary restenosis after PTCA. We have pursued the unique use of PTCA balloons inflated at low pressure with solutions of Re-188, since use of liquid-filled balloons provides the most uniform vessel wall dose delivery profile. Rhenium-188 has an attractive half-life (16.9 h), emits a high energy beta particle (2.12 MeV) and is readily available on demand from our alumina-based tungsten-188/rhenium-188 generator which has a useful shelf-life of several months. In the unlikely event of balloon rupture, Re-188-perrhenate exhibits rapid urinary excretion (T_{1/2} 10 h in rats) and thyroid uptake is displaced with oral perchlorate. Because of the very high specific-volumes (> 150 mCi/mL) required for angioplasty balloon inflation, we have developed simple and efficient post-elution concentration methods using "tandem" Dowex cation/ QMA "Light" SepPak® anion columns. The final Re-188-perrhenate is eluted from the anion column with saline or ionic contrast (i.e. Hypaque). Concentration ratios of > 20:1 are readily achieved with final specific volumes as high as 800 mCi/mL. Because of the importance of accurate dose planning, a Windows-based personal computer program has been developed for calculation of radiation dose to the vessel wall using MCNP 4B and EG54 Monte Carlo codes. The program allows selection of vessel diameter, comparison of different radioisotopes and either wire or solution sources, and also accounts for density of arterial plaque. The status of Phase I clinical trials which are now in progress with Re-188 liquid-filled balloons at several sites in the U.S., Europe and Australia for therapy of *de novo* and "in stent" lesions will be discussed. ORNL is managed by Lockheed Martin Energy Research Corporation for the U.S. DOE under contract DE-AC05-96OR22464 and ORAU under contract DE-AC05-76OR00033.

Oncology: Therapy

OS-187

B.Stolz, K. Pollehn and R. Haller

Research Oncology, Novartis Pharma AG, Basel, Switzerland

RADIOTHERAPEUTIC EFFICACY OF ⁹⁰Y-SMT 487 (⁹⁰Y-DOTA-DPHE¹-TYR³-OCTREOTIDE) VERSUS HIGH DOSE-¹¹¹IN-OCTREOSCAN IN A RAT TUMOR MODEL

Aim of the study: to compare the radiotherapeutic efficacy of the new beta emitter coupled somatostatin analog ⁹⁰Y-SMT 487 (⁹⁰Y-DOTA-DPHE¹-Tyr³-octreotide, OctreoTher™) and that of high dose treatment with the diagnostic [¹¹¹In-DTPA-DPHE¹]octreotide (¹¹¹In-OctreoScan) in a preclinical tumor model.

Materials and Methods: ¹¹¹In-OctreoScan and ⁹⁰Y-SMT 487 were prepared to yield specific activities of approx. 1 Ci/µmole. Thirty-nine Lewis rats bearing the CA 20948 rat pancreatic tumor (cumulative tumor size ~ 9000 mm³/rat) were randomized into five groups. Each animal received a single injection into the jugular vein of 10 mCi/kg, 20 mCi/kg or 30 mCi/kg of ¹¹¹In-OctreoScan, or of 10 mCi/kg of ⁹⁰Y-SMT 487 or of 13 µg/kg of DOTA-DPHE¹-Tyr³-octreotide (control) (n=6-10/group). The tumor volumes and body weights were measured twice weekly during the first two weeks and once per week thereafter.

Results: A single administration of ¹¹¹In-OctreoScan resulted in a regression of tumor (20 mCi/kg.) or produced stable disease (10 and 30 mCi/kg ¹¹¹In-OctreoScan) only up to three days post injection (p.i.) and the animals had to be sacrificed already at day 10 p.i. due to excessive tumor growth. The animals of the control group had to be sacrificed at 7 days p.i. In contrast to that, 80% of the tumor bearing rats that were treated with 10 mCi/kg of ⁹⁰Y-SMT 487 exhibited complete tumor remission at day 31 p.i.

Table: Effect of ⁹⁰Y-SMT 487 and ¹¹¹In-OctreoScan in tumor bearing rats

Compound	Dose(mCi/kg)	T/C %		Maximum Tumor Regression (%)
		day 3	day 7	
⁹⁰ Y-SMT 487	10	52	22	92, day 31
¹¹¹ In-OctreoScan	10	59	133	2, day 3
¹¹¹ In-OctreoScan	20	48	97	21, day 3
¹¹¹ In-OctreoScan	30	59	96	none
SMT 487, 13 µg/kg (control)	-	100	100	none

Conclusion: Both high-dose ¹¹¹In-OctreoScan and ⁹⁰Y-SMT 487 were active in a somatostatin receptor-expressing animal tumor model. However, a single high dose of the radiodiagnostic drug ¹¹¹In-OctreoScan yielded only a weak and transient tumor regression/stable disease. In contrast to that, a single treatment with the beta-emitting ⁹⁰Y-SMT 487 resulted in a complete tumor remission in 80% of the rats. Therefore, ⁹⁰Y-SMT 487 is considered to be the appropriate radiotherapeutic drug for effective treatment of somatostatin receptor-expressing tumors.

OS-188

A. Otte, M. Goetze, S. Dellas, R. Hermann, E.U. Nitzsche, E. Jermann, H.C. Bucher, A. Heppeler, J. Mueller-Brand, H.R. Maecke. Institutes of Nuclear Medicine and Departments of Oncology, University Hospitals Basel, Switzerland, and Freiburg, Germany

YTRITIUM-90-LABELLED SOMATOSTATIN-ANALOGUE: A PROMISING NEW ANTI-CANCER DRUG CONCEPT

Treatment of unresectable somatostatin receptor positive tumours of any histology has been a cause of concern for several years. Chemotherapy and/or radiotherapy often have failed. As a promising alternative, a new peptidic vector, DOTA-D-Phe¹-Tyr³-Octreotide (DOTATOC) that can be stably labeled with the β-emitting radioisotope yttrium-90, has recently been developed.

Intravenous Y-90 DOTATOC treatments have been started in up-to-now 10 patients with different receptor positive tumors: 6 patients received multiple treatments and 4 a single treatment. Treatment was monitored by CT, In-111-DOTATOC scintigraphy and laboratory parameters in all patients, and additionally by FDG-PET in 2 patients.

All 6 multiple-treated patients showed beneficial effects on tumour growth and symptomatology. We report two cases: A 44-year-old man with multiple metastases of a neuroendocrine carcinoma of unknown localization received 7 treatments with Y-90 DOTATOC (25, 25, 40, 50, 50, 60, 80 mCi). After he had experienced rapid metastatic spread, despite two cycles of chemotherapy, he showed a clear clinical improvement, no further metastases and no growth of the known tumour masses. His back and abdominal pain disappeared and he no longer needed treatment with morphine. Chromogranin-B decreased from 295 to 141 pmol/L, neuron specific enolase from 20 to <10 µg/L. A 52-year-old woman with unresectable and chemotherapy resistant metastasizing presacral neuroendocrine carcinoma received 5 treatments with Y-90 DOTATOC (40, 60, 80, 95 and 110 mCi). CT revealed shrinkage of a lymph node metastasis in the anterior superior mediastinum from 14 cm³ to 5 cm³. The presacral tumour mass exhibited a regression in size from 112 cm³ to 96 cm³. In-111-DOTATOC scintigraphy also revealed a 2-fold reduction of peptide uptake in the lymph node metastasis. In 2 of the 4 single-treated patients (both thymus carcinomas, 40 mCi and 60 mCi, respectively), FDG-PET revealed a marked reduction of glucose uptake in the tumour. Standardized uptake values decreased from 4.3 to <2 and from 6.5 to <2, respectively. The remaining patients (neuroendocrine carcinoma, 60 mCi, and multiple meningioma, 40 mCi) showed a stable disease. In 9/10 patients, toxicity of platelets and white cells did not exceed grade 1 of the National Cancer Institute grading criteria at any stage of the treatment cycles. One patient developed a grade 4 thrombocytopenia and a grade 4 anemia persisting over 3 months after 5 treatments with a total dose of 385 mCi. In 9/10 patients, a grade 3 lymphopenia developed from grade 2 at baseline within 1 week after each therapy injection, recovering within 6 weeks, but without clinical impact. In 9/10 patients, renal and hepatic toxicity was not seen, whereas one patient showed a grade 1 serum creatinine increase after 5 treatments with a total dose of 380 mCi.

On account of the demonstrable efficacy, Y-90 DOTATOC could be a potential and promising new therapeutic agent for anti-cancer treatment of somatostatin-receptor positive tumours. Whereas in 9/10 patients hematologic toxicity was restricted to lymphocytes, one patient receiving the highest total dose developed a grade 4 toxicity. Further studies with respect to the maximum tolerated dose are in progress.

OS-189

I. Virgolini, P. Smith-Jones, R. Moncayo, A. Kurtaran, M. Wenger, M. Raderer, E. Havlik, P. Angelberger, I. Szilvaszi, S. Zoboli, G. Paganelli, G. Riccabona.

Universities of Vienna, Innsbruck and Budapest, and European Institute of Oncology, Milano.

111In-90Y-DOTA-LANREOTIDE SCINTIGRAPHY AND THERAPY: INITIAL CLINICAL RESULTS OF „MAURITIUS“

We have developed the somatostatin (SST) receptor (R) seeking agent DOTA-lanreotide (i.e. MAURITIUS) which binds to SSTR2 through 5 with high affinity and to SSTR1 with low affinity. These R are frequently expressed on most human tumors. We report the first clinical results of MAURITIUS (Multicenter Analysis of a Universal Receptor Imaging and Treatment initiative, a European Study). In 111In-MAURITIUS (120 MBq; nmol) was administered as an i.v.-bolus injection and dynamic sequential imaging over one known tumor site was performed during the first 20-30 min p.i.. Thereafter, a serial whole body scans, blood and urine were obtained up to 72(96) h p.i. for tumor, whole body and organ dosimetry. SPECT dosimetry was also obtained in single patients. From 47 pts studied, 18 pts had carcinoid tumors, 5 pts other neuroendocrine tumors, 7 pts lymphomas, 11 pts intestinal adenocarcinomas, 3 pts de-differentiated radioiodine-negative thyroid carcinomas, 2 pts prostate and 1 pt breast cancer. In 43/47 pts known tumor sites were visualized by 111In-MAURITIUS scintigraphy. The calculated tumor uptake ranged between 1 (carcinoid under lanreotide treatment) and 100Gy/GBq (colorectal carcinoma for Y-90-MAURITIUS. Pts with favourable dosimetry (> 10 Gy/GBq tumor dose) were scheduled for treatment with 90Y-MAURITIUS (1 GBq per treatment dose, multiple doses given every 4 weeks). To date, in 4 pts with carcinoids, in 2 pts with intestinal adenocarcinomas and in 1 pt with gastrinoma up to 6 treatment doses were applied. Significant regression of tumor disease was indicated in the pt with gastrinoma (after 4 doses) and stable disease in 4 carcinoid pts (up to 3 doses). We conclude that 111In-MAURITIUS shows a high tumor uptake for a variety of different human tumor types and allows prediction of successful treatment intervention using 90Y-MAURITIUS.

OS-190

P.P.M. Kooij, M. de Jong, M. Boonzaaijer, and E.P. Krenning.

University Hospital Dijkzigt, Department of Nuclear Medicine, Rotterdam, The Netherlands.

THE CONSEQUENCES OF THE EFFECT OF COLD OCTREOTIDE TREATMENT ON PEPTIDE RECEPTOR RADIO-NUCLIDE THERAPY WITH [In-111-DTPA-D-Phe1]-OCTREOTIDE.

In several publications it has been suggested that administration of cold octreotide (CO) has a positive effect on the visualisation of tumors after i.v. administration of [In-111-DTPA-D-Phe1]-Octreotide (In-Oct). Our impression, however, was that the better visualisation of tumors, especially in the abdomen, was caused by a more pronounced reduction of uptake of In-Oct in the kidneys, liver and spleen, compared to the reduction of uptake in tumors. This a very important issue, since in peptide receptor radionuclide therapy (PRRT) maximal uptake in the tumor is essential.

Aim: To quantify the effect of CO treatment on the 24h uptake of In-Oct in the kidneys, liver, spleen and especially in tumors.

Method: In a prospective study the absolute uptake, expressed as percentage of the injected dose, in the forementioned organs after a diagnostic dose of In-Oct (220 MBq, 10 µg) was calculated in 6 patients who were scanned twice, during and without CO treatment. In 5 patients the scan without CO treatment was performed first. The interval between the scans varied from 1 to 12 months (mean=6.5). In none of the patients tumor shrinkage has been observed in this interval. The dose of CO varied from 300 to 1500 µg daily.

The ratio of the absolute uptake values during and without CO treatment was calculated (+/- ratio).

Results: In 3 of 5 patients the uptake in the kidneys was lower during CO treatment, thus +/- ratio < 1 (kidneys range 0.6-1.4). In all patients the +/- ratio for the liver, spleen and tumors was < 1 (liver range 0.3-0.7, spleen range 0-0.3, tumor range 0.2-0.9).

Conclusion: Treatment with CO negatively affects uptake in tumors. Although the results are based on In-Oct scintigraphy, it may be important with regard to PRRT with radiolabelled octreotide analogues in general. The lower uptake will reduce the effects of PRRT. If possible, the CO treatment has to be stopped before PRRT.

OS-191

R.S. Zhu, J.X. Ma, J. Zhu

Department of Nuclear Medicine, Shanghai Sixth People's Hospital, Shanghai 200233, China

58 CASES OF MALIGNANT PHEOCHROMOCYTOMA TREATED BY 131I-MIBG—THERAPEUTIC RESULTS AND ADVERSE EVENTS

Clinical experience in the treatment of 58 cases of malignant pheochromocytoma with soft tissue metastasis was hereby reported. Treatment regimen: intravenous 131I-MIBG 2590mBq -3700mBq (70 -100 mCi) monthly was instituted for 6 months in the first course, after which treatment was continued at 2-3 month interval for another 1-3 courses. MIRD was applied to estimate absorptive dose by the tumor. Results: Patients were classified into three groups according to tumor size. In the first group, tumor was under 8 cm³ (11 cases). In the second group, the size was from 8-20 cm³ (21 cases). In the third group, the tumor size was > 20 cm³ (26 cases). In the first group, the mean absorption dose was 12924.4 cGy. Absorption dose per gram of tumor was above 1000 cGy. After treatment, tumors disappeared in all, attaining treatment goal. In the second group, the absorption dose was similar, but the mean absorption per gram was 217.6 cGy, and tumor regression was only 36% (8 cases). 76% showed urinary reduction of catecholamines; However, 64% showed as regression of tumor size. In the third group, the mean absorption dose per gram tumor size was 277 cGy. After treatment, 30% demonstrated tumor progression, 20% died. The remaining cases showed symptomatic improvement with change in tumor size. In 58 cases, 3, 5, 10 years follow up was carried out. The results showed that 131I-MIBG did not demonstrate significant bone marrow suppression; only 5.1% had severe bone marrow suppression. In most cases, bone marrow suppression was only temporary. Furthermore, bone marrow suppression was not related to the dosage. Conclusion: 131I-MIBG exhibited certain therapeutic benefit with symptomatic improvement. Blood pressure could be controlled, and urinary catecholamine complete case—viz tumor disappearance was yet difficult. However, complete disappearance was possible in small tumors. Thus, treatment with 131I-MIBG should be instituted immediately after surgical resection to eradicate the remaining tumor and prevent recurrences. Bone marrow suppression was temporary and not dosage related. Treatment could be reinstated after several weeks.

OS-192

V. Rufini, A. Tornesello*, I. Saletnich, S. Mastrangelo*, R. Mastrangelo*, L. Troncone. Depts. of Nuclear Medicine and Pediatric Oncology*. Catholic University of the Sacred Heart, Rome - Italy

AN ORIGINALLY DEVELOPED TREATMENT OF ADVANCED STAGE NEUROBLASTOMA (NB): A NEW COMBINATION OF CHEMOTHERAPY AND I-131-MIBG

I-131-MIBG therapy is an effective and well tolerated treatment modality in advanced NB. However, the heterogeneity of MIBG uptake and/or the emergence of resistant clones can limit the efficacy of this radiopharmaceutical when used alone. Therefore, I-131-MIBG has been associated to chemotherapeutic agents. A previous study of MIBG therapy in combination with cisplatin (administered the day before the MIBG infusion) in 7 patients showed to be effective (2 CR, 1 VGPR, 3 PR, 1 MR); however the possible therapeutic utility of this approach was affected by a significant hematological toxicity. Cyclophosphamide was included in the regimen to reduce toxicity through a possible "priming" effect of the drug. Cisplatin (20 mg/m²/day i.v. for 4 days) and cyclophosphamide (2g/m² i.v. in 2 hrs) were administered followed ten days afterwards by 7.4 GBq of I-131-MIBG. Thirteen pts (16 mo-8 yrs) were treated: 10 with relapsed or refractory disease (group 1) and 3 at diagnosis (group 2). Patients were evaluated within 3-6 weeks. In the 10 relapsed pts 7 PR, 1 mixed response, 1 MR and 1 SD were obtained. In the 3 pts of group 2, 2 VGPR and 1 PR were observed. T/B ratios were evaluated with a tracer dose of I-131-MIBG prior to and after chemotherapy; no decrease of MIBG uptake was observed. Hematological toxicity was acceptable and short-lasting when compared to the protocol with cisplatin alone. These results demonstrate the feasibility and effectiveness of the combined treatment of high risk NB suggesting that chemotherapy may be intensified and successfully combined with MIBG therapy.

Paediatrics

OS-193

F.H. Schilling, H. Bihl, H. Jacobsson, T. Martinsson, U.G. Falkner, P. Borgström, P.F. Ambros, I.M. Ambros, J. Treuner, P. Kogner Nucl. Medicine, Pediatric Oncology (Katharinen-&Olghospital, Stuttgart); Nucl. Medicine, Pediatric Oncology, Pathology (Karolinska Hospital; Stockholm), CCRI (Vienna); Clinical Genetics Gothenburg/Sweden

SOMATOSTATIN RECEPTOR SCINTIGRAPHY (SRS) IS LESS SENSITIVE THAN MIBG-SCINTIGRAPHY IN THE IMAGING OF NEUROBLASTOMA (NB), BUT PROVIDES ADDITIONAL PROGNOSTIC INFORMATION IN VIVO.

Background: MIBG-scintigraphy is still regarded as one of the essential diagnostic tools in neuroblastoma (Nb) tumors. In a preliminary analysis of a prospective multicenter study comparing the clinical value of MIBG-scintigraphy and SRS in Nbs, we stated recently (1) that SRS tends to be less sensitive than MIBG, but (2) that positive SRS is correlated with biological parameters with a favorable prognosis of the disease.

Purpose: To analyse further the data of the ongoing study with respect to the two aspects above. Additionally, we were now able to correlate the imaging data with real survival data of the children.

Methods: 64 children with histologically proven Nb were investigated at diagnosis or relapse for Somatostatin Receptor (SR) expression *in vivo* by SRS with In-111-pentetreotide. I-123-MIBG scintigraphy was performed in all children. 46 children were followed for a minimum of 18 months. Tumor tissue was analysed for DNA content and chromosome 1p36 integrity in all these patients.

Results: SR expression was detected in 39/64 tumors. Thus, SRS proved to be less sensitive in detecting tumor tissue than MIBG (61% vs. 95%, $p = 0.055$). SR expression was mostly detected in Nbs exhibiting a cytometrically triploid DNA content (23/25). This is significantly different in tumors with di/tetraploidy (5/21, $p < 0.0001$). SR expression was predominantly absent in tumors with deletion of 1p36 (13/14) in contrast to non-deleted tumors (5/32, $p < 0.0001$). Tumors with concomitant adverse genetic features (1p-deletion and di/tetraploid DNA content, $n=13$) were all negative for SR expression, whereas those with one or both favorable features (triploidy and/or normal 1p) more often showed SR expression (6/9 and 22/24 respectively; $\chi^2 = 29.88$, d.o.f.=2; $p < 0.0001$). Survival probability according to Kaplan-Meier was better for children with SR expression: 96,4% at 4 years vs. 52.6% without SR expression ($p=0.005$).

Conclusion: MIBG is still the „gold standard“ in detecting Nb tissue but SR expression in Nb is highly correlated with favorable genetic features and good prognosis; such prognostic information can be of great clinical relevance in some situations.

OS-194

H.R. Nadel, A. Cahill, J.F. Magee, J. Davis

Children's & Women's Health Centre of British Columbia, Division of Nuclear Medicine

PATHOLOGIC CORRELATION OF THALLIUM SCINTIGRAPHY IN CHILDREN WITH OSTEOGENIC SARCOMA

Purpose: To compare the patterns on thallium (Tl-201) scintigraphy with the degree of post chemotherapy pathologic necrosis in children with osteogenic sarcoma (OGS).

Methods: Since 1989 we have performed 76 Tl-201 scans in 36 children with OGS (14 F; 22 M, age range 1.6-18.9 yrs). Scans were performed at diagnosis (N=36) and postchemotherapy/pre-surgery (N=28), with pathology available in N=27 (including 3 sites multifocal disease in 1 patient).

Results: Tl-201 activity in tumor is graded visually compared to heart and compared to % pathologic tumor necrosis:

	> 95%	90-95%	80-90%	50-80%	< 50%
Grade (gr) 1 <heart (N=6)		4			
Gr 2=heart (N=12)	1	5	1	3	
Gr 3>heart (N=20)		3	2	5	3

Tl-201 tumor activity is either $>(N=29)$ or $=(N=9)$ opposite epiphyseal plate activity. Tl-201 tumor uptake is either focal (gr1=5, gr2=11, gr3=14) or diffuse (gr1=1, gr2=1, gr3=6). The pattern of activity is either homogeneous (gr 1=5, gr2=3, gr3=8) or donut (gr1=1, gr2=9, gr3=12), and either in bone alone (gr1=5, gr2=10, gr3=12), or bone and soft-tissue (gr 1=1, gr2=2, gr3=8). These patterns compare to % necrosis as follows:

	> 95%	90-95%	80-90%	50-80%	< 50%
focal pattern		13	2	6	3
diffuse pattern	1	1	1	2	
homogeneous		8	2	2	1
donut	1	5	1	6	2
bone alone	1	11	2	5	1
bone & soft tissue		2	1	3	2
% change in ratio	35.2%	18-67%		-23-67%	

Conclusions: A higher initial visual grade, focal and donut shaped activity and associated soft tissue involvement correlates with the finding of less % tumor necrosis. Percent change in tumor to contralateral non-tumor ratios are worst in tumors showing less pathologic necrosis.

OS-195

Z. Burak¹, D.A. Yüksel¹, N. Çetingül², H. Özkılıç¹, J.L. Moretti³

Dept. of Nuclear Med¹ and Pediatrics², Ege University, TURKEY. Hospital Avicenne, Bobigny³. FRANCE

Tc-99m Sestamibi Scintigraphy at Initial Diagnosis and Post-therapy Follow up Stage IV Neuroblastoma in Comparison with I-131 MIBG and Tc-99m MDP Bone Scintigraphy

Neuroblastoma remains a significant problem in pediatric oncology. Accurate staging of disease is essential for the prognosis and the choice of treatment. In this preliminary study, we prospectively investigated the diagnostic role of Tc-99m MIBI in staging and predicting the therapeutic response of stage IV neuroblastoma (NB) in comparison with I-131 MIBG and Tc-99m MDP bone scintigraphy (BS).

So far, 9 patients (4 girls and 5 boys, between 1-7 ages) with 29 metastatic sites in MIBG diagnosed as stage IV NB were investigated with Tc-99m MIBI and BS. The data were also correlated with US, CT and/or MRI, VMA levels and bone-marrow biopsy. In a period of 11-17 months, MIBG scans, BS and MIBI imaging were repeated 2-3 times in all patients during follow-up after 3-4 cycles of chemotherapy. Scintigraphic findings were correlated with radiological skeletal survey and laboratory results.

Results: 1. Uptake of MIBG by the primary tumor occurred in 7 of 9 patients. Two were detected by BS, but none of the abdominal masses accumulated MIBI. 2. At diagnosis, only 5 of 29 MIBG avid metastatic sites were positive in MIBI scan. 3. At follow-up, period 3 of 5 MIBI avid metastases were resolved while clinical and laboratory data confirmed progressive recurrent disease. 4. Until now, 5 of 9 patients were accepted clinically as multidrug resistant.

The results of this preliminary study point at that Tc-99m MIBI has no role at initial staging of NB, however, it may provide information regarding the response of chemotherapy while its variable accumulation in metastatic sites needs to be investigated.

OS-196

T. Traub, R. Ladenstein, A. Becherer, U. Pötschger, K. Kletter, H. Gadner, I. Virgolini

University of Vienna, Department of Nuclear Medicine and St. Anna Children's Hospital, Vienna

THE IMPACT OF 123I-MIBG SCINTIGRAPHY IN THE CLINICAL LONG-TERM FOLLOW-UP OF NEUROBLASTOMA (NB).

The purpose of this retrospective study was to evaluate the impact of 123I-MIBG scintigraphy in the clinical follow-up of children with NB compared to conventional imaging techniques (CIT). **Methods:** 123I-MIBG scintigraphy and CIT (CT, US, MRT, x-ray, bone scintigraphy) results were analyzed in 33 NB patients (15 males, 18 females; age: 7 days-90 months; 9 pts Stage 2, 8 pts Stage 3, 14 pts Stage 4, 2 pts Stage 4s). The median observation time was 3.5 years. A total of 221 123I-MIBG scintigraphies were compared with 159 US, 100 CT, 90 MRT, 30 bone scintigraphies and 27 x-ray investigations with respect to the location of primary/recurrent tumor, skeleton, liver, lymph nodes or skin metastases. Results were scored as positive, inconclusive or negative and were evaluated for their impact in the clinical long-term follow-up.

Results: 3 of 15 pts with positive or inconclusive MIBG vs negative CIT results for the primary tumor had relapse of disease. In 2 of 9 pts 123I-MIBG scintigraphy indicated earlier the recurrent tumor and in 1 pt earlier absence of relapse. Based on positive MIBG results in the skeleton, alteration of staging and/or treatment of NB was indicated in 7 pts. In 5 of these 7 pts a larger number of skeleton lesions was detected only by 123I-MIBG scintigraphy. Lesion sites in liver, lymph nodes and skin yielded the most ambiguous results in the judgement at diagnosis as well as during follow-up for both 123I-MIBG scintigraphy and CIT. **Conclusion:** 123I-MIBG results as opposed to CIT results were confirmed in the long-term follow-up of NB pts and resulted in a change in staging and/or treatment 8/33 NB pts (24%). This evaluation suggests that 123I-MIBG scintigraphy has a stronger impact than CIT in the monitoring and management of NB pts during long-term follow-up.

Paediatrics

OS-197

K.Y. Tzen, T.C. Yen, W.P. Chen, C.Y. Lin.

Hospital: Chang Gung Memorial Hospital, Department of Nuclear Medicine, & Veterans General Hospital, Department of Pediatrics, Taipei, Taiwan.

IDENTIFICATION OF ACUTE PYELONEPHRITIS IN DAMAGED KIDNEYS USING Tc-99m DMSA-SPECT, Ga-67-SPECT AND CORRELATION WITH THE GRADE OF VESICoureTERAL REFLUX.

This prospective study is to compare (1) the value of planar versus SPECT of Tc-99m DMSA renal scans and (2) the value of Ga-67 SPECT (Ga-SPECT) versus Tc-99m DMSA renal SPECT (DMSA-SPECT) in the detection of acute pyelonephritis (APN) in a previously damaged kidney.

Seventy-two children (aged from 1 wk to 15 yr) with previous Tc-99m DMSA renal scans showing and proven to have renal scarring (118 kidneys) now have clinical and/or laboratory suspicion of APN are included for investigation. APN was defined as being present if all of the following were confirmed: fever (>38.5 centigrade), pyuria (WBC counts/HPF >10), and a positive urinary culture and/or a positive blood culture. DMSA-planar, DMSA-SPECT and voiding cystourethrography (VCUG) were performed in every case within 3 days of hospitalization. In a subgroup of 32 children (49 kidneys) (from 10 mos to 12 yrs) Ga-SPECT were performed in addition. The presence of vesicoureteral reflux (VUR) was graded on a scale from 0 to 5 according to the International Reflux Study.

Our studies showed that new APN lesions were observed with DMSA-SPECT in 56 kidneys (47%) and with DMSA-planar in only 38 kidneys (32%) ($p < 0.05$). None with negative DMSA-SPECT would have positive finding on DMSA-planar. In the subgroup of 49 kidneys, Ga-SPECT detected all but 1 (48 kidneys, 98%) APN lesions. However, DMSA-SPECT detected lesions only in 33 kidneys (67%) ($p < 0.05$). High grade VUR (grade >3) is more commonly associated with repeated APN than did low grade or no VUR. And this is better demonstrated by DMSA-SPECT than by DMSA-planar (46 vs. 30 and 10 vs. 8 respectively).

We thus concluded: In diagnosing repeated APN in previously damaged kidneys, (1) DMSA-SPECT is superior to DMSA-planar; (2) Ga-SPECT is superior to DMSA-SPECT. (3) There is a tendency of repeated APN to occur with high grade VUR than with low grade or no VUR. Previous reports underestimating chance of new renal scars were probably based on intravenous urography or planar DMSA scans.

OS-198

M. Vljakovic, A. Slavkovic, S. Ilic, M. Popovic

Department of Nuclear Medicine and Pediatric Surgery, Clinical Centre Nis, Yugoslavia

RADIONUCLIDE UROFLOWMETRY PATTERN IN CHILDREN WITH PSYCHOLOGICAL DISTURBANCES AND UNSTABLE BLADDER

The purpose of this study was to investigate if abnormal bladder parameters could be detected by radionuclide uroflowmetry in anxious, irritable children with unstable bladder. Radionuclide uroflowmetry was performed in 16 children aged between 8-12 yrs, without evidence of neurologic and nephrourologic disorders. Findings were compared with those obtained in 10 healthy volunteers aged between 7-10 yrs. The dynamics of the bladder emptying were studied after intravenous injection of 37 MBq/10 kg b.w. ^{99m}Tc -DTPA in the posterior views. Images of 90 frames every 2 sec were stored in the 64x64 computer matrix during voiding. The patients voided into a container and the volumes were measured. The parameters evaluated were: bladder capacity (% of expected volume) - BC, residual urine (% of BC) - RU, voiding time (sec) - VT, average flow rate (ml/sec) - AFR and peak flow rate (ml/sec) - PFR. There was a statistically significant difference between controls and children with unstable bladder in the following parameters: BC $98 \pm 6\%$ vs $80 \pm 4\%$ ($p < 0.001$), RV $16 \pm 8\%$ vs $8 \pm 4\%$ ($p < 0.001$), AFR 13 ± 5 ml/sec vs 9 ± 4 ml/sec ($p < 0.05$) and VT 23 ± 8 sec vs 15 ± 6 sec ($p < 0.001$), respectively. The PFR obtained from the control group of 26 ± 4 ml/sec did not differ significantly from the value of children with unstable bladder of 24 ± 5 ml/sec.

Our results show that the radionuclide uroflowmetry is a simple, noninvasive method suggested allows for a good separation of patients with unstable bladder from the normal voiding pattern in children.

Infection/inflammation/hematology: New radiopharmaceuticals in animals

OS-199

P. Laverman, W.J.G. Oyen, G. Storm, E.T.M. Dams, R. Prevost, N. Mullah, S. Zalipsky, J.W.M. van der Meer, F.H.M. Corstens and O.C. Boerman.

Departments of Nuclear Medicine and Internal Medicine, University Hospital Nijmegen, Nijmegen and Department of Pharmaceutics, Utrecht University, Utrecht, The Netherlands and SEQUUS Pharmaceuticals, Inc., Menlo Park, CA, USA.

AVIDIN INDUCED CLEARANCE OF Tc-99m-BIOTIN-PEG-LIPOSOMES TO IMAGE FOCAL INFECTIONS

Previous studies have shown that polyethyleneglycol-coated (PEG) liposomes are excellent vehicles for imaging infection and inflammation. However, due to their long-circulating characteristics, the blood activity remains high, which could hamper visualization of infections in well-perfused tissues. We developed a Tc-99m labeled liposome formulation with biotin-PEG-distearoylphosphatidylethanolamine (DSPE) incorporated in the bilayer. In this study we investigated their imaging characteristics and avidin-induced blood clearance in a rat model.

Liposome formulations with 0.1, 0.5 and 1.0 mol% biotin-PEG-DSPE were prepared and sized by extrusion to a mean size of 90 nm. Liposomes were radiolabeled with Tc-99m via HYNIC that was conjugated to DSPE in the lipid bilayer. In vitro binding assays with avidin were performed. The biodistribution of the liposomes was studied in rats with *Staphylococcus aureus* infection.

In the binding assays, maximal avidin binding capacities were found with the 0.5 and 1.0 mol% formulations. The avidin binding capacity of the 0.1 mol% biotin-PEG-liposomes was 4-fold lower. Twenty-four hours after induction of the *S. aureus* abscess in the left calf muscle, rats were i.v. injected with liposomes (10 MBq/rat). Four hours after liposome administration, when the liposomes had accumulated in the abscess, as determined scintigraphically, rats were i.v. injected with avidin (10 to 1000 μg). No enhanced clearance was found with the formulation with 0.1 mol% biotin, even at the highest avidin dose. The 1.0 mol% formulation showed some minor clearance after injection of 30 μg avidin and rapid clearance at higher avidin doses. Blood levels were reduced from 4.57 ± 0.40 %ID/g to 0.52 ± 0.05 %ID/g within 30 min, while abscess uptake only marginally decreased. Consequently, abscess-to-blood ratios increased 5-fold. Liposomes mainly cleared to liver (8.56 ± 0.64 %ID/g) and spleen (13.80 ± 2.00 %ID/g). Studies in rats infected with *Klebsiella pneumoniae* have been initiated to investigate the new approach in a clinical relevant animal model.

In conclusion, our studies have shown that efficient and rapid avidin-induced clearance of radiolabeled PEG-liposomes can be achieved by incorporation of 0.5 mol% biotin-PEG-DSPE. This liposomal formulation may be suitable to image infections in well-perfused tissues (e.g. vascular grafts).

OS-200

T. Nikula¹, K. Jaakkola² and S. Jalkanen²

¹ MAP Medical Technologies, Tikkakoski, Finland

² National Public Health Institute and MediCity Research Laboratories, University of Turku, Turku, Finland

RADIOLABELED SPECIFIC MAB AGAINST VAP-1 FOR IMAGING INFLAMMATORY DISEASES

Technetium-99m and indium-111 labeled unspecific IgGs and IgMs have been used to localize an inflammatory process. The mechanism underlying the accumulation of labeled mAbs in these processes has not yet been clarified.

VAP-1 is an endothelial cell molecule that in normal conditions is mainly expressed in intracellular granules. However, in inflammatory situations it is rapidly translocated to the endothelial cell surface, where it facilitates leukocyte entry into the tissue. VAP-1 has been found to be upregulated in the following inflammations: tonsil, synovium, bowel, skin and ischemia-reperfusion injury of heart.

1B2 is a IgM and TK8/14 is a IgG class monoclonal antibody against VAP-1. MABs have been labeled with iodine-123 and technetium-99m. The immunoreactivity fractions of labeled antibodies were determined by using A_x cell line, which was transfected with VAP-1 cDNA (positive cells) or vector alone (control cells). The immunoreactivities of the antibodies were found to be 30 to 70% after labeling.

In our first animal studies with radioiodinated TK8/14, IgG targeted in few minutes on the inflammatory areas and inflammation skin to normal skin ratio was over 20 after 4 h. However, in the first experiments the blood pool activity was high.

The unlabeled and radiolabeled antibodies have shown high specificity for inflamed tissue. We believe that imaging with the specific monoclonal antibody against VAP-1 improves specificity and sensitivity of the diagnosis of inflammatory diseases.

OS-201

C.J. van der Laken, O.C. Boerman, W.J.G. Oyen, M.T.P. van de Ven, J.W.M. van der Meer, and F.H.M. Corstens.
Dpts. of Nuclear and Internal Medicine, University Hospital Nijmegen, Nijmegen, The Netherlands.

EARLY IMAGING OF INFECTION AND STERILE INFLAMMATION WITH RADIOLABELED INTERLEUKIN-8

Several small receptor binding agents have been tested for imaging of infection and inflammation. The potential of chemotactic peptides and of interleukins is promising and seems to be superior to that of conventional radiopharmaceuticals. In the present study, we investigated the potential of radiolabeled interleukin-8 (IL-8) for imaging of infection and sterile inflammation in rabbits. IL-8 was radiolabeled with I-123 via the Bolton-Hunter method. 24 Hr after the induction of *Escherichia coli*, *Staphylococcus aureus* or zymosan abscesses in the left thigh muscle, rabbits were i.v. injected with 18 MBq of ¹²³I-IL-8. Gamma camera images were obtained at 5 min, 1, 4 and 8 h p.i. Biodistribution was determined at 8 h p.i. In all models, ¹²³I-IL-8 rapidly cleared from the blood. In circulation, the majority of ¹²³I-IL-8 was bound to erythrocytes. Accumulation of ¹²³I-IL-8 in the abscesses was visible as early as 1 hour p.i. The highest uptake of ¹²³I-IL-8 was obtained in the *E. coli* abscess at 4 h p.i., i.e. 2.6 ± 0.2 %ID. ¹²³I-IL-8 rapidly cleared from all non-inflamed tissues, resulting in increasing abscess-to-contralateral muscle ratios reaching values higher than 100 in the *E. coli* model and higher than 50 in the *S. aureus* and zymosan model, as determined in tissue biodistribution at 8 h p.i. The radioiodination method clearly affected the in-vivo biodistribution of IL-8, since IL-8 iodinated via the iodogen method cleared significantly slower from the blood and most other organs, resulting in poor visualization of the abscess. The abscess uptake of radiolabeled IL-8 reached high levels despite reduced migration of granulocytes towards the site of infection due to anti-inflammatory activity of i.v. injected IL-8. IL-8 could be injected without induction of neutropenia at a dose level of 2 mg/kg. In conclusion, the superior characteristics of IL-8 radioiodinated via the Bolton-Hunter method, i.e. high abscess uptake and rapid background clearance within a few hours, make IL-8 a promising agent for imaging of infection and inflammation.

OS-202

J.A. Barrett, T. Harris, S. Heminway, L. McKay, M. Vining, A. Crocker, J. Lazewatsky, M. Rajopadhye, S. Liu and D.S. Edwards
Dupont Merck Pharmaceutical Company, N Billerica MA, USA

RP517 A TECHNETIUM-99M LABELED LEUKOTRIENE B4 ANTAGONIST AS A POTENTIAL INFLAMMATION/INFECTION IMAGING AGENT

Our goal was to develop an agent which will rapidly detect sites of infection/inflammation and fulfill an unmet clinical need. A Hynic-derivatized LTB4 antagonists was evaluated in a neutrophil LTB4 binding assay, guinea pig peritonitis, rabbit focal infection, inflammatory bowel and primate dosimetry models. The unlabeled Hynic-derivatized LTB4 antagonist RP517 and Tc99m-RP517 bound to the neutrophil (PMN LTB4) receptor in a similar fashion (IC50 18 & 2nM, respectively). In the guinea pig peritonitis model a casenate soaked suture was placed in the abdominal cavity. 24 hrs later, the Tc99m- RP517 or Tc99m-PMN were administered at a dose of 1 mCi/kg.i.v. and a biodistribution performed at 1 and 4 hrs postinjection. Uptake at the site of infection in the guinea pig model was 0.6 and 0.4 % ID/g at 1 hr and 0.5 and 0.3 % ID/g at 4 hrs. RP517 was excreted via the hepatobiliary route. In the rabbit focal infection model, a thigh was infected with *E. Coli* and 24 hrs later the test agent was administered at 1 mCi/kg.i.v. In this model uptake was similar to that of the guinea pig with the target/background ratio (T/B: infected muscle/normal muscle) 16:1 and 2:1 at 4 hrs. RP517 was cleared from the blood moderately with approximately 25% of the injected dose present at 1hr. In a rabbit model of phorbyl ester-induced inflammatory bowel similar uptake was observed at the focal site (0.3 and 0.1%ID/g) with the target/background ratio (T/B: focal site/normal colon) 16:1 and 2:1 at 1 hr. Primate dosimetry was performed in 4 rhesus monkeys. Preliminary analysis indicates that an injected dose of 400 MBq will yield an Effective Dose of approximately 8 mSv. The organ receiving the highest dose was the gall bladder. In all cases no decrease in white blood cell count was observed.

It is concluded that RP517 was able to rapidly detect sites of acute inflammation/infection. Further this agent may have utility in the rapid diagnosis of acute inflammatory events throughout the body.

OS-203

E.Th.M. Dams¹, M. Reijnen¹, W.J.G. Oyen¹, O.C. Boerman¹, P. Laverman¹, G. Storm², J.W.M. van der Meer¹, F.H.M. Corstens¹, H. van Goor¹.
University Hospital Nijmegen¹, Nijmegen and Utrecht University², Utrecht, The Netherlands.

DETECTING EXPERIMENTAL INTRA-ABDOMINAL ABSCESES WITH Tc-99m-PEG-LIPOSOMES AND Tc-99m-HYNIC-IgG.

Rapid and accurate localization of intra-abdominal infections is a challenging problem for nuclear imaging techniques. Two newly developed technetium-99m-labeled agents, Tc-99m-PEG-liposomes and Tc-99m-HYNIC-IgG, have shown excellent imaging of experimental focal infection, but have not yet been studied in the detection of abdominal abscesses. We studied the performance of these two agents in a rat model of acute abdominal abscess including Ga-67-citrate as a reference agent. **Methods.** On day 0, abdominal abscesses were induced in rats by puncturing the caecum after dissection, backwards filling with faeces, and proximal ligation. The following day, the caecum was resected after rinsing the abdominal cavity with normal saline. On day 8, groups of rats were injected intravenously with Tc-99m-PEG-liposomes, Tc-99m-HYNIC-IgG or Ga-67-citrate. After the last image session at 24 hours postinjection, the rats were killed, and the uptake of the radiolabel in dissected tissues was determined. Macroscopic abnormalities and focal uptake on the images were independently scored on a semi-quantitative scale and compared. **Results.** Abscesses were clearly delineated by each of the agents from 4 hr postinjection onwards. Liposomes, IgG and Ga-67 all showed high absolute uptake in the abscess (2.3 ± 0.3 %ID/g, 2.8 ± 0.3 %ID/g and 2.8 ± 0.4 %ID/g, respectively), and did not differ significantly. Focal uptake of all three radiopharmaceuticals correlated well with the severity of inflammation (for liposomes r = 0.65, p < 0.03; for IgG r = 0.61, p < 0.05; for Ga-67 r = 0.73, p < 0.02). **Conclusions.** Tc-99m-labeled PEG-liposomes and Tc-99m-HYNIC-IgG show high focal uptake in experimental intra-abdominal abscess, similar to the standard agent Ga-67. The uptake correlated well with macroscopic inflammation. The lower radiation exposure and more favourable physical properties of Tc-99m make labeled liposomes and IgG attractive agents for imaging abdominal infection. In addition, PEG-liposomes could be valuable in the treatment of abdominal inflammation by enhanced local delivery of incorporated drugs.

OS-204

M. Rusckowski, T. Qu, F. Chang, R. Marcel, AC. Ley*, RC. Ladner*, DJ. Hnatowich.
University of Massachusetts Medical Center, Worcester, MA and *Dyax Corp., Cambridge, MA., USA.

INFECTION/INFLAMMATION IMAGING WITH A 99mTc-NEUTROPHIL ELASTASE INHIBITOR IN A MONKEY MODEL. A radiolabeled human neutrophil elastase peptide inhibitor (EPI-HNE2) may represent an improved imaging agent for inflammation/infection by localizing specifically to neutrophil elastase released in inflammatory sites by activated neutrophils. In this investigation, the EPI-HNE2 study peptide and a nonspecific control peptide, both about 6.5 kDa, were conjugated with NHS-MAG3 and radiolabeled with 99mTc at room temperature. A rhesus monkey inflammation/infection model was developed using a combination of arachidonic acid and/or sterile or live staphylococcus aureus. No toxicity, dosage effects or circulating antibodies were observed. Plasma clearance was rapid (T1/2 7 min) with kidneys being the major organ of accumulation. Specificity was established in 3 animals receiving labeled control peptide 2 hrs prior to the administration of radiolabeled EPI-HNE2, and in one study in which the radiolabeled peptides were administered 2 wks apart in an animal with a reproducible inflammation. In all 4 cases, the inflammation was more apparent in the EPI-HNE2 images. The ability of labeled EPI-HNE2 to image inflammation was evaluated in 8 additional studies in monkeys receiving only labeled EPI-HNE2 and with inflammations in the arm, shoulder or lower back. Positive images were obtained in all studies, uptake was apparent almost immediately and images were still positive 24 hrs later. Lesion to normal tissue ratios at 2 hrs were 3.5 increasing to 6 at 22 hrs. As an additional control, animal also received 99mTc labeled nonspecific IgG antibody. The lesion was apparent but with higher background levels in liver and heart. In conclusion, 99mTc-EPI-HNE2 localized specifically in inflammation in a monkey model and provided images of diagnostic quality.

Neurology/Psychiatry: Dopamine + serotonin studies

OS-205

C.-G. Swahn¹, C. Loc'h², K. Någren³, C. Halldin¹, I. Günther², J. Hietala¹, B. Mazière² and L. Farde¹.
¹Karolinska Institutet, Stockholm, Sweden, ²CEA, SHFJ, Orsay, France and ³Turku PET Centre, Turku, Finland.

PLASMA METABOLISM OF THE DOPAMINE D2 PET RADIOLIGAND FLB 457 IN HUMAN

The benzamide FLB 457 has one of the highest known affinities for the dopamine D2 receptor (20 pM). It has been labelled with ¹¹C or with ⁷⁶Br and is currently used as a PET ligand for examination of extrastriatal dopamine D2 receptors status in the human brain. It is essential to have a radioligand with a very high affinity as the density of receptors is very low in the extrastriatal brain regions. In connection with PET studies in human beings, blood samples were obtained and plasma was separated. Protein was precipitated and the samples were analysed by HPLC. The results are used for correction of the plasma input function.

The results obtained in three European PET centers are summarised in Table 1. FLB 457 was metabolised faster than the benzamide analog raclopride, which is the PET standard for striatal D2 receptors. One hydrophilic labelled metabolite, several minor labelled metabolites of intermediate polarity, the unchanged compound and also one labelled metabolite more lipophilic than FLB 457 were observed. The results demonstrate that the methods used are valid for a standardized use among European laboratories.

TABLE 1. Percentage of unchanged FLB 457 in plasma from human beings versus time

Time (min)	4	10	20	30	40	50	60
Healthy controls n=16 (KI)	95.0	81.0	52.1	39.4	31.7	26.2	27.8
Schizophrenics n=18 (KI)	92.6	75.8	48.8	36.4	29.2	27.3	24.7
Healthy controls n=63 (TU)	96.6	84.1	55.8	42.4	36.6	30.5	28.7
Schizophrenics n=12 (TU)	95.4	78.0	47.2	35.2	31.2	28.1	24.4
Healthy controls n=4 (CEA)	99	83	63	49	39	33	29

KI stands for Karolinska Institutet, TU for Turku PET Centre and CEA for Orsay. This work has been performed within the BIOMED 2 (BMH4-CT-96-0220)

OS-206

Y.-H. Chou, P. Karlsson, C. Halldin, L. Farde

Karolinska Institutet, Department of Clinical Neuroscience, S-17176, Stockholm, Sweden

LOW ENDOGENOUS DOPAMINE D1 RECEPTOR OCCUPANCY IN THE PRIMATE BRAIN

Several positron emission tomography (PET) studies have shown that radioligand binding to D2 dopamine receptor competes with endogenous dopamine. The purpose of this PET study was to examine the effect of amphetamine and reserpine on D1 dopamine receptor binding. Four Cynomolgus monkeys (A-D) weighing 3-4 kgs were examined with the D1 dopamine receptor radioligands [¹¹C]NNC 112 and [¹¹C]SCH 23390 at baseline conditions and at a series of times after i.v. injection of amphetamine 2 mg/kg and reserpine 1 mg/kg. The binding potential (B/F) in the striatum and the neocortex was determined at transient equilibrium. D1 dopamine receptor density (Bmax) and apparent affinity (Kd) were determined from a Scatchard analysis of two PET measurements with high and low specific radioactivity. The effect of amphetamine on D1 dopamine receptor binding varied between -14% and 6%. These changes can be considered as within the range of the test/retest reliability. Thus, there was no evident effect of amphetamine induced dopamine release on D1 dopamine receptor binding. Five hours after reserpine administration, there was no change in Bmax and Kd. The Scatchard analyses indicated a 13-20% reduction in Bmax without any evident change in Kd at 3, 23, 28 days. The lack of evident effects of amphetamine and reserpine on D1 dopamine receptor binding is markedly different from the 20% amphetamine induced decrease and 50% reserpine induced increase of that has been consistently reported for D2 dopamine receptor binding. The data indicate that endogenous dopamine D1 receptor occupancy is low at physiological conditions.

OS-207

S. Dresel, M.-P. Kung, X.-F. Huang, K. Plössl, C. Hou, C. Shiue, J. Karp, H. F. Kung

Department of Radiology, University of Pennsylvania, USA

SPECT IMAGING USING [Tc-99m]TRODAT-1: IN VIVO BINDING TO THE SEROTONIN TRANSPORTER

[Tc-99m]TRODAT-1 has proven to reliably assess dopamine transporter binding sites in the striatum. Additionally, in vitro and autoradiographic experiments demonstrated binding to the serotonin transporters in the hypothalamus-midbrain area. In this study [Tc-99m]TRODAT-1 was investigated as a potentially useful ligand to image serotonin transporters in the living brain of baboons.

A total of eight SPECT scans was performed in two baboons after iv injection of 740 MBq [Tc-99m]TRODAT-1 using a triple-head gamma camera equipped with UHR-fan beam collimators (scan duration: 210 min.). In four blocking studies, baboons were pre-treated with McN5652 (1 mg/kg) or methylphenidate (1 mg/kg) to block the serotonin or the dopamine transporter binding sites. After coregistration with MRI, ROI analysis was performed using predefined templates from coregistered MRI to calculate specific uptake (Target-Background/Background). Additionally two PET brain scans were performed after iv injection of 85 MBq [¹¹C]McN5652 to image serotonin transporter binding sites.

In [Tc-99m]TRODAT-1 SPECT scans, the serotonin transporter binding sites in the midbrain region were clearly visualized, which was supported by the co-registration of the [¹¹C]McN5652 PET scans. The specific uptake in the hypothalamus-midbrain area was blocked by pre-treatment with non-radioactive McN5652. Semiquantitative analysis revealed a specific uptake of 0.30 ± 0.02 for the scans without any co-injection, which decreased to 0.04 ± 0.005 after pre-treatment with McN5652. With pre-treatment of methylphenidate the specific binding to dopamine transporter sites decreased remarkably from 2.45 ± 0.13 to 0.32 ± 0.04, but no effect was observed on the binding of [Tc-99m]TRODAT-1 to the serotonin transporter sites.

This preliminary study suggests that specific binding of [Tc-99m]TRODAT-1 to the serotonin transporter can be detected by in vivo SPECT imaging, even if the target to background ratio is rather low. However, these promising findings provide impetus for further development of similar compounds with increased affinity to the serotonin transporter binding sites in the hypothalamus-midbrain area.

OS-208

P.D. Mozley, K. Plössl, S. Dresel, E.D. Barraclough, J.B. Stubbs, L.I. Araujo, A. Alavi, J. Saffer, R. B. Sparks, S. Meegalla, and H.F. Kung.

Division of Nuclear Medicine, University of Pennsylvania, Philadelphia, PA and Internal Dosimetry Systems of Oak Ridge, TN USA

BIOKINETICS OF A [Tc-99m] LABELED TROPANE FOR IMAGING DOPAMINE TRANSPORTERS IN THE BRAIN AND GI TRACT.

[Tc-99m]TRODAT-1 is an analog of cocaine that selectively binds dopamine transporters. The purposes of this study was to measure its whole body biodistribution and cerebral kinetics in 10 healthy human volunteers.

Methods: An average of 18 whole body scans were acquired sequentially on a dual-headed camera for up to 46 hours after the intravenous administration of 370 ± 16 MBq (10.0 ± 0.42 mCi) of [Tc-99m]TRODAT. SPECT scans of the brain were acquired on a triple headed scanner. The renal excretion fractions were measured from 13-24 discrete urine specimens voided over 22 to 46 hours. The percentage of the administered dose in 17 regions of interest (ROIs) and each urine specimen was quantified from the attenuation and background corrected geometric mean counts in conjugate views. Multiexponential functions were iteratively fit to each time-activity curve. Gender-specific radiation doses were then estimated from the residence times with the MIRD technique for each subject individually before any results were averaged.

Results: There were no pharmacological effects of the radiotracer. The early planar images showed differentially increased activity in the nose, pendum, and the left upper quadrant corresponding to the stomach. SPECT images demonstrated that the radiopharmaceutical localized in the basal ganglia with caudate to whole brain uptake ratios of up to 4 to 1. There was no metabolism to free perchlorate. Image analysis showed that kidneys excreted between 20 and 32% of the injected dose during the first 22-28 hours post administration. The dose estimates were significantly higher in women than in men because the females who participated in this study were taller and heavier than Reference Woman. Nevertheless, the dose limiting organ in both men and women was the liver, which received an average of 0.046 mGy/MBq (0.17 rads/mCi, range: 0.14-0.22 rad). In the worst case, it would have required 22.7 mCi to deliver 5 rads to the dose limiting organ.

Conclusions: TRODAT selectively binds the dopamine transporters in the brain and the GI tract. Pharmacological side effects are negligible, and its radiation dosimetry profile is highly favorable.

Supported by NIDA grant DA09469.

Neurology/Psychiatry: Dopamine + serotonin studies
OS-209

J.T. Kuikka, D. Guilloteau, J. Hiltunen, K.A. Bergström, P. Emond, C. Haldin, L. Farde, S. Chalon, L. Mauclore, B. Maziere, J.C. Besnard, J. Tiihonen. University of Kuopio, Finland, University of Tours, France, MAP Medical Technologies, Inc., Finland, Karolinska Institutet, Stockholm, Sweden, CIS bio international, France, SHFJ, Orsay, France.

PHARMACOKINETICS AND DOSIMETRY IN HUMANS OF IODINE-123 LABELLED PE2I, A SPECIFIC LIGAND FOR DOPAMINE TRANSPORTER IMAGING

βCIT is widely used for SPECT dopamine transporter imaging but it presents a poor selectivity and a low kinetics. To improve these properties we have developed a new cocaine derivative: the iodine-123 labelled N-(3-iodoprop-2E-enyl)-2-β-carbomethoxy-3β-(4-methylphenyl)nortropane also called (I-123)-PE2I. PE2I displays high specificity for the dopamine transporter and a valuable kinetics in monkey. According to this promising results obtained in non human primates (I-123)-PE2I was evaluated as a probe for selective dopamine transporter imaging in the human brain. Six healthy subjects (mean age of 32years) were imaged with a high-resolution single-photon emission tomography scanner. PE2I was obtained by iodination of the tributyltin precursor and purified by HPLC, the dose injected varied from 140 to 215 MBq. No adverse reactions were observed. High striatum contrasted images were obtained, the striatal radioactivity peak at 64-84 min after injection, leading to a transient equilibrium with a ratio striatum to cerebellum of about 9. The background radioactivity was low. The volume of distribution in the striatum was 94 ± 24 ml/ml (mean ± SD). The results were compared to those of (I-123)-β-CIT at 24 h (170 ± 27 ml/ml). There was no significant uptake of (I-123)-PE2I in serotonin-rich regions such as the midbrain, hypothalamus and the anterior ganglions suggesting that in vivo binding is specific for the dopamine transporter. One main polar metabolite of (I-123)-PE2I was found in plasma, and the parent plasma concentration decayed rapidly. Radiation exposure to the study subject is 0.022 ± 0.004 mSv/MBq (effective dose). The preliminary results suggest that (I-123)-PE2I is a high selective SPECT ligand with very low non-specific binding for imaging striatal dopamine transporter density in human. The dosimetry is acceptable for human use and the scan time is optimal (60-100 min p.i.) in daily clinical routine.

OS-210

R. Linke, J. Gostomzyk, K. Hahn, K. Tatsch
Department of Nuclear Medicine, University of Munich, Munich, Germany

[I-123]IPT-BINDING TO THE PRESYNAPTIC DOPAMINE TRANSPORTER: VARIATION OF THE INTRA- AND INTER-OBSERVER DATA-EVALUATION IN PATIENTS AND CONTROLS

Imaging the presynaptic dopamine transporter with cocaine analogs and SPECT has proven to be a potential diagnostic tool for classifying the extend and degree of dopaminergic nerve cell loss. For a correct interpretation of scan results in individual follow up studies, however, knowledge about the test/retest reproducibility and the intra-/inter-observer variation of repetitive data evaluation is mandatory. Focusing on the latter aspect was aim of the present study using I-123-IPT and SPECT to image the dopamine transporter.

The IPT-SPECT data of 15 controls and 15 parkinsonian pts with various degrees of reduced IPT-binding were analyzed twice by an expert (intra-observer) and once more by a less experienced nuclear medicine physician in training (inter-observer). For semiquantit. evaluation of specific IPT-binding, ratios between total striatum (S), caudate (C), putamen (P) and a background region were calculated. For statistical analyses a variation-index was defined as the absolute difference of the ratios of 1st/2nd evaluation, divided by the mean of the respective region. Mean values were compared by Student's t-test, and in addition regression analyzes were applied.

	Variation-Indices (%)			Significant differences were neither observed with intra- nor inter-observer analyzes. Variation was lower in controls than in the patient group. The highest variation was observed in the putamen, the most severely affected structure in the patient group.
	S	C	P	
Intra- total obs. controls pts	2.3±2.0	3.0±2.2	3.1±2.3	
Inter- total obs. controls pts	1.6±1.0	2.6±1.6	2.2±2.0	
	3.0±2.5	3.4±2.7	4.0±2.3	
	2.6±2.2	3.4±2.7	3.5±2.8	
	2.3±1.8	2.6±1.7	2.9±2.9	
	2.9±2.6	4.1±3.3	4.2±2.7	

In cases of severe disease reliability of data evaluation may be hampered by poor visualization of the putamen as well as inhomogeneous background activity within the putamenal region. As shown in the table overall variation-indices revealed only minor variations. Variation in intra- was only slightly smaller than in inter-observer results, indicating that the evaluations are mostly observer-independent. The intra-/inter-observer results showed highly significant correlations (r=0,94 up to 0,99).

Our results indicate that the specific presynaptic striatal dopamine transporter binding assessed with IPT-SPECT may be reproducibly analyzed by the same and different observers in controls as well as in pts with various degrees of reduced binding. Therefore, IPT-SPECT may be recommended as a useful tool to document the progression of nigrostriatal degeneration in longitudinal studies since even subtle changes indicate specific pathology rather than methodological based variation.

Radiopharmacy and radiochemistry: Tumor markers
OS-211

J. Bogatzky, H. Bender, P. Willkomm, J. Ruhlmann* and H.-J. Biersack
Dept. of Nuclear Medicine, University of Bonn, PET Center Bonn*, Germany

RESULTS OF THE TUMORMARKER S-100 IN COMPARISON TO FDG-PET IN MELANOMA PATIENTS

S-100 is a new promising tumor marker, which might play a role in melanoma screening. The aim of our study was to compare the results of S-100 (RIA) with FDG-PET.

S-100 is an acidic calcium-binding protein in the nervous system and it is present mainly in astrocytes and Schwann cells, but it has also been detected in other tissues and in certain tumors. In studies S-100 has been shown to be a prognostic marker for malignant melanoma and can also give additional information to clinical staging. Therefore it has been also suggested as a marker for treatment monitoring of malignant melanoma. The test is a monoclonal (sandwich) assay which discriminates between the α and β subunit and measures the β subunit of the protein S-100.

Whole-body positron-emission tomography employing [18F]-fluorodeoxyglucose (FDG) was performed in patients suffering from melanoma. Routinely, a multiple (4-6) bed position protocol, with 10-min emission and 10-min transmission acquisition per bed position was used, starting 45-60 min after i.v. injection of 287 Mbq. FDG accumulation was qualitatively graded depending on the intensity of uptake (intense uptake = malignant; moderate uptake: suspicious; minimal uptake: normal/inflammation).

At this time, 96 patients have been evaluated in detail. 56 pts. showed no evidence of disease (FDG-PET, CT, MRI, clinical follow-up > 6 months), 54 of them had values off-curve and 2 pts had values near the sensitivity of < 0,2 µg/L. Of 22 pts. with lymph metastasis showed 13 pts. values under the sensitivity and 9 pts. had values clearly above 0,2 µg/L. 17 pts had more than one FDG-positive lesion which proved to be melanoma. All patients showed measurable S-100 values above the sensitivity. One patients showed FDG-uptake (fals-positive), but presented S-100 values off-curve.

These data indicate, that S-100 may be useful in screening melanoma tissue and to select patients suitable for further staging by FDG-PET.

OS-212

B. Günalp, K.Okuyucu
Gülhane Medical School, Department of Nuclear Medicine, Ankara, Turkey

CLINICAL UTILITY OF FREE/TOTAL PROSTATE SPECIFIC ANTIGEN (PSA) SERUM RATIO AND PSA DENSITY IN THE DIFFERENTIAL DIAGNOSIS OF PROSTATE CANCER

The aim of this study was to evaluate diagnostic value of the proportion of free to total prostate-specific antigen (F/TPSA) and PSA density (PSAD) in enhancing the ability of PSA to distinguish prostate cancer from benign prostatic hyperplasia and decreasing the number of unnecessary prostate biopsies.

Serum samples were obtained from 110 untreated patients with total PSA levels more than 4ng/ml and 50 asymptomatic healthy male control. Total PSA (TPSA) and free PSA (FPSA) were determined by the dual monoclonal antibody immunoradiometric assay. Logistic regression was used to evaluate the importance of F/TPSA and PSAD for predicting of cancer.

The analysis revealed that when all subjects with PSA>4 ng/ml were included, the mean F/TPSA and PSAD values are statistically significantly different between the prostate cancer and BPH groups. (Table I)

	No	PSA (ng/ml)		F/TPSA		PSAD (ng/ml/cc)	
		Mean	SD	Mean	SD	Mean	SD
Normal control	50	2.8	0.8	0.24	0.07	0.12	0.05
BPH	58	9.8	7.3	0.17	0.06	0.20	0.60
Cancer	52	32.9	31.8	0.10	0.05	0.52	0.10
P value*		<0.0001		<0.0001		<0.0001	

Table I: Statistical analysis of total PSA, F/T PSA and PSAD for all subjects by patient group. (*Determined by t test); †SD: Standard deviation)

Cut-off levels were determined for F/TPSA and PSAD at the 0.50 probability. Cut-off levels were found 0.13 for F/TPSA and 0.33 for PSAD. Using logistic regression model and combining PSAD and F/TPSA (PSAD>0.011+2.48 F/TPSA) sensitivity and specificity increased to 73% and 100% respectively. However in the range of PSA between 4-10 ng/ml, F/TPSA alone was found to be superior to PSAD in distinguishing benign and malignant disease.

It is concluded that the differentiation between prostate cancer and BPH can be considerably improved by combining F/TPSA with PSAD and decreased the number of unnecessary biopsies remarkably. However especially in the PSA levels between 4 to 10 ng/mL measurement of F/TPSA alone increases the specificity of PSA in diagnosis of prostate carcinoma and enhances the diagnostic performance. Based on these findings, a diagnostic algorithm was suggested for the screening and the diagnosis of prostate carcinoma.

OS-213

K. Mardon, A. Katsifis, F. Mattner, B. Dikic, A. Donald, J. Chapman

Radiopharmaceuticals Division, ANSTO, PMB 1 Menai, NSW, 2234, Australia.

SYNTHESIS AND PHARMACOLOGICAL EVALUATION OF [123I] IMIDAZO[1,2- α] PYRIDINES AS POTENTIAL TRACERS FOR THE STUDY OF PERIPHERAL BENZODIAZEPINE RECEPTORS USING SPECT.

The peripheral-type benzodiazepine receptor (PBR) differs from the central-type benzodiazepine receptor in anatomical distribution, subcellular location and pharmacological functions. PBR are predominantly associated with the mitochondrial outer membranes of the peripheral organs as well as in the glial cells in the brain. PBR have been implicated in the control of cell proliferation and differentiation and shown to display increased levels in a variety of malignant tumours. A series of halogenated imidazo [1,2- α]pyridines have been prepared, of which, [6-chloro-2-(4'-iodophenyl)-3-(N',N'-dimethyl)-imidazo[1,2- α]pyridine-3-acetamide 1 was found to display potent *in vitro* binding for PBR (IC₅₀=2nM with 3H-PK 11195) compare to a low selectivity for central receptors (IC₅₀=170 nM with 3H-Flumazenil). The iodine-123 analogues of 1 was prepared by iododestannylation with NaI¹²³I in the presence of peracetic acid in acetic acid, followed by purification by RP-HPLC. Specific binding of [123I]1 to rat cerebral cortical, kidney and adrenal membranes was saturable with an equilibrium dissociation constant (K_D) of 9 ± 1.5, 6.1 ± 1.2 and 6.6 ± 1.3 nM, respectively, and a maximal number of binding sites (B_{max}) of 0.24 ± 0.03, 2.4 ± 0.32 and 24.4 ± 4.2 pmol/mg of protein, respectively. *In vivo* biodistribution in rodents indicated high uptake of activity in tissues with known PBR sites: adrenals (10), kidney (0.65), Heart (0.75), Liver (0.54) (% Kg Dose/gram organ 1h post-injection). Pre-treatment of the rats with PK 11195 and the cold material reduced significantly the uptake of activity in organs expressing the PBR. Other drugs such as flumazenil and haloperidol did not modify the uptake of activity in these organs. In Conclusion, [123I]1 indicated high and selective *in vivo* uptake in tissues expressing the PBR, with potential for further development as a SPECT radiotracer for studying the peripheral benzodiazepine receptors.

OS-214

N. Iznaga-Escobar¹, I. Luis², J. F. Amador¹, A. López¹, J. C. Izquierdo¹, R. Pérez¹.

Center of Molecular Immunology, Research Department, Havana 11 600, Cuba.

RADIOIMMUNOTHERAPY OF ¹⁸⁸Re-LABELLED ANTI-HUMAN EGF-R ANTIBODY *ior egf/r3* IN H-125 HUMAN LUNG ADENOCARCINOMA XENOGRAFTED NUDE MICE.

The use of ¹⁸⁸Re from a tungsten-188/rhenium-188 (¹⁸⁸W/¹⁸⁸Re) radionuclide generator system represents an attractive alternative radionuclide for radioimmunotherapy (RAIT). In the present report we have evaluated the biodistribution and the therapeutic effect of the ¹⁸⁸Re-labeled mAb *ior egf/r3* in nude mice xenografted with human H-125 lung adenocarcinoma tumor cell line. Biodistribution studies carried out following i.p administration of ¹⁸⁸Re-labeled mAb *ior egf/r3* to tumor-bearing nude mice indicated good tumor uptake of the radioimmunoconjugate 5.80 ± 1.77 % of the ID/g tissue at 24 hr post-injection. For RAIT when the mice were given ¹⁸⁸Re-labeled mAb *ior egf/r3* at 100 μ Ci/mouse, a significant difference of tumor growth from the untreated saline 0.9 % (p < 0.001) and unlabeled mAb *ior egf/r3* (p < 0.01) control groups was observed and animals that received the activity demonstrated a partial response to the treatment. In one of 12 mice under treatment, the tumor regressed at 1 week post-injection of the ¹⁸⁸Re-labeled mAb *ior egf/r3*. In these animals multiple doses of ¹⁸⁸Re-labeled mAb *ior egf/r3* led to 73 % of inhibition of tumor growth after 35 days of tumor xenografts with long-term survival, only one death (8 %) in a total of 12 grafted mice treated with 500 μ Ci of ¹⁸⁸Re-labeled mAb *ior egf/r3*. The mAb *ior egf/r3* labeled with ¹⁸⁸Re, can effectively control the growth of a tumors in nude mice and RAIT using ¹⁸⁸Re-labeled mAb *ior egf/r3* is able to destroy lung adenocarcinoma xenografts at an early stage.

OS-215

Luca Giovannella, Stefano La Rosa (*), Paola Erba, Carlo Capella (*), Silvana Garancini

Departments of Nuclear Medicine and Pathology (*), University Hospital "Ospedale di Circolo e Fondazione Macchi"- Varese (Italy)

Immunoradiometric assay of Cromogranin-A (CG-A) in diagnosis and staging of neuroendocrine tumours: comparison with Neurone Specific Enolase (NSE) and correlation with immunoistochemical data

Aim: aim of the study was the analytical and clinical evaluation of a new developed immunoradiometric method for CG-A assay in serum (CG-A RIACT Cis Diagnostici, Italy) and the comparison with NSE. Moreover, CG-A and NSE levels were correlated with pathological staging and immunoistochemical data.

Material and Methods: we selected 50 patients affected by neuroendocrine neoplasia. Serum levels of CG-A and NSE were evaluated by immunoradiometric methods (CG-A RIACT, Cis Diagnostici, Italy and NSE, Byk Gulden, Italy) at diagnosis time and correlated to the stage of tumor and immunoistochemical data. A group of 50 healthy subjects was used as control.

Results: quality control tests were performed and showed a CV intraassay minor than 5% while CV interassay was minor than 10% for both methods. Marker distribution in control and pathological groups showed a significative difference only in CG-A levels (p<0.0001) while NSE did not. Using ROC curves analysis we selected a cut off levels of 96 ng/mL for CG-A and 16 ng/mL for NSE, respectively. The correlation between the stage of disease and markers expression underline a good relationship for CG-A and a non significative correlation for NSE. Immunoistochemical data showed a strict link between CG-A serum concentration and its expression in tissues whereas NSE high positive immunoistochemical detection in patents with negative NSE serum level was found.

Conclusions: CG-A RIACT is an accurate method for CG-A serum detection. CG-A is a powerful marker of neuroendocrine tumours, which correlates both with pathological stage and immunoistochemical expression of CG-A. Serum NSE presents low sensitivity and its levels are not correlated with tissutal expression: for these reasons, NSE can not be considered an useful marker for neuroendocrine tumours.

OS-216

M. Filesi, G. Ventroni, A. Signore, F. Fiore Melacrinis, G. Ronga.

SS Nuclear Medicine, Clinica Medica II University of Rome "La Sapienza" - Italy

METASTASES FROM DIFFERENTIATED THYROID CARCINOMA CAN BE EARLY DETECTED BY THE COMBINED USE OF INITIAL 131-I WBS AND THYROGLOBULIN MEASUREMENT

Aim of this work was to evaluate the role of the first 131-I WBS (with and without Tg measurement) after thyroidectomy for the early diagnosis of metastases in differentiated thyroid carcinoma (DTC).

We studied 269 pts with metastases (184 papillary, 85 follicular : 95 lymph node, 174 distant; 53 non 131-I uptaking - follow-up 3 yrs minimum) and we evaluated the results of first 131-I WBS alone in 200 patients from 1958 to 1984, and both first 131-I WBS and first Tg results in 69 pts from 1985 to 1993. In all pts the first 131-I WBS detected the post-surgery remnant, and in 146/269 pts (54.3%) also metastases (60.3% of distant and 43.1% of lymph node - χ^2 P=0.01). In 46/69 pts (66.7%) Tg levels were above 60 ng/mL (76.7% of distant and 50% of lymph node metastases - χ^2 P=0.04). Pts with lymph node metastases had first Tg between 5-60 ng/mL in 11/26 cases (42.3%). In 4/69 pts (5.8%) first Tg was <5ng/mL. First 131-I WBS detected metastases in 11/23 pts with first Tg <60 ng/mL; 31 pts had a negative first 131-I WBS, but Tg were >60ng/mL in 19. In 73.3% (11/15) of pts with non 131-I uptaking metastases we observed a Tg >60ng/mL.

In conclusion, the combined use of WBS and Tg levels revealed in 82.6% of pts the presence of metastases also before the post-surgery remnant ablation.

Our data suggest the following outline: if first 131-I WBS is positive, regardless of Tg results, the presence of metastases is certain; if first WBS is negative, the metastases are rare for Tg levels <5 ng/mL and probable for levels >60 ng/mL: for values between 5-60 ng/mL metastases are possible (predominantly lymph node)

General nuclear medicine: Lung

OS-217

G. Calmanovici*, M. Zubillaga*, A. Lysionek*, A. Hager*, T. De Paoli*, M. Alak*, O. Degrossi*, H. Garcia del Rio*, J. Nicolini#, R. Caro* and J. Boccio*. *Radioisotope Laboratory, School of Pharmacy and Biochemistry, U.B.A., Argentina. #Instituto Argentino de Diagnóstico y Tratamiento, Argentina. # Bacon Laboratories, Argentina.

99mTc-ENS, A NEW RADIOPHARMACEUTICAL FOR AERIAL LUNG SCINTIGRAPHY.

Exogenous natural surfactants (ENS) are used with success in the treatment of the respiratory distress of newborns and seems a promising approach for the treatment of the adult respiratory distress syndrome. For these reasons we studied at our laboratory a new radiopharmaceutical with the purpose of evaluating the lung ventilation, labeling the exogenous natural surfactant with 99mTc (99mTc-ENS). This radiopharmaceutical is administered by inhalation as a fine aerosol, using a nebulizer. In order to evaluate the new radiopharmaceutical's specificity for the lung, we performed biodistribution studies in rats using 99mTc-ENS and compared the results with those obtained with 99mTc-DTPA and 99mTcO₄-. For this study, thirty female Sprague-Dawley rats, were used. Each radiopharmaceutical was placed in the chamber of a comp-air nebulizer to administer each radioaerosol to the rats for five minutes. Twenty five minutes after the aerosol inhalation, the animals were sacrificed to extract their organs. The activity of each organ was measured in a gamma counter. Results were given as the percentage of activity concentration (C%) of each organ. The labeling yield percentage was always higher than 95% for the 99mTc-ENS and the 99mTc-DTPA, even after the aerosolization procedure. Biodistribution studies performed after aerosolization are shown in the table below.

Product	Lungs (%)	Kidneys (%)	Liver (%)	Blood (%)	Spleen (%)	TGI* (%)
^{99m} Tc-ENS	98.7±1.3	0.3±0.4	0.1±0.1	0.6±0.6	0.4±0.4	0.1±0.1
^{99m} Tc-DTPA	77.8±20.6	16.9±16.5	0.5±0.6	2.6±2.6	1.7±2.6	0.5±0.4
^{99m} TcO ₄ -	22.4±7.5	15.6±1.9	14.1±2.4	28.8±3.0	10.2±2.6	9.0±1.7

* TGI is gastrointestinal system (gut + stomach).

The biological behaviour of 99mTc-ENS demonstrates that almost all the radiopharmaceutical concentrates in lungs, while its activity concentration is very low in all the other organs. Our results suggest that this new radiopharmaceutical may be effective for the diagnosis of ventilatory related pulmonary disorders and therefore it can be considered for clinical trials.

OS-218

Rakesh Kumar, Srikant Sharma*, M Sriram, A Malhotra, S Sharma, S Dilip, C Patel.

All India Institute of Medical Sciences, New Delhi-110029. Departments of Nuclear Medicine & Medicine.

RADIONUCLIDE VENTILATION & PERFUSION SCINTIGRAPHY IN THE EARLY DETECTION OF SMOKE INHALATION INJURY IN FIRE ACCIDENT VICTIMS.

Respiratory tract injury is the most common cause of death in the victims of fire accidents. In the present study we tried to find out the role of radiotracer ventilation-perfusion (V/Q) scan in fire victims.

Twenty six patients underwent 99mTc-DTPA aerosol lung ventilation and 99mTc-MAA lung perfusion scan within 2 weeks of smoke inhalation. Follow up V/Q scans were obtained after 6 weeks and 6 months. The scans were categorised as normal, matching defects and mismatched defects.

The study revealed normal V/Q scans in 19, matching defects in 3 and mismatched defects in 4 patients. The results were correlated with clinical history, pulmonary function tests and x-ray chest. Match and mismatch defects were seen in patients with significant smoke inhalation lung injury. Patients with normal V/Q scans were the ones discharged after an early recovery. Patients with abnormal scans showed significant improvement on follow-up.

In conclusion, radionuclide ventilation-perfusion scintigraphy is an easily performed procedure and can be a sensitive diagnostic test for early smoke inhalation injury. Inhalation lung injuries are largely reversible if diagnosed early and treated appropriately.

OS-219

S.I. Heiba, I. Loutfi, K. Al-Za'abi and A. H. Elgazzar. Dept. of Nuc. Med., Faculty of Medicine, University of Kuwait and Mubarak Hospital, Ministry of Health, KUWAIT

INTEROBSERVER VARIABILITY IN THE ASSESSMENT OF PERFUSION DEFECTS SIZE : EFFECT ON LUNG SCAN INTERPRETATION

Prospective Investigation of Pulmonary Embolism Diagnosis (PIOPED) study validated the concept of segment equivalent used in the interpretation of ventilation and perfusion (V/Q) scans. Controversy however still exists regarding the effect of assessing the size of perfusion defects on the interpretation of V/Q scans. The objective of this retrospective study was to evaluate the relationship between interobserver variability in the determination of perfusion defects' size and the final V/Q scan interpretation.

Seventy seven consecutive V/Q studies were reviewed independently by 3 experienced physicians who were blind to the patients' clinical information. Tc-99m DTPA aerosol and Tc-99m MAA were used for the ventilation and perfusion scans respectively. Defects size, number, shape, location and matchness to ventilation abnormalities as well as final scan interpretation using the modified PIOPED criteria were determined by each observer. The defect size was graded as small, moderate or large. Disagreement between observers was classified as minor disagreement for 1 grade difference and major disagreement for 2 grades difference.

Perfusion defects were identified in 49 out of 77 studies. Defect size agreement among the observers was 61% (kappa range 0.28 - 0.52). Minor disagreement was 32% (62% between small and moderate defects, and 38% between moderate and large defects), while major disagreement was only 7%. Nevertheless the final interpretation agreement was 81% (kappa range 0.66 - 0.70).

The interobserver disagreement in determining the size of perfusion defects is predominantly minor. Additionally, the lung scan final interpretation agreement among observers remains high and not influenced by the defect size interobserver disparity.

OS-220

Y.Sasaki, T.Imai, T.Shinkai, H.Ohishi, Y.Nishimoto, Y.Imai, H.Uchida, T.Yoneda, M.Yoshikawa, N.Narita. Dept. of Oncoradiology, Radiology and 2nd Dept. of Internal Medicine, Nara Medical University, Japan

EVALUATION OF REGIONAL LUNG FUNCTION WITH VENTILATION-PERFUSION SCINTIGRAPHY FOLLOWING LUNG VOLUME REDUCTION SURGERY

The purpose of this study is to evaluate the change of the regional lung function of pulmonary emphysema (PE) before and after lung volume reduction surgery (LVRS) using ventilation and lung perfusion scintigraphy.

Twenty-two patients with PE were examined. They all underwent LVRS by thoracoscopy. Ventilation and lung perfusion scintigraphy were performed using 133Xe gas and 99mTc-MAA in the sitting position, then ventilation (V), perfusion (Q) images and mean transit time (MTT) were evaluated. We compared three sets of data : 1.before LVRS ; 2.less than 6 months after LVRS ; 3.More than 6 months after LVRS. We examined the relation between the data and dyspnea on exertion (DOE) Using Hugh-Jones' classification and lung function tests (%VC, FEV1.0, FEV1.0%, %RV, %TLC, PaO₂, PaCO₂, VO₂max, VEmax and WRmax).

In patients who underwent the examination less than 6 months after LVRS, the images showed that V and Q distribution inhomogeneity had improved in fewer than 50% of all cases. MTT was significantly shortened in the whole lung and in each regional lung field. In patients who underwent examination more than 6 months after LVRS, the V and Q distribution data showed no appreciable improvement compared with the patients who were examined less than 6 months after LVRS. However, MTT tended to be longer. V distribution was related with DOE, FEV1.0. Q distribution was related with DOE, FEV1.0, FEV1.0%, VO₂max and VEmax.

We conclude that ventilation and perfusion scintigraphy are useful in the appraisal of the effect of LVRS and follow-up.

OS-221

O. Portnoy, M.L. Goris, H.W. Strauss
Stanford University School of Medicine, Division of Nuclear Medicine.

THE CONTRIBUTION OF SPECT TO THE DISCRIMINATING POWER OF VENTILATION PERFUSION IMAGING.

Following a study in which no significant difference was found between planar and SPECT VQ imaging in the overall classification of cases, where few cases are documented as positive or negative on angiography and where a preponderance of VQ outcomes is negative, we attempted to define if the discriminating power of the VQ classification was affected by the imaging technique.

As an hypothesis we assumed that symptoms which trigger the request for a VQ study would be evenly distributed amongst the classes of outcomes (positive, undetermined, negative), but risk factors and final disposition would favor one outcome over another.

We studied 193 cases, performed as planar and SPECT, read by 2 observers independently of the official clinical and each other's reading. The studies were performed either as simultaneous ^{99m}Tc -MAA and ^{99m}Tc images, or sequential MAA and DTPA aerosol images. Symptoms, risk factors and outcomes were compared for two modalities, two observers, and outcome classes.

Variable	Planar 1	Planar 2	SPECT 1	SPECT 2
Chest X-ray	NS	NS	0.048	NS
SOB	NS	NS	NS	NS
DVT	5.8E-08	5.0E-08	8.83E-11	1.55E-05
Final Dx=PE	6.42E-15	1.67E-15	8.98E-16	3.18E-12
Clinical PE	NS	NS	NS	NS
Angio +	0.072	0.060	5.85E-05	2.43E-06

By chi-square, symptoms were randomly distributed, but risk and outcome were non-randomly distributed. The discriminative power for angiographic confirmation was the greatest for SPECT in all cases, if the eccentricity of the distribution as determined by Chi-square is taken as a measure.

We conclude that SPECT may in fact have a marginal advantage, even if globally the results do not differ sensibly, because of the relative low frequency of positive cases and confirmed cases respectively.

OS-222

B. I. Kettner, D. Sandrock, R. Aurisch, *R. Ewert, D. L. Munz

Clinic for Nuclear Medicine, Charité, Humboldt University Berlin, *German Heart Center Berlin, Germany

VENTILATION/PERFUSION-INEQUALITIES AFTER LUNG TRANSPLANTATION

In patients with end-stage lung disease and lung transplants one should expect particular distortions of ventilation and perfusion, induced by ex- and transplantation, denervation, and disruption of lymphatic vessels of the lung. Aim of this prospective study was, therefore, to prove this hypothesis.

Overall, 37 consecutive patients with lung transplants (22 f, 15 m, age, 13-58 years) were enrolled. In all patients, a ventilation scan (200 MBq Xe-133) and a perfusion scan (150 MBq Tc- 99m microspheres) was performed. All scans were analyzed visually and semiquantitatively by two experienced nuclear physicians blinded. Special attention was paid to differences between ventilation and perfusion of > 10 % defined as being abnormal.

A normal ventilation and perfusion scan (difference between right and left lung < 20 %) was observed in 24/37 (65 %) and 27/37 (73 %), respectively. In 13 patients with abnormal ventilation pattern, FEV1 as a parameter of lung function was < 80 %. Bronchoscopy confirmed pathologic anatomical findings in 4 of them and, furthermore, 5 of them had also a pathologic perfusion pattern of the lung transplant. A difference between ventilation and perfusion of > 10 % was found in 13 patients (35 %).

In conclusion, the data warrant the hypothesis that in a large number of patients with lung transplants there is a "mismatch" between ventilation and perfusion indicating an impaired bronchial vascular response.

Cardiovascular: Function

OS-223

H.WU, HC.LIU, YX.MA, S.YU

Department of Nuclear Medicine and Cardiology, Tongji Hospital, Tongji Medical University, Wuhan, China

QUANTITATIVE COMPARISON OF DOBUTAMINE WITH EXERCISE ^{99m}Tc -MIBI MYOCARDIAL SPECT IN DIAGNOSIS OF CORONARY HEART DISEASE

Purpose: The purpose of the study was to compare the value of dobutamine with exercise ^{99m}Tc -MIBI myocardial imaging in diagnosis of coronary heart disease(CHD). **Method:** Twenty-one patients with suspected CHD (including 3 cases with myocardial infarction) underwent dobutamine stress ^{99m}Tc -MIBI myocardial SPECT(Dob-ECT) and exercise stress myocardial SPECT(Exe-ECT), with 24-48h interval between the two imaging procedures. Dobutamine was administered intravenously with a standardized protocol. Coronary angiography was performed on all subjects within two weeks after SPECT imaging. **Results:** Coronary angiography proved 14 out of the 21 patients with positive angiographic lesions and 7 negative cases. For detecting CHD, there was no significant difference between Dob-ECT and Exe-ECT in overall sensitivity (92.8% vs 92.8%), specificity (71.4% vs 85.7%), positive predictive value (86.0% vs 92.0%) and negative predictive value (83.3% vs 83.3%). There was also no significant difference between the two methods in sensitivity and specificity of detecting lesions of different specified vessels (i.e., LDA, RCA or LCX). The two methods showed similar diagnostic capacity for detecting single- or multiple-vessel disease. However, with quantitative analyses of polar map, the average ischemic area (blackout size) in Dob-ECT was bigger than that in Exe-ECT (22.8±11.4% vs 17.5±12.3%, p<0.001); the average uptake ratio of ischemic area in Dob-ECT was lower than that in Exe-ect (43.2±13.8% vs 57.4±14.6%, p<0.001). No serious adverse reaction was found in this study. **Conclusion:** Dob-ECT may have comparable efficacy in detecting CHD. In case of same diseased vessel, the perfusion defect of related territory seemed to be more obvious in Dob-ECT image than in Exe-ECT image. Whether Dob-ECT is more sensitive in detecting CHD with mild diseased coronary artery remains to be studied.

OS-224

N. Zafrii, B. Zlotikamin, N. Avraham, S. Sclarovsky

Hospital: Rabin Medical Center, Beilinson Campus, Nuclear Cardiology Unit

DOBUTAMINE RADIONUCLIDE VENTRICULOGRAPHY IN PATIENTS WITH ACUTE ANTERIOR WALL INFARCTION: LONG-TERM FOLLOW-UP

We previously reported on the utility of low dose dobutamine radionuclide ventriculography (RNV) in the detection of viable myocardium at day 3 of first acute anterior wall myocardial infarction (AMI) and in prediction of left ventricular (LV) improvement at discharge and at 3 months' follow-up after AMI. In this study the utility of dobutamine RNV on long-term follow-up (60 m) was investigated. The 32 patients (pts) who underwent dobutamine RNV after AMI were reevaluated after 60m±5mos; 3 pts died (one cardiac death). Revascularization was performed on 19 pts (66%) and 10 were receiving medical treatment; all 29 pts underwent repeated RNV. The change in ejection fraction (ΔEF) from day 3 of AMI at discharge, 3 and 60 mos. were calculated in pts who respond to dobutamine (Gr 1, N=19) and in pts with who did not respond to dobutamine (Gr 2, N=10). Gr 2 (ΔEF 3±3%) showed no improvement at discharge (ΔEF - 2±8%), at 3 mos. (ΔEF 0.3±8%) and at 60 mo (ΔEF 1±14%) (NS). However, Gr 1 (ΔEF 14±6%) did demonstrate an improvement in LV at discharge (ΔEF 6±8%) that was more pronounced at 3 mos. (ΔEF 14±10%, P<0.02), but then remained stable at 60 mo (ΔEF 17±10% NS). It is noteworthy that LV improvement in revascularized patients (ΔEF 16 ±11%) was more significant than that in the medically treated patients (ΔEF 8±3%, p<0.03) at 60 mo. We concluded that dobutamine RNV is a useful method for predicting functional improvement at 3 mo after AMI. However, no further improvement in LV function is found at 60 mo follow-up. The functional improvement was more pronounced in the revascularized pts compared to the medically treated pts.

OS-225

P.Rossini, A.Terzi, E.Milan, R.Giubbini.
Spedali Civili, Brescia, ITALY - Nuclear Medicine Department

CLINICAL VALUE OF GATED MYOCARDIAL PERFUSION SINGLE PHOTON EMISSION TOMOGRAPHY IN THE EVALUATION OF LEFT VENTRICULAR EJECTION FRACTION IN CAD PATIENTS

Gated myocardial perfusion single photon emission tomography (GSPECT) currently allows simultaneous evaluation of perfusion and global and regional left ventricular function. Aim of our study was the assessment of the accuracy of GSPECT in the calculation of global ejection fraction (EF) in comparison to gated blood pool ventriculography (MUGA) which is still considered a clinical reference standard in this specific measurement. This study was designed to verify 1) the correlation between MUGA and rest GSPECT. 2) the influence of ischemia on the GSPECT algorithm for EF calculation and 3) the ability of GSPECT to reveal EF modification occurring after revascularization.

20 subjects with history of previous myocardial infarction and documented CAD were investigated according to the following protocol:

MUGA, GSPECT acquired 1h after both rest and peak exercise injection (two day protocol): all studies were completed within one week. The same sequence was repeated after PTCA in 18 pts. The following correlations were found:

MUGA Vs rest-GSPECT (n.38 determinations)

r=.84; r square=.7; SE=5; slope=.78; intercept=11.7

MUGA Vs GSPECT after exercise injection (n. 38 determinations)

r=.84; r square=.8; SE=5; slope=.78; intercept=12.2

GSPECT after rest and GSPECT after peak exercise injection (n.38 determinations) r=.87; r square=.75; SE=5; slope=.89; intercept=6.7

12/18 patients showed an EF increase by MUGA after PTCA: in this group of pts equivalent results were observed in 10 subjects (83%) by GSPECT.

In conclusion GSPECT is an accurate method to calculate EF in comparison to MUGA. Ischemia does not affect significantly the algorithm. The method is an accurate tool for monitoring the effects of treatment.

OS-227

Y.Zhou, W.Lee, W.Y.Qu, X.Q.Liu, D.P.Liu
Department of Nuclear Medicine, Beijing Hospital, P.R.China

EVALUATING EFFECTS OF ISCHEMIC PRECONDITIONING ON FIRST INFARCT SIZE AND LEFT VENTRICULAR FUNCTIONS IN THE ELDERLY BY RADIONUCLIDE IMAGING

Purpose: To evaluate effects of ischemic preconditioning on first infarct size and left ventricular functions in the elderly. Methods: 53 patients were divided into two groups based on angina pectoris (AP) within 24 hours before AMI onset: AP group (n=25) and non-AP group (n=28). The size of infarction was detected by 99mTc MIBI SPECT myocardial perfusion imaging; the incidences of left ventricular enlargement and dyskinesia as well as the left ventricular ejection fraction (LVEF), peak ejection fraction (PER) and peak filling rate (PFR) were used as major indexes for cardiac function by radionuclide ventriculography. These data were compared between 2 groups. Results: Numbers of infarct segments were 3.16±2.61 and 5.57±2.57 between AP group and non-AP group respectively (P<0.005). Incidence rate of left ventricular enlargement and dyskinesia were 12% (n=3) and 39.29% (n=11) respectively (P<0.05). LVEF was 49.34 ± 8.56% and 41.82±11.36%, PER was 2.53±0.55edc/s and 2.15±0.65edc/s, PFR was 2.07±0.42 edc/s and 1.62±0.60edc/s, mean phase was 146.92±13.54° and 160.00±24.05°, the phase angle was 84.12±51.89° and 133.89±86.07° between AP and non-AP group respectively (P<0.05 or P<0.005). Conclusions: Our findings suggest that ischemic preconditioning by preinfarction angina pectoris within a short period before AMI is effective for the preservation of left ventricular functions and the reduction of infarct segment size in the aged patients with first AMI. These favorable effects can be acquired by appropriate rehabilitational training, so as to decrease the incidence rate of myocardial infarction or improve the prognosis.

OS-226

P.Weinmann, G.Baillet, JM.Rochisani, JL.Moretti
Avicenne Hospital, UFR L. De Vinci PARIS 13, Bobigny, France.

EFFECTS OF DIPYRIDAMOLE ON LEFT VENTRICULAR EJECTION FRACTION (LVEF) IN HEALTHY SUBJECTS AS ASSESSED BY MIBI GATED SPECT.

Dipyridamole (DIP) is a widely used test for diagnosis of coronary artery disease (CAD) in myocardial scintigraphy. However, the effects of DIP on myocardial function in healthy subjects have rarely been studied by radionuclide techniques. MIBI gated SPECT provides both myocardial perfusion and LVEF. Image acquisition is usually started 60 min after DIP and MIBI infusion. Therefore, we studied the amplitude and duration of change induced by DIP in 9 subjects (7 women, 2 men, mean age 60.2 ± 4.9 yr) with low likelihood of CAD. MIBI (740 MBq) was injected at rest, a provocative fatty meal was given and 3 consecutive gated SPECT were performed 60 min after MIBI injection: at rest (GS 1), 7 min after the beginning of the infusion of 0.76 mg/kg DIP over a 4 min period (GS 2), and 60 min after the DIP infusion (GS 3). No patient received aminophylline after DIP infusion. Heart rate (HR) and blood pressure (BP) were monitored for each patient. Results are as follows (mean ± sd):

	GS 1	GS 2	P GS 1 vs GS 2	GS 3
LVEF %	62.5 ± 9.4	73.3 ± 10.2	<0.0001	62.3 ± 8.5*
HR / min	79.4 ± 9.4	94.1 ± 8.5	<0.005	81.2 ± 10.1*
BP mmHg	136 ± 16.5 / 80.5 ± 10.4	130 ± 17 / 71.7 ± 10.3	NS	139 ± 25 / 86.7 ± 15.2*

* non-significant (NS): GS 1 vs GS 3

It is concluded that:

- 1) DIP increases LVEF and HR and has no significant effect on BP in healthy subjects.
- 2) at 60 min, DIP effect is no more noticeable.
- 3) therefore, DIP MIBI gated SPECT as performed in routine, provides a rest LVEF, unless stunned myocardium is present.

OS-228

N.Uno, J.Yamazaki, H.Hosoi, S.Ishiguro, H.Mutoh, S.Yamashina, H.Yamashina, S.Ishida, T.Morishita
The First Department of Internal Medicine, Toho University School of Medicine, Tokyo, JAPAN

THE RELATIONSHIP BETWEEN FATTY ACID METABOLIC ABNORMALITY AND REGIONAL WALL MOTION OF THE LEFT VENTRICLE: USING 123I-BMIPP MYOCARDIAL SPECT

<Purpose of study> Although 123I-BMIPP (BM) is reported to be useful in ischemic heart disease, the improvement mode of fatty acid metabolic abnormality has not been fully clarified in chronic stage after myocardial infarction. A study was conducted on the improvement mode of wall motion and fatty acid metabolic abnormality in cases of myocardial infarction. <Methods> Subjects were 80 cases of myocardial infarction; 40 cases at acute stage (those who underwent BM-SPECT within 30 days of onset), of whom 17 cases underwent it twice at acute and chronic stages; 40 cases at chronic stage. TI-SPECT, echo cardiography, and coronary angiography were performed in all cases over the same time period. Extent score (ES) and severity score (SS) were calculated by the Bull's eye method from the SPECT images obtained. As an index of wall motion of the left ventricle, wall motion score index (WMSI) was determined by UCG.

<Summary and Result> The acute stage group produced excellent correlations between BM-ES and WMSI (r=0.782), between BM-SS and WMSI (r=0.849) as well as between TI-ES and WMSI (r=0.743), between TI-SS and WMSI (r=0.712). For investigation, all cases were divided into four groups according to the time when BM-SPECT was performed: (1) 0-14 d, (2) 15-30 d, (3) 31-90 d, (4) 90 d. In groups (1), (2), and (3), a significant discrepancy in SS was noted between BM and TI (p<0.05). As for ES, the discrepancy was observed in groups (1) - (4). dSS denotes the difference in long-term phase BM-SS between acute and chronic stages. dWMSI is defined the same way. An excellent correlation was noted between dSS and dWMSI (r=0.603). The correlation was not shown in TI-SPECT.

<Conclusion> Fatty acid metabolic abnormality was thought to play a positive part in the improvement of wall motion of the left ventricle, while discrepancies were considered to remain between BM and TI over a long period, for 90 days and 90 days or more in SS and ES, respectively.

Oncology: Therapy

OS-229

T.M. Behr, E. Wehrmann, M. Béhé, C. Apostolides*, R. Molinet*, M. Löhr, S. Yücekent, S. Gratz, L. Koch*, and W. Becker.
Dept. of Nuclear Medicine of the Georg-August-University of Göttingen, and Institute for Transuranium Elements*, Joint Research Centre of the European Commission, Karlsruhe, Germany.

ALPHA-EMITTERS FOR RADIOIMMUNOTHERAPY OF SOLID TUMORS: TOXICITY AND THERAPEUTIC EFFICACY OF ²¹³Bi-LABELED CO17-1A Fab'

Recent data suggest that radioimmunotherapy (RIT) with high linear energy transfer (LET) radiation (such as Auger electrons) may have therapeutic advantages over conventional low-LET (e.g., β-) emissions (e.g., Welt *et al.*, *J Clin Oncol* 1996; 14: 1787; Behr *et al.*, *Int J Cancer*, in press). The aim of the present study was to assess the toxicity and anti-tumor efficacy of radioimmunotherapy with the α-emitter ²¹³Bi as compared to the conventional β-emitter ⁹⁰Y in a colon cancer model in nude mice.

Biodistribution studies of ²¹³Bi- or ⁸⁸Y-labeled DTPA-conjugated Fab' fragments of the murine monoclonal antibody CO17-1A (belonging to the IgG_{2a} subclass) were performed in nude mice, bearing subcutaneous human colon cancer xenografts. ²¹³Bi was readily obtained from an "in-house" ²²⁵Ac generator. It decays by β- and 440 keV-γ-emission with a t_{1/2} of 45.6 min. to the ultra-short lived α-emitter ²¹³Po (t_{1/2}, 4 μs). For therapy, the mice were injected either with unlabeled, ²¹³Bi- or ⁹⁰Y-labeled CO17-1A Fab', whereas control groups were left untreated. The maximum tolerated dose (MTD) of each agent was determined. The mice were treated with or without inhibition of the renal accretion of antibody fragments by D-lysine (Behr *et al.*, *Cancer Res* 1995; 55: 3825). Myelo- and potential second-organ toxicities (e.g., kidney, liver etc.), as well as tumor growth were monitored at weekly intervals.

In accordance to kidney uptake values of as high as ≥ 80% of the injected dose per gram, the kidney was the first dose-limiting organ with the use of both, ⁹⁰Y- and ²¹³Bi-labeled Fab' fragments. Application of D-lysine decreased the renal dose by approximately five-fold by inhibiting the tubular re-uptake of glomerularly filtered Fab'. Accordingly, myelotoxicity became dose-limiting with both conjugates; by using lysine protection, the MTD of ⁹⁰Y-Fab' was 250 μCi, the MTD of ²¹³Bi-Fab' was 700 μCi. At these very dose levels, no biochemical or histological evidence of renal damage was observed (kidney doses < 40 Gy). Both radioimmunoconjugates led to a significant tumor growth retardation as compared to untreated controls or animals given the unlabeled conjugate. At equitoxic dosing at their respective MTDs, ²¹³Bi-labeled Fab' fragments were significantly more effective than the respective ⁹⁰Y-labeled conjugates.

These data show that RIT with α-emitters may be more therapeutically effective than conventional β-emitters. Due to its short physical t_{1/2}, ²¹³Bi appears as especially suitable for use in conjunction with fast-clearing fragments; its γ-emission can be used for quantitation by external imaging. (Supported in part by DFG grant Be 1689/4-1).

OS-230

T.M. Behr¹, A. Salib¹, S. Gratz¹, M. Béhé¹, S. Yücekent¹, R.D. Blumenthal², R.M. Sharkey², D.M. Goldenberg², and W. Becker¹.

Department of Nuclear Medicine¹ of the Georg-August-University of Göttingen, Germany, and Garden State Cancer Center², Belleville, NJ, USA.

RADIOIMMUNOTHERAPY (RAIT) OF COLORECTAL CANCER IN SMALL VOLUME DISEASE: EVALUATION OF RADIOIMMUNOTHERAPY VERSUS STANDARD CHEMOTHERAPY IN A NUDE MOUSE MODEL OF HUMAN COLON CANCER METASTATIC TO THE LIVER.

At the time of surgery, occult (micro-)metastases are present in more than 50% of colorectal cancer patients, and the liver is the most frequent site of metastatic disease. Frequently, adjuvant chemotherapy is unable to prevent tumor recurrence. Therefore, novel therapeutic strategies are warranted. The aim of this study was to establish a model of human colon cancer metastatic to the liver of nude mice, and to assess, in this setting, the therapeutic efficacy of RAIT as compared to the most commonly used standard chemotherapeutic regimens (5-fluorouracil [5-FU]/leucovorin or irinotecan).

Multiple liver metastases of the human colon cancer cell line, GW-39, were induced by intrasplenic injection of 100 μl of a 10% tumor cell suspension into the spleen of anesthetized nude mice with subsequent splenectomy 2 min later. Whereas controls were left untreated, therapy was initiated on day 10 or 20 after tumor inoculation with the ¹³¹I-labeled, low affinity anti-CEA MAb, F023C5 (K_d=10⁷ l/mol), or the high-affinity anti-CEA MAb, MN-14 (K_d=10⁹ l/mol), or chemotherapy (5-FU/leucovorin or irinotecan ["CPT-11"]) at their respective maximum tolerated doses (MTD). The animals were monitored, and histology was obtained from mice surviving 6 months.

The untreated controls died from rapidly progressing hepatic metastases at 6 - 8 weeks after tumor inoculation. The lifespan of animals treated with 5-FU/leucovorin or irinotecan was prolonged for only 1-3 weeks. In these animals, the liver parenchyma was almost completely replaced by tumor. In contrast, at their respective MTDs, the ¹³¹I-labeled low-affinity anti-CEA MAb, F023C5, led to a 25%, the high affinity MAb, MN-14, even to a 85% permanent cure rate, when therapy was initiated at 10 days after tumor inoculation. Histologically, no remaining viable tumor cells could be demonstrated in these animals surviving > 6 months. In the 20-day-old tumor stage, although prolonging life, ¹³¹I-F023C5 was unable to achieve cures, whereas ¹³¹I-MN-14 was still successful in 30%.

These data suggest that, in small volume disease, RAIT may be superior to conventional chemotherapy. Antibodies of higher affinity seem to be clearly superior. Future studies will show whether combination strategies of RAIT and potentially radiosensitizing chemotherapy will help to further improve therapeutic results. (Supported in part by grant Be 1689/4-1 from the Deutsche Forschungsgemeinschaft).

OS-231

J. Pinkert, G. Wunderlich, W.-G. Franke, M. Andreeff, J. Kropp and F.F. Knapp Jr.

Dresden University, Dept. of Nuclear Medicine, Germany; Nucl. Med. Group, Oak Ridge, USA

LABELING OF MICROSPHERES WITH RE-188 FOR INTRAARTERIAL TUMOR TREATMENT

Radioembolisation of tumors by selective catheterization has been proven to be an effective radionuclide therapy. But so far particles labeled with a short-lived beta-emitter are not available as an approved radiopharmaceutical.

In this study we evaluated the labeling of different particles with Re-188 which can be obtained carrier free from a W-188/Re-188 generator (Oak Ridge). Labeling was performed for B-20 (Mallinkrodt, HSA microspheres, 15-30 μm), MAA (Amersham, HSA macroaggregates, 10-100 μm), Ultra Drivalon (Nycomed, polyvinylformaldehyde foam particles, 50-150 μm), Bio-Rex 70 Resin (BioRad, macroreticular-acrylic resin particles, 45-75 μm), Macro Prep High Q (BioRad, methacrylate particles, 50 μm) and Angiostat (Regional Therapeutics Inc., collagen particles, 1-15 μm). About 370 MBq of Re-188 sodium perchlorate (2 ml) were mixed with 6 mg gentisic acid, 7.5 mg of SnCl₄·2H₂O, and 0.5-5 mg of these particles in a glass vial. The vial was boiled and shaken for 1 h (100 °C). After centrifugation the supernatant was removed. The particle preparations were washed twice and resuspended in saline / contrast medium (ULTRAVIST 30, Nycomed) at equal shares. After incubation with human plasma up to 48 h the final preparation for injection was found stable for all preparations. The biodistribution was analyzed after intravenous injection in 3-4 wistar rats for each particle preparation using the lung as model of a well perfused tumor. Samples of various organs were obtained 48 h p.i. and counted to calculate the tissue concentration (see table). The release of activity from the lungs representing the metabolic destruction and the biological half-life (T_{1/2}) were determined from whole body scintigrams after 10 min, 1 h, 3 h, 6 h, 24 h and 48 h p.i.

	T _{1/2} [h]	liver	spleen	kidney	muscle	bone	bowel	blood	urine
		[% injected dose / g]							
B-20	214.1	0.083	0.144	1.013	0.003	0.012	0.018	0.016	0.271
MAA	51.7	0.303	0.894	1.777	0.006	0.045	0.025	0.017	0.184
Drivalon	120.1	7.515	11.997	0.317	0.022	0.268	0.058	0.007	0.065
Bio-Rex	>250	0.756	1.578	0.081	0.005	0.049	0.014	0.003	0.025
Macro Prep	>250	0.089	0.222	0.047	0.002	0.003	0.036	0.007	0.022
Angiostat	177.3	5.058	17.992	0.258	0.018	0.384	0.036	0.011	0.056

Our data demonstrate the successful labeling of different types of particles with Re-188. B-20 microspheres seem to be promising for intraarterial tumor treatment after labeling with Re-188 with good in-vivo stability and low uptake in non-target tissues.

OS-232

N. Sato, T. Saga, H. Sakahara, Y. Nakamoto, Z. Yao, M. Zhang, S. Zhao, Y. Iida, M. Kuroki, Y. Matsuoaka, K. Endo, J. Konishi.

Department of Nuclear Medicine, Kyoto University and 1st Department of Biochemistry, Fukuoka University, Japan.

REDUCTION OF BONE MARROW TOXICITY BY AVIDIN CHASE IN RADIOIMMUNOTHERAPY OF LIVER MICROMETASTASES.

Purpose: The purpose of the present study was to investigate the effect of avidin chase on the reduction of bone marrow toxicity, which is the major dose limiting factor in the radioimmunotherapy, along with its effect on biodistribution, tumor uptake, and anti-tumor effect using liver micrometastases model of nude mice. **Methods:** Seven days after intrasplenic injection of human colon cancer cells, mice got iv injection of 11.1 MBq of biotinylated I-131 labeled anti-CEA Ab (33-38 μg). Mice of the chase group received iv injection of avidin twice (24 and 30 hr, 99-114 μg each). Groups of mice were killed at various time points, number of peripheral WBC was counted, and the biodistribution was examined. Uptake of radiolabels in the liver metastasis was measured by quantitative autoradiography. Therapeutic effect was determined on day 23. **Results:** Avidin chase markedly facilitated the clearance of the radiolabeled Ab from the blood and normal tissues. WBC count of the chase group showed less decrease at nadir (day 6) with earlier recovery compared to that of the group without chase (data shown below). Radiolabel uptake in the liver metastasis also decreased significantly (12.95 vs 24.79 %ID/g on day 3) but metastases-to-background ratios were much higher in avidin chase group. Therapeutic effect on liver metastasis was almost comparable each other (2/8: very small, 6/8: no visible mets. vs 1/8 very small, 7/8: no visible mets.), making contrast to the non-treated group (3/5: massive, 2/5: moderate mets.). **Conclusion:** Bone marrow toxicity could be reduced by avidin chase without significant reduction of the therapeutic effect. Tumor uptake was affected probably because of decreased recruitment from the circulation. More stable radioiodination method to retain high tumor uptake for longer period could partially solve this problem.

		day 1	day 3	day 6	day 10	day 15
chase(+)	Tumor (%ID/g)	29.14	12.95	6.54	14.53	
	Blood (%ID/g)	16.10	2.08	1.42	1.19	
	WBC (/mm ³)	3238	3233	1448	3553	3841
chase(-)	Tumor (%ID/g)	29.14	24.79	14.43	22.81	
	Blood (%ID/g)	16.10	13.69	10.02	5.17	
	WBC (/mm ³)	3238	2550	976	1114	1800

OS-233

J.F.W. Nijsen*, J.R.W. Woittiez#, W. van Maurik* and A.D. van het Schip*

Dept. of Nuclear Medicine, University Hospital Utrecht*, Netherlands Energy Research Foundation, Petten#, and Dept of Molecular Cellbiology, EMSA, University of Utrecht*, The Netherlands

CONDITIONS DURING NEUTRON BOMBARDMENT INFLUENCING THE INTEGRITY OF ORGANIC HOLMIUM-165-POLY LACTIC ACID MICROSPHERES FOR RADIOTHERAPY OF HEPATIC MALIGNANCIES.

Intra-arterial administration of radioactive holmium-165-poly lactic acid microspheres (Ho-165-PLA-MS) for internal radiotherapy of liver metastases can potentially overcome the disadvantages of external beam radiation which is limited by the radiosensitivity of the healthy tissue. Irradiation of these MS must result in a dosage of 15 Gbq at end of bombardment and 7.5 GBq for therapy. Irradiation in a high flux reactor is necessary because of the limiting conditions: a maximum of 12% incorporation holmium, a maximum tolerable amount of MS 500 mg for therapy and short physical half-life of 26.8. Neutron-irradiations of organic materials resulting in such large dosages are very complex. Parameters were investigated that affect the integrity of organic MS during bombardment with thermic neutrons. **Methods:** Irradiation of Ho-165-PLA-MS was done in polyethylene or in quartz vials in a high flux nuclear reactor (Petten, The Netherlands). Amounts of 10, 200 or 400 mg of dried MS were irradiated with a neutron flux (ϕ) of 5.10^{13} n.cm⁻².s⁻¹ or 2.10^{14} n.cm⁻².s⁻¹, respectively. A droplet of water was added to 2 samples of 200 mg MS, $\phi=5.10^{13}$ n.cm⁻².s⁻¹, irradiation time 1 h. Irradiation time was 0.5, 1, 2, or 4 hours. Condition of MS after bombardment was investigated by scanning electron microscopy (SEM). **Results:** Irradiation time and water were the most important factors causing damage under the described circumstances. Neutron flux was less important than irradiation time, nevertheless irradiations with $\phi=2.10^{14}$ n.cm⁻².s⁻¹ during 1 h resulted in melted MS. Irradiation of 10 mg MS with $\phi=5.10^{13}$ n.cm⁻².s⁻¹ during 2 h resulted in useful spherical MS while 200 mg MS gave melted MS. Irradiations with a neutron-flux of 5.10^{13} n.cm⁻².s⁻¹, during 1 h resulted in intact spherical MS useful for therapy. **Discussion:** Irradiation time, presence of water and the amount of MS are the crucial factors that generate irradiation damage of organic material. This can be decisive for the successful application of organic components for radiotherapy.

OS-234

S. Oku*, P.Thedrez, A. Faivre-Chauvet, C. Sai Maurel, F. Kraeber-Bodere J. Le Boterff, E. Gautherot**, J. Barbet**, J.F. Chatal, and Y. Sasaki*. Research Unit 463 INSERM, Nantes, Immunotech**, Marseille, France and University of Tokyo*, Japan.

RADIOIMMUNOTHERAPY (RIT) WITH BISPECIFIC ANTIBODY AND I-131 LABELED HAPTEN IN NUDE MICE BEARING HUMAN SMALL CELL LUNG CARCINOMA (SCLC).

The purpose of this study was to determine the toxicity and efficacy of two-step RIT using an anti-NCAM/anti-histamine bispecific antibody (NKINBL1-679 BsmAb) and a bivalent hapten (I-131-di-histamine-succinimidyl-glycyl-lysine) with a model of SCLC bearing nude mice. **Methods:** Eight mice subcutaneously grafted with a human SCLC H69 were injected with 600 micro gram of NKINBL1-679 BsmAb followed 48 hours later by a second injection of 3 nmol (41.4 MBq) of I-131-bivalent hapten. A group of 8 mice bearing the same tumor was used as a control. Toxicity was evaluated by serial measurement of body weight and total number of white blood cells (WBC) and platelets. Efficacy was estimated by the change in tumor volume and of the serum neuron specific enolase (NSE) levels during 90 days. **Results:** Hematologic toxicity was maximal 13 days after the injection of radiolabeled hapten with a decrease of 89.7+/- 6.4% and 60.7+/- 10.6% of WBC's and platelets respectively. There were no deaths observed in the treated. Tumor volume decreased from 222 +/- 87 mm3 to 34.2 +/- 8.2 mm3 at 31 days after the second injection, which corresponds to a mean reduction of 81.8 +/- 6.0% of initial tumor volume. In this group of treated mice, tumor regrowth was observed in all mice after a period of 8 to 28 days relative to the minimal tumor volume. In the control, tumor volume increased from 190 +/- 78 mm3 to 1659 +/- 1404 mm3 during the same period of time. Serum NSE levels also decreased from an initial value of 64.5 +/- 20.8 to 13.3 +/- 2.7 mg/dl for the treated, whereas that of the control group consistently increased from 47.3 +/- 32.1 to 1011 +/- 913 mg/dl. This therapy produced a 62-day mean growth delay, which was slightly longer than that with the single-step RIT in the literature. **Conclusion:** A significant reduction of tumor volume was observed after two-step RIT using anti-NCAM/anti-histamine BsmAb and I-131-bivalent hapten, however, efficacy was transient with regrowth of all tumors. Further investigation with repeated two-step RIT and/or its association with chemotherapy may reveal improved efficacy.

Oncology: Single photon

OS-235

M. Zhang, Z. Yao, H. Sakahara, Y. Arano, H. Saji, and J. Konishi.

Kyoto University, Department of Nuclear Medicine and Department of Radiopharmaceutical Chemistry

ENHANCED ACCUMULATION OF ALBUMIN IN INTRAPERITONEAL TUMORS FOLLOWING MANNOSYL GLYCOSYLATION.

This study was undertaken to investigate the potential of mannosyl glycosylated albumin in targeting intraperitoneal (i.p.) cancer xenografts. Three human tumor xenograft models, including a colon cancer, LS180, an ovarian cancer, SHIN-3, and a gastric cancer, MKN45, were established by i.p. injections of the human cancer cells in nude mice. Human serum albumin (HSA) was conjugated with mannose or galactose. Mannosyl-neoglycoalbumin (NMA), galactosyl-neoglycoalbumin (NGA), or HSA was labeled with In-111 through SCN-Bz-EDTA conjugation. The radiolabeled proteins were administered i.p. into the tumor-bearing mice and the biodistribution of radioactivity was studied at 2 or 24 hours postinjection.

Biodistribution of radioactivity in LS180 tumor mice (%ID/g, 2 h)

	HSA	NGA	NMA
Blood	8.50±2.75	0.28±0.23	0.30±0.08
Liver	2.97±0.75	18.31±6.49	12.95±2.98
Tumor	3.61±0.75	6.17±1.12	19.30±4.07

The results show that glycosylation of albumin increased blood clearance and liver accumulation of radioactivity. However, the tumor uptake was only significantly increased with NMA, resulting in a high tumor-blood ratio. Similar biodistribution pattern of radioactivity was also observed 24 hour postinjection. The biodistribution in SHIN-3 or MKN45 tumor-bearing mice was similar to that in LS180. In conclusion, mannosyl glycosylation of albumin enhanced its accumulation in i.p. tumors when administered i.p.. The high targeting efficiency could make NMA a useful vehicle for delivering radionuclide or other therapeutic agents to such tumors for the diagnosis and therapy.

OS-236

A. Kurtaran, W. Schima, M. Raderer, Ch. Müller, J. Pidlich, G. Novacek, C. Osterreicher, P. Angelberger, and I. Virgolini. Dept. of Nuclear Medicine, University of Vienna, Austria.

RECEPTOR IMAGING USING 99mTc-NEOGALACTO-ALBUMIN (NGA) AND 123I-TYR-(A14)-INSULIN IN THE DIFFERENTIAL DIAGNOSIS OF LIVER LESIONS

Purpose: Hepatic imaging using 99mTc-NGA reflects specific hepatocellular function as this ligand is metabolized only by its specific receptor (R) on the hepatocytes. *In vitro* studies have demonstrated that the R binding does not occur in hepatocellular carcinoma (HCC) and metastatic tumors (MTS) because surface NGA-R are lost during malignancy. However, focal nodular hyperplasia (FNH) lesions express normal or an increased NGA-R. In an approach to differentiate focal liver masses we have used two hepatocytes specific ligands 99mTc-NGA and 123I-Tyr-(A14)-Insulin as hepatic imaging agents. We have investigated 61 patients with HCC, 31 patients with metastatic liver lesions (MTS) and 15 patients with focal nodular hyperplasia (FNH). After i.v administration of 100-150 MBq/50 nmol 99mTc-NGA, all HCC-lesions as well as MTS were identified as cold spots, whereas in all patients with focal nodular hyperplasia a normal or an increased accumulation of 99mTc-NGA was observed. While 99mTc-NGA scintigraphy enables the distinction between FNH and malignant liver tumors, another ligand is needed for the differentiation of HCC from MTS. For this purpose, 123I-Tyr-(A14)-Insulin has been applied in patients with malignant lesions, as *in vitro* studies demonstrated significant expression of high affinity insulin-R for HCC. After i.v-injection of 100-150 MBq 123I-Tyr-(A14)-insulin all HCC lesions showed a significant accumulation, however, no accumulation of 123I-Tyr-(A14)-insulin was present in patients with MTS.

Conclusion: Our study clearly indicates that this dual receptor imaging method is useful for the differential diagnosis of focal liver lesions.

OS-237

J. Le Cloirec, R. Lebtahi, C. Houzard, J.L. Raoul, L. Sarda, L. Serb, J.F. Bretagne, L. Dussaulx, G. Sassolas, P. Bourguet, D. Le Guludec. Rennes, Paris, Lyon, France.

DETECTION OF NEURO-ENDOCRINE TUMORS (NET) WITH Tc-99m-P829: RESULTS OF A FRENCH MULTICENTER TRIAL.

The aim of this study was to evaluate the diagnostic value of a new somatostatin analog, Tc-99m P829, compared with In-111 pentetreotide. Forty-five patients (34 males, 11 females, mean age 56 years, range 24-78) with biologically and/or histologically proven NET, were prospectively included: 12 pts with Zollinger Ellison Syndrome, 13 pts with carcinoid tumors, 10 with non secreting differentiated NET, and 10 with other types of neuroendocrine tumors. Tc-99m P829 planar images (head, chest, abdomen, pelvis) were performed at 1 hour and 4-6 hrs post injection of 50 µg of peptide labeled with 700 MBq of Tc-99m. Abdominal SPECT was performed 4-6 hrs post injection (p.i.). Within 7 to 60 days, In-111 Pentetreotide planar images were performed 4 hrs and 24 hrs p.i. of 111 to 222 Mbq and SPECT was performed 24 hrs p.i. Results. In-111 Pentetreotide detected 204 tumoral sites in 38 out of 45 pts (84%), while Tc-99m P829 detected 79 sites in 26 out of 45 pts (58%, p<0.005). In contrast, Tc-99m P829 showed 3 additional sites in 3 pts, not detected by In-111 Pentetreotide. Location of detected sites were as follow:

	In-111 Pentetreotide	Tc-99m P 829
Head	2	4
Chest	24	21
Liver	107	34
Duodenopancreatic area	28	10
Abdomen	27	7
Pelvis	16	3

In conclusion, in pts with neuro-endocrine tumors, detection rate of Tc-99m P 829 scintigraphy was lower than In-111 Pentetreotide scintigraphy, which appears more sensitive, especially for liver metastases.

OS-238

R. Barone, M. Chianelli, E. Procaccini, A. Annovazzi, U. Bottoni¹, C. Panetta¹, D. Innocenzi¹, S. Calvieri¹, A. Signore Medicina Nucleare, II Clin Med and ¹Dermatologia, University "La Sapienza" Rome, Italy.

99mTc-IL2 SCINTIGRAPHY IN PATIENTS WITH CUTANEOUS MELANOMA: DETECTION OF LYMPHOCYTIC INFILTRATION

Tumor infiltrating lymphocytes are often observed at histological evaluation of cutaneous melanoma. The degree of infiltration represents the immune reaction to the tumour. Patients with peri-tumoral infiltration may have better prognosis and may also benefit on IL2 therapy.

The aim of this study was to evaluate in vivo to what extent 99mTc-IL2 binds to lymphocytes infiltrating cutaneous melanoma and if the uptake correlates with immunological and histological data thus providing a possible prognostic factor for the successful of IL2 therapy. We studied 30 patients with clinical diagnosis of cutaneous melanoma. Planar gamma camera images over known sites of the tumour were acquired one hour after the injection of 2mCi of 99mTc-IL2. Peri-tumoral uptake of 99mTc-IL2 was measured as Target/Background (T/B) ratio. All patients underwent surgery. Histological and immunological parameters were studied and correlated with scintigraphic results. The percentage of different peripheral blood lymphocyte subsets (CD3, CD4, CD8, CD16, CD25) and the percentage of IL2R+ve cells in histological sections of the tumour were also measured. Results of this study showed that in vivo tumoral uptake of 99mTc-IL2 correlates with the severity of the disease (Clark level, p=0.01) and with the number of circulating CD3+(p=0.0001), CD4+(p=0.002) and CD16+(p<0.01) cells. No correlation was observed in patients with benign cutaneous lesions between T/B ratio and immunological parameters. In conclusion, 99mTc-IL2 scintigraphy can allow in vivo measurement of IL2R+ve cells infiltrating melanoma lesions suggesting its use for prognostic purposes and to select patients who may benefit of IL2 immunotherapy.

OS-239

F. Scopinaro,*O.Schillaci,O.Bagni,F.Montealeone,G.Bonanni,A.M. Mangano,M.Di Loreto,F.Capocchetti,A.Centi Colella Nucl.Med.Sect.,Dept.Exp.Med.and Urology, Univ."La Sapienza", Rome and *Nucl.Med.,Univ."L'Aquila",Italy

Tc-99m ANTI EPITHELIAL GROWTH FACTOR MOAB UPTAKE IN TRANSITIONAL CELL CANCER OF THE BLADDER.

Overexpression of epithelial growth factor receptors (EGFR) always occurs in transitional cell carcinoma (TCC) of the bladder. We developed an anti-EGFR, EGF competitive antibody and labelled it with Tc-99m, as previously reported.

15 patients, 13 with bladder cancer and 2 with ematuria of other causes (1 urethritis, 1 cystitis) were studied before cystoscopic operation and before the control cystoscopy that was performed 6 months later. Written informed consent was always obtained. The Tc-99m MoAb was administered via chateter into the bladder; 1 hour later the bladder was washed twice with water and the scintigraphic images acquired with a standard gamma camera fitted with high resolution low energy collimator.

Tc-99m anti EGFR MoAb detected 16 spots in the 12 patients with TCC, whereas only 14 tumours were detected and taken away by the cystoscopic exam. The second cistoscopy was able to detect and remove both the TCCs. Focal uptakes were observed neither in the 2 patients with non neoplastic pathologies, nor in the control scintigraphies performed in the 10 patients in whom the first cystoscopic and scintigraphic exam were in agreement. Tumour/bladder activity ratio was 5 ± 1.2 in the patients with TCCs..

In conclusions, intrabladder administration of Tc-99m anti EGFR MoAb is a powerful diagnostic method for TCC detection .

OS-240

T.M. Behr, M. Béhé, N. Jenner, E. Wehrmann, R. Mach, L. Hegemann, S. Gratz, S. Yücekent, and W. Becker.

Department of Nuclear Medicine of the Georg-August-University of Göttingen.

TARGETING OF CHOLECYSTOKININ (CCK-B) / GASTRIN RECEPTORS IN VIVO: PRECLINICAL AND INITIAL CLINICAL EVALUATION OF RADIOLABELED GASTRIN ANALOGS.

The high sensitivity of pentagastrin in detecting the presence of medullary thyroid cancer (MTC) suggests a widespread expression of the corresponding receptor. Indeed, autoradiographic studies demonstrated CCK-B (= gastrin) receptors not only in ≥ 90% of MTCs, but in a high percentage of small cell lung and ovarian cancers, among several other tumor types (Reubi et al., *Cancer Res* 1997; 57: 1377). The aim of this study was to develop suitable radioligands for targeting CCK-B receptors *in vivo*.

Among others, a variety of peptides, all bearing the CCK-receptor binding amino acid sequence Trp-Met-Asp-PheNH₂, but differing in their N-terminal structure, were radioiodinated by the Iodogen or Bolton-Hunter (BH) procedures: big-gastrin, gastrin-I and [Leu¹⁵]-gastrin, minigastrin, caerulein, cionin, non-sulfated (ns) and sulfated (s) CCK-8, as well as des-BOC-Pentagastrin and CCK-4. Their stability was studied *in vitro* and *in vivo*; their biodistribution was tested in nude mice, bearing subcutaneous human MTC xenografts, and initial therapy experiments were undertaken. Several chelator- (e.g., DTPA-) conjugated derivatives were synthesized for labeling with radiometals (such as ¹¹¹In, ⁹⁰Y, or ⁶⁷Ga). A pilot clinical study was initiated in patients with metastatic MTC.

The serum stability of those peptides was significantly higher (t_{1/2} ≥ 24 h at 37°C), which bear N-terminal pGlu residues (e.g., big gastrin, gastrin-I), which are known to protect from enzymatic degradation. Best tumor uptake, with tumor-to-blood ratios ≥ 10 as early as 30 min p.i., as well as targeting of physiological CCK receptors in the stomach, gallbladder, and pancreas were obtained with those peptides having high affinity to the CCK-B receptor (e.g., sCCK-8, gastrin-I). However, sulfated CCK analogs had higher uptake in the liver, pancreas and bowel than nonsulfated gastrin derivatives, due to their equally high affinity for both, CCK-A and -B receptors. Optimal tumor uptake and tumor-to-nontumor ratios were found for the members of the gastrin family, bearing a highly anionic Glu, sequence close to the N-terminus of the receptor-binding tetrapeptide sequence. Radiometal-labeled derivatives showed further improved tumor-to-nontumor ratios. Therapy experiments with ¹³¹I- or ⁹⁰Y-labeled peptides in MTC bearing animals showed significant anti-tumor efficacy as compared to untreated controls. In a pilot clinical study, excellent targeting of all physiological CCK-B receptor expressing organs (e.g., stomach, gallbladder) as well as of all known tumor sites was observed.

These data suggest that CCK and gastrin analogs may be a useful new class of receptor binding peptides for diagnosis and therapy of a variety of tumor types. Non-sulfated, CCK-B receptor selective ligands (e.g., gastrin) seem to be preferable, due to their lower accretion in normal organs. Further preclinical as well as clinical studies are ongoing.

Infection/inflammation/hematology: New radiopharmaceuticals in man

OS-241

C.J. van der Laken, P. Barrera, O.C. Boerman, W.J.G. Oyen, M.T.P. van de Ven, J.W.M. van der Meer, L.B.A. van de Putte, F.H.M. Corstens.

Dpts. of Nuclear Medicine, Internal Medicine and Rheumatology, University Hospital Nijmegen, The Netherlands.

RADIOLABELLED INTERLEUKIN-1 RECEPTOR ANTAGONIST TARGETS TO INFLAMED JOINTS IN PATIENTS WITH ACTIVE RHEUMATOID ARTHRITIS. A REPORT OF PRELIMINARY RESULTS

In animal studies, it was recently demonstrated that radiolabeled interleukin-1 receptor antagonist (IL-1ra) localizes in infectious and inflammatory foci. In the present study, the imaging properties of radiolabeled IL-1ra were investigated in patients with active rheumatoid arthritis (RA). Patients with active RA were selected since it has been shown that the disease activity of RA improved after IL-1ra treatment. IL-1ra may therefore specifically localize in inflamed joints. IL-1ra was radiolabeled with I-123 according to the Bolton-Hunter method. After radioiodination, the in vitro receptor binding capacity was determined on the murine thymoma cell line EL-4-6-1. Patients with active RA were i.v. injected with 74-185 MBq 0.5 mg ¹²³I-IL-1ra. Scintigraphic images were obtained at 5 min, 1, 4, 8 and 24 h p.i. Spot views of the inflamed joints were made from 1 h p.i. onwards. Three patients were investigated. ¹²³I-IL-1ra rapidly cleared from the blood and most other organs. After 8 h p.i. more than 50% of the activity had left the body, mainly by rapid excretion in the urine. ¹²³I-IL-1ra localized in the inflamed joints of two patients within 1 h p.i. The inflamed joints were clearly visible at least up to 8 h p.i. The uptake decreased thereafter. Inflamed joint-to-periarticular normal tissue ratios were already higher than 2 at 1 h p.i.. Peak values, higher than 2.5, were obtained within 8 h p.i. In these two patients with severe RA, most of the joints which were tender and/or swollen on clinical examination showed ¹²³I-IL-1ra uptake (>70%). None of the clinically unaffected joints showed uptake of ¹²³I-IL-1ra. One patient with mild activity of RA did not show any uptake of ¹²³I-IL-1ra in inflamed joints. In conclusion, these initial results demonstrate that radiolabeled IL-1ra localizes in inflamed joints in patients with active RA. The level of uptake of radiolabeled IL-1ra may reflect the activity of the inflammatory sites. Inflamed joints were visualized as early as 1 hour after injection while it was rapidly cleared from most background tissues, allowing early detection of both peripherally and centrally located inflamed joints.

OS-242

A. Signore, E. Procaccini, R. Barone, V. Fiore, M.G. Parisella, G. Di Leve, P. Giacalone, M. Chianelli.

Nu.M.E.D. Group, Servizio di Medicina Nucleare, II Clinica Medica, University "La Sapienza" Roma, Italy.

IL2-SCINTIGRAPHY DETECTS MULTIPLE ORGAN INVOLVEMENT IN AUTOIMMUNE PATIENTS

Radiolabelled IL2 is a radiopharmaceutical for the in vivo detection of chronic lymphocytic infiltration that can provide relevant information about the disease activity in patients with autoimmune diseases. It is known that in these patients multiple autoimmune pathologies are frequently associated and the immediate recognition of the diseased state may have relevant clinical consequences.

In this study we describe the results of IL2-scintigraphy in 129 patients in which we investigated the presence of an other tissue infiltrated by activated lymphocytes, as sign of multiple autoimmunity.

We have studied 24 patients with Graves' disease, 50 with Hashimoto's thyroiditis, 25 with Type 1 Diabetes at onset, 15 with Crohn's disease and 15 with Coeliac disease. Patients were analysed for the presence of IL2 accumulation in the thyroid, salivary glands, pancreas and bowel by the acquisition of planar or tomographic images 1 hr after the injection of 1 to 3 mCi of ¹²³I-IL2 or ^{99m}Tc-IL2.

Results showed that 7.5% of thyroid patients had salivary infiltration, 13% of patient with Coeliac disease had extra intestinal localisation (thyroid and salivary glands), 20% of patients with Crohn's disease had thyroid uptake of radiolabelled IL2. Finally, 5 out of 14 diabetic patients (35.7%) showing pancreatic uptake of radiolabelled IL2 had at least one extra accumulation of IL2 (thyroid, salivary glands or bowel).

Our data indicate that radiolabelled IL2 can provide relevant information on the detection of multiple sites of autoimmunity in patients with an organ specific autoimmune disease.

OS-243

M. Chianelli, M.G. Parisella, R. Barone, A. Annovazzi, G. Nardi, N. Visalli, P. Pozzilli, IMDIAB study group, A. Signore.

Nu. M.E.D. Group, Medicina Nucleare, II Clinica Medica, Università "La Sapienza" Roma, Italy.

IMAGING OF INSULITIS IN NEWLY DIAGNOSED DIABETIC PATIENTS BY ^{99m}Tc-IL2 SCINTIGRAPHY

Identification of type 1 diabetic patients with autoimmune aggression of insulin-producing beta cells (insulinitis) at diagnosis may have important implications for treatment of patients with immunomodulatory drugs to preserve residual beta-cell function.

We have studied 25 newly diagnosed, insulin-dependent, diabetic patients by ^{99m}Tc-IL2 scintigraphy a technique for the detection of organ infiltration by activated lymphocytes. Tomographic sections of the abdomen were obtained 1 hr after the injection of 2mCi ^{99m}Tc-IL2 and pancreatic radioactivity was calculated as pancreas to background (bone) ratio (P/B). In all patients metabolic status (C peptide, HbA1c, blood glucose, insulin requirement) was monitored every 3 months throughout the study.

Results showed that 33% of patients had a significant pancreatic accumulation of ^{99m}Tc-IL2 at time of diagnosis. C peptide values (a marker of beta cell function) 9 months after diagnosis were significantly higher in patients with pancreatic accumulation of ^{99m}Tc-IL2 compared to patients with a negative IL2 scintigraphy at diagnosis (1.3 vs 0.63 ng/ml; p=0.004).

These results suggest that a residual mass of insulin-producing beta cells and a pancreatic beta-cell inflammation are present in a subgroup of patients that can be identified by ^{99m}Tc-IL2 scintigraphy. This technique, therefore, may be used for the selection of patients to be treated with adjuvant immunotherapies in an attempt to preserve the residual beta-cell mass and improve long-term metabolic control.

*The IMDIAB Study Group: P Pozzilli, N Visalli, MG Baroni, R Buzzetti, L Nisticò, E Fioriti, C Mesturino, A Signore, MG Cavallo, L Lucentini, MC Matteoli, A Crinò, C Teodono, R Amoretti, F Paci, M Ruggeri, L Pisano, C Suraci, MG Pennafina, B Boscherini, S Stoduto, MT Fonte, F Batelli, G Multari, MA Suppa, GC De Mattia, M Cassone Faldetta, O Laurenti, ML Mancabitti, G Marietti, D Pitocco, F Ferrazzoli, C Bizzarri, AV Greco, G Ghirlanda.

OS-244

E.Th.M. Dams¹, W.J.G. Oyen¹, O.C. Boerman¹, P. Laverman¹, J.H. Beijnen², G. Storm³, J.W.M. van der Meer¹, F.H.M. Corstens¹.

University Hospital Nijmegen¹, Nijmegen, Slotervaart Hospital², Amsterdam, and Utrecht University³, Utrecht, The Netherlands.

FIRST CLINICAL EVALUATION OF Tc-99m-PEG-LIPOSOMES FOR THE DETECTION OF INFECTION AND INFLAMMATION.

Introduction. Labeled PEG-liposomes have shown excellent results in various models of experimental infection and inflammation. In this study, the scintigraphic application of Tc-99m-PEG-liposomes was evaluated in patients suspected of infectious or inflammatory disease, and directly compared to In-111-IgG scintigraphy.

Methods. Seventeen patients (7 females, 10 males; mean age 52 yr, range 20-75 yr) were prospectively studied. After administration of 740 MBq Tc-99m-PEG-liposomes, imaging was performed at 4 and 24 hr postinjection. To avoid cross-over activity, In-111-IgG was injected 24 hr after Tc-99m-liposomes, and imaged at 4, 24 and 48 hr postinjection. The scintigraphic results were confirmed by microbiological and histological methods, and clinical follow-up.

Results. All 6 patients with proven infection or inflammation had positive findings with Tc-99m-liposomes scintigraphy: one patient had an infected aorta prosthesis, two had soft-tissue infection, one had arthritis, one had colitis and one patient had a small abdominal abscess. In one patient with an uninfected pseudarthrosis of the tibia, Tc-99m-liposomes and In-111-DTPA-IgG scintigraphy were concordantly false-positive. In the 11 patients with negative Tc-99m-liposomes scan, absence of infection or inflammation could be confirmed. A false-negative In-111-IgG scan was recorded in a patient with mild soft-tissue infection. The sensitivity and specificity of imaging infectious or inflammatory foci with Tc-99m-PEG-liposomes in this group of patients was 100% and 91%, and with In-111-IgG 86% and 91%, respectively.

Conclusion. Scintigraphy with Tc-99m-labeled PEG-liposomes is at least as effective as In-111-DTPA-IgG scintigraphy for detection of infection and inflammation. Given the simple and safe preparation and the apparent physical and logistic advantages of a Tc-99m label, Tc-99m-labeled PEG-liposomes could be an attractive agent for infection/inflammation imaging.

Infection/inflammation/hematology: New radiopharmaceuticals in man OS-245

S. Gratz¹, T. Behr¹, H.A. Schmitt², M. Wüstner³, A. Morguet², J. Meller¹ and W. Becker¹
Department of Nuclear Medicine¹, Internal Medicine² and Surgery³ of the Georg August University, Göttingen, Germany

^{99m}Tc-LABELED ANTIGRANULOCYTE MONOCLONAL ANTIBODY FAB' FRAGMENTS (LEUKOSCAN®) FOR DIAGNOSTIC IMAGING OF BONE AND SOFT TISSUE INFECTIONS

Rationale: ^{99m}Tc-labeled antigenulocyte monoclonal antibody Fab' fragments have shown in prospective studies high sensitivity and specificity for detecting osteomyelitis. Aim of this study was to evaluate the overall diagnostic accuracy of LeukoScan® (Immunomedics, Morris Plains, N.J.) in the clinical routine of detecting bone and soft tissue infections. **Patients and Methods:** 73 patients (35 men, 38 women, mean age 56.76±21.29 years) with fever of unknown origin (n=32), suspected infection of peripheral-(n=9) and central bones (n=8), infection of prosthesis (n=8), arthritis (n=7), soft tissue infection (n=6), appendicitis (n=3), pericarditis (n=2), and vascular graft infection (n=2) were imaged after injection of 555-925 MBq ^{99m}Tc-labeled antigenulocyte monoclonal antibody Fab' fragments (LeukoScan®). In patients with suspected soft tissue- and bone infection histology (n=18), biopsy (n=12) and clinical follow up (n=43) were available for final diagnosis. In patients with fever of unknown origin (n=32) the revised Duke criteria were used for diagnosis. Wholebody images and planer view spots of the infected focus were performed 1h, 4h and exceptionally 24h p.i. In patients with suspected endocarditis SPECT imaging was performed 19 h p.i. of the thorax (n=32). ¹¹¹In-oxin (n=6) and ^{99m}Tc-HMPAO (n=5)-labeled white blood cells, planar radiography (n=25), MRI (n=6) and CT (n=12) were used for comparison. **Results:** A positive infection uptake was detectable in 63/81 lesions. The sensitivity and specificity were 77/75% respectively. In arthritis 7/7 foci could be detected, whereas false negative results were found in infections of the femoral bone in 6/9 and periprosthetic infections of long bones in 6/8 lesions. Good results were found in 5/6 soft tissue infections, 4/4 patients with endocarditis, 2/2 unclear cases of appendicitis, 2/2 infected vascular grafts and 1/1 patient with pericarditis. Subacute/chronic infections of the spine always showed „cold lesions“ in 8/8. If cold lesions were used as guide for diagnosing a pathologic finding, thus, the sensitivity and specificity became 91/67% respectively. **Conclusion:** 1.) ^{99m}Tc-labeled antigenulocyte monoclonal antibody Fab' fragments can be used for imaging acute infections of peripheral bones and soft tissues, as well as for positive diagnosing of endo-/pericarditis and appendicitis. 2.) False negative results have to be expected in patients with chronic infections, especially in case of infections of the spine. 3.) An increase in sensitivity with commensurate decrease in specificity can be achieved when adding cold lesions in the spine as pathognomic for localization of disease.

OS-246

C. Aprile¹, G. Merlino², F. Salvi³, R. Saponaro¹, G. Cannizzaro¹, G. Calsamiglia¹, E. Anesi², P. Garini²
¹Fond. "S. Maugeri", IRCCS and ²S. Matteo Hosp., IRCCS, Pavia;
³Bellaria Hosp., Bologna - Italy

AMYLOID DEPOSITS IMAGING WITH ^{99m}Tc-APROTININ: REPORT ON THE FIRST 92 PATIENTS (AL AND ATTR TYPE)

In 92 patients with biopsy proven amyloidosis (80 AL and 12 ATTR) 119 scintigraphic studies were performed 90 min after i.v. administration of 500-800 MBq of ^{99m}Tc Technetium labelled Aprotinin, a protease inhibitor from bovine lung (Trasylol®).

Scintigraphic results, supported by histology and/or clinical course in a follow-up time >6 months, showed cardiac uptake in 45, head & neck in 67, lung in 25, bone-marrow in 20, spleen in 17, GIT in 14, uptake in other sites including testes, skeletal muscle and ocular structures in 28 cases. The presence of renal/adrenal involvement was obscured by the high physiological renal uptake while hepatic activity, inversely related to residual renal function, rendered this area of difficult interpretation: only in the presence of amyloid deposits the activity remained stable or increased in a late scan (3-6 hrs p.i.). In about 30% of cases the scan allowed the detection of previously unknown sites of involvement, including the myocardium; this fact, considering the unfavourable prognostic significance of myocardial involvement, is of the utmost importance. Tc-Aprotinin scan showed positive heart uptake in 3 patients previously considered unaffected, ruled out the presence of heart involvement in 11 and confirmed it in 23 suspected patients; positivity was also confirmed in 19 patients with congestive heart failure. In 21 patients follow-up studies allowed to monitor the disease progression/remission after therapy.

In 31 control patients affected by various non-amyloid cardiac, renal and osteoarticular diseases, no extrarenal uptake was detectable, thus proving the specificity of the test.

We feel that Tc-Aprotinin, owing to its rapid blood clearance, the favourable characteristics of Tc^{99m} and the availability of the molecule, might become a useful tool for diagnosing extrarenal amyloid deposits and monitoring the evolution of the disease.

Neurology/Psychiatry: Dopamine + serotonin studies OS-247

C. Messa, R.M. Moresco, C. Gobbo, R. Cavallaro, K. Prato, C. Colombo, E. Smeraldi, F. Fazio
INB-CNR, University of Milan, Institute H S. Raffaele, Milano, Italy

DOPAMINERGIC AND SEROTONINERGIC RECEPTOR ACTIVITY IN DRUG-FREE SCHIZOPHRENIC PATIENTS USING PET AND [F-18]FESP.

An impairment of the dopaminergic and serotonergic systems is probably underlying different features of the symptomatology in schizophrenic patients. Also both typical and atypical neuroleptics act on schizophrenic symptoms by interacting with these systems. With the present study we wanted to evaluate: 1) the in vivo binding of [F-18]FESP (a D2 and 5HT2 antagonist) to the cortex (C) and basal ganglia (BG) of drug free schizophrenic patients compared with age matched normal control, 2) the relationship between in vivo [F-18]FESP binding and clinical presentation. 23 patients (16 males, mean age 34) free from neuroleptic treatment for at least 21 days, and 10 normal subjects (3 males, mean age 36) underwent a PET scan (GE Advance 3D acquisition) 120 minutes after the injection of 2.6 MBq/Kg of [F-18]FESP. Patients with prevalent negative (NEG) and positive (POS) symptoms were 17 and 6 respectively. [F-18]FESP binding index (BI) was calculated as the difference between the radioactivity concentration in C and BG and in the cerebellum, divided by cerebellum. Differences between groups (Normal, NEG and POS) were assessed by an analysis of covariance, adjusting mean BI for age. The only positive correlation found to be significant (Pearson p<0.005) was between BI in BG and negative symptoms subscale scores (r=0.61). A significant difference between groups was found in the BG (p<0.004) being the mean BI in this region 6.2, 5.1 and 6.2 for NEG, POS and normals respectively. In conclusion for the first time a differentiation in the same population of schizophrenic patients could be detected using PET to measure the activity of the D2 dopaminergic receptors in the striatum. This difference is related to the symptoms presented by the patients, indicating that different clinical subtypes of schizophrenic patients may be related to different underlying physiopathological mechanisms.

OS-248

R.M. Moresco, C. Colombo, C. Gobbo, A. Bonfanti, G. Lucignani, C. Messa, A. Del Sole, A. Lucca, L. Galli, E. Smeraldi, F. Fazio
INB-CNR, University of Milano, Institute H S. Raffaele, Milano, Italy.

EFFECT OF FLUVOXAMINE ON 5HT2 SEROTONINERGIC RECEPTORS OF DRUG NAIVE DEPRESSED PATIENTS STUDIED WITH PET AND (18F) FESP.

Pharmacological and postmortem studies have shown that an impairment of the serotonergic transmission occur in the pathogenesis of mood disorders. The effect of chronic treatment with the serotonin reuptake site inhibitor (SSRI) fluvoxamine on the in vivo binding of [F-18]FESP in the brain of depressed patients was evaluated. For this study, 15 patients with unipolar major depression never treated with antidepressants, antipsychotics or mood stabilizers were recruited. Each patient underwent a PET study (GE Advance), before and after four to six weeks of treatment. Images of the distribution of the tracer in the brain were acquired between 90 and 120 minutes after injection of ~2.5 MBq/kg of [F-18]FESP. A binding index (BI) was calculated as the difference between concentration of radioactivity in the target region and in the reference region (cerebellum), with respect to cerebellum. Target regions were the frontal cortex (FC) and basal ganglia (BG). Nine/15 patients recruited completed the study (4 males). All patients but one were responders to fluvoxamine therapy at the time of the second PET study. Fluvoxamine treatment significantly modified [F-18]FESP BI in the FC (Wilcoxon sum-rank test: p=0.055). In particular an increase in [F-18]FESP BI was found in the 8 responder patients (35±33%) but not in the non responder patient in which BI was reduced (-22.5%). In the BG a less marked increase of [F-18]FESP BI was found in 6 patients (from 6% to 44%), no change in two patients and a reduction in the nonresponder patient (-10%).

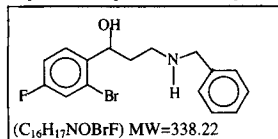
In conclusion an increase of (F-18)FESP BI in the FC is observed 4-6 weeks after SSRI therapy in patients with major unipolar depression. This finding may reflect a modification in 5HT2 binding capacity secondary to changes in cortical serotonergic activity.

OS-249

A. Bottoncetti, A. Pupi, A. Guarna, G. Menchi, F. Vannacci, R. Franceschini, A. Pecorale, S. Raspanti. Nuclear Medicine Unit and Organic Chemistry Department of the University of Florence, Florence and Amersham-Sorin, Saluggia, ITALY.

SYNTHESIS AND PRELIMINARY BIOLOGICAL CHARACTERIZATION OF A NEW POTENTIAL D₂ RADIOLIGAND.

With the aim to obtain potential radioligands to investigate for serotonin and dopamine receptorial systems and their connections, we designed a new molecular structure selecting fragments of serotonin and dopamine receptor's active compounds and joining them with flexible chains of different length. The design of the molecules has been accomplished taking into account for an easy, highly efficient and well controlled introduction of a radioisotopic atom and for a labelling procedure which guarantee an optimal analytical discrimination between the 'cold' and the 'hot' ligand to obtain a radioligand with a very high specific activity. In the present study we report the preclinical characterization of a molecule of this class, represented in the figure.



The molecule has been tested for the capacity to cross the blood brain barrier with a method which permits to measure simultaneously the unidirectional influx constant of the substance and the regional brain perfusion (rCBF), with the injection in the left hearth ventricle of a mixture of the test molecule and of microspheres. This measure has been performed in three Sprague-Dawley rats varying with hypercapnia the rCBF value between 0.7 and 4.5 ml/min/g. The extraction fraction was (mean±std) 0.56±0.14. In vitro binding studies has been conducted with ³H-spiperone on crude membrane preparation from rat striatum and frontal cortex. The data collected showed that the compound, which has been tested in its racemic form, has an undetectable affinity for serotonin receptors in frontal cortex while shows an affinity for the D₂ receptors in the striatum preparation, displaying a dose-related inhibition of the ³H-spiperone binding with an IC₅₀ of 200 µM. This compound is the first tested molecule of a novel series of putative D₂ receptor ligands for use in nuclear neurology.

OS-250

M. Kerner, R. Linke, J. Schwarz¹, P.D. Mozley², K. Hahn, K. Tatsch

Dept. of Nuclear Medicine, Univ. of Munich, ¹Dept. of Neurology, Univ. of Ulm, Germany; ²Dept. of Radiology, Univ. of Pennsylvania, USA

STRIATAL DOPAMINE TRANSPORTER BINDING IN PATIENTS WITH EARLY PARKINSON'S DISEASE: IMPLICATIONS FOR PRECLINICAL DIAGNOSIS ?

Previous SPECT studies with cocaine analogs such as β-CIT, FP-CIT or IPT have demonstrated progressive loss of striatal dopamine transporters in Parkinson's disease (PD) with increasing clinical stages. This study particularly focused on the assessment of the dopamine transporter in pts with early, unilateral PD (H&Y stage I) comparing the results with those of controls and pts with moderately advanced disease (H&Y stage II).

In 14 PD pts with H&Y stage I (mean disease duration 1.6±0.9 yrs), 14 PD pts with H&Y stage II (mean disease duration 3.0±1.6 yrs) and 9 age-matched controls [¹²³I]IPT-SPECT was performed 90 min p.i. of 120 MBq using a triple headed camera. For semiquantitative evaluation of specific IPT binding, ratios between striatum [S], caudate [C], putamen [P] and background activity [BG] were calculated.

	([S-BG]/BG)		([C-BG]/BG)		([P-BG]/BG)	
	ipsilateral	contralateral	ipsilateral	contralateral	ipsilateral	contralateral
controls	7.28±0.94	7.41±1.28	8.65±1.22	8.54±1.34	6.48±0.93	6.56±1.45
H&Y I	4.72±0.75	3.69±0.61	6.01±0.95	5.13±0.78	3.75±0.93	2.29±0.75
H&Y II	3.47±0.75	2.96±0.73	4.55±1.07	4.15±1.09	2.67±0.51	2.03±0.49

As compared to controls mean specific IPT-uptake was significantly reduced in pts with H&Y stage I, affecting not only the contralateral but also the ipsilateral S, C and P (p<0.0001). Binding ratios for the contralateral S, P and C were not in a single case, and those for the ipsilateral S, C and P were only in 1/14, 3/14 and 0/14 higher than the respective values observed in controls, suggesting only minor overlap between both groups. PD pts with H&Y stage II showed a significant lower binding than the H&Y I group.

IPT-SPECT is a valuable tool to assess the reduction of dopamine transporter binding already in pts with early, unilateral Parkinson's disease. Pathologic data obtained in the ipsilateral striatum of pts with H&Y stage I (reflecting the so far non affected side of the body) demonstrate the potential of this method for the detection of preclinical disease.

OS-251

R. Larisch, B. Schommartz, H. Vosberg, H.-W. Müller-Gärtner

University Clinic of Nuclear Medicine, Heinrich-Heine-University, Moonenstr. 5, 40225 Düsseldorf, Germany

INFLUENCE OF MOTOR ACTIVITY ON POSTSYNAPTIC STRIATAL DOPAMINE D₂ RECEPTOR BINDING - A STUDY USING 123I-IODOBENZAMIDE AND SPECT

Although a role of the dopaminergic neurotransmission in multiple brain functions as motor activity and emotional processing is undoubted, dopamine release as a consequence of neuro-psychological paradigms has not been examined yet *in vivo* with PET or SPECT. The aim of the present study was to test whether postsynaptic dopamine D₂ receptor imaging reflects presynaptic dopamine release. The basic hypothesis was that motor activity leads to an increased dopamine release resulting in increased competition of the endogenous ligand and IBZM for the postsynaptic D₂ sites.

Twenty subjects serving as the control group received 185 MBq of 123I-IBZM intravenously in a supine resting state. Another group of six subjects were asked to write a text. After two minutes of writing, IBZM was injected. Subjects had to continue writing for thirty minutes. SPECT imaging of the cerebral D₂ receptors was performed 90 minutes after injection. The study was approved by the local authorities in radiation protection.

Writing lead to a significant decrease of striatal IBZM binding normalised to the cerebellum both on the right (controls: 2.93 ± 0.24; writers: 2.59 ± 0.27; p < 0.01, t-test) and on the left side (controls: 2.86 ± 0.24; writers: 2.56 ± 0.25; p < 0.01). Similar results were obtained with other reference regions.

We conclude that writing compared to a resting state significantly influences dopamine D₂ receptor binding, as measured using IBZM and SPECT. We hypothesise that the motor activity involved leads to an increase of dopamine release into the synaptic cleft and that this additional amount of dopamine competes with the IBZM for the D₂ sites. This results in a decrease of postsynaptic IBZM binding. Thus, it is possible to depict presynaptic dopamine release with relatively simple methods. The data show the importance of standardised conditions during the cerebral accumulation of IBZM to control the effect of presynaptic mechanisms on postsynaptic binding.

OS-252

W. Pirker, S. Asenbaum, M. Willeit*, A. Neumeister*, N. Praschak-Rieder*, S. Kandhofer, P. Angelberger**, L. Deecke, I. Podreka, T. Brücke

Departments of Neurology and Nuclear Medicine, *Department of General Psychiatry, University of Vienna, **Forschungszentrum Seibersdorf, Austria

KINETIC ANALYSIS OF 123I-β-CIT BINDING TO SEROTONIN TRANSPORTERS IN HEALTHY HUMAN SUBJECTS

The cocaine congener β-CIT, labeled with 123I can be used as a tracer for SPECT to visualize dopamine (DA) and serotonin (5HT) transporters in the living human brain. Previous studies have demonstrated that due to different anatomical localizations and different binding kinetics it may be possible to investigate DA and 5HT transporter binding separately using β-CIT as a single ligand. However, no detailed study on the kinetics of β-CIT binding in 5HT transporter rich regions in human subjects has been performed. Methods: To obtain the optimal time frame for β-CIT SPECT imaging of 5HT transporters we performed SPECT studies in 2 healthy volunteers at 1, 2, 4, 7, 10, 13, 16 and 24 hrs post injection (p.i.). Consequently 14 volunteers were studied 4, 7, 10, 20 and 24 hrs p.i. of ~4mCi β-CIT. ROIs were placed over the striatum, thalamus and hypothalamus, frontal and occipital cortex and the cerebellar hemispheres, which served as reference region. Specific binding was defined as mean counts per minute in target minus reference regions corrected for time of injection and body mass (cpm/mCi x kg).

Results: Striatal uptake increased slowly reaching a plateau between 13 and 24 hrs p.i. (339±55 cpm/mCi x kg; 24hrs p.i.). Specific binding in thalamus and hypothalamus, a region known to contain 5HT transporters in high densities showed faster kinetics with a steep increase of binding up to 4 hrs p.i. and a plateau between 4 and 10 hrs p.i. (99±21 cpm/mCi x kg; 4hrs p.i.). Binding in frontal and occipital cortex decreased from 1 to 4 hrs and remained relatively stable from 4 to 10 hrs p.i. (12±4 and 11±5 cpm/mCi x kg; 4hrs p.i.). Conclusion: These results confirm previous findings of different binding kinetics of β-CIT in DA and 5HT transporter rich regions. A time frame between 4 and 10 hrs p.i. appears to be optimal for 5HT transporter imaging with β-CIT. SPECT imaging of serotonin transporters with β-CIT has been shown to be a useful tool for studying the action of antidepressant drugs in the living human brain and might provide better insight into the pathophysiology of different neuropsychiatric disorders.

Physics and instrumentation: PET

OS-253

T.D. Fryer, R.W. Barber, N.J. Bird, D. Visvikis

Department of Nuclear Medicine and Wolfson Brain Imaging Centre, Addenbrooke's Hospital, Cambridge, UK.

ASSESSMENT OF A 3D PET IMAGE RECONSTRUCTION ALGORITHM FOR USE WITH THE PICKER PCD SYSTEM: COMPARISON WITH A DEDICATED PET SCANNER FOR FDG BRAIN IMAGING

The aim of the study was to optimise the image quality attainable for brain imaging of dementia patients using a dual-headed gamma camera coincidence system (Picker 2000XP PCD). This involves optimising the data acquisition stage, using noise equivalent count analysis, and the image reconstruction methodology.

NEC analysis indicates that the optimum data quality is obtained by operating the system without septa with ~7 MBq in the brain. To preserve the resolution in such a data set, a 3D reconstruction algorithm is required.

The new algorithm is based on the backproject-then-filter method, which obviates rebinning the list mode data. The whole 3D data set is utilised by estimating the required missing data through Monte Carlo forward projection. Attenuation correction is shown to be the most important data correction. As transmission scanning is not available, an attenuation map is modelled using a quick 2D reconstruction of the data. Both uniform and non-uniform maps can be utilised; the inclusion of bone to model the skull gives superior results to a uniform soft tissue model, particularly in the cerebellum.

Correction of scattered events in the photopeak window (450-600 keV) involves smoothing, scaling and subtracting events where one photon lies in the photopeak and the other is in a scatter window (350-450 keV). As a delayed coincidence window is not provided, a Monte Carlo correction for random coincidences has been implemented.

The quality of the images produced was assessed through comparison against images of the same patients from a GE ADVANCE scanner. The images on the ADVANCE were reconstructed using the PROMIS algorithm with corrections for attenuation, scatter and randoms. The Picker and ADVANCE brain images were registered before regions of interest were superimposed. The ROI values (normalised to the cerebellum) agreed to within 8%, compared to discrepancies of up to 22% when using the software provided with the system.

Acquisition without septa, followed by reconstruction with the above 3D algorithm, now forms the basis of our brain imaging protocol.

OS-254

H. Erler, J. Zaknun, G. Riccabona, M. Oberladstätter

Hospital: Dept. of Nuclear Medicine, University of Innsbruck, Austria

ASSESSMENT OF OPTIMIZED IMAGING STRATEGIES FOR 18FDG-PET WITH A HYBRID DUAL HEAD CAMERA AND COINCIDENCE MODE

The particular features of new hybrid dual head PET cameras require specific tuning of imaging strategies to achieve optimal results in clinical 18FDG-studies, concerning energy window, matrix size, sensitivity and reconstruction algorithm. The aim of our study was to define the best approach to 18FDG-scanning with such a system and to test it in clinical routine. Methods: Using a Jaszczak-phantom with different inserts and 2D-Hofman brain in air, we varied energy window parameters to study the performance of our camera system. We studied the perceptibility of hot and cold lesions with and without photopeak/ Compton (PC) coincidences over photopeak window widths of 15%, 20% and 30% for target to background activity ratios ranging from 2:1 up to 8:1. Activity concentration at start was 7,4-55kBq/ml. All clinical studies were done with a two-head digital gamma camera (ADAC VERTEX) equipped with molecular coincidence detection (MCD). We performed 99 oncological studies in 95 patients (f = 45, m = 54), 13 studies in patients with lung cancer, 13 with thyroid cancer, 15 with lymphoma, 13 with CUP syndromes and 45 with other tumors. Moreover 10 patients with neurological symptoms were studied (7 epilepsy and 3 degenerative brain disorders).

Results: The accuracy of activity concentration estimates in studies using photopeak/ photopeak (PP) and photopeak/ Compton (PC)-coincidences was better with narrow photopeak windows. A further improvement was achieved with PC off settings. This effect was more pronounced in „lesions“ of larger volume. Only by using a 15% PP-window and PC-off the visualization of 13 mm hot spheres (target to background ratio of 4:1) and the detection of small cold structures was possible. We found no remarkable improvement in image quality using PC-on, indicating that mainly scattered events are responsible for loss in contrast. Based on these data, both brain and oncological 18F-FDG studies are therefore acquired using a 20% window over PP with PC-off. To compensate the loss of events we started the acquisition with singles-count-rates of 1,3x10E6 just below the threshold for „pearl-string“ artefacts, which required adjustment of applied activities (mCi = 0.05xBW[kg] + 1.2).

With this acquisition protocol an analysis of clinical studies showed 63 true positive, 27 true negative, 5 false positive and 1 false negative results in oncological studies (sensitivity 98%, specificity 84%). In neurological studies were 8 true positive and 1 true negative. In conclusion, the performance data regarding specificity and sensitivity for this camera system with optimized acquisition parameters are similar to those reported for ring cameras.

OS-255

M.A. Lodge, G. Cook, P.K. Marsden, A. Dynes and I. Fogelman.

Div. of Radiological Sciences, UMDS, Guy's & St. Thomas' Hospital, London, UK.

MINIMALLY INVASIVE DETERMINATION OF THE ARTERIAL INPUT FUNCTION FOR F-18 FLUORIDE PET.

The aim of this project was to develop a minimally invasive procedure to measure the arterial input function for F-18 Fluoride studies of the lumbar spine. An ECAT 951R PET scanner was used to perform dynamic (12x10s, 4x30s, 14x240s) acquisitions on 9 healthy volunteers after administration of 180 MBq of F-18. Arterial blood concentrations were measured using an on-line fluid analyzer in conjunction with discrete arterial sampling; 8 venous samples were also acquired; whole-blood (WB) and plasma (PI) concentrations were measured; and images were reconstructed using FBP (0.5 Hann, 2mm pixels, measured attenuation correction). We observed from these data that plasma input functions derived from time-activity curves over the aorta are subject to the partial volume effect and a PI-to-WB ratio which varied over the course of the acquisition (Arterial mean \pm s.d. : PI/WB = 1.47 \pm 0.16 at t=300s, 1.30 \pm 0.07 at t=3600s). In addition we noted that the PI-to-WB ratio for arterial blood was well approximated by the same ratio for venous blood and, at later times, the arterial and venous blood concentrations converged (WB mean \pm s.d. : Ven/Art = 1.01 \pm 0.06 at t=3600s). With these observations in mind, a software package was developed which: 1) automatically identified the aorta in each plane of an early frame and defined a 10x10mm ROI around the maximum pixel; 2) defined an additional background ROI in each plane; 3) applied the above ROIs to all frames of the dynamic image; 4) used the resulting image data in conjunction with the late venous WB samples to perform a partial volume correction; 5) converted the WB image data to PI values by applying time-dependent correction factors determined from the venous PI/WB data. For each patient an image-derived input function was compared with the one derived from arterial sampling in terms of the macroparameter K determined using Patlak graphical analysis. A mean bias in K of 1.06 \pm 0.06 was observed for the image-derived input functions with respect to the arterial input functions. The arterial functions had broader peaks and we partly attribute the differences in K to the dispersion of arterial blood in the line prior to measurement. These results confirm that an image-derived input function, requiring only a few venous blood samples, can be used to determine the uptake constant for F-18 in bone.

OS-256

E. Rota Kops, B.J. Krause, H. Herzog, H.-W. Müller-Gärtner

Institute of Medicine, Forschungszentrum Jülich GmbH, Jülich, Germany

3D PARTIAL VOLUME CORRECTION AND SIMULATED PET STUDIES

Partial volume effects can strongly influence the quantification of perfusion, metabolism and receptor density in brain PET. A fully 3D partial volume correction (3D-pvc) method was developed on the basis of the 2D "Grey Matter PET" method of Mueller-Gaertner [1]. By using a noiseless simulated brain volume, the accuracy of the method was tested with regard to basic parameters for this method as e.g., resolution of the PET camera, knowledge of the actual white matter value, misregistration and mis-segmentation. The evaluation of the first two parameters is presented here.

A segmented brain volume was used to model a MR volume dataset as well as to simulate a PET volume dataset with a grey matter (GM=100) to white matter (WM=20) ratio of 5:1 and a blurring 3D kernel (PET-res=8mm). The histograms of the GM pixels in the resulting corrected volume yielded information about the accuracy of the method. Using the correct values for WM and PET-res, the resulting histogram showed a peak at 100 \pm 0.8. Setting WM=20, we varied PET-res from 4 mm to 12 mm to simulate the influence of the PET scanner resolution (Fig.1). Setting PET-res=8mm, we varied the WM value from 5 to 40 (Fig.2). Finally, since the actual situation is the result of a combination of these parameters, we calculated the histogram of a 3D partial volume corrected dataset of a human brain (Fig.3, left) and compared it with simulated results for different combinations of the parameters (Fig.3, right, one combination shown). The plots in Fig.3 show similar shapes and indicate that a too low PET-res was chosen together with a too high WM value.

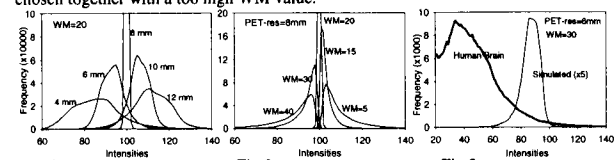


Fig.1 Simulations were used to determine the accuracy as well as the limitations of our 3D-pvc method. They helped to evaluate the optimum combination of the parameters for partial volume corrected data, the latter leading to a more accurate quantification of the original PET data.

[1] Müller-Gärtner et al. (1992): J Cereb Blood Flow Metab 12:571-583

OS-257

B. Pichler^{1,2}, G. Böning¹, E. Lorenz², M. Rafecas¹, M. Schwaiger¹, S.I. Ziegler¹

¹Nuklearmedizinische Klinik und Poliklinik der Technischen Universität München, ²Max-Planck-Institut für Physik München, Germany

STUDIES WITH A PROTOTYPE AVALANCHE PHOTODIODE PET

A prototype high resolution positron emission tomograph, based on lutetium-oxorthosilicate (LSO) read out by avalanche photodiodes (APD) was designed for imaging small animals. It uses four compact detector modules, each of them comprising 16 small LSO crystals (3.7x3.7x12 mm³, CTI, Knoxville TN) and a 2x8 APD array (4 mm detector spacing, Hamamatsu Photonics, Japan). Fast, low noise charge sensitive preamplifiers were developed for the APD arrays. The modules were mounted on a rotating gantry to simulate a full tomograph. Data were acquired in list mode and sorted into parallel projections using rebinning algorithms with different acceptance angles, either for a large field-of-view or homogenous sampling. Energy resolution was 16% (FWHM) for 511 keV gamma rays. The time resolution for two opposing LSO-APD detectors was 3.2 ns. Intrinsic spatial resolution, measured with a positron emitting point source scanned between 2 detector arrays was 2.2 mm (FWHM). The promising results of phantom measurements including F-18 line sources proved the feasibility of using this tomograph for the detection of small structures in vivo.

In addition, tests of a single LSO-APD channel in a high magnetic field (9.4T) showed no performance degradation. Further studies will evaluate the possibility of simultaneous magnetic resonance and coincidence imaging using this compact module. Future developments will concentrate on implementing new APD arrays with smaller detector distances and will also include novel detector structures based on the unique possibilities of APD arrays to facilitate two radial detector layers for improved detection efficiency and spatial resolution.

OS-258

A. Del Guerra, G. Di Domenico, M. Scandola, G. Zavattini, M. Giganti, L. Uccelli, A. Piffanelli

Department of Physics and Department of Clinical and Experimental Medicine, University of Ferrara, Italy

PET FOR SMALL ANIMALS: EXPERIMENTAL TEST OF THE YAPPET TOMOGRAPH

It is widely accepted that animal PET scanners are extremely valuable to assess new radiopharmaceuticals before their administration to humans. To accomplish this task a high spatial resolution scanner is necessary. At Ferrara University we have built and tested a small Field of View PET scanner for rats and mice with very good sensitivity and high spatial resolution.

The scanner is made of four detector modules: each one is composed of 400 YAP:Ce finger crystals (2x2x30 mm³) directly coupled to Hamamatsu Position Sensitive PhotoMultiplier (PSPMT). The modules are mounted on a rotating gantry and the opposite detector can be positioned at a distance ranging from 10 to 25 cm. The read-out data and data acquisition are handled by off-the-shelf electronics and are controlled by in-house developed programs. The scanner has a total FOV of 4x4x4 cm³ that is appropriate for small animal studies. The system operates in 3D acquisition mode and a 3D filtered back-projection algorithm is used for image reconstruction.

The spatial resolution has been measured with a ²²Na point-like source; values below 2mm (FWHM) are obtained within the useful FOV. The sensitivity is 730 counts/μCi at the centre of the scanner for a gantry diameter of 15 cm. These results are appropriate for small animal PET studies. The first images on biodistribution of FDG in rat brain have been obtained.

General nuclear medicine: Bone

OS-259

R. Kashyap, A. Babbar, A. Bhatnagar, A. Mondal, K. Swaroop, UPS Chauhan

Departments of Nuclear Medicine and Radiopharmaceutical Institute of Nuclear Medicine and Allied Sciences, Delhi-54, India

Tc-99m GLUCARIC ACID IMAGING; A NEW WAY TO ASSESS AVASCULAR NECROSIS OF FEMORAL HEAD.

Conventional bone scintigraphy has been used with variable success to assess avascular necrosis of the femoral head. At present, MRI is considered to be the best non-invasive modality to evaluate the same. The presence of a metallic prosthesis, its prohibitive cost and the feeling of claustrophobia in some patients limit the use of MRI in every possible case.

The ability of Tc-99m Glucaric acid to image necrosis prompted us to study its utility in imaging avascular necrosis. A kit to prepare Tc-99m Glucaric acid was developed by our group.

9 patients (7 males, 2 females) with 11 hips developing avascular necrosis of the femoral head was studied. All the patients underwent a conventional 3 phase bone scan with Tc-99m MDP and serial imaging with Tc-99m glucaric acid using LEAP collimator in a Siemens Integrated DICAM SPECT system. MRI scan was also performed on 4 of these 9 cases. Histopathological confirmation was obtained in all. 370-555 MBq of Tc-99m Glucaric acid was administered intravenously after an informed consent. Sequential images for blood flow were obtained for 2-min post-injection (PI) at the rate of 3 sec/frame. Images of 400 k counts were obtained at 5 min, 1 hr and 4 hrs PI. A SPECT data acquisition was done at 4 hrs PI in step and shoot mode in 64 x 64 matrix. Reconstruction of the data was done using filter back projection technique.

Reduced blood flow in the initial images could be appreciated in 4 of the 11 involved hips. The pattern of increasing Tc-99m glucaric acid concentration at the pathological femoral head and reduction in size of the central photopenia from the 1 hr to the 4-hr image was noted in 9 of the 11 hips studied.

The Tc-99m MDP scan could offer a relatively definite diagnosis with the image characteristics of increased concentration with central photopenia at 3 hours PI in 7 of the eleven cases. On comparing the appearance of the diseased site in the later images, the uptake with Tc 99m glucaric acid was seen in a much smaller area indicating that unlike Tc-99m MDP, Tc-99m glucaric acid possibly does not accumulate in fracture sites or reactive bone sites in delayed images. MRI could offer a diagnosis in all the 4 patients (6 hips) studied.

This preliminary and ongoing study shows that Tc-99m glucaric acid imaging is useful in avascular necrosis of bone and merits further critical evaluation.

OS-260

F. Paycha¹, B. Brunot², C. Houzard³, F. Salmon⁴, A. Fontaine⁵

Nuclear Medicine Working Party on Reflex Sympathetic Dystrophy, Société Française de Biophysique et Médecine Nucléaire (SFBMN), Dpts of Nuclear Medicine and Evaluation, Hôpitaux Louis Mourier (Colombes)^{1,5}, Hautepierre (Strasbourg)², Neuro-Cardiologique (Lyon)³, Cochin (Paris)⁴, France. FRENCH NATIONWIDE MULTIDISCIPLINARY SURVEY « BONE SCAN IN REFLEX SYMPATHETIC DYSTROPHY »:

USE AND EVALUATION OF BONE SCAN BY CLINICIANS

The aims of the survey were to delineate the indications of bone scan (BS) in reflex sympathetic dystrophy (RSD), to set the best criteria of interpretation of BS and to assess the role of BS in the current strategy of prescribing physicians for the diagnosis of RSD.

In April-May 1997, a questionnaire specifically dedicated to ordering physicians was designed by the RSD Working Party of Nuclear Medicine Physicians. A preliminary draft was submitted for modifications to rheumatologists subspecialised in RSD and eventually tested by unspecialised colleagues. The final form, containing 26 questions, was dispatched throughout France from June to October according to two independent routes: 1) the network of SFBMN Regional Delegates and Nuclear Medicine dpts, 2) the manifold French clinical scientific societies.

A total of 644 completed questionnaires were returned. The majority of respondents (61%) had a liberal practice. Rheumatologists provided most answers (54 %), followed by orthopedic surgeons (20 %) and physical medicine and rehabilitation physicians (14 %). RSD is a prevalent disease (1 to 2 % of patients seen each year). The 3 most frequently quoted contexts of referring patients for a BS were an atypical clinical picture (70 % of answers), an arduous differential diagnosis (55 % of answers) and medico-legal circumstances (45 %). The procedure was systematically performed by only 20 % of surveyed physicians. The "top three" differential diagnoses of RSD were osteonecrosis (75 % of answers), fracture (75 %) and acute arthropathy (45 %). For 70 % of respondents, BS confirmed the diagnosis suspected on clinical grounds. Only 20 % of correspondents quoted blood flow phase disturbances as interpretation criteria. The impact of whole body BS on the diagnosis of RSD was deemed high by only 15 % of clinicians.

Finally, for most clinicians, the diagnosis of RSD relied on the triptych of clinical (83 %), scintigraphic (72 %) and roentgenographic (55 %) arguments.

The survey met strong interest and general approval from specialists tackling with RSD but evidenced frequent knowledge deficiencies pertaining to BS technical aspects and semiological criteria in RSD.

Nevertheless, this survey emphasizes that, in current practice, BS remains the pivotal test in the diagnostic management of a disorder still challenging by a poorly understood pathophysiology, a protean clinical presentation and an unpredictable evolution.

OS-261

P.Predič, D.Hrastnik

Hospital Celje, Slovenia

QUANTITATIVE ANALYSIS HIP PERFUSION IN ALL STAGES OF ASEPTIC HIP NECROSIS

Since there has always been a question of the amount of perfusion in hips at different stages of aseptic hip necrosis, we tried to impartially examine the perfusion in hips at different stages (from early to late) of aseptic necrosis of one hip. Our study included 247 patients with proven aseptic necrosis of one hip. All patients were subjected to three-phase scintigraphy of hip, SPECT, and quantitative calculation of relative perfusion in the artery phase (3T). The examination was performed at the early stage and repeated at later stages. 550-740 MBq of Tc-99m - DPD were bolus injected. At the early stage of aseptic hip necrosis the obtained 3T was decreased, from 0.59-0.99 (3T=0.81). SPECT showed a moderate increase of diffuse accumulation. At the late stages we obtained 3T decreased from 0.32-0.76 (3T=0.62), thus evidencing hypoperfusion. SPECT showed an increased accumulation, partly diffuse and partly multifocal. In the group examinations of the very late stage 3T was extremely decreased, from 0.29-0.65 (3T=0.48), implying thus progressive hypoperfusion.

Conclusion: With the aseptic hip necrosis, quantitative analysis of perfusion 3T indicates that the perfusion is decreased at all stages of the process which however shows a significantly falling trend with the progress of the disease. 3T allows early diagnosis in the patients with aseptic hip necrosis, as well as the control of the disease progress.

OS-262

A.Furno, A. Palermo, D. Grigolato, P. Castellucci, *A. Toni, *A. Sudanese, *L. Busanelli, *C. Basile.

Nucl Med, Immunohematology Depts. Azienda USL Citta' di Bologna, *University Orthopaedics Clinic, Rizzoli Institute, Bologna, Italy.

SCINTIGRAPHIC DIAGNOSIS OF ARTHROPLASTY INFECTION: HAS THREE PHASE BONE SCAN STILL A ROLE? A PROSPECTIVE STUDY.

AIM OF THE STUDY: to assess the diagnostic value of three phase bone scan (TBS) versus ^{99m}Tc HMPAO granulocyte scintigraphy (GS) in the pre-operative phase of patients (pts) with suspected arthroplasty loosening needing surgery.

METHODS: in the last 2 years 95 consecutive pts were enrolled and 78 completed the follow up program after surgery (63 hip, 13 knee, 1 elbow, 1 shoulder). The remaining 17 pts were not considered for result analysis because of incomplete data. GS was considered positive if uptake of labelled cells, not present at 30 min images, was seen at late (3-24 h) scan in periprosthetic zone. TBS was separately evaluated for vascular (V) and equilibrium (BP) phase. Implants were considered infected (n=20) if: a) intraoperative cultures grew out organisms or b) gross purulence was evident at surgery. Aseptic loosening (n=58) was diagnosed when: a) operative smears revealed no leukocytes and intraoperative cultures were reported as no-growth and b) no signs of infection developed during a 6 months follow-up period, despite a positive culture result.

RESULTS: see table

	n	GS		TBS-V		TBS-BP	
		Set	SpI	Set	SpI	Set	SpI
HIP	63	92	98	78	74	85	70
KNEE	13	100	86	100	13	100	0
OTHERS	2	-	-	-	-	-	-
GLOBAL	78	95	97	75	68	89	60

CONCLUSIONS: this study confirms the high accuracy of GS in the diagnosis of bone implant infections. TBS is of limited value in hip arthroplasties and completely unhelpful or misleading in other orthopaedic implants.

OS-263

*P. Meyer, +H. Burkhardt, °W. Gründer, +E. Buchner, +E. Palombo-Kinne, *W. Becker, *F. Wolf, +J.R. Kalden, and #R.W. Kinne

*Departments of Nuclear Medicine and +Internal Medicine III, University of Erlangen-Nürnberg, Erlangen, and °Institutes of Biophysics and #Immunology, University of Leipzig, Leipzig, Germany

123I-ANTILEUKOPROTEINASE SCINTIGRAPHY REVEALS CARTILAGE ALTERATIONS ON THE CONTRALATERAL SIDE OF MONOARTHRITIC ANTIGEN-INDUCED ARTHRITIS (AIA)

PURPOSE: Involvement of the contralateral knee joint (CKJ) cartilage in "monoarthritic" AIA was assessed by scintigraphy with the cationic (11kD, pI > 10) 123I-labelled serine proteinase inhibitor antileukoproteinase (123I-ALP).

METHODS: AIA was induced in Lewis rats by intra-articular injection of 500µg bovine serum albumin/saline (mBSA) into the right knee joint following systemic immunisation; saline was injected into the CKJ as control. Rats were examined 80d later (chronic stage), when joint swelling and 99mTc-uptake of the arthritic knee joint (AKJ) had normalised. 123I-ALP or 123I-myoglobin, a control protein of comparable size, but different isoelectric point (pI = 7.3), were injected i.v. into normal or AIA rats (n = 6 each). AKJ, CKJ, and both ankles were examined scintigraphically 14h after radiotracer injection. Joint cartilage was examined *ex vivo* by magnetic resonance microimaging (MRMI), histopathology and for accumulated tissue radioactivity (well counter).

RESULTS: In normal articular cartilage, ALP accumulated to a significantly higher degree than myoglobin; this preferential accumulation was lost in rats with chronic AIA, both in AKJ and CKJ, but not in the ankles. In both knee joints, 123I-ALP target/background ratios (T/B) negatively correlated with the loss of toluidine blue staining in cartilage, which documents depletion of charged matrix molecules (T/B at 4h, AKJ: r = -0.92, p < 0.01 / CKJ: r = -0.68, p < 0.05; cartilage radioactivity, AKJ: r = -0.68, p < 0.02 / CKJ: r = -0.82, p < 0.01), while there was no correlation for the control protein. Histopathology confirmed mild cartilage alterations in the AKJ and, to a lesser degree, in the CKJ, whereas the ankle joints were unaffected. In contrast to clear abnormalities demonstrated with ALP scintigraphy, MRMI detected only very subtle signal changes in the cartilage in the AKJ, but failed to show changes in the CKJ.

CONCLUSION: Loss of ALP accumulation appears to document proteoglycan depletion in mildly altered arthritic cartilage. Bilateral knee joint cartilage alterations in "monoarthritic" AIA indicate that the use of the CKJ as a control is problematic. High diagnostic sensitivity and specificity of ALP scintigraphy may provide the basis for detection of early, pre-morphological cartilage alterations also in human arthritis.

OS-264

V. Zavadovskaja, I. Sukhodolo. Departments of Radiology and Morphology, Siberian Medical University, Tomsk, Siberia, Russia.

RE-EVALUATION OF DIAGNOSTIC EFFICIENCY OF ¹¹¹IN CITRATE SCAN IN DETECTION OF ACUTE AND CHRONIC BONE INFECTION

Purpose of the study was to evaluate usefulness of ¹¹¹In-citrate scintigraphy in differentiation of acute from chronic osteomyelitis and in detection of acute inflammatory focus in a relapse of chronic process.

39 patients (pts) with suspected osteomyelitis including 12 ones with diabetic foot were studied with ¹¹¹In-citrate scan 24h after i.v. injection of agent. Diagnosis was verified by surgery, follow-up, x-ray and morphologic studies. Focal areas of increased activity at site of bone inflammatory were classified to 3 types: as high, moderate and minimal. ¹¹¹In-citrate scan showed 26 true-positive, 11 true-negative and 2 false-negative results. The absence of false-positive scans resulted in a specificity of 100%. Sensitivity and accuracy were 92.8% and 94.9% respectively. Acute osteomyelitis, bone abscess at the site of neuroarthropathy, chronic osteomyelitis in the phase of activation appeared as focal areas of high activity. Autopsy studies indicated plentiful neutrophil infiltration in 9 cases. The patterns characterized by moderate or minimal uptake correlates with chronic infection or postantibiotic condition. Lymphocyte and plasmocyte infiltration was seen in five pts. True-negative scans were verified mostly by the follow-up and the morphologic data in two pts. Two rib osteomyelitis cases showed false-negative patterns.

Thus, ¹¹¹In-citrate scan is safe, sensitive and reliable technique to reveal both acute and chronic osteomyelitis and to evaluate the results of treatment and can be employed as replacement to labelled leucocytes when necessary.

Cardiovascular: Function

OS-265

C. Alexander¹, B. Schwaab², G. Fröhlig², D. Hellwig¹, J.B. Bader¹, H. Schieffer², C.-M. Kirsch¹; Dept of Nuclear Medicine¹ and Cardiology²; Saarland University Medical Center, D-66421 Homburg/Saar; Germany

INFLUENCE OF RIGHT VENTRICULAR STIMULATION SITE ON LEFT VENTRICULAR FUNCTION IN ATRIAL SYNCHRONOUS PACING

Purpose: Applying radionuclide ventriculography left ventricular contraction was studied during right ventricular septal and apical pacing in an atrial synchronous mode. **Methods:** In 14 patients with 3rd degree AV-block, AV-interval was optimized for septal and apical pacing. QRS time-interval in the 3 leads of the Frank electrode system was compared to septal and apical pacing. After in-vivo bloodpool labelling and acquisition of 64 frames per cardiac cycle, ejected counts (EC), ejection fraction (EF) and left ventricular phase analysis were determined randomly for septal and apical mode. Area under the curve (AUC) and full width at half maximum (FWHM) of the phase histogram were compared for both modes and were correlated to Frank's QRS time-interval. **Results:** QRS duration was shorter with septal than with apical pacing in 9 out of 14 patients (64 %), it was longer in 4 (29 %), and no difference was seen in 1 patient. There was a positive correlation between the change in QRS duration and the phase histogram ($\Delta AUC: r=0.66, p=0.01$; $\Delta FWHM: r=0.61, p=0.2$) and a negative correlation with the systolic function ($\Delta EF: r=0.63, p=0.016$; $\Delta EC: r=0.74, p=0.002$). **Conclusion:** Decreased QRS duration that is commonly obtained by right ventricular septal pacing is correlated with reduced dyssynergy of left ventricular contraction and increased systolic function. In atrial synchronous right ventricular pacing, this is commonly obtained by QRS-guided septal implantation when the AV delay is individually optimized.

OS-266

V. Gendreau, F. Archambaud, A. Ramadan, A. Terral, A. Prigent.

Hospital: Bicêtre, Nuclear Medicine Department, 78 Av Gal Leclerc, Le Kremlin Bicêtre, AP-HP Paris, France.

201-Tl MYOCARDIAL GATED SPECT (Th-GSPECT) VERSUS 99mTc GATED PLANAR EQUILIBRIUM VENTRICULOGRAPHY (Tc-GEV) TO ASSESS LEFT VENTRICULAR FUNCTION.

Tl-GSPECT was compared to Tc-GEV to assess rest left ventricular ejection fraction (LVEF) and qualitative wall motion analysis (QWMA). 31 patients referred for routine myocardial SPECT and Tc-GEV were prospectively included. 4 hours after a 120 MBq of 201-Tl injection for a stress test and 45 min after reinjection of 55 MBq, a rest Tl-GSPECT was performed. Without any delay, a Tc-GEV was acquired at the best septal and left lateral views while heart rate was unchanged.

Analysis and results: LVEF differences between Tl-GSPECT and Tc-GEV were analysed referring to the Tc-GEV LVEF values:

LVEF diff	Tc-GEV LVEF values				n patients
	≤ 15%	15%-40%	40%-60%	>60%	
≤ 5%	1	5	11	5	22
5%-10%	0	0	3	4	7
>10%	0	1	1	0	2
n patients	1	6	15	9	31
Mean diff	2%	5%	5%	4%	5%

QWMA was evaluated using a four point scale (normal(0), moderate(1) and severe(2) hypokinesis, akinesis(3), dyskinesis(4)) in 10 segments defined on best septal and left lateral views. The percentage of concordant QWMA (conc.%) were presented referring to each segment:

segment	Best septal view					Left lateral view					Total n=310
	inf apx	ant lat	ant bas	sep bas	ant sep	apx	ant apx	inf bas	ant apx	ant bas	
conc.(%)	97	84	97	68	84	90	84	77	87	87	265

Conclusion: Tl-GSPECT seems to be a promising technique to assess LVEF when compared to Tc-GEV. An unexplained large difference (14%) was observed in only 2 patients. LVEF and QWMA were concordant in 93% and 85% of the patients respectively.

OS-267

H. Xu, J.X. Luo, J. Chen, R.H. Lie, H. Huang and J.Q. Xie

Dept. of Nuclear Medicine, The First Affiliated Hospital, Jinan University Medical College, Guangzhou, China

AUTOMATIC QUANTIFICATION OF LEFT VENTRICULAR FUNCTION FROM GATED MYOCARDIAL PERFUSION SPECT IN PATIENTS WITH CORONARY ARTERY DISEASE

This study investigates the feasibility of routine clinical gated myocardial perfusion SPECT with ^{99m}Tc-sestamibi for automatic quantification of left ventricular (LV) function in patients with coronary artery disease (CHD), gated myocardial perfusion SPECT with ^{99m}Tc-sestamibi was performed in 49 ischemic patients (17 females and 32 men, mean±SD 58±10 years), 10 myocardial infarcts (MI) (1 female and 9 men, mean±SD 63±7 years) and 27 normal subjects (NS) (11 females and 16 men, mean±SD 44±14 years) on a dual-detector SPECT (APEX SPX HELIX with Xpert, Elscint). The LV functional parameters (LVEF, EDV and ESV) were calculated without operator interaction using an automated gated myocardial perfusion SPECT processing software (QGSPECT, Elscint). Thirty patients (10 females and 20 men, mean±SD 57±11 years) underwent rest gated blood pool imaging within 72 hr of gated ^{99m}Tc-sestamibi SPECT. **Results:** Automatic quantification of LVEF, EDV and ESV was successful in 86/86 (100%) of this study and was perfectly reproducible. The LV functional parameters (mean ± SEM) assessed by QGSPECT and gated blood pool imaging in 30 consecutive patients is in the following table:

	n	LVEF (%)	EDV (ml)	ESV (ml)
QGSPECT	30	44.7±3.3	118.4±15.9	77.6±15.8
Blood pool imaging	30	49.0±3.0	119.6±14.4	71.1±13.7
r		0.89*	0.94*	0.97*

* p<0.0001

The results (mean ± SD) of LV functional parameters from QGSPECT in patients with CHD (ischemia, MI) and NS are summarized in the table below:

	n	LVEF (%)	EDV (ml)	ESV (ml)
NS	27	57.3±4.8	85.3±4.8	77.6±15.8
Ischemia	49	55.1±10.8 #	87.7±27.6 #	71.1±13.7 #
MI	10	21.4±11.2*	203.4±107.2 §	169.5±103.6 ♦

p>0.05, * p<0.0001, § p<0.01, ♦ p<0.005 (compared with NS)

Conclusion: Automatic quantification of LV function from gated myocardial perfusion SPECT is as reliable as gated blood pool imaging and has clinical value in patients with CHD, for providing clinically useful information to complement myocardial perfusion studies.

OS-268

XJ Liu, ZH Tao, RF Shi, XL Zhang, ZM Yao, YZ Liu

Department of Nuclear Medicine, Cardiovascular Institute & Fu Wai Hospital, CAMS & PUMC, Beijing, China

ASSESSING THE HEMODYNAMIC EFFECTS OF THE CHINESE HERBAL MEDICINE HIGENAMINE AND THE POTENTIAL ROLE IN NUCLEAR CARDIOLOGY

Higenamine (dl-demethylcodaurine) (HG) which was isolated from aconitum japonicum. It has been used for treatment of patients with bradycardia. We considered it might be useful in pharmacologic stress test. A comparison of hemodynamic effects of HG and dobutamine (DB) was performed in 6 dogs: Heart rate (HR), blood pressure (BP), coronary blood flow (CBF), myocardial O₂ consumption (MOC) and cardiac output (CO) were measured during infusion of HG and DB. Results: The comparison of hemodynamic effects of HG and DB in 6 dogs was shown as follows:

	HR(beat/min)		CBF(increase%)		MOC(ml/min)		CO(increase%)	
	pre	post	pre	post	pre	post	pre	post
HG	148±22	192±14**	0	55±37**	3.2±0.8	7.6±2.0*	0	12±11
DB	158±19	197±42	0	46±35	4.27±0.6	6.4±1.9**	0	8±10

*P < 0.05, **P < 0.01.

Though the effects of HG and DB on heart were comparable, the increase of systolic BP of HG is lower than that of DB. No side effects were found. Conclusion: HG might be utilized in pharmacologic stress test as that of DB, particularly for patients with hypertension.

OS-269

S. Zhang, L. Li, W. Guo, X. Yan, L. Wang, C. Zhang, G. Hu

Hospital: Cardiology Department, First Hospital, Shanxi Medical University, Taiyuan, P. R. China

THE TIME COURSE OF LEFT VENTRICULAR DILATION IN ACUTE MYOCARDIAL INFARCTION

After an acute myocardial infarction(AMI), there will be regional dilation and global remodeling of infarcted left ventricle. This study aims to observe the features of the left ventricular remodeling, the size of left ventricle in 37 patients(pts) with AMI by resting myocardial gated SPECT(GSPECT). The pts were admitted to hospital within 3 hours(hrs) to more than 12 hrs after onset of symptom. Tc-99m MIBI were infused at admission and data of GSPECT was collected 2 hours later following the infusion. End-diastolic volume(EDV), end-systolic volume(ESV) and LVEF were calculated by the system. Stroke volume(SV) was calculated by SV=EDV-ESV. The EDV, ESV, SV and LVEF for 11 controls were collected too. EDV, ESV, SV and LVEF for 37 pts with AMI at admission to hospital and that for 11 normal controls were showed as following:

	Controls(11)		Patients(37)			
	≤ 3hrs(16)	>3hrs(7)	≤ 6hrs(7)	>6hrs(11)	≤ 12hrs(3)	>12hrs(3)
EDV(ml)	74.7±12.2	98.5±31.9	99.4±55.6	128.1±55.1*	140.0±25.3	
ESV(ml)	25.3±5.8	57.0±30.9	55.1±40.3	77.4±39.8	81.3±26.0	
SV(ml)	49.5±8.4	41.5±10.2	44.3±15.2	50.7±18.8	58.7±2.5	
LVEF(%)	66.4±4.6	44.6±13.1	49.7±13.1	42.8±13.5	42.7±8.6	

* P<0.05(>6-≤ 12Hrs compared with ≤ 3Hrs)

EDV and ESV in pts with anterior infarction admitted to hospital after 6 hrs were 148.6±51.8ml, 72.5±32.4ml respectively. EDV and ESV in pts with anterior infarction admitted to hospital in 6 hrs were 116.1±37.7ml, 94.0±36.0ml respectively. That in pts with inferior infarction admitted to hospital after 6 hrs were 148.6±51.8ml, 72.5±32.4ml respectively. That in pts with inferior infarction admitted to hospital in 6 hrs were 71.9±20.6ml, 31.4±12.0ml respectively. The results suggest that the left ventricular size enlarged in 3 hrs after AMI and EDV and ESV did not change in 6 hrs and the EDV, ESV increase gradually after 6 hrs after onset of the symptoms.

OS-270

C.G.Zhang, Q.H.Han, Z.Z.Zhang, S.W.Zhang, J.Z.Liu, S.J.Li, S.J.Han and G.Hu.

1st Hospital, Shanxi Medical University, Department of Cardiology and Nuclear Medicine, Taiyuan, P.R.China.

EFFECT OF THROMBOLYTIC THERAPY ON LEFT VENTRICULAR REMODELING FOLLOWING ACUTE MYOCARDIAL INFARCTION WITH A SERIES OF TC99M-MIBI MYOCARDIAL GATED SPECT

The aim of this study is to evaluate the effect of thrombolytic therapy on left ventricular remodeling(VR) following acute myocardial infarction(AMI) with a series of myocardial gated spect(MGS). 34 patients with AMI, 24 males and 10 females, average age of 60.65 years were studied using Tc99m-MIBI(925MBq) and dual-head gamma camera with a special software of quantitative gated spect(QGS). 23 patients were treated by thrombolytic therapy(TT). 20 patients obtained reperfusion. 3 patients failed to get reperfusion. Thrombolysis could not be used in 11 patients. MGS was performed at about 12 hr., 1 week(W), 2 weeks and 1 month after AMI.

The level of remodeling following AMI was divided into 3 grades: I was without global ventricular dilatation(GVD) and/or global distortion of shape(GDS); III was with GVD and/or GDS; II was between I and III. The change of remodeling level can be evaluated by a series of MGS. The normal values of end-diastolic volume(EDV), end-systolic volume(ESV) and ejection fraction(EF) were measured in 14 normal persons. The results were showed on the table below:

Group	Normal(14)	TT success(20 patients)			Non-TT(11 patients)	
		Before TT	After TT<1W	-2W	Before T	After T-2W
EDV(ml)	92±13	101±31*	102±38	94±31**	111±55*	121±66***
ESV(ml)	39±9	53±24*	54±33	47±22	66±51*	71±64***
EF(%)	58±6	49±12*	50±12	51±9	47±18*	49±18

*p<0.05(compare with normal);**p>0.05(compare with before TT); ***p<0.05(compare with after TT-2W). The change of VR level was listed on the table below:

Group	No.	III to II or II to I	I to II or II to III	Almost no change
TT success	20	8	2	10
TT failed	3		1	2
Non-TT	11	1	5	5

Those data showed that thrombolytic therapy can make a beneficial effect on VR. The EDV(mean value) was near normal in the patients with TT success after TT ~2 W but the EDV (mean value) was much bigger than that of before therapy in the patients with Non-TT. The level of VR was getting better in 40% of the patients with TT success but only ~10% of the patients with Non-TT. A series of myocardial gated spect with Tc99m-MIBI is a valuable technique for evaluating VR and the effects of thrombolytic therapy.

Oncology: Therapy

OS-271

L. Kabasakal, C. Nişli M. Halaç, O. Oğuz, Ç. Önsel, S. Taşpolatoğlu, S. Apaydın, M. Altıparmak, I. Uslu
Cerrahpaşa Medical Faculty, Department of Nuclear Medicine, Istanbul, Turkey.

MONITORING MULTIDRUG RESISTANT P-GLYCOPROTEIN FUNCTION WITH Tc-99m-MIBI: THE EFFECT OF CYCLOSPORIN-A.

The failure to cure cancer patients is primarily caused by the development of drug resistance by overexpression of p-glycoprotein (Pgp). Diverse group of drugs have been identified including cyclosporin-A (Cyc-A) which can reverse drug resistance by inhibiting Pgp transport. Recently Tc-99m MIBI (MIBI) has been shown to be a substrate for Pgp and may be used for imaging of Pgp transport. Pgp is normally expressed in biliary canalicular surface of hepatocytes and found responsible for the excretion of cationic metabolites from the liver. The aim of the present study was to evaluate the effect of Cyc-A on biological distribution of MIBI in vivo. For this purpose 5 patients with alopecia and 2 renal transplant patients who were treated with Cyc-A were selected for the study. All patients were studied before and at least 2 weeks after administration of Cyc-A. MIBI scintigraphy was performed by obtaining planar abdominal images at 5., 30., 60., 120. and 180. min. after injection and the liver/heart (LH) ratios were calculated. Plasma Cyc-A, bilirubin levels, liver enzymes and creatinine clearances were obtained from all patients. In 3 patients plasma Cyc-A level was increased above 400 pg/dl and in 2 patients clinical Cyc-A toxicity was observed. The LH ratio was increased significantly after Cyc-A administration (p<0.01). After Cyc-A administration MIBI excretion was delayed and the uptake in liver was increased as well. The difference was 18.5% at 5 min. and 45.9% at 180 min. The liver retention was highest in patients with Cyc-A toxicity. With limited number of patients this study suggested that MIBI excretion from liver was mediated by Pgp and inhibition of Pgp transport not only delays liver excretion but also increases the liver uptake of MIBI.

OS-272

L. Vini, S. Chittenden, B. Pratt, M.E.A. O'Connell, M. Flower, V.R. McCready, C. Harmer.
Thyroid Unit, Royal Marsden Hospital, Downs Road, Sutton, Surrey, SM2 5PT, UK.

IN VIVO DOSIMETRY OF RADIOIODINE IN PATIENTS WITH METASTATIC DIFFERENTIATED THYROID CANCER (PRELIMINARY REPORT).

Aim: 1) To calculate the radiation dose absorbed by metastatic differentiated thyroid cancer from therapeutic doses of iodine-131 2) To establish a dose-response relationship 3) To individualise administered activity so that a tumouricidal dose is achieved.

Methods-Patients: 24 hours after administration of a tracer dose of ¹²⁴I or ¹²³I, PET or SPECT imaging was performed in order to assess the functioning mass (m) of metastatic deposits. Following administration of a therapy dose of ¹³¹I (5.5 GBq), sequential quantitative scans using a dual-headed whole-body gamma camera were taken to produce activity-time curves for each metastatic site; by extrapolating the data to the time of administration the initial activity (Ao) in the tumour sites and the effective half-life (Te) were determined. Absorbed radiation dose was then calculated using the equation: D= 0.16x Ao x Te/m. Twenty-nine studies on 21 patients (14 female and 7 male, median age of 62 years). Nine patients had papillary and 12 had follicular carcinoma. Metastatic sites included: bone in 8, lung in 6, lymph nodes in 6 and brain in 1.

Results: Preliminary analysis of 18 studies showed that absorbed radiation dose from administered ¹³¹I activity of 5.5 GBq varies widely ranging from 6 Gy to 102 Gy. In 5 patients the result of the dosimetry study had a significant impact on patient management; radioiodine therapy resulted in subtherapeutic tumour doses and for this reason additional treatment (external beam radiotherapy) was given.

Conclusions: In vivo dosimetry of radioiodine therapy in patients with metastatic differentiated thyroid cancer showed a wide variation in radiation absorbed dose from a fixed administered ¹³¹I activity. Analysis of the dose-response data is awaited. In future based on the final results, we hope to improve effectiveness of treatment as well as minimise late morbidity, staff hazards and unnecessary expense.

OS-273

K.H. Bohuslavizki, S. Klutmann, W. Brenner, S. Kröger, W.U. Kampen, S. Tinnemeyer, and E. Henze.

Clinic of Nuclear Medicine, University of Kiel, Germany.

PROTECTION OF SALIVARY GLANDS BY AMIFOSTINE IN HIGH-DOSE RADIOIODINE THERAPY – RESULTS OF A DOUBLE-BLIND PLACEBO-CONTROLLED STUDY.

Parenchymal damage of salivary glands is a well-recognized side effect following high-dose radioiodine treatment (HD-RIT). Since differentiated thyroid cancer has an excellent prognosis, reduction of long-term side effects is important. Thus, the effect of amifostine, a radio-protective drug, was studied in HD-RIT.

Quantitative salivary gland scintigraphy was performed prospectively in 42 patients with differentiated thyroid cancer prior to and 3 months after HD-RIT with 6 GBq I-131 in a double-blind, placebo-controlled study. 22 patients were treated with 500 mg/m² amifostine intravenously prior to HD-RIT, and 20 patients served as controls. Parenchymal function was evaluated quantitatively as uptake of Tc-99m-pertechnetate in percent of the activity injected. Xerostomia was graded according to WHO criteria.

	Control group (n=20)		Amifostine group (n=22)	
	Parot. gl.	Subm. gl.	Parot. gl.	Subm. gl.
Prior to I-131	0.47±0.17	0.44±0.16	0.46±0.17	0.42±0.18
After I-131	0.29±0.11	0.27±0.12	0.45±0.16	0.41±0.17

In 20 control patients HD-RIT significantly (p<0.001) impaired parenchymal function by 35.4 ± 16.2 % and 37.7 ± 14.8 % in parotid and submandibular glands, respectively. Eight out of these 20 patients developed grade I (WHO) xerostomia. In contrast, there was no significant (p=0.691) decrease in parenchymal function in amifostine-protected patients, and xerostomia did not occur in any of them.

Parenchymal damage in salivary glands caused by HD-RIT can be reduced significantly by amifostine. This may improve quality of life of patients with differentiated thyroid cancer after HD-RIT.

OS-274

M. Zubillaga*, J. Boccio*, J. Nicolini#, R. Ughetti#, E. Lanari[†], J. Salgueiro* and R. Caro*. *Radioisotope Laboratory, School of Pharmacy and Biochemistry, U.B.A., Argentina. #Bacon Laboratories S.A.I.C., Buenos Aires, Argentina. [†]Nuclear Medicine Department, Mater Dei Sanatorium, Buenos Aires, Argentina.

PIROCARBOTRAT: A NEW RADIOPHARMACEUTICAL FOR THE TREATMENT OF SOLID TUMORS.

To evaluate the effectivity of a single intratumoral dose of Pirocarbotrat, a gelatin protected charcoal suspension labeled with chromic [32P] pyrophosphate, studies of bioelimination, biodistribution and therapeutic action were carried out in rats and the results thus obtained were compared with those of other 32P dispersions. To perform the study, 98 female Sprague Dawley rats with experimental mammary adenocarcinomas, were used. The radiopharmaceuticals were administered intratumorally. After the injection of the products, samples of urine and feces were collected. The size of the injected and not injected tumors was determined with a caliper along two axes as a function of time, and their mean diameters were compared. The not injected tumors were used as controls in order to determine the evolution of both the controls and the injected tumors in the same animal. Once the experiment was finished, 32 days after the injection of the radiopharmaceuticals, animals were anaesthetized with ethyl ether till death in order to extract their organs and the injected tumors. The organs and the tumors were disrupted and mineralized with sulfochromic mixture. The radioactivity of the urine, faeces, organs and tumor samples as well as a 32P standard were measured in a monochannel gamma spectrometer using the Bremsstrahlung photons of 32P. Percentage of the retained activity in each organ as well as the percentage of elimination for each product were referred to its 32P standard. We found that 78.3% of the treated tumors reduced its size after 32 days of treatment. Histopathological studies confirmed the therapeutic action studies. At that time, the total eliminated activity was 12.70±3.90 % distributed in urine (8.30±1.80)% and feces (4.40±3.50)%. Biodistribution studies demonstrate that 84.50±2.60 % of the injected activity remained in the tumor, with no significant concentration in the rest of the organism. The ratio dose to the tumor/dose to the rest of the organism is 1.17 x 10⁴. We conclude that Pirocarbotrat can be used as a safe agent for brachytherapy of solid tumors with beta particles. Even though, Pirocarbotrat is a non-sealed beta radiation source, the radiopharmaceutical behaves very closely to a sealed beta radiation source for the treatment of solid tumors.

OS-275

Turner JH, Rose AH, Glancy RJ, Barker AP and Penhale WJ

Fremantle Hospital, Fremantle WA 6160, Australia

A LARGE ANIMAL MODEL OF HUMAN CANCER RADIOIMMUNOTHERAPY

The purpose of this project was to create an animal model of human cancers which reproduced biodistribution and pharmacokinetic parameters of radioimmunotherapeutic agents more accurately than nude mice for preclinical evaluation. Cyclosporine was administered IV in immunosuppressed sheep to allow growth of human tumour xenografts. Following orthotopic inoculation of 10⁷ cells human tumour xenografts grew as: 1. Subcutaneous SKMEL melanoma. 2. Subcutaneous intrahepatic, peritoneal and rectal LS174T colon carcinoma. 3. Ovarian and peritoneal JAM ovarian carcinoma. 4. Intravesical J82 transitional cell bladder carcinoma. Metastases from orthotopic human melanoma and colonic and ovarian carcinoma xenografts were also evident in our sheep. Histopathological examination of human tumour xenografts in the sheep demonstrated no significant host rejection and the morphological characteristics of the tumour cell types were retained. The LS174T colon adenocarcinoma xenografts produced mucin and expressed CEA and uptake of Iodine-131 A5B7 anti-CEA IgG1 monoclonal antibody was 0.03% dose injected per gram. This is comparable with uptake of I-131-A5B7 in colonic carcinoma in patients but contrasts with uptake of 20% in nude mouse LS174T xenografts. A variety of human cancers may be orthotopically xenografted in immunosuppressed sheep. Our large animal model has the potential for pre-clinical evaluation of locoregional and systemic radioimmunotherapy of human tumours under controlled experimental conditions which approach the human condition much more closely than those prevailing in a nude mouse. Furthermore quantitative SPECT imaging of sheep may be used to measure dosimetry in vivo which can be validated by serial biopsy and gamma counting and extrapolated to humans to predict efficacy and toxicity of new radioimmunotherapeutic agents in patients.

OS-276

T.M. Behr¹, E. Wulst¹, S. Radetzky¹, S. Gratz¹, M. Béhé¹, F. Raue², W. Becker¹.

Department of Nuclear Medicine¹ of the Georg-August-University of Göttingen; and Dept. of Endocrinology² of the Ruprecht-Karl-University of Heidelberg, Germany.

IMPROVED THERAPY OF MEDULLARY THYROID CANCER AS A RADIO-RESISTANT TUMOR TYPE BY COMBINING RADIOIMMUNO- WITH RADIOSENSITIZING DOXORUBICIN CHEMOTHERAPY.

Whereas clinically in advanced medullary thyroid cancer (MTC), chemotherapy has achieved only limited success, more recently, radioimmunotherapy (RIT) with ¹³¹I-labeled anti-CEA MABs has shown promising results (e.g., Juweid *et al.*, J. Nucl. Med. 37 (1996), 875-881). The aim of this study was to compare, in an animal model, the therapeutic efficacy of RIT to most frequently used "standard" chemotherapeutic schemes, as well as to evaluate, whether combination strategies of both modalities may help to improve therapeutic results in this rather radioresistant tumor type.

Nude mice, bearing subcutaneous xenografts of the human MTC cell line, TT, were treated either with the ¹³¹I-labeled anti-CEA MAB, F023C5 IgG, or were administered chemotherapeutic regimens which had shown promising clinical results (e.g., doxorubicin ["adriamycin"], cisplatinum, 5-fluorouracil, dacarbazine, streptozotocin, as well as combinations thereof). The maximum tolerated doses (MTD) of each agent and its combinations were determined. Toxicity and tumor growth were monitored.

At equitoxic doses, RIT as well as doxorubicin were superior to all other chemotherapeutic agents tested. Myelotoxicity was dose-limiting with RIT (MTD at 600 µCi), as well as with the alkylating chemotherapeutic agents. In contrast, at its MTD (200 µg), only mild myelotoxicity was caused by doxorubicin, where gastrointestinal toxicity was dose-limiting. Accordingly, bone marrow transplantation (BMT) enabled dose-intensification with RIT (up to 1100 µCi), whereas it was unable to increase the MTD of doxorubicin. Due to the complementarity of toxic side effects, but an anticipated synergism of anti-tumor efficacy, combinations of RIT and adriamycin were tested. Administration of 500 µCi ¹³¹I-anti-CEA, followed 48 h later by 200 µg doxorubicin did not result in increased lethality. Therapeutic results of this combination therapy were superior to equitoxic monotherapy with either agent; indication for synergistic anti-tumor efficacy is given. At its respective MTD, combination radioimmuno-chemotherapy led to a 36% cure rate if given without, and to a 85% permanent cure rate, if given with BMT.

This animal model seems to be useful for the preclinical testing of systemic treatment of MTC. At equitoxic doses, RIT is equally effective as doxorubicin chemotherapy. Combination of RIT and doxorubicin seems to have synergistic therapeutic efficacy, which is most likely due to radiosensitizing effects of doxorubicin. Clinical studies, which have been designed accordingly, are ongoing.

Oncology: Single photon

OS-277

T.M. Behr, E. Kruck, T. Homayounfar, S. Gratz, M. Conrad, J. Meller, I. Schreivogel, and W. Becker.

Department of Nuclear Medicine, Georg-August-University of Göttingen, Germany.

DETECTION OF RECURRENT OR METASTATIC THYROID CANCER BY A RAPID CHROMATOGRAPHIC ASSAY OF THE PATIENT'S ABILITY TO ENDOGENOUSLY SYNTHESIZE THYROID HORMONES FROM ORALLY ADMINISTERED RADIOIODINE.

The determination of thyroglobulin (Tg) levels and Na¹³¹I whole-body scanning are, together with clinical examination and other imaging modalities (ultrasonography, CT, MRI etc.) the gold standard in the follow-up of differentiated thyroid cancer (DTC) patients. Bianchi et al. (*J. Nucl. Med.* 1993; 34: 2032) first described a relatively time-consuming chromatographic procedure (≥ 24 h) to identify endogenously synthesized ¹³¹I-labeled thyroid hormones (¹³¹I-T₃/T₄) as indicator of persistent differentiated thyroid cancer. The aim of this study was to establish and evaluate a simplified, more rapid procedure in comparison to conventional follow-up methods.

A total of 92 patients with DTC (45 papillary, 39 follicular, 5 Hürthle cell, and 3 anaplastic cancers) were given 2-300 mCi Na¹³¹I for diagnosis or therapy (all had TSH levels ≥ 40 µU/ml). Whole-body scanning was performed over at least 72 h after ¹³¹I administration, and Tg was determined (normal range in athyroid patients ≤ 1.0 ng/dl). Additionally, the patients' serum was analyzed for the presence of ¹³¹I-T₃/T₄ at 48 h after ¹³¹I administration. Briefly, thyroid hormones were liberated from protein-binding by adding 8-anilino-1-naphthalene sulfonic acid. Within < 1 h, this serum was analyzed chromatographically on a PD-10 column (15 x 50 mm; Pharmacia, Uppsala, Sweden). Elution of unbound iodide was performed with PBS, ¹³¹I-T₃/T₄ were eluted with thyroxin binding globulin from normal donors' sera.

Concordantly positive results between all three diagnostic procedures (i.e., Tg, ¹³¹I scans, and chromatography) were found in 46 patients, concordantly negative in 24. From the 22 pts. with discordant results, chromatography was positive in 21. It was the only positive method in 12 pts. (2 of them of Hürthle cell histology), in 8 cases were chromatography and scans positive at normal Tg values, whereas in one case, chromatography and Tg were positive. In one patient with an anaplastic cancer, ¹³¹I scans and chromatography were (obviously false-)negative, but Tg was elevated. Ten of those 12 patients, who were only chromatographically positive, lost their ability to synthesize ¹³¹I-T₃/T₄ at 4 - 6 months after therapeutic radioiodine administration.

The assessment of ¹³¹I-T₃/T₄ synthesis seems to be a sensitive procedure in detecting recurrent DTC, including scintigraphically negative Hürthle cell cancers. This simplified and more rapid chromatographic procedure provides reliable results within less than one hour as compared to > 24 h with earlier methods.

OS-278

Y. Duman, R. Erinc, Ü. Bilkay, E. Teber, Y Erşahin.

Departments of Nuclear Medicine and Pediatric Neurosurgery, Ege University, Medical School, Izmir, Turkey.

SPECT IMAGING OF BRAIN TUMORS WITH Tl-201 AND Tc99mGSH

The purpose of this study was to evaluate the feasibility of Tc99mGSH (GSH) and was to compare with Tl-201 in detecting primary brain tumors.

Twenty-seven pediatric patients (pts) (mean age: 6.3) were included in the study. 185-740 MBq Tc99mGSH was injected to the group 1 (11 pts) 4 hr. after injection, SPECT imaging was performed using double head gamma camera (Sophy DST). Group 2 included 16 pts and was evaluated by dual isotope SPECT imaging. Two hours after the injection of 185-740 MBq Tc99mGSH, 37-74 MBq Tl-201 was given to this group. The dual isotope SPECT images were acquired after 2 hours using the same equipment. In 2 pts with meningiomas delay SPECT ++images (24 th. hr.) were obtained additionally. ROI's were drawn over the lesions and contralateral normal brain tissue on transaxial slices. Thereafter lesion (L)/ normal tissue (N) ratios were calculated.

Group 1:

Diagnosis	L/N
A. Primary brain tm. (n: 9)	3,94±1,52.
B. Postop. primary brain tm (n:1)	(-)
C. Granulation tissue (n: 1)	(-)

Group 2:

Diagnosis	L/N	
	GSH	Tl-201
A. Primary malignant brain tm (n: 11, recurrence n:3)	3,15±0,94	2,69±0,80
B. Primary benign tm (n:3)	(-)	(-)
	p< 0,05	

	4 th hr.		24 th hr.	
	GSH	Tl-201	GSH	Tl-201
Meningioma 1	2,87	2,18	1,92	1,53
Meningioma 2	3,94	2,39	1,80	1,60

In conclusion, Tc99m GSH is a promising agent with its stability in late images, cost-effectiveness, easily accessibility and has physical advantages of being labeled with Tc99m. Tc99m GSH may be an alternative to Tl-201 in imaging of brain tumors.

OS-279

P. Lind, H.J. Gallowitsch, P. Mikosch, M. Molnar, I. Gomez, E. Kresnik, O. Unterweger, H.P. Dinges

Department of Nuclear Medicine & Endocrinology, LKH Klagenfurt, AUSTRIA

Tc-99m TETROFOSMIN WHOLE BODY SCINTIGRAPHY IN THE POST-THERAPEUTIC FOLLOW UP OF PATIENTS WITH THYROID CARCINOMA

The purpose of this study was to evaluate prospectively the reliability of the new non-specific tumor searching tracer tetrofosmin in the post-therapeutic follow-up of differentiated thyroid carcinoma (DTC) during TSH suppressive thyroid hormone treatment. **Methods:** Whole-body scintigraphy (WBS) was performed in 146 patients under TSH suppressive L-T4 treatment, 20 min after intravenous injection of 370 MBq Tc-99m tetrofosmin by means of a double-headed gamma camera followed by 3-D SPECT in case of suspicious tracer uptake. The results of serum thyroglobulin (Tg), ultrasonography (US) of the neck, I-131 whole-body scintigraphy (I-131 WBS), chest X-ray, transmission computed tomography (TCT) or magnetic resonance imaging (MRI), and bone scintigraphy were also available. **Results:** A group of 88 patients without thyroid remnants who were tumor free and had no history of metastases or tumor recurrence, showed negative Tc-99m tetrofosmin WBS. Another 32 patients (papillary carcinoma pT1N0M0) were also in complete remission, but had sonographically proven remnants (echonormal). Twenty one of them (63%) exhibited Tc-99m tetrofosmin accumulation in the thyroid bed which corresponded excellently to the localization of the remnant. The third group comprises 12 cases of local recurrence confirmed by histopathology after reoperation or by cytology after fine needle aspiration where tetrofosmin scintigraphy clearly revealed relapse of malignancy in all cases. A total of 17 patients had distant metastases (11 pulmonary, 3 bone, 2 bone and pulmonary, 1 bone and soft tissue) discovered by different modalities, resulting in 44 lesions to be evaluated. Of the 23 radioiodine negative metastases, 17 were detected by tetrofosmin (74%), whereas all 21 radioiodine accumulating lesions also showed tetrofosmin positive scans. The overall sensitivity of Tc-99m tetrofosmin in detecting distant metastatic lesions was 86%. Four additional cases with radioiodine-negative disseminated lung metastases showed diffuse pulmonary tetrofosmin uptake. **Conclusion:** Tc-99m tetrofosmin is a promising tracer to detect malignant recurrence and distant metastases in the follow up of DTC without the necessity of thyroid hormone withdrawal.

OS-280

VALUE OF INDIUM-111 OCTREOTIDE IMAGING IN PATIENTS

WITH UNKNOWN PRIMARY CARCINOMA

E.S. Delpassand, M. Vaseghi, Lenzi R., D.A. Podoloff. U.T. M.D. Anderson Cancer Center, Houston, TX.

Patients presenting with cancer of unknown primary origin make up 3-15% of all malignancies seen in cancer referral centers. The initial biopsy of presenting site (PS) is not contributory in 80% of the malignant neoplasm. We evaluated fifteen patients (pts) with carcinoma of unknown primary referred to Department of Nuclear Medicine, M.D. Anderson Cancer Center from August, 1994 to January, 1997. All pts. had exhaustive evaluation by other laboratory and imaging modalities (Histology, CT, MRI, US) that were unsuccessful in localizing the primary tumor. There were 11 female and 4 males, ages ranging from 44 to 70 with average of 55. Imaging was performed following IV administration of 5.0 mCi of Indium-111 Octreotide. Wholebody and SPECT images were obtained at 4 and 24 hours. Patients presented with metastasis to the bones, lungs, liver and lymph nodes. Three patients had complete excision of PS prior to scan. Ten out of 12 PSs showed Octreotide uptake (83%). Histological type of cancer on visualized lesions were adenocarcinoma, clear cell carcinoma from follicular thyroid cancer, and neuro endocrine tumors. Pathology on non visualized PSs were metastatic adenocarcinoma of the lungs (lesions <1 cm) and unclassified malignant neoplasia in fibrous tissue. Octreoscan was able to identify or suggest primary (i.e. hilar uptake suggesting lung primary) in 7 out of 15 cases (46%). The result is comparable to the yield of autopsy in patients with unknown primary carcinoma¹⁾. Based on the uptake in PS, identification, and/or suggestion of the primary cancer, pt. management was affected in 10 of 15 pts. (67%).

CONCLUSION: Indium-111 Octreotide is helpful when other imaging modalities fail to identify primary site of malignancy. Visualization of primary cancer or uptake in presenting site can make significant impact on pts. management and probably outcome.

REFERENCE: 1. Chevalier, T.L., Cvitkovic, E., et al. Early metastatic cancer of unknown primary origin at presentation. A clinical study of 302 consecutive autopsied patients. Arch Intern Med 148:2035-2039, 1988.

OS-281

M.Gasparini, P. Gerundini, *L.S. Maffioli, *L. Devizzi, M. Castellani, *C. Tondini, V. Longari, *JD Tesoro Tess, *M Zanini, *E. Bombardieri.
Nuclear Medicine Depts. IRCCS - Ospedale Maggiore - Milan and *Istituto Nazionale dei Tumori - Milan, Italy

PROGNOSTIC IMPORTANCE OF GALLIUM SCINTIGRAPHY (Ga-67) AND MAGNETIC RESONANCE IMAGING (MRI) IN RESTAGING LYMPHOMA PATIENTS AFTER CHEMOTHERAPY; AN 8-YEAR FOLLOW-UP STUDY.
This study was intended to assess the role of restaging by Ga-67 and MRI to distinguish between patients who still have active lymphoma and those who are true complete responders. Early identification of the former might increase the success of secondary salvage therapy. In order to evaluate the ability of the two techniques to define residual disease after treatment, 49 lymphoma patients (38 Hodgkin's disease-HD and 11 non-Hodgkin lymphoma-NHL, 24 males, age range 15-72 yrs) were prospectively studied for a period of 99 months (range 8-99 months). We investigated if the positivity of the scan and/or MRI after chemotherapy could predict the clinical outcome. All patients underwent restaging 2-4 weeks after the end of 4-8 cycles of chemotherapy and were examined 48-72 hours after i.v. injection of 185-300 MBq of Ga-67. Imaging included whole body planar imaging and in many cases SPET of the involved region. The restaging workup included physical examination, laboratory assessment with complete blood count and chemistry, radiographic baseline studies including chest X-rays, MRI and all diagnostic examinations performed at staging. A comparison was made between Ga-67 and MRI. The patients were divided into two groups according to the positivity or negativity of restaging Ga-67 and MRI. In the first group 14 patients showed persistent uptake of gallium. Of these, 8 (57.1%) died (in 7 pts no complete remission-CR was observed, while in 1 case the disease recurred 8 months from partial remission; follow-up 8-82 mths) and 6 were considered to be in CR (follow up 41-84 mths). MRI was positive in 19 of the 49 pts; 9 pts died (follow-up 8-82 mths), while 10 pts were considered in CR (follow-up 32-84 mths). The two techniques showed discordant results in 5 cases (2 false-negative results for Ga-67 and 3 false-positive results for MRI). In the second group 35 pts proved negative on restaging with Ga-67. Of these, 33 pts are alive without evidence of disease and 2 died (1 pt with no CR and 1 pt relapsed 6 months after CR; follow-up 32 and 50 mths). MRI was negative in 30 cases; 29 pts are currently alive, without evidence of disease, 1 pt died 50 mths after initial diagnosis. Statistical analysis of the association between Ga-67 and MRI results and survival was performed using the log-rank test. There was a statistically significant association between Ga-67 and MRI results and survival ($P < .001$ for both techniques). The 8-year overall survival rate was 93.9% for pts with negative scans (96.6% for MRI) and 33.3% for both gallium and MRI-positive pts. Restaging gallium scan and MRI seem to be excellent indicators of residual viable tumor and accurately distinguish complete responders from induction failures. But from a financial point of view Ga-67 is to be considered the more favourable.

OS-282

S Taki, K Kakuda, K Kakuma, K Kobayashi, M Ohashi, S Ito, M Yokoyama, Y Annen, and N Tonami.
Tonami General Hospital, Tonami, Japan and Kanazawa University Hospital, Kanazawa Japan

COMPARISON BETWEEN THE Tl-201 UPTAKE IN BRAIN TUMOUR AND THE DEGREE OF CONTRAST-ENHANCEMENT ON MRI.

The aim of this study was to elucidate the relationship and difference between Tl-201 (Tl) uptake in brain tumours and the degree of contrast-enhancement on MRI. Early (15min) Tl-SPET image and Gd-DTPA enhanced T1-weighted MRI were performed on 101 untreated various histological types of brain tumours. The histological types of tumours consisted of 16 metastatic tumours, 15 glioblastomas, 3 anaplastic astrocytomas, 3 malignant lymphomas, 4 miscellaneous malignant tumours, 35 meningiomas, 7 pituitary adenomas, 6 schwannomas, 3 cavernous hemangiomas, 2 craniopharyngiomas, and 7 miscellaneous benign tumours. Tl-uptake ratio was calculated by dividing the count density of tumour by that of the normal area. The grade of contrast-enhancement of the tumour on MRI was visually scored as; 0= none (group1), 1= faint (group2), 2= moderate (group3), 3= strong (group4). The mean Tl-uptake ratio of each group were; group1= 1.00±0.0(n=5), group2= 2.35±0.75(n=13), group3= 3.29±1.05(n=27), and group4= 4.96±2.24(n=56). There were significant differences among each groups ($p < 0.01$). A weak positive correlation was noted between Tl-uptake ratios and contrast-enhancement scores on MRI ($r = 0.62$). However, lesions with low Tl-uptake ratio (lower than 1.5) were also included in the group of high contrast-enhancement on MRI. The lesions of Tl-uptake ratio < 1.5 were noted in 14% (5/56) of the group4 lesions. Histological types of these 5 lesions included 2 schwannomas, 1 epidermoid cyst, 1 cavernous hemangioma and 1 metastatic tumour. In conclusion, Tl-uptake ratio is not always concordant with the degree of contrast-enhancement on MRI. This indicates the uptake of Tl reflects tumour activity or viability more accurately than the degree of contrast-enhancement on MRI, which provides additional informations for diagnosis of brain tumours.

Infection/inflammation/hematology: Clinical studies

OS-283

F.Chierichetti, D.Rubello, P.Zanco, P.Manente^o, S.Bissoli, G.Ferlin.
Nuclear Medicine - PET Centre, ^oOncology, Hospital of Castelfranco V.to (TV), Italy.

DIAGNOSTIC ROLE OF FLUORINE-18-DEOXYGLUCOSE (FDG) POSITRON EMISSION TOMOGRAPHY (PET) IN THE STAGING AND THE FOLLOW-UP OF MALIGNANT LYMPHOMAS.

From 1994 to 1997, 159 patients (pts) with malignant lymphoma were studied by means of FDG-PET in our centre. In 39 out of them complete information about therapy and follow-up were recorded. There were 16 F, 23 M (mean age 37.6 years), 25 (64%) affected by Hodgkin's Disease and 14 (36%) by Non Hodgkin Lymphoma. In 6 cases the PET study was performed before any treatment, for staging purpose, whereas the other 33 pts were evaluated during follow-up after chemio- and/or radiotherapy. In all cases the whole body FDG-PET results were compared to CT/MRI data.

In 3/6 pretreatment studied pts, PET revealed a greater number of lymphnode metastases (LNM), and in 1 case PET modified the therapeutic approach.

Pts studied during follow-up (range 8-32 mo.) were divided in two groups according to the disease outcome. There were 17 pts with persistent/recurrent disease (PRD) and 16 pts disease free (DF). In 11/17 (64.7%) pts with PRD, PET correctly identified the neoplastic foci, while CT/MR were negative or doubtful; in 5/17 cases (29.4%) both PET and CT/MR were positive; in 1 case (5.9%) CT showed recurrent LNM while PET was negative.

Considering the group of 16 DF pts, in 9/16 cases (56.2%) PET was negative, while CT/MRI revealed persistent LN disease (false positive results); in the other 7/16 pts (43.8%) PET provided negative results as well as CT/MRI.

We can conclude that PET represents an useful imaging technique in the staging and the follow-up of pts with malignant lymphomas. In particular, it is important to point out that during follow-up FDG PET appears able to accurately distinguish pts with persistent/recurrent from disease free pts and in more than half of cases it allows a change in the therapeutic strategy (more therapy/less therapy).

OS-284

D. Sandrock, M. Backhaus, D. Bollow, D. Loreck, G.-R. Burmester, and D.L. Munz

Clinics for Nuclear Medicine and Internal Medicine, Institute of Radiology, Charité, Humboldt University Berlin, Germany

MODERN IMAGING VERSUS TWO-PHASE BONE SCINTIGRAPHY IN RHEUMATOID ARTHRITIS

Aim of this prospective study was to evaluate the clinical usefulness of two-phase bone scintigraphy compared with modern imaging techniques in patients with rheumatoid arthritis of hand and finger joints.

Overall, 30 patients with and 30 patients without pathological findings on radiographs of the hands entered the study (40 women, 20 men, aged 47.1 +/- 13.8 years). Three-phase bone scintigraphy of the hands (600 MBq Tc-99m-MDP i.v., dynamic scintigraphy 12 x 5 s, early static image for 5 min, late static image 3 h p.i. for 5 min), sonography of hand and finger joints (7.5 MHz), and magnetic resonance imaging (MRI, half open system, 0.2 T, planar and dynamic sequences after administration of contrast media) were performed. All results were evaluated blinded and independently. The intensity of tracer accumulation in joints on bone scans was semiquantitatively scored (scale, 0 to 3) and, using ROI-technique, uptake ratios (PIP V as reference) for each joint calculated. Scintigraphs were defined as "positive" if the added scores of scintigraphic phase II and III were ≥ 2 or the ROI ratio was 1.5 fold higher than the ratio of the respective joint in a normal control group.

The overall prevalence of pathological findings (1080 joints studied) in the group without radiographic signs of arthritis was for radiography 27.9 %, for scintigraphy in phase II 19 %, in phase III 58.7 %, for sonography 35 %, for MRI 47.5 %, and for clinical investigation 36.4 %. In the group with radiographic signs of arthritis the prevalence was for radiography 65.2 %, for scintigraphy in phase II 32.6 %, in phase III 37.5 %, for sonography 37.4 %, for MRI 63.7 %, and for clinical investigation 31.5 %. Sonography yielded a high accuracy for soft tissue and tendons and MRI for tendons, cartilage, and bone structures.

Conclusion: The sensitivity of two-phase bone scintigraphy is still comparable to modern imaging techniques (sonography, MRI) for the assessment of arthritic findings.

OS-285

K. D. M. Stumpe, H. Dazzi, A. Schaffner, G. K. von Schulthess

University Hospital of Zurich, Department of Medical Radiology, Nuclear Medicine

PET IMAGING OF INFLAMMATORY LESIONS

Aim of the Study: to evaluate F-18 FDG Positron Emission Tomography for the detection of infectious foci and non-infectious inflammation.

Materials and Methods: Nineteen patients, 17 with suspected bacterial or fungal infections and 2 with other inflammatory diseases were examined with PET. All patients but one had at least one additional radiological cross-sectional imaging method performed within three days of the PET scan. Two patients had negative biopsies at sites suggestive of infection by other imaging modalities. The two non-infectious patients had an arteritis. All patients were examined using whole or partial body FDG-PET scans including transmission correction when the focus was in the trunk. The PET scans were obtained with a GE Advance PET camera with an axial FOV of 14.6 cm and a minimum of 5 cradle positions. Acquisition for each position was 4' to 5' for the emission and if applicable also for the transmission scan. Axial images were reconstructed and coronally and sagittally reformatted images were visually inspected.

Results: Of the 17 patients with presumed infections, 12 were proven to have an infection by imaging other than PET or proof by culture. PET scanning identified foci in all of the 13 patients with infections, correctly excluded the two who were positive on other imaging but negative on culture, and showed relatively weak accumulation in the patients with arteritis. In one patient who had two PET scans, the first identified an osteitis, which was prospectively overlooked on MR and after antibiotic therapy, the second PET scan showed normalization of FDG uptake in the focus while the second MR was still positive. In the other four patients, no focus could be identified on other imaging nor did the patients grow positive cultures despite elevated inflammation markers.

Conclusions: PET appears to be a highly sensitive method to detect acute infection foci. It also seems accurate in identifying non-infectious pathology as such, as was the case in one patient with presumed osteitis, one with presumed spondylodiscitis and one with presumed soft tissue abscesses. Thus it can distinguish involved from uninvolved sites. On two patients we also have preliminary data, that PET shows treatment response early compared to other imaging methods. While the use of PET in patients with infectious foci is very promising, the logistics of providing PET essentially on an emergency basis is still formidable.

OS-287

M.Liberatore*, D.Prosperi*, F.Ponzo*, A.P.Turilli*, C.Santini°, P.Baiocchi°, M.Galiè°, GD.Di Nucci^, A.Centi Colella*.

*Dip.di Med.Sperim., °Dip.di Med.Clinica, ^Ist.di Cardiochir., Univ.di Roma La Sapienza

STERNAL WOUND INFECTION (SWI) AFTER MEDIAN STERNOTOMY: THE ROLE OF ^{99m}Tc-HMPAO LABELLED LEUKOCYTE SCAN (WBCs) IN CLINICAL DECISION MAKING. SWI is a rare complication (1-3%) of median sternotomy in cardiac surgery. From the clinical point of view, the difference between superficial and deep SWI is considerable, even if distinguishing between the two forms is often difficult. The present work aims to evaluate the role of WBCs in clinical decision making. Twenty-seven consecutive patients with suspected SWI were categorised and treated as affected by superficial or deep SWI on the basis of clinical signs and microbiological findings. These patients were submitted to WBCs at the onset of the infection and then 2-3 months later. 10 patients without suspected SWI were also studied as control group. For the assessment of superficial or deep SWI, the gold standard was histological findings, when surgical exploration was undertaken, and a long-term follow-up in the other cases. The scintigraphic images (30 min., 4 and 20 hours) were reviewed by two nuclear physicians who were unaware of the patients' clinical conditions. WBCs was negative in the control group. All the deep SWI (n=11) were correctly detected by WBCs (100% sensitivity). In 7 of 16 superficial SWI, WBCs failed to assess the infection (56% sensitivity). Out of the 9 superficial SWI correctly detected by WBCs, 5 had been clinically judged as deep SWI. The results indicate that WBCs may have a role in the correct management of SWI in so far deep SWI is concerned. In patients affected by superficial SWI the observed sensitivity of WBCs was low, even if this result does not reduce the usefulness of the procedure from the clinical point of view.

OS-286

V. Ivančević, A. Wolter, S. Sen Gupta, D.L. Munz

Clinics for Nuclear Medicine and Bone and Joint Surgery, Charité, Humboldt University, Berlin, Germany

IMAGING INFLAMMATION WITH Tc-99m LABELLED MONOCLONAL ANTI-NCA 90 Fab' FRAGMENT AND NONSPECIFIC BOWEL ACTIVITY

The Tc-99m labelled monoclonal anti-NCA 90 granulocyte antibody Fab' fragment (AGFab) might be of interest for imaging abdominal inflammation. Since imaging inflammation in the abdomen could be hampered by nonspecific bowel activity, we prospectively investigated the appearance of bowel activity in AGFab imaging. Sixty-six scans in 58 consecutive patients (age range, 12-85 years; median age, 56 years) referred for suspected nonabdominal, mostly musculoskeletal infection were included. Abdominal inflammation was excluded clinically and there were no signs of inflammatory bowel disease in the patients' histories. One hour (n=66), 5 h (n=65) and 24 h (n=41) after intravenous injection of up to 1.1 GBq of AGFab and prior radiochemical purity testing, 10 to 20-min planar images of the abdomen were performed using a dual-head gamma camera and 256 word acquisition matrix. Bowel activity was graded visually as 0 (none), 1 (< bone marrow), 2 (= bone marrow), 3 (> bone marrow) or 4 (= liver or higher). For practical reasons the gut was divided into 6 segments (small intestine, ileocaecal region, ascending, transverse, descending colon and rectosigmoid). The 1 h, 5 h and 24 h images revealed 43, 140 and 129 accumulating bowel segments, respectively, in 34 (52%), 60 (92%) and 41 (100%) patients. The mean intensity score per segment amounted to 1.3, 2.3 and 3.2, respectively. The frequency of appearance of the individual segments is summarized in the following table:

Segment	n 1h	% 1h	n 5h	% 5h	n 24h	% 24h
Small intestine	28	42	38	58	8	20
Ileocaecal region	5	8	34	52	18	44
Ascending colon	5	8	46	71	35	85
Transverse colon	1	2	8	13	25	61
Descending colon	5	8	12	19	28	68
Rectosigmoid	0	0	3	5	15	37

In conclusion, significant bowel activity is often present in the early and almost always and more intense in the delayed images. The pattern of activity appearance in bowel segments with a shift towards the aboral segments with time indicates nonspecific activity in the bowel lumen being transported along with physiological bowel contents. Thus, nonspecific bowel activity can be anticipated to be a pitfall in imaging abdominal inflammation, especially inflammatory bowel disease, with AGFab.

OS-288

Lantto T., Soini I., Waahtera M. and Ylikangas P.

Clinical Physiology of Tampere University Hospital, Tampere, Radiology and Rheumatology of Rheumatism Foundation Hospital, Heinola and Nuclear Medicine of Päijät-Häme Central Hospital, Lahti, Finland
JOINT ACTIVITY IN ARTHRITIS EVALUATED WITH ^{99m}Tc-HIG, PHYSICAL EXAMINATION AND MAGNETIC RESONANCE IMAGING

The purpose of this study was to assess the efficacy of ^{99m}Tc-HIG scintigraphy (HIG) to detect joint inflammation by comparing it with physical examination and magnetic resonance imaging (MRI).

Altogether 208 peripheral joints of 4 patients with rheumatoid disease in different phases were clinically evaluated. In clinical evaluation joint swelling and/or pain were considered as signs of active inflammation. Within 2 days patients were imaged 30 min and 4 h after injection of 370 MBq HIG. Whole body and local images were obtained. Joint activity was scored from 0 (normal) to 3 (high) comparing it with the background vascular activity. MRI was performed during the same day. The results were interpreted independently.

Clinically 134/208 joints were normal, 67 swollen and 7 only painful. HIG uptake was normal in 123 and increased in 85 joints. 91 % of swollen joints were HIG positive; activity score was moderate or high in 80 % of these joints. One of the 7 only painful joints was HIG positive. Physical examination and HIG gave different result in 33 joints; swelling without HIG uptake was in 9 joints and HIG uptake without swelling in 24 joints. 59 % of 4 h images were positive 30 min p.i.

Five joint regions were imaged with MRI; 2 wrists, an ankle, a foot and a knee. MRI showed acute synovitis in all joint areas. MRI findings were in concordance with HIG findings.

As a conclusion HIG offers a sensitive imaging method for the evaluation of synovial inflammatory activity. It is readily available, detects reliably and objectively the inflamed joints. MRI is a sensitive method to localize acute synovitis but the reduced throughput limits the number of imaged joints. The results of HIG are in good agreement with the findings of MRI. HIG offers possibility for whole body screening of inflammatory activity.

Neurology/Psychiatry: Alzheimer's disease

OS-289

N.C. Friedman, D. Bova, W.E. Barnes, T.J. Milo, P.H. Shirazi

Hines V.A. Hospital, Nuclear Medicine Service, Hines, IL, USA

EVALUATION OF STATISTICAL PARAMETRIC MAPPING IN THE CHARACTERIZATION OF CEREBRAL PERFUSION ABNORMALITIES ASSOCIATED WITH ALZHEIMER'S DISEASE

PURPOSE: To analyze the changes in cerebral perfusion that occur with Alzheimer's Disease (AD) using Statistical Parametric Mapping (SPM96) as an objective analysis tool. In addition, SPM96 was evaluated as a tool to assist in identifying individuals with AD.

METHODS: Three groups were selected for the analysis: 13 patients (pts) with clinical and SPECT features of AD (age 74 ± 6.3); 14 aged matched pts with cortical atrophy (CT or MRI) and without an AD SPECT pattern (age 72 ± 9.8);

15 young, normal subjects with normal SPECT images (age 34 ± 9.9). Studies were acquired on a triple head gamma camera after administration of ^{99m}Tc HMPAO under standard conditions. Images were aligned, normalized, smoothed, and the three groups compared with SPM96.

RESULTS: Comparison of the AD to the normal group demonstrated extensive regions of statistically deviant clusters, without the characteristic abnormalities associated with the disease. This finding results from concurrent cortical atrophy that was present in the AD group. Comparison of the AD group to an age matched group with cortical atrophy demonstrated a pattern typical of AD. Bilateral temporo-parietal and posterior frontal hypoperfusion were identified ($p < 0.05$, $Z = 3.3$). Preservation of perfusion was noted in the post central gyrus bilaterally and in the cerebellum. In comparing individual AD pts to the atrophy group, most showed features of an AD pattern at $p < 0.1$ that, however, were confounded by the level of atrophy.

CONCLUSION: SPM successfully characterized the typical findings in AD patients when compared with an age-matched control group with cortical atrophy. However, the level of atrophy confounded the evaluation of individual patients. Enhancement of SPM is necessary to allow comparison of abnormalities identified in individuals to those of a disease group.

OS-291

O. Migneco¹, I. Digay¹, Ph. Robert², Ph. Desvignes¹, P.M. Koulibaly¹, F. Bussièrè¹, J. Darcourt¹,
Dpts of Nuclear Medicine¹ & Psychiatry², Centre A. Lacassagne and Hôpital Pasteur, Nice University, France.

BEHAVIORAL DISTURBANCES ARE RELATED TO FRONTAL LOBE INVOLVEMENT IN ALZHEIMER'S DISEASE.

Behavioral disturbances (BD) in Alzheimer's disease (AD) have been neglected for a long time compared to cognitive disorders. They are in fact very frequent (prevalance > 90%) and often lead to the patient confinement. To establish the relationships between BD and rCBF measure by SPECT in AD, we studied 20 patients (mean age: 77.4) fulfilling the NINCDS-ADRDA criteria for probable AD. The patients were clinically evaluated using the Mini Mental State Examination (MMSE, mean score: 20.6) and the Neuro-Psychiatric Inventory (NPI, Cummings 1994). This scale quantifies independently 12 behavioral domains. For each patient, 1100 MBq of ^{99m}Tc -ECD were injected via an IV line. One hour later, 120 projections of 55 sec each were gathered using a three headed gamma camera (Prism 3000 XP, Picker, Cleveland, Ohio) equipped with LEUHR fan beam collimators leading to a resolution of 8 mm on the reconstructed images. Referring to the literature, behavior is related to frontal lobe, therefore, to analyse the data, 5 regions of interest were manually drawn: anterior cingulate, orbitofrontal, medial and lateral dorsolateral prefrontal and temporal. Temporal uptake significantly correlates with the MMSE ($r = 0.49$ for the left, $p < 0.05$) and the NPI total score ($r = -0.55$ for the right, $p < 0.01$; $r = -0.49$ for the left, $p < 0.05$). Concerning the frontal lobes, there were significant correlations between the anterior cingulate uptake and the apathy score ($r = -0.53$ for the right, $p < 0.05$; $r = -0.48$ for the left, $p < 0.05$) and between the dorsolateral prefrontal regions uptake and the NPI total score ($r = -0.50$ for the left, $p < 0.05$) and the depression/apathy score ($r = -0.45$ for the right, $p < 0.05$). There was no significant correlation between frontal uptake and MMSE. These results suggest that BD in AD are related to specific frontal areas involvement rather than to the global cognitive decline.

OS-290

G. Rodriguez, F. Nobili, F. Copello, P. Vitali, M.V. Gianelli, G.Z. Taddei, E. Catsafados, and G. Mariani.
Nuclear Medicine Service, DIMI, Neurophysiology and Neuropathophysiology Units, DISM, and Institute of Occupational Medicine, University of Genoa Medical School; Genoa (Italy).

EVALUATION OF ALZHEIMER'S DISEASE BY COMPARATIVE ^{99m}Tc -HMPAO BRAIN-DEDICATED SPECT AND QUANTITATIVE ELECTROENCEPHALOGRAPHY

The pattern of regional cerebral blood flow (rCBF) changes observed by brain SPECT with ^{99m}Tc -HMPAO provides useful diagnostic information and pathophysiologic clues towards better understanding various degenerative neurological diseases. We report here the results of a study correlating the pattern of rCBF with quantitative electroencephalography (qEEG) in patients with Alzheimer's disease (AD).

Forty-three AD patients (mean age 72.4 ± 7.5 years) underwent rCBF evaluation with ^{99m}Tc -HMPAO employing a brain-dedicated gamma-camera (CERASPECT, Digital Scintigraphics, Waltham, MA). For each patient, rCBF values relative to the cerebellum were assessed for 16 ROIs (12 superficial cortical ROIs, 2 hippocampal and 2 thalamic ROIs), while qEEG analysis provided 7 relative power bands for each of 16 channels. Patients were also scored by Mini Mental Status Examination (MMSE). A complex, multi-step statistical analysis was applied to all these variables, based on preliminary sequential factorial analysis, then on multiple analysis of variance.

Full statistical analysis identified the following correlations: 1) the 2-5.5 Hz and 8-11.5 Hz qEEG powers were correlated with rCBF impairment in the parietal ROIs ($p = 0.0009$); 2) the 2-5.5 Hz power was correlated with rCBF impairment in the right hippocampal ROI ($p = 0.007$); 3) the MMSE score was correlated with rCBF impairment in the right ($p = 0.006$) and left ($p = 0.004$) hippocampal ROIs, and in the parietal ROIs ($p = 0.01$); 4) the MMSE score was correlated with both the 2-5.5 Hz ($p = 0.0005$) and the 8-11.5 Hz ($p = 0.004$) power bands on qEEG.

The present results show that both the relative rCBF values (especially hippocampal impairment, besides bilateral parietal impairment as already expected) and qEEG (especially the slow 2-5.5 Hz frequencies) are reliable indicators of AD severity. Perfusion pattern of hippocampal ROIs provides crucial information as to understanding AD pathophysiology.

OS-292

P. Charpentier¹, Lavenu I², A Duhamel³, Pasquier F², L Defebvre², Steining M¹

¹Unité d'Imagerie Fonctionnelle Cérébrale, ²Clinique Neurologique, ³CERIM, Centre Hospitalo Universitaire, Lille, France

^{99m}Tc -HMPAO SPECT IN DIFFERENTIAL DIAGNOSIS BETWEEN FRONTO-TEMPORAL AND ALZHEIMER'S DISEASE

Background: Alzheimer's disease (AD) and fronto-temporal dementia (FTD) are the most frequent neurodegenerative cognitive disorders. However, if FTD is representing about 9% of all dementia, it remains poorly recognised clinically. Several previous study have demonstrated the interest of SPECT in the positive diagnosis of AD and FTD, but there's actually very few comparative prospective study on this subject. **Aim of the study:** The aim of this study was to determine a simple algorithm, deduced from statistical analysis, which, if applied to regions of interest (ROIs), could improve the predictive value of SPECT in this indication, in order to support and comfort the visual analysis. **Patients and methods:** 40 patients were included: 20 with probable AD according to NINCDS-ADRDA criteria and 20 with probable FTD, according to Lund and Manchester criteria. All patients underwent brain SPECT imaging after intravenous injection of 555 MBq of ^{99m}Tc -HMPAO. 20 ROIs were determined on Fleschig's slice for each patient and normalized to the mean cerebellar activity. Mean value was calculated for each variable (20 ROI + Mini-Mental-State). A Wilcoxon test was applied to these 21 data, in order to determine where the difference was significative. Then, the two groups were separated by a discriminating analysis. At least, 21 variables were studied by a stepwise discriminative analysis in order to determine a sub-group of variable with the highest predictive value for DTF versus DTA. **Results and discussion:** Decreasing fixations in frontal areas were correlated with DTF and decreased fixations in parietal posterior areas were correlated with DTA. Among the 21 variables, 5 were selected. The 20 DTF patients were correctly classified by this algorithm (Predictive Positive Value: 100%) while 18/20 patients with probable AD were classified in the correct group. (PPV for DTA versus DTF: 81%). **Conclusion:** We conclude that this semi-automatic classification could be a precious tool to comfort clinical differential diagnosis between DTF and AD, if this result will be confirmed by other studies.

OS-293

ML Calcagni, A Giordano, A Cappa*, G Villa*, G Gainotti*, G De Rossi, G Galli. Dpts of Nuclear Medicine and Neurology*, Università Cattolica del Sacro Cuore, Largo A. Gemelli, 8 - 00168 Rome- Italy.

BRAIN PERFUSION IN «FOCAL TEMPORAL LOBE DYSFUNCTION»: A COMPARISON WITH CONTROL SUBJECTS AND WITH PATIENTS WITH ALZHEIMER DISEASE.

Patients with early Alzheimer Disease (AD) showing neuropsychological deficits in memory and language, have recently been classified as affected by «Focal Temporal Lobe Dysfunction» (FTLD) (Butters MA et al. Neurology 1996;46:687-92). The aim of our study was to compare the cerebral perfusion of pts with AD and with FTLD. We studied 32 subjects: 12 control subjects matched for age and sex (C group), 14 AD pts with a diffuse and homogeneous cognitive impairment (AD group) and 6 early AD pts with prevalent memory and language deficits, classified as FTLD according to Butters et al. (FTLD group). All pts underwent a complete neuropsychological assessment (including MMSE, Mental Deterioration Battery and a set of 15 neuropsychological tests in order to evaluate different cognitive abilities) and SPET imaging with ^{99m}Tc-HM-PAO using a four heads brain dedicated tomograph. Tracer uptake was quantified in 29 regions of interest, including temporal-mesial areas (hippocampal and para-hippocampal cortex) according to a previously validated procedure. Statistical analysis was performed by the Kruskal-Wallis test with Bonferroni's correction when appropriate. Results: FTLD group showed significant left temporal-mesial and temporal-lateral defects as compared to C group (p=0.003 and 0.006, respectively); the «typical» pattern of bilateral posterior-temporal-parietal defects was never observed in this group. AD group showed severe hypoperfusion in several cortical regions, constantly including the left posterior-temporal-parietal region (p<0.002 vs. C group); moreover, a significant correlation was found between the number of cortical regions involved and the number of «abnormal» neuropsychological tests (r=0.78, p<0.01).

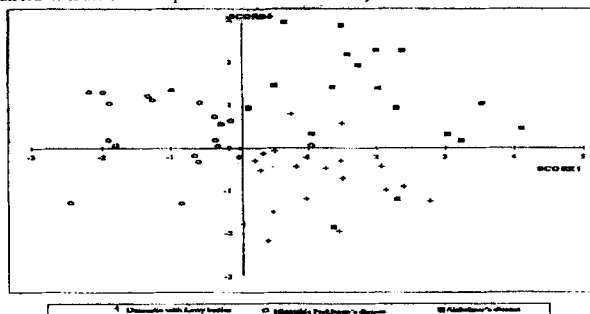
Conclusions: FTLD group showed a constant left temporal perfusion defect; this finding, not yet reported in the literature, confirms that FTLD may represent a distinct biological subgroup of AD. Brain perfusion SPET may help to identify these pts that have a slower rate of cognitive decline.

OS-294

L. Defebvre; V. Leduc; A. Duhamel; P. Lecouffe; F. Pasquier; Ch. Lamy-Lhullier; Destée; M. Steinling. University Hospital of Lille (France) ; Departments of Neurology A , Medical Informatics , Nuclear Medicine and Memory Center.

TECHNETIUM HMPAO SPECT STUDY IN DEMENTIA WITH LEWY BODIES, ALZHEIMER'S DISEASE AND IDIOPATHIC PARKINSON'S DISEASE.

The aim of the present study was to compare the regional cerebral blood flow measurements studied by SPECT with ^{99m}-Technetium HMPAO in Dementia with Lewy Bodies (DLB) and Alzheimer's disease (AD), to determine the contribution of SPECT to the differential diagnosis between these two diseases. Twenty patients with probable DLB, 20 patients with probable AD and 20 patients with idiopathic Parkinson's disease (IPD) were studied. Compared with IPD there was in the DLB group a global decrease of HMPAO uptake in cortical regions of interest excepted in the posterior frontal and occipital regions; in the AD group there was a limited left temporal and parietal hypoperfusion. In the DLB group frontal HMPAO uptake was significantly lower than in AD group. A factorial discriminant analysis allows to establish from cortical indexes and minimal state two predictive scores, which classified correctly 53/60 patients (83%) (DLB: 18/20, AD: 16/20, IPD: 19/20). These findings indicate the presence of diffuse cortical abnormalities in DLB and suggest that SPECT may be useful in discriminating in vivo DLB from AD. We estimate that SPECT study increase the possibility to separate DLB and AD, because both disorders share different patterns of CBF abnormality.



Physics and instrumentation: SPET

OS-295

J. Ryan, B. Penney, H. Al-Hallaq, R. Keast, I. Weissman

University of Chicago Medical Center, Chicago, IL, USA, Section of Nuclear Medicine, Department of Radiology

RAPID ACQUISITION SEQUENCE (RAS) IMAGING WITH DUAL OR TRIPLE HEAD GAMMA CAMERAS REDUCES BLADDER FILLING ARTEFACTS.

Bladder filling artefacts appear in tomographic imaging of the pelvis when significant bladder filling occurs during prolonged acquisition intervals customary with single head gamma cameras. The artefacts result from changing activity distribution during that interval as both bladder volume and bladder activity increase with time; however, typical SPECT reconstruction methods assume that the activity distribution remains constant during the imaging time and violating this assumption leads to artefacts. To address this problem we investigated the use of multihead gamma cameras operating in a rapid acquisition sequence (RAS) mode for SPECT imaging. The activity distribution changes less during each short acquisition period, and a summed composite image of all the images acquired serially can be formulated for analysis. We constructed a bladder phantom and compared images obtained using a standard extended acquisition technique of 30 minutes with those using a RAS technique of 10 three minute acquisitions. A balloon was chosen to model the bladder. It was suspended in a 22cm diameter tub phantom, and the specific activity in the "bladder" was set to 10 times that of the solution around it. During each acquisition the "bladder" was filled from a starting volume of 60mL to a final volume of 100mL over 30 minutes using an infusion pump. The phantom was not completely filled because the opening for the infusion tube was not sealed. The rapid acquisition sequences were added together prior to analysis. In the reconstructed composite RAS images there was considerably less artefact than in those based on the slow acquisition. The technique was applied to clinical studies, and improved ability to interpret the pelvic region was achieved despite significant bladder activity in the images. Another advantage of RAS imaging is the capability of examining each individual sequence for patient motion and omitting those with motion from the summed image. RAS imaging can also eliminate the need for decay correction of long acquisition SPECT studies. Thus, RAS imaging with a multihead gamma camera is recommended for tomographic imaging of the pelvis when significant bladder activity is present.

OS-296

L. Barnden and C. Rowe

Nuclear Medicine, The Queen Elizabeth Hospital, Adelaide, Australia

NON-UNIFORM ATTENUATION CORRECTION OF A MYOCARDIAL INFERIOR WALL ARTIFACT IS MORE ACCURATE WITH SCATTER SUBTRACTION AND RESOLUTION RECOVERY.

Attenuation correction (AC) using attenuation coefficient (mu) maps from transmission scanning improves myocardial SPECT, but inaccuracies remain. This work evaluates AC for Tc-99m when lower (112-125 keV) window scatter subtraction and distance dependent resolution recovery (RR) are also implemented. A realistic chest-heart-liver-lung phantom was configured to yield a -15% inferior wall artifact without AC. Scatter subtraction was applied either to the projections (SSp) or to the tomograms (SSt). Reconstruction of scatter for SSt included attenuation correction. Mu maps from a Tc-99m transmission scan after the emission activity had decayed were segmented into soft-tissue or lung with mu in the ratio 3:1. RR was achieved by incorporating the distance dependent spatial resolution within the iterative reconstruction (OSEM). Bullseye plots were generated and averages in the 3 coronary artery areas (as % of maximum) were used to compute two accuracy indices: inferior deviation (inf) = RCA - (mean of LAD and Cx), and right to left asymmetry = LAD-Cx. The truth was zero for both. Results in % are shown for soft-tissue mu = 0.15/cm and for the soft-tissue mu which rendered inf = 0. With no AC, inf = -15%, LAD-Cx = 8%.

	mu	inf	LAD-Cx	mu	inf	LAD-Cx
AC	.15	+7	11	.08	0	14
AC + RR	.15	+5	1	.10	0	5
AC + SSp	.15	+2	1			
AC + RR + SSp	.15	+2	2.5			
AC + RR + SSt	.15	-.3	4			

For mu = 0.15, AC alone over-corrected the -15% inferior wall artifact to +7% and yielded an 11% LAD-Cx asymmetry. Processing with either RR or SSp reduced both the artifact (inf) over-correction and LAD-Cx, although SSp was more accurate at the artifact. Scatter subtraction and RR together yielded optimal accuracy when SSt was used instead of SSp. Adjusting mu, instead of subtracting scatter, to remove the residual inferior wall artifact (inf=0) worsened the LAD-Cx asymmetry. Scatter subtraction and/or RR markedly improve the accuracy of myocardial emission-transmission tomography.

OS-297

D. McCool, R. V. Barlow, J.R. Buscombe, J. E. Agnew
Royal Free Hospital and School of Medicine; Department of
Nuclear Medicine. London; UK

EVALUATION OF SPECT FOR SCINTIMAMMOGRAPHY USING A NOVEL BREAST PHANTOM

Scintimammography is a valuable tool in evaluation of breast cancer. Low differential uptake of MIBI in tumour can make detection difficult. Scatter from heart and liver activity can significantly degrade the breast image. Phantom studies allow us to investigate optimum scanning technique. Using a collection of sources and items easily available we have put together a practical breast phantom. The breast itself is simulated with a saline bag providing a good match for typical breast size and attenuation; diluted activity in the bag represents normal breast tissue activity. A modelling balloon is inserted into the bag; this allows us to produce variable tumour size and uptakes with a good degree of control. Standard phantoms (thyroid, liver slice and rectangular 'flood' respectively) were used to simulate heart, liver and background chest wall activity. Lesion volumes ranging from 4ml to 22.5ml were obtained with diameters from 17mm to 38mm. Measurement with the phantom gave higher lesion to background ratios for SPECT with a 30% (range 13% to 43%) median improvement relative to planar imaging. All eleven studies with lesion to background ratio below 4 on planar images (patient study mean 4.1) improved with SPECT. Additionally we assessed the value of a standard 'triple-energy-window' method relative to the single energy 15% window used clinically. Planar and prone-SPECT images were acquired using the same protocols as for clinical imaging. Triple-energy-window (TEW) imaging utilised a central 20% window and two adjacent 2keV windows. Four lesion sizes and 5 lesion-to-background ratios were set up in the phantom - giving a total of 20 image-sets (planar and SPECT) acquired with 15% and TEW windows. TEW improved lesion to background ratios for planar but not SPECT imaging.

Technique	Median Improvement (TEW compared to 15%)	Range
Anterior Planar	8%	1-23 %
L Lateral Planar	9%	2 - 29 %
SPECT	-2	-12 -54 %

Thus TEW proved consistently helpful *only* in planar imaging. In conclusion our results provide quantitative evidence of contrast enhancement with SPECT and underline its scope for clinical application.

OS-298

A.M. Marques da Silva*, C.C. Robilotta**

*Departamento de Física, CCNE, Universidade Federal de Santa Maria, RS, Brasil

**Instituto de Física, Universidade de São Paulo, SP, Brasil

USE OF CONSISTENCY CONDITIONS TO ESTIMATE THE ATTENUATION MAP IN CARDIAC SPECT STUDIES, WITHOUT USING TRANSMISSION DATA

Most methods for estimating the attenuation map in SPECT studies use a transmission scan, performed simultaneously with the emission scan. An alternative approach, with lower cost, avoids the transmission imaging and estimates the attenuation map directly from emission data. It uses the consistency conditions of the attenuated Radon transform to estimate the attenuation coefficients distribution. The method is based on the fact that attenuated Radon transform obeys a set of consistency conditions which describes different relationships between the emission sinograms and the unknown transmission values (Welch, 1997).

The goal of this work is to use the consistency conditions for obtaining the attenuation map in cardiac SPECT studies, only from the measured emission projections. Since the method requires some prior information about the attenuation map, we adopted two constraint conditions: (i) restricting the transmission sinograms by assuming that the shape of the attenuation distribution is the boundary of the body, while the attenuation coefficients are kept as free parameters, and (ii) using a constant value for the attenuation coefficient, while allowing the shape of the attenuation distribution to be adjusted consistently.

To solve the set of consistency equations, a non-linear minimization algorithm (Levenberg-Marquardt method) is used.

The method is tested with Monte Carlo simulated projection data of a line source, a triple cylinder phantom and the inhomogeneous Mathematical Cardiac Torso - MCAT (University of North Carolina). All these simulations include the scattered radiation influence. The results with uniform attenuators recovers the true attenuation distribution boundaries. Comparisons between estimated non-uniform attenuation distributions and true attenuation maps are discussed.

OS-299

T. Mito, N. Sugo, T. Kano, I. Shibata, M. Takano, H. Takahashi, J. Sugita

Hospital: Toho University School of Medicine, 1st Department of Neurosurgery

CEREBRAL HEMODYNAMICS IN HYDROCEPHALUS EVALUATED BY THREE DIMENSIONAL IMAGES OF 123I-IMP SPECT AND MRI

[Background]

We employed three-dimensional (3-D) renderings and voxel analysis to examine the cerebral blood flow (CBF) of the entire brain accompanying pressure changes regulated by a Medos programmable valve in hydrocephalus patients. But this valve is needed several pressure change and is occasionally out of order post MRI examination. Recently we are using a Orbis-Sigma valve which is a continuously variable-resistance valve to automatically control CSF drainage. Therefore it does not have those demerits.

[Subjects and Methods]

Subjects were Hydrocephalus patients using a Orbis-Sigma valve. Before and after the operation, SPECT and MRI were performed. The SPECT data collected was analyzed by an Application Visualization System Medical Viewer(AVS) which plotted the number of voxels per 5% threshold change, taking the voxel with the highest RI count as 100%. SPECT/MRI fusion image was constructed by using workstation(TITAN) and software(AVS).

[Results]

The voxel distribution curve (number of voxels per 5% threshold change) of a normal subject was a bimodal curve with a trough at around the 40% threshold and a peak at around the 70% threshold. As the data processed by the surface rendering method could only discriminate two values, the shape of the image varied according to the threshold setting. Although setting different threshold values resulted in variations in size and shape of the 3-D images, the image obtained at the 50% threshold best matched the volume measured by CT. Therefore, the images at the 50% threshold were examined in the present study. In semi-transparent images of hydrocephalus cases, the area internal to the 50% threshold (i.e. area at below the 50% threshold) expanded, and in axial and coronal sections the CBF distribution at the 50% threshold and above were presented in different colours. 3-D images, including semi-transparent images at the 50% threshold and tomographic images of the CBF, were generated. The semi-transparent image revealed reduction of the hypoperfusion region at below the 50% threshold accompanying symptom improvement. In the voxel distribution curve, the increased voxel in the 40% threshold trough region decreased gradually and a trough shape approaching that of normal subjects was formed gradually, agreeing well with the changes in clinical symptom. In the voxel distribution curves of all the hydrocephalus cases, an increase in voxel in the 40% threshold region and a decrease in the 70% threshold region were observed. Improvement in clinical symptoms after the operation was accompanied by a tendency of the voxel distribution curve to return to a pattern close to that of normal subjects. 3-D SPECT/MRI fusion images revealed reduction of the periventricular hypoperfusion region at below the 50% threshold accompanying symptom improvement.

[Conclusions]

The 3-D SPECT image and voxel distribution curve findings correlated with symptomatic changes. And 3-D SPECT/MRI fusion images were useful to evaluate the periventricular cerebral hemodynamics. These techniques indicate clearly the cerebral hemodynamics in hydrocephalus patients.

OS-300

R. Jaszczak, C. Scarfone, L. Marks, M. Munley, K. Greer, D. Gilland

Duke University Medical Center, Departments of Radiology and Radiation Oncology, Durham, North Carolina USA.

INVESTIGATION OF SPECT QUANTIFICATION OF LUNG PERFUSION IMAGING: A PHANTOM STUDY. The purpose of this research was to evaluate quantitative filtered backprojection (QFBP) and maximum likelihood (QML) reconstruction techniques for measuring absolute and relative concentrations in the lungs. The envisioned application is pulmonary dose-response analysis for improved radiation treatment planning (RTP). SPECT scans of an anthropomorphic thorax phantom containing 99mTc activity dispersed in simulated lung tissue (Styrofoam beads/water mixture) were acquired. Hollow plastic spheres (1.4 to 5.6 cm dia.) containing air, water, and simulated lung tissue (sphere:lung concentration (S/L) ratios of 0:1 to 0.7:1) were placed in the lungs. Nonuniform attenuation compensation was performed using single iteration Chang (QFBP) and intrinsic modeling (QML). To obtain attenuation maps, gamma ray transmission computed tomography (TCT) scans were performed using a fan beam TCT geometry. Scatter compensation was performed using a dual energy window subtraction method (for QFBP) and an additive scatter modeling method (for QML). Absolute concentrations and concentration ratios were extracted from region-of-interest data using: 1) a calibration scan of a point source in air, and 2) a self-calibration method appropriate for lung perfusion imaging that is based on the known total activity in the lungs. Although both QFBP and QML resulted in similar quantitative accuracy, the QML method eliminated streak artifacts that were observed using FBP. Quantitative accuracy was influenced by the choice of the scatter subtraction parameter, and, for ML-EM, the iteration stopping number. Mean lung concentrations determined using quantitative SPECT resulted in errors of ~3%. For the 5.6 cm dia. water, air and simulated lung spheres, the SPECT measured S/L ratios had errors on the order of 5% to 10%. For the smaller spheres, the biases were affected by finite system resolution, partial volume effects, and the choice of post-reconstruction filters. Generally, the biases ranged between 25 to 50% for the smaller spheres. These results demonstrate the potential usefulness of SPECT lung quantification for improving RTP.

General nuclear medicine: Bone

OS-301

Z. Jurasinovic, Z. Pavlinovic, D. Dodig, M. Medvedec, D. Huic

University Hospital Zagreb, Clinical Department of Nuclear Medicine and Radiation Protection

BONE MINERAL DENSITY IN PATIENTS TAKING SUPPRESSION THERAPY WITH LEVOTHYROXINE

Conflicting data exist concerning influence of suppression therapy with levothyroxine on bone mineral density, some of them suggesting that osteoporosis occurs after prolonged use. We conducted a study of bone mineral density in 228 female patients (median age 47 years, range 20-77) with history of thyroid carcinoma and total surgical thyroidectomy and radioiodine ablation, performing bone densitometry in two skeletal sites: lumbar spine and femoral neck. Twenty-three patients were examined immediately after total surgical thyroidectomy, prior to radioiodine ablation and the onset of suppression therapy with levothyroxine, forming the control group. Other four groups are shown in the following table.

group	number of patients	median age	duration of suppression therapy (years)	mean Z-score in lumbar spine	mean Z-score in femoral neck
1	23	45,0	0	0.329	0.347
2	44	44,5	<1	0.219	0.372
3	66	46,0	1-3	0.168	0.165
4	51	47,0	3-5	0.306	0.485
5	44	49,5	>5	0.170	0.336

Average levothyroxine dose was 160 µg a day and TSH levels in all patients were suppressed, except in 23 patients from control group who had elevated TSH following thyroidectomy. Comparing mean Z-scores (age-matched) of control group with those of other four groups, as well as groups between themselves, no statistically significant differences were found, so we concluded that long-lasting suppression therapy with levothyroxine doesn't affect bone mineral density.

OS-302

J.C.H. Wong, P.J. Lewindon, R. Mortimer, R.W. Shepherd

Department of Nuclear Medicine and Bone Mineral Densitometry, Royal Brisbane Hospital & Department of Paediatric Gastroenterology, Royal Children's Hospital, Brisbane, Queensland, Australia

BONE MINERAL DENSITY AND NUTRITIONAL INDICES IN EARLY ADOLESCENT FEMALES WITH ANOREXIA

Anorexia nervosa (AN) has been shown to predispose to osteopenia/osteoporosis and fractures. This study evaluated the bone mass of early adolescent females diagnosed with AN within the preceding 12 months to determine whether there was any significant bone mass reduction at that early stage of diagnosis and evaluated the correlation between whole body (WB) and lumbar spine (LS) bone mineral densities (BMD) and bone mineral content (BMC), and nutritional indices (body weight, weight percentile, body mass index (BMI), lean mass, fat mass and percentage fat). 20 adolescent females aged between 12 to 17 years (mean = 14 years) diagnosed with AN less than 12 months earlier (range = 2.5-11 months; mean = 6.7 months) with a weight range at presentation to the Eating Disorder Clinic of 1st to 50th weight percentiles had bone density measurements of the WB and LS using a Lunar DPX-L densitometer (mean weight percentile = 15, mean BMI at presentation = 14.9, mean weight loss from premonitory weight = 19.8%). Comparison was made with values of age-matched controls available in the Lunar normative database. There were no significant difference in the WB and LS BMD of the anorexic subjects and age and sex-matched controls. Multiple regression analysis shows significant correlation between WB BMD and lean mass ($p < 0.01$; $r = +0.72$) and between WB BMC and lean mass ($p < 0.01$; $r = +0.88$) and weight ($p < 0.01$; $r = +0.70$). There was similar significant correlation between LS BMD and lean mass ($p < 0.01$; $r = +0.76$) and weight ($p < 0.01$; $r = +0.67$), and between LS BMC and lean mass ($p < 0.01$; $r = +0.88$) and weight ($p < 0.01$; $r = +0.78$). In addition, the weight percentile correlated highly with the LS BMD Z-score ($p < 0.01$; $r = +0.70$). Therefore, during adolescence, the lean mass in particular, and also body weight are good indicators of bone densities. Adolescent females do not appear to show bone mass reduction in the early stages of diagnosis of anorexia nervosa. This suggests early intervention may preserve gain of bone mass and attainment of normal peak bone mass.

OS-303

W. Brenner, K.H. Bohuslavizki, N. Sieweke, S. Kröger, S. Klutmann, W.U. Kampen, M. Clausen, E. Henze

Departments of Nuclear Medicine, Universities of Kiel and Hamburg, Germany

AGE- AND SEX-RELATED BONE UPTAKE VALUES MEASURED BY QUANTITATIVE BONE SCANNING

The reference method to quantify bone uptake is to measure 24 h body retention of Tc-99m-diphosphonate by a whole body counter. Recently, we introduced a new method for bone uptake measurement by ROI-technique based on three-phase bone scanning. The aim of this study was to establish age- and sex-related uptake values in normals. Studies were performed in 49 women (16-79 yrs) and 44 men (6-89 yrs) with normal bone scans. Images were acquired at 3 min and at 3-4 h after injection of 600 MBq Tc-99m-HMDP using a double head gamma camera. The activities for whole body, urinary bladder and both thighs - used as representatives for soft tissue - were measured by ROI-technique. Bone uptake was then calculated as total whole body activity at 3 min minus urinary excretion and remainder soft tissue activity.

Age- and sex-related bone uptake values in percent of initial total whole body activity are given both as mean \pm 1 SD and range:

age	men (n = 44)	women (n = 49)
< 18 yrs.	40.7 \pm 15.8 % (29.5-77.2)	40.4 \pm 4.5 % (35.9-44.8)
18-25 yrs	27.1 \pm 5.1 % (23.3-34.3)	20.2 \pm 3.9 % (13.6-23.1)
26-45 yrs	27.8 \pm 5.7 % (19.7-38.7)	26.9 \pm 8.6 % (14.1-41.4)
46-55 yrs	25.4 \pm 4.6 % (14.2-31.2)	24.0 \pm 5.4 % (14.7-35.3)
> 55 yrs	25.8 \pm 9.8 % (12.7-44.9)	25.9 \pm 3.9 % (21.1-35.5)

Significant differences between men and women were proven within the subgroup age 18-25 yrs only ($p < 0.02$). In patients < 18 yrs with active epiphyseal proliferation zones bone uptake was significantly higher than in any other subgroups ($p < 0.02$). In postmenopausal women a highly positive linear correlation between age and uptake was found ($r = 0.91$).

Thus, age- and sex-related uptake values of normals covering a wide range of age are presented for bone uptake of diphosphonates using a new method based on conventional three-phase bone scanning.

OS-304

P. E. Zouboulis (*), P. Meges (*), D. J. Apostolopoulos (**), K. Kalatzis (**), C. Giannakenas (**), D. Kostakiotis (*), E. Lambiris (*), P. J. Vassiliou (**), (*) Orthopaedic Department, (**) Department of Nuclear Medicine, Regional University Hospital of Patras, Greece.

PROGNOSIS OF CEMENTLESS TOTAL HIP ARTHROPLASTY, BY Q-SPECT ANALYSIS OF ^{99m}Tc-MDP UPTAKE.

Purpose: Cementless total hip implant fixation closely resembles a fracture's healing response. Prognosis of its final outcome becomes possible by an early detection of response disorders. A clinical prospective study was conducted to establish the potential prognostic value of Q-SPECT analysis of periprosthetic ^{99m}Tc-MDP uptake.

Material/Methods: 31 patients, 11 male and 20 female (33-71 years), scheduled for a total hip arthroplasty (THA) due to primary osteoarthritis were divided into 2 groups. Group A (n=18), using a CLS-Spotorno-Sulzer, press fit Ti prosthesis and Group B (n=13), using a Perfecta-Orthomet, proximal porous coated Ti prosthesis. The choice of implant was made using a CAD/CAM technique, based on the different design properties of each implant and the anatomic characteristics of each patient. Patients were imaged 1 week pre-operatively and 2, 8, 36 and 60 weeks postoperatively (p.op). Quantitative measurements were performed with a ROI technique. The 5 ROIs were planned to include Charnley's acetabular zones 1 and 2-3, and Gruen's femoral zones 1-2, 4 and 6-7. Q-SPECT analysis of the radionuclide uptake was performed in coronal, transaxial and sagittal projections. Elliptical angular analysis in the two latter was included.

Results: Preoperative scintigrams were used to exclude measurement errors, due to radiopharmaceutical concentrations of osseous pathology other than the surgical procedure itself. Elliptical angular analysis offers an estimation of the biomechanical type of fixation achieved by the cementless implant for the acetabular as well as the femoral side, leading to qualitative criteria of the design characteristics for each implant. In the majority of cases, the maximum concentration in each ROI was measured 15 days p.op, followed by progressively lower concentrations, up to 15 months p.op. Higher concentrations on the 2nd, 3rd or 4th p.op scintigrams are considered a significant prognostic factor for early detection of failure to achieve initial stability, probably leading to early aseptic loosening. Four distinct types of ^{99m}Tc-MDP uptake are obtained - Type I: adequate initial stability, Type II: secondary fixation, Type III: thigh pain and Type IV: failure of initial stability.

Conclusions: An evaluation of different biomechanical properties and different types of fixation of the cementless implants is possible through different patterns of periprosthetic radionuclide uptake. Quantitative SPECT analysis of ^{99m}Tc-MDP uptake seems to offer, an early prognostic sign for the final implant fixation right from the second p.op month. The surgeon is able to assess the achieved initial stability of the implant from the obtained curve patterns.

OS-305

R. Morita, I. Yamamoto, I. Yuu, M. Takada, Y. Hamanaka, T. Ohta, R. Matsushita, K. Masuda
Department of Radiology, Shiga University of Medical Science, Otsu, Japan

SCREENING FOR OSTEOPOROSIS BY QUANTITATIVE ULTRASONOMETRY AND BONE MARKERS IN JAPAN

Since quantitative ultrasonometry (QUS) is a portable, safe and inexpensive method, the QUS system is expected to become a screening tool for detecting those with a high risk of fracture.

A guideline for primary screening for osteoporosis by bone densitometry was released by the Japanese Ministry of Health and Welfare in 1995.

In this guideline those whose lumbar BMD is less than 80% of the Young Adult Mean (YAM) are advised to undergo further examination for osteoporosis.

The correlation between QUS and DXA, however, is rather poor, so that no matter what cut-off levels are set, fairly high false positive and false negative rates would result from QUS screening. So, what cut-off levels are practical?

Since 1993, we have carried out an osteoporosis screening program mainly focused on females between 30 to 60 years of age living in the community to assess the feasibility and practicality of a population based program.

In this program, Stiffness was measured in 1635 women by QUS, urinary deoxypyridinoline in 346 and Lumbar BMD in 569 by DXA. When the cut-off levels is set at a Stiffness value of 80, 20% of those with low bone density would not be detected, but 40% of the participants would be judged as having a high risk of fracture and referred for further examination.

With a cut-off level of 74 for Stiffness, the non-detection rate would rise to 30% and the proportion required for further examination would fall to less than 15% of the total number of participants. This is the most acceptable cut-off level from a practical point of view.

In conclusion: 1) QUS has advantages as a screening tool, because it is portable, inexpensive and radiation free. 2) The cut-off level of Stiffness 75, which is 84% of YAM is an acceptable level from a practical view point. 3) Measurement of metabolic bone markers is expected to improve the efficacy of QUS screening. 4) Mass screening motivates participants for the prevention of osteoporosis and provides chances for health guidance.

OS-306

S. Gratz, T. Behr, J. Meller, M. Conrad, S. Yücekent and W. Becker
Department of Nuclear Medicine of the Georg August University, Göttingen, Germany

SENSITIVITY AND SPECIFICITY OF SINGLE PHOTON EMISSION COMPUTED TOMOGRAPHY COMPARED TO PLANAR ^{99m}Tc BONE SCANNING

Rationale: Bone scintigraphy with ^{99m}Tc - MDP is a highly sensitive method with low specificity for detecting bone abnormalities. The aim of this study was to compare the sensitivities of single photon emission computed tomography (SPECT) and planar bone scanning. Furthermore, we wanted to evaluate whether SPECT can provide an increase in specificity. **Patients and Methods:** From 7/95-10/97 bone scanning was performed in 111 patients by SPECT. For evaluation, complete data sets were available. These 111 patients (43 men, 68 women, mean age 58.26±25.32 years) suffered from breast (n=36), prostate (n=14), kidney or bladder (n=10), colorectal cancer (n=9), bone/Ewing sarcoma (n=9), malignant melanoma (n=7), non-Hodgkin lymphoma (n=6), eosinophilic granuloma (n=5), M. Paget (n=3), M. Perthes (n=3), ovarian carcinoma (n=3), small cell lung cancer (n=2) or necrosis of foot/ankle bones (n=4). Imaging was performed 2 h after injection of 555 MBq ^{99m}Tc - MDP with a double headed gamma camera (Prism 2000, Picker) for planar imaging and a tripple headed gamma camera (Prism 3000, Picker) for SPECT. In all patients, a 256x256 matrix with preselected 500 kcts were applied. Whole-body images, planar spot views and SPECT were performed at 3 h to 4 h p.i.. For SPECT reconstruction, an iterative algorithm was used. For comparison, 158 radiograms, 82 CTs, 67 MRIs, 7 histologies, 6 biopsies, and all clinical follow-ups were available for final correlation. **Results:** Out of 188 known overall lesions, 109 were detected by planar scans and 163 by SPECT. Thus, the sensitivities were 58% and 87% respectively. Eight false negative lesions in the ribs and 4 false positive lesions in the iliosacral joint in planar scintigraphy were correctly diagnosed by SPECT. In the spine, planar scintigraphy detected 91/140 lesions, whereas 140/140 were detected by SPECT. Primarily, patients with known vertebral bone metastases were all seen by planar scintigraphy, but in two patients one further lesion for each patient was detected by SPECT. With SPECT, an increased uptake in the vertebral body and in the pedicles is often described as suspicious for malignancy. In our data set, this form of uptake corresponded in 9/25 (36%) to a metastatic lesion, in 44/110 (40%) to degenerative alterations and in 2/5 (40%) to vertebral osteomyelitis. Thus, the specificity was only 39%. Lesions limited to the vertebral body and especially to the pars interarticularis and facetal joints (n=15) were always correctly diagnosed as spondylarthrosis. **Conclusion:** 1.) SPECT increases the detectability of bone lesions significantly. 2.) In case of degenerative alterations in the spine, a specific diagnosis is possible with SPECT because of a better anatomical resolution.

Cardiovascular: Attenuation correction/transplantation
OS-307

D.S. Lee, Y. So, G.J. Cheon, M.M. Lee, J-K Chung, M.C. Lee.
Seoul National University College of Medicine, Seoul, Korea

PRE-TEST LIKELIHOOD, EXPERIENCE OF OPERATORS AND ADDITIVE DIAGNOSTIC EFFICACY OF GATED ATTENUATION-CORRECTED MYOCARDIAL SPECT IN CORONARY ARTERY DISEASE.

Diagnostic performance of gated or attenuation-corrected SPECT differed in relation to pre-test likelihood of coronary artery disease (CAD) and the performance of operators, i.e., the expertise of physicians. We investigated if gated and/or attenuation corrected SPECT improved performance of experienced or inexperienced operators in the diagnosis of CAD or stenosed arteries in patients having intermediate or high pretest likelihood.

Rest/dipyridamol stress gated attenuation-corrected SPECT (ADAC, vantage.1.5 simultaneous gating and attenuation correction) was performed in 81 patients who had a pre-test likelihood of high (n=38) or intermediate (n=43) degree for CAD. These patients (M:F=48:33, 62±/8.6 year old) were diagnosed by coronary angiography (>50% stenosis, 1 vessel; 14, 2 vessel; 19, 3 vessel disease; 31, normal 17). Two experienced physicians and one novice nuclear physician (6 month-trained) graded 1 (normal) to 5 (definitely abnormal) for each artery 1) by conventional rest Tl-201/stress Tc-99m-MIBI SPECT, 2) plus viewing gated SPECT (+gated) and 3) 2) plus attenuation-corrected SPECT (+attenuation corrected gated). Receiver operating characteristic (ROC) curves were drawn and areas under ROC curves (AUC) were compared using MedCalc software.

Regardless of the experience of physicians, AUC was larger in patients having high pre-test likelihood than those having intermediate likelihood (average 0.89 vs. 0.68), as was the case for each artery (average 0.75 vs. 0.65). Novice physician performed better when they diagnosed RCA stenosis (AUC: 0.53 for usual, 0.58 for +gated, and 0.66 for +attenuation corrected gated) in patients having intermediate pretest likelihood. Otherwise, not only in these patients having intermediate pretest likelihood but also in patients having high pretest likelihood, AUC was not different for the diagnosis of CAD and LAD or LCx. On the contrary, performance of experienced physicians was not different when they read usual, +gated, and +attenuation corrected gated SPECT, regardless of intermediate or high pretest likelihood. If we set positive as > grade 3 for CAD or arteries, novice operator's specificity increased from 53% to 73% (p>0.1) for CAD, and 62% to 89% (p<0.05) for RCA in patients having intermediate degree of pretest likelihood.

We concluded that gated attenuation-corrected SPECT was helpful only for novice physician's performance to diagnose RCA stenosis by increasing specificity in patients having intermediate pretest likelihood. Even for inexperienced physician, these methods were not helpful in patients with high pre-test likelihood or for LAD or LCX.

OS-308

G. Cantinho, H. Pena, V. Marques, J. Monteiro, F. Godinho

Atomical, Laboratório de Medicina Nuclear, Lisboa, Portugal

ATTENUATION CORRECTION IN THALLIUM 201 SPECT STUDIES

Stress/rest thallium (201Tl) protocol is widely used in the clinical setting for myocardial perfusion evaluation. The low thallium energy is potentially responsible for attenuation artefacts of men's left ventricle inferior wall and in the woman's anterior wall.

Attenuation correction represents an important recent development in cardiac single photon emission computed tomography. The aim of this study was to compare distribution between stress and rest thallium SPECT studies with and without attenuation correction.

We analysed 20 SPECT studies at dipyridamol stress and at rest (3h redistribution). The SPECT studies analysis was done using Cedars-Sinai quantitative tomographic 201Tl. The polar maps obtained reflect the area and severity of the disease. This approach expresses the percentage of myocardium involved with an initial perfusion defect.

Two groups of patients were considered: A - 11 women and B- 9 men.

These two groups of patients were subdivided in two more groups:

Group Aa- 7 patients (61 ± 4kg and 157 ± 8 cm), group Ab- 4 patients (80 ± 4kg and 162 ± 5 cm), group Ba- 5 patients (71 ± 6 kg and 167 ± 6 cm) and group Bb- 4 patients (85 ± 4 kg and 173 ± 6 cm).

We analysed the three artery territories of left ventricle: LAD, LCX and RCA. In all groups, we obtained values for severity and area of lesion, considering normal values the % area from the total < 12% for the LAD and LCX and < 9% for RCA. In the women's group, we verified an increased lesion severity in 2/7 of group Aa pts and a decreased in 2/4 of group Ab pts in the LAD territory. In the LCX territory, we found an increase of abnormal pixels in 4/7 pts of Aa group. The remaining studies were similar. In the RCA, the severity of the lesion increased in 2/7 and remained similar in the others. In men, in the LAD and LCX territories no significant changes were noted. In RCA territory we have found a decrease of the abnormal number of pixels in attenuation correction tomograms in 3/9 pts, one from Ba group and two pts from Bb group. Our study shows, in women, a predominantly anterior count density change and in the inferior wall, in men. The non-uniform changes in count density distribution obligate a careful interpretation, accounting pts obesity and sex in SPECT studies with or without attenuation correction.

OS-309

Hans Jürgen Gallowitsch¹, Josef Sykora², Peter Mikosch¹, Ewald Kresnik¹, Oliver Unterweger¹, Georg Grimm², Peter Lind¹

¹Department of Nuclear Medicine and Special Endocrinology, ²Department of Cardiology, Landeskrankenhaus Klagenfurt, Austria

Attenuation-corrected TI-201 - SPECT using a Gd-153 moving line source: Clinical value and the impact of attenuation correction on the extent and severity of perfusion abnormalities.

The aim of the study was to test the clinical value of attenuation-corrected TI-201 SPECT (AC) using a moving Gd-153 line source in a clinical setup of patients planned to undergo coronary angiography because of clinically suspected coronary artery disease. Furthermore, we wanted to test the impact of AC on the extent and severity of perfusion abnormalities. **Patients and method:** 107 patients, planned to undergo coronary angiography, were included in our study. In each patient, AC and NC (non-corrected)- TI-201 SPECT was performed. AC and NC were evaluated visually as well as by a 31-segment-semiquantitative analysis and correlated with angiographic results. Patients were assigned to two different groups: group A with angina and no previous cardiac infarction or intervention and group B with known CAD because of previous myocardial infarction or intervention. **Results:** With visual analysis, NC revealed a sensitivity of 88.9 % in group A and 74.3 % in group B compared to 94.4 % in group A and 94.3 % in group B with AC. Specificity was calculated for NC to be 68.7 % for group A and 91.3 % for group B. AC demonstrated significant higher specificity with 83.9 % and 100 % , respectively. This effect could be particularly demonstrated for males and bicycle workload. The extent and the severity of perfusion abnormalities were significantly influenced using AC by demonstrating significantly less abnormal and less severe abnormal segments in the segmental analysis compared to NC, especially for the vascular territory of the LAD and RCA. **Conclusion:** AC with a moving line source is feasible in a clinical setup of patients with all types of probability of CAD. AC has a significant impact on the severity and the extension of myocardial ischemia, especially in the posterior and septal wall

OS-310

A. Tausig, C. Spes*, P. Knesewitsch, V. Klaus*, P. Weisenseel*, C. Angermann*, B. Reichart**, H. Mudra*, K. Tatsch, K. Hahn. Departments of Nuclear Medicine, *Cardiology (Medizinische Klinik, Klinikum Innenstadt), and **Cardiac Surgery (Klinikum Großhadern), University of Munich, Munich, Germany

VALUE OF COMBINED DOBUTAMINE-MYOCARDIAL SCINTIGRAPHY AND STRESS-ECHOCARDIOGRAPHY FOR NON-INVASIVE ASSESSMENT OF CORONARY VASCULOPATHY AFTER HEART TRANSPLANTATION

Coronary angiography (CA) is commonly used for assessment of cardiac allograft vasculopathy (CAV), mostly on a routine basis. This study was designed to investigate the value of combined dobutamine (Dob) stress echocardiography (SE) and myocardial scintigraphy (MSz) in comparison to CA.

In 38 pts (52±13 years, 85±37 months after heart transplantation) a Dob-stress was performed (5 - 40µg/kg KG/min). For analysis of wall motion abnormalities (WMA) SE was performed simultaneously. For MSz Tc-99m-MIBI (250 MBq) was injected at peak stress and reinjected 3h later at rest (650 MBq). SPECT-data were acquired with a triple-headed gamma camera (PRISM 3000, Picker) applying patient-specific attenuation correction (STEP™). Visually abnormal MSz at rest and/or at stress or WMA were regarded as markers of CAV. Both, MSz and SE were read blinded to the results of CA, which was performed within 24h.

MSz in combination with SE identified 8/8 pts with stenosis >50% or severe and diffuse CAV. 7/14 pts with normal CA were read normal with both tests. 16/16 pts with moderate CAV (<50%) had an abnormal MSz or WMA at SE. PTCA was necessary in 2 pts, who were identified properly with both non-invasive methods.

All pts with abnormal coronary angiograms suggestive for CAV were detected with combined Dob-MSz and Dob-SE. SE might be more reliable in pts with diffuse disease, MSz is advantageous in pts with poor echocardiographic images. So far all pts in whom a cardiovascular intervention was necessary were properly identified by both. Thus, combined Dob-MSz and Dob-SE is a reliable non-invasive approach to screen for CAV, allowing CA to be performed on a more individual rather than a routine basis after heart transplantation. This strategy may be particularly important for pts with renal insufficiency in whom repeated injections of contrast-agent should be avoided.

OS-311

J.Mortensen, J.Toft, B.Hesse.

Rigshospitalet, Department of Clinical Physiology and Nuclear Medicine.

HIGH FREQUENCY OF ATRIOVENTRICULAR BLOCK BY ADENOSINE FOR PHARMACOLOGICAL STRESS TESTING IN HEART TRANSPLANT PATIENTS (HTX).

A normal myocardial perfusion scintigraphy 1 yr after HTX is an important predictor of 5-yr survival. We use annual myocardial perfusion scintigraphy with Tc-99m - tetrofosmin or Sestamibi and pharmacological stress testing at our centre to monitor coronary artery disease in HTX patients. Intravenous dipyridamole given as 140 µg/kg/min over 4 min. was our standard procedure, but due to the more transient and milder adverse effects from adenosine we recently changed to intravenous adenosine as 140 µg/kg/min over 6 min., during submaximal exercise as recommended by Pennell et al. (JACC 1995;25:1300-9). However, we experienced, apparently, markedly different safety profiles in HTX patients.

Therefore, we compared the incidence of second-degree and third-degree AV-block during adenosine stress testing in 9 HTX patients and in 25 non-transplant patients without a pacemaker. The incidence of AV-block of 1 of 25 (4%) non-transplant patients is similar to the frequency reported by Cerqueira et al. (JACC 1994;23:384-9) and Johnston et al. (Mayo Clin Proc 1995;70:331-6). The incidence of AV-block was 4 of 9 (44%) in HTX patients. The 10 times higher frequency in the HTX patients is statistically significant (p<0.01, Fisher's test). None of the 4 patients had sustained AV block, but the adenosine infusion had to be interrupted because of severe discomfort and chest pain in 2 patients. All of the HTX patients had earlier undergone dipyridamole stress testing without any significant changes in the EKG. Previously we have performed more than 350 dipyridamole stress tests in 95 HTX patients without occurrence of AV block.

In conclusion, there is a high risk of clinical significant AV-blockade during adenosine stress testing in heart transplant patients. In our opinion dipyridamole should be preferred for pharmacologic stress tests in these patients.

OS-312

J.Toft, J.Carlsen, S.A.Mortensen, H.Arendrup, J.Aldershvile, B.Hesse Rigshospitalet, Dpts.Clin.Physiol.Nucl.Med. and Cardiol., Copenhagen University, Denmark

HEART TRANSPLANT CORONARY ARTERY DISEASE: HIGH SENSITIVITY AND MODERATE PROGNOSTIC VALUE OF Tc-SESTAMIBI OR TETROFOSMIN MYOCARDIAL SPECT WITH CORONARY ANGIOGRAPHY (CAG) AS REFERENCE.

Background: Following heart transplantation (HTX) the diagnosis and treatment of graft coronary artery disease is a major clinical challenge. Although CAG is not a sensitive method for the diagnosis of HTX vasculopathy it remains the basis for deciding possible revascularisation. The purpose was to evaluate myocardial SPECT as a method of detecting coronary artery disease with CAG as the reference. **Patients and methods:** A total of 255 SPECT studies and CAGs were performed in a consecutive series of 67 pts. (mean age 43 y, range 11-63), once yearly after HTX for an average follow-up period of 5.6 years (range 2-11). Myocardial SPECT was performed as a 2-day protocol with Tc99m-Sestamibi or -Tetrofosmin, with dipyridamole for the stress test. The SPECT studies and CAGs were evaluated in a blinded fashion by 2 different teams. **Results:** Out of 9 pts. with reversible perfusion defects at SPECT 5 had significant coronary artery lesions. Two of the remaining 58 pts. also had coronary artery stenosis but SPECT was assessed as normal. Irreversible defects had no relationship to abnormal CAG. With CAG as the reference PV_{pos} was 56% for reversible defects at SPECT, PV_{neg} 97% and accuracy 91%. During follow-up 10 pts. died, 3 of them had abnormal CAG and 4 abnormal SPECT. **Conclusions:** 1) This study indicates that myocardial SPECT in HTX has high sensitivity in the diagnosis of significant coronary lesions. 2) The false positive SPECT studies may be true positive in the sense that they reflect myocardial ischaemia, considering the low sensitivity of CAG for HTX vasculopathy. 3) CAG and SPECT have similar moderate prognostic power regarding mortality.

Oncology: Peptide

OS-313

H. Mershed, N. Salehi, M. Lichtenstein, A.M. Baricevic,

Department of Nuclear Medicine, Royal Melbourne Hospital, Parkville, Victoria.

VASOACTIVE INTESTINAL PEPTIDE (VIP) LABELLING WITH Tc-99m USING CHELATING AGENTS

The detection of tumour cells by radiolabelled VIP is receiving a great deal of interest. Our Aim is to investigate a method of labelling of VIP with the regularly available radionuclide pertechnetate.

Methods: (1) two steps were used, Anhydride of diethylenetriaminepenta acetic acid (ADTPA) was attached to VIP and then radiolabelled with pertechnetate. (2) A three step method was developed, using a spacer to ADTPA prior to coupling to VIP and then radiolabelling was performed. The conjugates from both methods were separated through Sephadex G-50 and purified by G-25 and HPLC at flow rate 1 ml / min. UV absorbance at 280 nm confirmed the molecular weight of the radiolabelled VIP.

The labelling efficiencies were determined by using instant thin-layer chromatography (ITLC) LE = 91+ 3.4 % (1) and 83+ 4 % (2). Scanning was performed using GE-300 in control mice (n=3 in each method) at T0 +15 min

1 and 4 hr after IP injection of radiolabelled VIP, the biodistribution in mice at T0 + 4hrs confirmed that both conjugates were excreted by the kidneys and

there was little colloid formation in the liver (Kid:Bl = 58.7, Liv:Bl = 6.2

and Lungs: Bl = 4.1, (2) Kid:Bl = 21.2, Liv: Bl= 2.5 and Lung:Bl = 0.67 }.

Conclusion: Our in vitro experiments using a chelating agent such as ADTPA

and a spacer to ADTPA and in vivo work in control mice are in favour of a strong and stable radiolabelled VIP with Tc-99m. Further receptor binding assays

are in progress.

OS-315

C. Bischof, P. Angelberger, G. Hamilton, P. Smith-Jones, M. Shirzad, T. Traub, T. Pangerl, M. Raderer, M. Peck-Radosavljjevic, R. Breitenecker, I. Virgolini

University Hospital of Vienna, Department of Nuclear Medicine

123I/99mTc-CPTA-INSULIN-LIKE GROWTH FACTOR I (IGF-I): PREPARATION AND *IN VITRO* BINDING CHARACTERISTICS

The insulin-like growth factor I (IGF-I) is a single chain polypeptide structurally related to insulin. Recent data suggest the expression of IGF-I receptors on various tumor types. This study was aimed to create a cost-effective and stable radiolabeled IGF-I peptide and to evaluate its binding characteristics *in vitro*. IGF-I was labeled either with 123I (specific activity: 0.025 mCi/ μ g) or with 99mTc (specific activity: 0.3 mCi/ μ g) after coupling to CPTA. In *in-vitro* radioligand binding studies we used tumor cell lines (ZR75-1, BT20, MCF-7, T47D, PANC-1, ASPC-1, BXP-3, CAPAN-1, SKHEP1, HEPG2 and HEP3B), primary ductal breast cancers (n=10) and normal breast tissue (n=6). 123I/99mTc-CPTA-IGF-I bound with high affinity to the four breast cancer cell lines ZR75-1, BT20, MCF-7 and T47D (Bmax = ~ 0.1-2 x 10e9 sites/cell, Kd = 1-10 nM), to the pancreatic adenocarcinoma cell lines PANC-1, ASPC-1, BXP-3 and CAPAN-1 (Bmax1 = ~ 0.3-9 x 10e4 sites/cell, Bmax2 = ~ 0.3-4 x 10e5 sites/cell, Kd1 = 1-5 nM, Kd2 = 5-30 nM) and to the hepatoma cell lines SKHEP1, HEPG2 and HEP3B (Bmax = ~ 0.3-8 x 10e5 sites/cell, Kd = 1-4 nM). 123I/99mTc-CPTA-IGF-I also bound to primary breast cancers (Bmax1 = ~ 0.6-9 x 10e11 sites/mg, Bmax2 = ~ 0.9-1.4 x 10e13 sites/mg, Kd1 = 1-2 nM, Kd2 = 5-15 nM), whereas no saturable specific binding of 123I/99mTc-CPTA-IGF-I to normal tissues was found. Binding of 123I/99mTc-CPTA-IGF-I to the tumor cells and primary tumors was well displaced by unlabeled IGF-I (IC50 1-20 nM for tumor cell lines, 10-100 nM for primary tissues), less effectively by IGF-II and insulin. Northern Blot analyses confirmed the expression of IGF-I receptor mRNA in primary tumors and tumor cell lines.

A variety of tumor cells over-express IGF-I receptors which bind 123I-IGF-I and 99mTc-CPTA-IGF-I specifically. These peptide tracers seem to be suitable for localization diagnosis/treatment of respective tumors.

OS-314

A. D. Varvarigou, F. Scopinaro, L. Leontiadis, G. Romano G. P. Evangelatos and S.C. Archimandritis.

National Center of Scientific Research "Demokritos", 15310 Athens, Greece

Universita' "La Sapienza", 00161 Roma, Italia.

PREPARATION AND PRECLINICAL EVALUATION OF A NEW 99mTc-LABELLED BOMBESIN-LIKE PEPTIDE

In the present study we have synthesized a new bombesin-like decapeptide, containing the basic amino acid sequence that stimulates bombesin activity. The peptide synthesized was Cys-Aca-Gln-Arg-Leu-Gly-Asn-Gln-Trp-Ala-Val-Gly-His-Leu-Met-NH₂, which consists of the Bombesin 2-14 sequence, elongated by a cystein residue. This residue replaced the pyroglutamic acid, present in the original bombesin sequence, and served as the Tc-99m binding group in the synthetic peptide. An 6-amino-N-hexanoic acid (Aca) spacer-arm was incorporated between the cystein residue and the remaining synthetic peptide, for avoiding any stereochemical hindrance between the radiolabelled part (Cys-99mTc) and the biologically active peptide fragment. The peptide was synthesized by fmoc solid-phase technique and was purified by reverse-phase semipreparative HPLC. The elution profile of the purified synthetic peptide on analytical reverse phase HPLC showed a single peak at 17.8 min. Amino acid analysis revealed the expected amino acid content, while the synthetic compound had the expected molecular weight (1723), as determined by electrospray mass spectrometry. The biological efficacy of the new derivative was evaluated in smooth muscle cells circular layer of human colon. The synthetic bombesin-like peptide, tested in comparison to the same amount of Bombesin, was found to have similar effects (95%).

Labelling of the new peptide with Tc-99m was studied, using gluconate as an intermediate technetium exchange ligand. Labelling yield, studied by chromatographic techniques, was found >95%. HPLC analysis of the radiolabelled product, on a reverse phase chromatography column with linear gradient solvent system, showed the formation of a single radioactive species, detected both by UV and radioactivity detectors. This new labelled derivative was found stable at 4°C for 27 hrs. Biodistribution was studied initially in normal mice, by i.v injection. The % dose per organ and the % dose per gram were calculated in comparison to a standard of the injected dose. Results showed significant lung localization 15 min p.i. Lung values remained high for more than one hour. Excretion of the radiolabelled peptide was detected two hours p.i., mainly through the hepatobiliary tract. In vivo evaluation is continued in higher animals.

OS-316

R. Valkema, J. Burgers, J. van Meerbeeck, A.E.M. Reijs, E.P. Krenning. Departments of Nuclear Medicine and Pulmonary Medicine, University Hospital, Rotterdam, The Netherlands.

FLUORINE-18-DEOXYGLUCOSE COINCIDENCE ECT FOR THE DETECTION OF NON-SMALL CELL LUNG CANCER.

Aim: Positron emission tomography (PET) using 18-FDG is a sensitive method to detect pulmonary cancer lesions; it is useful for discriminating malignant from benign lesions and for the detection of metastases. In this preliminary study we compared gamma camera positron coincidence detection (PCD) with histology in patients with known or suspected lung malignancies.

Patients and methods: Sixteen patients (pts) were studied with PCD before surgery or mediastinoscopy. After overnight fasting, and 45 min after injection of 185 MBq of F-18 FDG, ECT of the chest incl. the adrenals was performed, followed by ECT of the head/neck region. Each ECT was acquired over 37 min with a dual-head camera (Picker PRISM 2000 XP) fitted with 3/4" crystals and axial filters. Rebinning in 128 x 128 matrices using photopeak/photopeak events was followed by MLEM iterative reconstruction, and wierner 3D post-filtering. All PCD studies were interpreted independent of other diagnostic results.

Results: FDG PCD was clearly positive in 11/13 pts (85%) with histologically proven malignancies (7 adenoca., 2 squamous cell ca., 1 large cell ca., 1 metastasis of colon ca.) In these pts the primary lung lesion and all confirmed lymph nodes, 1/2 brain, 1/1 vertebral and 1/1 adrenal metastases were seen with PCD. The brain metastasis in 1 pt showed no enhanced FDG uptake, although the other lesions in that patient were intense, and the edema around the metastasis was correctly identified by decreased FDG intensity. Additional-unconfirmed- lymph nodes were suspected in 4 pts, and a vertebral metastasis in 1 pt. One pt with a 2.5 cm adenoca. and 1 pt with bronchoalveolar ca. were negative with FDG PCD (2/13, 15%). In 3 pts with solitary pulmonary nodules no histology was obtained because of the clinically presumed benign character; 2 pts remained stable without growth over 3, resp. 4 months, and 1 pt had a probable hemangioma with successful shrinkage after embolization. All these pts had negative FDG PCD studies.

Conclusion: Based on these preliminary results, FDG imaging with PCD is a promising clinical tool for non-small cell lung cancer.

Oncology: PET
OS-317

A. F. Jacobson, M. N. Maisey

Clinical PET Centre, Guy's and St. Thomas' Hospital, UMDS, London, UK

TRENDS IN CLINICAL UTILISATION OF ONCOLOGIC PET IMAGING

Although PET imaging has been available as a research tool for more than thirty years, it has only become available as a routine clinical investigation during the past decade. The Guy's and St. Thomas' Clinical PET Centre began operation in 1992, and we have examined the utilisation of PET imaging in the evaluation of patients (pts) with known or suspected malignancies for the five-year period from 1993-1997. Clinical information supplied at the time of study request, as well as additional data obtained at the time of scanning and subsequently, were reviewed, and pts were categorized based upon the malignancy which PET imaging was intended to characterise. Data were analysed both in terms of the number (no.) of new pts studied and the no. of follow-up exams, with the second and all subsequent scans for a pt considered equivalent for the purposes of this tabulation.

Our primary observations are summarized in the following tables.

	1993	1994	1995	1996	1997	TOTAL
Total Scans	275	421	651	1100	1171	3618
No. New Pts	250	334	474	766	819	2643
No. Follow-up Scans(%)	25(9)	87(21)	177(27)	334(30)	352(30)	975(27)

FIVE MOST COMMON TUMOURS AMONG NEW PTS: No. (%)

	1993	1995	1997	TOTAL(% only)
Lung:	74 (29.6)	Lymphoma: 89 (18.8)	Lymphoma: 192 (23.4)	Lung: 18.8
Breast:	32 (12.8)	Lung: 71 (15.0)	Lung: 162 (19.8)	Lymphoma: 18.3
Head/Neck:	28 (11.2)	Sarcoma: 50 (10.5)	Melanoma: 66 (8.1)	Head/Neck: 7.6
Brain:	21 (8.4)	Melanoma: 47 (9.9)	Unknown 1 ^o : 50 (6.1)	Breast: 7.4
Lymphoma:	18 (7.2)	Head/Neck: 40 (8.4)	Brain: 38 (4.6)	Melanoma: 7.3

While overall PET utilisation quadrupled between 1993 and 1997, more than 1/3 of the new oncology pts studied in each year had either lung cancer or lymphoma. In contrast, lung cancer pts were only infrequently restudied (16 follow-up exams in 1997). Two tumour categories, lymphoma and sarcoma, dominated these studies (47% (n=166) and 15% (n=54) of the follow-up exams respectively in 1997). No other tumour accounted for more than 6% of these exams (that being breast) in 1997.

Subsequent to introduction of clinical oncologic PET, there is strong, progressive acceptance of the modality, particularly for evaluating pts with newly diagnosed lung cancer and lymphoma, and for following treatment response in lymphoma.

OS-318

M. Babar Imran, K. Kubota, S. Yamada, H. Fukuda, K. Yamada, T. Fujiwara, M. Itoh.

Institute of Development Aging and Cancer, Tohoku University, Sendai, Japan.

CAN ATTENUATION UN-CORRECTED IMAGES BE USED AS STANDARD FORMAT IN FDG WHOLE BODY PET ONCOLOGICAL STUDIES?

The purpose of this study was two fold: To compare the diagnostic efficacy of attenuation corrected and un-corrected whole body F-18 FDG PET images, and to search an adequate method that can semiquantitatively evaluate non-attenuation corrected images for their use in PET oncology. Whole body PET studies were performed, 40 minutes after a bolus injection of F-18 FDG on 24 fasting subjects with thoracic and breast tumors. Post-emission transmission data was acquired for measured attenuation correction. Reconstructed attenuation corrected images (ATT) and attenuation un-corrected images (ATN) were displayed simultaneously and the relative FDG uptake in lesions and corresponding background areas were evaluated by region of interest (ROI) method after visual interpretation of the scans. Tumor to background (T/B) ratio was calculated for each lesion and Weber's law was applied to correlate with visual interpretation. ATT and ATN images were also compared with X-CT scans and conventional nuclear medicine scans for diagnostic efficacy. A total of 55 lesions were evaluated. ATT and ATN images were found equally sensitive for the detection of both benign and malignant lesions. There was a strong linear correlation between T/B ratios of ATT and ATN images ($r=0.98$ $p < 0.001$). A significant difference in T/B ratio between ATT and ATN images was present in only 2 malignant lesions. Standardized uptake ratio (SUR) in ATN images did not correlate with SUR in ATT nor with T/B ratio in ATN images. On ATN images, certain areas vulnerable to artifacts were recognized and appropriate explanation was sought out. **Conclusion:** The efficacy of ATN FDG PET images in the evaluation of tumors is similar to that using ATT images. ATN images provide not only clinically useful but also quantitative information equivalent to those provided by ATT images. By this protocol, imaging time can be shortened and consequently throughput can be increased. However T/B ratio is the only available index that can be used for quantification of ATN images.

OS-319

K. D. M. Stumpe, N. Meier, G. K. von Schulthess

University Hospital of Zurich, Department of Medical Radiology, Nuclear Medicine

PHYSIOLOGICAL AND SECONDARY PATHOLOGICAL FLUORO-DEOXYGLUCOSE (FDG) ACCUMULATIONS IN PET SCANS

Aims: to identify physiological and secondary pathological accumulations in non-absorption corrected partial or whole body FDG-PET scans for tumor staging and to determine the frequency of occurrence and the intensity of accumulation.

Materials and Methods: 272 FDG-PET partial and whole body scans of patients obtained for tumor staging were examined and physiological FDG accumulations in the neck, trunk (excl. lung, liver and spleen) and extremities were graded from 0 to 4 (0: no FDG acc.; 4 FDG acc.), as were accumulations with potential secondary pathology such as arthrotic joint involvement. Non-transmission corrected scans were chosen because in most situations, such scans are adequate for tumor staging.

Results: Oropharyngeal accumulations occurred in 86.8% with grade 2-4, while nasopharyngeal, parotid and submandibular activity was much less frequent (6.9 - 10.9%, grade 2 - 4). There was FDG in the thyroid glands of 37.6% patients (grade 1 - 4). Muscular activity was most frequent in the calves (29.2 %, mean grade 2.2), while it was rare in the upper thigh (2.2%), and the same distribution pattern and almost equal frequency were observed in the upper extremities. Neck muscles showed in approximately 20% of all patients with an intensity average around 3. A substantial number of patients (20.8%) showed bowel activity of low grade (1 - 2). Vascular activity of grade 1 - 2 was frequently seen in the upper thighs (74.8%), but less so in the lower thighs and the upper and lower arms and neck (11 - 17 %). Joint activity of grade 1 - 2 was relatively frequently noted: the joints of the foot showed in 43.4 %, the knees in 50 %, the hips in 36.1 %, the shoulder in 79.2 % and the acromio-clavicular joints in 44.1%. weak bone marrow activity was seen in the femora in 53.6%, in the pelvis in 20.8% and the ribs in 9.5%, while the vertebrae showed activity in virtually every patient. Strong accumulation occurred in 6 patients under chemotherapy.

Conclusions: FDG accumulations in whole body PET scans are quite frequent. The most striking physiological accumulations are found in extremity muscles, the oropharynx and the thyroid. Activities in joints are probably due to mild to moderate arthrotic disease and frequently noted in the foot but also in the acromioclavicular joints. Bone marrow accumulation in the upper thighs pointing to some bone marrow expansion were frequent in our patient population and the vascular blood pool was quite noticeable in the extremities but much less so in the trunk. The latter is probably due to the fact that non-absorption corrected scans were evaluated as their image quality is far superior to the corrected ones. Knowing the sites and frequency of such accumulations is important when reading PET scans for tumor staging.

OS-320

J. Ruhlmann, P. Oehr, G. Stegemann, C. Menzel*, P. Willkomm*, H.J. Biersack*.

PET-Center Bonn; *Klinik für Nuklearmedizin, Universität Bonn, Germany.

CLINICAL VALUE OF WHOLE-BODY FDG-PET IN RECURRENT MALIGNANT MELANOMA.

Purpose: we wanted to assess the the sensitivity of whole body FDG-PET as a single diagnostic procedure compared to conventional staging procedures in patients with malignant melanoma.

Methods: 147 patients with a history of malignant melanoma and clinical evidence of recurrent disease were retrospectively analyzed. All patients underwent a conventional diagnostic work-up and an additional whole-body PET, performed on an ECAT Exact Siemens scanner (10 min /bedposition) starting 45 min after intravenous injection of 185-370 MBq F-18-FDG. PET findings were compared to conventional clinical work-up using histological results, additional imaging or clinical follow up as reference.

Results: In 90 of the patients without metastatic lesions PET and CT had 94% specificity. In addition, there were 57 patients with a total of 150 metastatic lesions. 66% of these lesions were detected by both PET and the block of conventional imaging procedures (CT, MR, SPECT and sonography). The number of additionally detected lesions was 34 by PET and only 16 by all other conventional imaging methods together. 37% of the lesions detected only by PET were in the abdominal region, where the other methods detected only 7% further lesions. The sensitivities for single lesions were 90% by PET and only 46% by CT.

Conclusion: At a comparable specificity for PET and CT it can be shown that the sensitivity of PET for metastatic lesions is superior to CT and to the combined use of all other conventional imaging methods. The advantage of PET is whole body imaging which leads to detection of metastases in regions normally not covered by other imaging methods. Our data give evidence that PET should be the first choice for imaging recurrent malignant melanoma.

Infection/inflammation/hematology: Basic studies

OS-321

J. Makarewicz¹, O.C. Boerman², W.J.G. Oyen², E.B. Koenders², P. Laverman², F.H.M. Corstens²
Department of Nuclear Medicine¹, Medical University, Lodz, Poland and Department of Nuclear Medicine², University Hospital Nijmegen, The Netherlands

THE EFFECT OF MOLECULAR WEIGHT ON ACCUMULATION OF Tc-99m LABELLED PEPTIDES AND PROTEINS IN INFLAMMATORY FOCI

Although several proteins have been tested for infection detection the most optimal characteristics of a protein for this application have not yet been determined. To determine the optimal size (molecular weight - MW) of a protein for the nonspecific detection of infections we compared the tissue distribution of Tc-99m labelled peptides and proteins of various MW in a rat model of infection.

Seven proteins and peptides: α-crystallin (Cry; MW 800 kDa), amylase (Amy; 206 kDa); IgG (150 kDa), bovine serum albumin (BSA; 66 kDa), carbonic anhydrase (Anh; 29 kDa), myoglobin (Myo; 17 kDa), insulin-A-chain (Ins; 2.5 kDa) were labelled with Tc-99m using S-HYNIC as a bifunctional chelator. The radiochemical purity as determined by HPLC (size exclusion or reversed phase) indicated that for each of the preparations > 90 % of the radioactivity was associated with the monomeric protein/peptide peak (molar conjugation ratio - HYNIC : protein < 2 : 1). The Tc-99m-labelled proteins/peptides were injected i.v. in rats (10 rats/agent, 8 µg/rat) with *S. aureus* infection and groups of 5 rats were killed at 4 and 24 hr p.i. The biodistribution of the radiolabel was determined by counting the radioactivity of selected tissues in a well-type gamma-counter. In addition, separate groups of three rats were injected i.v. with each of the Tc-99m-proteins/peptides and imaged by means of a γ-camera at 0, 1, 2, 4, 8 and 20 hr p.i.

The biodistribution study demonstrated slow blood clearance with predominant hepatic and splenic uptake of Cry, Amy, IgG and BSA and rapid blood clearance with predominant renal uptake of Myo and Ins. The abscess uptake of the agents (%ID/g, 24 h p.i.) was highest for proteins of intermediate MW: IgG (1.4) > BSA (0.9) > Amy (0.6) > Anh (0.5) > Ins (0.13) > Cry (0.08) = Myo (0.08) and correlated with their blood level (%ID/g, 24 h p.i.): IgG (1.8) > BSA (0.7) > Amy (0.3) > Anh (0.2) > Cry (0.03) > Ins (0.08) > Myo (0.02). The abscess/muscle ratios varied from 16.8 to 2.7 at 4 h p.i. and 10.8 to 2.1 at 24h p.i. with highest values for IgG > Amy > BSA > Anh > Cry > Ins > Myo whereas abscess/blood ratios in the range 1.4 - 0.3 at 4 h p.i. and 4.7-0.8 at 24 h p.i. were highest at both ends of MW spectrum: Myo > Cry > Amy > IgG = BSA = Anh > Ins. Quantitative analysis of the scintigrams revealed that the whole-body clearance was fastest for low MW agents (Myo; Ins) with kidneys being the main route of tracer elimination. Blood pool activity, hepatic and splenic uptake was higher for higher MW proteins. The abscesses were visualised with each of the Tc-99m-labelled proteins/peptides with best abscess/background ratios at 4 and 20hr p.i. for IgG (4.7-7.0) > Amy (4.2-5.4) > BSA (3.8-4.4) > Anh (3.1-3.9) > Cry (2.3-2.1) > Ins (2.2-1.7) > Myo (2.0-1.4).

This study demonstrates that although many inert proteins can be used to visualise inflammation in a rat model, the best localisation of inflammatory foci is obtained with a proteins with a MW around 150 kDa.

OS-322

I. Ak, E. Vardareli, B. Durak, Z. Gülbaş, S. Artan, N. Başaran

Osmangazi University Medical Faculty, Nuclear Medicine, Hematology and Medical Genetic Departments, ESKİŞEHİR, TURKEY

THE CYTOGENETIC PROFILE OF LABELED LYMPHOCYTES WITH Tc-99m HMPAO

It is known that In-111 causes chromosomal aberrations on labeled lymphocytes. As an alternative to In-111, Tc-99m HMPAO is clearly not mentioned the profile of radiotoxic effect to lymphocyte cytogenetic. To evaluate the radiation-induced damage in lymphocytes after labeling of mixed white cells, we used the cytogenesis-blocked micronucleus assay (MN) and chromosome aberration assay on lymphocyte cultures.

22 healthy donors (10 females, 12 males; mean ages 32.1±8.18 years) were included into study. 50 ml freshly blood was withdrawn from the each person and white cells were separated with erythrocyte sedimentation method. Tc-99m HMPAO was obtained by reconstituting a vial of HMPAO (Ceretek, Amersham) with 14-20 mCi sodium pertechnetate. Radiochemical purity and labeling efficiency were %85.15±1.73, %51.05±1.73. With Trypan blue exclusion, 92-98% of labeled cells (mean 95.45±1.76%) were viable. Lymphocyte cultures were obtained from before and after labeling process.

While MN score was 1-14/1000 (mean 5.65±1.04) cells before labeling, it was 62-611/1000 (mean 272.23±32.7/1000) of labeled cells, p<0.001, there was statistically significant difference. 30 metaphases from each person's cultures were evaluated for all types of chromosome aberrations. Before labeling with Tc-99m HMPAO, all metaphases of lymphocytes were defined as normal. But, all of labeled lymphocytes have had multiple asymmetrical aberrations including dicentric, acentric fragments and centric rings and also fivecentric fragments. Some metaphases have had double minute chromosomes (DM) which are define as oncogene amplification and seen malign transformations. Whether it was really DM or not, we used FISH technique with p53, erb2 and N-myc probes (2 cases). Increased signals were seen interphase cells and also on DM at metaphases. It was thought that increased signals related in translocations for p53, oncogene amplification for other.

In conclusion, we expect that the majority of the aberrated cells would die during the interphase period. We also believe that, having symmetrical aberrations including translocations, inversions and chromosomes with deleted segments will remain alive for a long time in the cell compartment with the ability of keeping immunological memory. Future studies are necessary to investigate the oncogene amplification at labeled lymphocytes.

OS-323

E. Vardareli, I. Ak, Z. Gülbaş

Osmangazi University Medical Faculty, Nuclear Medicine and Hematology Departments, ESKİŞEHİR, TURKEY

THE EFFECT OF LABELLING PROCESS TO FUNCTIONS OF LABELED LEUKOCYTES WITH Tc-99m HMPAO

The usefulness and success of labeled leukocytes with Tc-99m HMPAO will greatly depend on the functional integrity of the white blood cells after labeling which is necessary for their localization at the inflammation sites. The aim of the present study was to analyze the functional status of the leukocytes which were labeled with routinely used Tc-99m HMPAO dose and technique, before and after labeling the process with flow cytometry.

Twenty healthy donors (10 females, 10 males; mean ages 32.1±8.18 years) were included into study. 50 ml freshly blood was withdrawn from the each person and white cells were separated with erythrocyte sedimentation method. Tc-99m HMPAO was obtained by reconstituting a vial of HMPAO (Ceretek, Amersham) with 14-20 mCi sodium pertechnetate. Radiochemical purity and labeling efficiency were %85.15±1.73, %51.05±1.73. Before and after labeling process, CD14/CD16 expression, oxidative burst generation (OBG) and phagocytosis functions of neutrophils and monocytes were analyzed with flow cytometry (FACS Calibur, Becton Dickinson, CellQuest software). t-test was used for statistical analyses. With Trypan blue exclusion, 92-98% of labeled cells (mean 95.45±1.76%) were viable.

	Neutrophils		Monocytes	
	before	after	before	after
CD14/CD16 exp. %			18 ± 3.5	17.9 ± 2.7 *
Phagocytosis %	83.83 ± 2.3	77.0 ± 5.97 *	65.28 ± 4.9	71.44 ± 4.84 *
OBG				
E.Coli %	60.50 ± 7.8	47.8 ± 8.05 *	57.85 ± 6.98	47.30 ± 6.87 *
FMLP %	25.3 ± 2.19	15.75 ± 2.19 *	20.8 ± 5.86	18.35 ± 6.24 *
PMA %	81.7 ± 4.9	77.35 ± 5.04 *	68.75 ± 6.9	62.4 ± 6.5 *

*p>0.05

In conclusion, we found no difference in chemotaxis and phagocytosis function and oxidative burst generation of neutrophils and monocytes and also monocyte activation during the early period in routinely used Tc-99m HMPAO dose and labeling method. Labeling of leukocytes with Tc-99m HMPAO results in functionally intact cells.

OS-324

M. Liberatore*, D. Prosperi*, F. Ponzio*, AP. Iurilli*, F. Grammatico*, F. Roccella*, M. Roccella*, A. Centi Colella. *Sezione di Medicina Nucleare., *Cattedra di Genetica Medica, Dipartimento di Medicina Sperimentale, Università di Roma "La Sapienza"

THE EFFECTS OF 99mTc-HMPAO-LABELLED LEUKOCYTE SCAN (WBCs) ON HUMAN KARYOTYPE.

In a number of diseases WBCs is often used as a diagnostic tool. This scintigraphic method requires the separation and labelling of mixed leukocytes, which include particularly radiosensitive cells as lymphocytes. Reproducing themselves, these lymphocytes may transmit possible damage to other cells. The aim of the present study was to assess, in humans, the presence of a cause-effect relation between WBCs and the onset of kariotypic changes. The study was performed on patients with low pre-test probability of infection. Consecutive patients with suspected vascular graft or hip prosthesis infection were included and underwent scintigraphy. The subjects at high professional risk of having induced sporadic chromosomal aberrations as well as patients submitted to radiotherapy or chemotherapy or assuming antibiotics were excluded from the study. All of the patients underwent kariotype determination and sister cromathidic exchange (SCE) evaluation before WBCs. The same examinations were repeated 7 days and then 6 months after WBCs. The study protocol has been completed for 15 of the 23 enlisted patients. Results do not show a significant difference in the rates of chromosomal aberrations obtained before WBCs and after WBCs. By considering the high radiation dose received by lymphocytes during the labelling procedure, these findings should be interpreted as results of the dead of these cells.

Physics and instrumentation: Mathematical models

OS-325

A.R. Formiconi

University of Florence, Department of Pathophysiology

A GENERAL MATHEMATICAL FORMULATION FOR THE GEOMETRICAL RESPONSE OF MULTIHOLE COLLIMATORS

A general formula to describe the geometrical response of multihole collimators was determined in closed form in frequency space. This closed form allows to derive all the known efficiency and resolution formulas of multihole collimators for the first time in the framework of a unique theory. The approach is very general since parallel beam, fan beam, cone beam and astigmatic collimators as well as all the most frequent hole array patterns and hole shapes can be described.

The point spread function in the space domain for a certain collimator and source position can be calculated via a discrete fast Fourier transform.

Predictions of the theory were compared with line source data acquired with a fan beam collimator for a range of source distances and lateral locations. Agreement of theoretical predictions with experimental data was excellent within the experimental errors derived from Poisson statistics.

Beside the complete theoretical definition of multihole collimators response, this theory allows the definition of accurate models of the geometric response for SPECT reconstruction and it is also suitable for designing new collimators.

OS-326

H.Bergmann^{1,2}, E.Dworak³, B.König³, A.Mostbeck², M.Šámal⁴

¹Dept. of Biomed.Eng. & Physics, University Hospital AKH, Vienna, Austria,

²L. Boltzmann Institute of Nuclear Medicine, Vienna, Austria, ³Hanusch Hospital, Vienna, Austria, ⁴Charles University Prague, Czech Republic

ACCURACY OF AUTOMATIC DIFFERENTIATION OF RENAL STRUCTURES IN DYNAMIC RENAL SCINTIGRAPHY USING FUZZY REGIONS OF INTEREST

The aim of the study was to evaluate the accuracy of a new method for the automatic definition of mutually overlapping fuzzy regions of interest of renal parenchyma and pelvis in dynamic renal scintigraphy. Using factor analysis, the parenchymal ROI has been extracted from the initial interval of renal uptake in which it can be well separated from the vascular background. The pelvic ROI was obtained by factor analysis of the third phase of the renogram in which it can be easily separated from the parenchyma. Pixel values in the resulting ROIs are proportional to local values of a membership function of each pixel of the specific region. The renal ROIs, together with the associated optimized factor images of vascular background, were stacked as column vectors into matrix V , and used to extract time-activity curves C from the original data D using $C=D \cdot V(V \cdot V)^{-1}$. In contrast to former experience with factor analysis, the time-activity curves obtained by the new method reflect more closely the expected physiological function. The most prominent feature we could observe with the new approach was the delayed offset of the pelvic curve. In order to check whether the length of the initial zero interval of the pelvic curve is related to the minimum parenchymal transit time, we have analyzed 46 kidneys in 28 patients randomly selected from a data base. Each study (MAG3) consisted of 120 images 64x64 (2 bytes per pixel) recorded in 10s intervals. Time activity curves from the fuzzy ROIs have been obtained using factor analysis as described above. Renal retention function has been calculated by matrix deconvolution of the parenchymal factor curve. As input function, the time-activity curve has been used from a manually selected cardiac ROI. No smoothing has been applied to the curves. The offset of the pelvic factor curve (PFCO) has then been compared with the minimum parenchymal transit time (PTTM). The mean value of PFCO (151.3 ± 58.5 s) did not differ significantly from that of PTTM (156.9 ± 76.9 s, $p>0.05$), and the individual values of both PFCO and PTTM were closely correlated ($r=0.79$, $p<0.0001$). The numbers support a conclusion already assumed after visual inspection of the curves: the new approach provides reliable separation of renal parenchyma and pelvis and may contribute to objective and standard quantitative evaluation of dynamic renal scintigraphy.

OS-327

V.Oikonen, ²P.Nuutila, ¹U.Ruotsalainen

¹Turku PET Centre and ²Dept. of Medicine, University of Turku, Finland

IN SKELETAL MUSCLE FDG-PET RATE CONSTANTS ARE IMPROVED BY MEASURED BLOOD FLOW

The addition of tissue blood volume (V_b) compartment in the FDG three compartment model is essential. In regions of low blood flow the tissue time-activity curves can be affected by differences between pre- and post-capillary intravascular radioactivity (C_a and C_v).

The femoral regions of three healthy subjects were studied with 90-min FDG-PET in basal state, and four subjects were studied during euglycemic hyperinsulinemic clamp. In addition to the arterial blood compartment, venous compartment was included in the FDG three compartment model as a function of tissue activity (C_t) and measured blood flow (f) as $C_v(t) = C_a(t) - (1 - V_b) dC_t(t) / f$.

In the basal state, the rate constants for plasma-to-tissue transport (K_1) were 0.015 ± 0.001 min⁻¹ and for phosphorylation (k_3) 0.021 ± 0.003 min⁻¹. In the clamp studies, the estimates were 0.028 ± 0.002 min⁻¹ and 0.26 ± 0.13 min⁻¹, respectively. Estimated blood volumes were 1.4 ± 0.3 % in the basal state and 3.2 ± 1.1 % during the clamp. If the venous blood compartment was ignored, the estimates were increased for K_1 and decreased for k_3 , being closer to the values reported by Kelley et al. (1996), but blood volume estimates were too low. The FDG influx constants (K_i) from Gjedde-Patlak plots were 0.0015 ± 0.0004 min⁻¹ in the basal state and 0.019 ± 0.006 min⁻¹ during the clamp.

The estimation of FDG rate constants in the skeletal muscle was reliable in basal state, when the venous blood compartment was included in the model. However, in the clamp studies especially k_3 was uncertain, and good initial values and restraints were necessary to obtain reasonable estimates from non-linear fitting. The FDG uptake constants from Gjedde-Patlak plots were reliable both in basal and clamp studies, and only minor bias was caused by ignoring the blood compartments.

OS-328

J. van den Hoff, W. Burchert, H. Fricke, G.J. Meyer, W.H. Knapp

Klinik für Nuklearmedizin, Medizinische Hochschule Hannover Germany

INFLUENCE OF DIFFUSION EFFECTS ON THE QUANTIFICATION OF TISSUE PERFUSION WITH PET

Quantification of tissue perfusion with PET is based on the assumption that concentration gradients in tissue are negligible throughout the investigation. This is a prerequisite for the use of compartment models. It was the purpose of this study to investigate the validity of this assumption for freely diffusible tracers.

Methods: As a model system we used the Krogh cylinder consisting of a single capillary and concentric tissue cylinder. For different input functions and perfusion values numerical solutions of the coupled convection/diffusion problem were determined. The finite velocity of diffusive equilibration and restricted membrane permeability were taken into account in the computations. For the resulting tissue response curves the usual quantification procedure based on the Kety-Schmidt one-compartment model was used for determination of the perfusion.

Our results show that for light tracer molecules with diffusion coefficients $D \approx 10^{-5}$ cm²/s and perfusion values up to about 1 ml/min/ml perfusion is overestimated by at most 10-20% within the framework of the Kety-Schmidt model. At high flow values the behaviour is more strongly dependent on the precise value of the membrane permeability. For typical perfusion values in myocardial stress investigations (3-4 ml/min/ml) perfusion is overestimated by about 30-40% if the permeability of the tracer is too high. This error is reduced if the permeability is slightly restricted. We arrive at the conclusion that for ideally permeable tracers the assumptions underlying the Kety-Schmidt model can be strongly violated in high flow areas. Experimental findings that compartmental modelling can yield quantitative results even under these conditions might be explained by a restricted permeability of the corresponding tracers.

Endocrinology/Thyroid

OS-329

GENOTOXIC OXIDATIVE DAMAGE IN PERIPHERAL BLOOD AFTER TREATMENT WITH 131-IODINE IN PATIENTS AFFECTED BY THYROID CANCER

The role of oxidative stress in genotoxic effects by irradiation has been well established. Irradiation and other stimuli, like metabolism itself, generate oxygen free radicals, able to induce reactive species (Clastogenic Factors, CF), generated by superoxide radicals, which can perpetuate and enhance the damage itself. Natural antioxidants, in cells and blood, oppose against genotoxic effects of free radicals. Post-surgical I-131 treatment in the management of thyroid cancer (TC) is generally recognized as safe therapy. Nevertheless, a genetic damage after I-131 irradiation has been proven in peripheral lymphocytes (LC). Little agreement has been reached on the duration of radiation-induced genetic damage, be it temporary or long-lasting. The aim of our study was to evaluate the oxidative and genetic damage in 6 patients (pts), affected by differentiated TC, undergone to a single I-131 dose (2.96-4.81 GBq) and never irradiated before. Blood samples were drawn just before and 2, 5, 7, 14, 30, 60, 90, 180 days after I-131 administration and analyzed for the presence of cytogenetic damage in their LC. The formation of micronuclei (MN) was used as a parameter for the assessment of structural and numerical chromosome aberrations. Both types of mutations are considered potentially dangerous for the formation of a iatrogenic secondary malignancy. From the plasma of these pts, a fraction possibly containing CF, was isolated and tested against LC from healthy donors to evaluate the induction of MN. We studied variations in two free radical scavengers, plasma vitamin E (α -tocopherol) and serum coenzyme Q10 (CoQ10) (an important lipid-soluble antioxidant that humans can both synthesize and regenerate from its oxidized form), by correlation with the production of plasma lipoperoxides. Plasma α -tocopherol and serum CoQ10 were determined by HPLC fluorimetric detection. As a consequence of single I-131 dose a significant peak of MN was observed within the first 2 weeks, followed by a decline without turning down to the spontaneous level. When the plasma fraction possibly containing CF was tested against LC from healthy donors, a significant increase of MN frequency was detected, suggesting that I-131 therapy have induced the formation of CF. These data point out that the observed induction of MN is reasonably determined by the initial exposure to I-131, while MN persistence might be due to the presence of CF. Our preliminary results, on the 14th day after I-131 administration, also showed a decrease in α -tocopherol plasma levels, not corresponding to total cholesterol variations but correlating with an opposite increase of plasma lipoperoxides. These results suggest that an oxidation of circulating vitamin E may have occurred. We also found a clear decrease in serum CoQ10, reaching a nadir on the 14th day after irradiation, and a slight increase but no recover to the former state, during the following 2 months. These data show a change in antioxidant response of CoQ10, maybe due to an increased request in tissues, during oxidative stress.

OS-330

D. Sandrock, H.F. Deckart, H. Grambow, B. Schicke, K. Baba, D. Noack, B. Kettner, and D.L. Munz

Clinic for Nuclear Medicine, Charité, Humboldt University Berlin, Clinic for Nuclear Medicine and Endocrinology, Clinic Berlin-Buch, Germany

PROGNOSTIC IMPACT FACTORS IN DIFFERENTIATED THYROID CARCINOMA - RESULTS OF TWO CENTERS

Aim of this study was the evaluation of a large series of patients with thyroid carcinoma from two centers with the same therapeutic regimen. Special attention was paid to factors with impact on prognosis and the effect of an additional percutaneous radiotherapy.

Overall, 1205 patients with differentiated thyroid carcinoma (papillary, 558; follicular, 647; women, 916; men, 289; mean age at time of diagnosis, 48 years) were studied with a mean follow-up of 10 years. All had total thyroidectomy followed by repeated radioiodine therapy (3.7 GBq) in order to obtain normal whole body scans. Patients with papillary carcinoma had the following T stage (in brackets, numbers of follicular carcinoma): pT₁, 15.6 % (5.7 %); pT₂, 50.4 % (50.3 %); pT₃, 21.2 % (30.5 %); pT₄, 12.8 % (13.5 %). Lymph node metastases were found in 38.4 % of the papillary and 18.2 % of the follicular carcinomas, distant metastases in 4.6 % of the papillary and in 16.5 % of the follicular carcinomas (49 % lung, 45 % bone, and 6 % at other locations). The 5- and 10-year survival rates were 94 % and 86 %, respectively, for papillary and 86 % and 73 %, respectively, for follicular carcinomas. Additional percutaneous radiotherapy had been given to 41.5 % of the patients studied. This group encompassed more T_{3,4} stages than the group without radiotherapy (67.4 % vs. 31.2 %). However, by matching groups with equal stages there was no significant difference of the 5- and 10-year survival to be observed. In a multivariate analysis factors with impact on (worse) prognosis were: larger tumor size, metastases, and higher patient age at time of diagnosis.

Conclusion: The differentiated thyroid carcinoma treated conventionally by surgery and radioiodine has a relatively good overall prognosis. Prognostic factors are tumor stage and patient age. Additional radiotherapy does not improve survival.

OS-331

D. CASARA, G. SALADINI, R. MAZZAROTTO, D. RUBELLO*, A. FASSINA**, M.E. GIRELLI***, B. BUSNARDO***.

Radiotherapy and Nuclear Medicine, **Pathology, and ***Endocrinology, University Hospital of Padua; *Nuclear Medicine, Hospital of Castelfranco V.to (TV), Italy.

HAS DIFFERENTIATED THYROID CARCINOMA (DTC) IN CHILDREN AND ELDERLY A DIFFERENT BEHAVIOUR IN COMPARISON WITH ADULT PATIENTS ?

We evaluated 314 pts with DTC, taken out from the general series (GS) of 2,786 DTC pts followed-up in our center from 1967 to 1994 (minimum follow-up 3 yrs). There were 62 pts younger than 15 yrs old (group A), and 252 pts older than 65 yrs old (group B). F/M ratio was similar in the two groups (1.3:1 vs 1.4:1); it was 3.2:1 in the GS of DTC pts. Papillary/follicular ratio was higher in group A than in group B (4.9:1 vs 1:1, p < .01); it was 3.6:1 in the GS. Local extrathyroid tumor extension was high in both group A and group B (28.3% and 35%); it was 6% in the GS. Prevalence of loco-regional lymph node metastases - mts (LNM) was higher in group A than in group B (72.5% vs 48%, p < .05); it was 64% in the GS. Regarding distant mts (DM), in group A were found exclusively pulmonary mts (PM), 19.3%, in most cases not radiologically visible (microscopic pattern) (75%), while PM in group B were found in 21.9% of pts, radiologically visible (macroscopic pattern) in 100% of cases. Furthermore, bone mts (BM) were observed exclusively in group B (19% of cases). Prevalence of PM and DM in the GS was 11.6 and 8%, respectively. 131-I uptake was present in all pts from group A while in only 64.5% of pts from group B; it was 81.5% in the GS. Complete disease remission was observed in 93.5% of pts from group A and in 18.8% of pts from group B. Tumor-related mortality was 0% in group A and 28% in group B, after a minimum 3-yr follow-up. Due to the high frequency of local extrathyroid tumor spread, and of loco-regional LNM and of DM in both pediatric and elderly pts, an aggressive therapeutic approach is recommended, i.e. total thyroidectomy plus loco-regional lymph node resection and 131-I therapy. Furthermore, because of the high prevalence of non-functioning mts and BM in elderly pts, it has to be taken into account external radiotherapy and systemic chemotherapy in these pts.

OS-332

M.Geling, J.Farahati, P.Köck, S.Muffert, U.Mäder, Chr.Reiners

Department of Nuclear Medicine, Tumorcenter, University of Würzburg, Germany

PROGNOSTIC FACTORS FOR ANAPLASTIC THYROID CARCINOMA

Background: Anaplastic thyroid carcinoma (ATC) has a dismal prognosis. We reviewed our experience during a 15-year period to clarify prognostic factors and the effect of therapeutic regimens on outcome of patients with ATC.

Methods: The case records of all patients with anaplastic carcinoma (n=42) referred to our center between 1981 and 1995 were reviewed and all cases with histologically proven anaplastic carcinoma were included in our retrospective study. The influence of the prognostic factors tumorstage, lymphnode involvement, metastatic status (according to TNM-classification), sex and therapeutic regimen on survival time was tested by multivariate discriminant analysis. Life expectancy was calculated by Kaplan-Meier survival ship function.

Results: Mean age at time of diagnosis was 67.8 years (range: 45-84 years) with a sex ratio female to male of 5.3 : 1. Main symptom was a rapidly growing thyroid nodule (83%), other symptoms were dyspnea (31%), hoarseness (26%) and dysphagia (26%). 76% of all patients died during the first six months after diagnosis, only 4 patients survived more than one year.

		number	median time of survival (months) ± SD	P
tumorstage	pT1-3	6	6±3.6	=0.85
	pT4	36	5.3±8.6	
lymphnode-involvement	pN0	5	8±4.1	=0.07
	pN1	18	4.2±3.9	
metastases	M0	24	7.2±10.1	=0.08
	M1	18	2.8±2.2	
sex	female	34	7.3±14.1	=0.38
	male	8	5.1±3.5	
therapeutic regimen	operation (op)	12	1.9±1.8	=0.02
	op+radiotherapy	8	5.6±4.5	
	op+radiochemotherapy	12	1.9±1.8	<0.01
		9	7.1±3.3	

Conclusion:

In the light of the poor prognosis of anaplastic thyroid carcinoma sex, tumorstage, lymphnode involvement and the presence of distant metastases don't seem to have essential influence on survival time. Patients treated with a multimodal therapeutic regimen consisting of surgical resection, external radiation and chemotherapy have a longer median time of survival compared to those operated only.

Cardiovascular: Radiopharmaceuticals for CA

OS-333

S. Gerali, V. Prassopoulos, Th. Athanassoulis, N. Sifakis, E. Papadaki, J. Lekakis, S. Stamatelopoulos P. Kostamis
Depts of Nuclear Medicine and Clinical Therapeutics «Alexandra»
University Hospital, Athens, Greece

THE DIAGNOSTIC VALUE OF THE INDIUM-111-ANTIMYOSIN MYOCARDIAL SCINTIGRAPHY COMBINED BY VIRUS-BACTERIOLOGICAL CONTROL FOR THE ACCURATE DIAGNOSIS OF ACUTE MYOCARDITIS

Indium-111-antimyosin scintigraphy (IAS) is useful to detect the presence of myocyte lesion. Myocardial necrosis is an essential feature of myocarditis. IAS has been performed in relation with endomyocardial biopsy (EB) for definite diagnosis. In the present study we estimated the significance of IAS followed by virus-bacteriological control (VBC) in patients with suspect acute myocarditis.

Methods : Twenty-one patients (pts) presenting clinical figure of acute myocarditis were studied. Twelve pts (2 women, 10 men, mean age 36 ± 13 years) with EB formed Group A, and 9 pts mean age 32 ± 11 years with VBC formed Group B respectively. All pts underwent IAS 48 hours after intravenous administration $2mCi$ In-111-antimyosin. Heart to lung ratio (H/L) was calculated. A H/L ratio $>1,6$ was considered abnormal. As control group of 5 subjects with low probability of myocarditis were used.

Results: All pts in both Group (A,B) presented abnormal antimyosin uptake in myocardium (H/L in Group A was $2,1 \pm 0,3$ and $2,04 \pm 0,24$ in Group B respectively, ns). In Control Group H/L ratio was $1,3 \pm 0,1$, a difference was considered statistically significant ($p < 0,001$). In Group A 8/12 pts had positive endomyocardial biopsy (66%). In 6/9 pts of Group B the VBC was positive (66%).

In conclusion : In-111-antimyosin scintigraphy plays a primary role as a non-invasive method for diagnosing of pts suffering from acute myocarditis. A combined application of the IAS and VBC could be considered as an absolute confirmation in diagnosing of acute myocarditis. Consequently, the myocardial biopsy as an invasive method, and with low sensitivity could be omitted.

OS-334

C. Boizati, A. Boschi, L. Uccelli, A. Duatti, R. Pasquaini, A. Piffanelli
Laboratory of Nuclear Medicine, Department of Clinical & Experimental Medicine, University of Ferrara, Italy, CIS bio international, France.

MIXED DITHIOCARBAMATE-PHOSPHINE-THIOL Tc-99m COMPLEXES AS IMPROVED MYOCARDIAL PERFUSION AGENTS

Bis(N-Ethoxy, N-Ethyl-dithiocarbamate) nitrido Tc-99m (Tc-99mN-NOEt) is a new imaging agent currently under clinical evaluation as tracer for myocardial perfusion. This second-generation heart imaging agent exhibits a thallium-like behavior, and undergoes redistribution in viable-ischemic myocardium. Along with this major advantage, Tc-99mN-NOEt shows initial significant lung uptake and prolonged liver localization. In this work, we attempted to improve the biological behavior of Tc-99mN-NOEt by decreasing lung and liver retention. Following our previous finding that Tc-99m complexes with phosphine-thiol ligands exhibit significant heart uptake and fast lung and liver washout, we tried to assemble into the same complex one dithiocarbamate ligand and one phosphine-thiol ligand to produce a mixed complex. The final goal of this design was to impart to the resulting product properties originating from the presence of both type of ligands.

The high-yield synthesis of the mixed complexes was carried out through a two-step procedure involving the preliminary preparation of the complex Tc-99mN-NOEt followed by substitution of one dithiocarbamate ligand by one phosphine-thiol ligand. The biodistribution of the mixed complexes in rats showed that they are generally retained into the myocardium for a prolonged time, but that the uptake was approximately half of that observed for Tc-99mN-NOEt. Washout from the lungs was extremely fast, and liver activity was rapidly metabolized and eliminated into the intestine. The specific kinetic properties in organs of interest of each complex was determined and it was found to depend on the chemical nature of lateral substituents on phosphine-thiol ligands.

OS-335

M.J. Welch, J.S. Lewis, D.W. McCarthy, T. Sharp, P. Herrero, T.J. McCarthy, *Y. Fujibayashi.

Division of Radiological Sciences, Department of Radiology, Washington University Medical School; *Biomedical Imaging Research Center, Fukui Medical University.

EVALUATION OF COPPER-60 DIACETYL-BIS(N4-METHYLTHIOSEMICARBAZONE) (CU-ATSM), A HYPOXIA IMAGING AGENT, IN CANINE MODELS OF ISCHEMIA.

Fluorine-18 labeled fluoromisonidazole has been used for the PET imaging of hypoxia in brain, myocardium and tumors. Although uptake in ischemic tissue has been visualized, this agent suffers from several deficiencies including a long synthesis time and the fact that imaging needs to be carried out at 2 to 4 hrs post-injection to allow the washout of the tracer from normoxic tissue. Fujibayashi and co-workers have shown that copper-62-ATSM is effective in the rapid detection of hypoxic viable tissue (Fujibayashi et al., JNM 1997; 38:1155-1160). Copper-60 is a 23.4 min half-lived nuclide decaying 93% by positron emission which can be produced in high yield and at high purity using the proton beam of compact biomedical cyclotrons (Bass et al., J Label Compds Radiopharm 1997; 40:325-327). Copper-60-ATSM can be prepared in a time of ~1 hour including the cyclotron target irradiation, copper-60 purification and copper-60-ATSM preparation. Two canine models of ischemia were used to evaluate this tracer. In the first model, myocardial ischemia was caused by the occlusion of flow in the Distal Left Anterior Descending (LAD) coronary artery and secondly a non-acute model was used where the canine was subjected to a breathing atmosphere of 10% oxygen and 90% nitrogen. In the second model the oxygen blood saturation of the dog was directly monitored at all times and oxygen saturation decreased to approximately 35% of normal. In both models, blood flow was determined using oxygen-15 labeled water and in the non-acute model, fluorine-18 fluoromisonidazole was also studied. Copper-60-ATSM rapidly washed out of normoxic myocardium and was trapped in hypoxic myocardium. A simple two compartment model was used to model the uptake and washout of the tracer over the first ten minutes post-administration. In both animal models significant differences were obtained in the appropriate model parameters. When the model was applied to the uptake and washout of fluorine-18 fluoromisonidazole, no significant differences in these model parameters were seen. This study confirms the potential usefulness of copper labeled ATSM for the detection of ischemic myocardium; copper-60-ATSM can be readily prepared in any center with a biomedical cyclotron and be used for this purpose.

OS-336

R. Lebtahi, JL. Trouillet, M. Faraggi, L. Sarda, N. Delahaye, C. Labriolle-Vaylet, J. Chastre, C. Gibert, D. Le Guludec
Hôpital Bichat, Paris, France.

FOLLOW-UP OF SURGERY FOR MEDIASTINITIS AFTER STERNOTOMY : USEFULNESS OF ^{99m}Tc -HMPAO-LABELED LEUKOCYTES SCINTIGRAPHY

Management of patients suspected to relapse after initial surgical drainage for mediastinitis following cardiac surgery is difficult. To evaluate the usefulness of ^{99m}Tc -labeled leukocytes scintigraphy to decide a surgical re-debridement, 13 patients all treated by closed drainage technique using Redon catheters were consecutively included. Patients referred for radiolabeled leukocytes scintigraphy 3 weeks after a primary surgical drainage, because of cutaneous abnormalities (n=5), persistent fever (n=4) or positive bacterial cultures (n=4), despite a sustained antibiotic therapy. Primary thoracic surgery was aortic surgery (n=2), valvular replacement (n=3) or coronary artery bypass grafting (n= 8). Planar thoracic imaging in anterior, posterior and lateral views were performed during 10 minutes, 1 hr, 4 and 24 hrs after injection of 110 to 185 MBq of ^{99m}Tc -HMPAO-labeled leukocytes. The final diagnosis was assessed either by a 3 to 6 months clinical and biological follow-up (n=8) or by bacterial growth on cultures and/or histological samples obtained during surgical re-debridement (n=5). Radiolabeled leukocytes scintigraphy found sternal or mediastinal infection in 4 patients, without false positive cases but was falsely negative in 2 patients. The 7 other negative patients were true negative cases. Therefore, sensitivity, specificity, positive and negative predictive values were respectively 67, 100, 100 and 78 %.

We conclude that a positive ^{99m}Tc -HMPAO labeled leukocytes scintigraphy is useful to decide another surgery in patients suspected of persistent local infection following primary debridement for mediastinitis after sternotomy.

Oncology: FDG

OS-337

S. Stroobants, J. Vansteenkiste, P. Dupont, P. De Leyn, W. De Wever, E. Verbeken, G. Deneffe, L. Mortelmans.
Department of Nuclear Medicine, Pneumology, Thoracic Surgery, Radiology and Pathology, UZ Gasthuisberg KU Leuven, Belgium.

VALUE OF FDG-PET IN THE EVALUATION OF DOWNSTAGING AFTER INDUCTION CHEMOTHERAPY IN PATIENTS WITH NON-SMALL CELL LUNG CANCER (NSCLC)

Purpose: Clearance of viable tumor cells in mediastinal lymph nodes (MLN) by induction chemotherapy (IC), so called downstaging, is an important prognostic factor in patients with N2 NSCLC. Based on the good results obtained with PET in chemo-naïve patients and because CT is inaccurate and remediastinoscopy is technically not always feasible, we investigated whether FDG-PET after IC could accurately predict downstaging and therapeutic outcome.

Methods: Attenuation corrected PET images of the thorax were acquired before and at the end of IC. Any focal FDG uptake higher than mediastinal bloodpool activity was scored positive. PET results were correlated with survival and with pathology of the MLN when available.

Results: Fifteen pts with biopsy proven N2 NSCLC, were prospectively included. Final locoregional therapy after IC consisted of either surgery (n=9, group A) or radiotherapy (n=6, group B).

In group A, 3/9 pts had persistent focal FDG uptake in the mediastinum. Correlated with histology the accuracy for PET to predict downstaging was 100% whereas CT obtained only 67% (2 FP, 1 FN). All 3 pts with a positive mediastinal PET developed systemic relapse within 12 months, compared to only 1 pt when PET showed no abnormal mediastinal uptake (median follow-up: 10 months, range: 4.5 - 23.5 months).

In group B, 4/6 pts had a positive mediastinal PET, all died of systemic relapse within 12 months whereas the 2 pts with a normal mediastinal PET are still disease free (follow-up: 8 and 16 months).

Conclusion: A persistent positive mediastinal PET after induction chemotherapy predicts a poor prognosis probably because of the accurate detection of residual mediastinal tumor involvement. If these preliminary findings are confirmed in larger studies, PET is the first non invasive tool that can accurately predict downstaging and select patients for further intensive locoregional therapy after induction chemotherapy.

OS-338

B.M. Dohmen, C. Bokemeyer, K. Oechsle, A. Ch. Pfannenber, R. Lietzenmayer, M. Sötker, C.D. Claussen, L. Kanz, R. Bares
Dep. of Nuclear Medicine, Internal Medicine II and Diagnostic Radiology, University Hospital Tübingen, Germany.

HIGH-DOSE CHEMOTHERAPY IN GERM CELL CANCER: IS FDG-PET ABLE TO PREDICT THE FINAL OUTCOME?

According to current results long term remissions can be achieved by high-dose (HD) chemotherapy in only 30-40% of patients with advanced germ cell cancer. Thus, better selection of patients who will profit from this therapy is needed. The presented pilot study was initiated to evaluate the prognostic value of FDG-PET prior to HD-chemotherapy.

FDG-PET was performed approx. 3 weeks after completion of induction chemotherapy. Patients with complete remission at this moment were excluded. So far 12 patients were enrolled and have completed the study protocol (finished HD-chemotherapy, 3 month follow-up). PET-findings were analyzed visually and quantitatively by calculating SUV. Success or failure of high-dose chemotherapy was determined by clinical follow-up or biopsy.

All patients who reached a complete remission after HD-chemotherapy (n=5) had a completely normal PET-scan after induction chemotherapy. CT demonstrated stable disease (n=2) or partial remission (n=3) at that time. Failure of HD-chemotherapy occurred in 7 patients. 4 of them had residual tumor viability (SUV = 1.6 / 2.4 / 2.8 / 12), 3 were negative. In 2 of these patients PET showed faintly positive pulmonary lesions (SUV = 1.1 resp. 1.0) which turned out to be teratoma. In the third case (teratocarcinoma) the PET study was performed against protocol too early (< 3 weeks) after completion of the induction chemotherapy, which might have caused the false negative finding.

We conclude, that increased FDG-uptake after induction chemotherapy, is highly predictive for failure of subsequent high-dose chemotherapy. The prognostic value of normal PET-findings is limited due to the low FDG-uptake of teratoma. Thus, FDG-PET might be able to improve patient selection for HD-chemotherapy.

OS-339

M.P.M. Stokkel(1), H. Stevens(1), M.J.B Taphoorn(2), P.P. Van Rijk(1).

University Hospital Utrecht, The Netherlands, Departments of Nuclear Medicine,(1) and Neurology(2)

DIAGNOSIS OF RECURRENT BRAIN TUMOR: VALUE OF TL-201 SPECT VS 18F-FDG USING A DUAL HEAD COINCIDENCE CAMERA.

Introduction: CT and MRI imaging suffer from significant limitation when they are used to differentiate recurrent brain tumor from radiation induced necrosis. Measurement of 18F-FDG uptake using Positron Emission Tomography (PET) and Tl-201 SPECT are useful to distinguish local recurrence from radiation effects in the brain. However, dedicated PET scanners are not widely available. With a dual head SPECT scanner with coincidence module (ADAC MCD), PET scanning of 18F-FDG is possible, with a spatial resolution of 5 mm.

Methods and Materials: Sixteen patients suspect for having recurrent brain tumor were studied. After a 6 hours fast, at 30 minutes after intravenously injection of 120 MBq Tl-201, all patients underwent imaging of the head. Then 130 MBq 18F-FDG was injected and acquisition was started 1 hour p.i. Images were visually interpreted and quantified using the thallium-index and a FDG-grading scale. The final diagnosis of tumor recurrence was based on clinical course and/or follow-up CT or MRI.

Results: Mean follow-up was 9.6 months (range: 5-14 months). Twelve patients demonstrated local recurrence. Tl-201 SPECT scans correctly detected all, whereas 18F-FDG PET detected 8 of 12 recurrences. No false positive results were found. Tl-201 showed a significant higher detection rate compared with 18F-FDG (p=0.023). No correlation was found between the thallium-index and the FDG grade (r=-0.041).

Conclusion: 201Tl SPECT is superior to 18F-FDG using a dual head coincidence camera in distinguishing recurrent brain tumor from necrosis.

OS-340

L. Aloj, C. Caraco', W.C. Eckelman and R.D. Neumann

Nuclear Medicine and PET Departments, Warren G. Magnuson Clinical Center, NIH, Bethesda MD.

OVER-EXPRESSION OF GLUT-1 DOES NOT YIELD INCREASED FDG UPTAKE IN CANCER CELL LINES.

We are evaluating the relationship between GLUT-1 expression and FDG uptake in cancer cell lines. We have previously shown that there is high variability in the amount of GLUT-1 expressed by different cells. In the cell lines we have characterized, GLUT-1 levels do not correlate with FDG uptake, but there is a good correlation between FDG uptake and hexokinase activity. We have now over-expressed the GLUT-1 gene by transfection into two cancer cell lines to investigate if increasing the amount of GLUT-1 in a cell affects FDG uptake. Wild-type (WT) A431 cells, derived from a human epidermoid carcinoma, express 10-20 times more GLUT-1 mRNA and protein than WT T47D cells, derived from a human breast carcinoma. Both cell lines were transfected with a plasmid containing the entire coding region of the human GLUT-1 gene under a strong viral promoter. One positive A431 clone expressing GLUT-1 was selected (AGT1) and one T47D clone (TGT1). The AGT1 clone expresses ~ 5 times more GLUT-1 mRNA than WT A431, while TGT1 cells express >70 times more GLUT-1 mRNA than WT T47D. The initial transport rates of 3-O-methyl glucose (3OMG) and FDG were found to be virtually identical in the WT A431 compared to the AGT1 clone, as was the rate of FDG incorporation from 10 to 30 min. In TGT1 cells, the initial transport rates of 3OMG and FDG were found to be higher than for WT T47D. Surprisingly, the rate of FDG incorporation between 10 and 30 min was 30% lower in TGT1 cells than T47D. In conclusion, overexpression of GLUT-1 in these cell lines does not yield increased FDG uptake as one would expect. This suggests that the GLUT-1 alone does not regulate the amount of FDG taken up by cancer cells.

OS-341

R. Tiling, R. Linke, K. Brinkbäumer, G. Konecny, K. Tatsch, K. Hahn

Departments of Nuclear Medicine and Gynecology, University of Munich, Munich, Germany

FDG-PET AND SESTAMIBI-SPECT FOR MONITORING BREAST CANCER RESPONSE TO NEOADJUVANT CHEMOTHERAPY: PRELIMINARY RESULTS

The purpose of this comparative study was to evaluate whether FDG-PET and/or sestamibi-SPECT are suitable to monitor the response of extended breast carcinomas to high dose neoadjuvant chemotherapy.

Up to now, 3 patients with extended breast cancer (tumor size approx. 5 cm) under-went both, FDG-PET and sestamibi-SPECT before, during (day 8 and 28) and after chemotherapy. PET studies were performed acquiring emission and transmission data (200 MBq F-18 FDG). SPECT data were acquired using a 360° rotation (3° steps, 20 sec/step) after injection of 740 MBq Tc-99m sestamibi. Images were analysed visually and (semi)quantitatively calculating the mean standardized uptake value of the tumor (SUV) in PET and a ratio between sestamibi-uptake of tumor and lung tissue (T/L-ratio) in SPECT. The results of both methods were correlated and compared with the histopathologic findings.

The results are summarized in the table below. There was a good correlation

Pat.	tumor-size (mammogr.)	(SUV / T/L-ratio)				tumor-size (histopath.)
		pre-chemoth.	chemoth. (day 8)	chemoth. (day 28)	post-chemoth.	
N.M.	approx 5 cm	5.0 / 0.7	2.7 / 0.4	1.7 / 0.2	1.0 / 0.1	0.3 cm
P.J.	approx 5 cm	2.1 / 0.7	1.9 / 0.6	1.5 / 0.4	1.1 / 0.3	2.2 cm
W.C.	approx 5 cm	4.2 / 1.1	2.3 / 0.8	1.5 / 0.8	1.6 / 0.4	3.8 cm

between SUV and T/L-ratios ($r=0.63$, $p<0.05$). In all 3 patients significantly decreasing tracer uptake during chemotherapy was observed ($r=0.99$, 0.99 , 0.73). As an early sign of tumor response, SUV and T/L-ratios decreased already 8 days after the first chemotherapy. The further decline of FDG- and sestamibi-uptake correlated well with the histopathologic outcome. In the one case of nearly complete remission (N.M.) preoperative FDG-PET as well as sestamibi-SPECT were considered normal. The patients with proven residual invasive carcinoma showed visually a persisting clear (W.C.) and faint (P.J.) tracer uptake with both techniques.

The preliminary data indicate that sestamibi-SPECT may be as useful as FDG-PET for monitoring the response of breast carcinoma to neoadjuvant chemotherapy.

OS-342

H. M. Abdel-Davem, H. El-Zeftawy, G. Rosen, S. Naddaf, M. Kumar, S. Atay.

St. Vincent's Hospital and Medical Center, Nuclear Medicine Section, Dept. of Radiology, Dept. of Medical Oncology St. Vincent's Clinical Cancer Center, Valhalla, New York

How useful is repeated F-18 FDG scans in Evaluation of Therapy Response in Advanced Bone and Soft Tissue Sarcoma?

Aim of the study: Review the results of F-18 FDG studies for evaluation of treatment response (surgical, chemotherapy and radiotherapy) in patients with advanced bone and soft tissue sarcoma.

Material and Methods: 17 patients with known recurrent or metastatic bone and soft tissue sarcomas had 64 lesions detected by CT and/or MRI in different areas including the pelvis, retroperitoneum, head and neck, and lower limbs that we were able to follow on subsequent studies, and had 44 F-18 FDG studies. Patients were properly prepared by fasting over night (fasting blood sugar levels ranged between 60-100mg/dl), injected 5-7 mCi F-18 FDG, Laid supine for at least an hour and imaged using Dual Head Coincidence Imaging (DHCI) device (ADAC-MCD division). Data acquired in 32 projections for at least 40 seconds /projection. Data processed using iterative reconstruction without attenuation correction. Data interpreted visually by at least 3 observers and by calculating tumor to normal background (T/B) ratio. Results were confirmed by clinical data or a minimum of 3 months follow up. **Results:** FDG studies were true positive for viable tumor tissue in 42 lesions with T/B ratio ranged from 1.1 - 6.6. aver: 1.66 +/-1.03. False positive in 8 lesions that proved to be post operative changes on follow up, with T/B ratios ranging between 1.2 - 1.7. aver: 1.37 +/- 0.2. No FDG uptake (true negative) was identified in 14 sites (follow up after definitive treatment, surgical excision or adjuvant therapy) with T/B ratio ranged from 1 - 2.2. Aver 1.25 +/- 0.54. T/B ratio dropped in 41 of the 42 positive lesions from an average of 1.68 +/- 1.13 to 1.49 +/- 0.93 except for one lesion where T/B ratio increased from 1.3 before treatment to 1.7 after treatment (mixed response in the same patient). The ratio response correlated well with clinical response, X-ray CT and MRI.

Conclusion: repeated F-18 FDG imaging before and after treatment using DHCI is a reliable technique for evaluation of therapy response. T/B ratio is sensitive in detecting the variable response to treatment, its values are lower than expected because of absence of attenuation correction.

Oncology: Single photon

OS-343

Lamki, L.M., Dandia, F., Barron, B., Ephron, V., Fang, B.

The University of Texas Medical School and Hermann Hospital, Houston, Texas, USA

CORRECTING FOR SPECT ARTIFACTS DURING TC-99M LABELED MONOCLONAL ANTIBODIES IMAGING BY "CLAMPING" OF THE HIGH COUNTS REGIONS: A NOVEL APPROACH

PURPOSE: To overcome the "Flaring" and the "Shadow" artifacts observed in SPECT imaging of Tc-99m labeled monoclonal antibodies (Mab) due to the very high counts observed in liver, spleen, kidneys and bladder, which interfere with the detection of low count lesions in the vicinity.

METHODS: 17 patients studied with Tc-LL-2 (anti-Raji for lymphoma), Tc-MN3 (anti-Leukocyte for appendicitis) and Tc-Arcitumomab (anti-CEA for colon carcinoma) were included in this study. Organs with high physiologic accumulations were "clamped" down to the highest count per pixel of the neighboring low count background tissues using the raw ECT data and Trionix/SunSparc Station.

RESULTS: 10 new lesions were detected which would not have otherwise been seen because of the SPECT reconstruction artifacts of "Flare" or "Shadow" phenomenon. 14 other lesions were visualized more clearly than they were before "clamping". In addition, some suspected lesions were ruled-out, thus raising sensitivity and specificity. Anatomy of the spine & pelvis was also more clearly defined.

CONCLUSIONS: 1) SPECT artifacts of "Flare" & "Shadow" phenomenon can be overcome by "clamping" the raw ECT data of Tc-labeled monoclonal antibodies; 2) New lesions can be detected raising the sensitivity of SPECT imaging for lesions near liver, spleen, kidney & bladder; 3) Improved visualization of lesions can increase the physician's confidence in interpretation of antibody SPECT images and improve specificity; 4) Better delineation of spine & pelvis anatomy can also be achieved.

OS-344

M. Gómez-Río, M.D. Martínez del Valle, A. Rodríguez, M. Ureña, M.A. Muros, M.J. Acosta, J.M. Llamas,* F. Villanueva. Servicios de Medicina Nuclear y *Radioterapia. Hospital "Virgen de las Nieves". Granada. Spain.

RADIONECROSIS vs TUMORAL RECURRENCE IN BRAIN TUMORS: DIAGNOSIS USING Tl-201 SPECT.

Introduction: After the surgical and/or radiotherapeutic treatment of brain tumors is difficult for CT and MRI to differentiate gliosis and necrosis post treatment from viable tumour. **Objective:** Expose our experience in the diagnosis of tumoral recurrence vs radionecrosis in brain tumours using Tl-201 SPECT.

Patients: A total of 82 patients diagnosed of the primary tumor as: Astrocytoma (72%), Glioblastoma Multiforme (16%), Oligodendroglioma (4%) and others (8%).

Method: Fifteen min. after i.v. injection of 5mCi (185 MBq) Tl-201-Chloride SPECT acquisition was performed (64 frames, 30s/frame). ²⁰¹Tl was reported as: negative (no uptake), unclear (uptake 1-1.2% in comparison with the contralateral side), positive low-grade (uptake 1.2-1.5% in comparison with contralateral site) and positive high-grade (uptake >1.5%).

All patients were studied with neurostructural explorations (single and enhanced CT and/or MRI). Eighteen patients (22%) had pathological confirmation. The evolution of patients was examined as favorable or unfavorable using oncology criteria.

Results. Tl-201 scan: was inconclusive in 8% of the patients. All patients needed various neurostructural studies: CT ($\kappa=4.3$) which was inconclusive in 65% and MRI ($\kappa=2.6$) which was inconclusive in 17% of cases.

Findings between ²⁰¹Tl scan and neurostructural explorations coincided topographically in 79% of cases; in 18% Tl-201 scan showed tumoral activity in the foci and in another location and in 4% were completely discordant.

The best concordance with the clinical evolution was established using both MRI and ²⁰¹Tl scan ($p<0.01$ Chi-Square test), better than using only MRI or ²⁰¹Tl scan.

The best concordance with the pathological findings was found with Tl-201 scan ($p<0.05$ Chi-Square test). In patients with histological confirmation (n=18) sensibility was 83% and specificity 83%, PPV=90% and NPV=71. Two cases were false negatives (low grade astrocytomas) and one false positive (3 months after surgical treatment?).

OS-345

T.M. Behr¹, S. Gratz¹, M. Conrad¹, J. Meller¹, H.J. Hansen², G.L. Griffiths², C. Goldenberg², D.M. Goldenberg³, and W. Becker¹.
Dept. of Nuclear Medicine¹ of the Georg-August-University of Göttingen, Germany; Immunomedics, Inc.², Morris Plains, NJ, and Garden State Cancer Center³, Belleville, NJ, USA.

INTRAINDIVIDUAL COMPARISON OF COMPLETE IgG VERSUS Fab' FRAGMENTS OF THE ^{99m}Tc-LABELED ANTI-NCA-90 ANTIBODY, MN-3, FOR BONE MARROW SCINTIGRAPHY.

Immunoscintigraphy with antibodies which are directed against granulocyte-associated antigens (e.g., nonspecific crossreacting antigens [NCA]) has been shown to be a sensitive and reliable tool for the early diagnosis of focal bone marrow involvement, e.g., by bone (marrow) metastases. The aim of this study was to compare IgG and Fab' of the ^{99m}Tc-labeled monoclonal anti-NCA-90 antibody, MN-3, in this setting intraindividually.

A total of twenty patients with malignancies, which tend to metastasize into the bone (e.g., breast, prostatic, head and neck cancers, non-Hodgkin's lymphoma, plasmocytoma), underwent bone and bone marrow scintigraphy within 2 weeks. For bone marrow scanning, ^{99m}Tc-labeled MN-3 IgG and Fab' (15 mCi each) were administered to the patients in randomized order within 4 days. Five patients each received protein doses of 0.25, 0.50, 1.0, or 1.3 mg (identical protein doses of IgG or Fab' in the same patients). Whole-body scans were performed at 30-60 min., 4-6, and 18-24 h p.i. The final assessment was performed in correlation to the results of other diagnostic modalities (x-ray, CT, MRI, and bone marrow biopsy).

The overall lesion-based sensitivities of IgG and Fab' were 92% and 76%, respectively. Additional lesions, not known from bone scanning, were found in 4 pts. with Fab', as compared to 5 with IgG. Four lesions could be clearly diagnosed with IgG, but would have been completely missed by Fab'. In 4 patients, bone involvement, as suspected from bone scanning, was excluded by normal bone marrow scans, whereas both, IgG and Fab' were able to identify focal lesions in two plasmocytoma patients with a normal bone scan. No difference was found with respect to the various protein doses. However, IgG showed a significantly faster (!) blood clearance than Fab' (with rapid uptake in the bone marrow, liver and spleen; "endogenous background subtraction"). Therefore, diagnostically useful scans were obtained with IgG as early as 30 - 60 min. p.i., in contrast to 4-6, sometimes even at 24 h with Fab'.

These data show that the ^{99m}Tc-labeled anti-NCA-90 antibody, MN-3, is suitable for bone marrow imaging, and protein doses as low as 0.25 mg are sufficient. IgG is diagnostically clearly superior to its fragment, which is due to its more rapid clearance and, thus, better target/non-target ratios, probably because of the higher avidity and binding affinity of the bivalent IgG.

OS-346

C. Soler, JL Perrot, O. Thiffet, S. Boucheron, F. Cambazard, F. Dubois.

CHU Saint-Etienne, Hôpital Bellevue, Dept of Nuclear Medicine, France.

THE ROLE OF ^{99m}Tc-SESTAMIBI SPECT FOR THE DETECTION OF THE LYMPH NODE METASTASES DURING THE FOLLOW UP OF PATIENTS HARBORING CUTANEOUS MALIGNANT MELANOMA: A PROSPECTIVE STUDY (ABOUT 48 PATIENTS).

The potential of ^{99m}Tc-Sestamibi (MIBI) for the detection of lymph node metastasis (axillary, groin, or cervical areas) of cutaneous malignant melanoma was investigated in a prospective study. At the present time, after gaining their informed consent, 48 patients were included. The ^{99m}Tc-MIBI scintigraphy was assessed in comparison with the post surgical anatomopathological examination of the resected lymph nodes. In all cases, planar imaging and SPECT imaging of the clinical suspected sites were performed 15 minutes after intravenous injection of 1110 MBq of ^{99m}Tc-MIBI. A double field-of-view gamma camera and a high-resolution low-energy collimators were used. ^{99m}Tc-MIBI scintigraphy was positive for 26 patients showing uptake of ^{99m}Tc-MIBI in the axillae, groin and cervical areas. These results were histopathologically confirmed to be lymph node metastases from melanoma in 25 patients. No MIBI uptake was found in 24 patients. These results were also histopathologically confirmed for 22 patients. So, our preliminary results show a high sensitivity and specificity (93% and 96% respectively). Usually, the detection of the metastases of malignant melanoma is performed by radioimmunoscintigraphy, ¹²³I Iodoamphetamine, radioiodine-123-iodobenzamide or indium-111-pentetreotide. The availability of cyclotron production is a significant disadvantage with radioiodine-123 or indium-111, and, on the other hand, the radioimmunoscintigraphy is not easy to make us of. Furthermore, ^{99m}Tc-MIBI have been shown to be effective radiopharmaceuticals in the detection of various tumors, including, recently malignant melanoma and his lymph node and/or visceral metastases. So, ^{99m}Tc-MIBI seems to be a simple method for the detection of metastatic lymph node melanoma. In the future, if our preliminary results are confirming, we hope to avoid unnecessary surgical resection of lymph nodes and to detect much earlier lymph node metastases.

OS-347

R.Han, I. Žagar, S. Marković, T.Trčić, M.Jovanović, D. Đokić
Institute of Nuclear Medicine, Clinical Centre of Serbia, Belgrade

DIAGNOSTIC UTILITY OF ¹³¹I-MIBG AND ^{99m}Tc(V)-DMSA SCINTIGRAPHIES IN THE EVALUATION OF NEURAL CREST TUMOURS

Whole body scintigraphies with ¹³¹I-MIBG were performed, in 137 patients with various tumours of neural crest origin [39 with pheochromocytoma (PH), 60 with neuroblastoma (NB), 5 with paraganglioma (PG), 2 with malignant insulinoma and carcinoid, one with chemodectoma and Schwannoma], according to the routine protocol. Tumour uptake of ¹³¹I-MIBG was calculated using the "conjugated views" method. In 27 patients with medullary carcinoma of the thyroid (MCT) whole body scintigraphies were performed consecutively with ¹³¹I-MIBG and ^{99m}Tc(V)-DMSA. Sensitivity and specificity of ¹³¹I-MIBG scintigraphies were: 97.1 % and 95.2 % for PH, 89.5 % and 100 % in patients with NB and 100 % in patients with PG, respectively. In all patients with clinically suspected metastases of malignant insulinoma and carcinoid, secondary deposits were scintigraphically confirmed. The evolution of the disease and tumour uptake of ¹³¹I-MIBG were in significant positive correlation in all patients with PH and NB. In patients with MCT, scintigraphy with ¹³¹I-MIBG was much less sensitive than scintigraphy performed with the ^{99m}Tc(V)-DMSA (30 % and 100%, respectively). It may be considered that whole body scintigraphy with ^{99m}Tc(V)-DMSA was very sensitive for diagnosis and follow-up in patients with, both clinically apparent and occult MCT. Scintigraphy with both radiopharmaceuticals was particularly useful in detecting patients with MEN II syndrome.

OS-348

M.Leimer, A.Kurtaran, M.Raderer, P.Smith-Jones, C.Bischof, J. Valencak, W.Schirma, J.Lister-James and I.Virgolini.

Department of Nuclear Medicine, University of Vienna, Austria and Diatide Inc., New Hampshire.

IN VITRO AND IN VIVO BINDING OF ^{99m}Tc-P829 TO GASTRO-INTESTINAL ADENOCARCINOMAS.

Recent data suggest that the novel peptide tracer ^{99m}Tc-P829 binds with high affinity to somatostatin receptor (SSTR) subtypes 2, 3 and 5. The SSTR3 is frequently expressed on intestinal adenocarcinoma cells. In this study, we have characterized the *in vitro* binding properties of ^{99m}Tc-P829 using primary intestinal adenocarcinomas and HT29 colonic adenocarcinoma cells. In addition, the *in vivo* binding of ^{99m}Tc-P829 was evaluated in 16 tumor patients after injection of 370-550 MBq/20 µg ^{99m}Tc-P829. ^{99m}Tc-P829 bound to primary and immortal tumor cells with high affinity and high binding capacity. The dissociation constant Kd ranged between 1 and 15 nM. ^{99m}Tc-P829 scintigraphy revealed *in vivo* binding to primary and/or metastatic tumor sites in 8/9 pts with colorectal, in 4/4 pts with pancreatic and in 1/2 pts with gastric adenocarcinomas. Liver lesions were indicated by ^{99m}Tc-P829 in 3/5 colorectal, in 3/4 pancreatic and in 1/2 gastric cancer pts. Abdominal lymph node metastases were localized in 1/3 colorectal and in 1/2 pancreatic adenocarcinomas. In 2/2 pts with colorectal cancers peritoneal carcinosis was visualized by ^{99m}Tc-P829 and in one patient with unknown primary adenocarcinoma abdominal lymph node metastases were imaged by ^{99m}Tc-P829. In 4 pts focal accumulation suggested metastatic spread to the lung not detected by CT previously. Furthermore, ^{99m}Tc-P829 indicated abdominal lymph node metastases not seen on CT in one patient with pancreatic adenocarcinoma. In summary, our data show that ^{99m}Tc-P829 binds with high affinity to gastrointestinal tumor cells *in vitro* and *in vivo*. We conclude that ^{99m}Tc-P829 may be useful in the staging and follow-up of intestinal adenocarcinoma patients.

Endocrinology/Thyroid

OS-349

Jan H. Al-Yasi AR, Reardon W, Trembath RC, Sobnack R, Britton KE.

St. Bartholomew's Hospital and Institute of Child Health, London, UK.

PENDRED'S SYNDROME, PS, AND RELATED CONDITIONS EVALUATED WITH I-123 PERCHLORATE DISCHARGE, IN 69 PATIENTS.

Familial goitre and sensineuronal deafness constitutes Pendred's Syndrome, now related to the gene DFNB4 on chromosome 7. As a result this familial disease has other associations: lack of goitre, cochlear (Mondini) malformation and or dilated endolymphatic sac. Failure of organification of iodine is the specific feature of PS and is determined by the perchlorate discharge test, PD. This study evaluates an updated test using I-123.

I-123 10-20 MBq dependent on age/weight is given IV with the patient supine and neck supported under a gamma camera set with a low energy parallel hole collimator peaked at 159 Kev with a 15% window. At 30 minutes 100-200 mg sodium perchlorate is given IV recorded for 30 minutes more. A 10% or greater discharge is taken as abnormal. PS typically showed over 20% discharge. 33 patients with a positive I-123 PD had one or more family members with PS. 36 with negative PD, only one had PS. 90% patients with PD had an abnormality of the endolymphatic sac. Patients with this radiological finding and deafness are now having a PD.

In conclusion an I-123 PD takes only an hour and gives consistent and useful results in Pendred's Syndrome.

OS-350

D. Moka, K. Smolarz, V. Urbanek, E. Voth, H. Schicha

Department of Nuclear Medicine, University of Cologne, Germany.

Influence of antithyroid drugs on biokinetics and therapeutic dosimetry of 131-iodine in hyperthyroid patients with graves' disease

Aim: Although a radioiodine treatment (RIT) in thyrotoxic patients receiving antithyroid drugs (ATD) leads, in comparison to nonpretreated patients, to higher treatment failure rates, continuous taking of ATD is sometimes necessary in patients with concomitant diseases. Aim of this study was to examine the influence of ATD on biokinetics and on therapeutic dosimetry of 131-iodine in patients with Graves' disease receiving a RIT.

Methods: The influence of ATD was investigated in 70 selected hyperthyroid patients with Graves' disease with known elevated turnover of 131-I. In 35 patients ATD was discontinued 2 days after RIT (group B). The biokinetics of 131-I and the dosimetry of the RIT was compared to 15 patients under continuous taking of ATD (group A) and to 20 patients where ATD was stopped 2 days prior to the RIT (group C).

Results: There was a significant increase effective half-life of 131-I 2-3 days after discontinuation of the ATD (group B: 3.5 ± 0.2 d to 6.0 ± 0.2 days after stopping ATD). In comparison to group A in group C 131-I-uptake (A: $37.7\% \pm 4.8\%$; C: $61.4 \pm 2.1\%$) and effective half-life (A: 3.1 ± 0.3 d; C: 6.3 ± 0.4 d) were significantly higher in but there was no significant difference in comparison to group B.

Conclusion: In patients with concomitant diseases, where a continuous taking of ATD before RIT is necessary, therapy of choice is a short washout period of ATD of 2 to 3 days before RIT. The improved biokinetics of 131-I leads then to lower therapy dosis by similar thyroid radiation doses.

OS-351

Z. Grabowski*, J.Jenda*, M.Michalek*, K.Tobiasz**, E.Grabowska*, J.Tomczak*, A.Pawlak* and D.Galczyńska-Zych*.

*Nuclear Medicine Department County Hospital Siedlce. ** Department of Radiology County Hospital Siedlce. Poland.

THERAPY OF LARGE MULTINODULAR GOITRES WITH FRACTIONATED RADIOIODINE.

In Eur J Nucl Med No 12 1997 dr Howarth and co-workers published a paper about treatment of patients with large multinodular goitres with fractionated radioiodine. After giving 4 doses of radioiodine /555 MBq of I131 per month/ they achieved good improvement in compressive symptoms and reduction in goitres size, but 65% of patients were hypothyroid after therapy. We decided to present our method of therapy of large multinodular goitres with fractionated radioiodine.

In the years 1995-97 29 consecutive patients with large multinodular toxic goitres were treated with fractionated doses of radioiodine. 370-740 MBq of I131 were given in intervals of at least 3 months. Before and after therapy the volume of goitre was calculated using typical method based on ultrasound measurements. Scintigraphy with Tc99m before and after therapy, uptake of I131 after 24 hours before therapy and FT3, FT4, TSH calculations were made several times. Propylthiouracil was given at least 4 weeks before therapy, then for 5 days before radioiodine and 3-4 days after was discontinued, and then patients were treated according to the need.

All patients received 1,1-2,96 GBq /30-79mCi/ of I131 except 1, who received 4,99 GBq /135mCi/ for a very large toxic goitre. The therapy was well tolerated.

Before treatment the volume of goitres ranged 43-454 ml, average 129ml. After treatment it was 9-184ml, average 61ml. The volume decreased 14-87%, average 52%, and only in 6 patients it decreased less then 30%.

Among 29 patients after therapy, 17 were euthyroid, 8 hyperthyroid /but much less intensive then before therapy/ and only 4 were hypothyroid / 58%, 28% and 14% respectively /. Considering, that hyperthyroid patients have not completed the treatment and not taking them into account, only 4 of 21 patients were hypothyroid after therapy - 19%.

Our data suggest, that therapy of large multinodular toxic goitres with fractionated radioiodine given in intervals of 3 months is safe and effective and gives much less of hypothyreosis /19% corresponding to 65% in dr Howarth's report/.

OS-352

Rakesh Kumar, AK Pandey, AK Gupta, AK Padhy, GS Pant, AC Ammini

All India Institute of Medical Sciences, New Delhi-29, INDIA
Department of Nuclear Medicine, Radiology & Endocrinology.

EVALUATION OF DIFFERENT PROTOCOLS OF 131I TREATMENT IN PATIENTS OF GRAVES DISEASE AND THE ROLE OF LITHIUM.

Graves disease is one of the commonest causes of hyperthyroidism and I-131 administration is a well established modality for its treatment. However, choice of protocol using 131I remains controversial. We have made an attempt to summarise and compare the effectiveness of different protocols using 131I with and without lithium.

A total of 61 consecutive patients of Graves' disease were treated with I-131 in this study. They were randomised into four groups before work-up for treatment depending on whether or not they had received lithium along with radioiodine and the anticipated radiation dose (60 Gy or 90 Gy). The administered doses were calculated by using the weight of the thyroid gland, anticipated radiation dose to the thyroid (60Gy or 90Gy), effective half life of I-131 and RAIU at 24 hrs

The results showed no significant difference in the response rate of patients treated under different groups. The patients getting lithium required significantly lower doses of I-131 as compared to those in the non-lithium group, whereas the incidence of hypothyroidism was the same in both.

In conclusion the therapeutic doses of I-131 for the treatment of Grave's disease can be significantly reduced by administering lithium orally to the patients before and after administration of therapeutic doses of I-131.

OS-353

F. Dore, P. Solinas, M. D. Azzena, M. Piga, A. Serra, A. Falchi and G. Madeddu.
Depts. of Nuclear Medicine Universities of Sassari and Cagliari. Italy.

RISK OF BONE LOSS IN THYROID LATENT TOXIC CONDITIONS: ROLE OF MOC AND BIOCHEMICAL MARKERS.

The aim of this study is to clarify whether a risk of osteopenia exists in thyroid latent conditions. For this purpose we investigate 47 clinically euthyroid female pts, aged 42 to 66 yrs, with autonomous thyroid nodules (ATN), their size ranging between 16 and 35.5 mm and disease appearance time ranging 3 and 10 yrs; 16 of these pts were in pre (P) and 37 in post-menopause (M) stages. TSH levels were suppressed in all cases, mean values being $0.12 \pm 0.095 \mu\text{U/ml}$; means FT3 and FT4 concentrations were 3.5 ± 0.6 and $12.6 \pm 2.1 \text{ pg/ml}$, respectively. In all ATN pts, in 92 osteoporotic female pts (OP) without thyroid disease and in 173 sex-age matched controls (C), bone density (BD: g/cm^2) was measured in spine by multidetector DPA. Moreover, in all ATN pts, in 16 OP pts and in 56 C, osteocalcin (O) and bone alkaline phosphatase (BAP) in serum by IRMA and pyridinoline (PYR) in urine by ELISA were also assayed. Low BD was found in 29/47 ATN pts and the mean values were significantly ($p < 0.001$) lower ($0.841 \pm 0.170 \text{ g/cm}^2$) in respect of C (0.985 ± 0.121). When ATN pts were considered according to menopause stage, BD was significantly reduced only in M cases compared to C. However, BD was significantly lower in OP pts in respect of both ATN pts and C, independently of menopause. In ATN group, O, BAP and PYR levels were slightly elevated in 23, in 7 and in 25 cases, respectively. Marker mean values were significantly higher than in C (26.6 ± 10.2 vs $21.5 \pm 9.3 \text{ ng/ml}$ for O; 14.3 ± 6.3 vs $11.4 \pm 7.0 \text{ ng/ml}$ for BAP; 37.6 ± 9.3 vs $29.9 \pm 9.4 \text{ nM pyr/mM creat}$ for PYR). The three markers were more elevated in M pts in respect of P but the difference was significantly ($p < 0.001$) only for BAP. In ATN pts BD, O, BAP, and PYR did not correlate with both TSH, FT3, FT4 and nodule sizes as well as disease duration. Our data suggest that an apparently low turnover osteopenia may present in ATN pts with clinically euthyroidism, independent of TSH, FT3 and FT4 levels, nodule sizes and disease duration; however, menopause seems to play an additional important role in bone loss in our cases. Both BD and biochemical markers could be useful for a better selection of pts to submit to bone disorder therapy and for a more accurate follow-up in ATN pts.

OS-354

E. Kresnik, H.J. Gallowitsch, P. Mikosch, M. Molnar, O. Unterveger, I. Gomez, P. Lind.

Department of Nuclear Medicine and Endocrinology, Landeskrankenhaus Klagenfurt, Austria

Scintigraphic pattern in small thyroid nodules

Scintigraphy is routinely used in evaluating thyroid nodules. Functioning nodules are reported to have a low probability of being malignant. Therefore cancer should appear hypofunctioning or „cold“ on scintiscan. The aim of the study was to compare the scintigraphic pattern in different tumor stages of thyroid carcinoma. In addition, sonographic and cytologic results are evaluated. **Method:** In 151 patients with thyroid carcinoma $^{99\text{m}}\text{Tc}$ -pertechnetate scans were evaluated retrospectively by a visual inspection scoring method (A= no significant uptake to D= nodular uptake superior to normal thyroid tissue). Planar images were taken using a small field thyroid gamma camera (GAEDE[®], GKS I, Freiburg, Germany). All patients underwent sonographic examination (5MHz transducer) and 97 patients had fine needle-aspiration biopsy (FNAB) guided by ultrasonography. **Results:** There were 52 patients with pT1 carcinoma (2x follicular and 50x papillar). The mean tumor size was $0.56 \pm 0.26 \text{ cm}$. Most of the nodules showed similar tracer uptake compared with the surrounding thyroid tissue. (3x A, 3x B, 33x C, 13x D). On ultrasonography, 20 patients showed similar echogenicity, 29 had a decreased echo and 3 a complex echo structure. Out of 40 patients with pT2 carcinoma, 34 showed a papillar, 6 a follicular structure. Mean tumor size was $1.66 \pm 0.49 \text{ cm}$. On the scintiscan, most of the nodules showed similar or less uptake to normal thyroid tissue (5x A, 13x B, 16x C and 7x D). On ultrasonography, the nodules had decreased echogenicity. There were 11 patients with pT3 carcinoma (4x papillar, 7x follicular). The mean tumor size was $3.58 \pm 1.07 \text{ cm}$ in diameter. On ultrasonography, most of the nodules had decreased echogenicity. On the scintiscan, the vast majority of the tumors were cold. Therefore they were scored „A“. Among 48 patients with pT4 carcinoma (2x follicular, 1x non differentiated, 45x papillary), scan was cold in most of the patients (20x A, 7x B, 14x C, 7x D). The mean tumor size was $2.16 \pm 1.45 \text{ cm}$. On ultrasonography, the nodules showed a decreased echo structure. Fine needle aspiration biopsy was performed on 97 patients. Cytological specimens suspicious of malignancy were found in 73 patients. **Conclusion:** Tumor size plays an important role in routinely used planar scintigraphy. Nodules greater 2cm in diameter tend to appear cold but microcarcinomas ($\leq 1 \text{ cm}$) are mostly warm on scan. Therefore not all cancers are cold. On ultrasonography, small nodules often have a similar echo structure. The echo structure tends to decrease when the nodules enlarge. Especially for the diagnosis of non palpable carcinomas, ultrasonographically guided FNAB is necessary.

Neurology/Psychiatry: New insights

OS-355

J Pinkert¹, I Gerdens², R Foetzsch³, L Oehme¹ and WG Franke¹

Depts. of Nuclear Medicine¹, Neuroradiology² and Neurology³, Dresden University of Technology

SMA AND PREMOTOR CORTEX OVERACTIVATION IN PATIENTS WITH SPASMODIC TORTICOLLIS

Background: Recent studies have suggested a disturbed balance of excitatory or inhibitory modulation by distinct cortical areas, motor cortex hyperexcitability and task-specific defective motor program preparation in dystonia. This study was designed to test the hypothesis of motor system hyperexcitability during a standardized ocular motor task using functional SPECT and SPM 95 image analyses.

Methods: 20 schizophrenic, 20 depressive and 17 idiopathic torticollis patients were included. All patients underwent MRI and electronystagmographic examinations. Clinical observations comprised the Spasmodic Torticollis Rating Scale and the rating of psychopathology. Under resting conditions and following activation with a horizontally alternating visual target (0.4 Hz), 750 MBq $^{99\text{m}}\text{Tc}$ -ECD were given intravenously. Each subject was scanned 2h after tracer injection using a three headed rotating gamma camera system. Low-energy high resolution collimators were employed with images obtained at 64 projections in a 64×64 matrix (FOV $26 \text{ cm} \times 26 \text{ cm}$); 40 sec/frame (FWHM = 10mm). Images were reconstructed using the iterative maximum likelihood method (ML-EM). Attenuation correction was performed using the Chang algorithm. Calculations and image matrix analysis were conducted in MATLAB using SPM 95. The statistical analysis of SPM95 is described by a design matrix with two conditions: resting and activation. The condition effects were estimated according to the general linear model. The resulting set of voxel values for the contrast, activation-rest, constituted the statistical parametric map of the t-statistic (SPM(t)). The search-threshold was set to $p = 0.01$.

Results: SPM analysis showed activation in the right frontal eye field, right premotor and supplementary motor cortex (SMA), posterior parietal cortex, striate cortex, left extrastriate cortex and right cerebellar hemisphere. Deactivation was seen in the anterior cingulate and right dorsolateral prefrontal cortex. The most significant functional difference while performing a smooth tracking paradigm was the finding of right premotor Cortex and SMA overactivation in torticollis patients.

Conclusion: This data indicate the particular abnormal involvement of the SMA and premotor area in motor control of torticollis patients suggesting also impaired cortical control of movement initiation and timing. This findings support the hypothesis of hyperexcitability of cortical areas involved in motor control.

OS-356

H.H. Abu-Judeh, R. Parker, M. Singh, H. El-Zeftawy, S. Atay, M. Kumar, S. Naddaf, Aleksic, H.M. Abdel-Dayem.

St. Vincent's hosp and Med Ctr, Sec of Nucl Med and Dept. of Neurol+*, NY Med Coll Valhalla NY, and Dept. of Neurol, NYU Med Ctr, New York, NY**

SPECT BRAIN PERFUSION IMAGING (BPI) IN MILD TRAUMATIC BRAIN INJURY WITHOUT LOSS OF CONSCIOUSNESS AND NORMAL CT.

Purpose: Present SPECT brain perfusion findings in 32 patients (pts) suffering from mild traumatic brain injury without LOC and normal CT.

Patients: Non had any history of alcohol or drug abuse. Ages ranged from 11 to 61 years (mean=41). SPECT was performed in 20 pts (62%) within 3 months from the date of injury and in 12 pts (38%) 3 months after the date of injury. 19 pts (60%) were involved in MVA, 10 (31%) sustained a fall, and 3 pts (9%) received a blow to the head. The most common complaints were headaches in 26 pts (81%), memory deficits in 15 (47%), dizziness in 13 (41%), and sleep disorders in 8 (25%).

Method : The studies were acquired 2 hours after IV injection of 20 mCi (740MBq) of $^{99\text{m}}\text{Tc}$ -HMPAO on a triple head gamma camera (TRIONIX). Data was displayed on 10 graded color scale, 2 pixel thickness (7.4mm) and were reviewed without any knowledge of patients' history of symptoms. The cerebellum was used as the reference site (100% maximum value). Any decrease in cerebral perfusion in the cortex or basal ganglia under 70%, or <50% in the medial temporal compared to the cerebellar reference, was considered abnormal.

Results: 13 pts (41%) had normal studies, and 19 (59%) had abnormal studies (13 had their studies < 3 months and 6 had their studies > 3 months from the date of injury). 17 studies revealed 48 focal lesions, and 2 showed diffuse supratentorial hypoperfusion. The 12 abnormal studies performed early had 37 focal lesions averaged 3.1 lesions per patient, whereas there was a reduction to an average of 2.2 lesions per patient in the Sstudies (total 11 lesions) performed more than 3 months from the date of injury. In the 17 abnormal studies with focal lesions, the following regions were involved in descending frequency; frontal lobes 58%, basal ganglia and thalami 47%, temporal lobes 26%, parietal lobes 16%.

Conclusion: SPECT brain perfusion imaging is valuable and sensitive for evaluation of cerebral perfusion changes following mild traumatic brain injury; these changes can occur in the absence of LOC. SPECT BPI is more sensitive than CT in detecting brain lesions; and the changes may explain a neurological component of the patients' symptoms in the absence of morphological abnormalities in the other imaging modalities.

OS-357

C. Dannenberg, A. Bosse-Henck *, H. Barthel, K. Hohdorf, A. Weiser, P. Georgi

Departments of Nuclear Medicine and *Internal Medicine, University of Leipzig, Germany

ABNORMALITIES IN DAYTIME Tc-99m-ECD BRAIN SPET IN PATIENTS WITH SEVERE SLEEP APNEA SYNDROME BEFORE AND AFTER n-CPAP-THERAPY

Incidence of sleep apnea syndrome (SAS) is comparable to that of diabetes mellitus. Excessive daytime sleepiness and disturbances in ability of concentration, short time memory and learning function are common symptoms of SAS. Since neuronal activity is closely related to brain perfusion, the aim of the study was to clarify, whether there are abnormalities in daytime regional cerebral blood flow in SAS and if so, whether they are reversible after nocturnal transnasal continuous positive airway pressure breathing (n-CPAP-therapy).

Subjects: Patients: n = 58 (age 55 ± 11 a) with severe SAS (respiratory distress index > 30). Control group: Age matched (age 51 ± 12 a, n.s.). SPET before and after 6 month of n-CPAP-therapy. Acquisition after injection of 600 MBq Tc-99m-ECD at 8 a.m. using a high-resolution brain dedicated system (CERASPECT, DSI). Visual scoring regarding left and right frontal, parietal, temporal, occipital, cerebellar, striatal and thalamic activity uptake and homogeneity by 3 independent experts (scale 0 to 3, 0 = normal local activity, 1 = non significant deficit, 2 = significant deficit, 3 = large defect).

Results: 1. Before n-CPAP-therapy activity deficits were predominantly located in frontal and temporal lobes: 11/58 patients had mean values ≥ 2 in visual scoring of local activity in frontal and 8/58 in temporal cortices. Mean values of scores of 1.5 were found in 22/58 patients frontal and in 23/58 temporal. Activity uptake was significantly lower compared to that of the control group in left and right frontal, parietal and left temporal cortices and in homogeneity (p < 0.00001), on a lower level of significance in right temporal, left and right occipital and left cerebellar cortices (p < 0.01), too.

2. After 6 month of efficient n-CPAP-therapy activity uptake significantly increased in left and right frontal and temporal cortices (p < 0.01), right parietal lobe and homogeneity (p < 0.05) without reaching the level of the control group.

Conclusion: Cerebral perfusion deficits in SAS are predominantly located in frontal and temporal lobes and are partially reversible after n-CPAP-therapy. Therefore cortical perfusion deficits in SAS do not only reflect morphological changes, but may be due to functional neuronal deactivation caused by vigilance disturbances.

OS-358

H.-W. Mueller-Gaertner^{1,3}, S. M. Rubow^{1,2}, E. Rota Kops¹, M. Beu³, H. Herzog¹, H. Vosberg³

Institutes of ¹Medicine Research Center Juelich, Germany; ²Department of Nuclear Medicine, University of Stellenbosch, South Africa; ³Clinic of Nuclear Medicine, Heinrich Heine-University Duesseldorf, Germany

FUNCTIONAL CHARACTERISATION OF HIGH-AFFINITY CHOLINE TRANSPORTERS *IN VIVO*

Choline is carried across the cell membrane of neurones by means of two different transporters, one with a high and one with a low affinity. The high-affinity transporter primarily sustains acetylcholine synthesis, the low-affinity one predominantly serves phospholipid synthesis. We developed a kinetic model for cerebral choline metabolism in rabbits which may allow to differentiate the two transporter systems and to estimate *in vivo* the activity of the high-affinity choline transporter in humans.

Cerebral transport kinetics of [¹¹C]choline was studied in 17 experiments on 9 rabbits *in vivo* using PET. Hemicholinium-3 was employed as a specific blocker of the high-affinity choline transporter. The experimental data were evaluated using compartment modeling.

Using a model with one extraneuronal (vascular and extravascular space) and two parallel intraneuronal pathways, one mostly unidirectional for phospholipid synthesis and one bidirectional for acetylcholine turnover, we found the following results. Hemicholinium-3 suppressed the [¹¹C]choline entry into the acetylcholine pathway almost completely in hippocampus and cortex: K₁acetylcholine was reduced from 12,3 ± 1,3 and 9,8 ± 1,4 to 0,08 and 0,04 ml/g/min, respectively (mean ± SD of the model, data under the influence of hemicholinium-3 were associated with a relatively high statistical error). There was no effect on the choline entry into the phospholipid pathway: K₁phospholipids amounted to 0,4 ± 0,1 and 0,32 ± 0,12 before and 0,7 and 0,29 after hemicholinium-3. The data indicate that initial [¹¹C]choline uptake in cortex and hippocampus is driven by the high- but not the low-affinity transporter.

In summary, the data demonstrate that initial choline uptake kinetics in cortex and hippocampus reflects the transition of choline from plasma into the acetylcholine synthesis pathway of neurones via the high-affinity transporter *in vivo*. Because the high-affinity transporter serves as biochemical gate for acetylcholine synthesis, uptake kinetics of choline is proposed as functional probe of cholinergic neurones *in vivo*. Since the synthesis of acetylcholine is supposed to be closely coupled to the high-affinity choline transporter activity, we suggest that assessment of it's function may reflect acetylcholine turnover *in vivo* at the presynaptic and/or synaptic level.

OS-359

P. Colamussi, *G.Calo', L.Uccelli, *S.Sbrenna, R.Roveri, C.Cittanti, M.Giganti, C.Bolzati, *C.Bianchi, A.Piffanelli
Department of Experimental and Clinical Medicine, Section of Nuclear Medicine and *Section of Pharmacology, University of Ferrara, Italy

NEW INSIGHTS ON THE MEANING OF ^{99m}Tc-HMPAO HYPERFIXATION IN NERVOUS TISSUE: AN *IN VITRO* STUDY

"In vitro" and "in vivo" studies showed that metabolic status of neuronal cells can affect the brain distribution of the perfusion tracer ^{99m}Tc-HMPAO. To rule out any flow factor, a rat brain slice model was used and the effects of metabolic alterations both on intracellular trapping of ^{99m}Tc-HMPAO and on extracellular glutamate and lactate dehydrogenase (LDH) levels were evaluated. ^{99m}Tc-HMPAO uptake and release were measured in test tubes filled with standard Krebs solutions bubbled with 95% oxygen and 5% carbon dioxide. Control medium was then altered a) adding a metabolic poison (5mM azide), b) removing glucose and replacing oxygen with nitrogen to mimic transient ischemia (*in vitro* ischemia) and c) replacing Krebs solution with a hypotonic medium to evoke irreversible cell membrane damage.

Under control condition, the uptake of ^{99m}Tc-HMPAO was 11.9 ± 1.2 cpm slice/mg prot/cpm medium, whereas prelabeled slices released 10.8 ± 1.1% of tracer content; glutamate and LDH levels were 1.9 ± 0.2 nmol/mg prot and 95 ± 6 U/L/mg prot, respectively. Azide and *in vitro* ischemia both induced a significant increase in ^{99m}Tc-HMPAO release (15.8 ± 1.6%; 18.3 ± 2.2%, respectively), without any modification in LDH efflux. However only azide was able to reduce the uptake of the tracer (9.3 ± 0.9 cpm slice/mg prot/cpm medium). Conversely, the increase in glutamate release was massive during *in vitro* ischemia (=36 fold) and far lower (≈2 fold) during azide treatment. As expected, under hypotonic medium condition, the release of ^{99m}Tc-HMPAO as well as of glutamate and LDH were dramatically increased. Surprisingly, also a 5 fold increase of ^{99m}Tc-HMPAO uptake was found. Adding to the medium 1mM glutathione, which converted native lipophilic into hydrophilic ^{99m}Tc-HMPAO, tracer uptake was strongly reduced both under control and under hypotonic medium conditions.

In conclusion ^{99m}Tc-HMPAO brain retention depends not only on CBF but also on the metabolic status of the tissue. Azide poisoning and *in vitro* ischemia both induce a reduction in ^{99m}Tc-HMPAO retention, but with different mechanisms. Furthermore, we firstly demonstrate that injuries which induce cellular membrane disruption may cause hyperfixation of ^{99m}Tc-HMPAO.

OS-360

G. Demonceau, J. De Vuyst, H. Colaert, C. Monte.

Hospital: St Elisabeth, Dpt of Nuclear Medicine, Zottegem, Belgium.

GENDER-LINKED VARIATIONS OF THE NORMAL CEREBRAL PERFUSION DISTRIBUTION

We tested the hypothesis of different normal perfusion pattern between genders, using different perfusion tracers and age-matched populations.

The perfusion distribution of 126 normal patients (pts) (50% women, age between 20 and 88 years, age-matched, righthanded) was studied, on a 3-head camera, 10 minutes after injection of 1 GBq of either Tc-HMPAO (80 pts) or Tc-ECD (46 pts). The images were obtained on a 3-headed camera in a 128x128 matrix, 25 sec/step, 90 steps on 360°. After backprojection with adaptative filters, the images were fully automatically processed: the creation of database included activity normalisation based on the healthy cortex, warping and elastic transformation to correct for the different cerebral sizes and shapes and transfert into an anatomical atlas. The comparison within the different groups was based, slice by slice, on the ratio of the voxels and its level of significancy was based on the intensity as well as the area of the variation.

In comparison with the female subjects, the male's brain perfusion demonstrates a slightly significant increased activity of the medial aspect of both frontal and parietal lobes (maybe due to an higher enlargement of the interhemispherical space). The activity of the right middle frontal gyrus is also slightly increased in the man by comparison with the female subject.

The presence of these significant gender-linked variations of the cerebral perfusion distribution seems to reinforce the need of comparison with adapted normal database in the quantitative interpretation of brain imaging.

Physics and instrumentation: Data analysis

OS-361

A Cluckie, M Buxton-Thomas

Nuclear Medicine Dept, Kings College Hospital, London, UK

VOXEL-BASED SPECT IMAGE ANALYSIS: A PHANTOM STUDY TO ASSESS THE EFFECT OF DIFFERENCES IN ACQUISITION PARAMETERS BETWEEN SIMULATED PATIENT AND NORMAL TEMPLATE SCANS.

Voxel-based image analysis techniques may be used to identify abnormalities in SPECT 99mTc HMPAO distributions by comparing patient scans to a template obtained from scans of normal subjects. A new set of normal subject scans will be needed when any gamma camera acquisition parameter is modified.

Aim: To use phantom data 1) to demonstrate how changes in acquisition parameters affect the normal template and 2) measure percentage of correctly identified voxels on simulated patient studies when different parameters are used to acquire the normal template scans.

Method: A set of 20 Hoffman brain phantom SPECT scans was acquired using baseline acquisition parameters (A). Then 5 additional sets of 20 scans were acquired with one parameter changed for each set (B-F). 1) The baseline normal template was compared with the other five using voxel based t-tests. 2) Sub-cortical and cortical perfusion deficits (volume = 2.5, 5cm³; severity = 25%, 15%) were simulated on the baseline data set. The percentage of voxels with a z-value ≤ -2 relative to the normal template was derived using each of the 6 templates.

Results: 1) Large areas of significant difference were identified in grey matter, ventricles & outer edge of template B, and in the ventricles & outer edge of template D. 2) Percentage of voxels with z-value ≤ -2 are shown below:

Acquisition parameter	Baseline value	New value	Subcortical		Cortical	
			mean (%)	SD	mean (%)	SD
A Baseline	n/a	n/a	94.1	7.4	82.7	14.4
B Radius of rotation	15.5cm	30cm	54.0*	19.5	24.5*	9.5
C Total counts	10x10 ⁶	3x10 ⁶	40.3*	19.8	24.8*	17.4
D Matrix	128x128	64x64	88.4	9.3	24.7*	7.9
E No. azimuths	128	64	95	6.8	70.6	17.8
F Energy window	sym	asym	91.4	7.3	72.1	16.8

*significantly different from baseline template value (p<0.01)

Conclusion: Differences between acquisition parameters for simulated patient data and template scans may produce misleading results.

OS-362

J. Varga, A. Szanyi, I. Garai, L. Galuska

University Medical School of Debrecen, Hungary
Nuclear Medicine Centre

A METHOD FOR THE DOWNSCATTER CORRECTION OF DOUBLE ISOTOPE GAMMA CAMERA STUDIES

Double isotope studies guarantee that the two image sets reflect the same physiological state and the same organ position. However, scattered photons from the higher energy peak contaminate the image acquired in the lower energy window. Neither subtracting a constant portion of the high energy image, nor the use of an intermediate energy window is adequate for downscatter correction. We propose to convolute the high energy image with a suitable kernel to estimate the downscatter to the lower energy window.

To calculate the convolution kernel, images of patients were acquired in both energy windows after administering the high energy radiopharmaceutical alone. After scaling the images to have the same summed counts, one dimensional spectra were generated from the projection areas of the body in both images. A two-parameter exponential of the form $exp(-(x^{(2+P))/S})$ was fitted to the array of the amplitude ratios after removing the high frequency components. The low-pass filter defined by this formula was applied to the high energy image before scaling down and subtracting it from the image acquired in the lower energy window.

The method was tested on combined krypton-81 - technetium-99m macroaggregated albumin lung scintigrams. (a) Kernels calculated from different views and patients were compared and no major differences were found. (b) Estimated downscatter images were compared to the measured ones and showed minor differences along the body contours: our method slightly overestimates the scatter image outside, and underestimates inside the body contours. Inside and around the lung region our estimate is much more realistic than just a scaled-down high energy image. (c) Downscatter-corrected technetium images were compared to uncorrected ones and those acquired with no krypton present. The correction method significantly enhanced the contrast of hypoperfused areas, and resulted in images visually indistinguishable from the images with technetium alone.

We conclude that this method successfully corrects for the downscatter in double isotope studies, and is suitable for the routine clinical use.

OS-363

S. Lappi, S. Lazzari, G. Sarti, F. Del Dottore, G. Moscatelli, M. Agostini, P.L. Pieri

Hospital: Bufalini, Department of Health Physics and Nuclear Cardiology Unit, Cesena, Italy

IMPROVEMENT IN IMAGES RESOLUTION AFTER ATTENUATION CORRECTION AND INFLUENCE OF DOWN-SCATTER OVER ATTENUATION MAPS. A PHANTOM STUDY.

AIM: Geometrical distortion can occur in SPECT images due to nonisotropic attenuation, if they are reconstructed by the Filtered Back Projection (FBP) algorithm, that does not consider the attenuation along the various projection-rays. We investigated the resolution improvement (related to reduction of geometrical distortion) in attenuation corrected (AC) SPECT images, reconstructed by an iterative algorithm (ML-EM) that uses attenuation maps. Since the transmission data, provided by two Gd-153 sources mounted in a dual headed camera (ADAC-Vertex), are potentially affected by the down-scatter (DS) of Tc-99m, we also evaluated the influence of DS over the attenuation maps.

METHODS: To quantify the images resolution, a Tc-99m filled line source underwent a SPECT study in air and then placed in a cylindrical phantom, first in the center and later in a peripheral position (isotropic and nonisotropic attenuation). Non-attenuation corrected (NC) images were reconstructed with FBP algorithm, while AC images with ML-EM. To evaluate the DS of Tc-99m over Gd-153, we imaged an anthropomorphic phantom containing no activity firstly and containing activities in the various organs then. The attenuation maps were compared. **RESULTS:** The resolution improved in AC images, in the case of nonisotropic attenuation:

LINE SOURCE IN AIR	NC		AC	
	FWHM (mm)	FWTM (mm)	FWHM (mm)	FWTM (mm)
ISOTROPIC ATTENUATION	12±2	23±2	15±2	27±2
NONISOTROPIC ATTEN.	16±2	28±2	19±2	35±2

Due to DS, attenuation coefficients decreased in the hepatic area (16%) and in the spine (10%), but not in the lungs. **CONCLUSIONS:** In presence of nonisotropic attenuation, the resolution improves in AC images. The changes in attenuation maps, due to DS, does not affect the projection-rays originating from the heart.

OS-364

P.Almeida, B.Bendriem, O.de Dreuille*, A.Peltier*, C.Perrot*, O.Lamer, V.Brulon, P.Merceron, E.Petit*

Serv. Hosp. Frédéric Joliot-CEA, *Hopital du Val de Grace-Paris, †CES-SRI-CEA, ‡Univ. Paris XII-Créteil -FRANCE

DOSIMETRY OF TRANSMISSION MEASUREMENTS IN NUCLEAR MEDICINE: A STUDY USING ANTHROPOMORPHIC PHANTOMS AND THERMOLUMINESCENT DOSIMETERS

Introduction: Quantification in PET and SPECT rely on attenuation correction which is generally obtained with an additional transmission measurement. Therefore, the evaluation of the radiation doses received by patients needs to include the contribution of transmission procedures (dose-T).

Methods: In this work we have measured these doses for both PET and SPECT. PET dose-T was measured on a CTI/Siemens ECAT HR+ equipped with 3 rod sources of 68Ge (555 MBq total) and extended septa. SPECT dose-T was measured on a SMV/DST equipped with 2 collimated line sources of 153Gd (22.2 GBq total). Two anthropomorphic phantoms were used to estimate doses delivered in typical cardiac and brain transmission studies. Measurements were made with Thermoluminescent Dosimeters (TLD, consisting of Lithium Fluoride) having characteristics suitable for dosimetry investigations in nuclear medicine. Sets of TLD were placed inside small plastic bags and then attached to different organs of the phantoms (at least two TLD were assigned to a given organ). Before and after irradiation the TLD were placed in a 2.5cm thick lead container to prevent exposure from occasional sources. Ambient radiation was monitored and taken into account in calculations. Transmission scans were performed for more than 10 hours in each case to decrease statistical noise fluctuations.

Results: The doses delivered to each organ were calculated by averaging the values obtained for each corresponding TLD. These values were used to evaluate the effective dose equivalent (EDE) following guidelines described in ICRP-60. The estimated values were 7.70x10⁻⁴ mSv/MBq.h (1.94x10⁻⁶ mSv/MBq.h) for cardiac PET (SPECT) and 2.66x10⁻⁴ mSv/MBq.h (1.04x10⁻⁶ mSv/MBq.h) for brain PET (SPECT). In our institution, transmission scan (15 minutes) are usually performed prior to emission in PET and is simultaneous to emission in SPECT (usually 30 minutes for brain and 15 minutes for cardiac). Under these conditions, dose-T for PET (SPECT) estimated as EDE are 1.07x10⁻¹ mSv (1.08x10⁻² mSv) and 3.69x10⁻² mSv (1.15x10⁻² mSv) for cardiac and brain studies respectively.

Conclusion: These measurements show that the dose received by a patient during a transmission scan adds little to the typical dose received in a nuclear medicine procedure.

OS-365

J.A.K. Blokland, P. Dibbets, B.L.F. van Eck – Smit, E.K.J. Pauwels

Leiden University Medical Centre, Division of Nuclear Medicine
Leiden, The Netherlands

THE SMOOTHING EFFECT ON THE MEASUREMENT OF END-DIASTOLIC AND END-SYSTOLIC LEFT VENTRICULAR VOLUMES FROM SPECT MYOCARDIAL PERFUSION IMAGES.

End-diastolic (ED) and end-systolic (ES) left ventricular (LV) volumes can be measured from gated SPECT myocardial perfusion images (gSPECT). A computer program can automatically delineate the LV myocardium. However, the reconstruction filters will influence this detection of the endocardial contours. In this study we investigated the effect of the reconstruction filter on the measured volumes.

gSPECT studies (64²-matrix; 16 frames/RR cycle) were acquired after administration of 750 MBq ^{99m}Tc-tetrofosmin. Studies of 12 consecutive patients were reconstructed applying Butterworth reconstruction filters (order 8) with cut-off frequencies (COFs) ranging from 0.24 cycles/pixel (cpp) to 0.40 cpp. ED and ES LV volumes were computed using a standard software package (Germano, et al). For each patient study the measured volumes were normalised to the average volume obtained when reconstruction filters with a COF of 0.32 cpp or higher were applied. The results were presented as function of the COF.

For all studies we found increasing ED and ES LV volumes when the COF increased. For COFs above 0.30 cpp the measured volumes did not change much, but the visually assessed image quality decreased remarkably. At the lowest COF the average normalised ED and ES volumes were respectively 0.96 and 0.89, at high COFs these volumes were both equal to 1.01. The influence of the reconstruction filter was different for the ED and ES volumes: the ejection fraction decreased when the COF increased.

We conclude that the COF must be chosen as high as possible (≥ 0.28 cpp) to obtain stable volume measurements, but not too high as the poor image quality hampers the visual assessment of the perfusion images.

OS-366

M. J. Carroll, K.E. Britton

St Bartholomew's Hospital, Department of Nuclear Medicine

EIGENTEMPLATE TUMOUR DETECTION IN NUCLEAR MEDICINE

The objective of this study is to synthesise a set of matched filters for tumour detection based upon a principal component decomposition of a set of normalized training examples.

There are imaging tasks, for example detection of hyperplastic parathyroid glands in tertiary hyperparathyroidism (THP) which pose considerable technical difficulties due to low signal to noise and small gland size.

From a database of 15 previously analysed patients who had 44 glands surgically confirmed a set of constant sized regular ROI's are manually defined bounding the confirmed gland sites. Each training tumour site is reshaped into a vector and placed in a n x m matrix X where n is the number of pixels in the ROI and m is the number of tumour sites. The eigenvalues and thus the principal components of X are extracted. A set of eigentemplates are derived from a small number of significant eigenvalues of X. These eigentemplates encode the significant characteristics of the training set. By correlating these eigentemplates with a sliding n pixel size window throughout an image then a saliency map is generated for each pixel.

This technique is applicable in other areas of nuclear medicine in particular axillary lymph node involvement in breast cancer.

General nuclear medicine: Kidney varia

OS-367

A. Smokvina, N. Giroto, M. Subat, G. Saina
Clinical Hospital Center Rijeka, Croatia

THE RENAL PARENCHYMA EVALUATION: ANY ADVANTAGE OF MAG3 SCAN?

The purpose of this research was to assess the possibilities of using the initial phase of study with MAG3 for the evaluation of renal parenchyma. In 83 studied patients, 57 female and 26 male, of whom 34 children under the age of 15, scintiscans of the parenchymal phase of the study with MAG3 were compared with scintiscans in the same projection made with DMSA. The investigation was performed with the same gamma camera, under the exactly same conditions of detection. Three months was the longest period between the MAG3 and DMSA scans.

The analysis was performed independently first with MAG3, applying strict evaluation criteria of the appearance of the outlines and the accumulation of radiopharmaceuticals in particular segments of each kidney. The analysis with DMSA was performed in exactly the same way and finally both studies were compared by simultaneous analysis.

Results showed that in over 80% of cases scintiscans with MAG3 and DMSA correspond completely. The outlines of the kidneys were less distinct in the analysis with MAG3, so that in 20% of patients there was a suspect outline change, which was not visible on scintiscans with DMSA. Although DMSA produces sharper outlines and a superior quality presentation of the parenchyma, a clear outline defect or a parenchymal lesion visible on a scintiscan with DMSA could always be differentiated even when analysis was performed with MAG3. The differential function (ratio) of both radiopharmaceuticals also showed no significant differences. In obstructive renal disease MAG3 has proved to be superior to DMSA because collecting system in this phase contains no radioactivity.

OS-368

C.G. Zhang, D.S. Zhao, M. Zhao and Z.L. Lei

1st Hospital, Shanxi Medical University, Department of Nuclear Medicine, Taiyuan, P.R. China.

EXERCISE SCINTIRENOGRAPHY FINDINGS IN NON-HYPERTENSIVE YOUTHS WITH PARENTS OR GRANDPARENTS WITH HYPERTENSION.

The aim of this present study was to observe the findings of exercise scintirenoigraphy on non-hypertensive youths who have one or more parents and/or grandparents with hypertension. 22 non-hypertensive youths were studied and they were divided into two groups. Group A (GA) was youths without hypertensive family members; Group B (GB) was youths with one or more parents or grandparents with hypertension. There were 11 subjects in group A, 9 males and 2 females with mean age 22.7 ± 3.8 years. In group B there were 11 subjects, 4 males and 7 females with mean age 21.6 ± 2.7 years. All subjects have normal BUN, creatinine, ECG and no cardiovascular risk factors. DTPA imaging (5mCi) was done upright on a bicycle at rest (R) and during exercise (5 mCi) at 60% maximum predicted heart rate (220-age) for 20 min. (EX). Heart rate, blood pressure, ECG were monitored. Time to peak (TP), 20 min./peak count ratio (20/P) and mean transit time (MTT) were measured.

Group	Item	Time to Peak	20min./ Peak	Mean Transit Time
A	R	154.9 ± 28.7*	0.31 ± 0.04	106.7 ± 6.8***
	EX	167.7 ± 50.2**	0.39 ± 0.05	124.8 ± 31.3
B	R	186.5 ± 26.4*	0.34 ± 0.05	118.9 ± 21.6***
	EX	203.7 ± 37.4**	0.43 ± 0.09	141.4 ± 35.1

* GA-R/GB-R p<0.05; ** GA-EX/GB-EX p<0.05; *** GA-R/GB-R p<0.05.

An example of an abnormal exercise-induced scintirenoigraphy was demonstrated in a non-hypertensive 21 year old female who has a father with essential hypertension for 10 years. The rest and exercise scintirenoigraphy results were listed below.

	Time to Peak		20min./ Peak		Mean Transit Time	
	L	R	L	R	L	R
R	225	192	0.42	0.38	150	122
EX	258	207	0.73	0.62	240	243

These data demonstrate that exercise scintirenoigraphy may be abnormal in non-hypertensive youths with parents or grandparents with hypertension.

OS-369

A. Sankaya¹, S. Sen², T. F. Cermik¹, N. Aydin³, H. Sunar⁴, S. Berkarda¹.

Depts. of Nuclear Medicine¹, Nephrology², Neurology³, Cardiovascular Surgery⁴
Trakya University, Faculty of Medicine, Edirne, TURKEY

Tc-99m MIBI SCINTIGRAPHY FOR ASSESSMENT OF MYOPATHY IN THE END STAGE RENAL DISEASE(ESRD) and EFFECTS OF L-CARNITINE ADMINISTRATION IN THE ESRD PATIENTS SKELETAL MUSKLES.

Uremic Myopathy (UM) is not uncommon in ESRD and it is diagnosed difficulty by electromyography(EMG) and clinical findings in the early stage. The aim of this study was to show the value of Tc-99m MIBI in skeletal muscle perfusion scintigraphy to identify UM of the lower extremities in the early stage. Doppler ultrasonography was performed on all subjects and subjects and all patients without arterial disorder were taken into scintigraphy group. 47 ESRD pts. (26 M, 22F) (Mean age 43,1± 14 yr.) (32 haemodialysed, 17 peritoneal dialysed) and 18 healthy controls (HC) (10 M, 8 F) (Mean age 46,1±10,1 yr.) were performed and moreover 19 ESRD pts. were performed after L-carnitine (L-C) treatment period (2 gr./day during the 4 month + 25 unit/every other day during the 3 month). 740 Mbq Tc-99m MIBI was injected to three groups, and rest study was performed after 45 minutes. Posterior images were acquired over the thighs and calves. For the interpretation of studies every thigh uptake/ ankle uptake ratio (T/ Ar), calf uptake/ knee uptake ratio (C/Kr) were computed with semiquantitative. All patients were performed EMG and their plasma creatinekinase (CPK), parathormone (PTH), calcium (Ca), phosphorus (P) value were measured. EMG study showed that 21 (%45) ESRD pts. had polyneuropathy but only 2 (%4) pts. had myopathy. The scintigraphic results are shown in the following table.

47 pts.	ESRD Pts. Mean±SD	HC Mean±SD	P value
C/Kr	2,60±1,29	3,57±0,98	0,0088
T/Ar	1,85±0,59	2,60±0,51	0,0000
19 pts.	Before L-C	After L-C	P value
C/Kr	2,45±0,80	3,00±0,89	0,0290
T/Ar	1,79±0,67	2,38±0,52	0,0034

There was statistically significant difference between ESRD pts. and HC groups at the scintigraphic values and we observed that calf areas ratio 54/94 (%56) and thigh areas ratio 71/94 (%73) were lower than "HC Mean-1SD" value.

Underwent L-C administration pts. a significant increased in both thigh and calf areas ratio in comparison with before therapy.

In conclusion, our first results indicate that Tc-99m MIBI muscle perfusion scintigraphy may be useful for the identification and evaluation of the UM in ESRD pts. at the early stage before positive EMG signs and clinical symptoms, and second results indicate that Tc-99m MIBI may show positive effects of L-C administration in ESRD pts. with UM.

OS-370

D. Volterrani, A. Vella, L. Burrioni, P. Bertelli and A. Vattimo.

Department of Nuclear Medicine, University of Siena, Italy.

POSSIBLE EMPLOYMENT OF A DUAL DETECTOR GAMMA CAMERA FOR GFR MEASUREMENT

Kidney function can be evaluated by means of several radionuclide methods. The need of simplification has led to the use of gamma camera external counting methods which have also the advantage to enable the measurement of separate kidney function. However, patient attenuation and kidney geometry are some pitfalls that can affect the assessment of either global and separate kidney function. Aim of the study was to evaluate the possible benefits from the employment of dual head gamma cameras, that are still more present in many departments. Ten pts with differing degree of renal function underwent a dual detector dynamic renal study and a plasma clearance study (multiple blood samples up to 180 min. p.i., two compartment model) as a gold standard, after a single i.v. injection of ^{99m}Tc-DTPA (240 Mbq). The acquisition was performed with the two detectors in anterior (A) and posterior (P) position to calculate kidney depth and counts by means of a geometric mean approach. The distance (D) between the two collimators was registered to obtain patient thickness (after bed thickness subtraction). Patient attenuation was considered 0.12 cm⁻¹. One minute integral net background kidney counts (C) at different times after bolus arrival were calculated as follows:

$$C = \sqrt{Acounts \cdot Pcounts} / \exp(-0.12 \cdot D/2)$$

Counts corrected for kidney depth according to the Tonnesen algorithm were also calculated. All counts were normalized for the injected dose.

The best linear relationship (R²=0.99) with plasma clearances (GFR range 25-156 ml/min) was observed using 3rd minute counts obtained with the dual head approach. A worse relationship (R²=0.93) was found with the Tonnesen method. No correlation between kidney depth and a significant difference (p<.005) between separate kidney function were observed when comparing the two methods

The dual detector dynamic acquisition could be a promising approach to more accurately measure global and separate kidney function especially when abnormalities of kidney size, shape or site are present.

OS-371

M D Rutland, I M Hassan, L Que

Auckland Hospital [NZ]: Department Of Nuclear Medicine

COMPARISON OF QUANTITATIVE RENOGRAPHY WITH DTPA & MDP

Over half of the 99m-Tc-MDP injected is excreted via the kidneys, so that bone scans contain renal information. Over the past 18 years, some patients having bone scans for unexplained back pain, and patients having bone scans for analysis of bone activity in Paget's Disease have had quantitative renal studies performed using their MDP injection. This study compares the numerical results of such MDP renograms [from patients with apparently normal kidneys], with conventional 99m-Tc-DTPA renograms.

RESULTS 1 - Tracer Uptake Rates [per million seconds, both kidneys]:

AGE GROUP	20-29	30-39	40-49	50-59	60-69	70-79
[years]						
DTPA[mean]	410	399	380	305	311	206
DTPA [sd]	144	97	103	88	104	58
DTPA [n]	33	31	26	21	19	15
MDP[mean]	393	367	338	306	236	227
MDP [sd]	55	62	89	109	57	92
MDP [n]	10	12	14	25	36	20

RESULTS 2 - Vascular & Glomerular Analyses [ages 20-40 years]:

	Flow	Vascular	GFR	Renal	Cortical
	Index	Transit		Transit	Transit
	ml/sec	secs	ml/sec	secs	secs
DTPA[mean]	7.84	7.7	1.861	288	214
DTPA [sd] [n=64]	3.72	2.1	0.554	99	57
MDP [mean]	7.36	6.8	1.748	293	204
MDP [sd] [n=22]	1.77	1.5	0.271	66	27

CONCLUSION: The uptake rate for MDP is approximately 94% that of DTPA, and in all other respects [Flow, vascular, renal and cortical transit times] MDP renography produces similar numerical results to DTPA studies. In the majority of cases the coefficient of variation is lower for MDP than for DTPA.

OS-372

B. ERBAS, I. CIFTCI.

Hacettepe University, Medical School, Department of Nuclear Medicine, Ankara-TURKEY

A NEW FORMULA TO ESTIMATE CLEARANCE OF 99mTc-EC USING SINGLE SAMPLE METHOD.

Several alternative algorithms taking into account the individual body dimensions were proposed by investigators for the estimation of 99mTc-MAG3 clearance to be used in both adults and children. This approach provided more precise results. Since 99mTc-EC(ethylene-dicyteine) is a similar agent used for the assessment of tubular function, this study was intended to apply a similar algorithm for the estimation of EC clearance and to find an optimal time for blood sampling.

Following i.v. injection of 5 mCi 99mTc-EC, plasma clearance values of 83 subjects were measured using multi-sample plasma method. The clearance values ranged from 93 mL/min/1.73 m² to 518 mL/min/1.73 (mean=316±103 mL/min/1.73 m²).

The dose concentration reciprocals (ID/cn_t) were plotted against reference clearance values (ID=injected dose, cn_t=plasma concentration at time t normalized to 1.73 m²). For each patient, sampling times ranging from 30 to 75 min by one minute increments were tested. A logarithmic curve (y=A+B.lnx) was fitted to the data.

Sampling time(min)	s.e.e(mL/min)	correlation coeff (r).
40	26.685	0.961
50	23.936	0.969
55	23.263	0.971
56	23.201	0.971
57	23.163	0.971
58	23.150	0.971
59	23.160	0.971
60	23.194	0.971
70	24.600	0.967

The optimal time for the single plasma sampling appears to be between 50 and 60 min. with very close s.e.e and r values. New algorithm for the calculation of tubular extraction rate of 99mTc-L-EC is:

$$EC \text{ Clearance} = -869e - 0.00771 + 380e - 0.01031 \times \ln (ID/cn_t)$$

We have presented a new formula for estimating 99mTc-EC clearance from a single plasma sample based on the normalization of plasma counts to body surface area which can be used with an acceptable error.

■ Cardiovascular: Perfusion and coronary anatomy

Cardiovascular: Perfusion and coronary anatomy

OS-373

L. Ceriani, F. Verna*, L. Giovanella, G. Binaghi* and S. Garancini.

Department of Nuclear Medicine and * Division of Cardiology
University Hospital - Varese - Italy

POSITIVE MYOCARDIAL STRESS/REST SCINTIGRAPHY AND NORMAL CORONARY ANGIOGRAPHY IN PATIENTS WITH ANGINA: A FALSE POSITIVE RESULT FOR CAD? AN ANSWER FROM INTRAVASCULAR ULTRASOUND STUDIES.

Aim. Aim of the present study was to assess the significance of scintigraphic myocardial perfusion abnormalities in pts with angina and normal coronary angiography (CA) by means of intravascular ultrasound studies.

Methods. In 18 pts with a reversible perfusion defect detected by stress/rest Sestamibi SPET and normal CA, intravascular ultrasound (IVUS) was performed at the time of CA. Eleven pts also underwent doppler flow wire velocity measurements (DW). At least two major coronary arteries were tested in each pt. and vessels were grouped according to perfusion map as supplying hypoperfused (Group A, target vessels) or normoperfused territories (Group B, reference vessels). Presence and extension of occult atherosclerotic plaques (AP) was assessed by IVUS, and cross sectional luminal area (LA), vessel area (VA) and cross sectional narrowing (CSN= VA-LA/VA) were measured in 39 vessels. Coronary flow velocity reserve (CFR) was assessed during i.c. Adenosine induced hyperemia in 22 vessels and a CFR ratio (CFR_r = CFR target /CFR reference vessel) was calculated for each pt. A semiquantitative stress/rest perfusion score was used to describe extent and severity of the reversible perfusion defects.

Results. Occult AP were observed in 17/18 pts (94%). CSN was > 40% in 16 (89%). An abnormal CFR value (< 2.5) was found in 8 pts (66%). IVUS showed higher values of CSN in the Group A (n=21: 43.8% ± 16) compared with Group B vessels (n=18; 12.8% ± 17; p<0.0001). DW demonstrated a reduced mean value of CFR in Group A (n=11) with respect to Group B vessels (n= 11) (2.5 ± 0.5 vs 3.48 ± 0.5; p<0.0001). A weak linear correlation between CFR_r and perfusion score was also found (y= 0.85 - 0.04x ; R=0.62; p< 0.05).

Conclusions. Perfusion defects as detected by SPET images identify pts with anatomical and functional abnormalities of the coronary circulation which may be recognized by IVUS and DW studies. Mismatch between positive scintigraphic results and negative angiographic findings may be better understood after intravascular ultrasound studies.

OS-374

M. Kostkiewicz, W. Tracz, P. Podolec,
Department of Nuclear Cardiology, Department of Cardiovascular Surgery
Collegium Medicum UJ Kraków Poland

PROGNOSTIC VALUE OF A NORMAL MIBI MYOCARDIAL EXERCISE SCINTIGRAPHY IN PATIENTS WITH CORONARY ARTERY DISEASE.

In order to assess the prognostic value of normal MIBI myocardial scintigraphy with documented coronary artery disease, we compared the incidence of severe cardiac events in 3 groups of patients. First group of 75 patients (Group 1) with normal exercise MIBI scintigraphy, who demonstrated significant coronary lesions (stenosis >70%) on an angiogram performed within 3 months of scintigraphy was compared to a second group with abnormal exercise scintigram and coronary proven artery disease (Group 2) and to a third group of patients with normal exercise scintigraphy and normal coronary angiography (Group 3).

Over a mean follow up period of 5,8 years patients in Group 1 presented more frequently than in Group 2 single vessel disease and more distal lesions and the majority of patients in Group 1 were treated medically. There were no significant difference in the incidence of major cardiac events in patients with normal exercise scintigraphy and with or without documented coronary artery disease (Group 1 and Group 3), while the incidence was higher in Group 2.

	n	CD	MI	Revasc.
Group 1; MIBI -, coro. +	75	1	5	7
Group 2; MIBI +, coro. +	105	8	16	39
Group 3; MIBI -, coro. -	120	-	4	3

CD-cardiac death, MI-myocardial infarction

In conclusion, patients with coronary artery disease and normal exercise MIBI myocardial scintigraphy usually have mild coronary lesions and good long term prognosis, with a low incidence of cardiac death.

OS-375

M.O. Demirkol, N. Kurtoglu, B. Yaymaci, H. Silahci*, Ç. Önsel*, F. Turan.

Koşuyolu Heart and Research Hospital, Cardiology and Nuclear Medicine
Departments Istanbul, Turkey.

SLOW CORONARY FLOW: CORRELATIONS MYOCARDIAL PERFUSION TOMOGRAPHY AND CORONARY ARTERIOGRAPHY.

A patient with chest pain of recent onset, suggestive for angina pectoris, was referred for diagnostic coronary arteriography, which showed the typical phenomenon of "slow flow pattern" in the absence of any significant coronary artery stenosis. We assessed coronary arteriographic and scintigraphic properties in patients with a slow flow pattern (SFP).

Our study included 54 patients who revealed "slow coronary flow pattern" in their angiograms. The control group consisted of 50 patients with normal coronary arteries. The TIMI (thrombolysis in myocardial infarction) flow-grading system was used for the assessment of SFP. The arithmetic means of the number of cineframes required for contrast to fill three main coronary arteries (LAD, LCX, RCA) were used to calculate mean frame count for each patient. Single day rest-stress Tc-99m MIBI myocardial perfusion scintigraphy (SPECT) was performed to all patients. Patients with SFP revealed higher counts both native coronary arteries as well as mean frame counts:

	Mean	LAD	LCX	RCA
control	26.4±3.5	35.4±3.3	22.5±4.5	21.5±2.8
slow flow	63.6±19.6	86.2±35.5	55.5±18.7	49.1±23.2

Myocardial perfusion scintigraphy showed ischemia in 16 patients (group1), while 38 patients in group2 revealed no perfusion defect. There is no significant statistical difference between two groups.

	Mean	LAD	LCX	RCA
Group1	56.7±15.9	73.8±24.2	50.4±23.7	43.4±15.2
Group2	57.7±20.4	77.4±34.7	48.9±20.4	46.5±21.8

In conclusion, there is no correlation between the time needed to fill native coronary artery and ischemia, even if there is SFP.

OS-376

K. Morita, N. Tamaki, T. Nakata, T. Syogase, K. Hirasawa, M. Furudate and T. Kobayashi.
Multicenter Study in Hokkaido, Hokkaido, Japan

I-123-BMIPP CAN IDENTIFY CORONARY PATIENTS WITHOUT PRIOR MI, WHO REQUIRE REVASCULARIZATION THERAPY

The aim of this study is to clarify the clinical usefulness of I-123-BMIPP (BMIPP) SPECT in coronary patients without previous MI. This multicenter study in Hokkaido enrolled 86 patients, including 51 effort angina, 23 unstable angina, 8 vasospastic angina and 4 variant angina. BMIPP SPECT was obtained at 20 min. after injection at rest and compared with myocardial perfusion (MP) images at rest or delayed images after stress imaging. LV myocardium was divided into 13 segments to score BMIPP & MP uptake using 4 point grading system (0: normal to 3: severe defect). Total defect score (TDS) was defined as the sum of each defect scores. TDS of BMIPP was larger than that of myocardial perfusion (3.9±0.5 vs 2.8±0.4, p<0.01). Sensitivity for detecting coronary lesion (>75%) with BMIPP (53.2%) was higher than that with MP agents (41.4%). Sensitivity for detecting severe stenosis (>95%) was higher (BM: 71.8%, MP: 61.5%). In addition, in the follow-up study, patients who needed PTCA or CABG had higher TDS of BMIPP than those without interventional treatment.

	PTCA, CABG	No Intervention	P
BMIPP	3.9±0.5	3.0±0.6	<0.05
MP	3.3±0.9	2.4±0.4	n.s.
BMIPP-MP	1.9±0.5	0.6±0.5	<0.05

means±s.e.

These results suggest that myocardial fatty acid metabolism imaging with BMIPP at rest seems to be sensitive for detecting coronary vascular lesions in patients without prior MI. In addition, it is more useful to select the severe patients who require interventional treatment than MP alone.

OS-377

I. Tsuda, T. Yamaguchi, T. Miyajima
Kido Hospital, Department of Cardiology

UTILITY OF IODINE-123-BMIPP IN THE DIAGNOSIS OF PATIENTS WITH UNSTABLE ANGINA ASSOCIATED WITH CORONARY SPASM AND NO CORONARY STENOSIS

Coronary spasm has been considered to be a cause of unstable angina. In patients with unstable angina and no coronary stenosis, provocation test is required to detect the culprit lesion of coronary spasm. We investigated whether [¹²³I] BMIPP could be used in the diagnosis of patients with unstable angina associated with coronary spasm and no coronary stenosis. **Methods:** The study group consisted of 9 patients (6 men, 3 women, mean age 60 yrs) who were suspected of having unstable angina associated with coronary spasm. Resting BMIPP SPECT was performed within 1 week before provocation test. Reduced BMIPP uptake was semiquantitatively evaluated by polar map display. Patients with coronary stenosis were excluded. During coronary angiography, spasm was induced by provocative testing with acetylcholine or ergonovine, and only total or subtotal occlusion was considered positive. Wall motion analysis was performed by left ventriculography before coronary angiography and provocation test. **Results:** Provocative testing was positive in 14 coronary territories in all 9 patients. Four patients showed multi-vessel spasm and only two patients showed wall motion abnormality. On the other hand, 5 patients without multi-vessel spasm showed normal wall motion. Reduced BMIPP uptake was observed in 6 (67%) of 9 patients and at 8 (43%) of 14 coronary territories. In these 6 patients, four patients with multi-vessel spasm were included and had reduced BMIPP uptakes in one or two coronary territories. **Conclusion:** BMIPP can not detect myocardial damage effectively in unstable angina associated with coronary spasm and no coronary stenosis, but may be useful in estimating the severe cases with multi-vessel spasm.

OS-378

I. Karner, S. Šijanović, D. Dekanić
UNIVERSITY HOSPITAL OSIJEK, DEPARTMENT OF NUCLEAR MEDICINE

LONGTERM THYROXINE TRETMENT AND OSTEOPOROSIS

The aim of this study was to determine whether longterm thyroxine treatment is a risk factor in the case of osteoporosis. A selected group of women in premenopausal period (N=19), and a selected group of men (N=9) suffering from differentiated thyroid gland carcinoma in the average age of 39,0±8,0 years and 41,8±10,0 years were examined. To all of them, the total thyroidectomy was done and the thyroxine suppression therapy was introduced. The duration of the suppression therapy from the beginning of the research, for the female examinees, amounted 9,4±6,4 years, and 8,1±6,0 years for the male examinees. The prospective study of the bone densitometry was done to all of the examinees using the method of dual photon X-ray absorptiometry (DXA) of the spine and of the femoral neck, and also by the method of one-photon absorptiometry (SPA) of the distal radius. Statistically significant loss of bone tissue was registered only on the distal radius concerning male examinees (p<0,05). On the lumbar part of the spine and femoral neck, only a minor bone loss was registered in the small number of examinees, and it was of no statistical relevance nor for male or for female examinees. It is necessary to prolong the time of observation in the prospective studies, as well as to increase the number of examinees, in order to define relative risk involved in thyroxine suppression treatment of osteoporosis. Bone densitometry should already be included in diagnostic and therapy procedure, in order to discover persons with largest risk for osteoporosis on time, and to be able to undertake preventive treatment.

Oncology: FDG

OS-379

C.Landoni, L.Gianolli, G.Lucignani, P.Magnani, A.Savi, L.Travaini, F.Fazio.
INB-CNR, University of Milan, H SRaffaele, Milan, Italy.

COMPARISON OF DUAL-HEAD COINCIDENCE IMAGING PET (DHCI-PET) VS. CONVENTIONAL RING PET (RING-PET) IN TUMOR PATIENTS.

Seventy patients with primary tumor and/or metastatic dissemination were studied with [¹⁸F]FDG and both a dedicated positron emission tomograph with multiring detector (RING-PET) and a dual head coincidence imaging PET (DHCI-PET). Aim of the study was a comparison between RING-PET and DHCI-PET for restaging neoplastic patients following surgery and/or radio-chemotherapy. Patients received an iv dose of [¹⁸F]FDG (100 µCi/kg) under fasting condition; RING-PET studies were performed 45-75 minutes post [¹⁸F]FDG injection. DHCI-PET scan were performed ~3 hours post [¹⁸F]FDG injection, centred on the field of view of the lesion(s) detected by the RING-PET scan. RING-PET and DHCI-PET images were analyzed by three independent observers. The number and location of the hyper-metabolic lesions were recorded for each patient. DHCI-PET identified 14 of the 14 head/neck lesions identified by RING-PET, 53/63 of the thoracic lesions, and 36/45 of the abdominal lesions. A concordant restaging, based on location and number of lesions detected, was found in 14/14 pts with head/neck tumors, 28/30 pts with thoracic tumors, and 24/26 pts with abdominal tumors. Our preliminary results demonstrate a good agreement between RING-PET and DHCI-PET images assessment of oncological pts undergoing post-therapeutic restaging. In 4/70 pts discrepancies were found in restaging disease. The discrepancies found on the number of lesions detected by the two studies can be attributed to the lesions dimension.

	Number of lesions detected		
	Head/Neck	Thorax	Abdomen
DHCI-PET	14	53	36
RING-PET	14	63	45

OS-380

M. Zimny, HJ. Kaiser, U. Cremerius, P. Reinartz, B. Nowak, M. Schreckenberger, U. Bull
Department of Nuclear Medicine, University Hospital, Technical University Aachen, Germany

GAMMA CAMERA COINCIDENCE SYSTEM VERSUS FULL RING PET-SCANNER: FIRST RESULTS IN ONCOLOGIC PATIENTS.

Aim of this study was to compare the results of 18FDG positron imaging in oncologic patients using a coincidence gamma camera system (SoluS Epic MCD ADAC) and a full ring PET scanner (ECAT EXACT 922/47, Siemens). **Methods:** The study group consisted of 11 patients (age 56 ± 15 yrs) with a suspected diagnosis of primary or recurrent malignancy scheduled for PET. A conventional PET scan was performed 45-60 min after 187 - 313 MBq 18FDG i.v. 3 - 5 h p.i. a second scan of one body region was performed using a gamma camera coincidence system (FOV 35 cm). No attenuation correction was applied. PET data were reconstructed using filtered back projection (Hanning 0.4 cc), coincidence camera (CC) data by an iterative algorithm. In a first reading the CC images were interpreted unaware of the PET findings. In a second reading both modalities were analyzed together. Confining to the corresponding fields of view the number of lesions detected with CC or PET was compared. For semiquantitative analysis tumour/background (T/BG) ratios were calculated by ROI - technique for both methods in corresponding transaxial slices. **Results:** Both methods found focally increased glucose consumption indicating malignant disease in all patients. In the corresponding field of view PET detected a total of 45 lesions. By the first reading all but five lesions were clearly delineated by CC. By the second reading 4/5 lesions were accepted from the CC images in addition. The remaining lesion was most likely an axillary lymphnode metastasis in a patient with recurrent carcinoma of the breast. Due to technical reasons the CC scan was performed without elevated arms in this patient.

Table: Number of lesions (percentage) detected; tumour to background ratio

	1. reading	2. reading	T/BG	
PET	45 (100%)	45 (100%)	18.4 ± 27.1	p<0,001
CC	40 (89%)	44 (98%)	5.1 ± 8.3	

In two patients the CC findings of the first reading underestimated the tumour spread (1 axillary lymphnode metastasis in breast cancer and 2 lymphnode metastases in lung cancer). **Conclusion:** Even if the full ring PET scanner provides a higher image contrast the results for both methods in this small series of patients are comparable. Our first experience shows that only with careful reading of the CC images some „eye-catching“ PET - foci were reproducible with the gamma camera coincidence system.

OS-381

R.Burt, R.Witt, H.Park, A.Siddiqui, D.Schauwecker, H.Wellman, S.Das VAMC and Indiana University, Division of Nuclear Medicine

COMPARISON OF FDG-PET AND DELAYED FDG-SPECT FOR LUNG CANCER IMAGING

80 patients referred for evaluation of lung nodules or status of known lung cancer received both FDG-PET and SPECT imaging. All patients had direct pathologic confirmation or long followup.

The attenuation corrected PET study started 30 minutes after dose administration (total imaging time about 1.5 hours and the SPECT acquisition began about 1 to 2 hours later. A Siemens 931/35R PET scanner and a Trionix XLT (50 cm field of view, ultra high energy collimators) were used. The SPECT camera detected 7mm radioactive spheres in a standard Ga-68 PET Phantom while PET detected 4mm spheres.

Blinded interpretation were made of individually displayed PET and SPECT images and analyzed by the AFROC method. No difference in detection of lesions between instruments was found by the 5 member panel.

A retrospective direct review of an additional 40 patients whose images were compared side by side showed no clinically relevant differences.

The success of the SPECT method appears to be in large part from delayed imaging with clearance of FDG from normal tissues. At 2 hours there is retention of FDG in abnormal tissues and at times the heart. We now routinely use a 1 hour 45 minute to a 2 hour 15 minute delay when SPECT imaging is the only modality used.

FDG SPECT is an effective method of lung cancer or nodules evaluation with wider availability and lower costs than PET. The previously reported lower limits of resolution of lung lesions of 1.5 to 2.0 cm with other instruments are incorrect for this instrument.

OS-382

J.M.G. Chu, P. Lin, N. Pocock, T. Quach, B.M. Camden

Liverpool Hospital, Liverpool, Australia
Department of Nuclear Medicine & Clinical Ultrasound

18FDG PET WITH CO-INCIDENCE GAMMA CAMERA: INITIAL ONCOLOGY EXPERIENCE

Co-incidence Detection in gamma camera technology holds promise for the use of positron radiopharmaceuticals in non-dedicated PET facilities. We report our initial experience with this technique in the diagnostic evaluation of 40 patients with proven malignant tumours.

METHOD

All patients were scanned 60 minutes after 185MBq 18FDG was administered intravenously, in a fasting, well hydrated state and immediately after voiding. Emission Tomography was performed using an ADAC Solus, Molecular Co-incidence Detection (MCD) dual-head gamma camera. The scans were compared with standard conventional diagnostic imaging appropriate for each of the particular tumours (ie CT, MRI, plain X-rays, 67Ga scans, bone scans etc).

RESULTS

There were 25 males and 15 females. The average age was 60.5 years with a range of 26 to 83 years. 23 were studied prior to treatment, 5 during and 12 afterwards. The largest of the tumours demonstrable on conventional imaging was 6cm, the smallest was less than 2cm. The tumours were: Non-small cell lung cancer 7, colon 6, non-Hodgkins Lymphoma 6, adeno-carcinoma of unknown primary 5, breast 4, head & neck 3, testis 2 and 1 each of kidney, carcinoid, pancreas, pituitary, small cell lung, soft tissue sarcoma and Hodgkins Disease. Scan results of 43% were in concordance with conventional imaging. In 35%, the scan abnormalities were more extensive than those of conventional imaging. In the remaining 22%, conventional imaging abnormalities more extensive than those of the scans - but were commonly of patients who had prior treatment for their tumours.

CONCLUSION

Co-incidence Detection Positron Emission Tomography (Co-PET) with 18FDG has a promising role in Oncology. We have therefore commenced a prospective trial to evaluate the use of this technique in the pre-operative diagnosis and staging of solid tumours.

OS-383

AJ Green, KL Adamson, RHJ Begent

Department of Clinical Oncology, Royal Free Hospital School of Medicine
LONDON, NW3 2PF, UK

THE USE OF GAMMA CAMERA PET IMAGING IN CLINICAL TRIALS OF ANTI-CANCER TREATMENTS: A PILOT STUDY.

Gamma camera based 18F-FDG PET imaging may have an important role to play in the development of novel treatments for cancer. The measurement of the change in glucose metabolism over the course of a treatment will provide invaluable information about the efficacy of the treatment and may be considerably more sensitive than measurement of lesion size on CT or ultrasound.

We have used an ADAC dual headed camera in co-incidence mode (MCD) to image five patients taking part in a clinical trial of antibody directed enzyme drug therapy (ADEPT). The patients were imaged with 185 M Bq of 18F-FDG three days prior to starting the ADEPT treatment and on days 28 and 56 provided they had not started some other treatment by this time. For all the scans the patients were allowed a light breakfast and then nil by mouth for four hours. Approximately 185 M Bq of 18-F FDG was given i.v. and the precise administered activity recorded for later normalisation of the images. Imaging started 45-60 min after FDG administration, again the precise interval was recorded. Whole torso PET images were acquired using three rotations (ADAC recommend a 50% overlap to allow for the imaging characteristics of the camera in MCD mode) of 32 azimuths over 180 degrees: the average time per view was 40s (the acquisition software automatically compensates for 18F decay). Images were reconstructed using ordered subset maximum likelihood (2 iterations with 8 subsets) uniform elliptical attenuation was applied to aid visualisation of the lesions. Images were normalised for injected activity and radioactive decay during the interval between injection and imaging. Multi-slice regions were drawn around whole lesions, whole myocardium, whole kidney and sections of normal liver. Ratios of counts before and after treatment were calculated for tumour and normal tissues for both 28 and 56 day time points.

The ratios were not significantly altered by use of the simple attenuation correction method. Myocardium and liver showed small variations in FDG uptake with larger variations seen in the kidney uptake. Tumours showed significantly larger changes in glucose metabolism over the course of the study.

The consistency of normal tissue uptake and the change in tumour uptake in this pilot study show that gamma camera PET imaging has considerable promise for this application.

OS-384

Grahek D¹, Montravers F¹, Kerrou K¹, Younsi N¹, Wartski M², Zerbib E², Talbot J.N¹.

Services de médecine nucléaire, hôpital Tenon¹, centre chirurgical Marie Lannelongue², Paris-Ile de France, FRANCE.

STAGING OF LUNG CANCER BY [18F]-FDG ON A DUAL-HEADED GAMMACAMERA WITH COINCIDENCE DETECTION (CDET).

[18F]-FDG with positron emission tomography (PET) has been shown to be superior to conventional imaging (CI) for staging in non small cell lung cancer (NSCLC). Recently, our dual headed gamma-camera was equipped with CDET and thick crystals, to be able to detect FDG. Our aim was therefore to evaluate FDG-CDET in this indication, as part of a clinical trial (coordinator : JL Moretti).

Methods : Between July 1997 and March 1998, 47 patients (pts) (fasting for 6 h or more) had FDG-CDET for pre-operative staging of a NSCLC (diagnosed in 38 pts by biopsy before FDG-CDET). 45 min. after i.v. injection of 150-250 MBq of [18F]-FDG, a whole-body scan and at least one tomoscintigram on a PICKER Prism XP 2000 CDET camera were performed.

Results : Post surgical histology was obtained in 30 of 47 pts, 9 pts had chemotherapy for widespread tumor ; no result was obtained to date in the 8 last pts. All lung tumors clearly took up FDG, but in 1 case the counts ratio to contralateral healthy tissue was < 3 (46TP/47). In the staging of lymph node involvement, the agreement with histology for stages N0 or N1 was 20/25 (80%) for FDG vs 16/25 (64%) for CT; for N2 it was 5/5 for FDG vs 2/5 for CT. The histologic evaluation of suspected N3 lymph nodes (5 FDG+, 2 concordant with CT) was not done. All 8 metastatic sites confirmed histologically or highly probable on CI (3 lymphangitic carcinomatoses, 2 adrenal invasions, 2 bone metastases, 1 occipital lymph node only seen with FDG) were FDG+. FDG-CDET showed 7 others foci, without histologic evaluation until now. In 1 case, a FDG+ unknown focus was discovered in caecum which was endoscopically removed and proved to be a villous tumour.

Conclusion : These results indicate that FDG-CDET detected not only the primary lung tumor (Se=97,8%) but also its secondary deposits with a sensitivity (87%) similar to published values for FDG-PET and superior to that of CT (53%), and even evidenced other unsuspected tumours.

Radionuclide therapy

OS-385

S. C. Srivastava*, H.L. Atkins*, G.T. Krishnamurthy**, I. Zanzi^o, E.B. Silberstein*

*Brookhaven National Laboratory, Upton, NY **V.A. Med. Center, Tucson, AZ
^oNorth Shore Univ. Hosp., Manhasset, NY ^oUniv. of Cincinnati, Cincinnati, OH

LONG-TERM ANALYSIS OF PHASE II CLINICAL DATA FROM PATIENTS TREATED WITH TIN-117m DTPA FOR METASTATIC BONE PAIN

Purpose: This study was done to perform a detailed analysis of the Phase II data to assess the safety and efficacy of tin-117m DTPA for treatment of metastatic bone pain. **Methods:** 47 patients with metastatic bone pain (primarily prostate, breast and lung malignancies) were given a single i.v. administration of 185, 370, 462, 592, or 740 MBq/70kg of ^{117m}Sn DTPA. Urine and blood were collected during the 1st wk for dosimetry, along with images of ^{117m}Sn distribution. Patients were followed daily during the first wk, weekly for 2 months, and less frequently thereafter. Long-term follow-up for assessment of pain, analgesia requirements and hematological parameters continued for several months to over a year in surviving patients. **Results:** Overall, 30/40 assessable patients (75%) experienced complete response (CR) (12) or partial response (PR) (18) lasting for 4-60 wks (avg=98d). Time to onset of pain relief in CR was 5.3±4.3d, and in PR, it was 12.2±12.5d. Based on administered activity, those receiving <370 MBq/kg (n=10) experienced onset at 19±15d versus at 5±3d with >462MBq/kg (n=20) (p<0.05). Onset was modestly correlated with marrow dose, administered Sn-117m activity, and the bone index (r=-0.66, -0.59, and -0.49, resp.). The duration of response was more difficult to analyze since many patients died due to disease progression. CR were usually long lasting. 4/12 CR lasted until end of follow-up at 1.5, 2, 2, and 3 mo. 7/12 CR lasted until the patients died at 1.5, 3, 4, 4, 6, 12, and 14 mo. One patient was pain free for 11 mo; he was retreated at 12 mo and remained pain free until his death 5.5 mo later. 2/40 patients experienced grade 2 and 1/40 grade 3 WBC toxicity, but none showed platelet toxicity. This is much lower than what is reported for Sr-89 Cl₂, Sm-153 EDTMP, or Re-186 HEDP (p<0.01). **Conclusion:** At up to 10.6MBq/kg dose, ^{117m}Sn shows less hematological toxicity than the other β-emitting bone pain palliation agents (p<0.05). Overall response (avg. duration 98d) was 78% at 5.3-10.6MBq/kg doses. Time to onset of pain relief was shorter at higher doses (p<0.05). Two double-blind, randomized, multicenter clinical trials in 200 prostate and 75 breast cancer patients are currently in progress. This work was supported by the U.S. Dept. of Energy, Contract No. DE-AC02-98CH10886, and by Diatide, Inc.

OS-386

LUTETIUM-177-EDTMP FOR BONE PAIN PALLIATION. PREPARATION, BIODISTRIBUTION AND PRE-CLINICAL STUDIES.

G.A. Ruty Solá, D.L. Bottazzini, M.G. Arguelles, J.C. Furnari and H. Vera-Ruiz*
 Comisión Nacional de Energía Atómica, Centro Atómico Ezeiza, Buenos Aires, Argentina
 *International Atomic Energy Agency, Vienna, Austria

Beta emitting radionuclides have demonstrated excellent properties for radionuclide endotherapy using appropriate carrier molecules. In particular, ¹⁵³Sm-EDTMP is already in clinical use as an effective palliative agent for bone metastasis. In an effort to search for alternative radionuclides with different radioactive decay characteristics (half-life and particle energy) with improved therapeutic effectiveness and facilitate the logistics of transportation to distant centres from the production facilities (1/2 of ¹⁷⁷Lu 6.6 days as compared with 1.9 days for ¹⁵³Sm), the preparation of ¹⁷⁷Lu-EDTMP was undertaken. Natural Lu₂O₃ was irradiated at the RA-3 nuclear reactor of the Ezeiza Atomic Center at a neutron flux of 7 × 10¹³ n/cm sec for 5 to 7 days producing Lutetium-177 of high radionuclidic purity as controlled by high resolution gamma spectrometry with radioactive specific activities up to 180 mCi/mg. The optimal molar ratio of EDTMP: Lu that yields a product with the highest radiochemical purity (> 98 %), as well as adequate in-vitro and in-vivo stability was studied. At a molar ratio of 20:1 it was found that the complex is stable up to 7 days as tested by paper chromatography. Biological distribution in Wistar rats as follow by sacrificing the animals at different times post-injection and gamma camera imaging in New Zealand rabbits, shows high bone up-take (> 1% in femur) that does not decrease up to 6 days post-injection, high renal excretion, (> 40-50 % of the injected dose is eliminated in 2 hrs) and low hepatic up-take (< 1%). These biodistribution values do not change when solutions of ¹⁷⁷Lu-EDTMP were injected after 6 days of preparation, indicating an excellent in-vitro stability.

These results indicate that a) using naturally enriched inexpensive Lutetium oxide, ¹⁷⁷Lu of high purity for the preparation of Lutetium-177-EDTMP can be prepared, b) ¹⁷⁷Lu-EDTMP has comparable stability and biodistribution characteristics as its Samarium counterpart and c) an excellent alternative therapeutic radiopharmaceutical with extended time for clinical use after production, aspect of important significance for remote hospitals from the nuclear installations.

OS-387

V. Soukhov, L. Korytova, T. Khazova, O. Korytov

Central Research Institute of Roentgenology and Radiology, Saint-Petersburg, Russia

CLINICAL SETTING OF STRONTIUM-89 IN PATIENTS WITH PAINFUL METASTATIC CANCER IN BONE.

The study involved patients with multiple bone metastases demonstrated by scintigraphic evidence and increasing pain requiring palliation who were eligible for systemic administration of "Metastron" (n=47), local field radiotherapy (n=26) or hemibody irradiation (n=41). The objectives were to assess original and new sites of pain, requirements for further radiotherapy, toxicity and survival.

Patients with bone pain from endocrine refractory metastatic prostate cancer, breast and lung cancer and some other malignancies were treated with "Metastron" (Amersham International, Ltd., UK) - 4.0 mCi (40-70 micro-Curi/kg) of Sr-89 or received the external beam therapy.

All patients was followed with bone scintigraphy scans, pain, sleep and activity diaries, records of medications taken and Karnofsky index. They were adequately followed up and survived more than six months.

The majority of patients became pain free or obtained partial relief of pain without differences between therapeutic modalities. Patients noted the reduction of analgesics intake, requirement for external beam radiotherapy and the appearance of new pain sites. Tumor markers was also reduced and there was no new metastatic sites by bone scintigraphy. However, only after Sr-89 therapy response was maintained for at least 4 months and significantly fewer patients noted new sites of pain and required further radiotherapy at any (new or original) painful sites. Moreover, Sr-89 therapy associated only with mild and transient hematologic depression while external beam radiotherapy causes greater toxicity including gastrointestinal symptoms. Although there was no differences in survival between Sr-89 and external beam therapy groups, another prospective trial will help to estimate whether systemic radiotherapy offer survival advantage over other modalities.

"Metastron" has proven to be more efficacious than external beam therapy in patients with metastatic bone cancer for reducing progression of disease as evidenced by new sites of pain, the requirement of further radiotherapy and need for analgesic support thus improving the quality of remaining life with only little hematologic toxicity.

OS-388

ZY Pan, SL Zhu, DM Chen and W Fan*

Beijing Medical University, First Hospital, Beijing 100034, and Zhongshan Medical University, Cancer Hospital, Guangzhou*, China.

PHASE I STUDY OF ¹⁵³Sm-EDTMP DOSE-RESPONSE RELATIONSHIP IN RELIEVING METASTASIS BONE PAIN

Aim: Study relationship between ¹⁵³Sm-EDTMP dose and both toxicity and effect in relieving metastasis bone pain for recommendation of an optimal dose to be used in Phase II clinical trial.

Methods: ¹⁵³Sm-EDTMP was prepared by CIAE. Rp> 98%. 17 patients with significant bone pain induced by metastasis divided into 3 groups based on dose: 0.5mCi/kg, 1.0mCi/kg and 1.5mCi/kg. WBC>3.5 × 10⁹/L, PLT>85 × 10⁹/L.

Results:

1. Efficacy and dose

group (mCi/kg)	No. of cases	complete relief (1)	significant relief (2)	mild relief (3)	no response (4)	effective (1+2)
0.5	4	1	1	0	2	2/4
1.0	6	0	2	2	2	2/6
1.5	4	0	3	1	0	3/4

2. Haematology toxicity and dose

group (mCi/kg)	No. of cases	WBC ↓			PLT ↓		
		10 ⁹ /L	% nadir,wk	3	10 ⁹ /L	% nadir,wk	4
0.5	6	1.4	18.9	3	105	47.9	4
1.0	6	2.7	36.2	4	132	59.6	4
1.5	5	4.2	49.5	5	166	60.3	4

Severe haematology toxicity (grade IV) did not appear in any group.

Conclusion: In the range from 0.5 mCi/kg to 1.5mCi/kg, the efficacy of relieving bone pain seems to increase along with ¹⁵³Sm-EDTMP dose goes up and the haematology toxicity appears more significantly. But the toxicity is still temporary and tolerable. Therefore, 1.0mCi/kg and 1.5mCi/kg are recommended to be the main doses used in Phase II clinical trial of ¹⁵³Sm-EDTMP.

Being supported by IAEA CRP E1.30.13 and CIAE.

OS-389

M. Rutgers, C.K.M. Buitenhuis, L.A. Smets, C.A. Hoefnagel(&), P.A. Schubiger(#), I. Novak-Hofer(#).
Departments of Experimental Therapy and Nuclear Medicine (&), Netherlands Cancer Institute, Amsterdam, The Netherlands.
Center for Radiopharmacy (#), Paul Scherrer Institute, Villigen-PSI, Swiss.

TARGETED RADIOTHERAPY OF NEUROBLASTOMA XENOGRAFTS IN MICE: 131I-CE7 CHIMERIC ANTIBODY (CE7) vs 131I-MIBG (MIBG)

Using macroscopic and microscopic xenograft models we have demonstrated that 131I-MIBG can effectively debulk neuroblastoma but is decreasingly effective for microscopic tumors. Because the presence of non-storing cells can be a limiting factor in therapy with radioiodinated MIBG, we have investigated the feasibility of radiolabeled, neuroblastoma-specific, chCE7 antibody for complementary treatment. For both human SK-N-BE (BE) and SK-N-SH (SH) neuroblastoma growing as s.c. tumors in athymic BALB/c nude mice, we studied the biodistribution of radioactivity with time and the antitumor response after a single i.v. administration of 131I-MIBG (s.a. 1.5 GBq/mg) or 131I-CE7 (s.a. 150 MBq/mg). Peak tumor levels as percent injected dose/g (mean ± SD, n=4-8) were 22 ± 5 (BE) or 11 ± 2 (SH) for CE7 (24 h p.i.) and 2.5 ± 0.4 for MIBG in both xenografts (1 h p.i.). BE tumors cleared the MIBG significantly faster than the SH. Tumor/blood ratios were consistently higher with MIBG than CE7. Therapy results are expressed as days to reach 4 times the pre-treatment tumor size being 6 ± 1 (BE) and 8 ± 1 (SH) for saline-injected controls (n=6). Treatment with 17 MBq 131I-CE7 or 112 MBq 131I-MIBG significantly inhibited tumor growth (p < 0.05; n=5-6): 30 ± 5 or 9 ± 2 for BE and 42 ± 3 or 33 ± 4 for SH. With 17 MBq of a non-specific 131I-antibody (Ab35) the SH tumor size increased 4x in 17 ± 4 days. Thus for both neuroblastomas, a) the number of tumor volume doublings delayed by the CE7 treatment was similar, and b) the therapeutic efficacy of 131I-CE7 was superior to 131I-MIBG in agreement with a 13- (BE) or 2-fold (SH) increased tumor radiation exposure. The 131I-MIBG-induced body weight loss was mild but highly variable for the radioimmunotherapy groups, but the therapeutic ratio of 131I-CE7 was at least as high as with MIBG. **Conclusions:** This is the first study to show that 131I-CE7 very effectively inhibits neuroblastoma growth. Targeted CE7 radiotherapy seems a promising alternative in rare cases of MIBG-negative disease and a valuable tool to treat residual neuroblastoma after standard 131I-MIBG therapy.

OS-390

JM Connert, TL Buettner, DW McCarthy*, CJ Anderson*

Department of Surgery and Mallinckrodt Institute of Radiology, Washington University School of Medicine, St. Louis, MO., 63110 USA.

MAXIMUM TOLERATED DOSE STUDIES IN HAMSTERS WITH Cu-64-BAT-2IT MAb 1A3, AN ANTI-HUMAN COLORECTAL MAb

The purpose of this study was to determine the maximum tolerated dose (MTD), the highest possible dose resulting in no animal deaths and less than 20% weight loss) of Cu-64-BAT-2IT MAb 1A3 in hamsters. In previous studies we have found that 82% of hamsters with small (0.2-0.4 g) GW39 human colorectal tumors were alive and tumor free 7 months after treatment with 2 mCi of Cu-64-BAT-2IT MAb 1A3 (n=17). In contrast, saline control hamsters were sacrificed by 5 weeks due to large tumor burden (>10 g). In the current studies non-tumor bearing hamsters were injected with varying amounts of Cu-64-BAT-2IT MAb 1A3 (>10 mCi) normalized to mCi injected/kg of hamster body weight. The animals were weighed and observed daily for any change in gross physical appearance. Weight loss greater than 20%, lethargy, scruffy coat or diarrhea were indications of toxicity. Samples of blood from control and treated animals were taken by retroorbital bleeding at days 0 and approximately every week thereafter for 6 weeks for analysis of hematology and liver and kidney enzyme levels. Results indicated that the MTD was 150 mCi Cu-64/ kg of body weight. Hamsters receiving higher doses (170-190 mCi) lost greater than 20% of their body weight and all died between 8 and 13 days (n=3). All hamsters receiving doses 150 mCi/ kg (120-150 mCi, n = 13) survived to the experimental endpoint (6 weeks) with an overall gain in weight. WBC and platelet counts were depressed in all animals 7 days after treatment, but returned to normal values in the survivors by two weeks. We conclude that Cu-64-BAT-2IT MAb 1A3 is able to cause tumor growth inhibition and regression at doses > 7 fold lower than the MTD, suggesting that "Cu-labeled agents are excellent candidates for RIT.

Endocrinology/Thyroid

OS-391

P. MIKOSCH, H.J. GALLOWITSCH, E. KRESNIK, I. GOMEZ, P. LIND

Department of Nuclear Medicine and Special Endocrinology, General Hospital Klagenfurt, Austria

Interassay-Comparison and Interpretation on Clinical Data of Two Immunoradiometric Assays (IRMA) of Thyroglobulin

Aim: The aim of this study was to compare two different thyroglobulin-immunoradiometric assays (Tg-IRMA) with each other for interassay correlation, sensitivity, specificity, positive and negative predictive value (PPV, NPV) in the follow up of patients with differentiated thyroid cancer (DTC). The question was whether a decrease of the functional assay sensitivity from 0,5ng/ml to 0,3ng/ml can show an improvement of clinical results. **Material and methods:** All imaging data (ultrasonography of the neck, I-131 whole body scintigraphy, Tc-99m tetrofosmin whole body scintigraphy) were used for the interpretation of measured Tg levels and the clinical follow-up of up to 17 years was included, too. 432 samples of 286 patients (220 female, 66 male; age 16-83 for patients with DTC, age 1-81 for patients without DTC) were investigated. According to the clinical background groups included patients a) without any evidence of thyroid tissue b) with thyroid remnants and c) with recurrence or metastases of thyroid cancer. In addition a further differentiation was done according to the state of TSH level (L-T4 on and L-T4 off). **Results:** Mean values and standard deviations (SD) of the different groups showed comparable results for the two kits. The two assays also presented a good overall interassay correlation of 0,839. Correlation to clinical data using different clinically relevant cut off levels showed acceptable results for both kits, too, whereas the results for kit A were slightly better than those of kit B. The sensitivities and the NPV of both kits were comparably high due to different cut off levels. However, the specificity and the PPV showed a better performance with kit A especially at the low and critical cut off level of 0,5ng/ml. Therefore, the functional assay sensitivities as described by the producers could be already met to a high degree at the 0,5ng/ml level by kit A, but not at the 0,3 ng/ml by kit B. Kit B also presented worse results at the 0,5ng/ml cut off level in comparison to kit A. This difference was especially due to a higher spread of results in the very low range of Tg measurements with kit B in patients without any evidence of progressive disease. The presence of non-malignant thyroid remnants made the interpretation of Tg measurements more difficult with both kits and thus limited the value of the Tg measurements in these cases.

OS-392

A.Spanu, M.E.Solinas, P.Chiamida, A.Falchi, C.Bagella, P.Solinas, A. Masia, S.Nuvoli and G.Madeddu.
Dept. of Nuclear Medicine. University of Sassari. Italy.

TC-99m TETROFOSMIN (T) PINHOLE (P) SPECT IN NECK METASTASES FROM DIFFERENTIATED THYROID CARCINOMA (DTC).

To improve the effectiveness of T-scan used as alternative tool to 131I-WBS in the diagnosis of DTC neck metastasis, we studied 63 pts, 49F and 14M, aged 19 to 81 yrs: 6 cases (G1) in hypothyroidism after thyroidectomy and 59 cases (G2) on L-Thyroxin suppressive therapy in follow up after radioiodine ablation. Both planar and 360° SPECT images were acquired using a rectangular dual head gamma camera equipped with HR collimator, centered on the neck, 10 min after 740 MBq T injection. Neck P-SPECT images over 180° (from -90° to +90°) were then acquired using a tilted circular HR gamma camera with a 128x128 matrix and a zoom 2. Pinhole aperture size (4.45mm), angular step (6°) and time/frame (40 sec) were selected on the basis of our previous studies with an experimental phantom simulating different sized lesions in a hypothetical neck region. P-SPECT projections were reconstructed by a cone beam algorithm and filtered by a Metz filter. T studies were compared both to DS and Therapeutical (TS) radioiodine scans, and related to TG and histology. In G1 pts, there were 16 true positive areas (10 residual tissue, 6 metastatic lesions) at P-SPECT, 15 at SPECT, 7 at planar. Both DS and TS missed 4 metastases, all confirmed at histology. Only DS had 3 false positive results. In 11 G2 pts with high TG and negative DS, P-SPECT evidenced 24 malignant lesions ascertained at histology, SPECT 21 and planar 8; only 4 were positive at TS. In 4 other G2 pts with high TG and positive DS, P-SPECT, like TS, identified 6 lesions, SPECT 5 and planar 4; DS was positive only in 4. Moreover, both P-SPECT and SPECT were concordantly positive with DS for 3 lesions (planar only in one) in 3 further G2 pts with low TG, both during therapy and hypothyroidism. Finally, in 38/39 G2 pts with persistently negative DS and low TG, P-SPECT, SPECT and planar were true negative. In the remaining one case, only P-SPECT evidenced 2 metastases. Our preliminary data confirm T scan as a reliable method to identify DTC neck lesions, often providing better results than DS. Moreover, both P-SPECT and SPECT gave more information than planar in our cases, but P-SPECT apparently proved the best resolute diagnostic method.

OS-393

R. Lietzenmayer, M. Müller-Berg, M.H. Thelen, B.M. Dohmen, H. Dittmann, W. Müller-Schauenburg, R. Bares
Department of Nuclear Medicine
Eberhard-Karls-University, Tübingen, Germany.

CLASSIFICATION AND FOLLOW-UP OF DIFFERENTIATED THYROID CANCER (DTC) BY FDG-PET

Purpose: Recent reports have demonstrated, that recurrences of DTC have often lost the ability to concentrate radioiodine, while increased glucose metabolism measured by PET is present. Aim of this study was to analyze, whether this metabolic behavior already exists prior to radioiodine treatment or arises later during the course of disease.

Patients and Methods: 18 pts. (13 f, 5 m, 51±20 years) with DTC (7 follicular [f], 10 papillary [p], 1 pap. with an oncocyctic portion [onc]) and a TNM-stage of T=4 and/or N/M>0 were examined by Iodine-131 whole body scanning (WBS) and FDG-PET after total thyroidectomy. In 13 pts. (5 f, 8 p, 1 onc) with metastatic spread follow-up examinations were performed by WBS and FDG-PET (n=20). Data were compared intraindividually and correlated with tumor histology and clinical course (hTg, CT-findings).

Results: In 8 pts. (7 p, 1 f) with both negative WBS and PET scans clinical course (> 12 months) did not reveal any evidence of recurrent disease. Ten pts. had metastases (4 p, 6 f; 9x lymph node mets [LNM], 7x distant mets). Eight of these pts. revealed concordant findings of WBS and PET. In two pts. a discordant uptake pattern was found: 1) LNM: WBS +, PET - (f). 2) multiple mets: WBS -, PET + (onc). In the follow-up, 6 pts. showed concordant behavior of WBS and PET: 4 pts. => improvement (3 f, 1 p); 1 pt. => stable disease (p); 1 pt. => progress (f). In 4 pts. discordant findings were obtained: regression in WBS, increase in PET => progressive disease (n=1, onc); constant WBS, decrease in PET => tumor regression (n=2, p) or stable disease (n=1, f).

Conclusion: These data indicate, that iodine negative metastases in untreated differentiated thyroid cancer appear very rarely. The origin of iodine negative metastases might therefore be due to mutation and selection of tumor cells, which were not killed by preceding treatment courses. Most metastases reveal concordant behavior of glucose and iodine metabolism after radioiodine therapy. Increasing FDG-uptake appears to be an indicator of poor prognosis and should therefore initiate intensified treatment protocols, e.g. use of antiproliferative drugs.

OS-394

D. Rubello, U.P. Guerra^o, P. Gasparoni^{oo}, F. Chierichetti, E. Englaro^o, P. Zanco, F. Giacomuzzi^o, G. Ferlin.
Nuclear Medicine - PET Centre, ^{oo}Endocrinology, Hospital of Castelfranco V.to (TV); ^oNuclear Medicine, Hospital of Udine, Italy.

DIAGNOSTIC ROLE OF FDG PET IMAGING IN PATIENTS AFFECTED BY DIFFERENTIATED THYROID CARCINOMA (DTC) WITH HIGH SERUM TG LEVELS AND NEGATIVE 131-I SCAN.

A few studies, with discordant results, have been reported about the potential role of FDG PET imaging in DTC patients (pts). To better define this topic, we evaluated 29 consecutive pts (18 F, 11 M, mean age 49.3 years), of whom 4 preoperatively, and 25 after total thyroidectomy and radioiodine therapy: 5/25 of them had a positive 131-I scan for the presence of metastases (M), 17/25 had a negative 131-I scan but elevated serum Tg levels, and 3/25 had a negative 131-I scan, undetectable Tg serum levels but enlarged loco-regional lymphnodes (LN), suspected to be metastatic, at CT scan (inflammatory LN at biopsy). FDG PET results were compared with conventional imaging techniques (131-I scan, neck US, chest x-rays, chest and superior abdomen CT scan). In 2/4 preoperatively studied pts, PET revealed a greater number of M (in 1 case LNM, in 1 case pulmonary M - PM). Regarding the group of 17 pts with negative 131-I scan but elevated serum Tg levels: in 7 pts PET was superior to the other imaging techniques in visualizing M (3 cases with PM, 1 with PM + LNM, 2 with LNM, 1 with a local tumor relapse); in 6 pts PET provided the same information of the other modalities (3 cases with LNM, 1 with PM, 1 with PM + LNM); in 4 pts all the diagnostic techniques were negative for the presence of disease. In the 3 pts with false positive LN lesions at CT scan, FDG PET resulted correctly negative. In the group of 5 pts with positive 131-I scan, PET provided the same information of 131-I scan in 2 cases, revealed a greater number of loco-regional LNM in 1 case, whereas 131-I scan showed a greater number of LNM in the other 2 pts. On the basis of our results, we can conclude that FDG PET represents a highly sensitive technique in detecting metastases in DTC and the use of this imaging modality should be recommended in pts previously treated by surgery and radioiodine, with high serum Tg levels and negative 131-I scan.

OS-395

K. Brandt-Mainz¹, S.P. Müller¹, R. Gorges¹, B. Saller², A. Bockisch¹
Kliniken für Nuklearmedizin¹ und Endokrinologie²,
Universitätsklinikum Essen, Germany

FLUOR-18-FDG IN THE FOLLOW-UP OF MEDULLARY THYROID CARCINOMA.

The early detection of medullary thyroid cancer (MTC) metastases is important since the only potentially curative therapy is early surgical tumor resection. There is no sensitive diagnostic imaging modality for the localization of MTC metastases. Therefore, several tests are performed in patients with elevated tumor marker (ultrasonography, MRI, CT, Tc-99m-V-DMSA, In-111-Pentreoide). We investigated PET with Fluor-18-FDG in the follow-up of MTC in patients with elevated calcitonin-levels and/or sonographic abnormalities in the neck.

In a prospective study, we examined the neck and the thorax of 16 patients (12 males, 4 females) starting 30 min after injection of 370 MBq F-18-FDG using a Siemens CTI 953/15 PET-scanner. Attenuation correction based on transmission-scans was used in all patients. The validation was done by histology, CT, or selective calcitonin measurements.

In 12/15 patients, we detected tumor (9 patients were validated by histology, 3 by CT). 4 patients showed completely negative PET-scans (1 patient true negative, 3 patients false negative). Analyzing the different localizations of metastases separately, we found 11 of 12 known lesions in the neck, 3 of 4 known lesions in the mediastinum, 1/1 lesion in the thorax, and 1/1 lesion in the bone. 2 patients had FDG-accumulations in the mediastinum without correlation in CT. In addition, 1 patient with silicosis and 1 patient with pleural fibrosis showed FDG-accumulations.

Especially for cervical tumors, where complete remission can be achieved by surgery, FDG-PET seems to be a valuable diagnostic method in the follow-up of MTC.

OS-396

G. Ronga, M. Filesi, G. Ventroni, T. Montesano, C. Pace
SS Nuclear Medicine, Clinica Medica II, University of Rome "La Sapienza" - Italy

THE INFLUENCE OF 131-I UPTAKE BY METASTASES ON SURVIVAL OF PATIENTS DEAD FROM DIFFERENTIATED THYROID CARCINOMA

We retrospectively studied 84 patients dead because of differentiated thyroid carcinoma (DTC) (31 follicular, 53 papillary, M/F ratio 1:1.5). All pts underwent a total thyroidectomy and then were treated with 131-I for local and/or metastatic disease. These pts were classified for metastases site and presence (Group 1) or absence (Group 2) of 131-I uptake. Mean age at diagnosis and mean survival from surgery were calculated.

Site	Mean age ± SD (yrs)			Mean survival ± SD (yrs)		
	Group 1	Group 2	Total	Group 1	Group 2	Total
Bone (n=17)	50.1±12.8 n=14	58.3±14.1 n=3	51.6±13.0	7.4±6.2 n=14	3.3±2.5 n=3	6.7±5.9
Lung (n=22)	49.1±14.4 n=15	49.6±16.1 n=7	49.3±14.6	8.3±6.5 n=15	5.6±6.3 n=7	7.4±6.4
Other site (n=12)	54.7±4.3 n=4	51.2±18.8 n=8	52.4±15.3	8.7±7.0 n=4	15.0±8.9 n=8	12.9±8.6
Multiple (n=16)	47.5±13.3 n=8	44.2±11.0 n=8	45.9±11.9	7.9±6.7 n=8	6.7±7.4 n=8	7.3±6.9
Lymph n. (n=5)	---	---	59.4±14.5	---	---	5.0±4.5
Local rec. (n=12)	---	---	63.6±12.6	---	---	3.0±4.7
Total	49.7±13.1 n=41	49.4±15.8 n=26	52.2±13.6 n=84	7.9±6.5 n=41	8.6±7.3 n=26	7.2±6.5 n=84

Mean age and mean survival were significantly different between local recurrences and the remaining metastases site (p=0.015, p=0.02, respectively). No significant difference was observed among 131-I uptaking metastases and non 131-I uptaking ones. Local recurrences seem more frequent in older pts and may determine a lower survival, probably due to the high cancer aggressiveness. Finally, 131-I uptake by metastases seems not to influence significantly the natural history of disease. However, we observed very few deaths for lymph node metastases, because of their high sensitivity to 131-I therapy.

Neurology/Psychiatry: Dopamine + serotonin studies

OS-397

A.M. Catafau, J. Guardia, J.C. Martin, A. Flotats, C. Mari, B. Gonzalvo, L. Segura, M. Estorch, Ll. Bernà, M. Casas, I. Carrió. Hospital de Sant Pau. Nuclear Medicine and Addictive Behavior Depts. Barcelona, Spain.

INCREASED STRIATAL 123I-IBZM UPTAKE MAY PREDICT RELAPSE IN ALCOHOLIC PATIENTS

Several neurotransmitter systems seem to be involved in alcohol addictive behavior. A potential for dopaminergic agents to reduce alcohol consumption has been suggested, although the role of the dopaminergic system in alcohol addiction is still controversial. The aim of this study was to assess the utility of 123I-IBZM SPECT in the diagnosis and prognosis of relapse in alcoholic patients.

123I-IBZM SPECT was performed on 14 alcoholic inpatients during detoxification, and on 9 age-matched normal volunteers as a control group. Free post-synaptic D2 receptor density was estimated by a basal ganglia/occipital cortex (BG/O) uptake index at 90 min. post-injection. Six patients underwent a second SPECT 3 months after detoxification. Patients were followed up to detect relapse.

The mean BG/O index in alcoholic patients during detoxification was 1.77 ± 0.11 , and in controls 1.75 ± 0.11 ($p=NS$). The BG/O index was significantly higher in the subgroup of alcoholic patients which showed relapse than in the subgroup which remained abstinent (1.80 ± 0.8 , $n=9$ vs. 1.70 ± 0.8 , $n=5$; Mann-Whitney U-test $p<0.05$). In the 6 patients who underwent a second SPECT, an increase in the BG/O index was found in the 2 patients who subsequently relapsed, whereas a decrease was observed in 3 of the 4 patients who remained abstinent.

In conclusion, increased striatal IBZM uptake seems to identify alcoholic patients at risk of relapse, supporting a role for the dopaminergic system in alcohol addiction.

OS-398

E. Donnemiller, G.K. Wenning*, C. Brenneis*, J. Wissel*, W. Poewe*, G. Riccabona. Departments of Nuclear Medicine and Neurology*, University of Innsbruck, Austria.

STRIATAL DOPAMINE TRANSPORTER (DT) FUNCTION AND D2-RECEPTOR BINDING IN PATIENTS WITH SEVERE HEAD INJURY STUDIED BY SPET USING 123I-BCIT AND 123I-IBZM

Akinetic rigid syndromes are established sequelae of acute severe head injury (HI). So far, underlying nigrostriatal dysfunction has not been demonstrated in such patients (pts) using receptor ligand SPET.

We therefore studied changes in pre- and postsynaptic dopaminergic function in 10 pts with HI (2 females and 8 males, 3.9 ± 2.1 months after HI, mean Glasgow-Coma-Scale-Score=6) and evidence of either akinesia and/or rigidity with SPET using 148 MBq 123I-BCIT and 185 MBq 123I-IBZM as tracers. Average age was 33 ± 13 years and no drugs which could interfere with traceruptake were given at the time of SPET, which was performed with an ADAC Vertex dual-head imaging system in pts studies and a single head Siemens orbiter ZLC 3700 camera in normal controls (ncs) using a standardized protocol described previously.

Data of count ratios striatum/cerebellum (crS/C) were calculated 2h after tracer application for 123I-IBZM and crS/C for 123I-BCIT 3h and 18h after tracer injection. SPET data were compared with 6 age-matched ncs. Additional CT and/or MRI studies showed a variety of cortical and subcortical lesions, basal ganglia (BG) however and cerebellum appeared normal in 9 pts.

All pts showed unilateral or bilateral impairment of presynaptic DT binding on scans and a significant reduction of 123I-BCIT binding kinetics could be demonstrated (pts: crS/C18h 3.80 ± 1.34 versus ncs: crS/C18h 8.52 ± 0.82 , pts: crS/C3h 2.01 ± 0.44 versus ncs: crS/C3h 2.98 ± 0.28 , $p<0.001$). Decreased D2-receptor binding was found in all but two of the pts. (pts: crS/C2h 1.47 ± 0.11 , versus ncs: crS/C2h 1.74 ± 0.06 , $p<0.001$). Dopamine agonist therapy was administered to 5 pts and was beneficial in 2 of them, 1 had a normal IBZM study and the other unilaterally decreased IBZM binding. Our findings suggest that nigrostriatal dysfunction may be detected using SPET in pts with severe head injury despite a lack of structural lesions within the BG. The mechanisms of persistent posttraumatic down regulation of dopaminergic function remain to be explored.

OS-399

MJ Ribeiro¹, JL Baulieu², C Levilion-Prunier², C Janeiro¹, F Chossat³, D Guilloleau², AC Santos¹, L Mauclair³, J Marchand³, A Autret², L Cunha¹, JC Besnard², J Pedroso de Lima¹
¹HUC, Coimbra, Portugal ²INSERM U316 CHU Tours, ³CIS Biointernational Gif-sur-Yvette, France

SPECT AND 123I-IBZM UPTAKE (123I-ILIS) IN EXTRA-PYRAMIDAL SYNDROMES

The aim of this work was to evaluate 123I-ILIS as a radioligand of dopamine receptors in patients with extra-pyramidal diseases by using different cameras in different centers.

46 patients (P) (30M, 26F) were distributed by 2 centers (22 + 24 pts) and were divided in 2 groups: group 1 ($n=29$ age= 67.8 ± 3.5 yrs): idiopathic Parkinson disease, group 2 ($n=17$, age= 57.5 ± 7.1 yrs): other extra-pyramidal syndrom. 123I-ILIS, 1.7 to 2.8 MBq/kg, was injected after informed consent. Imaging was performed with a single head camera (camera A, GE400AC*, 21 studies 1 hr p.i.), a dual head camera (camera B, Helix Elscint*, 18 studies 1.5hr to 2.5hr p.i.), a triple head camera (camera C, Neurocam GE*, 17 studies 45mn to 2hr p.i.) and a brain dedicated annular detector (camera D, Ceraspect DSI*, 14 studies 1 to 3hr p.i.). Striatal /frontal cortex ratio (S/FC) was calculated from standardized, geometrical ROI's. No pt showed any undesirable effect. All SPECT images were interpretable. S/FC values were as follows:

cameras	group 1	group 2	
A	1.48 ± 0.20	1.26 ± 0.25	$p=0.036$
B	2.32 ± 0.27	1.75 ± 0.70	$p=0.025$
C	1.55 ± 0.22	1.34 ± 0.15	$p=0.033$
D	3.07 ± 1.30	2.11 ± 0.66	$p=0.039$

We conclude that 123I-ILIS is able to provide functional information about the striatal dopaminergic synapse in patients with extra-pyramidal degenerative disease. The clinical use of 123I-ILIS will require the normalization and standardization of the imaging and data processing procedures.

OS-400

İlgin N., Gökçora N., Atavcı S., Şenol S., Gücüyener K.

Department of Nuclear Medicine, Gazi University, Ankara-Turkey.

D2 RECEPTOR IMAGING WITH 123I-IBZM BRAIN SPECT IN ATTENTION DEFICIT HYPERACTIVITY DISORDER

Attention deficit hyperactivity disorder (ADHD) is a common condition of childhood the symptoms of which include inattention, excessive motor activity, impulsivity and distractibility. Dopamine is believed to play a major role in the manifestation of ADHD. The purpose of this study was to evaluate the striatal dopamine D2 receptor density in children with attention deficit hyperactivity disorder (ADHD) using ¹²³I-IBZM brain SPECT and to correlate the findings with the severity of ADHD as well as therapeutic outcome. Eight children (mean age 9.8 ± 2.3) who were diagnosed to have ADHD using the criteria of DSM IV were included in this study. ¹²³I-IBZM brain SPECT was performed at the time of the diagnosis and 3 months after methylphenidate ($0.2-0.5$ mg/kg/day) therapy. After an intensive thyroid blocking scheme ¹²³I-IBZM brain SPECT was performed 2 hours following i.v. injection of $50 \mu\text{Ci/kg}$ ¹²³I-IBZM. Specific binding ratios of striatal to occipital cortex (ST/OC) representing Bmax/Kd were calculated using 3 consecutive transaxial slices obtained parallel to the orbito-meatal line. The pre-therapy ST/OC ratios (mean 2.66 ± 0.70) were significantly higher (60-80%) from the previously reported healthy adult values, returning back to near-normal values after methylphenidate therapy ($p=0.04$). Therapeutic outcome was also determined by serial neuropsychiatric examinations and seven children had dramatic response to methylphenidate therapy while remaining one showed minimal benefit. The mean pre-therapy attention deficit and hyperactivity scores changed from 18 to 9 and 16 to 8 respectively in the post-therapy period. The results of this study suggest a baseline D2 receptor density abnormality in ADHD which is down-regulated back to near-normal adult values after methylphenidate therapy.

Neurology/Psychiatry: Dopamine + serotonin studies
OS-401

J. Booij, J.T.G.M. Hemelaar, J.D. Speelman, K. de Bruin, A.G.M. Janssen, and E.A. van Royen

Graduate School of Neurosciences, Department of Nuclear Medicine, Academic Medical Center, Amsterdam, The Netherlands

ONE-DAY PROTOCOL FOR IMAGING OF THE NIGROSTRIATAL PATHWAY IN PARKINSON'S DISEASE BY [123I]FP-CIT SPECT

The main neuropathological feature in Parkinson's disease (PD) is degeneration of dopaminergic neurons in the substantia nigra, resulting in loss of striatal dopamine (DA) transporters. Recently, a SPECT ligand (*N*- ω -fluoropropyl-2 β -carbomethoxy-3 β -(4-iodophenyl)tropane [FP-CIT]) with fast kinetics has been developed for in vivo imaging of DA transporters. In this study we developed an [123I]FP-CIT SPECT protocol for routine studies. We examined the time course of [123I]FP-CIT binding to DA transporters in 10 healthy controls (mean age 53 yr) and 19 patients with PD (57 yr; H&Y I-IV). 110 MBq 123I-FP-CIT was injected and SPECT studies were performed with a brain dedicated SPECT camera (SME 810) up to 6 h post-injection (p.i.). The time of peak specific striatal binding (striatal-occipital binding) was highly varied between subjects, but, specific binding peaked in all controls and patients within 3 h p.i. Between 3 and 6 h p.i., the ratio of specific to non-specific striatal FP-CIT binding was stable in both groups (non-parametric ANOVA), but significantly lower in patients (non-parametric Mann-Whitney U test) (Table).

Ratios of specific to non-specific striatal [123I]FP-CIT binding in controls and patients with PD (mean \pm SD)

	3 h p.i.	4.5 h p.i.	6 h p.i.
Controls	2.24 \pm 0.32	2.28 \pm 0.57	2.20 \pm 0.55
Patients	0.89 \pm 0.34*	0.89 \pm 0.34*	0.88 \pm 0.28*

*Significantly different from controls

In patients, [123I]FP-CIT binding in the putamen was more decreased than in the caudate nucleus, and contralateral striatal binding was significantly lower than ipsilateral binding (non-parametric Wilcoxon paired test). A subgroup of patients with hemi-PD showed loss of striatal DA transporters, even on the ipsilateral side. In conclusion, for routine [123I]FP-CIT SPECT studies, we recommend imaging at a single time point, between 3 and 6 h p.i. The [123I]FP-CIT SPECT technique is sensitive enough to differentiate patients with PD and controls, even at an early stage of the disease.

OS-402

P. Fang, B.C. Wang, J. Jin, Z.P. Chen, C.Y. Wu, X. Zhou and W.X. Wan

National Laboratory of Nuclear Medicine, Wuxi, P.R. China
 Department of Radiopharmaceuticals

99mTc LABELLED IMAGING AGENT FOR THE DOPAMINE TRANSPORTERS

The dopamine transporter, localized on dopamine neuron, is an effective marker for a number of pathologic states including Parkinson's disease. A neutral and lipophilic conjugated complex [2-[[[3-(4-chlorophenyl)-8-methyl-8-azabicyclo [3, 2, 1] oct-2-yl] methyl] (2-mercaptoethyl)amino]ethyl]amino]ethane-thiolato (3-)-N2, N2', S2, S2']oxo-[1R-(exo-exo)]-[99mTc] technetium (99mTc-Trodac-1) containing N2S2 and 99mTc(V)O center core, was prepared and evaluated as a potential CNS dopamine transporter imaging agent in rats, rabbits and monkey. Biodistribution displayed low initial uptake in rat brain (0.3% at 2min post injection), the striatal/cerebellar ratio reached 2.4 at 60min post injection. Blood clearance kinetics was performed in rabbits by means of bolus injection, data was analyzed with two-compartment model. The initial half-life of 1.18min, late half-life of 367.8min, apparent volume of distribution of 2.65L and total clearance of 5.0ml/min were obtained. Monkey was administered 99mTc-Trodac-1 intravenously and brain imagings were performed at the images revealed that the complex could cross the blood brain barrier and localize in the striatum. The above-mentioned results showed the 99mTc-Trodac-1 we prepared may turn to be an imaging agent for dopamine transporters.

Physics and instrumentation: Data analysis
OS-403

P.E. Radau, R. Linke,* P.J. Slomka, and K. Tatsch.*

Dept. of Nuclear Medicine, London Health Sciences Centre and University of Western Ontario, London, Canada. Dept. of Nuclear Medicine*, University of Munich, Germany.

Automated, Three-dimensional Quantification of Iodine-123-IBZM Uptake in the Striatum in Parkinson's Disease.

A three-dimensional (3-D), automated method of quantitative analysis of iodine-123-iodobenzamide (I-123-IBZM) striatal binding was developed and compared with a two-dimensional (2-D), manual approach to quantification. The specific I-123-IBZM binding measured by SPECT was retrospectively analysed in patients, 10 with a clinical diagnosis of non-idiopathic Parkinson's syndrome (NIPS), and 13 with idiopathic Parkinson's disease (IPD) for which the I-123-IBZM binding should be greater. Clinical diagnosis was based upon response to dopaminomimetic therapy that occurred after the scans. Studies of an additional 18 IPD patients were used to form mean and variation templates. All patient scans were automatically fitted to the mean template using a simplex-minimization technique that adjusts orientation, position and size (nine parameters). Two 3-D maps of regions of interest (ROIs) were tested: a fixed map corresponding to the template, and a map with ROIs derived from patient isocontours constrained by the template. These were used with all studies processed automatically. The manual technique had observers draw ROIs on each study, and the striatal binding was calculated as the ratio of the striatal to frontal cortex mean counts (BG/F). For the automated method the diagnostic criterion was calculated as the ratio of the BG/F value of the template to that of the patient study, minus 100% (BGD). The automated method was completely reproducible except in 3 of the 23 studies where manual fitting was needed, and in all cases it required less operator time. The isocontour ROI map was superior to the fixed ROI map for automated quantification. For the automated method, BGD \leq 7.6% was the optimal cutoff for diagnosis as IPD from receiver-operator curve analysis, whereas with the manual method a cutoff of BG/F \geq 1.60 indicated IPD. As compared to the clinical diagnosis, the automated method classified correctly 7/10 IPD, and 11/13 NIPS patients; the manual method classified correctly 8/10 IPD, and 10/13 NIPS patients. A 3-D, automated method using a template has been developed to quantify I-123-IBZM binding that eliminates inter- and intra-observer variability, and manual definition of regions of interest with accuracy comparable to the 2-D, manual approach.

OS-404

S. Both, O. Nickel, H. Armbrust-Henrich, G. Förster, J. Andreas

Department of Nuclear Medicine, Johannes Gutenberg-University Mainz, Germany

QUANTIFICATION OF IBZM-SPECT WITH STANDARDIZED 3-D ROIS

Aim of the study: The quantification of IBZM-SPECT data requires standardized regions of interest (ROIs) as well as an exact definition of their position in space relative to a standardized coordinate system. We developed a method, which allows an exact matching of anatomical 3-D-ROIs templates to the individual brain anatomy, independent of external markers or additional CT- or MR tomograms.

Materials and methods: We define, in analogy to the coordinate system of Talairach, a proportional system, which is given by the brain long axis and borderpoints of the outer cortex. This long axis is defined from a 2-3 cm thick mediosagittal slice by an algorithm, which finds the longest distance between the frontal and occipital cortex. Relative to this coordinate system we defined 3-D ROIs templates for measuring SPECT countrates. We constructed an individual data set for ten patients, consisting of three objects: frontal cortex, striatum and occipital cortex, separated for the left and right hemisphere. With these data sets we have calculated the ratios of striatum/frontal cortex and striatum/occipital cortex. The templates were constructed by processing the mean of the individual ROIs. Independently of this method we correlated our results with the conventional 2-D ROI method. A group of additional ten patients was selected for a normals database.

Results: The comparison of the 3-D ROIs and the conventional 2-D ROIs shows a high correlation of the calculated ratios. The method was usable on all examinations; it gives a reliable standardized reorientation. In the group of patients with suspected normal D2-receptor occupancy we found with this method normal ranges of 1,41 (\pm 0,09) for the ratio striatum/frontal cortex and 1,69 (\pm 0,17) for the ratio striatum/occipital cortex (mean values \pm SD)

Conclusions: The method allows a standardized semiquantitative measurement of dopamine receptors. This is a requirement for a comparison with a normals database to get a reliable quantitative information about brain perfusion or receptor kinetics.

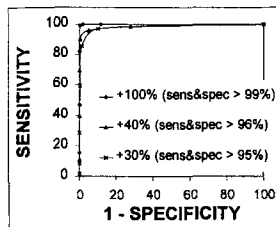
OS-405

R.deKemp, T.D.Ruddy, B.Safa, M.Dalipaj, T.Alvarez-Diez, M.Aung, R.S.Beanlands

University of Ottawa Heart Institute, Cardiac PET Centre

'PAIRED COMPARISON' OF MYOCARDIAL PERFUSION IMAGES TO EVALUATE THE TREATMENT OR PROGRESSION OF DISEASE

Myocardial perfusion is an important prognostic marker for patients with CAD. Diagnosis of CAD is performed typically by comparing to 'normal database' perfusion values. However, this diagnostic approach may not be optimal for monitoring individual changes over time, which may result from the treatment or progression of coronary disease. A sensitive test is required to detect small changes in myocardial perfusion in individual patients over time. We have developed a technique to perform direct 'paired comparisons' of quantitative parametric images of myocardial perfusion. The goal of this study was to determine the sensitivity and specificity to detect small changes in serial perfusion scans. Four repeated Rb-82 dynamic PET scans were performed in dogs both at rest and during pharmacological stress with dobutamine. Dynamic images were reoriented and resampled into polar map format automatically with no operator interaction. The arterial blood curve was obtained from an image region placed automatically at the base of the left ventricle. Polar map images of myocardial perfusion (and associated standard errors) were estimated using the net retention of Rb-82: mean uptake from 2.5-10 min divided by the integral of the blood curve from 0-2 min. The 'paired comparison' of two polar map images can then be performed using a t-test on each polar map sector. An ROC analysis was performed using 'paired comparisons' of the repeated rest and stress blood flow scans, i.e. sector-by-sector t-tests thresholded at various levels of statistical significance. The sensitivity for changes in perfusion was determined from the stress-rest comparisons, while specificity was determined from the rest-rest and stress-stress comparisons. The magnitude of the drug effect was estimated from stress-rest changes in the rate-pressure product (RPP) which were strongly correlated with increases in global perfusion ($r=0.91$, $n=12$, $p<0.001$). Sensitivity and specificity were $\geq 95\%$ for changes of 30% or more. These results indicate that the technique can detect small changes in myocardial perfusion as would be associated with small changes in RPP. This method may be beneficial for evaluating therapy or the progression of disease with serial measurements in individual patients.



OS-406

O. Geb, W. T. Kranert, H. Schmidt-Böcking, A. Hertel, G. Hör

Klinikum der Johann Wolfgang Goethe-Universität Frankfurt, Klinik für Nuklearmedizin

COMPUTER SUPPORTED PROGRAM FOR DESCRIPTION, ANALYSIS AND EVALUATION OF HEART WALL MOTION BY F-18-FDG PET

The aim was to develop a fully automatic program to quantify the wall motion of the heart, using 3-dimensional data produced by POSITRON-EMISSION-TOMOGRAPHY (PET).

This program uses the short axis slices of the left ventricle, received by F-18-FDG PET gated heart studies. The heart cycle was divided into 8 gates from which the 1st and 4th are representing the enddiastolic and endsystolic phase respectively. The reference-axis for wall motion is determined automatically in the enddiastolic phase (gate 1). The method is to calculate the center of masses (CM) for the count distributions for all slices across the ventricle. The CM pixels are the characteristic points of heart wall for motion analysis. The advantage of the method is that the reconstruction artefacts, which make the finding of the heart wall difficult, can be overcome.

Wall motion is received as the difference of the center of mass pixels of gate 1 and 4. It is presented in a polarmap. In this advantageous way of presentation all results are included in one picture. Heart wall motions are found to be in a range of 8 mm for parts with high FDG uptake and only a small motion (0.1 mm) for scars. In hibernating myocardium, found by mismatch with the MIBI-SPECT 0-2 mm was found.

Conclusion: With the program it is possible to calculate and present the regional heart wall motion from gated FDG-PET-studies in an easy, fully automatic way from the short axis slices. Additionally it is possible to extract the regional ejection fraction of the left ventricle.

OS-407

L.G. Strauss, G. Kontaxakis, A. Dimitrakopoulou-Strauss, S. Pavlopoulos, A. Santos Lleo

German Cancer Research Center, Heidelberg, Germany.

PARAMETRIC IMAGING OF DYNAMIC PET STUDIES, BASED ON COMPARTMENTAL AND NON-COMPARTMENTAL APPROACHES

Follow up studies with Positron Emission Tomography (PET) in oncological patients necessitate quantification of tracer uptake and kinetics. While uptake measurements are performed with a region-of-interest technique and the calculation of standardized uptake values (SUV), tracer kinetics can be evaluated by parametric images. Compartmental and non-compartmental methods were implemented for parametric imaging from dynamic PET studies on a PC system. The following modules were implemented: 1. Two compartment model (k21 and k12 images) 2. Patlak model (global influx images) 3. Fourier analysis (amplitude, phase) 4. Fractal dimension. Compartment methods require an input function, which can be defined by the user. The Fourier analysis and the calculation of the fractal dimension can be performed with or without the use of an input function. The fractal dimension was calculated based on the boxcount procedure. All parametric images are scaled and can be evaluated on PC systems using a dedicated software. The processing of the dynamic data is fast for the compartment and Fourier analysis (less than 2 minutes for 15 frames and 63 slices), while the processing time for the fractal dimension is mainly dependent on the evaluation parameters (e.g. box grid). The calculation of k21 and k12 images was helpful for transport tracers like C-11-Aminoisobutyric acid and O-15-Water. The delineation of colorectal tumors was superior with parametric imaging as compared to SUV images. Influx images using the Patlak approach were used in patients with liver metastases, lymphomas and breast carcinomas. Liver metastases were easily identified on the influx images due to the very low liver background. The Fourier analysis (phase images) can help to differentiate lesions with comparable FDG uptake. Amplitude and phase images were helpful for the distribution analysis of C-11-Ethanol and intratumoral therapy. The calculation of the fractal dimension provides a new approach for the analysis of tracers like O-15-Water and FDG. The results show, that parametric imaging can help to achieve a more accurate assessment of dynamic PET studies.

OS-408

M.J. Ribeiro*, B. Bendriem*, R. Trébossen*, V. Brulon*, P. Almeida*, P. Remy*
* - Serv. Hosp. Frederic Joliot-CEA - Orsay, FRANCE; † Serv. Biofisica - FMUC - Coimbra, PORTUGAL

PRODUCTION OF A NORMAL SUBJECT DATABASE FOR F-18-L-DOPA STUDIES OF PARKINSON'S DISEASE: THE PROBLEM OF SCANS ACQUIRED ON DIFFERENT PET SYSTEM WITH DIFFERENT ACQUISITION MODE

Introduction: PET studies of the F-18-L-Fluorodopa (F-18-L-DOPA) uptake in the basal ganglia (BG) of the brain have greatly contributed to the understanding of the progressive degenerative nature of Parkinson's disease (PD). Recently, PET systems with 3D acquisition capabilities have become available. They are characterized by increased sensitivity and improved spatial resolution from which the study of neurodegenerative diseases can greatly benefit, specially in small structures such as the BG. **Methods:** In order to correctly interpret these studies, a normal subject database needs to be available. However, in our institution such studies have been conducted either in 2D acquisition mode using an ECAT 953B (scanner 1) or in 3D acquisition mode on an ECAT EXACT HR+ (scanner 2). The aim of our study was to understand the influence of instrumental parameters on the quantification of the F-18-L-DOPA uptake in the BG. We have re-studied and compared 15 normal subjects studies, 8 of them were acquired on scanner 1, 7 on scanner 2. **Results:** It was found that 1)- scatter correction (SC) needs to be applied for the two scanners and 2)- the degradation of spatial resolution (DSR) (axial and transverse) of scanner 2 (which has the best spatial resolution) to match that of scanner 1 reduces the variance associated with F-18-L-DOPA uptake in normal subjects.

slope of the patlak plot (min-1)	ki (caudate nuclei)	ki (putamen)
scanner 1 with standard protocol	0.0098 ± 0.0016	0.0085 ± 0.0009
scanner 2 with standard protocol	0.0125 ± 0.0013	0.0115 ± 0.0010
scanner 1 with SC	0.0104 ± 0.0016	0.0090 ± 0.0006
scanner 2 with DSR	0.0107 ± 0.0014	0.0103 ± 0.0011

Even though such degradation leads to 17% and 12% decrease namely to the caudate nuclei and to the putamen of the uptake measured on scanner 2, it reduces the differences between measurement on the two scanners. **Conclusion:** The study demonstrates that the acquisition and reconstruction protocol greatly influences the results involving with F-18-L-DOPA. It has permitted us to define a protocol which allow pooling of data acquired on two scanners. Such protocol will be now applied to PD patients.

General nuclear medicine: Kidney disease

OS-409

Montravers F¹, Grahek D¹, Kerrou K¹, Younsi N¹, Gattegno B², Costa De Beauregard MA³, Rossert J¹, Talbot J N¹.
Services de médecine nucléaire¹, d'urologie², de néphrologie A³ et B⁴ hôpital Tenon, Paris, FRANCE.

EVALUATION OF [18F]-FDG UPTAKE BY RENAL MALIGNANCIES (PRIMARY TUMOR AND/OR METASTASES) USING A CDET GAMMACAMERA.

The aim of this study was to evaluate the utility of FDG scan performed on an ordinary gammacamera equipped with coincidence detection (CDET) in two indications of renal cancer : - characterization and evaluation of extension of renal masses before nephrectomy (NX) (11 patients (pat)) - search for recurrences after NX (3 pat).

Methods: Between September and January 1998, a whole-body scan and at least one tomoscintigram were acquired in 14 pat (fasting for 6 h or more) using a PICKER Prism XP 2000 CDET gammacamera, starting 45 min. after i.v. injection of 150-250 MBq of [18F]-FDG.

Preliminary results: Among the 11 pat who had FDG-CDET before NX, a post NX histological evidence was obtained in 6 : 3 renal tumors did not accumulate FDG (2 TN, 1 FN) and 3 renal tumors did (3 TP). In the 8 other pat, histology only concerned 3 FDG positive extrarenal foci: bone metastasis of a renal cell carcinoma in 2 cases and 1 lymph node metastasis of an epidermoid carcinoma (3 TP). As for the evaluation of extension of the disease before NX in the 4 pat with proven renal malignancy, the FDG scan was negative in 2 (2 TN on the negative exploration with several imaging modalities and at surgery) and positive in 2, but no histologic evaluation of their foci have been obtained until now. In the 3 pat with suspected recurrence of renal cell carcinoma several months after NX, FDG accumulated in lymph nodes in 2 cases (2 TP on the concordance of several imaging modalities and histology in one case). In the last pat, FDG-CDET was negative, in particular in a vertebra suspected of metastasis on bone scan (TN on the concordance with MRI).

Conclusion: FDG-CDET can be efficiently utilised for the detection of extension of renal tumours in staging (Se=3/3, Sp=2/2) or restaging (Se=2/2, Sp=1/1) and might be useful for the characterization of the primary renal tumour in doubtful cases (Se=3/4, Sp=2/2).

OS-410

O. Lang¹, K. Willms², F. Eisenberger², H. Bihl¹

Department of Nuclear Medicine¹, Department of Urology², Katharinenhospital Stuttgart, Germany

COMPARISON OF F-18-FDG-PET AND TUMOR MARKERS IN STAGING, THERAPY CONTROL AND RESTAGING OF GERM-CELL-TUMORS

Background: Therapy strategies in germ cell tumors are highly dependent on exact staging. In therapy control an accurate statement about viability of residual masses is still recommended since there exist effective therapy schedules even if complete remission is not achieved after first-line therapy.

Purpose: Comparison of F-18-FDG-PET and tumor marker profile (AFP, HCG) for initial staging, therapy control and restaging of germ cell tumors.

Methods: A total of 84 FDG-PET scans were performed in germ cell tumors (seminoma: 22, non-seminoma/mixed histology: 62). A Siemens ECAT EXACT 47 scanner was used and after injection of an average dose of 370 MBq F-18-FDG both emission and transmission scans were performed. 26 scans were performed for initial staging, 48 for therapy control and 10 for restaging (≥3 years after last therapy). For comparison, the tumor markers AFP and HCG were measured. Histological examination or follow-up was used for validation.

Results:

	true positive	false positive	true negative	false negative	Sensitivity	Specificity
FDG-PET	51	0	24	9	85%	100%
AFP/HCG	36	0	24	24	60%	100%

False-negative FDG-PET scans were mainly due to mature teratomas. False-positive FDG-PET scans were not seen in our series.

Conclusion: FDG-PET is more sensitive than tumor markers in defining tumor burden in patients with germ cell tumor. Both FDG-PET and tumor markers are highly specific methods. It has to be evaluated in the future whether FDG-PET is able to replace second-look surgery in certain clinical situations.

OS-411

D. Moka, F. Sülentrop*, J. Hahn*, H. Schicha
Department of Nuclear Medicine and *Institute for Inorganic and Analytical Chemistry, University of Cologne, Germany

Paraneoplastic and systemic effect of renal cell carcinoma: an investigation of the phospholipid metabolism using 31P-MRS

Objectives: High resolution magnetic resonance spectroscopy (MRS) is an important analytical tool for the detection and quantification of unknown substances. It is known that the concentration of phospholipids, which are the major components of (tumour) cell membrane, can be altered in blood plasma in malignant diseases especially with systemic effects. The aim of this study was to find out, whether there are also systemic effects of the renal cell carcinoma detectable using 31P-MRS in blood plasma and whether these effects are reversible after therapy.

Method: The plasma-phospholipids of 20 male patients with renal cell carcinoma (RCC) were measured preoperatively, using an 300 MHz MR-spectrometer (group 1). None of the patients showed a renal dysfunction. The pathological phospholipid spectra were compared to 8 male healthy volunteers (group 2). Furthermore the blood plasma of four patients of group 1 was investigated, 6 month after successful therapy (group 3).

Results:

mol/l	PM + SM	LPC 1*	LPC 2*	PI	PC
group 1	456±11	214±17	39±4	49±4	1501±84
group 2	489±20	297±17	68±8	57±7	1622±78
group 3	469±21	277±19	60±7	52±5	1599±88

PE+SM: phosphatidylethanolamine + sphingomyelin; LPC: lysophosphatidylcholine; PI: phosphatidylinositol; PC: phosphatidylcholine; *p<0,01, the other values were statistically not significant.

Patients with RCC show a significant decrease of the phospholipid concentration in the phospholipid class of the lysophosphatidylcholines, preoperatively, in comparison to healthy volunteers. Lysophosphatidylcholine returned to normal values, when patients are in remission.

Conclusion: Our preliminary results show the suitability of the in-vitro 31P-MRS to assess systemic effects of carcinoma and to assess alterations of phospholipid and cell membrane metabolism in patients with RCC.

OS-412

T. Home, M. Goldman*, M. Cohenpour, L. Mindlin, L. Pinkas, M. Aladjem*,
Hospital: Assaf Harofeh Medical Center, Zerifin, Israel, Institute of Nuclear Medicine & Department of Pediatrics *A.

DIMERCAPTOSUCCINIC ACID RENAL SCINTIGRAPHY IN CHILDREN WITH URINARY TRACT INFECTION, VESICoureTERAL REFLUX AND SCARS.

Traditionally, renal scar formation have been mainly attributed to the pyelonephritic process. Recently, a close association between vesicoureteral reflux (VUR) and its degree, and renal scars, independent of urinary tract infection (UTI) have been demonstrated. Renal cortical scintigraphy using dimercaptosuccinic acid (DMSA) has been shown to be the most sensitive examination in identifying renal scars. It is a common practice in infants having their first diagnosed URTI to be referred for routine diagnostic imaging using ultrasonography (US), voiding cystourethrography (VCU) and DMSA scan. The aim of the present study was to investigate, by a DMSA scan, the relative influence of the VUR and its degree, and pyelonephritis during infancy on the formation of renal scars. Seventy-four infants with pyelonephritis, 44 girls and 30 boys, were enrolled in the study. VCU and US were performed within 6 weeks following the infection. DMSA scan was performed at least 4 months after the latest UTI. Renal damage was defined as localized or generalized uptake defect or as split renal uptake less than 45%. Nineteen percent (14/74) of the children had renal damage as evaluated by DMSA scintigraphy. There was a positive correlation between renal scars and the degree of VUR: no abnormality was found in 51 renal units without reflux, in 9 with VUR grade 1/5, and 54 with grade 2/5. Renal scars were found in 9/24 renal units with VUR grade 3, 3/8 with grade 4 and 2/3 with grade 5. In conclusion, in developed countries, where treatment is initiated promptly, the main cause of scars is reflux associated renal dysplasia and not the infection. Renal scars observed following a UTI in a child with significant VUR reflux, most probably is a pre-existing renal dysplastic process, rather than being the consequence of the infection. We recommend that a DMSA scintigraphy should not be a part of the routine diagnostic imaging following UTI in every infant with pyelonephritis, and that it should only be performed in children with VUR grade 3 and above.

OS-413

M. A. Macleod, A. S. Houston, W. F. D. Sampson and C. Anagnostopoulos

Royal Hospital Haslar, Department of Nuclear Medicine

FACTOR ANALYSIS OF DYNAMIC STRUCTURES (FADS) COMPARED TO FRUSEMIDE RENOGRAPHY IN THE DIAGNOSIS OF OBSTRUCTIVE NEPHROPATHY

Doubts as to the sensitivity of frusemide renography in detecting obstructive nephropathies prompted us to compare MAG3 frusemide renography with factor analysis of dynamic structures (FADS) applied to DTPA renography in 11 patients (3 female, 8 male) presenting for assessment of renal obstruction.

Each patient had a ^{99m}Tc -DTPA renogram and FADS analysis performed followed on the next day by ^{99m}Tc -MAG3 frusemide renography. FADS analysis is applied to the DTPA image sequence isolating structures corresponding to both kidneys and bladder. Areas of obstruction in the kidney will be at least partially assigned to bladder. By displaying the kidney and bladder structures in different colours and superimposed on each other it is possible to determine the spatial extent of the obstruction. For the MAG3 study frusemide was administered at the time of injection and the diagnosis was based on the shape of the whole kidney time-activity curves.

Of the 11 cases studied FADS analysis indicated 4 to be obstructive uropathies and 7 to be obstructive nephropathies, whilst MAG3 frusemide renography showed 10 to be obstructive uropathies and 1 to be an obstructive nephropathy.

Following a full urological assessment all 4 patients with obstructive uropathies demonstrated by both methods required no further treatment. Of the 7 patients with obstructive nephropathies indicated by FADS, 6 required surgical intervention to relieve an obstruction. This included the patient with an obstructive nephropathy indicated by MAG3 frusemide renography. The remaining patient had a hydronephrosis which was managed conservatively.

We conclude from this preliminary study that MAG3 frusemide renography appears to be inferior to FADS applied to DTPA renography in demonstrating an obstructive nephropathy.

OS-414

A. Fotopoulos, J. Schina, K. Katopodis, E. Kolioussi, A. Katsaraki, J. Theodorou, H. Pappas, K.C. Siamopoulos
University Hospital of Ioannina, Dept. of Nuclear Medicine

THE CONTRIBUTION OF EACH KIDNEY IN THE RENAL FUNCTION OF PATIENTS WITH POLYCYSTIC KIDNEY DISEASE

Autosomal dominant polycystic kidney disease (ADPKD) is the most common hereditary renal disorder, responsible for 8 to 10 percent of cases of end-stage renal failure (ESRF). Once renal failure starts the progression to ESRF generally takes less than 10 years. However, to the best of our knowledge there is no information regarding the renal function of each kidney and the percentage of their contribution to the total glomerular filtration rate (GFR) during the progression of renal failure. The purpose of the present study was to determine the renal function of each kidney in patients with ADPKD during a two years follow-up. We studied initially (t_0) 25 patients with ADPKD (12 female and 13 male, aged 18-68 years). Serum creatinine (Pcr) and GFR were 1.47 ± 0.56 mg/dl and 65.66 ± 31.21 ml/min/1.73 m² respectively. Estimation of the renal function of each kidney was performed by DMSA renal scan. The mean \pm 1SD difference between left kidney DMSA (DMSA-L) and right (DMSA-R) was 14.56 ± 10.12 %. In 20 patients (80%) the left kidney had lower percentage of contribution in total renal function compared to the right kidney. Among 25 patients, 13 had a follow-up study (t_2), 2 years after the initial evaluation. The results of first vs second study are summarized in the table:

n=13	Pcr (mg/dl)	GFR (ml/min/1.73 m ²)	DMSA-L (%)	DMSA-R (%)
t_0	1.7 ± 0.64	67.02 ± 35.26	46.84 ± 7.16	53.15 ± 7.18
t_2	2.01 ± 1.66	57.15 ± 32.12	45.69 ± 6.68	54.30 ± 6.68

The mean \pm 1SD differences between DMSA-L and DMSA-R at t_0 and t_2 were not statistically different (12.7 ± 8.8 vs 13.6 ± 7.8).

In conclusion: In patients with ADPKD the contribution of each kidney to the total renal function is not equal and remains stable during the progression of renal failure.

Cardiovascular: Pharmacokinetics and metabolism

OS-415

N. Nguyen, J. Matsunari, F. Haas, G. Reidel, G. Stöcklin, R. Senekowitsch-Schmidtke, M. Schwaiger.

Technische Universität München and Deutsches Herzzentrum München, Munich, Germany.

DIRECT COMPARISON OF MYOCARDIAL RETENTION OF TETROFOSMIN, SESTAMIBI, AND Q-12 USING A SWINE MODEL.

Several Tc-labeled tracers are available for the evaluation of myocardial perfusion using SPECT. The purpose of this study was to directly compare the myocardial retention of Tetrofosmin (TF), Sestamibi (MIBI), and Q-12 at various blood flows. Six pigs with and 3 pigs without coronary occlusion were studied with dipyridamole-induced vasodilation. Animals were anesthetized and a left-thoracotomy was performed. Each animal was injected with a cocktail mixture of Sn-113 microspheres, MIBI, and either TF (group 1) or Q-12 (group 2) labeled with either Tc-99m or Tc-95m via a left-atrial catheter. Arterial blood were sampled throughout studies as arterial input function. Animals were sacrificed 5 min post injection, the hearts were excised, sectioned, and counted in a γ -well counter. Tissue and blood counts were corrected for decay and spillover. Myocardial retention (ml/g/min) was calculated by dividing tissue activity by the integral of the arterial input function. Retention of MIBI was significantly greater compared to retention of TF (0.27 ± 0.11 vs 0.16 ± 0.06 , $p < 0.01$) and Q-12 (0.32 ± 0.13 vs 0.09 ± 0.03 , $p < 0.01$). Linear regression analysis of myocardial retention vs microsphere-determined flow are shown below.

		≤ 1.5 ml/g/min	> 1.5 ml/g/min	
Gr. 1	MIBI	0.24 ± 0.08	$R=0.88$	
	TF	0.12 ± 0.06	$R=0.82$	n.s.
Gr. 2	MIBI	0.26 ± 0.05	$R=0.90$	$0.03 \times + 0.33$ $R=0.33$
	Q-12	0.06 ± 0.04	$R=0.86$	$0.01 \times + 0.09$ $R=0.48$

The co-injection of the Tc-95m and Tc-99m labeled tracers together with Sn-113 microspheres allowed direct comparison of the tracers. Results indicated that none of these tracers showed a direct proportion to microsphere-determined blood flow as expected, especially at higher flow rates (> 1.5 ml/g/min). The low retention of Q-12 in this pig model may limit its use as a blood flow tracer; however, species differentiation should be considered in the interpretation of the results. Nevertheless, MIBI showed the highest tissue retention at 5 min post injection with more sensitivity to changes in blood flow. Therefore, MIBI displayed the most favorable physiologic characteristics as a perfusion tracer in this study.

OS-416

A. Flotats, Ll. Bernà, M. Santaló*, J. Lloret*, C. Mari, J.C. Martín, M. Estorch, A.M. Catafau, I. Carrió.
Hospital Sant Pau, Barcelona, Spain. Department of Nuclear Medicine and Intensive Care Unit*

MYOCARDIAL UPTAKE OF Tc-99m GLUCARATE IN CLINICAL CONDITIONS LEADING TO MYOCYTE NECROSIS.

Aim: ^{99m}Tc -glucarate (GLU) has recently been described as a marker of acute necrosis. We assessed GLU scintigraphy as a noninvasive method to detect myocardial necrosis.

Methods: Five patients with acute chest pain (<9 hours of onset) suggesting AMI, two patients with dilated cardiomyopathy, two patients with heart transplantation, and one patient with acute myocarditis were studied after injection of 740 MBq of GLU. Anterior and 45° - 70° LAO images were obtained within 12 hours. All patients underwent ^{111}In -antimyosin (AMS) studies. Regional myocardial distribution of both tracers was compared.

Results: 1) Patients with acute chest pain: three patients showed focal myocardial GLU uptake, which was concordant with focal AMS uptake and consistent with acute infarction; one patient had absent GLU uptake and diffuse anterolateral AMS uptake, peak serum creatine kinase was 184 U/L ($N < 180$), troponin I was 6.2 ng/mL ($N < 0.45$) and ST elevation in leads V2-4 normalized two hours later; one patient had absent GLU and AMS uptake, precocious thrombolytic therapy had been administered with ECG abnormalities disappearing two hours later.

2) Patients with other clinical conditions: all patients had absent GLU uptake; diffuse AMS uptake was observed in one patient with dilated cardiomyopathy, one with heart transplantation and in the patient with acute myocarditis.

Conclusions: GLU is an infarct-avid imaging tracer. Myocardial damage leading to necrosis in other clinical conditions than acute ischemic heart disease may not present with GLU uptake.

OS-417

O. Schröder, R.P. Baum, A. Hertel, G. Hör

Department of Nuclear Medicine, University of Frankfurt/Main, Medical Center, Germany

COMBINED HYPERINSULINEMIC GLUCOSE CLAMP AND ORAL ACIPIMOX FOR OPTIMIZING METABOLIC CONDITIONS DURING F-18-FDG CARDIAC GATED PET IMAGING

Purpose: To obtain optimal image quality in myocardial viability studies, it is recommended to perform cardiac FDG studies during hyperinsulinemic glucose clamping. FDG imaging after oral administration of acipimox, a nicotinic acid derivative, yields comparable image quality to clamping. The aim of this study was to evaluate whether acipimox can be used to further improve myocardial PET imaging in patients with CAD with or without diabetes mellitus when administered in combination with the clamp technique.

Methods: 20 consecutive patients (7 with diabetes mellitus), all with angiographically confirmed coronary artery disease (CAD) and similar demographic and clinical profile underwent FDG gated cardiac PET (ECAT EXACT 47, Siemens/CTI) after i.v. injection of 300 MBq of F-18-FDG randomly under a standard hyperinsulinemic euglycemic clamp protocol (group A) or using a combination of oral administration of acipimox and the insulin clamping technique (group B). Plasma glucose, insulin and free fatty acids levels were monitored at several time points and image quality of gated cardiac FDG-PET studies, expressed as the myocardial to blood pool (M/B) activity ratio was evaluated for all patients.

Results: The image quality was superior in group B compared with group A (3.37 ± 1.46 vs. 2.27 ± 0.62, p = 0.037). During imaging, no significant differences in plasma insulin and free fatty acids levels between both protocols could be observed. However, plasma glucose levels in group A were statistically elevated compared with group B (11.1 mM/L ± 3.7 mM/L vs. 6.3 mM/L ± 3.0 mM/L during clamping, and 10.2 mM/L ± 3.3 mM/L vs. 5.5 mM/L ± 3.0 mM/L during acquisition).

Conclusion: Our prospective data clearly indicate that acipimox administration in addition to the hyperinsulinemic euglycemic clamp technique yields better F-18-FDG gated PET image quality compared with the insulin clamping study alone. Accordingly, the percentage of interpretable images in cardiac metabolic studies of patients with CAD and impaired left ventricular function may be further increased even in patients with diabetes mellitus.

OS-418

A. Barreto, J.C. Esquerre, J. Foulon, R. Itti, M.P., Larock, M. Levy, P. Rigo.
Nuclear Medicine Divisions : CHU Liege, Belgium; CHU Purpan, Toulouse, Hôpital Neurocardiologique, Lyon; Hôpital La Roseraie, Aubervilliers, France.

ACCURACY OF QUANTITATIVE EVALUATION OF FURIFOSMIN MYOCARDIAL SCINTIGRAPHY FOR CAD DIAGNOSIS

Furifosmin is a recently introduced technetium-labelled myocardial imaging agent. We have performed a phase IV multicenter clinical evaluation study in 219 patients (148 males) using a 1 day stress-rest protocol. Images were quantified using our semi-automatic bull's eye program and assessed by consensus reading of 3 observers simultaneously.

79.8% of studies were judged of optimal or good quality, 15.7% were adequate, 3.8% poor and 0.5% non evaluable. Reproducibility of reading evaluated in 38 patients provided identical reports in 34 patients, while minor differences in type (ischemia or necrosis vs. mixed) or extent of defects (i.e. RCA or LCx vs. RCA and LCx) were noted in 4 patients.

Coronary angiographic data was available in 76 patients (normal in 22 patients and abnormal in 54). Sensitivity and specificity to detect presence of CAD (>50% lesions) were 88% and 83% respectively. Sensitivity and specificity for LAD disease were 72% and 90% respectively. They were 78% and 81% for RCA and/or LCx.

We conclude that Furifosmin provides myocardial images of adequate quality for diagnosis of CAD and specific vessel lesions with sensitivity and specificity comparable to those of other Tc-labelled tracers.

OS-419

N. Nguyen, M. Schwaiger.

Technische Universität München, Department of Nuclear Medicine, Munich, Germany

COMPARISON OF THE LANGENDORFF VS THE WORKING RAT HEART PERFUSION MODELS FOR THE ASSESSMENT OF FDG UPTAKE IN RESPONSE TO INSULIN.

The suitability of the low-work load Langendorff model vs the working heart to study cardiac metabolism is debated. Therefore, the purpose of this study was to compare the glucose metabolic rate (MR) in the 2 perfusion models with respect to the uptake of FDG and D-[2-H-3]glucose in response to insulin. Isolated rat hearts were perfused with buffer containing 10mM glucose, FDG, and H-3glucose at baseline, then 100nM insulin was added. Five hearts underwent retrograde perfusion according to Langendorff, while 3 hearts were perfused with a moderate work load. FDG uptake was monitored using a pair of BGO detectors interfaced with a computer. 3H-glucose utilization was assessed by the appearance of H-3water in the effluent using columns containing converted AG-1X8 resin. Calculated MR expressed as µmol/g tissue/min are presented below.

	H-3 glucose	FDG
Langendorff		
Baseline	0.11±0.02	0.20±0.04
Insulin	1.54±0.05	0.96±0.09
Working Model		
Baseline	0.97±0.08	1.01±0.21
Insulin	1.43±0.09	0.66±0.13

Although FDG-MR were significantly lower than H-3 glucose-MR after the addition of insulin in the Langendorff hearts, there was a significant correlation between FDG and H-3 glucose-MR values (r=0.87, p<0.05). As expected, baseline MR of both tracers were significantly higher in the working hearts compared to Langendorff hearts with a lower work load (p<0.001). Following insulin, H-3 glucose-MR was not significantly different between working and Langendorff hearts. However, FDG-MR was decreased compared to baseline values in the working hearts, in contrast to the Langendorff hearts, despite similar H-3 glucose uptake. Substrate interaction and/or altered affinity to transport processes, as well as the use of glucose as sole substrate in this study may be responsible for the divergent FDG results in the 2 perfusions models. Therefore, FDG kinetics need to be interpreted with caution as a marker for glucose metabolism in the heart, and experimental models must be considered in the evaluation of FDG data.

OS-420

W.S. Richter¹, M. Khiabanchian¹, A.C. Borges², R. Aurisch¹, G. Baumann², D.L. Munz¹
Clinics for ¹Nuclear Medicine and ²Cardiology, Charité, Humboldt University Berlin, Germany

EXTRACTION OF I-123 IPPA IS INCREASED IN HYPOPERFUSED BUT VIABLE MYOCARDIUM AND REDUCED IN SEGMENTS WITH REVERSE REDISTRIBUTION AT REST

Considerable alterations of myocardial energy metabolism are to be expected in coronary artery disease. The aim of this study was to characterize the extraction of the long chain fatty acid analogon I-123 iodophenylpentadecanoic acid (IPPA) in hypoperfused but viable myocardium and in segments with reverse redistribution at rest.

Methods: TI-201 rest-redistribution imaging was performed in 26 patients suffering from coronary artery disease (PTCA, n=11; 1-vessel disease, n=4; 2-vessel disease, n=10; 3-vessel disease, n=8; LVEF, 53±20%). TI-201 SPECT was performed 5 and 90 min after injection for assessment of segmental perfusion and viability, respectively. Fatty acid uptake was registered 5 min after injection of 200 MBq I-123 IPPA. The ratio between fatty acid uptake and perfusion characterized regional fatty acid extraction.

Results: A total of 27 studies was obtained in the 26 patients. Based on a difference of at least 10 percent points between the two TI-201 studies, 45/189 segments (24%) were classified as hypoperfused at rest but viable ("hibernating"). 22/189 segments (12%) showed the phenomenon of reverse redistribution.

	IPPA FA uptake *	TI (5 min) perfusion *	TI (90 min) viability *	FA extraction
"hibernating"	69.7±30.8*	54.1±18.4*	73.1±18.6	1.3±0.6*
reverse red.	70.2±17.9 [‡]	82.9±19.7 [‡]	64.8±19.8	0.9±0.3*
control	70.4±33.1	66.9±26.7	66.9±26.8	1.1±0.34*

FA - Fatty acid; * - segmental uptake [%], [‡] - p<0.02

Conclusions: Hypoperfused but viable ("hibernating") segments are characterized by an increased extraction of the long chain fatty acid analogon I-123 IPPA. In contrast, fatty acid extraction is reduced in segments showing reverse redistribution at rest.

Oncology: PET

OS-421

E.U. Nitzsche, S. Hoegerle, T. Krause, M. Reinhardt, A. Otte, M. Mix

Division of Nuclear Medicine, University of Freiburg, Germany

NONINVASIVE DIFFERENTIATION BETWEEN BENIGN AND MALIGNANT FOCAL LESIONS OF THE PANCREAS: ARE RESULTS OF A KINETIC ANALYSIS SUPERIOR TO THOSE DERIVED BY SUV ANALYSIS.

Purpose: The diagnostic utility of FDG PET for differentiating noninvasively focal pancreatic lesions originating from cancer (PC) or chronic pancreatitis (CPT) by combined visual and SUV analysis has been documented. However, in the clinical routine there is still some misdiagnosis observed. This is, because there is potential overlapping of SUV values concerning active inflammatory lesions and cancer. Therefore, this prospective blinded study was undertaken to test the hypothesis that a kinetic analysis of focal pancreatic lesions based on FDG PET may more accurately predict the benign or malignant nature of such lesions based on the endpoint of the individual histology.

Methods: 30 patients (56±17 years) were studied dynamically with FDG PET for a time period of 90 minutes. Patients were randomized in controls (CON), CPT, PC and acute pancreatitis (AP). Three observers, blinded to the clinical data, analyzed the time-activity curves of FDG kinetics based on ROI analysis. Interobserver agreement was calculated with the use of the kappa statistic. **Results:** Analysis of FDG kinetics revealed significant differences of the shape of the time-activity curve for CON, PC and inflammatory disease. Surprisingly, there was no significant difference of the time-activity curve shape for CPT and AP which is, however, not a clinical issue. Interobserver agreement was 1. Based on these findings, noninvasive differentiation between PC and CPT was correct in all cases. Compared to the results obtained from SUV analysis, the specificity was increased. **Conclusion:** Therefore, a non-invasive differentiation between PC and CPT may be best achieved based on a dynamic FDG PET study including a kinetic analysis. This approach renders results superior to those obtained by SUV analysis of pancreatic lesions.

OS-422

O. Schröder¹, E. Staib-Sebler², M. Wanner¹, M. Lorenz², G. Hör¹, R.P. Baum¹

Department of Nuclear Medicine¹ and Surgery², University of Frankfurt/Main, Medical Center, Germany

VALUE OF WHOLE-BODY FDG-PET AND CT SCAN IN THE DETECTION OF EXTRAHEPATIC METASTASES BEFORE LIVER SURGERY IN RECURRENT COLORECTAL CARCINOMA: INTRAINDIVIDUAL COMPARISON IN 36 PATIENTS

Purpose: The diagnostic accuracy of imaging procedures takes decisive influence on the therapeutic strategy in the restaging of recurrent colorectal cancer. The aim of the present study was to assess the diagnostic value of FDG-PET value and its impact on patients' management in the detection of extrahepatic metastases before liver surgery compared to CT.

Methods: 36 colorectal cancer patients with suspected liver metastases planned for resection underwent CT scans of the abdomen and the thorax and a whole-body FDG-PET study (ECAT EXACT 47, Siemens/CTI) with additional regional emission and (hot) transmission scans of the liver/pelvis after i.v. injection of 370-500 MBq of F-18 FDG after a 12-16 hr fast. Each single lesion was confirmed by surgical histology (n=26) or by clinical follow-up for at least 6 months (n=10).

Results: Diagnostic work-up revealed local recurrences (n = 4), liver (n = 22), lung (n = 7) and retroperitoneal (n = 8) and mediastinal LN metastases (n = 4) as well as peritoneal carcinosis (n = 5). For all sites of recurrence sensitivity of FDG-PET was superior to CT, while there was no statistical difference in the specificity between both imaging procedures. Patients' management was changed by PET in 39%.

Lesions	No. of Lesions	Sensitivity	Specificity	PPV	NPV
Results in % per patient		PET/CT	PET/CT	PET/CT	PET/CT
Local Recurrences	4	100/100	97/100	66/100	100/100
Liver Metastases	101	100/86	100/93	100/95	100/81
Lung Metastases	18	100/88	100/100	100/100	100/83
Mediastinal LN	11	100/25	97/100	80/100	100/75
Retroperitoneal LN	22	100/38	96/100	88/100	100/85
Periton. Carcinosis	5	60/0	100/97	100/0	94/86

Conclusion: Our prospective data clearly indicate that whole-body FDG-PET is the most accurate non-invasive method in the restaging of colorectal carcinoma with liver metastases planned for liver surgery. Moreover, PET takes decisive influence on the therapeutic strategy in more than one third of the patients.

OS-423

H. Bender, N. Metten, P. Willkomm, M. Bangard, H. Palmedo, N. Bangard*, C. Menzel, F. Grünwald, and H.-J. Biersack
Depts. of Nuclear Medicine and *Internal Medicine;
University of Bonn

TUMOR MARKERS AND FDG-PET IN THE RESTAGING OF COLORECTAL CARCINOMA

Tumor markers CEA and CA19-9 are valuable in the follow-up of colorectal carcinoma (CRC). We have assessed the accuracy of these two markers to predict tumor recurrence in combination with F-18-deoxyglucose (FDG) positron-emission-tomography (PET) in CRC patients.

Patients (n=45) with (a) histologically confirmed CRC and suspected tumor recurrence (rise of tumor markers and/or morphological changes) or (b) suspected primary tumors were enrolled. CEA and CA19-9 were determined using commercially available assay-kits. Whole-body PET (ECAT Exact 921/47; Siemens/CTI), including transmission and emission scans (each 10 min. per bed position) were performed in fasted patients 45-60 min. after i.v.-injection of 5-8 mCi FDG. Tomograms were reconstructed by filtered back-projection and corrected for measured attenuation and qualitatively evaluated under blinded conditions. Pathological findings were verified by US, CT/MRI, surgery and/or clinical follow-up (gold-standard).

In n=34 pts., CRC was finally confirmed, whereas in n=11 pts. a malignancy could be ruled out. CEA correctly predicted the status in 31/45 pts. with 24 true-positive (TP) and 7 true-negative (TN). Sensitivity, specificity and accuracy was calculated as 71%, 64% and 69%, respectively. CA 19-9 correctly identified 26/45 pts. with 19 TP and 7 TN (sensitivity, specificity and accuracy: 54%, 78% and 59%, respectively). FDG-PET correctly identified 42/45 pts. with 34 TP and 8 TN and no false-negative case demonstrating a sensitivity, specificity and accuracy of 100%, 73% and 93%, respectively. In the presence of elevated CEA or CA19-9, FDG-PET correctly diagnosed 26/28 (93%) and 20/21 (95%) lesions. In patients with normal CEA and CA19-9 markers, FDG-PET correctly identified 16/17 (94%), 10 TP) and 22/23 (96%, 16 TP) lesions, respectively.

Our data indicate that (a) FDG-PET is more sensitive and accurate in the detection of CRC, and (b) normal tumor marker levels do not exclude the presence of malignant tissue, at least in CRC.

OS-424

R.P. Baum, A. Niesen, O. Schröder, S. Adams, A. Hertel, M. Osterloh, G. Hör

Department of Nuclear Medicine, University of Frankfurt/Main, Medical Center, Germany

A PROSPECTIVE EVALUATION OF WHOLE-BODY FDG-PET, CT SCAN, AND IMMUNOSCINTIGRAPHY IN THE DETECTION OF OVARIAN CARCINOMA RECURRENCES

Purpose: In suspected recurrent ovarian carcinoma, the diagnostic accuracy of imaging procedures takes decisive influence on the further therapeutic strategy. The aim of this prospective study was to assess the value of several imaging procedures in the detection of recurrent ovarian carcinoma.

Methods: 15 women previously treated for serous ovarian adenocarcinoma who presented with a progressive rise in serum CA 125 levels (> 35 U/ml) during follow-up monitoring, strongly suggestive of recurrence, underwent computed tomography (CT), ultrasonography (US) and planar & SPECT immunoscintigraphy (IS) using an intact Tc-99m-labelled anti-CA125 monoclonal antibody (B43.13), and a whole-body FDG-PET study (ECAT EXACT 47, Siemens/CTI) within 3 months. Each single lesion was confirmed by histology/biopsy or clinical follow-up for at least 6 months.

Results: PET was false negative (FN) in 2 patients with microscopic peritoneal carcinosis (confirmed by laparotomy and histology) and true positive (TP) in 12 out of 15 patients (1 patient true negative [TN]) revealing a total of 61 lesions (no false positive [FP]). 3 patients had complete resection of recurrences only detected by PET. IS was FN in 3 patients (FP peritoneal carcinosis also in 3 patients.). CT was FN in 8 patients (mostly peritoneal implants and lymphnode metastases).

	No. of Lesions				
	CT	IS	PET	SUV	Size (mm)
Pelvis	2	2	9	5.8	8-28
Abdomen	3	17	28	6.3	7-39
Thorax	6	0	22	7.9	7-35
Others	0	0	2	4.6	14-22
Total Lesions	11	19	61	-	-

Conclusion: This first prospective intraindividual comparison suggests that FDG-PET is the most accurate diagnostic procedure in suspected recurrent serous ovarian cancer by detecting significantly more lesions in each region examined. Moreover, PET may take decisive influence on patients' management.

OS-425

M. Reinhardt, V. Müller-Mattheis*, H.-G. Waltemath, H. Vosberg, R. Ackermann*, H.-W. Müller-Gärtner

Department of Nuclear Medicine and *Department of Urology, Heinrich-Heine-University Duesseidorf

STAGING OF RETROPERITONEAL LYMPH NODES IN NONSEMINOMATOUS GERM CELL CANCER BY FDG-PET

The aim of this prospective study was to assess the positron emission tomography with ¹⁸F-FDG (FDG-PET) in the staging of retroperitoneal lymph nodes in patients with nonseminomatous germ cell cancer (NSGC).

Thirty-four patients with NSGC were studied with FDG-PET and X-ray CT of the abdomen at time of diagnosis and after chemotherapy. Results were correlated with histological findings at retroperitoneal lymph node dissection (RLA) and clinical findings. Foci with increased FDG-uptake were classified as suspicious for metastases. In CT scans retroperitoneal lymph nodes larger than 10 mm were regarded as suspicious for metastases.

At time of diagnosis 28 patients were studied. FDG-PET detected metastatic foci in 17 patients, whereas CT detected metastases in 13 patients. Three patients without clinical signs of metastases were not treated and remained tumorfree during the follow-up. Six patients received a primary RLA, the other patients received a chemotherapy. At primary RLA 5/6 patients had micrometastases and one patient had no metastases. CT failed to detect these metastases in all 5 patients, whereas FDG-PET detected metastases in 2 patients. No false positive PET- or CT-scans were observed. The overall sensitivity was 81% for FDG-PET and 62% for CT.

The influence of chemotherapy on the FDG-uptake in metastases was monitored in 13 patients. After chemotherapy the FDG-uptake was normalized in all but one patient who had inflammatory lymph nodes.

After chemotherapy 20 patients received a secondary RLA. RLA detected mature teratomas (mT) in 6 patients and micrometastases in one patient. 13 patients were tumorfree. FDG-PET failed to detect any of the mT or the micrometastases. PET was false positive in one patient with inflammatory retroperitoneal lymph nodes. CT detected two mT correctly, one CT was false positive and six CT scans were not conclusive.

Conclusions:

FDG-PET is more sensitive for detection of retroperitoneal metastases in NSGC before chemotherapy than CT and should be applied especially in patients with normal CT scans. FDG-PET can be used to monitor the effects of chemotherapy and to differentiate residual masses after chemotherapy. Mature teratomas show no increased FDG-uptake.

OS-426

H. Bender, P. Albers*, H. Yilmaz*, F. Grünwald, SC. Müller*, and H.-J. Biersack

Depts. of Nuclear Medicine and *Urology; University of Bonn

FDG-PET IN THE CLINICAL STAGING OF TESTICULAR GERM CELL TUMORS

In a prospective study, we are evaluating the use of whole-body positron-emission tomography (PET) employing fluoro-18-deoxyglucose (FDG) as a diagnostic tool in patients suffering from testicular germ cell tumors (GCT).

A total of 50 patients (pts) were studied using an ECAT/Exact (Siemens/CTI) PET scanner. Pts. received a body-trunk transmission scan, followed by an emission scan 45-60 min. after injection of 185-333 MBq FDG; FDG-uptake was qualitatively scored and the results compared with conventional imaging (CT) and the final institutional diagnosis (gold standard). Following the PET study, 26/50 pts were staged surgically by retroperitoneal lymph node dissection and 24/50 were followed clinically.

Overall, 16/50 patients had metastases, 12/16 metastases were detected by PET, 11 by CT. 34/50 patients had no metastases and were correctly staged by PET, in 9/34 patients CT was false-positive. Comparing FDG-PET vs. CT showed a sensitivity of 75% vs. 68%, specificity of 100% vs. 73%, and accuracy of 92% vs. 72%, respectively.

Our data demonstrate that FDG-PET is useful to detect metastatic lesions (> 5mm) of GCT, reduces false-positive findings in stage II GCT, but does not discriminate mature teratoma from necrotic tissue.

General nuclear medicine: Lung

OS-427

D.A. Yüksel, H. Yüksel*, S.Erdem, Z. Burak, M. Kayahoglu, R. Tanaç*

Depts. of Nuclear Medicine and Pediatric Allergy*, Ege Univ., TURKEY

Evaluation of Changes in Pulmonary Epithelial Permeability of Children with Asthma by Using Tc-99m-DTPA

Brochial asthma (BA) is chronic, eosinophilic inflammation of airway. This inflammation causes bronchial epithelial denudation. Several studies have been reported about this issue. But the results are controversial. The objective was to evaluate whether there is a marked difference between PE of asthmatics and normal children and also there is an effect of inhaled steroids on parameters of PE. PE was measured quantitatively according to DTPA clearance rate in 19 children (mean age of 10.3±2.7 year) with BA, who sensitive to dermatophagoides, by using Tc99m-DTPA lung scintigraphy; and the results were compared with those in 10 nonasthmatic control children. They had been inhaled 20 mCi aerosolised Tc-99m DTPA, then dynamic posterior thorax images were obtained by using Toshiba GCA 602-A gamma camera. Also two independent observers evaluated and calculated the "homogeneity scores" (HS) of Tc99m-DTPA distribution in the airways. Asthmatic children were given inhaled steroids (400 µg/day dose of budesonide) after first scintigraphic study. Same scintigraphic studies repeated in the asthmatics two months later and their symptoms scores recorded regularly. After 2 months later, symptom scores of asthma significantly decreased from 6.58±0.7/mo to 2.6±1/mo. (p<0.05). HSs of asthmatics were significantly decreased from 1.33±0.4 to 0.41±0.3/patient (p<0.05). HSs was no abnormal in the images of controls. PE of asthmatics were significantly higher than control group; 1.3±0.2/min and 1±0.1/min, respectively (p<0.05). At the end of study, mean PE of asthmatics significantly increased to 1.7±0.3/min. (p<0.05). Our results suggested that PE of children with BA are higher than normals, and it is increased by the treatment with inhaled steroids. It is in contradiction with previous reports.

OS-428

G Panoutsopoulos, M Alchanatis, G Tourkochoritii, C Batsakis, G Douskas, S Kakourou, J Christacopoulou, J Jordanoglou.

Dept of Nuclear Medicine, Dept of Respiratory Medicine of Athens University, "SOTIRIA" Chest Hospital.

RADIOISOTOPIC EVALUATION OF VENTRICULAR FUNCTION IN OBSTRUCTIVE SLEEP APNEA PATIENTS.

In order to investigate the consequences of obstructive sleep apnea (OSA) to the ventricular function, 20 pts with OSA syndrome verified polysomnographically, without any evidence (clinical, ECG and ECHO) of heart disease or history of systemic hypertension, were studied. Furthermore, 8 normal individuals of the same age were studied as control group. All pts had Apnea/Hypopnea Index (AHI) greater than 51.1±4.6 (mean±SE) and none of them have had concomitant Chronic Obstructive Pulmonary Disease (COPD) or daytime hypoxaemia of any reason. All patients underwent First Pass and Equilibrium Radionuclide Ventriculography (MUGA). The ejection fraction of both ventricles and the peak filling/emptying rates of the left ventricle were calculated. The calculation of the right ventricular ejection fraction (RVEF) was based on the First Pass data, while the left ventricular indices on the MUGA data. Results (mean±SD) and statistics between the two groups are shown as follows:

	Age years	RVEF %	LVEF %	PFR edv/sec	T-PFR msec	PER edv/sec	T-PER msec
Pts	49±9	38±7	50±10	2.4±0.6	0.3±0.4	2.9±0.7	0.4±0.3
Norm	49±6	55±4	61±4	3.6±0.6	0.1±0.0	4.3±0.8	0.3±0.3
p	NS	<0.001	0.009	<0.001	<0.05	<0.001	0.40

PFR, peak filling rate, PER, peak emptying rate, T-, Time to

Despite the significant differences observed in the ventricular indices between pts and normal individuals, when we tried to determine factors that may influence ventricular function correlating by linear regression analysis, parameters of nocturnal oxygenation and severity of OSA with each one of the indices of ventricular function, there was no correlation between ventricular left and right indices and OSA severity or nocturnal oxygenation parameters of OSA patients. OSA syndrome has a deleterious effect on the function of both cardiac ventricles even in the absence of COPD and daytime hypoxaemia. This effect is independent of the severity of OSA expressed by AHI and nocturnal oxygenation indices in our group of patients.

OS-429

L. QUE and M. D. Rutland

Department Of Nuclear Medicine Auckland Hospital NZ

LUNG SCANS ARE PARTICULARLY USEFUL IN ELDERLY PATIENTS

A follow-up study of all the Ventilation-Perfusion [VP] lung scans performed from 1994 to 1997 was analysed to assess the value of lung scans in elderly patients, and also to compare the results of lung scanning in routine clinical practice with results from the PLOPED research study.

AGE	N	NORM	SCAN PROBABILITY			Angios	CPER
			LOW PROB	INTERM	HIGH PROB		
20-39	351	43%	34%	10%	13%	0.86	.184
40-49	288	37%	38%	12%	13%	0.53	.189
50-59	335	27%	44%	14%	16%	0.36	.224
60-69	379	20%	46%	14%	20%	0.46	.260
70-79	428	16%	44%	15%	24%	0.23	.295
80+	211	6%	49%	23%	22%	0.10	.304
Overall	1992	25%	42%	14%	18%		

These results showed that in routine clinical practice lung scans will produce results which are clinically useful in 86% of cases, and diagnostic results in 43%. This is better than the results implied by PLOPED [67% useful and 28% diagnostic].

Although increased age is associated with more "intermediate probability" scans, the change is not enough to markedly reduce the clinical value of scans in elderly patients. More importantly, the "angios" ratio [angiograms divided by intermediate scans] shows that the likelihood of getting a pulmonary angiogram declines rapidly with age, even though the calculated PE rate [CPER] rises.

The results imply that lung scans are particularly important in elderly patients, as there is an increasing incidence of pulmonary emboli, but the likelihood of having an angiogram is markedly reduced.

OS-430

P. Jackson, R. J. Baker¹, D. W. J. Mackey, H. Van der Wall.

Concord Hospital, Sydney, Australia: Department of Nuclear Medicine.
¹Prince of Wales Hospital, Sydney, Australia: Department of Nuclear Medicine.

THE THEORETICAL ENTHALPIES OF VARIOUS REACTIONS IMPLICATED IN THE GAS PHASE EVOLUTION OF THE ^{99m}Tc-LABELLED MICROAEROSOLS TECHNEGAS AND PERTECHNEGAS

As an extension of our investigations into the ^{99m}Tc-labelled microaerosols Technegas [Nucl Med Commun 1996; 17:504-513] and Pertechnegas [J Nucl Med 1997; 38:163-167], *ab initio* frozen core density functional theory (DFT) calculations have been undertaken to ascertain the enthalpies of various oxidation and carbidisation reactions implicated in the high temperature evolution of these agents. To ensure the DFT results for molecular binding energies were reliable at this level of theory, the ground state of the diatomic carbide of molybdenum (Mo: Z = 42, ³Σ⁻ MoC) was also investigated, while the DFT results for the Tc-oxides were compared with literature results from Modified Coupled-Pair Functional (MCPF) calculations [Langhoff SR *et al. Chem Phys* 1989; 132:49-58; Siegbahn PEM. *J Phys Chem* 1993; 97:9096-9102]. For MoC, the difference between the experimental and theoretical binding energies was 0.1 kcal mol⁻¹. Although differences between the DFT and MCPF binding energies for TcO spin isomers were noted, which are attributable to the MCPF neglect of higher order electron correlation effects, the DFT results are in very good agreement with available literature results, and should be very reliable for TcL_{2,4}, L = C, O.

The binding energies from the DFT calculations confirm that the molecules TcC_x, x = 1-4 are indeed stable and will exist in high temperature Tc+C vapours. Notably, the ground state of TcC has a slightly higher binding energy than the ground state ³Σ⁻ TcO, although the values are close. This essentially confirms the body-centred cubic assignment for the radionuclide phase associated with the colloidal carbon Technegas particle detected using high resolution transmission electron microscopy [Isawa T *et al. Nucl Med Commun* 1996; 17:147-152]. Similar TcC and TcO binding energies also suggests the ⁹⁹TcO₂-carbon association, confirmed by X-ray photoelectron spectroscopy and scanning-transmission electron microscopy [Nucl Med Commun 1996; 17:504-513], may be endohedral. The enthalpy for the reduction of TcO₂ to Tc and the enthalpy of carbidisation (Tc + 4C → TcC₄), derived from both DFT calculations and literature experimental results, will be presented. There are implications for a recently proposed mechanism of Technegas formation [Senden TJ *et al. J Nucl Med* 1997; 38:1327-1333].

OS-431

H. Hadjikostova, J.-L. Stiévenart, G. Jebrak*, G. Lesèche**, M. Fournier*, B. Bok

hôpital BEAUJON, Department of Nuclear Medicine, *Department of Pneumology, **Department of Thoracic Surgery

VARIATIONS OF LUNG PERFUSION CHARACTERISTICS AFTER UNILATERAL VOLUME REDUCTION SURGERY FOR EMPHYSEMA.

Material and method 16 patients with pulmonary emphysema (mean age 53.2 yrs; range 32-70 yrs. 9 panlobular, 4 centrolobular, 3 mixed) underwent perfusion lung scintigraphies after injection in supine position, before and 3 months after unilateral volume reduction surgery (UVRS). Relative variations of each lung to perfusion was calculated as well as the cranio-caudal perfusion gradient - ratio of the superior third perfusion to the inferior third one - in the non-operated lung (NOL). Computations were performed on planar images by arithmetically averaging the anterior and posterior incidences. Correlations with several functional parameters were looked for.

Results: The contribution of the operated lung was significantly increased (41.5% → 46% p=0.003, paired t-test). This improvement was significantly correlated to relative variations of global residual functional capacity and of forced expiratory volume in the first second. The cranio-caudal gradient in the NOL decreased (2.32 → 1.93 p=0.04). This was due to a relative greater perfusion decrease in its upper part (19.3% → 16% p= 0.009).

Discussion. the operated lung perfusion improvement is an expected result, related to mechanical strains removal. It is sometimes lacking and the clinical improvement is then explained by a better utilization of the available pulmonary blood flow which was not changed after the operation.

Conclusion. Perfusion scintigraphy shows how the lung perfusion is modified after UVRS. Concurrently with thoracic scan X, pre/post operative comparisons could help in the choice of the lung regions to be removed in patients with diffuse emphysema.

OS-432

N.Prandini, L.Feggi, G.Ciancio*, G.Galeotti**, R.LaCorte*, F.Trotta*

Nuclear Medicine and Rheumatology* Depts Azienda Ospedaliera Arcispedale S.Anna, Institute of Radiology** University - Ferrara

LUNG CLEARANCE AND HIGH RESOLUTION CT IN SYSTEMIC SCLEROSIS: A COMPARISON

Interstitial lung disease complicating systemic sclerosis (SS) has a grave prognosis and it is important to recognise it as soon as possible. The early lung involvement can be monitored by high resolution computerized tomography (HRCT) and by aerosol clearance times of ^{99m}Tc-DTPA, a measure of lung inflammation.

Twenty-four SS patients without clinical pulmonary manifestations, negative X-rays and normal ventilation parameters were studied by serial DTPA lung clearance studies (30 minutes) and HRCT.

Of the 24 patients, 8 had normal clearance rates of ^{99m}Tc-DTPA (T1/2 > 60 mins). A mild increase in the clearance rate was found in 10 cases (T1/2 between 40-60 min) and a significant increase in clearance rate in the remaining 6 (T1/2 < 40mins). An irregular distribution of ventilation was found in 14 patients with an asymmetric lung uptake and with basal ventilation defects. Three of these patients had a normal lung clearance. Totally, 79% (19/24) of SS patients have abnormal lung permeability. HRCT resulted positive in 21 of 24 patients with a sensitivity of 87.5%.

Our study suggests that the clearance of aerosol and HRCT are complementary studies to assess early alterations of interstitial lung involvement in SS and may facilitate early therapeutic intervention.

Endocrinology/Thyroid

OS-433

G.Ronga, M.Filesi, G.Ventroni, T.Montesano, F. Fiore Melacrinis, C. Pace, M.Ciancamerla, I.Baschieri.

SS Nuclear Medicine, Clinica Medica II, University of Rome "La Sapienza" - Italy

LYMPH NODE METASTASES FROM DIFFERENTIATED THYROID CARCINOMA: DIAGNOSIS AND TREATMENT WITH 131-I

The aim of this study was to evaluate the efficacy of 131-I in detecting and treating lymph node metastases from differentiated thyroid carcinoma (DTC). Of 1296 pts studied, 146 (11.3%, 24 follicular, 122 papillary) had lymph node metastases. On the basis of surgery, these patients were divided into two groups and a 131I dose (40-70 mCi) was given to 142 for remnant ablation.

Group A (58/146): a total thyroidectomy and lymphectomy had been performed. The 131I-WBS detected lymph node metastases in 42/58 pts (72.4%): the subsequent treatment was 131I therapy (31 pts), or lymphectomy and 131I therapy (10 pts), or lymphectomy alone (1 pt). Recurrence was observed only in 1 patient (1.7%).

Group B (88/146): only a total thyroidectomy had been performed. Lymph node metastases were detected by the first 131-I WBS in all patients: the subsequent treatment was 131I therapy (45 pts), or lymphectomy and 131I therapy (16 pts), or lymphectomy alone (4 pts). Recurrence was observed in 14 pts (15.9%). In 23 pts the lymph node metastases were detected at initial WBS but no later after 131I therapy for remnant ablation.

All recurrences were observed 3 to 9 yrs after surgery and occurred in 3/26 pts (11.5%) who underwent both lymphectomy and 131I therapy and in 12/111 pts (10.8%) treated with 131I therapy alone. We conclude:

- lymphectomy is often unable to eliminate all metastatic lymph nodes;
- WBS did identify 130/146 cases (89.04%) of lymph node metastases;
- low doses of 131I (1850-3700 MBq) can be enough to treat metastatic lymph nodes.

OS-434

RE O'Mara, P Klieger, S Cholewinski, KS Yoo, VU Chengazi

University of Rochester Division of Nuclear Medicine

Thyroid Stunning After 5mCi of I-131 for Whole Body Scanning

Recently, authors have reported a phenomenon called thyroid stunning which occurs when a diagnostic dose of I-131 reduces the observed radioiodine uptake on the subsequent post-therapy scan. This observation has led some authors to recommend smaller scanning doses of I-131 or the use of I-123 for diagnostic scanning. We compared the diagnostic scan and post-ablation radioiodine scan of 110 consecutive post-thyroidectomy patients to determine if thyroid stunning could be observed using our imaging protocol.

Each of the 110 patients underwent a diagnostic 72-hour whole-body radioiodine scan using 5 mCi of I-131 (185MBq). After confirming the presence of thyroid remnant or functioning thyroid tissue on the diagnostic scan, the patient received an ablation dose of I-131 ranging between 100mCi and 180mCi on the same day the diagnostic scan was completed. A post-ablation whole-body scan was then performed 72 hours later. Each post-ablation scan was correlated with the previous diagnostic scan for any observable reduction in the number of sites of radioiodine uptake or a decrease in the relative intensity of I-131 uptake that could be attributed to radioiodine stunning. After comparing the pre-ablation diagnostic whole-body scan with the post-ablation scan on each patient, we were unable to observe thyroid stunning in any patients. Therefore, we conclude that diagnostic whole-body scanning may be performed using a 5mCi I-131 dose without concern for thyroid stunning reducing the uptake of a planned therapy dose.

OS-435

M. Medvedec, D. Grošev, S. Lončarić, D. Dodig, Ž. Pavlinović

University Hospital Rebro, Department of Nuclear Medicine and Radiation Protection, Zagreb, Croatia

DOSIMETRIC QUANTITATION OF RADIOIODINE ABLATION AFTER SURGERY FOR THYROID CANCER

Despite complete ablation of postsurgical thyroid remnants in 95% of our patients using standard activity of up to 4.6 GBq I-131, the purpose of this work was to quantify our empirical procedure dosimetrically, in order to minimize the costs of treatment and unnecessary radiation exposure of patients, personnel and public. Twenty five patients thyroidectomized for thyroid cancer were studied up to seven days after mean activity of 80 MBq and 3070 MBq I-131 was administered for diagnostic (dg) and therapeutic purpose (th) approximately 4 and 5 weeks after surgery respectively. Remnant thyroid radioiodine uptake (RAIU) was measured by conventional probe system and beta-gamma exposure rate meter, and whole body retention by collimated whole body counter. The mass of thyroid remnant was determined from anterior and lateral pinhole gamma camera images assuming an ellipsoidal shape. The cumulated activity was calculated by analytic integration, and radiation absorbed dose using MIRD formalism. Thyroid stimulating hormone (TSH) concentrations were determined from blood samples taken on the day of activity administration. Mean uptake per gram of residual thyroid tissue was $RAIU_{dg}=4.1\%/g$, mean residence time $\tau_{dg}=145.2\text{ h}$ and absorbed dose $D_{dg}=750\text{ mGy/MBq}$ for thyroid remnant, and $\tau_{th}=19.5\text{ h}$ and $D_{th}=0.05\text{ mGy/MBq}$ for whole body. Mean TSH levels were $TSH_{dg}=52.8$ and $TSH_{th}=60.9\text{ mIU/l}$ ($p<0.01$). Mean relative observed vs. predicted radiation absorbed doses were 63.9% and 93.6% for thyroid remnant and whole body respectively, and significantly negative correlated with corresponding diagnostic dose ($r=-0.55$, $p<0.02$). However, complete ablation of residual thyroid tissue was observed in 24/25 (96%) patients six months after the treatment. 'Low' I-131 activity normally being used for diagnostic study delivered high amount of radiation to the remnant thyroid. This explains the observed effect of markedly 'stunned' or partially destroyed thyroid tissue by diagnostic dose. Consequently, further critical investigation of radioiodine ablation procedure would be very intriguing, because in case of the most favorable iodine kinetics either excellent ablation results seem to be achievable using activity even lower than 1 GBq, or radiation absorbed dose of 300 Gy recommended for successful radioiodine ablation of thyroid remnant needs a serious revision.

OS-436

Dorn, R., Kopp J., Vogt H., Heidenreich P.

Zentralklinikum Augsburg, Klinik für Nuklearmedizin, Postfach 101920, D-86009 Augsburg, Germany

TWELVE YEARS OF CLINICAL EXPERIENCE WITH RISC ADAPTED RADIOIODINE THERAPY IN METASTATIC DIFFERENTIATED THYROID CARCINOMA

Dosimetric technic is described and own clinical experiences (benefit and side effects) are discussed under the aspect of effectiveness versus risk.

The dosimetric approach to I-131 therapy (RIT) supports the decision whether a curative therapy is possible, i.e. the delivered dose to metastases exceeds 100 - 200 Gy. Simultaneously the dose to the organ at risk (mostly red bone marrow, RBM) is calculated. If no curative therapy is possible, either a palliative standard dose therapy (11 GBq) or no therapy is done. Thus an ineffective therapy and its radiation exposure can be avoided.

Since 1986 48 patients received intentional curative RIT at our hospital. The applied activity exceeded 11 GBq in 38 therapies (mean 20.1 GBq, max. 38.5 GBq). The dose delivered to RBM was 1 - 2.5 Gy in 17 pts. A 3 Gy dose delivered to the critical organ (healthy) RBM by risc adapted RIT in 22 patients has been proven to be safe. Other limiting organs were lung (limit 30 Gy, 4 therapies) and thyroid (limit 1000-2000 Gy, 6 therapies). Palliative therapy (11 GBq) was done in 8 pts.. 27 pts. received no therapy due to low I-131 uptake.

Risc adapted high dose RIT may stretch the intervals between consecutive RITs resulting in a longer period for the RBM to recover. Repeated therapies are possible in case of new metastases. One patient had RIT for 4 times (1989: 25.1 GBq, 1992: 17.5 GBq, 1994: 25.2 GBq, 1997: 13.9 GBq) Even after the latest therapy only a moderate decrease of thrombocytes (250,000⇒150,000) occurred and haematopoiesis recovered totally.

Meanwhile an increase in safety is offered by stem cell separation and the possibility of autologous transplantation.

OS-437

V. Shishkina, B. Sinyuta, E. Chebotareva, D. Dzhuha

Department of Nuclear Medicine, Ukrainian Research Institute of Oncology and Radiology, Kiev, Ukraine

THE CLINICAL EXPERIENCE OF USING RADIOIODINE THERAPY IN THE COMBINED TREATMENT OF DIFFERENTIATED THYROID CANCER IN CHILDREN AFFECTED BY THE CHERNOBYL ACCIDENT

With the aim of evaluating the efficiency of the radioiodine therapy (RIT) in the combined treatment of differentiated thyroid cancer (DTC) in children who were subjected to the pathogenic effects of the Chernobyl accident and fell ill in 1990-96 years we analysed the treatment results depending on age, histology and spread of the process.

RIT was made in 68 children aged 7-14 years after 4-6 weeks following total thyroidectomy. ¹³¹I whole body scanning and determination of serum Tg were performed before RIT and for control of the treatment results. If necessary, the repeated courses of RIT were given. During treatment the indices of ¹³¹I pharmacokinetics were recorded.

Ablation of the residual thyroid tissue was performed in 25 children, the treatment for lymph node metastases in combination with residual thyroid tissue was made in 18, the RIT for lung metastases was carried out in 25. The positive effects in these groups was reached after 1-3 courses in 20 pts (80.0%), 14 pts (77.8%), 15 pts (60.0%) respectively. The average effective activities in these groups were 1735.3 ±196.1 MBq, 1946.2±255.3 MBq, 10052.9±1665.0 MBq respectively.

RIT is an effective component of the combined treatment for DTC in children. The negative results in some patients are due to the individual features: tumor radioresistance, low initial ¹³¹I accumulation and rapid ¹³¹I excretion. To solve this problem it is necessary to investigate more deeply the ¹³¹I pharmacokinetics and individual planning of administered ¹³¹I activities.

OS-438

Chr. Reiners, J. Biko, J. Farahati, S. D. Kirinjuk, E. P. Demidchik

Clinic and Policlinic for Nuclear Medicine, University of Würzburg, Germany and Center for Thyroid Tumors, Minsk, Belarus

5 YEARS EXPERIENCE WITH RADIOIODINE TREATMENT IN 158 CHILDREN FROM BELARUS WITH THYROID CANCER AFTER THE CHERNOBYL ACCIDENT

Between 01.04.1993 and 31.03.1998 158 children with advanced stages of thyroid cancer from Belarus have been treated at the University Clinics of Essen and Würzburg. Totally 530 treatment courses have been applied to 95 girls and 63 boys who originated from the Gornel area (71 cases) and other parts of Belarus (87 cases). The mean age of the children at the time of diagnosis was 11.9 ± 2.5 years. Histologically, 156 cases have been typed as papillary and 2 cases as follicular cancers. 130 out of 158 cases had to be staged as pT4 after surgery, which has been performed in the Center for Thyroid Tumors in Minsk. 152 out of 158 cases presented with lymph node metastases. In 76 out of those 158 children, distant metastases have been detected (74 cases with lung and 2 cases with bone metastases).

After withdrawal of thyroid hormone supplementation for 4 weeks, radioiodine (¹³¹I) has been given (50 MBq/kg of bodyweight for ablation of thyroid remnants, 100 MBq/kg for treatment of residual tumor, tumor recurrences or distant metastases).

In the 134 children who had received more than one treatment course of radioiodine, it has been possible to judge the results of previous treatment with ¹³¹I. Up to the 31st of March 1998, 101 out of 135 cases (75 %) could be classified as complete remissions. The remission rate in cases with lymph node metastases amounted to 56/58 (97 %). In cases with distant metastases, the remission rate was 43/74 (58 %). However, at least partial remissions have been observed in all of the remaining children (evaluable by the decreasing levels of the tumor marker thyroglobulin). Finally, a considerable increase of the fraction (up to 70 %) of complete remissions in children with metastases of thyroid cancer from Belarus is expected, since the fractionated treatment with radioiodine is not finished in many of the cases.

The work has been sponsored by VDEW, Germany.

Neurology/Psychiatry: Psychiatry

OS-439

A. Conca*, H. Fritzsche**, Ch. Haas **, W. Peschina**, H. Wiederin**, P. König*, H. Schneider*.

Department of Psychiatry* and Department of Nuclear Medicine**, Landeskrankenhaus, Rankweil - Feldkirch, Austria.

REGIONAL CEREBRAL GLUCOSE METABOLISM AND REGIONAL CEREBRAL BLOOD FLOW CHANGES IN TEMPORAL LOBE STRUCTURES IN SCHIZOPHRENIA: MEASUREMENTS BY SIMULTANEOUS F-18 FDG AND Tc-99m HMPAO SPECT.

The aim of this study was to investigate the simultaneous pattern of glial and neuronal activities in chronic schizophrenic disorders in the temporal regions analysing the regional cerebral glucose metabolism (rCMR), the regional cerebral blood flow (rCBF) and the influence of gender respectively.

19 medicated patients (7 f, 12 m, mean age 37.8 ± 12.3 years, meeting ICD 10 diagnostic criteria for the schizophrenic syndrom F20.04) and 9 healthy volunteers comparable in handedness and age (4 f, 5 m, mean age 37.8 ± 9.3 years), underwent a simultaneous F-18 FDG and Tc-99m HMPAO double isotope study by a dual head gamma camera with a 511 KeV collimator. We semiquantitatively evaluated activities in the hippocampus (HIP), in the gyrus temporalis inferior (GTI) as well as in the gyrus temporalis superior (GTS), based on Podreka's analytical method. The rCBF and rCMR statistical patterns were analysed inter- as well as intrahemispherically by regression analysis and separately by the paired two t-test.

Schizophrenic males showed a positive correlation of rCBF and rCMR in the right (p< 0.03) and in the left side (p< 0.05) in HIP, also a significant high correlation in the right GTI (p< 0.005) and in the right GTS (p< 0.006)

Schizophrenic females had a marked correlation (p< 0.02) in HIP, no significant correlation in GTI and positive correlations bilaterally in GTS (p< 0.01 right ; p< 0.002 left).

Male controls showed a weak correlation in the left hemisphere (p< 0.06) in HIP and in GTI, a distinct correlation bilaterally in GTS (p< 0.02 right; p< 0.01 left). Female controls showed no correlation at all neither in HIP, nor in GTI, nor in GTS.

We observed a high positive correlation of rCMR between HIP and GTI (as a functional and regional entity involved in the syndrom) in both hemispheres only in schizophrenic males (p< 0.006 right; p< 0.05 left), the rCBF was slightly correlated (p< 0.07) only in the right hemisphere.

Our results suggest a different pattern of rCMR and rCBF in the chronic schizophrenic syndrom depending on marked temporal lobe structures and on gender.

OS-440

S.T. Zwas, E. Goshen, T. Hendler, M. Smekhov, Y. Sasson, E. Koren, M. Lustig, J. Zohar

Sheba Medical Center, Tel Hashomer, and Sackler School of Medicine, Tel Aviv University, Tel-Aviv, Israel.

Tc-99m-ECD BRAIN SPECT IN OBSESSIVE COMPULSIVE PATIENTS' COGNITIVE CHALLENGE PRE -AND POST- SERTRALINE TREATMENT

Preliminary brain SPECT studies in obsessive-compulsive disorder (OCD) showed inconsistent data, perhaps due to the patients' psychological state. Recently, treatment with the new Sertraline compound (Pfizer, USA) in OCD showed some encouraging results.

The aims of this study were to characterize brain perfusion patterns obtained in OCD patients during activated states (pre and post treatment) and to correlate the ultimate clinical response to Sertraline treatment with pretreatment SPECT findings. Thirty drug-naive OCD patients underwent four Tc-99m-ECD brain SPECT studies. For the first scan the patient was injected in a baseline relaxed state. For the second scan, the patient was injected at peak OC symptom provocation. Following six months of Sertraline treatment, the same set-up injection sessions were repeated and the third and fourth scans were obtained. Patients' clinical and neuropsychological states were assessed at each of the four stages of the study using a battery of tests including the Yale-Brown Obsessive Compulsive Scale (YBOCS) and the Anxiety Analog Scale.

Brain imaging was performed with a dual-head camera equipped with fanbeam collimators, 20-60 min. after I.V. injection of 740 MBq Tc-99m-ECD. A Metz filter was used for all studies, which were normalized to cerebellar activity. Following 3D reconstructions, each pair of studies (pre and post treatment) was computer-aligned for complete superposition. Then, each baseline study was computer subtracted from its paired activation study to obtain two net computer activity maps (CAM) of OCD brain perfusion activation changes (pre/post treatment). The transaxial frames of the CAM were color-coded into three grades of semi-quantitative relative activity percent differences from our normal data-base brain activity distribution (±10%) : ≤ ± 20% ; ≤ ± 30% and > ± 30% with hyper (+) or hypoperfusion (-). Statistical correlations between pretreatment SPECT CAM and treatment outcome revealed highly significant hyperperfusion changes in responders (R) vs nonresponders (NR), 15 patients each, in the following regions (presented in mean % of change) :

Regions	NR	R	P Values
Right temporal	+16	+4	= 0.03
Left caudate	+13	+3	= 0.052
Left thalamus	+12	-6	< 0.01

This study demonstrated well localized regional brain perfusion activation patterns in this group of OCD patients with highly significant differences observed among patients who responded to Sertraline treatment and those who did not. This information may be important in predicting treatment outcome.

OS-441

J. H. Zhao, X. T. Lin, K. D. Jiang, Y. C. Liu, L. Q. Xu,
Dept. of Nucl. Med. Hua Shan Hospital, Shanghai Medical University,
Shanghai 200040, China

Baseline and Cognitive Activated Brain SPECT Imaging in Depression

PURPOSE To evaluate the rCBF abnormalities through the semi-quantitative analysis of the baseline and cognitive activated rCBF imaging with the unmedicated depressed patients. **METHODS** 27 depressed patients, unmedicated by the anti-depressant drugs were enrolled. The diagnosis (depression of moderate degree accompanying somatization) was confirmed by the ICD-10 criteria. 15 age matched normal controls were studied under identical conditions. Both baseline and cognitive activated 99mTc-ECD SPECT were performed. The cognitive activated brain imaging: The cognitive task is Wisconsin Card Sorting Test (WCST). 1110MBq (30mCi) 99mTc-ECD was administered by intravenous bolus injection 5 minutes after the onset of the WCST. The images were reconstructed in the transaxial plane parallel to the OML. Semi-quantitative analyses were completed through the 7th, 8th, 9th, 10th, 11th slices of the transaxial imaging. rCBF ratios of every ROI were calculated using the average tissue activity in the region divided by the maximum activity in the cerebellum. **RESULTS** 1) The baseline rCBF values of left frontal (0.720) and left temporal lobe (0.700) were decreased significantly in depressed patients compared with the control subjects. 2) The activated rCBF values of left frontal lobe (0.719) and left temporal lobe (0.690) were decreased more evidently than that of the baseline images. There was additional decreased activated rCBF values in left parietal lobe (0.701) in depressed patients. **CONCLUSIONS** 1) Hypoperfusions of left frontal and left temporal cortex were identified in patients with depression. 2) The Hypoperfusions of left frontal and left temporal cortex may be the cause of cognitive disorder and depressed mood in patients with depression. 3) Cognitive activated brain perfusion imaging is useful to diagnose depression more accurately.

OS-442

D.O. Slosman¹, C. Ludwig^{1,2}, A. de Ribapierre², J. Billet¹, F. Herrmann¹, J.-P. Michel¹, E. Giacobini¹, C. Bouras¹, J.-M. Annoni¹, P. Magistretti³.
¹ HUG, Geneva (CH), ² FPSE, Geneva (CH), ³ CHUV, Lausanne (CH).

^{99m}Tc-HMPAO SPECT DURING NEUROPSYCHOLOGICAL ACTIVATION: A TOOL FOR CLINICAL DIAGNOSIS OF DEMENTIA.

Purpose: To assess the adequacy of neuropsychological (NP) activation with HMPAO SPECT to identify elderly with suspected dementia. **Material and method:** For this purpose, the initial phase of a prospective study conducted to follow elderly has been used. 38 subjects underwent HMPAO brain SPECT in standardized basal state (non word simple verbal repetition) and during NP activation (phonological verbal fluency) following the split-dose technique (i.v. injection of 7 and 28 mCi ^{99m}Tc-HMPAO with proportional time of acquisition) with a fan beam 3-heads Toshiba GCA-9300 camera. The population sample consists in 33 normal elderly aging 73.8±7.1 yr. (m±sd) and 5 mild Alzheimer (DAT) patients (73.0±10.3 yr). SPM analysis was performed in a) contrasting basal or NP activation for normal versus DAT and b) for basal versus NP activation on the whole sample and on 2 of its subgroups based on their cognitive performance on a Stroop Color task (tertile 1st versus 3rd). **Results:** Between DAT and normals, SPM analysis revealed the presence of a significant lower perfusion in the right lateral temporal area of the DAT population during base-line while a significant lower perfusion was observed in the same population in the left frontal area during NP activation. In addition, for the whole population as well as for the 3rd tertile (the most performant group), NP activation resulted in selective bi-temporal and parietal brain enhanced perfusion which did not exist for the 1st tertile. **Conclusion:** These results underline 1) the necessity to redefine basal conditions to perform brain perfusion SPECT and 2) the added value of a split-dose NP activation protocol to improve better identification of DAT patients.

OS-443

K. Lee, H. Kaushik, V. Arpadi, C. Kirkby, H. Dixson, A. Bell, T. Chey

Bankstown-Lidcombe Hospital, Department of Nuclear Medicine and Ultrasound

DIAGNOSTIC AND PROGNOSTIC VALUE OF SPECT HMPAO CEREBRAL PERFUSION SCANS IN ALZHEIMER'S DISEASE

The purpose of this study was to prospectively assess the clinical utility of SPECT HMPAO scans in the evaluation of unselected patients with cognitive impairment referred to the Memory Disorders Clinic. 72 consecutive patients (pts) with symptoms of cognitive impairment were studied. SPECT was performed 1 hour after administration of 1 GBq of Tc-99m HMPAO. Scans were obtained on a GE400T (pts 1-41) and Siemens MS2 (pts 42-72), using 40 minute scan acquisition. Scans were read by two physicians blinded to the psychiatric, neurologic and neuropsychologic evaluation (including Mini Mental State Exam-MMSE). Perfusion defects were categorised into bilateral temporoparietal pattern (BTP), unilateral temporoparietal pattern (UTP), vascular disease pattern (VDP= multiple asymmetric or severe wedge shaped perfusion defects), and frontal pattern (FP). Pts were then followed for three years. Scan results were compared to NINCDS/ADRDA diagnostic criteria, and to adverse patient outcome (progressive cognitive deterioration/neurologic death). BTP had a positive predictive value of adverse outcome of 80% (p<0.05, chi square test, 1 degree of freedom).

NINCDS-ADRDA criteria	Patient number	BTP	UTP	VDP	FD	Normal
Probable AD	27	23	3	0	0	1
No AD	27	2	2	10	4	9
Possible AD	18	5	6	1	1	5

	All TP defects	BTP alone	Mild cognitive impairment, (MMSE=19-29)	Moderate-severe cognitive impairment (MMSE<19)
Patient no.	54	54	36	18
Accuracy	90%	89%	89%	94%
Sensitivity	96%	85%	100%	92%
Specificity	85%	93%	82%	100%

In conclusion, SPECT HMPAO had prognostic value and was a valuable tool in the diagnosis of Alzheimer's disease. SPECT HMPAO demonstrated excellent correlation with NINCDS/ADRDA criteria in all degrees of cognitive deterioration.

OS-444

S. Dresel, T. Mager*, B. Rossmüller, K. Tatsch, K. Hahn

Departments of Nuclear Medicine and *Psychiatry,
University of Munich, Munich, Germany

[I-123]IBZM SPECT FOR ASSESSMENT OF STRIATAL D2-RECEPTOR BINDING IN VIVO UNDER TREATMENT WITH OLANZAPINE, A NEW ATYPICAL ANTIPSYCHOTIC DRUG

Olanzapine was recently introduced as a new atypical antipsychotic agent with similar properties as clozapine. The pharmacological efficacy was shown to be comparable to clozapine and remarkably higher than the one of risperidone, while exhibiting less bone marrow depressing effects than clozapine. Aim of the study was to evaluate the degree of D2-occupancy in relation to the neuroleptic dosage and to correlate the findings with the presentation of extrapyramidal symptoms (EPS). Additionally, the data were compared to our previous findings of IBZM-SPECT in patients under treatment with risperidone and clozapine.

In 20 patients treated with mean daily doses of olanzapine ranging from 0.05 to 0.6 mg/kg body weight (schizophrenics, DSM III R) SPECT data were obtained 2h after i.v. injection of 185 MBq I-123 IBZM (Picker Prism 3000, Matrix 128x128, HR-fan beam coll., filtered backprojection, Chang's attenuation correction). For assessment of EPS the "extrapyramidal symptom rating scale" (ESRS) was employed. Semiquantitative evaluation was performed calculating striatal/frontal cortex specific binding [STR-BG]/BG (normal > 1.8).

The dopamine D2-receptor binding was reduced in all patients treated with olanzapine ([STR-BG]/BG) % binding = 64%-14%). The D2-receptor occupancy revealed an exponential dose-response relationship (r = -0.85, p ≥ 0.0001). The slope of the curve was similar to that of risperidone and considerably higher than that of clozapine. EPS were observed in 1 patient, presenting with the highest D2 occupancy. EPS induction by olanzapine (4%) was comparable to clozapine and considerably less than under risperidone treatment (40%).

The findings suggest an exponential dose response relationship between the daily dose of olanzapine and the dopamine D2-receptor occupancy. These results are supported by in vitro experiments reporting a higher D2 receptor affinity and a similar 5HT2 receptor affinity of olanzapine as compared to clozapine. Thus, the decreased tendency to induce EPS at therapeutic doses is not due to limited occupancy of striatal D2 receptors in vivo. Protection from EPS, therefore, may be more likely mediated by other intrinsic effects of the drug, i.e. the combination of both D2 and 5HT2-receptor antagonism.

OS-445

G. Kontaxakis, L.G. Strauss, G. van Kaick, G. Sakas, S. Pavlopoulos

German Cancer Research Center, Heidelberg, Germany.

ORDERED-SUBSETS ACCELERATION OF THE ISRA, WLS AND SAGE IMAGE RECONSTRUCTION METHODS FOR EMISSION TOMOGRAPHY

The ordered-subsets (OS-EM) approach is shown to provide an order-of-magnitude acceleration over the maximum-likelihood expectation-maximization (ML-EM) iterative image reconstruction (IIR) method for positron emission tomography (PET), while maintaining image quality. The OS-EM technique is here extended to the case of other IIR algorithms. The image space reconstruction algorithm (ISRA) is shown to converge to a non-negative solution of the least-squares estimator (LSE) of the emission densities. The exponentiation form of acceleration of the EM algorithm, applied for the quadratic case, was shown to lead to a weighted least-squares (WLS) solution of LSE. The space-alternating generalized EM (SAGE) algorithm belongs to the class of penalized ML (PML) algorithms for PET. This method speeds convergence by sequentially updating voxels using a succession of appropriately chosen hidden data spaces. The measured data are grouped in an ordered sequence of s subsets for OS-EM. Each iteration is broken into s cycles and during each cycle the image vector is updated with the parameters estimated from a subset of the measured data. OS-EM is equivalent to ML-EM for $s=1$. All algorithms (ISRA, WLS, SAGE) compute estimates of the projection data to achieve correction factors for the image vector update during each iteration. OS-EM is then possible to be applied for accelerating their convergence. OS-ISRA, OS-WLS and OS-SAGE are implemented and compared to OS-EM. OS-SAGE generalizes the principle of sequential update in both measured data and image spaces. Although SAGE has been shown to converge faster than ML-EM at the expense of some additional CPU time per iteration, OS-SAGE does not show similar performance in comparison with the OS-EM. The OS-WLS approach shows faster convergence and better contrast recovery than the OS-EM, without significant increase in CPU time per iteration. The OS-ISRA shows slower convergence than the OS-EM, like the ISRA in comparison with the ML-EM. In addition, the produced images are contaminated with backprojection-like radial artifacts.

OS-446

W.Backfrieder¹, R.Schachinger¹, T.Leitha², H.Bergmann^{1,3}

¹Dept. Biomedical Engineering & Physics, ²Clin. Nuclear Medicine,

³L.Boltzmann Institute Nuclear Medicine, University of Vienna, Austria

NONUNIFORM ATTENUATION CORRECTION IN BAYESIAN RECONSTRUCTION OF SPECT DATA

Iterative reconstruction of SPECT images provides modeling of locally variant point spread function (PSF) and nonuniform body attenuation based on statistical properties of measured data. Using a maximum a posteriori (MAP) algorithm prior information is utilized in the reconstruction process.

We developed a MAP reconstruction algorithm with quadratic Gibbs priors for correction of nonuniform attenuation. Linear attenuation coefficients were derived from CT volume data showing respective body areas. CT and an overview reconstruction of the SPECT volume were registered using a surface-to-points matching algorithm. Different tissue types were segmented from the registered CT volume to access nonuniform attenuation. Standardized density values and mass absorption coefficients were used for calculation of the system matrix for iterative reconstruction. Registration and segmentation was done using the biomedical image processing package ANALYZE.

Phantom and in vivo studies were performed to demonstrate proper attenuation correction of the algorithm. Data acquisition was done on a three headed Picker Prism3000 gamma camera, with a LEUHR parallel collimator, 120 projections/360°, 128x128 matrix size and 3.6mm slice thickness. An elliptical Jaszczak phantom with 400 MBq ^{99m}Tc was measured for 60s/projection. In vivo data from patients with a squamous cell carcinoma in the head and neck region were measured for 15.5s/projection after application of 500MBq ^{99m}Tc Sesta-Mibi. Transaxial slices were reconstructed using filtered back-projection (FBP) with a Wiener filter, 0.5 f_{max} cut-off frequency, and absorption corrected ML-EM and MAP reconstruction.

MAP and ML-EM reconstruction show proper absorption correction in both phantom and in vivo studies. Spatial resolution is increased compared to FBP with Wiener filter. After 30 iterations the MAP algorithm shows sufficient smoothing of image data like FBP, whereas ML-EM increases noise artifacts by further increase of the number of iterations. Accepting slightly worse spatial resolution the implementation of ordered subsets in ML-EM and MAP increases the speed of reconstruction up to a factor 30.

OS-447

T. Kauppinen, S. Alenius, V. Turjanmaa, J. Kuikka and M. Koskinen

Clinical Physiology and Nuclear Medicine, Kuopio University Hospital, Kuopio, Finland, Tampere University of Technology, Tampere, Finland, Tampere University Hospital, Tampere, Finland.

COMPARISON BETWEEN ITERATIVE MEDIAN ROOT PRIOR ALGORITHM AND FILTERED BACK-PROJECTION IN SPET

The aim of this study was to compare filtered back-projection (FBP) method and a new type of Bayesian one-step late reconstruction method which utilizes a median root prior (MRP). That has been used with good results in PET, but for this study it was modified for SPET. Comparison between these methods was performed by using phantom measurements and clinical SPET heart studies.

MRP is mostly like the common EM-ML algorithm (expectation maximization - maximum likelihood). During the MRP iteration process each points of activity profiles are multiplied by a penalty function which is a factor depending on the difference between the actual pixel value and the median of its neighbourhood. MRP has effective noise reduction property and it is better than low pass filter, because it does not blur the important edge lines of object.

The phantom was a large plastic cylinder containing active water solution and small bottles filled up using different activities. Differences between reconstruction methods were evaluated by defining the recovery of activities in the phantom. 30 patients with coronary artery disease were studied. Differences in these stress-rest perfusion study were evaluated semi-quantitatively. Therefore the image of the heart was divided into 7 segments wherein a experienced physician rated perfusion into 4 classes.

It was found in phantom measurements, that MRP-method is more reliable and closer to the reality than FBP method. The true activity response curve was more linear in MRP than in FBP. Furthermore, typical streak artifacts outside the actual radioactive object were not present in MRP. These are remarkable advantages when aiming towards quantitative SPET. In the clinical heart studies MRP method gave a cleaner image than FBP. The number of perfusion defects was bigger in MRP than in FBP, but in paired t-test the p-value was only 0.085.

The MRP method, like iterative methods generally, produces cleaner images than FBP. By oneself MRP algorithm is slightly slow and it needs to be used with accelerating procedure like ordered subsets. Unfortunately, the lack of a golden standard makes it impossible to definitely say which gives more precise diagnose. However, MRP could be a useful reconstruction method also in SPET.

OS-448

C.Jeanguillaume, S.Begot, M.Quartuccio and P.Ballongue

Hopital Henri Mondor 94010 CRETEIL FRANCE and Faculté des Sciences d'Orsay 91405 ORSAY FRANCE

NEW FAST AND ROBUST DECONVOLUTION ALGORITHMS FOR COMPUTER AIDED COLLIMATION GAMMA CAMERA (CACAO).

We propose 2 new deconvolution algorithms useful for CACAO reconstruction. - Conventional parallel holes collimators produce poor resolution and poor sensitivity with gamma cameras. The problem is even worse in SPECT (Single photon emission tomography) due to the influence of noise in the reconstruction algorithm and variation of the spatial resolution with the source to detector distance. To overcome these drawbacks, a project called: computer aided collimation gamma camera (CACAO in French) has been proposed. Information theory has confirmed the potential benefit of the method, assuming the existence of an appropriate reconstruction program e.g. fast and robust. The huge amount of data produced by CACAO acquisition imposes a fast responding program. Robustness means good accuracy even in the presence of noisy data. We developed new methods of deconvolution using the Fourier Transform for a fast response. Usual drawbacks of the Fourier based deconvolution are avoided by several improvements. Two methods are combined for a maximum efficiency.

- The first method called Composite Kernel uses two kernels with two different widths corresponding to two different bore holes in the collimator. By dividing the raw data with the kernel of maximum value for each frequency, low value denominators are avoided. Thus the condition number of the problem is greatly reduced, and the noise amplification is equally reduced.

- The second method called PSBSFS (positive solution, bounded support and fixed sum) increases further the condition number by using a shifted difference of the kernel. In addition the method imposes 3 constraints on the solution: the search is limited to positive solution, bounded support and fixed sum. Constraining solutions is a well known method in solving ill conditioned problem.

-The robustness of the algorithm is evaluated by the signal to noise ratio (SNR) gain that is the ratio of the output over the SNR at the input. Hundreds of computer simulations for various random objects, affected by poisson noise and for various levels of SNR at the input were calculated. A 24 fold increase of SNR gain is obtained by the composite kernel method compared to the narrowest kernel deconvolution. The second method gives a further increase of SNR gain ranging from 18 to 2.2 when the SNR at the input range from 0.6 to 14 (number of photons 10 to 10 000). CONCLUSION: The algorithm presented here is sufficiently robust and rapid to make CACAO reconstruction successful and to improve both sensitivity and resolution of SPECT.

OS-449

Lindahl D¹, Toft J², Ali S³, Hesse B², Palmer J⁴, Lundin A⁵ and Edenbrandt L¹

Departments of ¹Clinical Physiology, ⁴Radiation Physics, and ⁵Radiology, Lund University, Lund, Sweden, and Departments of ²Clinical Physiology and Nuclear Medicine, and ³Cardiology, Rigshospitalet, Copenhagen, Denmark

VALIDATION FOR ARTIFICIAL NEURAL NETWORK CLASSIFICATION OF TECHNETIUM-99M MYOCARDIAL TOMOGRAMS

Background and purpose: Artificial neural networks is a form of machine intelligence. They have been shown capable of detecting coronary artery disease (CAD) from myocardial perfusion scintigrams. In clinical practice this type of neural networks will not take over the decision-making process from the physicians, but assist them by proposing an interpretation of the scintigram. Recently a study showed that physicians interpreting myocardial scintigrams benefit from the advice of these neural networks. These results show the high potential for neural networks as clinical decision support systems. However, the networks have been developed and tested at the same hospital using the same gamma cameras, acquisition techniques, and processing protocols. If the neural networks should be widely used they must be validated also in other clinical settings. The purpose of this study was to evaluate the performance of an artificial neural network at a hospital away from where it was developed. Further the performance of the network was compared to that of a human expert and another method for quantitative analysis.

Patients and Methods: A total of 203 patients (135 patients from Lund, Sweden and 68 from Copenhagen, Denmark) who had undergone both myocardial SPET (technetium-99m-sestamibi) and coronary angiography were included. The coronary angiography was used as gold standard and a lumen area reduction of 75% or more was defined as significant CAD. A three-layer feed-forward artificial neural network was trained on the Lund patients (87 of whom had angiographically verified CAD) and then the network's ability to detect CAD on the Copenhagen patients (52 of whom had angiographically verified CAD) were tested. Test results were compared to the results of a human expert and to the results of a method based on a commercially available program (CEqual®).

Results: The sensitivity was 86% (network), 69% (human observer) and 65% (CEqual®). The specificity was 81% for all.

Conclusion: An artificial neural network, trained on myocardial perfusion studies performed at one hospital, is able to detect CAD from studies performed at another hospital using different gamma cameras, acquisition, and processing protocols.

OS-450

S. Vandenberghe,¹ P. Lahore¹, Y. D'Asseler², M. Koole², K. Audenaert¹, I. Lemahieu², R. Dierckx¹

¹Department of Nuclear Medicine, University Hospital of Gent, Belgium;

²MEDISIP, Electronics and Information Systems Department, University of Gent, Belgium

STATISTICAL PARAMETRIC ANALYSIS OF ACTIVATION FOCI DETECTABILITY IN BRAIN SPECT IMAGING

Background and aim of the study: In the last few years, Statistical Parametric Mapping (SPM) has manifested itself as a very powerful technique in the analysis of PET- and fMRI neuroactivation studies. To the best of our knowledge SPM has however not yet been thoroughly validated with regard to the analysis of SPECT neuroactivation studies. We investigated the influence of foci dimensions and the number of scans included in the study on the detectability of activation foci in brain SPECT studies.

Methods: Spherical activation foci of varying size and percentage of hyperactivity were created at clinically relevant positions in the digital three-dimensional Hoffman brain phantom. Using shareware sinogram simulation software, an acquisition protocol was simulated for these phantoms on a triple-headed SPECT camera. The acquisition images were subsequently reconstructed with filtered backprojection and analyzed using the Statistical Parametric Mapping software package (SPM96)

diameter (mm) ↓	(A,B)⇒	(3,3)	(5,5)	(10,10)
8		100%	85%	70%
16		40%	30%	15%
24		20%	10%	5%

Table 1

Results: Table 1 shows the evolution of the minimum activity difference required for the detection of the activation foci in function of the foci diameter and the number of baseline (A) and activation scans (B) included in the study. The required minimum foci activity shows a marked decrease with increasing foci diameter and study size. For a balanced study consisting of 10 baseline and 10 activation scans, activation foci of 24 mm. in diameter, can be detected from an activity level (i.e. change in rCBF) of 5% on. Furthermore, differences were noted in the size of the detected foci relating to the position of the various foci in the brain.

Conclusion: As a first step in the systematic validation of the performance of statistical parametric analyses in functional SPECT brain mapping studies, we present results on the relative importance of study size and foci dimensions on the detectability of the activation foci.

General nuclear medicine: Kidney & liver transplantation
OS-451

A. Perera (1), F. Zayas (2), L. Torres (1), O. Pereztol (1), R. Fraxedas (2), J.F. Batista (1), M. Ramos(3), L. Reyes (2), L. del Risco (4), A. Hernández (1), I. Alvarez (1).

1. Center for Clinical Research, 2. Institute for Nephrology, 3. Center of Molecular Immunology, 4. Institute for Hygiene and Epidemiology, Havana, Cuba.

USE OF 99mTc-LABELLED MAb IOR T3 FOR THE EARLY DIAGNOSIS OF ACUTE TRANSPLANT REJECTION. PRELIMINARY RESULTS.

Monoclonal antibody IOR t3 is a murine IgG2a, directed against CD3 receptor of T-lymphocytes. The aim of the work was to assess the usefulness of 99mTc-labelled MAb IOR t3 for early immunoscintigraphic diagnosis of acute renal allograft rejection.

Materials and Methods: Labelling procedure was performed directly using 2-mercaptoethanol as reducing agent. A factorial design 2²⁺¹ was performed to assess the influence of different reaction parameters. Labelling efficiency was selected as response variable. DTPA and L-cysteine challenges were carried out to assess the stability of the label. Immunoreactivity fraction was determined. A sample of 6 patients (4 male and 2 female) with heart transplant was included to study pharmacokinetics, biodistribution and internal dosimetry. Six 6 patients with recent renal transplant (7-21 days) were studied. It was intravenously injected 1 mg of 99mTc-IOR t3 (962±53 MBq). **Results:** Experimental results showed that MAb:2-ME ratio and reduction time were the parameters with higher influence on labelling efficiency. Radiochemical purity of the 99mTc-IOR t3 was 97±2 %. It was detected no transchelation in presence of DTPA. In case of L-cysteine challenge, label was significantly transferred from antibody only at 1:30000 molar excess (80% at 24 h, p<0.001). It suggested that label should be stable in vivo. Immunoreactive fraction was 69±1 %. Plasmatic clearance in patients was fitted to a biexponential curve with T_{1/2α}=17.1 min. and T_{1/2β}=18.6 h. Liver and spleen were the organs with higher uptake of radiopharmaceutical. Target/background ratio was higher 2 for two patients underwent acute renal transplant rejection (one of them had no clinical symptoms) and close to 1 for the rest of patients. All results were confirmed by biopsy. **Conclusions:** 99mTc-IOR t3 could be a promising radiopharmaceutical for early diagnosis of acute renal allograft rejection. Further studies are necessary for it better evaluation.

OS-452

A.M.Omar, M. Samhri, T. Al-Saeed, A.A. Gawish, R. Castedio, M. Mousawi. Depts. of Nucl Med and Surgery, Organ Transplantation Center, Ministry of Public Health, Kuwait.

COMPENSATORY CHANGES OF EFFECTIVE RENAL PLASMA FLOW (ERPF) FOLLOWING LIVE DONOR NEPHRECTOMY.

Live donor renal transplantation has been increasingly performed over the last two decades. Significant compensatory changes occur in the remaining kidney, following nephrectomy.

The objective of this prospective study was to evaluate the early compensatory changes of effective renal plasma flow (ERPF) in the remaining kidney after donation. Sixteen consecutive live related kidney donors (11 females and 5 males) aged 22-45 were studied. ERPF was determined before, 3 days and 3 months after nephrectomy, using Tc-99m MAG-3 gamma camera method.

The following are the mean and range of the values obtained :

ERPF	Pre-nephrectomy		Post nephrectomy	
	Total	Remaining kidney	3 days	3 months
	710 (598-785)	350 (306-385)	610 (453-722)	629 (527-690)

The ERPF of the remaining kidney increased to near 2 folds of the pre-nephrectomy level of the same kidney reached 86% and 88% of the total pre-nephrectomy level at 3 days and 3 months after donation, respectively.

Rapid compensatory increase of ERPF occurs in the remaining kidney following live donor nephrectomy. Awareness of this change can be useful for proper interpretation of values in future incidents and follow up.

OS-453

T.A.F. El-Maghraby¹, J.A.J. Camps¹, J.A.K. Blokland¹, B.L.F. van Eck-Smit¹, A.H. Zwinderman², J.W. de Fijter³, S.I. El-Haddad⁴, E.K.J. Pauwels¹.
Departments of Radiology, Division of Nuclear Medicine¹, Medical Statistics², Nephrology³, Leiden University Medical Centre, Leiden, The Netherlands. Department of Oncology and Nuclear Medicine⁴, Cairo University, Egypt.

A NEW CAMERA BASED METHOD TO CALCULATE THE SLOPE OF THE EXTRACTION PHASE OF 99mTc-MAG3 RENOGRAM TO FOLLOW ATN PATIENTS IN THE EARLY POST TRANSPLANTATION PERIOD.

Delayed graft function remains a frequent complication in the early post-transplant period which may affect up to 50% of renal transplants. Acute tubular necrosis (ATN) is the most frequent cause of this delay in graft function. 99mTc-MAG3 is an actively secreted tubular renal radiopharmaceutical. This active transport of the tubular cells is affected in ATN leading to impaired 2nd phase of the renogram curve. We have developed a method to calculate the slope in a reproducible manner the renogram extraction phase in order to assess and to follow up the ATN cases. This study was carried out prospectively in 34 patients with 136 99mTc-MAG3 scintigrams. For each patient there was a baseline scan within 48 hours post-transplantation followed by at least two sequential studies on the subsequent days and one scan after 3 months. After injection of 100 MBq of 99mTc-MAG3, dynamic frames were recorded initially at 1-sec. interval for 2 minutes, followed by 90 frames of 20-sec. to complete the 32-minute study. The background subtracted-graft curve was generated for the first two minutes of the study. The injected dose was determined by counting the pre- and post-injection syringe on the camera with correction for decay. The graft curve was then normalized to the injected dose. To measure the slope a straight line was fitted through different intervals within the first two minute renogram. The most reproducible interval for slope measurements was from 50-110 sec. This quantitative parameter was defined as the tubular function slope (TFS). According to the clinical diagnosis given by an expert nephrologist on the scintigraphic days 18 scans were acquired during primary graft function (PGF), 31 during ATN, 32 after improvement of ATN and 52 in a normal functioning stage. Three studies from one patient who developed severe rejection were excluded. The TFS in normal scans was 2.58 ± 0.76 which was significantly higher than its value in the scintigrams of the ATN, improved ATN and PGF groups. ($P < 0.001$, $P < 0.001$ and $P = 0.002$ respectively). TFS was able to show improvement in the ATN condition as its value in ATN scans was 0.90 ± 0.52 which is significantly lower than its value in the improved ATN group (1.54 ± 0.41 , $P < 0.001$). The PGF group showed a higher TFS of (2.38 ± 1.42) than the ATN group with $P = 0.03$, while it was comparable to the improved ATN group ($P = 0.82$). In addition, the TFS showed a reasonable correlation with the serum creatinine ($r = -0.71$) and the creatinine clearance ($r = 0.65$) estimated on the scintigram days. In conclusion, our preliminary data suggest that TFS method is an easily quantified objective parameter which can assess the tubular cell function. TFS is helpful in the follow-up of ATN to monitor the severe prolonged cases and to detect improvement in the ATN condition.

OS-454

T.A.F. El-Maghraby¹, J.W. de Fijter², B.L.F. van Eck-Smit¹, A.H. Zwinderman³, S.I. El-Haddad⁴, E.K.J. Pauwels¹.
Departments of Radiology, Division of Nuclear Medicine¹, Nephrology², Medical Statistics³, Leiden University Medical Centre, Leiden, The Netherlands. Department of Oncology and Nuclear Medicine⁴, Cairo University, Egypt.

RENOGRAPHIC INDICES FOR ASSESSING THE CHANGES IN DELAYED GRAFT FUNCTION IN RENAL TRANSPLANTATION: A CRITICAL EVALUATION IN 43 PATIENTS.

Renal scintigraphy played an important role in assessing renal allograft function since the beginning of the renal transplantation era. Many quantitative radionuclide parameters were developed from analysis of the renogram to facilitate the detection of changes in perfusion and/or allograft function. We have evaluated the clinical usefulness of some of the frequently used quantitative radionuclide parameters in the early post-transplant period. The patient population in this study consists of 43 patients with 157 99mTc-MAG3 renograms. The quantitative methods studied were classified into perfusion parameters including: Global Perfusion Index (GPI), Cortical Perfusion Index (CPI) and the Vascular Transit Time (VTT) and parenchymal parameters: Uptake Capacity at 2 minutes (UC2) and Elimination index (K3/20). The findings of 8 studies were excluded (2 obstruction and 6 Cyclosporin-A toxicity) being insufficient for statistical analysis. Of the remaining 149 studies, there were 14 studies from stable functioning grafts (SGF), 105 studies done during ATN and 30 scans during Acute rejection (AR). The ATN group was further subdivided into 91 scans performed during acute episodes of tubular necrosis and 14 scans as improved ATN. The AR group was also subdivided into 21 scans of AR and 9 scans in improved AR. The perfusion indices GPI and CPI were able to differentiate between patients suffering from ATN or AR from cases with SGF ($P < 0.0001$). However, they were non-significant to differentiate ATN from AR (P values = 0.18 and 0.47 respectively). The VTT was prolonged in the AR group (14.8 ± 5.4 sec) which is significantly more than the SGF and ATN groups ($P < 0.01$ and $P < 0.05$) respectively. These perfusion indices, however, were of value in monitoring the improvement in the condition of the graft dysfunction. The changes in GPI were significant to show improvement in both AR and ATN subgroups ($P = 0.04$ and $P = 0.002$) respectively, whereas VTT could not show improvement in AR and ATN subgroups respectively. As for the parenchymal parameters both UC2 and K3/20 were able to differentiate between SGF versus AR and ATN groups ($P < 0.0001$) but with no ability to separate AR from ATN dysfunction ($P > 0.04$ for UC2 and $P > 0.08$ for K3/20). The ability of these parenchymal parameters to detect the improvement in the graft function was poor and statistically non significant. In conclusion, these quantitative numerical values are unable to unequivocally differentiate between grafts with ATN versus AR cases. The real value of these parameters, especially the GPI, is in the follow-up and detecting the improvement in the AR and ATN dysfunction processes.

OS-455

D. Fuster, F. Lomeña, J.V. Torregrosa¹, F. Oppenheimer¹, C. Píera, C. Laterza, J.J. Mateos, R. Herranz and J. Setoain. Nuclear Medicine Department and Renal Trasplant Unit¹. Clinical Hospital of Barcelona

111-In-LABELLED PLATELETS SCINTIGRAPHY CAN PREDICT THE IMMUNOLOGICAL ORIGIN OF PROLONGED FEVER IN PATIENTS WITH NON FUNCTIONING RENAL ALLOGRAFT

Purpose: 1) To evaluate the usefulness of labelled platelet scan in patients with non functioning renal allograft and prolonged febrile syndrome (PFS), and 2) to analyse if the use of steroids can artefactuate scintigraphic findings. **Method:** We have performed prospectively a 111-In-mercaptopyridine labelled platelet scan (PS) in 91 pat. (37 women, 54 men) with a mean age of 39.6 ± 12 years. The period of PFS was 35 days (range 7-322). 46/91 pat. underwent corticosteroid therapy (2-10mg/day). Platelet labelling was carried out following Thakur's method. PS was performed 48h after reinjection of labelled platelet. The platelet uptake index (PUI) was calculated dividing the cpm/pixel in allograft ROI by cpm/pixel in a mirror background ROI. The final diagnosis of PFS was established depending on the outcome after treatment. In 61/91 pat. the fever had an immunological origin (IF) because it disappeared after embolisation (8) or transplantectomy (53). In 30/91 pat. the PFS was non immunological and it was resolved after antimicrobial therapy. **Results:** Considering a PUI of 1.5 as the minimum level of platelet accumulation to establish an IF we obtained:

	IF	non IF	
PUI \geq 1.5	32	-	Sensit.=76% NPV=69%
PUI < 1.5	14	45	Specif.=100% PPV=100%

2) In pat. with IF, there was 1/18 false negative (FN) in pat. free of steroids and 13/43 FN in pat. under steroids. In these patients, the PUI was significantly lower than in patients with IF and free of steroids ($p < 0.05$). **Conclusions:** 1) PS can predict IF in patients with non functioning renal allograft. 2) Therapy with steroids can reduce the sensitivity of PS to detect IF.

OS-456

H.Sakahara, T.Kiuchi, S.Nishizawa, S.Kawase, T.Saga, Y.Nakamoto, N.Sato, T.Higashi, T.Fujita, K.Tanaka, J.Konishi.
Department of Nuclear Medicine and Diagnostic Imaging, Department of Transplantation Immunology, Kyoto University, Japan

ASIALOGLYCOPROTEIN RECEPTOR SCINTIGRAPHY IN EVALUATION OF AUXILIARY PARTIAL ORTHOTOPIC LIVER TRANSPLANTATION

Purpose: The purpose of the present study was to test asialoglycoprotein receptor scintigraphy in the post-transplant monitoring of liver graft and native liver functions in recipients of auxiliary partial orthotopic liver transplantation (APOLT) from living donors. **Methods:** We performed 31 asialoglycoprotein receptor studies in 11 patients who underwent APOLT for non-cirrhotic metabolic liver diseases or for small-for-size grafts. Anterior dynamic images including the heart and both livers were obtained for 16 min after intravenous injection of Tc-99m-DTPA-galactosyl human serum albumin and thereafter static SPECT images of both livers were taken. Rate constants of transfer from blood to the graft liver and from blood to the native liver were determined separately by the Patlak plot analysis with dynamic images. Total radioactivity counts present in each liver were calculated respectively by integration of counts in transverse SPECT images. A fraction of counts in the graft liver was expressed as the percentage of total counts in both livers. The volume of the graft liver and native liver was measured by computed tomography. **Results:** The rate constant in the native liver was variable according to the primary disease and decreased when the portal vein of the native liver was separated. In the graft liver without severe rejection nor other complications, the rate constant was high and the fraction of counts in the graft liver increased more dramatically than did the fraction of volume. Severely damaged graft liver, however, showed a slow rate constant and also a low fraction of counts in spite of a large fraction of volume. **Conclusion:** Asialoglycoprotein receptor scintigraphy is useful to distinguish and monitor the graft and native liver functions in recipients of APOLT.

Cardiovascular: Pharmacokinetics and metabolism

OS-457

S.Fukuzawa, S.Ozawa, M.Inagaki, J.Sugioka, M.Daimon, S.Kushida

Hospital: Funabashi Municipal Medical Center, Division of Cardiology

EFFECT OF ANGIOTENSIN-CONVERTING ENZYME INHIBITOR IN MYOCARDIAL FATTY ACID METABOLISM AFTER ACUTE MYOCARDIAL INFARCTION.

Angiotensin converting enzyme inhibitor (ACE-I) therapy has been shown to have an early mortality benefit in unselected patients with acute myocardial infarction (AMI). However, the effects of ACE-I on myocardial fatty acid metabolism in this population group have not been studied. We tested the hypothesis that ACE-I therapy improves myocardial fatty acid metabolism and decreases mortality in patients after AMI. 49 patients after first AMI were randomized to titrated oral enalapril (n=26) or conventional therapy (control, n=23). Iodine-123-betamethyl-p-iodophenyl-pentadecanoic acid (BMIPP) single photon emission computed tomography imaging underwent an average of 4 days and one month after AMI. The short-axis and vertical long-axis of myocardial tomograms were divided into 18 segments for each patient. These segments were assigned in 8 evenly spaced regions in the mid and basal short-axis views, and 2 apical segments were in mid-ventricular long-axis slices. Segments were scored using 4-points system (0=normal, 1=mild, 2=moderate, 3=severe reduction of radioisotope uptake). BMIPP defect score (DS) was provided from summated serial slices. There were no significant changes in baseline characteristics between enalapril-treated patients and control patients. However, BMIPP DS from acute phase to chronic phase was decreased in enalapril-treated patients (14.9 ± 7.2 to 9.8 ± 6.4 , $p < 0.05$), but not in control patients (16.6 ± 8.4 to 13.6 ± 4.8 , n.s.). We concluded that ACE-I therapy improved myocardial fatty acid metabolism in patients after AMI. It is suspected that the improvement of myocardial fatty acid metabolism may represent a sustained effect that is associated with a decrease in morbid events after AMI.

OS-458

N. David, N. Hassan, M. Angioi, C. Mercenier, P.Y. Marie, P. Olivier, P. Menu, D. Fagret, N. Danchin, G. Karcher, A. Bertrand. Departments of Nuclear Medicine and of Cardiology, CHU-Nancy, France.

THE KINETICS OF β -METHYLATED LABELLED FATTY ACIDS IN MYOCARDIUM SUBJECTED TO ISCHEMIA

β -methylated free fatty acids (FFA*) have been developed for myocardial SPECT imaging, but little is known about their kinetic in ischemic conditions. This study was aimed at determining the ischemic changes in the myocardial kinetics of a β -methylated FFA*: [123 I]-16-iodo-3-methylhexadecanoic acid (MIHA).

The kinetics of MIHA was analyzed: [1], on a blood perfused isolated heart model submitted to a 50 % reduction of coronary flow (moderate ischemia) and [2], in patients who had an exercise thallium-201 SPECT defect corresponding to either necrotic (n=13) or chronically ischemic and viable (n=15) myocardium, and who underwent 2 consecutive SPECT after MIHA-injection.

In animals, the myocardial early retention fraction of MIHA, but not MIHA clearance rate, was dependant on coronary flow, early retention fraction being higher in ischemic than in normoxic conditions (26 ± 9 % vs 15 ± 6 %, $p = 0.007$).

On patients SPECT, the uptake of MIHA calculated in ischemic and viable areas (74 ± 9 % of maximal LV value) was different from that calculated in necrotic (59 ± 5 %, $p < 0.001$) or normal (88 ± 6 %, $p < 0.001$) areas. By contrast, there was no difference between these 3 groups, for the MIHA-clearance calculated between the 2 consecutive SPECT.

Contrary to other FFA*, the myocardial clearance of MIHA is not decreased by ischemia. However, the uptake of MIHA is a reliable indicator of viability in chronically ischemic myocardium, a property which is facilitated by an increased early retention in case of moderate reduction of coronary flow.

OS-459

S. L. Chen

Hospital: Zhongshan Hospital, Department of Nuclear Medicine.

THE STUDY OF MYOCARDIAL ENERGY METABOLISM IN PATIENTS WITH HYPERTROPHIC MYOCARDIUM: COMPARED WITH SPECT AND PET

PURPOSE: To elucidate the energy metabolism of free fatty acid and glucose in myocardium of hypertrophic cardiomyopathy (HCM) patients.

METHODS: The compared study was performed with SPECT using 123 I-BMIPP, 201 Tl and with PET using 18 F-FDG in eleven patients with HCM and eight healthy volunteers who acted as controls. All eleven patients were male and they had a mean age of 56 ± 9 years old. For quantitative analysis, the relative regional uptake (RRU, %) in each segment was obtained by normalizing the frame of all segments to the maximal value. **RESULTS:** hypertrophic myocardium uptake of 123 I-BMIPP was markedly reduced in 10 patients. During fasting and after glucose loading, the hypertrophic myocardium uptake of 18 F-FDG was slightly or mild increased in ten and nine patients, respectively. Persistent defects were observed in six patients during thallium myocardial SPECT, whereas increased uptake or normal in 2 and 3 patients, respectively. **CONCLUSIONS:** Marked reduction in fatty acid utilization and increased in glucose during fasting and loading are observed at sites of myocardial hypertrophy. The hypertrophic myocardium is shown to have a wide variety of pathologic conditions in myocardial blood flow, fatty acid and glucose metabolism.

OS-460

K. Utsunomiya, I. Narabayashi, K. Sueyoshi, and R. Matsui. Osaka Medical College, Department of Radiology

CLINICAL EFFICACY OF ALDOSE REDUCTASE INHIBITOR AND VITAMIN B12 ON DIABETES MELLITUS, EVALUATED BY 123 I-MIBG MYOCARDIAL SCINTIGRAPHY.

This study was undertaken to examine the effects of aldose reductase inhibitor (ARI) and vitamin B12 (VB12) on myocardial uptake of Iodine-123-Metaiodobenzylguanidine (123 I-MIBG) in patients with diabetic autonomic disorder. Myocardial scintigraphy using 123 I-MIBG was performed on 20 healthy volunteers (Controls) and 56 patients with non-insulin-dependent diabetes mellitus (NIDDM), in order to obtain heart/mediastinum ratio in the initial images (HMi) and in the delayed images (HMd), and washout rate (%WR). Thirty-four of the 56 NIDDM patients might be diagnosed as having diabetic autonomic disorder by comparatively evaluating their scintigraphic findings to the Controls. Seventeen of the 34 patients received 150 mg/day of epalrestat (ARI group) in 3 divided doses before meals, and the other 17 patients received 1.5 mg/day of mecobalamin (VB12 group) in 3 divided doses after meals, for 3 to 5 months. According to the presence (+) or absence (-) of clinical symptoms of autonomic or peripheral somatic nerve disorder, the patients were subclassified into the ARIN (+) group, ARIN (-) group, VB12N (+) group, and VB12N (-) group. After the completion of the treatment, myocardial scintigraphy was performed again. Before and after the treatment, ARI improved only the HMi in the ARIN (+) group ($p=0.046$), whereas VB12 significantly improved HMi in the VB12N (+) group ($p=0.018$); and HMi, HMd, and %WR in the VB12N (-) group ($p=0.043$, $p=0.018$, $p=0.043$, respectively). We conclude that VB12 is more efficacious than ARI in treatment for diabetic cardiovascular autonomic disorder.

OS-461

N. Nguyen, S. Egert, M. Schwaiger.

Technische Universität München, Department of Nuclear Medicine, Munich, Germany

EFFECTS OF α - and β -ANTAGONISTS ON THE ISCHEMIA-INDUCED INCREASE IN FDG UPTAKE IN THE ISOLATED RAT HEART MODEL.

It has been shown in the isolated rat heart model that ischemia induces a translocation of the glucose transporter, Glut4, resulting in an increase in FDG uptake during reperfusion. The purpose of this study was to investigate whether the catecholamine release during ischemia is responsible for the ischemia-induced enhancement of glucose utilization. Isolated rat hearts underwent retrograde perfusion with Krebs-Henseleit buffer containing 10mM glucose and FDG. FDG uptake was monitored using a pair of BGO detectors interfaced with a computer. After 10min stabilization, all hearts were perfused without additives for 15 minutes as baseline, which provided internal controls for each heart. After baseline studies, 5 hearts underwent 15min no-flow ischemia then reperfusion. Nine hearts were perfused with either β -antagonist (propranolol, 10 μ M) or α -antagonist (phentolamine, 10 μ M) alone. Another set of 9 hearts were perfused with either antagonist prior to ischemia as well as during reperfusion. Time-activity curves were decay-corrected, normalized, then fitted to a linear function, and slopes were derived as an index of FDG uptake. Propranolol or phentolamine alone did not significantly effect baseline FDG uptake.

	Normalized FDG uptake (mean \pm sd, ml/g/min)		
	Baseline	Reperfusion	p-value
Ischemia	0.022 \pm 0.012	0.070 \pm 0.012	0.0002
Isch+Propranolol	0.014 \pm 0.008	0.060 \pm 0.004	0.004
Isch+Phentolamine	0.015 \pm 0.003	0.038 \pm 0.012	0.02

Although neither antagonists completely abolished the ischemia-induced increase in FDG uptake, phentolamine significantly reduced FDG uptake during reperfusion compared to ischemia alone (p=0.003), while propranolol did not (p=ns). These data suggest the involvement of the α -adrenergic mechanism in the ischemia-induced upregulation of FDG uptake. Further studies with specific α 1-, α 2-antagonists are necessary in order to further clarify the role of the α -adrenergic system in the regulation of glucose metabolism in ischemic heart disease.

OS-462

V. Yu. Soukhov, N.P. Fadeev, I. Yu. Savicheva, N.A. Kostenikov
Central Research Institute of Roentgenology and Radiology,
Saint-Petersburg, Russia

CLINICAL APPLICATION OF 123-IODINE LABELED 15-IODINEPENTADECANOIC ACID AND SPECT IN PATIENTS WITH CORONARY ARTERY DISEASE.

A study was underway to evaluate the diagnostic properties of radiopharmaceutical for cardiac imaging - 123-Iodine labeled 15-iodinepentadecanoic acid (123I-PDA) - synthetic radiolabeled free fatty acid with the ability to show differences in metabolism of myocardial tissue.

Eighty six patients with history of myocardial infarction (MI, n=19) and coronary artery disease (CAD, n=47) underwent SPECT heart imaging twice: at 3-5 and 35-40 min after i.v. injection of 400 MBq 123I-PDA using «APEX SP-6» camera (Elsint, Israel).

123I-PDA SPECT demonstrated the specificity up to 85% in diagnostics of perfusion defects. The sensitivity of the method to post MI scar and ischemia was 89% and 86%, respectively.

The delayed images (35-40 min p.i.) reflect the intensity of beta oxydation. The significantly lower activity was found in regions with normal metabolism rate as compared to ischemic ones, where the higher activity foci of more slowly metabolized triglyceride pool were revealed. Severe, fixed defects which don't change significantly over time were seen at the sites of postinfarction scar.

Conclusions: SPECT using 123I-PDA appears excellent characteristics in detecting of perfusion and metabolic changes in cardiac muscle in patients with CAD after single injection of radiopharmaceutical. It can also effectively assess the viability of ischemic myocardial tissue and thus lead to adequate pathogenetic therapy challenge. The safety and simplicity of the protocol make it suitable for the use in the assessment of treatment efficacy in cardiological patients.

Oncology: PET

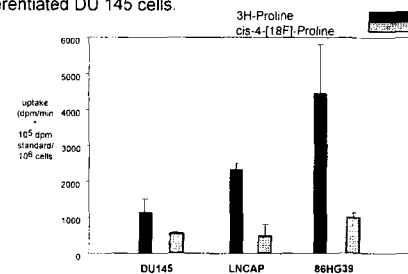
OS-463

A.R. Börner³, H. Mühlensiepen², K. Hamacher¹, M. Cremer², H.J. Peterson², K.J. Langen², H.W. Müller-Gärtner³, H.H. Coenen¹, Institut für Nuklearchemie¹ und Institut für Medizin², Forschungszentrum Jülich, Klinik für Nuklearmedizin³, Universitätsklinik Düsseldorf, Deutschland

UPTAKE OF CIS-4-[18F]-FLUOROPROLINE IN CULTURES OF HORMONE SENSITIVE AND HORMONE RESISTANT PROSTATE CANCER CELLS

Increased amino acid transport and utilisation in cancer cells has been demonstrated repeatedly. Considering the possible impact on tumor imaging we examined the accumulation of the positron emitting amino acid analog cis-4-[18F]-Fluoroproline (F-Pro) in comparison to [3H]-Proline (H-Pro) in the androgen sensitive prostate cancer cell line LNCAP and the hormone resistant DU145. The glioma cell line 86Hg39 served as a control. Transport assays were performed 3 days after seeding. Measurements were performed in HBSS medium at 37° C. The transport assay was started by addition of 185 KBq F-Pro and H-Pro. Incubation time was up to 30 min.

H-Pro uptake was higher than F-Pro uptake in all three cell lines. Uptake was highest in the glioma cells followed by the androgen sensitive LNCAP. Low but substantial tracer uptake was noted in the dedifferentiated DU 145 cells.



F-Pro shows lower cellular uptake in different tumor cell lines compared to H-Pro. Further evaluation of cis-F-Pro as a potential oncological PET tracer seems to be indicated. Similarly, the biochemical behaviour of the diastereomeric trans-F-Pro will be examined.

OS-464

A.R. Börner², K. Hamacher¹, H. Herzog², K.J. Langen², H.W. Müller-Gärtner², H.H. Coenen¹
Inst. für Nuklearchemie¹ and Inst. für Medizin², Forschungszentrum Jülich, Klinik für Nuklearmedizin³, Universitätsklinik Düsseldorf, Deutschland

[18F]-FLUOROPROLINE – BIODISTRIBUTION AND FIRST RESULTS IN PATIENTS WITH RENAL TUMORS

The amino acid analogue cis-4-[18F]-Fluoroproline (F-Pro) is the first positron emitting amino acid that can be produced in large quantities like FDG. The accumulation of proline, a substrate of the A-amino acid carrier, is influenced by oncogenes and proto-oncogenes on cellular level. This pilot study was performed to evaluate the distribution and kinetics of F-Pro in patients with suspected renal cell cancer.

5 patients were hospitalised for surgical removal of renal masses. Pretherapeutic evaluation consisted of CT, whole-body F-Pro and FDG PET on consecutive days immediately before surgery using a CTI HR+ scanner. Emission scans were carried out 1h, 3h and 5h after injection. During that time blood and urine were sampled.

In all patients, kidneys, urinary bladder and liver were visualized. With F-Pro, up to 50% of the injected radioactivity were excreted with the urine in 5 hours. F-Pro accumulation in the tumor was noted in 2 of 5 patients and FDG accumulation in 2 others. One patient with hemangioma showed neither FDG nor F-Pro accumulation.

	F-Pro	FDG	histology
pat 01	+	-	renal cell carcinoma
pat 02	-	-	haemangioma
pat 03	-	+	abscess
pat 04	+	-	renal cell carcinoma
pat 05	-	+	squamous cell cancer

F-Pro appears to be a useful additional tracer in the decisive differentiation of renal masses while FDG alone is not sufficient. No F-Pro accumulation was seen in inflammation so far and no false positive results were obtained. Drawbacks of F-Pro are relatively low tumor uptakes compared to the normal kidney and early and intense renal accumulation that can only be reduced by forced diuresis.

OS-465

A. Dimitrakopoulou-Strauss, D. Schadendorf, H. Naehrer, P. Mantaka, F. Oberdorfer, L.G. Strauss

German Cancer Research Center, Heidelberg, Germany.

FDG AND F-18-DIHYDROXYPHENYLALANINE IN PATIENTS WITH METASTATIC MELANOMAS

PET with F-18-Dihydroxyphenylalanine (F-18-DOPA) was used in patients with metastases from malignant melanomas to increase the specificity of PET for tumor diagnosis.

Eight patients with pretreated metastatic melanomas were studied twice with different tracers within one week. Dynamic PET multitracer studies with O-15-water (tissue perfusion) and F-18-Deoxyglucose (FDG, tumor viability) preceded F-18-DOPA (second study). The dynamic acquisition times are: O-15-water, 8 min; FDG, 60 min; F-18-DOPA, 120 min. ROIs were applied and SUV calculated. The transport constants k1 and k2 were evaluated for the perfusion series and the DOPA series using a two compartment model and the median uptake of a larger vessel was used for the input function. Parametric images of the influx and efflux of the tracer were reconstructed. The Patlak analysis was applied to the FDG data.

The FDG-scans showed an increased FDG metabolism in all subcutaneous metastases (n=3) and in 3/5 liver metastases. The DOPA-uptake was less than the FDG-uptake in 5/8 patients, equivalent to FDG in 1/8 patients, and higher than FDG in 2/8 patients. Two lesions with DOPA>FDG were treated with a combined immunotherapy and were false negative on the FDG scans. These lesions demonstrated an FDG-uptake of 2.45 and 1.94 SUV in comparison to 2.47 SUV for the normal liver parenchyma. The DOPA-uptake was 2.85 and 4.96 SUV for the lesions accordingly and 1.95 in the liver. A comparison of the transport constants for the O-15-water and the F-18-DOPA showed no statistically significant correlation between these parameters. Therefore, the DOPA-uptake is not perfusion dependent. The lesion dependent sensitivity was 77 % for each of the tracers and 82 % for both radiopharmaceuticals.

These preliminary results demonstrate, that F-18-DOPA is a promising tracer for the diagnosis of malignant melanomas and can help to optimize the differential diagnostics and therapy management in patients with treated metastases.

OS-466

P. Heiss, S. Mayer, H.-J. Wester, M. Herz, G. Stöcklin, M. Schwaiger, R. Senekowitsch-Schmidtko
Nuklearmedizinische Klinik der Technischen Universität München, , Munich, Germany

L-[F-18] FLUOROETHYLTYROSIN (FET) SHOWS A HIGH AND RAPID UPTAKE IN SW707 TUMOR TISSUE.

It has recently been shown that [F-18]FET seems to be a promising F-18-labeled amino acid derivative for tumor imaging (Wester et al., JNM 1997;38: 175). The aim of the present study was to further investigate the transport mechanism and uptake kinetic of L-[F-18]FET into human colon carcinoma cells SW707 in vivo and in vitro. SW707 cells were seeded in 24-well plates for two days. The cells were incubated with 185 MBq/ml [F-18]FET for 0, 1, 2, 4, 6, 10, 20, and 30 minutes at 37°C. After washing the samples three times with ice-cold PBS, the pellets were dissolved in 0.1 N NaOH plus 2% Triton X and counted in a γ -counter. To characterize the transport system of FET uptake, the incubation was performed by adding the specific transport inhibitors BCH and MeAIB plus serine. In addition mice xenotransplanted with SW707 tumors were injected i.v. with 37 MBq [F-18]FET with and without unlabeled FET or tyrosine. The animals were sacrificed by cervical dislocation at 10, 30, 60, and 120 minutes p.i., and the radioactivity in various organs was measured using a γ -counter. The uptake was expressed as % injected dose per gram tissue (%ID/g) \pm SD (n=6). The data of the biodistribution experiments demonstrated a high uptake of L-[F-18]FET into the tumor (at 30 and 60 minutes 6.42 \pm 1.35% and 6.34 \pm 1.70% ID/g). Only the pancreas had a higher uptake (18.9% ID/g at 30 and 60 minutes). The calculation of the tumor-plasma-ratio showed a linear increase up to 30 minutes followed by a plateau with a value > 2. Coinjection with unlabeled L-FET or L-tyrosine resulted in a reduction of [F-18]FET uptake into the tumor tissue. The transport inhibition experiments revealed that the uptake of [F-18]FET into the cells occurred mainly by the amino acid transport system L, similarly to the uptake of tyrosine. The in vitro kinetics showed a fast tracer uptake up to 6 minutes followed by a plateau with a substantial intracellular accumulation of the tracer. From these results the utility of L-[F-18]FET for imaging of brain and solid tumors in clinical studies can be expected

Supported by Deutsche Krebshilfe e.V., Dr. Mildred Scheel Stiftung.

OS-467

P. Willkomm, H Bender, P Decker*, E Ladwein*, J Bogatzky, J Ruhlmann**, F Grünwald, HJ Biersack. Departments of Nuclear Medicine and Surgery*, PET-Center Bonn**, University of Bonn, Germany

Comparative Efficacy of FDG-PET and Immunoscintigraphy with Tc 99m-labelled anti-body fragments for Detecting the Recurrence of Colorectal Carcinoma

Purpose: Multiple imaging methods are used in routine follow-up to detect the presence, location und extent of colorectal recurrence during follow up. But these procedures have only limited diagnostic reliability. FDG-PET and immunoscintigraphy with Tc -99m labelled anti-CEA antigen-binding fragments have both been shown to be suitable. The current study evaluates the efficacy of a new monoclonal antibody-based imaging agent, which comprises an anti-carcinoembryonic antigen monoclonal antibody FAB' fragment labeled directly with technetium-99m (CEAscan, Immunomedics, Mallinckrodt) and FDG-PET.

Methods: Twenty-five patients previously treated for colorectal carcinoma were examined by PET and immunoscintigraphy. The most common indications were elevation of serum CEA (17 cases) and CT lesions (9 cases). All patients had an i.v. administration of the anti-CEA- specific monoclonal antibody Fab-fragment labeled with 20 mCi Tc 99m. Planar and SPECT imaging was performed 6 hours after iv injection. FDG-PET imaging was performed 45 min after intravenous injection of 150-300 MBq FDG. Emission and transmission scans (Siemens, ECAT EXACT) were obtained sequentially using 5-6 bed positions (10 min for each bed position). Imaging with conventional diagnostic modalities was also performed and findings were confirmed by surgery and histology.

Results: N=8 local recurrences were correctly identified by PET and CEA-scan, while liver metastases were confirmed correctly in 9 patients by PET but only n=1 by CEA-scan. N=2 lymph node metastases were correctly identified by PET, none by CEA-scan. Bone metastases were identified in 1 case by PET but not with CEA-scan, whereas bonemarrow infiltration (n=1) was diagnosed by both imaging modalities.

Conclusion: The results indicate that PET as well as CEA-scan are suitable in diagnosing colorectal recurrence. PET is clearly superior in diagnosing liver or lung metastases and lymph node involvement.

OS-468

E.U. Nitzsche, S. Hoegerle, M.J. Reinhardt, I. Brink, A. Otte, T. Krause

Division of Nuclear Medicine, University of Freiburg, Germany

F-18 DOPA PET FOR THE DETECTION AND LOCALIZATION OF INSULINOMA: IS IT FEASIBLE AND REPRODUCIBLE?

Purpose: Insulinoma is overall a rare but the most common of all endocrine pancreatic tumors. The general diagnostic management involves endo-ultrasound, CT and/or MRI imaging, somatostatin receptor imaging or more invasively percutaneous transhepatic portal vein catheterization for selective measurements of insulin levels. In 30% of all cases the insulinoma is less than 1 cm in diameter. Because of that small size its preoperative localization is uncertain or impossible. This prospective study was undertaken to answer the following questions: Does F-18 DOPA PET permit proper detection/localization of suspected small insulinoma. Is it a reproducible approach?

Methods: 4 patients (54 \pm 10 years) underwent abdominal dynamic PET imaging for a period of two hours following i.v. injection of 200 \pm 20 MBq F-18 DOPA. To test the reproducibility, two patients underwent a repeat DOPA PET study 6 months later. Patients presenting with the following criteria were enrolled: positive Whipple triad, positive fasting test, negative noninvasive and invasive diagnostic imaging results. DOPA PET results were judged on the basis of the histological result. For quality control reasons, striatal D2 receptor binding was documented by brain PET after the abdominal study was completed. PET analysis was performed by two blinded investigators. Fusion of CT and PET images was available but not mandatory. **Results:** Four suspected insulinomas were diagnosed as a hot focal lesion in the head of the pancreas 120 minutes after injection. Three patients underwent surgery. Insulinoma localization was predicted by PET correctly in these cases. Histology confirmed the correct diagnosis. One patient denied surgery. He underwent medical therapy and is free of symptoms. F-18 DOPA PET of the abdomen is reproducible. Brain PET revealed unremarkable striatal findings in all patients. **Conclusion:** F-18 DOPA PET appears as a reproducible promising approach to detect small size insulinoma, if the diagnostic localization remains otherwise impossible.

General nuclear medicine: Gastroenterology

OS-469

M. Charron, F. del Rosario, S. Kocoshis

University of Pittsburgh, Children's Hospital of Pittsburgh, Departments of Nuclear Medicine and Gastroenterology

3D IMAGING OF INFLAMMATORY BOWEL DISEASE WITH WBC-Tc99m

Purpose: We evaluated the accuracy of three dimensional (3D) imaging of White Blood Cell labeled with Technetium 99m (WBC-Tc99m) compared to planar imaging in patients with inflammatory bowel disease (IBD).

Methods: Of the 215 patients evaluated with WBC-Tc99m, there were 80 Crohn's disease, 34 ulcerative colitis, 31 controls, 18 indeterminate colitis, and 52 patients who had nonspecific gastrointestinal (GI) complaints. In addition to planar images, 3D imaging (reprojected SPECT images in cine mode; volume rendered) were also performed on 97 of these patients. Biopsy results were available in 137 patients.

Results: When the WBC-Tc99m findings were compared to the biopsies, there were 9 false negative and 3 false positive studies; the sensitivity was 93% and specificity 98%. 3D imaging detected additional abnormal bowel segments in 8 patients who had normal planar findings. Localization of uptake was easier with 3D in 37 patients (especially separation of rectum from the bladder). Limitations included GI bleed, gastritis and anastomosis sites.

Conclusion: 3D imaging with WBC-Tc99m is accurate in evaluating inflammatory bowel disease. Identification and localization of bowel segments is substantially better with SPECT, however the gain in sensitivity is modest.

OS-470

M. Papós¹, T. Molnár², L. Kardos³, F. Nagy², E. Ambrus¹, Cs. Gyulai³, J. Láng¹, A. Palkó³, J. Lonovics², L. Pávics¹

A. Szent-Györgyi Med. Univ., Depts. of Nuclear Medicine¹, Medicine², Radiology³ Szeged, Hungary

HMPAO-leukocyte scintigraphy and computed tomography in Crohn's disease

The diagnostic value of HMPAO-leukocyte scintigraphy (LS) and of computed tomography (CT) was investigated in 16 clinically active Crohn's disease patients. The segmental extent (small intestine, ascending, transverse and descending colon and recto-sigmoidum) of the inflammation was determined by means of LS and CT and was compared with the endoscopic finding. The segmental activity of the process was scored by both methods. Activity indices (LA and CA) were calculated via summing of the segment scores, and compared with the clinical chemical parameters of the inflammation.

Both LS and CT revealed active Crohn's disease in 14, but different cases (sensitivity of 88%). For the segmental extent of the inflammation, the sensitivity and specificity of LS 75% and 84%. CT revealed a sensitivity of 51% and a specificity of 62%. Additionally, 3 abdominal abscesses were verified by surgery. All of these lesions were detected by CT, whereas LS was positive for only one of them. Statistically significant correlation were found between the segmental endoscopy scores and LS scores ($r=0.55$, $p<0.0001$), between the endoscopy scores and CT scores ($r=0.33$, $r<0.005$), between LA and the CRP level ($r=0.61$, $p<0.05$), between LA and the fibrinogen level ($r=0.59$, $p<0.05$) and between CA and the fibrinogen level ($r=0.55$, $p<0.05$).

Conclusions:

1. CT is neither sensitive nor specific enough for visualization of the extent of the inflammation.
2. The value of LS is higher than that of CT in the determination of the activity of Crohn's disease.
3. CT is superior to LS only in cases where there is a suspicion of abdominal abscess.

OS-471

J.C. Alonso, Soriano, C. Rubio*, J.L. Cuadra*, M. Zarca, A.G. Vicente, P. Guerra**, C. Molino
Nuclear Medicine Unit, Department of Rheumatology*, Clinical Research Unit **
C. Hospitalario de Ciudad Real, Plaza de Pio XII s/n 13002 Ciudad Real, Spain.

SERONEGATIVE SPONDYLARTHROPATHIES AND GUT

The factors that contribute to development of seronegative spondylarthropathies (SSp) are not completely known. Gut inflammation is frequent among patients with SSp, as demotrated by colonoscopy and histological examination of biopsy samples. The aim of this study was to evaluate the presence of positive abdominal scintigraphy in patients with SSp and without clinical symptoms or signs of inflammatory bowel disease (IBD) **Materials and methods:** A total of 86 patients were prospectively studied by technetium-99m hexamethylpropylene amine oxime (99mTc-HMPAO)- labeled leukocyte scintigraphy. 59 fulfilling the European Spondylarthropathy Study Group 1991 criteria, 23 ankylosing spondylitis, 7 psoriatic arthritis, 9 reactive arthritis and 20 undifferentiated SSp. 37 of them were men (62.71%), average age was 37.2±16.3. A total of 27 individuals without SSp, taking non-steroidal anti-inflammatory drugs, were used as control group, 11 Rheumatoid arthritis, 16 chronic low back pain, 3 lumbar disk herniation and one juvenile chronic arthritis. **Leukocyte labeling:** In vitro leukocyte labeling was achieved according to the method of Vorne et al with some modifications. **Imaging and interpretation:** Images were obtained in the anterior abdominal projection at 30 min and 2 hour after the injection of labeled leukocytes. The tracer uptake was scored in the whole series of images from 1 (lowest uptake) to 4. **Result:** The scan was positive in 33 patients with SSp (55.93%), 27 of them scored from 2 to 4 (50.94%). Four were positive in the control group (14.80%), 1 higher than 2 (4.17%). $\chi^2=12.78$, $p=0.00035$. Odds Ratio = 7.3. Interval of trust (95%) 2.24-23.74. Patients with scored from 2 to 4 the relationship was $\chi^2=13.07$, $p=0.0003$. Odds Ratio = 21.94. Interval of trust (95%) 2.79-172.46. **Conclusion:** These findings provide a evidence, as our previous studies, linking SSp with intestinal inflammation and suggest that in some cases a bowel - related process could contribute to the development of SSp.

OS-472

L. Sarikaya, A. Bektas*, E. Ibis, M.H. Yasa*, N. Ormeci*, G. Aras

Departments of Nuclear Medicine and Gastroenterology*, Ankara University Hospital, Ankara, TURKEY.

Tc-99m DEXTRAN AND Tc-99m HIG FINDINGS IN PATIENTS WITH ULCERATIVE COLITIS

In this study, Tc-99m Dextran and Tc-99m HIG have been studied in patients with ulcerative colitis (UC) for the evaluation of disease activity and extent. Twelve patients with active UC, 5 with remission and 5 healthy subjects were included in the study. All patients were evaluated by endoscopy. Disease activity were graded by endoscopy. Tc-99m Dextran and Tc-99m HIG studies were performed in two separate days. After the injection of both agents, static anterior images of the abdomen were acquired during the 6 hours with 1 hour interval. Images were evaluated by visually and scintigraphic grading were performed according to the uptake of both agents in the pathologic region and background.

Disease activity was detected in 83% of patients with active UC by Tc-99m HIG and 91% by Tc-99m Dextran. 58 colon segments were found active by endoscopy, 39 by Tc-99m Dextran and 31 by Tc-99m HIG. No intestinal activity was detected in control subjects. Grade 1 activity localization in the large bowel was detected in 3 patients with remissive UC by Tc-99m Dextran and 1 patients by Tc-99m HIG.

As a result, we found that Tc-99m Dextran is more sensitive for detection of disease activity and extent than Tc-99m HIG.

OS-473

Tutus A., Güven K., Yolcu T., Gürsoy S. and Kibar M.
Erciyes University, School of Medicine, Depts of Nuclear Medicine and Internal Medicine, Kayseri, Turkey.

ABNORMAL TC-99m DTPA AEROSOL SCINTIGRAPHY IN PATIENTS WITH ULCERATIVE COLITIS

Inflammatory bowel disease (IBD) only occasionally affects the lung. Abnormal pulmonary functions were reported in ulcerative colitis. This study was designed to determine the pulmonary clearance rate of Tc-99m-DTPA in asymptomatic patients with ulcerative colitis and the role of Tc-99m-DTPA aerosol scintigraphy in the early detection of the lung involvement. Twenty patients with ulcerative colitis (43.50±3.50 years), no clinical pulmonary symptoms, and normal chest radiograms were studied. As a control group, 10 healthy non-smokers (44.80 ± 9.71 years) were studied. Aerosol scintigraphy was performed in all patients and controls. On the basis of the scintigrams the percentage decline in activity per minute (Kep) was evaluated, which represented an accurate parameter of lung membrane permeability. The Kep values of healthy controls (0.719±0.133) were significantly lower than patients with ulcerative colitis (1.050±0.150, p<0.05). These values showed that even in patients with asymptomatic ulcerative colitis, abnormal Tc-99m-DTPA clearance may be frequently occurred. We think that Tc-99m-DTPA aerosol scintigraphy may allow early detection of subclinical pulmonary involvement in patients with ulcerative colitis.

OS-474

J. Naumovski, N. Simova, G. Pilovski, E. Kovkarova

Clinic Center, Clinic of Toxicology and Urgent Internal Medicine, Skopje, Macedonia

RADIOLABELED SUCRALFATE SCINTIGRAPHY IN INVESTIGATION OF CAUSTIC INJURIES

Clinical evaluation of caustic burns of the upper gastrointestinal tract (UGI) meets many difficulties with routine methods as fiberoendoscopy and roentgenography with a contrast swallow. The first is invasive with a risk of perforation and the second needs active patients collaboration. A study that included 27 patients was done in order to evaluate a noninvasive method suitable for seriously ill patients after ingestion of a caustic. The scan with per orally applied Tc-99m-DTPA labeled Sucralfate was performed under a gamma-camera. Scans and roentgenology findings were compared to the endoscopic results (as a objective superior method). Sensitivity (Sn), Specificity (Sp) and Accuracy (Ac) were calculated for topographic parts of the esophagus, stomach and duodenum, separately for each organ and whole UGI. The results showed Sn-91.5%, Sp 85.5%, Ac-85.7% for the radiolabeled Sucralfate scans and roentgenology contrast investigation revealed a Sn-40%, Sp-93% and Ac-79% in detection of mucosal lesions of the UGI. The statistical analysis approves the choice of scintigraphy in detection of caustic injuries (p=0.001, C2=0.49). These results in detecting mucosal lesions, non-invasivity and easy performance, recommend this scintigraphy technique as a valid supplemental method in investigation of UGI after a caustic ingestion. Combination of the three methods performed in adequate periods gives best visualization of the condition of UGI lesions.

Endocrinology/Thyroid

OS-475

O. Lang^{1,2}, C. Elbe¹, M.-L. Sautter-Bihl¹, H. Bihl²

Dept. of Radiooncology, Staedisches Klinikum Karlsruhe, Germany¹,
Dept. of Nuclear Medicine, Katharinenhospital Stuttgart, Germany²

PRE-OPERATIVE DIAGNOSIS OF THE PARATHYROID GLAND WITH DOUBLE-PHASE TC-99m SESTAMIBI SCINTIGRAPHY. ENHANCED SENSITIVITY WITH SPECT WITH A TRIPLE-HEAD CAMERA?

Background: Double-phase Tc-99m sestamibi scintigraphy is established in the pre-operative localization of parathyroid adenomas - especially in case of secondary surgery. The clinical value of this method, however, is based on relatively small patient collectives.

Purpose: Evaluation of double-phase Tc-99m sestamibi scintigraphy in the pre-operative localization of parathyroid adenomas in case of suspicion of primary hyperparathyroidism (pHPT), with special emphasis on the value of SPECT with a triple-head camera.

Methods: 113 patients (female: 69, male: 44) with suspicion of pHPT were examined pre-operatively with double-phase Tc-99m sestamibi scintigraphy. The scintigraphic results were all verified by surgery (extensive exploration of the thyroid bed) and histology. 10 min. and 2 h after injection of 555 MBq Tc-99m sestamibi planar images of head/neck/mediastinum were obtained. Subsequently SPECT was performed with a triple-head camera.

Results: Planar scintigraphy was able to identify 67/113 (59%) of the parathyroid adenomas, with 5 cases located in the mediastinum. With SPECT this result mounted to a total of 98/113 (87%), including 1 additional mediastinal adenoma previously not seen in the planar images.

Conclusion: Double-phase Tc-99m sestamibi scintigraphy - especially in combination with SPECT with a triple-head camera - is a powerful tool for the localization of parathyroid adenomas (sensitivity: 87% versus 59% in planar technique). It has to be stated, however, that experienced surgeons will do primary surgery of pHPT mostly without pre-operative imaging; this may change in case of secondary surgery, where sometimes a more conservative surgical strategy is necessary (Nervus recurrens!).

OS-476

C. Billotey, E. Sarfati, S. Fritsch, P. Cattani, C. Peker, J-D Rain.

Hospital Saint-Louis : Departments of General Surgery and of Nuclear Medicine, Paris, France.

MEDIASTINAL PARATHYROID GLAND'S DETECTION BY A MONOISOTOPIC SCINTIGRAPHY USING MIBI-Tc99m AND SPECT PERFORMED WITH EXTERNAL RADIOMARKERS.

Aim: Evaluate the sensitivity of a monoisotopic parathyroid scintigraphy (PS) using MIBI-Tc99m and SPECT performed with external radiomarkers to detect enlarged parathyroid glands in the mediastinum.

Patients and method: 20 patients (pts) suffering from hyperparathyroidism (HPT) [primary HPT for 10 pts, including 4 with hyperplastic HPT; secondary HPT for 10 pts] have had surgical removed mediastinal glands (MG). 1 MG/patient has been removed in 16 patients, 2 MG/pt in 3 patients, and 3 MG/pt in 1 patient. 21 SP were performed before 21 operations including 19 reoperations (4 performed only 1 to 3 days after a previous unsuccessful operation).

15-20 mCi of MIBI-Tc99m was injected. Dynamic acquisition (25 to 30 one-min images - matrix 128x128) performed with a pin-hole centered of the thyroid uptake area and lateral views of neck (600 kcts - matrix 128x128) allowed to detect cervical glands. Abnormal mediastinal uptake were demonstrated on planar views of thorax (800 to 1000 kcts - matrix 128x128) or on tomographic slices (360°-64 steps- 35 sec- matrice 64x64 to 128x128- filtered backprojection reconstruction with Wiener filter) performed with radiomarkers of Ba133 (2) placed on the sternum +/- 1 on clavicle (dual-isotope acquisition - two-slice superposition of tomographic slice by immunoscintigraphy software).

Results: 23 / 25 MG found by surgeon were demonstrated by SP, including 6/6 adenomas and 17/19 hyperplastic glands. In 1 pt, the 2nd MG was demonstrated only after the removal of 1st MG by cervicotomy because of both uptakes were superposed on 1st PS. The 3 MG placed in the middle mediastinum were correctly identified by PS. Minimal weight of detected MG was 125mg in the anterior mediastinum and 675mg in the middle mediastinum. Both no detected MG were removed in the same patient and weighed only 258mg.

Conclusion: A monoisotopic PS using MIBI-Tc99m and SPECT allowed to demonstrate MG with a high sensitivity (92 %), even if hyperplastic, posterior and small glands. The location of enlarged glands was more precisely defined by activity superposition of radiomarkers. Accurate location increased success rate of surgery.

OS-477

C. Marí, Ll. Bernà, E. Urgell, X. Rius, A. Flotats, JC. Martín, M. Estorch, A. Catafau, I. Carrió.
Hospital Sant Pau, Barcelona. Spain. Department of Nuclear Medicine

99mTc-SESTAMIBI SCINTIGRAPHY AND INTRAOPERATIVE MEASUREMENT OF PTH IN HYPERPARATHYROIDISM

Purpose: To assess the utility of double phase 99mTc-sestamibi (MIBI) scintigraphy and intraoperative quick parathyroid hormone measurement in ensuring excision of all parathyroid hyperfunctioning tissue.

Methods: 13 patients with hyperparathyroid disease were studied: eleven with primary hyperparathyroidism, one with tertiary hyperparathyroidism and one with MEN I. Mean PTH 44.88±47.38 pmol/L (nl: 1.5-6.7), mean calcium 2.84±0.25 mmol/L (nl: 2.14-2.54) and mean phosphate 0.83±0.27 mmol/L (nl: 0.85-1.33). MIBI scintigraphy was performed on all 13 patients before surgery. Intraoperative quick parathyroid hormone measurement was performed preincision, postmanipulation and postextirpation of hyperfunctioning parathyroid tissue. Exitous surgery was considered when postextirpation PTH was half or less than half of preincision PTH.

Results: MIBI scintigraphy localized 14 hyperfunctioning glands (one patient had two abnormal glands), one of them in the mediastinum. Surgery removed the 14 MIBI scintigraphy localized glands, all of them being histologically confirmed as abnormal during surgery. Eleven patients showed a decrease in preincision PTH >50%, one of 45.5% and the other of 47.7%. Mean preincision PTH was 33.48±23.62 pmol/L, postmanipulation PTH 27.36±17.20 pmol/L and five min. postextirpation PTH 7.05±4.68 pmol/L. At this moment, all patients are free of hyperparathyroid disease (maximum follow-up 10 months).

Conclusion: The combination of preoperative parathyroid MIBI scintigraphy localization and intraoperative quick parathyroid hormone measurement ensures excision of all parathyroid hyperfunctioning tissue in patients with hyperparathyroidism.

OS-478

A. Vignati, L. Mazzucchelli, L. Pedrazzini, G. Lomuscio, M.E. Dottorini, L. Colombo

Medicina Nucleare Ospedale di Busto Arsizio - Italy

99mTc-MIBI PARATHYROID IMAGING: COMPARISON AMONG FOUR METHODS.

99mTc-MIBI is used in parathyroid imaging both alone (double phase study) and combined with 99mTc-pertechnetate (PERT). The aim of this study was to compare the diagnostic value of four subtraction images obtained from MIBI and PERT images acquired at different times. We studied 35 pts with hyperparathyroidism (HPT): 20 with primary HPT (56.7±16.4 yr, 4 males) and 15 with secondary HPT (56.7±11.5 yr, 6 males).

Ten minutes after the injection of 74 MBq of PERT a cervico-thoracic image was recorded (P1). Then 740 MBq of MIBI were given and the early MIBI image (M1) was acquired after ten minutes. Two hours later, after repositioning the patient, the delayed MIBI image was obtained (M2). Ten minutes after another injection of PERT (180 MBq) the last image was recorded (P2).

The four images were aligned and interpolative background subtraction was applied. A step-by-step subtraction technique was used to obtain M1-a-P1, M2-b-P1, M2-c-M1 and M2-d-P2 where a..d are subtrahend coefficients. As P1 activity is negligible in comparison with MIBI activity, it affects neither M1 nor M2 images. M2-d-P2 is equivalent to M2-b-P1. In fact P2 is the sum of M2 and a PERT image and k(P2-M2)=b-P1. Then: M2-b-P1= M2-k(P2-M2)=(k+1)M2-k-P2=(k+1)(M2-k-P2/(k+1))=(k+1)(M2-d-P2) with d=k/(k+1). M2-b-P1 identified the largest number of regions of increased focal uptake of MIBI (41, 5 ectopic). When compared with these findings, M1-a-P1 M2-c-M1 and M2-d-P2 allowed correct localization of 39/41 (95%), 21/41 (51%) and 37/41 (90%) abnormal regions, respectively. Agreement in localization becomes 95, 37 and 95% if primary HPT are considered; 95, 63 and 86% if secondary HPT are considered.

In conclusion the detectability of areas suspected for parathyroid abnormal glands is not significantly different when subtraction techniques are applied between the early or delayed MIBI image and the PERT image (recorded before or after MIBI image), while double-phase MIBI procedure seems less sensitive. If PERT injection and image precede the early MIBI image (M1-a-P1) or follow the delayed MIBI image (M2-d-P2) time is saved (only 30 minutes) and patient repositioning is avoided.

OS-479

H.J. Gallowitsch, P. Mikosch, E. Kresnik, I. Gomez, P. Lind

Department of Nuclear Medicine and Special Endocrinology, Landeskrankenhaus Klagenfurt, Austria

99mTc tetrafosmin parathyroid imaging: Results with double-phase study and SPECT in primary and secondary hyperparathyroidism

The aim of our study was to evaluate the sensitivity, specificity and positive predictive value (PPV) of 99mTc tetrafosmin double-phase scintigraphy and SPECT in preoperative localization of parathyroid adenoma in case of primary and secondary hyperparathyroidism (HPT). Sixty-eight consecutive patients, biochemically or sonographically suspected of parathyroid adenoma were included in our study. Apart from biochemical analysis of serum calcium, phosphate and intact PTH, double-phase scintigraphy was performed in each patient 5 and 45 min. after injection of 370 MBq 99mTc tetrafosmin, followed by SPECT imaging. In consciousness of the scintigraphic results, ultrasound of the neck was performed as well to exclude false positive results due to thyroid adenomas. Depending on the results of the biochemical analysis in combination with the results of the scintigraphic and ultrasound examination, the patients were classified retrospectively into three groups: Group A with primary HPT (n=35), group B with secondary HPT (n=13) and group C without any biochemical suspicion of primary or secondary HPT (n=20). In group A, double-phase study localized 25/36 (69.2%) parathyroid adenomas (one double adenoma) as against 34/36 (94.4%) with SPECT. Nine adenomas could only be visualized by SPECT. The reason for non-visualization on planar scans was suspected to be an ectopic location in two cases (retrotracheal dislocation, retrovascular dislocation), a maximal diameter less than 15 mm (9 - 13 mm) in 6 cases, and oxyphilic-cell-poor cellularity in one case. Four false positive retentions (3 thyroid adenomas, 1 papillary thyroid carcinoma) were observed. SPECT showed a sensitivity of 94.4 %, a specificity of 85 % and a PPV of 91.9% in biochemically suspected primary HPT. In Group B, planar scintigraphy demonstrated 12 hyperplastic glands in 5 out of 13 patients scintigraphy and SPECT 20 hyperplastic parathyroid glands in 8 out of 13 patients, which corresponds to a sensitivity of 38 and 61.5 %, resp. 99mTc tetrafosmin seems to be a promising alternative tracer with similar capabilities to 99mTc sestamibi in localization of parathyroid adenoma. SPECT showed clear advantages in terms of sensitivity over planar scintigraphy and should be used at least in cases with poor or no uptake in double-phase study. In endemic goiter areas, ultrasound of the neck should be performed to exclude false positive retention in thyroid adenomas. 99mTc tetrafosmin, like 99mTc sestamibi, is not ideal for localization of hyperplastic glands in secondary hyperparathyroidism because of low sensitivity.

OS-480

A. Giordano (1), G. Meduri (1), G. Rubini (2), G. Di Giovine (2), P. Marozzi (3), A. Pagano (3), M. Cappagli (4), A. Montepagani (4).

Nuclear Medicine Depts of (1) Rome Catholic University, (2) Bari University, (3) Palermo Hospital and University, (4) La Spezia Hospital, Italy.

ITALIAN MULTICENTER STUDY ON 99mTc-TETROFOSMIN AND 99mTc-SESTAMIBI IN PARATHYROID SCINTIGRAPHY (PS): RESULTS IN 133 SUBJECTS.

In order to compare 99mTc-Tetrofosmin (TETR) and 99mTc- Sestamibi (MIBI) in PS, we carried out two studies: one in 62 pts with hyperparathyroidism (STUDY 1), and the other in 71 control subjects (STUDY 2). STUDY 1: 28 pts with primary and 34 with secondary hyperparathyroidism (HPT), underwent 99mTcO4- (37 MBq), TETR (370-740 MBq) and MIBI (370-740 MBq) scans in different days. Image evaluation was accomplished both by 99mTcO4- Subtraction technique (SUBTR) and by Dual-Phase technique (DP). Parathyroid uptake was evaluated by computing the parathyroid/thyroid ratio in 75 glands (all surgically confirmed).

	PRIMARY HPT (28 pts)		SECOND. HPT (34 pts)	
	TETR	MIBI	TETR	MIBI
SENSIT. SUBTR	93%	93%	82%	82%
SENSIT. DP	56%	88%	46%	60%

MIBI parath./thyr. ratio was 1.18±0.2 in early images and increased to 1.36±0.1 in delayed images (p<.009); TETR parath./thyr. ratio was 1.16±0.2 in early images and did not significantly change in delayed images: 1.13±0.2 (NS vs. early TETR images; p<.0001 vs. MIBI delayed images). STUDY 2: all subjects did not show any clinical or biochemical evidence of thyroid or parathyroid diseases; they underwent early (5 min) and delayed (2-4 hours) thyroid scintigraphies along with rest myocardial scintigraphy performed for known or suspected coronary artery disease. TETR was randomly injected in 43 pts, MIBI in 28 pts (740 MBq for both tracers). Tracers uptake was quantified as thyroid/Bkg ratio (T/B) and thyroid washout (WO) in % of early counts.

	Early T/B	Delay T/B	WO Tir
TETR	1.72 ± 0.3	1.45 ± 0.2	67 ± 11
MIBI	1.95 ± 0.3	1.34 ± 0.2	77 ± 12
P Value	0.006	0.026	0.0001

In conclusion: 1) both tracers showed identical high sensitivity using SUBTR; 2) DP was less valuable than SUBTR with MIBI and not acceptable with TETR; 3) thyroid early uptake of MIBI was higher than that of TETR (MIBI>TETR) while at 2-4 hours the opposite was found (MIBI<TETR); 4) TETR thyroid washout was significantly slower than that of MIBI; 5) our data show that failures of DP scintigraphy with TETR are due to the persistent thyroid retention of the tracer.

Radiopharmacy and radiochemistry: Peptides

OS-481

P.A. Schubiger, R. Alberto, A. Egli, L. Allemann-Tannahill, D. Tourwé*

Center for Radiopharmaceutical Science of ETH, PSI and USZ, CH-5232 Villigen PSI; *Faculteit Wetenschappen, Vrije Universiteit Brussel, Brussels

***Me(I)-CARBONYL COMPLEXES FOR HIGH SPECIFIC ACTIVITY LABELLING OF NEUROPEPTIDES (*Me = 99mTc, 186Re, 188Re)**

A direct and efficient method for the labelling of neuropeptides with *Me(I) (*Me= 99mTc, 186Re, 188Re) has been developed and tested on neurotensin analogues. The organometallic aquaion [**Me*(H₂O)₃(CO)₃]+1 is formed under ambient conditions and histidine is used as ligand. Different neurotensin analogues have been synthesized and labelled.

The labelling of 99mTc-carbonyls by simply adding ligand solutions gives rise to steep sigmoidal curves for each applied ligand representing the minimal concentration where complex formation occurs. The most impressive finding of this study shows histidine forming complexes at concentrations as low as 10⁻⁶ M. All other aminoacid-ligands have to be applied 1000 times more concentrated to obtain the corresponding 99mTc-compounds. Only cysteine is able to bind comparably good with 10 times higher concentrations.

We achieve a very high specific activity of up to 3.7 TBq (100Ci)/μmol histidine-peptide in a radiochemical purity of > 95 %. One 99mTc-neurotensin analogue retained its receptor affinity fully having a K_D-value of 0.25 nM on colon carcinoma HT29 cells. Biodistribution experiments in nude mice showed complete clearance from blood and no retention in the kidneys.

In conclusion, the new peptide labelling approach with *Me(CO)₃ combines highest specific activities with minimal influence on the biological properties of the neuropeptides.

OS-482

A. Heppeler¹, M. Behr¹, E. Jermann¹, S. Froidveaux¹, M. Hennig², I. Virgolini³, H.R. Mäcke¹

Institute of Nuclear Medicine¹, University Hospital Basel and Hoffmann LaRoche², Basel, Switzerland, Departement of Nuclear Medicine, University of Vienna, Austria³

Biodistribution Studies of Four Tumor Targeting Somatostatin Analogues and Correlation to Metal-Coordination Chemistry Aspects

Radiolabeled somatostatin (SRIF) analogues have been used successfully to localize SRIF receptor positive tumors in patients. The In-111 labeled compound OctreoScan® was also introduced for internal radiotherapy due to Auger electron emitting properties. Despite some favorable effects on tumor growth particle emitting isotopes would be more useful. We synthesised four peptides with affinity to the somatostatin receptor and coupled the macrocyclic chelator DOTA to them for stable labeling with hard Lewis acids as the β-emitter Y-90.

Aim: Comparative biodistribution studies of the four somatostatin analogues DOTA-D-Phe¹-Tyr²-octreotide (DOTATOC), DOTA-octreotide (DOTAOCT), DOTA-D-Phe¹-Tyr²-Val³-Trp-NH₂⁴-octreotide (DOTAVAP) and DOTA-D-β-Nal¹-Tyr²-Val³-Thr-NH₂⁴-octreotide (DOTALAN) labeled with Ga-67, In-111 or Y-90 in a tumor bearing mouse model, in vitro binding assays and analysis of the influence of the atomic radii of different radiometals on binding affinity and biodistribution.

Results: All four Y-90 labeled radiopeptides showed high and specific uptake in tumors and SRIF receptor positive organs. In the order of increasing lipophilicity (DOTALAN > DOTAVAP > DOTAOCT > DOTATOC, determined by RP-HPLC), the percentage of unspecific binding increased. The highest specific binding was found for Y-90-DOTATOC. In the same order liver and small intestine activity increased. Labeling with different radionuclides showed higher uptake in receptor positive organs in the order Ga-67 > Y-90 > In-111. This increasing uptake parallels the increase in receptor binding affinity and appears to be caused by the metal coordination sphere. X-ray single crystal structural data of the Ga- and Y-complexes of DOTA-D-Phe-amide, a model peptide conjugate, were used to explain these different properties. With Ga³⁺ DOTA-D-Phe-amide forms a hexacoordinated pseudooctahedral complex with a N₂O₂(carboxy) equatorial and a N₂ axial donor set whereas Y-DOTA-D-Phe-amide shows octacoordination and antiprismatic geometry involving the carbonyl oxygen of the linking amide function in the binding to the metal.

Conclusion: Modification of octapeptides with the essential pharmacophoric aminoacids contained but amino acid exchange otherwise leads to highly specific radioligands with rather different biodistribution with regard to uptake in different organs; also changes in coordination sphere of the radiometal appears to greatly influence tumor uptake and rate of kidney excretion. In a rat brain cortex membrane assay all four peptides labeled with Y-90 and In-111- show high specific binding in the nanomolar range.

OS-483

Marion de Jong, Wout Breeman, Bert Bernard, Arthur van Gameren, Willem Bakker, Leo Hofland, Theo Visser, Ananth Srinivasan, Michelle Schmidt, Joseph Bugaj, Jack Erion, Helmut Mäcke, Eric Krenning. Depts of Nucl Med and Intern Med III, Univ. Hospital Dijkzigt, Rotterdam, The Netherlands; Mallinkrodt Medical, St. Louis, USA; Kantonspital Basel, Basel, Switzerland.

COMPARISON OF In-111-LABELLED SOMATOSTATIN-ANALOGUES.

We evaluated the potential of In-111-labeled somatostatin analogues: [DTPA]octreotide (DTPAOC; "OctreoScan"), [DTPA,Tyr-3]octreotide (DTPAT3OC), [DTPA,Tyr-3]octreotate (DTPAT3TATE; Thr(ol) in octreotide replaced by Thr), [DOTA,Tyr-3]octreotide (DOTAT3OC) and [DOTA]lanreotide (DOTALAN; "Mauritius") as radiopharmaceuticals for in vivo detection and peptide-receptor-radionuclide-therapy (PRRT) of somatostatin receptor-positive tumors. In vitro receptor binding, internalization and rat in vivo metabolism was investigated. **Results:** All unlabeled compounds showed high and specific binding to somatostatin receptors in rat cerebral cortex microsomes in vitro, IC₅₀-values were in the nanomolar range. In vivo: specific uptake (%ID/g) of DTPAT3TATE in the octreotide receptor-expressing tissues (pancreas, pituitary, adrenals) and tumor (CA20948) was the highest of the compounds tested, while for DTPAOC and DOTALAN the lowest values were found (see Table: data %ID/g, 4 and 24 h p.i., mean, n≥4), in accordance with findings of in vitro internalization studies (not shown). a) P<0.01 vs. In-111-DTPAOC.

Table:	DTPAOC	DTPAT3OC	DOTAT3OC	DTPAT3TATE	DOTALAN
	4 h - 24 h	4 h - 24 h	4 h - 24 h	4 h - 24 h	4 - 24 h
Blood	.005 - .003	.006 - .003	.006 - .002	.007 - .003	.014a-.008a
Pancreas	0.99 - 0.69	3.51a-2.40a	2.57a-1.70a	11.2a-4.66a	0.89-0.59
Adrenals	1.69 - 1.33	6.53a-5.83a	3.62a-3.19a	13.15a-9.57a	1.76-1.50
Pituitary	0.53 - 0.51	2.10a-1.65a	1.48a-1.22a	2.40a-2.38a	0.34a-0.30a
Tumor	0.79 - 0.58	0.94a-0.96a	1.15a-1.12a	4.22a-1.20a	0.62-0.47

Uptake of all In-111-labeled peptides in pituitary, pancreas, adrenals and tumor was blocked by 0.5 mg unlabeled octreotide, indicating specific binding to octreotide receptors. High kidney uptake of radioactivity could be reduced by a single iv injection with 400 mg/kg D-lysine. **Conclusion:** In-111-labeled DTPAT3OC and DTPAT3TATE, and their DOTA-coupled counterparts, are very promising for scintigraphy and/or PRRT of human tumors. 3) Radiolabeled DOTALAN, recently introduced for PRRT, is less promising for this purpose.

OS-484

Marion de Jong, Eric Krenning, Bert Bernard, Arthur van Gameren, Wout Breeman, Willem Bakker, Theo Visser, Ananth Srinivasan, Michelle Schmidt, Jack Erion, Jean-Claude Reubi. Depts of Nucl Med and Intern Med III, Univ. Hosp. Dijkzigt, Rotterdam, The Netherlands; Mallinkrodt Medical, St. Louis, USA; Dept of Pathol, University of Bern, Switzerland.

In-111-DOTA-CCK, INTERNALIZATION AND BIODISTRIBUTION.

Cholecystokinin (CCK) is a peptide with many functions in the GI tract, mediated through CCK-B/gastrin and CCK-A receptors. CCK-B/gastrin receptors are abundant in medullary thyroid carcinoma, small cell lung cancer and stromal ovarian cancer. Recently, DOTA-CCK-8 (DOTA-D-Asp-Tyr-Nle-Gly-Trp-Nle-Asp-Phe-NH₂) was found to have a high affinity for CCK-B receptors, therefore radiolabeled DOTA-CCK-8 was proposed for tumor scintigraphy and radionuclide therapy. We investigated internalization of In-111-DOTA-CCK in receptor positive AR42J and CA20948 rat pancreatic tumor cell lines and furthermore biodistribution in rats was studied in comparison with non-sulfated I-125-CCK-decapeptide-analogue. Results internalization: our studies demonstrated that In-111-DOTA-CCK-8 was internalized by a receptor-specific, time- and temperature-dependent process (see Table, 60 min incubation, CA20948 cells). Results biodistribution: I-125-CCK was mostly cleared via the liver and bile to the intestines, whereas In-111-DOTA-CCK-8 was cleared more rapidly from the blood via the kidneys and excreted in the urine; the latter situation being much more favorable for our purpose. Receptor specific uptake of In-111-DOTA-CCK-8 was found in the stomach. Uptake in these and other organs studied was very low (see Table), resulting in a very low background radioactivity. Table (data of In-111-DOTA-CCK-8, biodistribution with mentioned peptide mass (3 MBq), 100 μg = blocking peptide dose):

Internalization, % dose/mg protein.	Biodistribution, %ID/g, 24h p.i.				
	37C	4C	0.5 μg	100 μg	
0.1 nM	2.01	0.52	blood	0.0046	0.0043
1 nM	1.73	0.50	kidney	0.21	0.24
10 nM	1.02	0.43	liver	0.016	0.021
1 μM	0.18	0.24	stomach	0.022	0.007

Conclusion: Internalization of In-111-DOTA-CCK-8 in vitro was found to be receptor specific, time- and temperature-dependent. Biodistribution studies in rats showed favorable low background radioactivity.

OS-485

K. Chavatte¹, E. Wong², D. Eshima², J. Thomback², D. Terriere³, J. Mertens³, D. Tourvé⁴ and A. Bossuyt¹.
AZ-VUB-Nuclear Medicine¹, VUB-Cyclotron³, VUB-Organic Chemistry⁴, Brussels-Belgium, Resolution Pharmaceuticals², ON Canada.

SYNTHESIS AND FIRST IN VITRO EVALUATION OF RHENIUM AND TECHNETIUM-99M OXO COMPLEXES OF NEUROTENSIN (8-13).

Radiolabeled neurotensin analogs have application as tumor imaging agents. Non-endocrine pancreas carcinoma, small cell lung carcinoma, human colon carcinoma and human meningiomas express high amounts of neurotensin receptors. DTPA coupled neurotensin(8-13) (N-Arg-Arg-Arg-Pro-Tyr-Ile-Leu-OH) analogs, which can be labeled with In-111, have an affinity for the receptors ($K_i = 3.5$ nM). As a continuation of the development of a neurotensin receptor targeting radiopharmaceutical, this study describes the synthesis and first in vitro evaluation of Re and Tc-99m complexes of neurotensin (NT) analogs with dimethylgly-ser-cys(aceto-amidomethyl)-gly (RP414) as the chelator. This chelator is linked to the N-terminus of the biological active carboxy terminal hexapeptide NT(8-13). Different RP414-NT(8-13) analogs with either Arg or Lys in positions 8 or 9 are synthesized. Room temperature labeling with Tc-99m is performed using stannous gluconate at pH 4.5 on 250 μ g of peptide and 10 mCi of pertechnetate. Labeling yields > 98% are obtained. To prepare the non radioactive Re complex, the acetoamidomethyl group in RP414-NT(8-13) was removed using mercuric acetate and the peptide was then reacted with Re dioxo ethylene diamine. As required, the Re and Tc-99m complexes showed identical retention times on HPLC. Inhibition of the binding of 3H-NT on HT29 colon adenocarcinoma cells yielded K_i values of 1 nM for NT(1-13) and 0.8 nM, 5.5 nM and 4 nM for the Re complexes of RP414-NT(8-13), RP414-Lys-Arg-NT(10-13) and RP414-Lys-Lys-NT(10-13) respectively. Biological stability in human plasma of RP414-NT(8-13) showed biological half-times up to 30 minutes. The results of this study show that RP414 can be used for labeling peptides with Tc-99m and Re without affecting receptor affinity and indicate that RP414-NT(8-13) analogs have potential application in diagnosis and therapy of neurotensin receptor positive tumors.

OS-486

L. Allemann-Tannahill, N. Rémy, P. Bläuenstein, M. Willmann, *D. Tourvé, P. A. Schubiger

Center for Radiopharmaceutical Science, Paul Scherrer Institute Villigen PSI, Switzerland, *Vrije Universiteit, Brussels, Belgium

FIRST STUDIES OF THE CELL BINDING AND THE METABOLISM OF A Tc-99M LABELLED NEUROTENSIN FRAGMENT.

Neurotensin (NT) has been shown to bind to a receptor which is expressed on many tumour cells. Thus it may be a useful vehicle to transport radionuclides for diagnosis or therapy into tumours.

We have selected a fragment of neurotensin (NT8-13), coupled with histidine to give HisNT8-13 (His-Arg-Arg-Pro-Tyr-Ile-Leu) and labelled it with Tc-99m for diagnostic purposes. To provide a therapeutic agent the congeners Re-186 or Re-188 will be used. For labelling the carbonyl method was applied: First the Tc(I)-tricarbonyl complex is prepared which then is bound to the histidine.

Tc-99m-HisNT8-13 was tested on a human colon carcinoma cell line (HT29). It showed a specific binding with a $K_d = 0.64$ nM.

After binding at 4°C the cells were incubated at 37°C. After 5 min about 80% of the cell-bound activity was internalised. Later, the ratio of surface bound and internalised activity remained constant, while these values decreased compared to the total applied activity.

After internalization the cells were lysed in 0.1 M hydrochloric acid with heating for 1.5 min at 100°C. The suspension was centrifuged, the remaining proteins precipitated with 30% ethanol and the supernatant analysed with HPLC (reversed phase RP18, acetonitril/water gradient from 16/86 to 40/60). Three main peaks representing the intact Tc-HisNT8-13 and two not yet identified peptide fragments were found. Pertechnetate, the free Tc-tricarbonyl complex, the Tc-99mHis and Tc-99mHis-Arg were expected metabolites but were absent.

Based on the results of receptor affinity and internalisation we can conclude that neurotensin derivatives can be used as vehicles for a systemic application of radionuclides. Metabolism in cell culture, however, seems to be fast and thus metabolically more stable NT8-13 analogues have to be prepared and tested.

Physics and instrumentation: Registration

OS-487

O. Sipilä, P. Nikkinen, S. Savolainen, K. Liewendahl, E. Gaily, V.-P. Poutanen, H. Pohjonen, M.-L. Granström

Helsinki University Central Hospital, P.O. Box 280, 00029 HUT, Helsinki University of Technology, P. O. Box 2200, 02015 HUT, Finland

TRANSMISSION IMAGING FOR REGISTRATION OF ICTAL AND INTERICTAL SPECT, MRI AND VIDEO-EEG STUDIES

The purpose of this study was to develop a method for registration of ictal and interictal SPECT, MRI and video-EEG studies for improved localization of epileptogenic foci. In registration, the advantages introduced by SPECT transmission imaging were utilized. For SPECT studies, Tc-99m-ECD (950 MBq) was injected intravenously while the patient was monitored on video-EEG to document the ictal or interictal state. Imaging was performed using a triple-head Picker Prism 3000XP gamma camera and a STEP transmission imaging device with a Gd-153 source. The images (128 x 128 pixels, voxel size 3.6 x 3.6 x 3.6 mm³) were reconstructed using an iterative ML-EM algorithm and postfiltered with a Wiener filter. Video-EEG monitoring was performed using Beehive equipment (Telefactor Corp.) with a maximum of 128 digital EEG channels and analog video. Gold plated silver electrodes were glued to the patient's scalp and were also utilized as markers for registration of the ictal and interictal SPECT images, as these metallic markers were clearly seen in the transmission images. Fitting of the marker sets was based on a non-iterative least squares method. The RMS residual of the marker sets was approximately 3 mm after the fitting. Transmission imaging also allowed reconstruction of emission images with accurate attenuation correction. This was important since the patient's scalp was covered with metallic electrodes attenuating emission radiation. Utilization of the electrodes as markers in registration defined the EEG coordinate system in the SPECT images without any further transformations. MR images (Siemens Magnetom Vision, 1.5 T) were obtained before video-EEG monitoring and SPECT imaging without any external markers for registration. Surface fitting methods could be utilized for registration of MR and SPECT images since the surface of the head could be segmented from transmission SPECT images more reliably than the surface of the brain from emission SPECT images. Conclusion: SPECT transmission imaging enabled accurate and easily implemented registration of ictal and interictal SPECT, MRI and video-EEG data.

OS-488

D. Dey, P.J. Slomka*, L.J. Hahn, R. Kloiber.

University of Calgary, and Division of Nuclear Medicine, Foothills Hospital, Calgary, Canada; *London Health Sciences Centre, University of Western Ontario, London, Canada.

ROBUST AUTOMATED MULTOMODALITY REGISTRATION UTILIZING RADIONUCLIDE TRANSMISSION ATTENUATION MAPS.

Co-registration of images from a single subject, acquired by different modalities, is important in clinical diagnosis, surgery, and therapy planning. The purpose of this work was to evaluate a novel, fully automated method for three-dimensional (3-D) image registration of X-ray Computed Tomography (CT) and SPECT, using radionuclide transmission (RNT) attenuation maps.

We obtained CT scans, and SPECT scans paired with RNT maps of an anthropomorphic cardiac phantom. RNT attenuation maps were acquired using an uncollimated Tc-99m-filled flood source. RNT and SPECT scans were acquired in the same spatial orientation (usual clinical practice in non-uniform attenuation correction). In addition, CT attenuation maps (CTMAP) for Tc-99m SPECT were generated from CT by linear energy scaling. RNT maps were registered to CT and CTMAP by iterative simplex minimization of count difference, and uniformity index (sum of RNT map intensity variances corresponding to each intensity level in the CT volume). In each iteration, 3 shifts and 3 angles were adjusted. To register SPECT to CT, we apply the RNT transformation parameters to SPECT.

RNT maps could be registered to CT images using uniformity index criterion and to CTMAP images using both criteria. The average 3-D difference between landmark and automated registration was 2.5 +/- 1.2 mm for count difference and 3.3 +/- 1.3 mm for uniformity index. The 3-D reproducibility errors were 1.2 +/- 0.7 mm for count difference, 2.1 +/- 0.5 mm for uniformity index, and 2.3 +/- 1.0 mm for manual marker registration. The minimization of uniformity index was robust when up to 50% CT or RNT slices were missing, and was not affected significantly (< 2mm) by realistic variation in CT values (+/- 10 Hounsfield units).

In addition to typical use in non-uniform attenuation correction, radionuclide transmission maps can be used for fully automated 3-D registration of SPECT to CT. In contrast with other proposed registration methods, our method is independent of abnormal features or quality of the SPECT images; it also avoids difficulties associated with the use of fiducial markers. Our method can potentially be applied to multimodality registration of various organs such as brain, heart, lungs, breasts and abdomen, including oncological scans and receptor imaging of the brain.

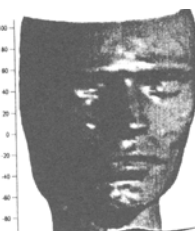
OS-489

C.Scheiber, O. Musse, Y. Mallet and G. Sirat
 Institut de Physique Biologique - Service de Médecine Nucléaire
 Faculté de Médecine - rue Kirschleger 67085 Strasbourg France

NM IMAGE REGISTRATION BY NON-COHERENT INTERFEROMETRY

Matching the external contour of the body is one approach used to perform inter or intra-modality registration of medical images or of non-imaging medical data, to improve diagnostic efficiency and/or to guide surgery/radiotherapy. When dealing with brain examinations, contour registration has a theoretical advantage over volume image matching techniques, i.e. it does not use the organ of interest itself but a common reference with the surface of the body. The nature of NM data and the spatial resolution of the gamma-camera do not allow a direct measurement: an intermediary system have to be used. For routine use the system has to be integrate in the gamma-camera, to be robust, precise (1/10 mm) and affordable. The calibration should be easy to perform. To our knowledge, no commercially available sensors fulfill all these criteria. Conoscopy is a new telemetry system based on non-coherent interferometry which has been initially developed for industrial purposes. The optical system of the conoscope is housed in a 10*15*10 cm case which includes all dedicated miniaturized electronics. To obtain a head contour as the first step of brain registration, the conoscope was mounted on the SPECT gamma-camera (Helix, Elscint) at 90° with reference to the detector's plane. Under these conditions the telemetric system and the gamma-camera have the same referential thus decreasing the systematic error in the second step of the registration process: matching of the face and the NM data.

Bidimensional profiles (256 points, XYZ data, 12 pts/sec) were recorded for selected angle of the gantry (2°) during a conventionnal SPECT procedure of an antropomorphic 3D brain phantom (Nuclémed, BR005) and volunteers. Accurate calibration allowed fusion between the face profiles (in mm) and the brain-study.



OS-490

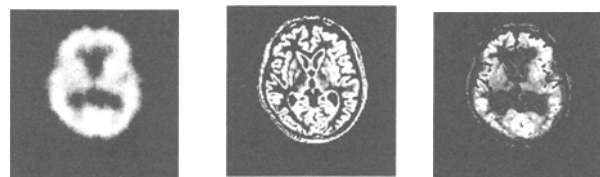
V.Barra, A.Colin, J-Y.Boire

ERIM - Faculté de Médecine - CLERMONT FERRAND

SYNTHESIS OF A HIGH RESOLUTION FUNCTIONAL IMAGE BY AN IRM/SPECT FUSION PROCESS

The aim of this study is to create a high resolution functional synthetic image. This is achieved by a fusion process, which takes into account both anatomical data coming from MRI and functional information of the SPECT image. The tissue characterisation, which may improve the diagnosis, the treatment and the general understanding of the pathology, is the first step of our fusion process.

We first generate our tissues models by analysing the grey-levels histogram of each image, and more particularly its modes and fingerprints. The relevant "tissues" chosen were grey matter, white matter, cerebrospinal fluid and the background of the image. The result is a set of fuzzy images, each of those being a fuzzy map of a given tissue. More precisely, the grey-level of a voxel V in a fuzzy map F represents the degree of possibility of V to belong to the tissue mapped by F. We now propose a new approach for the MRI image, based on a possibilistic clustering of the wavelet coefficients sets associated to each voxel. This method classifies all the voxels according not only to their spatial localisation, but also to their frequency properties, which makes this method more robust than the first approach. The classification gives a relevant separation of the different types of tissues, with a better definition of local anatomical structures (grey nuclei, cortical fissures). We present here the results of the two methods, and we compare them. We demonstrate the interest of the synthetic image, which allows for example to discriminate between a hypoperfused zone in the cortex and a low signal in SPECT due to the presence of a large fissure. Both fuzzy maps of tissues and the synthetic image shed light on future prospects for the exploration of cerebral degenerative diseases.



Original SPECT Image Grey Matter Fuzzy Map Synthetic Image

OS-491

Habraken, J*; Koot, R**; Verbeeten, B***; Paans, A****, Royen-van, E.A*

* Dept. Of Nuclear Medicine, AMC Amsterdam,
 ** Dept. Of Neuro-surgery, AMC Amsterdam,
 *** Dept. Of Radiology, AMC Amsterdam,
 **** PET Centre, AZG, Groningen, The Netherlands

MULTIPLE IMAGE MODALITY FUSION FOR THERAPEUTIC PLANNING OF PATIENTS WITH GLIOBLASTOMA MULTIFORME TUMOURS.

Patients with malignant brain tumours of the type glioblastoma multiforme can be treated with brachyradiotherapie. It is known that this treatment induces radionecrosis. In case of recurrent symptoms it is difficult to differentiate tumour recidive from radionecrosis on CT or MRI images. It has been claimed that Tyrosine PET and Thallium-201 SPECT images can differentiate between tumour and radionecrosis. Fusion of the images obtained by these various modalities may be helpful in solving this difficult clinical problem.

We utilized the chamfer matching technique for fusion of all four modalities. The implementation performs an automatic contour detection in 3D of the edge of the skull, and then minimizes the distance between the 3D contours by adjusting 6 parameters using simplex method. (3 translation and 3 rotation parameters). The result of the image registration was tested by circle matching; comparing the mean voxel distance of the SPECT study that was matched directly onto the MRI and the SPECT study that was matched first onto the CT study and then reoriented by the CT-MRI transformation onto the MRI study.

Chamfer matching proved to be a suitable technique for the fusion of Tyrosine PET and Thallium-201 SPECT images with CT and MRI images. For the SPECT to MRI matching we reached accuracies that were within SPECT resolution (8mm). Further research will concentrate on :

- Further determination of the accuracy by comparing chamfer matching with other matching techniques like mutual information matching or matching with artificial markers.
- What is the clinical efficacy of the method.

OS-492

A. S. Houston

Royal Hospital Haslar, Department of Nuclear Medicine

THE USE OF RESAMPLING METHODS FOR TESTING A NORMAL BRAIN ATLAS

This paper investigates the use of resampling methods for testing the validity of a normal rCBF atlas based on a database of SPECT images of 50 normal volunteers.

A normal atlas may be constructed by extracting a mean image, several eigenimages and a residual SD image from a database of normal images. A significance image for a new subject may be formed by dividing the subject's residual image (reconstituted image minus original image) by the atlas's residual SD image, allowing assessment of any suspected abnormalities.

Cross-validation on a "leave-one-out" basis is a useful method for assessing the quality of the atlas, while jackknifing the images in the atlas may be used to remove bias and test its stability. Both methods involve omitting each subject in turn and constructing an atlas from the remaining 49 images. The state of normality of the omitted image is determined using this atlas providing cross-validation for this image. An unbiased (or jackknifed) estimate of each image in the atlas, together with an image of its standard error, is obtained from the multiple atlases thus formed using the standard jackknife technique. In addition, the jackknifed image divided pixel-by-pixel by its standard error image produces an image of the t-statistic. This may be used to test if a value on the jackknifed image is significantly different from zero. This is particularly useful for eigenimages.

It is also possible to jackknife the significance image for each subject in the database. The subject in question must first be omitted from the database. A set of atlases is obtained from the remaining images in the database by omitting each subject in turn and constructing an atlas from the remaining 48 images. A set of significance images is obtained from these atlases for the subject in question. The jackknife technique is then applied producing a jackknifed significance image, its standard error image and its t-image. In this case the t-image may have diagnostic potential.

The images of the atlas and the significance image of each subject are shown in every case to be little altered by jackknifing. It may be concluded, therefore, that both the atlas and the significance image it provides are stable. The diagnostic potential of the t-image is under investigation.

General nuclear medicine: Bone

OS-493

Li Peiyong Yu Junfeng* Jiang xufeng Chenmo Zhu

RuiJin Hospital, Shanghai, Dept. of Nucl. Med. ; *Shanghai institute of Nucl. Research, Academia Sinica, P.R.China

RHENIUM-188 SULFIDE SUSPENSION: POTENTIAL RADIOPHARMACEUTICALS FOR RADIATION SYNOVECTOMY

Rhenium sulfide suspension was prepared by the reaction of Na₂S₂O₃ and KReO₄ in way of dispersion and assessed for its applicability as a particle carrier for use in radiation synovectomy. **Materials and Methods:** 1) *Production of 188Re sulfide suspension.* The rhenium sulfide suspension was formed by acid reduction of sodium thiosulfate in the presence of perchlorate. The solution was centrifuged and particles was subjected to ultrasonic bath for 20 min in order to assure uniformity of the suspension prior to administration to animals. 2) *In vitro studies.* The labeling efficiency and radiochemical purity was tested by centrifugation method and paper chromatography, respectively. The particle size was examined under microscope. The in vitro stability studies were performed by adding aliquots of 188Re sulfide suspension in to tubes containing normal saline, PBS (pH=7), BSA and synovial fluid for incubating at intervals of 1 day, 3 days and 5 days 3) *Animal models.* Eight New Zealand white rabbits weighing 3 kg were used in an antigen-induced arthritis model as described by Steinberg. 1 wk after induction, the rabbit knees were injected with 0.2ml suspension containing approx. 0.5mCi of 188Re sulfide suspension. 4) *Biodistribution.* The rabbits were slaughtered 24h and 72h after intra-articular injection of 188Re sulfide suspension. Samples of different organs were weighed and counted in a well-type counter to calculate the %ID/g tissue. **Results** The labeling efficiency and radiochemical purity was more than 96% and 99%, respectively. Particle sizing indicated that 94.7% were 1-5µm, 3.5% were 5-9µm. In vitro stability tests revealed that 99% of radiochemical purity remained over 5 days period of incubation. 79% of particles were 1-5µm and 18% were 5-10µm at 48h after production of 188Re sulfide suspension. The results of biodistribution was as following table

Time (days)	%ID/g tissue x 10 ⁻²						
	liver	lung	kidney	spleen	muscle	bone	blood urine
1 (n=4)	0.0062	0.0078	0.012	0.0088	0.0045	0.0042	0.0013 0.017
3 (n=4)	0.0028	0.0025	0.0062	0.0031	0.0030	0.0063	0.0023 0.0074

Conclusion: Our preliminary results indicate that 188Re sulfide suspension is an effective radiopharmaceutical for radiation synovectomy.

OS-494

Zehra Özcan, Zeynep Burak, Dündar Sabah, Ayşenur Memiş, Gülçin Başdemir, Hayal Özkılıç.

Ege University Medical Faculty, Nuclear Medicine, Radiology, Pathology and Orthopedic Surgery Departments, İzmir, Turkey

SEQUENTIAL SCINTIGRAPHIC FINDINGS IN PATIENTS WITH TUMOR RESECTION AND LIMB-SPARING RECONSTRUCTION

Improvements in preoperative chemotherapy has facilitated limb-salvage surgery procedures in patients (pts) with extremity tumors. However, follow-up after surgery and detection of complications may be difficult by using CT/MR due to metal components. The present study aimed to review the sequential scintigraphic findings with emphasis on normal patterns and abnormal findings of reconstructed extremities. The study group included 26 pts with tumor resection and prosthetic replacement. Substitution with vascularized fibula/iliac grafts was performed in 8 pts. Primary tumor was osteosarcoma in 19, Ewing sarcoma in 5, chondrosarcoma in 1 and MFH in 1. There were 17 male and 9 female and age range was 10-42 yr. Three phase dynamic bone scintigraphy after iv injection of 7.4 MBq/kg activity was obtained. First-pass, blood-pool and delayed phase images were evaluated visually using a three-point scale as mild +, moderate ++ and marked +++, for abnormal tracer accumulation. Ten pts had 3, 14 pts had 2, 5 pts had 1 post-operative scans with a mean interval of 6 months for each. First postoperative scans were obtained within 3 weeks after surgery in cases with autografts for the assessment of viability of the implant, otherwise within the following 3-6 months. Totally 63 examinations were evaluated and radiological examination was also performed. Baseline postop scans of all pts showed mild hyperemia, rim-like activity accumulation surrounding the prosthetic components, moderate tracer accumulation in host junction and marked intensity in autografted areas which declined gradually after 6 months. Pts with loosening (n:3), pseudoarthrosis (n:1) showed markedly increased tracer uptake. Areas of non-union (n:1), infection (n:2), fracture (n:1) and local recurrences (n:2) demonstrated well-defined hyperemia and focal markedly increased osteoblastic activity. In conclusion, it is important to establish normal patterns of scintigraphic findings after reconstructive surgery, since pts with extremity malignancies are regularly referred for bone scintigraphy for the assessment of metastatic involvement. Therefore, baseline postoperative scans obtained before any clinical symptomatology are useful for the evaluation of long-term scintigraphic findings. It seems that any abnormal persistent focal activity after six months is probably associated with a complication which requires further investigation.

OS-495

Zehra Özcan, Zeynep Burak, Dündar Sabah, Gülçin Başdemir, Kamil Kumanloğlu, Hayal Özkılıç.

Ege University Medical Faculty, Nuclear Medicine, Pathology and Orthopedic Surgery Departments, İzmir, Turkey.

SCINTIGRAPHIC FEATURES IN EWING SARCOMA: CLINICAL EXPERIENCE WITH HISTOLOGICALLY PROVEN 22 CASES

The scintigraphic appearance of primary bone tumors has not achieved a major role in differential diagnosis. In this study it was aimed to review the abnormal scan findings at initial presentation and follow-up and to test whether a characteristic pattern can be described for Ewing sarcoma (ES). Between 94 and 97, 22 patients with histologically confirmed ES, examined with Tc-99m-MDP three phase scintigraphy were included in the study group. The age range was 10 to 25 and the female/male ratio was 9/13. The follow-up scanning was available in 16 pts with a mean duration of 9 months. Early and delayed phases of bone scintigraphy (BS) was evaluated semi-quantitatively using a 3-point scale. The vascularity of tumor, intensity of tracer accumulation, distortion/destruction in bony outlines were graded as mild, moderate and marked. The pattern of activity distribution within the tumor was classified as homogenous, patchy, cold-on-hot or dough-nut like appearance. The primary tumor location was extremities in 16 (femur: 9, tibia: 6, radius: 1), axial skeleton in 6 (pelvis: 5, rib: 1) cases. Tumor vascularity was markedly increased in 10, moderately in 9 and mildly in 3 patients. The overall intensity of the lesion was markedly increased in 12 and moderately in 10. Activity distribution was patchy in 12, homogenous in 8, cold-on-hot in 1 and doughnut like in 1. Destructive/distorted bone margins were noted in 7 lesions mostly on tumors with patchy uptake. Multicentric diseases was diagnosed in 4 (multifocal bone involvement : 2, and pulmonary metastases: 2) pts in whom primary tumor axially located. Of the 5 metastatic nodules in lungs, none were detected on bone scintigraphy. Follow-up BS after radio/chemotherapy demonstrated decreased regional hyperemia and tracer uptake. However, unsuspected metastases were visualized in 2 cases. In conclusion, ES seemed to not to have a unique scintigraphic pattern, however markedly increased vascularity, patchy distribution of high intensity levels and moderately distortion in bony outlines was the most striking feature in this series. It was also noted that pts with axially located tumors must be interpreted with great caution, since the primary tumor located in axial bones is more frequently associated with metastatic disease. It is suggested that BS should be an essential part of imaging strategies both at initial presentation and follow-up of Ewing sarcoma.

OS-496

Y. Nishiyama, Y. Yamamoto, Y. Fukuda, Y. Kawasaki, M. Ohkawa, M. Tanabe

Kagawa Medical University, Asada General Hospital, Department of Radiology

THE CLINICAL VALUE OF 201TI AND THREE-PHASE BONE SCINTIGRAPHY FOR BONE AND SOFT TISSUE TUMORS

While 201Ti (Ti) has been shown to be highly sensitive in the detection of bone and soft tissue tumors, its accumulation is not specific for malignancy. The purpose of the present study was to assess differentiation of benign and malignant lesions using Ti imaging and three-phase bone scan. A total of histologically confirmed 25 bone and soft tissue tumors (12 malignant and 13 benign) were investigated. Ti static images were acquired after 10 min (early) and 2 hours (delayed). Within 7 days, a three-phase bone scintigraphy was performed using 99mTc-HMDP with the patient in the same position as for Ti imaging. The count ratio of the lesion to the contralateral or adjacent site (L/C ratio) was measured. With Ti, all malignant lesions except one (myeloma) were clearly visualized. Mean (± S.D.) values of early and delayed L/C ratio were: 3.5 ± 1.3 and 2.9 ± 1.4, respectively, in malignant lesions; and 2.2 ± 1.3 and 1.6 ± 0.9, respectively, in benign lesions. Ti accumulation of benign lesions was significantly lower than that of malignancies, except for giant cell tumor (n=2) and schwannoma (n=1). No such significance was detected on three-phase bone scintigraphy (L/C ratios of benign and malignant tumors were 2.7 ± 0.9 and 2.8 ± 3.3, respectively for 1st phase; 2.3 ± 0.8 and 2.3 ± 1.9, respectively for 2nd phase; and 3.5 ± 2.4 and 3.2 ± 4.5, respectively for 3rd phase). When we assumed that the tumor was malignant in cases in which delayed Ti L/C ratio exceeded the 2nd phase L/C ratio, the sensitivity was 77%, specificity 100%, and accuracy 88%. In the present study, Ti scan for bone and soft tissue tumors was better than three-phase bone scintigraphy alone but was not enough to clearly differentiate malignant lesions from benign ones. However, when the delayed Ti L/C ratio exceeded the 2nd phase L/C ratio, the specificity for detecting bone and soft tissue tumors was 100%.

OS-497

G. Berding, H. Schliephake, W. Burchert, J. v.d. Hoff, W.H. Knapp

Klinik für Nuklearmedizin und Klinik für Mund-, Kiefer- und Gesichtschirurgie, Medizinische Hochschule Hannover

EVALUATION OF BONE HEALING AND EARLY DETECTION OF COMPLICATIONS AFTER FIBULAR TRANSPLANTATION FOR MANDIBULAR RECONSTRUCTION USING ¹⁸F-FLUORIDE PET

Purpose of the study: Bone blood flow and osteogenic activity (fluoride influx) can be measured using ¹⁸F-fluoride PET. The aim of the present study was to establish the range of flow and F⁻ influx in the early and delayed phase after mandibular reconstruction with revascularized fibular bone grafts in case of uncomplicated healing and in case of complications.

Methods: In 11 patients dynamic PET-studies with simultaneous arterialized blood sampling were performed 1-4 weeks post mandibular reconstruction (n=6) and after a delay of 8-32 weeks (n=10). 5 patients had complications (transplant necrosis, n=2, and pseudarthrosis, n=3). PET was quantitated using a 3-compartment model and multilinear least squares fitting. Regional blood flow and F⁻ influx were determined for 3 areas: transplant, area of osteosynthesis, vertebra (reference).

Results: In the early postoperative phase flow in grafts with uncomplicated healing was significantly elevated compared to the delayed phase (0.1487 vs. 0.0801; p=0.0065) as well as compared to the reference area (0.0888; p=0.0216). In contrast, there were no significant differences in F⁻ influx. Early postoperative flow and F⁻ influx were significantly elevated in osteosyntheses (0.1351 vs. 0.0888; p=0.0170 and 0.0728 vs. 0.0418; p=0.0017). In comparison to transplants and osteosyntheses with uncomplicated healing fluoride influx was significantly reduced in transplant necrosis (0.0072 vs. 0.0289; p=0.0199) and mobile pseudarthroses in the osteosynthesis region (0.0247 vs. 0.0474; p=0.0438).

Conclusions: Despite high blood flow of revascularized transplants of cortical bone in the early phase post operation, osteogenic activity is in the same range as that of the vertebrae. Our data suggest that complications can be predicted in case of reduced fluoride influx in the transplant or in the osteosynthesis area.

OS-498

L. Lauer, N. Czech, J. Zieron*, M. Baehre, E. Richter

Clinic of Radiotherapy and Nuclear Medicine, *Clinic of Maxillofacial Surgery, Medical University of Luebeck, Germany

EARLY EVALUATION OF MICROVASCULARIZED BONE GRAFT VIABILITY IN MANDIBULAR RECONSTRUCTION BY BONE SPECT AND SEMIQUANTITATIVE ANALYSIS

Objective: Performing tumor resection of carcinomas affecting the mandible, the resulting defects can be replaced by microvascularized bone graft from the fibula or radius. Following this operation, complications as necrosis or infection may occur. This retrospective study investigates the value of bone scintigraphy with SPET and semiquantitative analysis in the early detection of bone graft necrosis.

Patients and methods: We evaluated 61 scintigraphies of 36 patients with 39 bone grafts. 3 patients received two grafts because of tumor recurrence or necrosis. 34 SPECT were performed 6-11 days and 27 up to 11 months postoperatively (po). 19 patients had only an early and 6 only a late investigation. In 11 cases we could perform 2-4 controls. 3 hours after application of 550 MBq ^{99m}Tc-MDP a SPECT study was performed (Prism 2000XP or 3000XP, Picker, LEUHR; 128 matrix, 6°, 50 sec/frame). The data was reconstructed iteratively (Luig). The scans were evaluated visually and semiquantitatively using ROI technique. Using transoblique slices ROIs of the transplanted bone and the cranium were formed and the ratios (T/C) were calculated.

Results: (1) 28 patients (29 SPECT) with uncomplicated healing showed 6-11 days po a T/C > 1.0 (M = 3.24); in 5 cases with necrosis T/C was below 1.0 (M = 0.88). This difference was significant (p < 0.004, U-Test). (2) 20 SPECT (normal healing) 1.5-6 months po showed a T/C between 1.13 and 5.56 (M = 2.74); in 5 SPECT (necrosis) T/C ranged from 0.67 to 1.5 (M = 0.92). Also these values were significantly different (p < 0.035). (4) T/C in one patient with partial necrosis due to osteomyelitis following dental implant was 0.89 (11 months po).

Conclusion: Our data show that bone scintigraphy with SPECT can reliably assess graft viability in the early stages after surgery. Already 6-11 days po an increased tracer uptake demonstrates viability and indicates a normal healing process. Especially no false positiv or false negativ results were observed in the early SPECT. The T/C ratio could clearly differentiate between vital and non-vital bone grafts.

Cardiovascular: Comparison of techniques

OS-499

J.J. Bax*, J.H. Cornel**, F.C. Visser#, A. van Lingen#, P.M. Fioretti##, C.A. Visser##.

University Hospital Leiden*, Medical Center Alkmaar**, Free University Hospital Amsterdam#, Netherlands and Istituto di Cardiologia##, Udine, Italy.

AGREEMENT AND DISAGREEMENT BETWEEN METABOLIC IMAGING AND DOBUTAMINE ECHOCARDIOGRAPHY.

Preserved metabolism and presence of contractile reserve are different aspects of cellular viability. However, not all viable cells exhibit all characteristics; in the present study we performed a direct comparison between metabolic imaging with F18-fluorodeoxyglucose (FDG) SPECT and assessment of contractile reserve with low-dose dobutamine echocardiography in akinetic myocardium.

Forty patients with a depressed LV function (mean LV ejection fraction 31 ± 16%) were studied. All underwent FDG SPECT, resting thallium-201 SPECT (to assess perfusion) and resting echocardiography to identify segments with akinesia at rest. Low-dose dobutamine echocardiography was also performed. For all techniques a 13-segment model was used. 165 (32%) segments were akinetic at rest. The majority (n=154, 93%) of these segments demonstrated resting hypoperfusion. FDG imaging revealed a perfusion-metabolism mismatch in 41 segments and a match in 113 segments. Contractile reserve was present in 33 (80%) of the segments with a perfusion-metabolism mismatch and in 7 (6%) segments with a match (P < 0.0005). Of the 11 segments with normal perfusion, only 5 (45%) showed contractile reserve. The agreement between SPECT and dobutamine echocardiography was 87%. While 94% of the scintigraphically nonviable segments did not show contractile reserve, the disagreement between SPECT and dobutamine echocardiography was mainly due to absence of contractile reserve in 27% of the scintigraphically viable segments.

Conclusion. This study shows a good agreement between SPECT and dobutamine echocardiography, although a substantial number of segments with preserved viability on SPECT do not exhibit contractile reserve, indicating underestimation of viability by dobutamine echocardiography as compared to FDG imaging.

OS-500

J. de Boer, W. Kool, P.K. Blanksma, A.T.M. Willemsen, P.L. Jager, A.M.J. Paans, W. Vaalburg, D.A. Piers.

Departments of Nuclear Medicine, Cardiology and PET, University Hospital, Groningen, The Netherlands.

COMPARISON OF F-18-FLUORODEOXYGLUCOSE (FDG) Tc-99m-SESTAMIBI (MIBI) DUAL ISOTOPE SIMULTANEOUS ACQUISITION SPECT (DISA) WITH REST/STRESS-MIBI SPECT (RM/SM) FOR THE ASSESSMENT OF MYOCARDIAL VIABILITY.

Purpose: Evaluation of myocardial viability with DISA has the advantage of simultaneously obtaining information on myocardial perfusion using MIBI and metabolism using FDG, saving time, cost and patient burden. Prerequisite is that MIBI images are not degraded by scatter of 511 keV photons and poor count statistics. Therefore, we compared MIBI images of DISA (DM) with MIBI images of RM in 11 patients with coronary artery disease and only irreversible perfusion defects on prior RM/SM.

Methods: At 45 min after oral glucose (75 g) loading 600 MBq MIBI and 185 MBq FDG were injected i.v. at rest and 60 min later DISA was performed with a Siemens Multispect-2 gammacamera (UHE collimators, single head, 180°, 64 views, each 30 s) using 3 windows: 140 (15%) keV (MIBI), 170 (10%) keV (scatter correction) and 511 (15%) keV (FDG). After scatter correction of the MIBI window (counts in 140 keV minus counts in 170 keV window) DM and FDG images were reconstructed and reorientated with identical axis. DM and RM images were displayed in polar maps with 128 segments normalized to the maximum study value.

Results: In all 1408 segments the activity of DM and RM correlated well (r=0.93) and the SD of the difference between DM and RM was 8%. Visually there were no differences between DM and RM images. Quality of FDG images was excellent in 9 patients and acceptable in 2 patients. Myocardial viability defined as metabolism perfusion mismatch was visually scored in 9 segments per heart in 49 irreversible perfusion defects observed on the prior RM/SM. DISA showed viability in 4 segments which included 3 patients.

Conclusion: Without loss of MIBI image quality DISA may be used routinely for viability assessment in patients with coronary artery disease. DISA shows viability in 8% of the segments that were classified as infarct with RM/SM.

OS-501

ZM Yao, XJ Liu, RF Shi, RP Dai, SX Zhang, YZ Liu

Department of Nuclear Medicine, Cardiovascular Institute & Fu Wai Hospital, CAMS & PUMC, Beijing, China

A COMPARISON OF ^{99m}Tc-MIBI MYOCARDIAL SPECT WITH ELECTRON BEAM CT IN ASSESSMENT OF CORONARY ARTERY DISEASE IN TWO DIFFERENT AGE GROUPS

Our previous study showed that ^{99m}Tc-MIBI myocardial perfusion SPECT has higher specificity and accuracy than those of electron beam CT (EBCT) in detection of coronary artery disease (CAD). To compare SPECT and EBCT in assessment of CAD in different age groups, ^{99m}Tc-MIBI SPECT (stress-rest), EBCT and coronary angiography (CAG) studies were performed in 64 patients with suspected CAD. The patients were classified into two subgroups: group A: 40 patients over 45 years of age and group B: 24 patients ≤ 45 years of age. There were 31 and 14 patients with coronary stenosis ≥ 50% proved by CAG in group A and B, respectively. Thirty CAD patients (67%) had both abnormal ^{99m}Tc-MIBI SPECT and coronary calcification 14 non-CAD patients (73%) had normal ^{99m}Tc-MIBI SPECT and normal EBCT. In group B, the sensitivity of SPECT for detecting CAD was significantly higher than that of EBCT (92.9% vs 42.9%, P < 0.01). When individual coronary artery disease considered, the specificity of SPECT was significantly higher than that of EBCT in group A (94.1% vs 66.7%, P < 0.001), the sensitivity of SPECT was significantly higher than that of EBCT in group B (85.7% vs 38.1%, P < 0.005), the accuracies of SPECT in both subgroups (82.5% and 93.1%, respectively) were higher than those of EBCT (67.5% and 76.4%, respectively), P < 0.01. In conclusion, ^{99m}Tc-MIBI myocardial perfusion SPECT has higher sensitivity in detection of CAD in patients ≤ 45 years old and higher specificity in detection of CAD in patients > 45 years old than those of EBCT. Combination of SPECT and EBCT may be much better in evaluating CAD.

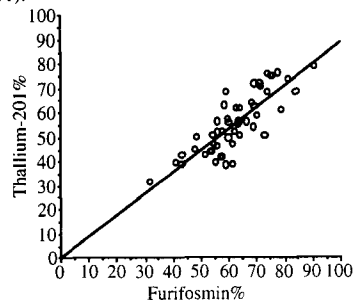
OS-502

A. Giorgetti, S. Stefanini, A. Gimelli, G. Sambucetti, E. Ferdeghini, P. Marzullo

CNR-Institute of clinical physiology, Pisa-Italy

COMPARISON OF SPECT THALLIUM-201 AND TECHNETIUM-99m FURIFOSMIN FOR DETECTION OF TISSUE VIABILITY IN PATIENTS WITH LEFT VENTRICULAR DYSFUNCTION

Recent studies have demonstrated that Thallium-201 (T) and Furifosmin (F) show similar accuracies in identifying transient myocardial ischemia. However, the potentiality of F in assessing tissue viability is still to be defined. To this aim we compared rest T (111 MBq) and rest F (3700 MBq) SPECT in 10 patients (5 male, mean age 66±10 yrs) with coronary artery disease and depressed ejection fraction (0.34±0.9). Tomographic analysis was performed in segments with echocardiographic baseline dysfunction, in 4 short axis planes; perfusion defects were visually identified and scored using a 4 point scale (0=normal, 3=severe defect). Furthermore, both severity and size of each defect were expressed as normalized % uptake and pixel number, respectively. Of 50 segments analyzed, 47/47 had concordant moderate or severe defect by T and F, respectively. Quantitative analysis showed a good correlation between T and F in terms of normalized uptake (r²=.67, p<.0001) and defect size (r²=.79, p<.0001).



In conclusion, in patients with overt left ventricular dysfunction F scintigraphy appears suitable in the assessment of myocardial viability.

OS-503

J.R. Buscombe, J.L. Davarashvili, W.L. Smith, G.J. Coghlan, T.R. Evans, D.P. Lipkin, A.J.W. Hilson
Royal Free Hospital and school of Medicine, Departments of Nuclear Medicine and Cardiology, London UK

MYOCARDIAL PERFUSION ECHOCARDIOGRAPHY: HAS RADIONUCLIDE PERFUSION IMAGING MET ITS NEMESIS.

Though stress dobutamine echocardiography has been used as an alternative to radionuclide myocardial perfusion imaging (MPI) for many years it has relied on changes in wall motion to determine ischaemia and is the two types of studies have been seen as complimentary. A new approach however has been to combine stress echocardiography with a perfusion ultrasound agent-Optison (octafluorprpane). The aim of this study was to compare dobutamine myocardial perfusion echocardiography (DPE) with MPI.

Twenty patients (15 males) with mean age of 62 years with known or suspected coronary artery disease underwent both studies within a 13 day period.

MPI SPECT was performed after Adenosine or Dobutamine stress with Tc-99m isonitriles. DPE was performed in two modes harmonic-11 patients and fundamental-9 patients. The Optison was injected at peak Dobutamine stress. Each study was reported blind of the other modality and was reported as normal, ischaemia or infarct.

The Optison was well tolerated overall concordance between the two modalities was 75%. The concordance for each coronary artery territory is given below.

Mode of imaging	LAD	LCX	RCA
Harmonic-11 pts	91%	81%	78%
Fundamental-9 pts	78%	78%	56%

In cases when the MPI and DPE were discordant the wall motion abnormalities favoured the DPE results.

Myocardial perfusion echocardiography can potentially be used instead of radionuclide myocardial perfusion imaging. The two methods appear competitive not complimentary

OS-504

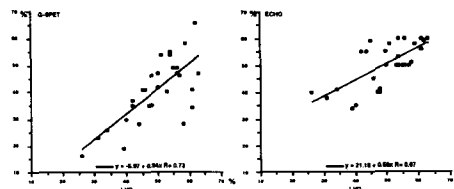
A. Bruno, F. Zito, *A. Finzi, M. Castellani, G. Marotta, *G. Cali, P. Gerundini.

Nuclear Medicine and *Cardiology Departments, IRCCS - Ospedale Maggiore, Milan, Italy

LEFT VENTRICULAR EJECTION FRACTION IN INFARCTED PATIENTS: G-SPECT, ECHOCARDIOGRAPHY AND LEFT VENTRICULOGRAPHY EVALUATION.

The addition of ecg gating to myocardial SPECT (G-SPECT) can provide potentially useful information for the assessment of ventricular function. The purpose of this study was to determine if G-SPECT calculation of the left ventricular ejection fraction (LVEF) in infarcted pts. was reliable in comparison with echocardiography (ECHO) taking left ventriculography (LVG) as the reference technique. **Methods:** 29 pts. referred for recent (1-6 months) myocardial infarction were included. G-SPECT acquisition began 30'-45' after Tc99m-tetrofosmin injection at rest (1110 MBq); 60 projections/360°, supine, 60 sec/projection, 64x64 frame, 8 frames/cycle. The G-SPECT images were processed using automated commercially available software. All pts underwent basal ECHO and LVG within 1 month from G-SPECT.

Results: The only parameter considered was LVEF. The R values of G-SPECT and ECHO versus LVG were similar, 0.73 and 0.67 respectively (see figure). G-SPECT tended to underestimate LVEF compared to LVG. but if only the 15 pts with LVG values of LVEF <50% were considered, the correlation with GSPET improved (r=0.86), whereas the correlation with ECHO significantly worsened (R=0.41).



Conclusions: In addition to perfusion evaluation, myocardial G-SPECT, allows a reliable quantification of LVEF. There are several factors that may cause inaccuracies and require improvement and expertise (8 frames/cycle sampling inadequate to obtain an accurate end diastolic phase, edge detection in pts with large defects, severe cardiac arrhythmias, low QRS complexes, etc.) but G-SPECT has shown a better ability than ECHO to assess LVEF, particularly at low values. The differences between G-SPECT and LVG are acceptable for a large-scale clinical application.

Oncology: PET

OS-505

H. Minn, JM. Nuutinen, M. Haaparanta, J. Bergman, J. Knutti. Department of Oncology and Radiotherapy; Turku University Central Hospital and Turku PET Centre; FINLAND

FATTY ACIDS DO NOT INTERFERE WITH GLUCOSE UPTAKE IN MALIGNANT LYMPHOMA: FDG-PET STUDY

PURPOSE: To study whether blood free fatty acids (FFA) interfere with glycolytic metabolism of lymphoproliferative neoplasms as assessed with FDG PET.

PATIENTS: Twelve patients with untreated Non-Hodgkin lymphoma (4 low, 3 intermediate, 2 high grade / WHO classification) and Hodgkin's disease (n=3) participated in this study.

METHODS: Two FDG PET studies were performed within one week after overnight fast. Blood FFA concentrations were reduced pharmacologically in the second study by giving orally 1.5 and 1 h before scanning 250 mg acipimox (Olbetam[®]). Acipimox is a nicotinic acid derivative used for treatment of hyperlipidemia by decreasing blood FFA concentration through inhibition of lipolysis. In all cases, 60 min dynamic acquisition over tumor area was performed with ECAT 931/08 PET-scanner after injection of a median dose of 363 MBq FDG. Both graphical analysis (rMR_{FDG}) and single scan approach (SUV) were used to compare tumor uptake of FDG under high fasting FFA concentrations (PET_{BL}) and after pharmacologically decreased FFA concentrations (PET_{ACI}).

RESULTS: Median FFA concentrations under PET_{BL} were 0.80 mmol/l (range 0.51-2.34) and under PET_{ACI} 0.20 (range 0.02-1.59), respectively (p=0.0001). By contrast, blood glucose, insulin and lactic acid concentrations were similar in PET_{BL} and PET_{ACI}. Median rMR_{FDG} of total of 12 involved lymph nodes was 0.219 (range 0.087-0.825) in PET_{BL} and 0.201 (range 0.107-0.817) in PET_{ACI} (NS). The respective figures for median SUV were 7.8 (range 3.6-18.6) and 6.0 (range 4.1-20.2). Tumor imaging was unchanged during the two approaches.

CONCLUSIONS: Blood fatty acids appear to have minor significance for FDG uptake in lymphoma, suggesting that glucose metabolism in neoplastic tissue is not regulated by supply of free fatty acids.

OS-506

A. Dimitrakopoulou-Strauss, L.G. Strauss, M. Schwarzbach, S. Hohaus, F. Oberdorfer, G. van Kaick.

German Cancer Research Center, Heidelberg, Germany.

C-11-AMINOISOBUTYRIC ACID (AIB) IN ONCOLOGICAL PATIENTS

The relevance of amino acids in oncological patients is still an open question. We used a synthetic amino-acid, AIB, which reflects the "Alanine-like transport" (A-type) and has the advantage of a clear C-11-signal, because AIB is not further metabolized.

AIB was applied in recurrent lymphomas (n=15), colorectal recurrences (n=10), hepatocellular carcinomas (n=6) and soft tissue sarcomas (n=12). Multitracer studies were performed using AIB and FDG. In selected cases O-15-Water was used to evaluate the tumor perfusion. Dynamic PET studies were performed for 30 min (AIB) or 60 min (FDG). ROIs were used to obtain time-activity curves for the tumor, the normal tissue, and the aorta. Parametric images of the influx and efflux were calculated using a two compartment model. The ROI data obtained from a large vessel were used as an input function. The transport constants k1 and k2 were calculated on a pixel by pixel basis. The same model was used for the evaluation of the perfusion studies. The influx constant was calculated for FDG using the Patlak approach.

The AIB-uptake was lower than FDG in all tumor lesions. All malignancies were identified with FDG, except for histiocytoma (n=1) and well differentiated hepatocellular carcinomas (n=4). Two false positive results were obtained with FDG in patients with a suspected recurrent lymphoma. Surgery revealed an abscess in both patients, without evidence of tumor recurrence. Both inflammatory lesions were negative in the AIB scans. AIB-scans were helpful for the differentiation of colorectal recurrences (n=3). Recurrent malignant lymphomas demonstrated background equivalent AIB concentrations, independent from the histological subtype. Hepatocellular carcinomas demonstrated low AIB-uptake and could not well delineated. We noted no significant correlation between k1 for AIB and the FDG influx constant, while a low correlation was found for the influx of O-15-water and AIB (r=0.6). Comparable results were observed for k2 of O-15-water and AIB (r=0.54). The results show, that combined AIB studies can help to characterize tumor biology and are promising for the improvement of cancer treatment planning.

OS-507

R.S. Liu, C.C. Yuan, C.P. Chang, K.L. Chou, C.W. Chang, H.T. Ng and S.H.Yeh.

Taipei Veterans General Hospital, National PET/Cyclotron Center, and National Yang-Ming University School of Medicine, Taipei, Taiwan.

POSITRON EMISSION TOMOGRAPHY (PET) WITH [C-11] ACETATE (ACE) IN DETECTING MALIGNANT GYNECOLOGIC TUMORS.

[F-18]fluorodeoxyglucose (FDG) PET has been used to detect gynecologic cancer in the abdomen and pelvis. However, intense FDG accumulation in the bladder due to excretion of FDG in the urine may disturb the imaging of pelvic tumors. This limitation can be partly corrected by irrigation of the bladder or iterative reconstruction technique. ACE is a promising tracer for detecting nasopharyngeal carcinoma, brain tumor, and renal cell carcinoma. It is cleared from the renal parenchyma without any urinary excretion, and consequently it is a potential tracer for abdominal and pelvic PET imaging in detecting malignant tumors. The purpose of this study was to assess the feasibility of imaging of gynecologic cancer with ACE-PET.

Five women with recurrent ovarian carcinoma and 3 women with cervical carcinoma, were studied with ACE and FDG-PET in the same day. For FDG study, we had the patients void before scanning and image the pelvic area first. Sixteen min dynamic ACE-PET imaging was carried out following iv injection of 370 MBq (10 mCi) ACE. Attenuation corrected emission data from overlapping planes over the entire abdomen and pelvis were acquired and tomographic images were generated. PET images were visually analysed to identify areas of increased tracer uptake compared to the surrounding tissues. The operation and pathology results were then correlated with PET data. All patients demonstrated tumoral uptake of ACE uptake that correlated with the local distribution of tumors found at laparotomy. FDG-PET was inferior to ACE-PET in six cases due to interference of intense urine radioactivity. FDG-PET showed reduced lesion detectability in the vicinity of the bladder and dilated renal pelvis.

In conclusion, these preliminary data indicate the feasibility of ACE-PET imaging in gynecologic oncology patient.

OS-508

P. Shreve

University of Michigan, Ann Arbor, U.S.A.

C-11 ACETATE PET IMAGING OF CANCER

Neoplastic transformation is characterized by alterations in cellular metabolism, including lipid metabolism. C-11 acetate can act as a probe of tissue intermediary metabolism through acetyl-CoA mediated entry into catabolic or anabolic lipid synthetic pathways. The purpose of this study was to investigate C-11 acetate as a metabolic tracer for the identification and characterization of malignant neoplasms.

Fifty-five patients with histopathologically proven malignant neoplasms underwent dynamic attenuation corrected positron emission tomography following intravenous administration of 740 MBq C-11 acetate. Time-activity curves and tracer activity 10-20 minutes post tracer administration (SUV₁₀₋₂₀) of different neoplasms was compared to normal tissues.

Twenty-five renal cell carcinomas studied demonstrated variable uptake and retention of C-11 acetate, with SUV₁₀₋₂₀ ranging from 2.9 to 15.2. Ten non-small cell lung carcinomas revealed modest uptake and retention of C-11 acetate with SUV₁₀₋₂₀ ranging from 3.5 to 7.8, while three small cell lung carcinomas demonstrated low uptake and retention with SUV₁₀₋₂₀ less than 3.0. Likewise, minimal C-11 acetate uptake and retention with SUV₁₀₋₂₀ less than 3.0 was observed in fourteen pancreatic adenocarcinomas, as was the case with two non-Hodgkin's lymphomas and a hepatocellular carcinoma. The time-activity curves the C-11 acetate avid neoplasms revealed a pattern of rapid (within 5 minutes) tracer uptake and then slow clearance similar to that observed in non-neoplastic tissues with active anabolic lipid pathways such as pancreas and adrenal tissue.

Some malignant neoplasms, particularly renal cell carcinoma and non-small cell lung cancer, demonstrate marked uptake and retention of C-11 acetate. The retained tracer activity as early as 10 minutes post tracer administration is comparable in degree to retained FDG at one hour in FDG avid neoplasms. C-11 acetate represents a new radiotracer for detection and characterization of malignant neoplasm, distinct in participating metabolic pathways from FDG or labeled amino acids.

OS-509

A. Dimitrakopoulou-Strauss, L.G. Strauss, F. Gutzler, D.K. Kim, G. Irrngartinger, G. Kontaxakis, F. Oberdorfer, G. van Kaick

German Cancer Research Center, Heidelberg, Germany

POSITRON EMISSION TOMOGRAPHY WITH C-11-ETHANOL AND F-18-DE-OXYGLUCOSE IN PATIENTS WITH HEPATOCELLULAR CARCINOMAS RECEIVING PERCUTANEOUS ETHANOL INJECTION.

PET was used in patients with nonresectable hepatocellular carcinomas scheduled for intratumoral ethanol therapy. One aim of the study was the investigation of the kinetics during treatment with intratumoral ethanol. Furthermore, FDG follow-up studies were performed to assess the tumor viability and to monitor the response to therapy.

The ongoing study includes 8 patients with child A cirrhosis and HCC (UICC stage III-IVA; tumor size 3-6 cm). Dynamic PET studies (60 min) with FDG were performed prior to therapy (day 0), immediately after treatment (day 1), one day (day 2), and one week after therapy (day 8). C-11-Ethanol (37-80 MBq) was applied together with the nonlabeled therapeutic dose of the drug, at day 1 via a biopsy needle positioned by ultrasound guidance. Parametric images, based on the Fourier transformation, were calculated for further analysis of the local distribution pattern of C-11-Ethanol.

Five out of eight tumors demonstrated almost constant C-11-uptake values after the initial distribution phase. PET documented a rapid elimination of C-11-Ethanol in 3/8 tumors. The time-activity curves of the liver up to 45 min gave evidence of a slow but steady increase of the tracer uptake with time. The use of the Fourier transformation demonstrated different inhomogeneous areas in the amplitude images (7/8 tumors) and a rather random redistribution in the phase images (6/8 tumors). The evaluation of the FDG data demonstrated a liver equivalent uptake in six of the tumors (well and moderate differentiated HCC) prior to therapy. One moderately differentiated HCC showed an increased FDG metabolism. The tumors were hypometabolic in the center with a rim-like FDG-accumulation at day 2 and day 8. CT follow-up studies four weeks after the first ethanol therapy showed no significant change of the tumor volume.

C-11-ethanol can be used to guide intratumoral therapy and visualize a possible tracer redistribution. FDG follow-up studies are not conclusive within one week after therapy.

OS-510

F. Najjar, G. Jerusalem, P. Paulus, G. Fillet, P. Rigo

Divisions of Nuclear Medicine and Onco-Hematology, University Hospital, Liege, Belgium

WHOLE-BODY FDG-PET FOR THE EVALUATION OF PATIENTS WITH AGGRESSIVE NON-HODGKIN'S LYMPHOMA

Accurate staging of non-Hodgkin's lymphoma (NHL) is important for treatment management. We studied 35 patients with histopathologically proven aggressive NHL to assess the value of whole-body FDG-PET as an imaging modality for staging NHL at initial diagnosis (n=27) and disease recurrence (n=8). All patients in this comparative analysis were submitted to clinical examination, enhanced CT and whole-body PET study before starting the treatment.

Results : There were 127 abnormal lymph node regions seen by FDG-PET in 35 patients; 72 were peripheral lymph nodes; 37 observed by clinical examination (8 TP, 1 FP and 28 unconfirmed) in 18 patients (14 at initial diagnosis and 4 at disease recurrence) and 35 clinically undetected (2 TP and 33 unconfirmed) in 17 patients (13 at initial diagnosis and 4 at disease recurrence) whereas the clinical examination showed 3 additional nodal lesions in 3 patients at disease recurrence. In 22 of the 32 patients with comparative CT, 55 thoracic and abdomino-pelvic lymph node regions were demonstrated by FDG-PET, 44 lesions were identified by CT (in 23 patients, 16 at initial presentation and 7 at disease recurrence), while 11 had negative CT findings (in 8 patients at initial diagnosis). CT showed 3 additional nodal lesions in 3 patients at initial diagnosis. Extranodal lymphomatous localisations in the liver (n=3), lungs (n=3), pleura (n=5), spleen (n=10) and others (n=11) were histologically verified in 8 patients (7 TP and 1 FP). Bone marrow infiltration demonstrated by PET was confirmed by biopsy in 4/6 patients, however known medullar invasion was not seen by PET imaging in 4 patients.

PET staging was concordant to overall clinical staging and CT findings in 30 patients (22 at initial presentation and 8 at disease recurrence). Lymphoma invasion diagnosed by FDG-PET led to a downstaging in 3 cases and to an upstaging in 2 cases.

Conclusion : FDG-PET is an efficient, non-invasive method for staging and restaging aggressive NHL but marrow biopsy remains indicated.

General nuclear medicine: Gastroenterology

OS-511

M. Zubillaga*, P. Oliveri#, H. Panarello*, M. Buzurro*, J. Adami*, M. Alak**, O. Degrossi**, A. Lysionek*, D. Sragowicz*, R. Caro* and J. Boccio*.

*Radioisotope Laboratory, U.B.A. Argentina; #German Hospital, Argentina.

^Quilmes Model Sanatorium, Argentina; °INGEIS, CONICET, Argentina;

**Argentine Institute of Diagnostic and Treatment, Argentina.

MODIFICATION OF THE 13C-UBT AND ITS CUT-OFF POINT DETERMINATION

In the last few years, the use of respiratory tests that uses 13C-urea for the control of Helicobacter pylori (H. pylori) eradication has been widely known. The aim of our work is to determine the cut-off point of the 13C-Urea Breath Test (13C-UBT) for breath samples collected as gas and for breath samples collected in a solution of triethanolamine. The results were compared with those obtained with the 14C-Urea Breath Test performed at different times and combined with the study of the gastric basal transit (MIN 14C UBT).

One hundred 13C-UBT determinations were performed in 15 control non-infected patients and in 25 infected patients, determined by culture, histology, rapid urease test and MIN 14C UBT. The 13C UBT was performed on patients who fasted for at least 6 hours. Basal samples were taken five minutes before of the administration of 65 mg of 13C-urea in aqueous solution. Samples of exhaled air were taken 10, 30 and 60 minutes after the administration of the labeled solution. All the samples were collected in gas collectors and in glass vials containing 1 ml of a 7% triethanolamine solution. Samples absorbed in triethanolamine were made to react with 100% of phosphoric acid. The obtained CO₂, after cryogenic purification, was measured in a mass spectrometer Finnigan Delta-S, triple collector, multipoint inlet system, mass spectrometer against a reference from a CO₂ tank. Results were given in permil deviations (δ 13C). The non-infected patients showed Δ13C average values of 2.32‰, 0.9‰ and 0.6‰ after 10, 30 and 60 minutes, with maximum values of 3.3‰, 1.5‰ and 1.1‰ for gas collected samples and 2.4‰, 2.1‰ and 2.0‰, with maximum values of 5.0‰, 3.0‰ and 3.4‰ for the samples collected in triethanolamine solution. The H. pylori infected patients showed Δ13C average values of 11.2‰, 8.7‰ and 11.5‰ after 10, 30 and 60 minutes, with minimum values of 5.4‰, 4.0‰ and 5.1‰ for gas collected samples and 19.1‰, 20.9‰ and 18.0‰, with minimum values of 10.1‰, 8.1‰ and 12.6‰ for the samples collected in triethanolamine solution. We conclude that the obtention of 4 breath samples (basal, 10, 30 and 60 minutes) allows a better differentiation between H. pylori infected and non infected patients with cut-off points of 5.0‰, 3.0‰ and 3.4‰ for the 10, 30 and 60 minutes samples collected in triethanolamine solution.

OS-512

P. Oliveri*, M. Zubillaga*, M. Calcagno*, C. Goldman*, R. Caro*, J. Adami#, M. Buzurro#, M. Sarabia*, H. Garcia del Rio**, O. Degrossi**, M. Alak** and J. Boccio*. *German Hospital, Argentina. °Radioisotope Laboratory, University of Buenos Aires, Argentina. #Quilmes Model Sanatorium, Argentina. **Argentine Institute of Diagnostic and Treatment, Argentina.

COMBINATION OF GASTRIC BASAL TRANSIT AND 14C UREA BREATH TEST FOR THE DETECTION OF HELICOBACTER PYLORI INFECTION.

None of the methods used in the diagnosis of the gastric infection produced by H. pylori can be considered as a reference standard, because the samples are obtained by an endoscopic biopsy, which is focal in nature and it does not represent the whole surface of the stomach. The purpose of this study is to demonstrate that the combination of the basal gastric transit study with the 14C-Urea Breath Test performed at different times (MIN 14C UBT) has the advantage of being representative of the whole stomach surface and constitutes a non-aggressive test. The test was performed on 180 patients with gastrointestinal disorders. All the patients had had an upper gastrointestinal endoscopy and specimens for histology and culture were taken. The determinations of the MIN 14C UBT were performed within 7 days of the endoscopy. 62 normal control volunteers were studied to find out the MIN 14C UBT cut off values for each time under study (limit curve). Two basal samples of the exhaled air were taken. Patients ingested 185 kBq (5 µCi) of 14C- urea and 11.1 MBq (300 µCi) of 99mTc-colloid. The patients were imaged with a gamma camera at 0, 5, 10, 15, 20, 25, 30, 45 and 60 minutes after the ingestion of the labeled solution. At the same times, the samples of exhaled air were collected, by duplicate, into glass vials containing Soluene-350, ethanol and phenolphthalein as pH indicator. Each breath sample was counted in a Liquid Scintillation Counter after the addition of Insta-Gel XF. The results were expressed according to Marshall and Surveyor (1988). The external detection of the 99mTc activity permits the determination of the probable location of H. pylori colonization in the gastroduodenal mucous membrane. The collection of multiple breath samples at different times, as well as the obtention of them by duplicate, assures the obtention of more reliable results and determines a decrease of false negative and positive cases, rising the sensitivity to 98% and the specificity to 96%. So, it is possible to determine simultaneously the production of 14CO₂ and the place where this process occurs. Due to its non-aggressiveness, we consider, that the MIN 14C UBT combined with the gastric basal transit allows a better interpretation of the localization of the H. pylori infection in the gastroduodenal tract, in the initial diagnosis of this pathology, as well as in the control of the treatment for its eradication.

OS-513

C. Galleguillos, P. González, T. Massardo, A. Morales, C. Pimentel, J.C. Gil, M. Rivera, R. Alay, S. Otárola. Nuclear Medicine and Gastroenterology, University of Chile.

SHOULD CARBON-14-UREA BREATH TEST BE THE GOLD STANDARD FOR HELYCOBACTER PYLORI DETECTION?

It is known the well demonstrated role of *Helicobacter Pylori* (HP) in the pathogenesis of gastritis, peptic ulcer disease and, perhaps, gastric carcinoma. Gastric biopsy and bacteria culture have been considered the gold standard for HP detection, even though, they have some shortcomings (invasiveness, cost, and their limited stomach sampling). Direct bacteria visualization in fresh frosts stained with Giemsa and urease tissue activity (CLO test) are also used. C-14-urea breath test is an alternative recently validated for the same purpose. It could replace the initial gold standard due to it represents urease activity in the whole stomach. We studied 77 patients (67% females; mean age 44±15 y.o.) referred for gastric endoscopy with diverse gastrointestinal symptoms. All had gastric biopsy (Giemsa, H-E and urease test) and C-14 breath test in the same day, using 1 uCi capsules. In the analysis: 1) if biopsy was considered the gold standard (55 positive and 22 negative) sensitivities for frosts and urease were 93% and 66% and specificities 55% and 68%, respectively. 2) if C-14 was considered the gold standard (65 positive and 12 negative) sensitivities for frosts and urease were 88% and 72% and specificities 66% and 75%, respectively; (p=ns for all) 3) if biopsy was the standard, C-14 sensitivity was 93% and specificity 36% 4) if C-14 was the standard biopsy sensitivity was 78% and specificity 67% 5) if a global standard was considered (frosts/biopsy/ureasa being ≥2 of them positive or negative) sensitivity of C-14 was 94% and specificity 62%. Concluding, it appears that there is no any real good gold standard for HP detection, but theoretically, C-14 could be a possibility that needs to be explored.

OS-514

G. Mariani, C. Mansi, G. Villa, G. Taddei, P. Calza, R. Fiscer, A. Remagnino, R. Costa, C. Maragliano, G. Curti, V. Savarino. Nuclear Medicine Service, and Gastroenterology Unit, DIMI, University of Genoa, Genoa (Italy)

SIMULTANEOUS DOUBLE ISOTOPIC EVALUATION, BY ¹³C-OCTANOIC BREATH TEST AND RADIOLABELED SOLID MEAL, FOR ASSESSING GASTRIC EMPTYING IN CONTROLS AND IN DYSPEPTIC PATIENTS.

The ¹³C-octanoic acid breath test has recently been developed for evaluating gastric emptying. This method is based on a solid meal labeled with octanoic acid tagged with the stable isotope, ¹³C. Octanoic acid, which is totally non absorbable in the stomach, is promptly absorbed in the proximal duodenum and oxidized in the liver to ¹³C-dioxide which is in turn exhaled; thus, ¹³C rapidly appears in the breath as a function of gastric emptying. This study reports a comparison of the results of the ¹³C-octanoic test with those of conventional gamma-scintigraphy.

A total of 22 subjects were studied: 10 healthy controls and 12 patients with chronic dyspepsia (8 idiopathic, 4 diabetic). The solid test meal was labeled simultaneously with both ¹³C-octanoic acid (100 mg) and with ^{99m}Tc-DTPA (74 MBq), mixed with scrambled eggs and bread toast. A dynamic scintigraphic acquisition over the abdomen was recorded for 1 hr (1 frame/min), while mass spectrometry was employed to measure mass enrichment in exhaled air at various intervals throughout the same period. In the dyspeptic patients the double-labeled study was repeated after a single test dose (25 mg) of the gastrokinetic drug, levosulpiride.

There was an excellent correlation (r=0.81, p<0.001) between the T_{1/2} of gastric emptying measured in controls by scintigraphy (59±9.7 min) and those derived by the ¹³C-octanoic test (64.5±11.2 min). The baseline gastric emptying T_{1/2} values were quite longer in the dyspeptic patients (122.7±26.7 min by scintigraphy versus 142.6±30.3 min by the breath test). In these patients acute treatment with levosulpiride resulted in T_{1/2} values significantly shorter with respect to baseline (83.8±26.9 min by scintigraphy versus 96.1±20.3 min by the breath test), although still longer than the values observed in control subjects.

The present results indicate that either the conventional radioisotopic scintigraphic method or the new stable isotopic method provide virtually superimposable results for evaluating gastric emptying.

OS-515

R. Bennink, M. Peeters, V. Van den Maegdenbergh, B. Geypens, M. De Roo, P. Rutgeerts, L. Mortelmans.

Dept. Nuclear Medicine UZ Leuven Belgium.

GASTRIC EMPTYING FOR SOLIDS IS SLOWER IN HEALTHY FEMALE- AS COMPARED TO MALE VOLUNTEERS.

There is increasing evidence of gender related differences in gastric emptying. The purpose of this study was first, to confirm the difference in a larger series for both solid and liquid test meal between men and women, and secondly, to investigate the origin of this difference by studying regional gastric emptying and antral motility.

Methods. 20 healthy women (studied in the first 10 days of the menstrual cycle) and 31 healthy age matched men underwent a standard gastric emptying test of a solid (Tc99m sulfur colloid, 230Kcal) and liquid (In111 DTPA water) test meal. Geometric mean gastric emptying data were fit to a modified power exponential function to determine the half-emptying time (T_{1/2}), lag phase (TLAG) and terminal slope. Additionally compartmental (proximal and distal) evaluation and dynamic imaging of the antrum for solids was performed.

Results. In concordance with previous reports, women had a longer halfemptying time for solids as compared to men (86.2 ± 5.1 vs. 52.2 ± 2.9 min. p<0.05). In our observations this seemed to be related to a significantly prolonged lag phase (43.7 ± 4.7 vs. 25.2 ± 2.2) and a significant decrease in terminal slope (1.5 ± 0.1 vs. 2.4 ± 0.1). Dynamic antral scintigraphy did not show a significant difference. The distribution of the test meal within the stomach (proximal vs. distal) showed more early proximal retention in women as compared to men. The terminal slope of the distal stomach was significantly lower in women. We did not observe a significant difference in gastric emptying of the liquid test meal between gender.

Conclusion. Gastric emptying of solids is significantly slower in healthy women as compared to men. These findings emphasize the importance of using different normal-values for clinical and research purposes in gastric emptying scintigraphy in men and women. It also enhances our previous opinion that slower gastric emptying in premenopausal women is not related to a decrease in antral motility.

OS-516

Zehra Özcan, Coşkun Özcan, Rüya Erinc, Ahmet Çelik, Ebru Teber and Oktay Mutaf. Ege University Medical Faculty, Nuclear Medicine and Pediatric Surgery Departments, İzmir, Turkey.

SCINTIGRAPHY IN DETECTION OF GASTROESOPHAGEAL REFLUX IN CHILDREN WITH CAUSTIC ESOPHAGEAL STRICTURES: A COMPARATIVE STUDY WITH BARIUM STUDIES AND 24 hr pH MONITORING

Gastroesophageal reflux (GER) is a frequent complication of caustic ingestion. Conventional therapy usually fails and an antireflux surgery becomes necessary. However, motility disturbances and strictures in esophagus may lead to misinterpretation in radiologic findings of GER. The present study aimed to determine the ability of scintigraphy to detect GER in children with caustic esophageal injuries in comparison with 24 hr pH metry and barium gastroesophagography studies. The study group consisted of 21 children with a previous history of caustic ingestion (mean duration 4.2 years). There were 5 girls and 16 boys. Age range was 22 months-16 years. All patients (pts) underwent gastroesophageal scintigraphy, barium gastroesophagography and 24 hr distal esophageal pHmetry within a period of one week. 24 hr ambulatory pH monitoring was performed using a glass electrode positioned 2 cm proximal to the upper limit of manometrically defined lower esophageal sphincter. Tc99m SC labelled milk/juice, with a volume adjusted to age, was administered orally (n: 13), otherwise through a nasogastric tube (n:3) or gastrostomy tube (n: 5) in cases with severe esophageal strictures to avoid poor esophageal clearance of orally ingested tracers which could lead to diagnosis of a false positive GER. Following feeding, 60 sec images of 64x64 matrix were recorded continuously for ≈ 45 minutes without any provocation. Gastric emptying was also assessed for each case. Scintigraphy correctly identified GER in 10 out of 15 cases who are found to have increased esophageal acid exposure documented by 24 hr pH metry. Barium studies could only detect reflux in 6 pts in whom scintigraphic studies were also positive. Up to date 7 pts with GER underwent antireflux surgery and were investigated by the above-mentioned modalities for the assessment of post-surgical outcome. Postoperative studies demonstrated no evidence of GER and gastric emptying rate was shortened (mean 48 %) when compared with the preoperative data. In conclusion, scintigraphy seems to be a useful method in the detection of GER even in cases with serious esophageal strictures and/or motility disturbances and offers reliable results in the assessment of follow-up after surgery.

Endocrinology/Thyroid

OS-517

I. Žagar, R.Han, S.Marković
Institute of Nuclear Medicine, Clinical Centre of Serbia, Belgrade

DIAGNOSTIC UTILITY OF THE ADRENAL CORTEX SCINTIGRAPHY WITH ⁷⁵Se-METHYLCHOLESTEROL

The aim of this study was to summarize the results of adrenocortical scintigraphy in 75 patients with clinically proven disfunctions of the adrenal cortex [21 with ACTH-dependent and 9 with ACTH-independent Cushing's disease, 35 with primary hyperaldosteronism (PH), 7 with hirsutism, 2 with congenital adrenal hyperplasia (CAH), 1 with adrenogenital syndrome], 25 patients with low-renin essential hypertension (LREH), and 13 with incidentally discovered clinically silent adrenal masses (INC). Adrenal cortex images were acquired (with/without Dexamethasone suppression) 2 to 7 days after i.v. injection of 11 MBq of ⁷⁵Se-methylcholesterol. Adrenocortical uptake was calculated according to Hawkins, using rectangular ROIs. In 88.8% of patients with Cushing's disease, early unilateral high adrenal uptake (mean 0.59 %) corresponded to glucocorticoid secreting adenoma, and in 90.4% bilateral visualization indicate hyperplasia of the adrenal cortex due to excessive pituitary ACTH secretion. When Dexamethasone suppression was performed prior to the adrenocortical scintigraphy in patients with PH, the initial sensitivity of 86.4% was enhanced to 100%. In 91% of patients with LREH normal suppressibility of the glomerular zone was found with significantly lower uptake than in patients with PH. The highest uptake was found in patients with CAH and adrenogenital syndrome (1.22%). In 4 of 13 subjects with INC (2 with the adrenocortical metastases of the lung carcinoma, 1 with the adrenal cyst and 1 with the metastases of unknown origin) uptake of the ⁷⁵Se-methylcholesterol was significantly reduced or absent. In 7 of 13 subjects with INC, unilateral visualization (by ultrasound, CT and MRI) was in accord with clinically "silent" adenoma. In a patient with asymmetrically enlarged glands, adrenal carcinoma was histologically confirmed.

OS-518

F.Tenenbaum, J.Samuel-Lajeunesse, JY Devaux, N Prat-Jude, J Pitre, Y Chapuis, B Richard.
Services de Médecine Nucléaire et de Chirurgie générale.
Hôpital Cochin, Paris, France.

USE OF QUANTITATIVE MYOCARDIAL UPTAKE OF ¹²³I-MIBG TO PREDICT PEROPERATIVE RISK IN PATIENTS WITH PHEOCHROMOCYTOMA.

An inverse relationship between visual cardiac uptake with ¹³¹I-MIBG and circulating catecholamines has been reported in pheochromocytoma (*Nakajo et al. J Nuc Med 1983*). The aim of this study was to determine if quantitative myocardial uptake of ¹²³I-MIBG could be a pronostic factor of peroperative complications in pheochromocytoma.

Methods: 10 patients with a benign pheochromocytoma and 10 controls (suspected but with no pheochromocytoma) were studied during the last 2 years, with urinary catecholamines assay. ¹²³I-MIBG scintigraphy was performed after injection of 100 MBq, at 4 hrs (for controls) and 24 hrs (for patients and controls). No patient received labetalol. Cardiac MIBG uptake was assessed by the heart to mediastinum activity ratio commonly used in severe chronic cardiac failure before transplantation (*Merler et al. Q J Nucl Med 1995*).

Results: Cardiac uptake at 4 hrs and at 24 hrs were correlated (p: 0.06). There is an inverse correlation between cardiac uptake and urinary metanephrines (p: 0.02). Six patients had a normal cardiac uptake (ratio>1.2) and no anesthetic complications. Four patients had a decreased cardiac uptake and needed more adrenergic drugs during surgery: one had a cardiogenic shock, one a pulmonary edema.

Conclusion: Quantitative myocardial uptake of ¹²³I-MIBG may be used to select patients with an increased peroperative risk. Measuring heart to mediastinum ratio during MIBG adrenal scintigraphy is a simple method which may be useful for anesthetic monitoring.

OS-519

R Barone, M Chianelli, A Giordano², WJM Looman¹, G Ronga, G Capriotti, G Galli², the "IMDIAB Study Group, A Signore Nu.M.E.D. Group, II Clinica Medica University "La Sapienza" and ²Medicina Nucleare, University "Cattolica del Sacro Cuore", Rome, Italy. ¹Mallinckrodt BV, Holland.

99mTc-HIG SCINTIGRAPHY IN NEWLY DIAGNOSED TYPE 1 DIABETES PREDICTS BETTER METABOLIC CONTROL

Approximately 10-20% of newly diagnosed type 1 diabetes (IDDM) patients benefit of an adjuvant immunotherapy. We previously described that 40% of newly diagnosed IDDM patients accumulate 99mTc-HIG in the pancreas. In this study we evaluated if this subgroup of patients have a different clinical response to an adjuvant immunotherapy. We studied longitudinally for 1 year 40 recent onset IDDM patients (13 females e 27 males, mean age 16.05±8.61) undergoing the IMDIAB V trial where nicotinamide and the BCG vaccine are given at diagnosis. Metabolic and immunological parameters (HbA1c, C-peptide, insulin requirement, lymphocyte subsets, autoantibodies) were studied at diagnosis and every 3 months. SPET HIG scan of the abdomen was performed at time of onset and after 1 year and pancreatic/bone (P/B) ratio was calculated and correlated with metabolic and immunological markers. Results showed that patients with positive HIG scan at time of IDDM onset (n=10; P/B > 4.49) had a lower daily insulin requirement at 9 months follow-up (p<0.04) and higher C-Peptide values (p<0.05) after 1 year compared to IDDM patients with a negative scan at diagnosis. Thus HIG scintigraphy may contribute to select patients with residual beta-cell mass at time of diagnosis who benefit of an adjuvant therapy.

*The IMDIAB Study Group: P Pozzilli, N Visalli, MG Baroni, R Buzzetti, L Nisticò, E Fioriti, C Mesturino, A Signore, MG Cavallo, L Lucentini, MC Matteoli, A Crinò, C Teodonio, R Amoretti, F Paci, M Ruggeri, L Pisano, C Suraci, MG Pennafina, B Boscherini, S Stoduto, MT Fonte, F Batelli, G Multari, MA Suppa, GC De Mattia, M Cassone Faldetta, O Laurenti, ML Mancabitti, G Marietti, D Pitocco, F Ferrazzoli, C Bizzarri, AV Greco, G Ghirlanda.

OS-520

G Blomqvist, G von Heijne, M Ingvar, JO Thorell, S Stone-Elander, M Alvarsson, K Ekberg, L Widén
INSERM U334, SHFJ, CEA, Orsay France, and Departments of Clinical Neuroscience, Endocrinology and Physiology, Karolinska Hospital, and Karolinska Pharmacy, Stockholm Sweden

THE EFFECT OF HYPERKETONEMIA ON THE CEREBRAL UPTAKE OF KETONE BODIES IN HEALTHY CONTROLS AND IDDM PATIENTS

In a previous study of the cerebral uptake of ketone bodies in healthy humans using R-β-[1-¹¹C]hydroxybutyrate ([¹¹C]-βHB) and PET it was found that the net uptake of ketone bodies increases almost linearly with increasing concentration of ketone bodies in the blood and, further, that the brain tissue concentration of ketone bodies is very low, indicating that the transport across the blood-brain barrier is the rate limiting step. In the present study the ketone body utilization in healthy controls and in IDDM patients were compared at hyperketonemia using the same tracer method.

Six healthy subjects and six well controlled IDDM patients participated in the study. Infusion of unlabeled β-HB started one hour before the bolus injection of [¹¹C]-βHB (PET scan duration 10 min). The time course of the radioactivity in blood and the concentrations of β-HB, [β-HB], were measured. For kinetic analysis a two tissue compartment model with three rate constants was applied.

The resulting [β-HB] in blood was found to be constant in time within 5% during the PET scan: 0.97±0.33 μmol/ml (average±SD) for the controls and 1.28±0.31 μmol/ml for the IDDM patients, compared to 0.043±0.029 μmol/ml found at normoketone (previous study).

The ketone body utilization was found to be nearly proportional to [β-HB] also at hyperketonemia. No significant difference in this relationship could be detected between the controls and the IDDM patients. Further, the ratio between the concentrations of β-HB in the brain tissue and the blood was found to remain very low in both groups (0.0032 ±0.0025 for controls, 0.0074±0.0019 for IDDM patients, compared to 0.0065±0.009 found at normoketone in the previous study). In conclusion, the brain tissue concentration was found to increase with increasing [β-HB]. The results indicate that also at high blood levels the brain increases the metabolism of ketone bodies in response to increased delivery of these compounds. No difference in ketone body utilization could be detected between IDDM patients and healthy controls.

Endocrinology/Thyroid

OS-521

H.-J. Baumgart¹, K. Badenhoop², H. Donner², L. Gebhard¹, I. Kobel¹, H. Langhammer¹, C. Hirsch¹, R. Senekowitsch-Schmidtko¹, M. Schwaiger¹

¹Nuklearmedizinische Klinik, Klinikum rechts der Isar, TU München, FRG
²Medizinische Klinik I, Zentrum der Inneren Medizin, Klinikum der J.W. Goethe-Universität, Frankfurt/M., FRG

HLA DQA1*0501 AND CTLA4 (ALA-17) DO NOT CONFER SUSCEPTIBILITY TO IMMUNO-HYPERTHYROIDISM AFTER IODINE 131 THERAPY OF AUTONOMOUS GOITRE

Autoimmunhypertyreoidismus ist eine organ-spezifische autoimmune disease and shares susceptibility alleles of major histocompatibility complex class II human leucocyte antigen (HLA) DQA1 genes. Another candidate gene for susceptibility is the cytotoxic T-lymphocyte antigen 4 (CTLA4) gene located on chromosome 2. The development of immunohypertyreoidismus after iodine 131 treatment of autonomous goitre is a rare disorder whose etiologic factors are still unknown. In view of a possible genetic predisposition we investigated the distribution of HLA DQA1*0501 and CTLA4 exon 1 polymorphism (49 A/G) in 24 patients (8 m, 16 f) who developed hyperthyreoidismus after iodine 131 treatment of autonomus goitre. The polymorphism was analysed by SSP-PCR, single strand conformation polymorphism, and restriction fragment length polymorphism analysis. There was no higher frequency of HLA DQA1*0501 in comparison to healthy controls (n=271; 33 vs 43%). Also no association could be found with the CTLA4 Ala-17 allele (37vs 36%). However, HLA DQA1*0501-positive patients had higher levels of TSH receptor autoantibodies than negative patients (158±48 U/l vs 53±18 U/l, p<0.05). In conclusion, there seems to be no immunogenetic predisposition controlling susceptibility to immunohypertyreoidismus in patients after iodine 131 therapy of autonomous goitre, with the exception of high levels of TSH receptor autoantibodies in patients sharing HLA DQA1*0501 alleles.

OS-522

Ph.Rondogianni, G.Ioannidis#, I.Lekatsas*, V.Vassiliou#, H.Giannopoulou, E.Houssianakou, N.Thalassinos#, K.Alevizaki, M.Kesse-Elias.

Dpts of Nuclear Medicine and Medical Physics, First Cardiology* and Endocrinology#, «Evangelismos» Hospital, Athens, Greece.

TI-201 TOMOGRAPHIC SCINTIGRAPHY IN TYPE II DIABETES MELLITUS: CORRELATION WITH THE PRESENCE OF MICROALBUMINURIA AND DIABETIC RETINOPATHY.

Introduction: The presence of reversible defects in TI-201 tomographic cardiac scintigraphy (TI-SPECT) is a strong prognostic index of severe cardiac events. In this study we examined whether the presence of microalbuminuria (MG) or/and diabetic retinopathy (DR) in patients with diabetes mellitus, correlates with high prevalence of ischemia in TI-SPECT, probably due to a common pathogenetic mechanism.

Patients and methods: Twenty three patients, all with type II diabetes mellitus, 19 men and 4 women, aged 46-68 years (m.v.58.2±1.39yrs), were studied. The values of glycosylated haemoglobin (HbA1c) were 5.5-11.6% (mv=8.08±0.36%) 6/23 patients had MG, 8/23 had DR, while 13 patients had none of the two. All patients have had a TI-SPECT study after i.v. infusion of dipyridamole followed by a 4h redistribution TI-SPECT. If necessary a 1mCi TI-201 reinjection study was then performed. The presence of reversible defects was then evaluated. Results were analyzed statistically by the X2 test, Spearman Rank Correlation or ANOVA analysis.

Results: The presence of reversible defects in TI-SPECT had positive correlation with the presence of DR (p<0.043). A similar trend, but not statistically important (p=0.06) was found with the presence of MG. The presence of of none (group 0), only 1 (group 1), or both (group 2) factors had positive correlation with the presence of reversible defects in TI-SPECT (15%, 50% and 75% of the patients respectively had abnormal TI-SPECT study p<0.02). There was no correlation between the presence of ischemia in TI-SPECT and the age, hypertension, hyperlipidemia, and the levels of HbA1c.

Conclusions: TI-SPECT seems to be a useful method for the early diagnosis of ischemic cardiopathy, in patients with type II diabetes mellitus, especially in the presence of MG and/or DR.

Radiopharmacy and radiochemistry: Molecular biology/peptides

OS-523

L.G. Strauss, Y.M. Zhang, A. Dimitrakopoulou-Strauss, M. Schwarzbach, F. Willeke, T. Heichel, F. Oberdorfer, M. Voim

German Cancer Research Center, Heidelberg, Germany.

FUNCTIONAL STUDIES WITH F-18-DEOXYGLUCOSE, C-11-AMINOISOBUTYRIC ACID, O-15-WATER, AND Tc-99m-SESTAMIBI: CORRELATION WITH MULTIDRUG RESISTANCE, MULTIDRUG RESISTANCE-ASSOCIATED PROTEIN, AND GLUCOSE TRANSPORTER GENE EXPRESSION

Positron Emission Tomography (PET) was performed with F-18-Deoxyglucose (FDG), C-11-Aminoisobutyric acid (AIB), and O-15-Water in patients with soft tissue sarcomas and bone tumors during the initial tumor staging or for the detection of tumor recurrence. Dynamic PET studies were acquired and iteratively reconstructed cross sections (256x256 matrix) were quantitatively evaluated using a ROI technique and the calculation of standardized uptake values (SUV). Dynamic studies with Tc-99m-Sestamibi were performed prior to the PET examination. All patients were examined prior to any chemotherapeutic treatment. Tumor tissue specimens were obtained by surgery and analysed with the semiquantitative reverse transcription-polymerase chain reaction (RT-PCR) assay for the multidrug resistance gene expression (mdr1), the multidrug resistance-associated protein gene expression (mrp) and the glucose transporter 1 (glut1) expression. The evaluation of the ongoing study includes 14 patients. We were able to compare the experimental results to 14 FDG patient studies as well as to 7 multitracer studies. A significant correlation was found for the FDG accumulation in the tumors and the glut1 expression (r=0.6679, p<0.009). The multiple regression analysis demonstrated a correlation coefficient of r=0.7045 for mdr1 (dependent variable), FDG and O-15-Water. Multidrug resistance was associated with both low perfusion values and FDG uptake values. The mrp expression was lower than the mdr1 expression in all tumors and no significant correlation was observed for mrp and the PET tracers. The Tc-99m-Sestamibi uptake was significantly increased in all tumors and did not correlate with the mdr1 and mrp expression. The results show, that multidrug resistance is associated with low tumor perfusion and FDG uptake.

OS-524

S.C. Srivastava, S.J. Gately, G.E. Meinken, P. Freimuth, B. Pyatt, N.D. Volkow.

Brookhaven National Laboratory, Upton, NY.

DETERMINATION OF VIRAL BINDING SITES IN RODENTS USING I-131 LABELED ADENOVIRAL FIBER PROTEIN (AVFP)

Purpose: This study was undertaken to quantify rodent tissue binding sites for adenoviruses. Adenoviruses are good candidate vectors for gene therapy because of their easily manipulated genomes and high frequencies of foreign gene expression. **Methods:** Studies with cultured cells have shown that the initial step in infection is binding of a type-specific "adenoviral fiber protein" (AVFP) to cell membrane receptors. AVFP from adenovirus type 2 was labeled with I-131 in >85% yield using the lodogen method in pH 7.0 phosphate buffer. Free I¹³¹ was removed by repeated ultrafiltration. I-131 AVFP was incubated with tissue homogenates (30°C for 2h) in tris buffered physiological medium. Biodistribution and ARG studies were also carried out. **Results:** Rat tissue binding sites from a saturation analysis were in the order: liver>brain, kidney, heart>spleen>lung. Kd and β_{max} values of 2 nM and 12.5 pmol/g tissue wet wt were obtained in brain. Linear Scatchard plots suggested one class of sites and both association and dissociation rates were consistent with a nanomolar value for Kd. Similar results were obtained in mice except that β_{max} values were lower and Scatchard plots suggested >1 binding site. ARG in rats after i.v. injection of AVFP revealed high concentration of radioactivity in the thyroid and spleen but exclusion of AVFP from the brain and spinal cord. The lung showed the next highest concentration. The liver, trachea, testis and kidney cortex were also visualized. Mouse biodistribution studies gave similar results. **Conclusion:** Our studies document for the first time the widespread distribution of high affinity binding sites for labeled AVFP. Although I-131 AVFP is not the ideal radioligand, these studies do support the possibility of quantifying adenoviral binding sites in human tissues, which could be important for gene therapy using modified viral vectors.

This work was supported by the U.S. Dept. of Energy, Office of Biological and Environmental Research, under Contract No. DE-AC02-98CH10886.

OS-525

W.H. Bakker, D.J. Kwekkeboom, M.E. van der Pluijm, J. Erion, and E.P. Krenning.

Departments of Nuclear and Internal Medicine. University Hospital Rotterdam, The Netherlands and Mallinckrodt Medical, St Louis, Missouri, USA.

IN-111 LABELING EXPERIENCES WITH DOTA-CHOLECYSTOKININ

Tumors with receptors for cholecystokinin (CCK), e.g. medullary thyroid carcinoma and small cell lung cancer, are potentially suitable for visualisation and treatment with radiolabeled analogues of CCK. In this study the labeling of a newly synthesized CCK-analogue, DOTA-D-Asp-Tyr-Nle-Gly-Trp-Nle-Asp-Phe-NH₂ (DOTA-CCK-8) was investigated with the ultimate goal of preparing a kit-formulation for human use. The DOTA-chelating group was chosen because it can be stably labeled with radiometals for scintigraphy as well as for future radionuclide therapy. To improve labeling yields, strictly metal-free components were used throughout the whole procedure to circumvent many problems which are usually encountered in labeling DOTA-ligands. Coupling radiometals to the DOTA-group requires a heating step. Therefore, the stability of the compound was investigated by HPLC (UV-absorption) after various heating times at different temperatures. In contrast to our experiences with the stable (cyclic) DOTA-octreotide, HPLC showed major degradation of the (linear) CCK-analogue after heating during 1 h at 100 C, but not at 60 C. A formulation was developed on the basis of 50 % of a future human injection, i.e. 10 µg DOTA-CCK-8 in 10 µL 0.005 M sodiumbicarbonate in MilliQ-water, 42 µL of 12 mg gentisic acid /mL in 0.05 M acetic acid in MilliQ-water, 24-50 µL 0.2 M ammoniumacetate buffer (pH 5) in MilliQ-water and 111 MBq In-111-chloride in 177-360 µL 0.05 M HCl. Less reaction volume (e.g. 24 µL buffer and 177 µL In-111-chloride) was used depending on the precalibration of In-111. All labeling experiments were done with a 100-fold excess of peptide over radionuclide on different days before and on the calibration date of In-111 with various reaction volumes. As the speed of coupling is dependent on the concentration of the peptide as well as the radionuclide: $v = k * [In-111] * [DOTA-CCK-8]$ the highest yields are expected in the smallest reaction volumes, i.e. far before the calibration time of In-111-chloride. The reaction volume could be further reduced during the heating step by removing the radiation quencher (gentisic acid), without deteriorating the peptide as shown by HPLC. Typically, labeling yields exceeded 95 % but occasionally low labeling yields (till 50 %) occurred. From experiments done under various conditions it was shown that the lowest labeling yields were obtained from vials which contained 185 MBq In-111 (in 0.5 mL) on the calibration date ($p < 0.01$). This indicates that the volume of HCl in the In-111-chloride manufacturer vial can become surprisingly a yield limiting parameter in labeling of DOTA-containing peptides with In-111, probably due to higher concentrations of contaminants (metals and/or organic compounds) in smaller delivered volumes of In-111-chloride solution.

OS-526

HK Lu, RS Zhu, J Zhu

Department of Nuclear Medicine, Shanghai Sixth People's Hospital, Shanghai 200233, China.

BIODISTRIBUTION OF 125I-LABELLED ANTISENSE PROBE TO c-myc ONCOGENE mRNA IN NUDE MOUSE BEARING HUMAN COLON CANCER

Purpose: We have radiolabelled the antisense oligonucleotides to c-myc messenger RNA (mRNA) with 125I and intended to use the radiolabelled-antisense probe as a suitable non-invasive imaging technique and also an enhanced treatment to human colon cancer. **Methods:** 15-mer oligonucleotides specific for hybridization with c-myc mRNA was synthesized in both phosphodilester (oxo) and phosphorothioate (thio) forms, with the sense sequence (oxo) synthesized for control. Each sequence was iodinated with 125I by modified TICl₃ labelling method and free 125I was eluted by Sephadex G-50 column. Iodinated-oligonucleotides were conjugated with diethylenetriamine pentaacetate (DTPA) and purified through DAEA sephadex column. The radiolabelled compounds (about 50 uCi/ each) were injected into 54 nude mouse bearing solid human colon cancer with tumor sizes varying from 0.5 to 1.2 g. The c-myc mRNA expression in the colon cancer cells was pre-determined by histoimmunoassay. **Results:** The uptakes of antisense probes in the tumor tissues were significantly higher than those of the sense probes ($P < 0.001$). The peak uptake of oxo antisense in the tumor appeared earlier (at 2 hr after the injection) than that of thio antisense (at 4 hr) and also much higher ($p < 0.01$), but the tumor and blood clearances of thio probe were much slower than those of oxo probe. **Conclusion:** The study indicates that the radiolabelled antisense probe to oncogenes may be a feasible technique for tumor imaging and treatment. However, higher and stable tumor uptakes of the antisense probes should be developed before this technique comes to be a reliable practice.

OS-527

Y.M. Zhang, L.G. Strauss, A. Dimitrakopoulou-Strauss, M. Schwarzbach, F. Willeke, T. Heichel, M. Volm

German Cancer Research Center, Heidelberg, Germany.

ASSESSMENT OF MULTIDRUG RESISTANCE GENE EXPRESSION, MULTIDRUG RESISTANCE-ASSOCIATED PROTEIN GENE, AND GLUCOSE TRANSPORTER IN SARCOMAS

The multidrug resistance gene expression (mdr1) and the multidrug resistance-associated protein gene (mrp) were evaluated with the semiquantitative reverse transcription-polymerase chain reaction (RT-PCR) assay using tumor tissue specimens. Furthermore, the glucose transporter 1 (glut1) was assessed and compared to mdr1 and mrp. All tissue samples were collected from surgically removed tumor specimens from soft tissue sarcomas and bone sarcomas. All tissue samples were obtained prior to any chemotherapeutic treatment.

Eighteen tissue specimens were included in the evaluation. The semiquantitative evaluation was based on a RT-PCR method, and mdr1, mrp and glut1 were quantified with reference to beta-actin. The mdr1 expression was increased (>50 % of the reference level) in 4/18 tumor tissue samples (mdr1/reference ratio: mean: 0.346, standard deviation: 0.281), whereas the mrp levels were generally significantly lower (mrp/reference ratio: mean: 0.054, standard deviation: 0.055). The mrp expression in all samples was less than 20 % as compared to the reference probes. Furthermore, no measurable mrp expression was observed in 6/18 tumor samples. In contrast, the glut1 expression was increased in 14/18 specimens (glut1/reference ratio: mean: 0.872, standard deviation: 0.498). No significant correlation was observed for mdr1, mrp and glut1. However, cluster analysis using the weighted pair-group average method with squared Euclidean distances identified a subgroup (n=3) with high mdr1 expression levels and low glut1 expression. In contrast, the mdr1 expression was generally low in all samples if glut1 was increased. This directs to an association of low tumor metabolism and resistance to chemotherapy.

The results demonstrate, that the mdr1 expression is increased in 22 % of the untreated sarcomas, while the mrp expression is low in all malignant lesions. The cluster analysis gave evidence for an association between low glut1 expression and presence of multidrug resistance.

OS-528

J.E. Vazquez, ¹G. Pimentel, ²A. Perera, J. Gaviñondo, ¹J. Oliva, ³R.P. Baum.

Center for Genetic Engineering, Div. of Immunotechnology; ¹National Institute of Oncology, Dept. of Nuclear Medicine; ²Center for Clinical Research, La Habana, Cuba; ³Central Clinic (PET Center), Bad Berka, Germany

PRODUCTION AND PRECLINICAL EVALUATION OF AN ANT-CEA scFv-ANTIBODY FRAGMENT FOR IMMUNO-SPET/PET

The purpose of our efforts is to produce a biomolecule of small size, therefore rapid biokinetics, fast penetration capabilities, and low (or no) immunogenicity which binds specifically to the carcinoembryonic antigen (CEA) for immuno-SPECT (Tc-99m) and immuno-PET (Tc-94m) studies.

Methods. From hybridoma cells genetic material, we have generated a recombinant single-chain antibody fragment (scFv-antibody) specific to CEA and able to substitute an intact murine monoclonal IgG1 antibody also developed by our group which is used in clinical routine since many years.

Results. Expression in methylotrophic yeast (*Pichia pastoris*) using 5 liter fermentors (Biolaffite, France) yielded 0.6 gram per liter of soluble and active protein as was demonstrated by ELISA. Immunocytochemistry studies showed a positive recognition of LoVo cell line, a CEA-expressing human carcinoma, by the scFv-molecule.

Under GMP conditions, the protein was purified at 90% or higher by Metal Affinity Chromatography employing a pH gradient. Labeling with Tc-99m yielded 96% radiochemical purity of the product, without major effects on biologic activity. Biodistribution studies were done in mice, in comparison to non-recombinant Fab' fragments and the whole antibody molecule. Results showed a normal organ distribution up to 24 hrs. Clinical studies with the Tc-99m labeled product are currently underway.

Physics and instrumentation: Quality assurance

OS-529

D. Lange ⁺, U. B. Noelpp ⁺⁺, A. Nagel ⁺, P. Ritter ⁺⁺

⁺ Department of Nuclear Medicine, University of Heidelberg, FRG
⁺⁺ Department of Nuclear Medicine, University of Berne, Switzerland

DEADTIME PERFORMANCE OF SINGLE-HEAD AND COINCIDENCE CAMERA-SYSTEMS AT EXTREMELY HIGH COUNTRATES

NEMA-evaluated countrate-losses embellish the more the instruments performance the worse it responds to the input countrate. This is due to wrong assumption the lowest measured countrate might be unaffected by countrate-losses.

Materials and Methods: Different sources are measured at strictly constant conditions. Source strength is varied by radioactive decay of one single source, or for several different sources by pipetting well known volumes from a stock solution of (in principle unknown) activity. Each countrate is corrected specifically for the decay of each individual source. Countrates per normalized activity - i.e. the efficiency - is plotted (on log scale) against the normalized activity (lin scale).

Exponential decrease of efficiency (paralyzable model) with increasing activity is verified far beyond the measurable countrate maximum. Linearized results are fitted simply. Results are extrapolated to activity zero yielding the ideal countrate per activity without any countrate-loss. From this the 10 % loss-values (in accordance to NEMA recommendations) and the deadtime itself are calculated directly. The efficiency curves are independant on the losses, even of the lowest source, which is the main dissimilarity to the known NEMA procedure.

Results: Our procedure discovers instruments that broaden the energy-window to yield higher countrates without any better performance i.e. with constant or even increased countrate loss at the same photon fluence. The influence of correcting circuits - i.e. homogeneity - on deadtime can be demonstrated quantitatively.

camera system	deadtime (µs)	output cps 10 % loss	input cps 10 % loss	maximal output cps	maximal input cps
slow, 10 y old	4.40	21.6 kcps	24 kcps	84 kcps	227 000
fast, 10 y old	1.40	68 kcps	76 kcps	262 kcps	720 000
2 head, single m.	0.11	900 kcps	1 mill cps	3.5 mill cps	9.5 mill cps

Conclusions: The method is simple and reproducible. With pipetted activities the deadtime of any counting system can be measured unambiguously within less than one hour. Using decaying sources not more than 3 halflives are necessary for a complete evaluation. Integral correction factors for countrate loss are calculable from output countrate. The method opens an outlook to solve the question whether there might be a basic deadtime parameter inherent to the instrument that is independant on the chosen window width.

OS-530

E. Gremillet, A. Champaillet, S. Guillot

Centre d'Imagerie Nucléaire, Saint-Etienne, France

TWO-DIMENSIONAL KOLMOGOROV-SMIRNOV (2DKS) TEST AND GAMMA-CAMERA UNIFORMITY CONTROL: EXPERIMENTAL COMPARISON WITH OTHER INDEXES.

The 2DKS test compares an observed 2D distribution to a theoretical one and thus could be used to assess gamma camera uniformity. We compared the 2DKS results with NEMA integral uniformity (IntUnif) and the variance-to-mean ratio (VtoM) at various total counts (TC), point source off-axis shift (OAShift), and energy window shift (EShift). 256x256 floods were acquired on an uncollimated camera with a Tc-99m point source placed 2.5m away. CFOV was considered for IntUnif and a similar ROI for VtoM and 2DKS. Immediately after a 100Mcts uniformity correction matrix acquisition with a 20% energy window at 140keV, a 1Mcts flood was first acquired and then 16 other floods by varying: i)TC: 2, 4, 8 and 16Mcts; ii)OAShift: 5, 10, 15 and 20cm; iii)EShift: -10, -5, +5 and +10keV. The probability level p by the 2DKS test was obtained using a formula previously established from Monte-Carlo simulations performed in our lab, suited to large numbers of events; p values above 0.05 were considered NS (ie the flood image was not significantly different from a uniform one).

Total Counts (Mcts)	1	2	4	8	16
IntUnif(%)	5.46	3.78	3.10	1.85	1.67
VtoM	1.033	1.028	1.046	1.060	1.093
2DKS p	NS	NS	NS	NS	NS
Off-Axis Shift (cm)	0	5	10	15	20
IntUnif(%)	5.46	5.98	5.77	6.11	5.98
VtoM	1.033	1.032	1.034	1.038	1.022
2DKS p	NS	NS	NS	NS	0.033
Energy Shift (keV)	-10	-5	0	+5	+10
IntUnif(%)	10.12	6.25	5.46	5.21	6.28
VtoM	1.079	1.052	1.033	1.043	1.044
2DKS p	0.000	0.000	NS	NS	0.000

Conclusion: in contrary to IntUnif and VtoM, the 2DKS test was not sensitive to TC, thus suggesting its usefulness for fast uniformity controls at relatively low TC, while being at least as sensitive to other perturbations like OAShift or EShift.

OS-531

B.H. Brinkmann, M.K. O'Connor, T.J. O'Brien, B.P. Mullan, R.A. Robb

Departments of Physiology, Radiology and Neurology, Mayo Foundation, Rochester, Minnesota, USA

DUAL ISOTOPE TOMOGRAPHIC STUDIES OF Tc-99m HMPAO AND I-123 IMP IN THE BRAIN: VALIDATION IN A PHANTOM MODEL USING MULTI-SPECTRAL ACQUISITION

Purpose: The aim of this study was to develop and validate an accurate method for the simultaneous acquisition of Tc-99m and I-123 SPECT images of the brain. **Methods:** A multi-compartment 2-D Hoffman brain phantom was filled either with Tc-99m, I-123 or a 3:1 mixture of the 2 isotopes. Planar and SPECT images were acquired on a dual-head gamma camera system equipped with fan-beam collimators. Thirty-two energy windows (2 keV width) were acquired over the energy range 120-184 keV. From the planar data, the signal to noise characteristics and crosstalk was measured for each energy window and used to devise an energy window acquisition strategy. This strategy was then applied to the SPECT data. From the 32 energy bands, 3 summed energy windows were created: a primary Tc-99m image (11.5% asymmetric window from 130-146 keV), a primary I-123 image (10% asymmetric window from 152-168 keV), and a secondary Tc-99m/I-123 crosstalk image (4.3% asymmetric window from 134-140 keV). A fraction (0.041) of this crosstalk image was subtracted from the I-123 image to compensate for Tc-99m crosstalk. No crosstalk correction was performed on the Tc-99m image, as I-123 contamination in the Tc-99m window was small and was dominated by spatially uncorrelated scatter and septal penetration. Planar and SPECT studies of both isotopes acquired using a 20% standard energy window and a 10% asymmetric window were used as reference standards. **Results:** Planar Images: Results showed 1.3% crosstalk in the I-123 image compared with 19.7% for a 10% asymmetric energy window alone. I-123 crosstalk into the Tc-99m window was 2.8% and was fairly constant with changes in the position of the Tc-99m energy window. **Tomographic Images:** Results showed 1.5% crosstalk into the I-123 image compared with 12.4% for the uncorrected image. There was 3.7% crosstalk from I-123 into the Tc-99m image. The difference image between the reference I-123 image and the crosstalk-corrected I-123 image (normalized to mean cerebral pixel count) was dominated by reconstruction noise, suggesting that residual artifacts due to the dual isotope acquisition were small. **Conclusion:** An effective technique for the simultaneous acquisition of Tc-99m HMPAO and I-123 IMP distribution in the brain has been developed and validated in a phantom model. This technique should have clinical application in functional activation studies of the brain with these two radiopharmaceuticals.

OS-532

AJ Green, KL Adamson, RHJ Begent

Department of Clinical Oncology, Royal Free Hospital School of Medicine LONDON, NW3 2PF, UK

INITIAL VALIDATION OF GAMMA CAMERA PET IMAGING FOR SERIAL MEASUREMENTS OF 18F-FDG UPTAKE.

Dual head gamma cameras capable of imaging in coincidence mode can make serial measurements of 18F FDG uptake over the course of an anti cancer treatment. This promises a relatively cheap and accessible tool for following the time course of tumour glucose metabolism in clinical trials and in routine practice. In order to make serial measurements the imaging system must have a linear response for the range of activity densities expected in patients. We have used phantom studies to investigate the response of a dual headed ADAC gamma camera.

A standard elliptical phantom (Data Spectrum) was filled with a solution containing 18F FDG; images were acquired with a range of activities in the phantom (340 M Bq - 11 M Bq). Acquisition data sets consisted of a single rotation of 32 azimuths over 180 degrees; two energy windows were set for each head, one centred on the 511 keV photopeak the other in the Compton region. peak-peak and peak-Compton coincidence events were acquired; the average time per view was 40s (the acquisition software automatically compensates for 18F decay). The singles rate seen by each head was recorded for each acquisition.

Images were reconstructed using the ADAC ordered subset maximum likelihood method (2 iterations with 8 subsets) uniform elliptical attenuation was applied. The uniform section of the phantom covered 8 slices of the reconstructed images. A region of interest was set at half the maximum pixel count for the image in the centre of the uniform section and applied to all slices in this section; the total counts in this region for each slice were recorded on a spreadsheet for analysis.

The singles rate was seen to be linear with phantom activity when the activity was less than 100 M Bq. Reconstructed image quality deteriorated with phantom activity greater than 100 M Bq with no interpretable image from activities greater than 150 M Bq. Only data sets with phantom activity less than 100 M Bq were used for further analysis. In all these image sets the total counts in the region increased towards the centre of the phantom (towards the centre of the camera face). Image counts were linear with phantom activity with phantom activity less than 50 M Bq.

The usable range of the camera is in accordance with the manufacturers recommendations. These results emphasise the need for strict adherence to tight administration and imaging protocols and careful repositioning of patient and camera for serial studies. Under these conditions valuable information can be obtained from gamma camera PET systems.

OS-533

B. E. Zimmerman and J. T. Cessna

Physics Laboratory, National Institute of Standards and Technology, Gaithersburg, MD, USA; *Nuclear Energy Institute, Washington, DC, USA.

DEVELOPMENT OF A TECHNIQUE TO DETERMINE EXPERIMENTAL DOSE CALIBRATOR SETTINGS OF VERY SHORT-LIVED ISOTOPES: THE CALIBRATION OF CU-62PTSM

A new method will be presented that enables the experimental determination of dose calibrator factors for short-lived radionuclides without requiring knowledge of the activity of the solution prior to measurement on the dose calibrator. The method was utilized in the recent calibration of Cu-62PTSM by the National Institute of Standards and Technology (NIST). This NIST-traceable calibration is one of the requirements for approval by the United States Food and Drug Administration for new radiopharmaceuticals marketed in the United States. Because of the extremely short (9.67 min) half-life of the Cu-62, the conventional method of measuring the activity and consequently "dialing in" the correct setting on the dose calibrator cannot be applied. In this new technique, we determine a response curve of apparent activity versus dial setting for the dose calibrator using solutions of the radionuclide in the geometry in which it will be counted in the hospital. The specific activity of the Cu-62 solution is then determined using 4πβ liquid scintillation counting with H-3 - standard efficiency tracing on samples that are gravimetrically related to those used to determine the dose calibrator response curve. The dose calibrator setting can then be determined from a polynomial fit to the response curve. Using this method, we determined dial settings for Cu-62PTSM in NIST-standard 5 mL glass ampoules and 35 mL polyethylene syringes using the NIST Capintec CRC-12. These newly-determined calibrator settings differ from the manufacturer's suggested setting by 11 % in the activity and now enable radioassays of Cu-62 to be made with an accuracy of better than 3 %. Details of this protocol and source preparation will be presented. Analysis of associated uncertainty components will be discussed, as will planned extensions to other positron-emitting radionuclides.

OS-534

U. Jaeger, O. Lang, H. Bihl

Department of Nuclear Medicine, Katharinenhospital Stuttgart, Germany

FDG-PET IMAGING OF TUMOR PATIENTS WITH IMPLANTED METALLIC MATERIAL.

Background: In FDG-PET studies of oncological patients, an increased F-18-FDG signal was observed in the surroundings of metallic implantations (e.g. hip-endoprothesis). This effect may either be caused by malignant tumor or by reconstruction artifacts due to the high density gradient between metallic material and human tissue.

Purpose: FDG-PET phantom study for the evaluation of the FDG signal in the surroundings of metallic material.

Method: As phantom, an original hip endoprothesis in a water-environment of uniform activity concentration (AC; 50 kBq/ml F-18-FDG) was used. FDG-PET scans in this experimental setting were performed and quantitative analysis of the above effect was done. A Siemens ECAT EXACT 47 scanner was used and acquisition time for the emission and transmission scans were 10 and 6 min., respectively. Image reconstruction was done by two methods, (1) by a filtered back projection method (FBP) and (2) an iterative maximum likelihood method (IRT).

Results: Although the water (background) AC in the phantom was uniform, an increase of the F-18-FDG-signal up to 50% using the FBP method and 20% using IRT was found in the direct surroundings of the prothesis. This effect was mainly present in the attenuation corrected scans. The smoothing effect of the transmission scans (due to their poor count rates) could be identified as main reason for these artifacts.

Conclusion: At the present time, IRT without attenuation correction seem to be the most adequate method for FDG-PET image generation to avoid false positive results in patients with metallic implantations.

General nuclear medicine: Bone

OS-535

R. Kashyap, A. K. Mishra, R. Sharma P. Mishra, M. K. Chopra, V. Jain

Depts of Nuclear Medicine, Radiopharmaceuticals, and Biocybernetics Institute of Nuclear Medicine and Allied Sciences, Delhi-54, India

CLINICAL EVALUATION OF A NEW Tc-99m LABELED BIFUNCTIONAL CHELATING AGENT-IBz-EDTPA

A new phosphonate ligand, Isothiocyanato-Benzyl-Ethylene Diamine Tetramethylene Phosphonic Acid (IBz-EDTPA) has been developed by our group with an idea to use it for targeting cancer. This bifunctional agent would eventually be used to label specific peptides with radiometals. After standardizing the labeling technique with Tc-99m, the biodistribution of the agent was measured in rabbits, which showed promising potential in imaging the skeletal system.

A group of patients with various pathologies like metastases bone disease (5), Ewing sarcoma (1), polyarthritis (2) and infected prosthesis (1) were studied within a week after a conventional bone scan with Tc-99m-MDP. Serial imaging was performed at 15 min, 1hr, 2hr, 3hr, 4hr, 6hr, 24 hrs after administration of 370-600MBq of radiotracer, using Siemens Integrated DIACAM Camera. Blood samples at 15 min, 1hr, 2hr, 3hr, 4hr, and 6hr were also collected from 3 patients to study blood kinetics. The biodistribution at different time interval was estimated using regional ratio computer program.

There was no untoward reaction observed on administration. The radiotracer was seen to accumulate in bones appreciably from 1 hr onwards and concentration increased marginally with time. The lesions in bone showed higher concentration compared to normal bone. There was no thyroid or stomach noted in any patients.

The pharmacokinetic parameters were determined from the percentage of injected dose per mL of blood in a one-compartment model. With IBz-EDTPA, distribution and retention half-lives and mean residence time were shorter than with MDP.

Mean uptake ratios for bone metastatic site.

	15 min	1 hr	2hr	3hr	4hr	6hr	24hr
Bone to soft tissue	1.64	2.09	2.86	2.96	2.74	2.66	2.76
Lesion to normal bone	1.86	2.57	3.15	3.70	3.46	4.14	4.34

This new bifunctional chelating agent appears to have (1) efficient blood clearance; (2) an ability to image the skeleton earlier than conventional Tc-99m-MDP besides reducing the radiation burden (3) can be used to estimate the radiation burden to marrow and the tumor when IBz-EDTPA is labeled with Re-188 for therapy.

OS-536

O. Israel, F. Nakhoul, Z. Keidar, A. Moscovici, J. Green, D. Front.

Rambam Medical Center and the Faculty of Medicine, Technion - Israel Institute of Technology, Haifa, Israel.

EVALUATION OF BONE TURNOVER IN PATIENTS WITH END STAGE RENAL DISEASE (ESRD): COMPARISON OF QUANTITATIVE BONE SPECT (QBS) TO BONE HISTOMORPHOMETRY (HTM).

Purpose: To evaluate the ability of QBS for diagnosis of high and low bone turnover disease (HTOBD, LTOBD) in patients with ESRD and for prediction of future bone loss.

Materials and Methods: 12 patients with ESRD were examined. QBS measurements of the lumbar spine (LS) and femoral neck (FN) were performed. QBS values were expressed as the percent of injected dose of Tc-99m methylene diphosphonate per gram of bone tissue QBS values were elevated if above mean +1 SD of normal data-base.. HTM was performed in samples of bone obtained by transiliac biopsy following double tetracycline labeling. Bone samples were evaluated for the presence of static and dynamic bone formation parameters. Bone mineral density (BMD) of the LS and FN was performed at entering the study and after one year.

Results: HTOBD was diagnosed by both QBS and HTM in the LS of 5 patients and in the FN in 6 patients. LTOBD was diagnosed by both QBS and HTM in the LS and the FN of 3 patients. Discordant results were found in the LS of 4 patients. The change in BMD showed QBS measurements to be correct in 3 patients (2 with LTOBD and 1 with HTOBD) and supported HTM findings in 1 patient with LTOBD. Discordant results were found in the FN in 3 patients. The change in BMD showed QBS measurements to be correct in 2 patients. (1 with HTOBD and 1 with LTOBD) and supported HTM results in 1 patient with LTOBD.

Conclusion: QBS is a sensitive, non-invasive test for diagnosis of high or low bone turnover disease in patients with renal osteodystrophy. It may obviate the need for bone biopsy and suggest the appropriate treatment modality for preventing bone loss in the individual patient.

OS-537

M.Fjälling, M.Suurkula, J.Grétarsdóttir, L.Jacobsson.

Hospital: Sahlgrenska University Hospital, Department of Nuclear Medicine, Göteborg, Sweden.

COUNT DENSITY AND DIAGNOSTIC ACCURACY IN BONE SCANS
The amount of administered activity for nuclear medicine investigations varies between different hospitals for the same type of investigation. Image quality depends not only on administered activity, but also on type of gamma camera (age of camera, collimator, uniformity, spatial resolution), mode of displaying images and length of acquisition time. **The aim** of the present study was to see the influence of count density diagnostic accuracy in bone scans. **Method:** 65 consecutive patients irrespective of age, sex and diagnosis, were included in the study. Image was performed 3 h after iv injection of 500 MBq ^{99m}Tc MDP. Dynan acquisition was done in a 256 x 256 matrix with 1 min/frame for 5 min. From the dynamic study static images were created with registration times of 1, 2, 3 and 5 min, thus creating images with four different count densities = image qualities for the same patient study. Totally 15 images were created. The study was performed on one gamma camera. **Image interpretation:** Images were interpreted and coded independently by two experienced physicians. The images were displayed on a black and white, and a colour screen. The images with the shortest acquisition time were viewed first, i.e. first the 1 min, then the 2 min and then the 3 min images. The last image to be interpreted and coded was the 5 min image simulating the highest administered activity and representing the final diagnosis. The images were displayed automatically and randomly on the screen one at a time and with neither patient identification nor clinical information. **Results:** In the 5 min images totally 168 findings were coded as pathological. With the 5 min images as the final result the number of false positive findings was roughly the same ~ 5% for the 1, 2 and 3 min images and the number of true positive findings was 65% for the 1 min images, increasing to 73% for the 2 min and 78% for the 3 min images. **Discussion:** The count density interval studied corresponds to 0.4 - 2 times the count density routinely used at our department and simulates an injected activity of 167 - 833 MBq for a registration time of 3 min. As there were 22% false negative findings for the 3 min images and 500 MBq it can be considered to increase the administered activity to 800 MBq or increase the registration time to 5 min.

OS-538

B. Klemenz, H. Wieler, J. Katzwinkel, K.P. Kaiser

Central Military Hospital of Germany, Dept. of Nuclear Medicine, P.O. Box 7460, 56064 Koblenz, Germany

HYDRATION DOES NOT IMPROVE BONE TO SOFT TISSUE CONTRAST AND IMAGE QUALITY IN BONE SCINTIGRAPHY

Purpose of this prospective study was to evaluate the effects of different drinking amounts on bone to soft tissue (B/ST) ratio and image quality of bone scans carried out with Tc-99m-MDP. **Materials and methods.** 160 patients with no renal disease were divided in 3 groups (I: 0.25 l; II: 1.0 l; and III: 1.5 l fluid intake), image quality was assessed with a semiquantitative score. B/ST ratio was calculated using a ROI over the whole femoral diaphysis compared to a contralateral adductor area (mean of anterior and posterior projections). There were no differences regarding demographic parameters, thigh circumference, fluid intake prior to injection and the start of bone scan p.i. (555 MBq Tc-99m-MDP; one-head gamma camera, SMV Sophera-DSX, scan speed 20 cm/min; LEAP-collimator). One-way ANOVA, Kruskal-Wallis-test and Spearman rank order test were used, with a p<0.05 considered to be significant. **Results and Discussion.** No significant differences in B/ST ratio or image quality were demonstrated with different amounts of fluid intake. The median values of B/ST ratios were 1.90 (I), 1.93 (II), and 1.84 (III). It is likely that the fluid volume ingested by our patients was insufficient to achieve an accelerated renal excretion. Filled urinary bladder was associated with higher fluid intake, consequently restricting the assessment of pelvic structures. B/ST ratio and image quality positively correlated with the post injection time interval and inversely with age. In most patients undergoing bone scan for staging of non skeletal malignancies fluid restriction might be advisable to achieve improved image quality, despite the cancer risk due to higher radiation burden. **Conclusion.** Large drinking amounts are not necessary for patients' preparation because they do not increase B/ST ratios nor improve image quality in bone scintigraphy.

OS-539

I. Szilvási, Zs. Varga, L. Bohár, L. Bucsi*

Haynal University of Health Sciences, Dept. of Nuclear Medicine and Semmelweis University of Medicine, Dept. of Orthopaedics*, Budapest

DIAGNOSTIC IMAGING ALGORITHM FOR PATIENTS WITH UNEXPLAINED LOW BACK PAIN. THE ROLE OF BONE SPECT

Cost-effective diagnostic imaging strategy for patients with unexplained low back pain (LBP) is of great economic importance because of high number of patients and possible overuse of sophisticated diagnostic techniques like CT or MRI. Aim of our study was to evaluate diagnostic role of bone scintigraphy (planar, whole-body and lumbar SPECT) in patients with unexplained LBP lasting more than three months. 18 patients (5 male, 12 female, median age: 54.5 years) were prospectively studied. All patients underwent to X-ray, CT and 12 patients to MRI of the lumbar region. Whole-body bone scintigraphy (WBS) with planar spot images and SPECT of the lumbar region were performed using a dual-head SPECT system with elliptical rotation (180 degree rotation with 90 degree of relative angles of the two detectors). Conventional tomographic slices and 3-D display were interpreted qualitatively by two experienced NM physicians without knowledge of clinical data. Diagnostic value of all imaging techniques were evaluated by orthopaedic surgeon, radiologist and NM physicians based on surgical/biopsical findings or clinical follow-up of patients. Results: incremental diagnostic values of consecutive imaging techniques were: X-ray was diagnostic in 6 patients (degenerative disc disease, osteoarthritis, spondylolisthesis), planar scintigraphy in 2 patients (osteoporotic compression fractures, sacroiliitis) WBS for 1 patient (metastatic lesion), SPECT was diagnostic for 3 patients (osteoarthritis), CT/MR were diagnostic in 6 patients (degenerative disc disease, stress fracture, haemangioma). In conclusion: combined use of X-ray and WBS with SPECT of the lumbar region is cost-effective in patients with unexplained low back pain, because number of unnecessary CT/MRI examinations can be significantly decreased.

This project was supported by IAEA

OS-540

A.N. Babichev¹, N.A. Pocock¹, K. Lee², H. Dixon², R. Babicheva²

Liverpool Hospital¹, Bankstown/Lidcombe Hospital², NSW, Australia

CORRELATION OF DUAL ENERGY ABSORPTIOMETRY (DEXA) OF SPINE AND FEMUR WITH QUANTITATIVE ULTRASOUND OF THE HEEL.

Calcaneal ultrasound (CU) has been proposed as an independent measurement for assessment of osteoporosis. We measured a sample of 67 patients had previously suffered pathological fractures. All subjects were 40 years old or older. Patients were divided to 5 groups: 40-50, 50-60, 60-70 and 70 and over years old. Our aims were: 1) to compare the ability of CA and DEXA to distinguish between patients with and without osteoporosis 2) to determine if there is any difference in CU and DEXA correlation in different age groups and between men and women 3) to assess calcaneal ultrasound as an independent screening tool for osteoporosis. We measured calcaneal ultrasound parameters (broadband ultrasound attenuation (BUA) speed of sound (SOS) and stiffness, combination of BUA and SOS [%]) at the os calcis (Achilles+, Lunar) and BMD at lumbar spine and femoral neck by DEXA (DPX-IQ, Lunar). We used the WHO criteria for BMD measured by DEXA to determine osteoporosis (T<-2.5SD) and osteopaenia (-2.5≤T<-1.0SD). Correlations between DEXA and CU stiffness were 1) femur BMD and CU 0.72, 2) spine BMD and CU 0.59 and 3) femur BMD and spine BMD 0.78. Correlation between BMD and stiffness decreased with age. CU is only moderately correlated with DEXA BMD and this correlation decrease with age.

Cardiovascular: Comparison of techniques

OS-541

A. Fikrlé, E.P. Ritter, D. Lüscher, J.A. Kinser, W. Mering, M. Hummel, H. Ledermann
Department of Nuclear Medicine, University of Berne/Inselspital, CH 3010 Berne, Switzerland

DETERMINATION OF THE LEFT VENTRICULAR EJECTION FRACTION FROM GATED 99mTc-MIBI SPECT BY TWO DIFFERENT METHODS: CORRELATION WITH CONTRAST LEFT VENTRICULOGRAPHY

Myocardial perfusion and function can be simultaneously demonstrated with gated SPECT (GSPECT). The purpose of this study was to compare two different methods for the determination of the ejection fraction (EF) with GSPECT and their correlation with contrast left ventriculography (VCG). 57 patients (pts.) were examined according to a 2-day protocol using the 3-head camera (Picker PRISM 3000). The first GSPECT was performed at rest 30 minutes after exercise-stress MIBI-injection, the second on the next day 60 minutes after the MIBI-injection at rest. Each patient underwent cardiac catheterization within 2 weeks of the GSPECT. Two independent observers determined the EF from the stress (S) GSPECT and from the rest (R) GSPECT. The EF was determined with two different methods: 1) semiautomatic using „perfusion motion map (PMM)“ according to T.L. Faber and 2) automatic using „quantitative gated SPECT (QGS)“ according to G. Germano. The average EF (%) for the 57 pts. was: VCG=58±14; S-PMM=53±12; S-QGS=53±15; R-PMM=54±10; R-QGS=54±15. The differences between VCG-EF and GSPECT-EF were significant ($p<0.05$) in all groups. The correlation with VCG in 57 pts. was: S-PMM=0.81; S-QGS=0.85; R-PMM=0.87; R-QGS=0.88. The best correlation was found for VCG-EF in the range of 40-60 %, followed by the VCG-EF <40 % and VCG-EF >60 %. The correlation of PMM vs QGS was 0.90 both for S and R. There was no significant difference found between the two observers for both methods: the correlation was S-QGS=1.0; R-QGS=1.0; S-PMM=0.98; R-PMM=0.97. The determination of the EF with GSPECT correlated well for PMM and QGS with VCG (for QGS slightly better). Both methods slightly but significantly underestimate the EF in comparison to VCG (mainly in the higher area of EF >60 %, PMM more than QGS). Both methods are reproducible (QGS somewhat better) and render clinically useful quantitative information about the systolic function. In all compared parameters, QGS was slightly better than PMM, most likely due to the automatic processing.

OS-542

Zhibong Tang, Yili Liu, Xiao Gao, Zuhan Huang
Nanfang Hospital, Department of Nuclear Medicine
Guangzhou, China

SIMULTANEOUS EVALUATION OF EXERCISE ECHO AND 99mTc-MIBI TOMOGRAPHY FOR DETECTING CAD

Aim of the study was to compare the diagnostic efficiency of 99mTc-MIBI tomography and echocardiography (Echo) with the same stress in detection of CAD. We performed stress test 99mTc-MIBI SPECT and Echo in single exercise in 52 cases of suspected CAD undergoing coronary arteriography. Among them, 7 cases had normal coronary vessels, 28 patients one-vessel, 13 two-vessels and 6 three-vessels (>50% coronary stenosis). 99mTc-MIBI was injected at peak of treadmill exercise and Echo was simultaneous performed. A rest study was performed on a separate day. Results: the sensitivity, specificity and predictive accuracy for detection of stenosed vessels were 88%, 79% and 82% for 99mTc-MIBI and 76%, 68% and 71% for Echo. Conclusions: Exercise 99mTc-MIBI SPECT is more accurate than exercise Echo in the diagnosis and localization of CAD.

OS-543

C. Corbelli¹, R. Casanova², F. Matteucci³, A.L. Patroncini⁴, P.L. Guidalotti⁵, M. Dondi⁶, M. Sanguinetti⁷, A. Maresta⁸.
¹Nuclear Medicine Dpt and ²Cardiology Division, Faenza (Ra), ³Cardiology Division, Ravenna, ⁴Nuclear Medicine Dpt, AUSL "Città di Bologna", ⁵Nuclear Medicine Dpt, Azienda S.Orsola-Malpighi, Bologna (Italy).
PATIENT ASSESSMENT WITH 99mTc-MIBI-SPET AFTER ACUTE MYOCARDIAL INFARCTION (AMI): COMPARISON BETWEEN ADENOSINE (AD) AND PREDISCHARGE MAXIMAL EXERCISE (EX).

It has become routine practice to risk stratify patients with uncomplicated AMI at the time of discharge using stress testing; however the strategy and stress modalities to be used are controversial. Aim of this study was to assess the feasibility and safety of AD infusion and EX in the early post-AMI period and their accuracy when used in conjunction with MIBI-SPET. Forty pts (29 male and 11 female; mean age 56 ± 9), with uncomplicated AMI, all treated with thrombolytic therapy underwent AD-Tc99m-MIBI-SPET, EX-Tc99m-MIBI-SPET and coronary angiography (CA), respectively 5+2, 10+3 and 16+5 days after AMI. AD infusion was performed with single-port (n=20 pts) or double-port infusion protocol (n=20 pts); exercise test was performed according to Bruce protocol. Mild secondary effects after AD (flushing, headache, palpitation, dizziness) were observed in 24 pts (60%), transient AV-block and ST in 2 and 4 pts, irrespective of protocol infusion. No adverse reactions occurred during symptom-limited EX. No pts had normal perfusion pattern; compared with CA, both AD-SPET and EX-SPET identified 32 pts with one-vessel disease (100%) and 6 of 8 pts with multi-vessels disease (75%). Out of 74 coronary arteries with <50% stenosis, both AD-SPET and EX-SPET were negative in 72 (97%), while in 2 cases AD-SPET and EX-SPET gave false-positive patterns. In 26 pts (65%) AD-SPET and EX-SPET demonstrated reversibility: in 24 of these pts (92%) CA revealed >50% stenosis and in 2 pts occluded infarct-related artery. In 14 pts AD-SPET and EX-SPET showed fixed defects: in these pts CA showed occluded infarct-related artery in 4 (28%) and stenosis >50% in 10 pts. Comparison of AD-SPET and EX-SPET failed to show any significant difference. Our data suggest that extent of coronary artery disease and presence and extent of jeopardized myocardium can be early and safely documented in post-AMI period with either AD-SPET and EX-SPET to formulate further management strategies; AD-SPET may be utilized even earlier (within 5 days), especially when pts are unable to exercise.

OS-544

J. Knuuti, C. Kato, M. Luotolahti, I. Kantola, A. Jula, P. Nuutila, H. Laine.
Turku University Departments of Medicine and Clinical Physiology and Turku PET Centre, Finland.

THE EFFECTS OF LEFT VENTRICULAR HYPERTROPHY ON MYOCARDIAL PERFUSION, OXYGEN CONSUMPTION AND SUBSTRATE UTILIZATION

To determine whether myocardial oxygen consumption, blood flow and substrate metabolism are altered in LV hypertrophy induced by hypertension we studied 9 hypertensive (HTN) men with LVH (LVH, age 42±2 years, LV mass 161±8 g, BP 145±16/88±10 mmHg), 9 HTN men without LVH (LVH -, age 40±5, LV mass 109±15, BP 143±18/93±14) and 10 normotensive men (CONT, BP 127±16/75±16). The HTNs were studied during medication. Myocardial blood flow (F), oxygen extraction (OEF) and consumption (MMRO2) and glucose uptake (GU) were measured during euglycemic hyperinsulinemia (insulin ~70 mU/L) using PET. Efficiency (EFF) was calculated to estimate the produced myocardial work per oxygen consumption.

	CONT	LVH -	LVH
Minute work (mm Hg·mL·min ⁻¹ ·g ⁻¹)	5.0(1.6)	6.25(1.3)*	4.7(0.9)
Flow (mL·g ⁻¹ ·min ⁻¹)	0.84(0.16)	1.06(0.22)*	0.81(0.09)*
OEF	0.59(0.02)	0.71(0.03)*	0.73(0.04)*
MMRO2 (mL·g ⁻¹ ·min ⁻¹)	0.09(0.02)	0.14(0.03)*	0.11(0.01)*
GU (μmol·100g ⁻¹ ·min ⁻¹)	81(21)	92(17)	96(26)
EFF (mmHg·kg·min ⁻¹)	76(19)	62(10)	58(7)*

* $p<0.05$ vs CONT, * $p<0.05$ vs LVH-

Hypertension increases myocardial blood flow and work load. This appears to be compensated by development of LVH. OEF and MMRO2, however, remain increased in patients with LVH and this leads to reduced myocardial efficiency. No significant changes in GU exist suggesting that oxidative metabolism is shifted to alternative substrates.

OS-545

Jun Zeng, Li-Hua Zhang, Wen-Hui Xie, Zhi-Chang Yu

Department of Nuclear Medicine, Shanghai Chest Hospital, 241 Huaihai West Road, Shanghai 200030, P.R. of China

ENHANCEMENT OF THE MISMATCHED UPTAKE BETWEEN ^{99m}Tc-MIBI AND ²⁰¹Tl IN ISCHEMIC MYOCARDIUM BY PRECONDITIONING WITH NIFEDIPINE

PURPOSE: The effects of nifedipine on vasodilation of coronary artery and improvement of contractile dysfunction and mitochondrial calcium overload in postischemic myocardium have been demonstrated recently. Thus, there is a possibility of inducing the different uptake between ^{99m}Tc-MIBI and ²⁰¹Tl with nifedipine in ischemic myocardium. **METHODS:** Our study was made up of 33 patients with coronary artery disease demonstrated by coronary angiography. Patients with myocardial infarction were excluded. 21 patients who received 10mg of sublingual nifedipine (group A) 15 minutes before dobutamine-stress test and 12 patients without nifedipine administration (group B) were injected venously with a mixture of 4mCi ²⁰¹Tl and 15 mCi ^{99m}Tc-MIBI at patient's maximum heart rate. The double isotopic SPECT myocardial imaging was performed 15min and 3-4 hours after injection. **RESULTS:** The maximum systole blood pressure was higher in group B (165.5 +/- 31.7mmHg) than in group A (133.3 +/- 13.6mmHg) during stress test, but there were no differences between the 2 groups in basic and maximum heart rate and diastolic pressure. Comparing with group B, the defect segments of ^{99m}Tc-MIBI and the segmental agreement with ²⁰¹Tl were significant lower in group A (P<0.001). The defect segments of ^{99m}Tc-MIBI were 10.1% (67/667) and 7.4% (49/667) on early and delay images in group A while 19.4% (62/319) and 17.2% (55/319) in group B. The segmental agreement with ²⁰¹Tl was 34.5% in group A and 66.3% in group B. The values of subtracting ²⁰¹Tl uptake from ^{99m}Tc-MIBI uptake in ischemic over normal zone of early images were 0.316 +/- 0.201 in group A, were significant higher than that of 0.146 +/- 0.138 in group B (P<0.001). Even in the ²⁰¹Tl fixed defect segments, the values still higher in group A (0.217 +/- 0.158) than in group B (0.099 +/- 0.097), P<0.001. **CONCLUSIONS:** Preconditioning with nifedipine may enhance the detection of ischemic but viable myocardium with ^{99m}Tc-MIBI and ²⁰¹Tl double isotopic imaging and avoid the high systole blood pressure during stress test.

OS-546

E.Milan, A.Terzi, P.Rossini, M. Volpini, R.Giubbini.

Spedali Civili, Brescia, ITALY - Nuclear Medicine and Cardiology Departments

COMPARISON BETWEEN STANDARD AND HIGH DOSE DIPYRIDAMOLE IN DETECTION OF CORONARY ARTERY DISEASE BY TC-^{99m} SESTAMIBI SPECT.

Dipyridamole is a widely used stressor for myocardial perfusion imaging in CAD patients. Its indirect mechanism of action may lead to suboptimal coronary vasodilation. The purpose of this study was to evaluate the potential benefits of an increased dose of Dipyridamole for ^{99m}Tc Sestamibi (MIBI) myocardial SPECT. 49 pts, all with previous myocardial infarction and recent catheterization, underwent MIBI SPECT after 0.84 mg/Kg/5min of Dipyridamole (STUDY GROUP) (SG). The control group (CG) consisted of 100 pts, with comparable characteristics, submitted to the same procedure using the standard dose of Dipyridamole (0.56 mg/Kg/4min). Extension (expressed as a percentage of left ventricle surface) and severity (expressed as arbitrary units) of reversible uptake defects were quantified by evaluation of gender matched polar maps. Both groups were divided into pts who had (SG1 & CG1) and hadn't (SG2 & CG2) been submitted to previous procedures of revascularization. Moreover both SG2 and CG2 were divided into pts with 1 vessel (1V), 2 vessel (2V) and 3 vessel (3V) disease. No major side effects were observed after Dipyridamole high dose administration. **Results:** significant difference in severity of reversible defects was found between SG2 and CG2 (1997 ± 340 vs 1277 ± 2455; p<0.005), but not in extension. Significant difference in severity of reversible defects was found between SG2-1V & CG2-1V (2373 ± 2301 vs 1278 ± 1013; p<0.02) as well as between SG2-2V & CG2-2V (1753 ± 912 vs 901 ± 823; p<0.02). Taking into account the extension of the reversible defect, significant difference was found between SG2-2V & CG2-2V (15 ± 9 vs 7 ± 8; p<0.02) but not between SG2-1V & CG2-1V. SG2-3V & CG2-3V as well as SG1 & CG1 showed no significant differences both in the extension and in the severity of the inducible defect. **Conclusions:** the use of a high dose of Dipyridamole does not hamper the safety of the test and seems to be helpful in increasing sensitivity of Tc-^{99m} MIBI SPECT.

Oncology: PET

OS-547

S.Kosuda, S.Kusano

Hospital: National Defense Medical College, Department of Radiology, Japan

DECISION TREE SENSITIVITY ANALYSIS FOR COST-EFFECTIVENESS OF CHEST FDG-PET IN PATIENTS WITH A PULMONARY NODULE (NON-SMALL CELL CARCINOMA) IN JAPAN.

All Japanese people are covered by the national health care systems. Decision tree analysis was used to assess cost-effectiveness of this study, based on the data of the current decision tree. Decision tree models were constructed with two competing strategies (CT alone vs. CT plus chest FDG-PET) in 1,000 patient population with 74.1% prevalence. Baseline of FDG-PET sensitivity and specificity on detection of lung cancer and lymph node metastasis, and mortality and life expectancy were available from references. Chest CT plus chest FDG-PET strategy increased a total cost by 10.5% when a chest FDG-PET study costs 0.1 million yen, since it increased the numbers of mediastinoscopy and curative thoracotomy despite reducing the number of bronchofiberscopy to half. However, the strategy resulted in a remarkable increase by 115 patients with curable thoracotomy and decrease by 51 patients with non-curable thoracotomy. In addition, an average life expectancy increased by 0.607 year/patient, which means increase in medical cost is 218,080 yen/year/patient when a chest FDG-PET study costs 0.1 million yen. In conclusion, chest CT plus chest FDG-PET strategy might not be cost-effective in Japan, but we are convinced that the strategy is useful in cost-benefit analysis.

OS-548

R.P.Baum¹, D. Rinne², O. Schröder¹, A. Hertel¹, G. Hör¹, R. Kaufmann²

Department of Nuclear Medicine¹ and Dermatology², University of Frankfurt/Main, Medical Center, Germany

WHOLE-BODY FDG-PET IN PRIMARY STAGING AND FOLLOW-UP OF HIGH-RISK MELANOMA PATIENTS: RESULTS OF A PROSPECTIVE STUDY OF 100 PATIENTS

Purpose: Retrospective PET studies revealed encouraging results in malignant melanoma. In order to test the hypothesis that whole-body PET could be used as a first line procedure in the primary diagnosis and follow-up, we prospectively studied 100 consecutively patients with high-risk melanoma. **Methods:** In all patients whole-body FDG-PET (ECAT EXACT 47, Siemens/CTI) and conventional imaging (MRI of the brain, chest x-ray, CT thorax/abdomen/pelvis, ultrasound abdomen, high-resolution lymph node sonography, and skeletal scintigraphy) were performed comparing each single abnormal lesion detected by any method. 52 patients were studied at primary diagnosis (group A), and 48 in the follow-up when there was suspicion of recurrence/progression (group B). Each single lesion was confirmed by histology. Interpretation of attenuation corrected/non-AC studies was performed blindly. **Results:** In group A, sensitivity of PET was 100% and specificity was 94%, whereas the conventional methods did not identify any of the metastases (true positive rate 0%) and demonstrated a lower specificity (80%). In Group B, a total of 121 lesions were detected, 111 by PET and 69 by conventional imaging. On a patients' basis, sensitivity/specificity/accuracy of PET were 100%/96%/98% (92%/94%/92%, when counting each single metastasis, respectively). Conventional imaging did not identify all patients with progression (sensitivity 85%) and detected significantly fewer metastases (sensitivity 58%) with much lower specificity (68% on a patients' basis and 45% for single lesions); therefore accuracy of conventional imaging was 77% on a patients' basis and only 56% for single metastases. Results also depended on specific sites: While PET yielded a higher sensitivity in discovering cervical (100% vs. 67%) and abdominal metastases (100% vs. 27%), CT scan proved to be superior in small lung metastases (87% vs. 70%). **Conclusion:** With the possible exception of the brain whole-body PET can replace the standard battery of imaging tests currently used in high risk melanoma patients by detecting significantly more metastases. When used as a first line procedure PET might also lead to a significant saving of costs.

OS-549

P. Lind, H.J. Gallowitsch, O. Unterweger P. Mikosch, M. Moinar, M. Starlinger, H.P. Dinges

Department of Nuclear Medicine & Endocrinology - PET Center, LKH Klagenfurt, AUSTRIA

FDG PET IN THE FOLLOW UP OF THYROID CANCER: COMPARISON WITH Tc-99m TETROFOSMIN AND I-131 WHOLE BODY SCINTIGRAPHY

After thyroidectomy and radioiodine ablation several imaging modalities are used to follow up patients with thyroid cancer. Recent studies were able to demonstrate that non-specific tracers are superior compared to I-131 in detecting metastases, because not all malignant lesions accumulate iodine. **Aim** of the present study was to evaluate FDG PET in patients with suspicion of recurrent or metastatic disease and to compare the results with Tc-99m tetrofosmin (TETRO) and I-131 whole body scintigraphy (WBS). **Patients and Methods:** In eighteen patients with elevated thyroglobulin (3-21045 ng/ml; SelcoTg IRMA, Medipan) TETRO WBS (5 min after i.v. injection of 370 MBq Tc-99m tetrofosmin using a double headed high resolution gamma camera with LEHR collimator, Elscint, HELIX HR, Haifa) and FDG PET (70 min after i.v. injection of 180 MBq F-18 deoxyglucose using a Siemens/CTI Ecat Art Scanner) was performed. All patients received a high dose radioiodine therapy (5550- 7400 MBq) and a post-therapeutic WBS was done 5 days after therapy (Elscint Sp-6 , HEAP). **Results:** On a patient basis five different pattern of tracer accumulation were seen. I: I-131 pos/ TETRO pos/ FDG pos (n=6), II: I-131 neg/ TETRO pos/ FDG pos (n=5); III: I-131 neg/ TETRO neg/ FDG pos (n=4); IV: I-131 pos/ TETRO neg/ FDG neg (n=2); V: I-131 pos/ TETRO pos/ FDG neg (n=1). On a lesion by lesion evaluation, the 6 patients of group I demonstrated 8 I-131 pos, 15 TETRO pos and 37 FDG pos lesions; also in group II with complete neg pt I-131 WBS, FDG PET showed more lesions (24) compared to TETRO WBS (10). **Conclusion:** In patients with suspicion of metastatic thyroid cancer due to elevated thyroglobulin most of the I-131 pos patients show additional I-131 neg but TETRO and/or FDG pos lesions. Compared to Tc-99m tetrofosmin FDG PET gives better image quality and demonstrates more lesions. The value of additional I-131 high dose therapies with the need of thyroxine withdrawal in patients with additional FDG pos lesions is questionable.

OS-550

A. Hertel, P. Mantaka, S. Adams, R.P. Baum, A. Niesen, G. Hür

Department Nuclear Medicine, Universitätsklinik der Johann Wolfgang Goethe-Universität Frankfurt/FRG

WHOLE BODY FDG-PET PERFORMANCE FOR EVALUATION OF CANCER OF UNKNOWN PRIMARY (CUP)

Diagnostic management of patients with unknown primary or suspected metastases of unknown origin represents a clinical and diagnostic challenge. Conventional imaging (CI) usually has a very low sensitivity below 30% in correctly identifying the primary site. We evaluated the performance of FDG whole body PET in this patient group.

Patients and methods: 29 patients could be evaluated on the basis of a clinical follow-up from 6 months to 3 years to confirm PET findings. 21 patients presented lymph node metastases prior to PET imaging, the other 8 presented various signs of involved tumor spread (pulmonary, abdominal, elevated tumor markers). All patients underwent whole body FDG imaging (Siemens ECAT 47, 16.2 cm axial FOV) in a routine protocol. All patients underwent extensive conventional imaging (CT, US, MRI, x-ray thorax, mammography, coloscopy) prior to PET with no conclusive results demanding final PET imaging.

Results: In 13/29 patients surgically or clinically (more than 1 year after PET) proved tumor primaries could be found: bronchogenic (6), mammary (3), stomach, ovarian, pancreatic and lymphoma each in one case. In 11 patients the correct outcome could not finally be decided, no tumor was detected, they were therefore termed undecided. 4 patients were false positive (benign tumors and inflammatory lesions) and one patient false negative (parotis tumor). From these data a sensitivity of 76.4 % for FDG-PET was calculated (undecided cases excluded). In contrast CT displayed a sensitivity of 18.2 %.

Conclusion: FDG-PET is highly efficient in contrast to CI in detecting cancer of unknown primaries and should be earlier included in the work-up of these patients.

OS-551

I. Brink, *T. Klenzner, T. Schumacher, *U.H. Ross, E. Moser, M. Mix, E. Nitzsche

Department of Nuclear Medicine, *Department of Oto-Rhino-Laryngology, Albert-Ludwig-University, Freiburg, Germany

ASSESSMENT OF METASTATIC DISEASE OF SLIGHTLY ENLARGED LYMPH NODES IN HEAD AND NECK CANCER BY FDG-PET

Introduction: For individualized therapy decisions in patients with head and neck tumors lymph node staging is mandatory. Sonography has been shown to have a high sensitivity in the detection of lymph nodes enlargement but is often unable to characterize malignancy versus benignancy of lesions, especially in nodes less than 2 cm in diameter. The purpose of this study was to investigate the efficiency of FDG PET in correctly identifying the presence or absence of metastatic disease in slightly enlarged small lymph nodes of the head and neck.

Methods: 66 patients with histologically proven squamos-cell carcinoma and sonographically detected lymph nodes in 77 neck sides were examined with FDG-PET. After 90 min uptake period, attenuation correction and reconstruction by filtered back projection images were displayed in three orthogonal planes. Suspicious lesions were semiquantitative valued by standard uptake value analysis. Partial volume effects were corrected using the node diameters measured by ultrasound. The PET determinations were correlated with histopathologic findings in neck specimens after neck dissections and/or clinical follow-up studies.

Results: Metastatic involvement in lymph nodes up to 1 cm (31 neck sides) were correctly identified by PET with a sensitivity of 71,4% and a specificity of 95,8%. Sensitivity (83,3%) and specificity (100%) increased for lymph nodes between 1,1 and 1,5 cm (22 neck sides). PET characterized all lymph nodes between 1,6 and 2,0 cm accurately (16 neck sides). PET as well as histopathology showed metastasis in all lymph nodes larger than 2 cm.

Conclusion: FDG PET provides an effective method to assess malignancy in slightly enlarged head and neck lymph nodes. Considering sonographic size measurement for correction of partial volume effects in small lesions it is a adequate and practicable procedure.

OS-552

J.M.Llamas, M.A.Muros, A.Rodríguez, M.Gómez, A.Ferrón*, A. Maldonado**, M.J.Pérez**, J.L. Carreras**.

Nuclear Medicine and *Surgery Departments. Virgen de las Nieves Hospital.Granada.**PET Center.Complutense University. Madrid. Spain.

FDG-PET IN DIFFERENTIATED THYROID CARCINOMA: CONTRIBUTION FOR PATIENTS WITH NEGATIVE RADIOIODINE SCAN AND ELEVATED SERUM THYROGLOBULINE LEVELS

Purpose: This study was to determine the role of FDG-PET in the follow of patients who have been treated for differentiated thyroid cancer (total thyroidectomy and total I31I thyroid ablation) and that show thyroglobulin levels rise and negative I31I and 201 Tl scans.

Methods: Seven patients with differentiated thyroid carcinoma (6 women, 1 man, mean age 38.7 yr) were evaluated. Two patients with papillary carcinoma and five with follicular tumours underwent total thyroidectomy and I31I therapy up to negativity of I31I scans. After patients preparation with discontinuing exogenous thyroxine replacement for five weeks, I31I and 201Tl scans were performed with negative results. Concomitantly serum thyroglobulin measurements were obtained and in all cases reach positive results (mean value 248 ng/ml) with negative serum thyroglobulin auto-antibodies. One week after I31I scan, whole body FDG-PET scans were performed.

Results: An unique pathological foci of uptake of FDG in a lymph node metastasis (with subsequently histologic confirmation) were found in three patients by FDG-PET scans. Multiple pathological foci in brain, neck and chest were found by FDG-PET scan in one patient. The sensitivity of whole body FDG-PET scan for detecting metastatic thyroid cancer was 57% (4/7) in our study. Other patient showed several pathological foci in mediastinum by FDG-PET scan no confirmed by other imaging techniques, and two patients showed uncertain uptakes. This patients were considered negative in the study.

Conclusion: This study indicates that whole body FDG-PET scan is useful in the follow of patients with differentiated thyroid cancer with negative I31I and 201 Tl scans and thyroglobulin levels rise. Whole body FDG-PET scan detects metastatic foci in more than 50% of this patients that can be followed by surgical therapy in accessible lesions.

General nuclear medicine: Miscellaneous

OS-553

G. Taddei, G. Curti, G. Agnese, A. Rahimi Mansour, F. Martini, R. Costa, C. Maragliano, F. Boccardo, C. Campisi, and G. Mariani. Nuclear Medicine Service, DIMI, and Microsurgery Unit, University of Genoa; Genoa (Italy).

COMBINED SUPERFICIAL AND DEEP LYMPHOSCINTIGRAPHY FOR EVALUATING PERIPHERAL LYMPHEDEMA

This study was aimed at optimizing the diagnostic potential of lymphoscintigraphy in order to improve its reliability in the evaluation of patients with peripheral lymphedema.

A total of 46 pts (34 women, 12 men, age 47.6±14 yr, range 4-76 yr) underwent lymphoscintigraphy because of either primary (PL, 18 pts) or secondary (SL, 28 pts) lymphedema of the upper or lower limbs (16 and 30 pts, respectively). According to classical methods, the superficial lymphatic circulation (SLC) was explored in all pts by injecting ^{99m}Tc-albumin microcolloids intradermally. In 25 of the pts in whom the tracer did not drain through the SLC, a second injection was performed close to the periosteal space, to explore the deep lymphatic circulation (DLC). Activity/time curves from 0-30 min were generated for ROIs defined at the injection sites and at distance, to derive T_{1/2} values (min), clearance (μl/min), and lymph flow velocity (cm/min). These parameters were also evaluated for SLC in 8 adult volunteers.

A normal lymphoscintigraphic pattern was observed in 13 pts (6 PL, 7 SL): in 9 of these pts (5 PL, 4 SL) SLC only had been explored, while in 4 pts (1 PL, 3 SL) the DLC had also been evaluated. Either the SLC and/or the DLC pattern was abnormal in the remaining 33 pts. Flow kinetic parameters in controls and in pts with abnormal SLC pattern:

	T _{1/2} (min)	Clearance (μl/min)	Flow velocity (cm/min)
Controls (n=15)	72.8±11.5	28.7±3.6	4.9±1.1
Patients (n=12)	156.3±20.1	12.6±1.9	2.0±0.5

These results confirm the first-choice diagnostic potential of lymphoscintigraphy in pts with lymphedema. DLC exploration helps to avoid misinterpretations on false drainage patterns of lymph node destruction or lymphatic aplasia when no superficial lymph drainage is observed in the first 45 minutes after intradermal injection.

OS-554

P. Shreve

University of Michigan, Ann Arbor, U.S.A.

CLASSIFICATION OF PANCREAS EXOCRINE FUNCTION WITH PET IMAGING USING C-11 L METHIONINE AND C-11 ACETATE

Early chronic pancreatitis is characterized by diminished pancreas exocrine function as demonstrated on a secretin-pancreozymin test, but no specific changes on anatomic imaging. C-11 L methionine can serve as a tracer of amino acid uptake in pancreas acinar tissue and C-11 acetate a tracer of pancreas tissue lipid metabolism. The purpose of this study was to investigate the use of PET imaging to quantify pancreas functional tissue mass as a non-invasive measure of pancreas exocrine function.

Twenty patients with varying degrees of pancreas exocrine function as classified by secretin-pancreozymin test underwent dynamic attenuation corrected positron emission tomography for 40 minutes following intravenous administration of 740 MBq C-11 acetate, and then a subsequent imaging acquisition following 740 MBq of C-11 L methionine. Total tracer activity in the pancreas was determined by region of interest analysis at 10-20 minutes post tracer administration.

Normal subjects had C-11 L methionine activity in the range of 13.5-26.4 (%injected dose/ml x 1k) and C-11 acetate activity in the range of 9.2-12.9, while those patients with early chronic pancreatitis had C-11 L methionine activity in the range of 5.3-14.1 and C-11 acetate activity in the range of 3.3-8.8. Severe chronic pancreatitis, with little if any pancreatic exocrine function on secretin-pancreozymin test and CT and ERCP findings diagnostic of chronic pancreatitis, had very low PET measures of C-11 methionine, <2.3 or of C-11 acetate, < 2.1. While the range of tracer uptake in the pancreas tissue was greater with C-11 L methionine than with C-11 acetate, the accuracy of classification as normal, abnormal-early chronic pancreatitis, or severe abnormal was the same with either tracer.

Positron emission tomography using physiologic tracers C-11 L methionine or C-11 acetate can be used to assess functioning pancreatic exocrine mass as an indirect measure of pancreatic exocrine function for the purposes of non-invasive diagnosis of early chronic pancreatitis.

OS-555

O. Lang, H. Bihl

Department of Nuclear Medicine, Katharinenhospital Stuttgart, Germany

NEUROENDOCRINE GASTROENTEROPANCREATIC (GEP) TUMORS: IN WHICH CLINICAL SITUATIONS IS THE USE OF F-18-FDG-PET REASONABLE?

Background: The use of whole-body FDG-PET for detection of malignant tumor tissue is increasing. However, there is little experience concerning the diagnostic value of FDG-PET in neuroendocrine GEP tumors. So far, somatostatin receptor scintigraphy (SRS) represents the method with the highest sensitivity (70% - near 100%) for the localization of these tumors.

Purpose: To evaluate in which clinical situations the use of FDG-PET is reasonable.

Methods: 32 whole-body FDG-PET studies of patients with neuroendocrine GEP tumors (carcinoids: 18, nonfunctioning pancreatic tumors: 8, gastrinomas: 3, insulinomas: 3) were performed. Corresponding SRS studies were available for comparison. FDG-PET was performed after injection of an average dose of 370 MBq FDG with a Siemens ECAT EXACT 47 whole body scanner. SRS was performed 30 minutes, 4 and 24 hours after injection of In-111-octreotide (OctreoScan-111[®]) (mean dose: 190 MBq) as planar whole body and spot views and as a SPECT study.

Results: FDG-PET showed hypermetabolism in 63% of SRS-positive studies (patient per patient analysis) and in 49% of SRS-positive tumor lesions (site per site analysis). When carcinoids and neuroendocrine pancreatic tumors were analysed separately, these figures changed to 47%/35% and 84%/79% respectively. It appeared remarkable that FDG-PET revealed 12 localizations which were SRS-negative and that SRS was able to demonstrate 26 sites without hypermetabolism in FDG-PET.

Conclusion: Since FDG-PET is far less sensitive than SRS in carcinoid tumors, FDG-PET is no alternative in this tumor entity. For neuroendocrine pancreatic tumors FDG-PET shows a sensitivity in the nearly same range as SRS. Therefore, FDG-PET should only be used in neuroendocrine pancreatic tumors and/or in case of SRS-negative carcinoid tumors.

OS-556

Persson E¹, B-Barnekow B², B-Stigmar E², Bajc M¹

¹Department of Clinical Physiology, Lund University Hospital

²Department of Ophthalmology, Lund University Hospital

OCTREOSCAN AND ⁶⁷Ga SCINTIGRAPHY IN PATIENTS WITH POSTERIOR UVEITIS

Posterior uveitis may be the first and very early symptom in sarcoidosis. To investigate the underlying cause, the diagnostic procedure sometimes includes both ⁶⁷Ga and Octreoscan scintigraphy. Retrospectively, we have compared the results from these two types of examinations and related it to clinical status. In addition some younger patients were examined with only Octreoscan.

Patients and methods: 11 patients, aged 23-84 years, were examined with both ⁶⁷Ga and Octreoscan within a month. Whole body scintigraphy was performed after 48 hours with ⁶⁷Ga, and after 5 and 24 hours with Octreoscan. Tomography (SPET) of head and thorax was also done. The patients are followed up clinically. Moreover, 5 younger patients, aged 10 to 15 years, were examined with Octreoscan only. Lung clearance with DTPA was measured as well.

Results: In 8 patients both tracers showed increased uptake in the mediastinum and/or in the eye. In 1 patient there was normal finding with ⁶⁷Ga, while Octreoscan showed increased uptake in mediastinum/lungs. Another patient showed increased uptake with ⁶⁷Ga, while Octreoscan was normal. In one patient, both tracers showed normal distribution of activity.

In the 5 patients examined with only Octreoscan, increased uptake was found in the mediastinum/lungs. One had also focally increased uptake in the abdomen. Pathological findings on ⁶⁷Ga influenced the therapy - steroid treatment. However in the case when only ⁶⁷Ga was pathological, Borrelia has later been found. In the case where only Octreoscan was pathological, clinical follow up has indicated sarcoidosis.

The scintigraphic findings with Octreoscan showed better signal to noise ratio. No correlation was found between increased lung DTPA clearance and increased uptake with ⁶⁷Ga and/or Octreoscan in the lungs.

Conclusions: Octreoscan showed increased uptake in all patients with sarcoidosis. Compared to ⁶⁷Ga, Octreoscan had the advantage of possible visualisation of pathology in lacrimal glands. Furthermore, in some cases Octreoscan yields a better visual signal to noise ratio.

OS-557

L. Vargas, F. Hernández, J. de los Santos, J. Querol, M. Moreno

Xalapa Medical Centre, Department of Nuclear Medicine, Xalapa, México.

PENILE BLOOD FLOW MEASUREMENTS USING PROSTAGLANDIN E1

Actually, for an appropriate treatment of impotence, it is necessary to know the factors which participate in its etiology. Intracavernous injection of vasoactive agents induces an erection in men with an intact penile vascular tree. We previously reported our results using papaverine. Now, with the advent of prostaglandin E1 and its less potential collateral effects we have a new drug to study the impotence, thus we evaluate a series of patients.

48 patients were evaluated. In the group were included impotent and potent men. In all of them were evaluated age, response erectile to prostaglandin, blood flow in ml/min/100 ml and collateral effects.

An intravenous dose of PYP to tagg eritrocites was injected 20 minutes before the procedure. The base of the penis was tied with a rubber garter to isolate the blood of corpus cavernosum. A dose of 555 to 925 MBq of Tc99m was injected in an antecubital vein. A lead sheet was used to shield the radiation from the thighs and testicles. Patient was positioned under the gamma camera and checked for effective blockade of penile circulation. An intracavernous dose of 10 mcg of prostaglandin E1 was injected by a midium lateral puncture using a 25 gauge needle.

Penile volume was calculated using a geometric formula and the penile flow was calculated according to the slope of the initial portion of the time-activity curve, the volume of the penis and the value of a blood sample withdrawn at the end of the procedure. We evaluated the erectile response in a scale of 0 to 3.

Our results show no difference between papaverine and prostaglandin in the erectile response and in the flows calculated in potent and impotent men. We obtained the following values: For the normal group: Age 50.1 ± 12.4 , flow 130.0 ± 20.8 , response 1.8 ± 0.7 ; for the impotent group: Age 49.9 ± 12.2 , flow 42.4 ± 15.1 , response 1.9 ± 0.9 . There were an intermediate group: Age 62.2 ± 9.6 , flow 89.8 ± 7.3 , response 1.8 ± 1.0 . In 8 men there were penile and/or perineal pain. In 3 men the slope of the curve showed a double component.

OS-558

G. Brezinskis, J. Dumpis

Department of Oral and Maxillofacial Surgery, Medical Academy of Latvia

SIALOSCINTIGRAPHY FOLLOWING EXTRAORAL IDEAL SIALODOCHOLITHOTOMY OF SUBMANDIBULAR DUCTS

STATEMENT ON THE PURPOSE OF THE STUDY

After extraoral microsurgical sialodocholithotomy of submandibular ducts, scintigraphy was conducted to allow assessment of the submandibular ducts condition and gland regeneration following treatment of salivary calculi disease.

METHODS USED

Operations were conducted on patients with small (<8mm) intraoral unpalpable salivary stones in the origin of the submandibular duct or in the lower interlobar duct.

Scintigraphy with ^{99m}Tc -pertechnetate was performed on each of 7 patients once during a 1 to 4 month period after operation. Intravenous injection of 100 MBq ^{99m}Tc -pertechnetate was administered. The observation period was 30 min; after 16 min, salivary secretion was stimulated by peroral administration of 2-3 ml 5% citric acid solution. The data were digitised to obtain time-activity curves for accumulation and excretion of isotope from the treated and normal salivary glands. The time-activity curves were described using the Mita et al. (1981) classification. Cmax ratio, secretion rate, secretion rate ratio and function index (Nishi et al., 1987) were calculated for the curves.

SUMMARY OF THE RESULTS

The mean function index value was 0.76. In one case, the duct was closed after operation, causing an accelerated curve. Four treated patients were observed 5-6 years after operation. Scintigraphy indicated a good function in three patients, showing capacity for functional recovery of the gland after removal of concrement. The closure case was diagnosed as a non-functioning scintigramm type.

CONCLUSION

Scintigraphy of salivary glands, in contrast with sialography, could be used in all cases, including when duct orifice was damaged. The obtained data also allowed to assess the regeneration of salivary glands after treatment of salivary calculi disease.

Endocrinology/Thyroid

OS-559

N. Olsen, S. Nielsen, S. Møllekjær, T. Bacher, J. Mortensen, L. Rasmussen, J. Astrup, J. Weeke, J. Jørgensen

Aarhus University Hospital, Departments of Nuclear Medicine, Endocrinology and Neurosurgery, Aarhus, Denmark

SOMATOSTATIN RECEPTOR SCINTIMETRY AND RECEPTOR SUBTYPES IN HUMAN PITUITARY ADENOMAS

Somatostatin receptor scintimetry was performed in patients with pituitary adenomas to evaluate the discriminative capacity of an uptake index (UI) and correlate the index to the expression of somatostatin receptor mRNA. In total 18 patients were investigated in a prospective study. Six patients had Cushing's disease (ACTH), 6 had non-functioning adenoma (NF) and 6 had acromegaly (GH). The size of the adenoma was measured by MR imaging. A lateral view of the head was imaged by a Siemens Orbiter gammacamera 21 hrs after i.v. injection of 111 MBq In-111 pentetreotide. In total 300.000 counts were acquired in a 128 x 128 matrix. Standardized regions of interest were placed on the pituitary projection and the hemispheric brain. UI was the activity ratio of the normalized regions. UI ≥ 2.5 was considered positive. Tissue samples were obtained from transphenoidal adenectomy. The expression of mRNA encoding SSTR1-5 was assessed by a method using reverse transcription followed by a polymerase chain reaction. This mapping was obtained in one ACTH, 6 NF and 5 GH.

UI was 2.7 (2.3-6.9) in NF which was higher than 2.3 (1.9-2.4) in ACTH ($p < 0.01$) and smaller than 4.3 (3.6-7.0) in GH ($p < 0.05$). UI was negative in all 6 ACTH and positive in all 6 GH ($p < 0.01$). The width of adenoma (WA) was 3 mm (3-8) in ACTH which was smaller than 26 mm (5-34) in NF and 17 mm (11-25) in GH ($p < 0.01$). WA did not differ between NF and GH ($p > 0.10$). UI correlated slightly with WA in the 18 patients ($R = -0.59$, $p < 0.02$) but not in the 12 with NF and GH ($R = -0.02$, $p > 0.10$). SSTR4 was only found in ACTH. SSTR2 was detected in various combinations with receptor subtype 1, 3 and 5 in all 5 GH and in 5 of 6 NF but not in ACTH.

The results indicate that UI may be suitable to differentiate between NF and GH and characterize GH by a positive UI. An increased UI was mainly associated with SSTR2. NF and GH had the same WA and expression of mRNA. Thus the difference in their UI may reflect a difference in the density of the activated SSTR2. The normal UI in ACTH may be explained by the small size of the adenomas or the absence of SSTR2.

OS-560

THYROID-ASSOCIATED OPHTHALMOPATHY : OCTREOSCAN 111® SCINTIGRAPHY

Nocaudie M., Itti E., Bailliez A., Decoux M., Wemeau J.L., Marchandise X. - CHRU de Lille, 59037 Lille Cedex, France.

Objective. Management of thyroid-associated ophthalmopathy remains controversial. Specific treatment has to be applied at peak disease activity, before increase of disease severity. Somatostatin receptors expressed on the cell membrane of activated lymphocytes allow a scintigraphic imaging (Octreoscan-111®) of inflammation in extraocular muscles and retrobulbar fat. In order to see if octreoscan scintigraphy reflects the disease activity, we compared its results to pre and post-treatment changes.

Material and methods. We led a prospective study with 17 patients presenting a severe exophtalmia (11 Graves diseases, 4 Hashimoto disease, 2 Meigs disease). Each patient performed an hormonal and immunological assessment, an orbital computed tomography and a visual functional examination (giving 3 severity criteria), before and after undergoing a potential treatment (steroids and/or radiation therapy). Patients were clinically followed-up during 6 months at least. After intravenous injection of 111 MBq of ^{111}In -Octreotide, planar imaging was carried out focusing the head (anterior front view, right side and left side), at 4 and 24 hours. Retrobulbar uptake was assessed by a semiquantitative analysis (grading given by 2 independent and trained observers).

Results. All 10 cases in whom scintigraphy showed an important or moderate uptake were clinically improved. In 7 cases in whom uptake was indistinct from background or uncertain, orbitopathy activity did not change in 6 of them, but showed a substantial therapeutic response in 1 patient ($\chi^2 p < 0,01$).

Conclusion. Radiolabelled octreotide scan appears to reflect the thyroid associated ophthalmopathy activity predicting therapeutic response.

OS-561

Muros MA, Llamas-Elvira JM, Acosta MJ, Ramirez A, *Vilchez R, *Muros T, *Garcia-Calvente C. Department of Nuclear Medicine, *Department of Internal Medicine. Virgen de las Nieves Hospital. Granada. Spain.

SUPERIORITY OF 111IN-PENTETREOTIDE OVER 123I-MIBG SCINTIGRAPHY FOR CHEMODOCTOMAS DIAGNOSIS AND LOCALISATION.

Purpose: Chemodectomas or Glomus tumours are unusual head and neck paragangliomas. The non-invasive imaging technique metaiodobenzylguanidine (MIBG) scintigraphy has been used for the diagnosis of all type of paragangliomas during years. The purpose of this study is to evaluate and to compare the classic 123I-MIBG scintigraphy and the recent 111In-pentetreotide scintigraphy in the diagnosis and localisation of chemodectomas or glomus tumours.

Method and results: In order to get it, we have performed 123I-MIBG and 111In-pentetreotide scintigraphy in eight patients (seven women and on men) with histologic or radiologic confirmation of chemodectoma (five carotid body and three yugulotympanic chemodectomas). 123I-MIBG uptake were visualized in four patients on planar views and SPECT images (sensitivity 50%), and uptake was low to moderate in all patients. Using 111In-pentetreotide scintigraphy all chemodectomas of our eight patients were visualized (sensitivity 100%), and 111In-pentetreotide uptake intensity was high in all cases.

Conclusion: In conclusion, this study indicates that 111In-pentetreotide scintigraphy is superior to 123I-MIBG scintigraphy in diagnosis and localisation of chemodectomas or Glomus tumours. Moreover, 111In-pentetreotide scintigraphy permits a good classification of patients with or without somatostatin receptors in the chemodectoma in order to intend a pharmacological therapy with somatostatin analogues in inoperable tumours.

OS-562

Michael Hejna, Amir Kurtaran, Markus Raderer, Thomas Pangerl, Bruno Niederle, Fritz Vorbeck, Heinrich Vierhapper, Peter Angelberger, and Irene Virgolini. Departments of Oncology and Nuclear Medicine, University of Vienna, Austria.

123I-VASOACTIVE INTESTINAL PEPTIDE (VIP) RECEPTOR AND 111IN-DTPA-D-PHE1-OCTREOTIDE SCANNING IN PATIENTS WITH INSULINOMA

Introduction: Recent data suggest the expression of functional receptors (R) for vasoactive intestinal peptide (VIP) on various tumor cells. The high level expression of these R provided the basis for the successful clinical application of 123I-VIP for the *in vivo* localization of endocrine tumors. In this article, we report our experience in 15 patients suffering from insulinoma as compared to scanning with the somatostatin (SST) analog 111In-DTPA-D-Phe1-Octreotide (111In-OCT).

Patients and Methods: 15 patients with a histologically verified diagnosis of insulinoma were investigated using 123I-VIP scintigraphy (~150 MBq/1µg) and/or 111In-OCT scintigraphy (~150 MBq/10µg). The time span between both scintigraphies was 3-6 weeks. Scan results were compared to results of conventional imaging including CT, MRI and sonography. In addition, also results of surgical exploration were taken into account in case of discrepancies between conventional and scintigraphic imaging. Also *in vitro* investigation of SST subtypes in tumor specimens obtained during surgery was performed (Northern Blotting).

Results: 123I-VIP localized primary insulinomas in 83% (size 1-5 cm in diameter) and metastatic tumor spread in 80% (local lymph nodes or liver metastases). In comparison, 111In-OCT scanning had a sensitivity of 60% for primary tumors as well as metastases, while conventional radiologic imaging disclosed primary tumoral lesions in 55%. *In vitro* examination of tumor samples disclosed a predominant expression of the SST subtype 3 in all specimens investigated.

Conclusion: Our data implicate that 123I-VIP-receptor scanning has superior potential to 111In-OCT for the *in vivo* localization of small-sized primary insulinomas. This peptide scan is able to provide valuable additional information to conventional radiologic imaging.

OS-563

M. Shirzad, A. Leimer, J. Lister-James, B.R. Moyer, P. Angelberger and I. Virgolini. Department of Nuclear Medicine, University of Vienna, and Diatide Inc., Londonderry, USA.

PRECLINICAL CHARACTERIZATION OF A 99mTECHNETIUM LABELED VASOACTIVE INTESTINAL PEPTIDE (VIP) RECEPTOR IMAGING PEPTIDE

Colorectal cancer is a major health problem. 123I-VIP has been implemented for the staging and follow up of patients with intestinal adenocarcinomas. Among a variety of VIP peptide analogs we have identified [S-(CH₂CO-Gly-Gly-Cys-Lys-amide)Hcy]17-des-Met17]VIP (i.e. P1666) suitable for *in vivo* application to human. 99mTc-P1666 was purified by preparative HPLC resulting in a high specific activity product. The oxorhenium(+5) complex of P1666 was prepared by ligand exchange using Bu₄NReOBr₄ (product P1671). 99mTc-P1666 and 123I-VIP were compared for their *in vitro* binding to HT29 colonic adenocarcinoma cells, PANC1 pancreatic adenocarcinoma cells as well as to primary colonic cancer tissues. A comparable binding affinity in terms of the dissociation constant K_d was obtained for 123I-VIP and 99mTc-P1666 (K_d ≈ 5 nM). The binding of 123I-VIP was displaced by VIP (IC₅₀ 5 nM), P1671 (IC₅₀ 20 nM) and P1666 (100 nM). The binding of 99mTc-P1666 was displaced by VIP (5 nM), P1671 (15 nM) and P1666 (100 nM). No binding of both compounds to normal blood cells was observed. Biodistribution studies of 99mTc-VIP in Sprague-Dawley rats indicated rapid blood clearance, high lung and low gastrointestinal uptake. Based on its binding affinity for VIP receptors, and its biodistribution we conclude that 99mTc-P1666 has the potential to identify primary and recurrent adenocarcinomas as well as their metastases.

OS-564

E. Procaccini, M. Chianelli, M.G. Parisella, R. Barone, G. Di Leve, M. Filesi, G. Ronga, A. Grossman*, A. Signore. Nu.M.E.D. Group, II Clinica Medica University "La Sapienza" Rome, Italy. *St. Bartholomew's Hospital, London, UK.

99mTc-IL2 SCINTIGRAPHY AUTOIMMUNE THYROID DISEASES

Autoimmune thyroid diseases are characterized by lymphocytic infiltration of the gland and increased circulating antibodies. Aim of this study was to investigate the thyroid uptake of 99mTc-IL2 and quantify *in vivo* the severity of infiltration in different autoimmune thyroid diseases. 50 pts with Hashimoto's thyroiditis (HT) and 24 pts with Graves' diseases (GD) were studied before therapy onset. As control group, 30 normal subjects were evaluated. 15 pts with HT thyroiditis were studied after 1 year treatment with L-thyroxine; 5 pts with GD were also studied after the withdrawal of antithyroid therapy (18 months). Planar gamma-camera images of the thyroid region were acquired after 1 hour and specific uptake was expressed as thyroid to background (T/B) ratio. Autoantibodies were measured at the time of the study. Results showed a significant 99mTc-IL2 accumulation in patients with HT (1.67±0.26, p<0.0001 vs NS) and in patients with GD (1.60±0.28, p<0.0001 vs NS). After LT-4 therapy no significant differences were found in the 99mTc-IL2 accumulation in HT pts. Three out of 5 GD pts studied after therapy, had a positive IL2 scintigraphy and had a disease relapse within 3 months despite the absence of anti-thyroid antibodies; the other 2 pts (1 positive, 1 negative IL2 scan) are still disease free after 6 months follow-up. We conclude that L-thyroxine therapy does not modify lymphocytic infiltration in the thyroid of HT patients during the first year; in GD patients IL2 scintigraphy may be useful for therapy follow-up and for prediction of disease relapse.

Radiopharmacy and radiochemistry: Miscellaneous

OS-565

M.J. Welch, M.R. Lewis, J.B. Downer, D.W. McCarthy, T.J. McCarthy, *B.J. Hughey, *R.E. Klunkowstein, *R.E. Shefer.

Division of Radiological Sciences, Department of Radiology, Washington University Medical School; *Newton Scientific, Inc., Cambridge, MA.

HIGH YIELD PRODUCTION OF METAL AND HALOGEN RADIONUCLIDES FOR BIOMEDICAL APPLICATION USING A SMALL CYCLOTRON.

We have developed a simple, remotely-operated target system for producing high yield, high specific activity copper-64 using a biomedical cyclotron (McCarthy et al., Nucl Med Biol 1997; 24:35-43). We have adapted this target for the production of the shorter lived radionuclides copper-60 and copper-61 (Bass et al., J Label Compd Radiopharm 1997; 40:325-327). In this work we have also adapted the targetry and processing systems to produce gallium-66, yttrium-86, technetium-94m, bromine-76, bromine-77 and iodine-124. Yield measurements for our production of these nuclides approach literature values in all cases. For high yield production, gallium-66 is produced from zinc metal, yttrium-86 from strontium oxide and technetium-94m from molybdenum trioxide. These target materials are backed by gold disks and can be mounted in the copper-64 target system. The system allows automatic removal of the disc and transportation to a hot-cell. Techniques for the separation of the nuclides and recycling of the target material have been developed. For the production of the bromine and iodine radionuclides, selenium and tellurium targets were irradiated in the chemical forms of copper (I) selenide or telluride. For these irradiations, tungsten, a good heat conductor with a melting point of 3410°C, is substituted for gold due to the high melting points of the copper selenide/telluride. During target preparation and nuclide release, heating to greater than 1100°C is required. An indentation in the disc was filled with copper and the mole equivalent amount of selenium or tellurium and heated in a furnace. After irradiation, the target was returned to the furnace and reheated to release the halogen, which is then trapped on a cooled surface. We have shown that targets prepared in this way can be recycled. Work is in progress to use a specially designed inductive heating system to prepare these targets and obtain the radiohalogens. This system is compact and can heat to the required 1100°C in 2 minutes. This work demonstrates the successful adaptation of our copper-64 production method to high yield production of a variety of nuclides useful for PET imaging (gallium-66, yttrium-86, technetium-94m, bromine-76 and iodine-124) and for therapy (gallium-66, bromine-77 and iodine-124).

OS-566

J. Baranowska-Kortylewicz, Z.P. Kortylewicz, B. Toth, D. Hoffman

University of Nebraska Medical Center, Departments of Radiation Oncology and Radiology, J. Bruce Henriksen Laboratories, Omaha, NE
Funded by the LB595 Grant from the NE Department of Health

RADIONUCLIDE THERAPY OF COLORECTAL CANCER WITH ORAL 125IUdR

5-Iodo-2'-deoxyuridine (IUdR) radiolabeled with Auger-electron emitters is exceptionally effective as a radiotoxic agent *in vitro* but it failed to produce comparable results in the *in vivo* systems. Primary reasons for this failure are the efficient and rapid catabolic and anabolic degradation of IUdR *in vivo*. We postulated that by temporarily altering physicochemical properties of IUdR, an improved pharmacologic outcome will be achieved. Bioreversible modifications of a structure of IUdR yield inert precursors which must undergo a specific metabolic transformation to release IUdR. Such an approach is novel in the field of radiotherapeutic agents and nuclear oncology.

The GI tract represents a hostile environment for any drug or drug dosage form. 125IUdR prodrugs for local delivery to colon must survive this environment and be released only in the specific segments of the GI tract. To assure the sustained delivery of 125IUdR to the site of colorectal cancer, we have prepared a series of glycoside-based prodrugs of limited permeability in the stomach and small intestine, and digested only by enzymes of the colonic microflora. We have already reported on the *in vivo* fate of these glycosidic prodrugs in normal mice. This report describes the outcome of studies conducted in tumor-bearing mice.

Female mice received carcinogen (ten weekly doses of 1,2-dimethylhydrazine) and then were treated p.o. with either 125IUdR-prodrugs or 125IUdR. One week after treatment with radionuclides, mice were killed and full biodistribution studies conducted. The radioactivity levels in selected tissues and blood were determined and the entire GI tract fixed for histopathology and autoradiography. The selective uptake of 125IUdR in experimental animals was observed in all segment of the large intestine and liver (Figure above). Autoradiographic studies indicated nuclear localization of the radioactivity which confirmed the site-specific release of 125IUdR from its prodrugs and its availability for the uptake by dividing cells. This class of prodrugs can also be applied to the oral delivery of IUdR-based radiosensitizers.

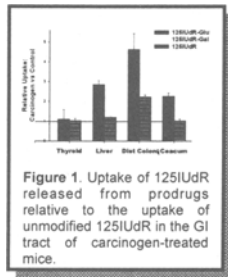


Figure 1. Uptake of 125IUdR released from prodrugs relative to the uptake of unmodified 125IUdR in the GI tract of carcinogen-treated mice.

OS-567

U. Häfeli, and C. Grüttner

Cleveland Clinic Foundation, Radiation Oncology Dept. T28, 9500 Euclid Ave., Cleveland, OH 44195, USA; Microcaps GmbH, Friedrich-Barnewitz Str. 4, D-18119 Rostock, Germany

MICROSPHERES FOR SELECTIVE BINDING AND MAGNETIC TARGETING OF 111IN, 90Y, 99mTc, 186Re AND 188Re ISOTOPES IN RADIOTHERAPY

Targeted radiotherapy approaches using biologically selective molecules (e.g. antibodies) have shown limited success, primarily due to the relatively small percentage of radioactive material that actually reaches the tumor sites. One method to overcome this situation is to prepare tissue-compatible microspheres which can selectively bind very high concentrations of diagnostic and therapeutic radionuclides and then apply them locally (e.g. embolization therapy) or by magnetic targeting. Our aim was to prepare polymer-derivatives which are able to form microspheres and then bind currently used radionuclides after a short incubation time with high efficiency.

The polymer poly(lactic acid) (PLA) was successfully derivatized with the tetraazacrown ether DOTA for the selective complexation of 111In and 90Y. The aliphatic N₃S-ligand MAGG together with the analogous N₂S₂-ligand was also bound to PLA after terminal introduction of aliphatic amino groups. Both derivatives selectively complex 99mTc and 186Re / 188Re. The PLA derivatization did not influence their ability to form 10-30 µm microspheres using a solvent evaporation method. Radiolabeling of these microspheres is short (<30 min) and shows high labeling efficiencies (>90%).

The surface modification of the microspheres was followed by the study of Zetapotential-pH-profiles of the various microspheres in comparison to unmodified PLA microspheres and microspheres with covalently bound DTPA on the surface. The introduction of ligands leads to significant changes of the surface potential of the particles.

The prepared microspheres containing specific, covalently bound chelators are potentially useful carriers for the diagnostic and therapeutic delivery of radionuclides. Applications include the local injection of beta-emitting microspheres into tumors and for radioembolization therapy. The use of magnetite filled microspheres of different size would further allow to reach target areas within the body through the use of an external magnetic field.

OS-568

T.S.T. Wang, R.A. Fawwaz, and R.L. Van Heertum

College of Physicians and Surgeons, Columbia University, New York, NY.

A STUDY OF PREPARATION, QUALITY CONTROL, AND *IN VITRO* STABILITY OF Re-188-MAG3: A POTENTIAL AGENT FOR INHIBITION OF RESTENOSIS AFTER PTCA.

Re-188-MAG3 (I) (t_{1/2}=16.9 h, 2.1 MeV, β⁻) is used in our IND clinical trials to prevent restenosis after coronary angioplasty or stent implantation. The aim of this study is to evaluate conditions for the preparation, quality control and *in vitro* stability of I, which may be important in its clinical application.

Re-188-perrhenate (10-18 GBq/ml) was obtained by elution through a W-188/Re-188 generator under the following conditions: A). In each buffer solution at pHs 2,3,4, & 5, aliquots of 0.5, 1, & 2 mg of SnCl₂ were dissolved. B). A MAG3 kit was mixed with SnCl₂ and perrhenate solutions, and kept at 100°C for 15, 30, 45, & 60 min. C). Sep-Pak column, 0.001N HCl, and EtOH-N.S. eluents were used for quality control. D). I was stored with and without 1 mg of ascorbic acid (II), at room temperature for 0-6 hr. The results revealed that: 1). >1 mg SnCl₂ was required to produce I. 2). The yield of I was not affected by pH. 3). At least 30 min incubation at 100°C was needed. 4). Without the presence of II the *in vitro* stability of I decreased from 99 to 84%. In the presence of II, I was stable (99%) after 6 hr of storage. In conclusion: The addition of SnCl₂, >30min of heating and the presence of II are needed for successful preparation of I.

OS-569

S.C. Srivastava, G.E. Meinken, and J.L. James*

Brookhaven National Laboratory, Upton, NY, and *Diatide, Inc., Londonderry, NH.

CHARACTERIZATION AND IN-VIVO TESTING OF HPLC-PURIFIED Sn-117m STANNIC DTPA PREPARATIONS.

Purpose: In the formulation of Sn-117m(IV) DTPA for use in the treatment of metastatic bone pain, a 20-fold molar excess of DTPA has been used to ensure complete complexation of tin. We carried out a study to separate stannous DTPA, stannic DTPA, and free DTPA using anion exchange HPLC based on the charge difference between the various chemical species, and to determine the in-vivo properties of stannic DTPA as a function of the DTPA/tin molar ratio in the final product. **Methods and Results:** Using a 7.5x75mm DEAE column and an inverted parabolic gradient using 0.05-0.4M pH 4.5 phosphate buffer, the following retention values (K') were obtained: Sn-117m (IV) DTPA= 1; Sn-117m (II) DTPA = 4.2; DTPA = 4.6. Purified Sn-117m (IV) DTPA fraction (i), free of uncomplexed DTPA, was evaluated in mice. Results were compared with other similar fractions (ii, iii and iv) to which an additional 2, 3, and 5-fold molar excess of DTPA were added based on the amount of tin present. The original pre-HPLC preparation (v) was used as a control. For each sample, 5 normal mice were injected i.v. and the biodistribution determined at 24 h and 7 days. There was no difference in the bone uptake, blood clearance, or the total whole body retained activity among the various samples. However, liver (L) and spleen (S) uptakes (% ID per g at 24h respectively) were slightly higher in the case of preparation (i) (L: 0.63; S: 0.34), and very slightly increased for preparations (ii-iv) (L:0.47 avg; S:0.27 avg), as compared with the control (v) (L:0.29; S:0.08). The difference between ii-iv and v was not statistically significant (p<0.05). **Conclusion:** The HPLC method developed in this study provides a means for determining stannous and stannic content of Sn-117m DTPA as well as a method for removal of excess free DTPA. We conclude that once the tin is thoroughly complexed, there is no significant difference in the biodistribution of purified Sn-117m stannic DTPA containing between a final 3-20 fold molar excess of DTPA. This work was supported by the U.S. Dept. of Energy, under Contract No. DE-AC02-98CH10886, and by Diatide, Inc.

OS-570

C B Sampson

Hospital: Addenbrooke's Hospital, Department of Nuclear Medicine, Cambridge, UK.

DOES PATIENT MEDICATION AFFECT THE RADIOLABELLING OF WHITE BLOOD CELLS? A SIXTEEN YEAR SURVEY

Failure to properly radiolabel white cells (WBCs) can lead to poor quality scintigrams or, at worst, abandonment of the nuclear medicine test. As a major UK blood labelling centre we have experienced unexplainable difficulties in labelling with both Tc-99m and In-111. A survey was therefore carried out for the period 1981-1997 to examine whether patient medication was responsible for unusually low labelling efficiencies (LE) of labelled WBCs. Respondents were asked to report the patient's medication regime on the day of the test. Before sending in the report they were asked to discount other causes of poor labelling such as low yields of WBCs.

54 adverse reports were received. Nearly all the patients were on multi-drug therapy and many were taking at least two drugs which are known to have marked pharmacological effects on the biochemistry and/or chemotaxis of WBCs. Six patients were taking cyclosporin, azathioprine and prednisolone; six were taking cephalosporins other than cyclosporin; five patients were taking mesalazine or mesalazine derivatives; three were taking either cyclophosphamide or methotrexate and two were on nifedipine.

To assess whether there was a causal association between the pharmacological effect of the drugs on WBCs and a low LE, Bradford-Hill's criteria for the assessment of a causal association between two variables were applied. These criteria are *strength of association, consistency, specificity, biological gradient, plausibility, temporal relationship and coherence*. Six out of the seven criteria were found to be positively correlated. We conclude that there is a high probability that cyclosporin, other cephalosporins, azathioprine, cyclophosphamide, methotrexate, nifedipine and mesalazine cause a low LE. We suggest that in patients taking these drugs, or combinations of these drugs, increased amounts of radioactivity should be used for the labelling process to overcome the poor LE.

Physics and instrumentation: Others

OS-571

Slomka PJ, Cheng D, Driedger AA. Nuclear Medicine and Diagnostic Radiology. University of Western Ontario. London Health Sciences Centre, London, Ontario, Canada

JAVA BASED NUCLEAR MEDICINE VIEWING AND PROCESSING STATION: NEW PARADIGM FOR TELEMEDICINE AND PACS.

In nuclear medicine practice, the situation often arises where images have to be reviewed and reported from many locations outside the department. However, expensive PACS stations, cannot be easily deployed at numerous locations. To solve this problem, we propose to utilize Java language, internet browser technology and existing standard computer base for reading and providing the reports of nuclear medicine images.

Java viewing station (JarViS) interfaces to the Interfile-based clinical patient database on a departmental nuclear medicine workstation. All software resides on a nuclear medicine server. The contents of the clinical database can be searched via a browser interface after providing a password, which can be specific for each referring physician. Compressed images with the Java applet and color lookup tables are downloaded on the client side. This paradigm does not require nuclear medicine software installation on remote computers, which simplifies support and deployment of such systems in contrast to traditional PACS design. To enable versatile reporting of the images, color tables, and thresholds can be interactively manipulated and images can be processed displayed in a variety of ways, including 3-D SPECT reorientation. Image filtering, frame grouping, and movie display are available. Final reports can be stored as HTML files.

JarViS runs on Windows 95/NT, Solaris and Macintosh platform with Netscape Communicator or Microsoft Internet Explorer. The performance of Java code with just-in-time compiler approaches that of standard imaging workstation for bilinear interpolation, cine display and filtering, and SPECT reorientation. Time for spatial filtering of 100 frames of a dynamic kidney study is 2 sec on Pentium 233Mhz computer with Netscape 4. Time to download compressed 14 frames of 128x128 static study together with the applet and color tables via a 28.8 modem is 120 seconds, and less than 1 second on the local area network

We conclude that it is feasible to setup a remote nuclear medicine viewing and reporting station using Java and an inter- or intranet browser. No software is required on the remote site, thus images can be made easily and cost-effectively available to referring physicians, cancer clinics within and outside of the hospital, providing a viable alternative to film media or traditional PACS systems. We also find this system useful in home reporting of emergency procedures such as lung ventilation perfusion scans or dynamic studies.

OS-572

V. Bosnjakovic

Center for High Technology, CCS, Belgrade, Yugoslavia
ADAC Laboratories, USA

THEORETICAL PRINCIPLES AND EVALUATION OF THE DESIGN OF UNIVERSAL NUCLEAR MEDICINE IMAGER (UNMI)

A UNMI has been designed based on position sensitive (PS) area detectors. The detector head, incorporated in a dual headed machine to provide for planar, SPECT and PET studies, uses a thick layered NaI(Tl) crystal to enable the determination of depth-of-interaction (DOI) of gamma events in particular crystal layers. Insertion in a thick crystal of thin glass layers with different refraction indices (RI), forms the internal light collimators (LC) within DOI crystal layers. Thus, according to the Snell's law light photons exceeding "critical" angle shift from the direction toward the PS PMTs to the lateral side(s) of the crystal layer(s), providing for DOI determining signal; by the external LCs (fiberoptics mounted on crystal sides) and DOI electronics, a DOI signal, as put in coincidence with the PS signal coming from the same event, shifts an x,y, address to a particular DOI memory stack. A possible optimal design of the detector head might consist of the following: the total NaI(Tl) crystal (RI, 1.85) thickness of 0.75" is divided into two layers each 3/8" thick, separated by a thin (1/32") light flint glass (RI, 1.61) layer; on top of the upper NaI(Tl) layer is a light flint layer, 2/8" thick, facing PS PMTs array as a light guide (LG); a heavy flint glass (RI, 1.695) layer, 1/32" thick, on bottom of the lower NaI(Tl) layer (facing aluminium cage), as externally diffusely reflectively painted, increases by its RI the solid angle of view and thus the amount of light to be diffusely back reflected towards PS PMTs. The optical couplings of the two crystal layers with three glass layers are made specularly reflective. By selecting the glasses of various RIs, one can control the amount of scintillation light directed to both the DOI determining system and the PS system influencing energy and spatial resolution. Also, one can physically confine the range of direct and diffusely reflected light directed towards PS PMTs to a local 7 (3") PMTs array (fitting a local centroid position calculation), as enabled by the above given design. The geometric light collection efficiency was found to be 50.2% for the PS system, and 28.5% per crystal layer for the DOI system, enabling by 3:1 a clear discrimination of the two 3/8" DOI crystal layers. The UNMI design is likely to retain the intrinsic spatial resolution of the recent MCD detectors for low energy single photon emitters, and improve the efficiency for the medium energy ones. In PET studies, the 6/8" NaI(Tl) thickness (a probably upper limit at PS area detectors) should still improve the rate of detected true coincidences by improving sensitivity due to a thicker crystal and wider angle of acceptance; the latter being enabled by a known DOI allowing for a proper correction for "parallax error", which in turn improves the spatial resolution, too.

OS-573

S.A. Benjegård, V. Sauret, P. Bernhardt, B. Wängberg, H. Ahlman, E. Forssell-Aronsson
Sahlgrenska University Hospital, Departments of Radiation Physics and Surgery

EVALUATION OF THREE GAMMA DETECTORS FOR INTRAOPERATIVE DETECTION OF TUMOURS USING ¹¹¹IN-LABELLED RADIOPHARMACEUTICALS

Attempts with intraoperative scintillation detection using tumour-binding radiopharmaceuticals has been intensified recently. In some cases previously unknown lesions have been found, but in most cases no additional lesions were detected. In the present study the physical characteristics and the ability to detect tumours, accumulating an ¹¹¹In labelled radiopharmaceutical, have been investigated for three different detector systems: one sodium iodide (NaI(Tl)) detector (ScintiProbe), one caesium iodide (CsI(Tl)) detector (TecProbe1) and one cadmium telluride (CdTe) detector (TecProbe2).

METHOD: A clinical measurement situation was simulated by a body phantom and tumour phantoms (diameter 5 mm to 20 mm), made of water, agarose gel, or epoxy, with similar density and attenuation coefficient as soft tissue. The activity concentration in the body phantom was based on reported values of ¹¹¹In-octreotide in normal tissue in man. The ¹¹¹In activity concentration in the tumour phantoms was varied from 3 to 80 times the ¹¹¹In activity concentration in the body phantom. Data were processed to determine tumour detection levels.

RESULT: ScintiProbe showed the lowest FWHM-values due to the best collimation leading to a high ratio between counts from tumour and background, i.e. small tumours could be detected. Due to high efficiency, TecProbe1 required a shorter acquisition time to reach a statistically significant difference between tumour phantom and background. For deep-lying tumours ScintiProbe was superior, while TecProbe2 was best suited for superficial tumours with high activity concentration of the underlying tissue.

CONCLUSIONS: At a maximum acquisition time of 30 seconds almost all superficial tumours with a diameter of 10 mm diameter, or larger, were detected, if the ratio between the ¹¹¹In concentration in tumour and background exceeded 3. However, in the clinical situation the biological variation of the uptake of ¹¹¹In-octreotide in tumour and normal tissue makes it difficult to determine a distinct detection level. For such clinical condition ScintiProbe is the best choice of the detectors investigated, due to its good resolution, despite lower efficiency. Documentation of detector characteristics is of importance for the clinician to make an adequate device in relation to tumours location and receptor expression by the tumour.

OS-574

A. van Lingen, A.M. Bosma, V. Prat, T. IJbema, R. Pijpers.
Free University Hospital, Nuclear Medicine, Amsterdam,
PI Medical, Almere, Netherlands and Eurorad, Strasbourg, France.

THE EFFECT OF DETECTOR SIZE AND DETECTOR MATERIAL ON GAMMA PROBE PERFORMANCE.

By the introduction of the sentinel node concept in Nuclear Medicine routine the interest in gamma probes has increased. However, acceptance tests have not been devised. Although acceptance tests exist for large counting units (thyroid uptake probe, contamination counters), the special feature of small gamma probes used during surgery is the combination of sufficient sensitivity and the ability to localize small nodes. The detector size (diameter) and the detector material affect both performances. We used probes (Eurorad) of different sizes and detector materials: P1: CdTe, 5 mm diam, 3 mm thick; P2: CdTe, 8 mm diam, 3 mm thick; P3: CsI (coupled to photodiode), 5 mm diam, 10 mm thick. All probes were shielded with tungsten (2.5 mm for CdTe and 5 mm for CsI) and connected to the same electronics. The sensitivities (cps/kBq) were determined from a 1 MBq ⁵⁷Co reference source centered in holders closely fitting the probes.

The localisation accuracy at a certain depth was assessed by the FWHM of a profile measured at lateral displacements (0-70 mm) of the source at depths of 1, 2 and 5 cm. Relative sensitivity (%) at a depth was obtained by normalization to the sensitivity at 1 cm depth. All measurements were performed within an energy range of 100 - 140 keV:

Probe	Sensitivity		FWHM (mm) / Relative sensitivity (%)		
	cps/kBq	Depth:	1 cm	2 cm	5 cm
P1	1.2		19.2 / 100%	30.8 / 40%	63.2 / 10%
P2	2.4		18.4 / 100%	30.0 / 42%	73.8 / 9%
P3	2.4		22.0 / 100%	28.0 / 55%	51.8 / 14%

The FWHM may reflect the "field-of-view" of the probe, in which it is able to detect a source effectively. However, to choose the probe with the best overall performance, a figure of merit needs to be established.

OS-575

J.H. Kim, Y. Choi, H.S. Kwon, J.Y. Kim, S.E. Kim, Y.S. Choe, M.H. Kim, K.S. Joo, B.T. Kim
Samsung Medical Center, Department of Nuclear Medicine
Myongji University, Department of Physics
Konkuk University, Department of Computer Engineering

DEVELOPMENT OF A MINIATURE GAMMA CAMERA USING NaI(Tl) - PSPMT FOR BREAST IMAGING

Scintimammography performed with a conventional scintillation camera and tumor seeking radiopharmaceutical such as ^{99m}Tc MIBI and ²⁰¹Tl has been shown to be useful for detecting malignant breast tumors. The conventional gamma camera, however, is not ideal for scintimammography because of its large size (~50 width) causing high cost and low image quality. We are developing a small gamma camera, consisting of a NaI(Tl) crystal (60 mm × 60 mm × 6 mm) coupled to a Hamamatsu R3941 position sensitive photomultiplier tube (PSPMT), resistor chain circuit, preamplifier, nuclear instrument modules, analog to digital converter and PC employed for control and display. The PSPMT was read out using a standard resistive charge division which multiplexes the 34 cross wire anode channels into 4 signals (X+, X-, Y+, Y-). Those signals were processed individually through a four-channel line driver and preamplifier board, shaped and amplified. The signals were discriminated and digitized via triggering signal and used to localize the position of an event by applying the Anger logic. The intrinsic energy resolution of the system was 18% FWHM at 140 keV. The spatial resolution was obtained using a line phantom and ^{99m}Tc point source and was 2.7 mm FWHM. The intrinsic sensitivity of the system was approximately 8000 cps/μCi. High quality flood image and hole mask images were obtained. Breast phantom containing 2~7 mm diameter spheres was successfully imaged with a parallel hole collimator. The obtained image displayed accurate size and activity distribution over the imaging field of view. Linearity and uniformity correction algorithms are being developed. The small gamma camera developed in this study may improve the diagnostic accuracy of scintimammography by optimally imaging the breast.

OS-576

C. Bagnara, P. Bianchi, F. Buffoni, T. Torreggiani, G. Agnese, G. Villa, G. Taccini, and G. Mariani.
Health Physics, S. Martino Hospital, and Nuclear Medicine Service, DIMI, University of Genoa; Genoa (Italy).

PHYSICAL PERFORMANCE PARAMETERS OF A NEW INTRA-OPERATIVE GAMMA-PROBE DESIGNED FOR SENTINEL LYMPH NODE LOCALIZATION

Utilization of intraoperative gamma-probes extends now well beyond radioimmunoguided surgery. In fact, radiopharmaceuticals other than anti-tumor radiolabeled antibodies allow to explore the expression of receptors on the surface of tumor cells, or the pattern of lymph flow from primary tumors scheduled for surgery, searching for the sentinel lymph node. Physical performance of the gamma-probe is instrumental in achieving good target localization, also considering that most of these probe-guided procedures rely now on gamma emission different from ¹²⁵I, such as ^{99m}Tc or ¹¹¹In. In this study we characterized the physical performance of a gamma-probe specifically designed for sentinel lymph node localization (ScintiProbe MR100, Pol.hi.tech, Italy).

The probe, supplied with a cylindrical 8x10 mm CsI(Na) crystal shielded laterally by an internal tungsten collimator, has an intrinsic 99% counting efficiency for incident 140 keV photons. Performance of the system was characterized by phantom measurements in air and in water, to derive attenuation-transmission coefficients of ^{99m}Tc point sources.

Counting efficiency showed the expected pattern related to distance from the source up to 15 cm, while perfect linearity of response was found up to about 400 μCi (measured at 10 cm). The angular coefficient of response, measured in air, showed counting efficiencies below 80% for detection angles over 23-24° at 5 cm, and below 80% for angles over 18° at 10 cm, while slightly wider angular coefficients were observed in water. The measured global counting efficiency at 1 cm was 13300 cps/MBq in air and 430 cps/MBq in water.

The experimental data obtained with phantom measurements support the excellent target localizing properties observed *in vivo* with this probe, based essentially on optimal lateral shielding (narrow detection angle) which helps in the intraoperative localization of the sentinel lymph node by markedly reducing background activity, thus increasing the target-to-background ratio.

General nuclear medicine: Gastroenterology

OS-577

L. Madácsy*, H.V. Middelfart, P. Matzen, L. Højgaard and P. Funch-Jensen
Depts. of Med. and Surg. Gastroenterology and Clinical Physiology/Nuclear
Medicine, Hvidovre Hospital, University of Copenhagen, Denmark, and *1st
Dept. of Internal Medicine, Albert Szent-Györgyi Med. Univ., Szeged, Hungary

ASSESSMENT OF FLOW-PRESSURE RELATIONSHIP IN THE BILIARY TRACT BY COMPARISON OF THE RESULTS OF QUANTITATIVE HEPATOBILIARY SCINTIGRAPHY (QHBS) AND ENDOSCOPIC SPHINCTER OF ODDI MANOMETRY (ESOM)

Introduction: In cholecystectomized subjects with normal liver function, the bile flow from the liver into the duodenum is regulated by the motor function of the sphincter of Oddi (SO). The aim of the present study was to compare the results of QHBS and ESOM to assess the flow-pressure relationship in the biliary tract.
Patients and methods: 20 patients (PTs) with suspected SO dysfunction (SOD) of biliary type II or III (SOD group) and 20 cholecystectomized asymptomatic subjects (control group) were investigated. QHBS was performed in every PT, but ESOM was attempted only in the SOD group. ESOM was successful in 13 PTs, 7 drop-outs were due to poor PT co-operation and technical difficulties. The time to peak activity (Tmax), the half times of excretion (T1/2) of the liver parenchyma (LP), the hepatic hilum (HH) and the common bile duct (CBD), and also the duodenum appearance time (DAT) were determined by means of QHBS. The SO basal pressure (SO BP) and the amplitude (A), frequency (F) and peristalsis (P) of phasic contractions (PCs) were measured by means of ESOM. The quantitative parameters of QHBS and ESOM were compared.
Results: The upper limits of the normal values of QHBS were determined in the control group. QHBS revealed delayed transpapillary drainage in 10 of the 20 PTs with suspected SOD. The ESOM recording was normal in 5 and abnormal in 8 PTs. A comparison of the results of ESOM and QHBS demonstrated a good overall agreement, with concordant results in 10 PTs (6 abnormal and 4 normal). Only 3 PTs exhibited discordant results (2 PTs with abnormal and 1 PT with normal ESOM), all of them had normal SO BP. The T1/2 for the LP, HH and CBD, the Tmax for the HH and CBD, and also the DAT showed significant, linear correlations with the SO BP (r: 0.80, 0.83, 0.75, 0.76, 0.57, 0.85, respectively), but there was no correlation with the A, F and P of the PCs.
Conclusions: QHBS and ESOM are comparable and equally sensitive methods for the diagnosis of SOD, therefore non-invasive QHBS is preferable. Not the PCs, but the SO BP is the main regulator of the transpapillary bile transit.

OS-578

A. Szepes, L. Madácsy, M. Lázár*, B. Velösy, J. Lonovics, L. Pávics*
First Department of Internal Medicine and Department of Nuclear Medicine*,
Albert Szent-Györgyi Medical University, Szeged, Hungary

DIFFERENTIATION BETWEEN INTRAHEPATIC AND EXTRAHEPATIC CHOLESTASIS BY MEANS OF QUANTITATIVE HEPATOBILIARY SCINTIGRAPHY (QHBS)

Introduction: Scintigraphic features of the sphincter of Oddi (SO) dysfunction (SOD) associated with impaired transpapillary bile flow are well established, however, such features have not yet been characterized in intrahepatic cholestasis caused by primary biliary cirrhosis. The aim of the present study was to determine those quantitative scintigraphic parameters that may be used to differentiate between different forms of cholestasis.
Patients and methods: 8 patients (PTs) with typical intrahepatic cholestasis caused by primary biliary cirrhosis (PBC group), and 7 PTs with impaired transpapillary bile flow caused by SOD (SOD group) were investigated by QHBS, and the scintigraphic parameters were compared with normal values determined in 20 asymptomatic cholecystectomized PTs (Control group). QHBS was performed with our standard protocol, and the time to peak activity and the half- times of excretion (T1/2) of the liver parenchyma (LP), the hepatic hilum (HH) and the common bile duct (CBD) were calculated. The T1/2 ratio of CBD/LP was expressed as a new parameter: the obstructive factor (OF).
Results: Normal values of T1/2 over the LP, HH and CBD were determined in the control group (T1/2: 19.3±2.3, 19.3±2.4, 18.8±2.6 min, respectively). In PBC group, there was a primary increase in T1/2 over the LP, which determines the slower emptying parameters of the HH and CBD (50.1±12.3, 51.7±9.0 and 55.4±18.4 min, respectively). However, in SOD group, T1/2 was normal over the LP, but enhanced over the HH, reaching its maximum over the CBD (25.3±6.4, 45.1±20.9, 72.9±22.0 min, respectively). OF was significantly increased in the SOD group as compared with the PBC group and also the control group (2.91±0.79 vs. 1.1±0.2 and 1.0±0.1).
Conclusions: These results indicate that intrahepatic cholestasis caused by PBC and impaired transpapillary bile flow induced by SOD are associated with completely different scintigraphic patterns, and QHBS seems to be a valuable method in their differential diagnosis

OS-579

R. Róka, T.T. Várkonyi*, Cs. Lengyel*, P. Légrádi*, L. Madácsy*, B. Velösy*, P. Kempler**, J. Lonovics*, L. Pávics
Department of Nuclear Medicine, First Department of Medicine*, Albert
Szent-Györgyi Medical University, Szeged, First Department of Medicine**,
Semmelweis Medical University, Budapest, Hungary

EVALUATION OF GALL BLADDER AND STOMACH MOTILITY IN LONG-STANDING DIABETES MELLITUS

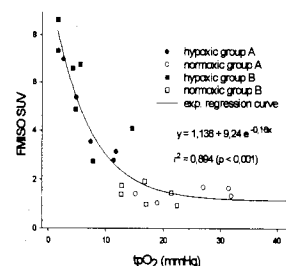
Gallstone disease and gastroparesis are frequent complications of diabetes mellitus (DM).
AIM: To evaluate the relation of the gall bladder (GB) and stomach motility to the neuropathy status and the severity of symptoms in patients with long-standing DM.
PATIENTS AND METHODS: 9 patients with DM and 6 healthy subjects were examined. The GB motor function was measured by means of quantitative hepatobiliary scintigraphy. The gastric emptying rate was determined by solid meal gastric scintigraphy. The presence of autonomic and peripheral neuropathy was determined. In order to characterize the severity of digestive complaints, a gastrointestinal symptom score was calculated.
RESULTS: Scintigraphic studies revealed a marked gall bladder (GB) and stomach hypomotility in DM patients (GB ejection fraction (GBEF): 35.3±7.0 vs 78.2±5.8%, half -time of gastric emptying(HTE): 107.6±15.5 vs 55.8±7.5 min, p<0.05, DM vs controls). A positive correlation was found between the gastric HTE and the autonomic neuropathy (AN) score (r=0.68, p<0.05) while a negative correlation was observed between GBEF and the AN score (r=-0.68, p<0.05). Analysis of the symptom scores did not reveal any relation between the severity of complaints and the degree of gastrointestinal motor disorders or the progression of neuropathy.
CONCLUSION: GB and stomach hypomotility is frequently associated with long-standing DM. The severity of the motility disorders is related to the progression of the neuropathy, but not consequently related to digestive complaints. Our observations demonstrate the important role of simple and non-invasive scintigraphic methods in the early diagnosis and objective follow-up of gastrointestinal complications of DM.

OS-580

M. Piert*, H.-J. Machulla**, P.D. Dißmann*, P. Aldinger*, G. Becker**,
W. Lauchart*, H. Fischer*, H.D. Becker*, R. Bares**
*Department of General Surgery and **Department of Nuclear Medicine
University of Tübingen (Germany)

SIMPLE SUV ANALYSIS OF F-18-FLUOROMISONIDAZOLE UPTAKE ALLOWS ACCURATE MEASUREMENT OF REGIONAL LIVER HYPOXIA

Purpose: Lacking clinically available methods, **Results:** Measured by PET, the mean FMISO metabolic effects of liver hypoxia have not been SUV in normoxic liver tissues was 1.33 in investigated in detail. F-18-Fluoromiso- group A and 1.35 in group B. In hypoxic re- nidazole (FMISO) accumulates in hypoxic gions, the SUV increased to 3.8 in group A (p tissue by means of covalent binding to cyto- < 0.01) and to 5.5 in group B (p < 0.001). In plastratic proteins following intracellular radi- comparison to normoxic regions, the tpO₂ cal formation. This study was undertaken to decreased by 69 % in group A (p< 0.01) and evaluate whether - despite the physiological 72 % in group B (p < 0.001), respectively. The metabolism of nitroimidazoles - FMISO PET exponential function stated below accurately can quantify liver hypoxia on a regional basis. describes the relationship between tpO₂ and **Materials and methods:** To establish the re- FMISO SUV (see Fig.). lationship between FMISO uptake and the extent of tissue hypoxia, we evaluated the FMISO uptake of normal and hypoxic liver in 13 domestic pigs. For induction of an arterial flow reduction, branches of the hepatic artery of varying size and localization were occluded yielding different degrees of tissue hypoxia in the dependent liver regions. The portal venous blood flow to the liver was not mechanically impaired. A 3-hour dynamic PET study with FMISO followed while ventilating the animals either by O₂/N₂O (group A, FIO₂=0.67, n=6) or room air (group B, FIO₂=0.21, n=7). The tissue pO₂ (tpO₂) was measured directly via pO₂-histography (Eppendorf) in normoxic and hypoxic liver regions. In addition, the regional **Conclusion:** Our results suggest that the arterial blood flow was measured prior to and FMISO uptake is directly related to the severity after arterial occlusion by ⁵¹Cr- and ¹⁴¹Ce- la- of the tissue hypoxia. In this experimental belled microspheres. The standard uptake model, liver hypoxia can be quantified by sim- value (SUV) for FMISO was calculated from ple SUV analysis of FMISO PET results. late images (150-180 min).



OS-581

A.Maini, S.Gambhir, * A Srivastava, * G.Chaudhary, T.C. Kalawat, B.K. Das
Hospital: Sanjay Gandhi P.G.I., Department of Nuclear Medicine and Gastroenterology.

CCK-AUGMENTED QUANTITATIVE HEPATOBIILIARY SCINTIGRAPHY (QHBS) FOR DIAGNOSIS OF SPHINCTER OF ODDI DYSFUNCTION IN PATIENTS OF IDIOPATHIC PANCREATITIS.

8-25% of patients with acute pancreatitis are labeled as "idiopathic". This figure is lower if sphincter of Oddi manometry and microscopic study for microlithiasis have been done after the first or second attack of "idiopathic" pancreatitis. The aim of this study was to detect SOD using QHBS in patients of idiopathic pancreatitis where microlithiasis is also associated. 18 normal volunteers and 8 patients of idiopathic recurrent pancreatitis underwent QHBS after injection of 37 Mbq of 99m Tc-mebrofenin IVI. Study was acquired in 128x128 matrix, 1 frame/min for 90 mins. CCK (0.01 µgm/Kg x 3 min) was injected at 60min. Computer generated T-max and T-1/2 parameters were calculated over liver parenchyma and CBD. Gall bladder ejection fraction was also calculated. Biliary microliths were analysed by polarised microscopy after endoscopic bile drainage.

	N	Liver Parenchyma		CBD	
		Tmax(min)	Tl/2(min)	Tmax(min)	Tl/2(min)
Controls	18	9.8±2	24.4±9.1	21.7±5.47	21.0±11.0
Patients	8	9.6±2.3	25.4±12.5	21.4±4.9	17.0±10.7

There was no significant difference between the control subjects and patients. However using mean +2SD as upper reference limit in controls, 2/8(25%) patients had a higher CBD Tmax. Both underwent endoscopic papillotomy. They are subsequently asymptomatic. This study shows that QHBS is a useful non-invasive procedure for detection of SOD in patients of idiopathic pancreatitis.

OS-582

Y. Fukuda, Y. Nishiyama, Y. Yamamoto, M. Ohkawa, M. Tanabe

Kagawa Medical University, Department of Radiology

EVALUATION OF LIVER FUNCTION USING 99mTc-GSA LIVER DYNAMIC SPECT

99mTc-DTPA-galactosyl human serum albumin (99mTc-GSA) is a ligand that binds specifically to asialoglycoprotein receptors in hepatocytes. The purpose of the present study was to study correlation between parameters of an original predictive index and those of hepatic function capacity test and severity of liver disease. Liver dynamic SPECT using 99mTc-GSA was performed in 25 patients with liver diseases. Dynamic SPECT with continuous 35 rotations was performed to obtain the K value (K) according to the accumulation curve in each voxel (0.34 cm×0.34 cm×0.68 cm) of the liver immediately after bolus injection of 185MBq 99mTc-GSA. Each rotation consisted of 360° turn in 64 steps in a 64×64 matrix. The acquisition time of each rotation was 35 sec.

After preprocessing the data by 9-point weighted smoothing, the filtered back-projection method was used for image reconstruction using the Shepp and Logan filter to suppress high frequency noise. We devised an original predictive index by combining the K value (K) with liver volume (V) and effective liver volume (Fv) which were measured by liver dynamic SPECT. Correlations between these parameters and the results of hepatic function capacity test (ICGR 15, PT, HPT, Alb, Bil) and the grade of liver disease severity were analyzed. Result showed that K correlated well ICGR 15 and HPT. K was more sensitive to the grade of liver disease severity than Fv and V. In conclusion, liver dynamic SPECT using 99mTc-GSA may provide a novel method for evaluation of hepatic functional reserves.

Cardiovascular: Perfusion and coronary anatomy

OS-583

W. Burchert, H.G. Wolpers*, J. van den Hoff, M. Hakimi, G.J. Meyer, D. Hausmann*, K.Pethig**, W.H. Knapp
Klinik für Nuklearmedizin, *Abt. Kardiologie and **Abt. Herz-,Thorax- & Gefäßchirurgie; Medizinische Hochschule Hannover; Germany

DIAGNOSIS OF CARDIAC ALLOGRAFT VASCULOPATHY. A COMPARISON OF N-13-AMMONIA PET WITH ANGIOGRAPHY AND INTRACORONARY ULTRASOUND.

The cardiac allograft vasculopathy (CAV) could not be detected reliably with conventional perfusion scintigraphy. Therefore, myocardial perfusion and coronary flow reserve was measured quantitatively with N-13-ammonia PET, and compared with the findings of angiography and intracoronary ultrasound (ICUS). **METHODS:** 35 consecutive patients (pts) were investigated 52±26 months after heart transplantation. In all pts. dynamic PET-scans (Siemens ECAT 951) with N-13-ammonia (740 Mbq) were performed at rest and after vasodilation with dipyridamole (0,56 mg/kg i.v). Absolute flow values were derived from a two-tissue-compartment model. Grade of coronary artery stenosis was assessed with angiography. Minimal luminal cross-sectional area was determined with ICUS (20 pts). **RESULTS:** In pts without significant CAV (angiography, ICUS) the coronary flow reserve was 3.0±0.8 on average. No significant reduction of flow reserve was found (2.7±0.8), if only ICUS indicated CAV (<40% luminal area stenosis; negative angiography). A severe reduction of the flow reserve was found (1.3±0.4; p<0.05) in pts with more than a 50% coronary stenosis in angiography. The coronary resistance was correlated with the grade of stenosis, but not with the time after transplantation. **CONCLUSION:** Only minimal impairment of coronary reserve was found in vasculopathy detected bei ICUS only. A reduction of the coronary reserve to values lower than 2.0 indicates reliably the existence of angiographically relevant stenosis.

OS-584

E.I. Skaliadis*, S. Koukouraki, N.E. Mezilis*, E.A. Zacharis*, P.E. Vardas*, N. Karkavitsas.,
Hospital: Dpts. of Nuclear Medicine and *Cardiology, Heraklion University Hospital, Heraklion, Crete, Greece.

REDUCED EARLY DIASTOLIC CORONARY FLOW AND CORONARY FLOW RESERVE IN PATIENTS WITH LEFT BUNDLE BRANCH BLOCK. EXERCISE THALLIUM-201 PERFUSION DEFECT AND NORMAL CORONARY ARTERIES

The high frequency of septal or anteroseptal defects on exercise perfusion scintigraphy in patients (pts) with LBBB in the absence of coronary artery disease has been well documented. In this study we assessed the coronary flow reserve (CFR) and velocity (CFV) pattern in these pts in an attempt to explain the underlying mechanism.

Method: Eleven pts with LBBB, normal coronary arteries and perfusion defect on exercise TI-201 scintigraphy were studied. Nine normal subjects were the control group. Coronary flow velocities were recorded during routine cardiac catheterization using a 0.014-in Doppler guide wire in the proximal left anterior descending coronary artery before the 1st septal branch (LAD) and the right coronary artery (RCA). Average peak velocity (APV) was measured before (R) and after (H) intracoronary adenosine administration to achieve maximal hyperemia. CFR was calculated as the ratio of APV-H to APV-R. We also measured the time from the beginning of diastolic flow to maximum peak velocity (TimeMPV) and the slope of the velocity waveform leading to the maximum peak velocity (Acceleration in cm s⁻²).

Results:

	CFR-LAD	TimeMPV (ms)	Acceleration	CFR-RCA
LBBB	2.7 ± 0.2*	158 ± 16*	210 ± 70*	3.7 ± 0.8
Controls	3.2 ± 0.6	104 ± 13	310 ± 74	3.8 ± 1.2

*p<0.05 compared to controls

Conclusion: Coronary flow reserve in the LAD area is reduced in pts with LBBB and exercise TI-201 perfusion defects in the same region. Although the reduction in CFR is not in itself sufficient to cause perfusion defects, in combination with the reduced early diastolic flow (whose contribution to coronary flow becomes more important during tachycardia, when the diastolic period shortens), it may explain the scintigraphic findings in these pts.

OS-585

M.Kostkiewicz, P.Rudziński, J.Sadowski, W.Tracz, A.Dziatkowiak
Department of Nuclear Cardiology, Department of Cardiovascular Surgery
Collegium Medicum UJ Kraków Poland

TRANSMYOCARDIAL LASER REVASCLARIZATION, THE RESULTS ASSESSED BY PERFUSION MIBI SCINTIGRAPHY

Transmyocardial laser revascularization (TMLR) is a relatively novel treatment for coronary artery disease in patients (pts) in suitable for conventional myocardial revascularization by CABG or PTCA. In order to determine whether TMLR led to an increased myocardial perfusion in lased segments, MIBI exercise scintigraphy and low dose dobutamine echocardiography was performed at the baseline, 3 to 6 months after surgery. Twenty eight pts (6 women and 22 men, mean age 56,9 yrs) underwent TMLR, which was combined with single or multiple CABG to nonlased segment in 19 cases. The Eximer Max 20 Laser and the Eclipse 2000 Laser was used. Three pts died before the first follow up. Thirteen pts after 3 months and 7 pts after 3 and 6 months had scintigraphic investigation. Nine pts had CABG + TMLR, 4 TMLR procedure. Comparing to the baseline, that was perfusion improvement in 11 pts (7 after CABG + TMLR, 2 after t stress / rest before operation did not change in all pts after a follow-up of 3 months and 6 months, respectively. Our study shows that perfusion of previously ischemic myocardium was improved by TMLR, however better results was after CABG + TMLR. Perfusion of scar tissue did not changed in both groups.

OS-586

Y.S. Lee, D.H. Moon, J.W. Shin, S.W. Park, S.J. Park, and H.K. Lee.
Asan Medical Center, University of Ulsan, Seoul, Korea.

DIPYRIDAMOLE TI-201 SPECT IMAGING IN PATIENTS WITH MYOCARDIAL BRIDGING

Myocardial bridging has been reported to be associated with exercise induced myocardial perfusion abnormalities. The purpose of this study was to evaluate dipyridamole induced myocardial ischemia by TI-201 SPECT imaging in patients with myocardial bridging.

Twelve patients with myocardial bridging ($\geq 50\%$ systolic narrowing) on coronary angiography who performed dipyridamole TI-201 SPECT were included. Eight were associated with left ventricular hypertrophy. Myocardial bridging was present in left anterior descending artery (LAD) territories: 2 in mid-LAD, 7 in distal LAD, and 5 in septal branches. Three of 6 with 50 to 70% of systolic narrowing had an dipyridamole induced perfusion abnormality. In 7 of 8 with more than 80% systolic narrowing, dipyridamole TI-201 SPECT showed a reversible perfusion defect. All five patients with septal branch compression had a perfusion defect in mid anteroseptal wall without apical abnormality. In control group of consecutive 118 patients with fixed LAD disease, no patient had a isolated perfusion defect in mid anteroseptal wall associated with septal branch disease (5/12 vs. 0/118, $p < 0.001$).

Perfusion abnormalities on dipyridamole TI-201 SPECT are observed in LAD or its branches in patients with high grade myocardial bridging. Isolated perfusion defect in mid anteroseptal wall without apical abnormality may be a characteristic finding of septal branch compression, because fixed lesion involving septal branch only is rare.

OS-587

M.O.Demirkol, B.Yaymacı, Y.Başaran, N.Ekşi, H.Silahçı*, Ç.Önsel*, F.Turan.

Koşuyolu Heart and Research Hospital, Cardiology and Nuclear Medicine* Departments, İstanbul, Turkey.

DIPYRIDAMOLE MYOCARDIAL PERFUSION TOMOGRAPHY IN PATIENTS WITH SIGNIFICANT AORTIC STENOSIS.

Exercise cardiac stress testing has low specificity in detecting coronary artery disease among patients with aortic stenosis. Also because of complications like hypotension, syncope and sudden death the safety of exercise testing is controversial. This study assessed the safety and diagnostic accuracy of dipyridamole stress myocardial perfusion scintigraphy (MPS) for the detection of coronary artery disease (CAD) in patients with significant aortic stenosis (AS).

The study included 36 patients with moderate to severe AS (aortic valve area $0.97 \pm 0.17 \text{ cm}^2$, maximal gradient $68.4 \pm 10.9 \text{ mmHg}$, mean gradient $45.2 \pm 11.8 \text{ mmHg}$). All patients underwent dipyridamole myocardial perfusion scintigraphy (SPECT), coronary arteriography, catheterization, as well as doppler echocardiography. MPS was applied with Tc-99m MIBI by single day rest-dipyridamole infusion protocol. Hemodynamic, electrocardiographic and clinical response were compared with 50 control patients without AS. Hemodynamic responses during dipyridamole stress testing between the study and control patients demonstrated no significant difference in systolic blood pressure, heart rate, rate pressure product or incidence of headache (%25-%24) or chest pain (%22-%20) or dyspnea (%19-%18), burning sensation (%16-%16). No atrioventricular conduction defect was observed. Reversible perfusion defect was observed in twelve patients with MPS. The existence of coronary lesions were determined by coronary arteriography in ten of twelve (sensitivity 100%, specificity 92%).

The preliminary results showed that MPS performed with dipyridamole is well tolerated in patients with significant AS and has a high diagnostic value in assessing coronary artery disease.

OS-588

D. Daou, N. Delahaye, R. Lebtahl, D. Vilain, M. Faraggi, C. Peker, D. Le Guludec.

Nuclear Medicine department, Bichat hospital, Paris, France.

DETECTION OF EXTENSIVE CORONARY ARTERY DISEASE (CAD) WITH TI-201 SPECT: THE INCREMENTAL VALUE OF DIFFERENT PARAMETERS.

Patients with extensive CAD (3-vessel, 2-vessel, proximal left anterior descending or left main coronary artery stenoses) benefit most from revascularization in terms of survival. Exercise (ex) TI-201 multiple perfusion defect finding should identify these patients but defects are frequently limited to the culprit lesion. High risk ex-ECG and indirect TI-201 SPECT findings (left ventricular (LV) transient ischemic dilation, increased lung to heart ratio-L/H) were previously reported for the identification of these patients. We evaluated the incremental value of these criteria as compared to multiple perfusion defect finding by comparing patients with extensive CAD (n=248; diameter stenosis $> 50\%$) and a control group with limited CAD (no CAD or 1-vessel CAD other than proximal left anterior descending artery; n=90). Results :

CRITERIA	Se	Sp	L(+)	L(-)	WE(+)	WE(-)	EWE
(1) = Ex-HR < 120 bpm	49	67	1.5	0.8	40	-27	0.5
(2) = High risk ex ECG	15	89	1.4	1	31	-5	0.1
(3) = Multiple Defects	48	94	8	0.6	208	-59	6.9
(4) = L/H ratio (quantitative)	39	90	3.9	0.7	136	-39	2.9
(5) = LV dilation (visual)	31	87	2.4	0.8	87	-23	1.1
(6) = (3) or (4)	60	87	4.6	0.5	153	-78	6.1
(7) = (3) or (5)	60	82	3.3	0.49	120	-72	4.4
(8) = (3) or (4) or (5)	67	78	3.1	0.4	111	-86	4.6
(9) = (2) or (3) or (4) or (5)	73	72	2.6	0.4	96	-98	4.3

HR: heart rate; WE(+) and WE(-): positive and negative weight of evidence; EWE: expected WE; L(+) and L(-): positive and negative likelihood ratio.

Conclusions : 1/ Exercise ECG criteria alone are not accurate for the detection of extensive CAD. 2/ Presence of multiple perfusion defects is highly specific but is not enough sensitive. 3/ The combination of high risk ECG, quantitative lung to heart ratio and LV transient dilation to multiple perfusion defect criteria strongly improves the detection of extensive CAD.

■ Cardiovascular: Perfusion and coronary anatomy

Cardiovascular: Perfusion and coronary anatomy

PS-1

A.Aktaş, N.Elahi, M.Uluçam, V.Şimşek

Başkent University Hospital, Ankara-TURKEY

PERI-INFARCTION ISCHEMIA IN PATIENTS WITH ANTEROAPICAL TRANSMURAL MYOCARDIAL INFARCTION HAVING BLACK-HOLE SIGN

It's known that areas of reduced left ventricular cavity activity (black-hole sign) both in stress and rest myocardial perfusion images appearing in conjunction with a transmural perfusion defect has a high correlation with the presence of a left ventricular aneurysm. The aim of this study was to find the incidence of peri-infarction ischemia in patients with a black-hole sign and to compare the sensitivity of myocardial perfusion scintigraphy and echocardiography for detecting anteroapical aneurysm.

Thirty-one patients having black-hole sign on myocardial perfusion scintigraphy were included for this study. All patients had an anteroapical ventricular aneurysm detected on contrast left ventriculography. Myocardial perfusion scintigraphy (MPS) was performed using 3 mCi Tl-201. All patients had post-exercise, 3h redistribution and late redistribution imaging (18-24 h after 1 mCi Tl-201 reinjection). Based on the relative orientation of anterior and inferior left ventricular wall toward the apex in long-axis sections, myocardial perfusion images were grouped into divergent, parallel and convergent. Scintigraphic images were evaluated both visually and quantitatively for the presence of peri-infarctional ischemia.

On the distribution of myocardial perfusion defect, echocardiography demonstrated dyskinesia in 9, akinesia in 20 and hypokinesia in 2 patients. None of the patients with a divergent orientation of left ventricular free walls had peri-infarction ischemia (both at 3 and 24 h imaging). 60 % of the patients with a convergent or parallel orientation had redistribution demonstrable on either early or late redistribution images. The presence of dyskinesia or akinesia did not predict the reversibility of defect on MPS.

In conclusion, MPS appeared to be more sensitive than echocardiography for detecting an anteroapical ventricular aneurysm. Patients with a divergent orientation of left ventricular free walls on MPS do not demonstrate peri-infarction ischemia, hence excluding the need for a 24 h image.

PS-2

A. Alector¹, M. Yüksel¹, T. Kürüm², F. Özçelik², M. Kaya¹, T.F. Çermik¹, F.Yorulmaz³, G. Özbay², Ş. Berkarda¹
T.U. Faculty of Medicine, Depts. of Nuclear Medicine¹ and Cardiology², Public Health³, Edirne, TURKEY

ASSESSMENT OF MYOCARDIAL VIABILITY USING REST-REDISTRIBUTION (MRR) AND NITRATE (MN) Tc-99m MIBI SPECT IMAGING.

The aim of this study was to compare the ability of Tc-99m MIBI rest-redistribution (MRR) and Tc-99m MIBI nitrate (MN) SPECT imaging to detect viable myocardium in patients with myocardial infarction 3-8 months previously.

We studied 27 patients (23 men, 4 women; mean age 55 ± 11.28 yr.) with angiographically documented coronary artery disease and left ventricular dysfunction. All patients underwent resting Tc-99m MIBI SPECT with initial (45-60 min) and delayed redistribution (4 hr) images. On the subsequent day, Tc-99m MIBI SPECT was performed after nitroglycerine (0,5 mg/kg sublingual) administration. A week after, all patients also underwent rest-redistribution Tl-201 imaging (TRR). For each study, tomograms were divided into 14 myocardial segments and regional Tc-99m MIBI and Tl-201 uptake were quantitatively analyzed.

On the initial Tc-99m MIBI images 223 segments were normal, 141 showed abnormal tracer uptake. In each patient corresponding MRR and MN with TRR tomographic images were evaluated for direct comparison.

	MRR		MN	
	viable	nonviable	viable	nonviable
TRR viable	24	34	31	27
TRR nonviable	12	71	24	59
	Sensitivity	Specificity	PPV	NPV
MRR	%41	%85*	%66*	%67
MN	%53*	%71	%56	%68#

*p<0.05; # p>0.05; PPV: Positive Predictive Value; NPV: Negative Predictive Value

As a conclusion, it was found out; that when compared to MRR, MN study was more sensitive, yet due to its high specificity and positive predictive value, MRR study for the patients who are to be underwent coronary revascularization after MI, was superior to MN study.

PS-3

I. Aslanidis, M. Vakhromeeva, I. Berishvili, Z. Katsitadze

Hospital: Bakoulev Scientific Center for Cardiovascular Surgery, Laboratory of Radionuclide research methods

THALLIUM-201 IMAGING IN ANOMALOUS LEFT CORONARY ARTERY FROM PULMONARY ARTERY (ALCAPA)

Purpose: to analyse diagnostic potentials of the 201TL in the patients with ALCAPA.

Patients and methods: 40 patients with ALCAPA aged 0-50 have been examined. Preoperative (40 pts) and postoperative (19 pts) 201TL imaging has been performed. 12 pts were evaluated resting and 28 - stress TL imaging. Preoperative (9 pts) and postoperative (6) 99mTc radionuclide ventriculography has been performed.

Results: Preoperative patients were classified into III age groups. I group consisted 10 pts (0-1 year), II - 25 (1-16 years) and III - 5 (>16 years). According to the type of the surgical treatment, all the patients were classified into V groups. I group consisted 8 pts after ligation LCA, II - 1 pt after ligation left anterior descending artery, III - 3 pts after LCA ligation and aortocoronary bypass, IV - 6 pts after reimplantation of the LCA into the aorta and V - 1 pt from Hamilton procedure. The preoperative imaging findings were consistent with myocardial scar and ischemia of the anterolateral and posterolateral walls. Detection of the myocardial scar with the sings of cardiomegaly is a pathognomonic sings of ALCAPA in infants and most of the children. Radionuclide ventriculography has revealed regional and global left ventricular (LV) systolic dysfunction in all the patients. Stress-redistribution (3, 24-hour) imaging has evaluated ischemic but viable myocardium in adults. The identification of viable myocardium in patients with ALCAPA has important implications for surgical choice and prognosis. Postoperative 201TL imaging allows to evaluate efficiency of the surgical procedure.

Conclusions: planar 201TL myocardial perfusion imaging and radionuclide ventriculography are well accepted as a efficient non-invasive diagnostic method in the detection of myocardial scar and ischemia, regional and global function of the LV for ALCAPA and has been used to differentiate ischemia due to an ALCAPA from the diffuse ischemia secondary to congestive cardiomyopathy.

PS-4

T. Athanasoulis, L. Karaloizos, N. Sifakis, Ch. Kalliontzi, E. Papadaki, S. Gerali

Dept of Nuclear Medicine «Alexandra» University Hospital, Athens, Greece

TL201 REVERSE REDISTRIBUTION PHENOMENON AFTER INJECTION AT STRESS PERSISTS AND IN SUBSEQUENT REINJECTION-REDISTRIBUTION STUDY

The explanation of Tl201 reverse redistribution phenomenon (TL-R-R), often found in TL201 stress-redistribution studies, is unclear. Proposed mechanisms are related to different patency of collateral vessels during stress compared to rest, or accelerated Tl201 washout from myocardial cells. The aim of the study was to investigate which is the most possible mechanism that is responsible for the TL-R-R. Ten consecutive pts were included in the study who demonstrated TL-R-R in Tl 201-stress study. Five had an anterior stress perfusion defect, four had an inferior and one had a lateral perfusion defect. All pts had an previous myocardial infarction. After redistribution imaging (RED-I) pts were reinjected with 1mCi Tl201 and two more spect images were obtained, reinjection image (RJ-I) and late reinjection image (L-RJ-I), 30 min and 4h post reinjection respectively. Visual comparison of the spect images was done. Comparison of the RED-I and RJ-I revealed that all perfusion defects demonstrated Tl201 fill-in and became as similar in size as those found in stress images. Comparison of the RJ-I and L-RJ-I revealed that all perfusion defects were increased again in size and were similar to those found in RED-I. We conclude that Tl-R-R occurs both after injection at stress and after injection at rest, implying that it is independent on any hemodynamic changes that occurs during stress, and that it is rather related with accelerated Tl201 washout from myocardial cells. Furthermore, if accelerated Tl201 washout is present in combination with ischemia at stress, it may interferes fill-in during redistribution resulting in a balanced RED-I that underestimates viability comparing with reinjection image.

PS-5

M. Bangard, M. Hümmelgen*, H. Bender, H. Palmedo, P. Willkomm, J. Risse, F. Grünwald, B. Lüderitz* and H.-J. Biersack. Dept. of Nuclear Medicine and Dept. of Internal Medicine*, University of Bonn, Germany

MYOCARDIAL UPTAKE OF TECHNETIUM-99M-FURIFOSMIN (Q12) VERSUS TECHNETIUM-99M-SESTAMIBI (MIBI)

Aim: Comparison of Tc-99m-Q12 and Tc-99m-MIBI myocardial uptake in correlation to the whole body uptake under resting conditions.

Methods: 21 patients (mean age 56 yrs., range 36-75 yrs., m:f = 18:3) with coronary artery disease and no rest ischemia were examined (Q12: n = 13; MIBI: n = 8). For both tracers 370 MBq were injected and a whole body scan (ADAC Vertex, wb-speed 20 cm per min.) was done 60 min. p.i. under resting conditions. A region of interest was drawn around the heart and the whole body in anterior and posterior projection. The mean value of the decay-corrected total counts of the heart-ROI was divided by the counts of the whole-body. Additionally, a heart/lung ratio was calculated using the heart-ROI and an lung-ROI (right lung). The whole procedure was part of a routine rest/stress study using a split-dose one day protocol. Student's t-test unpaired was used to test the statistic significance.

Results:

	heart/ whole body	heart/ lung
Tc-99m-Q12	0.027 ± 0.012	1.56 ± 0.191
Tc-99m-MIBI	0.026 ± 0.004	1.94 ± 0.197
significance	n.s.	p < 0.01

Conclusion: These data show that under resting conditions the total myocardial uptake of Tc-99m-Q12 does not differ significantly from that of Tc-99m-MIBI. However, the pulmonary uptake of Tc-99m-Q12 is higher, resulting in a significant lower heart/lung ratio.

PS-6

M. Yu, E. Vanninen, K.A. Bergström, J.T. Kuikka, J. Yang, H. Mus-salo, A. Airaksinen, S. Lötjönen, E. Lämsimies. Department of Clinical Physiology, Kuopio University Hospital and Department of Chemistry, University of Kuopio, Kuopio, Finland.

RADIOCHEMICAL IMPURITIES OF [Tc-99m]Q12 AND IMAGE QUALITY IN MYOCARDIAL PERFUSION SPECT IMAGING

In clinical myocardial perfusion SPECT studies with [Tc-99m]Q12, we observed that some patients had high liver uptake interfering severely with the assessment of inferior wall of left ventricle. This study was designed to test whether the radiolabeled impurities of [Tc-99m]Tc-Q12 contribute to the high liver uptake.

Thirty clinical patients undergoing routine myocardial perfusion SPECT study using Siemens E.CAM gamma camera were evaluated. The radiochemical purity of [Tc-99m]Q12 was detected with HPLC. Venous blood samples taken at 50 minutes after injection of [Tc-99m]Q12 at rest were analyzed with HPLC. Liver uptake was expressed liver/heart ratio. In addition, the SPECT images were classified by two experienced nuclear medicine specialists in three groups representing studies with good quality images, images with high general background activity, and images with high liver and/or intestinal uptake.

Quantitatively, the liver/heart ratio correlated with radiochemical purity of [Tc-99m]Q12 ($r = -0.65, p < 0.001$), radiolabeled polar impurity in [Tc-99m]Q12 ($r = 0.51, p < 0.01$), [Tc-99m]Q12 in plasma ($r = -0.44, p < 0.02$), and radiolabeled polar compound in plasma ($r = 0.46, p < 0.02$). The radiochemical purity of [Tc-99m]Q12 was significantly lower in the studies with high liver uptake ($60.1 \pm 4.2\%$) than in the studies with good quality images ($81.8 \pm 5.6\%$, $p < 0.01$) or in studies with high background activity ($82.3 \pm 2.5\%$, $p < 0.01$). The radiolabeled polar impurity in [Tc-99m]Q12 was significantly higher in studies with high liver uptake ($24.7 \pm 6.9\%$) than in studies with good quality images ($8.3 \pm 6.0\%$, $p < 0.05$) or with high background activity ($5.7 \pm 1.1\%$, $p < 0.01$).

In conclusion, the radiochemical purity of [Tc-99m]Q12 is associated with high liver uptake interfering severely with the assessment of inferior wall. This suggests that adequate pre-test quality control is mandatory for the clinical use of this new myocardial perfusion tracer.

PS-7

S. Betker, J. Holzinger, R. Weise, T. Kuwert

Heart Center North Rhine Westfalia University of Bochum, Department of Nuclear Medicine, Bad Oeynhausen, Germany
ASSESSMENT OF REGIONAL CORONARY FLOW RESERVE IN 74 PATIENTS WITH HYPERTROPHIC OBSTRUCTIVE CARDIOMYOPATHY USING POSITRON EMISSION TOMOGRAPHY (PET)

The aim of this study was to assess the regional coronary flow reserve (CFR) in 74 symptomatic patients with hemodynamically important hypertrophic obstructive cardiomyopathy (HOCM) but without coronary artery disease.

Baseline data : 74 HOCM patients : males:46, females:28; mean age:49,4 +/- 15,5 years. Controls (C) : 8 persons(51,5 +/- 12,6 years) with normal coronary angiogram and without significant septal hypertrophy.

Methods : Regional myocardial blood flow (MBF) was measured at rest (MBFr) and after pharmacological stress (MBFd) with dipyridamole (0,56mg/kg) using PET with N-13-ammonia as flow tracer. Coronary dilator capacity was assessed from minimal coronary resistance (Rmin: mean arterial pressure/MBFd), maximally obtainable flow (MBFd) and instantaneous flow ratio (MBFd/MBFr).

Results (means +/- SD) : Averaged MBFr was normal in HOCM at rest: 91 ± 22 ml/minx100g. Overall averaged CFR was significantly reduced: $2,04 \pm 0,63$ vs C: $3,9 \pm 1,1$ ($p = 0,01$). MBFd was lower: 178 ± 51 vs C: 372 ± 75 ; ($p = 0,01$) and Rmin significantly increased: $0,56 \pm 0,18$ mmHg/ml/minx100g vs C: $0,25 \pm 0,05$ ($p = 0,01$). Regional MBFd was lowest in the septal layer.

PS-8

G. Cannizzaro¹, G. Calsamiglia¹, R. Sara², D. Massa², R. Saponaro¹, R. Mingrone¹, C. Aprile¹

¹Fond. "S. Maugeri", IRCCS, Pavia; ²Niguarda Hospital, Milano, Italy

EFFECTS OF NITROGLYCERIN ON RESTING MYOCARDIAL HYPOPERFUSION BY 99m Tc MIBI SPET IN PATIENTS WITH PREVIOUS MYOCARDIAL INFARCTION WITHOUT SEVERE REDUCTION OF LEFT VENTRICULAR FUNCTION

In patients with previous myocardial infarction (MI) and left ventricular dysfunction the administration of nitroglycerin (ntg) before 99m Tc MIBI injection can improve the tracer uptake in resting hypoperfused but still viable myocardium. In this study the efficacy of ntg MIBI SPET was investigated in subjects without severe reduction of left ventricular function.

METHODS

Eighteen consecutive patients (pts) (all male, median age 60, range 46-71) with previous MI, FE 44 ± 7 , all with multivessel disease, referred for revascularization (REV), underwent rest echocardiography (ECHO) and, within one week, rest MIBI SPET. A second study with injection of the tracer during intravenous infusion of nitroglycerin (ntg MIBI SPET) was then performed (1-2 days after the first). Nine pts underwent a second rest ECHO and a third rest MIBI SPET three months after a successful REV (nine drop-outs: two deaths, two perioperative infarctions, two incomplete REV, one post operative angina, two losts for follow up).

RESULTS

Twenty-three out of one hundred and eight (21.3%) segments (sgts) had an uptake <60% of the maximum in the rest scintigraphy: "likely scar". Only 3/23 (13%) had an improved uptake after ntg. Moreover these segments were "viable" in the pre-REV ECHO (slightly hypokinetic or normokinetic). Seventeen out of twenty-three sgts (74%) resulted akinetic or dyskinetic in pre REV ECHO; in 16/17 (94%) neither perfusion nor function improved after REV. The few sgts with improved perfusion in ntg MIBI SPET confirmed the improvement after REV.

CONCLUSIONS

In patients with previous myocardial infarction, multivessel disease and only mild or moderate reduction of left ventricular function, the evaluation of myocardial viability with MIBI SPET after ntg does not seem to be useful, probably because in these subjects the residual inducible ischemia is prevalent and the extent of the hibernated myocardium is negligible.

Poster presentations

■ Cardiovascular: Perfusion and coronary anatomy

PS-9

I. Casáns, A. Llácer, JA Ferrero, J. Ciudad, J. Manjón

Nuclear Medicine and Cardiology Departments.
Hospital Clínico Universitario. Valencia. Spain.

ASSESSMENT OF LEFT VENTRICULAR FUNCTION AND EXTENT OF CORONARY DISEASE BY LUNG UPTAKE OF ^{99m}Tc-TETROFOSMIN.

Our purpose was to evaluate the clinical value of ^{99m}Tc-Tetrofosmin (^{99m}Tc-TF) lung uptake in SPECT myocardial perfusion to assess left ventricular dysfunction and extent of coronary disease. In a group of 76 coronary patients proven by cardiac catheterization, we have determined a lung to heart ratio (LH) from stress SPECT images, the extent of stress perfusion defect (EX) by quantification of bull's eye, and left ventricular ejection fraction (EF) at rest from equilibrium radionuclide ventriculography, obtained 24 h later. Previously we have obtained an high and significant correlation between LH from SPECT and LH from a conventional anterior planar image acquired immediately before SPECT in a separate group of 37 patients (r: 0.95, p<0.001).

In the 76 coronary patients, LH (0.21-0.86, X±SD: 0.36±0.11) showed with EF(10-70%, X±SD: 40%±17.1) a significant negative correlation (r: -0.65, p<0.001). With EX (12-78%, X±SD: 41.5%±17.8), we also found a significant correlation (r: 0.50, p<0.001). Mean LH was higher in patients with EF<40% (0.42±0.12) than in those with EF≥40% (0.29±0.05), p<0.001. In the group with EX<30%, LH was lower (0.32±0.06) than in patients with EX≥30% (0.40±0.12, p<0.01).

In conclusion, lung uptake of ^{99m}Tc-TF from usual SPECT perfusion images, provides additional clinical information about ventricular dysfunction and extent of coronary disease, similar to that seen with 201-Tl.

PS-10

J. Castell, A. Muxi, J. Martín-Comin, J.A. Nuño, M.J. García, S. Aguadé, R. Puchal, J. Pavia, I. Casans, J.J. Martínez-Sampere, I. Carrió, M.D. Abós, J.M. Castro, L. Campos, J. Freire, P. Labanda, C. Gómez, M.D. Marín, Y. Ricart. Grupo de Trabajo Español de Cardiología Nuclear.

^{99m}Tc-TETROFOSMIN NORMAL DATA BASE. SPANISH MULTICENTRIC TRIAL.

The aim of the study was to obtain a pool of SPET perfusion images with an stress/rest one-day protocol in normal volunteers.

They underwent an exercise stress test with injection of 300 MBq of Tetrofosmin. Rest study was obtained after tracer injection of 900 MBq. The study was completed in 4 hours. After a phantom validation of the SPET systems, 15 Hospitals were involved. 178 volunteers with a pretest probability <5% CAD (Forrester and Diamond) were recruited. All of them had clinical, laboratory parameters, ECG and echocardiographic normal evaluation. Two cases were rejected for low quality images and seven after stress test positive criteria. Finally 169 were accepted.

Results:

Group	M<30y	M30-50y	M>50y	FpreM	FpostM
n	30	31	30	35	32
Age	25.9	38.3	54.8	33.9	55.5
echoEF	64.5	66.1	63.2	66.3	66.4

M: male, F: female, preM: premenopausal, postM: postmenopausal, y: years, n: number, echoEF: echocardiographic ejection fraction.

High intestinal activity was observed in 8 stress studies and in 48 rest studies. 24 segments were analysed in each study which were classified in 5 uptake degrees. No severe perfusion defects were observed. Two moderate-reversible defects were observed in the infero-basal region. 67 (1.6%) segments showed mild-reversible perfusion defects, without significant location. All segments with mild-non reversible defect (25, 0.6%) were located in the inferior wall.

Conclusion: We have obtained a wide normal data base including five age-gender subsets. We observed a low false positive rate (below the pre-test CAD likelihood) which validate the feasibility of stress-rest one-day protocol.

PS-11

J. Castell, G. Romero, J. Candell, S. Aguadé, M. Soler, C. Santana, M. Simó, M.J. Díez, F. Porta.

Servicios de Medicina Nuclear y Cardiología*.
Hospital General Universitari Vall d'Hebron. Barcelona.

SIGNIFICANCE OF REVERSE DEFECTS IN MYOCARDIAL SPET TETROFOSMIN ONE DAY PROTOCOL

The aim of the study was to review the significance of reverse segmental defects (RD) (stress uptake > rest uptake) in myocardial SPET images.

Methods and results: We analysed 1124 consecutive SPET one-day studies: 1st stress (300 MBq), 2nd rest (900 MBq). We identified 80 (7%) RD: 38 (47.5%) were attributed to an artefactual effect due to a high extracardiac activity (29 inferior, 9 anterior), 42 (52.5%) were considered true RD (35 post-exercise, 6 post-exercise/dipyridamole, 1 post-dipyridamole).

Twenty one out of 42 RD had previous myocardial infarction in the same region (15 inferior, 6 anterior). Nine patients out of 11 who underwent coronary arteriography presented patency of infarction related artery. All of them had myocardial viability (uptake > 40% of the maximal in more than half of the extent in everyone of the four left ventricular regions: antero-septal, inferior, lateral and apical); 13 out of 21 without previous myocardial infarction presented RD in the inferior region and 8 in the anterior region. Eight patients underwent coronary angiography: 3 no CAD, 5 with 50-70% coronary stenosis.

Conclusion: A low rate (3.5%) of true RD were observed in this one-day/stress-rest Tetrofosmin SPET protocol. Half of RD were observed in regions with previous myocardial infarction and viability criteria. Patients without myocardial infarction showed RD in regions with normal coronary arteries or with moderate stenosis.

PS-12

V. Chernov¹, A. Garganeeva², Yu. Lishmanov¹

Institute of Cardiology, Tomsk, Russia, ¹Department of Nuclear Medicine, ²Department of Rehabilitation

^{99m}Tc-MIBI SPECT IN EVALUATION OF CALCIUM ANTAGONIST INFLUENCE ON MYOCARDIAL PERFUSION IN CAD PATIENTS.

The aim of the study was to assess calcium antagonists (CA) effect on myocardial perfusion in CAD patients using ^{99m}Tc-MIBI SPECT.

Seventeen CAD patients were treated with CA adalat during two weeks. ^{99m}Tc-MIBI SPECT was performed at rest and during bicycle exercise before and after treatment. The next indices were assessed: perfusion defect size (PDS), ^{99m}Tc-MIBI accumulation in perfusion defect (APD) and integral index of perfusion defect (IPD).

Adalat treatment led to improvement in clinical status and myocardial perfusion in 14 patients. The dynamics of myocardial perfusion parameters in these patients are presented in the Table.

Indices	Before treatment		After treatment	
	Rest	Exercise	Rest	Exercise
PDS, %	23,5±4,8	28,9±4,6	19,7±4,2*	23,4±4,6*
AD, %	45,2±4,1	41,3±4,2	52,3±4,5*	48,1±4,3*
IPD, %	8,3±0,7	12,0±2,1	5,0±0,4*	7,3±1,5**

* - p < 0,05, ** - p < 0,01 -compared with initial parameters

Adalat worsened clinical status and myocardial perfusion, which may be a result of steel syndrome, in 3 patients.

Conclusions: ^{99m}Tc-MIBI SPECT provides useful information for evaluation of CA effect on myocardial perfusion and revealing of steel syndrome as a result of CA treatment. The IPD is one of the most sensitive signs of improvement in myocardial perfusion after treatment.

PS-13

K.Cho, S. Kumita, S. Mizumura, T. Kijima, H. Nakajo, M. Ishihara, M. Sakurai, S. Okada, T. Kumazaki
Nippon Medical School, Department of Radiology

COMPARISON OF MYOCARDIAL WALL THICKENING BETWEEN THE COUNT-INCREASE AND GEOMETRY METHODS USING ECG-GATED MYOCARDIAL SPECT WITH Tc-99m MIBI IN PATIENTS WITH ACUTE MYOCARDIAL INFARCTION.

Purpose: To elucidate the differences of left ventricular wall thickening between count-increase and the geometry (gaussian fit) methods, myocardial SPECT with Tc-99m MIBI was performed in 34 patients with acute myocardial infarction (28 men and 6 women, 64 ± 9 years) during the sub-acute phase. **Methods:** Forty minutes after the administration of 555 MBq MIBI, ECG-gated myocardial SPECT data were acquired over 360 degrees using a 3 head gamma camera. Subsequently, another ECG-gated data set was collected with 180-degree circular orbit using a dual-detector camera. The regional count increase rate (WT-CI) from end-diastole to end-systole using the first data set was computed with manual correction of left ventricular rotation. The regional wall thickening using geometry (WT-GF) was also determined using an automatic method for defining endocardial boundaries of the heart from the second acquired images. The WT-CI and WT-GF distributions were displayed on the polar map and the mean values in 9 myocardial segments were calculated on the polar map, as well as perfusion distribution (% uptake) using summed gated (=non-gated) data. The damaged segments (n=99) were determined by coronary angiography (>75% stenosis). The Z-values of % uptake, WT-CI and WT-GF by segment were calculated using the normal data base and the damaged segments were divided into two groups by the % uptake limit; moderately damaged (MD) segments (n=43) with the Z-value more than -2 and severely damaged (SD) segments (n=56) with the Z-value below -2. **Results:** The MD segments showed comparable Z-values of WT-CI and WT-GF (-2.9 ± 1.7 vs. -2.8 ± 1.2). However, the mean Z-values of WT-GF were significantly lower than those of WT-CI in SE segments (-2.8 ± 1.6 vs. -4.0 ± 1.1, p < 0.001). In apical infarction with the restrictions of 2 damaged segments or less within a subject, the mean Z-values of WT-GF were significantly higher than those of WT-CI (-4.1 ± 0.6 vs. -3.0 ± 1.1, n=9, p < 0.05). **Conclusion:** In damaged segments both WT-CI and WT-GF showed lower Z-values than % uptake, suggesting the diagnostic benefits. However, WT-CI could underestimate regional contractility in segments with severely reduced perfusion and WT-GF may also underestimate apical thickening in small infarction probably due to rotation of the heart.

PS-14

M.L.DeRimini; L.Piazza*; D.Capobianco; A.Mollo*; A.Martino; M.Cotrufo*; L.Mansi.
Nuclear Medicine-Inst.of Radiol, Cardiac-Surgery*
2 University - Naples

TL-201 SPET IN THE ASSESSMENT OF TRANSMYOCARDIAL LASER REVASCULARIZATION (TMLR).

TMLR creates a series of channels between left ventricular cavity and myocardium, allowing perfusion of CAD affected walls (CADW). To assess TMLR induced early perfusion improvement we performed Tl201 Stress/Rest/Reinjection (S/R/Rj) SPET before (T0), at 3(T1), at 6(T2) and 12(T3) months after TMLR in six males (mean age: 57) with infarct multivessels CAD, refractory to routine treatment angina.

Tl201 uptake was quantified in 120 segments (S) as % of peak in a 4 points scale, using a 20 S scheme. Defects were classified as fixed (F) or, in presence of a 10% increase at R/Rj with respect to S, partially reversible (> 50% of peak PRev) or reversible (>60% Rev). TMLR was performed in inferior-basal CADW where, at T0, 20 pathological S (8F, 8PRev and 4Rev) were defined.

	Fixed	PRev	Rev	Tot.S
To:	8 (40%)	8 (40%)	4 (20%)	20
T1/2/3:	10 (52.%)	6 (31.%)	3 (15%)	19

Overlapping results were obtained at T1, T2 and T3, in comparison with T0 data, 1 S Rev before surgery became normal, 2 S PRev at T0 became F nevertheless clinical improvement.

Our data confirm that no significant perfusion improvement TMLR induced has been detected at 3, 6 and 12 months in Tl201- T0 F and PRev defects, stimulating further investigations in a larger number of case.

PS-15

E. Derebek, S. Güneri, E. Özbilek, Ö. Kırımlı, B. Değirmenci, G. Çapa, H. Durak.

Dokuz Eylül University Hosp, Depts of Nuclear Medicine and Cardiology, İzmir, Turkey.

GATED Tc-99m SESTAMIBI SPECT IN CAD: INCREMENTAL ROLE OF WALL MOTION AND THICKENING ON SPECIFICITY

The purpose of this study was to investigate the role of gated SPECT in discriminating soft tissue artefacts as a cause of low specificity. Thirty-five patients (11 F, 24 M) with the suspicion of CAD were enrolled in the study. Same-day rest (8 mCi)-stress (23 mCi) gated imaging protocol was performed using dual-head gamma camera (Siemens Multispect, LEHP collimator, 180°, 64x64 matrix, 32 projections, 40 sec / projection, 8 frame / R-R, 45 min after the injection). Coronary angiography was performed in all patients within one month after the imaging (CAD in 21, and normal in 14). Five observers interpreted the non-gated images in one session and the gated images in another session, according to their own experiences. Thereafter, segmental uptake (9 segment for each study) was scaled as greater than 80%, 60-80%, 40-60% and lower than 40% in each non-gated images. Wall motion / wall thickening (WM / WT) was evaluated in each segment as normal (inward motion and at least 50% increment in ES image) and abnormal (no motion and less than 50% increment in ES image). Sensitivity and specificity of non-gated and gated SPECT in detecting CAD for each observer (1-5) are:

		Obs.1	Obs.2	Obs.3	Obs.4	Obs.5
Non-Gated	Sens (%)	80	90	85	85	95
	Spe (%)	53	60	60	60	26
Gated	Sens (%)	80	90	85	85	95
	Spe (%)	60	86	66	86	80

Segmental uptake was %80-60 in 15, 60-80% in 19 and less than 40% in 27 MI related segments. Whereas in segments attributable to soft tissue attenuation, uptake of 80-60%, 60-80% and less than 40% existed in 45, 4, and 1 segments, respectively (p < 0.01). We conclude that gated SPECT rules out soft tissue artefacts, increasing the specificity of Tc-99m sestamibi myocardial perfusion imaging in detecting CAD.

PS-16

Khaled El. Sabun, MD; Soliman Ghurieb, MD**; Medhat El Rifaie, MD**; Taher El Kady, MD**; Ahmed Zayed, MBCh***
Nuclear medicine department, Cairo University. ** Cardiology department, Cairo University. *** National heart institute

Dobutamine echocardiography versus ²⁰¹Tl SPECT In Detection of Myocardial Viability

Background: Although both Thallium scintigraphy & dobutamine echocardiography (ECHO) have been used to assess left ventricular dysfunction in patients CAD, the mechanisms by which these two methods identify viable myocardium are different.

Aim of The Study: Investigate the value & limitation of low dose dobutamine (LDD) during stress ECHO & thallium scintigraphy (TI) & the cost benefit of each of the two non Invasive tests.

Patients & Methods: 40 patients (31 male & 9 female) with their mean age of 49 ± 14 years were included in the study. All of them had clinical & angiographic proof of CAD. Patients underwent clinical examination, coronary angiography, resting & dobutamine ECHO. at rate of 5 & 10 ug/kg/min & ²⁰¹Tl SPECT. The left ventricle was divided into 20 segments for analysis of ECHO & TI images.

Results: Out of 800 myocardial studied segments of the 40 patients, there were 320 abnormal segments during resting ECHO. Whereas 178 (55.6%) segments were detected to be viable by LDD ECHO versus 154 (48.1%) segments which were detected to be viable by TI imaging. On the other hand, the two methods were in agreement in detection of 125 viable segments (39.1%) & 113 non viable segments (35.3%) (i.e. 238/320 (74.4%) segments show agreements by the two methods) (P < 0.05). On adding LDD to TI study, the number of viable segments detected by TI imaging increased to be 197 (61.6%) versus 178 (55.6%) segments which could be detected to be viable by LDD ECHO i.e. TI become more sensitive in detection of viable myocardium than before. Furthermore, the two methods were in agreement in detection of 168 viable segments (52.2%) & 113 non viable segments (35.3%) (i.e. 281/320 (87.8%) segments show agreement by the two methods) (P < 0.001).

Conclusion: Although both TI & LDD ECHO have nearly the same cost, the proportion of segments with preserved thallium uptake is greater than those showing a positive response to dobutamine & despite the difference is statistically insignificant, yet it is physically significant.

Poster presentations

PS-17

TRANSIENT ISCHEMIC DILATION OF LEFT VENTRICULAR CAVITY (TID): WHY IS IT OF LOW SENSITIVITY, THOUGH HIGHLY SPECIFIC?

El-Sabban, Kh^{*}, El-Kady, T.^{**}, Gharieb, S.^{***}, El-Gably, M.^{**}, and Imam, A.^{**}
Nuclear Cardiology division of Faculty of Medicine, Cairo University, Nuclear Cardiology and cardiology divisions of National Heart Institute^{**}, Cardiology department, Faculty of Medicine Cairo University^{***}

ABSTRACT:

Background: Several authors reported that TID is a marker for multivessel disease and $\geq 90\%$ stenosis, with high specificity (90-100%) and low sensitivity. On the other hand, the etiology of this finding varies from left ventricular dysfunction to diffuse subendocardial ischemia. So, the aim of this work is to try to find the cause of the low sensitivity, and its main etiology.

Patients and methods: One hundred and seventy five patients with known high risk for CAD had been reviewed for TID using thallium-201 SPECT (stress-redistribution protocol), radionuclide gated study at rest and stress, and coronary angiography. Patients had been subdivided into two groups: Group 1 (105/175, i.e. 60%) showed no TID, and Group 2: (70/175, i.e. 40%) showed TID.

Result: Group 2 showed statistical high prevalence of: (1) Multivessel disease (55/70 [i.e. 78.6%]) had 3 VD and 13/70 [i.e. 18.6%] had 2 VD, (2) Proximal lesions (55/70, i.e. 78.6%), and (3) $\geq 90\%$ stenosis of the affected vessels (55/70, i.e., 78.6%). On the other hand, quantitative assessment of TID can be used to get cut-off level between cases with TID and those with no TID.

Conclusion: The lower sensitivity of TID as a marker of extensive multivessel disease and 90% stenosis, though highly specific, is due to the necessity of multiple factors to be present together.

PS-18

Nicholas Friedman, Sharon Bernhardt, P Shirazi, Edward Hines VA Medical Center., Hines, IL.

COMPARISON OF GROUPED END-DIASTOLIC VS END-SYSTOLIC TOMOGRAPHIC SLICES IN MYOCARDIAL PERFUSION IMAGING.

Purpose: Routine SPECT myocardial imaging uses data acquired throughout the cardiac cycle to create 3 view tomographic slices. In addition, 8 frame cardiac gated acquisitions are performed to evaluate wall motion. However, gated information is not used to evaluate defect size due to the degradation of image quality associated with gated acquisitions. This study evaluated the ability to perform routine 3 view tomographic perfusion images using grouped end-systolic (ES) and end-diastolic (ED) acquisition frames.

Methods: Sixteen patients, either known or suspected of coronary artery disease, were injected with 925-1110 MBq of ^{99m}Tc-Sestamibi during stress. Cardiac acquisitions were performed using 8 frames/cardiac cycle on a triple head gamma. In addition to routine processing, the acquisition data was grouped into relative ES (frames 3, 4, 5, 6) and ED (frames 7, 8, 1, 2) acquisition bins. Processing of the reformed data was done with ES and ED images displayed in standard vertical long, horizontal long and short axis comparison views. Two physicians reviewed the ED and ES tomographs in a blinded fashion for the presence of myocardial perfusion defects.

Results: Image quality of grouped ES and ED frames was judged the same compared to standard images. Nine of the sixteen patients (56%) studied with ^{99m}Tc-Sestamibi identified larger defects in the ED tomographs. In three cases, ED images demonstrated apical defects which were not present on the ES images. Seven of the sixteen (44.0%) showed no change in the two tomograph. These seven patients were identified as demonstrating poor systolic function.

Conclusion: Reduction of acquisition data to grouped ED and ES frames resulted in no perceptible degradation in image quality compared to routine images. Visual image analysis demonstrates that limiting data collected during myocardial perfusion imaging to ED frames achieves a greater sensitivity in detection of myocardial perfusion defects, however some defects, especially in the apex, could represent false positive abnormalities, reducing the specificity of the rest. In contrast, limiting acquisition data to ES frames, resulted in images with fewer defects or defects of smaller size and intensity. Further evaluation of this method, with both stress and rest gated acquisition is warranted.

PS-19

L. Galuska, I. Garai, Z. Csiki*, J. Varga, E. Bodolay*, A. Szanyi

University Medical School, Nuclear Medicine Centre and
*3rd Department of Medicine, Debrecen, Hungary

FINGERS-TO-PALM RATIO: A NEW INDEX OF THE MICROCIRCULAR ABNORMALITIES OF THE FINGERS

The purpose of the study was to develop a non-invasive nuclear medical method potentially for screening patients (pts) with painful hands, which can separate patients with normal from those with abnormal microcirculation of the hands, as the other methods available are either subjective or rather complicated.

Method and patient groups: The pts lying supine placed their hands overhead, below the surface of the gamma camera detector. 400 MBq ^{99m}Tc-DTPA was given in a bolus through the footback vein. After waiting for 10 sec, 60 frames (1 sec each) were acquired and stored by a computer. Regions (ROIs) were drawn on the summed images around the fingers, and over the palmar region, and fingers-to-palm ratio (FPR) was calculated from the total counts inside these ROIs separately for both hands. 9 normal adults, 21 pts with Raynaud syndrome, and 12 pts with mixed connective tissue disease (MCTD) were involved in the study.

Results: The FPR of the normals was 0.94 ± 0.18 (0.71-1.25), in the MCTD group 0.57 ± 0.22 (0.21-1.11), and for the Raynaud pts 0.40 ± 0.14 (0.18-0.77); variance analysis proved that these differences were highly significant ($P < 0.001$). There was also significant difference between the 6 MCTD pts in positive (mean 0.48) and in negative (mean 0.66) state (2-sample t-test, $P < 0.05$). There was no significant difference between FPR values of the two hands.

Conclusion: The method is able to separate pts with normal and abnormal microcirculation of the hands. Though the FPR is not specific, it is useful both for staging and in the follow-up of patients.

PS-20

R.Z. Gao, C.Y. Huang, S.H. He

Liuhua Qiao Hospital: Department of Nuclear Medicine

PROGNOSTIC VALUE OF ^{99m}Tc-SESTAMIBI MYOCARDIAL PERFUSION IMAGING IN PATIENTS WITH CORONARY ARTERY DISEASE

The purpose of this study was to describe the clinical outcome of ^{99m}Tc-sestamibi myocardial perfusion imaging in patients with coronary artery disease

Methods: The study cohort consisted of 164 patients with known coronary artery disease (CAD), referred for myocardial perfusion imaging. The patients were divided into two groups according to cardiac imaging: (a) A group of 34 patients with normal myocardial perfusion, and (b) a serious of 130 patients with abnormal myocardial perfusion. The patients ranged in age from 61 to 75 years. A total of 164 patients were followed up for from 1 to 6 years, the average follow-up period being 4.9 years.

Results: Of a total of 34 patients of group a, cardiac events occurred in only 1 patient, the annualized event rate was 0.6% per year. Of group b of 130 patients, 10 patients of cardiac death and 12 patients with nonfatal myocardial infarction, the annualized event rate was 3.4%. There was significant difference between the two rates ($\chi^2 = 5.737$, $p < 0.05$).

Conclusions: Our data confirm that the prognostic value of ^{99m}Tc-sestamibi myocardial perfusion imaging is likely to be comparable to 201TI imaging. The benign outcome of patients with normal ^{99m}Tc-sestamibi perfusion cardiac imaging, at least over an intermediate follow-up period.

PS-21

J.M. González, J. Castell, J. Candell*, A. Garcia-Burillo, S. Aguadé, T. Canela, C. Santana, M. Soler, D. Ortega. Servei de Medicina Nuclear. Servei de Cardiologia*. Hospital General Universitari Vall d'Hebron. Barcelona.

PREDICTION OF WALL MOTION RECOVERY AFTER REVASCULARIZATION BY MEANS OF QUANTIFIED ^{99m}Tc-MIBI SPET

Aim: To determine the usefulness of the quantitative analysis of ^{99m}Tc-methoxy-isobutyl-isonitrile (MIBI) single photon emission tomography (SPET) for the diagnosis of myocardial viability in coronary patients with severe segmental wall motion alterations, 40 patients (60.8 ± 10 years, 5 females) with at least one severe dysinergic segment in radionuclide ventriculography, who were revascularized, were studied.

Methods and results: Rest ^{99m}Tc-MIBI SPET before revascularization and gated blood pool ventriculography of three projections before and 4 - 6 months after revascularization were performed to all patients. Left ventricular wall motion was studied by visual and Fourier analysis (amplitud and phase). Quantification of ^{99m}Tc-MIBI SPET was performed on polar maps. Different viability criteria were adopted: uptake > 50%, > 40% and > 30% of the maximal in more than half of the extent in everyone of the four left ventricular regions: antero-septal, inferior, lateral and apical. A segment was considered viable when its motion improved after revascularization. Eighty-two out of 160 regions showed severe contractility dysfunction and 73 were revascularized. Fifty of the latter (68%) improved their contractility after revascularization. The highest accuracy for diagnosis of viability was obtained with the 40% level of uptake: 47 out of 66 viable regions improved their motion while 6 out of 7 non viable regions did not (sensitivity: 98%, specificity: 24%, global value: 73%, positive predictive value: 71%, negative predictive value: 86%).

Conclusion: Quantification of the intensity and extent of the rest ^{99m}Tc-MIBI uptake on polar maps allows to identify with high sensitivity and predictive values, although with low specificity, viable myocardium in severe dysinergic regions. The criterium with the highest diagnostic accuracy is an uptake >40% of the maximal in more than half of the extent for each left ventricular region.

PS-22

M.L.Goris, M. Petersen, A Kwan and W. Pace
Stanford University School of Medicine and Kaiser Permanente, Divisions of Nuclear Medicine.

THE EFFECT OF LESION MODULATION ON THE OPERATING CHARACTERISTICS OF MYOCARDIAL PERFUSION STUDIES.

In previous work a method of myocardial perfusion analysis, based on elastic registration of the SPECT volume images to a template, was presented. We had hypothesized that the method had two putative advantages: First, in the 3D volume, differences, either between stress and a normal population, or stress and rest images, could be defined as defects, by an erosion-dilatation technique which relies on proximity of aberrant points. Second that the defects could be characterized by type (the reference volume is either a normal population or a resting image), size, depth, and location and third, that the diagnostic implication could be modulated by the defect attributes.

Results are given for 68 angiographically defined cases. Of those 55 were positive, and 13 negative. Since the analysis was not used in the clinical management of the patient, selection bias is minimized. In the clinical interpretation (with selection bias) the sensitivity was 85%, the specificity 25%. When all lesions types are accepted (OR) and are given equal weight, the sensitivity is 94%, the specificity 61%. When, still in an OR combination, the lesions are weighted according to their location, the sensitivity becomes 87%, with a specificity of 100%. Intermediate results are obtained by more complex classifications: If only stress abnormalities are accepted, the sensitivity is 89%, or 82% with lesion modulation, and the specificities are respectively 69% and 100%.

The data do not directly show that the quantitative test, with defect analysis, out-performs clinical interpretation. However, if there was selection bias, this bias would favor high sensitivities for the clinical interpretation. In this case, the modulation of the defect attributes did not result in a lower than the clinical sensitivity. What the data show, however, is that modulation can be used to regulate the specificity at which one wants to operate.

PS-23

W. Guo, S. Zhang, L. Li, H.Chen, X.Yan, L.Wang, C. Zhang, S.Li, G.Hu.
Hospital: Department of Cardiology, First Hospital, Shanxi Medical University, Taiyuan, Shanxi, P. R. of China

EARLY LEFT VENTRICULAR REMODELING IN ACUTE MYOCARDIAL INFARCTION ASSESSED BY GATED TOMOGRAPHIC MYOCARDIAL PERFUSION IMAGES

Left ventricular remodeling is an important sequela of myocardial infarction. Infarct expansion is the major early contributor to left ventricular remodeling, which is associated with an increase in cardiac volumes. To examine the early changes in left ventricular volume for first acute myocardial infarction (AMI) by Gated SPECT(GSPECT), 40 patients(pts) were performed resting GSPECT after onset of symptoms. The result showed end-diastolic volume (EDV) for pts and control was 113.9 ± 48.5ml versus 74.7 ± 12.2ml (p<0.05). End-systolic volume (ESV) for pts and control was 67.3 ± 39.5ml versus 25.3 ± 5.8ml (p<0.05). EDV in anterior infarcts and in inferior infarcts was 126.4 ± 42.1ml, 75.1 ± 29.7ml respectively. (p<0.05). ESV in anterior infarcts and in inferior infarcts was 79.2 ± 32.2ml, 37.7 ± 15.7ml respectively, (p<0.05). Stroke volume (SV) for pts and control was 46.7 ± 14.2ml versus 49.5 ± 8.4ml (P>0.05). SV was directly related to EDV and ESV (r=0.92, 0.91 respectively) in pts. There was no correlation between SV and EF in AMI. The study indicates that left ventricular remodeling may be detected by GSPECT within 2 hours after onset of symptoms of first AMI, and infarct expansion is not a delayed phenomenon. The degree of left ventricular dilation is larger in anterior infarcts than in inferior infarcts. SV is maintained at expense of increment in EDV and ESV at the early stage of AMI.

PS-24

A.Hitze¹, A.Manrique^{1,2}, V.Pontvianne¹, P.Véra¹.
Nuclear Medicine¹, Cardiology², University Hospital, Rouen, France

QUANTITATIVE MEASUREMENT OF THALLIUM LUNG UPTAKE FOR MULTIVESSEL CAD DETECTION: EFFECTS OF MEASUREMENT SITE AND HISTORY OF MYOCARDIAL INFARCTION.

Increased Thallium-201 SPECT lung uptake during exercise is related to LV dysfunction, extent of coronary artery disease (CAD), and patients prognosis. This parameter may be assessed by the lung/heart Thallium-201 uptake ratio (L/H). However, it is unclear whether measurement site of lung uptake or history of myocardial infarction (MI) could influence quantitative measurement of L/H.

Methods: We studied 113 Pts (M: 84, F: 29, mean age: 59±11y) referred to our center for stress Tl-201 SPECT. 37/113 Pts (33%, G1) had proven multivessel disease (MVD) on coronary angiogram, and 76/113 (67%, G2) had either single vessel disease, normal coronary angiogram, or a low likelihood of CAD (<5%). Twenty-seven Pts (24%) had history of MI. Post-stress quantitative analysis was performed on a 5 projections summed image, centered on the anterior projection. A 4x4 pixels ROI was placed over the hottest myocardial region (H). Lung uptake was successively measured using 3 ROIs: a 8x8 pixels left lung ROI (LL), a 8x8 pixels right lung ROI (RL), and a manual ROI encompassing the whole right lung (RLt). The lung/heart ratio was calculated for each lung ROI. The effect of MI on stress lung uptake specificity for MVD detection was assessed by ROC curves.

Results: RLt/H showed the most significant difference between G1 and G2:

	RL/H	RLt/H	LL/H
G1	0.434 ± 0.100*	0.458 ± 0.155**	0.421 ± 0.115
G2	0.382 ± 0.097	0.384 ± 0.090	0.379 ± 0.090
G1+G2	0.395 ± 0.100	0.402 ± 0.011†	0.390 ± 0.009

*p = 0.02 and **p = 0.003 (G1 vs G2), †p = 0.05 (RLt/H vs LL/H)

With a specificity ≥ 85% for MVD detection, the RLt/H cutoff value varied with history of MI (cut-off = 0.53 in Pts with MI, else 0.44).

Conclusion: Stress thallium lung uptake is increased in Pts with MVD, and is at best evaluated by RLt/H. The specificity of RLt/H for MVD detection is influenced by history of MI.

Poster presentations

PS-25

S.C. Cherng, C.C. Shen, M.S. Yang, M.S. Lin, R.S. Liu and W.S. Huang, National Defense Medical Center, Taipei Veterans General Hospital, and Cheng-Hsin General Hospital, Taipei, Taiwan, R.O.C..

IS HIGH-DOSE DOBUTAMINE 201TL PERFUSION SCAN SUITABLE FOR ALL PATIENTS WITH CORONARY ARTERY DISEASE?

A high-dose (40 $\mu\text{g}/\text{kg}/\text{min}$) dobutamine 201TI myocardial perfusion scan has been widely applied to patients with suspicious coronary artery disease (CAD). Two hundred and eight patients who received 201TI scans due to suspected CAD were analysed retrospectively for the possible side effect of dobutamine administration. Changes of heart rate (HR) and blood pressure (BP) of these patients were monitored throughout the whole procedure. The concentration of dobutamine began from 5 to 10 $\mu\text{g}/\text{kg}/\text{min}$ in the first 3 min. The infusion rate maintained an increment of 10 $\mu\text{g}/\text{kg}/\text{min}$ per 3 min until reaching the maximum dose (40 $\mu\text{g}/\text{kg}/\text{min}$) or patient displaying symptoms and signs of severe hypoxia or other side effects. Then, the infusion stopped. 201TI (74 MBq) was administered intravenously 1 min prior to the end of dobutamine infusion. Scans were performed at 5 min and 4 hr postinjection. We found that only 37% of patients could tolerate the maximum dose. 54% and 9% of patients stopped after receiving 30 $\mu\text{g}/\text{kg}/\text{min}$ and 20 $\mu\text{g}/\text{kg}/\text{min}$, respectively, due to unusual HR (descending, failing to reach 85% of maximum HR) and BP (failing to pass beyond 200 mmHg of systolic pressure) patterns or appearance of side effects including marked arrhythmia. These symptoms and signs subsided after discontinuing infusion of dobutamine. Two incidents of cardiac arrest happened and were revived following emergency procedures. Both of them were old women and were not on any exercise regimen. We, therefore, suggested that the application of high-dose dobutamine 201TI for the detection of CAD should be cautious especially for those women older than 65 years of age without regular exercise. For those patients, the infusion rate of dobutamine should be slow after 30 $\mu\text{g}/\text{kg}/\text{min}$, and terminate infusion whenever unusual HR and BP patterns appeared.

PS-26

Hubalewska-Hola A., Grodecki J., Bacior B., Królkowski T., Szybiński Z., Kawecka-Jaszcz K. Jagiellonian University, Collegium Medicum, Chair and Department of Endocrinology, 1-st Department of Cardiology Institute of Cardiology

LEFT VENTRICULAR EJECTION FRACTION AFTER MYOCARDIAL REVASCULARIZATION IN PATIENTS WITH CAD VERSUS BASELINE ASSESSMENT OF MYOCARDIAL VIABILITY BY LOW DOSE DOBUTAMINE (LDD) ECHOCARDIOGRAPHY AND Tc99m MIBI SPECT AT REST

Myocardial revascularization in patients with CAD permits improvement of left ventricular ejection fraction (LVEF), relief of pain and prolongation of life. Beneficial effect of myocardial revascularization is a result of improved blood supply to the areas with poor contractility. However, the associated LV dysfunction increases the risk of surgical procedure. Therefore, it is of vital importance to select the patients who are most likely to benefit from CABG. Improvement of global LV function manifested by increased LVEF despite correct assessment of myocardial viability varies from study to study. The aim of the study was to assess LVEF in patients after myocardial revascularization in relation to the amount of viable myocardium revealed by low dose dobutamine echocardiography and Tc99m MIBI SPECT at rest. **Material and Methods:** We studied 30 patients with echocardiographic LV wall motion abnormalities who were selected PTCA or CABG by coronary arteriography. 26 patients had myocardial infarction. LDD echocardiography (5-10 $\mu\text{g}/\text{kg}/\text{min}$) was performed immediately before the procedure. Tc99mMIBI SPECT with semiquantitative evaluation of tracer uptake in myocardial segments corresponding to echocardiographic segments was performed twice: before and 3 months after the surgical intervention. LVEF was assessed by radionuclide ventriculography. CABG was performed in 18 patients, PTCA in 12. **Results:** In 12 patients LVEF increased after the procedure by over 5%. Out of 84 revascularized segments with initially abnormal wall motion in 48% segments showed a positive dobutamine test. In all these segments at least minimal tracer uptake was observed, and in 68% segments the uptake was considerably better after the procedure. In 55% of the patients LVEF did not change significantly. In this group of patients of 47 segments 45% responded to dobutamine with an increase of contractility before the procedure, and tracer uptake was increased in 60% of the segments after the procedure. A significant difference was observed in the number of revascularized segments in both groups (7:2.9). In 2 patients LVEF decreased; one of these patients had a perioperative infarction. **Conclusions:** The improvement of LVEF after PTCA and CABG is determined mainly by the number of revascularized segments, to a lesser degree by increased tracer uptake after the procedure and the result LDD echocardiography at baseline.

PS-27

H Jan, H Al-Sakhri, M Ibbotson*, R Sobnack, M Granowska, DS Dymond*, SJ Edmondson+, KE Britton.

Department of Nuclear Medicine and Departments of Cardiology*, and Cardiac Surgery+, St. Bartholomew's Hospital

THALLIUM-201 SPECT IN TRANSMYOCARDIAL REVASCULARIZATION (TMR): PRE AND POST-TMR ASSESSMENT

TMR is being evaluated in 17 patients, age range 38-77 years, with Tl-201 SPET, prior to operation, at 6 and 12 months, m. Selection for TMR was according to clinical and angiographic criteria in patients with diffuse coronary artery disease who were unsuitable for coronary by-pass surgery or angioplasty. TMR used 1000 W CO2 laser machine, SPET with Cardial gamma camera, 180°, 30 frames, 30 sec/frame, Adenosine or Dobutamine stress/reinjection at rest. Results in 12 of the 17 treated patients evaluated at 6 m are given. All will complete 12 m by August 1998. 8 patients had angina class 4 and all improved to an average class of 1.35 at 6 m. 5/8 improved on SPET at 3m, 6/8 at 6m. 4 patients had angina class 3 and all improved to class 1 at 6 m. 3/4 improved on SPET at 3m, 4/4 at 6m. At 6 m all 12 patients were free of angina at rest. In conclusion, Tl-201 SPET is a suitable method for evaluating TMR and has demonstrated its benefits.

PS-28

A. Jiménez-Heffernan, A. Ortega-Carpio*, A. Sanchez**, C. Herrera, AC Rebollo, A. Tobaruela**.

Hospital Juan Ramón Jiménez. Services of Nuclear Medicine, Critical Care and Emergency*, and Cardiology**., Huelva. SPAIN.

SIDE-EFFECTS OF ATP AS A PHARMACOLOGIC STRESS AGENT IN MYOCARDIAL PERFUSION SCINTIGRAPHY.

Side-effects of ATP as a pharmacologic stress agent in myocardial perfusion scintigraphy (MPS) are frequent and seldom serious. We analyzed the type and frequency of side-effects in 991 patients undergoing MPS with either Tl (392) or Tc-Tetrofosmin (562), and related them to patient age, sex, body weight, radiopharmaceutical (RF), history of angina, results of treadmill testing (TT) and MPS findings.

Patients were 565 men and 389 women with mean age: 60.5 \pm 0.74, range 19-84 years. ATP was infused i.v. at a rate of 140 $\mu\text{g}/\text{kg}/\text{min}$ for 6 minutes. One-day stress and reinjection protocols were used with both RF. Dobutamine was the stress agent in 32 patients with contraindications for ATP administration. These were excluded from the analysis. Side-effects were accounted for as symptoms reported by patients or signs obtained by physical examination or ECG and BP monitoring and were classified as cardiopulmonary (CP) (dyspnea, chest or throat pain, palpitations, and ECG or BP changes) or nonspecific (NS) (hotness, nausea, headache, dizziness and gastrointestinal discomfort). We used the Chi-square test to identify the variables associated with development of side-effects, and logistic regression for control of confusion factors.

Almost half (49%) of the patients presented side-effects with ATP. Of these, 29% were NS and 20% CP. The most frequent effects were hotness (22%), chest pain (14%), throat pain (14%), dyspnea (8%) and headache (6%). ECG changes were seen in 74 patients (8%). In 12 cases ATP infusion was discontinued because of severe discomfort but not requiring treatment or further workup. In the rest of patients effects reported were mild and self-limited.

Bivariate analysis revealed that side-effect development was associated with patient sex, age, history of angina, TT results, RF choice and MPS findings. Logistic regression confirmed the higher frequency of effects in women (OR: 1.79), tetrofosmin (OR:1.52), inconclusive TT (OR: 2.68), and normal MPS (OR:1.52) or nonischemic MPS defects (OR:1.79). When we analyzed only CP effects the variables RF and MPS lost their predictive value; feminine sex (OR: 1.53) and inconclusive TT (OR: 2.58) were maintained, and positive TT (OR: 2.37) and typical angina (OR: 1.76) proved their association with side-effect development.

We therefore conclude that side-effects of ATP administration are frequent (\approx 50% of our patients), mild and well tolerated. Women and patients with inconclusive TT are especially prone to develop both types of effects (CP and NS). In addition, CP effects were also increased in patients with positive TT and typical angina.

PS-29

M. Kamínek, M. Mysliveček, M. Skvařilová¹, V. Hušák, O. Lang²
 Dept. of Nuclear Medicine and ¹Dept. of Internal medicine I, University Hospital, Olomouc, Czech Republic. ²Dept. of Nuclear Medicine, University Hospital, Prague - Vinohrady, Czech Republic

REST 201TI/STRESS 99mTc TETROFOSMIN DUAL-ISOTOPE MYOCARDIAL PERFUSION IMAGING IN THE DIAGNOSIS OF CAD: COMPARISON WITH 201TI STRESS-REDISTRIBUTION AND 2-DAY 99mTc TETROFOSMIN PROTOCOL.

A dual-isotope protocol with rest 201TI followed by a stress 99mTc tetrafosmin combines optimal techniques for accurate detection of CAD and viability and seems to be the universal protocol. The aim of this study was to compare dual-isotope imaging with 201TI stress-redistribution and 2-day 99mTc tetrafosmin protocol. **Materials and methods:** A total of 209 patients - 115 without prior myocardial infarction (MI) and 94 after MI - underwent exercise myocardial perfusion SPECT and coronary angiography (CAD was defined as a luminal narrowing $\geq 50\%$). 77 patients (33 without prior MI and 44 after MI) were investigated with the dual-isotope protocol. 93 patients (43 without MI and 50 after MI) underwent 201TI stress-redistribution study. Thirty-nine patients (all without prior MI) were assessed with 2-day 99mTc tetrafosmin protocol.

Results: Group I: Patients without prior MI (n= 115).

	Dual-isotope (n=33)	201TI (n=43)	2-day tetrafosmin (n=39)
Sensitivity	95% (21/22)	92% (22/24)	96% (22/23)
Specificity	82% (9/11)	89% (17/19)	88% (14/16)
Accuracy	91% (30/33)	91% (39/43)	92% (36/39)

Group II: Patients after MI (n= 94)

	Dual-isotope (n=44)	201TI (n=50)
Sensitivity	92% (34/37)	95% (42/44)
Specificity	71% (5/7)	83% (5/6)
Accuracy	89% (39/44)	94% (47/50)

Conclusion: The dual-isotope imaging didn't improve diagnostic accuracy for determining the presence or absence of CAD in both groups of patients. However, the principal disadvantages of dual-isotope protocol include the added cost and radiation dose associated with administration of two tracers. Now we prefer 2-day tetrafosmin study for patients without prior MI and 201TI stress-redistribution-reinjection for patients after MI.

PS-30

C. Kato, U. Ruotsalainen, H. Laine, S. Alenius, H. Iida, P. Nuutila, J. Knuuti

Turku PET Centre, Turku University, Finland and Research Institute for Brain and Blood Vessels-Akita, Akita City, Japan

A NEW ITERATIVE RECONSTRUCTION METHOD BASED ON MEDIAN ROOT PRIOR IN QUANTIFICATION OF MYOCARDIAL METABOLIC RATE OF OXYGEN WITH PET

The aim of this study was to examine the clinical advantage of an iterative Bayesian reconstruction method based on median root prior (MRP) against the standard technique of filtered backprojection (FBP) in quantitative myocardial PET study.

Myocardial blood flow (rMBF), oxygen extraction fraction (rOEF) and myocardial oxygen consumption (rMMRO2) were quantified in 27 subjects. For each subject, regions of interests (ROIs) were drawn twice on both MRP and FBP images to test the variability and reproducibility of the metabolic parameters.

The image quality was visually clearly improved by MRP reconstruction. The correlation coefficients of the repeated measurements of rMBF, rOEF and rMMRO2 in a total of 324 myocardial regions were significantly higher in MRP images than in FBP images (rMBF: MRP $r=0.896$ vs. FBP $r=0.762$, $p<0.001$; rOEF: 0.915 vs. 0.877, $p<0.02$; rMMRO2: 0.954 vs. 0.900, $p<0.001$). Significantly higher correlations were also obtained in different myocardial anatomical regions in MRP images as compared to FBP images but this was especially clear in the septal regions. Coefficient of variation for each parameter was significantly lower in MRP images than in FBP images (rMBF: MRP $23.5\pm 11.3\%$ vs. FBP $27.0\pm 13.6\%$, $p<0.01$; rOEF: $21.0\pm 11.1\%$ vs. $29.7\pm 19.0\%$, $p<0.001$; rMMRO2: $23.1\pm 13.2\%$ vs. $27.7\pm 18.3\%$, $p<0.01$). Thus, the new MRP reconstruction method provides higher reproducibility and lower variability in the quantitative myocardial parameters as compared with the traditional FBP method. The MRP reconstruction algorithm clearly improves the stability of quantitation of myocardial blood flow and oxygen metabolism with PET.

PS-31

Kneifel S., Burger C., Buck A.
 Clinic for Nuclear Medicine, University Hospital Zurich, Switzerland

PIXELWISE QUANTIFICATION OF MYOCARDIAL PERFUSION WITH N-13 AMMONIA PET

Purpose:

Quantitative assessment of myocardial perfusion with N-13 ammonia PET is normally done using kinetic modeling (KM) with one or more tissue compartments. Time-activity curves for KM are derived from regions of interest (ROIs). This method has several disadvantages: a) only one global perfusion value per ROI can be obtained, b) the results depend upon the location of the ROIs, thus resulting in an inter-observer variability. The aim of our investigation was to evaluate an observer-independent method for the quantitation of myocardial perfusion.

Methods:

Dynamic ammonia PET at rest and after intravenous injection of dipyridamole was performed on 6 young, healthy volunteers. The data were analyzed with 2 different methods: In the first method (KIN) tissue and blood ROI's were defined on a midventricular slice. The time-activity curves were then analyzed using a one-tissue compartment model (K_1 , k_2 , spillover correction) with K_1 representing perfusion. In the second method (PIX) myocardial pixels were first corrected for ventricular spillover using a factor determined from kinetic modeling. In a second step K_1 values were calculated pixelwise using an integrated version of the K_1, k_2 model (Alpert et al.) and an arterial input curve derived from a left-ventricular ROI.

Results:

The values obtained with both methods were highly correlated: $K_1 \text{ pix} = 0.245 + 0.633 K_1 \text{ kin}$, values in ml/min/g; $r = 0.965$.

Conclusion:

Pixelwise assessment yields quantitative parametric maps of myocardial perfusion. The calculation of these maps can be fully automated, yielding objective values for myocardial perfusion. The method therefore eliminates disadvantages of conventional tracer kinetic modeling where the placement of ROIs is often subjective.

PS-32

T. Kolokolova, V. Chernov, V. Markov, Yu. Lishmanov

Institute of Cardiology, Tomsk, Russia

CAPOTEN INFLUENCE ON MYOCARDIAL PERFUSION IN MYOCARDIAL INFARCTION PATIENTS

Aim: The aim of this study was to assess capoten influence on myocardial perfusion in acute myocardial infarction (AMI) patients during one year treatment.

Methods: Forty AMI pts received effective thrombolytic therapy (ILT). Pts of the 1 gr. (n=20) were treated with capoten before TLT by dosage of 25-50 mg daily during one year. Another 20 pts of the 2 gr. received the same therapy without capoten. Dipyridamole 199Tl myocardial scintigraphy was performed on the third week of AMI and 12 months later. The next indices were assessed: perfusion defect size (PDS), volume of fixed and reversible defects (VFD, VRD), minimal TI accumulation in perfusion defect (MA) and coronary fraction of accumulation (CFA). **Results:** are presented in the Table.

Indices	1 Group (Capoten)		2 Group (Controls)	
	3 weeks AMI	1 year AMI	3 weeks AMI	1 year AMI
CFA	1,86 ± 0,18	1,88 ± 0,13**	1,88 ± 0,34	2,5 ± 0,13 *
PDS, %	16,61 ± 2,22	11,5 ± 2,26***	21,04 ± 2,68	21,63 ± 2,9
VFD, %	11,08 ± 2,43	6,83 ± 2,18**	14,6 ± 2,21	12,68 ± 2,2
VRD, %	7,26 ± 1,76	5,77 ± 1,0**	7,64 ± 1,76	8,8 ± 1,4
MA, %	40,51 ± 3,67	45,3 ± 3,52***	36,46 ± 5,62	31,32 ± 4,3

* - $p < 0,05$, ** - $p < 0,01$ -compare with initial parameters, # - $p < 0,05$, ## - $p < 0,01$ -control versus capoten.

Administration of capoten decreases perfusion defect size with fixed defects and increases minimal accumulation what improves myocardial microcirculation obviously. Deterioration of CFA in control gr. can be sign of the left ventricle remodelling. Five pts of the 2 gr had unstable angina (UA) and one pt had recurrent AMI throughout 12 months of follow up. Two cases of UA and one recurrent AMI were in the 1 gr throughout the year.

Conclusions: Capoten given in the early AMI period and later one year leads to significant improvement of myocardial microcirculation and clinical state of patients.

PS-33

M. Kostkiewicz, W. Tracz, M. Olszowska, T. Przewlocki, P. Pieniążek
Department of Nuclear Cardiology, Department of Cardiovascular Surgery
Collegium Medicum UJ Kraków Poland

THE EVALUATION OF MYOCARDIAL PERFUSION AND FUNCTION AFTER INTRACORONARY STENT PLACEMENT USING Tc99m SESTAMIBI EXERCISE SCINTIGRAPHY AND LOW DOSE DOBUTAMINE ECHOCARDIOGRAPHY.

Coronary stent placement has gained clinical acceptance as a treatment for coronary artery disease. However there are limited number of reported myocardial perfusion and function studies on stent implantation. The aim of this study was to compare the results of low-dose dobutamine 2D echocardiography and Tc 99m sestamibi perfusion scintigraphy before and after revascularisation achieved by intracoronary stent placement.

Fifteen patients (13 men, 2 women, mean age 54 ± 10 years) were included in this study. Eight patients had LAD, 5 RCA, 2 LCx lesions. All patients underwent low dose dobutamine ($5 \mu\text{g/kg/min i.v.}$) 2D echocardiography and two days protocol perfusion scintigraphy within 1 week before and 30-40 days after stent placement. Regional Tc 99m sestamibi activity and systolic function in echocardiography were assessed in 16 segments per patient.

Results. Stress perfusion defect was detected in 45 out of 300 segments. After revascularisation, the number of ischemic segments were significantly reduced and exercise perfusion scores were improved ($p < 0.001$). Of the 53 segments with severe dysfunction at rest of dobutamine echocardiographic study, 40 showed contractive reserve before revascularisation. Myocardial function improved also with dobutamine infusion after stent implantation. Only in 21 segments impaired function and contractive reserve was observed.

We conclude that Tc 99m sestamibi myocardial perfusion scintigraphy and low dose dobutamine 2D echocardiography provides a good documentation of the myocardial perfusion and function improvement after intracoronary stent placement. However significantly greater changes were observed in the perfusion in comparison with the myocardial function assessed by echocardiography.

PS-34

J.Y. Ahn, D.S. Lee, S.K. Kim, K.M. Kim, S.A. Shin, J-K Chung, M.C. Lee

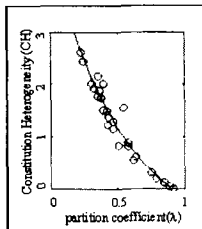
Seoul National University Hospital and Ewha Womans University, Seoul, Korea

DEVELOPMENT OF METHOD TO QUANTIFY AND ESTIMATE HETEROGENEITY OF MYOCARDIAL FLOW DISTRIBUTION USING ESTIMATED PARTITION COEFFICIENT IN O-15-H₂O PET.

In this study, we propose how we could quantify tissue heterogeneity and investigate if we could use (estimated) partition coefficient to represent the degree of heterogeneity of flow distribution in myocardium using O-15-H₂O PET and modeling. We estimated 6 parameters including perfusable tissue index (PTI) and partition coefficient (λ) using modified single compartment model with the data obtained from rest/dipyridamole stress O-15-H₂O PET in normal dogs.

With computer simulation, we made heterogeneous tissue composed of different sized blocks, each of which had different homogeneous flow and whose flow distribution was varied. We devised the concept of constitution heterogeneity, which implied the degree of heterogeneity of blood flow and its gradient. O-15 H₂O PET scan was performed in 4 normal dogs at rest and dipyridamole stress. Total 36 paired data were obtained from ROIs in LV (input) and myocardium at rest and stress. Recovery coefficient (F_{rm}), spillover fractions (F_{bm}, F_{vm}), PTI, λ , and flow were estimated using our modified model by two non-linear least square fitting methods.

In the simulation study, flow and λ decreased as constitution heterogeneity increased. Estimated λ and heterogeneity was inversely related (Figure). Flow estimated from O-15 H₂O PET was 1.3 ± 0.3 ml/min/g at rest and 4.4 ± 1.4 ml/min/g at stress. Estimated λ was $0.92-1.01$ ml/g and $0.84-1.01$ ml/g and PTI was $0.91-1.0$ and $0.93-1.07$ at rest and stress. We suggest that the degree of flow heterogeneity could be quantified and represented by estimated partition coefficient. In animal experiment, flow and partition coefficient was estimated successfully both at rest and at stress. This study suggests that we could use partition coefficient to represent flow heterogeneity in ischemic or infarcted myocardium having heterogeneous flow.



PS-35

D.S. Lee, J.Y. Ahn, S.K. Kim, M.M. Lee, J-K Chung, M.C. Lee.

Seoul National University College of Medicine, Seoul, Korea

LIMITED FEASIBILITY FOR INTERCHANGEABLE USE OF QUANTITATIVE INDICES AND WALL MOTION OF TI-201 GATED MYOCARDIAL SPECT WITH Tc-99m-MIBI GATED SPECT.

Tc-99m-MIBI gated SPECT is used with good reproducibility to quantify enddiastolic volume (EDV), endsystolic volume (ESV) and ejection fraction (EF) as well as to evaluate wall motion and systolic thickening. We investigated if we could use TI-201 gated SPECT to quantify EDV, ESV and EF and wall motion interchangeably by studying agreement with Tc-99m-MIBI gated SPECT using correlation and Bland-Altman plot analysis.

In consecutive 40 patients (M:F=30:10, 60.4 ± 9.8 year old) during our clinical routine we acquired another rest gated Tc-99m-MIBI (925MBq) SPECT 24 hours after rest gated TI-201 (111MBq) SPECT. As control, we acquired two consecutive Tc-99m-MIBI gated SPECT in the other 20 patients. Vertex camera with 16 frames per cycle was used both for TI-201 gated and Tc-99m-MIBI gated SPECT. Two independent operators graded wall motion using 5 point scores (normal: 0 to dyskinesia: 4) for 13 segments using slice cine images or using surface display of Cedars quantitative gated SPECT (QGS) software. The same software was used to obtain EDV, ESV and EF. QGS succeeded in giving surface display to let us have volumes and fractions and determine wall motion in every case, while we could not score wall motion in 53% (TI-201) or 8% of segments (Tc-99m-MIBI) using conventional slice cine viewing methods because of poor image quality. Kappa values for the intra- and inter-observer agreement of scoring wall motion using TI-201 gated SPECT was 0.66 and 0.55. Though correlation between EDV, ESV and EF of TI-201 and Tc-99m-MIBI was good ($r = 0.99, 0.98, 0.86$, respectively), Bland-Altman plot revealed that the range of 2 standard deviation (SD) of agreement was 33 ml, 28 ml, 13% for EDV, ESV, and EF between TI-201 and Tc-99m. The range of 2 SD of agreement between Tc-99m-MIBI gated SPECT and Tc-99m-MIBI SPECT was 16 ml, 16 ml, 6%.

We concluded that QGS software helped much determine wall motion and volumes and fraction, however, volumes and ejection fraction obtained using TI-201 gated SPECT was not interchangeable with Tc-99m gated SPECT because of intolerable degree of agreement. If we assume that 2 SD should be lower than the reproducibility of Tc-99m-MIBI gated SPECT itself we would not recommend routine use of TI-201 gated SPECT in stead of Tc-99m-MIBI one.

PS-36

XJ Liu, ZH Tao, RF Shi, ZM Yao, XL Zhang, YZ Liu, YQ Tian

Department of Nuclear Medicine, Cardiovascular Institute & Fu Wai Hospital, CAMS & PUMC, Beijing, China

EVALUATING A NOVEL PHARMACOLOGIC STRESS AGENT, THE CHINESE HERBAL MEDICINE HIGENAMINE, IN ASSESSING CAD WITH ^{99m}Tc-MIBI SPECT

Higenamine (HG), which was isolated from aconitum japonicum, has significant inotropic and chronotropic effects on the heart. It might be utilized in pharmacologic stress test in detecting coronary artery disease (CAD). HG stress and exercise (Ex) ^{99m}Tc-MIBI myocardial SPECT were performed in 21 patients documented by CAD (16 patients with CAD, 5 normal). Higenamine was infused with the start dose of $0.5 \mu\text{g/min/kg}$, gradually increased ($0.5 \mu\text{g}$ every 3 min) to top dose $4 \mu\text{g/min/kg}$. Twenty-two four mCi ^{99m}Tc-MIBI was injected intravenously and myocardial SPECT was performed 1 hour later with Siemens multi SPECT 3. Next day, submaximal exercise and resting SPECT were performed. Results: The sensitivity, specificity and accuracy of HG stress test were 89.6%, 88.5% and 88.9%, respectively. During HG stress, 33 segments shown reversible defects and while 28 shown defects during Ex. The concordance between HG and Ex was 90%. No significant side effects were found. Conclusion: HG ^{99m}Tc-MIBI stress testing might be useful and safe technique in detection of CAD.

PS-37

K. Machida, N. Honda, T. Takahashi, M. Hosono, T. Takahashi, T. Kamano, A. Kashimada, H. Osada, Y. Shimizu, T. Iwase, H. Toyoda, K. Ogawa, W. Watanabe, S. Dei, M. Ohmichi, K. Ochiai and T. Takishima
Hospital: Saitama Medical Center, Department of Radiology

ASSESSMENT OF REGIONAL WALL MOTION BY GATED MYOCARDIAL PERFUSION TOMOGRAPHY WITH ^{99m}Tc-TETROFOSMIN

Diagnostic ability for regional wall motion with ^{99m}Tc-Tetrofosmin ECG-gated cardiac SPET (TF-g-SPET) was investigated. Thirty-eight patients with ischemic heart disease were entered the study (M:F = 28:10, mean age of 61.2 years). The patients underwent TF-g-SPET, echocardiography (US) and contrast left ventriculography (LVG) within a month. Regional wall motions of the left ventricles (rWM) were assessed with cine displays of TF-g-SPET images by two experienced nuclear medicine physicians blinded to the clinical information to correlate with US and LVG. US and LVG were performed and evaluated by cardiologists not blinded to the clinical information. The diagnoses of rWM were not statistically different between US and TF-g-SPET (concordance rate 72.5% [103/142 segments], p<0.05) and between LVG and TF-g-SPET (58.3% [28/48], p<0.05). These rates were not statistically different from that between LVG and US (61.2% [30/49], p<0.05). Percent wall thickening (%WT), count increase rate between end-systolic and end-diastolic phases calculated from short-axis images, were correlated with LVEF derived from LVG (r = 0.56, n = 12, p<0.05) and from US (r = 0.66, n = 38, p<0.05). Mean %WT's were significantly declined as the rWM worsened (p<0.05): mean %WT was 35.4 ± 13.5% (n = 106) in normokinetic segments, 25.0 ± 12.4% (n = 83) in hypokinetic segments and 20.3 ± 11.5% (n = 19) in dys- or a-kinetic segments. In conclusion, TF-g-SPET can evaluate rWM both visually and quantitatively by %WT in addition to myocardial perfusion. Its performance of rWM assessment was comparable with that of US and LVG. Thus TF-g-SPET is clinically useful.

PS-38

A. Manrique^{1,2}, M Faraggi¹, P Vera², L Sarda¹, R Lebtahi¹, D Le Guludec¹

Nuclear Medicine, Bichat¹ and Rouen² university hospitals, France.

COMPARISON OF 2 METHODS FOR GATED SPECT LVEF MEASUREMENTS IN PATIENTS WITH LARGE MYOCARDIAL INFARCTION AND SEVERE LV DYSFUNCTION:

Gated myocardial SPECT (gSPECT) allows evaluation of LVEF, but its accuracy is still controversial in pts with large perfusion defects. This study aimed to compare LVEF measurements from equilibrium radionuclide angiography (ERNA) and from gSPECT using 2 different commercially available softwares, in patients with myocardial infarction (MI), large perfusion defects and LV dysfunction.

Method: 50 consecutive patients (43 men, mean age 61±17) with history of MI (anterior: 26, inferior: 18, lateral: 6) and ERNA LVEF = 38±12% enrolled the study. All had large fixed perfusion defects on rest non-gated SPECT (35±17% of the LV planimetered surface by bull's eye polar map). All underwent rest gSPECT, either 4 hours after the injection of 203 MBq of Thallium-201 or 1 hour after the injection of 1110 MBq of Tc-99mMIBI. Acquisition parameters were: 90° dual-head camera, LEHR collimator, 8 frames/cycle, 32 64x64 projections of 60s (Tc-99m MIBI) or 120s (Tl-201), energy window: 140±10keV (Tc-99m) or 70±20KeV and 167±20KeV (Tl-201). After prefiltering with a 2-dimensional Butterworth filter [order 5, cut off .25 (Tc-99m) or .20 (Tl-201)], projection data were reconstructed with ramp-filter backprojection and no attenuation correction. LVEF was calculated from reconstructed gSPECT with 2 different softwares: Multidim™ (SMVi; operating from 3D myocardial volume) and QGS™ (Cedars Sinai; operating from short axis slices).

Results: LVEF was significantly different between Multidim™ and QGS™ (respectively 36.3±13% and 34±12%, p<.01). Both software underestimated LVEF compared to ERNA:

	ERNA vs Multidim™	ERNA vs QGS™
difference ERNA-gSPECT:	2.3 ± 9%	4.7 ± 7.3%*
linear regression:	y = 8.258 ± .727 x**	y = 4.911 ± .753 x**
r:	.74	.82
SEE:	.097	.078

*p <.0001: ERNA vs QGS™, **p<.0001: gSPECT vs ERNA

Conclusion: gSPECT underestimates LVEF in pts with LV dysfunction and large perfusion defects. Although maximizing this underestimation, QGS™ software provides the best correlation to ERNA.

PS-39

G. Marotta, A. Bruno, R. Benti, A. Finzi*, C. Canzi, S. Costantino*, R. Perondi*, S. Romano*, F. Boccagna, P. Gerundini
Department of Nuclear Medicine and *Dept of Cardiology, IRCCS-Ospedale Maggiore, Milan, Italy

LEFT VENTRICULAR FUNCTION WITH GATED SPECT ASSESSED BY TWO SOFTWARE PACKAGES: COMPARISON BETWEEN TWO Tc^{99m}-LABELED PERFUSION AGENTS AND CONTRAST VENTRICULOGRAPHY

Noninvasive assessment of left ventricular function (LVF) by G-SPECT is emerging as a novel powerful tool in clinical cardiology. However, the role of the choice between different perfusion agents and software analysis has not yet been fully investigated. The aim of this work was to compare the quantification of LVF with G-SPECT as obtained by using Tc^{99m}-tetrofosmin (Tf) and Mibi as perfusion agents, and by 3D-Perfusion/Motion Map (3D-PFM) and Quantitative Gated SPECT (QGS) as analysis software; contrast left ventriculography (CVG) was taken as the reference. After having given their informed consent, 40 patients (mean age 58 yrs, range 41-75) with a history of recent (1-6 months) myocardial infarction were enrolled in a cardiological trial on myocardial viability and underwent two myocardial G-SPECT rest studies with Tf and Mibi within three days and a CVG within 3 months. Nuclear imaging was started 30-45 minutes after Tf and 60-90 minutes after Mibi injection at rest: 64x64 frame, 60 projections/360°, supine, 60 sec/projection, step and shoot mode, 8 time bins and a beat acceptance window of 40%. The evaluated parameters were ejection fraction (EF), end-diastolic volume (EDV), end-systolic volume (ESV) and stroke volume (SV). The table shows the coefficient of correlation (Pearson r) between Tf and Mibi G-SPECT and CVG of the parameters of LVF.

	EF (3D-PFM)	EF (QGS)	EDV (QGS)	ESV (QGS)	SV (QGS)
Tf vs Mibi	0.695	0.929	0.967	0.975	0.798
Tf vs CVG	0.491	0.720	0.565	0.738	0.518
Mibi vs CVG	0.593	0.753	0.563	0.732	0.533

Good correlations (all statistically significant, p<0.001), best with QGS, were observed between the quantitative LVF assessed by G-SPECT with Mibi and Tf and by CVG. The EF calculated by 3D-PFM was systematically lower than the EF assessed by QGS and by CVG. Measurements of LVF obtained by QGS correspond well with those of CVG, even in patients with severe and extensive perfusion defects. EF differences observed with QGS comparing the two Tc^{99m}-labeled perfusion agents were similar to the reported variability in EF serial measurements made by Mibi G-SPECT. In conclusion, estimation of EF by QGS was more reliable and reproducible than by 3D-PFM and quantification of LVF obtained by QGS should be considered as an integral part of myocardial perfusion studies. Moreover, it is possible to study LVF in the follow-up of myocardial infarction irrespective of which of these two Tc^{99m}-labeled perfusion agents is used.

PS-40

Ch. Maunoury, P. Acar, Th. Antonietti, S. Sébahoun, L. Barritault

Hôpital Necker-Enfants Malades, Paris

USEFULNESS OF 201TI MYOCARDIAL SPET AFTER ARTERIAL SWITCH OPERATION FOR TRANSPOSITION OF GREAT ARTERIES

Selective coronary angiography (SCA) is the gold standard to detect coronary artery lesions after arterial switch operation for transposition of great arteries. Our aim was to assess the usefulness of 201Ti myocardial SPET (MS) to study myocardial perfusion after switch. **Methods:** Twenty-four children (16 male, 8 female, mean age: 6 years, range: 4 months-12 years) an average of 6 years after neonatal switch underwent MS and SCA at an interval of 3 days. SCA was defined as abnormal in case of arterial stenosis greater than 50% or complete obstruction. MS was defined as abnormal in case of perfusion defect(s) on stress images. **Results:**

	normal SCA	coronary lesions
normal MS	9	2
perfusion defects	1	12

Sensitivity for MS was 86% and specificity 90%. Negative and positive predictive values were 82% and 92%, respectively. **Conclusion:** MS is very useful to assess perfusion and to discuss a revascularization.

Poster presentations

PS-41

S. Koukouraki, N.E. Mezilis*, I. Manousakas, E. Skalidis*, M.K. Kanakarakis*, P.E. Vardas*, N. Karkavitsas.
Hospital: Depts. of Nuclear Medicine and *Cardiology, Heraklion University Hospital, Heraklion, Crete, Greece.

EFFECT OF STRESS INDUCED ISCHEMIA ON POST-STRESS GATED Tc-99m SESTAMIBI TOMOGRAMS AFTER ACUTE MYOCARDIAL INFARCTION.

This study investigated the impact of stress induced ischaemia on post stress gated Tc-99m sestamibi tomograms and correlated the rest and post stress gated studies with the resting echocardiogram.

Methods: Fourteen pts with first MI underwent 1-day rest/reinjection stress Tc-99m sestamibi scintigraphic study and dobutamine-atropine stress echo (DASE) at a mean of 8 ± 1 days after MI. Dobutamine was infused at an initial dose of $5 \mu\text{g}/\text{kg}/\text{min}$, rising to $40 \mu\text{g}/\text{kg}/\text{min}$ every 3 minutes. Regional LV wall motion was analysed from the 16-segment model. The analysis of the tomographic images used the same 16 left ventricular segments, to match the echocardiographic analysis.

Results: The segmental correlations of rest echo/rest gated and rest echo/post stress gated were 84% and 78% respectively. The pts were divided into 3 groups. Group A (6 pts) with the same segmental agreement, group B (5 pts) with lower rest echo/post stress gated agreement, and group C (1 pt) with lower rest echo/rest gated agreement. In group B, 5 pts (83%) had inducible peri-infarction or remote ischaemia on either stress Tc-99m SPECT or DASE.

Groups	No.	Echo/ rest gated	Echo/ stress gated	Ischaemia on Tc-99m or DASE
A	7	90%	90%	3 (43%)
B	6	81%	69%	5 (83%)
C	1	69%	81%	1 (100%)

Conclusion: In acute MI, post stress gated images of regional left ventricular function do not reflect resting left ventricular function when compared with the resting echocardiogram. This mismatch is caused by peri-infarction or remote stress induced ischaemia and it is likely to represent post ischaemic stunning.

PS-42

E. Milan, A. Terzi, P. Rossini, R. Giubbini.

Spedali Civili, Brescia, ITALY - Nuclear Medicine Department.

ULTRA-SHORT ONE DAY PROTOCOL COMBINING Tc 99m TETROFOSMIN AND Tc 99m SESTAMIBI IN THE DETECTION OF MYOCARDIAL SCAR AND ISCHEMIA.

Tc-99m tetrofosmin (T) allows earlier imaging in comparison to sestamibi (S), due to its faster hepatic clearance. Therefore, an increase in Lab output might be hypothesized. But, the lower myocardial extraction factor in comparison to S makes controversial its choice in presence of increased myocardial blood flow, due to a possible underestimation of perfusion defects. Therefore, the combination of both tracers in the same patient (pt) might allow an imaging optimization. Aim: to analyze the accuracy of an ultra-short one day protocol in the evaluation of inducible ischemia using rest-T and stress-S.

Twentythree pts with previous myocardial infarction were evaluated according to the following protocol:

day1 → rest T → SPECT within 30', stress S → SPECT within 1h (=2h 10' for the entire procedure);

day2: rest S → SPECT within 1h.

Results: quality of rest T and S images was evaluated by 2 physicians (P1 and P2) aware of pt's sex and medical history. P1 found the rest-T images adequate and comparable in terms of quality to those obtained using S in all but 3 pts, while P2 found rest T to be worse than rest S images in 2 pts. No significant difference between T and S was found using quantitative analysis in the evaluation of infarct size (13.1 ± 15.4 vs 13.1 ± 15.1 ; $p=NS$). Moreover, comparing the ultra-short single day protocol (rest T + stress S) to standard two day protocol (stress S + rest S) no significant difference was found by quantitative analysis in the evaluation of reversible ischemia (26.4 ± 25.8 vs 24.4 ± 26.5 ; $p=NS$).

Conclusion: ultra-short protocol seems to allow an accurate evaluation of infarct size and inducible ischemia, comparable to that obtained by two day protocol.

PS-43

E. Moraliqis, G. Arsos, K. Karakatsanis, A. Kontopoulos*.

Dept. of Nuclear Medicine, 2nd Dept. of Internal Medicine*, University of Thessaloniki Medical School, Hippokraton Hospital.

A SINGLE SESSION "STRESS 201TI+REST RADIONUCLIDE VENTRICULOGRAPHY" (S 201TI+rRVG) SHORT PROTOCOL IN THE ASSESSMENT OF MYOCARDIAL PERFUSION.

The widely used «stress-rest 201TI» protocol (S-R 201TI) lasts 4 hours and it often necessitates additional wall motion evaluation for a complete assessment of myocardial status. The aim of this study was to assess the efficacy of the 45min long «S 201TI+rRVG» protocol versus both the «S-R 201TI» and the «S-R 201TI+rRVG», which allows for wall motion evaluation.

Twenty-two patients (17 men, 5 women, 14 after an acute ischaemic event) were routinely referred for coronary artery disease investigation. In each patient a «S-R 201TI» planar gated study (ANT, LAO, LL views) was performed, immediately followed by rRVG (LAO, LL views). These techniques have been previously evaluated in our department. Both segmental perfusion and wall motion were semiquantitatively assessed by two independent experienced observers and a final diagnosis was reached for each patient based on: 1) S-R 201TI, 2) S-R 201TI+rRVG and 3) S 201TI+rRVG.

Ninety-six myocardial segmental defects were detected at stress (53 with significantly reduced perfusion), 28 of which showed significant redistribution and another 68 showed partial or no redistribution 3 hours later. Using rRVG 22 segments with severe hypokinesis or akinesis were detected, 12 of which showed significantly reduced perfusion and 10 normal or slightly reduced perfusion at stress. Using the «S-R 201TI» protocol 10 of 22 patients (45%) were adequately assessed while results were ubiquitous in the rest 12 patients (55%). Using the «S-R 201TI+rRVG protocol» diagnosis was considered satisfactory in all cases. Using the «S 201TI+rRVG» protocol diagnosis was judged as satisfactory in 17 cases (all men) and ubiquitous in 5 cases (women).

Conclusion: These results suggest that the «S 201TI+rRVG» protocol is equally efficient to the «S-R 201TI+rRVG» and superior to the «S-R 201TI» in assessing myocardial perfusion in men. This is accomplished in a single short session, at no excess cost and it can additionally offer assessment of both global and segmental myocardial function.

PS-44

M. Onur Demirel*, N. Kurtoglu, M. Degertekin, H. Silahci*, C. Onsel*, F. Turan

Koşuyolu Heart and Research Hospital, Cardiology and Nuclear Medicine* Departments, İstanbul, Turkey.

CLINICAL SIGNIFICANCE OF EXERCISE-INDUCED ST SEGMENT ELEVATION AFTER MYOCARDIAL INFARCTION: A MYOCARDIAL PERFUSION TOMOGRAPHY COMPARISON WITH CORONARY ARTERIOGRAPHY.

After myocardial infarction (MI), ST segment elevation in exercise testing in infarct related leads can be interpreted as left ventricular dyskinesia. In fact, some studies indicate residual viable tissue in infarct zone. We investigated the relation between ST segment elevation and viable tissue in infarct zone, coronary perfusion scoring, left ventricle segment scoring and collateral perfusion.

Sixty patients with previous MI were admitted to the study. Exercise testing with Bruce protocol and TI-201 stress-reinjection myocardial perfusion scintigraphy (SPECT) were performed in all of the patients. We accepted at least 1mm ST segment elevation in infarct related leads (mean 1.8 ± 0.7 mm, range 1-4.5mm). Coronary arteriography and left ventriculography were performed and left ventricle segment scoring (LVSS), coronary perfusion scoring (CPS) were done. ST elevation was seen 31 patients (group 1), while 29 patients did not show ST elevation (group 2). Previous myocardial infarctions and its locations were in correlated with scintigraphy. Viable tissue in infarct region was seen in 28 patients in group 1, and 16 patients in group 2 ($p<0.05$). LVSS was 4.10 ± 0.31 in group 1 and 3.53 ± 0.39 in group 2 ($p>0.05$). CPS also is not different between two groups (32.35 ± 5.73 vs 26.21 ± 3.61 , $p>0.05$).

In conclusion; ST elevation in infarct related leads after MI especially early period could be demonstrated residual viable tissue. MPS could be performed in this patient group.

PS-45

G Panoutsopoulos, E Savari, C Batsakis, A Petrou, I Ilias, L Oros, C Karidis, J Christacopoulou.

Depts of Nuclear Medicine & Cardiology, "SOTIRIA" Chest Hospital, Athens

COMBINED PROTOCOLS IN HYPERTENSIVE PATIENTS FOR MYOCARDIAL PERFUSION IMAGING

Hypertensive patients submitted to exercise test for myocardial scintigraphy often respond with excessive elevation of the blood pressure (BP) resulting in interruption of the test or false positive results for coronary artery disease (CAD). Alternatively, pharmacologic testing with Dipyridamole alone (DP) can be used. DP diminishes BP mildly but often provokes undesirable non-cardiac side effects (NCSE) and increases splanchnic activity. Moreover, left ventricular function cannot be adequately evaluated with DP.

The aim of the study was to evaluate the hemodynamic changes and the safety of the combined protocols: DP plus handgrip (DP-HG) and DP plus symptom limited exercise test on a treadmill (DP-TM) in hypertensive patients. Two hundred and forty hypertensive patients suspected for CAD, divided in 3 groups, underwent perfusion imaging. Group I (DP) of 27 pts (16 M, 11 F, age: 63±7.2 y) underwent IV DP administration (0.142 mg/kg/min for 4 min). Group II (DP-HG) of 126 pts (70 M, 56 F, age:63±6.5 y) underwent DP administration plus handgrip. Group III (DP-TM) of 87 pts (56 M, 31 F, age: 57.6± 7.7) underwent DP administration plus a 2 min step treadmill symptom limited exercise test. One min before the end of the exercise and 4-8 min after the infusion of the DP 111 MBq of Tl-201 was injected and the SPECT study was acquired. During the tests BP, HR, ECG, cardiac and NCSE were noted. The results for each group are as follows:

Group	N	M-HR, %c.	M-S-BP, %c.	M-DP	NCSE
DP	27	100±20 32±17	162±31 -8±14	16984±5145	44%
DP-HG	126	111±21 64±23	191±18 19±21	23362±6247	25%
DP-TM	87	149±19 88±24	180±28 16±22	27430±5583	21%

M, maximum, %c. % change, S,systolic, DP, double product. All the relative comparisons between DP-HG and DP-TM Vs DP are statist. signif. (P<0.5), as well as between DP-TM Vs DP-HG, except M-S-BP and NCSE.

Only 2 pts of the DP-HG group presented M-S-BP above 230 mmHg (240, 260) and 2 pts of the DP-TM group above 220 mmHg (230, 240). No major cardiac complication (Death, MI, Unstable Angina) were observed in any group.

In conclusion both combined protocols for myocardial SPECT scintigraphy in hypertensive pts are safe, increase HR without an elevation in BP, diminish NCSE, consequently, they can be recommended for clinical use.

PS-46

J.E. Roeters van Lennep, E.E. van der Wall, A.H. Zwinderman, E.K.J Pauwels

Leiden University Medical Centre, The Netherlands

NO GENDER BIAS IN REFERRAL FOR CORONARY ANGIOGRAPHY AFTER SPECT TECHNETIUM 99M TETROFOSMIN MYOCARDIAL SCINTIGRAPHY

Objectives: Previous studies have shown a potential gender bias regarding the use of coronary angiography in patients with an abnormal non-invasive test. In the present study we sought to determine whether gender-related differences could be found in referral for coronary angiography in patients who underwent SPECT 99mTc-tetrofosmin stress myocardial perfusion scintigraphy .

Methods: The patient population consisted of 1219 consecutive patients with suspected or known coronary artery disease who underwent nuclear stress testing. For the purpose of the current study we analysed 755 patients (437 men and 318 women) who were suspected for coronary artery disease; 464 patients were excluded because of prior invasive cardiac procedures. Patients with one or more reversible or persistent perfusion defects were considered to have a positive test. The rates of subsequent coronary angiography within 90 days post-testing were determined and separately analysed for men and women.

Results: Baseline characteristics were non-significantly different for age, Quetelet-index, and use of beta-blocking agents. Women had more atypical angina than men (27.7% vs. 41.5%, p<0.01), also the use of pharmacological stress in women and men was different (41.8% vs. 33.9%, p<0.05). Men had significantly more abnormal scintigraphic images than women (60.2% vs. 33.5%, p<0.001). However, within the group of patients with a positive nuclear test, the post-test referral rate for coronary angiography was similar for men and women (17.7% vs. 17.9%, p = NS).

Conclusions: Although there were some gender differences in pre-test referral, no substantial evidence for a gender bias in post-test referral rates to coronary angiography after a positive 99mTc-tetrofosmin stress test could be found. This finding underscores the objective indiscriminate power of myocardial perfusion scintigraphy.

PS-47

S. Roy, A. Lalande, Y. Cottin, F. Guy, C. Touzery, M. Toubeau, P. Walker, P. Louis, J.E. Wolf, F. Brunotte.

Service de Médecine Nucléaire, Centre G.F. Leclerc, Dijon, France.

Service de Cardiologie, CHU Dijon, France.

DOES THALLIUM UPTAKE PREDICTS THE REST FUNCTION OF MYOCARDIAL SEGMENTS ?

The purpose of this study was to evaluate the relation between the thallium uptake after reinjection, which is known to reflect viability, and the myocardial function at rest. Diastolic and systolic wall thicknesses measured by MRI at rest permit to study the contraction of each myocardial segment.

Method : Sixty-one patients, studied after myocardial infarction, underwent stress-redistribution-reinjection ²⁰¹Tl myocardial SPECT. The myocardium was divided into 13 segments and thallium uptake was quantified and expressed as the percentage of activity of segment with maximal uptake. They also underwent MR imaging (1.5 T MR imager) using breath-hold cine MRI. Contiguous short axis slices (thickness of 5 mm) were obtained covering the left ventricle from the base to the apex. End-diastolic (DWT) and end-systolic (SWT) wall thicknesses were measured using the centerline method on each short axis slice. Wall thickening (WTh) was expressed as SWT-DWT, and data were grouped into 13 segments to allow comparison with SPECT data.

Result : The table indicates values of DWT and WTh in groups determined by percentage of thallium uptake at reinjection for the 793 segments.

Tl Reinj	< 50 %	51-60 %	61-70 %	71-80 %	> 80 %
n	61	98	144	160	330
DWT (mm)	6,0 ± 2,4	7,3 ± 3,1	7,5 ± 2,3	8,2 ± 2,5	8,4 ± 2,2
WTh (mm)	0,9 ± 1,2	1,2 ± 1,2	1,8 ± 1,4	2,5 ± 1,8	3,1 ± 2,0

Regarding wall thickening, each class is significantly different from the others except between class <50 % and class 51-60 %.

Conclusion : We showed a relation between thallium uptake at reinjection and myocardial wall thickening at rest. The level of the thallium uptake at reinjection reflects the myocardial contraction at rest.

PS-48

A. Sankaya, G. Altun, A. Altun*, M. Kaya, S. Berkarda

Trakya University Faculty of Medicine Department of Nuclear Medicine and *Cardiology, Edirne, TURKEY.

THE RELATION OF DIPYRIDAMOLE STRESS TEST TC-99M SESTAMIBI LUNG UPTAKE AND MYOCARDIAL ISCHEMIA

The value of lung uptake in exercise Tc99m sestamibi scintigraphy, as a sign of extensive coronary artery disease, was demonstrated using planar imaging. Recently, correlation between Tc-99m sestamibi exercise and resting lung uptake and left ventricular ejection fraction (LVEF) was shown. In pharmacological stress with dipyridamole, the scintigraphic findings may differ from those of treadmill test, due to different stress hemodynamics, tracer kinetics and imaging techniques.

The aim of this study was to determine whether the evaluation of lung to heart ratio (LHR) with dipyridamole stress test (DYP) Tc-99m sestamibi imaging may provide valuable information.

In 91 subjects (53 female, 38 male; age 50.93±11.80 years) about myocardial ischemia underwent DYP Tc-99m sestamibi SPECT for known or suspect CAD. All of the patients were imaged by same-day stress-rest protocol. The lung imaging was started after 20 min after iv 8-10 mCi Tc-99m sestamibi, before the SPECT study. LHR was calculated from anterior planar using 5x5 pixel ROI's drawn in the left lung and the most active area of the heart. The ischemia was examined visually and scored.

DYP LHR values who had normal myocardial perfusion (n=55, LHR= 0.33±0.07) was significantly lower from those of patients with abnormal perfusion (n=36, LHR=0.37±0.03) (p<0.05). The LHR values were correlated with ischemia scores (IS) (r=0.55, p<0.01). The relation between DYP LHR and IS were determined from multivariate regression analysis;

$$DYP LHR = 0.383 + (0.034 \times IS) \quad (R = 0.47, R^2 = 0.22).$$

Dipyridamole Tc-99m sestamibi LHR show good correlation to presence and extend of myocardial ischemia. Dipyridamole stress test Tc-99m sestamibi LHR is valuable for detecting myocardial ischemia as exercise Tc-99m sestamibi LHR.

PS-49

A. Sarikaya, G. Altun, M. Kaya, F. Özçelik, S. Berkarda
Trakya University Faculty of Medicine Department of Nuclear
Medicine and *Cardiology, Edirne, TURKEY.

HEMODYNAMIC INDICES OF MYOCARDIAL FUNCTION CORRELATED WITH Tc-99m MIBI CAVITY-TO-MYOCARDIUM RATIO

The aim of this study was to assess the value of cavity to myocardium ratio (c/m ratio) calculated in resting and dipyridamole (Dyp) Tc 99m sestamibi SPECT images to identify patients with left ventricular dysfunction who had known or suspected coronary artery disease.

In 41 patients (mean age 47.2±13.1 years, 22 male and 19 female) were studied, resting and dyp c/m ratios were calculated from the midventricular short axis slices using 5x5 pixels ROIs drawn in the centre of the cavity and in the most active area of ventricular wall. The resting and Dyp c/m ratio was compared with resting Doppler transmitral flow variables.

The Dyp c/m ratios were correlated left ventricular ejection fraction (LVEF) ($r=0.76$, $p=0.001$), LV ejection time (LVET) ($r=0.45$, $p=0.01$), isovolumic contraction time (IVCT) ($r=-0.45$, $p=0.01$), and Dyp heart rate ($r=0.57$, $p=0.01$). The resting c/m ratios were correlated left ventricular ejection fraction (LVEF) ($r=0.63$, $p=0.001$) and systolic blood pressure ($r=-0.60$, $p=0.001$).

The resting and Dyp Tc 99m sestamibi SPECT c/m ratios show good correlation to hemodynamic indices of resting left ventricular systolic function. The c/m ratios easily obtainable, requires minimal processing time and highly reproducible. Dyp Tc 99m sestamibi SPECT c/m ratio may enable to add supplementary information regarding left ventricular function in addition to perfusion from Tc 99m sestamibi SPECT imaging.

PS-50

M. Schmidt, P. Theissen, J. Crnac *, E. Voth, F. Baer *, H. Schicha

Clinic for Nuclear Medicine and * Medical Clinic III,
University of Cologne, Germany

MAGNETIC RESONANCE IMAGING OF MORPHOLOGICAL AND FUNCTIONAL PARAMETERS OF CORONARY ARTERY DISEASE

With the development of ultrafast gradient echo sequences magnetic resonance imaging (MRI) is able to image coronary arteries. After administration of a contrast agent dynamic MRI allows to characterise myocardial perfusion due to changes in myocardial signal intensity. Patients with angiographically documented coronary artery disease underwent MRI for imaging coronary arteries. Haemodynamic relevance of coronary stenosis were evaluated by MRI perfusion and myocardial scintigraphy.

12 patients (pts) (11 men, 1 woman) with angiographically documented coronary artery disease (stenosis > 70%) were imaged with MRI. A k-space segmented 2D, navigator-controlled pulse sequence was used for imaging coronary arteries. Slice thickness was 5 mm with 1 mm overlap. After administration of a contrast agent a dynamic short axis view of the left ventricle was acquired under dipyridamole stress (0,75 mg/kg body weight) for detection of perfusion defects. All pts underwent myocardial scintigraphy with polar map evaluation.

From 15 angiographically documented stenosis 12 stenosis were haemodynamically significant as proven by myocardial scintigraphy. MRI detected 9 of 15 coronary artery stenosis (sensitivity 60%), six stenosis were missed. From 12 haemodynamically relevant stenosis MRI perfusion demonstrated a regional delayed contrast enhancement in 7 coronary stenosis (sensitivity 58%). Five haemodynamically relevant stenosis did not demonstrate a regional delayed contrast enhancement.

Thus, with the development of ultrafast gradient echo sequences MRI is a potential tool for noninvasive diagnosis of coronary artery disease. It has the potential for combined evaluation of morphology and function in coronary artery disease because this technique allows to image coronary arteries and can measure myocardial perfusion. However, further technical improvements are necessary.

PS-51

M.A. Saidova, E.N.Khodareva, V.V.Kostrova, O.Yu.Atkov, V.B.Sergienko.
Cardiology Research Center, Department of nuclear medicine.

MYOCARDIAL VIABILITY ASSESSED BY THALLIUM REINJECTION AND LOW-DOSE DOBUTAMINE ECHOCARDIOGRAPHY (LDDE) IN PATIENTS WITH SEVERE LEFT VENTRICULAR DYSFUNCTION.

The aim of our study was: 1) to correlate the extent of myocardial perfusion abnormalities with dobutamine-induced contractile reserve evaluated by echocardiography 2) to compare the sensitivity of both tests in identifying viable myocardium in pts with severe left ventricular dysfunction. 31 pts with coronary artery disease & previous myocardial infarction (LVEF 31,4 ± 1,1%) underwent dipyridamole-redistribution-reinjection 201TL-SPECT (Dip-R-RI) and low-dose dobutamine echo (LDDE) (5-10 mkg/kg/min). All studies were analyzed by semiquantitative visual scoring using the same 5-point scale for wall motion & perfusion abnormalities. A 16-segments model was used to compare 201TL Dip-R-RI & LDDE. A wall motion score index (WMSI), global EF and index of perfusion abnormalities (IPA) were derived in each patient. Mild to moderate defects of perfusion (>40% of max. activity or 0-2 points of scale) & reversibility of stress-induced (Dip) perfusion defects on R or RI images for the 201TL-SPECT were defined as a presence of potentially viable myocardium. The results of 201TL-SPECT showed a significant improvement of regional myocardial perfusion on R (37.5%) and RI (50.5%) images compared with DIP abnormal segments (136/277) in 17 pts (I gr) and an absence of any TL reversibility of stress-induced perfusion abnormalities (10/141) in 14 pts (II gr). The all number of viable segments detected by 201TL-SPECT & LDDE was 80% & 60% respectively in the I gr. of pts.: 25% & 19% in the 2 gr. of pts. In the I gr there were significantly higher changes of IPA & global and regional myocardial function after low-dose dobutamine infusion compared with II gr of pts.: I gr - IPA Dip/RI 0,84 ± 0,06 → 0,31 ± 0,03; $p<0,01$; EF rest/LDDE 34,8±1,4% → 53,8± 2,1%, $p<0,01$; WMSI 1,4 ± 0,04 → 1,1 ± 0,08; $p<0,01$; II gr - IPA Dip/RI 1,79 ± 0,06 → 1,6 ± 0,05; $p>0,05$; EF rest/LDDE 27,4 ± 1,5% → 31,1 ± 1,7%, $p>0,05$; WMSI 2,2±0,09 → 2 ± 0,1; $p>0,05$. We revealed strong correlation between WMSI and IPA in both groups (I gr - $r=0,89$, $n=17$; II gr - $r=0,71$, $n=14$). Conclusion: our results demonstrates a good agreement between the extent of myocardial perfusion abnormalities and improvement in the global and regional contractile function after LDD infusion. 201TL-Dip-R-RI is more sensitive than LDDE in identifying of viable myocardium in the patients with severe left ventricular dysfunction.

PS-52

Li Si-Jin, Wang Jin, Zhang Zhong-Zheng, Hu Guang, et al

The First Affiliated Hospital of Shanxi Medical University

QUANTITATIVE EVALUATION OF MYOCARDIAL PERFUSION IMAGING IN PATIENTS WITH ACUTE MYOCARDIAL INFARCTION PRE AND POST THROMBOLYSIS

Purpose: Evaluate the effectiveness of thrombolytic therapy in pts with AMI using SPECT. **Methods:** 21 pts with proven AMI were divided into 3 groups. G1, 13 pts with proven successful thrombolysis; G2, 3 pts with unsuccessful thrombolysis; G3, 5 pts without taking thrombolysis. 925 MBq 99mTc-MIBI was injected in all pts and then the thrombolysis was performed in G1 and G2, the first myocardial SPECT is performed 3.9 ± 2.2h after thrombolysis and the second one 3 days later (6.9 ± 2.9d). For each study, tomograms were divided into 21 segments, and the segment with the maximum counts was taken as 100%. 99mTc-MIBI uptake in all other segments were then expressed as the percentage of this maximum. For quantitative analysis of the SPECT data, a four-point scoring system was used in each myocardial segment, 0=normal, 99mTc-MIBI uptake is ≥ 70%; 1=mild decrease, uptake is 50-69%; 2=moderate decrease, uptake is 30-49%; 3=severe decrease, uptake is <30%. **Results:** Of the 273 segments in G1, 126(46.2%) segments were abnormal and the mean score for each pt was 16.4 ± 8.4 pre thrombolysis, and 82(65%) segments were improved significantly post thrombolysis, and the mean score was 8.9 ± 7.1 ($p<0.01$ vs pre). Of the 63 segments in G2, 39(61.9%) were abnormal and the mean score was 25.7 ± 6.3 ($p<0.05$ vs G1) pre thrombolysis, and only 10(25.6%) segments were improved post thrombolysis, the mean score was 23.3 ± 7.3 ($p>0.05$ vs pre). Of the 105 segments in G3, 52(49.5%) were abnormal and the mean score was 17.6 ± 6.9 ($p>0.05$ vs G1 and G2) at the first SPECT, and only 11(21.1%) segments were improved at the second SPECT, the mean score was 16.6 ± 9.7 ($p>0.05$ vs pre). **Conclusion:** Our results suggested that it had a significant clinical value to assessing the effectiveness of thrombolysis in pts with AMI using this quantitative method of myocardial SPECT.

PS-53

M. Soler, S. Aguadé, J. Castell, J. Llevadot, C. Santana, T. Canela, J. Candell-Riera, D. Ortega.
 Servei de Medicina Nuclear. Servei de Cardiologia. Hospital General Universitari Vall d'Hebron. Barcelona.

GATED-SPET LEFT VENTRICULAR EJECTION FRACTION AND VOLUME MEASUREMENT IN PATIENTS WITH MYOCARDIAL INFARCTION.

Aim: To compare the results of gated-SPET automated EF and volume measurements with echocardiographic (ECHO) and equilibrium radionuclide ventriculography (RNV) values in subacute myocardial infarction patients. **Methods:** We consecutively studied 109 patients (14 women, 56.2 years mean age) admitted with an uncomplicated myocardial infarction during 1997. All of them underwent myocardial perfusion SPET imaging stress/rest protocol and a gated-SPET study in rest acquisition. Automated EF and volumes were quantitated by Germano method and also by ECHO (Simpson) and RNV (Massardo). Technical reasons excluded 10 (9.2%) patients for ECHO evaluation and 10 (9.2%) for gated-SPET: 3 ECG arrhythmia, 3 poor quality imaging, 4 poor endocardial delineation.

Results:	n	EF (%)	EDV (ml)	ESV (ml)	
Gated-SPET	99	47.1 ± 10.3	105.1 ± 35.9	57.1 ± 29.4	
ECHO	99	55.0 ± 11.5	68.8 ± 26.9	31.8 ± 16.7	
RNV	47	52.0 ± 10.4	121.7 ± 43.2	58.4 ± 28.2	
		EF		ESV	
		r	Error	r	Error
Gated-SPET/ECHO		0.735'	5.1	0.581'	8.4
Gated-SPET/RNV		0.796'	6.8	0.851'	13.6
ECHO/RNV		0.735 ^k	7.7	0.529'	10.7
				0.728'	4.9

p < 0.001, * p < 0.002

Conclusion: Good correlation was found between gated-SPET and RNV quantitative values. Suboptimal results were obtained when comparing the ECHO results with both radionuclide methods.

PS-54

A. Teresińska, S.Koniczna, B.Szumilak, E.Gosiewska, J.Potocka
 National Institute of Cardiology, Department of Nuclear Medicine, Warsaw, Poland

RELATION BETWEEN REGIONAL PERFUSION AND VENTRICULAR FUNCTION IN PATIENTS WITH SEVERELY DEPRESSED EJECTION FRACTION

Patients with low left ventricular (LV) ejection fraction (EF) and with regional or global LV dysfunction, considered for myocardial revascularisation, are often submitted to myocardial perfusion study to prove perfusion preserved and to approximate viability. The aim of this work is to evaluate, to what extent SPECT with Tc-99m-MIBI (SPECT-MIBI) additionally differentiates and enlarges the information on LV contractility achieved from radioisotopic ventriculography (RNV).

Sixty-five patients with EF=0.11-0.35 (mean: 0.26±0.06, calculated from RNV) were studied. Planar gated RNV and SPECT-MIBI were performed within 2 months (mean: 15±14 days). RNV, after in vivo red cells labeling with Tc-99m, was recorded in rest in LAO45 and RAO30 views. Global EF and contractility of 5 regions (anterior, posterior, lateral walls, septum and apex) were evaluated. Assessment was performed by means of LV in 'cine' mode, ED and ES outlines and amplitude-phase images. Regional contractility abnormalities were classified as dyskinesia, akinesia and hypokinesia. SPECT-MIBI was performed in rest and stress. Perfusion abnormalities in 5 above mentioned regions was classified as large (intense) or small persistent defects (DEFpers), large or small partially reversible defects (DEFpart-rev), large or small completely reversible defects (DEFrev).

Hypokinesia was detected in 216/325 regions (66%), dyskinesia - in 51 (16%), akinesia - in 34 (10%), normokinesia - in 24 (7%). In dyskinetic regions, there existed large DEFpers (78%) or large DEFpart-rev (22%). In akinetic regions, there also existed large DEFpers (71%) or large DEFpart-rev (29%). In hypokinetic regions, there were no perfusion defects (31% of regions), small DEFpers and DEFrev (19%), large DEF part-rev (22%) and also large DEFpers (28%). In most of normokinetic regions, different types of perfusion defects were observed (large DEFpers existed in 30% of regions). In summary: In dyskinetic and akinetic regions, most often large persistent perfusion defects exist, but in approx. 30% of the regions transient perfusion defects are found. In hypokinetic and normokinetic regions, most often perfusion is normal, slightly persistently decreased or decreased transiently, but in approx. 30% of the regions large persistent defects are found.

In conclusion: In patients with low EF, with dysfunction existing in more than 90% of regions, performance of perfusion study (SPECT-MIBI in rest and stress) allows: 1) to diagnose at least 30% of dyskinetic and akinetic regions with viability preserved; 2) to diagnose up to 30% of hypokinetic and normokinetic regions with high probability of necrosis.

PS-55

A.Teresińska, M.Sliwiński, J.Potocka, B.Szumilak, E.Gosiewska, A.Biederman, Z.Juraszyski, P.Hendzel, L.Chojnowska, S.Koniczna
 National Institute of Cardiology, Warsaw, Poland

CHANGES IN PERFUSION AND IN FUNCTIONAL CAPACITY IN PATIENTS AFTER TRANSMYOCARDIAL LASER (CO₂) REVASCULARISATION

Transmyocardial laser revascularisation (TMLR) is a new surgical procedure for the treatment of otherwise inoperable coronary artery disease. Transmural channels are created by the CO₂ laser in the left ventricle (LV) in an attempt to improve the flow of oxygenated blood into the ischemic tissue. The possible mechanism for the symptomatic improvement after TMLR is the stimulation of angiogenesis with regional perf [perf] augmentation. The goal of this work was to analyse the impact of TMLR on myocardial perf and on functional capacity during first 6 months after operation.

Twenty-seven pts (3F, 24M; age range 38-73y, mean 59y) were studied with Tc-99m-MIBI SPECT in rest and stress, including 15 pts after one myocardial infarction [MI], 6 after two and 2 after three MI. Perf studies were performed before TMLR [Study-0], in the earliest possible (from clinical point of view) term after TMLR [Study-I], 3 mo after TMLR [Study-II] and 6 mo after TMLR [Study-III]. Besides Study-0, all the pts had Study-I, 24 pts had Study-I and -II, and 20 pts had Study-I, -II and -III.

Perf was evaluated in 17 segments [seg] of the LV. Four septal seg were excluded from comparisons, as the seg not treated by laser, it was assumed that all the other seg - if with transient perfusion defects (DEFtrans) - were submitted to lesser therapy. Only perf changes in seg with DEFtrans are presented. Perf improvement [improv] in the patient (always in comparison to Study-0) was stated if it was perf improv in at least one seg and it was no perf deterioration.

In Study-0, 2 pts had persistent defects only; in 25 pts left there were 164 seg with DEFtrans. In Study-I, in 10/25 (40%) pts perf improv was diagnosed; in 27% of DEFtrans perf improved, in 54% did not change, and in 18% deteriorated. In Study-II, in 11/22 (50%) pts perf improv was diagnosed; in 36% of DEFtrans perf improved, in 49% did not change, and in 15% deteriorated. In Study-III, in 8/18 (44%) pts perf improv was diagnosed; in 36% of DEFtrans perf improved, in 48% did not change, and in 17% deteriorated. There was no significant difference among the results of the post-TMLR perf studies.

Angina was the end-point of exercise test (during stress perfusion study) in 56% of pts in Study-0, in 30% in Study-I, in 42% in Study-II and in 40% in Study-III (NS). Functional capacity, measured by rate-pressure product increment between rest and stress, presented systematic growth tendency between Study-0 and Study-III (from 7393 to 9632, NS). Work activity measured in METs showed similar tendency (from 6.3 to 7.7, NS).

Conclusions: During first 6 months after TMLR, postoperative perf improvement is observed in 40-50% of pts. In seg with DEFtrans, perf improves in 27-36% of seg, perf does not change in 48-54% of seg, and perf deteriorates in 15-18% of seg. No significant difference in mean perfusion results between the earliest post-TMLR study (approx. 4 weeks) and the later studies is observed. Functional capacity shows systematic growth tendency in this period of observation in comparison to pre-operative state.

PS-56

^{1,2}A.Kapur, ^{1,2}K.A.Latus, ¹G.Davies, ²PH.Jarritt, ¹MC.Young, ¹G.Roussakis, ²PJ.Elli, ¹SR.Underwood, on behalf of the ROBUST Study Group ¹Royal Brompton Hospital, Department of Nuclear Medicine, and ²University College School of Medicine, Institute of Nuclear Medicine, London, UK

THE ROBUST STUDY: A RANDOMISED COMPARISON OF THREE TRACERS FOR MYOCARDIAL PERFUSION SCINTIGRAPHY

Three tracers of myocardial perfusion and viability are available commercially: thallium-201 (Tl), ^{99m}Tc-MIBI (MIBI), ^{99m}Tc-tetrofosmin (Tf). There are no large studies available to guide the selection of tracer for routine use.

We have randomised 2540 patients to receive one of the three tracers during routine clinical myocardial perfusion imaging (MPI). At the time of abstract submission, data had been analysed from 1503 patients. A one day stress/rest protocol was used for MIBI and Tf with ECG gating in a subset of patients. Tomograms were scored visually in 17 segments and defects were quantified from a polar plot. Quality and artefact scores were assigned (0 to 3), and ratios of heart (H), liver (L), sub-diaphragmatic (S) and lung activity were measured.

The groups were similar in terms of risk factors for coronary artery disease, reason for referral, and proportion of abnormal studies (Tl 63%, MIBI 59%, Tf 61%, χ^2 P=NS). Mean quality scores were 2.12, 2.28, 2.33 (P<0.001 between Tc and Tl). For attenuation artefact MIBI=Tf<Tl (P<0.05) and for low count artefact Tf<MIBI<Tl (P<0.001). For H/S, Tl>MIBI=Tf, for H/L Tl>Tf>MIBI, and for H/Lung Tf>Tl=MIBI (max P<0.02). Stress defects in the abnormal scans were more severe for thallium than for the other tracers (mean summed score out of 68 = 51.5 [Tl], 54.7 [MIBI], 55.2 [Tf], P<0.01), but mean rest scores were similar (57.7, 59.1, 58.5, P=NS).

We conclude that there are technical differences between all the tracers. They all perform well in clinical terms, but overall image quality is superior using technetium.

Poster presentations

PS-57

S. Atavci, M.Ünlü, M.T Kitapçı, T. Atasever, A. Çengel, L. Gökğöz
Gazi University, Medical Faculty, Departments of Nuclear
Medicine, Cardiology and Cardiovascular Surgery, ANKARA

REVERSE REDISTRIBUTION PATTERN OF 201THALLIUM IN REST-REDISTRIBUTION MYOCARDIAL PERFUSION SPECT AS A SIGN OF AREA AT RISK IN CHRONIC CAD PATIENTS WITH PREVIOUS MI.

The aim of the study was to investigate the role of rest-redistribution 201Tl SPECT study perfusion patterns in the determination of area at risk in infarct related and other stenosed coronary artery areas in chronic CAD patients with previous MI. A total of 35 chronic CAD patients (29 male, 6 female; mean age: 61 ± 7.4 , with EFr lower than 40%) were included to the study. All patients had coronary angiography (CA) within a month. Following the iv. injection of 111 MBq of 201Tl, at 15 min. and 3 hours rest-redistribution SPECT study was performed. Infarct area to total myocardium ratio (I/T) was quantified. 201Tl perfusion patterns were classified as reversible defect (RD: >10% of improvement in redistribution), irreversible defect (IR: no change) and reverse redistribution (RR: >10% of worsening in redistribution). According to CA results, 16 patients had single vessel (13: LAD, 3: LCX), 14 two vessel (LAD: 11, LCX: 7, RCA: 10) and 5 multivessel disease. In 24 coronary arteries (LAD: 4, LCX: 10, RCA: 10) stenosis was not related with the infarction. There was a significant difference between rest I/T $25 \pm 12\%$ and redistribution I/T: $36 \pm 18\%$, $p < .05$. Mean value of perfusion worsening in infarct area as a sign of RR was $11.8 \pm 4.2\%$. In infarct area; 70% RR, 19% RD and 11% IR perfusion patterns were observed. 83% of the patients who had worsening of the perfusion in infarct area had greater than 90% of stenosis in infarct related artery. In 24 non-infarction related coronary artery stenosis 60% RD and 40% RR perfusion pattern was observed. In conclusion, RR pattern that was observed in rest-redistribution 201Tl myocardial perfusion SPECT studies, as a sign of area at risk in chronic CAD patients after MI, could be frequently detected in infarct related or other stenosed coronary artery vessel territories and it is strongly correlated with the degree of stenosis in multivessel CAD patients.

PS-58

P.Véra¹, A.Manrique^{1,2}, V.Pontvianne¹, A.Hitze¹, R.Koning², A.Cribrier²

Nuclear Medicine¹, Cardiology², University Hospital, Rouen, France

THALLIUM GATED SPECT IN PATIENTS WITH LARGE MYOCARDIAL INFARCTION : COMPARISON WITH EQUILIBRIUM RADIONUCLIDE IMAGING AND LEFT VENTRICULOGRAPHY, EFFECT OF FILTERING AND ZOOMING.

Effect of filtering and zooming on thallium 201 gated SPECT was evaluated in patients with major myocardial infarction.

Methods. Rest thallium gated SPECT was performed on a 90° dual-detector camera (DST-XL, SMVi; 120 sec/proj), 4 hours after injection of thallium 201 (185 MBq) in 32 patients (61 ± 11 years) with large myocardial infarction ($33 \pm 17\%$ defect on bull's eye). End diastole (EDV), end systole (ESV) volumes and LVEF were calculated using a commercially available semi-automatic validated software (SMVi, Vision 4.1.0, Multidim™). First, images were reconstructed using a 2.5 zoom, a Butterworth filter (order = 5), and 6 Nyquist cut-off frequencies: 0.13 (B5.13), 0.15 (B5.15), 0.20 (B5.20), 0.25 (B5.25), 0.30 (B5.30), 0.35 (B5.35). Second, images were reconstructed using a zoom of 1 and a Butterworth filter [(order = 5, cut-off frequency 0.20 (B5.20Z1)] (total = $32 \times 7 = 224$ reconstructions). LVEF was calculated in all patients using equilibrium radionuclide angiography (ERNA). EDV, ESV and LVEF were measured with contrast left ventriculography (LVG).

Results. LVEF was $39 \pm 10\%$ for ERNA and $40 \pm 13\%$ for LVG ($p = NS$). With B5.20, gated SPECT LVEF was similar ($39 \pm 11\%$) and correlated with ERNA ($r = 0.87$) and LVG ($r = 0.70$). Correlation coefficients between ERNA or LVG LVEF, and gated SPECT ranged from 0.26 to 0.88. Correlation coefficients between LVG and gated SPECT volumes ranged from 0.87 to 0.94. There was a significant effect of filtering and zooming on EDV, ESV and LVEF ($p < 0.0001$). Low cut-off frequency (B5.13) overestimated LVEF ($p < 0.0001$ vs ERNA and LVG). Gated SPECT with 2.5 zoom and high cut-off frequencies (B5.15, B5.20, B5.25, B5.30, B5.35) overestimated EDV and ESV ($p \leq 0.04$) compared to LVG. Zoom of 1 underestimated EDV, ESV and LVEF compared to 2.5 zoom ($p \leq 0.02$). **Conclusion.** Accurate LVEF measurement is possible with thallium gated SPECT in patients with major myocardial infarction. However, filtering and zooming greatly influence EDV, ESV and LVEF measurements.

PS-59

S. Watanabe, H. Matsuo, K. Watanabe, K. Suzuki, A. Goto, M. Arai*
Y. Uno*, H. Takatsu*, M. Ishiguro**

The Division of Cardiology, Gifu Prefectural Hospital, Gifu. *The 2nd Department of Internal Medicine, Gifu University School of Medicine. **The Department of Internal Medicine, Hirano General Hospital. JAPAN

IS ST RE-ELEVATION JUST AFTER REPERFUSION A SIGN OF MYOCARDIAL REPERFUSION INJURY ?

Objective; To evaluate the clinical value of ST re-elevation in terms of myocardial salvage effect by reperfusion therapy .

Method; 55 consecutive patients with anteroseptal AMI with TIMI 0 or 1 flow, who were subsequently treated with acute interventional therapy, underwent quantitative evaluation of area at risk (AAR) and infarct size (IZ) by 99mTc-tetrofosmin (TF) SPECT. Pts were divided into 3 groups according to the presence or absence of ST re-elevation just after successful reperfusion and patients with no reperfusion. **Result;** Pts with successful reperfusion resulted in greater myocardial salvage than unsuccessful group regardless of the presence or absence of ST re-elevation. Interestingly, the patients without ST re-elevation showed larger amount of myocardium salvaged than the patients with ST re-elevation (ST \rightarrow : $62.4 \pm 28.1\%$. ST \uparrow : $30.3 \pm 21.1\%$. no reperfusion: $0.0 \pm 43.1\%$, $p < 0.01$).

Conclusion; ST re-elevation can be regarded as indirect evidence of myocardial cell damage caused by reperfusion.

PS-60

M. Watanabe, K. Gotoh, K. Nagashima, Y. Uno, T. Noda, K. Nishigaki, M. Takemura, M. Kanoh, N. Yasuda, S. Minatoguchi, H. Fujiwara
Second Department of Internal Medicine, Gifu University School of Medicine

COMPARISON WITH THALLIUM-201 MYOCARDIAL SPECT AND ENDOMYOCARDIAL BIOPSY IN DILATED CARDIOMYOPATHY

The purpose of this study was to compare between thallium-201 myocardial SPECT, endomyocardial biopsy and contrast left ventriculography in dilated cardiomyopathy (DCM).

Methods: Eleven patients with DCM (mean age 55 ± 13 years, 8 men, 3 women) were studied. Early image was obtained 10 min. after thallium (111MBq) injection and delayed image was obtained 2 hours after injection at rest. Each Bull's eye map was made by using short axis image composed again from early image and delayed image. The followings were calculated from them. 1. Washout rate (WR). 2. The mean counts per pixel (M). 3. The standard deviation of the counts per pixel (SD). SD/M was calculated as an index of heterogeneity. In endocardial biopsied specimen the degree of the fibrosis were assessed histologically i.e., 0 = normal, 1 = mild, 2 = middle, 3 = severe. And the diameter of myocyte was measured. Ejection fraction (EF) and end diastolic volume index (EDVI) were obtained from contrast left ventriculography. **Results:** There was a close correlation between the followings. 1. Fibrosis and WR ($r = -0.784$, $p < 0.01$). 2. Diameter of myocyte and EF ($r = -0.617$, $p < 0.05$). 3. SD/M of the delayed image and EF ($r = -0.791$, $p < 0.01$) 4. SD/M of the delayed image and EDVI ($r = -0.785$, $p < 0.01$) The WR decreased as the fibrosis of myocardium increased. Diameter of myocyte increased as EF decreased, suggesting the compensative hypertrophy of myocyte. The degree of heterogeneity of the thallium increased the dilation of the left ventricle and the decline of EF. **Conclusion:** It is suggested that WR reflects the myocardial fibrosis, and SD/M is a good indication of myocardial injury in patients with DCM.

PS-61

H.WU, Z.Q.HU, S.YU, J.ZHOU, M.ZHAO, J.HU, Z.Q.XUANYU.

Department of Nuclear Medicine, Tongji Hospital, Tongji Medical University, China

^{99m}Tc-MIBI MYOCARDIAL SPECT IN THE ASSESSMENT OF PERCUTANEOUS TRANSLUMINAL CORONARY ANGIOPLASTY (PTCA).

The purpose of this study was to evaluate the role of cardiac SPECT in the assessment of PTCA. **Methods:** The subjects included 18 patients with severe coronary artery disease who were diagnosed by coronary angiography. Totally 29 vessels were revealed with occluded lesions. There were 12 of the patients with myocardial infarction. All patients underwent repeated exercise/rest ^{99m}Tc-MIBI SPECT before and one month after PTCA. 3 cases received the third scan 6 months after PTCA. Qualitative and quantitative analyses were used to assess the scan data from pre- and post-PTCA. **RESULTS:** Twenty-two out of 29 diseased vessels were successfully dilated with average diameter from 84.14±9.64% preoperatively to 31.14± 9.39% postoperatively. At dilated vessels allocated territory, perfusion was improved in 91.2% (31/34) of those segments with reversible defects on pre-PTCA scan. 20% of the segments with irreversible defects on pre-PTCA scan showed perfusion improvement. However, none of these segments with uptake ratio < 30% showed perfusion improvement after successful PTCA. In 8 cases with multivessel lesions, incomplete revascularization were carried out on 6 of them. Of these 6 patients only one case whose major perfusion defect related vessel failed to be revascularized did not show scintigraphic and symptomatic improvement after PTCA, although the other stenosed branch was dilated. In 3 cases who underwent 3 times of scintigraphy, one with worse segmental perfusion on the third scan was proved with vascular restenosis. **CONCLUSION:** Exercise/rest ^{99m}Tc-MIBI SPECT, combining with qualitative and quantitative analysis, may be very valuable in assessing the effects and monitoring vascular restenosis after PTCA. It also may be helpful in selecting the patients who may benefit from coronary revascularization. For cases with multivessel lesions, SPECT imaging may define the "prime criminal vessel" on which revascularization is indicated.

PS-62

D.C.Yang, K.Kulkarni, J.Kalani, M.Makan, M.K.Das, A.Reddy, R.Steiner

NY Methodist Hospital, Division of Nuclear Medicine, Department of Radiology and Division of Cardiology, Department of Medicine

STRESS MYOCARDIAL PERFUSION STUDY WITH SIMULTANEOUS DUAL ISOTOPE IMAGING TECHNIQUE AND GATED SPECT STUDY: A NEW PROTOCOL

PURPOSE: We are introducing a new protocol combining simultaneous dual isotope imaging technique (SDII) devised by the author (Yang et al) and gated SPECT technique for performing stress myocardial perfusion study.

PROTOCOL: At the peak of exercise or pharmacological stress, 15 mCi (555 MBq) Tc 99m-Sestamibi or Tetrofosmin is injected intravenously. 30 minutes later gated SPECT study is performed. If the results are normal, the study is terminated. If perfusion defects are seen, 3.5 mCi (130 MBq) of Tl-201 is given intravenously and simultaneous dual isotope myocardial perfusion images are obtained. If reperfusion is seen in the areas of perfusion defects, diagnosis of reversible myocardial ischemia is established and the study is terminated. If the defect is fixed, delayed 4 hour or 24 hour redistribution thallium images are obtained after reinjection of 1 mCi (37 MBq) of Tl-201. If wall motion study and LVEF are normal on gated SPECT, the findings favor soft tissue attenuation. If wall motion abnormality is noted on gated SPECT images in addition to the persistent fixed defect on delayed perfusion images, a diagnosis of MI is considered. **RESULTS:** We have performed 256 cases (124M & 132F, Age 41-87yrs) from July 1997 to February 1998. Ninety eight cases (38%) were negative and required only gated SPECT study, and most of them were completed in 1 hour. 158 cases (62%) had fixed perfusion defects and required SDII technique and the procedure was over in 2 hours. 14 cases (5%) required delayed redistribution thallium images. Initial correlation of 32 available coronary angiography results revealed 2 cases were false positive, 1 was false negative, 4 were true negatives and 25 were true positives. The overall accuracy of the procedure is 91%.

CONCLUSION: This protocol is accurate, time saving and 38 % of all cases can be completed in one hour and 95% within 2 hours. Gated SPECT study provides wall motion and LV functional information and at the same time it also helps to reduce false positives resulting from soft tissue attenuation. SDII technique allows precise alignment of the stress and rest images for comparison. The protocol offers the advantage of Technetium resolution and Thallium viability and avoids the pitfalls of other existing protocols.

PS-63

S.Zhang, W. Guo, L. Li, L. Wang, C. Zhang, S. Li

Hospital: First Hospital, Shanxi Medical University, Taiyuan, P. R. China.

LEFT VENTRICULAR SIZE OF EARLY ACUTE MYOCARDIAL INFARCTION ASSESSED BY SERIAL GATED SPECT.

The purpose of the present study was to assess the left ventricular size of AMI by serial gated SPECT(GSPECT). A serial myocardial perfusion imaging with Tc-99m MIBI was performed and end diastolic volume (EDV), end systolic volume(ESV), and stroke volume(SV) were collected at admission, one week and two weeks after onset of AMI in 15 patient(pts). In 11 normal controls, EDV, ESV, and SV were 74.7±12.2ml, 23.5±5.8ml, 49.5±8.4ml. In 15 pts with AMI, the EDV, ESV and SV at admission were 101.7±3.1ml, 59.1±27.4ml, 46.0±17.0ml. EDV at admission, one and two weeks later for 11 pts received urokinase were 108.8±30.5ml, 97.2±19.7ml, 91.6±16.6ml respectively. Among the 11 pts with AMI treated with urokinase, 7 of them were reperfused based on clinical data. EDV of 7 pts with nonperfused or without receiving thrombolytic therapy unchanged or enlarged during this period. ESV enlarged with increasing of EDV in all pts. SV did not change significantly, although EDV and ESV enlarged in all pts. The result suggests that left ventricular dilatation may be detectable in early AMI, thrombolytic therapy could prevent or attenuate this process.

Cardiovascular: FDG

PS-64

D. Agostini¹, O. Citerne², M. Hamon², G. Grollier², JC Potier², G. Bouvard¹

Departments of Nuclear Medecine¹ and CYCERON-CEA, Cardiologie², CHU de Caen, France.

IMPAIRMENT OF MYOCARDIAL GLUCOSE METABOLISM BY ¹⁸FDG AND PET IN PATIENTS WITH INFARCTION AND NORMAL CORONARY ARTERIES.

Positron emission tomography (PET) metabolic studies have investigated the pathways involved in glucose metabolisms and the impairments which occur in myocardial infarction (MI) with coronary arteries lesions. The purpose of the study was to assess myocardial metabolic glucose rate (MMGR) in patients with MI and normal epicardial coronary arteries. **Methods.** We selected 10 pts (age : 49±9 yrs old) with anterior MI based upon chest pain, ECG and CPKMB abnormalities and normal epicardial coronary arteries on the angiogram. No coronary spasm was detected and no biological abnormalities were found. All patients underwent dipyridamole-rest Tl201-SPECT imaging. LVEF was evaluated by radionuclide imaging. Each pt received a glucose load of 50 g before PET (TTVO3-LETI). After transmission scanning with ⁶⁸Ge, a bolus of 185 MBq of ¹⁸FDG was intravenously injected. Data were reconstructed with the following image frame sequences: 10x1,4x5,3x10 min. For each pt, 5 regions of interest (ROI) were drawn on the LV (anterior, septal, lateral, apical) and LV cavity. Logan-Patlak graphical analysis was applied to the myocardium (three-compartment) time-activity data for all the ROIs. 201Tl-SPECT data showed 5 fixed, 3 reversible defects and 2 normal myocardial perfusion in infarcted regions. LVEF was significantly low 49±6%. PET data showed severe reduction of MMGR (.31±.21 vs .58±.14 μmol/min/g) in infarcted regions when compared with lateral control region. **In conclusion,** these data show that using FDG and PET, MMGR rate is impaired in the infarcted zone in spite of heterogeneity of perfusion in pts with MI and normal coronary arteries.

PS-65

A. Hertel, A. Niesen, W.T. Kranert, R.P. Baum, M. Osterloh, C. Psallas, R. Aljazzar, S. Adams, G. Hör
Department Nuclear Medicine, Universitätsklinik der Johann Wolfgang Goethe-Universität Frankfurt/Main, FRG

COMPARISON OF DUAL HEAD COINCIDENCE GAMMA CAMERA FDG IMAGING WITH A RING-PET TOMOGRAPH IN ONCOLOGY AND NEUROLOGY - FIRST RESULTS

We report about comparative studies in oncologic and neurologic patients undergoing coincidence gamma camera FDG imaging and immediately afterwards imaging with a PET ring-tomograph in order to assess the performance of FDG imaging on a gamma camera compared to a PET tomograph set as gold standard. These results are the first ever reported on the newly PET-designated SMV dual head camera which is also routinely used for SPECT.

Methods: 22 patients underwent a one day protocol. First a mean 35.8 MBq (24-46 MBq) of F-18 FDG was injected and after a mean 58 min (oncology 64 min, neurology 43 min) Coincidence FDG imaging on a dual head gamma camera (Sopha Medical Vision, Frankfurt,FRG) equipped with a half inch Nal collimator and a 54 cm axial FOV was performed. Immediately afterwards, additional F-18 FDG was injected to achieve a mean of 354 MBq for all patients (206 MBq in neurologic and 397 MBq in oncologic patients) for conventional PET imaging (Siemens ECAT Exact 47). 17 patients were studied for evaluation of suspected or known malignancies (primaries 9, recurrences 8) and 5 patients were evaluated for Alzheimers disease.

Results: In oncology 5 patients did not show any hypermetabolic lesions in FDG PET. The other 12 demonstrated 20 lesions (1-6) ranging from 0.7 to 8.5 cm, mean 2.9 cm). 12 lesions were larger than 1 cm and 8 lesions were smaller or equal than 1 cm (ECAT 47 imaging). In Coincidence gamma camera imaging 10/12 lesions larger 1 cm and 3/8 lesion smaller or equal 1 cm were positive. In neurology 1 patient had a normal and 4 a typical Alzheimer brain metabolic pattern. All 5 had comparable patterns, still less pronounced in coincidence gamma camera imaging. Under current conditions (3D imaging, iterative reconstruction) coincidence FDG imaging should be considered for future applications on oncologic lesions larger than 1.5 cm and in neurology for evaluation of dementia.

PS-66

W.S. Richter, R. Aurisch, S. Fischer, D.L. Munz
Clinic for Nuclear Medicine, Charité, Humboldt University Berlin, Germany

MYOCARDIAL F-18 FDG UPTAKE: EFFECT OF ACIPIMOX IN ADDITION TO ORAL GLUCOSE LOADING

The lipid lowering substance acipimox has been introduced for effective stimulation of myocardial glucose uptake in F-18 FDG studies. The aim of this investigation was (1) to examine whether acipimox given in addition to 50g glucose can further increase myocardial F-18 FDG uptake, and (2) to identify parameters which are correlated with a high myocardial glucose uptake.

Methods: 78 patients with coronary artery disease were studied (66m, 12f; age, 58±17 y; LVEF, 34±15%). 60 min before F-18 FDG injection, 48/78 patients received 500 mg acipimox in addition to 50 g glucose for stimulation of myocardial glucose uptake, the remaining 30 patients received 50 g glucose only. Blood samples were obtained 60, 30, and 5 min before as well as 60 min after injection of F-18 FDG for laboratory investigations (glucose, cholesterol, triglycerides, insulin, HbA1c). Myocardial glucose uptake was assessed as heart-to-lung ratio (HLR) from planar views (Siemens MultiSPECT 2).

Results: Bivariate correlations between the HLR and laboratory parameters were obtained for plasma glucose concentrations with coefficients between $r=-.34$ and $r=-.42$ for the different samples ($p<0.05$) and the HbA1c value ($r=-.44$; $p<0.05$). In a linear regression model, only the HbA1c value was an independent predictor of myocardial glucose uptake ($R^2=0.16$). The HLR was not different between the groups with and without acipimox.

Conclusions: Adding acipimox to oral glucose loading does not further enhance myocardial glucose uptake. With the parameters tested, the stimulation of myocardial glucose uptake can only be imperfectly predicted. A good long-term control of glucose metabolism (low HbA1c value) was correlated with a higher myocardial F-18 FDG uptake.

PS-67

O. Satake, K. Masuyama, N. Takekoshi, S. Matsui, H.Tsugawa, S. Kanemitsu, M. Kitayama, J. Sanma, T. Yamagata, E. Murakami.
Department of Cardiology, Kanazawa Medical University, Uchinada, Japan

THE CHARACTERISTICS OF MICROVASCULAR SYNDROME (SYNDROME X) BY CARDIAC PET, 201TI-SPECT AND MYOCARDIAL BIOPSY

[Purpose] To evaluate the pathophysiological characteristics of microvascular angina, we studied the patients with Syndrome X by using cardiac PET, 201TI-SPECT and myocardial biopsy.

[Subjects and methods] Eight patients (3 men and 5 women, mean age 57 years) with Syndrome X were studied. They had typical or atypical chest pain and exercise-induced ST depression (particular II, III, aVF, V3-6) with angiographically normal coronary arteries without acetylcholine or ergonovine-induced vasospasm. In all patients, 201TI, FDG-PET and myocardial biopsy were procedured to investigate the ischemic change with a viability and histopathological findings.

[Results] Five of eight patients (63%) showed hypoperfusion area by 201TI-SPECT and all patients had a ischemic but viable pattern by 18FDG-PET. In the biopsied samples, the luminal narrowing of the intramural small arteries was found in most cases by light microscopic observations.

[Conclusions] It is suggested that Syndrome X may be a microvascular ischemic disease by cardiac imaging and histological characteristics.

PS-68

T. Schumacher, I. Brink, T. Krause, E. Nitzsche, E. Moser

Department of Nuclear Medicine, Albert-Ludwig-University, Freiburg, Germany

MYOCARDIAL VIABILITY IN PATIENTS WITH LOW LEFT VENTRICULAR EJECTION FRACTION (LVEF)

Introduction: The knowledge of myocardial viability preceding coronary bypass grafting is of great importance especially in patients with low LVEF to avoid revascularization of scarred myocardial areas and to reduce perioperative mortality. This study was performed to determine, whether mismatch patterns are found in at least five anatomical segments (more than 20% of left ventricular mass) especially in patients with end-stage heart disease.

Methods: 60 patients (mean age 64 years) were investigated prior to coronary revascularization with Hybrid-PET (99m-Tc-MIBI-SPECT (stress/rest) and 18-FDG-PET) to confirm ischaemia, match (M) and mismatch (MM) patterns. The images of the myocardium were divided into 20 anatomical segments. Analysis was performed by three independent investigators, PET-results were correlated with angiographic and echocardiographic findings.

Results: 20 patients showed a severe low cardiac output syndrome with a LVEF $\leq 30\%$ (av. 23.3 %). Beside ischaemia, MM-myocardium was found in 11 patients in an average of 7.3 segments (range 4-12). In 23 of 40 patients with better left-ventricular function (EF avg. 50%, range 35-80%) hibernating myocardium was found in an average of 6.3 segments (range 2-13)($p=n. s.$).

Four patients (7%) died perioperatively, three with preoperative low LVEF. In all of them, preoperative FDG-PET showed complete viability in all eligible bypass-regions.

Conclusions: Patients with severely decreased LVEF show a high percentage of hibernating myocardium (up to 60% of left ventricular mass) and thus could benefit from revascularization functionally. However, this patient group shows an increased risk of perioperative mortality.

Cardiovascular: Pharmacokinetics and metabolism

PS-69

Bönisch H*, Dutschka K#, Farahati J§

Departments of Pharmacology University of Bonn*, Nuklearmedizin University of Essen# and Nuklearmedizin University of Würzburg§

EVALUATION OF K_M AND V_{MAX} OF MIBG TRANSPORT FOR SK-N-SH NEUROBLASTOMA CELLS.

Introduction and Methods. The affinity and maximal transport rate of I-125-mIBG (mIBG) was compared to H-3-Norepinephrine (NE) for SK-N-SH Neuroblastoma cells. MIBG was synthesized by Cu(I)-assisted, non-isotopic exchange with a specific activity of 2.1 Ci/ μ mol and chemical purity of >99%. NE was purchased from NEM-Dupont and SK-N-SH cells from ATCC. Cells were cultured on tissue culture dishes in minimum essential medium supplemented with 10% fetal calf serum. Uptake of radiolabeled mIBG or NE was determined in HEPES-buffered Krebs-Ringer solution. Finally cells were washed three times with ice-cold buffer and thereafter solubilized in 0.3 M NaOH (mIBG-uptake) or 0.1% Triton (NE uptake). Radioactivity was counted either in a gamma counter (mIBG) or in a liquid scintillation counter (NE). The Lowry method was used to determine protein content of the culture dishes. A time course for uptake and accumulation of 0.1 nM mIBG in SK-N-SH cells was determined in the absence (total uptake) and presence (nonspecific uptake) of 10 μ M nisoxetine. Specific uptake was subtracted from total uptake to determine the specific uptake. In order to evaluate the K_m and V_{max} of specific mIBG transport, 1-min uptake rates were determined in SK-N-SH cells incubated with various concentrations of mIBG (0.1-10 μ M). In a parallel series of experiments, K_m and V_{max} values for uptake of NE (0.03-10 μ M) were measured under identical conditions but in the presence of inhibitors of NE metabolizing enzymes 10 μ M U-0521 (COMT+1 μ M Pargiline). Values for three independent experiments carried out in duplicates are expressed as mean values \pm SEM. **Results.** Rate of specific (nisoxetine-sensitive) uptake remained constant for about 2 min and declined thereafter, i.e. specific intracellular accumulation tended to approach a steady state which, however, was not yet reached within 60 min. From the 1st to the 60th min specific accumulation of mIBG increased by a factor of 20 \pm 1.2, whereas non-specific accumulation increased only by a factor of 2.4 \pm 0.1. 95% of total cellular mIBG accumulation after 60 min was due to specific uptake. Initial rates (1 min) of specific uptake of mIBG or NE in SK-N-SH cells at various substrate concentrations revealed K_m values of 1.6 \pm 0.8 and 1.0 \pm 0.2 μ M, respectively. **Conclusions.** mIBG is transported into the neuroblastoma cells by the nisoxetine-sensitive NE transporter and accumulates in these cells. Transport (determined as initial rates of uptake) of mIBG exhibits about the same affinity for the transporter as NE and the maximum rate of specific uptake is even higher than that of NE.

PS-70

T.Hashizume, M. Gouda, K. Maeda, H. Yamahata, Y. Hayashi, Y. Sakai, S. Hayashi, K. Moriwaki
National Minamiwakayama Hospital, Department of Cardiology and Neurosurgery, Tanabe, Wakayama, JAPAN

ASSESSMENT OF MYOCARDIAL FATTY ACID UPTAKE IN PATIENTS WITH HYPERTENSIVE INTRACRANIAL HEMORRHAGE USING IODINE-123-BMIPP

An evaluation of myocardial fatty acid metabolism in hypertensive patients with major complication has not been previously established. To assess the myocardial fatty acid metabolism in hypertensive patients with intracranial hemorrhage(IH), we performed myocardial image using ¹²³I-15-p-iodophenyl-3-methyl pentadecanoic acid(BMIPP). Fourteen hypertensive patients with IH(Group I;n=14, age 62 \pm 11yrs) and 25 hypertensive patients without IH(Group II;n=25, age 65 \pm 12yrs) were studied. All patients had no history of coronary artery disease. A dose of 111Mq of BMIPP was injected intravenously at rest, and a myocardial image was recorded 30 minutes after the injection. Myocardial perfusion image using ²⁰¹Thallium(Tl) was also performed within 2 weeks after BMIPP study. The regional myocardial uptakes of BMIPP and Tl were visually assessed in 17 segments with a four-point scoring system (0=absent to 3=normal uptake). Cardiac hypertrophy was evaluated by electrocardiography(ECG) and two-dimensional echocardiography. IH volume was calculated by computed tomography. Results: Tl score BMIPP score LVMI sV1+RV5(ECG) IH volume

	(points)	(points)	(g/m ²)	(mm)	(ml)
Group I	43 \pm 5	35 \pm 9*	170 \pm 92	3.4 \pm 2.6	14 \pm 7
Group II	46 \pm 4	43 \pm 4	130 \pm 31	3.1 \pm 0.9	---

LVMI : left ventricular mass index *:p<0.005

Conclusion: These results suggest that hypertensive patients with IH have a more impaired myocardial fatty acid metabolism compared to the hypertensive patients with similar cardiac hypertrophy. BMIPP imaging in hypertensive patients might be useful to evaluate the severity of myocardial fatty acid metabolism.

PS-71

Y. Ishino, H. Nakata.

University of Occupational and Environmental Health, Kitakyushu, Japan.

QUANTITATIVE EVALUATION OF SEVERITY OF THE ISCHEMIC HEART DISEASE USING 123I-BMIPP SPECT.

There are many reports about the usefulness of myocardial SPECT using 123I-BMIPP for the evaluation of the ischemic heart disease (IHD). But few evaluate the clinical significance of BMIPP SPECT in comparison to the result of coronary arteriography (CAG). The purpose of this study is to quantitatively compare BMIPP SPECT and Tl SPECT (at stress and rest) to the result of CAG on 62 patients with IHD. For relative quantification, each SPECT image was segmented in 23 and defect scores were classified into four grades (0:normal, 1:mild low uptake, 2:severe low uptake, 3:defect). Severity of coronary artery disease was evaluated using coronary severity score by Gensini (G-score).

The results are shown below (correlation between SPECT and G-score):

		BMIPP	Tl(stress)	Tl(rest)
Angina (n=15)	R	0.66	0.51	0.49
	P	<0.01	ns	ns
Infarction (n=47)	R	0.62	0.51	0.53
	P	<0.0001	<0.001	<0.0001
Total (n=62)	R	0.53	0.47	0.44
	P	<0.0001	<0.001	<0.001

BMIPP defect score was correlated well with G-score similar to Tl score (stress). These data suggest that for assesment of severity of the IHD, 123I-BMIPP SPECT is useful and this method may be used to estimate severity of coronary artery with little intervention.

PS-72

T. Mochizuki, K. Murase, M. Miyagawa, T. Kikuchi, Y. Kimura, and J. Ikezoe.

Ehime University School of Medicine, Department of Radiology

“MEMORY IMAGE” OF ACUTE MYOCARDIAL INFARCTION (AMI) OF I-123 BMIPP AFTER DIRECT PTCA: A COMPARISON WITH Tl-201 AND Tc-99m PYROPHOSPHATE (PYP) DUAL SPECT.

“MEMORY IMAGE” is a phenomenon of I-123 BMIPP in which AMI lesion (or damaged myocardium) could be detected as a defect during a couple of weeks even after successful reperfusion therapy.

Purpose of this study was to clarify the incidence and usefulness of the “Memory Image” of 123-I BMIPP in patients with AMI by comparing Tl-201 and Tc-99m PYP Dual SPECT.

Materials consisted of 14 pts with AMI and 20 pts with old myocardial infarction (OMI). All of the 14 AMI lesions were confirmed with positive Tc-99m PYP and Tl-201 dual SPECT. All pts performed both BMIPP and Tl/PYP Dual SPECT within two weeks. Extent and severity of the defect of BMIPP and Tl were scored into four grades; 0 = no defect, 1 = small or mild defect, 2 = intermediate defect and 3 = large or severe defect. These scores were compared.

In 12 out of 14 AMI pts, extent and/or severity score of BMIPP was greater than that of Tl. In two pts, BMIPP and Tl scores were the same. Positive PYP lesions were concordant with defects of the BMIPP (“Memory Image”). Differences (BMIPP - Tl) of extent and severity scores were greater in AMI pts {0.86 \pm 0.54 (mean \pm SD) and 0.93 \pm 0.73 respectively }, than in OMI pts {0.10 \pm 0.31 and 0.25 \pm 0.44} (P<0.05).

In conclusion, the “Memory Image” by BMIPP is a common phenomenon in pts after reperfusion therapy and quite helpful in evaluating area of the damaged myocardium (or rescued myocardium by comparing perfusion study) in acute phase even after normalized or successful reperfusion therapy.

Poster presentations

PS-73

M. Toba, Y. Ishida, K. Fukuchi, K. Hayashida, M. Takamiya.

Hospital: National Cardiovascular Center, Department of Radiology.

Significance of myocardial perfusion/metabolism mismatch estimated by ECG-gated Tc-99m sestamibi and I-123 BMIPP SPECTs in the follow-up study of AMI.

Scintigraphic myocardial perfusion/metabolism mismatch (normalized perfusion, but reduced uptake of free fatty acid or augmented glucose utilization) has been observed in acutely ischemic and reperfused myocardium. To clarify clinical significance of the mismatch in the follow-up study of AMI, we performed serial ECG-gated Tc-99m sestamibi (MIBI) and I-123 β -methyliodophenyl pentadecanoic acid (BMIPP) SPECTs in acute and subacute stages (1 week and 1 month after the onset, respectively) for 12 patients with AMI receiving reperfusion therapy. For each imaging, we generated Bull's eye polar map and determined %peak activity (%PA) in 8 segments of the map corresponding to those for estimating regional wall motion (RWM) in biplane LVG. The difference of %PA between MIBI and BMIPP was calculated in each segment as an index of the segmental mismatch (%SMM). The %SMM in acute stage was higher in the ischemically compromised segments (Gp A) with improved RWM during the follow-up ($n=13$, $12\pm 9\%$, $p<0.02$) than in those (Gp B) without the improvement ($n=22$, $5\pm 7\%$). Thus, the mismatch determined in acute stage of AMI provides prediction of functional recovery hereafter. Observing the serial changes from acute to subacute stage, segmental %PA of both MIBI and BMIPP showed significant improvement in Gp A (MIBI: 56 ± 9 to $73\pm 10\%$, BMIPP: 45 ± 10 to $61\pm 10\%$, $p<0.001$ in both) but not in Gp B, and hence %SMM did not show significant change in both Gps. However, ECG-gated MIBI imaging demonstrated that segmental %PA of Gp A increased only in the end-systolic image significantly (53 ± 14 to $66\pm 12\%$, $p<0.005$) but not in the end-diastolic image, indicating that the change in the non-gated %PA is mainly affected by those in the end-systolic %PA which reflects the improvement of RWM. Thus, the non-gated imaging may have limitations in assessing the serial changes in myocardial perfusion or metabolism independent of those in RWM for patients with AMI.

PS-74

N. Uno, J. Yamazaki, H. Hosoi, H. Nakano, S. Ishiguro, H. Mutoh, S. Yamashina, H. Yamashina, S. Ishida, T. Morishita

The First Department of Internal Medicine, Toho University School of Medicine, Tokyo, JAPAN

EVALUATION OF MYOCARDIAL DISORDER IN PATIENTS WITH LEFT VENTRICULAR ECCENTRIC HYPERTROPHY OF VALVULAR HEART DISEASE: USING 201-TL AND 123I-BMIPP

<Purpose of study> A study was conducted on the usefulness of 201Tl (Tl) and 123I-BMIPP (BM) for myocardial disorder in volume load valvular disease. <Subject> 23 cases of valvular heart disease excluding ischemic heart disease (14 males and 9 females with an average age of 58.7 ± 12.4 years); 8 cases of aortic regurgitation, 8 cases of mitral regurgitation, 7 cases of aortic and mitral regurgitation.

<Methods> BM-SPECT, Tl-SPECT, and Echo cardiography were performed in all cases over the same time period. Rest initial images were used for investigation in BM and Tl. On the SPECT images obtained, the left ventricle was divided into 16 portions and defect score (ds) was calculated by visual evaluation. In addition, ejection fraction (EF) and left ventricular end-diastolic dimension (LVDd) were determined from the tomographic echocardiogram.

<Result> A tendency for reduced uptake in the inferoposterior wall, especially at the apex, was noted in BM and Tl. Furthermore, positive correlations were observed between BMds and LVDd ($r=0.577$), between Tlds and LVDd ($r=0.555$). Negative correlations were indicated between EF and BMds ($r=0.649$), between EF and Tlds ($r=0.585$). For investigation, all cases were divided into 2 groups according to the tomographic echocardiogram: a normal wall motion of the left ventricle group with EF ≥ 0.5 ($n=15$) and an abnormal wall motion group with EF < 0.5 ($n=8$). BMds were 17.5 ± 1.6 and 20.6 ± 4.2 in the WMn group and the WMa group, respectively, showing a significant difference ($p<0.05$). No significant differences in Tlds and LVDd were noted between the WMn group and the WMa group.

<Summary> A tendency for reduced uptake in the inferoposterior wall, especially at the apex, was observed in BM and Tl. Both Tl and BM were considered to be useful in evaluating the severity of myocardial disorder. In addition, fatty acid metabolic abnormality could cause enlarged left cardiac chamber and abnormal wall motion in severe cases, while the abnormal wall motion extended globally on the echocardiogram in the WMa group, without reflecting the BM defect portions.

PS-75

T. Wakabayashi, T. Nakata, N. Nakahara, H. Kobayashi, S. Shimoshige, K. Miyamoto, K. Tsuchihashi, K. Nagao, T. Takada, K. Shimamoto.

Sapporo Medical University and Hakodate Goryoh-kaku General Hospital, Hokkaido, Japan.

PERFUSION-METABOLISM MISMATCH ASSESSED BY THALLIUM AND BMIPP INDICATES GREATER RECOVERY OF FATTY ACID METABOLISM FOLLOWING CORONARY REVASCULARIZATION

Perfusion-metabolism mismatch is often observed in viable but ischemic myocardium but the recovery process following coronary revascularization is not clear. To determine the effect of coronary revascularization on the correlation between myocardial perfusion and fatty acid metabolism, tomographic imagings with iodinated methyl-branched fatty acid analogue, BMIPP, and thallium were performed in 32 patients with stable coronary artery disease before and after coronary revascularization by coronary angioplasty or bypass grafting. The uptakes of BMIPP and thallium were semiquantitatively assessed as a total defect score (TDS) by a 4-point scoring system, normal 0 to defect 3. The mean intervals between the first and second scans were 70 days for thallium and 59 days for BMIPP. BMIPP TDS was significantly greater than that of thallium (pre-intervention, 7.9 ± 7.6 vs 6.3 ± 6.8 ; post-intervention, 6.1 ± 6.6 vs 4.4 ± 5.4), indicating perfusion-metabolism mismatch, and both BMIPP and thallium TDSs significantly reduced after revascularization. The patients were divided into 2 groups based on the presence (group A) or absence (group B) of reduction of perfusion-metabolism mismatch after coronary intervention. Group A showed greater perfusion-metabolism mismatch before revascularization compared to group B and BMIPP TDS significantly reduced after revascularization, resulting in no mismatch. In group B, despite no significant difference in thallium and BMIPP TDSs, a greater reduction of thallium TDS compared to BMIPP TDS after revascularization resulted in mismatch appearance. Thus, perfusion-metabolism mismatch might be an indicator of greater metabolic recovery following coronary revascularization; in contrast, less mismatched myocardium may show delayed recovery of fatty acid metabolism despite myocardial perfusion improvement.

PS-76

S. Yamashina, M. Takata, J. Yamazaki, T. Morishita, M. Takano, M. Inoue, S. Ishida

The First Department of Internal Medicine, Toho University School of Medicine, Tokyo, JAPAN

UTILITY OF 9-METHYLPENTADECANOIC ACID (9MPA) MYOCARDIAL SCINTIGRAPHY TO ADRIAMYCIN INDUCED CARDIOMYOPATHY

Purpose; In order to examine the abnormal metabolism of fatty acid in myocardium caused by the administration of Adriamycin (ADR). 9-methylpentadecanoic acid (9MPA) myocardial SPECT was performed. Object and methods; Male New Zealand White rabbits (3 months of age), weighing 2.3 ~ 2.8kg, were used for the experiments. These rabbits were divided into the A group (8 rabbits) that were administered isotonic saline for 8 weeks, and the B group (the group which cardiomyopathy, 10 rabbits) to which ADR was intravenously administered 3 times a week, for 8 weeks. These animals were subjected to the measurement of bodyweight, blood pressure, heart rate, ECG and hematological biochemical data. After the administration of the drugs, these rabbits were examined for the cardiac echo, 9MPA myocardial scintigraphy, and pathological examination of myocardium. Measurement of 9MPA was carried out, after 0.1 mCi 125I-9MPA, and 5 mCi 123I-9MPA were administered, 60 min and 5 min before the autopsy, respectively. After sacrifice of the animals, the accumulation rate of 9-MPA in myocardium (%Dose/g) was measured. Results; The accumulation rate of 9MPA in myocardium (%Dose/g) was significantly decreased in the B group, among the animals in which 0.1 mCi 125I-9MPA was administered, 60 min before the autopsy. Conclusion; From these results, it was suggested that 9MPA myocardial scintigraphy was useful for the detection of abnormal metabolism of fatty acid in myocardium caused by the administration with ADR, and for the progressive observation of the effects of ADR on myocardium.

Cardiovascular: Neural function and receptors

PS-77

K. Aoyagi, Y. Tomaru, T. Inoue, K. Endo, A. Hasegawa
Department of nuclear medicine and the second department of internal medicine, Gunma University school of medicine, Gunma, Japan

IODINE-123-MIBG MYOCARDIAL SCINTIGRAPHY IN PROFESSIONAL CYCLE RACERS.

The aim of this study is to evaluate the relationship between myocardial autonomic nerve activity and Iodine-123-metaiodobenzylguanidine (MIBG) myocardial scintigraphy of athletic heart. MIBG scintigraphy was performed in 10 professional cycle racers and 10 healthy volunteers. Anterior planar images and SPECT images were taken at 15 minutes and 240 minutes after injection of MIBG. To evaluate autonomic nerve activity, power spectral analysis (PSA) of heart rate variability was conducted during the MIBG study. The heart / upper mediastinum MIBG uptake ratio (H/M ratio) on the planar image obtained at 240 minutes and the regional MIBG uptake in the inferior wall normalized by individual maximal uptake among all pixels (percent U) in racers were significantly lower than those in healthy volunteers ($p < 0.01$). In the group of racers, the H/M ratio showed significant correlation with the percentage of high frequency component of PSA, which is an index of parasympathetic nerve activity ($r = 0.75$, $p < 0.05$). Percent U and the H/M ratio were significantly correlated with mean R-R interval in a resting ECG ($r = 0.76$, $r = 0.80$, $p < 0.05$, respectively). These results may indicate that myocardial MIBG uptake correlates with vagal tone in professional cycle racers, rather than sympathetic nerve activity.

PS-78

M. Alonso, J. Márquez (1), I. Castejón, M. Escribano, E. Mariño, I. Freile, V. Peiró, T. Torres, I. Lozano (1), M.J. Tabuenca, J. Ramos, J. Ortiz Berrocal
 Departments of Nuclear Medicine and Cardiology (1). Clínica Puerta de Hierro. Madrid, Spain.

123I-MIBG PLANAR SCINTIGRAPHY AND SPECT IN THE EVALUATION OF ADRENERGIC SYMPATHETIC ACTIVITY IN PATIENTS WITH MALIGNANT VENTRICULAR ARRHYTHMIAS

Selective myocardial denervation has been proposed to be an important mechanism in the genesis of ventricular tachycardia (VT).

Objective: To evaluate the utility of sequential planar scintigraphy (SG) and SPECT with 123I-MIBG as radiolabel in the assessment of adrenergic innervation in patients with malignant ventricular arrhythmias (MVA).

Material and methods: Twenty-two patients with MVA who had undergone implantation of an automatic implantable cardioverter defibrillator (AICD) after suffering an episode of sudden cardiac death (SCD) were studied. Three groups were established according to the underlying disease: dilated cardiomyopathy ($n=9$), ischemic heart disease ($n=10$) or primary ventricular fibrillation (VF, $n=3$). Planar SG and SPECT were performed 15 min and 3 hr after injection of 185 MBq of 123I-MIBG; plasma catecholamines were also measured. The images were subjected to qualitative and semiquantitative analysis and the heart/mediastinum (H/M) indices obtained in each phase of the study were assessed, while the percentage of global washout (%Wg) was determined on the basis of the planar images and percentage of regional washout (%Wr) using a bull's eye map. In addition, three clinical parameters were assessed: ejection fraction, NYHA functional class and recurrences/year according to the AICD; features of the myocardial infarction and those of the VT.

Results: The findings were compared with those in a control group. The MVA patients were found to have a decreased uptake, abnormal radiolabel distribution and accelerated washout. The results of the semiquantitative analysis appear in the table.

	Index H/M		% Wg	% Wr			
	15 min.	3 h.		Anterior-Septal-	Lateral-	Inferior	
Control	1.92	1.80	16.80	-0.29	1.82	4.33	3.26
Dilated Cardiom.	1.43	1.40	34	1.42	6.79	1.83	16.48
M. Infarction	1.36	1.31	15.7	1.86	-0.16	4.33	12.26
Idiopathic VF	1.03	1.04	-29.4	-6.12	-5.36	-1.98	-0.25

Conclusions: 123I-MIBG scintigraphy is a valid method for assessing the status of myocardial adrenergic activity in patients with MVA, suggesting its utility as a new parameter for risk stratification.

PS-79

M. Estorch, A. Flotats, C. Marí, A.M. Catafau, Ll. Berná, R. Serra, T. Prat, I. Carrió. Hospital Sant Pau, Barcelona. Spain. Department of Nuclear Medicine and Cardiology.

REGIONAL MYOCARDIAL MIBG UPTAKE AT REST RELATES TO REGIONAL MYOCARDIAL PERFUSION AT EXERCISE IN PATIENTS WITH CAD.

To assess the relationship between myocardial MIBG uptake at rest and myocardial perfusion at exercise, we studied 17 patients with known coronary artery disease and previous myocardial infarction who underwent MIBG studies at rest and rest/exercise tetrofosmin studies within the same week.

Regional tracer uptake was quantified and expressed as percentage of peak activity. On MIBG studies, 24 segments had uptake of $\leq 35\%$ of peak activity, 45 of 36-50%, 36 of 51-65%, 78 of 66-80%, and 72 of $> 80\%$. On exercise tetrofosmin studies, 15 segments had uptake of $\leq 35\%$ of peak activity, 18 of 36-50%, 57 of 51-65%, 81 of 66-80%, and 84 of $> 80\%$ ($p < .0001$, $r = .784$).

Fourteen patients had decreased myocardial MIBG uptake at rest and decreased exercise tetrofosmin uptake in the same segments. In nine of them, MIBG defects were more extensive and severe than tetrofosmin exercise defects. Patients with more severe ischemia at rest/exercise tetrofosmin studies had more severe MIBG defects at rest. Two patients had similar decrease in uptake of one or more myocardial regions in the three studies. One patient had decreased regional MIBG uptake with normal exercise/rest tetrofosmin uptake.

We conclude that resting myocardial MIBG defects relate to myocardial perfusion defects at exercise, suggesting that repetitive episodes of ischemia can induce a permanent loss of neuronal MIBG uptake in the myocardium.

PS-80

S. Ishida, J. Yamazaki, S. Yamashina, N. Uno, M. Takata, T. Morishita

The First Department of Internal Medicine, Toho University School of Medicine, Tokyo, JAPAN

STUDY OF CARDIAC SYMPATHETIC NERVE DISORDER IN CASES TREATED WITH ADRIAMYCIN

<Object> Cardiac sympathetic nerve disorder in cases treated with Adriamycin (ADR) was studied with MIBG for a dose-response relationship.

<Methods> MIBG myocardial SPECT images were acquired using the PRISM3000 (PICKER Inc.) fitted with a general purpose collimator 20 minutes and 4 hours after MIBG injection. Washout rate (WR), Extend score (ES), and Severity score (SS) of the whole left ventricle were calculated by the Bull's eye method from the initial and the delayed (4 hours later) images. Furthermore, the Bull's eye images were divided into four portions and WR was calculated for the left ventricular anterior and inferior walls. <Subjects> 27 cases of malignant hematopoietic disease (11 cases of multiple myeloma and 6 cases of malignant lymphoma); male-female ratio, 17: 11; average age, 60 years (range: 34 to 74 years); average ADR dosage, 354 mg/sm.

<Result> (1) The initial images showed a correlation coefficient of 0.526 between ADR dosage and ES, 0.520 between ADR dosage and SS. (2) The delayed images produced a correlation coefficient of 0.593 between ADR dosage and ES, 0.600 between ADR dosage and SS. (3) There was a correlation coefficient of 0.586 between ADR dosage and the WR of the left ventricle. (4) The WR of the anterior wall was significantly increased in the group dosed with ADR 300 mg/sm or more compared with the group dosed with ADR less than 300 mg/sm. As for the WR of the inferior wall, no significant difference was noted between the two groups.

<Discussion> In cases dosed with ADR less than 300 mg/sm sympathetic nerve disorder in the inferior wall was observed, while damaged sympathetic nerve was suggested in the anterior wall as well in cases dosed with ADR 300 mg/sm or more.

PS-81

H. Kobayashi, K. Kusakabe, M. Momo, S. Ohnishi, H. Kasanuki, T. Okawa
Tokyo Women's Medical College Hospital, Department of Radiology

DECREASED CARDIAC SYMPATHETIC ACTIVITY IN BRUGADA SYNDROME (IDIOPATHIC VENTRICULAR FIBRILLATION)

Background. Brugada syndrome is a new clinical entity of idiopathic ventricular fibrillation (VF) with right bundle branch block and persistent ST elevation. The purpose of the present study was to clarify the cardiac sympathetic activity in patients with Brugada syndrome by using ¹²³I-metaiodobenzylguanidine (MIBG) scintigraphy. **Methods.** Eight patients with Brugada syndrome, 11 with Long QT syndrome (LQTS), 11 with arrhythmogenic right ventricular tachycardia (ARVD), 13 with dilated cardiomyopathy associated with ventricular tachycardia (DCM) and 8 controls were studied. Planar and single photon emission computed tomography (SPECT) MIBG images were obtained 15 min and 4 hr after MIBG injection. **Results.** The MIBG washout rate in the Brugada syndrome group (1.4±12%) was significantly lower than that in the control group (13.4±9%). The MIBG washout rate in the LQTS group (11.3±6%) was not significantly different from the control group value, whereas the rates in the ARVD (21.1±12%) and DCM (34.3±15%) groups were significantly higher than that of the control group. In the SPECT images, a severe MIBG defect was not found in any of the Brugada syndrome patients. These results indicated that the cardiac sympathetic activity was significantly decreased in Brugada syndrome. **Conclusion.** In the Brugada syndrome patients, regional cardiac sympathetic denervation was not found, but the cardiac sympathetic activity was significantly decreased. Decreased sympathetic activity might be an important mechanism of the induction of VF in patients with Brugada syndrome.

PS-82

L. Lumbregas¹, I. Carrió², C. Puentes³, B. Fernández¹, M. Estorch², J. Ruiz², A. Flotats², A. Posada², D. Becerra¹ and JIM Sampere¹.
(1) Hospital Universitario, Granada; (2) Hospital Sant Pau, Barcelona; (3) Hospital Carlos Haya, Málaga (Spain).

EXTENT OF CARDIAC SYMPATHETIC DENERVATION AND RELATION TO ANGINA IN PATIENTS WITH CORONARY ARTERY DISEASE

Objectives. To evaluate regional adrenergic dysfunction in necrotic and ischemic territories in patients with coronary artery disease (CAD) and to relate its extent with the development of anginal pain. **Methods.** The study comprised 58 patients with diagnosis of CAD. According with their clinical data and the results of ^{99m}Tc-tetrofosmin (TF) stress/rest study, they were divided into three groups: **Group A:** Myocardial infarction (MI) (n=13); **Group B:** Myocardial ischaemia without MI (n=20); **Group C:** Myocardial infarction with post-infarction ischaemia (n=25). We compared the cardiac distribution of ¹²³I-MIBG and ^{99m}Tc-TF in a segment-by-segment basis: Three shortaxial slices at basal, midventricular and distal levels, and the apical portions of one vertical and horizontal long-axis images at the mid-left ventricle were selected for analysis of segmental activity, obtaining a total of 16 roi's. The extent of defects was calculated adding the defect scores for each study. Heart to Mediastinum (H/M) ratios and washout rate were calculated from anterior planar images acquired at 15m and 3h. Parameters about left ventricle ejection fraction (LVEF) and wall motion were obtained from echocardiography. **Results.** Abnormalities in adrenergic function (uptake ≤30% of the maximal cardiac activity) were more extensive than the associated in myocardial perfusion in the three groups (overall 9.45 ± 3.08 vs 6.26 ± 3.06, p<.0001), keeping a correlation with TF stress (r= .43; p<.0000) and rest (r= .69; p<.0000) defects. The MIBG defects in the Group B are also more extensive than the ischemic defects (8.55±3.32 vs 4.31±2.36). There were no differences in MIBG washout rates among the groups. A significant correlation was found between MIBG global defect and the area of nonischemic but denervated myocardium (r=0.77; p<.000). We also found a significant inverse correlation between MIBG defect score and LVEF in the groups with MI (**Group B:** r=-.759; p<.003. **Group C:** r=-.439; p<.028). HMR was lower in patients with angina (15m: 1.82±.20 vs 1.66±.31; p<.007. 3h: 1.82±.25 vs 1.64±.27; p<.011). Both, the ischemic area detected with perfusion tracers (1.68±2.18 vs 3.0±1.63; p<.005) and the extent of ischemic but denervated myocardium (4.32±2.64 vs 6.89±3.07; p<.005) are bigger in painful CAD patients. The logistic analysis shows that the extent of non-necrotic but denervated myocardium (MIBGR) is an independent predictive factor for the appearance of angina $Prob. (angor) = 1/[1 + EXP. (-3.152 \times MIBGR - 2.2273)]$. **Conclusions:** These results suggests that cardiac sympathetic denervation is common in patients with ischemic and necrotic CAD. The extent of non-necrotic denervation seems to be associated with the presence of pain.

PS-83

L. Lumbregas¹, M. Fernández-Soto², A. Nevado-Jiménez², D. Becerra¹, R. Nieto¹, B. Fernández¹, MC Bermudez¹, O Padilla¹, F Escobar-Jiménez², JIM Sampere¹.
¹Nuclear Medicine, ²Endocrinology and ³Pediatric Units. Hospital Universitario, Granada (Spain)

EVALUATION OF CARDIAC SYMPATHETIC INNERVATION WITH MIBG IN DIABETIC PATIENTS AND RISK OF CARDIAC AUTONOMIC NEUROPATHY

Objectives: To evaluate the pattern of cardiac sympathetic innervation in patients with diabetes mellitus (DM) in relation with presence of cardioneuropathy (CAN) and other long-term complications, and variables of metabolic control.

Methods: n=52 patients (11 controls and 41 DM patients -11 type 1 and 30 type 2-) without myocardial perfusion abnormalities (^{99m}Tc-tetrofosmin) were submitted for ¹²³I-MIBG evaluation. Mean duration of diabetes was 13.6 ± 8.6 years and mean HbA1c was 7.3 ± 1.7. Presence of CAN was evaluated with conventional ECG-based cardiac tests. Global uptake of MIBG was evaluated by Heart to Mediastinum (H/M) ratios calculated from anterior planar images acquired at 3h. Regional variations were analyzed with a polar map created using short-axis SPET images, in which the left ventricle was divided into four regions (anterior, septal, inferior, lateral) of 8 roi's each one. In each roi we calculate the percent of the maximal cardiac activity. We considered for the analysis the relative uptake (%) and the coefficient of variation (cv) obtained in each region. For functional analysis, FEVI parameters (LVEF, V. Ejection_{MAX}, V. Ejection_{PROM}, y V. Filling_{PROM}) were determined from radionuclide ventriculography.

Results: We don't found differences in clinical characteristics or presence of long-term complications between the two groups of DM defined by type (1 or 2) or presence of CAN. A reduction of uptake was observed globally (HMR: 1.77 ± 0.26 vs 2.01 ± 0.28; p<.001), and in the inferoposterior regions (p<.001) in the DM group respect the control group. The mean inferior and lateral uptake was also smaller in the CAN-positive diabetic group. In both cases there is an increased CV values. We don't found significative differences between LVEF, V. Ejection_{MAX}, V. Ejection_{PROM}, y V. Filling_{PROM}. There is a significative correlation between inferior uptake and HbA1c levels (r=.407; y=97.16 - 4.642 X; p<.05) independent of age and sex. The inferior uptake index (MIBGINF) was an independent predictive value for the presence on CAN:
{Probability = 1/[1 + EXP. (-0.097 x MIBGINF + 4.836).}

Conclusions: Direct assessment of CAN with ¹²³I-MIBG allows a detection previously of ECG-based conventional tests. The relation between a progression of the inferoposterior sympathetic dysinnervation and HbA1c levels suggests that metabolic control can play an important role in the basis of this complication.

PS-84

K. Sakata, R. Nawata, M. Shirohata, H Yoshida.

Hospital: Shizuoka General Hospital, Department of Cardiology.

EFFECTS OF ENALAPRIL AND NITRENDIPINE ON CARDIAC SYMPATHETIC NERVOUS SYSTEM IN ESSENTIAL HYPERTENSION.

Angiotensin-converting enzyme inhibitors and long-acting calcium channel blockers have been widely used in the treatment of many cardiovascular diseases. However, little information is available on the effects of these drugs on the cardiac sympathetic nervous system. ¹²³I-MIBG cardiac imaging and measurement of plasma norepinephrine were performed before and 3 months after the start of drug administration in 46 patients with mild essential hypertension. Twenty-two of the patients (E group) were treated with 5-10 mg of enalapril once a day, and the other 24 (N group) with 5-10 mg of nitrendipine once a day. For comparison, 20 normotensive subjects were also studied. There were no significant differences between the basal characteristics in the 2 hypertensive groups. In both hypertensive groups, both the systolic and diastolic blood pressures were significantly reduced to similar levels after the 3-month drug treatment, although the heart rate did not change significantly. The plasma norepinephrine concentration did not change significantly in either group. Before the drug treatment, the 2 hypertensive groups had a significantly higher washout rate and lower MIBG uptake compared to the normotensive subjects. In the E group, the heart/mediastinum ratio significantly increased (p<.0001) with decreased (p<.002) washout rate after drug treatment, but there were no significant changes in the N group. In conclusion, without affecting the systemic sympathetic activity, enalapril might suppress cardiac sympathetic activity and nitrendipine had no effect on it.

PS-85

N. Takahashi¹, H. Ochiai¹, H. Ashino¹, T. Ebina¹, S. Sumita¹, T. Ikegami², S. Matubara², M. Ishii¹. Department of 1st Internal Medicine and 2nd Radiology, Yokohama City University, Yokohama, Japan.

MYOCARDIAL SYMPATHETIC NERVOUS ACTIVITY IS MORE SENSITIVE MARKER THAN NEUROHUMORAL FACTORS FOR DETECTING LEFT VENTRICULAR DYSFUNCTION

Plasma norepinephrine concentration (PNE), atrial natriuretic peptide (ANP), brain natriuretic peptide (BNP) and left ventricular ejection fraction (LVEF) are important determinants of prognosis of chronic heart failure. The Sympathetic nervous system is activated in patients with congestive heart failure but it is unclear how cardiac sympathetic nerve function is affected neurohumoral factors in patients (pts) with LV dysfunction. We studied 42pts (age 52±11) with ventricular tachycardia (n=16), dilated cardiomyopathy (n=9), mitral valve disease (n=4), aortic valve disease (n=3), old myocardial infarction (n=4), stable angina pectoris (n=3) and WPW syndrome (n=3). Pts were rest at supine position in a quiet room for 30 min before venous blood samples. 111MBq of Iodine-123 meta-iodobenzylguanidine were injected intravenously and scintigrams were obtained in the anterior view at 15 min and 4 hours after injection. Then heart to mediastinum ratio (H/M) of delayed image and washout ratio (WO) were measured. Pts were classified into 3 groups according to LVEF: EF was >60% in 14 pts(A), >40% but <60% in 18pts(B) and <40% in 10pts(C). Results are shown in the table. In conclusion, the changes of H/M and WO were observed earlier than that of neurohumoral factors in pts with LV dysfunction.

	PNE(pg/ml)	ANP(pg/ml)	BNP(pg/ml)	H/M	WO
A	231±108	58±22	24±28	2.76±0.45	28.0±10.3
B	265±113	83±57	57±60	2.40±0.37#	37.1±9.8#
C	372±217	132±70	181±99**	1.95±0.37**	46.1±8.5*

#p<0.05 vs A, *p<0.05 vs B,**p<0.01 vs B

PS-86

M. Takata, S. Yamashina, J. Yamazaki, T. Morishita, M. Takano, M. Inoue, S. Ishida

The First Department of Internal Medicine, Toho University School of Medicine, Tokyo, JAPAN

INHIBITORY EFFECTS OF LOPRONONE HYDROCHLORIDE ON THE DISTURBANCE OF CARDIAC SYMPATHETIC NERVE OCCURRING IN THE ADRIAMYCIN INDUCED CARDIOMYOPATHY

Purpose; Effects of Lopronone Hydrochloride (LH) on the preservation of myocardium and the inhibition of the disturbance of sympathetic nerve were examined, using an Adriamycin (ADR) administered rabbit cardiomyopathy model. Objects and method; Male New Zealand White rabbits (3months of age), weighing 2.3 ~ 2.8kg , were used for the experiments. These rabbits were divided into the A group (8 rabbits) that was administered with isotonic saline, for 8 weeks, the B group (the group with cardiomyopathy, 10 rabbits) to which ADR was intravenously administered 3 times a week, for 8 weeks, and the C group (10 rabbits) to which both ADR and LH were continuously administered after 3 times administration of ADR. These groups were subjected to the measurement of bodyweight, blood pressure, heart rate, ECG and hematological biochemical data. After the administration of the drugs, these rabbits were examined for the heart echo, 123I-MIBG myocardial scintigraphy and pathological examination of myocardium. Results; The accumulation rate of myocardial MIBG(%Dose / g) of the C group was higher than that of the B group. The accumulation rate of myocardial MIBG of the C group was higher than that of the B group, and approximated to that of the A group. The washout rate of the C and D groups was improved. The ratio between myocardium and upper mediastinal space (H/B ratio) of the C group approximated to that of the A group. Conclusion; From these results, it was found that LH is useful for the prevention and treatment of myocardial disturbance induced by the abnormality of sympathetic nerve activity by ADR.

Cardiovascular: Others

PS-87

G. Altun, A Sarikaya, *A. Altun, M. Kaya, S. Berkarda Trakya University Faculty of Medicine Department of Nuclear Medicine and *Cardiology, Edirne, TURKEY.

RELATION OF CAVITY-TO-MYOCARDIUM RATIO IN Tc-99m SESTAMIBI SPECT TO LEFT VENTRICULAR MORPHOLOGY

The value of a low Tc 99m sestamibi cavity to myocardium count ratio (c/m ratio) to identifying patients with depressed left ventricular ejection fraction (LVEF) was published, however, to our knowledge relation between c/m ratio and LV morphology with non-ischemic subjects was not investigated. We studied the relation with dipyridamole (Dyp) Tc99m sestamibi SPECT c/m ratio and LV morphologic parameters in non-ischemic patients.

The study cohort consisted of 47 patients with a low (<5%) likelihood of coronary artery disease (CAD) referred for evaluation of CAD with dipyridamole stress Tc 99m sestamibi myocardial perfusion imaging. All patients underwent both a standard same day stress-rest Tc 99m sestamibi imaging and 2D-echocardiography. The c/m ratio was calculated from the dipyridamole stress Tc 99m sestamibi images midventricular short-axis slices using regular regions of interest drawn in the centre of cavity and the hottest area of myocardium. The c/m ratios were compared with LV echocardiographic dimensions.

The c/m ratio was correlated with LVEF (r=0.60, p=0.01), LV internal dimension (r=-0.66, p=0.001), septal wall thickness (r=-0.65, p=0.0001), posterior wall thickness (r=-0.66, p=0.0001) at the end-diastol and LV mass indices (LVMI) (r=-0.60, p=0.01). The c/m ratio of patients with abnormal LVMI were significantly different than those of subjects with normal LVMI (0.132±0.098, 0.211±0.163, p=0.0002).

We concluded that the c/m ratio measured by SPECT perfusion image was not only a useful parameter for identifying patients with depressed LVEF but also valuable in assessing LV morphology.

PS-88

H. Asano, K. Sakai, M. Ajioka, H. Matsui, T. Mizuno

Tosei general Hospital, Division of cardiology, the department of internal medicine, Seto, Japan

CLINICAL SIGNIFICANCE OF REVERSE REDISTRIBUTION IN TECHETIUM-99M TETROFOSMIN MYOCARDIAL SINGLE PHOTON EMISSION COMPUTED TOMOGRAPHY IN PATIENTS WITH ACUTE MYOCARDIAL INFARCTION

It is already reported the phenomenon of reverse redistribution of technetium-99m tetrofosmin (TF) in patients with acute myocardial infarction. It is the purpose to estimate of myocardial viability and investigate clinical significance of reverse redistribution of TF. Methods : Thirty-six consecutive patients with acute myocardial infarction and without previous one, who underwent successful direct angioplasty within 48 hours after onset, were investigated single photon emission computed tomography (SPECT) using I-123-beta-methyl-p-iodophenylpentadecanoic acid (BMIPP) within 5 days and TF within 2 weeks. TF SPECT was performed 30 minutes and 180 minutes after injection of TF 540 MBq at rest. Activity of both tracers was scored in 18 segments, using a 4-point grading system as defect score (extent score (ES) as a total number of segment deteriorated of uptake, and severity score (SS) as a total score of defect score). Wall motion abnormality of left ventriculogram was analyzed with centerline methods 1 month later. Results : ES of early image of TF, delayed image of TF and BMIPP were 5.3 ± 2.8, 6.4 ± 2.9, 6.9 ± 2.8, respectively. There was a significant correlation between ES of delayed image of TF and the one of BMIPP shown as area at risk (r = 0.955). SS of early image of TF, delayed image of TF and BMIPP were 8.0 ± 5.2, 11.4 ± 6.3, 13.9 ± 6.1, respectively. There was a significant correlation between SS of early image of TF, and total area and total deviation of wall motion abnormality (r = 0.824 and 0.857, respectively). In 29 patients with reverse redistribution, the ratio of ES of early image of TF and ES of BMIPP was significantly less than that in patients without reverse redistribution (0.729 vs. 0.9358, p < 0.05), demonstrated that salvage of myocardium with direct angioplasty was greater. There were no difference with reperfusion time, peak creatine kinase activity, wall motion abnormality, ejection fraction between in patients with and without reverse redistribution. In conclusion, reverse redistribution of TF SPECT reflect viable myocardium salvaged by early reperfusion therapy, and with the early image of TF SPECT left ventricular wall motion abnormality will be predicted. Furthermore the delayed image of TF SPECT can demonstrate area at risk.

PS-89

T. Athanasoulis, Ch. Kalliontzi, N. Sifakis, L. Karaloizos, E. Papadaki, C. Palestidis, S. Gerali
Dept of Nuclear Medicine, 'Alexandra' University Hospital, Athens, Greece.

RIGHT TO LEFT VENTRICULAR END DIASTOLIC VOLUME RATIO IN NONINVASIVE ASSESSMENT OF PULMONARY ARTERY PRESSURE BY GATED BLOOD POOL IMAGING

The aim of this study was to test the hypothesis that the right to left end diastolic volume ratio (R/L EDV) calculated by gated spect blood pool imaging (GSI), should be a reliable non invasive index for the assessment of pulmonary artery pressure (PAP), in pts with pulmonary hypertension since the separation of cardiac chambers is excellent and quantitation of end diastolic volumes are not significantly degraded by partial volume effect. Furthermore, the calculation of absolute volumes is not necessary and tricuspid regurgitation possibly does not adversely affects the correlation between R/L EDV ratio and PAP. In 29 pts with pulmonary hypertension and normal left ventricular function (19 pts had chronic obstructive pulmonary disease, 6 primary hypertension and 4 mitral stenosis) and in 15 controls we performed first pass radionuclide ventriculography (FP) followed by GSI. Right ventricular ejection fraction (RVEF) was calculated by FP and R/L EDV ratio by the horizontal long axis slices of the end diastole tomogram using the count-based method. The patients' mean PAP studied by right heart catheterization was 30 ± 12 mmHg. The RVEF mean value of the controls was $47 \pm 5\%$ and of the patients $39 \pm 9\%$ ($p < 0.01$). The R/L EDV ratio mean value of the controls was 1.12 ± 0.15 and of the patients 1.71 ± 0.57 ($p < 0.001$). A negative weak correlation was found between mean PAP and RVEF ($r = -0.43$, $p < 0.05$) and a strong positive correlation between mean PAP and R/L EDV ($r = 0.82$, $p < 0.001$). In conclusion R/L EDV ratio calculated by GSI is useful for the noninvasive assessment of pulmonary hypertension when left ventricular function is normal and for this purpose it is preferable to RVEF.

PS-90

B. Günalp, S. Ilgan, S. Işık

Gülhane Military Medical Academy, Department of Nuclear Medicine and Department of Plastic and Reconstructive Surgery, Ankara, Turkey

EVALUATION OF PLASMINOGEN ACTIVATOR EFFECT ON SAVING THE ZONE OF STASIS IN BURNS BY Tc-99m MIBI SCINTIGRAPHY AND AUTORADIOGRAPHY: AN EXPERIMENTAL STUDY IN RATS

Vessel-thrombosis under or near burned areas is well-observed postburn complication. The present study was designed to determine the effect of recombinant tissue-type plasminogen activator (r-tPA) on vessels thrombosis in zones of stasis postburn.

Twenty rats were assigned to experimental and control groups (n: 10). After shaving the backs, a 'comb burn' was given bilaterally on the back of the rats 0.5 cm lateral and parallel to the midline by using a brass probe consisting of four rows (10x20 mm) and three interspaces (5x20 mm). Standardized full-thickness burns of the experimental group were treated with r-tPA via femoral veins 2h after the burn, while the control group rats were infused the same volume of saline. Interspaces between the rows and vertical space area were evaluated as zone of stasis. To evaluate perfusion of panniculus carnosus muscle, which is beneath the burned area of skin, each rat received 3 mCi of ^{99m}Tc MIBI on the first or seventh day postburn. After one hour, the rats were killed by decapitation. The entire back skins including the panniculus carnosus muscle layer were dissected away. The specimens were immediately put under the gamma camera and images were obtained with pinhole collimator. After imaging, specimens were used for direct autoradiography.

Gamma camera images revealed that in the experimental group ^{99m}Tc MIBI uptake in the interspace areas 60-90% more than the burned areas while in the control group 20-50% more uptake by the interspace area when compared to burned areas. Autoradiographs gave excellent results that showed the necrotic area borders exactly. The mean percentage of survived interspace and vertical space areas was higher in experimental group than in the control group at either 24h or day 7. On day 7, the average surviving interspace and vertical space areas was 87.8% of the total evaluated area of 8.5 cm². The average surviving percentage was 31.8% in the control group at this time ($p < 0.05$).

These results confirm that treatment with this selective fibrinolytic agent (r-tPA) after burn injury would have some benefits on saving the zone of stasis in burns and Tc-99m MIBI scintigraphy and autoradiography are useful means for the evaluation of different drug effects on burn injuries in the experimental burn models.

PS-91

N.Ö.Küçük, E.İbis, İ.Dinçer*, İ.Köylüoğlu, E.Diker*, G.Aras, K.M.Kır, G.Tokuz.
Ankara University Medical School, Depts. of Nuclear Medicine and Cardiology*. Ankara/TÜRKİYE

EVALUATION OF SHORT TERM EFFECTS OF AMIODARONE THERAPY WITH MUGA IN PTS WITH LEFT VENTRICULAR DYSFUNCTION

Using of amiodarone infusion therapy for malignant ventricular arrhythmia is common. But, its short term side effects are not well established yet. The aim of this study was to illuminate the short term effects of the amiodarone infusion therapy in depressed left ventricular function.

19 patients (13 males, 6 females, mean age 58.8 ± 7.5) with LV dysfunction due to different etiologies (coronary artery disease in 12, dilated cardiomyopathy in 4 and hypertension in 3) were examined. Amiodarone was administered 1000 mg/day for at least 2 days. Diastolic and systolic functions were evaluated with rest MUGA and ECHO in the pre and post therapy periods.

ECHO showed no changes in systolic and diastolic parameters except prolonged E wave deceleration time. However, systolic (EF, TPE, PER) and diastolic (PFR, TPF) parameters obtained from MUGA were found slightly recovered ($p < 0.05$).

MUGA	Pretherapy	Posttherapy	Change (%)
EF (%) :	24.7±1.4	28.3±2.2	14.5
TPE :	129±24	166±28	28.6
PER :	1.45±0.2	1.67±0.3	15.1
PFR :	0.95±0.2	1.16±0.2	22.1
TPF :	268±32	205±25	23.5

As conclusion, any cardiac side effect of amiodarone in pts with depressed left ventricle was not detected by either MUGA or ECHO. Contrary, MUGA showed an increase in the systolic and diastolic functions. This leads us to the conclusion that MUGA can be an effective method of evaluating the short term effects of amiodarone therapy.

PS-92

C. Nguyen, C. Peker, J. Bardet, JB. Michel, E. Rouvier, A. Meulemans, D. Le Guludec.
Faculté Bichat et ImmunotechPharma, Paris, France.

COMPARATIVE TARGETING OF EXPERIMENTAL INFARCTION USING ONE AND TWO-STEP SYSTEMS.

In order to evaluate the interest of pretargeting by two-step systems in cardiac immunoscintigraphy, the myocardial uptake, the infarct avidity (quantitative autoradiography), the biodistribution and the image quality were compared with three different systems after experimental infarction obtained by left descending coronary artery ligation in male rats. 1/ One-step antimyosine antibody (AM-AB, Myoscint, $10 \mu\text{g} \pm 1 \mu\text{g}$ and $300 \mu\text{Ci}$); 2/ Antimyosine Fab'-streptavidine (Sav, $11 \mu\text{g} \pm 2 \mu\text{g}$) followed 24 hours later by ¹¹¹Indium-DTPA-Biotine(In-B, $300 \mu\text{Ci}$) 3/ Antimyosine anti-Indium-DTPA bispecific AB (BSIC) followed 24 hours after by ¹¹¹Indium labeled bivalent hapten at two different dosages : BSAM $10 \pm 2 \mu\text{g}$ and $100 \pm 5 \mu\text{g}$ and In-hapten $600 \mu\text{Ci}$). The optimal blood to myocardial ratio was first determined : 48 hours for Myoscint and BSAM, 18 hours for Sav-B. Myocardial uptake (% injected dose per g of tissue per g of rat), myocardial to liver ratio (M/L), infarcted to non-infarcted ratio (I/NI) at autoradiography were as follow :

	myocardial uptake	M/L ratio	I/NI ratio
Myoscint	0.88 ± 0.3	0.32 ± 0.09	4.3 ± 1
Sav-B	0.03 ± 0.005	0.75 ± 0.08	5.7 ± 0.9
BSAM low dose	0.04 ± 0.007	1.15 ± 0.09	4.4 ± 0.9
BSAM high dose	0.17 ± 0.03	1.61 ± 0.05	19 ± 1.3

Image quality was dramatically improved with both two-step systems since liver cannot be visualized. We conclude that two-step systems with similar AB doses than one-step system both equally improve signal to noise ratio in spite of a reduction of myocardial uptake. Similar uptake with higher infarcted to non infarcted ratio can be reached by increasing AB doses in this particular model of artery occlusion.

PS-93

D.S. Lee, G.J. Cheon, W. J. Kang, Y.K. Kim, M.M. Lee, J-K Chung, M.C. Lee.

Seoul National University, Seoul, Korea

EFFECT OF NITROGLYCERINE ON MYOCARDIAL FUNCTION IN ACUTE MYOCARDIAL INFARCTION EXAMINED BY GATED MYOCARDIAL SPECT.

Though nitrate treatment was recommended in acute myocardial infarction, the effects of nitroglycerine (NTG) in individual patients were often unpredictable. Preload, global or regional effect of nitroglycerine upon myocardial perfusion and so function could synergize or antagonize each other. We investigated whether gated myocardial SPECT could be used to find the effect of NTG upon myocardial function in acute myocardial infarction.

We studied 30 patients with AMI (M:F=26:4, 57±13 year old, 13±10 days after infarction, anterior wall: inferior wall=17:13, EF=40±11%(range 20-60%), 18 thrombolytic treatment, 6 adjuvant revascularization) using rest Tl-201/dipyridamole-stress gated Tc-99m-MIBI SPECT. After post-stress acquisition, we acquired another gated SPECT after administering sublingual NTG. We divided 13 segments per patient and found 151 dysfunctional segments of which 28 were stunned ones. Wall motion was compared side by side on the same monitor for paired images before and after NTG and was graded 0 (normal) to 3 (dyskinesia). Enddiastolic volume (EDV), endsystolic volume (ESV) and ejection fraction (EF) were calculated with Cedars quantitative gated SPECT software. Reproducibility (coefficient of variation over Bland-Altman plot) of quantitative indices without NTG (in another group of 20 subjects) yielded coefficients of variation (CV) of 5.9% for EDV, 4.9% for ESV and 2.2% for EF without any bias from zero.

EDV decreased more than 2 CV (i.e. significantly) in 9 patients after NTG and so was ESV in 12 patients. Cardiac output decreased in 7 among 17 patients, increased in 5, did not change in the other 5. Global LVEF decreased significantly in 12 patients and increased in 5. Global contractility, expressed as maximum elastance Emax, calculated using applanation radial artery tonometry and peripheral to central transfer function (PWV) and gated SPECT (ADAC), decreased in 2, increased in 2, and did not change in 3 among 7 data-available patients. NTG improved regional function in 18%(5/28) of stunned segments and 25%(38/151) of all the dysfunctional segments. Wall motion aggravated in 14%(4/28) of stunned segments and in 17%(26/151) of all dysfunctional segments.

We found that gated myocardial SPECT enabled us to evaluate loading effect and beneficial or harmful effect of nitroglycerine on dysfunctional myocardium with quite precision. We suggest that gated SPECT before and after drug challenge be used to individualize medication or treatment in patients with acute myocardial infarction, as we found so varied response of myocardium to nitroglycerine.

PS-94

H.Maruno, M.Onoguchi, K.Mori, N.Komiyama, K.Saito, H.Toyama, A.Uki, Y.Takizawa, A.Okazaki, H.Murata

Hospital: Toranomon Hospital, Division of Nuclear Medicine

ASSESSMENT OF REGIONAL LV FUNCTION USING ECG GATED SPECT AND FUNCTIONAL G-MAP METHOD.

We have developed a new quantitative program to analyze gated SPECT data and generate Functional G-maps automatically. The Functional G-maps are polar maps displaying several functional parameters and enable us to evaluate left ventricular regional function and myocardial perfusion simultaneously and quantitatively. In this study, the utility of Functional G-maps for clinical use was investigated. Ten normal subjects, 25 patients with coronary artery disease (CAD), and 12 patients with hypertrophic cardiomyopathy (HCM) were studied. Myocardial wall thickening and thinning in a cardiac cycle was analyzed for the optimal short axis images. The epicardial boundaries of LV were automatically defined and each short axis image was divided by 40 radii into 40 segments. The regional time-activity curve was made from subsequent images. The following quantitative parameters were calculated in each segment by means of the regional time-activity curve and Fourier expansion, and polar maps were generated using the parameters of all short axis slices. [1] Minimum count (MIN), [2] Maximum count (MAX), [3] Count increase (CI) [4] % count increase (%CI), [5] Peak contraction rate (PCR) [6] Peak distension rate (PDR) and [7] Contraction time (CT) were calculated. In CAD, CI and %CI in the ischemic segments were lower than those in normal segments, and CT were useful for assessment of asynergy. PCR and PDR could demonstrate myocardial contractility and distensibility in HCM. In conclusion, the Functional G-maps were useful for evaluation of regional LV function in clinical use.

PS-95

K.Minami, K.Ejiri, S.Tachiki, M.Tokuda, T.Kondo, M.Kato, T.Sawai, K.Yoshimura, T.Nishimura, K.Yokoyama, H.Toyama, T.Orito, and S.Koga

Departments of Health Physics, Cardiology and Radiology, Fujita Health University, Toyoake, Japan

USEFULNESS OF SEMI DUAL ISOTPE SPECT USING Tl-201-CHLORIDE AND I-123-BMIPP

To diagnose myocardial function, dual isotope SPECT of Tl-201-chloride and I-123-BMIPP is very useful, but image quality of this SPECT is more wrong than usual SPECT, because image background is increased by photon cross-talk between Tl-201 and I-123. So, we developed a new imaging method by which the cross-talk affection is perfectly corrected. This imaging method consists of a series of two scans, the first scan is I-123-BMIPP SPECT started at 30 minutes after I-123-BMIPP injection and the second scan is dual isotope SPECT continuously started at 10 minutes after Tl-201-chloride injection. In the first scan, energy windows of gamma camera were set up to the Tl-201 photo-peak (71±10 keV) and the I-123 photo-peak (159±7.5 keV), and in the second scan, a window was set up to the Tl-201 photo-peak (71±10 keV). The first scan provided usual I-123-BMIPP images and the cross-talk images, in the Tl-201 window, scattering from I-123-BMIPP, and the second scan provided the Tl-201-chloride image (71±10 keV) with the I-123 photon scattering. Tl-201-chloride image (71±10 keV) without scattering was obtained from an image processing to subtract the scattering image (71±10 keV) in the first scan from Tl-201-chloride image (71±10 keV) in the second scan. To evaluate this method, we carried out a fundamental test with a myocardial phantom (RH-2, Kyoto Kagaku Co., Ltd.) using the same process with patient study. In this test, it was recognized that the Tl-201-chloride image subtracted I-123-BMIPP scattering photon equaled to the original Tl-201-chloride image in terms of count profile curves, image contrast and background level.

As everybody knows, different scattering magnitude is observed in the individual dual isotope SPECT of patients. The most advantage of this method is that the scattering images of each patient are obtained from first scan and photon cross-talk between Tl-201 and I-123 can be completely corrected by subtraction. We think that this method provides the images to quantify the Tl-201-chloride and I-123-BMIPP uptake in myocardium at the same time.

PS-96

V.Prassopoulos, J.Lekakis, M.Mavrikakis, S.Gerali, N.Sifakis, S.Stamatelopoulos, P.Kostamis

Depts of Nuclear Medicine and Clinical Therapeutics «Alexandra» University Hospital, Athens, Greece

ANTIMYOSIN SCINTIGRAPHY IS USEFUL IN DETECTING SCLERODERMA HEART DISEASE

Systemic sclerosis (SS) is a multisystem disease involving the skin and internal organs. Primary cardiac involvement is common in SS. Indium-111-antimyosin has been shown to bind specifically to cardiac myocytes that have lost membrane integrity and exposed myosin to extracellular space.

Methods : Four patients (pts) with diffuse systemic sclerosis were included in the study, all were women, 61±9,3 years. The duration of the disease was 16,5±9,9 years and all patients presented Raynaud's phenomenon. Four women without signs of cardiac disease formed a control group, 57±10,6 years. In-111-antimyosin scintigraphy was performed 48 hours after intravenous injection of 2mCi In-111-antimyosin. Planar imaging was performed and heart to lung (H/L) ratio was calculated. A H/L ratio >1,6 was considered abnormal.

Results : All controls subjects had normal antimyosin study (H/L ratio ranged 1,3 to 1,5, mean 1,37±0,1). In the group of patients with systemic sclerosis H/L ratio ranged from 1,7 to 1,9 (mean 1,8±0,08, p<0,001). Diffuse uptake was observed in all patients. The four patients presented normal ejection fraction.

In conclusion, antimyosin scintigraphy is a valuable non-invasive method for the detection of early cardiac involvement in patients with systemic sclerosis. A positive antimyosin scanning may be present before deterioration of left ventricular function and the early detection of ongoing myocardial necrosis may be of value in the prognosis of these patients.

PS-97

V. Prassopoulos, J. Nanas, S. Gerali, J. Lekakis, G. Alexopoulos, Z. Margari, N. Sifakis, Ch. Kalliontzi, S. Stamatelopoulos, P. Kostamis
Depts of Nuclear Medicine and Clinical Therapeutics «Alexandra»
University Hospital, Athens, Greece

THE SIGNIFICANCE OF INDIUM-111-ANTIMYOSIN SCINTIGRAPHY IN PATIENTS WITH CHRONIC OR SUBACUTE DILATED CARDIOMYOPATHY AND ACUTE MYOCARDITIS

A high prevalence of monoclonal antimyosin (MA) uptake has been detected in patients (pts) with idiopathic dilated cardiomyopathy (IDC). The purpose of this study was to assess the evolution of antimyosin uptake in patients with short and long history of the disease and to compare these findings to those of acute myocarditis (AM).

Methods : Twenty four pts, 44±12 years, with IDC and 11 pts, 36±15 years, with AM were studied. The diagnosis was verified by endomyocardial biopsy. These pts underwent antimyosin scintigraphy twice, the first on the initial evaluation and the second after the first year of follow up. Planar imaging was performed and heart to lung ratio (H/L) was calculated. A H/L >1.6 was considered abnormal. Pts with IDC were divided into 2 groups according to the duration of symptoms (DOS). Group I (n=16) included IDC pts with DOS>12 mo (45±20 mo, chronic IDC). Group II(n=8) included IDC pts with DOS<12 mo (4±3 mo, subacute IDC). Pts with AM consisted group III(n=11)with DOS of 0.8±0.9 mo.

Results : On the initial evaluation the heart to lung ratio of MA uptake was: group I: 1.66±0.19, group II: 1.88±0.19 (p=0.016 vs group I) and group III: 2.05±0.46 (p=0.0019 vs group I and p=0.322 vs group II). On the late evaluation the MA uptake remained stable in group I (1.69±0.23, p=0.563) and was decreased in group II (from 1.88±0.19 to 1.66±0.21, p=0.008) and group III (from 2.05±0.46 to 1.63±0.30, p=0.014). The MA uptake on the late evaluation was similar in the three studied groups (1.69±0.19, 1.66±0.21 and 1.63±0.30, respectively).

In conclusion, it seems that in patients with chronic IDC the antimyosin uptake is relatively lower compared to the value obtained in patients with subacute IDC and AM, and remains unchanged overtime suggesting a stable condition of the disease. On the contrary antimyosin uptake is decreased overtime in both subacute IDC and AM, a finding associated with clinical improvement according the NYHA. These data may suggest that subacute IDC and AM may represent similar entities.

PS-98

G. Schulz, E. Ostwald, K.CH. Koch*, J. vom Dahl*, O. Sabri, M. Schreckenberger, U. Buell.
Departments of Nuclear and *Internal Medicine I, RWTH Aachen

DOES NITRATE INFUSION ENHANCE MYOCARDIAL VIABILITY DETECTION BY QUANTITATIVE MIBI SPECT ? A COMPARISON TO REST MIBI SPECT AND FDG PET.

The repeatedly proposed use of MIBI SPECT to predicted myocardial viability is still controversial. 11 patients (age 64 ±11 y.) with previous myocardial infarction, angiographically proven advanced coronary artery disease, severe abnormal wall motion and continued individual drug therapy underwent SPECT with 400 MBq [^{99m}Tc] MIBI twice: at rest and during infusion of 0.5 mg/min isosorbide dinitrate (MIBI injection if systolic blood pressure decreased ≥ 20 mmHg or 15 min after start). 360° SPECT included a triple energy window based attenuation and scatter correction. Transmissive attenuation corrected PET was performed at rest with 250 MBq [¹⁸F] FDG 30 min after oral glucose load. All three data sets (filtered backprojection 128² matrix) were threedimensionally matched, quantified into 25 regions and normalized to rest perfusion maximum. According to previous studies only in regions with rest MIBI uptake < 50% viability is questionable: FDG uptake ≥ 70% was defined as viable (mismatch), FDG uptake < 50% as scar (match) and the FDG range from 50 to 69% as "intermediate".

rest MIBI < 50%	ROI (n)	MIBI rest	t-test nitrate	MIBI nitrate	t-test	FDG
mismatch (viable)	21	41 ± 7%	n.s.	47 ± 12%	p<0.001	127 ± 43%
match (scar)	31	31 ± 10%	n.s.	34 ± 11%	n.s.	32 ± 11%

6 mismatch and 8 match regions showed a MIBI uptake difference of nitrate - rest ≥ 10% and revealed a positive predictive value of 0.43 (⁶/₍₆₊₈₎). However, 2 mismatch and 11 match regions showed a difference of nitrate - rest < 0% and revealed a negative predictive value of 0.85 (¹¹/₍₁₁₊₂₎). These preliminary results suggest that additional nitrate infusion does not improve detection of viable myocardium by MIBI SPECT significantly compared to FDG PET.

Oncology: Diagnosis

PS-99

Hayati Akın, Zehra Özcan, Tuncay Göksel, Sezai Taşbakan, Didem Yüksel, Günel Erenel, Duran Efe, Mustafa Kayaloğlu, Kamil Kumanlioğlu and Tulin Aysan.
Ege University Medical Faculty Depts of Nuclear Medicine and Chest Disease, Izmir, Turkey.

A COMPARATIVE STUDY WITH Tl-201 AND Tc-99m(V)DMSA IN THE DETECTION OF LUNG TUMORS AND EVALUATION OF THERAPEUTIC CHANGES

The purpose of this study was to evaluate the clinical value of Tc-99m(V)DMSA and Tl-201 in patients (pts) with a suspicion of lung cancer (LC) and to determine the role of these agents in differentiation between small cell (SCLC)/non-small cell (NSCLC) LC. It was also aimed to test the ability of these agents in differentiation of post-therapeutic fibrosis from tumor recurrence. The study group included 44 pts. with histological proven lung lesions (LL) with a mean age of 51 ± 6 yrs. All pts were examined with Tl-201 and Tc-99m(V) DMSA in the same week as well as other radiological modalities. Planar and SPECT images were recorded 3 hr. after iv inj. of 555 MBq Tc-99m(V)DMSA. Early (20 min) and late (3 hr) planar and SPECT studies were acquired after inj. of 111-129.5 MBq Tl-201. Early (A) and delayed (B) Tl-201 uptakes and Tc-99m(V)DMSA (D) of the lesion (L) and contralateral normal tissue (N) were calculated using ROI's techniques. The degree of Tl-201 retention (retention index: RI) in LL was calculated. The sensitivity, specificity and accuracy of Tl-201 and Tc-99m(V)DMSA in differentiation malign and benign lesions were %82, %86, %83 and %82, %40, %67 respectively. T/N ratios in malignant and benign lesions were presented in table.

	A	B	D	RI
Malignant (n:29)	1.44±0.25	1.55±0.23	1.49±0.53	8.17±11*
SCLC (n:7)	1.48±0.20	1.59±0.30	1.51±0.15	6.71±11
NSCLC (n:22)	1.43±0.26	1.53±0.21	1.49±0.26	8.66±11.8
Benign (n:15)	1.12±0.20	1.12±0.22	1.45±0.55	-0.44±4.1*

*indicates statistical significance

In 6 pts evaluated for the suspicion of viable tumor, Tc-99m(V)DMSA showed abnormal accumulation in 5 whose radiological findings and clinical follow-up revealed no evidence of tumor recurrence. However Tl-201 correctly identified one case of local recurrence and 5 pts of post-therapeutic fibrosis. It is concluded that, Tc-99m(V)DMSA scintigraphy may not distinguish the malignant/benign LL and both Tl-201 and pentavalent DMSA seem to be unable to discriminate SCLC from NSCLC. However, Tl-201 RI appears to be the most reliable parameter in differentiation of malignancy. It is suggested that Tl-201 scintigraphy offers higher accuracy in the evaluation of post-therapeutic changes.

PS-100

O. Alonso, M. Martínez, F. Mut, L. Delgado, G. Lago, M. Núñez, D. De Boni, J. Cánepa, I. Muse, J. Espasandín, J. Priario, and E. Touya.
Nuclear Medicine Centre and Melanoma Unit of the Clinical Hospital, University of Uruguay, Montevideo, Uruguay.

CLINICAL VALUE OF 99mTc-MIBI SCINTIGRAPHY IN THE ROUTINE STAGING OF PATIENTS WITH MELANOMA.

We are currently evaluating the use of 99mTc-MIBI in an ongoing prospective study, as a routine diagnostic technique in patients (pts) with melanoma (ML). We studied 82 pts referred for staging following removal of the primary tumour. Twenty-nine with known recurrent lesions and 53 without evidence of disease. Whole-body images were acquired 10 minutes post-injection of 740 MBq of 99mTc-MIBI. Additional planar and/or SPECT studies were also included on selected cases. The injection site was carefully chosen depending on the topography of suspected/known lesions. All pathological MIBI findings were controlled by conventional imaging (CT, MRI, US, bone scan) and/or resection. MIBI results were confirmed by histology/conventional imaging or clinical follow-up for at least 8 months. Innumerable lesions were classified as a single focus of disease for the purpose of counting. The technique correctly detected 69 (92%) of 75 metastatic lesions in the following sites: regional lymph nodes (n=24), non-regional lymph nodes: (n=10), skin/subcutaneous tissue (n=16), brain/cerebellum (n=6), lung (n=8), bone (n=4), and breast (n=1). MIBI scanning failed to detect: Three subcutaneous regressive lesions (<1 cm), one liver metastasis, one spleen metastasis and a case of multiple small lesions of the duodenal mucous membrane. Only two false positive cases were identified. Additionally the technique was negative in 4 pts with histologically proven benign lymph node enlargements. In 8 pts MIBI scan proved metastatic progress not previously known, and revealed more extended disease in 6 pts claiming immediate clinical effect. In summary, we calculated a diagnostic accuracy of 94% (sensitivity 92%, specificity 96%). Therefore, 99mTc-MIBI may provide a valuable tool for screening ML pts with the potential of influencing treatment planning.

PS-101

J. Arbizu, V. Vanaclocha*, I. Peñuelas, A. Cabrera, A. Crespo, JA. Richter. Clínica Universitaria de Navarra. Department of Nuclear Medicine and Neurosurgery. Pamplona. SPAIN

CONTRIBUTION OF 11C-METIONINE TO 18FDG IN THE CLINICAL EVALUATION OF BRAIN TUMORS

The aim of this study is to evaluate the usefulness of concurrent PET 18FDG and 11C-Metionine (11C-MET) in the evaluation of malignancy grade and recurrent-persistent and/or dedifferentiation of brain tumors.

For this purpose 24 patients with 36 lesions previously shown by MRI were examined. Final diagnosis was achieved by means of pathology and clinical evolution. Tumoral etiology and/or malignancy grade was studied in 13 untreated lesions, and recurrent-persistent and/or dedifferentiation in 23 previously treated tumors.

Both PET studies were performed in a ECAT EXACT HR + scanner 40 min. after the administration of 370 MBq of 18FDG and 20 min. after 185-370 MBq of 11C-MET. The maximal interval between the studies was 15 d. Quantitative analysis was carried out by means of SUV in the tumor lesion and contralateral cortex, obtaining the lesion to tumor ratio (L/C).

The mean values of L/C ratio in the high grade lesions was 1.19 with 18FDG and 1.94 with 11C-MET, and 0.5 with 18FDG and 1.53 with 11C-MET in the low grade lesions. All untreated tumoral lesions and the recurrent or persistent treated tumors were detected with MET (sensitivity and specificity 100%), with 18FDG the sensitivity was 80% and the specificity 100%. Nevertheless, 18FDG showed the high grade malignancy in 6/13 untreated tumors and the dedifferentiation of 9/13 tumors previously classified as low grade.

Conclusion: 11C-Metionine PET study improves the accuracy of 18FDG in the evaluation of brain tumors, mainly in low grade tumors and after recent quimio-radiotherapy.

PS-102

V. Artiko, V. Obradović, B. Davidović, N. Petrović, M. Petrović, Z. Krivokapić, D. Kecmanović, G. Adanja, R. Rebić Institute for Nuclear Medicine, CCS, Beograd - YU

111-In LABELLED ANTIBODIES IN THE DETECTION OF COLORECTAL CARCINOMAS

The aim of the study is detection of the recurrences and metastases of colorectal carcinomas using 111-In labelled antibodies B72.3.

14 patients has been examined (13 with adenocarcinomas of caecum, colon and rectum and one with squamocellulare colonic carcinoma) from 4 months till two years after surgery, two of them after two months after the end of radiotherapy. Radiochemical purity of the radiopharmaceutical was over 97%. Planar anterior, lateral and posterior scintigrams of thorax, abdomen and pelvis are done after 10 min, 24h, 72 and 96h after i.v. injection of Oncoscent CR-103, containing monoclonal antibodies B72.3 labelled with 150MBq 111-In while tomographic scintigrams of the pelvis are done after 72h. In 12 patients recurrences of carcinomas (5-12 cm), in 6 recurrences with liver metastasis, and in two only liver metastases were detected and confirmed by surgery. Planar immunoscintigraphy was positive in 8/8 patients with liver metastases and 9/14 patients with recurrences while in 5/14 recurrences were detected only by tomography. US was positive in all patients with liver metastases, CT finding was false negative in two patients with recurrences, while MRI in one. In three patients with recurrences, CEA was not increased. In 4 patients intensive accumulation of labeled antibodies was observed in colostomas, in one with granuloma, as well as in one with recurrence of squamocellulare carcinoma.

With tomography, we can access better distinction of tumour in comparison to other structures and estimation of its size. Other imaging methods (CT,US) have advantage in detection of liver metastases, while immunoscintigraphy is more specific for the assessment of malignant abdominal tumors and extrahepatic metastases. The first results point out that Oncoscent CR-103 can be useful in diagnosis of recurrences and metastases of colorectal carcinoma, viability assessment after radiotherapy and in the choice of the adequate surgical treatment in dependence of the spread of the disease.

PS-103

Tanık Başoğlu, Candan Coşkun, İrem Bernay, Murathan Şahin, Fevziye Canbaz, Tuncay Önen, Selahattin Albayrak Department of Nuclear Medicine, Ondokuz Mayıs University Hospital, Samsun TURKEY

EVALUATION OF Tc-99m TETROFOSMIN UPTAKE AS A PARAMETER IN MONITORING RESPONSE TO THERAPY IN PRIMARY LUNG CANCER

Uptake of cationic myocardial perfusion agent Tc-99m-Tetrofosmin (TF) in different malignant tissues has been reported in recent years. Its usefulness in detecting primary lung cancer has been evaluated in limited number of clinical investigations. Laboratory research has shown that TF shares with Tc-99m-MIBI the property of being a substrate for P-Glycoprotein (P-gp) and may be useful for functional imaging of tumor P-gp status. The objective of our study was to evaluate the uptake and kinetics of TF in malignant lung lesions before and after radio- and/or chemotherapy. 9 patients presenting with well-diagnosed and untreated malignant lung lesions (7 squamous cell carcinomas (SCC), and 2 small cell carcinomas (SC)) showing TF uptake were included in the study. The patients were treated with radiotherapy (RT), chemotherapy (CT) or with combination of both (RCT). An initial 30- minute dynamic acquisition and following static images were obtained in all patients after intravenous injection of 740 Mbq TF. Lesion / contralateral normal lung (L/CN) ratios were calculated for 25-30 p.i. before and 1-2 months after therapy. Tracer washout (TW) in the lesion at 30 minutes post-injection (p.i.) was determined. As clinical response parameter, reduction in radiological tumor size (RTS) was used. The results are presented in three groups: (1) significant decrease of TF uptake was observed in four patients with squamous cell carcinomas (SCC). Mean L/CN ratio fell from 1.43 to 1.13 in these patients. In 3 of 4, also decrease in RTS was observed. In one patient the RTS remained the same. (2) 3 patients with SCC showed no meaningful difference of TF uptake after therapy. In 2 of 3 minimal increment in RTS was observed. In one patient the RTS remained the same. (3) In 2 patients, both with small cell carcinomas, increase of tracer uptake was observed. In one patient increase in RTS was observed and in the other RTS remained the same. No relation could be detected between the changes in RTS and TW in the whole group. With the exception of increment of TF uptake solely in the patients treated with CT (group 3), there was no relation between the therapy regimen and therapy response. CONCLUSION: Tc-99m-Tetrofosmin may be useful in monitoring response to therapy in lung cancer. Broader and well-defined trials on this matter are needed for further clarification.

PS-104

Ü. Bilkay, K. Kumanloğlu, R. Erinç, E. Teber, M. Töbü, E. Göker, Z. Burak, Z. Özcan, A. Dirlik. Ege University, School of Medicine, Department of Nuclear Medicine, Izmir, Turkey.

THE VALUE OF Ga-67 AND Tc99mMIBI IN DIAGNOSIS AND FOLLOW-UP MALIGNANT LENFOMA

Although CT and MR have major role in the initial presentation of patients (Pts) with malignant lymphoma, these are known to be less accurate in the differentiation of posttherapy changes and active residual disease. Ga-67 has major advantage over CT and MR in posttherapeutic evaluation of lymphoma lesions. Tc99mMIBI is used in the detection of some malignant tumours. It is also reported that tumours that are resistant to therapy do not accumulate Tc99mMIBI.

The aim of our study was to compare the value of Ga-67 and Tc99mMIBI scintigraphy in different clinical settings comparatively. 29 pts (8 female, 21 male, age range: 7-65) with 73 lesions were included in the study. 8/29 pts. were evaluated before any therapeutic intervention (group 1), 5/29 pts; after 1 or 2 course of therapy (group 2) and 16/29 pts. after completion of therapy for the differential diagnosis of fibrotic changes and active residual disease (group 3). All pts. undergone high dose Ga-67 and Tc99mMIBI scintigraphies within the same week. Results interpreted visually (5 point semiquantitative analysis) and quantitatively. Final diagnosis of residual masses were done according to biopsy or clinical follow-up.

	Ga-67	Tc99mMIBI
Group 1	TP: 30, FN: 2, FP: 1 sens: 93%, acc: 90%	TP: 15, FN: 17, TN: 1 sens: 46%, spes: 100%, acc: 48%
Group 2	TP: 7, FN: 1 sens: 87%, acc: 87%	TP: 1, FN: 7 sens: 12%, acc: 12%
Group 3	TP: 14, FN: 5, FP: 4, TN: 9 sens: 73%, spes: 69%, acc: 46%	TP: 4, FN: 14, FP: 1, TN: 13 sens: 22%, spes: 92%, acc: 53%
Overall	TP: 51, FN: 8, FP: 5, TN: 9 sens: 86%, spes: 64%, acc: 82%	TP: 20, FN: 38, FP: 1, TN: 14 sens: 34%, spes: 93%, acc: 46%

In groups 1 and 3, Ga-67 accumulation was statistically superior to that of Tc99mMIBI both in quantitative and semiquantitative analysis (p<0.005).

Additionally, response to therapy could be evaluated in the 1st. group. While 7/8 pts. who had positive Tc99mMIBI uptake had complete response to therapy, 1/8 pts. with negative Tc99mMIBI scan failed to respond.

In conclusion, our preliminary results indicate that, Ga-67 is more sensitive than Tc99mMIBI, but Tc99mMIBI has higher specificity and could be used in the prediction of therapy response.

PS-105

Budihna NV*, Markovič S*, Milčinski M**

*Institute of Oncology, ** Nuclear Medicine, University Medical Center, Zaloška 2, Ljubljana, Slovenia

MALIGNANT NEUROENDOCRINE TUMORS: FOLLOW UP WITH SOMATOSTATIN RECEPTOR SCINTIGRAPHY

Aim: [¹¹¹InDTPA D Phe¹]octreotide scintigraphy (SRS) was used for follow-up of pts with carcinoid and other malignant neuroendocrine tumors. **Methods and patients:** 36 pts (22 men, 14 women, 52±11 years) were investigated with SRS for possible metastases of carcinoid (30 pts), mixed neuroendocrine tumor (2 pts), somatostatinoma (1 pt) or undetermined neuroendocrine tumor (3 pts). The mean follow-up period was 2.5 (±2.5) years. Whole body planar and liver SPET was performed 1.7 (±2.4) years after surgery (20 pts) or tumor discovery (16 pts), 4 and 24-48 h after iv application of octreotide (220 MBq). **Results:** 22 pts were true pos (TP), 6 true neg (TN), 3 false pos (FP), 5 false neg (FN). Sensitivity of SRS was 81%, specificity 67%. Lesions were in the liver (21), abdomen (18), skeleton (3) and pancreas (2). Liver-SPET was positive in 25 pts (FP in 3 pts, in 2 pts faint accumulation after 48 h). Eight pts died of rapidly progressing tumors (3 somatostatin receptor neg, FN pts). Thirteen pts were disease free. Fourteen pts were alive with residual disease, 1 of them FN. One pt was lost from follow-up. **Conclusion:** follow up after surgery for neuroendocrine tumors with SRS enables early detection of metastatic disease. Careful interpretation of liver SPET-SRS is needed. Indication for somatostatin-receptor antagonist therapy can be supported with SRS.

PS-106

J.M. Park, J.Y. Choi, K.H. Lee, S.E. Kim, Y. Choi, Y.S. Choe, G.J. Cheon, J.-K. Chung, S.-M. Lim, B.-T. Kim

Sung Kyun Kwan University, Samsung Medical Center, Seoul National University, Korea Cancer Center Hospital

FDG-PET EVALUATION OF SOLITARY PULMONARY NODULES INDETERMINATE ON CHEST CT

Chest CT has been widely accepted in patients with solitary pulmonary nodule (SPN) to differentiate malignancy from benign lesions, but invasive histologic diagnosis is usually required for the decision of appropriate treatment. Noninvasive FDG-PET has been proved to have high sensitivity and specificity in the characterization of SPNs. We evaluated whether it is true in SPNs which is indeterminate on chest CT.

Forty-three patients out of 66 patients (M:26, F:17; age: 32~78 yrs) with SPN (size 8~40 mm) were included in this study because chest radiologists could not characterize the mass as definite malignant or benign lesion considering patient's age, nodule size, margin, presence of calcification, pattern of contrast enhancement and associate lymphadenopathy on chest CT. Emission scan of the mass was acquired from 46 min to 56 min after intravenous injection of ~370 MBq of [¹⁸F]FDG and corrected with 20-min transmission data. Whole body emission scan was also performed. The final diagnoses (22 malignant, 21 benign) were established by histology (N=31) and clinical follow-up for more than 1 year (N=12).

As the cut-off peak SUV (maximum SUV in ROI) for the malignant lesion was set at 3.5, the accuracy of FDG-PET was 70.0% (30/43). Seven of 22 malignant SPNs were falsely negative; 5 adenocarcinoma (size 8~20 mm) and 2 bronchioalveolar carcinoma (size 14 and 40 mm). All false positive SPNs (6/21) were active inflammatory lesions; 2 bacterial abscess, 2 tuberculosis, 1 aspergiloma and 1 non-specific inflammation. The relative lower accuracy of FDG-PET in this study compared to previously reported data is probably due to strict subject selection.

The results suggest that FDG-PET may provide with more conclusive information in SPN indeterminate on chest CT.

PS-107

C.D.Ramos, H.M.Braga, S.Epelman, E.C.S.Camargo-Etchebehere, A.M.Silva, J.C.B.Gonçalves, S.Brandalise, E.E.Camargo.

Division of Nuclear Medicine, Department of Radiology and Centro Infantil Boldrini, Campinas State University (Unicamp), Campinas, Brazil.

[Tc-99m] SESTAMIBI TO EVALUATE RESPONSE OF HIGH GRADE SARCOMAS TO CHEMOTHERAPY IN CHILDREN.

Several reports in the literature have shown that the radiopharmaceutical [^{99m}Tc] sestamibi is a marker of tumoral viability. We have used this tracer to evaluate the response of bone and soft tissue high grade sarcomas to preoperative chemotherapy in children and young adults.

Eight patients (6 females, 2 males; 9-19 years of age) with biopsy-proven high grade sarcomas of the extremities (bone or soft tissue), were studied by planar imaging with [^{99m}Tc] sestamibi before and after preoperative chemotherapy. A dynamic study of 1 frame/2 seconds for 1 minute was obtained immediately after the intravenous injection of 370-740 MBq (10-20 mCi) of the tracer to assess regional blood flow. An early planar image for 500,000 counts was then acquired at 10 minutes and a whole body scan performed 1 hour later.

Tumor uptake of [^{99m}Tc] sestamibi before and after chemotherapy was graded visually as follows: 0= absent; 1= mild; 2= moderate; 3= intense. Histopathological classification divided the specimens into two groups: good responders with 95% or higher cellular necrosis; and poor responders with less than 95% of cellular necrosis.

All patients had uptake grade 2 or 3 prior to chemotherapy. After chemotherapy, all good responders had significant reduction of tumor uptake to grades 1 or 0. One of the two poor responders had a non-significant reduction of uptake to grade 2; however, the other poor responder had a significant reduction to grade 1.

These results support the concept that the reduction of [^{99m}Tc] sestamibi tumor uptake reflects the response to chemotherapy in most cases. The method was also able to detect one poor responder in this series. The reduction of uptake in a poor responder should be further investigated and may be related to the expression of the multidrug resistance glycoprotein P.

PS-108

F.A.Severiche, A.I.Joaquim, E.C.S.Camargo-Etchebehere, C.D. Ramos, L.G.Oliveira, A.S.Oliveira, S.Q.Brunetto, E.E.Camargo.

Division of Nuclear Medicine, Department of Radiology, Division of Clinical Oncology, Department of Anesthesiology and Center of Biomedical Engineering, Campinas State University (UNICAMP), Campinas, Brazil.

PHARMACOLOGICAL INTERVENTION WITH MORPHINE IMPROVES ABDOMINAL IMAGING WITH [Tc-99m] SESTAMIBI.

[^{99m}Tc] sestamibi cannot be effectively used for abdominal imaging because of its hepatobiliary excretion. The use of a substance capable of delaying the hepatobiliary excretion of [^{99m}Tc] sestamibi would theoretically prevent this problem. Morphine could be such an agent due to its direct action on the sphincter of Oddi causing functional obstruction, by a dose-dependent mechanism mediated by receptors.

The aim of this study was to evaluate the effect of morphine on the hepatobiliary excretion of [^{99m}Tc] sestamibi. Ten normal volunteers without abdominal pathology (6 males, 4 females; 22-58 years of age) were studied. After a 4 hour fasting, 0.04 mg/kg of morphine (the same dose used for hepatobiliary imaging) were injected intravenously, followed by 740 MBq (20mCi) of [^{99m}Tc] sestamibi 10 minutes later. Planar images of the abdomen in the anterior and posterior projections were performed at 10 and 60 minutes. The images showed marked retention of the [^{99m}Tc] sestamibi in the liver and gallbladder, and minimal intestinal activity.

The pharmacological intervention with morphine delayed the hepatobiliary excretion of [^{99m}Tc] sestamibi, and improved the evaluation of the abdomen at 10 and 60 minutes, without side effects. This method may be useful in the investigation of abdominal neoplasms with [^{99m}Tc] sestamibi scintigraphy.

PS-109

A.L.Joaquim, J.Y.Shinzato, C.D.Ramos, E.C.S.Camargo-Etchebehere, R.F.Vargas, F.A Severiche, M.Alvarenga, E.E.Camargo.
Division of Nuclear Medicine, Department of Radiology; and Division of Pathology, Department of Obstetrics and Gynecology, Campinas State University (Unicamp), Campinas, Brazil.

[Tc-99m] SESTAMIBI SCINTIMAMMOGRAPHY TO EVALUATE RESPONSE OF BREAST CARCINOMA TO NEOADJUVANT CHEMOTHERAPY

Accurate assessment of locally advanced breast carcinoma response to presurgical neoadjuvant chemotherapy is crucial in planning subsequent treatment. Conventional evaluation by clinical examination and mammography is not always reliable. [Tc-99m] sestamibi scintigraphy has been shown to be useful in the evaluation of response to therapy of several types of tumors such as bone and soft tissue sarcomas and brain tumors.

We have investigated the usefulness of this method to assess the response of breast carcinoma to neoadjuvant chemotherapy. Fifteen patients (35-69 years of age) with locally advanced breast carcinomas were studied with [Tc-99m] sestamibi scintimammography prior to the first cycle and 21 days after the last cycle of chemotherapy. We used prone planar images obtained 10 minutes after an intravenous injection of 925 - 1,111 MBq (25-30 mCi) of the tracer. Tumor uptake of [Tc-99m] sestamibi before and after chemotherapy was graded visually as absent, mild, moderate and intense.

Tumor response to chemotherapy was conventionally assessed by mammography, clinical evaluation and histopathological examination of the specimens in all patients. Seven patients who did not demonstrate significant change in tumor uptake were found to be poor responders to chemotherapy. Of the remaining 8 patients who were good responders to chemotherapy, 5 demonstrated significant reduction in tumor uptake and 3 showed no significant reduction in tumor uptake. The overall agreement between scintimammography and the conventional classification of tumor response, including mammography, clinical evaluation and histopathology, was 80%. The sensitivity of scintimammography for detection of good responders was 62.5%, with a specificity of 100%. On the other hand, its sensitivity for detection of poor responders was 100%.

Scintimammography with [Tc-99m] sestamibi seems to be an important adjunct in the assessment of response of locally advanced breast carcinoma to neoadjuvant chemotherapy.

PS-110

G.Capa, H.Durak, B.Değirmenci, E.Özbilek, A.Kargı, E.Derebek, A.Barutcu

Dokuz Eylül University School of Medicine Departments of Nuclear Medicine, Plastic and Reconstructive Surgery and Pathology.

IN-111 PENTETREOTIDE SCINTIGRAPHY IN MALIGNANT MELANOMA: Evaluation of residual tissue and lymph node involvement.

The aim of this study is to determine the utility of In-111 pentetrotide whole body (WB) scintigraphy to show residual or nodal metastases in patients with malignant melanoma(MM). In-111 pentetrotide was also given intradermally around the lesion site in order to determine the utility of "In-111 pentetrotide lymphoscintigraphy" in the diagnosis of lymph node metastases of MM. 8 patients(4 male, 4 female, mean age: 48±8) with a diagnosis of cutaneous MM after the excision of the primary lesion were included in the study. In 4 patients 250µCi In-111 pentetrotide was injected intradermally around the lesion. In 7 patients 3mCi In-111 pentetrotide was given intravenously. Planar and WB imaging were obtained 10min.,4h.,24h. after the injection to investigate the residual tumor and nodal involvement We found that In-111 pentetrotide lymphoscintigraphy results were false(-) in 1 patient with nodal involvement and true(-) in 3 patients without nodal involvement. In-111 pentetrotide WB scintigraphy was true(+) in 2 patients with residual tumor and true(-) in 5 patients with no residual tumor. In one patient there was a diffuse uptake pattern at the lesion site and this pattern was not evaluated as a residual tissue. In-111pentetrotide scintigraphy was false(-) in one patient with nodal involvement and true(+) in 6 patients with no nodal involvement.

In-111 pentetrotide scintigraphy may be used to evaluate the residual tissue after resection of MM.Lymph node involvement may not be visualized by In-111 pentetrotide scintigraphy.Lymphoscintigraphy with In-111 pentetrotide seems not feasible to use in evaluating lymph node metastasis.

PS-111

D. CASARA, G. SALADINI, R. MAZZAROTTO, D. RUBELLO*, G. TOMASELLA, M.E. GIRELLI***, B. BUSNARDO***.**
Radiotherapy and Nuclear Medicine, **Radiology and ***Endocrinology, University Hospital of Padua, *Nuclear Medicine, Hospital of Castelfranco V.to (TV), Italy.
Tc99m-MIBI SCAN IN PATIENTS WITH NON-FUNCTIONING METASTASES OF DIFFERENTIATED THYROID CARCINOMA. (DTC): A COMPARATIVE STUDY WITH CONVENTIONAL RADIOLOGY.

We investigated the diagnostic role of Tc99m-MIBI scan in a group of 125 pts with DTC evaluated during clinical follow-up after surgery and 131-I treatment: 101 pts had elevated serum thyroglobulin (Tg) levels, 9 with functioning (positive 131-I scan) loco-regional lymph node metastases (mts),(LNM), and 82 with non-functioning (negative 131-I scan) LNM (n. 71) and/or distant mts (DM) (n. 10). Twenty-four pts had normal serum Tg levels both during and after L-thyroxine discontinuation and were considered to be tumor-free; they were taken as controls. A comparison with neck ultrasonography (US), X-ray computed tomography (CT) scan and/or resonance magnetic imaging (RMI) was made. The presence of disease was established on the basis of histologic or cytologic findings (n. 82 pts) or of clinical findings. In the 9 pts with functioning loco-regional LNM, a close agreement between 131-I scan and MIBI scan findings was observed. In the 82 pts with metastatic disease but negative 131-I scan, MIBI scintigraphy revealed the presence of mts in 83% of cases, in most pts to neck or mediastinum LNM; moreover out of them 5 cases with LNM were positive with MIBI scan but negative with US, while 3 cases were positive with US but negative with MIBI scan. MIBI scan was positive in all the cases with mediastinal mts while CT scan and/or RMI revealed tumoral foci only in 54% of cases. MIBI scintigraphy was negative in all the 24 pts considered to be tumor-free. On the basis of these data, MIBI scintigraphy associated with neck US can be proposed as the first line diagnostic approach in the follow-up of DTC pts with high serum Tg levels and negative 131-I scan.

PS-112

CW.Choi, SM Lim, JS Lee, WI Yang and SW Hong
Korea Cancer Center Hospital, Seoul, Korea

FDG-PET IN PATIENTS WITH THYROID CARCINOMA AS A ROUTINE FOLLOW-UP PROCEDURE.

I-131 whole body scan, which needs discontinuation of thyroid hormone replacement to elevate serum TSH level, is used as a routine procedure for the evaluation of metastasis or recurrence in thyroid carcinoma patients. FDG-PET showed higher sensitivity than conventional imaging modalities in various cancers. We performed FDG-PET in 28 thyroid well differentiated thyroid carcinoma patients in order to find out whether FDG-PET can localize tumor sites. Whole body emission scan was performed 60 minutes after injection of 370 MBq of F-18 FDG and additional regional emission scan (usually neck) was taken. We compared FDG-PET results with I-131 scan (study interval within 2 months) in 10 patients with thyroid carcinoma. Twenty patients had persistent disease confirmed by I-131 scan, serum thyroglobulin (Tg) level, FDG-PET, other imaging studies (chest PA, ultrasonography, CT, MRI, etc.) and clinical observation.

Lesions with high FDG uptake were detected in 18 patients (sensitivity 90%). Among these patients 4 patients had undetectable serum thyroglobulin (Tg) level and serum Tg levels were elevated in 16 patients (sensitivity 80%). Two patients showed negative FDG-PET scan with elevated serum Tg level. Of 8 patients with remission, 7 patients had negative FDG-PET (specificity 87.5%). In comparison study of FDG-PET and I-131 scan, two patients shows no abnormal uptake in I-131 scan with multiple uptakes in FDG-PET. FDG-PET detected cervical LN metastasis in 7 patients (70%), lung metastasis in 7 (70%), and bone metastasis in 5 (50%), while I-131 scan detected cervical LN metastasis in 5 patients (50%), lung metastasis in 3 (30%), and bone metastasis in 3 (30%).

In conclusion, FDG-PET could be used as a routine follow-up procedure in thyroid cancer patients to avoid the discontinuation of thyroid hormone replacement.

Poster presentations

PS-113

E. Crippa, F. Belli, F. Gallino, M. Leutner, C. Chiesa, C. Pascali, A. Bogni, D. Decise, V. De Sanctis, M. Greco and E. Bombardieri.
National Cancer Institute, Milan (Italy)

WHICH KIND OF NODAL METASTASES CAN FDG-PET DETECT ? A CLINICAL STUDY ON MALIGNANT MELANOMA.

To determine the feasibility of FDG-PET in the detection of nodal metastases from melanoma, we are comparing FDG-PET with postoperative histopathology in patients with a clinical diagnosis (physical examination and ultrasound or CT) of nodal relapses. The current total number of evaluable nodal basins is 36 in 26 pts. A total of 511 nodes were surgically removed and metastases were histologically diagnosed in 72 of these. The metastases had a mean size of 12 mm (range 0.4-45). FDG-PET detected 100% (38/38) of the metastases > 10 mm and 26.5% (9/34) of those ≤ 10 mm (21 metastases were ≤ 5 mm). As regards the type of nodal involvement, FDG-PET detected 100% (18/18) of the massive metastases, 87.5% (7/8) of the subtotal metastases and 94% of the metastases with perinodal infiltration, regardless of the type of metastatic involvement. By contrast, FDG-PET detected only 25% (5/20) of the partial metastases and no nodes (0/8) with embolic or pluriembolic metastases. FDG-PET was correctly negative in 439 nodes without metastases ranging in size from 1.2 to 54 mm. In conclusion, our current results indicate that in melanoma FDG-PET may give an important contribution to the evaluation of enlarged nodes (sensitivity and specificity of 100%) with an equivocal clinical and/or instrumental diagnosis. However, FDG-PET cannot ensure an accurate diagnosis in metastatic nodes ≤ 5 mm and/or partial or embolic involvement.

PS-114

M. Emri, O. Ésik, F. Németh, I. Repa, L. Trón
PET Centre, Medical University, Debrecen, Hungary
Dept. of Radiotherapy, National Institute of Oncology, Budapest, Hungary
Diagnostics Centre, Pannon Agricultural University, Kaposvár, Hungary
ONCOLOGICAL APPLICATIONS OF REGISTERED AND FUSED CT, MRI AND PET IMAGES

An investigation was made of the applicability of an interactive and an automatic image registration and fusion method involving the use of morphological (CT or MRI) and functional (PET) modalities for routine daily diagnostics.

Seventeen patients (with solid tumours or malignant lymphomas) were included in the study, all presenting complex diagnostic problems. CT and MRI investigations were performed under standard conditions, and PET examinations were carried out by using 18-fluorodeoxyglucose or methionine as tracers. Data files obtained with the different imaging modalities were collected in a file server. Registration was performed with a multimodality image processing system based on the programs *Register* (Montreal Neurological Institute) and *AIR3*, automated image registration software (Laboratory of Neuro-Imaging of UCLA). The registered and resliced images were exported into the Image Display Analysis program of the PET camera for fusion, image analysis and definition of volumes of interest (VOIs). The defined VOIs (planning target volume and organs at risk) were exported into the TOMAS and VIRTUOS (developed by the German Cancer Research Centre) software package and served as input information for 3D radiotherapy planning.

Image registration and fusion proved to be very effective tools for routine daily diagnostics, providing the anatomical localization of viable tumorous tissue. These methods were of fundamental help in all 17 investigated cases, for biopsy guiding (1 case), the planning of surgical intervention (4 cases) and 3D radiotherapy (7 cases) or the solution of differential diagnostic problems (5 cases).

PS-115

L. Feggi, GL Scapoli*, N Prandini*, N Piva*, S Moretti*
Nuclear Medicine and Haematology*. Azienda Ospedaliera Arcispedale S. Anna and University*, Ferrara.

SCINTIGRAPHY WITH SESTAMIBI AND GALLIUM IN LYMPHOMA PATIENTS: PRELIMINARY RESULTS IN THE DETECTION OF RESIDUAL TUMOR DOUBTFUL ON CT

In order to evaluate residual disease in malignant lymphoma (ML) patients Ga scintigraphy is considered a very useful tool. In the present study we evaluated the usefulness of Ga67 citrate versus 99m-Tc Mibi and both in comparison with standard morphological techniques. **Material and methods:** In 18 patients (10 males and 8 females) affected by ML (9 NHL, 10 HD) aged between 14 and 69 (median age 34 yrs) we performed a total body scintigraphy with Mibi (MS) and Ga (GS), associated to tomography for a total of 48 studies. The first examination was performed 10 min after the administration of 740 MBq of the radiopharmaceutical while the second was performed on the third day after the injection of 370 MBq of Ga. To enable a further monitoring of the therapy response, scintigraphy was done as a part of the work up at the staging and at the restaging of the disease (at least 4 weeks after the end of the treatment). **Results:** All patients had a positive CT scan. Before treatment all but one patients had a positive GS, while MS was always positive. After treatment patients with a residual mass on CT were negative in all but two at GS and all but one at MS. Negative scintigraphies were confirmed by clinical evolution or biopsy or mass disappearance at consecutive CT. GS demonstrated a higher T/NT ratio in comparison to MS. Mibi uptake, in histologically confirmed cases, correlated with P-glycoprotein expression. **Conclusions:** Scintigraphy demonstrated a higher accuracy in the evaluation of residual disease in comparison to conventional diagnostic modalities (CT), affected by indetermined results. We could not demonstrate a significative difference between GS and MS due to low number of patients. Further patients are necessary to better clarify the role of Mibi versus Gallium in providing informations predicting the response to treatment in ML patients.

PS-116

C.R. Bellina, M. Grosso, G. Boni, G. Manca, B. Alberti, D. Volterrani, F. Boldrini, and R. Bianchi.
Division of Nuclear Medicine, Department of Oncology, University of Pisa, Italy

USEFULNESS OF ^{99m}Tc-TETROFOSMIN SCINTIGRAPHY IN THE PRE-SURGICAL STAGING OF THYROID CARCINOMA
Ultrasound study (US) of the neck combined with fine needle aspiration biopsy (FNAB) is extensively employed in the pre-surgical staging of thyroid carcinoma. CT and MRI are usually used when an extracervical extension of the tumor is suspected. However, these techniques cannot identify distant metastases, such as bone metastases, which are present in 5-15% of patients (pts) at the time of the diagnosis. Aim of this study was to evaluate the usefulness of ^{99m}Tc-Tetrofosmin in pts affected by thyroid carcinoma.

Eighteen pts (11F, 7M; age 23-76 yrs) with a cytologic diagnosis of thyroid carcinoma underwent an US of the neck, a FNAB of suspected lymph nodes and a scintigraphy with ^{99m}Tc-Tetrofosmin (740 Mbq). Whole body images, planar and SPECT acquisitions over the neck and the thorax were obtained after tracer i.v. injection in all pts. A CT-scan of the neck and the upper mediastinum was performed in 4 pts. A total thyroidectomy was performed in all pts and a laterocervical lymph nodes dissection in 2 pts. All pts underwent a subsequent post-therapeutic radioiodine WBS. Histology showed a well differentiated papillary carcinoma in 12 pts and poor differentiated in 3, a follicular carcinoma in 1 pt, an insular carcinoma in 2 pts. Three pts presented multiple bone metastases. US of the neck combined with FNAB was positive in all pts with laterocervical and jugular lymph node metastases but did not identify infiltrations under the jugulum. ^{99m}Tc-Tetrofosmin scintigraphy was positive in all the lymph node metastases showed by US. Moreover, scintigraphy showed a mediastinal lymph node involvement in 2/2 pts and bone metastases in 3/3 pts with a poor differentiated carcinoma.

These preliminary data confirm the usefulness of ^{99m}Tc-Tetrofosmin scintigraphy in the pre-surgical staging of thyroid carcinoma, especially for identifying the presence of mediastinal lymph node and bone metastases in pts with poor differentiated carcinomas.

PS-117

H.Hadjikostova, S.Sergieva*, D.Damjanov*, G.Kirova*, D.Mihov

Medical University, *National Oncology Center, Sofia, Bulgaria

Clinical application of 99mTc-MIBI in imaging and follow-up of patients with lung cancer

The aim of this study was to establish the diagnostic utility of 99mTc-MIBI in diagnosis and follow-up of patients(pts) with lung cancer (LC). Planar and tomographic imaging was performed 30 and 90 min. post i.v. injection of 99mTc-MIBI (555 - 740 MBq)in 150 pts with different lung tumors. Primary lung cancer was proved in 127 of them (58 were with squamous LC, 35-with small cell LC and 34-with adenocarcinoma),8 were with fibromas and 15 - with metastatic lung lesions. Control group of 53 pts without any tumor disease was studied. In order to quantify 99mTc-MIBI uptake Tumor/Background ratio(T/B) was calculated. Data were statistically managed using Excel 7.0 Statistical tools and paired and unpaired T-test. Twenty of pts with SCLC were examined before and after carrying out III-VI courses chemotherapy. Out of 20 pts 9 showed complete or partial response to this treatment and parallel reduction of the mean T/B ratio 1.26(range 1.17-1.32, p<0.001). Bone and brain suspected metastases were visualized in 14 pts. Sensitivity for 99mTc-MIBI diagnosis of LC was 95.8%, specificity -65.4% and accuracy -85%,PPV(positive predictive value)was83.5%,NPV (negative predictive value) was 91.5%. In conclusion 99mTc -MIBI scintigraphy is a non-invasive, high sensitive and useful method in the diagnosis and evaluation of clinically suspicious lung cancer and in the visualization of unknown distant metastases and follow-up the pts with this tumors .

PS-118

V. Ivancević, M. Plauth, S. K pferling, D. Sandrock, H. Lochs, D.L. Munz.

Clinics for Nuclear Medicine and Gastroenterology, Charit , Humboldt University, Berlin, Germany.

Tc-99m TETROFOSMIN SCINTIGRAPHY IN HEPATOCELLULAR CARCINOMA

Since some malignant tumours have been shown to accumulate Tc-99m 1,2-bis [bis (2-ethoxyethyl) phosphino] ethane (tetrofosmin), we prospectively investigated the potential value of tetrofosmin scintigraphy in the non-invasive diagnosis of hepatocellular carcinoma (HCC). Sixteen patients (age range, 34-78 years; median age, 59 years) with suspected HCC were included. In all of them ultrasound, CT, MRI, and/or angiography were performed prior to scintigraphy. Histopathology verified 8 HCC, 3 focal nodular hyperplasias/adenomas, and 1 dysplasia, cyst, and cirrhosis each. In 2 patients histopathological examination was omitted, because the respective lesions were considered to be benign which was proven by follow-up. After intravenous injection of 750 MBq of Tc-99m tetrofosmin as a bolus a dynamic study was performed for 60 min (1 frame/min) using a 128 word acquisition matrix followed by SPECT of the upper abdomen (128 word matrix in 64 frames, 30 s each).

The dynamic study revealed moderate tetrofosmin accumulation in the area of the tumour in 7/8 patients with HCC, while 6/8 benign lesions were true negative. Two cases of focal nodular hyperplasia showed transient uptake in the early dynamic phase only. An encapsulated HCC of 12 cm in diameter was false negative. The SPECT studies did not yield any significant additional information.

In conclusion, tetrofosmin accumulates in HCC. Uptake might be diminished or absent, if the respective tumour is encapsulated. A more sophisticated kinetic analysis could enhance differentiation between HCC and focal nodular hyperplasia.

PS-119

H. Jan KE Britton, MR Feneley, M Granowska, SJ Mather, D Ellison, AR Granowski.

Departments of Nuclear Medicine and Urology, St. Bartholomew's Hospital, London.

IMAGING PROSTATE CANCER WITH¹¹¹INDIUM LABELLED MONOCLONAL ANTIBODY.

An antibody against prostate membrane specific antigen, PMSA, is labelled with In-111 (Cytogen Corp, Proscint) and used to evaluate patients with prostate cancer either prior to radical surgery or during follow up with rising PSA and a negative bone scan as in our previous experience with ^{99m}Tc anti-PMSA. 100MBq ¹¹¹In anti-PMSA, was given to 52 men with prostate cancer imaged at one, 24 and 48h using a gamma camera (Siemens Orbiter) set with a medium energy collimator and peaked for both energies, with SPET, 64 steps, 40 s per step. 30 studies have followup. Of 23 men with clinically localised cancer, 14 had evidence of extra-prostatic extension and five also had positive nodes; nine had scans showing cancer confined within the prostatic margins, one of whom had nodal involvement. Six had previous radical prostatectomy. Of these, five had evidence on imaging of local recurrence, with positive lymph nodes also in two; and one had a true negative scan. One patient with para-aortic lymphadenopathy was scan positive confirmed by biopsy. In conclusion, residual and recurrent disease, and local extension of prostate cancer and soft tissue metastases prior to primary surgery may be detected. Radical prostatectomy was been avoided in three on the basis of the scan alone. Evidence of a soft tissue cause of a rising PSA aids patient management.

PS-120

S. Klutmann, K.H. Bohuslavizki, S. H ft, J.A. Werner, W. Brenner, S. Kr ger, E. Henze

Clinics of Nuclear Medicine and Otorhinolaryngology, Head and Neck Surgery, University of Kiel, Germany.

LYMPHOSCINTIGRAPHY USING DOUBLE TRACER TECHNIQUE IN SQUAMOUS CELL CARCINOMA OF THE HEAD AND NECK

In preoperative planning of head and neck cancer it is most desirable to predict possible lymph node involvement in a non-invasive fashion in order to identify individual aberrant lymphatic drainage. Lymphoscintigraphy enabling an accurate localization of lymph nodes may facilitate surgery. We report on a new method of lymphoscintigraphy in double tracer technique with simultaneous body-contouring.

Lymphoscintigraphy was performed preoperatively in 78 patients with squamous cell carcinoma of the head and neck. Patients received 100 MBq Tc-99m-collloid dissolved in 0.1-0.2 ml in 3-4 peritumoral sites. 2 ml of perchlorate solution were given orally in order to block the thyroid gland. 20 min later all patients received 50 MBq Tc-99m-pertech-netate i.v. for body-contouring. Planar images were obtained over 5 min each at 30 min and 4 h from anterior, right lateral and left lateral views using a LFOV-gamma camera equipped with a LEAP-collimator. Lymphatic drainage was assessed by visual inspection and correlation of lymphatic drainage to the six known cervical compartments.

The thyroid gland was seen in any of the patients. 28/78 = 36 % of the patients showed no lymphatic drainage at all. Lymph nodes could be easily assigned to the six cervical compartments in 50/78 = 64 %. 36/78 = 46 % showed unilateral, and 14/78 = 18 % exhibited bilateral lymphatic drainage. Although in 13 out of these 14 patients the primary tumor was localized unilateral, lymphatic drainage was observed on both sides of the neck. In one of these patients scintigraphic findings resulted in a more extended bilateral neck dissection.

Lymphoscintigraphy using double tracer technique allows an accurate correlation of lymphatic drainage to cervical lymph node compartments. This may provide the basis for a re-evaluation of its impact in preoperative planning in tumors of the head and neck.

PS-121

T.Komori, I.Narabayashi, R.Matsui, K.Sueyoshi, I.Adachi, T.Shimizu, K.Utsunomiya, Y.Nakata and K.Doi.
Osaka Medical College, Osaka, Japan.

Evaluation of Uptake and Release with Technetium-99m MIBI SPECT in Pulmonary and Mediastinal Lesions.

We evaluated the uptake and release of Tc-99m MIBI in pulmonary and mediastinal lesions (6 benign, 30 malignant). Thirteen patients underwent surgical operation and malignant involvement was examined in 21 mediastinal lymph nodes. Tl-201 SPECT was also performed in 10 patients. Tc-99m MIBI SPECT was performed 30 minutes and three hours after intravenous injection 600MBq of Tc-99m MIBI with three gammacamera detectors, GCA-9300A on transverse SPECT image. Regions of interest were set in the area of abnormal uptake of Tc-99m MIBI and in that of the contralateral normal lung. The uptake ratio of the lesion to the contralateral normal lung was obtained on early image (early ratio:ER) as well as delayed image(delayed ratio:DR). Retention index(RI) was calculated as follows: $RI = (DR - ER) / ER \times 100$. There existed significant difference between benign and malignant lesions for the ER and for the DR (benign and malignant; ER, 1.3 ± 0.3 , and 1.9 ± 0.5 , $p < 0.05$, DR, 1.4 ± 0.4 and 1.8 ± 0.5 , $p < 0.05$). There was no significant difference by RI. The DR of Tl-201 SPECT was significantly higher than that obtained with Tc-99m MIBI SPECT ($p < 0.05$). On the macroscopic diagnosis of mediastinal lymph node metastases, the sensitivity, specificity, and accuracy were 71.4%, 85.7%, and 80.9%, respectively on early images and 71.4%, 92.9%, and 85.7%, respectively, on delayed images. These results suggest that the uptake ratio of Tc-99m MIBI is a useful index of assessing benign or malignant pulmonary and mediastinal lesions.

PS-122

P. Koranda, M. Kala, M. Mysliveček, O.Lang*, V.Hušák
Depts. of Nucl. Med. and Neurosurg., Palacký Univ., Olomouc,
Dept. of Nucl. Med., Charles Univ. Prague, Czech republic

COMPARATIVE STUDY WITH 99mTc-MIBI SPECT AND 99mTc-DTPA SPECT IN GLIOMAS

99mTc-MIBI SPECT has been used in the assessment of the degree of a brain tumor malignancy. The aim of this study was to compare the tumor-avid uptake of MIBI with the DTPA-accumulation indicating the blood-brain barrier damage.

Eleven patients with histologically verified gliomas (5 low-grade tumors I,II and 6 high-grade tumors III,IV) were studied with double-headed gamma camera equipped with fan-beam collimators. The SPECT acquisition was started 20 min and 60 min after injection of 600 MBq 99mTc-MIBI and 600 MBq 99mTc-DTPA, respectively. The identical acquisition parameters (3° and 30 sec/step, matrix 128x128) were used in both studies. Besides the visual analysis the tumor/non-tumor (T/NT) ratio was calculated.

All high-grade gliomas revealed an increased MIBI- and DTPA-uptake, however, the distribution of the radiopharmaceuticals in lesions was different. In one patient DTPA-uptake was present in the peritumoral lesion without concurrent accumulation of MIBI. In the group of low-grade gliomas pathological accumulation of MIBI was not detected, but one tumor exhibited intensive uptake of DTPA.

Pat.	Grade	T/NT MIBI	T/NT DTPA
1	IV	15.5	21.3
2	IV	15.3	4.5
3	IV	6.2	9.9
4	IV	2.8	5.1
5	III	6.8	6.1
6	III	5.6	11.1+peritum.
7	II	1	6.8
8,9,10	II	1	1
11	I-II	1	1

Although statistical significance cannot be achieved by this data due to small sample size, the results suggest that MIBI-uptake in gliomas does not reflect the deterioration of the blood-brain barrier. It is concluded that MIBI-SPECT is a valuable tool for evaluation of the biological characteristics of brain tumors.

PS-123

L. Krollicki, J. Stelmachow, J.B. Cwikla
Medical Academy II; Departments MRI and Nuclear Medicine; and Obstetrics and Gynaecology; Warsaw, Poland.

EVALUATION OF Tc99m MIBI UPTAKE IN PATIENTS WITH SUSPECTED OVARIAN CANCER. INITIAL STUDY.

The diagnosis of ovarian cancer particularly in the early stages of the disease can be problematical. CT and ultrasound could be unhelpful in early stage of disease and often underestimate the extent of disease, particular in mesenteric and peritoneal deposits.

To determine if functional imaging using Tc99m MIBI may be accurate to be used in patients with suspected ovarian cancer a prospective trial was performed in 14 women (mean age 53, range 21-82) with a clinical suspicion of ovarian cancer.

Each woman was imaged at 5min post injection of 750MBq Tc-99m MIBI. Planar image of the pelvis and abdomen was performed using 256x256 matrix, with LEHR collimator.

Laparotomy was done in all patients within 5 days of the Tc-99m MIBI scan. There were 12 cancers verified by histological examination of biopsy material obtained at laparotomy. All these cancers were positive on imaging with Tc-99m MIBI. It was noted that Tc99m MIBI was able to identify peritoneal metastatic disease not seen on previously done ultrasound and CT. We noted 2 benign lesions. There was 1 polycystic ovary and 1 dermoid cyst. No one had uptake of Tc99m MIBI. In this initial study we noted 12 cases true positive and 2 cases true negative.

Using Tc-99m MIBI it is possible to identify all patients who have cancer (including sites not detected in ultrasound and CT as well).

It has been suggested that uptake of Tc-99m MIBI is affected by the expression of drug resistance, like products of genes encoded Pgp or MRP. In those patients with widespread disease whom chemotherapy is treatment of choice, information about potential drug sensitivity of the tumour seems to be very useful.

Further study after cytotoxic chemotherapy of those patients with higher grade of disease, also clinical and/or pathological follow-up should be performed to confirm usefulness of this functional study.

PS-124

Lamki, L., Barron, B., Stroehlein, K., Tamm, E., Bull, J. Holoye, p., Fang, B. Requenez, E., Ephron, V.

The University of Texas Medical School and Hermann Hospital, Houston, Texas, USA

TC-99M-LL2 (MONOCLONAL ANTIBODY AGAINST RAJI CELLS) IN THE INITIAL STAGING AND FOLLOW-UP OF B-CELL LYMPHOMA; UTILITY AFTER THERAPY

PURPOSE: To evaluate the role of Tc-99m-LL2 in the initial staging and follow-up of B-cell lymphoma, and compare it to current diagnostic modalities (CDMs).

METHODS: 13 patients were studied with Tc-99m labeled monoclonal antibody (Mab) Fab fragment against Raji cells (CD22) in the initial staging protocol. Nine of these patients had a repeat follow-up study after completion of chemoRx. Degree of uptake was correlated with flow cytometry and histologic cell type -- as well as Ga-67 imaging and CT/MRI/US scans. 30mCi of Tc-99m-LL2 I.V. were followed by imaging planar and SPECT at 4 and 20 hours.

RESULTS: 52 sites of abnormal localization were detected by Tc-99m-LL2 in the 2 protocols. 33 were known, but Tc-LL2 missed 7 lesions, and detected additional 20 "occult" lesions. Residual unsuspected disease was detected in 7/9 patients by the follow-up study. All specimen tested were positive for CD20 or CD22 antigens. In addition, large cell type showed greater Tc-99m-LL2 antibody localization than did small cleaved cells.

CONCLUSIONS: 1) Tc-LL-2 has a definite potential role to play in staging of B-cell lymphoma and complimentary to CT scans; 2) Tc-LL2 may have even a greater role in restaging/follow-up of these patients.; 3) In follow-up of patients, it was more sensitive in detecting activity of disease than CDMs and; 4) Tc-LL2 may be used to determine end-point of ChemoRx.; 5) Tc-LL-2 has a potential role in selecting patients for radio/immunotherapy with CD20 and CD22 antibodies.

Supported by Immunomedics, Inc.

PS-125

Z. Lengyel, O. Ésik, A. Rosta, L. Galuska, L. Trón

PET Centre, Medical University, Debrecen, Hungary
National Institute of Oncology, Budapest, Hungary
Dept. of Nuclear Medicine, Medical University, Debrecen, Hungary

FDG PET FOR LYMPHATIC STAGING AND RESTAGING IN PATIENTS WITH HODGKIN'S DISEASE (HD)

The role of FDG PET examinations in the lymphatic staging and restaging of HD was investigated. Thirty-eight consecutive whole-body (cervical, thoracic and abdominal) FDG PET investigations were performed in 34 HD patients with a GE 4069 Plus camera. The number of involved lymphatic regions was determined retrospectively by using the Ann Arbor nomenclature. The results of the PET examinations were compared with those numbers obtained with the combined information provided by physical examination, radiological diagnostics (CT, US, MRI) and gallium scintigraphy.

The number of involved lymphatic regions, determined on the basis of non-PET methods vs. FDG PET examinations, were as follows: Waldeyer ring 0 vs. 2, right cervical and supraclavicular 0 vs. 17, left cervical and supraclavicular 1 vs. 21, right infraclavicular 0 vs. 5; left infraclavicular 0 vs. 5, right axillary 1 vs. 8, left axillary 2 vs. 10, mediastinal 26 vs. 37, right pulmonary hilar 3 vs. 7, left pulmonary hilar 4 vs. 5, paraaortic 4 vs. 21, splenic 3 vs. 17, right mesenteric 1 vs. 11, left mesenteric 0 vs. 13, right parailiacal 1 vs. 9, left parailiacal 1 vs. 10. The inguino-femoral, epitrochlear and popliteal areas were not always fully included in the investigations, and thus they were not evaluated.

Due to its high sensitivity, FDG PET provides more complete and precise information about the anatomical extent of the HD than physical examination or conventional radiological and nuclear medicine methods do. The distribution of the involved lymphatic regions showed basically similar trends to those reported by Kaplan et al. (Natl. Cancer Inst. Monogr., 36: 291, 1973). The relatively high rates of mediastinal and mesenteric involvement are attributed to the leading cause of PET indication, and the advanced stage of the disease, respectively. Routine application of FDG PET examination for primary staging and restaging (including therapeutic monitoring) of HD is highly advocated.

PS-126

GS Limouris¹, V Voliotopoulos¹, A Iovanovic², D Tsoutsos², SK Shukla³, A Frantzis¹, I Vlahos¹, A Stauraka¹;

¹Nuclear Medicine Div, Areteion Hosp, Univ Medical Faculty, Athens;²Gen Civ Hosp G.Gennimatas, Plast Surg Dept, Athens;³Nucl Med Dept, St Eugenio Hosp collab CNR, Rome

TWO PHASE SCINTIGRAPHIC MAPPING OF LYMPHATIC DRAINAGE IN CUTANEOUS MELANOMA USING ^{99m}Tc-S-MICROCOLLOID/¹¹¹In PENTETREOTIDE

The purpose of lymphoscintigraphy in patients with melanoma before surgery is to image the lymphatic drainage net and particularly to detect the sentinel node; the purpose of somatostatin receptor scintigraphy before or after surgery is to characterise the malignancy, map the lymphatic drainage and detect a possible secondary spread towards the lymph nodes surrounding the surgical field or more distal regions. The aim of the present was to assess the sensitivity of a two phase procedure with ^{99m}Tc-S-microcolloid and ¹¹¹In-pentetreotide for exploring possible spread of melanoma.

Twenty-seven melanomectomized patients were enrolled into the study. The melanomas were situated on the head, back, arm, buttock and feet of these patients. Intracutaneous lymphoscintigraphy with ^{99m}Tc sulphur microcolloid [Lymphoscint, Solco, Basel] and i.v. scintigraphy with ¹¹¹In pentetreotide [Octreoscan111, Mallinckrodt, BV, Petten] in a dosage of 55 MBq and 111 MBq respectively, was performed in 27 patients to define possible infiltration of lymph nodes after surgery with a time interval of 1 week between the two examinations. ^{99m}Tc sulphur microcolloid preceded the ¹¹¹In pentetreotide scan. The scintigrams were evaluated by three experienced nuclear physicians.

The method correctly detected 50 out of 81 suspicious nodes as malignant. Combined two phase technique improves the diagnostic and staging accuracy of cutaneous melanoma affected population and appears extremely useful in the surgical confrontation of the lymphatic spread.

PS-127

C.P. Chang, R.S. Liu, J.K. Wang, S.H. Yen, L.C. Wu, S.M. Yu, S.Q. Liao, L.S. Lee, F.Q.H. Ngo, and S.H. Yeh.
Taipei Veterans General Hospital, National PET/Cyclotron Center, and National Yang-Ming University School of Medicine, Taipei, Taiwan.

DISCORDANT DISTRIBUTION OF [F-18]FLUORODEOXYGLUCOSE (FDG) AND [F-18]FLUOROMISONIDAZOLE (FMISO) IN BRAIN TUMORS.

Accumulation of both FDG and FMISO in tumor may be substantially enhanced by hypoxia. However, FDG uptake is more complicated than FMISO, because its accumulation may also be caused by an enhanced glucose utilization, tumor-associated macrophages and granulation tissues. In this study we compared the distribution of FMISO and FDG in brain tumor to assess if increased FDG uptake in tumor could be as useful to be a hypoxic marker as FMISO.

Fourteen patients with brain tumors were studied with FDG and FMISO PET in alternative days. FMISO imaging was carried out at 2 hr after iv injection of 370 MBq (10 mCi) of tracer. Side-by-side visual interpretation of FDG-PET images, FMISO-PET images, and CT or MRI images was performed. FMISO uptake ratio was also generated from the tracer uptake in the tumor divided by the uptake in cerebellum. Tumor uptake ratio greater than 1.24 was considered to be hypoxic (Yeh, et al. Eur J Nucl Med 1996; 23:1378-83). Interstudy fusion of FDG and FMISO images was done using similar measure image registration technique. Hypoxia was found in 10 out of 14 brain tumors (71%). Four tumors had both increased FMISO and FDG uptake and three had decreased uptake of the two tracers. Six hypoxic tumors with high uptake of FMISO had decreased FDG uptake and one normoxic tumor without accumulation of FMISO had enhanced FDG uptake. Only four hypoxic tumors (40%) had high uptake of FDG. The registered images demonstrated discordant distribution of FMISO and FDG in all hypoxic tumors.

In conclusion, hypoxia is commonly seen in brain tumors, and FMISO is more sensitive than FDG in detecting hypoxia. The facts of low sensitivity and discordant FDG and FMISO uptake in brain tumor discourage the FDG-PET in evaluation of hypoxia in brain tumor.

PS-128

Y.K. Chu, R.S. Liu, S.H. Yen, C.P. Chang, L.S. Chu, S.M. Yu, K.L. Chou, L.C. Wu, S.Q. Liao, K.Y. Chen, and S.H. Yeh.

Taipei Veterans General Hospital, National PET/Cyclotron Center, and National Yang-Ming University School of Medicine, Taipei, Taiwan.

THE PROGNOSTIC VALUE OF [F-18] FLUOROMISONIDAZOLE IN PATIENTS WITH NASOPHARYNGEAL CARCINOMA RECEIVING RADIATION AND CONCURRENT CHEMOTHERAPY.

Positron emission tomography (PET) with [F-18]fluoromisonidazole (FMISO) demonstrates hypoxia in primary as well as metastatic cervical lymph nodes in nasopharyngeal carcinoma (NPC). This study was undertaken to verify if imaging with FMISO could be used to predict the outcome of patients with NPC receiving radiation and concurrent chemotherapy.

Forty NPC patients were studied with FMISO and [F-18]FDG before treatment. PET imaging was performed at 2 hr after intravenous injection of 370 MBq (10 mCi) of FMISO. Tomograms were reconstructed and evaluated visually. ROI analysis was carried out to calculate tumor/muscle retention ratio (TMRR) of NPC or cervical nodal metastases over the suboccipital muscles. Threshold of TMRR of FMISO was set at 1.24 to separate tumor hypoxia versus normoxia (Eur J Nucl Med 1996; 23: 1378-83). FMISO and FDG images were fused using similar measure image registration technique. Extent of abnormal FMISO and FDG uptake was visually interpreted according to the registered images. The clinical outcome was evaluated at least one year (average:20 months) after completion of treatment. All patients were subdivided into groups of complete remission and poor outcome (persistent disease, recurrence or mortality). Tumor hypoxia occurred in 75% (30/40) NPC patients. In 25 patients with complete remission of NPC, tumor hypoxia was observed in 64% of lesions. 88% hypoxic tumors had less extent of FMISO uptake than FDG, only 12% had equal extent FMISO and FDG uptake. In patients with poor outcome, the incidence of tumor hypoxia was 93%. 71% hypoxic tumors had greater or equal extent of FMISO uptake than FDG, and 29% hypoxic tumors had less extent of FMISO uptake than FDG. TMRR (mean ± s.d.) was 2.13 ± 0.92 in patients with complete remission, and 1.91 ± 0.47 in patients with poor outcome. There was no statistical difference between the two groups (p>0.5).

In conclusion, tumor hypoxia is rather common in NPC, and the extent of hypoxia determined by FMISO PET imaging is a useful prognostic factor to predict the outcome of patients with NPC receiving radiation and concurrent chemotherapy.

Poster presentations

PS-129

St. Lourens, J.P. Wielepp, D. Lüscher, A. Crazzolaro, J.A. Kinser, Ch.U. Brand*, A. Banic*, A. Barth*, L.R. Braathen*, H.-B. Ris*. Department of Nuclear Medicine in conjunction with the Melanoma Board*, University of Berne and Inselspital, Switzerland

SENTINEL LYMPH NODE LYMPHOSCINTIGRAPHY AND SELECTIVE LYMPHADENECTOMY IN PATIENTS WITH MALIGNANT MELANOMA

Purpose: In the management of malignant melanoma, demonstration of the first line of lymphatic drainage, the sentinel lymph node, prerequisite to selective lymphadenectomy, is of critical therapeutic and prognostic importance, second only to excision of the primary lesion. This prospective study compared the results of sentinel lymph node mapping with the histological findings following selective lymphadenectomy.

Methods: We performed lymphoscintigraphy in 106 patients (52m, 54f), mean age 53 years (range 25-83) presenting with malignant melanoma. The distribution of melanoma location among patients was: upper limb, 23; lower limb, 42; trunk, 31; head and neck, 10. ^{99m}Tc-Nanocolloid (Nanocol™) was injected intracutaneously along the periphery of the melanoma or operative scar in healthy, non-oedematous skin. A dynamic acquisition of the lymphatic drainage basin was performed over 10 min, followed by static images in two orthogonal planes every 5 min. Images of the contralateral side were also acquired. The location of the demonstrated lymph nodes was marked on the skin with indelible ink.

Results: Selective lymphadenectomy was performed in 104 patients (not performed in 2 patients with double carcinomas). The sentinel node was not found in 3 patients. Of the remaining 101 patients, metastatic involvement of the sentinel lymph node was established in 17 (17%) (histology: n=10, immunohistochemistry: n=7). In 9% of patients with Breslow I lesions (<1.5mm) and in 21% of those with Breslow II lesions (>1.5mm), nodal metastatic involvement was found. Bilateral lymphatic drainage was found in 3 patients with trunk lesions.

Conclusion: Sentinel lymph node mapping (anatomically predictable as well as unpredictable divergent lymphatic drainage) effectively facilitates selective lymphadenectomy, whereby only the primary draining lymph nodes are excised for histological examination and staging purposes. In the case of histologically proven metastatic nodal involvement, an elective radical lymph node dissection is subsequently performed. In the case of histologically negative nodes, the patient can be spared this procedure and its associated morbidity. It is important to note that, although selective lymphadenectomy is usually considered unnecessary with lesions <1.0mm, in 9% of patients with Breslow I lesions (<1.5mm), nodal metastatic involvement was found.

PS-130

I. Makajová, F. Makai+, S. Kováčová, J. Kordoš+, M. Vívodová, R. Hajtš, J. Veselý, J. Tomeková, K. Hamarová, Š. Podaná, Nuclear Medicine Clinic Medical Faculty UK and St. Elisabeth Oncological Institute, +First Univer. Department of Orthopedic, BRATISLAVA, Slovak Republic

THE SIMPLEST METHOD FOR DIFFERENTIATION OF A BONE LESION IN HYPERNEPHROMA (M. GRAWITZ)

Hypernephroma is a tumor with a very high vascularization. Therefore in radionuclide perfusion study a „tumor blush“ is demonstrated during the perfusion phase, indicating increased microcirculatory flow. For this reason we can expect, that also the bone metastases of this tumor will have the high vascularization rate, while the osteogenesis is lower often with appearance of „cold lesions“ or „false negative“ lesions.

Therefore we performed radionuclide angioscintigraphy (flow study) in suspicious bone region, followed with „blood pool“ and bone imaging.

From a selected group of 32 patients in 20 from them there was a very high „blush“ flow detected. In 19 of them the presence of metastases was confirmed with other methods or surgically. In one case the reason of high flow was a fresh bone graft.

The sensitivity and specificity of this „flow study“ was 1.0 resp. 0.92, with the positive predictive value 0.95 and negative predictive value 1.0.

Conclusion: The radionuclide angioscintigraphy, resp. the three-phase bone scan allows with high predictive value differentiate the nontreated viable bone metastasis in renal cancer.

PS-131

M. Malešević, Lj. Stefanović

Institute of Oncology in Sremska Kamenica, Department of Nuclear Medicine

TECHNETIUM 99m-MIBI SCAN IN THE FOLLOW UP OF PATIENTS TREATED FOR DIFFERENTIATED THYROID CARCINOMA

Aim of this paper is to estimate the contribution of ^{99m}Tc-MIBI, in comparison to ¹³¹I scintigraphy in the follow-up of patients with differentiated thyroid carcinoma. All patients underwent total or near-total thyroidectomy with 96.7% of patients receiving an additional radioiodine therapy. In the course of scanning with these two markers, we checked thyroglobuline (Tg) and thyrostimulating hormone (TSH) levels. **Results:** the whole-body scintigram with ^{99m}Tc-MIBI and ¹³¹I was performed on 61 patients. There were 11/61 (18.03%) patients with follicular, and 50/61 (81.97%) with papillary thyroid carcinoma. Comparing these two types of scintigrams we obtained the following results: true positive (TP) ^{99m}Tc-MIBI scintigrams in 13/61; true negative (TN) in 40/61; false positive (FP) in 5/61, and false negative (FN) in 3/61 patients. Based on these data we determined: sensitivity (Se=81.2%), specificity (Sp=88.8%) and accuracy (A=86.8%) of diagnostic scintigram obtained with ^{99m}Tc-MIBI. In the group of TP scintigram findings there were 9/13 (69.2%) patients with increased Tg levels. These patients were in stage IV of the disease. In these patients the Tg level was increasing under the endogenous stimulation of TSH. Only in 7/13 (53.8%) patients with TP scintigram findings, Tg level was increased under a good suppressive/substitutional l-thyroxine therapy. **Conclusion:** We showed that the diagnostic scintigram ^{99m}Tc-MIBI has a very good sensitivity, accuracy and especially specificity. According to our opinion, ^{99m}Tc-MIBI scintigram can only be an addition but never an absolute substitution of diagnostic ¹³¹I scintigram in the follow-up of the patients with treated differentiated thyroid carcinoma.

PS-132

C. Marí, LL. Bernà, JA. Lopez-Pousa, A. Flotats, JC. Martín, A. Catafau, M. Estorch, I. Carrió. Hospital Sant Pau, Barcelona. Spain. Department of Nuclear Medicine.

EVALUATION OF TUMOR RESPONSE TO PRESURGICAL CHEMOTHERAPY IN MUSCULOSKELETAL SARCOMAS WITH THALLIUM-201 (Tl) AND TETROFOSMIN-Tc99M (TTF)

Aim: To evaluate the efficacy of Tl and TTF as indicators of the response to presurgical chemotherapy in musculoskeletal sarcomas.

Methods: 15 patients, 9 males and 6 females (mean age 32±17 years), with the following biopsy-proven tumours: 7 osteosarcomas, 4 Ewing's sarcomas, 2 sinovial sarcomas and 2 soft tissue sarcomas, were studied pre and post presurgical chemotherapy. Tumoral activity was evaluated obtaining a tumor/control ratio (TCR) pre and post chemotherapy. The percentage of change in the tumor/control ratio before and after chemotherapy (variation ratio) was correlated with the percentage of tumor necrosis observed in the surgical specimen. Tumoral necrosis was classified into 3 grades: Grade I (>90%), grade II (60-90%) and grade III (<60%).

Results: The mean value of tumor/control ratio pre and post presurgical chemotherapy was, Tl: 3.33±1.68 and 2.48±1.71, TTF: 2.74±1.49 and 1.74±1.01. The mean percentage of observed necrosis was 47.5±43.9. The mean percentage of variation ratio with Tl was 37.17±68.89 and with TTF 72.83±39.78. The variation ratios with Tl and TTF in patients with necrosis grade I (mean 95%) were: 85.5±20.5 and 100±0, with grade II (mean 65%): 82.14±0 and 90.82±0 and with grade III (mean 10±17.32%): -10±70.53 and 48.67±46.65. The ratios obtained with Tl correlated well with the histologic grades (p=0.019, r=0.88), the correlation with TTF and between both tracers was not significant.

Conclusion: Tl seems to be a better indicator of the response to presurgical chemotherapy in musculoskeletal sarcomas than TTF.

PS-133

J. Markwardt, Sprenger, H.-J., Michel, M., Henker, C.

Humboldt-University, Robert-Rössle-Clinic, Nuclear Medical Dept.
D 13122 Berlin, Lindenberger Weg 80

EXPERIENCES WITH AUTOMATIC COMPARISON OF BONE SCINTIGRAMS

The aim of the study was to assess the clinical value of the automatic evaluation of whole body bone scintigrams. It is performed by a method described earlier (SPIE Proceedings 1357:117-125, 1989). The results of the automatic procedure were compared with the results of the conventional procedure. Two different bone scans of 14 patients - one actual and one up to 3 years old - were used.

Central point of the automatic procedure are comparisons of congruent scans. After the anterior and posterior whole body bone scans are adapted to a normal skeleton by a geometrical transform, normalizing of the pulse content and elimination of background pulses the IBM Risk computer compares the actual whole body bone scan with a "normal" scan, with a previous one or its left with its right side.

Mean values of 28 images (anterior and posterior) are given below:

Comparison:	left/right side	with normal	in time
skull	3.5/0.1/4.4	2/0.2/1	0/0/0
spine	5/0.1/3.3	0.5/0.5/0.04	0.1/0.1/0
chest	7.6/0.2/18	2.4/0.6/5.5	3/0.1/3.7
pelvis	3/0.03/5.7	1.1/0.1/0.2	0.1/0.4/0.1
extremities	15.3/0.2/12.8	6.4/0.6/5.3	0.2/0.9/0.7
all	34.4/0.6/44.4	13.3/2.1/12.1	3.4/1.6/4.5

(correct positive / false negative / false positive of more than 300 locations)

The sensitivity is acceptable but the number of false positive is relatively high, esp. in left to right comparisons and in some comparisons with normal. For getting the scans congruent, the determination of landmarks with high accuracy is the major problem, which in part is interactively assisted. The refinement of automatic landmark determination procedure will improve the situation.

Despite some problems, the results indicate the possibility to detect automatically gross and minor changes of bone metabolism, partially not perceived by the observer. It helps in education and gives assistance in the evaluation of bone scans. It has been introduced into clinical use.

This system was developed in COST B2 activities and has been sponsored by the DFG.

PS-134

J. Mora, J. Ponce, M. Gil, Y. Ricart, A. Muñoz, A. Fernández, A. Benítez, M. Roca, E. Balagueró and J. Martín-Comin
S. Medicina Nuclear. CSUB Hospital de Bellvitge. Hospital de Llobregat. Spain

Monoclonal Antibody B 72.3 scintigraphy interpretation in ovarian carcinoma.

The aim of the work was to evaluate the usefulness of B 72.3 scintigraphy in the management of patients with ovarian carcinoma (OC).

16 patients were studied, mean age 60.4 years. All patients but 1 were studied 24-120 h before surgery. In the remaining patient a spleen recidive was suspected.

Planar abdominal scans were from 24 to 96 h post-injection of 5 mCi of ¹¹¹In-B72.3; an abdominal SPECT was performed at 48 h p.i. Surgery and histological confirmation was obtained in all cases. 9 OC were correctly identified, in 3 cases the OC was correctly discarded and in 2 cases the scintigraphy was falsely suggestive of OC. The scan identified 12/14 OC focus. The spleen recidive was not seen in the scintigraphy. The increase of activity from 24 to 96 h corresponded in most cases to OC while in the true negative cases activity did not change significantly. The SPECT showed extended disease in 2 cases not seen in the planar images.

In summary: B72.3 scanning may be of help in the evaluation of patients with OC. Attention has to be paid to the evolution of activity in the suspected focus. SPECT increases the sensitivity of the method.

PS-135

R. Matsui, T. Komori, K. Utsunomiya, I. Adachi, M. Shimizu, K. Sueyoshi, I. Narabayashi and T. Kageyama*

Osaka Medical College, Osaka, Japan, Department of Radiology and Internal Medicine*

BONE MARROW APPEARANCE WITH ^{99m}Tc-MIBI IN MULTIPLE MYELOMA

^{99m}Tc-MIBI scintigraphy was performed in patients with multiple myeloma and the relationship between accumulation in bone marrow and staging of multiple myeloma was examined.

[Materials and Methods] The chest SPECT was performed 10 minutes after 600MBq intravenous injection followed by whole body imaging. The subjects were 12 patients with multiple myeloma whose average age was 70.4 years old. Seven patients were in Stage 1, 3 in Stage 2 and 2 in Stage 3. The bone marrow findings of the sternum and thoracic vertebra by chest SPECT and those of the thigh bone marrow in the whole body image were classified into four grades (-, ±, +, ++). Next, ROI was set in bone marrow (M) of the sternum and thoracic vertebra (superior and inferior) and normal lung (L) by chest SPECT axial image and M/L ratios were calculated by the average for each pixel count.

[Result] The bone marrow grade for the sternum and thoracic vertebra was - in 1 case, ± in 2, + in 4 and the thigh bone marrow grade was - in 5, ± in 1, + in 1 among Stage 1 cases. The bone marrow grade for the sternum and thoracic vertebra was + in 1, ++ in 4 among Stages 2 and 3 cases and the thigh bone marrow grade was ± in 2 and + in 3. The M/L in stage 2 and 3 (2.43 ± 0.42) was significantly higher (P=0.007) than that (1.61 ± 0.14) in stage 1. The M/L was significantly correlated with reticulocyte(%), and Hg(g/dl) (r=0.91, p<0.0001 and r=-0.799, p=0.001, respectively). The M/L was not correlated with serum Ca, or M-protein.

[Conclusion] The accumulation of ^{99m}Tc-MIBI in bone marrow may be a useful index of bone marrow involvement in multiple myeloma.

PS-136

P. Mikosch, H.J. Gallowitsch, A. Pitschek, E. Kresnik, P. Lind

Department of Nuclear Medicine and Special Endocrinology, General Hospital Klagenfurt, Austria

Value of Ultrasound-Guided-Fine-Needle Aspiration Biopsy (US-FNAB) of Thyroid Nodules in the Preoperative Assessment and Additional Intraoperative Frozen Sections (IO-FS) in Cases of Suspicious Malignancy

Aim: The study had the aim of comparing the cytological results of fine-needle aspiration biopsy performed with ultrasound guidance (US-FNAB) with those of histology after thyroid surgery and whether an intraoperative frozen section (IO-FS) is of additional benefit. **Material and methods:** In order to select patients for surgery, all out-door patients who presented hypoechoic nodules with ultrasound and/or hypofunctional nodules with the scintiscan had an US-FNAB. The biopsy was performed free handed with ultrasound guidance during all phases of the biopsy procedure by operators experienced in the performance of US-FNAB. The cytological results of the US-FNAB were graded as 1) non-malignant (n = 59), 2) follicular proliferation (n = 31), 3) suspicious for malignancy other than follicular proliferation (n = 10), 4) inadequate (n = 6) and 5) malignant (n = 26). 132 patients underwent surgery and histological results were compared with the cytological results of the US-FNAB. In 42 cases an additional IO-FS was performed due to suspicious, malignant or inadequate results of the US-FNAB.

Results: US-FNAB allowed to biopsy nodules as small as 5mm in diameter with representative cytological results. This fact is due to the visual control of the fine-needle's location during all phases of the biopsy. US-FNAB reduced the time to perform the biopsy. No major complications occurred, only a few patients reported about local pain within 24 hours after the biopsy. For group 1 the non-malignant status could be confirmed in 56 cases (56/59, 94.9%). Patients with follicular proliferation (group 2) presented in 3 cases a thyroid cancer (3/31; 9.6%), one of these three cases was a papillary pT1 carcinoma of 3 mm in diameter in a nodule contralateral to the performed US-FNAB. In group 3 histology was malignant in 3 cases (3/10; 30%); 1 papillary, 1 follicular and 1 undifferentiated thyroid carcinoma. For the patients with US-FNAB presenting malignant transformation (group 5), histology could confirm malignancy in 73.1% (19/26). In group 4 (inadequate cytological results), three patients had a thyroid cancer (3/6; 50%). All in all US-FNAB distinguished correctly in 70.1% between malignant and non-malignant thyroid status. However, it was inconclusive for results with follicular proliferation. Especially for these cases the IO-FS was of additional benefit. IO-FS was correct in 90.1% (38/42) and in conclusive in another two cases. **Conclusion:** The application of both methods allowed an optimised preoperative and intraoperative management of suspicious thyroid nodules in order to minimise unnecessary primary surgery and re-operations in cases of thyroid malignancies.

Poster presentations

PS-137

D. Moka, M. Dietlein, K. Raffelt*, J. Hahn*, H. Schicha
Department of Nuclear Medicine and Institute for Inorganic and Analytical Chemistry*, University of Cologne, Germany.

Correlation of membrane metabolism assessed by phospholipid-31P-MRS with 18-FDG-PET, MRI and 131-iodine whole body scintigraphy in patients with metastatic thyroid cancer

Aim: Recently published studies showed that tumour growth is correlated to phospholipid-/tumour membrane metabolism. In vitro 31P magnetic resonance spectroscopy (MRS) is a new important tool to study systemic alteration of plasma phospholipids in patients with malignant diseases. Aim of this study was to correlate systemic effects in cancerous phospholipid metabolism (tumour membrane metabolism) in patients with metastatic thyroid cancer with different imaging methods (MRI, 18-FDG-PET and 131-I whole body scintigraphy).

Methods: Plasma phospholipid concentrations (phosphatidyl-ethanolamine, sphingomyelin (SM), 1- and 2-acyl-lyso-phosphatidylcholines, phosphatidylinositol and phosphatidylcholine(PC)) were measured using in-vitro 31P-MRS in 30 hypothyroid patients with thyroid cancer in preparation to a diagnostic whole body scintigraphy. All patients were thyroidectomized and had received at least 1 radioiodine therapy for thyroid ablation. Whole body scintigraphy, PET, MRI and measurement of TG-values in hypothyroidism were used to classify between patients in remission and patients with metastasis.

Results: In dependence of actual tumour-/metastasis extend there is a significant decrease of systemic sphingomyelin (0.45 ± 0.05 vs. 0.21 ± 0.02 mmol/ml) and phosphatidylcholine (1.9 ± 0.1 vs. 1.2 ± 0.1 mmol/ml) concentration. The size of the phospholipid alterations seems to depend only from the aggressiveness of tumour growth and from glucose metabolism but not from 131-iodine accumulation. There is also no dependence regarding histological classification (follicular or papillary thyroid cancer). Residual thyroid tissue showed a smaller decrease in systemic phospholipids (SM: 0.38 ± 0.02 mmol/ml; PC 1.7 ± 0.2 mmol/ml). After successful therapy systemic phospholipid concentration returned to normal values.

Conclusion: Our preliminary data showed that by usage of in vitro 31P-MRS in hypothyroid patients with thyroid carcinoma it might be possible to differ between residual thyroid tissue, thyroid metastasis and remission. Therefore in future, plasma spectroscopy could be developed to an additional diagnostic tool in the aftercare of thyroid cancer patients.

PS-138

S. Nezam Mafi, S. Hoda
Jam Hospital, Department of Nuclear Medicine
Tehran, Iran

TECHNETIUM-99M MIBI SCAN IN DETECTION OF THYROID

CANCER IN MULTINODULAR GOITER

Usefulness of MIBI scan in a single cold nodule has been documented, purpose of this study is to investigate if it is also of value in a multinodular goiter.

Material and Method: 143 patients with multinodular goiter who presented with multiple foci of diminished to absent radiotracer accumulation were studied, there were 119 females and 24 males, mean age 36 years. 555 MBq Tc99m MIBI was injected and scan in 15 minutes and 3 hours were performed, results were compared with Tc99m scan and fine needle biopsy FNA.

Results: 59 patients had hypoactive or cold nodules in both procedures, 32 were operated, 29 or 90.6% had benign lesions, 3 or 9% were malignant, among these 1 or 0.03% had a negative FNA. In 84 patients with warm MIBI nodules, 48 were operated, 6 or 12% were malignant and among these 2 or 0.04% had negative FNA.

Conclusion: warm MIBI nodules have 12% risk of malignancy, while a cold nodule has a 90.6% chance of being benign. False FNA in 0.07% were observed, therefore absent MIBI uptake is a good indicator of a benign lesion, while a warm one could not be relied upon for malignancy, although FNA remains a first diagnostic procedure, MIBI could be used as an additional method of investigation.

PS-139

S. Novikov, S. Kanayev, L. Jukova.
Research Institute of Oncology, Department of Radiation Oncology and Nuclear Medicine, 189646, Pesocny-2, St.-Petersburg, Russia.

BONE AND BONE MARROW SCANNING IN DIAGNOSIS OF SKELETAL METASTASES OF HODGKIN'S DISEASE.

PURPOSE: This study has been conducted to compare the sensitivity of bone marrow (BMS) and bone (BS) scintigraphy in patients with Hodgkin's disease (HD).

MATERIAL: From 1993 to 1997, 155 patients with HD underwent whole body BS (with 7-8 MBq/kg of 99mTc-MDP) and BMS (with 8-10 MBq/kg of 99mTc-colloids). Following scintigraphic changes were considered as the signs of skeletal metastases: for BMS - focal defects or diffusely diminished tracer uptake, for BS - "hot" spots or focal defects. All lesions detected by only one method (BS or BMS) were evaluated by biopsy, X-ray or magnetic resonance imaging.

RESULTS: 55 patients had scintigraphic signs of skeletal metastases on BMS: focal defects were revealed in 53 cases and diffusely diminished tracer uptake - in 2 patients. Positive results of BS were mentioned in 31 cases: 29 patients had hot spots and another 2 - focal defects.

Results of both BS and BMS were abnormal in 23 cases and normal in 92 patients. Thirty two patients had focal defects on BMS and normal results of BS (metastatic character of lesions was proved in 29 cases). On the contrary, in another 8 cases BMS was normal and BS showed hot spots in ribs and/or extremities (5 lesions verified as bone metastases).

Sensitivity for BMS was 88% and for BS - 46% ($p < 0.05$).

CONCLUSION: In screening for skeletal metastases of Hodgkin's disease BMS is more sensitive than BS.

PS-140

B. Nowak, U. Cremerius, S. Jänicke¹, E. Di Martino², G. Adam³, U. Buell
Departments of Nuclear Medicine, Oral and Maxillofacial Surgery¹, Otolaryngology² and Radiology³, University Hospital, Technical University Aachen, Germany

MALIGNANT HEAD-AND-NECK-TUMORS: STAGING BY 18F-FDG-PET IN COMPARISON TO CT.

Purpose: Aim of this study was to evaluate the use of 18F-FDG-PET in staging of patients with known or suspected primary or recurrent head-and-neck-tumors and to correlate the results to corresponding CT-findings.

Methods: 22 static PET-Scans from neck to upper thorax in 21 patients (age 64 ± 12 yrs.) with known or suspected primary (9) or recurrent (13) head-and-neck-tumor were obtained 60 min after i.v.-injection of 231 ± 61 MBq 18F-FDG using an ECAT EXACT 922/47 Siemens Scanner. A post-injection-transmission for attenuation correction was performed. PET-data were reconstructed by an iterative algorithm. Contrast-enhanced CT-Scans were performed with 5 mm slice thickness (Siemens Somatom Plus) in these patients. Resulting images were evaluated visually using routine criteria (CT: lymph node size > 1 cm; PET: increased focal uptake). The results were validated by histology or clinical follow up. PET and CT images were judged for: 1) detection of the primary or recurrent tumor, 2) detection of regional lymph-node-metastasis in the corresponding ipsi- and contralateral neck-sides.

Results: 13 of 22 patients with suspected local tumor-lesions had a proven tumor. 11 of 44 neck-sides were affected by regional lymph-node-metastasis.

	true (+)	false (-)	true (-)	false (+)	Sens.	Spez.
Local Tumor PET	9 / 13	4 / 13	8 / 9	1 / 9	0.69	0.89
Local Tumor CT	8 / 13	5 / 13	6 / 9	3 / 9	0.62	0.67
Neck-sides PET	11 / 11	0 / 11	30 / 33	3 / 33	1.00	0.91
Neck-sides CT	11 / 11	0 / 11	30 / 33	3 / 33	1.00	0.91

4 of the 5 false negative findings in local tumor sites in CT and 2 of the 4 false negatives in PET occurred in cases of recurrent disease.

Conclusion: Our first results in this small series of patients reveal a similar value of PET and CT in the local evaluation of primary or recurrent head-and-neck-tumors with a slight tendency of better accuracy in PET-findings. Especially in local recurrence, probably due to morphological alterations following primary therapy, PET tends to be slightly more sensitive. Both methods are valuable for staging of neck-sides.

PS-141

J. Oliva¹, G. Pimentel¹, M. Borron¹, F. Casanova², R. Peralta¹, J. Guerra³, N. Gonzalez⁴, J. Leonard⁴, R. Ortiz⁴, B. Oliver¹, M. Abreu¹, M. Hernandez¹, N. Diaz¹, R. Baum⁵

Instituto Nacional de Oncología ,Department of Nuclear Medicine¹, Abdominal Surgery², Gastroenterology³, Biostatistics⁴, University Hospital „C.García“ Department of Oncology⁵, Klinik für Nuklearmedizin, Universität Frankfurt/M⁶

RADIOIMMUNOSCINTIGRAPHY OF COLORECTAL TUMORS WITH THE CUBAN MONOCLONAL ANTIBODY IOR-CEA-1

Purpose: IOR-CEA-1 is a murine monoclonal antibody (Mab) developed in 1989 at the National Institute of Oncology and Radiobiology (INOR) characterized in collaboration with the Center for Genetic Engineering and Biotechnology, and produced at the Center of Molecular Immunology in Havana, Cuba. This Mab was developed to detect colorectal tumors and their metastases. Clinical trials phase I and I-II have been performed to evaluate the in vivo diagnostic qualities of radiolabeled IOR-CEA 1. This paper presents the results obtained at the Nuclear Medicine Department of INOR in the detection of colorectal tumors, their recurrences and metastases in 61 patients. Patients studied with radioimmunoscintigraphy (RIS) in comparison with computed tomography (CT) showed rising CEA or clinical suspected tumor.
Methods: Each patient received 1.48-2.22 GBq of the 99m-Tc labeled Mab. Anterior and posterior images of the thorax, abdomen, and pelvic region were taken at 10 minutes and 18-24 hours post administration of the Mab. SPECT studies were performed at 18-24 hours.
Results: The RIS was able to detect all the primary tumors and 21 of the suspected recurrences. Sensitivity was 91.3% in recurrences. Serum CEA and CA 19.9 levels and the RIS positivity did not correlate in all patients. HAMA response was seen in 17 patients beginning from the 15th day after Mab application and declined after 6-9 months. No toxicity was observed in this group of patients.
Conclusion: The cuban Mab IOR-CEA-1 is able to detect colorectal tumors, their recurrence and metastases superior to CT evaluation.

PS-142

N. Oriuchi, T. Inoue, K. Tomiyoshi, Y. Sando, M. Tsukakoshi, K. Aoyagi, Y. Tomaru, S. Amano, K. Endo
Gunma University School of Medicine, Gunma, Japan

COMPARATIVE F-18-FLUORO- α -METHYL-TYROSINE (FMT) AND FDG PET IN PATIENTS WITH PULMONARY TUMORS

The aims of this study were to compare the clinical usefulness of F-18-fluoro- α -methyl-tyrosine (FMT) and FDG PET in patients with pulmonary tumors, and to clarify the value of FMT in estimating therapeutic effect. PET was performed 40 min after intravenous injection of 200 MBq of FMT or FDG by a simultaneous transmission emission acquisition method in 12 patients. They included eight patients with lung cancer: three small-cell cancer (SCLC) and five non-SCLC; and four benign tumors: two atypical mycobacteriosis and two sarcoidosis. Standardized uptake values (SUVs) of pulmonary lesions were calculated for both FMT and FDG. In three patients with SCLC, follow-up examination was performed after treatment.

Seven of eight lung cancers were visualized with both FMT and FDG, and FMT PET was accurate for nodal staging. Although FDG showed increased uptake in a patient with suspicious of recurrent lung cancer and in four patients with benign lesions, FMT showed no uptake in these five patients without malignancy. SUVs for FMT decreased after chemotherapy (from 1.8 to 1.2) and correlated with SUVs for FDG (from 7.8 to 4.5).

In conclusion, FMT could localize lung cancer and appeared to be a better tracer than FDG for differentiating benign pulmonary lesions. FMT may also has a role in evaluating therapeutic effect for lung cancer .

PS-143

C Batsakis, G Tourkochoriti, G Panoutsopoulos, P Papanastassi, S Boutsali, D Bofos, J Christacopoulou.
Nuclear Medicine & 5th Pulmonary Medicine Depts, “SOTIRIA” Chest Hospital, Athens.

ASSESSMENT OF SMALL CELL LUNG CANCER WITH Indium-111- OCTREOTIDE SCINTIGRAPHY

Aim of the study was to evaluate the use of In-111-octreotide scintigraphy in staging and the therapeutic effect in patients with small cell lung cancer (SCLC).

Patients and method. We studied ten patients with histologically proved SCLC before and at the end of the chemotherapy with whole body scan at 4 and 24 hours after IV administration of 200 MBq of In-111-octreotide. Furthermore, we calculated the tumor to body background ratio.

Results. In all patients the primary tumor was visualized, but it's distinction from the involved lymph node was difficult when the primary tumor was centrally located. Less than 50% of the bone metastases seen on the bone scans were evident in octreotide scintigraphy.

After the end of chemotherapy there was a substantial decrease in the size of the primary tumor with an accompanied reduction of the count ratio and the survival of the patients. Small reductions were associated with short survival. Conventional x-ray studies at this point of the study showed almost complete disappearance of the tumor.

Conclusions. In-111-octreotide scintigraphy has a limited value in staging of small cell lung cancer. On the contrary, estimation of therapeutic effects seems to be more reliable with this method in comparison with other radiological techniques.

PS-144

A. N. Rahn¹, R. P. Baum³, I. A. Adamietz¹, S. Adams², S. Sengupta², St. Mose¹, S. B. Bormeth¹, G. Hör², H. D. Böttcher¹

¹Klinik für Strahlentherapie und ²Klinik für Nuklearmedizin, J. W. Goethe-Universität, Frankfurt/Main; ³PET-Zentrum, Zentralklinik Bad Berka

FDG-POSITRON-EMISSION-TOMOGRAPHY IN RADIATION TREATMENT PLANNING OF HEAD AND NECK TUMORS

Purpose: An individualized radiation treatment planning in patients with head and neck tumors requires an exact definition of tumorspread. Despite of high reliability of methods like computed tomography, sonography or magnetic resonance imaging used in daily routine, the correct diagnosis of lymphonodal tumor infiltration is often not possible. In a prospective trial, we examined whether an additional FDG-PET gives a relevant gain of information for radiation treatment planning.

Patients and methods: We studied data of 34 patients with histologically confirmed squamous cell carcinoma of the head and neck who received a FDG-PET prior to treatment planning additionally to conventional staging procedures. The extent of changes of treatment strategy or target volume due to additional FDG-PET findings were analysed.

Results: In 41% of patients with primary tumors and in 58% of patients with recurrent disease FDG-PET detected additional tumor manifestations. In all cases, changes of treatment strategy or target volume were necessary. Regarding patients with primary tumors the percentage of treatment modifications was highest in patients with large tumors (T3 and T4) (58%) and patients with advanced lymph node involvement (N2 and N3) (46%).

Conclusions: Especially in patients with recurrent disease and patients with advanced tumor stages FDG-PET is able to give clinically relevant information compared to conventional staging procedures. Therefore, in these group of patients a FDG-PET study prior to radiotherapy planning should be considered.

Poster presentations

PS-145

A. N. Rahn¹, R. P. Baum³, A. Hertel², S. Sengupta², S. B. Bormeth¹, St. Mose¹, D. Jacob-Heutmann¹, C. Niehoff¹, K. Wagner¹, G. Hör², H. D. Böttcher¹

¹Klinik für Strahlentherapie und ²Klinik für Nuklearmedizin, J. W. Goethe-Universität, Frankfurt/Main; ³PET-Zentrum, Zentralklinik Bad Berka

FDG-PET IN STAGING AND THERAPY MONITORING OF ESOPHAGEAL CANCER UNDER RADIOTHERAPY

Background: In staging and therapy monitoring of esophageal carcinoma secondary inflammatory tissue involvement and morphological changes due to former treatment are still a differential diagnostic problem for modern imaging techniques. Scar tissue and edema due to radiotherapy, local chemotherapy or resection can often not be distinguished from recurrent or residual tumor-tissue. Results of regional lymphonodal staging by CT or MRT are still not satisfactory. Purpose of the study was to evaluate whether FDG-PET is able bring a relevant gain of diagnostic information compared to other imaging techniques.

Patients and methods: Until April 1998 12 patients with histologically proven SCC of the esophagus were included into the study. All patients were scheduled for definitive or preoperative radiochemotherapy or radiotherapy alone. (3 female, 9 male; age ranged from 41 to 69 years). In addition to conventional staging procedures (CT, ultrasound, endoscopy) all patients received FDG-PET before radiotherapy, after 30 Gy and during follow up.

Results: FDG-PET detected all primary tumor sites. In eight cases additional tumor spread was diagnosed by PET (regional lymphnodes n=6, distant metastases n=6). 9 out of 11 tumors showed decrease of FDG-uptake under radiation therapy. Regional inflammatory involvement (mucositis) due to irradiation may lead to long lasting increased local FDG-uptake.

Conclusions: As known in head and neck cancer, FDG-PET may also be a useful diagnostic tool in patients with esophageal cancer. PET may give additional diagnostic information in tumor-staging and therapy monitoring and therefore may facilitate decisions about treatment strategy. Inflammatory involvement of irradiated tissue may cause diagnostic problems in posttherapeutic PET-studies and have to be taken into account.

PS-146

M. Ramos, N. Iznaga, A. Morales, L. Torres, J.P. Oliva, G. Pimentel, N. Rodriguez, N. González, A. Perera, Llorente F, Neninger E, González N, Leonard I, Martínez I, Martínez F.

Center of Molecular Immunology, Havana, Cuba.

A NEW MONOCLONAL ANTIBODY FOR RADIOIMMUNODIAGNOSIS OF COLORECTAL CANCER.

Colorectal cancer is the third cause of death among malignant neoplasms in Cuba. Different labeled monoclonal antibodies (MAb) have been used for the diagnosis and follow-up of this tumors by immunoscintigraphy. Recently, a new MAb ior c5 have been developed at Center of Molecular Immunology, Havana, Cuba. It recognizes a new tumor-associated antigen: IOR C2, found in most of colorectal adenocarcinomas. The aim of the present work was to assess the diagnostic utility of this antibody, labeled with ^{99m}Tc, as well as to study its pharmacokinetics, biodistribution and internal dosimetry. Forty five patients suspected of having colorectal cancer were studied in a phase I/II clinical trial. Three milligrams of ^{99m}Tc-ior c5 was administrated to the first 10 patients and 1 mg to the rest of them. Plasmatic clearance was fixed to a biexponential curve with $T_{1/2\alpha} = 5$ h and $T_{1/2\beta} = 38$ h. Just 4.8 ± 0.5 % of the injected dose eliminated via urine. Liver, heart, lung, kidneys, spleen and urinary bladder received higher dose. Sensitivity and specificity of the immunoscintigraphy with ^{99m}Tc-ior c5 was 100%. New metastases or recurrent lesions were detected in 55.6% of the cases. No adverse reaction was observed. **Conclusion:** This monoclonal antibody is useful for the diagnosis an follow-up of colorectal cancer.

PS-147

M. Ramos (1), N. Rodriguez (2), J.P. Oliva (3), N. Iznaga (1), A. Perera (4), A. Morales (1), N. Gonzalez (2), M. Cordero (2), L. Torres (4), G. Pimentel (3), M. Borrón (3), J. Gonzalez (3), O. Torres (1), T. Rodriguez (1).

1. Center of Molecular Immunology, 2. Center for Medical-Surgery Research, 3. National Institute for Oncology and Radiobiology, 4. Center for Clinical Research, Havana, Cuba.

DIAGNOSIS OF TUMORS OF EPITHELIAL ORIGIN WITH ^{99m}Tc-LABELLED MURINE MONOCLONAL ANTIBODY ior egfr3.

Despite of the advantages on antitumoral therapy, cancer of epithelial origin constitutes one of the first causes of death worldwide. That kind of tumors have a 10-30-fold overexpression of the epidermal growth factor receptor (EGFr). Monoclonal antibody (MAb) ior egfr3 is a IgG2a, which recognizes the epidermal growth factor receptor (EGF-R). The aim of the present work was to evaluate the diagnostic efficacy of the ^{99m}Tc-labeled ior egfr3 for the detection of epithelial-derived tumors, its metastasis and its recurrences. One hundred forty eight patients aged 53 ± 13 years old, suspected of having cancer of epithelial origin, were studied. Labeling efficiency was 97 ± 3 %. No adverse reaction or side effects were observed. The results of biopsy showed that 126/148 patients had tumors of epithelial origin (85.1 %), 21 were negative of cancer (14.2 %) and 1 non-Hodgkin lymphoma (0.7 %). Most of the patients were in stages III-IV of the disease (109/148). Liver, spleen and heart showed the highest uptake among all organs. Radioimmunoscintigraphy identified 106 of 126 patients suffering from cancer of epithelial origin and 22 of the 22 true negative persons. The sensitivity by organs was: brain 100%, digestive tract 90%, head and neck 89%, lung 84% and breast 79%. The overall sensitivity, specificity, accuracy, positive predictive value and negative predictive value of the immunoscintigraphic imaging were 84.1%, 100%, 86.5%, 100% and 52.4% respectively. New metastases were detected in 50% of the cases.

Conclusions: Immunoscintigraphy with ^{99m}Tc-ior egfr3 is useful for the diagnosis and follow-up of cancer of epithelial origin.

PS-148

F. Chierichetti, D. Rubello, S. Pedrazzoli^o, P. Zanco, P. Gasparoni^{oo}, C. Paspuali, G. Ferlin.

Nuclear Medicine, PET Centre, ^oSurgical Pathology, ^{oo}Endocrinology, Hospital of Castelfranco V.to (TV), Italy.

PROGNOSTIC ROLE OF FDG PET IMAGING IN NEUROENDOCRINE TUMORS (NETs): A COMPARATIVE ANALYSIS WITH ¹¹¹In-OCTREOTIDE SCAN AND RADIOLOGIC IMAGING.

We prospectively investigated 27 patients (pts) affected by NETs (13 M, 14 F, mean age 49.2 years) with cytologically or histologically proven NETs. They were divided into 2 groups accordingly to the clinico-pathologic criteria related to prognosis: slow growing NETs (no. 8: sporadic gastrinoma = 4, insulinoma = 3, somatostatinoma = 1) and aggressive NETs (no. 14: MEN I = 3, MEN II = 1, non functioning pancreatic NETs = 3, insulin producing ca. = 1, sporadic medullary thyroid ca. = 4, carcinoids = 2). Twenty pts were preoperatively evaluated, 2 pts with medullary thyroid carcinoma were studied at the moment of a disease relapse, and 5 pts were considered to be tumor-free after surgery for a slow growing NET and were taken as controls. In all the cases were performed FDG PET, ¹¹¹In-octreotide scintigraphy (OS) and RM/TC scan. OS was positive in 18/22 pts with disease (82% sensitivity), 10 slow growing and 8 aggressive NETs. OS was negative in 2 pts with insulinoma and in 2 cases with a medullary thyroid ca. recurrence. FDG PET was positive exclusively in aggressive NETs (13/14, 92.8%); moreover, in 2 out of these pts PET was the only method able to identify the primitive tumor, and in other 4 pts PET revealed a greater number of metastases to lymphnodes and/or liver than the other imaging modalities. RM/TC were positive in 12/22 pts (59% sensitivity), 4 slow growing and 8 aggressive NETs; moreover, we recorded 2 false positive lesions with CI (9%). All the diagnostic techniques were negative in the 5 tumor free pts. In conclusion: a) OS remains the highest sensitive imaging modality for detection of NETs, with both slow and aggressive pattern, b) FDG PET appears to be a highly sensitive technique for the visualization of both primitive and metastatic NETs with aggressive behaviour, and it seems able to accurately identify NETs with a bad prognosis.

PS-149

D. Rubello, *R. Mattei, F. Chierichetti, A. Fini, S. Cargnel, S. Bissoli, G. Ferlin.
Nuclear Medicine -PET Centre, *ORL Department, Hospital of Castelfranco V.to (TV), Italy.

ROLE OF FDG PET IMAGING IN PREOPERATIVE LOCALIZATION OF LYMPHNODE METASTASES (LNM) IN PATIENTS WITH HEAD/NECK NEOPLASMS: A GUIDE TO CONSERVATIVE SURGERY.

FDG PET is widely used in preoperative staging of various types of neoplasms with the aims to perform an accurate removal of all neoplastic lesions or to avoid unnecessary surgery in patients (pts) with distant metastases. In the present study we prospectively investigated 24 pts with head/neck neoplasms (5 F, 19 M, mean age 54.6 years). In all the cases a preoperative evaluation with FDG PET, MR/CT of the head and neck region was obtained within a 2-weeks interval, and subsequent surgery was performed by the same surgical team within 1 week. In addition, in pts with advanced disease, chemotherapy and radiotherapy were performed. Post-therapeutic follow-up ranged 8-34 mo. FDG PET was evaluated both with visual and quantitative analysis by means of calculation of the standardized uptake value (SUV; n.v. in our center < 2.5). The primitive tumor was correctly identified in all the pts both by RM/CT and FDG PET (visual analysis). However, RM/CT provided better information about size, border and local infiltration of the primitive tumor. On the other hand, FDG PET (visual analysis) provided better results regarding the localization of LNM (sensitivity: PET = 87.5%, MR/TC = 53.1%; specificity: PET = 99%, MR/TC = 87.8%). Also the NPV was higher for PET than MR/TC (99% vs 96%, respectively) as well as the PPV (87.5% vs 24.6%, respectively). In other words, MR/TC provided a significantly higher number of false negative and false positive cases in comparison with FDG PET. The smallest LNM revealed by FDG PET was 7 mm in diameter. SUV values ranged from 1.4-7.9 in the LNM, and were significantly higher in neoplastic than in inflammatory LN (3.9 vs 1.8, p < .05). However, it has to be pointed out that using SUV analysis, i.e. considering pathologic a SUV > 2.5, 7 LNM in our series should be considered negative (false negative). On the basis of our data we can conclude that FDG PET is a highly accurate imaging technique in preoperative identification of LNM in head/neck neoplasms; PET could be proposed as a guide to perform a conservative surgery in these pts. From a technical point of view, visual analysis appears to be more sensitive than quantitative analysis in the evaluation of LNM in pts with head/neck neoplasms.

PS-150

Lucilia Salgado, Ana Teresa Fonseca, Duarte Salgado, M. Rosário Vieira

Instituto Português Oncologia Lisboa, Portugal. Nuclear Medicine and Neurology Departments

201TI-SPECT IN THE EVALUATION OF PRIMARY BRAIN TUMOUR RECURRENCES: RELATION WITH HISTOLOGICAL GRADE AND PROGNOSIS

The aim of our study was to evaluate the role of brain tomography with 201TI (201TI-SPECT) in the detection of recurrence and its relation with histological grading and prognosis of primary brain tumours.

We studied 30 patients(pts), 7 female and 23 male, with a mean age of 53 y (14-75y), with clinical or radiological evidence of primary brain tumour recurrence. Initial histological diagnosis was: astrocytoma - 27 pts (grade I-II, 16 pts; grade III-IV, 11 pts), anaplastic oligodendroglioma - 3 pts. All pts, except one, were submitted to external radiotherapy. Twenty two pts were operated and chemotherapy was administered in 16 pts. SPECT was performed after e.v. administration of 74 Mbq of 201TI (64 images, 360°, 30s/image). Each study was visually evaluated by two independent observers. Tumour/background ratios (TR) were calculated from irregular ROIs of the lesion and contra-lateral brain.

Twenty seven pts had focal uptake of 201TI in the lesion. TR had a mean value of 2.64 (0.96 - 9.84). Mean TR in the group of pts with grade I-II tumours (n=16) was 1.8+0.7; in the group of pts with grade III-IV tumours, 3.6+2.27 (p<0.05). In the follow-up, 12 pts died (one to 17 months after recurrence). Mean time of follow-up of remaining 18 pts was 7.3 (3-17) months. Mean TR was higher in the deceased pts (3.8+2.8 (1.57-9.84) vs 2+0.7 (0.96-2.88); p<0.05).

Tumour/background ratio of 201TI at recurrence correlates with histological aggressiveness of primary brain tumours and can be a valuable prognostic index.

PS-151

K. Scheidhauer, M. Jungehülsing*, U. Pietrzyk#, P. Theissen, E. Stennert*, H. Schicha.

Departments of Nuclear Medicine, ENT-Medicine*, and Max-Planck-Institute#, University of Cologne, Germany.

FDG-PET IN PATIENTS WITH CUP-SYNDROME.

This investigation was undertaken to evaluate positron emission tomography (PET) using [F-18]-fluorodeoxyglucose (FDG) for detection of primary tumor sites in patients with carcinoma of unknown primary (CUP-syndrome), as the latter implies unfavourable prognosis. Out of 477 patients presenting in the ENT-ambulance between May '94 and August '97 because of malignant disease, n = 16 patients (3.3 %) were defined as a CUP-syndrome due to failing diagnosis of a primary by conventional diagnostics including panendoscopy, X-ray and CT. In these patients PET was performed in 2-3 bed positions on a CTI ECAT Exact scanner, covering an axial FOV of the ENT-area as well as thorax and upper abdomen (370 MBq FDG, fasting state). 'Hot' transmission scans for attenuation correction and transmission images were acquired in each patient. PET evaluation was done using a software program (MPI-Tool: multi purpose imaging) providing simultaneous depiction of emission and transmission images as well as fused images for sufficient anatomical orientation. Focally increased uptake was qualitatively judged suspicious for malignancy. PET yielded unexpected focal FDG-uptake in 7 of 16 patients (44 %) to be found cancer of lung (n=3), pharynx (n=3) and glandula parotis (n=1). This enabled a possibly curative therapeutic attempt. The results indicate, that FDG-PET in patients with CUP-syndrome represents a fast non-invasive diagnostic tool, which allows accurate detection of unknown primary tumors. Prognostic impact of early FDG-PET in unclear tumor disease, however, needs to be proven.

PS-152

O.Schröder¹, J. Trojan², St.Zeuzem², G. Hör¹, R.P. Baum¹

Department of Nuclear Medicine¹ and Internal Medicine², University of Frankfurt/Main, Medical Center, Germany

HEPATOCELLULAR CARCINOMA IN PATIENTS WITH CHRONIC HEPATITIS C: EVALUATION WITH F-18-FDG-PET AND RELATION TO p53 EXPRESSION

Purpose: In the present study the results of whole-body FDG-PET in primary hepatocellular malignancies suspected by ultrasonography and/or elevated serum levels of alpha-fetoprotein (AFP) in patients with chronic hepatitis C were compared with serum antibodies to the p53 tumor suppressor gene (anti-p53), whose product - a nuclear protein - regulates growth and apoptosis in both normal and neoplastic cells, and p53 immunohistochemistry.

Methods: Whole-body FDG-PET and transmission-corrected regional PET scans of the liver (ECAT EXACT 47, Siemens/CTI) were obtained in 10 patients after i.v. injection of 370 MBq of F-18-FDG. Standardized uptake values (SUV) were determined 60-90 min after injection. The results obtained by FDG-PET were compared with ultrasound (US), computed tomography (CT), serum anti-p53, histology and p53 immunohistochemistry (p53-IHC).

Results: Histologic examination revealed 5 hepatocellular carcinomas (HCC), 2 metastatic liver tumors and 3 benign regeneration nodules. In patients with HCC and metastatic liver tumors, the median AFP level was 46.0 ng/mL and 5.3 ng/mL, respectively. Serum anti-p53 was negative in all patients. p53-IHC was positive in two patients with HCC and in one patient with metastases of a rectal adenocarcinoma. FDG-PET detected hepatic metastases of the rectal adenocarcinoma as well as 2/5 HCCs and showed normal FDG metabolism in all benign lesions, in three HCCs and a metastatic carcinoma. Both tumors with a high expression of p53 presented with highly elevated glucose metabolism. Extrahepatic malignant disease detected by whole-body FDG-PET included lymph node metastases (n = 2), bone metastases (n = 2) and peritoneal carcinomatosis (n = 1). US and CT detected all HCC (5/5) as well as both metastatic liver tumors. In patients with benign lesions, US and CT were false positive in 2/3 and 1/3 patients, respectively.

Conclusion: Since FDG-PET does not reliably identify hepatocellular carcinomas in patients with chronic hepatitis C, ultrasound, CT-studies, and histologic examination remain the 'gold standards' for the assessment of hepatic malignancies. Our data demonstrate for the first time a correlation of liver tumor glucose metabolism and p53-antigen expression.

PS-153

Sergieva S., H.Hadjikostova*, D.Darnianov, G.Kirova, I.Trifonova
National Oncology Centre, Sofia & *Medical University, Sofia, Bulgaria

¹¹¹In-PENTETREOTIDE SCINTIGRAPHY IN PATIENTS WITH SMALL CELL LUNG CANCER

Small Cell Lung Cancer (SCLC) is characterized neuroendocrine properties and like other endocrine tumors that have APUD characteristics, SCLC have been demonstrated to possess high somatostatin receptor affinity. The purpose of this work was to investigate the clinical application of ¹¹¹In-pentetreotide scintigraphy in patients (pts) with histologically proven SCLC for diagnosis and follow-up of patients (pts) with histologically proven SCLC. Sixteen untreated SCLC pts- 9 with limited disease and 7- with extensive disease (4F, 12 M; age range: 42-67 years) were scanned. Staging was carried out according to current criteria (chest X-ray, CT scan, bronchoscopy, bone scintigraphy). Pts underwent combined chemotherapy. They received a 7-day course of treatment with somatostatin analog (Sandosten) in dose of 200µg/day in the intervals between the courses of standard chemotherapy. 12 pts were also investigated after a cycle of chemotherapy. Somatostatin receptor scintigraphy (SRS) was carried out using ¹¹¹In-pentetreotide (OctreoScan, Mallinckrodt) 110-185MBq. Planar and/or tomographic images were performed 24 and 48 hours after i.v. inj. In order to quantify ¹¹¹In-pentetreotide uptake a Tumor/Background (T/B) ratio was calculated. SRS results were compared with the data of the conventional imaging methods. Results: The primary SCLCs were visualized in all 16 pts- 100%. The mean T/B ratio was 2.02 (range 1.75 - 2.9). Liver metastases were scanned in 2 pts, brain metastases- in 1 pt; tumor spread to the contralateral lung - in 2 pts, hilar and mediastinal lymph nodes - in 2 pts, supraclavicular lymph node - in 1 pt. Sensitivity of SRS for detection of loco-regional and distant metastases in 7 pts with extensive disease was 57% (8/14). In 1 pt with limited SCLC unsuspected uptake was obtained in the contralateral lung, leading to an up-staging of this pt. Out of 16 pts, 12 pts showed complete or partial response to the combined chemotherapy and Sandosten treatment and parallel reduction of the mean T/B ratio - 1.55 (range 1.3 - 1.8). Second SRS was not carried out in 4 pts because of the tumor progression and worsened status of these pts. In conclusion SRS is an useful diagnostic method for detection of primary SCLC -100%. Sensitivity of this method is lower in the visualisation of SCLC metastases - 57%. Semiquantitative assessment of SRS in SCLC related to the tumor response after a cycle of therapy and it may be used for evaluation and follow-up of pts with this disease.

PS-154

S. Severi, P. Cristofolini*, E. Lorenzi, S. Boi*, S. Girlando*, R. Togni*, P. Dalla Palma*, M. Camerani.

Nuclear Medicine - Dermatology* - Pathology*
S CHIARA HOSPITAL - TRENTO - ITALY

THE SENTINEL NODE (SN) STUDY IN MELANOMA STAGING. WHICH ACCURACY THE LYMPHOSCINTIGRAPHY (LS) AND THE PATHOLOGY REPORT ARE REQUEST TO HAVE?

INTRODUCTION The LS is the only modality able to locate the first node draining from a site. The patients treatment needs a precise lymphatic mapping and SN evidentiating usefull also in case of double basin localization. On the other hand the development of techniques able to investigate the presence of mRNA Tyrosinase gene, that is considered a melanocytic marker (PCR), allows to wonder if the histologic routinary exams may be responsible of an high number of false negative results. **MATERIALS** We selected 35 patients for day surgery approach of SN study. Inclusion criteria were: stage 1 melanoma, thickness >= 1 mm, melanoma af the limbs or of the trunk. Each patients underwent LS with a dynamic acquisition, a static view to mark the SN projections in the skin and a postoperative static to confirm the SN excision. We inject, in 3 subcutaneous site all around the excision, 74 MBq of ^{99m}Tc Lymphoscint in 0.2 ml saline. The skin incision was no more than 5 cm and a probe mapping of the operatory field was done before and after surgery. After removing, the SN was immediately send to pathology lab where immunohistochemical and PCR modalities were performed. **RESULTS** 35 SN were located (32 excised, 1 in the axilla and 2 in the groin not found). In 5 cases double SN were detected and 2 of them were excised. Metastases were found in 5 patients with the routinary method whereas of the 19 SN studied with PCR (2 were in second basin) 10 were positive. The 5 positive histology assay were PCR positive too. The gamma probe study always predict the surgical result in accord with the static control. **DISCUSSION** An accurate LS is mandatory to obtain the selective SN location also in secondary basin. The success in excision (there is a learning curve) is conditioned by wound dimension and deep nodes exclusion. The high sensitivity of PCR investigation seems very important but at present further cases with an adequate follow up are needed to know if these patients are at risk of a worse biological outcome.

PS-155

D.O. Slosman, P. Bang, M. Allaoua, M. Becker, J.P. Papazyan, E. Piperkova, C. Morel, A. Allal, W. Lehmann. Geneva University Hospital, Switzerland.

LEAN BODY MASS, STANDARDIZED UPTAKE VALUE (SUV) AND FDG-PET: A STUDY OF PATIENTS WITH ENT CANCER.

Purpose: To determine the optimal cut-off for SUV to diagnose ENT cancer and to identify possible improvement in using lean body mass correction.

Material and methods: The goal of our longitudinal study is to prospectively assess the efficacy of FDG-PET to detect recurrence of ENT cancer after therapy in reference to MRI. We have initially evaluated 66 patients with FDG-PET. The protocol includes transmission scan and emission scans 45 minutes after injection of 5 mCi(185MBq)/70kg of body weight. Total body mass (TBM) and lean body mass (LBM) were determined by dual X-ray absorptiometry in order to calculate SUV adjusted to both parameters. Furthermore, reconstruction with and without scatter correction was applied. ROC curves were used to compared the 4 sets of results (SUV corrected with LBM or TBM, with scatter correction or not). Histopathological examination was used to assess the presence of the disease.

Results: Among these 66 patients, 114 foci were measured; 102 were positives and 12 were negatives. There was no significant difference in the area under the ROC curves between the 4 sets of SUV evaluation while lean body mass and total body mass scatter corrected ROC had area greater than 0.9. The optimal cut-off TBM SUV value was 1.8 that resulted to a sensitivity of 88.2% and a specificity of 91.7% while the optimal LBM SUV value was 1.7 that resulted to a sensitivity of 76.5% and a specificity of 91.7%.

Conclusions: In ENT cancer patients, LBM SUV was not better than TBM SUV while scatter correction only slightly improved the results. Such approach could be perform in other type of cancer in order to validate the use of LBM in cohort of patients with more important fat body compartment.

PS-156

C. Soler, A. Augusseau-Caillet, P. Beauchesne, F. Dubois, H. Rousset.

CHU Saint-Etienne, France, Dept of Nuclear Medicine.

THE ROLE OF ^{99m}Tc-SESTAMIBI SCINTIGRAPHY IN DIAGNOSING METASTATIC HÜRTHLE CELL CARCINOMA OF THE THYROID.

Aim: Hürthle cell carcinoma is known to usually no concentrate iodine-131. On the other hand, ^{99m}Tc-Sestamibi (MIBI) has been reported to localize in several tumors, including Hürthle cell carcinomas. We present two patients with metastases of Hürthle cell carcinoma wich was successfully imaged with ^{99m}Tc-MIBI. **Case 1**, a 51 year old female underwent sub-total thyroidectomy for multiple nodulars goiter 15 years previously. 14 years after the initial surgery a palpable mass in the neck was resected, revealing Hürthle cell carcinoma. ¹³¹I whole body scan at this time (3 months prior to MIBI) revealed iodine-accumulation tissue in the neck for wich the patient received an ablative dose of 3700 Mbq of ¹³¹I. Serum thyroglobulin level at this time was high, conflicting with the unique iodine-accumulation tissue. The X ray and CT scan of the chest were negative. Two months later, the patient complains of painning of his right rib. ^{99m}Tc-HMDP bone scan and ^{99m}Tc-MIBI scintigraphy were performed for further-MIBI evaluation of the lesions and for comparison of the image quality and detectability of the metastatic foci on the scintigraphic images obtained using these two radiotracers. ^{99m}Tc-HMDP bone scan disclosed an increased radiotracer uptake in the 10th right rib. ^{99m}Tc-MIBI scintigraphy showed a MIBI uptake in the 10th right rib and four metastatic foci was highlighted by MIBI SPECT in the 4th, 5th, 6th left rib and in the 7th right rib. **Case 2**, a 54 year old female underwent total right thyroidectomy for a cold nodular 20 years previously. A Hürthle cell carcinoma of the thyroid was diagnosed by histopathology. The clinical follow-up until march 1995 was free. However, serum thyroglobulin levels were gradually rising from march 1995 at june 1995 reaching a value of 180 ng/ml and a total thyroidectomy was performed. A local recurrent Hürthle cell carcinoma was found. On november 1995, the serum thyroglobulin level was high and a iodine-131 total body scan (injection of 100 mCi) was normal. The patient was referred for a MIBI scintigraphy demonstrating two foci of abnormal MIBI uptake (anterior mediastinal and left lung). Pathologic examination showed Hürthle cell carcinoma. In conclusion, our cases reports contribute to the hypothesis that MIBI scintigraphy could be interesting for the detection of Hürthle cell carcinoma's metastases.

PS-157

S. Szakáll, O. Ésik, L. Balkay, S. Lehel, M. Füzy, E. Berényi, L. Trón

PET Centre, Medical University, Debrecen, Hungary
Dept. of Radiotherapy, National Institute of Oncology, Budapest, Hungary
Diagnostics Centre, Pannon Agricultural University, Kaposvár, Hungary

ROLE OF FDG PET IN DETECTION OF LYMPH NODE (LN) METASTASES OF RESIDUAL OR RECURRENT MEDULLARY THYROID CARCINOMA (MTC)

Results of FDG PET scans were compared with serum tumour marker levels and findings of other imaging methods to assess the diagnostic value of FDG PET examinations in MTC with regional (cervical and mediastinal) LN-only metastasis.

Sixteen patients with a history of MTC were investigated. The serum tumour marker (calcitonin and CEA) levels were determined systematically during the follow-up. Each patient underwent regular posttherapeutic (surgery and external irradiation) cervical and mediastinal CT and/or MRI and/or US, and whole-body planar ¹³¹I MIBG scintigraphy. The inclusion criterion for FDG PET examinations was a discrepancy between the measured tumour marker levels and the findings of conventional imaging methods.

Tumour marker levels during the follow-up were elevated in 15 patients and within the normal range in 1 case. The radiological investigations were conclusive for regional LN metastasis in 7 cases, while MIBG scintigraphy yielded positive results in only 3 cases. Both radiological investigations and MIBG scintigraphy revealed LN involvement in the patient with normal serum tumour marker levels. Tumorous tissue was successfully detected in LNs by FDG PET in all cases, and PET identified LN lesions undetected by other imaging modalities. The FDG PET findings were confirmed during the follow-up by histology/cytology in 6 cases, and by other imaging methods and the clinical data in 4 patients.

FDG PET scans may be instrumental in diagnosing (occasionally widespread) LN involvement in patients with residual/recurrent MTC, establishing a rationale for further therapeutic interventions.

PS-158

L. Vaggelli, V. Briganti, L. Borgognoni*, A. Castagnoli, R Masi

UO Medicina Nucleare Azienda Ospedaliera di Careggi, Firenze, *UO Chirurgia Ospedale di SM Annunziata Azienda Sanitaria di Firenze, Italia

RADIOISOTOPIC LYMPHATIC MAPPING OF SENTINEL NODE IN MELANOMA PATIENTS: A PRELIMINARY EXPERIENCE.

Elective lymph node dissection (ELD) for patients with malignant melanoma is still controversial. A possible solution could be the biopsy of the first tumor draining lymph node, sentinel node (SN), which can be identified by means of radionuclide techniques. Preliminary data from our experience are reported. We performed lymphoscintigraphy (LS) in 50 melanoma patients (28 with melanoma of the legs, 3 of the arms and 19 of the trunk): our protocol consists of preoperative peritumoral i.d. injection of ^{99m}Tc labeled microlloid (Albures) to define the regional lymphatic basin and identify the sentinel node by means of planar scintigraphy and cutaneous mapping 30 min to 3 hours later. In 14 out of 50 cases, gamma probe (GP) was also used during surgery in tracing SN. Vital blue dye was used during surgery in all the cases. SNs were excised for pathological examination. The pathological status of SN was defined by means of examinations of frozen sections, hematoxylin-eosin staining and immunohistochemistry for S-100 and HMB-45 MoAb.

Results. At least one separate focus of activity was identified by LS in all the cases (16 in axillary and 34 in inguinal basin): in all 14 cases out of 50 where GP was used, it was successful in tracing SN. LS with cutaneous mapping of SN successfully drove surgical excision in 43 out of 50 cases: in the 7 remaining cases, which are 7 out of 16 cases with SN in the axillary basin, GP was not used and elective node dissection not performed. Micrometastases were found in 10 out of these 43 cases. In all 10 cases SNs were the only positive nodes in the basin. The results of our preliminary experience confirm the feasibility of SN targeting with LS and GP tracing to select patients for ELD in malignant melanoma: we stress the importance of GP tracing in axillary basin where LS with cutaneous mapping alone may not be successful in surgical retrieving of SN.

PS-159

S.Vidal-Sicart, F.Pons, R.Herranz, J.Piulachs¹, J.Palou², T.Castel², J. Setoain.
Nuclear Medicine, Surgery¹ and Dermatology² Departments.
Hospital Clinic. University of Barcelona. Spain

LYMPHOSCINTIGRAPHY AND GAMMA PROBE DETECTION OF THE SENTINEL LYMPH NODE IN MALIGNANT MELANOMA PATIENTS

The sentinel lymph node (SN) is defined as the first node in a lymphatic basin to receive lymphatic drainage from malignant melanoma. If the SN is free of tumour, then radical lymphadenectomy may be avoided in order to prevent morbidity.

AIM: To assess the usefulness of lymphoscintigraphy and intraoperative gamma probe in the SN detection.

METHOD: We studied prospectively 40 patients with malignant melanoma (MM) (24 in stage I/II and 16 in stage III). The day before surgery a lymphoscintigraphy with 4-6 doses (18.5 MBq each) of ^{99m}Tc-nanocolloid was performed. Dynamic flow images at 20 second per frame were obtained immediately after radiotracer injection followed by static images at 30 min and 2 hrs. The first lymph node identified was considered as SN and was marked on the skin. For intra-operative mapping a hand-held gamma probe was used as well as a blue dye injection just previously to surgical incision.

RESULTS: SNs were successfully identified in 39/40 patients (97.5%). In 23 patients with stage I/II 34 SNs were detected. Six (18%) of them were positive for MM and 28 (82%) negative. A total amount of 161 regional lymph nodes was removed, all of them being negative for MM (no "skip metastasis"). In 16 patients with stage III, 22 SNs were located (14 positive and 8 negative for MM). A total of 89 regional lymph nodes were excised in SN positive patients (44 positive and 45 negative for MM) and 41 lymph nodes in SN negative patients, all of them negative for MM.

CONCLUSIONS: Surgical localization of the sentinel node is facilitated with lymphoscintigraphy and the use of the gamma probe. This technique is very useful in selecting patients with malignant melanoma for lymphadenectomy.

PS-160

V.Voliotopoulos¹, A. Stauraka¹, A. Manetou², A. Frantzis¹, L. Vlahos¹, GS Limouris²;

¹Nucl Med Div, Areteion Hosp Univ Med Faculty, Athens, ²Med Phys Unit, NIMTS Hosp, Athens

Tc-99m FURIFOSMIN vs Tc-99m TERTAFOSMIN IN PARATHYROID ADENOMAS

Tc-99m furifosmin (Q₁₂, Mallinckrodt Medical BV, Petten) and Tc-99m tetrofosmin (Myoview, Amersham International Ltd) were used to evaluate 26 patients suspicious for parathyroid adenomas. In all patients serum calcium, phosphor, PTH, calcitonin, FT₃, FT₄ and TSH were assayed by standard clinical chemistry techniques or by using commercially available radioimmunoassay kits. In all patients echography for thyroid and parathyroid was performed. All removed parathyroid were histologically examined.

Both radiotracers were administered on different days to the same patients. Anterior view planar scintigrams were obtained 10 min and 2h p.i. In all subjects a pertechnetate image of the thyroid was followed immediately after the 2h delayed acquisition either of tetrofosmin or furifosmin injection for subtractive reasons.

Regarding the thyroid/parathyroid tracer ratio, different kinetic between furifosmin and tetrofosmin was demonstrated. In particular, the thyroid retention half-times of furifosmin ranged from 0.42 to 1.76 h (mean 1.23) in patients with parathyroid adenomas and from 0.32 to 1.24 h (mean 0.9) in normal subjects.

As compared to tetrofosmin, furifosmin showed a shorter retention to the thyroid gland, while the relevant tetrofosmin half-times appeared significantly longer (p<0.05) in parathyroid adenoma and normal thyroid tissue.

In early (10 min) scans both radiopharmaceuticals had the same sensitivity, while in the delayed images tetrofosmin appeared not to have a diagnostic impact, since in only 5 out of 16 adenoma patients the delayed acquisition was positive.

Furifosmin use for parathyroid adenoma detection seem to be a very promising tracer compared to tetrofosmin, since in both images (early and delayed) all scans were positive.

Poster presentations

PS-161

K.Yoshikawa, K.Tamura, Y.Imai, N.Matsuno, M.Koga, M.Kanai, S.Kandatsu, T.Suhara, H.Tsujii
National Institute of Radiological Sciences, Division of Radiation Medicine, Chiba, JAPAN

EVALUATION OF USEFULNESS OF C-11 METHIONINE PET FOR DETECTING MALIGNANT NEOPLASM

We evaluated the usefulness of C-11 methionine PET for detecting various kinds of malignant neoplasm. We evaluated the degrees of C-11 methionine accumulation in twenty hundred fifty six patients with malignant neoplasm. All patients were examined using PET with C-11 methionine before heavy ion beam irradiation therapy. All patients had malignant neoplasm of which diagnosis was made by histopathology of the specimens obtained by biopsy. Brain tumors, head and neck cancers, lung cancers, uterine cervical cancers, and bone or soft tissue cancers were entered in this study. There were astrocytoma grade two and three, glioblastoma multiform, metastatic brain tumor and others in the brain. Squamous cell carcinoma, adenocarcinoma, melanoma, adenoidocystic carcinoma, acinic cell adenoma and others were in the head and neck region. Adenocarcinoma, squamous cell carcinoma, bronchogenic carcinoma and metastatic lung cancer were in the lung. Adenocarcinoma and squamous cell carcinoma were in the uterine cervix, and so on. We use ECAT EXACT 47 PET scanner and ECAT HR+ PET scanner. Spatial resolutions were six millimeter and four millimeter respectively. From 555 MBq to 740 MBq of C-11 methionine was injected each patient. A static scan was started at 24 minute after injection of C-11 methionine. Fifteen minutes emission scan by EXACT 47 or thirty minutes emission scan by HR+ was done respectively. Axial images obtained by static scan were displayed on the monitor screen so that some reference normal soft tissue were visible at a standard level. The accumulation level of methionine in the tumor were evaluated visually and classified into five grades. The accumulation level was grade zero when no accumulation was seen in the tumor. Faint accumulation was grade one, fair accumulation was grade two, strong accumulation was grade three, and excessive accumulation was grade four. One percent of all our cases were in grade zero, 14% were in grade one, 31% were in grade two, 48% were in grade three, and 6% were in grade four. There were two sarcomas in grade zero which received chemotherapy over four weeks before PET study. There were chordomas, adenocarcinoma of the lung and small squamous cell carcinoma in grade two. Tumors near the liver tended to be evaluated in lower grade under the influence of high accumulation of the liver. From grade two to four came to 85% altogether. This means that the 85% of tumors in our study were detected well by C-11 methionine PET. We concluded that PET with C-11 methionine is powerful and useful imaging tool for detecting malignant neoplasm.

PS-162

M.Yükseç, T.F.Çermik¹, C.Yerlikaya², N.Gülşen², T.Çağlar², Ş.Berkarda¹
T.U. Medical Faculty Depts. of Nuclear Medicine¹ and Thoracic Disease², Edirne, TURKEY

IS Tl-201 SUPERIOR TO Tc99m-MIBI IN THE EVALUATION OF PRIMARY LUNG CANCER ?

Tl-201 and Tc99m-MIBI are achieved as useful tumor seeking agents in primary lung cancer. Our aim was to evaluate the role of Tc99m MIBI (MSc) vs. Tl-201 (TSc) in planar and SPECT scintigraphies in patients with suspicious primary lung cancer.

For this purpose 23 patients (66.25±11.63y) were underwent MSc after the injection of 15-20mCi Tc99m MIBI at 30th minute and 4th hour and TSc after injecting 5mCi Tl-201 at 15th minutes and 4th hour. Planar and SPECT images were evaluated visually and quantitatively. L/NL ROI's were drawn in all transversal and planar images from which early (ER), delayed (DR) ratios and retention indexes (RI=(DR-ER)x100/ER) for SPECT and planar images were obtained.

	SPECT		Planar	
	TSc	MSc	TSc	MSc
ER	4.38±2.94	6.12±6.86	1.5±0.59	1.51±0.33
DR	6.17±3.73	6.79±6.76	1.57±0.28*	1.33±0.19*
RI	68.94±120.52	24.03±55.18	11.49±20.89	-9.75±15.68*

* p<0.05; \$ p<0.01; # p<0.001

Although there weren't any significant difference in SPECT studies between TSc and MSc for ER, DR and RI, in planar studies TI DR and RI were significantly higher than MIBI DR (p<0.001) and RI (p<0.01). Also ER was significantly higher than DR in planar MIBI images (p<0.05).

In conclusion; our results indicate that while in SPECT images Tl-201 is similar to Tc-99m MIBI, in planar images it is superior to Tc-99m MIBI in primary lung cancer evaluation.

Oncology: Peptide

PS-163

M.Bäder¹, C.Hessenius³, M.Böhmig², S.Faiss², U.Pape³, H.Meinhold¹, E.O.Riecken¹, B.Wiedenmann³
Dpt. of Nuclear Medicine¹ and Dpt. of Gastroenterology² Benjamin Franklin Medical Center, Free University of Berlin and Dpt. of Gastroenterology, Charité, Campus Virchow Medical Center, Humboldt University of Berlin³, Germany

VASOACTIVE INTESTINAL PEPTIDE RECEPTOR SCINTIGRAPHY IN PATIENTS WITH PANCREATIC TUMORS.

Recent data suggest that vasoactive intestinal peptide (VIP) receptor expressing tumors can be detected in vivo by I-123-VIP receptor scintigraphy (VIPS). This study was conducted to examine the value of VIPS in solid gastrointestinal tumors.

Methods: Synthetic VIP (Bachem, Switzerland, pharmaceutical grade) was labeled with iodine-123 (carrier free) using a modified chloramine T method. To obtain "carrier free" monoiodinated VIP, radiolabeled products were purified by semipreparative reversed phase high performance liquid chromatography. 200 MBq I-123-VIP (< 0.5 µg) were applied in a single bolus intravenously. Repeated planar whole-body acquisition was performed in anterior and posterior view using a dedicated digital gamma camera system. I-123-VIP whole body biodistribution was revealed by applying Region Of Interest (ROI) technique. Scanning results were compared with abdominal ultrasonography and CT-scan.

Patients: Up to now 13 patients with histologically proven metastatic pancreatic adenocarcinomas (PA) (n=11) and non functional neuroendocrine pancreatic tumors (NET) (n=2) were investigated by VIPS.

Results: Apart from mild transient hypotension no side effects were observed. After intravenous injection I-123-VIP was rapidly cleared from the circulation. Whole body measurements expressed as radioactivity in % of injected dose revealed a very high uptake in lung (43,5% ± 4,7% at 36 ± 4 min, 18,8% ± 3,2% at 4,1 ± 0,3 hr and 1,0% ± 0,3% at 22,9 ± 0,8 hr). Only a low uptake was found in abdominal organs. Main excretion route is the urinary tract (78,4% ± 7,4% in 24 hr) compared to faeces (0,06% ± 0,09% in 24 hr). VIPS showed uptake in the primary of 3/11 PA and 1/2 NET. Liver metastases were visualised in 5/8 PA and 2/2 NET.

Conclusion: Iodine-123 labeled VIP remains stable for in vivo application. Reproducible biodistribution with major uptake in lung and minor uptake in abdominal organs was found. In addition to normal organs an increased uptake of I-123-VIP is observed in pancreatic adenocarcinomas and in neuroendocrine pancreatic tumors. To evaluate this procedure in further detail more patients as well as stable VIP-analogues have to be studied.

PS-164

L.Carp, P. De Bondt, P. Blockx.
Department of Nuclear Medicine, Antwerp University Hospital, Wilrijkstraat 10, B-2650 Edegem, Belgium.

THE CONTRIBUTION OF SOMATOSTATIN RECEPTOR SCINTIGRAPHY TO DECISION-MAKING IN THE CLINICAL MANAGEMENT OF NEUROENDOCRINE TUMORS.

The use of somatostatin receptor scintigraphy (SRS, In-111 Pentetreotide) has been reported in a wide variety of tumors of neuroendocrine origin. In view of the high cost of the examination we were interested in the actual contribution, in terms of new or unique data, of SRS to the clinical management of these tumors, with respect to strict observation of the indications accepted in literature.

We retrospectively studied 46 consecutive patients (24 females, 22 males) with a "good" indication for SRS, according to literature: known or suspected carcinoid (n=12), insulinoma (n=6), gastrinoma (n=4), melanoma (n=7), ectopic ACTH-secreting tumor (n=4) and other neuroendocrine tumors (n=13). Findings were correlated with CT, MRI, ultrasound and with final outcome.

The interpretation in terms of sensitivity or specificity was considered as not relevant, since both the presence and the absence of somatostatin receptors yields clinical important and unique information, especially decisive regarding a possible treatment with octreotide. The contribution of SRS was therefore also evaluated on the basis of this receptor status.

In only 4/46 (9%) patients the contribution of SRS was not relevant.

In 63% of patients, findings were decisive for therapy:

- radical change of an already defined therapeutical course: 8/46 (17%)
- information on the receptor status, regarding treatment with octreotide: immediate treatment in 7/46 (15%); as second-line treatment after other initial therapy in 8/46 (17%); no octreotide treatment in 6/46 (13%).

In 5/46 (11%) patients, findings were determining for the stage of disease by excluding (somatostatine receptor-positive) metastases of a receptor-positive primary tumor. In 8/46 (17%) patients, findings could exclude the presence of a somatostatine receptor-positive neuroendocrine tumor.

Conclusion: In 29/46 (63%) patients, findings of SRS were decisive for therapeutical management. In another 13/46 (28%) patients, a global negative work up, regarding the possible presence of a neuroendocrine tumor or metastases, could be concluded, because of the negative findings of SRS.

This high yield justifies the use of SRS in the work up of neuroendocrine tumors, provided strict observation of the indications accepted in literature.

PS-165

M. Lázníček, A. Lázníčková, F. Trejtnar, H.R. Mäcke

Faculty of Pharmacy, Charles University, Hradec Králové, Czech Republic, and Institute of Nuclear Medicine, University Hospital, Basel, Switzerland

PHARMACOKINETICS OF Ga-67-[DFO]-OCTREOTIDE IN RATS

Biodistribution and elimination characteristics of Ga-67-[DFO]-octreotide - a potential radiopharmaceutical for imaging of somatostatin receptor-positive tumors - were studied in rats.

The agent was prepared by adding of 4 µl of 1 mM [DFO]-octreotide to 100µl of ammoniumacetate pH 5.6 together with 10 µl of Ga-67-(NO₃)₃. Molar-concentration ratio of [DFO]-octreotide-to-no carrier added Ga³⁺ was 32.05. After 60 min incubation, 2 µl of this mixture was diluted 100 times to 20 mM ammonium acetate. Radiochemical purity, determined by HPLC, was over 99%.

Biodistribution studies were performed on male Wistar rats. Ga-67-[DFO]-octreotide was administered intravenously in a volume of 0.2 ml. At selected times post-injection, a blood sample and selected organs and tissues were removed to determine the distribution of the radiopharmaceutical. Whereas the radioactivity in blood and most of organs and tissues decreased rapidly with time, the radioactivity in kidneys decreased very slowly and in later time intervals remained relatively unchanged (about 6% of administered dose). Long term retention and high concentration of radioactivity in the octreotide receptor-expressing organs adrenals and pancreas were determined. The radioactivity found in bowels was evidently due to a partial elimination of the agent by bile. Binding of Ga-67-[DFO]-octreotide to rat plasma proteins was 42.2±10.3%. In blood, a negligible passage or binding of the radiopharmaceutical on/to blood cells was found. Elimination studies showed that the radioactivity after Ga-67-[DFO]-octreotide administration was eliminated relatively rapidly mostly via urine. About 8% of the administered dose was excreted also by faeces.

For the analysis of renal elimination mechanisms of Ga-67-[DFO]-octreotide, a rat kidney perfusion *in situ* was employed. The results confirmed that the agent is partially secreted in renal tubules, as renal clearance of free Ga-67-[DFO]-octreotide slightly exceeded the value of glomerular filtration rate.

The results may contribute to the explanation of Ga-67-[DFO]-octreotide pharmacokinetics.

Work was supported by the Grant Agency of Charles Univ. - grant No. 127 96 C

PS-166

O. Schillaci**, F. Scopinaro, P. Cannas, F. Monteleone, R. Danieli, S. Angeletti*, V.D. Corleto*, B. Annibale*, G.F. Delle Fave* Nucl. Med., Dep. Exp. Med. Path. and *Gastroenterol., Univ. "La Sapienza", Rome and **Nucl. Med., Univ. L'Aquila, Italy

EFFECT OF In-111 PENTATREOTIDE (In-pe) SCINTIGRAPHY (S) ON CLINICAL MANAGEMENT (MA) OF PATIENTS WITH GASTRINOMA (G). In-pe S has recently shown to be accurate in detecting neuroendocrine tumours. To assess its ability to alter clinical ma in patients (pts) with g, 25 pts with biochemical evidence of Zollinger-Ellison syndrome (ZES) and secretin test positive were studied prospectively. Conventional imaging modalities (CIM), including US, CT, MRI and bone scan, were performed, and ma was proposed, dividing pts in 4 groups: with indication of explorative laparotomy for unknown primary tumour (n=12); with indication of surgery for single known primary tumour (n=4); with indication of liver surgery for metastases (n=4); excluded from surgery due to known extrahepatic metastases (n=5). Then all pts underwent total body planar images (at 4 and 24 hours) and abdominal (ab) SPECT (at 4 hours) following In-pe injection, and treatment's plan was reassessed. SRS was superior to all CIM combined in detecting gs: it was the only positive imaging method in 10 pts and visualized 38 lesions (1e, 19 ab extrahepatic, 15 hepatic and 4 extraab) in 24 pts, whereas CIM detected only 29 1e (13 ab extrahepatic, 13 hepatic and 3 extraab) in 14 pts. These outcome resulted in changing man in 12/25 pts; therefore, primary tumour localizations and clarification of questionable findings of CIM were the major reasons for changing man. In-pe imaging was equally useful both in pts with and without metastatic liver involvement. In conclusion, our results show that In-pe imaging alters clinical man in 48% of pts with g and indicate that SRS must be performed before treatment decisions in ZES, especially when the disease has not been already localized. Moreover, due to its high sensitivity, greater than that of CIM also in pts in whom it did not change man, In-pe scintigraphy should be performed as the initial imaging method to evaluate pts with g.

PS-167

R. Valkema, P.M. Lugtenburg, A.C. Fröberg, J.M. van Muiswinkel, A.E.M. Reijts, P.P.M. Kooij, H.Y. Oei, E.P. Krenning. Depts. of Nuclear Medicine, Hematology, and Radiology, University Hospital, Rotterdam, the Netherlands.

ITERATIVE RECONSTRUCTION OF SOMATOSTATIN RECEPTOR SPECT IN LYMPHOMA.

Aim: Somatostatin receptor scintigraphy (SRS), including SPECT, is less sensitive for the detection of abdominal lymphoma lesions than for lesions elsewhere. We investigated whether the image quality and sensitivity of abdominal SRS SPECT improve after maximum likelihood estimation maximization (MLEM) iterative reconstruction compared to standard filtered backprojection (FBP).

Methods: Abdominal SRS SPECT studies of previously untreated patients (pts), 12 with Hodgkin's disease (HD) and 12 with non-Hodgkin lymphoma (NHL), were reanalyzed. Raw data had been acquired 24 h. after 220 MBq In-111-DTPA-octreotide with a 3-head camera (Picker PRISM 3000), 3x40 projections of 30 sec. The raw data were reconstructed twice, with standard FBP and with MLEM, 20 iterations. Iterative reconstruction took 30 sec. per study. In either case a 3D postfilter (low pass, cut-off 0.32 cycles/pixel, order 8.0) was used. The sets of all FBP and all MLEM images were separately read by a panel of 3 experienced observers. Lesions were scored by consensus. A visual grading was used: grade 0: no lesion, 1: equivocal, 2: lesion with intensity lower than liver, 3: intensity higher than liver, 4: very intense. The quality of the SPECT images was scored as 1:poor, 2: fair, 3:reasonable, 4: good. The corresponding CT scans were independently reanalyzed with focus to the location of lesions, to enable accurate comparison with SRS SPECT.

Results: In all FBP studies "star" artifacts were seen, in 22/24 studies these artifacts interfered with the interpretation. The MLEM studies were visually clearer, with only in 1 patient a slight circular artifact around an intense kidney. The mean quality score of FBP SPECT was 2.3 vs 3.8 for MLEM (p<0.001).

CT was positive for para-aortic or other abdominal lymph nodes in 12 pts (4 HD, 8 NHL). With FBP SPECT 1 study was poor due to artifacts, 2 pts were negative, 3 pts equivocal and 7 pts positive. With MLEM 9 pts were positive and 3 pts were equivocal (incl. the 2 negative pts with FBP). In 1 NHL pt CT, FBP and MLEM were all equivocal. CT was negative in 11 pts (8 HD, 3 NHL). In most patients spots with equivocal or low intensity were seen with FBP as well as with MLEM. The meaning of this is unclear, since CT is not a true gold standard.

Conclusion: MLEM iterative reconstruction of SRS SPECT allows better interpretation than FBP, and it is fast enough for clinical application.

PS-168

Jing Wang, Jinglan Deng and Hongqin Qiao

Hospital: Department of Nuclear Medicine, Xijing Hospital, Xi'an, Shanxi 710032, P.R.China

EXPRESSION OF SSSTR1~5 mRNA IN LUNG CANCER

The purpose of this study was to observe expression of the subtypes of somatostatin mRNA in lung cancers. There were 4 kinds of lung cancer tissue, totaling 24 specimens which were obtained from surgery, involved. Radioisotope[α-³⁵S]dATP labelled probes which were composed of complementary sequence of SSSTR1~5 mRNA were applied to *in situ* hybridization. Expression of multiple subtypes of SSSTRs occurred in all kinds of tissues of lung cancer. Each kind or each specimen of lung cancer registered a quite distinctive pattern of expression. The expression rates ranked as follows: S1=S4>S2=S3=S5 in Ad.; S1>S5>S2=S3=S4 in Sq.; S2>S5>S1=S4>S3 in SCLC.; S1>S3=S4 in GC.; From the result, it can be seen that S2 had a dominant expression in SCLC. while in NSCLC. S1 expression was dominant. Expression densities of S1~S5 in tissues of lung cancer ranked as follows: Sq.>Ad.>GC.>SCLC. in S1; Sq.=Ad.>SCLC.>GC. in S2; Sq.=Ad.>GC.>SCLC. in S3; Sq.>Ad.>GC.>SCLC. in S4; Sq.=Ad.>SCLC.>GC in S5. All results were statistically significant. In tissues of different kinds of lung cancer, S1, S3~S5 expression rates and expression density higher in NSCLC. than in SCLC., suggesting that SSA target-oriented agents also promise optimistic prospects for its use in treatment of NSCLC..

Poster presentations

Oncology: FDG

PS-169

H.M. Abdel-Dayem, H.A. El-Zeftawy, E. Bonfils, P. Teitgin, A. Gagliardi J. Luo, S. Naddaf, M. Kumar, S. Atay, B. Degirmenci. St. Vincent's Hosp, Nucl Med Sec, Dept. of Rad, St Vincent's Comp. clinical Cancer Ctr, and chest service of med. NY Med Coll, Valhalla, NY.

Evaluation of F-18 FDG Dual Head Coincidence Imaging (DHCI) in Detection of solitary pulmonary nodules (SPN) less than 3 cm

DHCI is an emerging modality for F-18 FDG imaging.

Purpose: to report results of F-18 FDG using DHCI in 20 patients (pts) with solitary lung nodules less than 3 cm seen in CT/MRI of the chest. **Methods:** After fasting overnight blood glucose levels were 60-100 mg/dl, pts injected 5-7 mCi (18.5-25.2 MBq) F-18 FDG, imaged after waiting for at least 60 minutes using ADAC Vertex/MCD dual head gamma camera with 30% photopeak window at 511 KeV and 30% Compton window at 330 KeV, 32 projections, 40 secs /view. Images prefiltered with Butterworth filter for FBP or Wiener filter for ml-em reconstruction, no attenuation correction used. Studies read visually and by calculation of lesion to normal background (L/N) ratios. Visual interpretation by at least 3 observers was positive for only high grade and intermediate FDG uptake agreed upon by all readers. Confirmation of results was by surgical biopsy or excision in 14 pts and more than 6 months follow up in 6 pts.

Results: All of the 9 pts with pathologically proven malignant lesions had positive FDG uptake with L/N ratio ranging from 1.1-2.8 aver 1.7+/- 0.47. Of the 10 pts with benign nodules, 3 had positive FDG uptake (false positive) L/N ranged from 1.1-1.28 aver 1.12+/-0.06 and 7 had negative FDG studies (all were true negative). Only one pt had recurrent nodule after excision of her primary.

Conclusion: FDG DHCI in our series for SPN <3cm had sensitivity of 100%, specificity 70%, PPV of 76.9% and NPV of 100%. L/N ratios are less than expected because of high scatter and absence of attenuation correction.

PS-170

M. Baehre, B. Meller, I. Lauer, *H. Luig, E. Richter
Clinic of Radiotherapy and Nuclear Medicine, Medical University of Luebeck, *Nuclear Medicine Department, University of Goettingen, Germany.

IMAGING PROPERTIES OF A GAMMA CAMERA COINCIDENCE PET SYSTEM AND CLINICAL RESULTS IN 210 PATIENTS

The use of coincidence gamma cameras for positron emission tomography decreases high investment and maintenance costs dramatically. Thus, a wider section of patients can profit from this diagnostic method, esp. in oncology. However, there is still a controversé discussion whether clinical information provided by the new method is sufficient when compared to conventional PET imaging. This is why the present study reports the strategies when introducing coincidence imaging (PRISM 2000 XP PCD, Picker) in our department and the clinical results in 210 patient investigations after application of 200-250 MBq [¹⁸F]FDG.

Primarily, basic imaging properties of the system were determined. Phantom studies were performed to register imaging of patient body cross-sections at common tumour/non-tumour uptake ratios. In the second stage, acquisition and reconstruction were optimized and a newly developed multiplicative iterative reconstruction technique was implemented. Reconstruction parameters were modified to achieve both maximum homogeneity of tomograms and recognizability of small tumour sites. Only in the third stage of the project, 210 patient studies were performed, 200 of them for oncologic questions.

Using the body phantom, recognizability of hot lesions reached to 10-12 mm (diameter) for an uptake ratio of 6:1. The smallest tumour detected in vivo (breast cancer) was 5 mm in diameter (histologically proven). Intrahepatic metastases were depicted down to lesions of 12 mm by now. 88 investigations were performed within defined oncologic studies. Non-oncologic questions existed in 10 patients. In the remaining 112 cases no active tumour was found in 38 patients, active tumour masses in 74 patients. In 8 out of 9 cases with CUP syndrome, tumour manifestations were proven.

Conclusions: Phantom studies and as well patient investigations demonstrated indisputably high clinical benefit of coincidence imaging in oncology. This new variant of PET seems to provide a useful completion of routine diagnostic tools - not only because of the limited funds in medicine even in many developed countries.

PS-171

M.E. Bellemann, G. Brix, L. Gerlach, H. Trojan, U. Haberkorn

Research Program „Radiological Diagnostics and Therapy“, German Cancer Research Centre, Heidelberg, Germany

PHARMACOKINETIC ANALYSIS OF [F-18]FDG UPTAKE IN HETEROGENEOUS TISSUES

For quantitative analysis of dynamic [F-18]FDG PET data, the well-established 4k model of Huang *et al.* is commonly employed. Recently, K. Schmidt *et al.* introduced a pharmacokinetic model for use in heterogeneous tissues (HT model) which describes the tissue compartment as an aggregation of small homogeneous subregions. In the HT model, the dephosphorylation of FDG-6-phosphate is neglected (*i. e.*, $k_4 = 0$). The purpose of this PET study is the evaluation of the 4k and the HT model in the framework of an experimental animal study.

Twelve male ACI rats with untreated *s. c.* transplanted Morris hepatoma (cell line MH3924A) were examined with a whole-body PET scanner. An extra-corporeal loop was placed between the carotid artery and the jugular vein for continuous measurement of the arterial input function with an external BGO fluid monitor. After *i. v.* bolus injection of 40-60 MBq of [F-18]FDG, the PET examination was performed dynamically (40 frames) over 90 min. The 4k and the HT model were used to determine the rate constants K_1 , k_2 and k_3 and the global metabolic rate of FDG turnover MR_{FDG} in the Morris hepatoma.

In both models, the quality of curve fitting was comparably good; the small differences in the residual weighted sums of squares were not significant. According to the Schwarz criterion and the Akaike information criterion, however, the 4k model described the PET data significantly better than the HT model ($P < 0.05$). Significant differences were found for the rate constants K_1 ($P < 0.05$), k_2 and k_3 ($P < 0.005$) as well as for the metabolic rate MR_{FDG} ($P < 0.005$). The coefficients of variation were not significantly different in the two models.

The HT model represents an interesting alternative to the 4k model. The differences in the rate constants can be explained by the different model configurations (*e. g.*, effective time-dependent parameters in the HT model, or the influence of $k_4 \neq 0$ on K_1 , k_2 and k_3 in the 4k model). Further biochemical studies on the glucose-6-phosphatase activity and the metabolic compartments in the hepatoma are warranted to decide in which model the FDG tumour uptake is most accurately described.

PS-172

M.E. Bellemann, G. Brix, F. Oberdorfer, L. Gerlach, U. Haberkorn

Research Program „Radiological Diagnostics and Therapy“, German Cancer Research Centre, Heidelberg, Germany

ASSESSMENT OF NEUTRAL AMINO ACID TRANSPORT: PET OF α -(N-[1-C-11]ACETYL)-AMINOISOBUTYRIC ACID

The study of amino acid transport in solid tumours provides information on the grade of the malignant transformation. The non-physiologic amino acid α -(N-[1-C-11]acetyl)-aminoisobutyric acid ([C-11]NA-AIB) is an ideal PET substrate for the investigation of the neutral Na⁺-dependent amino acid transport (system A). The purpose of this animal study is (i) the measurement of the biodistribution of [C-11]NA-AIB and (ii) the kinetic analysis of system A amino acid transport.

Seven male Copenhagen rats with *s. c.* transplanted Dunning prostate carcinoma (R3327-AT1) were examined with a whole-body PET system. The arterial input function was measured with an extra-corporeal loop placed between the carotid artery and the jugular vein. After *i. v.* bolus injection of 20-58 MBq [C-11]NA-AIB, the PET examination was performed dynamically (40 frames, 40 min). The organs were removed and the [C-11]NA-AIB uptake (*SUV*, 40 min *p. i.*) was measured by scintillation counting. The activity-time curves of tumour, liver, brain, and muscle were analysed with different kinetic models.

Both *in vivo* and *in vitro*, NA-AIB was not metabolised. In cell culture, 79 % of the substrate entered the prostate carcinoma by system A amino acid transport, whereas 21 % was taken up by the Na⁺-independent system. The [C-11]NA-AIB uptake 40 min *p. i.* was: tumour: *SUV* = 0.77 ± 0.06; liver: *SUV* = 0.83 ± 0.05; brain: *SUV* = 0.69 ± 0.05; muscle: *SUV* = 0.64 ± 0.02. According to the Schwarz criterion and the Akaike information criterion, the best model configuration was a two-compartment heterogeneous-tissue model with weighted forward transport rate K_1 (in ml/min/g) and effective backward transport rate k_2 (in min⁻¹), revealing the rate constants: tumour: $K_1 = 0.30 \pm 0.05$, $k_2 = 0.31 \pm 0.06$; liver: $K_1 = 0.84 \pm 0.13$, $k_2 = 0.59 \pm 0.13$; brain: $K_1 = 0.35 \pm 0.08$, $k_2 = 0.37 \pm 0.07$; muscle: $K_1 = 0.36 \pm 0.05$, $k_2 = 0.38 \pm 0.07$.

Since NA-AIB is not metabolised, amino acid transport can be studied separately from protein synthesis which provides higher accuracy. The kinetic analysis shows elevated amino acid transport rates in the liver (with $K_1 > k_2$) compared to the tumour and the other organs ($K_1 \approx k_2$).

PS-173

H. Bender, J.P. Frohmann*, M. Grapow, A. Schomburg, C. Menzel, F. Grünwald, J. Ruhlmann, and H.-J. Biersack
Depts. of Nuclear Medicine and *Dermatology;
University of Bonn

VALUE OF WHOLE-BODY FDG-PET IN THE ROUTINE STAGING OF MALIGNANT MELANOMA

The aim of this study was to evaluate the diagnostic value of whole-body positron-emission tomography (PET) employing fluoro-18-deoxyglucose (FDG) in the staging of melanoma as compared to conventional imaging modalities.

After resection of the primary tumor, high-risk melanoma patients (n=96; Breslow >0.75 mm, Clark Level >2) were prospectively enrolled for whole-body staging using a dedicated PET scanner (EcatExact 921/47; Siemens/CTI). Transmission-corrected emission tomograms were reconstructed and qualitatively evaluated employing a 4-point scoring system. Results were compared to CT/MRI, immunoscintigraphy, histology and final clinical diagnosis (gold standard) at a follow-up time of at least 6 months.

A total of 214 lesions (multiple lesions at the same site are counted as 1 lesion!) were identified: 49 with intensely, 45 with moderately and 120 with minimally enhanced glucose-uptake, respectively. Lesions with an intense uptake demonstrated a sensitivity, specificity, and accuracy of 90%, 97% and 94%, respectively, in predicting malignant tissue. In contrast, lesions with moderate uptake showed only a sensitivity, specificity, and accuracy of 64%, 73% and 72%, respectively, as an indicator for tumor tissue. Furthermore, only 65% of true positive and PET-positive lesions were identified by CT and 42% by immunoscintigraphy (Tc99m-TECHNEMAB). In some cases, FDG-PET identified lesions 3-6 months prior to CT and was most beneficial in the evaluation of lymph-node involvement.

FDG-PET (a) is a sensitive and accurate tool for the staging of high-risk melanoma, and (b) is most beneficial in the assessment of lymph-node involvement. FDG-PET should be used in the primary staging of high-risk melanoma patients.

PS-174

R.Burt, R.Witt
VAMC and Indiana University, Division of Nuclear Medicine

DUAL ISOTOPE IMAGING OF F-18 FDG AND Tc99M RBC IMAGING FOR BETTER LUNG TUMOR LOCALIZATION

SPECT F-18 FDG tumor imaging is sensitive; however the images contain little anatomic information. This is exacerbated when delayed imaging is performed. Two hours after FDG administration, the only anatomic landmarks are the kidneys, the liver is faintly seen and uptake in the heart is variable. Accurate localization of tumors or metastasis is sometimes difficult even with direct comparison with CT imaging and does not provide localization information when lesions are not identified by CT.

We studied 10 patients on an IRB protocol and 25 more clinically referred for FDG imaging with a dual isotope technique. Windows set at 511keV and 140 keV using a Trionix XLT20 gamma camera. Patients were premedicated with "cold" PYP and 3700 to 555 mBq FDG and were injected and 370 to 555 mBq of Tc-99m about 30 minutes later. After a 2 hour delay after FDG/Tc dual isotope images were acquired. Images were reformatted on a MedImage viewing station into 3-D and transverse formats. They were then fused into one image set with different colors representing blood pool and FDG distribution. Images were displayed in rotating and transverse format. The blood pool images were also subtracted from the FDG images which nearly eliminated background.

Location of lesions in relationship to the major blood vessels including those in the neck was easily discerned.

Use of the 2 isotope technique adds additional anatomic information on location and when images are subtracted less obvious lesions are better seen.

PS-175

A.Crespo, C.Gámez, JM. Aramendia, A.Cabrera, R.Cañón, J.Arbizu, J.Richter. Department of Nuclear Medicine-PET. Clínica Universitaria of Navarra. Pamplona. Spain.

¹⁸FDG-PET AND BONE SCINTIGRAPHY IN LUNG CANCER.

The purpose of this study is to compare diagnostic value with ¹⁸FDG-PET and conventional ^{99m}Tc MDP scintigraphy (BS) for detection of bone metastases in lung cancer patients.

Material and Methods : PET-[¹⁸F]FDG and ^{99m}Tc MDP studies were compared in 47 patients with proven diagnosis of lung cancer; maximum period between both explorations was less than two weeks in any case. PET scans were obtained in thorax, abdomen and, in some cases, in pelvis. BS were carried out by conventional whole-body scanning. The final diagnosis of bone metastases was achieved by means of CT, MRI and / or clinical evolution.

Results: No differences between PET and BS were found in 42 patients. Thirty-seven showed no bone lesions while in 5 patients bone metastases were found with both techniques. From 5 remaining patients, with discordant findings, PET confirmed 2 true-negative and 1 true-positive cases. In one case, reported as positive by BS, PET field of view did not include the lesion. BS detected a sacrum metastasis informed as presacrum focus by PET.

Conclusion: Using a whole-body PET-¹⁸FDG for lung cancer evaluation, BS could be avoided for bone metastases detection.

PS-176

A.Dimitrakopoulou-Strauss, M. Schwarzbach, F. Willeke, Y.M. Zhang, T. Heichel, G. Mechttersheimer, G. Irngartinger, L.G. Strauss

German Cancer Research Center, Heidelberg, Germany.

MULTITRACER STUDIES IN PATIENTS WITH SARCOMAS

PET multitracer studies were used to differentiate viable tumor tissue and to delineate the tumor extension. The evaluation comprises 23 patients with suspected sarcomas (15 soft tissue tumors, 6 bone tumors; scar tissue was found in two patients). PET and SPET studies were performed for tumor staging with F-18-Deoxyglucose (FDG) and Tc-99m-Sestamibi. In selected cases O-15-Water (tissue perfusion) was used to support the differential diagnosis. Dynamic PET studies were performed for 60 minutes (FDG) or 8 minutes (O-15-Water). Planar acquisitions as well as SPET studies were performed with Tc-99m-Sestamibi on the same day prior to PET.

Twenty-one of twenty-three lesions showed an increased uptake of FDG. One patient with a lesion classified as tumor recurrency in MRI, due to Gd-DTPA enhancement, revealed a low uptake of all three tracers in PET and was classified as a scar tissue. This patient did not undergo surgery but the result was confirmed by the clinical follow-up data. Another lesion was classified as scar tissue, which was confirmed by histology. Large lesions demonstrated a very inhomogenous uptake with enhanced uptake values in the rim of the lesions and a low uptake in the central parts due to necrosis, hemorrhage etc.

The quantitative evaluation of the tumors revealed:

FDG: 1.9-4.6 SUV (60 min p.i.); tumor/muscle 1.88-4.18

O-15-Water: 1.8-3.8 SUV (5 min p.i.); tumor/muscle 2.25-4.35

The uptake was lower for liposarcomas with grade I as compared to grade III. An increased uptake was found for all tracers in the malignant tumors. Scar tissue was correctly identified only with PET. The distribution patterns within the sarcomas were different for FDG and O-15-Water. Tc-99m-Sestamibi was positive in all malignant tumors and in one of the two scar lesions. The results support the preferential use of FDG for tumor diagnosis due to the superior spatial resolution, the specificity as compared to Sestamibi, and the quantification capabilities.

PS-177

H. Fujii, M. Ide, S. Yasuda, W. Takahashi, A. Shohtsu, T. Suzuki, K. Nakamura, F. Kinoshita, A. Kubo
HIMEDIC Imaging Center at Lake Yamanaka and
Department of Radiology, Keio University School of Medicine

INCREASED FDG UPTAKE IN THE RIGHT ATRIAL WALL ON THE PEOPLE WHO PARTICIPATED IN CANCER SCREENING PROGRAM WITH WHOLE BODY PET.

We have studied cancer screening with whole-body PET using F-18 FDG. We have encountered several cases of increased FDG uptake in the right atrial walls. In this study we evaluate the characteristics of these rare cases.

We reviewed the findings for 2367 cases (1523 male, 844 female, mean age 52.4 yr) who underwent whole-body FDG PET. All of these participated in our cancer screening program between October 1994 and January 1998. A PET study was carried out 45 to 60 minutes after the administration of 260 to 370 MBq of F-18 FDG during a fasting state of several hours. The cases with high FDG uptake in the right atrial walls were selected and we examined their illness, the size of their right atria, the results of treadmill ECG tests (5 cases), and myocardial perfusion tests with N-13 ammonia PET (6 cases).

Increased activity in the right atrial wall was found in 7 of 2367 cases. All 7 cases suffered from cardiac disorder. Five suffered from atrial fibrillation, one had congestive heart failure with tricapsid regurgitation, and the other had atrial septal defect. The maximum diameter of the right atrium was greater than 5 cm in 6 of 7 cases. But no remarkable myocardial ischemic change was detected on the treadmill ECG tests or ammonia PET studies.

In conclusion, increased FDG uptake in the right atrial wall was observed in the 7 cases of cardiac disorders. As most of them had enlarged right atria, overload of right atria could induce the high metabolic state of glucose. Since increased activity in the right atrial wall would be a false positive finding in the cancer screening with FDG PET, attention should be paid to cases with right atrial overload.

PS-178

C. Gámez, MJ García Velloso, M Giménez, I Azinovic, JM Aramendia, J Arbizu, J Richter. Servicio de Medicina Nuclear. Clínica Universitaria. Universidad de Navarra. Pamplona. Spain.

COMPARISON OF WHOLE-BODY F-18-FDG-PET AND Tc-99-ANTI-CEA FOR DETECTION AND STAGING OF RECURRENT COLORECTAL CARCINOMA.

Since several agents seem to be suitable for detection and staging of recurrent colorectal carcinoma, a comparative evaluation of the different methods available is needed. Hence, we investigated F-18-fluorodeoxyglucose (FDG)-PET and Tc-99-anti-CEA during the same week in an intraindividual comparative study. Six patients, clinical or radiographical suspicious of recurrent or metastatic colorectal carcinoma were prospectively studied. PET-FDG was performed in the whole-body mode 60 min after iv injection of 370 MBq of FDG using bladder catheter and furosemide iv in order to force diuresis and minimize bladder activity. Anti-CEA imaging was conducted 2 to 5 hours after the iv administration of 750 MBq of Tc-99-anti-CEA, using both planar scintigraphy and single-photon emission CT (SPECT), and further planar images were procured at 18 to 24 hours postinfusion, but no forced diuresis or bladder catheter were used. All patients were further evaluated by additional imaging procedures (chest X-ray, liver ultrasound, pelvis CT, bone scan), CEA levels, colonoscopy or surgery. The mean follow-up was 7.7 months (min. 6.5, max. 10.5). Overall malignancy was present in 5 patients, either local, distant or both. FDG-PET correctly identified 4 recurrences, 2 hepatic metastatic disease and 1 tumoral adenopathy in the pelvis, but overevaluated 1 patient with no proved presacral recurrence by biopsy. Anti-CEA scintigraphy missed 1 pt with liver metastases and 1 pt with a isolated tumoral adenopathy in the pelvis. Both procedures correctly excluded a local relapse in 1 pt confirmed by laparotomy.

Our data suggest that F-18-FDG-PET is more accurate for detecting recurrence of colorectal cancer than Tc-99-anti-CEA and affords a high-quality, same day imaging, but anti-CEA scintigraphy could improve its results minimizing the bladder activity.

PS-179

C. Gámez, T Ramón y Cajal*, MJ García Velloso, I Azinovic*, M Giménez, JA Richter.
PET-CUN Center. Department of Oncology*. University Hospital School of Medicine. University of Navarra. Pamplona. Spain

DETECTION AND STAGING OF RESIDUAL OR RECURRENT COLORECTAL CANCER WITH 18F-FDG PET.

Purpose: To evaluate accuracy and possible clinical utility of PET and 18F-FDG in the diagnosis of residual or recurrent disease in patients with colorectal carcinoma.

Material and methods: Forty-one whole-body PET scans were obtained from 37 patients (22M/15F, Mean Age=58 years) following iv administration of 370 MBq of 18F-FDG. Attenuation corrected scans were performed on 17 studies. The results were compared to histopathological examination, other imaging procedures, tumoral markers and follow-up (>3 months).

Results: A total of 57 potential malignant sites in 28 patients were suspected on the basis of a hypermetabolic uptake: 52 true positive (site of initial resection=14, liver=8, extra-hepatic abdominal=9, lung=13, bone 2, other=6) and 5 false positive in local sites (4 post-radiotherapy fibrosis and 1 acute infection). PET also disclosed malignant sites not previously suspected in 13 patients. Seven patients were confirmed to be free of disease. In 2 different patients, the suspected mediastinal adenopathies and a solitary pulmonary nodule showed no uptake in the PET study and proved to be malignant in the subsequent follow-up. Both patients were receiving chemotherapy at the time of PET performance.

Conclusion: Our data indicate that PET-FDG appears to be an accurate procedure for imaging residual or recurrent disease in patients previously treated with colorectal carcinoma. PET scans analysis should be carefully interpreted in patients receiving chemo or radiotherapy.

PS-180

MJ García Velloso, M Giménez, J Alcalde, C Gámez, I Azinovic, J Arbizu, J Richter. Department of Nuclear Medicine-PET. Clínica Universitaria and Hospital of Navarra. Pamplona. Spain.

POSITRON EMISSION TOMOGRAPHY WITH [18F]FDG IN HEAD AND NECK TUMORS AFTER IRRADIATION

The purpose of this study was to evaluate the clinical utility of PET-[18F]FDG imaging in diagnosing recurrency in head and neck tumors after irradiation.

Material and Methods: PET-[18F]FDG imaging was performed 45 minutes after 370 MBq of [18F]FDG administration in 30 patients, 26 males and 4 females, being squamous-cell carcinoma the most common tumor (19 patients, 63.3%). CT was performed in 24 patients, MRI in 2 and 4 patients had CT and MRI. Histopathologic analysis compared recurrent tumor with findings on CT, MRI and PET images.

Results: PET imaging accurately detected 24 cases (S=96%), was true negative in 4 cases (E= 80%) false positive in one patient with infection and equivocal in 1 patient with recurrency. CT or MRI identified accurately 15 cases (S=60%) and there were 3 true negatives (E=60%), but in 9 patients the results were equivocal and there were 3 false negatives. Combining the information from CT, MRI and PET imaging 25 cases with recurrency (S=100%) and 4 cases negatives (E=80%) were accurately diagnosed, remaining a false positive study in a patient with infection.

Conclusion: PET-[18F]FDG imaging is highly effective in evaluating patients for recurrent head and neck tumors, although the best results are obtained combining morpho-functional information from PET, CT and MRI.

PS-181

MJ García-Velloso, A Gorosquieta*, C Pérez-Equiza *, M Giménez, A Cabrera, J López **, JA Richter. Departments of Nuclear Medicine-PET, Haematology* and Oncology**. Clinica Universitaria and Hospital of Navarra. Pamplona. Spain.

PET-FDG VERSUS CT IN THE STAGING AND DETECTION OF RELAPSE IN PATIENTS WITH HODGKIN'S DISEASE OR NON HODGKIN LYMPHOMA. TWO YEARS EXPERIENCE.

Purpose: To retrospectively evaluate the effectiveness of FDG-PET and CT in the staging and in the detection of residual disease or recurrence in patients with Hodgkin's disease (HD) or Non-Hodgkin lymphoma (NHL).

Materials and Methods: 53 whole body FDG- PET and 51 CT scans were performed in 12 patients with HD (5f/7m) and 32 with NHL (17f/15m). PET-[18F]FDG imaging was performed 45 minutes after 370 MBq of [18F]FDG administration. Nine evaluations were pretherapeutic. PET and CT scans were validated by histology (n=12) or clinical follow-up (n=41).

Results: In 9 patients undergoing initial staging FDG-PET was true positive in 8 patients and true negative in one. A pathological CT scan, however, was found in only 6 patients and 3 studies were inconclusive. In 44 studies performed after treatment PET was true positive in 18/19 (S=95%) and true negative in 22/25 (E=88%), whereas CT was true positive in 6/19, true negative in 8/25, there were 24 inconclusive residual mass, a false positive and 3 false negative scans.

Conclusion: FDG-PET may provide an accurate means of staging and detecting relapse in patients with Hodgkin's disease or Non-Hodgkin lymphoma.

PS-182

U. Haberkorn, R. Kinscherf, H. Kamencic, I. Morr, M. Eisenhut, G. van Kaick. German Cancer Research Center (dkfz), Heidelberg.

CHANGES IN TUMOR METABOLISM AND APOPTOSIS IN HEPATOMA CELLS AFTER GENE THERAPY WITH HSV THYMIDINE KINASE.

This in vitro study investigates the relation of tumor metabolism to the appearance of apoptosis after gene therapy with the suicide gene HSV thymidine kinase (HSVtk). HSVtk-expressing Morris hepatoma cells were incubated for 24 h with 0.5, 5 and 25 µM ganciclovir (GCV). Thereafter, FDG, 3-O-methylglucose and thymidine (TdR) uptake studies were performed immediately and 24 h after the end of GCV incubation. The uptake was normalized to the viable cell number. Furthermore, the amount of apoptotic cells was determined using the TUNEL reaction. FDG uptake and apoptosis were also measured after exposure of the cells to cytochalasin B, which binds to the inner site of the glucose transporter. Immediately after incubation with GCV the FDG and 3-O-methylglucose uptake increased up to 186%. At 24 h after the end of treatment, the FDG uptake normalized, whereas the 3-O-methylglucose uptake remained elevated. The TdR uptake decreased in the acid-insoluble fraction to 27% and 11%, whereas the TdR accumulation in the acid-soluble fraction increased to 228% immediately after therapy and to 172% at 24 h after treatment. Significant amounts of apoptotic cells were found only 1 day after therapy, where a lower uptake of FDG and TdR was observed. After additional incubation with 10 µM cytochalasin B a decrease of FDG uptake to 20% and an increase in apoptosis were seen. The increase in FDG and 3-O-methylglucose uptake early after therapy onset is interpreted as stress reaction of the tumor cells. Inhibition of glucose transport may be used to enhance the effectiveness of gene therapy with HSV thymidine kinase.

PS-183

U. Haberkorn, M.E. Bellemann, R. Kinscherf, H. Kamencic, G. Brix, H. Trojan, J. Doll, J. Blatter, G. van Kaick. German Cancer Research Center (dkfz), Heidelberg, Germany and Lilly Deutschland.

TUMOR METABOLISM AND APOPTOSIS AFTER GEMCITABINE THERAPY OF MORRIS HEPATOMA.

This combined in vivo/in vitro study investigates the application of positron emission tomography (PET) for monitoring of gemcitabine therapy. Furthermore, apoptotic changes were related to changes of tumor metabolism. Morris hepatoma cells were transplanted into ACI rats and dynamic PET measurements of FDG uptake were done in animals prior to therapy (n=7), one day (n=6) and 2 days (n=6) after the onset of therapy with 90 mg gemcitabine/kg using an extracorporeal circulation. The PET studies were evaluated by SUV and a pharmacokinetic analysis. The thymidine (TdR) incorporation into the DNA of these tumors was determined after DNA extraction. Also in vitro measurements of FDG and TdR uptake were performed immediately and 24 h after the end of 24 h incubation with different doses of gemcitabine and the amount of apoptotic cells was determined using the TUNEL reaction. The kinetic constants increased significantly at 2 days after treatment, whereas the values for SUV and the metabolic rate were not different. TdR incorporation declined to 8% and 34% of the controls at 1 and 2 days after treatment, respectively. In vitro studies showed an increased uptake for FDG (60%) immediately and a normalization at 24 h after therapy. TdR uptake revealed a decrease in the acid-insoluble fraction (16% and 25%) and a 320% increase in the acid-soluble fraction which normalized at 24 h after the end of gemcitabine incubation. Significant amounts of apoptotic cells were found only 1 day after therapy, where FDG uptake and TdR metabolism normalized. These data indicate that PET with FDG and TdR may be applied for therapy monitoring of gemcitabine therapy. The increase in glucose uptake and TdR metabolism early after therapy onset is interpreted as stress reaction of the tumor cells and may protect the cells from apoptosis at least during this period after exposure to cytotoxic drugs.

PS-184

U. Haberkorn, M.E. Bellemann, L. Gerlach, I. Morr, F. Oberdorfer, H. Trojan, J. Doll, G. van Kaick. German Cancer Research Center (dkfz), Heidelberg, Germany.

PET STUDIES OF FDG UPTAKE DURING GENE THERAPY WITH HSV THYMIDINE KINASE IN MORRIS HEPATOMA.

This combined in vivo/in vitro study investigates the application of positron emission tomography (PET) with tracers of tumor metabolism for monitoring of gene therapy with the suicide gene HSV thymidine kinase (HSVtk). After generation of HSVtk-expressing Morris hepatoma cells by transfection with a retroviral vector, these cells were transplanted into ACI rats and dynamic PET measurements of FDG uptake were done in animals prior to therapy, two days and 4 days after the onset of therapy with 100 mg/kg ganciclovir (GCV). Also uptake measurements were done in a tk-expressing cell line and in control cells (bearing the empty vector) using FDG, 3-O-methylglucose, and thymidine in the presence of different doses of GCV. These experiments were done up to 72 hours after the onset of therapy. Two days after therapy an increase of K1 was seen in almost all animals (n=9) as compared to controls (n=9), although an overlap was observed. Four days after therapy the value declined. Furthermore the thymidine incorporation into the DNA of these tumors declined to 25% of the controls. To simulate the clinical situation, 6 animals were After 2 days therapy with ganciclovir the SUV increased in all animals. The metabolic rate and K1 increased in 4/6 animals. Thereafter a decline of FDG uptake was seen in 3/6 animals after 4 days treatment. The in vitro studies showed an increased uptake for FDG and 3-O-methylglucose up to 200% and a 96% decrease of thymidine incorporation into the nucleic acid fraction. These data indicate that PET with FDG and thymidine may be applied for therapy monitoring of gene therapy with HSVtk. The increase in FDG and 3-O-methylglucose uptake early after therapy onset is interpreted as stress reaction of the tumor cells.

PS-185

L. Lauer, B. Meller, M. Baehre, B. Jaeger, E. Richter

Clinic of Radiotherapy and Nuclear Medicine, Medical University of Luebeck, Germany

STAGING AND RADIOTHERAPY FOLLOW-UP OF MALIGNANT LYMPHOMA WITH PET USING A COINCIDENCE GAMMA CAMERA

Objective: Aim of the study was to investigate the value of PET with a gamma camera coincidence system for staging, restaging and radiotherapy follow-up of malignant lymphoma. PET findings were compared with conventional diagnostic procedures and the clinical follow-up.

Patients and methods: Up to now we examined 15 patients with malignant lymphoma (8 NHL, 4 Hodgkin's disease, 3 Burkitt Lymphoma). 4 patients had 3 to 6 investigations for radiotherapy follow-up, usually performed prior to irradiation, after administration of half dose (HD), at the end and 4 weeks after irradiation. Altogether 30 PET studies were performed with a double-head coincidence gamma camera (PRISM 2000 XP PCD, Picker). Patients were fasting for 4 hours (blood glucose < 7 mmol/l) and were not diabetic. PET studies were started 45 min after administering 250 MBq ¹⁸F-FDG. We generally performed 3 tomographies (180°, 6° step, 80 sec/step (prolonged due to decay)) for complete imaging of neck and trunk, except for the studies at HD, where only the irradiated volume was investigated. The data were reconstructed iteratively (Luig). For determination of irradiation response the scans were evaluated visually. Additionally, a tumour uptake ratio was calculated semiquantitatively.

Results: (1) 20/30 PET studies were true pos., 9/30 true neg., 1/30 was false pos. (inflammatory lymphatic tissue in oropharynx). (2) 6/30 studies revealed additional information not found by the conventional diagnostics. (3) In 5 cases only PET could distinguish between active lymphoma and scar (3/5 true pos., 2/5 true neg.). (4) The effect of radiotherapy (4 patients) could be visualized prior to CT or MRI using ROI technique. In one patient irradiation planning was changed because of PET results.

Conclusion: Our data demonstrate the value of PET with a coincidence system in staging and follow-up of patients with malignant lymphoma. Especially, no false negative findings were observed. When compared to the conventional diagnostics, PET revealed enhanced information and showed radiotherapy response earlier.

PS-186

N. Lemmens, S. Stroobants, M. Gysen, G. Vandenbosch, I. Vergote, P. Dupont, G. Bormans, L. Mortelmans
Departement of Nuclear Medicine, U.Z. Gasthuisberg, K.U. Leuven, Belgium.

FDG-PET IN THE DETECTION OF PERITONEAL AND RETROPERITONEAL METASTASES OF OVARIAN CANCER.

Aim of the study : to evaluate the performance of FDG-PET, compared with CT, for the preoperative detection of peritoneal and retroperitoneal metastases of ovarian cancer.

Methodology : Patients, suspected to have advanced ovarian cancer and scheduled for laparoscopy and/or laparotomy, were prospectively included. Prior to surgery, patients underwent a contrast enhanced abdominal CT and a FDG-PET scan. Attenuation corrected images were obtained 60 min. p.i. of 6.5 Mbq/kg FDG on a ECAT 9318/12 camera (10 min. emission in 4 bedpositions). For data analysis, the abdomen was artificially divided into 6 regions (right and left subphrenic region, right and left paracolic gutter, retroperitoneum and omentum). Each region was visually scored both on PET and CT on a 3-point scale (negative, positive and equivocal). Equivocal results were considered positive in the further analysis. PET results were compared with those of CT, using the surgical data as gold standard.

Results: Until now 13 patients were included (7 with newly diagnosed ovarian cancer and 6 with suspicion of recurrent/residual disease after prior surgery or chemotherapy). In total, 73 regions were evaluable. Correlated with final diagnosis. PET scan was correct in 58 regions, 2 regions were false positive and 13 regions false negative, whereas CT scan was correct in 55 regions, false positive in 8 and false negative in 10 regions. Sensitivity was slightly better for CT than for PET (73% versus 66%). Metastases of less than 5 mm were missed with both techniques. Specificity, however, was clearly better for PET than for CT (94% versus 77%), especially in post-surgical patients, where postoperative adhesions and fibrosis caused false positive as well as false negative results. PET correctly diagnosed retroperitoneal involvement in all patients whereas CT was false positive in 2.

	all		new diagnosed		postsurgical	
	PET	CT	PET	CT	PET	CT
sens	66	73	66	74	53	53
spec	94	77	94	77	100	79

Conclusion: Given the low sensitivity of both PET and CT for the detection of peritoneal metastases, invasive staging remains the only adequate tool in the initial staging. Because of the clearly better specificity, especially in post-surgical patients, PET might be preferred for evaluating residual or recurrent disease.

PS-187

M. Lonneux, G. Lawson, C. Ide, M. Minet, V. Gilain, M. Remacle and S. Pauwels. UCL PET Laboratory, Louvain-la-Neuve, Belgium and Dpts of ENT, Radiology, Mont-Godinne UCL University Hospital, Yvoir.

Positron emission tomography (PET) for the detection of recurrence or second localisation in head and neck cancer.

Background: morphological changes induced by therapy are frequent and can reduce the accuracy of conventional imaging modalities such as CT or MRI in the follow-up of patients with head and neck cancer. In this study, we investigate the potential role of fluorodeoxyglucose (FDG) PET imaging in the workup of patients suspected for head and neck cancer recurrence.

Methods: 25 pts were prospectively included in the study. All had been treated for a head and neck tumor and presented with clinical symptoms evocating tumor recurrence. Conventional workup included physical examination, CT-scan and MRI of the head and neck region. FDG-PET was obtained and interpreted blinded to the results of conventional workup. Final diagnosis was obtained by biopsy in 19 pts, and the clinical follow-up (6-15 mo.) was used for the remaining 6 pts.

Results: 21 tumor sites were demonstrated in 16 patients. 9 pts were free of disease. Results are detailed in Table.

	Tumor + (n=16)	Tumor - (n=9)
PET +	15	3*
PET -	1	6
	sens 94 %, spec 67 %, PPV 83 %, NPV 86 %	
CT/MR +	11	5
CT/MR -	5	4
	sens 69 %, spec 44%, PPV 69%, NPV 44%	

* 1 pt with inflammatory tracheal stenosis, treated by laser 1 week before PET, 1 pt with recent (<2days) biopsy.

Conclusion: PET-FDG is a powerful tool to help differentiate between tumor recurrence and post-therapy changes in patients previously treated for head and neck cancer. However, it has to be reminded that highly inflammatory sites show high FDG uptake, and that clinical context is mandatory to avoid these false positive findings.

PS-188

H. Moustafa, A. Zaher, S. Eissa and H. Abd El Dayem

Dept. of Nuclear Medicine in Kasr El Aini Hosp.
and Cancer Institute, Cairo University, Egypt.

Value of 99mTc-Furifosmin (Q 12) as tumour imaging agent

A prospective study using 99mTc-Q12 a myocardial perfusion imaging in detection of malignant tumours in 82 patients. The group is formed of 44 males, 38 females with bone, brain, lung, breast and head and neck cancer as proved histopathologically. Patients were injected with 740 mBq of Tc-Q12 with imaging within 5 minutes. Planner and SPECT images were done using Trionex dual head gamma camera. 61 patient showed different grade of tumour uptake and 11 patients had no evidence of tumour uptake following radiation therapy. Whereas 10 patients had false negative results, such finding may be related to multidrug resistance. The sensitivity, specificity and accuracy of 99mTc-Q-12 in tumour detectability was 85%, 100% and 74% respectively.

To conclude 99mTc-Q12 can be used as tumour imaging agent.

PS-189

T. Okamura, J. Kawabe, K. Koyama, M. Shakudo, H. Sakamoto, M. Matsuda, H. Ochi, R. Yamada

Hospital: Osaka City University Medical School, Department of Radiology, Division of Nuclear Medicine, Department of Otolaryngol.

EVALUATION OF FDG PET FOR THE DIAGNOSIS OF HEAD AND NECK LESIONS

The purpose of this study was to evaluate the usefulness of FDG PET for diagnosis and monitoring of treatment of head and neck lesions. A total of 109 patients with head and neck lesions (82 malignant, 11 benign and 17 inflammatory lesions) other than salivary gland lesions were included in the study. All patients underwent FDG PET, and PET images were evaluated quantitatively with SUV (standardized uptake value). The SUV of malignant tumors (average 7.8) was significantly higher than that of benign lesions (av. 3.3). With a cut-off value of 3.0, accuracy was 82%. Seventy-one malignant tumors were localized in 6 different sites: hypo-, meso-, or epipharynx, larynx, maxillary sinus and tongue · oral floor. There was no significant differentiation of SUV in each localization. Fifty-two squamous cell carcinomas (SCC) were histologically classified as well, moderately, poorly or undifferentiated. A histological classification was not correlated with tumor SUV (av. 7.4~8.2). These SCC included T1~ T4 stages. SUVs of T4 stages were significantly higher than those of T2 and T3 stages. FDG PET was performed after chemoradiation therapy in 38 patients with malignant tumors. After chemoradiation, SUVs of 21 cases were over 3.0 and SUVs of 17 less than 3.0. Residual tumors were proven in 17 out of 21 with SUV over 3.0 and 6 out of 17 with SUV under 3.0 histologically. With a cut-off value of 3.0, accuracy was 79%.

In conclusion, FDG PET was useful in differentiating between malignant and benign head and neck lesions and in the evaluation of residual tumor after treatment using SUV. However, no correlation was found between SUV and localization, and none between SUV and histological classification.

PS-190

S. Oku, K. Nakagawa, T. Ohtake, M. Tateno, T. Momose, S. Saegusa, Y. Sasaki.

University of Tokyo, Japan

FDG-SPECT AS A SUBSTITUTE OF FDG-PET IN THE PATIENTS MANAGEMENT WITH MALIGNANT NEOPLASMS.

FDG-SPECT attracts increasing interest as a substitute of FDG-PET because of its lower installation cost. The present study was designed to evaluate the feasibility of FDG-SPECT using a gamma-camera equipped with 511keV collimators (Vertex, ADAC Laboratories, Milpitas CA) as a monitoring tool of external radiotherapy (XRT).

Methods: PET and SPECT were performed with an identical pool phantom to determine the calibration coefficients. Six patients of colorectal cancer underwent two times a combination of FDG-PET and consecutive FDG-SPECT before and after whole pelvic XRT of 50Gy. The XRT was aimed as an adjuvant of either Miles' operation or low anterior resection. SUV corresponding to maximal concentration of FDG in the tumors were calculated by use of above mentioned calibration coefficients. Changes in SUV were compared between the modalities.

Results: The efficacy of XRT was assessed by a decrease of SUV with SPECT (SUV-S) from 12.8±5.4 to 8.4±4.1, as well as by that with PET (SUV-P) from 13.5±4.1 to 5.8±3.9. The difference between SUV-P and SUV-S ranged from -35% to 44%. For two patients out of six, the regions of interest after therapy were hardly delineated because of poor SPECT image quality. Correlation coefficient between SUV-S and SUV-P was 0.84.

Conclusion: SUV-S with the collimator method showed suboptimal correlation with SUV-P and the feasibility of FDG-SPECT as a monitoring tool for XRT was suggested. Coincidence imaging technique may further enhance the quantitative significance in SPECT.

PS-191

Ramackers J.M., Frappaz D., Honnorat J., Jouvet A., Fischer G., Sindou M., Galy G., Pujol J.F., Cinotti L. CERMEP, Centre L. Bérard, Hôpital Neurologique, LYON, FRANCE.

METABOLIC FOLLOW-UP OF OLIGODENDROGLIOMAS (ODG) USING C11-METHIONINE (MET) AND F18-FDG IN PET.

Chemotherapy may cause a volumic reduction of brain tumors like ODG. Despite this reduction, as shown by anatomic imaging, a residual mass persists, and no prognosis can clearly be carried out. Metabolic activity evaluation by means of PET markers could contribute to evaluate the prognosis of this mass. Therefore, we used MET and FDG for a semi quantitative evaluation of the tumor activity.

Seven patients (age : 41,6 ± 14,2 years), with biopsy or surgery proven ODG, (1 grade A, 4 grade B and 2 grade C of Smith's classification) underwent, at least, 2 PET studies using MET and FDG during their follow-up (20,3 ± 5,7 months) : 6 before and after the same chemotherapy protocol and one for a simple follow-up. Maximum tumor over normal contralateral cortex ratios (T/N) were computed.

Before treatment, these tumors presented with a normal or reduced FDG uptake (T/N = 0.89 ± 0.22; 6/7 pts), except for one grade C (2.35). On the other hand, MET showed a high uptake (2.13 ± 0.5; 6 pts, and 5.79 for the same grade C). After therapy, MET demonstrated a reduced volume of the tumor. Uptake ratios decreased for MET in 5 patients presenting a tumor response to therapy (T/N-FDG : 0.88 ± 0.17 and T/N-MET: 1.49 ± 0.36) but remained stable in one symptomatic patient. In one patient, initially stabilized by therapy, PET detected an secondary increase of T/N-MET, suggestive of evolutive disease, that was confirmed later. The non treated patient presented with a T/N increase and this evolution was also confirmed. This preliminary study shows that MET gives visual and semi-quantitative informations, more sensitive than FDG, to evaluate the proliferative potential of ODG. MET also appears to offer the possibility of chemotherapy effect assessment in ODG.

PS-192

M.J. Reinhardt, B. Kracke, H. Guffler, C. Ihling, S. Högerle, T. Bauknecht, E. Nitzsche, T. Krause
Departments of Nuclear Medicine, Gynecology and Obstetrics, and Diagnostic Radiology, and Institute of Pathology, Albert-Ludwigs-University, Freiburg, Germany

DETECTION OF METASTATIC LYMPH NODES BY MRT AND BY F-18 FDG PET IN PATIENTS WITH CERVICAL CANCER

The purpose of this study is to compare the diagnostic accuracy of MRT and F-18 FDG PET for detection of metastatic lymph nodes in cervical cancer.

Therefore, 23 patients with cervical cancer FIGO IB - IIB (age 50 ± 14 yrs.) are investigated with F-18 FDG PET and MRT prior to hysterectomy and radical lymphadenectomy. The results are compared on the basis of histology. PET is performed 90 min. after i.v. injection of 370 MBq F-18 FDG (Siemens Ecot Exact). Urinary bladder was continuously rinsed during emission scan. Images are reconstructed with photon absorption correction and filtered back projection technique in 13 patients and with iterative reconstruction in 10 patients. MRT is performed on a 1.5 Tesla system (Siemens Magnetom Vision) using a body coil and standard T1 and strong T2 weighted spin-echo sequences. Out of 784 lymph nodes (LN) dissected, 26 are metastatic. PET identified 21 metastatic LN's and MRT identified 12, respectively (p < 0,01 Fisher's exact test). On a lymph node by lymph node basis, the sensitivity of F-18 FDG PET is 81 % and of MRT is 46 %, and the specificity is 99 % and 98 %, respectively. 2 of 5 metastatic LN's not identified on PET sized 5 mm in diameter or less and 3 were on LN-regions containing multiple metastatic LN's. With iterative reconstruction, only one 3 mm LN-metastasis was missed. In conclusion, detection of metastatic lymphadenopathy can be done more accurate by F-18 FDG PET than by MRT. F-18 FDG PET might be used in the first place instead of MRT for predicting the site of metastatic lymph nodes in patients with cervical cancer.

PS-193

J.H. Risse, F. Grünwald, H. Strunk, H. Bender, P. Willkomm, C. Menzel, Hj. Biersack
Departments of Nuclear Medicine and Radiology, University of Bonn, Germany

18-FDG-PET AND 3-PHASE HELICAL LIVER CT IN INTRA-ARTERIAL THERAPY WITH I-131-LIPIODOL IN PRIMARY LIVER CANCER.

Purpose: Evaluation of PET changes after i.a. therapy with I-131-Lipiodol in patients with primary liver cancer, and comparison with liver CT.

Methods: 9 patients with hepatocellular cancer (HCC) and 1 pt. with cholangiocellular cancer (CCC) were angiographically treated with 16 intraarterial applications of I-131-Lipiodol (1110 - 1850 MBq) into the hepatic artery. Each patient had CT and 9 patients had 18-FDG-PET controls before therapy. 6-8 weeks after each application tumor response was controlled by CT (all patients) and PET. 1 patient (HCC) had 3 PET controls, 1 patient (HCC) 2 and 3 patients (2 HCC, 1 CCC) 1 PET control, respectively.

Results: Pretherapeutic PET showed a high interindividual variability in tumor tracer accumulation, ranging from 3 lesions equivalent to normal liver tissue (3 HCC) to different grades of hot lesions (5 HCC, 1 CCC). After the first treatment control PET scans could be achieved in 5 patients. One HCC (therapy responder) had no PET change. Another responder without pretherapeutic PET showed no change of the cool lesion in all further PET controls despite obvious tumor changes in the CT controls. In contrast, PET showed progression of the CCC earlier than CT. In 2 patients control findings of PET and CT were concordant with progressive disease in both.

Conclusions: PET and CT controls in our first 10 patients with primary liver cancer treated by I-131-Lipiodol show in part discordant findings. The combination will be most sensitive for tumor changes and thus yield the best results.

PS-194

M.P.M. Stokkel(1), FW ten Broek(2), P.P. Van Rijk(1).

University Hospital Utrecht, The Netherlands, Departments of Nuclear Medicine(1), Oral and Maxillofacial Surgery(2).

ASSESSMENT OF CERVICAL LYMPH NODE METASTASES IN HEAD AND NECK CANCER WITH 18F-FDG USING A DUAL HEAD COINCIDENCE CAMERA.

Introduction: An accurate evaluation of metastatic cervical lymph nodes plays a decisive role in the treatment and prognosis of patients with squamous cell carcinoma of the head and neck. FDG-PET seems to be a valuable imaging technique for the detection of cervical lymph nodes. However, dedicated PET scanners are not widely available. With a dual head SPECT scanner with coincidence module (ADAC MCD), PET scanning of 18F-FDG is possible, with a spatial resolution of 5 mm. **Methods and Materials:** Twenty-seven patients with primary head and neck cancer were studied. In 7 of these patients the primary tumor had already been resected. All patients underwent clinical examination of the neck. CT-scan and US with FNAC was performed in 21 and 23 patients, respectively. After a 6 hour fast, at 60 min. after the injection of 130 MBq of 18F-FDG imaging of the neck was performed during 32 min. Twelve histologically proven neck sides were found. **Results:** The sensitivity of FDG-MCD and CT for detecting the primary tumor were 100% and 67%, respectively. In three patients, an unknown second primary tumor was found by FDG-MCD. The smallest tumor detected with 18FDG-MCD was 5 mm in diameter. The sensitivity and specificity for detecting lymph node metastases are:

	Sens. (%)	Spec. (%)
18FDG-MCD	100	97
CT	91	94
US	75	48
US + FNAC	50	100

Conclusion: Measurement of 18F-FDG with a dual head coincidence camera seems to be a valuable imaging technique for the detection of cervical lymph node metastases. These results justify a prospective study on staging head and neck tumors.

PS-195

M.P.M. Stokkel, J.W. van Isselt, A. Hoekstra and P.P. Van Rijk.

University Hospital Utrecht, The Netherlands, Department of Nuclear Medicine.

LESIONS OF 4 MM AND 5 MM DETECTED WITH 18F-FDG USING A DUAL HEAD COINCIDENCE CAMERA.

Introduction: Accurate evaluation of tumor and lymph nodes plays a decisive role in the treatment and prognosis of patients with head and neck cancer. In this respect, FDG-PET seems to be a valuable imaging technique. However, dedicated PET scanners are not widely available. With a dual head SPECT scanner with coincidence module (ADAC MCD), PET scanning of 18F-FDG is possible, with a spatial resolution of 5 mm. Two cases are presented in which very small lesions were detected by using a dual head coincidence camera. Neither of these lesions were visible on CT.

Case 1. In November 1997, a resection of a T1 tumor of the upper lip was performed without a neck dissection in a 44-year old female. In December 1997, the patient was suspected for having a metastasis. After the injection of 130 MBq 18F-FDG imaging was performed using a dual head coincidence camera. Besides metastatic uptake there was intensely increased uptake in the thyroid area. A second primary tumor in the thyroid was suspected. Lymph node biopsy revealed a metastasis from a papillary thyroid carcinoma. After thyroidectomy the primary tumor appeared to have a maximum diameter of 5 mm.

Case 2. In January 1996, a 74-year old man was treated for a T1N0 laryngeal carcinoma by means of external beam radiotherapy. In December 1997, he was suspected for having a local recurrence. FDG-PET was performed (protocol see case 1) demonstrating focally increased uptake in the laryngeal region. Biopsy revealed local tumor recurrence. Laryngectomy was performed and histologic examination showed a tumor with a maximum diameter of 4 mm.

Conclusion: Tumor imaging with 18F-FDG using a dual head coincidence camera is capable of detecting lesions as small as 4 mm in the head and neck region.

PS-196

H.J. Straehler-Pohl*, H. Bender, D. Linke, C. Ponath, A. Schomburg, P. Willkomm, J. Ruhlmann, F. Grünwald, and H.-J. Biersack
Depts. of *Head and Neck Surgery and Nuclear Medicine; University of Bonn

VALUE OF F-18-DG-PET IN THE STAGING OF HEAD AND NECK TUMORS UNDER CLINICAL ROUTINE CONDITIONS

The aim of this study was to evaluate the clinical utility of F-18-Deoxyglucose (FDG) positron-emission tomography (PET) as a routine diagnostic tool in the pre-surgical staging of defined head-and-neck tumors.

PET-scans (Ecat/Exact 921/47; Siemens/CTI) were performed in more than 180 patients (pts) employing a whole-body protocol. Transmission corrected emission scans (filtered backprojection), 45-60 min after i.v. injection of 185-333 MBq FDG) were qualitatively assessed using a 4-point scoring system. Results were compared to histology (gold-standard), ultrasound, CT and/or MRI.

In a pilot study, pts. (n=50) with large tumors (pT2) were scanned in order to establish malignancy-typical criteria. Primary tumors and metastases showed intense FDG-uptake and high contrast as compared to normal tissue (sensitivity 100%, specificity 80%). FDG-uptake comparable to cerebellum was established as "malignancy-typical". In continuation, pts. with suspected recurrence (n=63), large primary (n=47), or cancer of unknown primary (n=37) were assessed according to these criteria. FDG-PET showed an overall sensitivity, specificity, and accuracy of 94%, 72% and 89%, respectively, and was able to present important functional information. FDG-PET was most beneficial in assessing lymph-node involvement, scar tissue vs. recurrence, and identification of a primary in CUP. Prior knowledge of the PET result, would have changed therapeutic intervention in 34% of the patients, due to up- or downstaging.

We conclude, that FDG-PET is a useful tool in the pre-surgical staging of selected cancer patients and in the restaging of treated patients with suspected tumor recurrence.

PS-197

J. G. Strauss, L. Schad, A. Dimitrakopoulou-Strauss, J. Debus, M. Knopp, F. Oberdorfer, G. van Kaick.

German Cancer Research Center, Heidelberg, Germany.

POSITRON EMISSION TOMOGRAPHY (PET) AND MAGNETIC RESONANCE IMAGING (MRI) IN PATIENTS WITH BRAIN TUMORS RECEIVING RADIOTHERAPY.

The correlative assessment of PET and MRI studies necessitates common landmarks. This is important in particular for the radiotherapy of brain tumors. Vital as well as necrotic tumor tissue must be identified and associated with morphological structures.

We used an individual, dedicated head mask and a stereotactic device in patients scheduled for radiotherapy due to brain tumors. External marks were used during the imaging procedures and evaluated with a software program in order to correlate the corresponding cross section levels. The MRI examination was dynamically performed in each patient using the intravenous application of contrast material (Gd-DTPA), parameter: TR=170 ms, TE=5 ms, FL=900, RFOV=160*270 mm², MA=128*256, TH=5 ms, 15 sections, acquisition time 22 sec). Double tracer PET studies were performed with O-15 labeled water and F-18-Deoxyglucose. The PET images were corrected for scatter and attenuation and iteratively reconstructed. Identical ROIs were used for MRI and PET and time-signal and time-activity concentrations were calculated. Furthermore, models (two and three compartment) were used for the quantitative evaluation of the MRI kinetics, for O-15 labeled water and FDG.

The preliminary evaluation of the ongoing study comprises 5 patients. The spatial error was less than 3 mm in all patients. All tumors were well delineated in the MRI images. The PET data demonstrated in 2 patients inhomogeneous tumor tissue with hypo- and hypermetabolic areas, which were associated with hypo- and hyperintense regions in MRI. The quantitative evaluation gave evidence for a two compartment distribution of Gd-DTPA in tumors. The FDG accumulation was associated with the contrast material kinetics, when the evaluation was confined to the tumor area. PET multi-tracer studies were used to differentiate viable tumor tissue and to delineate the tumor extension.

PS-198

A. J. Sun, Q. Y. Sun, J. M. Li, J. Zhao, M. F. Wang, D. B. Qiu
Zibo Wanjie Hospital

PET center, Department of Nuclear Medicine

DETECTION RECURRENCE OF HEAD AND NECK CANCER AFTER TREATMENT WITH 18F-FDG PET

To evaluate 18F-FDG PET in detection of suspected recurrence of head and neck cancer after treatment and to compare with CT imaging.

Thirty eight patients with clinical suspected recurrence of head and neck cancer were performed with 18F-FDG PET, twenty eight patients also underwent CT imaging. The images were interpreted visually and semiquantitated as tumor-to-normal (T/N). The accumulation of tumor was graded into four grade: 0 grade (no FDG uptake), I grade (slight uptake), II grade (moderate uptake), III grade (intensive uptake), the accumulation of tumor in grade II or grade III was defined recurrence, the final diagnoses of recurrence were based on histological or clinical follow up.

The sensitivity and specificity of visual interpretation of PET for recurrence was 90.6% (29/32), 83.3% (5/6) respectively, CT imaging was 63.6% (14/22), 50% (3/6) respectively. The ratio of T/N of recurrence was higher than benign.

In conclusion: Compared with CT images, PET has a higher accuracy in the detection of recurrent head and neck cancer post treatment.

PS-199

Y. Suzuki, S. Nasu, S. Yasuda*, M. Ide*, A. Shohtsu*, S. Kuge and Y. Tokuda.

Tokai University Medical School. and *HIMEDIC Imaging Center

THE WHOLE-BODY FDG-PET FOR DIAGNOSIS OF BONY METASTASIS IN THE PATIENTS WITH BREAST CANCER: COMPARISON WITH 99mTc-MDP BONE SCAN

This study was done to evaluate the potential role of FDG-PET(PET) for diagnosis of bony metastasis in the patients(pts) with breast cancer. In the total 48 female patients, 56 PET and bone scan(B-scan) with 99mTc-MDP images obtained within one month each other, were retrospectively evaluated. The whole body PET was obtained 45min after injection of 256 to 370MBq of F-18 FDG in the fasting patients with a whole body PET camera(ECAT EXACT 47, Siemens). Attenuation correction was done with a transmission method. The whole body B-scan was obtained 3hr after injection of 740MBq of 99mTc-MDP. The presence or absence of bony metastasis was confirmed by CT, MRI and clinical follow up more than 10 months. True negative and positive images of the PET were 41 and 13, and those of B-scan were 36 and 8, respectively. The false negative and positive images the PET were one of each, and those of B-scan were 5 and 7, respectively. The false positive findings of the B-scan were found in the rib(3 studies), thoracic spine(2 studies) and lumbar spine(2 studies). The false negative findings of the B-scan were found mainly in the thoracic spine, lumbar spine and pelvic bone. The sensitivity (13/14 studies, 92.8%) and specificity (41/42 studies, 97.6%) of the FDG-PET in diagnosis of the bony metastasis was very high. In conclusion, the PET appears to be useful in diagnosis of bony metastasis difficult to diagnose by B-scan among the patients with breast cancer.

PS-200

M. Tokunaga, S. Amano, K. Aoyagi, N. Oriuchi, T. Inoue, J. Aoki and K. Endo
Gunma University School of Medicine, Department of Diagnostic Radiology and Nuclear Medicine

THE EVALUATION OF SOFT TISSUE LESIONS USING FLUORINE-18-FDG PET

PURPOSE: To evaluate benign and malignant soft tissue lesions with 18F-fluoro-2-deoxy-D-glucose (FDG) PET and to determine whether malignant tumors can be distinguished from benign lesions using standardized uptake value (SUV). **METHODS:** PET was performed in 9 patients with malignant tumors and 26 patients with benign lesions, administrating 172-390MBq of FDG. The SUVs were calculated in all lesions. The correlation between the SUV and contrast enhanced ratio (CE ratio: the volume of intratumoral enhancement/ the tumor volume) was also investigated in 9 lipomas and 4 liposarcomas. **RESULTS:** The mean \pm s.d. of SUV were 3.98 ± 1.87 in 9 malignant tumors and 1.40 ± 1.12 in 26 benign lesions. A significant difference of the mean SUVs between malignant tumors and benign lesions was demonstrated with Student's t-test. The SUVs of some benign lesions (1 calcifying epithelioma, 1 elastofibroma, 1 PVNS and 2 schwannomas) were greater than those of the lowest value among the malignant lesions. When the SUV value of 1.9 was used as a cut off to divide malignant lesions from benign lesions, the sensitivity for correctly diagnosing malignancy was 100% with a specificity of 79% and an overall accuracy of 85%. Furthermore, liposarcomas were clearly differentiated from lipomas by using SUV value of 1.9 with 100% accuracy. The SUV correlated to the CE ratio in lipomas and liposarcomas ($r=0.80, p<0.01$). **CONCLUSION:** Evaluation of SUV is useful to predict malignant soft tissue lesions. SUV values in liposarcomas and lipomas possibly depended on intratumoral vascularity.

PS-201

G. Weir, D. Rushing, J. Priem

Hospital: St. Joseph's Hospital/Marshfield Clinic, Department of Radiology

FDG IMAGING ON SPECT CAMERA, FIRST 50 CASES

Purpose: Evaluate clinical utility and accuracy of F-18 fluorodeoxyglucose (FDG) imaging.

Methods: Coincident detection of F-18 FDG on a SPECT camera was evaluated. Imaging was 1 hour after 5 mCi FDG. 2 or 3 circular orbits with 32 stops and decay-corrected time imaging (nominal 40 secs) was used. Data is fused for whole body depiction. Reconstruction is with a Wiener (0.7) filter.

Results: 50 cases with minimum follow up of 5 months are analyzed. All studies were for evaluation of malignancy. Eight cases were studied on protocol to investigate NSCLC, 42 specifically for patient care. Cases included: Melanoma 14, Pulmonary Carcinoma 14, Lymphoma 7, Colorectal 4, Breast 2, Others 9. 34 studies benefited patient management, 13 had no effect and 3 insufficient follow up to allow assessment. None of the studies adversely affected patient management. Seven resulted in major change in patient management, all in areas where CT was equivocal or negative. Four TN areas where CT was equivocal confirmed lack of need for further therapy. 75 areas were specifically evaluated for involvement. 36 were TP, 18 TN, 3 FP, 12 FN, 6 not yet assessed. FN results were slow growing tumors, cases on therapy at time of imaging, and small (<1 cm) lesions. FP studies were in the abdomen or pelvis. Intestinal and/or urinary activity may be the cause.

Conclusion: F18 FDG imaging on standard SPECT cameras is technically feasible. Patient management was enhanced in 34 of 47 evaluable cases (72%) and of major help in 11 (23%). No studies were deleterious to patient management.

PS-202

P. Willkomm, H. Bender, F. Grünwald, M. Wolf*, J. Ruhlmann**, H.J. Biersack
Depts. of Nuclear Medicine and Surgery*, PET-Center Bonn**,
University of Bonn, Germany

FDG-PET and MIBI SPECT for preoperative lymph node staging in Non Small Cell Lung Cancer

The aim of this study was to evaluate FDG-PET and MIBI-SPECT in the staging (TNM) of non small cell lung cancer (NSCL). Whole body PET (measured-transmission corrected emission scans) was performed after i.v. injection of 6-10 mCi F-18-FDG on a Siemens PET scanner (ECAT EXACT 47) including 5-6 bed positions. MIBI-SPECT (chest) was performed after injection of 20 mCi sestamibi using dual head camera (Picker Prism 2000, ADAC Vertex) and commercially available reconstruction algorithms.

We investigated 33 patients with suspected non small cell lung cancer. The FDG-PET and MIBI-SPECT results were compared to histological findings (after surgery) or bronchoscopic biopsies and CT.

The results were as follows: FDG-PET was true positive in 29/33 patients and true negative in 4/33. MIBI-SPECT identified 25/33 true positive, 4/33 false negative and 4/33 true negative cases. With respect to the lymph node staging, FDG-PET confirmed 10 true positive and 3 false negative cases. MIBI-scintigraphy gave 7 true positive and 5 false negative results. Both examinations found 1 bone metastases, in two cases distant metastases were found only with PET. The tumor/background ratio was higher with PET (2.5 v. 1.8).

Despite the limited numbers of patients it may be concluded that FDG-PET as compared to MIBI SPECT, is more suited to correctly stage lung cancer especially with respect to lymph node involvement. However, the negative findings in MIBI-SPECT may indicate multidrug resistance in some of these tumors.

PS-203

J. Zhao, Q. Y. Sun, J. M. Li, M. F. Wang, A. J. Sun, J. L. Wu

Hospital: Zibo Wanjie Hospital, PET center

COMPARISON OF WHOLE BODY 18F-FDG PET IMAGING AND 99mTc-MDP BONE SCINTIGRAPHY IN THE DIAGNOSIS OF BONE METASTASES

The purpose of this study was to compare 18F-FDG PET imaging to bone scintigraphy with 99mTc-MDP in the diagnosis of bone metastases in patients with various tumors, and to assess the value of whole body 18F-FDG PET imaging in the diagnosis of bone metastases.

Fifty seven patients with various tumors were underwent whole body 18F-FDG PET imaging and bone scintigraphy simultaneously. No attenuation-corrected whole body FDG PET imaging was performed 1h after i.v. administration of 185-370MBq 18F-FDG. Abnormal bone FDG uptake or MDP uptake was considered probability of bone metastasis. The final diagnoses of bone metastases were based on histological findings, or the other imaging studies (CT, MRI), and the clinical follow-up.

114 bone metastases were detected in 57 patients. The sensitivity of FDG PET and bone scintigraphy for detecting bone metastases were 61.4%, 87.7% respectively ($p < 0.01$). 14 additional bone metastases with positive FDG uptake were not identified in 99mTc-MDP bone scintigraphy. 6 benign bone lesions with positive MDP uptake were not identified in FDG PET imaging. Overall, the sensitivity of PET is lower for detecting the metastases in ribs and skull, and the location of lesions accurately is often difficult only by PET imaging.

In conclusion, it should be cautious for the diagnosis of bone metastases by whole body 18F-FDG PET imaging, and it is essential to combine with 99mTc-MDP bone scintigraphy.

Oncology: Breast

PS-204

O. Alonso, L. Delgado, F. Mut, I. Alonso, G. Lago, M. Núñez, Y. Afonso, P. Guisoli, G. Sabini, I. Muse, J. Gaudio, and E. Touya.
Nuclear Medicine Centre and Department of Clinical Oncology of the Clinical Hospital, University of Uruguay, Montevideo, Uruguay.

99mTc-MIBI SCINTIGRAPHY IN ADVANCED BREAST CANCER: PREDICTION OF CHEMOTHERAPY RESPONSE AND EVALUATION OF DISEASE EXTENSION.

Although 99mTc-MIBI scintigraphy has been extensively studied in the evaluation of early breast cancer, the clinical value of the technique in patients (pts) with advanced disease has been less documented. Multidrug resistance (MDR) is a major therapeutic problem limiting advanced breast cancer (ABC) treatment. 99mTc-MIBI has been reported to be extruded from tumoural cells by the P-glycoprotein (Pgp), encoded by the MDR1 gene. The aim of this study was to investigate the potential of the technique in the detection of ABC lesions and to evaluate whether or not the degree of 99mTc-MIBI tumoural uptake correlated with response to chemotherapy. We studied 27 (pts) with ABC (median age: 53, range: 35-83). Twelve with advanced locoregional disease, 5 with locoregional and metastatic disease, and 10 with recurrent disease. In pts with locoregional disease, two lateral (prone imaging) and one anterior thoracic views were obtained 10 minutes and 1 hour after the i.v. injection of 740 MBq of 99mTc-MIBI. A whole-body acquisition was performed in all pts and additional static views on selected cases. All pts with indication of cytotoxic treatment received combination chemotherapy containing doxorubicin. In these pts lesions were imaged 2-8 days prior chemotherapy and after a minimum of 2 cycles according to UICC criteria. Tumour-to-normal tissue uptakes ratios (T/N) were calculated in each assessable lesion. Response to chemotherapy was grouped as response (complete and partial remissions) and no remission. The technique detected 93% of tumoural lesions (18/18 breast tumours, 16/17 pts with axillary nodes, 4/4 local relapses, 3/4 pts with non-regional lymph nodes, 6/7 pts with bone, 2/2 with lung and 1/2 with liver metastases). Thirty lesions were evaluated for response to chemotherapy. Early T/N were significantly higher in lesions that responded to chemotherapy than in non responding lesions (1.95, 1.4-2.9 vs. 1.3, 0-1.6; median, range respectively; $p = 0.000007$). We conclude that 99mTc-MIBI scintigraphy could be useful for the evaluation of disease extension with the potential of guiding chemotherapy in ABC pts.

PS-205

S. Amano, T. Inoue, K. Aoyagi, J. Aoki, K. Endo

Gunma University School of Medicine, Department of Diagnostic Radiology and Nuclear Medicine

THE EVALUATION OF DELAYED SCINTIMAMMOGRAPHY WITH TECHNETIUM-99M-TETROFOSMIN

The aim of this study is to evaluate the usefulness of delayed scintimammography with ^{99m}Tc tetrofosmin in patients with breast cancer. We studied 25 patients who received 555 MBq ^{99m}Tc-tetrofosmin intravenously in the contralateral arm to the suspected breast tumor. Planar images were obtained in the lateral view with an acquisition time of 10 min at 30 and 180 min post-injection, and semiquantitatively evaluated by using a lesion to non-lesion (L/N) ratio and washout ratio. Excisional biopsy was performed within 2 weeks after scintimammography in all patients. There were totally 26 breast lesions (13 invasive ductal carcinoma; 2 scirrhous carcinoma; 1 non-invasive ductal carcinoma; 4 fibroadenoma; 3 mastopathy; 1 phyllodes tumor; 1 granuloma; 1 lipoma). Among 16 breast cancer lesions, there were 13 and 12 true positive lesions on 30 and 180 min images, respectively. There were two benign lesions (fibroadenoma and phyllodes tumor) with false positive scintimammographic result on 30 min images. The sensitivity of 30 and 180 min images was 81.3% and 69.4%, respectively. The specificity was 80% and 90%, and the accuracy was 80.8% and 76.9%, respectively. The L/N ratio of carcinoma on 30 min images was significantly higher than that of benign lesions (2.48 vs 1.22). The L/N ratio on 180 min images also revealed no significant difference between cancerous and benign lesions. The washout ratio showed no significant differences between cancerous and benign lesions. ^{99m}Tc-tetrofosmin scintimammography obtained at 30 min and 180 min post-injection has a high sensitivity and specificity, however, delayed scintimammography at 180 min does not contribute to improvement of the diagnostic accuracy.

PS-206

G. Cantinho, J. Inacio, T. Martins, H. Pena, J. N. Santos Junior, F. Veiga Fernandes, F. Godinho

Inst. Medicina Nuclear, Serv. Prop. Cirúrgica – Fac. Med. Lisboa H.Santa Maria Lisboa, Portugal

ROLE OF TECHNETIUM 99m SESTAMIBI SCINTIMAMMOGRAPHY IN THE DIAGNOSIS OF BREAST LESIONS

Breast carcinoma is the most frequently diagnosed female malignancy. It is also known that early detection improves survival and that the most successful screening procedures are physical breast examination and mammography (MG). The low positive predictive value of MG results in a large number of biopsies and invasive procedures with a high cost.

The aim of this study was to establish the value of ^{99m}Tc-sestamibi scintimammography (SMG), as a non invasive method of selecting those patients (pts) who would benefit the most from biopsy and thus reduce the number of negative biopsies.

24 women (mean age: 50,0 ± 11,9 y) were included in this study. All pts were submitted to physical breast examination by a surgeon and to MG.

Inclusion criteria consisted of either positive MG findings or a palpable mass on a physical examination, requiring biopsy. There were 19 palpable lesions and 5 no palpable lesions.

13 patients were submitted to surgical intervention and histopathological analysis. SMG was performed using a single head gamma camera equipped with a LEAP collimator (GE 4001). Pts were imaged in prone position using SMG positioning pad. Each patient received an intravenous injection of 20mCi (740 MBq) ^{99m}Tc-sestamibi in the contralateral arm to the breast lesion. Images consisting in two lateral and one anterior views obtained, 10 to 20 min later, in a 256x256 matrix for 10 min.

Two nuclear medicine physicians blinded to the clinical presentation and MG results evaluated all images. Any disagreement was settled by consensus. SMG was positive for carcinoma if there was any area of increased focal uptake in the breast and was negative if there was diffuse uptake.

In the 13 patients with histopathologic results 4 had the diagnosis of invasive ductal carcinoma. MG was suspect in all 4 and another 5 patients (5FP). SMG was positive in all 4 and also in another 2 (2FP). No false negatives have been detected. The false positives of SMG are true negatives in MG and would never be submitted to biopsy. The false positives of MG are all true negatives in SMG.

Our results seem to show that SMG may be used to clarify suspected MG studies improving the specificity and reducing the number of biopsy candidates.

PS-207

S L Chen, Y Q Yin, J X Chen, X G Sun, Y Xiu, W G Liu, W G Li, Y B zhang Hospital: Zhongshan Hospital, Department of Nuclear Medicine.

CORRELATION BETWEEN ACCUMULATION OF 99MTC-MIBI AND CELL PROLIFERATION AND ANGIOGENESIS

Purpose: To research the correlation between accumulation of ^{99m}Tc-MIBI in breast cancer and cell proliferation and angiogenesis. **Methods:** ^{99m}Tc-MIBI positive imaging was performed on 38 patients with palpable mass of breast. Cell proliferation and angiogenesis was assessed by immunostaining using proliferating cell nuclear antigen and UEA-I. Data was analyzed by correlation and regression analysis. **Results:** The diameter of mass (4.00±1.95cm) and the percentage of PCNA positive cell (74.13%±13.84) in patients with positive ^{99m}Tc-MIBI scans was significantly higher than in patients with negative scans (2.14±1.00cm, 43.76%±20.78%, p=0.01) but there was no evident difference in the number of vessels of two groups (181.32±71.66, 138.33±102.99, P=0.1407). The accumulation of ^{99m}Tc-MIBI was most strongly correlated with the percentage of PCNA positive cell (r=0.565, p=0.000), but had no relationship with the number of vessels (r=0.312, p=0.056). In stepwise regression analysis, the variance number of vessels was not entered in the model. **Conclusion:** The accumulation of ^{99m}Tc-MIBI in breast cancer is an indicator of cell proliferation, but had no relationship with angiogenesis.

PS-208

E. Crippa, E. Seregini, R. Agresti, C. Chiesa, C. Pascali, A. Bogni, D. Decise, V. De Sanctis, M. Greco, M.G. Daidone and E. Bombardieri.

National Cancer Institute, Milan (Italy)

[¹⁸F]FDG UPTAKE IN BREAST CANCER AND HISTOPATHOLOGY, STEROID-HORMONE RECEPTOR STATUS, THYMIDINE LABELLING INDEX AND P53 ASSAY.

To investigate the possible role of PET with [¹⁸F]FDG in the prognostic evaluation of primary breast cancer, we studied 86 patients with T1-3 (TNM classification) breast tumours before surgery and compared the tumour FDG uptake, calculated as a Standardized Uptake Value (SUV), with postoperative histopathological findings, steroid-hormone receptor status of the tumour, thymidine labelling index (LI) and tissular expression of p53. SUV was significantly higher in infiltrating ductal carcinomas (n = 68; median SUV = 5.6) than in lobular ones (n = 18; median SUV = 3.7) and in grade 3 carcinomas (n = 26; median SUV = 5.8) than in grade 1-2 ones (n = 60; median SUV = 4.4). Moreover, SUV was significantly higher in carcinomas with high levels of p53 (n = 12; median SUV = 9.5) than in those with low p53 levels (n = 48; median SUV = 4.25). By contrast, there was no significant correlation between SUV and the steroid-hormone receptor status and LI of tumours. In conclusion, our data show that in breast cancer the determination of FDG tumour uptake using PET and a simple non-kinetic method could provide oncologists with a new non-invasive tool to evaluate tumour aggressiveness. The value of SUV as a prognostic factor in the management of breast cancer patients must obviously be further evaluated by means of follow-up studies.

Partially supported by an AIRC grant and by the "Progetto Finalizzato" of the Ministry of Public Health.

PS-209

J.B. Cwikla, J.R. Buscombe*, S.P. Parbhoo*, D.S. Thakrar*, J.Hinton*, A.Deery*, J. Crow*, A.J.W. Hilson*
 PSK 2; Department of Radiology and Nuclear Medicine; Otwock; Poland
 Royal Free Hospital and School of Medicine*. Departments Nuclear Medicine,
 Breast Surgery, Radiology, Histology and Cytopathology; London; UK.

VALUE OF Tc99m MIBI IMAGING IN PATIENT WITH SUSPECTED RECURRENT BREAST CANCER

A prospective trial was performed to assess the accuracy of Tc-99m MIBI scintimammography (SMM) and X-ray mammography (XM) in 54 patients (mean age 60, range 39-85 years) with suspected recurrent breast cancer in the breast, or loco-regional tissues. All patients had been diagnosed with breast cancer 1-23 years, (mean 6.2 years) before the SMM. Twenty Four patients had undergone mastectomy so that a total of 84 breasts were studied with SMM and 80 with XM.

In both XM and Tc99m SMM the breast any abnormal uptake of Tc-99m MIBI was reported. Additional local or nodal uptake of Tc-99m MIBI was noted in each case. Confirmation of clinical suspicion of recurrence was by cytological or histological examination of tissue samples, correlative imaging and/or a minimum of 6 months clinical follow-up.

There were 31 patients with recurrent cancer. XM identified 13 of these cancers in the 29 cases in which it was performed. Tc99m MIBI SMM identified 21 of 31 recurrent cancers occurring in the breast. The sensitivity of Tc-99m SMM was 70%, better than XM at 45%. There were 4 false positive SMM and 2 false positive XM giving specificity of SMM of 83% and XM at 91%. Loco-regional recurrence including nodal disease was confirmed histopathologically in 19 patients. 15 of them had positive Tc99m SMM scan, XM found enlarged axillary nodes 5 of the 16 patients in which it was performed. The Sensitivity for detection of loco-regional recurrence was 79% for SMM and 31% for XM.

Tc-99m MIBI scintimammography is able to detect recurrent breast cancer both within the breast and in loco-regional tissues with a sensitivity higher than standard imaging. Its use in patients with suspected recurrent breast cancer should be considered.

PS-210

J.B. Cwikla, J.R. Buscombe*, S.P. Parbhoo* D.S. Thakrar*, A.L. Jones*, A.J.W. Hilson*

PSK2, Department of Radiology and Nuclear Medicine, Otwock, Poland
 Royal Free Hospital and School of Medicine*, Departments of Nuclear Medicine,
 Breast Surgery, and Medical Oncology, London, UK

DIFFERENT UPTAKE OF Tc99m MIBI AFTER CYTOTOXIC CHEMOTHERAPY AND ANTIESTROGEN THERAPY IN PATIENTS WITH BREAST CANCER-INITIAL STUDY

The chief goal in cytotoxic chemotherapy (CTX) and adjuvant hormonal therapy (AHT) is to obtain the high rate of survival and reduce the probability of local recurrence. It has been suggested that uptake of Tc-99m MIBI is affected by the expression of drug resistance. The aim of this study was to compare changes in uptake of Tc-99m MIBI in patients treated with CTX and AHT.

The study was performed prospectively in 22 patients with primary breast cancer, not receiving initial surgery, 15 underwent standard CTX and 7 patients with receptor rich tumours had AHT. Tc99m MIBI scintimammography was performed before and after treatment (interval 4-6 months). The mean age of patients in the CTX group was 46 years (SD 9), compared to 59 (SD 5) in the AHT group. Planar images using standard prone-lateral both breast and anterior-supine position was used in each case. The uptake of tracer in the tumour was calculated by drawing an irregular region of interest (ROI) around the suspected lesion on the prone lateral image and a similar size of region in adjacent ipsilateral normal breast a tumour to background ratio (TBR) was calculated. The resulting change in tumour uptake was compared with histological and clinical changes in the tumour.

There was a significant drop in mean TBR in all cancers receiving CTX from 2.38 (SD 0.7) before treatment to 1.35 (SD 0.4), after treatment (paired t test, p<0.0001). Though there was a reduction of TBR in all patients treated with CTX the reduction was more significant in the 8 patients with evidence of clinical response than non-responders (p<0.01). In those patients given AHT, 5 patients had a reduction in TBR, 2 were unchanged. However there was no significant change in TBR before and after AHT. (1.80 vs 1.76)

Changes in uptake of Tc-99m MIBI in the initial few months after CTX or AHT may be related to the type of treatment given. However despite the rather non-specific response to CTX initial changes do appear to reflect clinical response. Tc-99m MIBI may therefore be more useful in following patients receiving CTX than AHT.

PS-211

L.Feggi, P Carcoforo*, N Prandini, A Sartori*, S Corcione**, D Beccati***, GC Candinì§ and I Donini*
 Nuclear Medicine, Radiology** and Heath Physics§ of Azienda Ospedaliera Arcispedale S.Anna of Ferrara and *Clinical Surgery and Pathology *** of the University of Ferrara

SCINTIGRAPHIC AND RADIOSURGICAL IDENTIFICATION OF SENTINEL NODE (SN) IN EARLY STAGE BREAST CANCER: A PRELIMINARY EXPERIENCE

Axillary lymph nodes dissection for breast cancer remains the most important prognostic factor and guide adjuvant therapy. We tested the scintigraphic and radiosurgical mapping of SN to verify if an adequate axillary staging and regional control is possible without radical axillary procedures. **Material and methods:**The study, began in October 1997, comprised 16 patients, aged between 35 and 78 (mean 60 years), with T1 tumor localized in 14 cases at the external superior region of the breast and in 2 case at the internal superior. All the patients underwent preoperatively two kinds of lymphoscintigraphy: 1- injection of 99m-Tc-collid (30 MBq) the evening before the day of the surgery with scintigraphic imaging after about 15 hours; 2- injection of 99m-Tc-nanocolloid (10 Mbq) in the morning of the surgery with scintigraphic imaging after 1 hour. We utilize a low energy LFOV camera with high resolution collimator for the scintigraphy (planar in two orthogonal projections); during the surgery we utilize a probe (Pol.hi.tech srl) specific for SN collimation. After induction of general anesthesia, Isosulfan blu vital dye was injected into the breast mass and surrounding breast parenchyma. **Results:** The accuracy of lymphatic mapping was examined by comparing the histopathology of SN and non SN specimens. The SN accurately identifies axillary node status in all the patients. Only in 1 case (sensitivity 93.7%) it was not possible to identify the SN because the lymphatic drainage was dramatically modified by radical mastectomy 1 month before: the SN was found only by blu dye. In 1 patient the SN was identified only by probe and not with scintigraphy. In the two tumors localized in the internal superior region the SN was found not in the axilla but in the internal mammary chain. Finally in 2 case the SN was located in interpectoral region and in 2 cases in claverar omolateral region. **Conclusions:** This study is at the beginning and the number of the patients is too low for a conclusion but the experience indicates that lymphatic mapping by scintigraphic and radiosurgical technique can accurately identify the SN (wich is located in the axillary nodes only in 50% of our cases) and could guide to a less radical axillary procedure in the patients with tumour T1 N0, with obvious benefit for the patients and inducing a reduction in overall costs.

PS-212

TC Ferreira, MR Vieira, A Moreira, ML Orvalho, S André, A Gaspar, C Santos-Costa, J Menezes-Sousa, A Fernandes, J Oliveira, JL Passos-Coelho

Instituto Português de Oncologia/ Dept. Medicina Nuclear, Lisboa, Portugal.

USE OF 99mTc-TETROFOSMIN SCINTIMAMMOGRAPHY IN THE EVALUATION OF RESIDUAL TUMOUR IN PATIENTS WITH LOCALLY ADVANCED BREAST CANCER TREATED WITH DOXORUBICIN AND PACLITAXEL: COMPARISON WITH MRI AND PATHOLOGY

To evaluate the use of 99mTc-Tetrofosmin scintimammography (SCM) in detecting residual tumour in pts with locally advanced breast cancer treated with doxorubicin and paclitaxel we compared our findings with MRI and postoperative pathology data.

We studied 15 pts who received four cycles of doxorubicin (dox) and paclitaxel (ptx) before mastectomy. Pts underwent SCM and MRI before and after dox and ptx to assess response to treatment and the extent of preoperative residual tumour. The SCM was performed after iv injection of 740 MBq of 99mTc-Tetrofosmin in an antecubital vein in the arm contralateral to the breast with the tumour. Imaging was started ten minutes after injection. Lateral (prone), anterior and medial (supine) planar images, 10-min. each, of both breasts were acquired (matrix size of 128x128) using a single head gammacamera (GE Starport System) equipped with a LEGP collimator. In all pts both before and after therapy a lesion / non-lesion (LNL) ratio was calculated by drawing a ROI around the lesion and a similar ROI in the contralateral, normal breast. All pathology specimens showed residual tumour; in 5 pts the area of residual tumour in the mastectomy specimen was less than 1cm². One pt had a false-negative SCM at diagnosis; of the remaining 14 pts with initial tumour uptake, the SCM had become negative in 3 pts preoperatively (2 pts with < 1cm², 1 pt with >= 1 cm² of residual tumour at surgery), precluding LNL ratio analysis. Of the 11 pts in whom the LNL ratio was evaluable pre and postchemotherapy, the ratio showed a significant decrease (mean decrease 24 %, range 1%-45%, p<0,005 paired student t test). All pts had tumour detectable in the preoperative MRI, including the 5 pts with less than 1 cm² of residual tumour in the surgical specimen. MRI therefore, estimated accurately the presence of viable, Gadolinium enhancing tumour in all pts.

In conclusion, measured decrease in LNL ratio does not seem to be related to loss of viability as measured by Gadolinium enhancement.

PS-213

M. Grosso, C.R. Bellina., M. Roncella *, G. Boni, G. Manca, D. Volterrani, D. Fontanelli, F. Morini, R. Albertelli, F. Mosca* and R. Bianchi. Division of Nuclear Medicine, Division of Surgery*, Department of Oncology, University of Pisa.

THE CLINICAL USEFULNESS OF Tc-99m SESTAMIBI PRONE SCINTIMAMMOGRAPHY IN THE DETECTION OF BREAST CANCER AND AXILLARY LYMPH NODE INVOLVEMENT

Physical examination and mammography are currently the most used diagnostic tools for the early detection of primary breast cancer and axillary lymphnode involvement. However, mammography (MMx) shows high sensitivity but low specificity (positive predictive value 10-40%) for an high percentage of misdiagnosed breast nodules, namely in younger women with dense breast tissue or fibrocystic disease. The aim of this study was to evaluate the clinical usefulness of ^{99m}Tc-SESTAMIBI prone scintimammography (SMM) in patients (pts) with breast lesion to select who would benefit from excisional biopsy and reduce the number of negative breast biopsies. We studied 87 women (mean age 52±15 years) with 60 palpable and 27 nonpalpable breast lesions. All pts underwent surgery within 4 weeks after SMM. There were 57 primary breast cancer and 30 benign lesions (prevalence 65%). Lymph node involvement was surgically detected in 18 pts. The size of primary breast lesion ranged from 0,5 to 5 cm. SMM was performed 10 and 60 minutes after i.v. injection of Tc-99m SESTAMIBI (740 Mbq). Planar breast images were obtained in lateral prone position and in anterior erect projection to better visualize the axilla and medial breast regions. SMM was positive in 52/57 breast cancers, while MMx was positive only in 46/57 lesions. SMM was true-negative in 27/30 benign lesions (MMx in 17/30). Ten out of eighteen metastatic lymphnodes were seen by SMM. Therefore, in primary breast lesions the sensitivity of SMM was 91%, specificity 90%, PPV 94%, NPV 84% and accuracy 91%. In conclusion this study confirms the high diagnostic accuracy of SMM as previously reported, suggests the complementary role of this technique to MMx and its utility to reduce the number of negative breast biopsies.

PS-214

T.Ikegami, S.Koike, M.Saito, N.Takahashi and S.Matsubara Hospital : Yokohama City University, Department of Radiology

PREDICTING THE PROGNOSIS OF BREAST CANCER BY THALLIUM-201 SPECT.

The aim of this study was to verify the feasibility of using pre-surgical Thallium-201 SPECT (TI-SPECT) in managing breast cancer patients for post-surgical prognosis after a 5-year follow up. Among the patients who underwent TI-SPECT and surgery from August 1991 to July 1992, 48 had been confirmed as breast cancer and were followed up along the regimen of the surgical department. SPECT images were taken at 15 min after injection of 111 MBq of Thallium-201 and regions of interest were placed on the tumor and normal lung field in the axial plane that showed the most intense uptake on the tumor. The relationship between ratio of the counts in the tumor to normal lung (T/N value) and outcome of the patients were examined. The average T/N value in 10 patients who showed distant metastasis (group A) after operation was 1.78 and that in 33 patients without metastasis (group B) was 1.21 which was statistically lower than the former(p=0.0015). (Five patients did not show uptake in the tumor.) Only one showed T/N value above 1.8 among group B patients, however 5 in group A showed T/N value above 1.8. In group A, 4 out of 5 with T/N value above 1.8 died, whereas 2 out of 5 patients died with T/N value under 1.8. On the other hand, no one died in group B. These results suggest that TI-SPECT is useful for predicting the post-surgical outcome in patients with breast cancer.

PS-215

Lj.Jauković, R.Spaić, U.Zoranović, M.Štrbac, S.Marković Military Medical Academy, Institute of Nuclear Medicine, Clinic of Sugery, Institute of Pathology, Belgrade

99m TECHNETIUM - TETROFOSMIN SCINTIMAMMOGRAPHY IN THE DIAGNOSIS OF PRIMARY BREAST CANCER

^{99m}Tc tetrofosmin is a cationic complex used in myocardial perfusion imaging, as well as in the diagnosis of patients with various malignancies. The aim of this study was to assess the value of scintimammography with ^{99m}Tc tetrofosmin in breast cancer. Fifty patients with lesion suspicious for malignancy, detected by palpation and (or) mammography, were studied. In eighteen of them biopsy and surgery were performed for histological evaluation. An amount of 600 mBq ^{99m}Tc tetrofosmin was injected intravenously in the arm opposite to the side of breast lesion. Ten minutes after injection planar breast 7 minutes scans were performed in supine (anterior) and prone (left and right lateral views). The results of ^{99m}Tc tetrofosmin scintimammography were compared to the final histological findings. Out of 18 patients, scintimammography was true positive in 16 patients(14 ductal invasive, one lobular carcinoma and one cystosarcoma phylodes - malignant type). The smallest detectable carcinoma measured 0.6 cm. True negative result was observed in one patient with fibrocystic disease, false positive scan in one patient with fibroadenoma. The overall sensitivity was 100%, specificity 50% and accuracy 94%. Our preliminary results suggest that ^{99m}Tc tetrofosmin scintimammography can be utilized in the diagnosis of breast carcinoma.

PS-216

U. Kabasakal, M. Halaç, C. Nisli, B. Kanmaz, G. Ersavasti, C. Onsel, A. Altug, K. Sönmezoglu, H.B. Sayman, I. Uslu.

Cerrahpaşa Medical Faculty, Department of Nuclear Medicine, Istanbul, Turkey.

COMPARISON OF Tc-99m MDP AND Tc-99m MIBI SCINTIMAMMOGRAPHY IN DETECTION OF BREAST CANCER.

Functional imaging of breast cancer with Tc-99m MIBI (MIBI) has gained a wide interest and significant experience has already been obtained. Recently, Tc-99m MDP(MDP) has also been used in diagnosis of breast cancer. Although the exact mechanism of uptake is unclear the low cost and its wide utilization for bone scanning are important advantages of MDP. The aim of the present study was to compare the value of MDP and MIBI scintimammography in detection of breast cancer. For this purpose 44 patients with suspicious breast lesions were included to the study. All patients had mammography, ultrasonography MIBI and MDP scintimammography. The final diagnosis was achieved by histopathology. MIBI scintimammography was performed by obtaining two lateral prone and an anterior planar images after injection of 5000-700 MBq Tc-99m MIBI. Within a week a MDP scintigraphy was performed 5-15 min after injection of 500-700 MBq Tc-99m MDP. Whole body scans were also obtained from all patients. All images were evaluated by two physicians independently and randomly. Any asymmetric activity accumulation was considered as abnormal. In 25 patients breast lesions were proven to be malignant and in 19 patients lesions were proven to be benign. Either MDP or MIBI detected 17 of 25 malignant lesions (sensitivity 68%) and 11 of benign lesions (specificity 58%). False (-) rate was higher among the lesions smaller than 1 cm (4 of 9 lesions, 44%). There were no discordant results between MDP and MIBI scintimammography. However, with MIBI in 9 of 25 patients (36%) additional axillary lesions were detected. On the other hand with MDP in 3 of 25 patients (12%) additional bone lesions detected which may be evaluated as bone metastases. Subjectively, readers were evaluated MIBI images as higher quality for interpretation as compared to MDP. In conclusion this study suggested that either MDP or MIBI can be used for scintimammography with equal value in detection of early breast cancer.

PS-217

S. Kanayev, S. Novikov, L. Jukova.
 Research Institute of Oncology, Department of Radiation
 Oncology and Nuclear Medicine, 189646, Pesocny-2,
 St.-Petersburg, Russia.

**ROLE OF SCINTIGRAPHY IN VISUALISATION AXILLARY
 LYMPH-NODES REMAINED AFTER MASTECTOMY WITH
 "COMPLETE AXILLARY LYMPH-NODES DISSECTION".**

Adjuvant irradiation of the regional lymph nodes (LN) in node-positive patients treated by mastectomy and complete axillary dissection (M&CA) can significantly improve local control. On the other hand, radiotherapy to axillar region in this patients is omitted because all LN are considered to be removed by surgery.

PURPOSE: To evaluate role of LN scintigraphy with radiocolloids in visualisation axillary nodes remained after "complete dissection".

METHODS: M&CA was performed by experienced surgeons (more than 10 years of surgical practice) in 10 women with T2-3 N1 breast cancer. Postoperative lymphoscintigraphy was performed in static mode 1hr after interstitial injection of 0.1-0.3 ml (100-150 MBq) of 99mTc-milicolloids into interdigital space of both hands. For better anatomical localisation of the visualised LN 74-148 MBq of radiocolloids were administered i/v.

RESULTS: Nine of 10 evaluated women had residual axillary LN. They all manifested as the small well defined areas of significantly increased tracer uptake. In 8 cases size of detected axillary LN was estimated as 1cm or less. One patient had 3 distinct small LN directly in the axillary region. Additionally, 4 of 9 women with visualised axillary LN had supraclavicular LN detected by LN scintigraphy.

CONCLUSION: LN scintigraphy can be effectively used for visualisation LN left in the axillar region after M&CA. Prognostic value of this findings remain undefined. Optimal loco-regional therapeutic strategy in this patients needs further determination.

PS-218

I-H. Kim, H.K. Lee *, J.W. Seo**, N.S. Cho**, K.H. Cha**,
 Gachon Medical College, Chung-Ang Ghil Hospital, Incheon, Korea
 Department of Nuclear Medicine, Radiology* and General Surgery**.

**Diagnostic accuracy of quantitative scintimammography
 using 99mTc-MIBI according to ROC curve analysis**

99mTc-sestamibi scintimammography(SMM) has been shown to be a useful diagnostic test in the detection of breast cancer and the receiver operating characteristic (ROC) curve analysis provides detailed information of a diagnostic test. The purpose of this study was to evaluate the feasibility and efficacy of quantitative indices of SMM in the detection of malignant breast lesions according to ROC analysis.

Method: Prone anterior, lateral planar and supine SPECT imagings were performed on 48 female patients (mean age=44.1 yr) with breast mass (size>0.8cm) after intravenous injection of 20-30 mCi 99mTc-sestamibi. 28 Malignant (Invasive ductal ca(22), Inv lobular ca(3), Inv duc+lob(1), Ductal CIS(1), Inv tubular ca(1)) and 20 benign (fibroadenoma(10), fib cyst(6), Inflammation(1), Fat necrosis(1), papilloma(1), lipoma(1)) lesions were histologically proven. Data were analyzed by creating three regions of interest (ROIs) over designated areas both on the planar and SPECT: lesion, normal breast and right chest wall. Lesion to normal (L/NL) and lesion to chest wall (L/CW) ratios were calculated for each patient. The area under the ROC curve (AUC) was calculated and compared among four semiquantitative indices and an average scintimammographic index(SMM(mean)) from arithmetic mean.

Results: ROC curve analysis revealed both L/NL and L/CW ratios of SMM on planar and SPECT images provide comparable diagnostic accuracies for detection of malignant breast lesions without statistically significant difference. The sensitivity(SN) and specificity(SP) of quantitative SMM(mean) were 75% respectively.

	SPECT(L/NL)	Planar(L/NL)	SPECT (L/CW)	Planar (L/CW)	SMM(mean)
AUC	0.757	0.799	0.754	0.715	0.782
SN	71.4	75.0	71.4	78.6	75.0
SP	70.0	70.0	75.0	60.0	75.0
Cut-off	>2.49	>1.33	>2.31	>1.13	>1.81
Normal	1	1	0.87 ± 0.47	0.87 ± 0.25	0.94 ± 0.18
SE	0.069	0.063	0.069	0.074	0.066
95% CI	0.612 -	0.658 -	0.608 -	0.567 -	0.639 -
	0.869	0.901	0.866	0.836	0.888
+LR	2.38	2.50	2.86	1.96	3.00
-LR	0.41	0.36	0.38	0.36	0.33

Conclusion: Quantitative SMM is an useful objective method for differentiating malignant from benign breast lesions. Correlation with other imaging modalities are in progress.

PS-219

P. Lind, H.J. Gallowitsch, P. Mikosch, M. Molnar, E. Kresnik,
 O. Unterweger, J. Oman, H.P. Dinges

Department of Nuclear Medicine & Endocrinology,
 LKH Klagenfurt, AUSTRIA

**Tc-99m TETROFOSMIN SCINTIMAMMOGRAPHY IN THE PRE-
 OPERATIVE EVALUATION OF MAMMOGRAPHICALLY SUSPICIOUS
 BREAST LESIONS**

Breast cancer, the most common malignancy in women, still poses a challenge to diagnostic procedures and therapy. Despite low specificity routine mammography is the method of choice to screen women for breast cancer. **Aim:** The purpose of our study was to evaluate prospectively the sensitivity, specificity, PPV and NPV of scintimammography with a new cationic complex Tc-99m tetrafosmin in patients with suspicious mammographic lesions. **Methods:** One hundred and fifty three patients in whom mammography and/or high resolution ultrasonography (10MHz) revealed suspicious breast lesions were studied with Tc-99m tetrafosmin scintimammography. In 93 of them surgery was performed for histological evaluation. After intravenous injection of 555 MBq Tc-99m tetrafosmin planar images in anterior and lateral projections (5 min.p.i.) and SPECT imaging including 3-D-reconstruction (20 min.p.i.) were performed. Scintimammography was evaluated as negative, equivocal (+), probably (++) or definitely (+++) positive. **Results:** Planar scintimammography with Tc-99m tetrafosmin was negative in 50 patients (47 true negative-t.n.; 3 false negative-f.n.) and positive in 43 patients (31 true positive-t.p.; 12 false positive-f.p.). Using SPECT imaging Tc-99m scintimammography was negative in 46 cases (44 t.n.; 2 f.n.) and positive in 47 cases (32 t.p.; 15 f.p.). Sensitivity of Tc-99m tetrafosmin scintimammography in this prospective study was 91%, specificity 80%, PPV 72% and NPV 94% for planar imaging and 94%, 76%, 68% and 96% for SPECT, respectively. **Conclusion:** Scintimammographic results in patients with suspicious breast lesion show, that Tc-99m tetrafosmin accumulates in breast cancer as well as in some fibroadenoma with high cellularity. However, the high NPV of 94 and 96% respectively excludes breast cancer in suspicious mammographic lesions to a very high degree and therefore reduces the need of biopsy and/or surgery in most of these patients.

PS-220

P. Madariaga, I Almuquera, A Alonso¹, JL Escat², O Vegazo, ML Martinez,
 JM Pérez-Vázquez.
 Hospital General G. Marañón. Departments of Nuclear Medicine,
 Oncology¹ and Surgery². Madrid.

**ROLE OF 99mTc-TETROFOSMIN IN THE RECURRENCE OF BREAST
 CANCER AFTER CONSERVATIVE SURGERY AND RADIATION
 THERAPY.**

OBJECTIVE: The aim of this study was to evaluate the feasibility of diagnosing recurrent breast cancer using 99mTc-Tetrofosmin in patients treated with conservative surgery and radiotherapy because of breast carcinoma.

MATERIAL AND METHODS: Thirty-five female patients (age range:32-83 years) with suspected breast cancer recurrence (23 palpable and 12 non-palpable lesions) underwent scintigraphy with 99mTc-Tetrofosmin. All patients had conventional mammography. Breast imaging begun 20 min after i.v. injection of 740 MBq 99mTc-Tetrofosmin in the arm opposite side to the suspected breast. Acquisition was performed in a large field of view camera equipped with high resolution collimator. The patient was imaged in supine and prone position (anterior and lateral views) during 10 min per image.

RESULTS: All patients had a non conclusive mammography. Twenty-three patients showed focal uptake in scintigraphy. Surgery confirmed 20 recurrences of breast cancer. The rest three patients, had benign diseases. Eleven patients had no abnormalities that were confirmed by biopsy. Only one patient showed no pathological uptake but surgery confirmed recurrence at the site of the scar. Our study sample has a sensibility of 95%, specificity of 78% and accuracy of 88%.

CONCLUSION: Our findings suggest that: 1) 99mTc-Tetrofosmin can play an important role in evaluating recurrence of breast cancer after conservative surgery and radiotherapy, 2) it can diminish the number of unnecessary biopsies.

PS-221

P. Weitz, P. González, T. Massardo, M. Quiroz, P. Behm, B. Durán, S. Torres, N. Garcés.

Nuclear Medicine, University of Chile Clinical Hospital.

COMPARISON BETWEEN ^{99m}Tc-SESTAMIBI AND ^{99m}Tc-MDP SCINTIMAMMOGRAPHY IN THE EVALUATION OF BREAST CANCER.

In order to compare the value of Tc^{99m} radiopharmaceuticals in breast cancer assessment, we studied 31 women (56±14 y.o., range 36-80), 5 of them with prior breast tumor. They were referred because of a nodule or a suspicious mammogram. Histological confirmation of carcinoma was obtained in 23/33 breasts and in 11/19 axillas through biopsy (mean difference: 47 days), 61% were ductal and infiltrant and 8% lobular carcinoma. Fibrocystic disease was confirmed in 6 patients. All had lateral and anterior views using 740 MBq of ^{99m}Tc-MDP and ^{99m}Tc-Sestamibi. Blind independent observers defined the lesions as positive or negative for malignancy, describing possible benign appearance; discrepancies were submitted to consensus. Mammogram was also compared in 28 patients. Interobserver concordance ranged between 78% and 88% for MDP and Sestamibi for breast and 100% and 95% for axilla, respectively. Concordance between both radiopharmaceuticals were 81% and 93% for breast and axilla.

Results are shown in the following table:

	BREAST						AXILLA		
	RX MAMMOGRAM	MDP	MIBI	MDP	MIBI				
ACCURACY (%)	72	61*	91*	47	63				
SENSITIVITY	95α	57#α	91#	9	36				
SPECIFICITY	28β	78	90β	100	100				
PPV	71ω	87	96ω	100	100				
NPV	75	41&	82&	44	53				

p test: α γ β: 0.003 # 0.007 * 0.01 ω 0.02 & 0.03

Two false negative with Sestamibi corresponded to carcinoma in situ in the same patient (with microcalcifications in one breast).

Concluding, ^{99m}Tc-Sestamibi appears as a significant better tool than ^{99m}Tc-MDP in the evaluation of breast carcinoma.

PS-222

K. Melis, A. Makar, L. Van Leuven, J. Goiris, A. Vervaeke, M. Kockx, J. Vandevivere, L. Denis* AZ Middelheim, Department of Nuclear Medicine, *Oncology Centre Antwerp, Belgium

PRE- AND INTRAOPERATIVE LOCALISATION OF THE SENTINEL NODE IN BREAST CARCINOMA : LYMPHOSCINTIGRAPHY AND GAMMA PROBE GUIDED SURGERY.

Elective axillary lymph node dissection (ALND) is part of the treatment of breast cancer due to its prognostic value. To avoid the morbidity of this procedure the sentinel node (SN) concept has been evaluated, which states that the first draining lymph node is representative for the remaining axillary LNN. The SN can be traced by preoperative lymphoscintigraphy and intraoperative gamma probe detection.

Patients and methods In a prospective trial 20 patients with recently diagnosed infiltrating ductal breast carcinoma without palpable axillary lymph nodes were injected peritumorally the day before surgery with 40 MBq ^{99m}Tc nanocolloid. After 3 hours a lymphoscintigraphy was performed using a gammacamera with LEHR collimator. Anterior and lateral static and transmission images were obtained. Using a radioactive penmarker a tattoo with indelible ink was made on the skin during the acquisition to guide the surgeon. The intraoperative lymphatic mapping was performed with a hand-held gamma probe (C-Trak, Care Wise). All patients underwent lumpectomy or mastectomy with ALND.

Results The SN identification percentage was 85% (17/20). In the remaining 3/20 the LS was also negative. No false negative SN's (skip meta's) were found. In 4 cases (23%) the only positive node was the sentinel node.

Discussion Our results show that the SN can be localised easily by combination of lymphoscintigraphy and intraoperative gamma probe guided detection and that when identified the SN accurately can predict the axillary nodal status in all cases.

PS-223

A. Mudun, I. Aslay, M. Aygen, M. Muslumanoglu, Y. Bozfakioglu, S. Cantez.

Istanbul University, Faculty of Medicine, Dept. of Nuclear Medicine, CAPA 34390, Istanbul, TURKEY

CAN PREOPERATIVE LYMPHATIC MAPPING BE USED AS A GUIDE IN THE TREATMENT OF BREAST CANCER ?

Aim of the study was to evaluate the lymphatic drainage patterns in patients (pts) with breast cancer and to see whether this helps to determine radiotherapy indications following the breast surgery.

Methods: Sixteen women with breast cancer were included into the study. Technetium^{99m}-Rhenium sulphide colloid (CIS-TCK17) with a total dose of 40 MBq in 0.5 ml divided in 4 syringes (10 MBq/0.125 ml each) were injected in 4 quadrants around the palpable breast lesion. Ten-minutes early dynamic images and at 2 hours, delayed 600-second static images were obtained from anterior and lateral positions. All patients had modified radical mastectomy and axillary dissection and results of lymphoscintigraphy were correlated with axillary histopathology.

Results: The lymphatic drainage sites in scans and the results of axillary histopathology were presented in the following table (n.pts):

Lesion site	Outer quadrant lesions (10 pts)			Central breast lesions (4 pts)			Inner quadrant lesions (2 pts)			Total (16)
	No drainage	Axilla* alone	Axilla and IM**	Axilla alone	Axilla and IM	IM alone	Axilla alone	Axilla and IM	IM alone	
Lymphoscans (n:pts)	1	5	4	1	2	1	0	1	1	16
Axillary tumor positive	1	1	2	1	1	0	0	1	0	7

*: Axillary drainage, **: Internal Mammary lymphatic drainage

Nine pts showed either axilla+IM or only IM lymphatic drainage on scintigraphy whom 4 of them had no axillary lymph metastasis.

Conclusion: In those pts who had IM drainage and no axillary tumor, radiotherapy portals may include parasternal regions as well. These preliminary findings indicate that preoperative lymphatic mapping may be used as a guide in the pathologic evaluation of lymphatic metastasis and in the management of radiotherapy portals in patients with breast cancer.

PS-224

Y.Nishimoto, T.Imai, Y.Sasaki, T.Shinkai, Y.Imai, Y.Nishimura, A.Ohkura H.Ohishi and H.Uchida. Dept. of Radiology, Oncoradiology, Nara Medical University, Dept. of Radiology, Nara Prefectural Mimuro Hospital, Kashihara, Japan

USEFULNESS OF ^{99m}Tc-HMDP (HMDP) SCINTIMAMMOGRAPHY IN CASES WITH BREAST CANCER.

We examined early phase images of breast cancer with HMDP scintimammography and evaluated the clinical usefulness of this method. This study included 67 patients. Twenty-three patients were suspected of having primary breast cancer upon examination by ultrasonography (US) and either mammography or spiral CT, and then HMDP scintimammography to detect breast tumor before operation (final histological diagnosis: breast cancer 23 nodules in 21 patients, benign tumor 4 nodules in 2 patients). Forty-four other patients were examined by scintimammography after mastectomy. Early and late phase spot images of breasts were obtained 15 minutes and 3 hours after intravenous injection of 740 MBq of HMDP. In 10 patients with breast cancer, dynamic study was performed for 2 minutes and then spot images were obtained 5 and 10 minutes after intravenous injection. In early phase images, HMDP accumulation was observed in 21 of 23 (91.3%) breast cancer nodules. The long axes of 2 nodules without accumulation were 8 and 18mm. Of 4 benign nodules, HMDP accumulation was observed in 2 nodules of fibroadenoma. These nodules showed contrast enhancement and abundant blood flow. In late phase images, HMDP accumulation was seen in 5 breast cancer nodules (21.7%), but in none of the benign tumor nodules. In the 44 postoperative patients, no tumors were detected by US, and HMDP accumulation was not seen. In the 10 dynamic study patients 2 breast cancer nodules showed no accumulation in dynamic study; however HMDP accumulation was seen in all 5 and 10 minutes spot images. HMDP accumulation was most marked 5 to 10 minutes after intravenous injection, and was slightly reduced 15 minutes after injection. There was no relation between HMDP accumulation and tumor histotype. It was suggested that HMDP accumulation correlates with tumor size and its blood flow. Adding spot images 5 to 10 minutes after intravenous injection to scintimammography may be useful for diagnosis of breast cancer and post operative follow-up.

PS-225

A Notghi, EA Clarke, M. Wadley, LK Harding

City Hospital, Birmingham, UK Physics and Nuclear Medicine

SCINTIAMMOGRAPHY OR MAMMOGRAPHY - A QUESTION OF SENSITIVITY.

In patients with known carcinoma of the breast, we have related Scintimammography (SM) and x-ray mammography (XM) with histology. Patients with palpable breast lesions were referred for scintimammography prior to surgery to assess the extent of the disease and the lymph node involvement. 750 MBq ^{99m}Tc^m tetrafosmin/MIBI was injected and standard planar breast images were acquired. Following surgery, the pathology of lesion and nodes was assessed and compared with scintimammography and mammography results. Both sensitivity and accuracy of scintimammography for breast lesions was 88% but varied with the type of pathology :

Histology	(n)	Sensitivity (SM)	Sensitivity (XM)
Ductal	(31)	90%	81%
Lobular	(6)	100%	50%
Tubular	(3)	67%	67%
Others	(2)	50%	50%

Scintimammography localised lesions in six patients which could not be localised by mammography and identified bilateral involvement in two patients. It appears useful in lobular carcinoma when mammography could identify only three out of six lesions. Scintimammography had an accuracy of 62%, sensitivity of 43% and specificity of 84% in lymph node detection.

Scintimammography is more sensitive than x-ray mammography and helps in determining the extent of lymph node surgery.

PS-226

V.Papantoniou¹, A. Stipsanelli¹, A. Arka¹, A. Keramopoulos², P. Kostamis¹, S. Michalas¹
¹Dept of Nuclear Medicine and Therapeutic Clinic «Alexandra» Hospital, University of Athens,
²Dept of Obst. and Gyn. «Alexandra» Maternity Hospital, University of Athens

COMPARISON OF TECHNETIUM-99M [V]-DMSA WITH TECHNETIUM-99M-MDP IN DIAGNOSIS OF BREAST LESIONS

The aim of the study was to compare the diagnostic accuracy of both radiopharmaceuticals in the detection of primary breast cancer. Methods: 22 breast lesions (20 women mean age ±SD: 57±25,9 ys) with suspected palpation and/or mamography have been investigated preoperatively. Tc-99m MDP (during a routine study for bone metastasis) & Tc-99m-[V]-DMSA scintimammographies (SM) were performed in 2 time periods (15-50 min and 60-150 min) and with a time interval of 2 days between the 2 studies. Anterior and oblique views of both breasts were obtained in an upright position after administration of 15-20 mCi of each radiotracer mentioned above. Tumor to background ratio (T/B) and also plasma levels of CA 15-3 and CEA were determined. Scintigrams and mammographies (M.M.) were correlated with biopsies. Results : Histopathology confirmed breast cancer in 13 and benign ones in 9 cases. Tumor size ranged from 10mm-43mm (m±SD:22,8±12,1mm). Malignancies were all but one palpable while 5 out of 9 benign lesions were not palpable. MM was definitely positive in 8, indeterminate in 3 and negative in 2 breast cancers. It was also definitely negative in 4 and indeterminate in 5 benign lesions. SM with Tc-99m[V]-DMSA and Tc-99m-MDP for breast cancer, revealed:

	Tc-99m-V-DMSA		Tc-99m-MDP	
	15-50 min	60-150 min	15-50 min	60-150 min
Sensitivity	85%(11P, 2FN)	92%(2TP, 1FN)	76%(10TP, 3FN)	53%(7TP, 6FN)
Specificity	88%(8TN, 1FP)	77%(7TN, 2FP)	44%(4TN, 5FP)	55%(5TN, 4FP)
Accuracy	85%	86%	63%	54%
PPV	91%	85%	66%	63%
NPV	80%	87%	57%	45%

T/B for malignant and benign lesions and for contralateral normal breast (CNB)¹ was:

Time	Tc-99m-V-DMSA		Tc-99m-MDP	
	Malignant	Benign	Malignant	Benign
(15-50 min)	1,93±0,34 (1,15±0,10)*	1,28±0,25 (1,15±0,21)*	1,74±0,41 (1,39±0,45)*	1,62±0,36 (1,28±0,14)*
(60-150 min)	1,88±0,28 (1,25±0,3)*	1,30±0,31 (1,22±0,25)*	1,54±0,35 (1,29±0,35)*	1,50±0,32 (1,16±0,10)*

Tc-99m-V-DMSA had a significantly higher difference in T/B ratio between malignancies and benign lesions than Tc-99m-MDP. T/B remained stable for V-DMSA during time while it was lower for MDP in the late phase. Conclusion : Tc-99m-V-DMSA appears to be more sensitive, specific and accurate than Tc-99m MDP in the detection of primary breast cancer. It also seems to have better imaging properties such as higher T/B ratio, stability over time and absence of chest wall activity.

PS-227

V.Papantoniou¹, A. Stipsanelli¹, C. Galeros², E. Feida³, P. Kostamis¹, A. Keramopoulos², S. Michalas²
¹Dept of Nuclear Medicine and Therapeutic Clinic «Alexandra» Hospital, University of Athens, ²Dept of Obst. and Gyn. «Alexandra» Maternity Hospital, University of Athens, ³Dept of Radiology «Alexandra» Hospital

SIMILARITY BETWEEN Tc-99m-V-DMSA AND Tc-99m SESTAMIBI IN THE DETECTION OF PRIMARY BREAST CANCER. PRELIMINARY RESULTS The study is part of a project IAEA

The scope of the study was to compare the diagnostic accuracy of the two radiotracers to recognize primary breast cancer. **Material and Methods.** 10 women (mean age ±SD: 66,7±10,7) with suspicious palpable lesions and/or mammographic evidence of breast abnormalities were included into our study. Lateral and anterior views of both breasts have been acquired in a prone position using a positioning pad after administration of 20-22 mCi of Tc-99m-sestamibi and Tc-99m-V-DMSA with a time interval of 48h at least between the two tests. Acquisitions have been performed at 10-30 min and 60-90 min postinjection. T/B ratio and max / min activity (for contralateral normal breasts) have been calculated using (ROIS) with standardized shape and size. Linear regression analysis has also been performed correlating T/B ratio of both radiotracers. Scintigraphic results and mammograms (MM) were compared with the histological findings. **Results.** Breast cancer (3 different types) was histologically confirmed in 8 patients while benign lesions were proven in 2. Tumor size ranged from 1,5cm-15cm (4,5±4,4 cm). MM was suggestive for cancer in 7 patients and indeterminate in 3. The indeterminate MM were concerning an infiltrating lobular carcinoma, a cystic dilatation and an amartoma. Tc-99m-V-DMSA as far as Tc-99m-sestamibi were truly positive in 8/8 breast cancers and truly negative in 2/2 benign diseases. The patients with indeterminate MM have been correctly recognized by both radiotracers. T/B ratio was almost equal for both agents:

	Tc-99m-V-DMSA		Tc-99m-MIBI	
	Malignant mean ± SD	Benign mean ± SD	Malignant mean ± SD	Benign mean ± SD
10-30 min	1,71±0,53	1,14±0,03	1,65±0,47	1,07±0,02
60-90 min	1,75±0,49	1,14±0,01	1,66±0,47	1,10±0,03

Linear regression analysis revealed statistically significant coefficient of correlation between the 2 radiotracers: r(10-10 min): 0,731, p<0,001
 r(60-90 min): 0,798, p<0,001.

Conclusions: Tc-99m-V-DMSA and Tc-99m-MIBI presented similar characteristics, imaging properties, and an excellent ability to detect primary breast cancer. Because of the limited number of observations we believe that further investigation would allow the estimation of the effectiveness of Tc-99m-V-DMSA as an accurate and inexpensive breast tumor seeking agent.

PS-228

E.Pons, R.Herranz, C.Laterza, M.Muñoz¹, S.Vidal-Sicart, J.Pavía, A.Palacín², J.Estapé¹, J.Setoain.
 Departments of Nuclear Medicine, Medical Oncology¹ and Pathology². Hospital Clinic, University of Barcelona, Spain.

99mTc-MIBI UPTAKE AS A PROGNOSTIC FACTOR FOR RESPONSE TO CHEMOTHERAPY IN ADVANCED BREAST CANCER

The resistance of some neoplasms to chemotherapy has been associated with the presence of high levels of P-glycoprotein in the tumoural cells which, simultaneously, have shown a relationship to 99mTc-MIBI uptake.

AIM: To assess whether the quantitation of 99mTc-MIBI uptake can predict the response to chemotherapy in patients with advanced breast cancer who initially cannot be operated on.

METHODS: Seventeen patients (age 62 ± 15 years) with advanced breast cancer were studied prospectively prior to neoadjuvant chemotherapy. Breast scintigraphy was performed after i.v. injection of 740 MBq of 99mTc-MIBI. Three patients had two lesions, therefore the total number of lesions was 20. Tumour/normal tissue uptake was calculated by drawing the region of interest manually as well as semiautomatically. Treatment response was evaluated upon completion of chemotherapy.

RESULTS: There was a very high correlation between tumour/normal tissue uptake obtained by manual quantitation and semiautomatic quantitation (r=0.99, p<0.0001). 70% of tumours showed a complete or partial remission to treatment while the remaining 30% did not show any response. Tumour/normal tissue uptake was significantly higher in the lesions which responded to chemotherapy (7.65 ± 5.5) than in non responding lesions (2.36 ± 1.2) (p<0.05).

CONCLUSION: These results suggest that breast scintigraphy with 99mTc-MIBI can be useful in the assessment of patients with advanced breast cancer prior to chemotherapy treatment.

This work was supported by Grant FIS 96/1559

PS-229

M. R. Quastel, S. Lantsberg, *L. Lantsberg, *B. Kirshtein

Institute of Nuclear Medicine and *Department of Surgery "A", Soroka Medical Center and Faculty of Health Sciences, Ben Gurion University of the Negev, Beer-Sheva, Israel.

MAMMOSCINTIGRAPHY WITH ^{99m}Tc-SESTAMIBI IN THE ASSESSMENT OF BENIGN AND MALIGNANT BREAST DISEASE

Ninety eight women and 3 males (age range 16-88 yrs; mean-46 yrs) with 103 lesions (101 palpable and 2 non-palpable mammographic findings) underwent technetium-99m methoxyisobutylisonitrile (^{99m}Tc-sestamibi) breast scintigraphy prior to biopsy to assess the value of this technique for the detection of breast carcinomas and for their differentiation from benign breast masses. In this double blind study, scans of 29 patients were ^{99m}Tc-sestamibi-positive and 72 were ^{99m}Tc-sestamibi-negative. Scintimammographic findings were true positive in 21 (72%) biopsies confirmed carcinomas and true negative in 65 (89%) benign lesions. ^{99m}Tc-sestamibi scans were false-negative in 7 cases of breast cancers: 4 infiltrating ductal carcinomas and 3 infiltrating ductal with intraductal component. There were 8 false positive scans with 4 fibroadenomas, 2 papillomas and 2 chronic inflammations. The mean size of the ^{99m}Tc-sestamibi-positive carcinomas was 2.9 ± 1.2 cm, in contrast to the size of ^{99m}Tc-sestamibi-negative breast malignancies, which averaged 1.8 ± 0.6 cm (p<0.005). The sensitivity of using ^{99m}Tc-sestamibi for detection of breast carcinoma was 75% and its specificity 89%. The positive predictive value was 86%, and negative predictive value 88%. Interobserver agreement between the 2 independent nuclear medicine physicians was 98%.

We suggest that the size of the tumors and invasive component plays an important role in sestamibi uptake in carcinomas. ^{99m}Tc-sestamibi can help in surgical strategy together with other noninvasive tests such as mammography and ultrasound.

PS-230

R. Obwegeser, S. Müllauer-Ertl, P. Berghammer, M. Rodrigues, E. Kubista, H. Sinzinger
University Hospital, Departments of Nuclear Medicine and Special Gynecology, Vienna, Austria

ROLE OF ^{99m}Tc-TETROFOSMIN SCINTIGRAPHY IN MONITORING NEOADJUVANT CHEMOTHERAPY IN PATIENTS WITH BREAST CANCER

^{99m}Tc-tetrofosmin scintigraphy (TS) has become recently a valuable method for detecting primary breast cancer (BC) as well as BC metastases. Resistance of tumors to chemotherapeutic drugs is one of the major causes of failure of cancer therapy. The aim of this ongoing, prospective study was to evaluate whether the uptake of ^{99m}Tc-tetrofosmin is affected by chemotherapy and whether any such effect might be correlated to reduction or progression in tumor size.

22 female patients (pts), aged from 31 to 68 years, with histologically confirmed BC in an advanced stage with poor prognosis were evaluated so far. All breast tumors were palpable (size between 3 and 6 cm). In all pts TS was performed before the beginning and after 3 or 4 cycles of a neoadjuvant chemotherapy regimen (cyclophosphamide, methotrexate and fluorouracil), before surgery. 6 pts were already operated. Tumor size was evaluated clinically, with ultrasound, mammography and TS. In all pts TS showed BC clearly, whereas in 3/6 pts mammography and in 1/6 pts MRI were negative. TS detected in 1 pt lung metastases, which were confirmed by CT and not seen by conventional X-ray. Furthermore, in all the pts TS could clearly decide between therapeutic success or tumor progression under therapy. TS was thus helpful for decision on further therapeutic regimen.

PS-231

A. Spanu, G. Dettori, P. Chiaramida, G. Meloni, C. Bagella, P. Cottu, M.E. Solinas, A. Porcu, A. Falchi, P. Solinas, S. Nuvoli and G. Madeddu.
Depts. of Nuclear Medicine, Surgery and Radiology.
University of Sassari. Italy.

TC-99m TETROFOSMIN (T) PINHOLE (P) SPECT IN AXILLARY LYMPH NODE METASTASIS DETECTION: A PRELIMINARY STUDY.

To assess the performance of high resolution P-SPECT, in comparison with planar and conventional SPECT, in axillary lymph node metastasis detection in breast cancer pts, we studied 30 pts, 27 with non operated breast cancer (Group 1), including 4 pts with palpable axillary nodes, and 3 pts (Group 2) previously operated for primary lesion with suspect axillary lymph node enlargement. In all pts, 10 min. after 740 MBq Tc-99m T injection, planar followed by SPECT images were acquired in supine anterior position with the arms raised over the head, using a rectangular dual head gamma camera equipped with parallel hole collimators. P-SPECT images were then acquired by 180° rotation around the involved axilla, using a circular HR gamma camera equipped with a pinhole collimator with a 128x128 matrix and a zoom 2. The pinhole aperture size (4.45 mm), the distance between COR and collimator face (within 15 cm), the angular step (3°) and the time/frame (30 sec), had been chosen on the basis of the results obtained in our previous study using an experimental phantom simulating different sized lymph nodes in a hypothetical axillary region. P-SPECT projections were reconstructed by a cone beam algorithm and filtered by a Metz filter, obtaining a final set of 4 pixel wide coronal slices. P-SPECT images were compared with both planar and SPECT images and related to histology. P-SPECT was positive in 13/13 Group 1 and in 3/3 Group 2 pts with axillary lymph node metastasis, while planar imaging was positive in only 8/13 Group 1 cases, including the 4 pts with palpable nodes, and in 3/3 Group 2 pts. SPECT showed the same per-patient sensitivity as P-SPECT in both Group 1 and Group 2 pts; however, P-SPECT showed, in respect of SPECT, a better visualization of small and non palpable axillary lymph node metastases and also identified more lesions in 9 pts with non palpable nodes, determining in 5 the exact number of lesions. Our preliminary data seem to indicate Tc-99m Tetrofosmin P-SPECT may be a reliable method to detect breast cancer axillary lymph node metastasis, particularly when non palpable, since it was positive in all our cases. Moreover, P-SPECT could give more information than conventional SPECT to determine the number of lesions.

PS-232

A. Spanu, G. Dettori, G. Meloni, P. Chiaramida, C. Bagella, A. Porcu, M.E. Solinas, P. Cottu, A. Falchi, P. Solinas and G. Madeddu.
Depts. of Nuclear Medicine, Surgery and Radiology.
University of Sassari. Italy.

TC-99m TETROFOSMIN (T) SCAN IN THE DIAGNOSIS AND STAGING OF PRIMARY BREAST CANCER: ROLE OF SPECT.

To assess the role of T-SPECT in primary breast cancer and axillary lymph node metastasis detection, we studied 83 pts, aged 31 to 83 yrs: 73 had suspect primary breast cancer (Group 1), while 10, scheduled for mastectomy and axillary lymph node dissection, had previously undergone nodular excisional biopsy (Group 2). Ten min. after 740 MBq Tc-99m T injection, planar (supine anterior, prone and lateral views) followed by SPECT images were acquired with the arms raised over the head, using a rectangular dual-head gamma camera. Both planar and SPECT data were related to histopathological findings. In 63 Group 1 pts with ascertained primary breast cancer, T-SPECT detected 66/70 malignant lesions (sens. 94.3%), while T-planar 48/70 (sens. 68.6%). T-SPECT and T-planar sensitivity for lesions ≤15 mm were 88.9% (24/27) and 40.7% (11/27), respectively; for lesions >15 mm they were 97.7% (42/43) and 86% (37/43), respectively. For non palpable lesions, T-SPECT and T-planar sensitivity were 90% (9/10) and 30% (3/10), respectively. In the remaining 10 Group 1 pts, T-SPECT and T-planar were true negative in 11/14 and in 12/14 benign lesions at histology, respectively. T-SPECT and T-planar specificity were 78.6% and 85.7%, respectively. T-SPECT was false positive in 3 fibroadenomas, 2 of which also positive at T-planar. Moreover, T-SPECT was true positive in 3/3 Group 2 pts (T-planar only in 1) who had residual breast cancer after excisional biopsy as ascertained at mastectomy. Both tests were true negative in the remaining 7 Group 2 pts. In the 71 pts submitted to axillary lymph node dissection (61 Group 1 and 10 Group 2), T-SPECT was true positive in 32/35 cases (sens. 91.4%), while T-planar was in 20/35 (sens. 57.1%). T-SPECT sensitivity was 100% (12/12) for palpable and 86.9% (20/23) for non palpable nodes, while T-planar was 75% (9/12) and 47.8% (11/23), respectively. Only T-SPECT, but not T-planar, showed false positive results (4 cases, spec. 88.9%). Our data suggest that T-SPECT may be useful to detect both primary breast cancer and axillary lymph node metastasis, as well as to identify residual breast cancer after nodular excisional biopsy, showing a better accuracy than T-planar.

Poster presentations

PS-233

G.Vural, E. Özalp, T. Çalikoğlu*, A. Üçer*, S. Durmuş*, N. Erçakmak

Ankara Oncology Hospital, Departments of Nuclear Medicine and Radiation Oncology*, Ankara-TÜRKİYE

VALUE OF AXILLARY LYMPHOSCINTIGRAPHY (ALS) IN PATIENTS WITH OPERATED BREAST CARCINOMA

It has been reported that adjuvant therapy increases local control and survive in patients (pts) with operated breast carcinoma. Axillary nodal status and tumor size are the most important factors to decide for adjuvant therapy. The aim of this study was to evaluate axillary nodal status with ALS after axillary dissection and its role in adjuvant therapy planning. 52 pts (mean age: 49.8yrs., range: 24-71yrs.) who had undergone modified radical mastectomy were included to this study. Interpretations of complete (C) and incomplete (IC) axillary dissection were defined according to number of axillary lymph nodes (LN) removed by surgery (≤ 10 LN:IC ; > 10 LN:C). ALS was performed by alternating bilateral interdigital subcutaneous injections of 14 MBq (0,5mCi) of ^{99m}Tc Nanocolloid. Anterior images of chest and axilla were obtained 1-2 hr later using a large field of view gamma camera. ALS was interpreted as C if no accumulation was shown, and IC if accumulation was shown in axillary region. Comparison of ALS and axillary dissection results are as follows;

ALS	Axillary dissection	
	Complete	Incomplete
Complete	28	1
Incomplete	16	7
Total	44	8

Totally, 16 of 44 pts (36 %), interpreted as C after operation, showed uptake of radiocolloid in axillary region and were interpreted to be scintigraphically IC. 4 of 6 pts (66 %) who had been removed ≤ 10 LN but stated as C dissection by the surgeon were found to be IC according to ALS. 12 of 38 pts (32%) who had been removed > 10 LN and claimed to be C dissection showed IC axillary dissection after ALS. We concluded that, in addition to surgical and pathological information, ALS known as a noninvasive and physiological method, should be performed to detect the patients needing adjuvant therapy, who otherwise could be missed. Hence, evaluation of axillary dissection with ALS can be useful in selecting pts (especially >10 LN removed) who actually need axillary irradiation.

PS-234

H.Q. Zhu, X.T. Lin, S.J. Jin, C.C. Ren, W.T. He

Dept. of Nucl. Med. Huashan Hospital, Shanghai Medical University
Shanghai 200040, China

COMPARISON OF ^{99m}Tc -MIBI SCINTIMAMMOGRAPHY WITH X-RAY MAMMOGRAPHY FOR DIAGNOSIS OF BREAST CANCER

PURPOSE: To evaluate the ^{99m}Tc -MIBI scintimammography and X-ray mammography for differentiation of malignant breast lesions from the benign ones. **METHODS:** 46 patients ($49.2 \pm 7.4y$) with a suspected mass detected by palpation or nonpalpation but highly suspicious were taken with X-ray mammography and scintimammography. Excisional biopsy or surgery was performed in all patients for pathological findings. All patients received intravenously 740 MBq ^{99m}Tc -MIBI in the arm, contralateral to the suspicious breast. At 5-6 min postinjection, planar images were obtained in the anterior, anterior oblique, lateral and prone position and each had an acquisition time of 10 min. **RESULTS:** In the total patient group of 46 patients, 34 Patients were pathologically confirmed malignant and others were benign. Sensitivities of scintimammography and mammography were 91.3% , 75.9%, respectively, $P < 0.01$; and specificity of both were 80% , 57.1%, $P < 0.01$. The smallest detectable tumor in scintimammography measured was 11 mm in diameter. **CONCLUSION:** Scintimammography with ^{99m}Tc -MIBI is a more sensitive than conventional X-ray mammography, particularly in patients with dense breast.

Oncology: Therapy

PS-235

C.Alexander, B.Sax, J.B.Bader, D.Hellwig, C. Finke, C.-M. Kirsch; Dept. of Nuclear Medicine; Saarland University Medical School; D-66421 Homburg/Saar; Germany

LONG-TERM SIDE EFFECTS AFTER HIGH DOSE RADIOIODINE THERAPY IN THYROID CARCINOMA PATIENTS

The present investigation is an evaluation of side effects in patients after high-dose radioiodine treatment.

Material an Methods: The study was performed in a group of 203 thyroid carcinoma patients at least one year after the last therapy. The cumulated activities ranged between 4.4 and 69.0 GBq I-131. Present symptoms were checked by an experienced physician and documented in a standardized interview-form.

Results: Twenty-three percent of patients reported no complaints. The remaining patients presented: reduced salivation: 43 %; sialoadenitis: 33 % (parotid gland: 81 %, submandibular gland: 46 %); transitory alopecia: 28 %; transitory loss of taste or smell: 27 %; increased influenza rate: 14 %; chronic conjunctivitis: 23 %; xerostomia: 4 %. Haematological abnormalities were found in 9 cases. Further changes of blood were not registered. For sialoadenitis, loss of taste and dry mouth the dependence on accumulated activity was significant.

Conclusions: Severe long-term side effects are rare after high-dose radioiodine treatment. Moderate side effects are common. Mostly they are the result of radiation damage to the salivary glands. The frequency of such complaints advocates a regular protection of the salivary glands. Transient alopecia and chronic conjunctivitis after treatment of thyroid carcinoma have not been reported before.

PS-236

MT. Bajón, JR. García, S. Mañé

Centre de Tecnologia Diagnòstica

EFFECT OF DIAGNOSTIC DOSE OF ^{131}I IN POSTSURGICAL THYROID REMNANT

BACKGROUND: Stunning of thyroid tissue following diagnostic scanning with ^{131}I has been studied in the last years, and the concern is that this effect may limit ^{131}I therapy. But the follow-up, scan and serum thyroglobulin, of such patients has not been well documented.

OBJECTIVES: 1) To determinate how often less and/or smaller uptake were seen on post-therapy scan and 2) To study evolution of stunned thyroid tissue.

METHODS: We examined 901 scans, obtained before and after 303 treatments (mean dose: 4033 MBq ^{131}I) in 234 patients (182 papillary and 52 follicular carcinomas) undergone to total or nearly total thyroidectomy. Scans were performed 48 hours after 180 MBq ^{131}I or 5 days after therapeutic doses. In all patients pre and post-treatment scan were performed. In 157 patients follow-up scans were also performed. The time between diagnostic scan and therapy was 8.5 weeks. In all patients serum thyroglobulin level evolution was determined.

RESULTS: Post-therapy scan showed less uptake than diagnostic scan or even become negative in 54 cases (23.08%). The time between diagnostic scan and therapy in these cases was 8.9 weeks. In 29 out of these 54 cases (53.71%) follow-up scans continued or become negative and serum thyroglobulin was < 3 ng/ml and antibodies antithyroglobulin were negative. In 21 patients (38.88%) don't undergo to posterior scans yet. In 4 patients (7.41%) posterior scans become negative but serum thyroglobulin level continued high.

CONCLUSIONS: In the studied group it is not possible to talk about stunning effect, but therapeutic effect of diagnostic dose. So that, the tendency to decrease diagnostic scan dose would have to be reconsidered.

PS-237

Basmanov V., Kolesnik O., Ignatova A.
Ministry of Russian Federation for Atomic Energy, Institute of Physics and Power Engineering, Obninsk, Russia

RHENIUM-188 CHROMATOGRAPHIC GENERATOR AND THERAPEUTIC RADIOPHARMACEUTICAL

The aim of this study was to develop the prototypes of rhenium-188 chromatographic generator and cold kit for clinical preparation of bone-seeking radiopharmaceutical for treatment of patients with bone metastases of prostate and breast cancer. 3700-4400 MBq experimental rhenium-188 generators have been manufactured based on tungsten-188 with high specific activity (3,8 Ci/g). The specially pretreated Al₂O₃ (2,5-4,5 g) and Y₂O₃ (0,5-1,0 g) were used as adsorbents. HEDP and tin (II) chloride were selected as an osteotropic agent and a reductant respectively for the cold kit formulation. Under elution of the generators twice per week for 4 months rhenium-188 yield was 80-90%; rhenium-188 concentration activity in the eluate at the beginning of the generators operation - 270-300 MBq/ml; tungsten-188 content - not more than 10⁻⁴%, content of stable impurities - not more than 10 µg/ml (Al, Zr). The production technology of the cold kit for rhenium-188 generator has been developed. The radiochemical purity of HEDP based reconstituted radiopharmaceutical is not less than 95% and it is suitable for intravenous injections. Preliminary investigations of perrhenate-ions distribution in the tissues of laboratory animals have been done. The next step is to continue animal testing of the radiopharmaceutical and the generator eluate.

PS-238

WAP Breeman, GD Slooter, R Marquet, CHJ van Eijck, EP Krenning.
Depts of Nuclear Medicine & Surgery, University Hospital Dijkzigt, Rotterdam, The Netherlands.

Characteristics of peptide receptor radionuclide therapy (PRRT) of the somatostatin receptor (SSR) positive tumor CA20948 in a rat liver model with [¹¹¹In-DTPA⁰]octreotide (In-111-OC).

Lesions expressing SSR in rats and in man enabled PRRT in vivo using In-111-OC. This radioligand is internalised via the SSR and radioactivity (In-111) has a long lysosomal residence time, e.g. > 700 h in humans. PRRT with high doses of In-111-OC was investigated in SSR-positive tumor-bearing rats. CA20948 cells were injected into the portal vein on day 0. Exp 1: PRRT with 370 MBq In-111-OC (0.5 µg) per rat on day 1 or 8 or 1 and 8. Control rats received 0.5 µg unlabeled DTPA-octreotide. Exp 2: PRRT on day 6 or 12. Exp 3: in order to determine the minimal effective dosage the rats received 3.7 or 37 or 370 MBq on day 1. The rats were sacrificed on day 20 and tumor colonies in the liver were counted.

We conclude: Peptide receptor radionuclide therapy is effective with 370 MBq [¹¹¹In-DTPA⁰]octreotide, and even 12 days after inoculation of the tumor.

Exp		tumor colonies in liver						rats
		0	+	++	++	++	+++	
1	day 1	-	2	2	1	-	-	5 *
	day 8	-	-	3	2	-	-	5 *
	day 1,8	3	2	-	-	-	-	5 *
	Control	-	-	-	-	-	6	6
2	day 6	3	-	-	5	-	-	8 *
	day 12	1	-	3	4	-	-	8 *
	Control	-	-	-	-	-	8	8
3	3.7 MBq	-	-	-	2	5	1	8
	37 MBq	-	-	-	-	4	4	8
	370 MBq	-	-	4	4	-	-	8 §
	Control	-	-	-	-	-	4	4

* : p<0.01 vs Control; † : p<0.05 vs day 1,8;
§ : p<0.01 vs 3.7 MBq, 37 MBq and Control; Mann-Whitney u-tests

PS-239

M.R. Castellani, M. Resnik, L. Maffioli, R. Luksch, A. Trevisan, E. Bombardieri.
Istituto Nazionale per lo Studio e la Cura dei Tumori, Milan, Italy

TEN YEAR EXPERIENCE OF ¹³¹I-mIBG THERAPY IN NET TUMORS: WHICH PATIENTS AND WHICH DISEASES HAVE TO BE TREATED?

Our ten-year experience with ¹³¹I-mIBG therapy in NET tumors is revised with the aim to perform a balance of efficacy.

16 patients (pts) with neuroblastoma (12 advanced and 4 minimal residual disease), 8 pts with pheochromocytoma, 3 pts with paraganglioma, 6 pts with medullary thyroid carcinoma and 4 pts with carcinoid tumors, for a total of 37 pts, are evaluable.

2.96-5.55 Gbq of ¹³¹I-mIBG (specific activity >1.85 GBq/mg) were administered by 90 min infusion, after thyroid blocking (if not previously resected). In children with neuroblastoma, hydro-electrolytic and diuretic therapy was given to reduce whole body irradiation. The therapy was repeated at variable intervals, depending on the clinical extent and disease aggressiveness (8 weeks- 12 months). The main results are summarized in the table:

tumor	N pts	extent	Response (PR+NC)	duration (months)
neuroblastoma	12	advanced	7/12	4-30
neuroblastoma	4	minimal residual	4/4	6+-60+
pheochromocytoma	8	loc. advan. or metastatic	6/8	6+-44+
paraganglioma	3	metastatic	3/3	8+-66
medullary carcinoma	6	metastatic	2/6	6+-17+
carcinoid	4	metastatic	3/4	9-22

The data confirm that mIBG therapy induces a good palliative effect, consisting in tumor reduction, hormone response (in hormone secreting tumors) or long-lasting stabilization of disease in most of NET. The worst results are observed in advanced neuroblastoma and in medullary thyroid carcinoma. The therapy has been well tolerated and significant bone marrow toxicity has been observed only in advanced neuroblastoma patients.

PS-240

Simin Dadparvar, M.D., John E. Lahaniatis, Fariba Asrari, Athar A. Shaikh, Nasrin V. Ghesani, Mark Tulchinsky, Mingzhi Pan, Walter J. Slizofski, Luther W. Brady
Division of Nuclear Medicine, Departments of Radiation Oncology and Radiology, Allegheny University--Hahnemann, Philadelphia, PA

MANAGEMENT OF THYROID CARCINOMA: HAHNEMANN EXPERIENCE

The primary treatment of thyroid carcinoma is surgery and the outcome depends on its extent. The post-operative management alternatives in thyroid carcinoma include thyroid hormone, radio-iodine ablation (I-131 Na), external beam radiation therapy (EBRT) and occasionally adjuvant chemotherapy. This retrospective study analyzes the management of 153 patients (102♀, 51♂), age range 10-96 years, mean age 50.2 years treated for thyroid carcinoma. The range of follow-up was 1.0 - 294 months with median follow-up for 60.4 months. Twenty patients without therapy were excluded. Group A included 87 patients treated with I-131. Group B consisted of 13 patients received EBRT. Group C included both therapies in 33 patients. The therapies in all different stages of thyroid carcinoma and with various histopathologies were reviewed.

	Stage I	Stage II	Stage III	Stage IV
Group A = 87	12	29	34	12
Group B = 13	0	0	2	11
Group C = 33	0	0	14	19

The I-131 Na therapy was applied in all stages of thyroid carcinoma, but the need for EBRT or combined therapy was only in advanced stages of the disease (p<0.0001).

	Papillary	Papillary	Follicular	Follicular	Medullary	Anaplastic
Group A = 87	29	32	22	2	2	
Group B = 13	1	2	3	3	4	
Group C = 33	11	6	12	1	3	

The I-131 Na therapy was applied in the management of well differentiated thyroid carcinoma vs EBRT in aggressive histopathology (p<0.0001). I-131 Na and/or combined therapy were used in similar histopathologies (p=ns).

We conclude that I-131 Na therapy in post operative patients is the primary method of treatment in all disease stages and in majority of well differentiated thyroid carcinomas (WDTC). EBRT is commonly used in follicular carcinoma and the histopathologies other than WDTC. In the management for local control of the disease, or in patients with aggressive or unresectable tumors, combined therapy is commonly applied.

Poster presentations

PS-241

J.M.H. de Klerk, B.A. Zonnenberg, A.W.L.C. Huiskes, A.D. van het Schip, A. van Dijk and P.P. van Rijk.
University Hospital Utrecht, Department of Nuclear Medicine
The Netherlands

VALUE OF BONE MARROW SCINTIGRAPHY FOR THE PREDICTION OF PLATELET DECREASE IN PATIENTS TREATED WITH Re-186-HEDP

Thrombocytopenia has been identified as the dose-limiting organ in rhenium-186(tin)-1,1-hydroxyethylene diphosphonate (Re-186-HEDP) therapy in patients with painful bone metastases. Previously, a good relationship between the the Bone Scan Index, as an index of the extent of bone involvement and the percentage of platelet decrease (%DEC) was reported*. Because the normal bone marrow distribution is disturbed by metastatic tissue, bone marrow scintigraphy might result in an even better prediction of platelet toxicity. The aim of the present study is to evaluate the value of bone marrow scintigraphy in predicting the platelet toxicity. Twenty-nine prostatic cancer patients with multiple painful bone metastases were treated with Re-186-HEDP (administered doses ranging from 986 to 3067 MBq Re-186-HEDP. From a pre-therapy Tc-99m-nanocolloid bone marrow scintigram a Bone Marrow Index (BMI) was determined by scoring for functioning (not tumor invaded) bone marrow. The nadir of platelet count was at week 4 following therapy. From this value and the pretreatment level the percentage of platelet decrease (%DEC) was determined ($44 \pm 17\%$, range 14 - 72%). The BMI ranged from 19 to 90 (mean: 59 ± 20). Multiple regression analysis between (%DEC) versus BMI and administered dose normalized to standard body surface area (ADN), showed no improvement as compared with regression analysis between %DEC and ADN alone.

In conclusion, in contrast to bone scintigraphy, the additional value of bone marrow scintigraphy for prediction of platelet toxicity after administration of Re-186-HEDP is negligible. This can be explained by the fact that using bone scintigraphy not only the metastatic load is taken into account, but also the radiation dose to the bone marrow.

*De Klerk JMH et al. J Nucl Med 1994; 35: 1423-1428

PS-242

Oberdorfer, G. van Kaick

German Cancer Research Center, Heidelberg, Germany.

PET STUDIES OF THE FLUOROURACIL (FU) TRANSPORT WITH F-18-FU AND O-15-WATER IN PATIENTS WITH METASTATIC COLORECTAL CARCINOMA

Intraarterial chemotherapy can potentially increase drug delivery at the tumor sites and has therefore been used for the therapy of metastatic colorectal cancer. Dynamic positron emission tomography (PET) and F-18-Fluorouracil (F-18-FU) were used in patients with liver metastases from colorectal cancer to examine the pharmacokinetics of the drug up to 120 min p.i. following intravenous and intraarterial administration of the same dose of FU. All patients included in the study (n=15) had a surgically implanted catheter in the gastroduodenal artery. Dynamic PET studies (up to 5 min) with O-15-water were performed for the evaluation of the access to the lesions immediately prior to the F-18-FU study using both administration routes. The final evaluation includes 24 metastases obtained in 15 patients. 21/24 (87.5 %) of the lesions showed an improved access using the intraarterial approach. 20/24 (83.3 %) of the lesions demonstrated a better FU influx after intraarterial F-18-FU infusion. Metastases reached the highest F-18-FU concentrations after intraarterial administration with a maximum uptake of 18.75 SUV for the FU influx and of 5.03 SUV for FU trapping. 8/24 (33.3 %) of the metastases demonstrated an enhanced FU trapping following the intraarterial administration. Cluster analysis revealed a group of metastases (n=6) with a non-perfusion dependent FU transport using the intravenous application. 5/6 (83.3 %) of these lesions did not show any enhancement of the F-18-FU trapping after intraarterial application. The data gave evidence for at least one different, energy-dependent transport system, which can be saturated even after intravenous administration of the drug. The data show, that the main limiting factor for a therapy response is the very high and rapid elimination of the cytostatic agent out of the tumor cells. Furthermore, it was not possible to predict the pharmacokinetics of FU after intraarterial application using an intravenous PET-study. It may be possible using intravenous PET double tracer studies to identify metastases having a non-perfusion dependent transport system and exclude them from an intraarterial treatment protocol.

PS-243

G. Dimitrakopoulou, A. Dimitrakopoulou-Strauss, L.G. Strauss, P. Schlag, F. Oberdorfer, G. van Kaick

German Cancer Research Center, Heidelberg, Germany.

PERFUSION STUDIES OF LIVER METASTASES USING PET AND O-15-WATER IN PATIENTS WITH LIVER METASTASES

The evaluation of perfusion patterns of liver metastases is a major problem in patients scheduled for regional chemotherapy via single or multiple catheter systems.

We used Positron Emission Tomography (PET) and O-15-Water in patients with liver metastases from malignant melanomas and colorectal tumors. All patients had surgically implanted catheters and subcutaneous systems. Fifteen patients with eighteen liver metastases had a catheter in the gastroduodenal artery, three had a double catheter system with a second catheter implanted in the portal vein and two patients had a triple catheter system with a third catheter in the lienal artery. Repeated flow studies with O-15-Water were carried out after intravenous, intrarterial (hepatic artery), intraportal, and intralial tracer injection (2100-3700 MBq). Five to eight one-minute images were acquired. The quantitative evaluation was performed with Regions of Interest (ROIs) in the metastases and the normal liver parenchyma. We noted the highest tracer concentrations following the intraarterial tracer injection in 15/18 metastases. One patient with small liver metastases (<2 cm) from a melanoma demonstrated the highest perfusion of the lesions following the injection via the portal vein. In two other patients a mixed perfusion through the hepatic artery and the portal vein was observed.

The results indicate, that the intraarterial approach is not always sufficient for regional treatment and double catheter systems may be superior for therapy. The preliminary results demonstrate, that PET is an appropriate tool for repeated perfusion studies during one patient examination. Furthermore, in case of intraarterial chemotherapy the evaluation of the tumor perfusion is a prerequisite for a sufficient therapeutic result and should be examined prior to onset of treatment.

PS-244

El-Tannir O *, and El-Sabban Kh **

*Pediatric Oncology Unit, National Cancer Institute, Cairo University

**Nuclear Medicine Unit, Faculty of Medicine, Cairo University, Cairo, Egypt

¹³¹I-MIBG THERAPY IN ADVANCED NEUROBLASTOMA

Objectives: To evaluate role of ¹³¹I MIBG therapy as second line of treatment in advanced neuroblastoma.

Patients and Methods: Thirty nine children with advanced neuroblastoma who were either refractory to conventional therapy (C/T) or showed disease relapse after initial successful treatment, received ¹³¹I MIBG as therapy with a dose of 100 mci at each dose. They were 23 males and 10 females. 10 cases had stage III and 29 cases stage IV according to Evan's system. 15 cases received one course, 8 cases (2 courses), 14 cases (3 courses) and 2 cases (4 courses). Assessment of response has been done using CT, bone scan, MIBG, and VMA.

Results: 6/39 (15.4%) showed disease progression and 3/39 (7.7%) showed no response. While the rest (30/39 [76.9%]) showed varying degrees of response starting from stationary disease 10/30 (25.6%), minimal response 1/39 (2.6%), partial response 14/30 (35.9%) and complete response 5/39 (12.8%). Concerning survival 26 patients (66.7%) are still alive, while the rest were dead (33.3%), two of them were dead due to medical causes not related to neuroblastoma. Two cases were bed ridden (K.I. 30) on the start of MIBG therapy. They became in good performance (KI 80).

Conclusions: MIBG therapy at dose 100 mci is a safe and effective line of therapy in advanced neuroblastoma. Being a first line of treatment should be considered.

PS-245

A. Festa, R. Sciuto, A. Tofani, A. Ferraironi, S. Rea, R. Cucchi and C.L. Maini
Hospital: "Regina Elena" Cancer Institute, Department of Nuclear Medicine, Rome

PRELIMINARY RESULTS OF A CONTROLLED TRIAL WITH CISPLATIN AND 89Sr IN PROSTATE CANCER BONE PAIN PALLIATION

Purpose: a controlled randomized trial was designed to evaluate the effect of cisplatin radiosensitization in 89Sr metabolic radiotherapy on symptomatic bone metastases in prostate cancer patient. **Methods:** 16 patients entered the study and were randomized into two arms. Eight patients (Arm 1) received 89Sr 148 MBq plus Cisplatin 50 mg/mq in two administrations (immediately before and 10 days after 89Sr injection) and eight patients received 89Sr plus two placebo administration (Arm 2). Clinical response was evaluated at 2 months in terms of pain palliation (graded as complete, partial, minimal and absent by a modified Wisconsin test) and performance score evaluated by Karnofsky Index (KI) variation. Hematological toxicity was evaluated weekly and graded according WHO criteria. **Results:** overall pain palliation response rate was 87% in Arm 1 and 62% in Arm 2. Grade of pain response is illustrated in the Table 1.

	Complete	Partial	Minimal	Absent
Arm 1	2	4	1	1
Arm 2	2	3	-	3

Performance score effectively improved in 50% patients of Arm 1 while was slightly increased only in one patients of Arm 2. KI variations are reported in Table 2.

	Improved KI	Unmodified KI	Worsened KI
Arm 1	4	2	2
Arm 2	1	3	2

Mean platelet decrease was 23 % in Arm 1 (with a grade 1 of toxicity in 1 patient) and 36 % in Arm 2. Mean WBC decrease was 21% in Arm 1 (with a grade 2 of toxicity in 3 patients) vs 31% in Arm 2 (with a grade 2 of toxicity in 1 patients). **Conclusions:** radiosensitization with low-dose cisplatin may be effective for 89Sr pain relief and performance score improvement than 89Sr alone. Hematological toxicity is only slightly enhanced by cisplatin.

Supported by Ministry of Health, Grant RF/96, 287

PS-246

M. Fözy, O. Esik, B. Vincze, *J. Környei

National Institute of Oncology and *Institute of Isotope Co. Ltd., Budapest, Hungary

I-131-MIBG THERAPY OF RECURRENT AND/OR METASTATIC MEDULLARY THYROID CARCINOMA

Aim of study: To assess the value of high dose of I-131-MIBG treatment in 20 pts suffering from recurrent and/or metastatic medullary thyroid carcinoma.

Methods: All pts underwent different type of operation of the thyroid gland and lymph node dissection. Eighteen pts received p. op. external irradiation and two cytostatic treatment. After a tumor free period lasting from four months to 13 years in 14 pts lymph node metastases, in four pts lung or liver metastases and in two pts only elevated calcitonin level were observed. The extension of the disease was determined by physical examination, X-ray, computer tomography and in 11 pts by PET, too. I-131-MIBG was applied in high dose (2,000-4,000 MBq) in slow drop infusion. The treatment was repeated in 7 cases, in one case four times. I-131-MIBG uptake was observed by scintigraphy on the fourth day in five pts.

Results: In four pts partial remission was achieved that lasted for more than one year, in three pts progression and in 11 pts steady state were observed. The serum level of calcitonin diminished after I-131-MIBG treatment in all cases except in progression of the disease.

Conclusion: I-131-MIBG therapy has a temporary beneficial effect in recurrent and/or metastatic MTC.

PS-247

N. Guerrero Mejia, A. Normandia Almeida, R.M. Garcia A., G. Ferro Flores and R. Vega Serrano.

Hospital de Especialidades del. Centro Medico Nacional La Raza del. I.M.S.S., Departments of Nuclear Medicine and Urology. Instituto Nacional de Investigaciones Nucleares. Mexico City, Mexico.

TREATMENT OF BONE PAIN WITH SAMARIUM-153-EDTMP IN PATIENTS WITH PROSTATIC CANCER.

Bone pain as a consequence of metastatic prostatic cancer is frequently observed in the disease process and it is characterized for its resistance to subside with standard therapeutic methods including anti-inflammatory drugs, analgesics, external radiation and root nerve blockage. Several radioactive compounds such as 32-P and 89-Sr have been used to relieve bone pain in these patients, but the results are inconsistent and the risk of bone marrow suppression is high. Samarium 153 (153-Sm) is a beta emission radioisotope that has proved to be the best alternative way to relieve bone pain in patients with metastatic prostatic carcinoma.

Herein we report a prospective and control study of 18 patients with metastatic bone pain due to prostatic carcinoma who underwent 153-Sm treatment. Patients were divided in 2 groups: the first group (nine patients) received I.V. 1.5 mCi/Kg/ideal weight of 153-Sm-EDTMP and conventional analgesia. The control group received conventional analgesia. In both groups the pain level was evaluated

by a semiquantitative method called visual analogical scale. We used the statistics methodology of t-Student.

Thrombocytopenia was observed during the first week of treatment with 153-Sm, being the difference with the control group statistically significant (p < 0.00025).

Thrombocytopenia was a transitory side-effect that subsided after 8 weeks and without haemorrhagic manifestations.

Pain relieve was statistically significant in patients treated with 153-Sm (P<0.0006), while in patients receiving narcotic analgesia, bone pain far from subsiding, became worse.

In summary, 153-Sm treatment of bone pain in patients with metastatic prostatic carcinoma with 153-Sm-EDTMP is a useful method to be used in patients with refractory pain to conventional analgesia

PS-248

U. Haberkorn, I. Morr, M. Eisenhut, G. van Kaick. German Cancer Research Center (dkfz), Heidelberg.

ENHANCED EXPRESSION OF THE HUMAN THYROID PEROXIDASE GENE IN HUMAN ANAPLASTIC THYROID CARCINOMA CELLS DOES NOT INCREASE IODIDE TRAPPING.

Radioiodine therapy represents an attractive and highly effective treatment of differentiated thyroid carcinoma. Peroxidase activity seems to be a critical parameter for the accumulation of radioiodide in thyroid tissues which may be lost in anaplastic carcinoma. Therefore, transfer of the human thyroid peroxidase (hTPO) gene in anaplastic carcinoma cells may be used to restore the iodide trapping capacity in these tumors. A bicistronic retroviral vector based on the myeloproliferative sarcoma virus which carries the genes for hTPO and neomycin resistance and the internal ribosomal entry site from polio virus was constructed. Using this vector two human anaplastic thyroid carcinoma cell lines (C643 and SW1736) were transfected and neomycin resistant cell lines were generated. Thereafter, the hTPO expression and activity were measured using a luminescence kit and the guaiacol assay. Furthermore, the iodide uptake was determined after 4 h incubation with Na¹²⁵I and normalized to the viable cell number. We found different levels of hTPO expression in the neomycin resistant cell lines, indicating different sites of integration into the host genome. The hTPO expression was up to 600-fold higher in the genetically modified cells than in the wild type cells. The hTPO expression and hTPO activity were not correlated. Furthermore, no enhancement of iodine uptake was observed even in the cell lines with very high hTPO expression. In conclusion, the transfer of the hTPO gene is not sufficient to enhance the iodide accumulation in human anaplastic carcinoma cells. Therefore, the hTPO gene cannot be used for gene therapy of these tumors.

Poster presentations

PS-249

Qing Lan, Qiang Huang, Yuanfang Hu

Second Affiliated Hospital, Suzhou Medical College, Neurosurgery Department & Brain Tumor Research Laboratory

PRECLINICAL STUDY ON IMMUNORADIOTHERAPY WITH 35S LABELING MONOCLONAL ANTIBODY SZ39 AGAINST HUMAN BRAIN GLIOMA

Purpose: To evaluate the effect of the immunoradiotherapy agent, 35S labeling monoclonal antibody(MAb) SZ39, in vitro and in vivo. **Methods:** The cytotoxicity of 35S-MAB SZ39 against glioma cell line SHG-44 was tested with MTT method, to get a cell growth inhibition rate comparing with 35S-nIgG, 35S+MAB SZ39 and 35S control groups. Target treatment effect and pharmacokinetics of 35S-MAB SZ39 were assessed in 42 glioma-bearing nude mice. The radioactivity values of blood samples of 35S-MAB SZ39 were calculated with a PKBP-N1 pharmacokinetics computer procedure package to get the kinetic parameters and linear model. The nude mice were sacrificed in group of 3 at 24h,72h and 120h. The radioactivity uptake in glioma and main organs were calculated. To assess the inhibition of growth of solid tumor in vivo, 3 group(5 animals for each) were designed:(1)35S-MAB SZ39; (2)35S-nIgG; (3)PBS. The tumor inhibitory rate(I) was calculated with the formula: $I=(\text{Volume group3}-\text{Volume group2})/\text{Volume group3}$. The statistical significance of differences was determined with $P=0.05$ for all statistical analysis. **Results:**35S-MAB SZ39 had a strong cytotoxic effect to SHG-44 cells with 4.2-fold and 4.0-fold more toxic to "target" cells than 35S-nIgG and 35S+MAB SZ39. In the glioma-bearing nude mice, 35S-MAB SZ39 could specially localize in glioma. The special indexes of 35S-MAB SZ39 to 35S-nIgG and 35S were 4.1 and 4.87 separately. Its pharmacokinetics fitted 3 compartment's model. The dose-time equation was $Ct=1559276e^{-3.49t}+977313e^{-0.5t}+21682e^{-0.017t}$, $T_{1/2\alpha}$ was 0.23h, $T_{1/2\beta}$ was 1.46h, $T_{1/2\gamma}$ was 42.9h. Tumor growth delay of one week was observed with 103.6MBq 35S-MAB SZ39. The tumor inhibition rate was 50% at 26 days after 35S-MAB SZ39 administrated, and no evidence of marrow inhibition was observed. **Conclusion:** 35S, as a pure β -emitting radionuclide, has a superiority of itself. 35S-MAB SZ39 has a good prospect as a immunoradiotherapy agent and is worth further studying.

PS-250

GS Limouris¹, M Lyras¹, N Baziotis², D Mourikis¹, A Hatzioannou¹, A Gouliamos¹, A Stauraka¹, L Vlahos¹; ¹Nucl Med Div, Areteion Hosp, Univ Med Faculty, Athens, ² Nucl Med Dept St Savvas Anticancer Inst, Athens

AUGER AND CONVERSION ELECTRON THERAPY WITH 111In PENTETREOTIDE IN NEUROENDOCRINE AND NONE-TUMORS

In a 42 year male with hepatocellular carcinoma, a 58 year lobectomized male with lung cancer and two 52 and 39 year females with abdominal carcinoid, biopsy confirmed, all four positive for somatostatin receptor scans, was decided to be treated with high therapeutic doses of [¹¹¹In-DTPA-D-Phe]-Octeotride (Mallinckrodt, BV, Petten). Conventional and, in the majority of the cases, hopeless cytostatic therapy was abandoned.

So far, 6 months after 4 sessions in a dosage of 4070 MBq each, via i.v. infusion for the lung/carcinoid cases and intrahepatic artery catheterization, for the hepatocellular case, all 4 patients are in excellent clinical condition, without any site effect from renal, pituitary, bone marrow or thyroid function. A transient diarrhea was noticed the first two days after every infusion in all patients. In all cases on CT/MRI sequential images, tumor size remained stable. A progressive increase of the cystic/necrotic area in dispense of the surrounding thick pericyclic/perinecrotic tissue was particularly seen on hepatocellular carcinoma scans. Dosimetric calculations of each session are presented below.

Organ	Hepatic cancer	Neuroend cancers
	Mean absorbed dose (rads)	Mean absorbed dose (rads)
Tumor	4346.20	325.00
Liver	1241.50	600.00
Kidneys	440.60	225.00
GI tract	361.08	378.00
Spleen	141.30	192.26
Red marrow	272.00	268.00

The marked dosimetric diversity between the hepatocellular and lung/carcinoid cases is the result of the different tracer application mode (i.v. perfusion vs intrahepatic catheterization; in the latter the fractional radioactivity distribution is practically equal to 1).

PS-251

H.K. Lu, R.S Zhu, J.F Zhu, et al. Department of Nuclear Medicine, Shanghai Sixth People's Hospital, Shanghai 200233, China

STUDY OF CLINICAL FEATURES AND 131I THERAPEUTIC EFFICIENCY IN PATIENTS WITH PULMONARY METASTASES OF DIFFERENTIATED THYROID CANCER.

Purpose: A retrospective analysis on 38 Chinese patients with pulmonary metastases (PM) of differentiated thyroid cancer (DTC) was carried out to study their clinical features and the results after 131I treatment. **Materials & Methods:** At diagnosis of PM, the patients' mean age was 52.9 y (11-71), female / male ratio 2.3 /1.0. Eighteen patients (41.5%) exhibited no obvious chest symptoms. Eight came up with only mild chronic chest symptoms, and the rest with severe situations (distress and short of breath in exertion in 10 cases, chest pain and /or blood stained or hemoptysis in 4). The severity of chest X-ray findings, with abnormal ones in 29(76.3%) cases, was roughly classified into four degrees. In addition to PM, cervical lymphnodes' and /or other distant metastases were found in 30 patients. As to treatment, 5254 ± 445 MBq 131I (120 -160mCi) was given to each patient per time. **Results:** The presence of pulmonary symptoms and its severity tended to be in concord with their abnormal degrees of chest X-rays, both of which were adversely correlated with outcomes of 131I treatment ($r_1=-0.74$, $p<0.01$; $r_2=-0.65$, $p<0.01$). The overall 131I therapeutically efficiency (complete remission and favourable improvements included) was up to 73.6%. 131I therapeutically efficiency was significantly higher in the group of patients with PM alone and plus only cervical lymphnode metastases (89.5%) than that of the group of patients with PM and other distant metastases concomitant (57.9%) ($p<0.01$). **Conclusion:** Absence of chest symptoms without or with only mild abnormal chest X-rays in patients with PM of DTC predicates benign outcomes after 131I treatment. On the other hand, the presence of pulmonary symptoms with severe morphologic changes in chest X-rays probably proceeds with poor consequence of 131I treatment. 131I therapy is less effective on PM of DTC when other distant metastases are concomitant.

PS-252

M.Malesevic, J.Vojcic, Lj. Stefanovic, J. Mihailovic, B. Guduric, J.Bogdanovic, N. Slijapic, Lj. Miljkovic Institute of Oncology, Sremska Kamenica, Yugoslavia

20 YEAR FOLLOW-UP OF PATIENTS WITH DIFFERENTIATED THYROID CARCINOMA TREATED SURGICALLY AND WITH RADIOIODINE

From 1977 to 1997, 239 patients with differentiated thyroid carcinoma received radioiodine therapy (¹³¹I-Th) after total or near total thyroidectomy. Afterwards, all patients began life-long L-thyroxine therapy and had regular check-ups. **Aim** of our study was to evaluate survival rate of the patients. **Results:** There were 177 (74.1%) female pts (13-75 yrs; $\bar{x}=45.8\pm13.1$) and 62 (25.9%) male pts (11-75 yrs; $\bar{x}=48.1\pm11.9$). Female: male ratio was 2.8:1. 33 pts (17.8%) received ¹³¹I-Th more than once. There were 44 (16.7%) pts with follicular and 195 (83.3%) pts with papillary carcinoma. Divided into clinical stages, according to TNM classification: I=112 (47%) pts, II=48 (20.1%) pts, III=57 (23.4%) pts and IV=22 (9.5%) pts. At the moment of survival rate evaluation (26/12/97), there were: 213 (89.1%) living pts, 11 (4.6%) who died of differentiated thyroid cancer and 15 (6.3%) who died of other causes or with no current data. Kaplan-Meier's method was used in the paper. The results show that after 18 years of follow-up, survival rate (SR) is 0.91. Presented through the clinical stages, SR is: I-0.99 after 18 yrs, II-0.91 after 12 yrs, III-0.93 after 14 yrs and IV-0.33 after 15 yrs. According to hystological type: in pts with follicular cancer it is 0.85 after 18 yrs and with papillary cancer it is 0.93 after 18 yrs. There is no statistically significant difference between pts with follicular and ones with papillary cancer ($p>0.5$). Also, there is no statistically significant difference in SR of I/II, II/III and III/IV clinical stages ($p>0.05$). There is highly significant difference in SR of I/IV clinical stages ($p<0.001$) and statistically significant difference in SR of I/III and II/IV clinical stages ($p<0.05$).

CONCLUSIONS: Survival rate of patients with differentiated thyroid cancer treated according to our Protocole, in given periods of time, is very high for the first three clinical stages. It is especially high for the first stage and it is getting close to $p=1$. Survival rate of patients with clinical stage IV is low, but satisfying from the oncologists' point of view.

PS-253

J.C. Martín, L.I. Bernà, C. Marf, A. Flotats, J.M. Tabernero, C. Alonso, M. Estorch, A. Catafau, I. Carrió
Hospital de Sant Pau. Barcelona

BONE PAIN PALLIATION WITH STRONTIUM-89 IN BREAST AND PROSTATE CANCER PATIENTS WITH BONE METASTASES AND REFRACTORY BONE PAIN

Aim: To assess the effectiveness of strontium-89 in the palliation of pain from bone metastases in breast and prostate cancer patients.

Materials and methods: A total of 43 patients were studied from October 1992 to October 1997. Group I: 22 females with breast cancer, mean age of 61 ± 9 years; time of evolution since the diagnosis of skeletal metastases had been made was 63 ± 39 months. Group II: 21 males with prostate cancer, mean age of 68 ± 5 years; the time of evolution since the diagnosis of skeletal metastases was 28 ± 20 years. Inclusion criteria were: multiple bone metastases demonstrated on bone scintigraphy, bone pain in areas of higher uptake, bad response to conventional analgesic therapy, normal renal function, white cell count > 3x10⁹/L and platelet count > 100x10⁹/L, and life expectancy of at least 3 months. Karnofsky performance status, severity of bone pain, and dependency on analgesics were evaluated before, 4, 8 and 12 weeks after strontium-89 administration. Patients received 2MBq/Kg (118-148 MBq) of strontium-89 by i.v. injection (Metastron (R), Amersham). Monitoring of peripheral blood cells was carried out at baseline, at 6 and at 12 weeks after treatment.

Results: Pain relief and a reduction in analgesic requirements were observed in 12 of 22 (55%) patients of Group I and in 9 of 21 (43%) patients of Group II. Duration of the response oscillated from 3 to 7 months. Eighteen of the 43 patients died before the end of the third month of follow-up. In Group I, 9 of the 12 (75%) patients who survived a minimum of 3 months responded to therapy; in Group II, 8 of 13 (62%) patients who were alive at third month improved after treatment. A decrease in peripheral blood cell count was observed in 14 patients: a 15-66% reduction in white cell count and a 14-75% reduction in platelet count. Hematologic toxicity grade 3 or 4 was observed in 5 patients.

Conclusion: We conclude that strontium-89 is effective for bone pain palliation in bone metastases from breast and prostate cancer.

PS-254

H. Oyamada

Tokyo Eastern Blood Center, Japanese Red Cross Society, Tokyo

PRESENT STATUS OF UNSEALED RADIOISOTOPE THERAPY IN JAPAN

In Japan, clinical application of unsealed radioisotopes is strictly regulated. Especially in the field of therapy, we are allowed to use only NaI-131 at present. Therefore, target diseases are limited only to Graves' disease and thyroid cancer. Only recently has the phase III clinical trial of strontium-89 chloride been concluded, and as for I-131-MIBG, we have no idea when it will be available. Under such circumstances, the present status of therapeutic nuclear medicine in Japan was surveyed by means of a nation-wide questionnaire in 1997, conducted in 193 hospitals. Then, 113 hospitals replied to such questionnaire (recovery rate: 58.5%), and it was found that in 77 hospitals, radioisotope therapy is being performed for Graves' disease and/or thyroid cancer. The questionnaire covered the following points: for Graves' disease --- the basic strategy of I-131 therapy, its indications (especially concerning the patient's age), absorbed dose planned to be administered, whether the therapy had been conducted on out-patient basis or in-patient basis, standard of discharge in case of in-patient basis, method of the thyroid weight estimation, interval of administration in case of multiple doses, number of patients treated per year (1996) etc.; and for thyroid cancer --- strategy for thyroid remnant, the dose to be administered for treatment, the maximum dose permitted by the authority in each hospital both per day and per year, handling of highly contaminated urine in each hospital, interval for the administration of the second dose, number of patients treated per year (1996) etc. The present status in Japan seems to be quite different from other advanced countries, but I believe the problem partly lies in the existence of the peculiar regulation which I hope to look into and pursue further.

PS-255

H. Oyamada*, I. Uchida**, M. Koizumi**, A. Kubo***, J. Hashimoto***
* Tokyo Eastern Blood Center, Japanese Red Cross Society, Tokyo
** Dept. of Nuclear Medicine, Cancer Institute Hospital, Tokyo
*** Dept. of Radiology, Keio University Hospital, Tokyo

SOME CONSIDERATIONS ON THE URINATION FREQUENCY IN REGARD TO THE AVOIDANCE OF EXCESS BODY BURDEN AFTER HIGH-DOSE RADIOIODINE-131 THERAPY OF THYROID CANCER.

In case of radioiodine-131 treatment of metastatic thyroid cancer, multiple doses are often given to the patient. Therefore, unnecessary exposure must be kept as low as possible. The administered radioiodine is excreted mainly through urinary system. On the assumption of a continuous evacuation of the urine through the bladder, we set one case having a particular pattern of the whole body retention curve after the dose of 160mCi(5.92GBq), which is represented by the formula as follows: $Y=150\exp(-\lambda_1 \cdot t)+10\exp(-\lambda_2 \cdot t)$, where $\lambda_1=0.693/10$ and $\lambda_2=0.693/(7 \times 24)$. Under the physiological state, however, intermittent urinations will cause a stepwise decrease, basically following the curve introduced by the formula. Then, two different modes of urination were considered; mode A indicates every 2 hour-urination x 6 times followed by every 6 hour-urination x 2 times, and mode B indicates every 6 hour-urination x 4 times. Focusing on the different amount of urine in the bladder upon the different modes of urination, radiation exposures from the urine to the neighbouring organs, such as bladder wall, uterus, ovary and testis, and also to the whole body were calculated. As the results, it was found that the urination mode B would cause radiation exposure from the urine in the bladder twice as much as the urination mode A to the neighbouring organs as well as to the whole body. This study will supply arguments for the necessity of frequent urination in the cases receiving radioiodine-131 treatment for metastatic thyroid cancer.

PS-256

H. Palmedo, S. Guhlke, H. Bender, J. Sartor, F.F. Knapp², J. Risse, H.J. Biersack. **Dept. of Nucl. Med., Univ. of Bonn, Germany, Nuclear Medicine Group², ORNL, Oak Ridge, TN, U.S.A.**

RHENIUM-188 HEDP FOR PAIN PALLIATION OF MULTIPLE BONE METASTASES: A DOSE-ESCALATION-STUDY.

Rhenium-188 (Re-188) emits a high energy beta radiation (2.11 MeV, T_{1/2}=17h) and is available from the tungsten-188/rhenium-188 generator. The option of very cost effective radiolabeling with Re-188 and the physical properties suitable for therapy led us to investigate Re-188 HEDP as a compound for pain palliation. We used a clinical-scale generator (18 GBq, weekly checked for sterility and apyrogenicity). Laboratory and animal studies have shown that only carrier-added (c.a.) Re-188 HEDP accumulates significantly in bone tissue. We have performed 16 injections of c.a. Re-188 HEDP in 12 patients (6 prostate cancers, 6 breast cancers) using increasing doses: 3 injections (inj) with 1295 MBq (35 mCi), 5 inj with 2405 MBq (65mCi), 6 inj with 3330 MBq (90 mCi) and 8 inj with 4440 MBq (120 mCi). A whole body Re-188 scan was performed 3 and 24 h. p.i. An eight-week follow-up included: weekly control of physical examination, blood count measurements, standard biochemical parameters and pain diary. All patients showed high Re-188 HEDP uptake in bone metastases. In the 35 mCi group, there was no alteration of blood counts. In the 65 mCi group, there was one case of thrombopenia grade I. In the 90 mCi group, there was one case of thrombopenia grade I and two times thrombopenia grade II. 2 patients showed a leukopenia of grade I. All alterations of the blood counts have been reversible within 7 weeks. Seven patients reported a significant pain relief. We feel that Re-188 HEDP is well suited for therapy of painful bone metastases. A decrease of thrombocytes appeared with a dose of 65 mCi first. The study is continued to evaluate the maximally tolerated Re-188 HEDP dose.

Poster presentations

PS-257

CH Rhee, JS Jang, SH Lee, CW Choi, SW Hong and SM Lim.
Department of Nuclear Medicine and Neurosurgery, Korea Cancer Center Hospital, SEOUL, KOREA

HOLMIUM-166-CHITOSAN AS A NEW INTRACAVITARY RADIONUCLIDE THERAPY FOR CYSTIC BRAIN TUMORS : PRELIMINARY CLINICAL TRIAL.

Ho-166 is a good therapeutic radionuclide because of its suitable half-life (26.8 hrs), high beta energy and 6% gamma ray for imaging. Chitosan is a kind of N-glucosamine, which chelates metal ions and degrades slowly in vivo. We synthesized Ho-166-chitosan complex (Ho-166-chico) and treated the unresectable eight cystic brain tumors (3 cases of metastatic brain tumors from lung cancer or breast cancer, 1 case of recurrent trigeminal neurinoma, 3 cases of recurrent low grade cystic astrocytomas, and 1 case of craniopharyngioma). The cyst volume and wall thickness were measured by MRI before Ho-166-chico injection (cyst vol.:6.3-60 ml). After installation of the Ommaya reservoir in cystic tumor, the activity of Ho-166-chico injected into the cyst was prescribed to result in 2,500 rad of dose to a cyst wall at a depth of 4 mm (EGS4 code, Monte Carlo simulation). After Ho-166-chico injection, the distribution of isotope was monitored by gamma camera. Two injections were administered in four cases, three injections in one case, and one injection in two cases. The response was evaluated with MRI. Five of 8 cases were shrunk in size with thinning of the cyst wall (one case of complete response, 4 cases of partial responses), 2 of 8 cases showed growth arrest, and one case (astrocytoma) showed progression. Every patient except one showed neurological improvement. The Ho-166-chico did not leak from the cyst, and no systemic absorption happened. No one showed infection or systemic absorption of Ho-166-chico, and other specific complications associated with isotope injection. Ho-166-chico intracavitary radiation therapy for cystic brain tumor is safe and reliable method, and deserves further evaluation.

PS-258

J.H. Risse, F. Grünwald, H. Strunk, R. Kleinschmidt, T. Bultmann, H. Palmedo, H. Biersack
Departments of Nuclear Medicine, Radiology and Internal Medicine, University of Bonn, Germany.

SUCCESS OF I-131-LIPIODOL THERAPY IN LIVER NEOPLASMS.

Purpose: Success, safety and effectiveness of intraarterial liver radiation therapy with I-131-Lipiodol in malign liver disease was assessed.
Methods: 11 patients with hepatocellular cancer (HCC, 9) with or without portal vein thrombosis, cholangiocellular cancer (CCC, 1), and multiple liver metastases due to breast cancer (BCM, 1) were treated by 17 cycles of selective intraarterial delivery of 1110 - 1924 MBq of I-131-labeled Lipiodol during hepatic angiography. 1 patient with HCC had three and 4 patients two therapy applications, respectively. The patients were monitored for distribution of lipiodol by CT, of the applied activity by planar scintigraphy and SPECT, and for evaluation of therapy success by CT and 18-FDG-PET.
Results: CT and SPECT showed pronounced I-131-lipiodol accumulation in the tumor tissue in all patients with variable distribution patterns. In 2 HCC a significant reduction in tumor size was achieved after the first treatment. 7 patients (6 HCC, 1 CCC) with huge tumors had stable disease (5) or showed progressive disease (2); 1 patient died because of renal failure. The BCM patient proved significant reduction in metastases number and size. 7 patients suffered from post embolisation syndrome (6 mild, 1 moderate), and 2 patients showed a transient elevation of pancreatic enzymes. All patients had a transient rise in liver enzymes. No severe side effects occurred.
Conclusions: Our first 11 patients with liver neoplasms treated by intraarterial I-131-Lipiodol show tumor mass dependent therapy response. Side effects are tolerable. The procedure is safe and effective for tumors up to a moderate mass. In general, the results are encouraging, and further studies are being conducted.

PS-259

T.Saga, H.Sakahara, N.Sato, Y.Nakamoto, S.Zhao, M.Kuroki, Y.Matsuoka, J.Konishi.
Department of Nuclear Medicine, Kyoto University, Kyoto and 1st Department of Biochemistry, Fukuoka University, Fukuoka, Japan

RADIOIMMUNOTHERAPY OF EXPERIMENTAL LIVER MICROMETASTASES: PHARMACOKINETICS, SHORT-TERM AND LONG-TERM EFFECT AFTER INJECTION OF THERAPEUTIC DOSE OF I-131 LABELED ANTIBODY

Purpose: Small metastatic lesion is the good target of antibody(Ab)-based therapy, since antibody uptake is high and intratumoral Ab distribution is good in small-sized tumors. In the present study, pharmacokinetics of intravenously injected therapeutic dose of I-131 labeled Ab was investigated along with its short-term and long term therapeutic effect in experimental liver micrometastases in nude mice.
Methods: Liver metastasis was established by intrasplenic injection of human colon cancer LS174T cells. Mice received 8.88 MBq of I-131 labeled anti-CEA Ab and the biodistribution was studied 1, 2, 4, 6, and 10 days later. Short-term and long term therapeutic effect was studied after injection of various dose of I-131 labeled anti-CEA Ab and compared with I-131 labeled irrelevant Ab, and non-treated mice. **Results:** Uptake of I-131 labeled anti-CEA Ab to the metastases remained high until 4 days after injection (21.6 - 24.0 %ID/gram) and gradually decreased thereafter with the biological half life of 6.5 days. Distribution of the radiolabeled antibody in metastatic nodules of several hundred microns in diameter determined by autoradiography was quite homogeneous at each time point. Estimated absorbed dose to the metastases was 16 Gy. Short-term effect determined 3 weeks after injection of radiolabeled Ab showed dose dependent therapeutic effect where no visible metastasis was observed after injection of more than 9.25 MBq of I-131 labeled anti-CEA Ab. Treated mice also showed dose dependent life prolongation effect and those who received 9.25 MBq lived more than 4 months with no sign of liver metastasis. Treated mice, however, showed significant bone marrow suppression. **Conclusion:** Liver micrometastases is a good target of radioimmunotherapy using I-131 labeled Ab and can even be cured. Bone marrow toxicity, however, is the major side effect and necessary administration dose should be reduced or clearance of unbound Ab should be facilitated to reduce bone marrow toxicity.

PS-260

I.Saletnich, V.Rufini, MC Garganese, G.Fadda*, L.Romano, G.Meduri, M.Salvatori, ML.Maussier, L.Troncone
Depts of Nuclear medicine and Human Pathology and Histology*, Catholic University of Sacred Heart, Rome, Italy

INSULAR THYROID CARCINOMA: HISTOPATOLOGICAL AND CLINICAL BEHAVIOUR AND THERAPEUTIC CONSIDERATIONS.

Insular thyroid carcinoma represents an entity situated morphologically and biologically in an intermediate position between the well-differentiated and undifferentiated carcinomas and is commonly considered to be an aggressive tumor. It may have focal or predominant insular component (IC). The aim of our study is to investigate whether a high or a low percentage of IC influences the biological behaviour of this cancer, including I131 uptake in metastatic lesions and Thyroglobulin (TG) production.
Out of 506 thyroid cancer pts submitted to total thyroidectomy during the period 1992-1997, 15 cases (2.9%), had histopathological findings showing the presence of IC. It was predominant (≥90%) in 7 pts, focal (≤50%) in 8. They were 7 males and 8 females, aged 14-74 yrs. Surgical staging was: T2 in 7, T3 in 6 and T4 in 2. Two pts showed lymph node metastases at surgery. Four pts, all with predominant IC, had distant metastases (bone and/or lung) detected by radiological imaging at post-surgical evaluation. All pts were studied with I131-whole body scintigraphy and TG assay and were treated with I131 therapy (average dose 300 mCi). Among metastatic pts, TG values were elevated (>1000 ng/ml) in all cases; I131 WBS was negative in 2/4 even after a therapeutic dose of I131. They were treated with radiation therapy and/or chemotherapy and 2 died six months and 18 months post diagnosis respectively. Of the remaining 11 pts, 2 (with predominant IC) developed local recurrence and 2 (with focal IC) lymph node involvement in a follow-up period varying from 3 months to 3 yrs. All 11 pts are still alive.
In conclusion, the prevalence of IC influences the clinical behaviour of thyroid cancer. In fact the predominant pattern is associated with a high incidence of local recurrence and metastases, a low rate of radioiodine uptake and a poor survival, while in the focal pattern the presence of differentiated areas suggests that I131 may have an important diagnostic and therapeutic role.

PS-261

R. Sciuto, A. Tofani, A. Semprebene, R. Pasqualoni, R. Cucchi, S. Rea and C.L. Maini
Hospital: "Regina Elena" Cancer Institute, Department of Nuclear Medicine, Rome

131I THERAPY IN LOCALLY ADVANCED THYROID CANCER (LATC): A 5 YEARS EXPERIENCE

Purpose: to analyze the incidence, characteristic and therapy outcome of LATC on a series of 400 differentiated thyroid cancer patients followed at our Institute during 5 years. **Methods:** 128 out of the observed 400 pts. were selected as LATC according to the presence of one or more of the following histopathological criteria: local tumor invasion (pT4), regional lymph node metastases (pN1), multiple intrathyroidal tumors (>3). **Results:** baseline feature of 128 pts. are illustrated in table 1:

Gender	Age	Histotype	pTNM
female	88 < 45	80 papillar	108 T1
male	40 > 45	48 follicular	14 T2
		insular	3 T3
		Hurtle	3 T4
			NO 42
			NI 87

Over 60% pts. were at low risk for age (<45 years) and lymph node metastases were present in 25% of pts. with primary tumor <1 cm. Lung or bone metastases were revealed only after 131I diagnostic or post-therapy whole-body in 14 pts. Whole-body scan findings and therapy outcome (complete, CR, or partial response, PR) are shown in table 2:

Radioiodine uptake Type	no. pts.	Outcome		131I Therapy	
		CR	PR	cumulative MBq	no. cycles
thyroid remnant	77	100%		2960-9250	1-3
residual tumor	5	100%		7400-12210	2-3
lymph node	32	32%	68%	3700-17020	1-4
lung	7	16%	84%	7400-14060	2-4
bone	7	16%	84%	7400-17760	2-5

Conclusions: conventional risk factors may underestimate tumor spread and recurrence in LATC; lung and bone metastases can be unexpected findings and tracheal involvement is also not unusual. The response to radioiodine treatment, if correctly performed, is very good.

PS-262

M.G. Steffens, M.H.G.C. Kranenborg, O.C. Boerman, E. Oosterwijk, F.M.J. Debruyne and F.H.M. Corstens.

Departments of Nuclear Medicine and Urology, University Hospital Nijmegen, The Netherlands.

TUMOR RETENTION OF THREE MONOCLONAL ANTIBODY G250 PREPARATIONS - LABELED WITH ¹⁸⁶Re-MAG3, ¹¹¹In-DTPA AND ¹²⁵I - IN NUDE MICE WITH RENAL CELL CARCINOMA XENOGRAFTS.

Despite the recent advances of radioimmunotherapy in patients with hematological malignancies, the results of radioimmunotherapy in solid tumors have been much less successful. Much effort is put in optimization of this relatively new therapeutic approach, including the choice of radionuclide. The physical properties of ¹⁸⁶Re - a high energy β emission in combination with only 10 % abundance imitable γ emission - seem to be ideal for radioimmunotherapy. In contrast to radioiodine, it has been shown that radiometals such as ⁹⁰Y and ¹¹¹In, are retained in the tumor cell after internalization of the antibody. In the current study we compared the tumor retention and biodistribution of monoclonal antibody G250 labeled with ¹⁸⁶Re-MAG3, ¹¹¹In-DTPA and ¹²⁵I in nude mice with s.c. renal cell carcinoma xenografts.

Radioiodination was done according to the IodoGen method, DTPA was used as chelator for ¹¹¹In, MAG3 was used as chelator for ¹⁸⁶Re. ¹³¹I-labeled monoclonal antibody MN14 was used as non-specific control. Antibody preparations were i.v. injected and 72 hours post injection uptake (% ID/g) was determined in the tumor and normal tissues (blood, muscle, lung, spleen, liver, kidney and intestines).

Blood levels of all G250 antibody preparations were remarkably low (mean: 2.38, 1.40 and 1.43 % ID/g for respectively ¹²⁵I, ¹¹¹In and ¹⁸⁶Re) whereas blood levels of the non-specific antibody MN14 were much higher (mean: 12.3 % ID/g), indicating that the antibody G250 was processed by the tumor. Retention of ¹¹¹In in the tumor (18.6 ± 6.2 % ID/g) was significantly higher than of ¹⁸⁶Re and ¹²⁵I (10.7 ± 5.2 and 5.9 ± 4.5 % ID/g respectively). Tumor retention of ¹⁸⁶Re and ¹²⁵I did not differ significantly. Enhanced retention of ¹¹¹In was also observed in the liver and was almost as high as uptake in the tumor.

The results of this study indicate that after processing of the antibody the ¹⁸⁶Re-label is not retained in the tumor cell and thus has no additional advantage for radioimmunotherapy in terms of tumor retention following internalization.

PS-263

M.G. Steffens, O.C. Boerman, E. Oosterwijk, W.J.G. Oyen, J.A. Witjes, G.O.N. Oosterhof, F.M.J. Debruyne and F.H.M. Corstens.

Departments of Nuclear Medicine and Urology, University Hospital Nijmegen, The Netherlands.

TUMOR DISTRIBUTION OF TWO SEPARATE, DIFFERENTLY RADIOLABELED, INJECTIONS OF CHIMERIC MONOCLONAL ANTIBODY cG250 IN PATIENTS WITH PRIMARY RENAL CELL CARCINOMA.

Tumor uptake of chimeric monoclonal antibody (mAb) G250 (cG250) in patients with primary renal cell carcinoma (RCC) is amongst the highest reported in solid tumors but is often highly heterogeneous, which might limit effective radioimmunotherapy. Analysis of mAb cG250 uptake related to antigen expression, (neo)vascularization and tumor viability showed that this heterogeneity could not be attributed solely to one of these factors. A number of physiological factors have been postulated that might affect antibody uptake; enhanced interstitial fluid pressure, heterogeneous blood supply and large transport distances in the interstitium. These factors may vary from one tumor to another as well as from one day to the next. A clinical study was performed to investigate whether mAb cG250 uptake is dependent on factors that change with time over a period of days.

All patients entered (n=9) had a clinical diagnosis of primary RCC and were scheduled for surgery. Nine days before surgery a 1st injection of ¹²⁵I-cG250 (5mg cG250, 50 μCi ¹²⁵I) was administered followed by a 2nd injection of ¹³¹I-cG250 (5 mg cG250, 3.5 mCi ¹³¹I) four days later. Whole body immunoscintigrams were made 1, 48 and 96 hours after the 2nd injection. Postsurgery, a tumor slice was mapped and cut into 1 cm³ cubicles. Each cubicle was analyzed for ¹²⁵I-cG250 and ¹³¹I-cG250 uptake and in each tumor slice the distribution of both isotopes were compared with each other.

All tumors analyzed showed a heterogeneous distribution of both isotopes throughout the tumor; intratumoral mAb cG250 uptake ranged between 0.0052-0.1804 % ID/g. However, the behaviour of both injections was identical: without any exception, in all 1 cm³ samples analyzed (>650) uptake of ¹²⁵I-cG250 was similar to ¹³¹I-cG250 uptake. Computerized reconstruction of ¹³¹I-cG250 throughout a tumor closely resembled the in vivo tumor images.

The results of this study show that, within a time interval of nine days, mAb cG250 uptake is not influenced by factors variable in time. Thus, in primary RCC, these factors seem to play a less important role as assumed in the literature. This implicates multiple injections, given within a short period of time, does not solve the problem of heterogeneity of antibody uptake by the tumor.

PS-264

M.G. Steffens, O.C. Boerman, E. Oosterwijk, W.J.G. Oyen, P.H.M. De Mulder, J.A. Witjes, G.O.N. Oosterhof, F.M.J. Debruyne and F.H.M. Corstens.

Departments of Nuclear Medicine and Urology, University Hospital Nijmegen, The Netherlands.

RADIOIMMUNOTHERAPY WITH ¹³¹I-LABELED CHIMERIC MONOCLONAL ANTIBODY cG250 IN PATIENTS WITH METASTATIC RENAL CELL CARCINOMA, A PHASE I/II STUDY.

In previous clinical studies with chimeric monoclonal antibody (mAb) G250 (cG250) in renal cell carcinoma (RCC) patients excellent tumor targeting was observed. Dosimetric analysis showed that therapeutic responses might be achieved when high doses of ¹³¹I-cG250 (>100 mCi) will be administered. Furthermore, chimeric mAb G250 appears to be immunosilent in contrast to murine mAb G250, potentially allowing multiple dosing. It was concluded that this antibody is a promising candidate for radioimmunotherapy in patients with RCC and therefore we initiated a phase I/II activity dose escalation study to determine the safety, the maximum tolerable dose (MTD) and the therapeutic potential of I-131 labeled chimeric mAb G250.

All patients entered received a diagnostic i.v. infusion of 5 mg cG250 labeled with 6 mCi I-131 followed by acquisition of 5 whole body scans on different time points up to 1 week p.i. In case accumulation of the antibody in metastatic lesions was visualized, patients (n=7) were hospitalized and a second, therapeutic, i.v. infusion of 5 mg cG250 labeled with a high dose of I-131 was administered. Three patients were entered per dose level, starting at 45 mCi/m². Toxicity was monitored up to 10 weeks p.i. according to the WHO toxicity criteria. If no dose limiting toxicity was observed three more patients were entered at the next dose level (15 mCi/m² increase).

The treatment was well tolerated by all patients. Most patients experienced mild nausea, without vomiting. No other complaints were reported. All patients showed a drop in platelet count with a nadir at 4-5 weeks p.i. In one patient (60 mCi/m²) a grade III haematological toxicity was observed (platelet count 39 x 10⁹/l). Dose limiting toxicity has not been observed yet. In one patient entered at 60 mCi/m² stable disease (3 month post therapy) was achieved while there was clear progression of disease prior to study entry.

The preliminary results of this study indicate that radioimmunotherapy might be applied successfully in the management of renal cancer. The achievement of stable disease without any serious side effects of treatment, while MTD has not been reached, is considered encouraging. However, more objective responses need to be observed before a conclusion can be drawn concerning the efficacy of this treatment.

PS-265

J. Tennvall, P.-A. Abrahamsson, G. Ahlgren, L. Darte, P. Flodgren, M. Garkavij, S.-E Strand
Depts of Oncology, Urology and Radiophysics, Lund University, S-22185 Sweden

PALLIATIVE RADIATION WITH RHENIUM-186 ETIDRONATE IN PATIENTS WITH DISSEMINATED PROSTATE CARCINOMA

The objectives of the present study were to evaluate the safety and efficacy of Re-186 etidronate in the treatment of painful skeletal metastases in patients with hormone refractory prostate cancer. Rhenium-186 is a beta-emitting radionuclide with a maximum β -emission of 1.07 MeV (74% abundance) and a physical half-life of 89.3 hours. It has a 9% abundant gamma -ray of 137 keV which is suitable for scintigraphic imaging.

Material and Methods: The series included 15 patients with disseminated prostatic carcinoma and morphine-requiring pain who received iv. 2590 MBq (70 mCi) Re-186 etidronate. They were permitted to leave hospital 4 hours postinjection after a scintigram had been performed. The patients assessed once weekly pain intensity, performance ("daily activity"), and analgesic consumption for a 24 hr period during a time span of at least 8 weeks, viz. from one week prior to therapy to at least 6 weeks post therapy. Additionally they indicated on an anatomic outline specific sites of pain including specification of the most painful site. The pain intensity was evaluated on a pain related behavioural scale graded from 0-6, the daily activity according to a Zubrod scale, graded 0-4. The criteria as an indication of positive response were: reduction in pain intensity with 1 step (=15%) during at least 4 consecutive weeks without deterioration in performance ("daily activity") or analgesic consumption.

Results. Pain-relief to Re-186 etidronate therapy was observed in 11 of 14 evaluable patients (79 %). Besides reported pain relief, 4 of the responding patients also noted an improvement in daily activity ($\geq 20\%$) and 3 had markedly reduced or discontinued morphine medication. Pain relief occurred within one week in 4 patients, within 2 weeks in 8 responding patients. The duration of pain relief after the first course of Re-186 etidronate averaged 6 weeks, range 4 - 10 weeks. Of the 11 responders, 4 became completely free from pain during 1-5 weeks. 3 patients experienced a flare response. The toxicity was mild, transient and restricted to haematological toxicity only (Table 2). The nadir for thrombocytes occurred at 4 weeks postinjection. A grade 2 thrombocytopenia was observed in 3 patients with a duration of 1-2 weeks. A grade 2 leukopenia was seen for 1 week in 2 patients and for 3 weeks in a third patient. All patients but one were hematologically eligible for a repeat treatment 6 weeks after therapy. Re-186 etidronate was repeated in 4 patients, of whom one has received 5 injections.

Conclusion: Re-186 etidronate gives a fast pain-relief with a mild toxicity in most patients with disseminated hormone refractory prostatic carcinoma.

PS-266

M. Tristram

Nuclear Medicine, Southampton University Hospitals NHS Trust, Southampton, United Kingdom

CONSENSUS AND CONTROVERSY IN DOSIMETRY FOR BIOLOGICALLY TARGETED THERAPIES

With development of new radiopharmaceuticals and growing use of radionuclides in cancer treatment, the demand for accurate dosimetric assessments increases. We have reviewed literature on methods of measurement and computational techniques relevant to targeted therapy dosimetry. This revealed a diversity of approaches, with biologic data obtained from different imaging modalities as well as clinical and *in vitro* studies, and conventional MIRD formalism augmented by, or replaced with, microdosimetry. The aim of this study was to summarise the concepts of *macro*- and *micro*dosimetry in the context of targeted therapy at a time when clinicians and physicists face the exigencies of new treatment regimes.

The need for improved precision in dosimetry is motivated by two factors. Firstly, in therapies which attempt cure, strategies involve administration of activities pushed to the limits of toxicity and assessment of doses to bone marrow and other dose limiting organs is essential. Techniques such as fluorescence *in situ* hybridisation (FISH) offer tools for retrospective biological dosimetry. Secondly, therapy agents labelled with short-range particle emitters targeted to micrometastases, require microdosimetry and the use of Monte Carlo simulations to calculate energy absorbed in individual clonogenic cells and subcellular targets. The demands of dosimetry are met by progress in scintigraphy, especially coincidence imaging, and in computer technology. Addition of microautoradiography data to clinically measured biokinetics makes realistic modelling of small-scale dosimetry possible, perhaps with application of fractal analysis as a method for the description of its complexity. These new developments will be discussed in the light of their impact on dosimetry.

Centres around the world report dosimetric results. In our extensive review of over a hundred published papers, we encountered controversy as well as consensus: these we submit for arbitration.

PS-267

I. Novak-Hofer, R. Waibel, M. Meli, F. Carrel, *H. Moch, #H. Amstutz, P.A. Schubiger
Center for Radiopharmaceutical Science, Paul Scherrer Institute, CH-5232 Villigen-PSI, *Institute for Pathology, University of Basel, CH-4003, Basel and #Central Laboratory of the Swiss Red Cross, Berne, Switzerland

ANTI NEUROBLASTOMA MAB chCE7 TARGETS A L1-CAM VARIANT PROTEIN WHICH IS ALSO EXPRESSED IN SOME RENAL TUMORS

The high affinity chimeric mAb chCE7 was developed originally as a targeting vehicle for neuroblastoma and 131I-chCE7 has shown excellent tumor uptake in patients with disseminated neuroblastoma. We have identified the target antigen for this mAb by biochemical purification from tumor cells using immunoaffinity chromatography with mAb chCE7. N-terminal peptide sequencing and partial cDNA cloning showed that the antigen is a form of the cell adhesion molecule L1-CAM, bearing a deletion of 5 amino acids close to the N-terminus, corresponding to exon 2. The same exon 2- deleted protein was partially purified from a renal carcinoma cell line which showed high levels of mAb chCE7 binding. When mRNA expression in renal cancer cells was investigated by Reverse Transcriptase Polymerase Chain Reaction (RT-PCR) methods using L1-CAM specific primers, the predominant transcripts were found to be specific for a form of L1 deleted in exon 2 and in exon 27. In contrast, neuroblastoma cells were found to contain the full length L1 transcripts in addition to the exon 2/27 deleted form. Subsequent Western blot analysis of a number of renal carcinoma cell lines revealed that 6 of the 7 tested cell lines expressed L1-CAM. The two embryonal renal cell lines tested showed high levels of expression, whereas normal adult kidney tissue reacted only very weakly with mAb chCE7. We have so far investigated 15 different renal tumor samples by Western blotting with mAb chCE7 and found that 5 tumors showed a strong reaction with mAb chCE7. It is planned to analyse a larger number of renal tumors in order to assess the clinical significance of L1 expression in renal tumors. Because genetic aberrations involving the Xq28 chromosomal region, where the L1-CAM gene is localized, were found in a significant portion of renal cancers a possible correlation between these genetic changes and the expression of L1-CAM will be investigated. The results obtained so far justify the further assessment of an application of radiolabeled mAb chCE7 in diagnosis/therapy of renal carcinomas.

PS-268

Z. Yao, M. Zhang, H. Sakahara, and J. Konishi.

Kyoto University Hospital, Department of Nuclear Medicine

IMPROVED SURVIVAL OF MICE WITH MALIGNANT ASCITES AFTER IN-111-AVIDIN RADIOTHERAPY.

We have shown that radiolabeled avidin targeted intraperitoneal (i.p.) tumors efficiently and reported preliminary radiotherapy results in tumor bearing mice with In-111-avidin. This study was undertaken to further investigate the efficacy of the radiotherapy method in improving the survival of tumor-bearing mice. Human tumor xenograft models, including an ovarian cancer, SHIN-3, a colon cancer, LS180, and a gastric cancer, MKN45, were established by i.p. injections of 5-10x10⁶ tumor cells in nude mice. The mice were randomly divided into therapy and control groups and there were 16 mice in each group. Avidin was labeled with In-111 through DTPA-biotin. Mice in therapy groups were i.p. injected twice with 11.1 and 9.25 MBq of In-111-avidin (100 μ g) at day 2 and 4, respectively, after i.p. injections of human cancer cells. Mice in control groups were injected with the same doses of unlabeled avidin. In the three tumors studied, average survival time of mice in therapy groups was significantly increased compared to that in control groups as shown below.

Average survival time (days)

	Control group	Therapy group	p-value
SHIN-3	41.06	53.25	< 0.025
MKN45	35.31	46.31	< 0.005
LS180	35.13	51.13	< 0.005

In conclusion, radiolabeled avidin is an effective treatment agent for malignant ascites. Metallic radionuclide with beta emitter would be more suitable for labeling avidin to treat tumors.

PS-269

L.Faris, G. Ziada, S. Yacoub : Dept. of Radiotherapy & Nuclear Medicine, Ain Shams University; Cairo, Egypt, and Dept. of Nuclear Medicine, Kuwait University, Kuwait .

EVALUATION OF EFFICACY AND TOXICITY OF Re-186 HEDP THERAPY OF METASTATIC BONE DISEASE.

Control of bone pain in patients with multiple skeletal metastases is a significant clinical problem. Palliative treatment of bone pain with less dependence on narcotics is crucial to improve the life quality of patients with cancer.

The objective of this prospective study was to assess the efficacy and toxicity of Re-186 HEDP in treating bone pain secondary to metastases.

Twenty six patients with bone pain from metastatic cancer were treated with 35 mCi of Re-186 HEDP administered intravenously in the outpatient clinic. Patients were followed with pain diaries, records of medication taken, mobility, sleep patterns, serial bone scans and a karnofsky index. Twenty five patients with complete records were evaluated. Patients were grouped according to the extent of bone metastases as seen on bone scans.

Sixteen patients (64%) showed clinical response of whom, 4 became completely pain free. Pain relief typically began 10 and 20 days after Re-186 HEDP administration, while maximum benefit was normally achieved by 6 weeks. Relief of pain was maintained for 4 to 15 months (mean 6 months). No immediate adverse reactions were observed following the administration of Re-186 HEDP. Only mild transient fall in platelet levels was noted which normalized by 6 weeks.

Rhenium-186 HEDP appears safe, convenient (outpatient use) and effective palliative treatment for pain secondary to bone metastases in cancer patients.

Oncology: Miscellaneous

PS-270

A. S. Arbab, K. Koizumi, M. A. Karim, T. Araki

Institute of Nuclear Medicine, Bangladesh. Yamanashi Medical University, Japan.

INVOLVEMENT OF SODIUM AND CALCIUM CHANNELS IN THE INFLUX AND EFFLUX OF Tc-99m-MIBI

Possible involvement of cell membrane ion transport systems in the uptake and extrusion of Tc-99m-MIBI was investigated using various buffers with or without Na⁺ and Ca⁺⁺, and ion transport inhibitors in a tumor cell line. The following ion transport modulators; dimethyl amiloride (DMA), verapamil, flunarazine, and monensin were used. The uptake of Tc-99m-MIBI was significantly increased in all buffers containing either Na⁺ or Ca⁺⁺ alone or none of them. There was significantly increased uptake of Tc-99m-MIBI especially in buffers without Na⁺. Verapamil, a L-type Ca⁺⁺ channel blocker, increased Tc-99m-MIBI uptake in all buffers. Flunarazine, which inhibits Ca⁺⁺/Na⁺ exchange, caused significantly increased accumulation of Tc-99m-MIBI only in buffer containing both Na⁺ and Ca⁺⁺. Monensin, a sodium ionophore, significantly increased uptake of Tc-99m-MIBI. DMA, a potent Na⁺/H⁺ antiport inhibitor, significantly inhibited the uptake of Tc-99m-MIBI in all buffers. In conclusion, Tc-99m-MIBI behaves like Na⁺ during its uptake and extrusion. Extrusion of Tc-99m-MIBI involves both L-type Ca⁺⁺ channel and Ca⁺⁺/Na⁺ exchange channel.

PS-271

E.V.Barysheva, A.M.Peters, Ju.E.Riannel, S.L.Stukanov, S.A.Velichko, M.Myers, V.V.Slastion, W.Yu.Usov. Tomsk Medical Research Centre, Tomsk, Russia and Hammersmith Hospital, London, UK

QUANTIFICATION OF BLOOD FLOW IN MUSCULOSCELETAL SARCOMAS FROM PATLAK ANALYSIS OF ^{99m}Tc - MIBI UPTAKE

Although ^{99m}Tc-MIBI has been well shown as radiopharmaceutical providing visualising of musculoskeletal sarcomas, quantitative analysis of ^{99m}Tc - MIBI uptake remains unemployed in clinical practice of oncology.

We analysed uptake kinetics of ^{99m}Tc-MIBI in bone sarcomas aiming to develop a technique for quantification of blood flow in the neoplasm. Assuming ^{99m}Tc-MIBI uptake to sarcoma unidirectional for early few minutes after injection, the equation can be applied: $dA / dt = K * C_h$, where A is radioactivity in sarcoma, C_h-blood concentration of ^{99m}Tc-MIBI, K - transport constant. The equation can be converted to classic Rutland-Patlak one when integrated and divided by C_h: $A/C_h = K * (\int C_h dt)/C_h + V_0$. Plotting $\{(\int C_h dt)/C_h\}$ as X, and (A/C_h) as Y, the K can be obtained as slope. K is neoplasm clearance constant equal to product (retention fraction) * (blood flow): $K = E * Flow$. Blood flow can be then calculated as ratio K/E.

Dynamic of ^{99m}Tc-MIBI uptake (after injection of 370-540 MBq as intravenous bolus) was acquired in 14 patients with osteoblastoclastoma (N=9), angiosarcoma (N=3) and rhabdomyosarcoma (N=2) synchronously with half-minute sampling of arterialised blood. Dynamic studies with ^{99m}Tc-human serum albumin were performed in ten subjects for subtraction of intravascular component and with ^{99m}Tc-MAA as standard marker of blood flow in seven. E was calculated from A(t) and C_h(t) time series as asymptote of ^{99m}Tc-MIBI retention function $h(t)=F^{-1}\{F[A(t)]/F[C_h(t)]\}$, where F is Fourier transforms, and corrected for intravascular component.

E values have shown acceptable uniformity over the groups varying from 0.49 up to 0.64 (mean 0.56 sd 0.06). The blood flow values varied from 8 ml/min/100 cm³ (rhabdomyosarcoma case) to 36 ml/min/100 cm³ (osteoblastoclastoma) and correlated well (r = 0.87, P < 0.01) with ^{99m}Tc-MAA uptake in the sarcomas.

Hence we conclude dynamic analysis of ^{99m}Tc-MIBI kinetics in sarcomas provides correct information on blood flow in the neoplasm and can be employed routinely in clinical studies and also in pharmacokinetic analysis.

PS-272

H. Bender, N. Bangard*, N. Metten, M. Bangard, C. Ponath, J. Mezger*, A. Schomburg, H-J. Biersack.

Depts. of Nuclear Medicine and *Internal Medicine, University Bonn, Germany

EARLY CHEMOTHERAPY OUTCOME PREDICTION WITH FDG-PET IN LIVER METASTASES OF COLORECTAL CARCINOMA..

Liver metastases of colorectal carcinoma (CRC) show a failure rate of around 70% following high-dose chemotherapy (CHx), which can not be established earlier than 3 month post CHx. The aim of this pilot study was to correlate acute and early changes of glucose metabolism in liver metastases following high-dose CHx with final therapy outcome.

In patients (n=10) with histologically confirmed, non-resectable liver metastases positron-emission tomography (PET) of the liver was performed prior and 48 hrs after the first infusion of high-dose 5-FU. Patients were followed up in 3-monthly intervals (physical examination, blood-tests, ultrasound and/or CT) and response was graded according to WHO-definitions. Emission scans of the liver were performed in fasted patients 45 min. after intravenous injection of 5-8 mCi F-18-Deoxyglucose (FDG) on an ECAT Exact 921/47 scanner (Siemens/CTI). Tomograms were reconstructed by filtered back-projection, corrected for measured-attenuation, and normalized for body-surface and injected dose in order to determine standard uptake values (SUV).

Sofar, n=8 pts. were evaluated (5 female, 3 male). In 5 pts. post CHx glucose-uptake decreased between 6-160%; 3 pts. showed an increased (>30%) glucose-uptake. Clinical follow up, revealed tumor remission (tumor volume reduction > 50%, >3 months) in 2 pts., both had decreased SUV >70%. In 4 pts., tumor progression was found, with 2 pt having a SUV-reduction of <10% and 3 pts.with an increase of >30%. One pt. had a short-term remission (<3 mo.) presenting with a SUV reduction of between 30-60%.

Our preliminary data suggest, that quantitative assessment of glucose-metabolism prior and early after one CHx cycle might be a sensitive indicator of therapy response, thus, allowing early identification of responders versus non-responders.

Poster presentations

PS-273

M. Cimitan, E. Borsatti, R. Ruffo, M. Tavio, D. Errante, M. Spina, G. Nasti, U. Tirelli

Centro di Riferimento Oncologico Aviano (IRCCS), Departments of Nuclear Medicine and AIDS Oncology, Aviano ITALY

COMBINED USE OF GALLIUM AND THALLIUM SCANS FOR DEFINITIVE DIAGNOSIS OF AIDS RELATED MALIGNANCIES

Although Gallium imaging may have high accuracy in the assessment of AIDS related diseases, especially in pulmonary pathogen evaluation, a more definitive diagnosis may be needed in those patients in which therapeutic response is poor. We tested the ability of Thallium scan associated with Gallium scan to improve the specificity of nuclear medicine in AIDS related pathology, including the detection of the exact malignancy, such as Kaposi Sarcoma (KS) and lymphoma, or infection.

28 HIV positive individuals with suspicion of malignancy were selected for nuclear medicine tests. Gallium and Thallium scans (planar and SPET) of the brain (4 cases), chest (21 cases) and abdomen (8 cases) were performed using a Sophycamera DSX by injecting 185-320 Mbq of ⁶⁷Ga citrate and 90-130 Mbq of ²⁰¹Tl chloride. Scan interpretation was made on the basis of previous reports and the results of nuclear medicine tests were correlated to CT or MRI, as well as to clinical data (bronchoscopy/mediastinoscopy, brain biopsy or cerebral liquor analysis). We found 11 cases with KS, 8 with lymphomas, 8 with infections and 1 with lung adenocarcinoma. In one patient KS and lymphoma co-occurred, in another one lymphoma was associated with mycobacterial infection. Almost all patients (91%) with KS and 60 % of patients with lymphoma had positive Thallium scan. However, no patient with KS but 70% of patients with lymphomas had positive Gallium scans. The primary lung tumour showed both Thallium and Gallium uptake.

Almost all infections (87%) showed Gallium uptake but 37% of them (mycobacterial infections) had Thallium uptake too.

The positive predictive value (TP/TP+FP) of ²⁰¹Tl positive scan associated with ⁶⁷Ga negative scan for KS was high (92%), whereas that of ²⁰¹Tl positive scan associated with ⁶⁷Ga positive scan for lymphoma was 55% and that of ²⁰¹Tl negative scan associated with ⁶⁷Ga positive scan for infections was 66%.

Dual isotope imaging with Thallium/Gallium may play a role in the definitive diagnosis of AIDS related pathology, showing high specificity to distinguish KS from lymphoma or infection and providing sufficient justification for initiating therapy.

PS-274

P. Colarinha, O. Almeida, A. Fernandes, M.Ferreira, M. Sousinha, P.Oliveira, L. Salgado, M.R.Vieira
Instituto Português de Oncologia, Lisboa, Portugal

ROLE OF THALLIUM-201 IN THE EVALUATION OF THE THERAPEUTIC RESPONSE IN BONE SARCOMAS

Objective: A research was undertaken to evaluate serial Tl-201 scintigraphy in assessing the effectiveness of neoadjuvant chemotherapy in bone sarcomas.

Methods: in 22 bone sarcoma cases, serial Tl-201 scintigraphy was prospectively performed and evaluated with a quantitative based method and a visual systematic analysis.

All pts were treated with chemotherapy and in 19 pts tumour surgery was also performed. For all surgical specimens a slab section of the entire tumor was evaluated. The criterion for a good histologic response to neoadjuvant chemotherapy was a tumor necrosis greater than 95%. Each patient underwent a Tl-201 scan both before and after completion of neoadjuvant chemotherapy.

Tl-201 scintigraphy was performed 5 min. after iv injection of 74-111MBq of Tl-201. Planar images were acquired with a preset time of 10 min. .

Tumour-to-normal tissue Tl-201 uptake ratio (T/N) was calculated in all scintigraphy. Tumour Tl-201 uptake was also visually analysed and classified according to the tumour uptake pattern on pre and posttreatment evaluations.

Results: all pts showed tumour Tl-201 uptake, however two groups of pts were found when histologic response was considered. Group 1- (good histologic response) - 4 pts showed a T/N ratio decrease and a presurgery tumour uptake pattern transformation. Group 2 - (poor histologic response) - 15 pts, where 5 pts showed an increase of the T/N ratio and 10 pts showed a decrease of the T/N ratio, but in all 15 pts the tumour uptake pattern did not change.

Conclusion: these data suggest that Tl-201 scintigraphy was able to identify the sort of histological response to neoadjuvant chemotherapy. A T/N ratio decrease associated to a tumour uptake pattern transformation was the best criterion to predict bone sarcoma response to chemotherapy.

PS-275

Fjälling M, Ekman M, Mattsson J.

Hospital: Sahlgrenska University Hospital, Department of Nuclear Medicine, Göteborg, Sweden.

ASSESSMENT OF LEAKAGE DURING SELECTIVE LIMB PERFUSION IN MELANOMA PATIENTS USING A PORTABLE GAMMA DETECTOR SYSTEM AND COMPARISON WITH BLOOD SAMPLING.

Metastases to a limb from malignant melanoma can be treated by adding drugs to the perfused limb during hyperthermal perfusion. Using ^{99m}Tc RBC or ^{99m}Tc HSA minimal leakage has been reported when analysing blood samples from the body circulation or when measuring radioactivity over the heart. In order to measure the leakage more adequately, a gamma detector system with online registration of radioactivity (as well as temperature and blood flow) was used and compared with the radioactivity of blood samples from the perfused limb and the body circulation.

METHOD: ^{99m}TcRBC was added to the perfusion fluid of 10 patients and ^{99m}TcHSA (Albures) to that of 10. A computerised gamma detector probe for continuous registration of radioactivity was used and data was stored for later analysis. The probe was placed over the limb and radioactivity was continuously registered during the entire perfusion period. Blood samples were collected at regular intervals from the perfused limb and the body circulation.

RESULTS: The measurements showed leakage of ^{99m}Tc RBC from the limb to the body circulation, which was confirmed by analysis of the blood samples. After 60 min an equilibrium was reached with a steady state between the concentration of radioactivity of the two systems. RBCs leak into the body circulation via collaterals, which may also serve as a route of leakage of drugs added to the perfusion fluid. When using ^{99m}Tc albures there was a continuous decrease of concentration of radioactivity in the limb without a corresponding increase in the body circulation. Instead radioactivity was accumulated in the liver confirmed by gamma camera imaging.

CONCLUSION: Our results indicate a gradual leakage from the perfused limb to the main circulatory system until equilibrium between the two systems is reached. A high concentration gradient between the perfusion fluid and body circulation can be expected only to exist initially.

PS-276

U. Haberkorn, K. Khazaie, I. Morr, A. Altmann, M. Müller, G. van Kaick.

German Cancer Research Center (dkfz), Heidelberg, Germany.

GANCICLOVIR UPTAKE IN HSV- THYMIDINE-KINASE EXPRESSING HUMAN MAMMARY CARCINOMA CELLS.

Assessment of suicide enzyme activity would have considerable impact on the planning and the individualization of suicide gene therapy of malignant tumors. This may be done by determining the pharmacokinetics of specific substrates. We generated ganciclovir (GCV) sensitive human mammary carcinoma (MCF7) cell lines after transfection with a retroviral vector bearing the Herpes Simplex Virus thymidine kinase (HSV-tk) gene. Thereafter uptake measurements and HPLC analyses were performed up to 48 hours in a HSV-tk-expressing cell line and in a wild type cell line using tritiated GCV. Furthermore bystander experiments and inhibition/competition studies for ganciclovir transport were done. HSV-tk-expressing cells showed higher GCV uptake and phosphorylation than control cells, whereas in wild type MCF7 cells no phosphorylated GCV was detected. In bystander experiments the total GCV uptake was related to the amount of HSV-tk expressing cells. Furthermore, the uptake of GCV correlated closely with the growth inhibition (r=0.92). Therefore, the accumulation of specific substrates may serve as an indicator of the HSV-tk activity and of therapy outcome. Inhibition and competition experiments demonstrated slow transport of GCV by the nucleoside carriers. The slow uptake and low affinity to HSV-tk indicate that GCV is not an ideal substrate for the nucleoside transport systems or for the HSV thymidine kinase. This may be the limiting factor for therapy success as well as for radionuclide imaging, necessitating the search for better substrates of HSV-tk.

PS-277

C. Germann, A.F. Shields, J. R. Grierson, U. Haberkorn.

German Cancer Research Center, Heidelberg, Germany. Harper Hospital Detroit and Dept. of Med. and Radiology, Univ. of Washington, Seattle, USA.

IN VITRO STUDIES OF FFUDR UPTAKE IN HSV- THYMIDINE-KINASE EXPRESSING MORRIS-HEPATOMA CELLS.

The planning and individualization of gene therapy with suicide genes as Herpes Simplex Virus thymidine kinase (HSV-tk) necessitates the assessment of the enzyme activity induced in the tumor. This can be done by uptake measurements of specific substrates for HSV-tk. Due to its molecular structure 5-Fluoro-1-(2'-deoxy--fluoro-β-D-ribofuranosyl)uracil (FFUDR) may be a substrate not only of human thymidine kinase, but also of Herpes Simplex Virus thymidine kinase. Using a HSV-tk-expressing rat hepatoma cell line (MH3924A) and a control cell line (bearing the empty vector) the uptake of ³H-FFUDR was determined after different incubation periods. Furthermore measurements with different mixtures of HSV-tk-expressing cells and control cells were done and compared to the growth inhibition after a 72 h and 96 h incubation period with 5 μM ganciclovir. To elucidate the transport mechanism of FFUDR inhibition/competition experiments with different inhibitors or competitors for the nucleoside and the nucleobase transport systems were performed. Uptake studies with tritiated FFUDR revealed a higher accumulation in the HSV-tk-expressing cell line than in the control cell line. The FFUDR uptake was 3-4-fold higher than the ganciclovir uptake in these cells. Furthermore the FFUDR accumulation was dependent on the amount of HSV-tk-expressing cells. FFUDR uptake and growth inhibition were highly correlated with $r = 0.96$. Inhibition/competition experiments showed that FFUDR is transported mainly by the equilibrative and the concentrative nucleoside transporter but not by the nucleobase transport systems. FFUDR is a promising radiotracer for the measurement of HSV-tk activity during gene therapy of malignant tumors.

PS-278

J. Heřmanská, J. Zimák, M. Kárný*, L. Jirsa*, K. Vořmíková

Clinic of Nuclear Medicine, Faculty Hospital Motol V úvalu 84, 150 06 Prague 5, Czech Republic
*Inst. of Information Theory and Automation, AV ČR
POB 18, 182 08 Prague 8, Czech Republic, school@utia.cas.cz

JODNEW SUPPORTS TREATMENT OF THYROID DISEASES

A novel in-house developed software system JODNEW is tested in our Clinic. It aims at:

- increasing quality of raw biophysical data exploited in diagnosis and therapy of thyroid diseases by ¹³¹I;
- exploiting all relevant information contained in data;
- estimating cumulated activity so that MIRD methodology can be safely used for dose evaluation;
- decreasing working load on staff.

JODNEW is an extensive data-base system cooperating with advanced data-processing algorithms coded in C-language. The algorithms provide Bayesian estimates of:

- weak signals on a strong background;
- mass of thyroid gland using palpation, sonographic and scintigraphic measurements;
- calibration factors (with a test on its invariance);
- accumulated activities and effective half-lives;
- rates of the activity elimination by urine;
- compound biophysical quantities like specific irradiation of blood.

The adopted Bayesian methodology allows us to exploit expert knowledge, models of observed processes and data in a consistent and efficient way. It is important in the considered case when the number of measurements is quite limited and influence of biological and physical variations high. Moreover, all resulting estimates are qualified by the remaining uncertainty. It was demonstrated on thousands of available patient records that the advanced data processing led to significant improvement of the estimates found. For instance, just physically meaningful estimates of effective half-life are found and the precision increased by 15-30%. The system is outlined in the contribution. The gained experience with JODNEW, problems encountered and development perspectives are discussed.

PS-279

M. Hosono, M. N. Hosono, F. Kraeber-Bodéré, A. Devys, P. Thédréz, A. Faivre-Chauvet, K. Machida, E. Gautherot, J. Barbet, and J.F. Chatal. Saitama Medical Center, Saitama, Japan, INSERM Research Unit 463, Nantes, Immunotech SA, Marseille, France

LOCALIZATION OF SMALL-CELL LUNG CANCER XENOGRFT BY TWO-STEP METHOD WITH BISPECIFIC ANTIBODY AND BIVALENT HAPTEN

Two-step immunoscintigraphy using bispecific antibody (BsAb) and radiolabeled bivalent DTPA-indium hapten was previously reported to be useful for CEA-expressing tumors. The purpose of this study was to evaluate the efficacy of this method for targeting human small-cell lung cancer (SCLC) using histamine hapten in place of DTPA-indium hapten. Anti-neural cell adhesion molecule (NCAM)/anti-histamine BsAb NK1NBL1-679 were prepared by coupling an equimolecular quantity of a Fab' fragment of NK1NBL1 to a Fab fragment of anti-histamine 679 activated beforehand by o-phenylene-dimaleimide. Athymic mice inoculated s.c. with NCI-H69 SCLC cells expressing NCAM were administered with BsAb, and then 48 hr later, with I-125-labeled histamine hapten. I-125-labeled intact NK1NBL1 was injected into other groups of mice. Biodistributions were examined at 5, 30 min, 5, 24, 48, and 96 hr for the two-step method, and 1, 5, 24, 48, and 96 hr for the one-step method. In mice of the two-step targeting, tumor uptake was 2.5 ± 0.2 , 3.2 ± 0.4 , 6.3 ± 2.0 , 7.2 ± 2.7 , 6.1 ± 2.1 , 2.2 ± 0.4 %ID/g at 5, 30 min, 5, 24, 48, and 96 hr and tumor-to-blood, -to-liver, -to-kidney ratios were 1.4 ± 1.1 , 10.8 ± 13.2 and 4.6 ± 4.7 at 5 hr, whereas I-125-labeled NK1NBL1 showed a tumor uptake of 5.7 ± 0.4 %ID/g and tumor-to-blood, -to-liver, -to-kidney ratios of 0.3 ± 0.1 , 1.1 ± 0.2 and 0.9 ± 0.1 at 5 hr. Thus, high tumor accumulation and good tumor-to-normal tissue ratios were achieved as early as at 5 hr by the two-step technique. These results were confirmed by autoradiographic studies demonstrating clear tumor-to-normal tissue contrast. In conclusion, this two-step targeting seems very potent for the diagnosis and therapy of SCLC as it combines high tumor uptake and low normal tissue background.

PS-280

S. Kanayev, S. Novikov, L. Jukova.

Research Institute of Oncology, Department of Radiation Oncology and Nuclear Medicine, 189646, Pesocny-2, St.-Petersburg, Russia.

ROLE OF NUCLEAR MEDICINE IN RADIOTHERAPY PLANNING IN PATIENTS WITH HODGKIN'S DISEASE.

PURPOSE: Bone marrow (BMS), lymph-node (LNS) and spleen (SS) scintigraphy are not routinely used in patients (pts) with Hodgkin's disease (HD). In this presentation we evaluate our experience in terms of contribution of each modality to treatment decision (CTD).

METHODS: Three separate groups of pts with HD were analysed: 49 HD pts of the 1-st group had BMS after the end of routine staging and "primary" planning of therapy strategy. Changes in the extent and/or shape of radiation fields (RF) were considered as CTD. Lumbar and iliac-inguinal LNS was performed after abdominal X-ray CT examination in 32 HD pts of the 2-nd group. All cases of normal CT and subsequent abnormal LNS were considered as CTD. Verification of "spleen field" designed during conventional (without contrast material i/v injection) simulation procedure was made by SS in 13 patients of the 3-rd group. All changes in the shape of RF were considered as CTD.

RESULTS: 1-st group. BMS results influenced strategy of radiotherapy in 8 pts: shape of RF was modified in 3, their extent - in 2 cases. Multifocal BM invasion was the reason for radiotherapy reduction in 3 pts. 2-nd group. 3 pts with normal CT had abnormal LNS (in all cases RF were extended in order to irradiate all regions suspected for involvement by HD). In 26 cases results of both CT and LNS were similar: in 20 - normal, in 6 - abnormal. 3 pts with normal LNS had abnormal CT. 3-rd group. Spleen borders on SS were covered by simulated radiation portals in 7 pts, but in 3 of them radiation volume was reduced after SS. In another 6 cases RF shape was changed after SS because part of spleen image was outside of simulated portals. SS resulted in minor CTD in 23% and significant CTD - in 46% of pts.

CONCLUSION: BMS influenced treatment decision in 16%, LNS - in 9% and SS - in 69 % of evaluated pts with HD.

Poster presentations

PS-281

M.Kotb¹, R.A Valdés Olmos², S. El-Badawy³, K. El-Ghamrawy⁴, H. Farag¹, C.A. Hoefnagel² and H.K. Awwad³.

¹Nuclear Medicine Unit, National Cancer Institute, Fom El-Khalig, Cairo, Egypt, ²Nuclear Medicine Department, Netherlands Cancer Institute, ³Radiotherapy Department, National Cancer Institute, Kasr El-Eini Centre for Oncology and Nuclear Medicine.

THE USE OF GALLIUM-67-CITRATE, THALLIUM-201 CHLORIDE AND Tc-99m SESTAMIBI SCINTISCANNING TO PROBE CHEMORESISTANCE IN MALIGNANT LYMPHOMAS.

Background. Overexpression of P-glycoprotein (P-gp) may be associated with both multidrug resistance (MDR) and suppression of tumour Tc-99m Sestamibi uptake while not influencing Ga-67 or Tl-201 uptake.

Objective. Testing whether a negative pretreatment Tc-99m Sestamibi uptake together with positive Ga-67 and Tl-201 could predict chemoresistance in non-Hodgkin's lymphomas (NHL) and Hodgkin's disease (HD).

Material and Methods. Thirty-five (12 HD, 23 NHL) patients with nodal and extranodal tumour localizations already detected by clinicoradiological procedures were included. Pretreatment evaluation included scintiscanning. Patients were treated with combination chemotherapy and radiotherapy. Response was assessed after 3 courses, end of treatment and 22-30 months later.

Results. Six NHL patients had negative pretreatment Tc-99m Sestamibi together with positive Ga-67 and Tl-201 scans. All failed to show a complete remission (CR) either during the midtreatment or post-treatment periods. In contrast, all NHL patients having a positive pretreatment scans entered a CR and remained disease-free throughout the observation period. The predictive capacity of pretreatment Tc-99m Sestamibi scans with respect to MDR was less remarkable in patients with HD.

Conclusion. A negative pre-treatment Tc-99m Sestamibi uptake together with positive Ga-67 and Tl-201 scans seem to be a good probe for chemoresistance in NHL.

PS-282

T. Krause, M. Reinhardt, E. Nitzsche, E. Moser

Departm.: Universitätsklinik Freiburg, Department of Nuclear medicine;

BONE MARROW SCINTIGRAPHY WITH Tc-99m ANTI-NCA-95. IS THERE A RELEVANT INFLUENCE OF BENIGNE LESIONS ON THE INTERPRETATION OF BONE MARROW INFILTRATIONS IN MALIGNANT TUMOURS?

There are several reports stressing the specificity of detection of bone marrow (BM) metastases by using immunoscintigraphy (IS) for BM imaging.

Thus, in a retrospective study IS of 141 consecutive patients with fever of unknown origin and without tumour disease were evaluated. IS was acquired 5 hrs. after i.v. injection of Tc-99m anti-NCA-95.

IS showed defects in 16 patients (11%). With help of the typical scintigraphic defect pattern, in 4 pat. the cause of the lesions was identified to be due to degenerative changes and in 1 patients due to previous sternotomy. There was an increasing frequency of defects starting from 50-59 years in 10% of the patients, 60-69 years in 9%, to 70-79 years in 30%, and 80-89 years in 33% of the pat. IS was not hampered by tracer uptake to liver or spleen in 93 pat. In 48 pat. with intense tracer uptake to the spleen left caudal ribs were obscured. Patchy tracer uptake to the bone marrow of the limbs was found in 13/62 pat. with BM expansion in the lower limbs and 14/55 with BM expansion in the upper limbs.

Conclusion: The present study reveal that photopenic lesions of the BM by using Tc-99m NCA-95 are rarely seen in patients without known malignant disease. The occurrence of benign lesions is age related. In about 50% of the cases the benign cause of the lesion was obvious from location and pattern of the lesion or from case history. Evaluation of lesions in upper and lower limbs may be hindered due to physiologic variation of marrow distribution. Nevertheless, IS appears to be well suited for the detection and localization of bone marrow metastases.

PS-283

R. Lebtahi, A. Meulemans, K. Farahat, D. Daou, L. Sarda, M. Faraggi, G. Cadiot, M. Mignon, D. Le Guludec, Hôpital Bichat, Paris, France.

VALUE OF A NEW IMMUNO-ASSAY OF CHROMOGRANIN A IN PATIENTS WITH GASTROENTEROPANCREATIC ENDOCRINE TUMORS.

Serum levels of specific and/or non specific peptide tumors markers is useful for the diagnosis and follow-up in patients with endocrine tumors. Recently, the use of Chromogranin A (Cg A) level has been reported as a marker. We evaluated, a new immunoradiometric sandwich assay using 2 monoclonal antibodies whose epitopes are localized in the median part of the protein and are unfrequently affected by proteolysis. These monoclonal antibodies are likely to bind the majority of the circulating intact and degraded forms of Cg A. Forty-two patients with gastro-entero-pancreatic tumors were investigated: 29 with Zollinger Ellison Syndrome (ZES), 6 with carcinoid tumors and 7 with other endocrine pancreatic tumors, including 4 with non functioning tumors. Normal serum levels values were defined in 100 normal individuals: 36 ± 18 ng/ml, range 10 to 100 ng/ml., cut off > 100ng/ml. Chromogranin A levels were increased in 31 out of 42 (74%) patients, including 3 out of 4 patients with non functioning tumors and in 25 out of 29 (86%) patients with ZES. In patients with ZES, no correlation was found between Cg A and gastrin levels ($r=0.32$, $p=0.13$).

Serum Cg A levels are increased in 74% of patients with gastro-entero-pancreatic tumors. Chromogranin A level does not correlated to gastrin level in patients with ZES. These preliminary results suggest that serum Cg A assay may be interesting as a new distinct marker in the diagnosis and/or follow up of patients with gastroenteropancreatic endocrine tumors.

PS-284

J. Lemberger, M. Takacs-Kucsera, M. Bogar, D. Štrbac and I. Csernetics

General Hospital, Medical Centre, Depts of Nuclear Medicine, Oncology and Surgery, Subotica, Yugoslavia
GROWTH RATE OF THE COLORECTAL TUMORS MEASURED BY CIRCULATING CEA

In this study we investigated the growth rate of resected colorectal cancer using two dynamic concepts: marker production doubling time (MPDT) and doubling time (DT) of CEA. Sequential CEA determinations were performed by IRMA (approximately at 3 months intervals) in 26 patients with metastatic carcinoma of colon and rectum: in group of 7 patients who received no therapy and in 19 patients who underwent various modalities of oncologic treatments. MPDT and DT were calculated for the same period of time taking into account the exponential increase of serum CEA in at least 3 successive times. No significant difference was found either MPDT or DT between both groups, indicating no response to treatment. In all patients MPDTs and DTs ranged (with 95% confidence) within 33-68 days and 45-66 days, respectively. No correlation was found between MPDT and DT. Evaluating the results by inverse distribution function it was established that MPDT and DT are distinct parameters. Comparing of MPDT with survival after initial CEA increase showed that patients with MPDT > 100 days have longer time of survival than those with MPDT < 20 days. In conclusion, MPDT appeared to be more precise measure than DT of the tumor growth rate.

PS-285

R.S. Liu, C.P.Chang, L.C. Wu, J.K. Wang, S.Q. Liao, L.S. Lee, F.Q.H. Ngo, and S.H. Yeh.

Taipei Veterans General Hospital, National PET/Cyclotron Center, and National Yang-Ming University School of Medicine, Taipei, Taiwan.

COMPARISON OF CARBON-11-ACETATE AND CARBON-11-METHIONINE IN BRAIN TUMOR.

This study evaluated the effectiveness of [C-11]-acetate (ACE) as tumor-detecting tracers in positron emission tomographic (PET) study of brain tumor and compared the tumor uptake of ACE and [C-11]-methionine (MET).

Five male and nine female patients with 16 brain tumors were studied. Five patients had glioma of various grade, four had meningioma, three had metastatic brain tumors, and two had Schwannoma. All tumors were histologically verified. ACE-PET and MET-PET imagings were carried out for all cases in alternative days. Following injection of 370 MBq (10 mCi) of MET, serial scans were collected for a period of 30 min. Dynamic PET imaging was acquired after intravenous injection of 370 MBq (10 mCi) of ACE for a period of 16 min. Tomographic images obtained from the above procedures were analysed. Tumor uptake of ACE and MET was measured using the standard uptake value corrected by body surface (SUVs):

$$SUVs = \frac{\text{Tracer concentration (KBq/ml)}}{[\text{Injected dose (KBq)/Body surface (m}^2\text{)]}}$$

The ROI with the maximum average tracer concentration on the tumor, corrected for calibration and decay, was chosen for the SUVs analysis. All 16 brain tumors (12 primary, 4 metastases) were detectable by ACE and MET-PET. Distribution of ACE and MET in the tumor was almost identical, except for 2 tumors of which a little discrepancy was noted. SUVs (mean ± 1 s.d.) of ACE in the brain tumors were 1.32 ± 0.51 and of MET were 1.33 ± 0.49. No significant difference was found between tumoral uptakes of ACE and MET (p>0.5). A good correlation was found between SUVs of the two tracers (r=0.91, p<0.0001).

In conclusion, both ACE and MET are effective in PET imaging of brain tumor, and the uptake of the tracers seems to be closely related.

PS-286

A. Llamas Olier, A. De Los Reyes, MC. Martínez, G. Terselich, A. Suárez.

Instituto Nacional de Cancerología. Departments of Nuclear Medicine and Pediatric Oncology. Santafé de Bogotá. Colombia.

TECHNETIUM-99m TETROFOSMIN UPTAKE IN OSTEOGENIC SARCOMAS PREDICTS THERAPEUTIC RESPONSE AND CLINICAL OUTCOME.

OBJECTIVES: Tumor uptake of thallium-201 and Tc-99m-sestamibi has been shown to correlate with the histologic response of osteosarcomas (OS) to neoadjuvant chemotherapy. This study was undertaken to evaluate the efficacy of Tc-99m-tetrofosmin (Tfos) in assessing tumor response to preoperative chemotherapy (preop-CTx) and to predict survival in patients (pts) with high grade OS of the lower extremities. **METHODS:** 19 pts with biopsy-proven OS underwent Tfos imaging before and after preop-CTx. Average pixel counts taken over the tumor, divided by those taken from its normal counterpart, yielded a T/NT ratio. The preop T/NT ratio was correlated with the percentage of tumor necrosis (%TN) and with the patients' outcome. **RESULTS:** A preop T/NT ratio ≤ 1.5 was obtained in 13/19 pts, 8 of whom had a favorable tumor response (%TN ≥ 90%). Only one of the remaining 5 died, and he did so from unrelated causes, whilst the rest are still alive and free from disease after a mean follow-up period of 25 months, although one had a successfully resected lung recurrence. All pts with pulmonary metastases at diagnosis (n=5/19) died within a mean follow-up period of 11.5 months, despite the fact that 2 of them had a preop T/NT < 1.5 and %TN ≥ 90%. All 6/19 pts with a preop T/NT > 1.5 also had a %TN < 90%. They all died within a mean follow-up period of 15.7 months. **CONCLUSIONS:** Our results suggest that tumor uptake of Tfos in high grade OS, is capable of predicting survival preoperatively, regardless of the histologically determined tumor response to preop-CTx, given that no distant metastases are found at diagnosis.

PS-287

L.Maffioli, G.F.Gallino, A.Gerali, F.Belli, E.Seregni, M.R.Castellani,

M.Testoni, M.Greco, E.Bombardieri

Nuclear Medicine and Surgical Oncology "B" Divisions
Istituto nazionale per lo studio e la cura dei tumori, Milano - ITALY
**SENTINEL NODE LYMPHOSCINTIGRAPHY
IN PATIENTS WITH CUTANEOUS MELANOMA.**

Introduction: Sentinel node (SN) biopsy allows selective lymphadenectomy, sparing node-negative patients the morbidity and cost of the procedure. We evaluated the routine use of lymphoscintigraphy in the detection of the SN in patients with cutaneous melanoma.

Methods: The day before surgery, 43 patients underwent lymphoscintigraphy by means of 4 intradermal injections for a total of 40 MBq of Tc-99m microcolloid (Albu-res) around the lesion. Dynamic acquisition of 5 frames of 5 minutes was started immediately to visualize the lymphatic drainage. In some cases a flood source of Co-67 was used for simultaneous transmission imaging to facilitate orientation. A mark was drawn on the skin in correspondence with the sentinel node.

Results: The lymphoscintigraphic results were compared with those obtained in 121 patients operated on without lymphoscintigraphy. Hence a total of 164 patients were included in the study. In the group without LSG 22 SNs were missed (9 axillary, 11 inguinal and 2 atypical regions). In the group with LSG, the SN was identified in all patients but two. In 5 cases we found two SNs per patient: in 2 pts the SNs were located in both axillae, in 2 pts in the groins, and in 1 pt. in axilla and homolateral groin.

SN identification	Axillary	Inguinal	Others
without lymphoscintigraphy	30/39 (77%)	67/78 (86%)	2/4
with lymphoscintigraphy	18/19 (95%)	21/22 (95%)	2/2

Conclusions: LSG is a simple and feasible method that simplifies the surgical procedure. Its main usefulness seems to be in the recognition of the real lymphatic drainage to the axilla. In these cases, SN was identified in 95% of cases with vs. 77% without LSG.

PS-288

L Mansi*, PF Rambaldi*, F Masone*, N Panza°, M Sacco°, S Ialuna*, M Maccauro*.

*Ist Radiol Sciences, II Univ Naples.

°Cardarelli Hosp, Naples.

MIBI IN MULTINODULAR GOITER PATIENTS PRESENTING A TYPE II/III LAGALLA PATTERN AT ULTRASOUNDS: PREDICTIVE VALUE FOR NEOPLASMS.

14 pts (3M/11F, age 35-65 yrs) with multinodular goiter displaying cold nodules at thyroid scan and Lagalla (L) type II and/or III patterns at Echocolor Doppler (ECD) were included into the study. Scans were performed 10 minutes and 2 hrs after i.v. injection of 555 MBq of MIBI. Circular ROI were drawn on the nodule (N), normal thyroid (T) and background (B). N/T, N/B, T/B ratios were obtained at 10 min and 2 hours and a percent wash-out (W) was calculated. All pts underwent surgery and data were compared to histological findings. N/T ratio (1.2±0.59) and W (61.4±26.17) were significantly different (P<0.05) in 5 pts with thyroid neoplasms (follicular adenoma or thyroid carcinoma) compared to 9 pts with colloidocystic goiter (0.79±0.44 and 45±20.38). This preliminary report suggests the possible predictive role for neoplasms of MIBI dual phase scintigraphy in pts with multinodular goiter presenting Lagalla type II/III pattern at ECD.

Poster presentations

PS-289

C. Marí, LL. Bernà, P. Serret, LL. Puig, A. Flotats, JC Martín, M. Estorch, A. Catafau, I. Carrió.
Hospital Sant Pau, Barcelona. Spain. Department of Nuclear Medicine

ACCURATE STAGING AND LOWER MORBIDITY FOR THE PATIENT IS PROVIDED WITH SENTINEL LYMPH NODE BIOPSY IN MELANOMA

Aim: To assess the utility of sentinel lymph node biopsy in providing accurate staging of the melanoma and a lower morbidity for the patient.

Methods: Over a 1-year period, 13 patients with skin melanomas (Clark III-IV, Breslow 2-9mm) located in different places were studied twenty-four hours prior to surgery. One mCi of sulfur ^{99m}Tc(Re)colloid was intradermally injected around the site of the primary melanomas. Once the first draining lymph node (sentinel node) was identified, it was selectively removed with minimal dissection and histologically studied. In patients with evidence of metastases in sentinel nodes a regional lymphadenectomy was performed.

Results: Surgeon successfully resected the radiolabeled sentinel lymph nodes in all patients. Regional lymphadenectomy was performed in the 2 patients who showed evidence of metastases in the sentinel node. To this point, no patient has developed regional disease (maximum follow up one year).

Conclusion: Sentinel lymph node biopsy provides accurate staging of the melanoma and a lower morbidity for the patient.

PS-290

T. Mochizuki, Y. Karube, K.E. Baidoo, H.N. Wagner, Jr.
Division of Nuclear Medicine and Radiation Health Sciences, The Johns Hopkins Medical Institutions

^{99m}Tc SESTAMIBI UPTAKE IN SUBCLONES OF HUMAN CANCER CELL LINES RESISTANT TO DIFFERENT CHEMOTHERAPEUTIC DRUGS

The expression of the transmembrane P-glycoprotein (Pgp) pump in cancer cells plays an important role in the resistance of many tumors to chemotherapeutic drugs. The purpose of this study was to examine the accumulation of the Pgp substrate, ^{99m}Tc sestamibi, in human uterine sarcoma cell lines known to be resistant to different chemotherapeutic drugs. Three cell lines investigated in this study were: the wild type MES-SA (SA) which is susceptible to both doxorubicin and mitoxantrone (used as control), and two drug resistant subclones MES-SA/DX (DX) and MES-SA/MX (MX) which are resistant to doxorubicin and mitoxantrone respectively. The accumulation of ^{99m}Tc sestamibi in SA, DX and MX cells was studied as a function of time in cell suspensions (10⁶ cells) at 37 °C in the presence or absence of verapamil, the potent modulator of Pgp. At 2 hr incubation without verapamil, there was statistical significance (p < 0.01) between the uptake of SA [2.60 ± 0.10 %dose/10⁶ cells (mean ± SD)] and resistant cells [DX (1.15 ± 0.09) or MX (0.39 ± 0.03)]. There was also statistical significance (p < 0.01) between the uptake of DX and MX. Thus there was a marked reduction in the retention of ^{99m}Tc sestamibi in drug resistant clones of human uterine sarcoma in the absence of the modulator verapamil. In the presence of 100 mM verapamil, the ratio of the uptake of ^{99m}Tc sestamibi in the cells incubated with verapamil to cells incubated without verapamil were 1.73, 3.17 and 6.69 for SA, DX and MX cells respectively. Therefore, verapamil caused a greater increase in the uptake of sestamibi in the resistant cells than in the wild type. These results show that it may be possible to use ^{99m}Tc sestamibi imaging in this tumor type to predict response to chemotherapeutic drugs.

PS-291

N.Prévôt, J.P.Vuillez*, D.Marti-Battle*, J.P.Mathieu*, F.Dubois, M.Comet*.

Hospital: Departement of Nuclear Medicine
CHU Saint Etienne, CHU Grenoble* FRANCE

INFLUENCE OF GLUCOSE IN THE UPTAKE OF MIBI-Tc-99m BY TUMOR CELLS.

Introduction:

We wanted to study the relation between glucose metabolism of tumor cells and MIBI-Tc-99m captation. Is there a relation between this métabolism and mitochondrial and plasma membrane potentials ?

Material and methods

We have studied the uptake of MIBI-Tc-99m on a human ovarian tumor cell line (IGROV1) and evaluated the influence of a strong extracellular concentration of glucose (5mM = control, 35 mM, 70 mM, 100 mM).

We have first of all characterized our cellular model (uptake kinetics reached a plateau by 120 min with a half-life of 60 min) and verified that our methodology was correct by having agreement results with the literature (uptake of MIBI-Tc-99m determined by both mitochondrial and plasma membrane potentials).

Results

The intensity of the cellular uptake of MIBI-Tc-99m increases linear manner with the extracellular concentration of glucose, without modifying the uptake kinetics. We used a high K⁺ buffer (130 mM) and Valinomycine (1 µg/mL), to show that intensity of the uptake was linked to an increase of the plasma membrane potential (stability of the mitochondrial membrane potential).

Conclusion

These results support the hypothesis that a relationship could exist between the cellular uptake of MIBI-Tc-99m (illustration of plasma membrane potential) and the cell glycolysis activity.

PS-292

F. Chehne, M. Rodrigues, P. Berghammer, G. Karanikas, H. Sinzinger

University Hospital, Departments of Nuclear Medicine and Oncology, Vienna, Austria

COMPARISON OF UPTAKE OF ^{99m}Tc-TETROFOSMIN AND ^{99m}Tc-FURIFOSMIN INTO TUMOR CELL LINES.

^{99m}Tc-tetrofosmin (TF) and ^{99m}Tc-furifosmin (FU) are lipophilic monovalent cations that were introduced for myocardial imaging but found additional application as tumor-imaging agents. However, little is known about the mechanism of uptake of TF and FU into tumor cells. The aim of this study was to evaluate and compare the uptake characteristics of these complexes in vitro by breast cancer and sarcoma cells. Breast cancer- [MCF-7 (cloned carcinoma), ZR-75-1 (human adenocarcinoma) and SKBR-3 (human adenocarcinoma)] and sarcoma cell lines [A-204 (rhabdomyosarcoma), SW 684 (fibrosarcoma), SW 872 (liposarcoma), SW 982 (synovial sarcoma) and SW 1353 (chondrosarcoma)] were investigated. The influence of density of tumor cells (1.10⁵-1.10⁶ cell/ml), temperature-(4°C, 22°C, 32°C, 37°C) and time (10-60 minutes) of incubation on the radioactivity uptake (100 µCi ^{99m}Tc) were analysed.

TF showed in breast cancer lines a higher uptake for SKBR-3 and in sarcoma cell lines for SW 1353, whereas the highest uptake of FU were found for MCF-7 and SW-684, respectively. The uptake was highest at a cellular density of 1.10⁶ cell/ml and at a temperature of incubation of 32°C, followed by 37°C. In breast cancer lines the uptake reached a maximum at 20-40 minutes after incubation, starting to decline after about 60 minutes, whereas in sarcoma cell lines it reached its maximum as early as after 10-20 minutes. Data indicate that the uptake of TF and FU by breast cancer- and sarcoma cells occurs by different metabolic mechanisms. TF and FU seem to be taken up by these tumor cell lines by a mechanism predominantly related to high mitochondrial activity, besides cation channel transport, thus strengthening the hypothesis that these malignant cells may be imaged with TF- or FU scintigraphy at a very early clinical stage due to the high number or the high activity of mitochondria in these cells.

PS-293

A. Sarıkaya, N. Erkmen, T.F. Çermik, M. Kaya, G. Hüseyin*, M. E. İrfanoğlu**, S. Berkarda.
Trakya University Medical Faculty Department of Nuclear Medicine, *Pathology and **Surgery, Edirne, TURKEY.

COMPARISON OF THYROID NODULES WITH Tc-99m MIBI SCANNING and ELECTRON MICROSCOPY EXAMINATION

The aim of this study was twofold: firstly to evaluate how Tc 99m MIBI accumulates in the cold nodules as identified on the pertechnetate scan, and secondly to assess whether this uptake is influenced by the histological type of nodule.

70 patients who showed a cold thyroid nodule on a Tc-99m pertechnetate scan have been studied using Tc-99m MIBI double-phase imaging. 62 were female, and 8 male. The mean (\pm SD) age was 41.25 ± 12.3 years. Thirty three patients underwent surgery and the histological results were compared with the findings on Tc 99m MIBI scintigraphy. Fifteen of them were Tc-99m MIBI positive. Two of patients who Tc-99m MIBI positive had papillary Ca, three hurtle cell Ca., ten follicular adenoma. In our study, the sensitivity and specificity of Tc-99m MIBI imaging were 62,5 %, 60 %, respectively, in the operated group. Sixteen patients were evaluated by electron microscopy. Electron microscopy results were classified as A, D, B, C cells. Five patients out of ten with A cells, three patients out of six with B cells were Tc 99m MIBI positive.

Our results indicate that Tc-99m MIBI scanning is of little value preoperatively in distinguishing thyroid carcinoma from other thyroid nodules.

PS-294

S. Granegger, M. Rodrigues, R. Obwegeser, E. Kubista, H. Sinzinger

University Hospital, Departments of Nuclear Medicine, Gynecology and Oncology, Vienna, Austria

99mTc-TETROFOSMIN SCINTIGRAPHY IN MALIGNANT DISEASE. DISCUSSION OF UNUSUAL FINDINGS.

99mTc-tetrofosmin is a lipophilic cation that shows a preferential uptake by cells with high mitochondrial activity. 99mTc-tetrofosmin is currently under investigation for its tumor seeking properties in breast, lung and thyroid cancer, and musculoskeletal sarcomas, among others. After i.v. injection, 99mTc-tetrofosmin rapidly evades the circulation, with a blood clearance of more than 95% 10 minutes after injection. 99mTc-tetrofosmin is mainly excreted via the renal and hepatobiliary pathways. A significant uptake is seen in the liver and gallbladder as well as in the salivary, thyroid and parathyroid glands. Bowel, kidneys and lungs also show increased tracer uptake, rendering diagnosis of tumors in these organs difficult.

Unusual findings in patients studied with 99mTc-tetrofosmin scintigraphy related to the uptake or excretion of the tracer, namely ulcerated lesions, mammary implants and supravescical impression, among others, are discussed.

Data indicate that 99mTc-tetrofosmin is excreted through apocrine and eccrine glands („sweat spots“) and benign and malignant-, venous and arterial ulcerations as well.

PS-295

C. Soler, P. Beauchesne, J. Brunon, F. Dubois.

Hôpital Bellevue, CHU Saint-Etienne, Dept of Nuclear Medicine, France.

THE ROLE OF ^{99m}Tc-SESTAMIBI BRAIN SPECT IN THE MANAGEMENT OF MALIGNANT GLIOMAS.

^{99m}Tc-Sestamibi (MIBI), a radiopharmaceutical used to study myocardial perfusion has been proposed for use as a tumor imaging agent, in breast cancer, lung cancer, lymphomas and brain tumors. After the routine radiation therapy, deteriorating clinical status may be due to radiation changes or recurrent tumor. However, CT and MRI offer imperfect discrimination between these conditions. Thirty six patients with clinical deterioration were studied retrospectively (34 grade 4 and 2 grade 3), a tomoscintigraphy was performed 15 mn after intravenous injection of 1110 Mbq (30 mCi) of ^{99m}Tc-MIBI. We demonstrated a MIBI uptake for 33 patients with grade 3 and 4 gliomas. MIBI uptake occurred only in tumor recurrence. In the 3 remaining patients with radiative necrosis, no MIBI uptake was found. So, ^{99m}Tc-MIBI brain SPECT seems to be capable of discriminating tumor recurrence from radionecrosis in patients harboring grade 3-4 gliomas when treatment failure occurred. In order to investigate the role of ^{99m}Tc-MIBI brain SPECT for follow-up of these patients, we have undertaken a prospective study of 45 patients with high grade glioma. 25 patients underwent total or partial surgical resection and stereotactic biopsy was performed in 20 patients. The quality of surgical resection was determined by ^{99m}Tc-MIBI brain SPECT and CT in first 72 hours, and all patients underwent ^{99m}Tc-MIBI brain SPECT and CT at the end of radiotherapy and 2 courses of chemotherapy and then every two months until death. The results are :

- * ^{99m}Tc-MIBI brain SPECT as more sensitive than CT for evaluating residual tumor after surgery.
- * Volumes and index ratio of tumor are excellent for predicting efficacy of treatment and correlate with clinical progress of patients.
- * For patients with complete resection, ^{99m}Tc-MIBI brain SPECT was positive on post-treatment control as well as CT brain.
- * ^{99m}Tc-MIBI brain SPECT showed in many patients a « silent » residual tumor. In the light of these preliminary results, ^{99m}Tc-MIBI brain SPECT seems to be excellent for follow-up of patients treated for malignant gliomas.

PS-296

A. Soricelli, P.P. Mainenti, L. Florimonte, A.M. Della Morte, M. Salvatore

Dept. of Diagnostic Imaging and Center for Nuclear Medicine of the National Research Council, Univ. of Naples Federico II, Italy

ROLE OF LYMPHOSCINTIGRAPHY FOR THE DETECTION OF SENTINEL NODE IN CUTANEOUS MELANOMA

It has been shown that in cutaneous melanoma the first lymph node draining the tumor, the "sentinel node" (SN), reflects the lymphatic involvement of the entire regional basin: a negative SN virtually excludes the presence of lymphatic metastasis. In patients with CM without clinical evidence of regional lymph nodes involvement (stage I) a wide local excision of the primary tumor is performed followed, if the SN is positive for metastasis, by the elective dissection of the lymphatic basin. We have investigated the utility of LS with 99mTc-colloid albumin associated with intraoperative lymphatic mapping (ILM) in the identification of the SN in 41 patients with a clinical diagnosis of stage I CM, histologically proven in all cases (22 f, mean age 48.2 ± 14 years, age range 21-80 years; localization: trunk 12, shoulders 4, head and neck 3, upper limbs 5, lower limbs 17). The LS and the ILM were performed with the primary lesion in situ. Dynamic and static images were acquired up to 120 min. after 4 subcutaneous injections peripherally to the lesion (for a total of 80-100 MBq). Intraoperative lymphatic mapping for SN identification was performed by injection of dye (patent blue-V) around the CM. A total of 53 SN were found with LS (a double SN in different lymphatic basins was evident in 11 patients), 49 (92%) were identified during ILM, while two were not found during surgery, and two were not colored with patent blue. At the histological examination 4 SN nodes were positive for micrometastases and 2 for metastases. The six corresponding basins were excised. At the follow up (mean 30 months; median 32 months) the absence of metastases in the same or different lymph basins, compared to those predicted from LS indicates that this procedure and ILM, performed with the primary lesion in situ, identifies accurately the SN in all patients. In conclusion although LS does not indicate lymph node metastatic involvement, it is an accurate technique to identify the SN. Moreover the preoperative assessment of the SN with LS can reduce the surgical timing, identifying the lymphatic drainage basin and its number, specially when the primary lesion is localized at the level of the trunk, head and neck.

Poster presentations

PS-297

A.Spanu, A.Farris, P.Solinas, S.Nuvoli, C.Bagella, A.Masia, M.E.Solinas, A.Falchi and G.Madaddu.
Depts. of Nuclear Medicine and Oncology. University of Sassari. Italy.

TC-99m TETROFOSMIN (T) SCAN IN MONITORING MALIGNANT MELANOMA PATIENTS. PRELIMINARY RESULTS.

To verify the usefulness of T-scan in monitoring melanoma pts, we studied 28 consecutive pts (17 F and 11 M), aged 22 to 74 yrs, surgically treated for primary tumor 39.72±35.92 months earlier: 21 pts had no evidence of disease (NED), while metastases were suspected in the remaining 7 pts. Among the latter, 3 pts had suspect regional lymph node enlargement (inguinal in 2 cases and axillary in 1 case), both clinically and at Echotomography (Echo); 2 pts had a hot area at anti-melanoma Mab 225.28S Radioimmunosintigraphy (RIS) in the left inguinal and parietal brain regions, respectively; 1 patient had a hot area at bone scan; in the remaining patient a local recurrence (dorsal region) and supraclavicular lymph node involvement were suspect at physical examination. Ten min. after 740 MBq Tc-99m Tetrofosmin injection, whole body scan, and additional planar and SPECT images in selected sites were acquired. The scintigraphic data were compared with conventional imaging procedures, including RIS, which had been performed in all cases with the exception of the two pts with suspect inguinal lymph node enlargement. T-scan was true negative in 20/21 NED pts, as were conventional imaging procedures, including RIS, while it was positive in the left inguinal region of one patient, subsequently positive also at RIS. T-scanigraphy was true positive at SPECT in 3/3 pts (at planar in 2/3) with regional lymph node metastases (inguinal in 2 cases and axillary in 1 case), suspected clinically and at Echo, while it was true negative in the inguinal region of the patient positive only at RIS. Moreover, T-SPECT was positive in the patient with local recurrence and supraclavicular lymph node involvement and in the patient with positive bone scan, both negative at RIS. Finally, T-scan was negative in the patient with a parietal brain hot area at RIS, corresponding to angiomatous dysplasia at CT. Our preliminary results suggest that T-scan, and in particular SPECT, may be useful, together with conventional imaging procedures, in monitoring malignant melanoma patients, to detect local recurrence, lymph node and distant metastases.

PS-298

T.Suzuki, K. Nakamura, A. Kubo

Keio University School of Medicine, Department of Radiology

EVALUATION OF TC-99M LABELLED HL91(4,9-DIAZA-3,3,10,10-TETRAMETHYLDODECAN-2,11-DIONE DIOXIME) "PROGNOX" UPTAKE AND DISTRIBUTION IN HUMAN TUMORS

The purpose of this study is to evaluate the distribution of Tc-99m-HL91, which has been developed to detect tumor hypoxia, in tumors which were transplanted into athymic mice. Mice bearing human tumors; epidermoid carcinoma:KB-3-1, lung adenocarcinoma:HLC, gastric cancer:MKN45, and colon cancer:COLO205, were injected with Tc-99m-HL91 intravenously. The oxygen tension (pO2) in the tumor tissue was measured using a polarographic electrode system. Tumors removed 4 hours after injection were studied by autoradiography to determine intratumoral distribution of Tc-99m, and by HE-staining to distinguish necrotic from viable areas pathologically. The tumor oxygenation (pO2) ranged from 9 to 52 mmHg, and was not dependent on the type of tumor. In the large tumor tissues weighing c.a. 1.0 g, necrotic and viable fractions were present, and high intratumoral variations of pO2 were observed. On the other hand, for the big colon tumor the pO2 range was relatively small. Total Tc-99m-HL91 tumor uptake was more variable for the tumors with the greater pO2 range, and was slightly less variable for the small HLC tumor and COLO205 with the smaller pO2 range.

Tumors	pO2 (mmHg)	Tumor/Blood (SD)
KB-3-1	27-57	1.09 (0.19)
HLC (big)	31-44	1.73 (0.89)
HLC (small)	31-32	1.10 (0.12)
MKN45	29-52	0.89 (0.17)
COLO205	15-20	0.80 (0.02)

Autoradiography and pathological findings indicated that Tc-99m-HL91 was not distributed in the necrotic fraction, and that the highest activity was located in the hypoxic border areas between the viable and necrotic regions. Uptake in non-necrotic regions was highly heterogeneous, especially in the big MKN45 and KB-3-1 tumors. It should be noted that the distribution of Tc-99m in the HLC and COLO205 tumors was heterogeneous although pathological findings appeared to be homogeneous. Tc-99m-HL91 will have potential as a tumor hypoxic marker, and the tumor distribution provides information which is additional to pathological and CT findings.

PS-299

Tabuena MJ, Vargas JA*, Varela A**, Ramon y Cajal S***, Salas C***, Durántez A*. Ortiz Berrocal J.
Services of Nuclear M, Internal M*, Thoracic Surgery** and Pathology*** Clínica Puerta de Hierro. Madrid.

CLINICAL CORRELATION OF P-GLYCOPROTEIN EXPRESSION IN LUNG CANCER ACCORDING TO 99mTc-TETROFOSMIN UPTAKE AND IMMUNOHISTOCHEMISTRY

Objectives: P-glycoprotein (Pgp) is encoded by the multidrug resistance gene (mdr1). Its overexpression by lung cancer cell lines is associated with an increased efflux of many cytotoxic drugs from the cells. Tetrofosmin (TF), a lipophilic cation, is also a substrate for Pgp. We performed this study to determine clinically the Pgp distribution in non-small cell carcinoma (NSCLC) by immunohistochemistry (IHC) and correlate it with 99mTc-TF uptake. **Material and Methods:** We studied 18 patients with NSCLC: 16 men, 2 women; mean age: 66.3 yr (range: 52-83 yr); histology: 7 adenocarcinomas (AC) and 11 squamous cell carcinomas (SCC). Prior to surgery, planar images were acquired 10 and 60 min after the injection of 740 MBq of 99mTc-TF and SPECT images at 70 min. Image processing included quantitative study of regions of interest, after which we obtained a TF uptake ratio: lung cancer/normal lung. IHC studies were performed on paraffin sections using a monoclonal antibody, JSB-1, which reacts with an internal epitope of Pgp. We considered the IHC results to be positive when Pgp immunostaining was detected in >10% of the specimen.

Results: Immunostaining for Pgp was positive in 12 tumor sections (4 AC, 8 SCC) and negative in 6 (3 AC, 3 SCC). Our results showed an inverse correlation between the TF uptake ratio and the density of Pgp expression by IHC in tumor tissues: the TF uptake ratios were significantly lower (1.18±0.28) for tumors expressing Pgp than in negative specimens (2.05±0.67).

Conclusions: There is a good correlation between the expression of Pgp by immunohistochemistry and 99mTc-Tetrofosmin uptake. 99mTc-Tetrofosmin is useful to determine the presence of Pgp in lung cancer.

This work has been partially supported by Fundación Lair.

PS-300

L.Vini, B. Pratt, A. Al-Saadi, V.R. McCready, C. Harmer
Thyroid Unit, Royal Marsden NHS Trust, Downs Road, Sutton, Surrey, SM2 5PT, UK

TESTICULAR DOSE FROM IODINE-131 TREATMENT FOR THYROID CANCER AND MALE FERTILITY

Aims: 1) To evaluate the dose to the testes from ¹³¹I treatment. 2) To assess fertility of males following radioiodine therapy for thyroid cancer.

Methods: Radiation dose to the testes was measured prospectively using thermo-luminescent dosimetry in 12 consecutive male patients; 7 received an ablation dose of 3GBq and 5 were treated with 5.5GBq of ¹³¹I. Fertility was assessed retrospectively in 94 men under the age of 40 years when treated. All had well-differentiated thyroid cancer (58 papillary and 36 follicular). Sixty-three patients received a single iodine dose (3GBq) and 31 were given more than one dose (cumulative activity 8.5-32 GBq) for residual, recurrent or metastatic disease.

Results: Ablation of thyroid remnants with 3GBq resulted in a radiation dose to each testes ranging from 5.4cGy to 9.8cGy (6.81±1.72); from 12.9cGy to 19.2cGy (15.66±2.76). Sixty eight children were fathered by 48 patients; the remainder had no wish to have children. Malformations have not been reported.

Conclusions: The risk of damage to the gonads of male patients treated with ¹³¹I appears to be low and lacks clinical impact.

PS-301

D. Gludovacz, S.R.Li, P. Angelberger, E.Koller, P. Valent and I. Virgolini
Departments of Nuclear Medicine, Physiology and Haematology, University of Vienna, Research Center Seibersdorf, Austria

EFFECTS OF VASOACTIVE INTESTINAL PEPTIDE (VIP) AND SOMATOSTATIN (SST) ON LIPOPROTEIN RECEPTORS EXPRESSED ON A431 TUMOR CELLS

Recent data suggest that lipoprotein receptors may play a regulatory role in the development of tumor cells. In this study we investigated the effect of vasoactive intestinal peptide (VIP) and somatostatin-14 (SST-14) on the binding of ¹¹¹Indium-labeled lipoproteins (¹¹¹In-LDL, ¹¹¹In-HDL and ¹¹¹In-VLDL) onto A431 cells, the epidermoid mammary carcinoma cells. Scatchard analyses of the binding data indicated specific binding sites for LDL, HDL and VLDL (one class of high affinity binding sites for ¹¹¹In-LDL (maximal binding capacity (B_{max}): 3.25±0.42 µg/10⁶cell; dissociation constant (K_d): 18.6±7.6 nM) and one class of high affinity binding sites for ¹¹¹In-HDL (B_{max}:23.75±2.14 µg/10⁶cell, K_d: 70.3±22.6 nM) as well as for ¹¹¹In-VLDL (B_{max}:10.23±1.75 µg/10⁶cell, K_d: 3.6±1.9 nM). After preincubation of A431 cells with vasoactive intestinal peptide (VIP, 1 µM), the binding of ¹¹¹In-LDL onto the cells was significantly (p<0.01) increased, whereas, SST-14 (1 µM) had no influence on the binding of ¹¹¹In-LDL onto A431 cells, however, after preincubation of A431 cells with SST-14 as well as VIP, no VIP-induced increase of ¹¹¹In-LDL binding sites was shown. VIP and SST-14 did not interfere with ¹¹¹In-HDL and ¹¹¹In-VLDL binding onto A431 cells. Our results suggest a direct effect of VIP and SST-14 on LDL-binding onto tumor cells. The complex interactions between LDL, VIP and SST-14 may play a role in tumor cell growth.

PS-302

Yang-SE, Yu-YL, Yu-ZC, Zeng-J

Hospital: Shanghai Chest Hospital, Department of Nuclear Medicine

RADIONUCLIDE CARDIAC RESERVE FUNCTION FOR THE PREDICTION OF POSTOPERATIVE PERFORMANCE IN PATIENTS WITH PRIMARY LUNG CANCER

PURPOSE: To evaluate the clinical efficacy of preoperative radionuclide left ventricular function for the prognosis in patients with primary lung cancer.
METHODS: 132 patients (101 men, 31 women, mean age 67years.) were demonstrated as adenocarcinoma in 35 cases, squamous cancer 61, small cell lung cancer 5, undifferentiated cancer 3 and adenosquamous carcinoma 28. Before operation, the lung resection candidates underwent rest and stress testing with ^{99m}Tc-labeled red blood cells (RBC) gated SPECT or radionuclide stethoscope and pulmonary function testing within 2 wk. to obtain the values of left ventricular ejection fraction (LVEF), peak filling rate (PFR) and forced expiratory volume in one second (FEV1), forced vital capacity (FVC) etc. According to the observed LVEF,PFR undergoing rest and stress testing, the candidates were divided four groups. (Tab.1) Pulmonary function's data were collected and divided two groups: Group 1 (n=104): FEV1 / FVC was > 60%; Group 2 (n=28) FEV1 / FVC was ≤ 60%.
RESULTS: The incidence of postoperative complications in patients showed as follows: the Group 1, there were 6 postoperative complications / 29 patients for Group A, 3 / 19 for Group B, 11/31 for Group C and 11/25 for Group D. the Group 2, there were 1 postoperative complications / 6 patients for Group A, 1/2 for Group B, 4/11 for Group C and 6/9 for Group D. respectively. In 43 postoperative complications, there were 22 complications of cardiac, 10 of pulmonary, 6 of cardiopulmonary and 5 of others, thus it can be seen that cardiac events (22/43) are more than pulmonary (10/43). Among 8 deaths, there were 5 cases in Group D, 3 in Group C; half and half in Group 1,2. respectively.
CONCLUSION: The measurement of radionuclide cardiac reserve function has clinical significance in selecting indication and assessing prognosis. For postoperative performance, the prediction of radionuclide cardiac reserve function in lung resection candidates at increased risk for complications is much better than pulmonary function.

TABLE 1
Changes of LVEF,PFR After Stress

GROUP	n	LVEF	PFR
A	35	↑	↓
B	21	↑	↓
C	42	↓	↑
D	34	↓	↓

PS-303

M. Zhang, Z. Yao, H. Sakahara, Y. Nakamoto, T. Higashi, and J. Konishi.
Kyoto University Hospital, Department of Nuclear Medicine.

RELATIONSHIP OF GLYCOSYLATION AND ISOELECTRIC POINT WITH THE TUMOR ACCUMULATION OF AVIDIN.

We have shown that radiolabeled avidin targeted intraperitoneal (i.p.) tumors efficiently and treated the tumors effectively. This study was undertaken to investigate the mechanism of avidin accumulation in tumor. Avidin was deglycosylated through endoglycosidase-H digestion and/or neutralized by acetylation of its lysine amino acids with acetic acid N-Hydroxysuccinimide ester and the modified avidins were analyzed by SDS page and isoelectric focusing. Tumor model was established by i.p. injection of human colon cancer cells, LS180, in nude mice. The proteins, labeled with In-111 using DTPA-biotin, were administered i.p. into the tumor-bearing mice and biodistribution of radioactivity was examined at 2 or 24 hours postinjection. Deglycosylated avidin (Avid-E) revealed a major band of smaller molecule on SDS page while undeglycosylated avidins did not show the band. Isoelectric points of acetylated avidin (Avid-N) were reduced to less than 5, while those of unacetylated avidin were more than 9.5. Biodistribution study demonstrated that the liver uptake and kidney accumulation of radioactivity were decreased by deglycosylation and acetylation, respectively, of avidin. The tumor uptake of radioactivity was reduced by either deglycosylation or neutralization. Avid-E with neutralization (Avid-E/N) cleared from the circulation slowly and its accumulation in the tumor was low.

Tumor uptake of radioactivity in the tumor-bearing mice (%ID/g)

	Avid	Avid-E	Avid-N	Avid-E/N
2 h	69.3±16.6	30.4± 7.1	53.4±16.2	11.7±4.8
24 h	54.3±19.4	26.8±13.3	19.3± 6.3	10.7±1.3

In conclusion, both high glycosylation and positive charge of avidin contributed to its high tumor accumulation. This study may be helpful in finding new vehicles in delivering therapeutic agents to the tumors.

Neurology/Psychiatry: Epilepsy

PS-304

J.E. Keough, S. Dadparvar, M. Assadi, J. Mack, A.A. Shaikh, W.J. Slizofski, M. Jacobson,

Nuclear Medicine, Allegheny University Hospitals-Hahnemann & MCP Divisions, Philadelphia, PA

INTERICTAL TC-99M HMPAO SPECT FUNCTIONAL BRAIN IMAGING IN PATIENTS PRESENTING WITH SEIZURE

Evaluation of seizure disorder is a complex neurological problem requiring a multimodality approach. The current use of surface or scalp electroencephalogram (EEG) monitoring alone is inadequate to fully assess these patients. This retrospective study evaluated the role of Tc-99m SPECT functional brain imaging in adult patients presenting with seizure disorders.

During 1994-1996, 35 consecutive adult patients with seizure were referred for functional SPECT brain imaging. The group included patients with simple partial seizure, complex partial seizure, generalized seizure, S/P stroke seizure, pseudoseizure and frontal or temporal lobe epilepsy. Patients included 17♂ and 18♀, age range 19-76 years, mean age 44.1 years, with range of onset of first seizure from birth to 74 years. The SPECT functional brain imaging was performed with a triple headed camera following intravenous injection of 21.6 mCi Tc-99m HMPAO. The images were interpreted as abnormal if there was hyperperfusion or hypoperfusion in the anatomical area. Images were otherwise interpreted as normal. Clinical, EEG and anatomical correlations were performed. There were 35 concomitant EEGs and 26 CT/MRIs (anatomical imaging of the brain) available for comparison.

The concordance of the Tc-99m HMPAO SPECT brain imaging with clinical diagnosis was 28/35 (80%) and with EEG was 21/35 (60%). The concordance of EEG with clinical diagnosis was 27/35 (77%). There was 19/26 (73%) concordance between Tc-99m HMPAO SPECT and anatomical imaging of the brain.

Although the SPECT brain imaging was performed on the patients during the interictal phase, there was a high correlation among the SPECT brain imaging and the clinical diagnosis. The value of the functional SPECT brain imaging in clinical neurology during interictal phase may further be improved by simultaneous EEG monitoring of these patients while undergoing the functional brain imaging.

PS-305

E. Klemm, *H. Urbach, *J. Reul, **W. Koehler, *D. Brechtelsbauer, **A. Piotrowski, F. Grünwald, **D. B. Linke, ***M. Kurthen, **J. Schramm, *H. Schild, H.-J. Biersack.** *Departments of Nuclear Medicine, *Radiology, **Neurosurgery, and ***Epileptology, University of Bonn, D-53127 Bonn, Germany, and ****Department of Nuclear Medicine and Magnetic Resonance, University of Warsaw, PL-03285 Warsaw, Poland*

FUNCTIONAL INACTIVATION OF THE HIPPOCAMPUS IDENTIFIED BY HIGH RESOLUTION INTRAARTERIAL ^{99m}Tc-HMPAO SPECT AND ANGIOGRAPHY: COMPARISON OF THE INTRACAROTIDAL AND THE SELECTIVE POSTERIOR CEREBRAL ARTERY AMOBARBITAL TEST

The intracarotid amobarbital (WADA) test is used to assess memory function in patients prior to temporal lobe surgery. Since the major part of the hippocampus is supplied by branches of the posterior cerebral artery (PCA), selective injection of amobarbital into the PCA should result in functional inactivation of the hippocampus to a higher degree than after injecting into the ICA that usually supplies the hippocampal head via the anterior choroidal artery (AChA). To evaluate areas anaesthetized, we compared the amobarbital distribution to 10 hemispheres following selective injection into the PCA or the middle cerebral artery (MCA) with that obtained after injection into the internal carotid artery (ICA, 136 hemispheres). A special technique developed by us enabled fusion of SPECT images, angiograms and MRIs in the same patient. Following the routine angiography and an additional angiography of the ICA using the same procedure as for the WADA test, or subsequent to selective catheterization of either the P2 segment of the PCA or various branches of the MCA, ^{99m}Tc-HMPAO was injected into the ipsilateral ICA or the respective artery along with amobarbital. SPECT was performed using a high resolution dedicated brain gamma camera (ASPECT, FWHM 6 - 8 mm). The ICA procedure visualized the entire hippocampus only in hemispheres with a 'fetal origin' of the PCA (N = 25, 18 %). However, the hippocampus did not accumulate tracer in one fifth of these cases despite marked filling of the PCA. If the PCA was opacified only poorly or shortly by angiography, solely the uncus, amygdala, and parts of the hippocampal head were visualized. In contrast, selective injection into the PCA opacified the hippocampus without exception. When branches of the MCA were injected, homogeneous delivery to the irrigated territory was observed. In conclusion, high resolution SPECT after intraarterial injection of ^{99m}Tc-HMPAO can visualize the respective territories with high accuracy depending on their vascular supply and thus identify the areas actually inactivated by amobarbital.

PS-306

B.A. Krishna, V.P. Udani, Sangeeta Tikko

P.D. Hinduja National Hospital & Medical Research Centre, Mahim, Mumbai 400 016, India.

HMPAO BRAIN ICTAL SPECT IN PATIENTS WITH INTRACTABLE SEIZURES.

Epilepsy is an important clinical application of Brain SPECT studies in determining epileptic focus. The ictal SPECT is found to be more sensitive than CT or MRI examination. We present our data on ICTAL HMPAO Brain SPECT in paediatric patients with intractable seizures.

Methods: Totally 16 patients underwent ICTAL Brain SPECT with 15 mCi ^{99m}Tc-HMPAO administered intravenously at the onset of convulsions. There was simultaneous video EEG recording which was used as a guide to assess the time of injection of tracer for an ictal SPECT. If the injection was made during the generalised phase of convulsions then the study was considered Non-ictal. The data was compared to CT or MRI scan and EEG.

Findings: Of the 16 patients, the SPECT study was positive in 12 patients and CT or MRI was positive in 7 patients. In 3 patients, the MRI showed 3 focal abnormalities and SPECT study demonstrated the site of active focus in one of the 3 sites. The EEG correlated with the SPECT focus in 8 patients. 5 out of 12 SPECT positive patients underwent surgery and 4 of them are seizure free while one patient worsened after surgery.

Conclusion: The HMPAO Ictal Brain SPECT study is very sensitive for detection of ictal focus and is superior to CT and MRI. In our experience video EEG recording acts as a reliable guide to assess the time of tracer administration and the onset of convulsions. Ictal SPECT study also aids in pinpointing the most active focus when more lesions are seen on CT/MRI.

PS-307

D.S. Lee, S.K. Lee, KH Chang, CK Chung, KY Choi, J-K Chung, M.C. Lee.

Seoul National University College of Medicine, Seoul, Korea

DIFFERENTIATION OF MEDIAL FROM LATERAL TEMPORAL LOBE EPILEPSY BY F-18-FDG PET

Extensive lateral temporal lobe hypometabolism in medial temporal lobe epilepsy (TLE) obliterates the differentiating ability of F-18-FDG PET between medial TLE and lateral TLE on the basis of lateral temporal lobe metabolism. We investigated whether symmetric uptake of F-18-FDG uptake in medial temporal lobe could differentiate lateral from medial TLE. In 113 patients (83 medial TLE, 30 lateral TLE) who underwent anterior temporal lobectomy and had good surgical outcome (Engel class 1 or 2), we compared visually both medial temporal lobes with focus on the presence or absence of medial temporal hypometabolism. On pathologic examination, all the patients with medial TLE had hippocampal sclerosis except one congenital abnormal hippocampus. Lateral TLE included various pathologic findings of cerebromalacia, microdysgenesis, arteriovenous malformation, old contusion, and tumors.

Twelve patients were normal on F-18-FDG PET. The other 101 patients had lateral temporal hypometabolism. Among 88 patients (80 lesional, 8 cryptogenic) who showed medial temporal hypometabolism, 70 were medial TLE patients and 18 were lateral TLE. Positive predictive value of medial temporal hypometabolism for medial TLE was 79%. Among 13 patients (9 lesional 4 cryptogenic) who did not show medial temporal hypometabolism, 4 were medial TLE patients and 9 were lateral TLE. Negative predictive value of normal metabolism of medial temporal lobe against medial TLE was 69%. Normal MR findings, on their own, stood against medial TLE, whose negative predictive value was 66%.

We suggest that normal metabolism of medial temporal lobe in addition to no structural lesion on MR could be referred as evidence against medial temporal lobe epilepsy. Lateral temporal lobe epilepsy should be suspected when we found no asymmetry of F-18-FDG uptake in medial temporal lobe.

PS-308

C. Menzel, F. Grünwald, S. Brückner, P. Willkomm, H. Bender, J. Risse, R. Otte, J. Ruhlmann, C.E. Elger, and H.J. Biersack.

Departments of Nuclear Medicine and Epileptology, PET-Center Bonn and University of Bonn, Germany

SUV-CORRELATION OF F-18-FDG PET TO MORPHOMETRICAL AND RELAXOMETRICAL ASSESSMENT OF PATHOLOGY AS SHOWN BY MRI IN PARTIAL EPILEPSY OF TEMPOROMESIAL ONSET.

Acquisition of quantitative data of functional and morphological imaging to evaluate a potential correlation of functional and morphological findings in patients with partial epilepsy of temporomesial onset.

33 patients with partial epilepsy (mean age 31.5 yrs., range 8-53 yrs., m:f = 16 : 17) of left (N = 20) or right (N = 13) temporomesial onset underwent functional imaging with F-18 FDG PET (Siemens / CTI, ECAT EXACT) including SUV-analysis within the hippocampus, ncl. amygdalae, and temporopolar, -basal, and -lateral neocortical structures and a MRI study (Philips Gyroscan ACS II) including a coronal T2w TSE sequence (THK 2mm) for morpho-/volumetrical analysis and a sequence for T2-relaxometry (THK 5 mm).

Mean hippocampal volume of all patients was 2.12 ml +/- 0.59 for diseased hippocampi and 2.62 ml +/- 0.40 for the healthy side (normal range 1.9 - 3.0 ml). Mean T2-relaxometry was 117.7 ms +/- 11.5 and 107.9 ms +/- 5.10 (normal < 114 ms). In contrast mean SUV within the hippocampus was 3.69 +/- 0.74 (side of seizure onset) and 3.79 +/- 0.79 („healthy“ side). Correlation of the results showed no positive or negative correlation of any pair of metabolic and morphological data. E.g. Spearman's correlation of hippocampal T2-signal, as a measure of hippocampal sclerosis, and hippocampal SUV analysis was - 0.06 / N = 33 / sig. 0.737. In addition, if only those patients with clearly pathological T2-relaxometry (> 120 ms) were correlated to their hippocampal SUV values, the correlation remained insignificant (r = -0.17, N = 14, mean T2-signal 129 ms, range 121 - 144 ms; mean SUV 3.61, range 2.5 - 6.32). Similar results were obtained for volumetric data and SUV-values of the temporal neocortex.

In conclusion, functional and morphological anomalies are not correlated. Pathological findings as detected by F18-FDG PET that involve temporal structures exceeding the temporomesial region in those pts. with seizures of temporomesial onset do not only reflect a mere consequence of temporomesial pathology but must instead be noticed as an individual factor of disease extent.

Neurology/Psychiatry: Cerevascular

PS-309

E. Ambrus, R. Szent-Györgyi, E. Vörös, P. Barzó, M. Bodosi, L. Csernay, L. Pávics
Albert Szent-Györgyi Medical University, Szeged, Hungary

THE VALUE OF ACETAZOLAMIDE-ENHANCED HMPAO-SPECT IN THE EVALUATION OF BILATERAL OCCLUSIVE DISORDERS OF THE INTERNAL CAROTID ARTERIES

The complementary role of acetazolamide-enhanced HMPAO SPECT was investigated in the presurgical evaluation of bilateral occlusive disorders of the internal carotid arteries (ICA). 20 patients with different grades of bilateral stenosis of the ICA were investigated by means of HMPAO SPECT at rest and after acetazolamide administration (one-day protocol), with selective cerebral angiography (DSA), color-coded Doppler sonography (US), and CT-angiography (CTA). All patients underwent carotid reconstruction surgery. The results of the DSA, US and CTA investigations and the surgical findings were utilized to make a final classification of the degree of carotid stenosis. The degree of stenosis of the ICA ranged mildly stenosed (0-29%) to occlusion. In 9 of the 20 patients, the perfusion abnormality correlated well with the degree of stenosis. As concerns the 3 cases with the same degree of bilateral stenosis, HMPAO SPECT revealed in 1 case a side dominance of the perfusion abnormality, in 1 bilateral hypoperfusion and in 1 no perfusion abnormality. The acetazolamide-enhanced rCBF study demonstrated a decreased vascular reserve capacity only in 6 cases (6/20, 30%). The side of acetazolamide-enhanced hypoperfusion matched with the higher degree of ICA stenosis in 4 cases, but not in 2. It was concluded that the combination of resting and acetazolamide-enhanced rCBF SPECT gives additional information compared to the angiography modalities, which is of importance in the decision concerning carotid surgery.

PS-310

R. Benti, *M. De Marchi, *N. Grimoldi, *M. Croci, A. Bruno, M. Gasparini, M. Castellani, V. Longari, G. Marotta, C. Canzi, *N. Stocchetti, P. Gerundini. Nuclear Medicine and *Neurosurgery Departments, *Neurologic-Care Unit, IRCCS-Ospedale Maggiore, Milan, Italy

"MISERY FLOW" SURROUNDING ISCHEMIC BRAIN LESIONS ASSESSED BY Tc-99m ECD BRAIN SPET AND INVASIVE O₂ PRESSURE MEASUREMENT (PtiO₂).

Seventeen patients (13 subarachnoid hemorrhage-SAH; 3 severe head trauma, 1 meningioma) were studied 3-7 days after ischemic brain injury and CT development of hypodense foci (mean volume 56±42ml). In this phase some rCBF impairment (misery flow) occurs in the perifocal tissue with possible instauration of metabolic penumbra. PtiO₂ measurement/monitoring is an invasive means to study cortical oxygenation for intensive neurologic care in-patients. This measurement was obtained by neurosurgical implantation of a flexible polarigraphic probe close to 21 focal brain lesions. CT results only were used for 10 foci (8 pts, Group A), whereas for 11 foci (9 pts, Group B) pre-implantation assessment included brain SPET imaging 60-120 min after i.v. injection of Tc-99m ECD (740 MBq). Point sources and radiopaque markers were used to match SPET/CT sections and guide PtiO₂ probe placement in group B. Device position corresponded to predicted in 8/10 (group A) and 8/11 (group B) foci. Adequate localization of misery flow areas was obtained if the selected site had a baseline PtiO₂<25mmHg :4/10 lesions in group A, 7/11 lesions in group B. The mean PtiO₂ was lower in group B: 22±8 vs 29±7 mmHg (p<0.05). SPET changed the neurosurgical access in 3/11 cases as well as 2 CT suggested probe sites. In all these zones low PtiO₂ (<25mmHg) was measured and ECD uptake ranged between 39 and 58% (mean 47%) with respect of contralateral cortex. The misery flow SPET pattern partially involved the margins of the lesion, with a sharp edge between nonperfused and most of the severely hypoperfused tissue. Diffuse hypoperfusion/misery flow around CT hypodense lesions was seen only in 2/3 patients with middle cerebral artery vasospasm following SAH. Reduced ECD uptake (40-60% vs. normal cortex) in low flow areas studied was significantly correlated (p<0.01) with low PtiO₂ values (<25 mmHg). Probe positioning was poor around 2/3 smaller (<30 ml) and 1/1 larger (>130 ml) CT lesions or hampered due to problematic neurosurgical access in 6/17 patients. In conclusion, ECD SPET is able to localize, better than CT alone, areas of reduced rCBF (misery flow) surrounding hypodense lesions at CT, with a good definition of their cortical extension. ECD retention in these misery flow/penumbra cortical areas positively correlated with invasively measured PtiO₂ values.

PS-311

A. Berbellini, U. Pasquini, S. Fattori, E. Brianzoni

Nuclear Medicine, Macerata and *Neuroradiology, Ancona-Italy

HMPAO SPET FOLLOW-UP STUDY WITH TRIPLE HEAD CAMERA IN BRAIN ANEURYSMATIC AND ARTERIOVENOUS MALFORMATION PATIENTS ENDOVASCULAR TREATED

The aim of our work is the evaluation of brain SPET study in the follow-up of a group of patients (P) submitted to endovascular treatment with Guglielmi Detachable Coil (GDC) for aneurysmatic (AN) and arteriovenous malformation (AVM). In these patients the endovascular metallic devices disuade from RM scan. We studied 14p (6 F, 8 M, 18-77 y) after GDC treatment (internal carotid artery AN (2), anterior communicating artery (7), Sylvian artery (2), vertebrobasilar system (1), left temporal lobe AVM (1) and right parietal lobe AVM (1). The GDC treatment was done 24h-17 days after the symptoms onset. All P showed stable improvement of clinical signs. In the follow-up study all P were submitted to neurological, angiographic and TC evaluation and classified: no TC lesion, group A (8) and residual TC lesion, group B (6). At 3-24 months from GDC treatment was performed SPET study (900 MBq ^{99m}Tc-HM-PAO, Siemens MS3 triple-head gamma camera; fan beam collimators; FWHM: 7-8 mm; 126 views, matrix 128×128; 20-25×10⁶ counts). We performed a visual and semiquantitative analysis. In group A the brain SPET identified 4 mild perfusion defects in 3 asymptomatic patients (in brain region near the treated lesions); in group B all patients had abnormal SPET data in abnormal TC regions, but a P had one more perfusion defect in TC silent region. In vertebrobasilar a patient we found an unexpected mild cerebellar perilesional hot spot without any clinical and TC sign. In our opinion the brain SPET study is a suitable method to complete the follow-up of GDC treated patients.

PS-312

F. BERK, Ç. BERK*, K. M. KIR, N. EGEMEN*, G. ARAS

Department of Nuclear Medicine and Neurosurgery*, Ankara University, Faculty of Medicine, Avicenna Medical Center, Ankara, Turkey

OUTCOME PREDICTION AFTER SUBARACHNOID HEMORRHAGE WITH ACETAZOLAMIDE ACTIVATED SPECT

Change in brain perfusion due to vasospasm is one of the most important determinants of the clinical course and outcome of patients after aneurysmal subarachnoid hemorrhage (SAH). Acetazolamide activated SPECT measures tissue perfusion and autoregulatory capacity of smaller resistance vessels and changes in these may be demonstrated with acetazolamide activated SPECT even before clinical or radiological findings appear.

Twenty four patients with angiographically proven aneurysmal SAH had baseline and acetazolamide activated brain SPECT studies between 4th and 12th days after SAH, using 370 MBq ^{99m}Tc HMPAO (baseline) followed by 925 MBq ^{99m}Tc HMPAO after one gram diamox injection (stress). The SPECT results were evaluated both visually and quantitatively. The final evaluation of the patients were made according to Glasgow Outcome Scale in the 3th post SAH weeks.

At baseline SPECT, 20 patients (%83.33) had perfusion defects at watershed area. After acetazolamide activation, the perfusion is found to be worsened in 6 (%25), unchanged 9 (%37.5) and improved in 9 (37.5) patients on visual evaluation. The cerebrovascular reactivity is found to be preserved in 15 (62.5) and disturbed in 9 (%37.5) patients with quantitative analysis. Glasgow Outcome scores of the patients with preserved cerebrovascular reactivity found to be significantly better in the clinical follow-up (p<0.05).

Acetazolamide activated SPECT is a promising, easily applicable and noninvasive tool for the prediction of outcome after aneurysmal SAH with increasing application in clinical practice and outcome prediction.

PS-313

Sheng-Pin Changlai, Thomas S.M. Chiou

Chung Shan Medical & Dental College Hospital
Department of Nuclear Medicine, Department of Neurosurgery

Technetium-99m hexamethyl-propyleneamineoxime (Tc-99m HMPAO) brain images, in combination with fan-beam single-photon emission computed tomography (SPECT) and surface three-dimensional (3-D) display, were used to detect cerebral cortex and basal ganglion anomalies in Creutzfeldt-Jakob disease (CJD). Fourteen CJD cases received brain Tc-99m HMPAO imaging, computed tomography (CT), magnetic resonance imaging (MRI) and electroencephalogram (EEG) were also performed for comparison. Tc-99m HMPAO brain images demonstrated multiple, diffuse and uneven hypoperfusion areas over cerebral cortices and basal ganglia in all 14 patients. In 2 of 14 cases and 2 of 10 cases, respectively, brain CT and MRI showed brain atrophy. EEG reveals periodic lateralizing epileptiform discharge (PLEDs) over bilateral hemispheres in all 14 patients. This study suggests that, in comparison with brain CT and MRI, Tc-99m HMPAO brain imaging is a sensitive tool for the detection of brain anomalies in CJD patients.

Tc-99m HMPAO brain imaging in Creutzfeldt-Jakob disease

PS-314

D. Chowdhury, V.R. Lele, Kshama Kundley, R.D. Lele

Hospital: Jaslok Hospital & Research Centre
Department of Nuclear Medicine.

ROLE OF BRAIN SPECT IN NEONATES WITH HYPOXIC ISCHEMIC ENCEPHALOPATHY AND ITS CORRELATION WITH NEURODEVELOPMENTAL OUTCOME

Literature on brain SPECT in neonates with hypoxic ischaemic encephalopathy (HIE) is very scanty and inconclusive. Twenty four term neonates (13M, 11F) of 7 days age, with Hypoxic Ischemic Encephalopathy (HIE) stage II or III were studied. Cerebral perfusion scan was performed with 99mTc-ECD (74 MBq/dose) using Triple Head Gamma Camera with LEUHR fan beam collimators. USG (24 Pts) & CT (7 pts) were also performed within 2 days of the SPECT study and were correlated with immediate neurological status and neurodevelopmental outcome at 3m (15 pts) and 6m (9 pts) of age. SPECT studies were normal in 12 & abnormal in 12 patients. Commonest SPECT abnormality was parasagittal hypoperfusion (41.66%), bilateral focal hypoperfusion (25%), global hypoperfusion (16.6%) and left focal hypoperfusion (16.6%). USG was normal in 19 & abnormal in 5. CT was normal in 4 & abnormal in 3. Neonates with severe perfusion defects had increased frequency of seizures which were difficult to control and had longer period of altered sensorium. Normal SPECT scan was found to predict normal neurodevelopmental outcome at 3m. (negative Predictive value 100%). However, abnormal SPECT studies did not correlate well with abnormal neurodevelopmental outcome at 3m. (positive predictive value 75%). The negative & positive predictive value of SPECT (100%, 75%) was greater than USG (76%, 60%) and CT (50%, 66.6%) in predicting neurodevelopmental outcome at 3 months and 6 months.

PS-315

G. Demonceau, J. De Vuyst, H. Colaert, C. Monte

St Elisabeth Hospital, Zottegem, Belgium.

COMPARISON BETWEEN Tc-ECD AND Tc-HMPAO NORMAL DATABASES, ACCORDING TO AGE.

Differences in the cerebral distribution of both tracers in healthy subjects have been reported. However, to our knowledge, the way in which these differences evolve with age, has not yet been reported.

The perfusion distribution of 215 normal patients was studied, 10 minutes after injection of 1 GBq of either Tc-HMPAO (120 patients) or Tc-ECD (75 patients) on a 3-head camera. The patients were classified according to age in 4 categories: between 20 and 30, between 30 and 50, between 50 and 70 and over 70 years. Images were obtained in a 128x128 matrix, 25 sec/step, 90 steps over 360°. Backprojected reconstruction and filtering of the data were the same for both tracers.

The creation of database included activity normalisation based on the healthy cortex, linearity correction for the tracer uptake, warping and elastic transformation to correct for the different cerebral sizes and shapes and transfer into an anatomical atlas. The comparison within the different subgroups was based, slice by slice, on the ratio of the voxels and its level of significance was based on the intensity as well as on the area of the variation.

Tc-ECD, by comparison with Tc-HMPAO, demonstrates at all ages a relative increase of the activity of the cuneus and the cingulate and lingual gyri of both hemispheres. A more moderate increase of activity was noted for the internal part of both superior frontal gyri, but this difference was only seen in the patients over 30. On the other hand, the activity of Tc-HMPAO was superior to that of Tc-ECD in both pulvinars, in the databases of patients between 30 and 70. The activity of both sylvian fissures was also slightly higher for the group between 30 and 50, probably related to the higher meningeal activity.

The presence of these significant variations of the cerebral perfusion distribution, not only with the tracer, but also with age, reinforces the need of databases adapted to both the patient and the workconditions.

PS-316

I. Dygai, I. Shvera, N. Krivonogov, Yu. Lishmanov

Institute of Cardiology, Tomsk, Russia

POSSIBILITIES OF THE ¹⁹⁹Tl-DIETHYLDITHIOCARBAMATE SPECT FOR CEREBRAL AND MYOCARDIAL PERFUSION EVALUATION

The aim of this study was to investigate the possibility of ¹⁹⁹Tl-diethyldithiocarbamate (¹⁹⁹Tl-DDC) SPECT in cerebral and myocardial perfusion estimation.

Thirty six pts with stenosing brachiocephalic arteries (BCA) atherosclerosis were studied using ¹⁹⁹Tl-DDC SPECT. Twelve pts among them with accompanying coronary artery disease (CAD) were examined also using myocardial scintigraphy after one i.v. injection of ¹⁹⁹Tl-DDC. The control group included 16 pts without cerebrovascular insufficiency.

The best brain images and maximal tracer uptake were obtained in 25-30 min after ¹⁹⁹Tl-DDC i.v. injection. By all pts cerebral hypoperfusion zones (HZ) corresponding to regions of affected artery were found. Moreover, in 70-80 min after ¹⁹⁹Tl-DDC injection was possible to visualize myocardium. ¹⁹⁹Tl-DDC myocardial uptake was in this period of time 2,5-3% of injected dose. ¹⁹⁹Tl-DDC myocardial scintigraphy allowed to observe perfusion defects in CAD pts. The same perfusion defects were obtained by using ¹⁹⁹Tl-chloride.

Thus, ¹⁹⁹Tl-DDC can be used as agent for simultaneous cerebral and myocardial perfusion estimation.

PS-317

M. Hosono, K. Machida, N. Honda, T. Takahashi, T. Takahashi, S. Dei, Y. Shimizu, T. Kamano, A. Kashimada, H. Osada, T. Matsui, and T. Asano.
Depts of Radiology and Neurosurgery, Saitama Medical Center, Kawagoe, Saitama, Japan

DETECTION OF VASOSPASM IN PATIENTS WITH ANEURYSMAL SUBARACHNOID HEMORRHAGE (SAH) BY NON-INVASIVE CEREBRAL BLOOD FLOW QUANTIFICATION

In monitoring SAH patients (pts), early detection of cerebral vasospasm after clipping aneurysms is essential, because vasodilative agents could be effective. We conducted cerebral blood flow (CBF) quantification using Tc-99m ethyl cysteinate dimer (ECD) based upon the Patlak analysis reported by Matsuda et al. (Eur J Nucl Med 1995;22:633) without arterial blood sampling, and SPECT on 1, 7, and 30 days after surgery in 29 consecutive SAH pts (17 females and 12 males, age 55.4 ± 12.4 yr). Scans were visually interpreted by 2 nuclear medicine physicians. mCBF decrease more than 10 % on day 7 in comparison with day 1 was considered significant since the coefficient of variation was 5 % for mCBF measurement with our equipment. In total, 7 out of 29 pts had cerebral vasospasm and consequent ischemia and/or infarction which were confirmed by CT, MRI, and/or angiography. With a cut-off value of 10 % decrease on day 7, mCBF measurement detected 6 of 7 vasospasm pts, showing sensitivity 85.7 % (6/7), specificity 81.8 % (18/22), and negative predictive value 94.7 % (18/19). Vasospasm pts had mCBF of 57.6 ± 9.1 and 51.9 ± 8.9 ml/100g/min on days 1 and 7 (p = 0.002), while pts without vasospasm 46.8 ± 5.3 and 46.5 ± 5.7 ml/100g/min (p = 0.78). SPECT demonstrated decreased perfusion in 22 pts and increased perfusion in 2 pts at craniotomy sites in frontal and/or temporal regions on day 1, which might represent transient abnormal perfusion due to surgery and should not be misread as vasospasm. In conclusion, non-invasive mCBF measurement with Tc-99m ECD is a reliable tool for detecting vasospasm in SAH pts.

PS-318

IY Hyun, JH Na*, IG Lee*, CG Ha*, W Choe

Inha University Hospital, Incheon, Korea:
Department of Nuclear Medicine, and Neurology*

DIRECT COMPARISON OF Tc-99m ECD AND Tc-99m HMPAO UPTAKE IN THE SAME PATIENTS WITH ACUTE/SUBACUTE ISCHEMIC STROKE

Purpose: We studied to compare the differences between Tc-99m ECD and Tc-99m HMPAO uptake in the same patients (pts.) with acute/subacute ischemic stroke. **Methods:** Sixty-seven pts. (M/F:36/31, range:34-81 yr; mean age 62.4 yr ± 10.7) had MRI, and sequential Tc-99m ECD/HMPAO SPECT at same position during the acute/subacute phase of their stroke (range:1-13 day, mean delay:4.2 day ± 2.8). **Results:** Among 67 pts., we found hypoperfusion in 40 pts. and mismatched uptake of Tc-99m ECD and Tc-99m HMPAO in 20(50%) of 40 pts. Among 25 lesions with mismatched uptake of 20 pts., Tc-99m ECD uptake was always less than Tc-99m HMPAO in all lesions. We observed 8 hypoperfusion by Tc-99m ECD SPECT only, and 4 luxury perfusion by Tc-99m HMPAO SPECT. Among 13 hypoperfusion discovered in both of Tc-99m ECD and Tc-99m HMPAO SPECT, the severity of mismatched uptake was ranged from mild degree(6) to severe degree(7).

	mismatched uptake (total No. of lesion)	luxury perfusion	Tc-99m ECD only*
cerebral(cb.) cortex	12	2	2
cerebellar cortex	2	0	0
BG	9	1	5
thalamus	2	1	1

(*hypoperfusion in Tc-99m ECD SPECT only)

Conclusion: Our intrasubject comparison of pts. with acute/subacute ischemic stroke showed that the difference between Tc-99m ECD and Tc-99m HMPAO uptake was observed in half of pts. We found more hypoperfusion in cb. cortex, thalamus, and especially BG with Tc-99m ECD SPECT.

PS-319

H.K. Lee, D.Y. Kang, J.S. Ryu, D.H. Moon, S.R. Choi, J.S. Kim, G.E. Kim.
Asan Medical Center, University of Ulsan, Seoul, Korea.

A COMPARATIVE STUDY OF ACETAZOLAMIDE (AZ) AND DIPYRIDAMOLE (DP) STRESS BRAIN SPECT IN CEREBROVASCULAR DISEASE (CVD).

AZ brain SPECT is a well established procedure to assess cerebrovascular perfusion reserve in CVD. The purpose of this study was to evaluate the efficacy of DP as a pharmacological stress agent in the assessment of cerebrovascular perfusion reserve by comparison with AZ brain SPECT.

We performed both AZ and DP brain SPECT in 17 CVD pts (age 8-72, mean 52) using one day protocol. AZ SPECT was performed first, and then DP SPECT within 5 days. Four of the 17 pts were diagnosed as moyamoya disease, and 13 pts had various CVD including 10 with cerebral infarction and 3 without infarction. Baseline brain SPECT was done for 20 min using three headed SPECT camera (TRIAD XLT20, Trionix) after injection of 555 MBq of Tc-99m ECD. For DP SPECT, 1110 MBq of Tc-99m ECD was injected while patients were receiving 0.56 mg/kg of DP, and then DP SPECT was done for 10 min. AZ SPECT was acquired according to the conventional one day protocol using the same dose and imaging time. Perfusion reserve was assessed on subtraction images, and graded visually into 4 grades: 0 normal, I slightly, II moderately and III severely diminished perfusion reserve. The resulting distribution of perfusion changes is summarized in the table.

	Cerebrovascular perfusion reserve				total
	Dipyridamole				
grade	0	I	II	III	
Diamox	3	1	1	3	5
	1	4	1	3	4
	1	1	1	3	5
total	4	6	4	3	17

There was no significant difference of perfusion reserve between AZ and DP SPECT (p=0.17), and they were significantly correlated (Spearman's rho=0.679, p<0.01).

In conclusion, DP brain SPECT may be equally effective as AZ SPECT, but it does not provide diagnostic advantage over AZ SPECT in the assessment of cerebrovascular perfusion reserve in CVD.

PS-320

T. Ogura, S. Takikawa, K. Hida, T. Masuzuka, H. Saitoh.

Sapporo Azabu Neurosurgical Hospital, Department of Radiology

QUANTITATION OF REGIONAL CEREBRAL BLOOD FLOW USING TECHNETIUM-99m ECD AND SPECT BY A SINGLE BLOOD SAMPLING.

Can an input function of technetium-99m ECD be accurately estimated by scaling a standard input function using one blood sample as reported in iodine-123-IMP/SPECT studies?

Methods: Fifteen subjects (9 male and 6 female; age 54 ± 19 years) were analyzed. 10 minutes after a standardized pump injection (10 ml in 1 minute) of 740MBq of ECD a static 20 min scan was obtained using a three-head SPECT system (TOSHIBA GCA9300A/HG). Arterial blood was sampled frequently from the radial artery for 10 minutes after injection, and the whole blood radioactivity concentrations and octanol extraction fraction (lipophilic fraction) were measured. The standard input function was generated by averaging the 15 individual input functions derived by multiplying the whole radioactivity concentration by the octanol extraction fraction. The optimal time to calibrate the standard input function was determined to minimize the difference of time integral (from 0 to 10 min.) of the calibrated standard input function from that of the real input function measured in each of the 15 studies. Values of regional cerebral blood flow (rCBF) in the middle cerebral artery territory were calculated based on a microsphere model using two input functions: (1) their real input function, and (2) the estimated input function obtained by calibrating the standard input function by the activity of the single blood sample.

Results: The mean percentage of difference in the time integral between the calibrated standard input function and the real input function was found minimal (6.9 ± 8.3%) at 2.5 min. post injection, which was considered as the optimal time for calibration. Values of rCBF calculated using the two input functions mentioned above were in good agreement (r=0.91, p<0.001).

Conclusion: Our results validate the use of estimated input function for rCBF quantitation using ECD and SPECT. The use of this technique would make the quantitative study simpler and less invasive.

PS-321

R. Quirce, I. Uriarte, A. Montero, A. Hernandez, NK. Vallina, C. Guede, I. Banzo, J. Jiménez-Bonilla, JA. Amado, JM. Carril

Servicio de Medicina Nuclear. Hospital Universitario Marqués de Valdecilla. Santander. España.

BRAIN BLOOD FLOW SPECT IN THE FOLLOW-UP OF DIABETICS PATIENTS WITH PREVIOUS SUBCLINICAL ABNORMALITIES OF BRAIN PERFUSION

In previous studies with HMPAO-Tc99m SPECT we appreciated subclinical abnormalities of the brain perfusion in the patients with Diabetes Mellitus (DM). DM is a risk factor to develop cerebrovascular disease. To analyse the evolution of perfusion abnormalities detected in a first SPECT with HMPAO-Tc99m in patients with DM and no history of neurological symptoms we performed a follow-up SPECT. We have evaluated 37 patients (25 type I, 12 type II) with a mean age of 45 ± 12 (range: 23-28 years) with a mean time of DM evolution of 17 ± 7 (range: 7-30 years). The interval between SPECTs was 21 ± 4 months (range: 15-37) and no patients showed neurological symptoms during this time. No patients showed clinical symptoms of hypo or hyperglycaemia. Both SPECTs were evaluated by semiquantitative method and we analysed 50 ROIs/patients (1850 ROIs in total). In the first SPECT 240 of the 1850 ROIs analysed (13%) showed perfusion abnormalities: 160 with hypoperfusion and 80 with hyperperfusion.

RESULTS: The second SPECT showed perfusion abnormalities in 201 of the 1850 (11%) ROIs evaluated: 117 hypo and 84 hyperperfused. Of the 240 ROIs with abnormal perfusion in the first SPECT 78 (33%) remained altered in the second SPECT (33%). Of the 160 hypoperfused ROIs in the first SPECT 52 (33%) remained hypoperfused and of the 80 hyperperfused ROIs 26 (33%) remained hyperperfused. In the second SPECT 123 ROIs showed abnormalities not detected previously: 65 ROIs hypoperfused and 58 hyperperfused. Of the 37 patients with perfusion abnormalities in the first SPECT, in 28 one of the abnormalities at least was shown in the follow-up SPECT, and 32 of the 37 showed new abnormalities.

CONCLUSION: In the population studied, a 33% of subclinical brain perfusion abnormalities detected in diabetic patients remained in the follow-up scans.

PS-322

A. Pupi, MTR De Cristofaro, L. Emmi, T. Marchione, S. Sestini, F. Li Gobbi, M. Cellerini. Nuclear Medicine, Radiology and Clinical Immunology, University of Florence; Florence, Italy.

BRAIN CORTICAL HYPOPERFUSION IN BEHÇET DISEASE: HMPAO STUDY WITH ACETAZOLAMIDE CHALLENGE.

Central nervous system (CNS) involvement in Behçet Disease (BD) may be considered a negative prognostic factor, due to vascular (mainly vasculitic) alterations. Brain hypoperfusion areas (HPAs) can be found with HMPAO-SPECT in BD patients, but frequently there is a lack of spatial correspondence between HPAs and the brain alterations detected with structural brain imaging. We have investigated the behavior of the HPAs, detected in HMPAO-SPECT executed in basal conditions (BI-SPECT), with an HMPAO-SPECT after an acetazolamide challenge (Acz-SPECT).

Eleven BD patients (3 females and 8 males, mean age 38 ± 9 years), six of them with neurological involvement, underwent two consecutive HMPAO-SPECT studies in a single day session. SPECT studies were acquired with a PRISM 3000 camera equipped with fan beam collimators, and were reconstructed and reoriented so as to be spatially matched. ROIs were manually extracted covering the HPAs detected in the BI-SPECT and, then, repositioned on the corresponding images of the Acz-SPECT. A corresponding number of ROIs were also positioned in normal perfusion areas (NPAs) in BI-SPECT and repositioned in the Acz-SPECT. ROI mean pixel activity (RMPA) was normalized by the mean pixel activity of the whole brain in the respective SPECT study. Data were then analyzed with a 2x2 MANOVA (hypoperfusion versus normal perfusion and BI-SPECT versus Acz-SPECT).

In 7 of the 11 pts. of this study, we found in total 19 HPAs (volume 4.1 ± 2.6 ml mean \pm SD). RMPAs were 1.09 and 1.37 in the HPAs, and 1.35 and 1.33 in the NPAs (BI-SPECT and Acz-SPECT respectively). Given a MANOVA significant interaction effect ($p < 0.0002$), the significance of the differences was tested with Scheffe' post-hoc test, which showed that the 26% increase of RMPA between the BI-SPECT and the Acz-SPECT was highly significant ($p < 0.0001$) while the difference was not significant for the NPAs.

Our results demonstrate that the HPAs found at brain cortical level in BD pts. can depend on functional rather than structural local alterations, probably related with distant vasculitic involvement of the CNS. Therefore, the spatial correspondence with the structural brain imaging techniques is not necessarily expected. Then HMPAO-SPECT has an important role in the study of neurological symptoms in BD pts.

PS-323

N.G. Hartman, J-P. Soucy, J. Raymond, C. Janicki, W. Wierzbicki, J-P. Bahary, D. Roy

University of Montreal Medical Centre, Campus Notre-Dame, Departments of Nuclear Medicine, Radiology, Radio-Oncology and Physics

IN SITU BETA-IRRADIATION OF A BRAIN ARTERIOVENOUS MALFORMATION MODEL: WORK IN PROGRESS

Bucrylate embolization and stereotactic radiosurgery may both be used in the treatment of brain arteriovenous malformations (AVM). Coupling the effects of the two techniques by mixing a β -emitter with the embolic agent may be advantageous. The purpose of this preliminary study was to evaluate the distribution of the isotope after selective intravascular injection. The pig *rete mirabile* was used as the AVM model. Eight *rete mirabile* (8 animals) were selectively injected with a freshly prepared mixture of 33% n-butyl, 2-cyanoacrylate and 66% lipiodol labeled with I-131 (2.57 to 4.7 mCi/ml) after femoral catheterization using standard endovascular techniques under general anaesthesia. Whole body γ -scintigraphy was performed immediately after injection. Animals were then sacrificed and tissue counts were obtained of the whole injected *rete mirabile* as well as samples of blood, brain, kidneys, liver, lungs and spleen. *Rete mirabile* specimens were cut in 50 micron slices and exposed to dedicated films for low dose β -emitters (BetaMax™). In addition, two pigs were injected with 6 mCi/ml of the same mixture and kept for 6 weeks during which serial γ -scintigraphies were performed. After sacrifice, the same tissue counts were obtained. In the first group, activity retained in the *rete mirabile* ranged from 0.26 to 1.8% of the total activity in the syringe prior to the injection. γ -scintigraphy showed minimal lung activity in 2/8 animals. In the tissue counts, 3 animals showed lung activity of less than 0.6%, 3 showed ipsilateral brain activity of less than 0.57% and one showed blood activity of less than 0.39% as compared to the *rete mirabile*. In the second group, there was no detectable activity outside the *rete mirabile* either scintigraphically or using tissue counting. Autoradiography showed inhomogeneous activity in the injected *rete mirabile*. In conclusion, this preliminary study demonstrated the feasibility of selective deposition of a β -emitter inside the pig *rete mirabile* with the same embolization technique used in clinical practice for the treatment of brain AVMs. Erratic deposition was negligible. Future investigation will address dosimetry and histological effects of *in situ* beta irradiation.

PS-324

K. Schomäcker, H. Ebel, A. Balogh, M. Volz, J. Funke, N. Klug, H. Schicha *Departments of Nuclear Medicine and Neurosurgery, University of Cologne, Germany

HIGH CERVICAL SPINAL CORD STIMULATION (CSCS) INCREASES REGIONAL CEREBRAL BLOOD FLOW AFTER INDUCED SUBARACHNOID HAEMORRHAGE IN RATS

Purpose of the study: The objective of our study was to investigate the effects of high cervical spinal cord stimulation on regional cerebral blood flow after experimentally induced subarachnoid haemorrhage (SAH) in rats.

Methods: The experiments were carried out on a total of 25 Wistar rats, divided in three groups [control group I(5): native examination, control group II(7): intracisternal application of 0.5ml autologous blood for SAH induction, after 24 h Tc-99m-HMPAO-application, experimental group III (13): cervical spinal cord stimulation (frequency 50 Hz, impulse width 200 μ s, intensity 5V) for 3 hours 24 hours after blood application, after that-HMPAO-application]. The amount of Tc-99m-HMPAO was separately determined 5 min p.i. in heart, blood, muscle, cerebrum and cerebellum. The quotients cerebrum/blood and cerebellum/blood were calculated to ascertain the "extraction-rates" in the samples differentially. The statistical analysis was performed using non-parametrical methods.

Results: The following mean values were calculated for the cerebellum/blood quotients: Group I: 1.266, s 0.076; Group II: =.660, s =.210; Group III: 1.010, s 0.394. Comparing the mean values of group II and group III by the Wilcoxon-test a high significance could be found for the extraction rate of the cerebellum ($p=0.0280$, < 0.05 , Z-value -2.197). Comparing the mean values of the cerebral perfusion rate no significant difference could be found ($p=0.1730$).

Conclusion: After having induced subarachnoid haemorrhage the electrical cervical spinal cord stimulation enhances cerebellar blood flow in rats. The "extraction rate" of the perfusion marker Tc-99m-HMPAO increases after stimulation to values comparable to those measured under normal conditions. No significant difference could be found for the cerebral perfusion. Possibly, the high cervical spinal cord stimulation constitutes a new approach treating the disturbed regional cerebral blood flow after subarachnoid haemorrhage.

PS-325

S. Takikawa, T. Ogura, K. Hida, T. Masuzuka, H. Saitoh.

Hospital: Sapporo Azabu Neurosurgical Hospital, Department of Neurosurgery

COMPARATIVE ASSESSMENT OF VARIOUS METHODS TO QUANTITATE CEREBRAL BLOOD FLOW USING IODINE-123-IMP AND SPECT.

Although a variety of analytical methods have been developed to quantitate regional cerebral blood flow (rCBF) using I-123-IMP and SPECT, little is known about their comparative assessment of quantitative accuracy. To address this issue, we compared rCBF values and its reactivity to Acetazolamide obtained from various quantitative methods with those from the nonlinear least-squares fitting (NLLSF) analysis as a golden standard. Seventeen subjects (5 normal volunteers and 12 patients with chronic cerebrovascular disease; age 51 ± 18 years) were analyzed. Each subject underwent two SPECT studies; at rest and after intravenous administration of Acetazolamide (15mg/kg) at an interval of 2 to 7 days. The dynamic SPECT scan was obtained for 60 minutes following intravenous injection of 222MBq of IMP using a three-head SPECT system. Continuous arterial blood sampling for 5 minutes after injection as well as frequent arterial blood sampling throughout the study were done from the same arterial line using three way valve. Values of rCBF in the middle cerebral artery territory were calculated using a NLLSF technique based on a two compartment model and following four quantitative method: (i) microsphere method (continuous blood sampling, mid-scan time 40 min, corrected by the ratio of whole brain count at 5 and 30 min post injection), (ii) super early microsphere method (continuous blood sampling, mid-scan time 5 min), (iii) autoradiographic method developed by Iida (one blood sampling at 10 min for scaling the standard input function, mid-scan time 40 min, $V_d=30$ ml/ml), and (iv) super early autoradiographic method proposed by us (continuous blood sampling, mid-scan time 10 min, $V_d=30$ ml/ml). Correlation analysis was used to compare rCBF and rCBF response to Acetazolamide $[(rCBF_{Diamox} - rCBF_{rest}) / rCBF_{rest}]$ obtained by these methods. rCBF values by all four methods were in good agreement with those by NLLSF ($r = (i) 0.971, (ii) 0.984, (iii) 0.909, (iv) 0.982$). Correlations of Acetazolamide response were also significant ($p < 0.01$; $r = (i) 0.777, (ii) 0.876, (iii) 0.793, (iv) 0.905$), but both super early methods showed better agreement than two other methods. These results suggest that considerable early scan is preferable both to increase the quantitative accuracy in microsphere and autoradiographic technique in IMP/SPECT.

PS-326

H.Toyama, K.Matsumura, H.Nakashima, T.Yoshida, K.Takeda, A.Takeuchi, S.Koga.

Fujita Health University, Toyoake, Mie University, Tsu, Japan.

EVALUATION OF SELECTIVE NEURONAL LOSS WITH IOMAZENIL AFTER TRANSIENT MIDDLE CEREBRAL ARTERY OCCLUSION IN RATS: POTENTIAL FOR THE MORE ACURATE THERAPEUTIC INDICATOR OF THE THROMBOLYTIC THERAPY.

Early successful reopening in embolic stroke should lead to partial salvage of an ischemic area. However, it is difficult to evaluate the extent and the severity of sublethal injury in CT negative lesion. The purpose of this study is to evaluate the neuronal distribution with benzodiazepine receptor (BZR) antagonist in permanent vs. transient brain ischemia in rats. The right middle cerebral artery (MCA) was occluded by inserting a nylon. The arterial occlusion was permanent in Grp A (n=4) and transient for 60 min in Grp B (n=6). At 1 wk after the occlusion, I-125-iomazenil for BZR and 45 min later I-123-IMP for cerebral blood flow (CBF) were injected. The affected and contralateral cerebral MCA regions were dissected, weighed and counted. The uptake ratios of the affected to contralateral regions were measured. The BZR as well as the CBF in Grp A were significantly lower than those in Grp B (BZR:0.71 vs 0.89, CBF:0.48 vs 0.92). In Grp A, the BZR was significantly higher than the CBF. However, in Grp B, the BZR was significantly lower than the CBF. The BZR could reflect the severity of the insult in where even the CBF shows the apparently recovered reperfused lesions. The BZR imaging with I-123-iomazenil might be promising for more accurate indicator of neuronal damage in therapeutic interventions.

PS-327

A. Kobayashi*, H. Toyama, T. Nariai**, K. Uemura*, K. Oda, M. Senda, A. Uchiyama*.

Positron Medical Center, Tokyo Metropolitan Inst. Gerontology, *Waseda Univ. and **Dept. Neurosurg., Tokyo Medical and Dental Univ., Tokyo, JAPAN

VISUALIZATION OF CORRELATED HEMODYNAMICS IN CEREBROVASCULAR DISEASE BY A CLUSTER ANALYSIS WITH PET ACTIVATION STUDY.

We developed a method of clustering the brain pixels into three or four regions with different stage of hemodynamic deficiency using three sets of PET images and applied it to evaluate the regional vasodilative and vasoconstrictive reactivity before and after revascularized surgery in chronic occlusive cerebrovascular disease. First, a three-dimensional correlation map was generated, in which the value of resting CBF, the acetazolamide (AZ) response (= CBF increased by AZ loading minus CBF at rest), and the hyperventilatory (HV) response (= CBF decreased during HV minus CBF at rest) was plotted on X-, Y-, and Z-coordinates, representing the three variables, respectively. Second, the pixels were clustered by the agglomerate hierarchical method, and each pixel was assigned its cluster number. Finally, a clustered brain image was created by referring to the clustered 3-D correlation map, where each pixel in the brain was labeled with the color representing its cluster number. With this method, the stage of hemodynamic deficiency was evaluated in a patient with the occlusion of internal carotid artery and in another with moyamoya disease before and after revascularized surgery. With four clusters, four anatomically and pathophysiologically different areas were delineated: #1= normal cortex, #2= cortex with abnormal value in all three variables, #3= cortex with impaired vasodilative response to AZ and normal vasoconstrictive response to HV, #4= white matter. In both patients, the area of cluster #3 (impaired AZ and normal HV responses) in the pre-operative image turned into cluster #1 (normal) with revascularization in the post-operative image. In the patient with moyamoya disease, however, we observed that the area of cluster #3 apart from revascularized region turned into cluster #2 (abnormal). We consider that this method is useful for multivariate staging of hemodynamic deficiency in obstructive cerebrovascular disease and that it is suitable for objective representation of multiple PET parameters obtained in the activation study as well as in a study with ^{15}O labeled CO_2 , O_2 and CO gases.

PS-328

M. Mirza, A.Tutus, M. Kula, F. Erdogan
Erciyes University, School of Medicine, Depts of Nuclear
Medicine and Neurology, Kayseri, Turkey.

TECHNETIUM-99m HMPAO BRAIN SPECT IN UNMEDICATED PATIENTS WITH MIGRAINE WITHOUT AURA DURING INTERICTAL PERIOD: COMPARISON NORMAL CONTROL SUBJECTS

Migraine is considered to be a functional neurological disorder. Cerebral blood flow abnormalities are observed in cerebral blood flow studies during migraine attacks and pain-free intervals. Migraine with aura is more likely to present with persisting decreased HMPAO uptake during the headache-free intervals. We performed this study to evaluate the brain perfusion in unmedicated migraine patients without aura during the headache-free intervals. Total 44 migraine patients without aura (2 males, 42 females; 34.4 ± 7.2 years old) and 17 age matched normal controls (2 males, 15 females; 32.2 ± 12.2 years old) were included in the study. The SPECT imaging was performed after 20 minutes following the injection of 550 MBq Tc-99m HMPAO. Data were obtained with a LEAP collimator interfaced to computer system in a 64×64 matrix through 360° rotation at 6° intervals, for 30 s per arc interval. For the semiquantitative analysis of the data, rectangular region of interest (ROI) drawn over upper and lower frontal, temporal, parietal and occipital regions were used to obtain activity ratios, taking cerebellum as reference. Mean cortical/ cerebellar ratios (C/ C) calculated for each ROI in patient and control groups. There was no statistically significant difference flow abnormalities between two groups, but a clear interhemispheric asymmetry especially in the upper frontal and occipital parts of the brain was observed in migraineurs as compared to controls. It is suggested that an impaired regional cerebral vascular autoregulation may exist even during headache-free intervals in migraine patients without aura. We think that many factors may contribute to the development of migraine and it may be that migraine is not a single pathogenic entity.

Poster presentations

Neurology/Psychiatry: PET

PS-329

L. Bigic, L. Meyer, J. Fandino¹, Y. Yonekawa¹, G.K. von Schulthess

University of Zürich, Clinical Center, Department of Radiology, Division of Nuclear Medicine and Clinic for Neurosurgery¹, Zürich, Switzerland

DIAGNOSTIC ACCURACY OF FDG-PET IN EVALUATION OF LOW GRADE GLIOMAS

The aim of this retrospective study was to evaluate the clinical usefulness and accuracy of F-18-Fluoro-Deoxyglucose (FDG) and Positron Emission Tomography (PET) in confirming a clinically and radiologically suspected diagnosis of a low grade tumor.

Methods: From May 1994 to September 1997 totally 50 patients (age 2 to 77 ys) who were diagnosed with a „low grade tumor“ by FDG-PET were retrospectively evaluated. PET images were acquired with transmission correction 30 min. after IV injection of 92 to 268 MBq (mean 148 MBq) FDG and prospectively evaluated by visual examination only. „Low grade tumors“ were diagnosed if the lesion demonstrated less FDG uptake than the surrounding cortex. Retrospectively, clinical data were obtained and, the histologic diagnosis included whenever possible. The PET studies, which were incorrectly classified as „low grade gliomas“ were semiquantitatively analyzed by means of regions-of-interest (ROIs). According to the preoperative MRI or CT images, ROIs were drawn around the lesion and normalized to the contralateral white matter. Lesions with ratios of > 1.5 were considered to be „high grade“.

Results: Histologic diagnosis could be obtained in 44 patients (88 %). Thirty-one of these patients had histologically proven low grade gliomas (70 %), whereas seven patients showed histological evidence of high grade glioma (anaplastic astrocytoma n=3, GBM n=4). The other histopathologic diagnoses were as follows: 1 abscess, 2 gliosis, 1 hamartoma, 1 epidermoid tumor, 1 tuberoma. In 7 patients, only clinical and radiological follow up could be obtained. In 2 patients, disappearance of the lesions and blood analysis suggested inflammatory disease. One patient had radiologically proven multiple subcortical infarcts, 1 has had stable disease, suggesting a low grade tumor. Another patient showed stable disease for 10 months, but deteriorated afterwards and was diagnosed with a high grade glioma by histology. One patient died 3 months after the PET study, suggesting a high grade brainstem glioma. Semiquantitative data analysis of the high grade lesions (n=8) showed tumor to white matter ratios of 0.92, 1.06, 1.09, 1.14, 1.36, 1.43, 1.46 and 1.85. Therefore, semiquantitative analysis changed only one patient into the high grade group.

Conclusions: FDG-PET was able to correctly diagnose low grade tumors or non-tumorous lesions in 84 % of the patients. With semiquantitative data analysis, the diagnostic accuracy improved only in one case (to 86 %).

PS-330

^{*}K. Borbely, [^]RA. Brooks, ^{^^}T. Chase, P. Del Dotto, [^]P. Jacob, [^]R. Miletic
^{*}National Institute of Neurosurgery, Department of Nuclear Medicine, Budapest, Hungary; [^]National Institutes of Health, Neuroimaging Branch, ^{^^}Experimental Therapeutics Branch, Bethesda, USA

MAPPING OF CEREBRAL METABOLIC DYSFUNCTION IN ASYMMETRIC PARKINSONISM

PURPOSE: To assess quantitative information on cerebral metabolic dysfunction in early parkinsonism and, in particular, to differentiate metabolic changes in the basal ganglia by Positron Emission Tomography (PET) with 18-F-deoxyglucose (FDG).

METHODS: Twenty-two Parkinson's Disease (PD) patients who displayed predominantly or exclusively unilateral symptoms and thirteen age matched normal controls underwent PET scanning with a standard technique for each patient. Examinations were started following 185 MBq of FDG. Regional metabolic rates were obtained using a special software program. Templates containing a total of 242 circular regions of interest 8 mm in diameter were placed on these slices. Normalized rates were obtained by dividing the regional values by the whole-brain metabolic rate. The metabolic asymmetry for each region in the patient population was calculated by subtracting the ipsilateral (unaffected) rate from the contralateral (affected) rate and dividing by the ipsilateral rate. For normal subjects, the right side was arbitrarily chosen as the reference, so %asymmetry=100(L-R/R).

RESULTS: We found 7,8% hypermetabolism in the contralateral lenticular nuclei (p<0.0001) of the parkinsonian patients and the thalamic metabolism was bilaterally elevated by 13% (p<0.001). Metabolic changes in the caudate nuclei were small and not significant, either in terms of asymmetry or magnitude. The cortex generally showed a small metabolic asymmetry in the opposite direction (relative contralateral hypometabolism) (p<0.05). The putamenal asymmetry decreased with disease duration while the cortical asymmetry increased.

CONCLUSION: The results demonstrate in humans that hypermetabolism in the basal ganglia is found primarily in the lenticular nuclei, thereby validating the current theory of neurological effects of PD. The correlations with disease duration help to bridge the gap between differing reports in early and advanced parkinsonism. Due to its high sensitivity the PET-FDG method might be a useful and reliable diagnostic tool in differentiation patients for PD surgery.

PS-331

M. Bruchmeier (1,3), K.L. Leenders (1), J. Th. Locher (3), J. Missimer (1), U. Roelcke (1,3), A. Curt (2), V. Dietz(2)

(1) Paul Scherrer Institute, CH-5232 Villigen, Switzerland
(2) University Hospital Balgrist, Paraplegic Centre, CH-8008 Zürich, Switzerland
(3) Cantonal Hospital, Department of Nuclear Medicine, CH-5001 Aarau, Switzerland

ALTERED BRAIN ACTIVATION IN PARAPLEGIC AND TETRAPLEGIC PATIENTS DURING HAND MOVEMENTS. A [15-O]-H2O PET STUDY.

Objective: To assess plastic changes of the brain following deafferentation and deafferentation by spinal cord injury (SCI).

Background: The primary sensorimotor cortex (SMC) of the adult brain possesses a great capability to reorganize after deafferentation. Recent studies in men using transcranial magnetic stimulation have shown a re-mapping of the SMC after limb amputation, peripheral nerve blockades and SCI. Little is known, however, about plastic changes of deep brain structures and the cerebellar hemispheres in SCI patients.

Methods/Design: We studied the brain activation associated with two motor hand tasks in 7 paraplegic (PARA, mean age 32 yr, range 23 - 40 yr) and 7 tetraplegic patients (TETRA, mean age 26 yr, range 18 - 46 yr) and compared the results with 8 healthy subjects (CON, 27 yr, range 24 - 32 yr). Using [15-O]-H2O, we determined regional cerebral blood flow (rCBF) as a measure for neuronal activity. Auditively cued, repetitive hand extension and joystick movements were used as activation paradigms. Brain areas of significant (p<0.0001) rCBF increase during motor performance were identified by statistic parametric mapping (SPM).

Results: Hand movements of CON induced rCBF increases in the contralateral SMC and the supplementary motor area (SMA), and, during more complex joystick movements, in the ipsilateral cerebellum. The maximum activation in the contralateral SMC of 7 PARA shifted towards the deafferented "leg cortex". There was abnormal bilateral activation in the thalamus and cerebellum, and to a lesser extent in the insula, the inferior parietal cortex and the putamen. Less successful hand extensions of TETRA led to little activation in the SMC and the SMA, whereas the better performed joystick paradigm caused an abnormal brain activation pattern similar to PARA.

Conclusions: Tetraplegic and surprisingly also paraplegic patients (with a normal motor hand performance) show an abnormal brain activation pattern during hand movements. These changes are most likely a consequence of a partial body disconnection by the SCI. Our findings confirm expected plastic changes within the SMC, but the involvement of deep brain nuclei and the cerebellum is surprising. Data suggest that pathological thalamic and cerebellar activation results in secondary reorganisation of cortical (SMC) and subcortical circuits.

PS-332

Sheng-Pin Changlai, C.H. Kao

Chung Shan Medical & Dental College Hospital

Department of Nuclear Medicine

FDG-PET AND Tc-99m HMPAO SPECT OF BRAIN IN SJOGREN'S SYNDROME

Involvement of the brain is one of the most important complications of Sjogren's syndrome (SS). However, diagnosis of brain involvement in SS patients is difficult due to the lack of effective imaging methods.

Sixteen primary females SS patients (age 30 to 61 years) with neuropsychiatric manifestations, but normal brain MRI findings were enrolled in this study. FDG-PET (30min after IV of 10 mCi FDG, GE advance PET scanner) and Tc-99m HMPAO SPECT (1hr after IV of 30mCi Tc-99m HMPAM, Elscint Helix with a fan-beam collimator) were performed in the 16 SS patients to detect glucose metabolism of the brain and regional cerebral blood flow (rCBF).

The results show that (1) Tc-99m HMPAO SPECT findings were abnormal in 13 (81%) patients. Parietal (11,69%) and temporal lobes (9,56%) were the most common areas of involvement. Basal ganglia (5,31%), frontal lobe (4,25%), and occipital lobe (3,19%) were less common areas of brain involvement. (2) FDG-PET findings were abnormal in 3 (19%) patients. Temporal lobes (3,19%) were the most common areas of brain involvement.

In our patients, no changes in anatomic structure of the brain were detected (normal brain MRI findings). We conclude that changes in rCBF are more sensitive to detection than metabolic changes in the brain, such as fluctuations in glucose metabolism, in SS patients with brain involvement.

PS-333

K.Ahmed, T.Inoue, K.Tomiyoshi, M.Sarwar, N.Oriuchi, H.Mizunuma, and Keigo Endo, Gunma University, School of Medicine, Department of Nuclear Medicine, Showa Machi, 3-39-22, Maebashi Shi, Gunma Ken, Japan.

COMPARATIVE STUDY OF PET AND QUANTITATIVE DIGITAL RADIOGRAPHY(QDR) IN DETECTING EFFECTS OF AGING AND DIET ON BONE METABOLISM OF GUINEA PIG.

The purpose of this study was to compare PET and QDR in detecting the effects of aging and diet on bone metabolism. Bone imaging of guinea pigs was performed with ¹⁸F fluoride ions using a high-resolution animal PET system to analyze bone metabolism quantitatively in different age groups of guinea pigs, young, adult aged groups and also in a dietary manipulation group (low calcium and low vitamin D3 diet for 1, 2, and 3 weeks). A three-compartment kinetic model was applied for the analysis of bone metabolism to evaluate the rate constant (K, K1--K4). There was a significant difference in K-constant between the young and other groups. The K-constant was higher(0.100 ± 0.005ml/min/ml) in the young group than in adults(0.028 ± 0.001 p<0.001) and the aged group(0.047 ± 0.020). This high value of the K-constant in the young group may indicate high turnover in bone metabolism. Bone mineral density (BMD) was lower in the young group (0.15 ± 0.026 g/cm²) than in the adult (0.230 ± 0.021)(p<0.001) and aged groups (0.26 ± 0.03). Although there was no difference in BMD between the control and dietary manipulation groups, PET study revealed a significant difference in K-constant between them (0.028 ± 0.001 vs 0.090 ± 0.009 ml/min/ml)(p<0.001). The quantitative skeletal dynamic PET study with ¹⁸F fluoride ions was more sensitive and superior in the early detection of metabolic disorders in bone disease than QDR.

PS-334

M. Holschbach*, C. Boy[§], H. Herzog[§], W. Wutz*, T. Schmitz[§], H. Mühlen-siepen[§], J. Shah[§], M. Grosse-Ruyken[§], M. Cremer[§], H.-W. Müller-Gärtner[§], R.A. Olsson*, H.H. Coenen*
 Institute für *Nuklearchemie und [§]Medizin, FZ Jülich GmbH, D-52425 Jülich; [†]Dpt. of Int. Medicine, University of South Florida, Tampa, FL, 33612

PRECLINICAL EVALUATION OF THE NEW A1 ADENOSINE RECEPTOR (A1AR) ANTAGONIST [18F]8-CYCLOPENTYL-1-PROPYL-3-(3-FLUORO-PROPYL)XANTHINE ([18F]CPFPX)

The A1AR plays an important role in central neuromodulation and perhaps in the pathogenesis of neuropsychiatric diseases. The present study evaluated the feasibility of imaging A1AR using the new antagonist, [18F]8-cyclopentyl-1-propyl-3-(3-fluoropropyl)-xanthine ([18F]CPFPX, s.a. 7.5 Ci/μmol) in different rodents ex vivo and primates in vivo. In rat brain autoradiographs a high accumulation of radioactivity can be demonstrated for several regions including thalamus, striatum, cortex, and cerebellum. I.v. blockade of A1AR by the specific antagonists 8-cyclopentyl-1,3-dipropylxanthine CPX and N-0840 or by carrier added [18F]CPFPX (s.a. 8, 40 and 200 Ci/mmol) indicates reversible specific binding (SB) of [18F]CPFPX to A1AR in cortical and subcortical regions of interest. In rodent blood at least two polar metabolites were formed during 60 min after tracer application. Analysis of brain homogenates showed that >98% [18F]CPFPX remained intact. The influence of two anesthetics (methohexital and isoflurane) on the binding of [18F]CPFPX to A1AR in the rat brain was examined. The distribution pattern of [18F]CPFPX was unchanged, however, the brain uptake under isoflurane was 50% higher than under methohexital. The biodistribution of [18F]CPFPX was studied with positron emission tomography (PET) in the baboon (*Papio hamadryas*, n=3) anesthetized by isoflurane. Measurements of regional radioactivity and sampling of arterial blood for metabolite analysis continued for 60 min after the i.v administration of [18F]CPFPX, 0.8 mCi/kg, 28 ng/kg. Overlays of PET scans on whole body MRIs identified regions of interest (ROIs). Residual radioactivity (% iD/g) 40 min after [¹⁸F]CPFPX injection was: lower intestine ≤ 0.005, brain ≤ 0.005, heart ≤ 0.008; liver ≤ 0.037 kidneys ≤ 0.046; gallbladder ≤ 0.6. At 0.5, 1, 2, 3, 5, 10, 20 and 60 min the relative plasma fraction of unchanged [18F]CPFPX was 92, 91, 83, 67, 44, 31, 22 and 11%. The binding pattern in brain corresponds to the known distribution of A1AR and suggests that [18F]CPFPX may be a suitable radioligand for the non-invasive imaging in investigational and clinical PET.

PS-335

K.H. Ma, S.D. Wang, S.Z. Lin, W.S. Huang, C.W. Chang, S.E. Wang, J.C. Peng, R.S. Liu, and J.C. Liu. National Defense Medical Center, Taipei Veterans General Hospital, National PET/Cyclotron Center, Taipei, Taiwan, R.O.C..

ESTABLISHMENT OF PARKINSONIAN SWINE MODEL FOR POSITRON EMISSION TOMOGRAPHIC STUDY

Parkinson's disease (PD) is a progressive neurodegenerative disorder characterized by the motor disturbance. This experiment was undertaken to establish an animal model for basic investigation of positron emission tomographic (PET) studies of human PD. Swine (*sus vittatus*) was selected for this experiment due to its long life span, comparable dopaminergic system with human's and abundant source. Lesion was created by unilateral injection of 6-hydroxydopamine (6-OHDA) into medial forebrain bundle under MRI guide to eliminate the dopamine content of corpus striatum. Repair surgery was performed by grafting swine fetal ventral mesencephalic tissues (from 22 to 26 days of embryos) into dopamine-denervated striatum. Amphetamine-induced rotation, [F-18]-6-fluoro-L-DOPA PET scan, and immunocytochemistry were used to evaluate the severity of the lesion and the effectiveness of the lesion and graft surgery. After unilateral injection of 6-OHDA, swine developed amphetamine-induced ipsilateral rotations. PET study found significant decrease of radiouptake at the lesion side. Immunocytochemical study also showed significant decrease of tyrosine hydroxylase (TH) immunostaining at both ipsilateral striatum and substantia nigra compacta. The increased glial fibrillary acidic protein immunostaining represented reactive astrocytes at the striatum lesion site. One to 2 months after graft surgery, PET scan showed increased uptake at the grafted area. The rotational behavior was decreased. TH immunostaining indicated that grafts survived in the host striatum. Notably, the incomplete lesions could cause spontaneous recovery, but the degree of their recovery was less remarkable than that of the grafted group. The results of [F-18]-6-fluoro-L-DOPA PET scan, amphetamine-induced rotation, and immunocytochemistry provide convincing evidence that the swine can be a useful animal model for PET studies of human PD.

PS-336

J.S. Lee, D.S. Lee, S-K. Lee, H. Nam, S.K. Kim, J.M. Jeong, K.S. Park, J-K. Chung, and M.C. Lee
 Seoul National University, Department of Nuclear Medicine, Neuropsychiatry, and Biomedical Engineering, Seoul, Korea.

LOCALIZATION OF NEURAL BASIS FOR VERBAL AND VISUAL WORKING MEMORY IN HUMAN HEALTHY VOLUNTEERS.

To localize and compare the neural basis of verbal and visual human working memory, we performed functional activation study using O-15 water PET. Repeated PET scans with successive four tasks, which consist of one control and three different activation tasks, were performed on six right-handed normal volunteers during 2 min with bolus injections of 925MBq O-15 water at intervals of 30 min. Each activation task was composed of 13 matching trials to activate the brain regions associated with verbal or visual working memory. On each trial, four targets, a fixation dot and a probe were presented sequentially. Subject's task was to press a response button to indicate whether or not the probe was one of the previous targets. Short meaningful Korean words and simple drawings, which evoke the association of specific words in mind, were used as matching objects for verbal memory (VERBAL I and II, respectively) and monochromic pictures of human faces were used for visual memory (VISUAL). One control task was performed before the activation tasks to remove the effect of visual stimulation and activation due to the movement of finger to push the button. All images were spatially normalized and the differences between control and activation states were statistically analyzed using SPM96. The verbal working memory tasks activated predominantly left-sided structures, and the visual memory activated right hemisphere. Areas of significant activation (P<0.05) identified by SPM are tabulated with their Z-scores.

	BA	VERBAL I	VERBAL II	VISUAL
Left Broca's & Premotor	44, 6	2.89	3.35	
Superior Temporal	22		3.35	
BG & Thalamus			2.85	
Cerebellum		2.85	2.67	
Right Inferior Frontal	47, 44		2.08	3.26
Cingulate	23, 31, 32	2.64	2.71	3.02
SMA & Premotor	6			2.65
Superior Parietal	7			2.20

The results are consistent with the hypothesis of the laterality and dissociation of the verbal and visual working memory from the invasive electrophysiological studies and emphasize the pivotal role of frontal cortex and cingulate.

PS-337

G.-J. Meyer, R. Höfs, W. Burchert, J. van den Hoff, and W. H. Knapp.
Klinik für Nuklearmedizin der Medizinischen Hochschule Hannover

NORMAL VALUES OF [¹¹C]-L-METHIONINE TRAPPING IN GREY AND WHITE MATTER OF THE CORTEX AND IN THE CEREBELLUM

The rate constants of methionine trapping were determined in at least 10 brain regions of each of 98 patients who received positron emission tomography with L-11-C-methionine. The regions were localized and sized according to anatomically identifiable structures down to a size of about 2 cm². Quantitative analysis was performed using the Gjedde-Patlack method. For the analysis of rate constants in normal brain, regions of interest were placed in areas which according to CT, MRI and PET were opposite and at least 5 cm apart from any confirmed or suspected malignant process.

To analyse any effect of the established or suspected disease on the data in normal brain regions, patients were grouped in three classes: Patients with highly malignant processes (n=32) patients with mildly malignant processes (n=35) and patients without malignant processes (n=31). No significant differences were found in the three groups.

Rate constants in grey and white matter as well as in cerebellum varied by ±35% in all three groups. The mean values are 0,0291 min⁻¹ for grey matter, 0,0157 min⁻¹ for white matter and 0,0282 min⁻¹ for the cerebellum. The differences in the brain regions are typical and correlate significantly in all three patient groups. Other brain structures with significantly elevated rate constants are the occipital visual cortex and the pituitary gland. The individual right left symmetry varies by 4,9%±4,4%. The ratios of grey over white matter and grey matter over cerebellum are very stable in all three patient groups with an overall variability of less than 10%.

The larger inter-patient variability is due to individual differences in the systemic methionine concentration, which, on average, is in the order of 21 μmol/l, but may vary more than twofold with the nutritive status.

The results confirm that rate constants of amino acid trapping in brain and especially the ratio of these constants in grey and white matter are a stable physiological parameter. Knowledge of its variability in normal brain tissue is a prerequisite, however, before it can be used as a tool for the detection of pathophysiological states.

PS-338

A. Newberg, A. Alavi, C. Clark.

Hospital of the University of Pennsylvania, Philadelphia, PA, Division of Nuclear Medicine and Department of Neurology

THE METABOLIC IMAGING SEVERITY RATING SCALE (MISRS) IN ALZHEIMER'S DISEASE: COMPARISON WITH QUANTITATIVE DATA.

Purpose: FDG PET imaging studies have been frequently utilized to examine patients with suspected Alzheimer's disease (AD) to determine severity. We previously described a qualitative scoring system which correlated well with tau protein levels and severity of cognitive dysfunction. We now present a validation of this method by comparing the qualitative scores with quantitative data.

Methods: FDG PET scans on 10 well characterized patients with AD were acquired on the PENN-PET scanner 40 minutes following the intravenous administration of 8mCi of FDG. All FDG-PET scans were read blindly by an experienced reviewer and the MISRS consisted of a four point scoring system of the activity of the temporal, frontal, and parietal areas and dividing the sum of these scores by the sum of the scores for the basal ganglia, thalami, cerebellum, visual cortices, and sensorimotor areas. A template with regions of interest (ROIs) was developed to determine the activity in the brain structures described above. Counts were obtained for each slice on which a given region appeared. A comparison was then made between the qualitative scores and the quantitative values for individual regions and for the MISRS. These values were also compared to the Dementia Severity Rating Score (the DRS is a functional measurement incorporating both cognitive impairment and activities of daily living), and the level of Tau protein in the cerebrospinal fluid as determined by enzyme linked immunosorbent assay. **Results:** The values obtained for the quantitative MISRS correlated highly with the qualitative MISRS (R=0.95, p=0.00002). The quantitative MISRS correlated inversely with the level of Tau protein (R = 0.76, p=0.046) and the DRS (R = 0.84, p=0.02) which are values similar to those obtained with the qualitative MISRS. **Conclusion:** The results of this study quantitatively validated a simple and practical rating scale that can be used to assess severity of cognitive dysfunction in AD. This approach may provide a means to stage the disease when initially diagnosed and follow the natural course of the disease with or without medical intervention.

PS-339

K. Oda, H. Toyama, K. Uemura*, Y. Ikoma*, M. Senda, K. Kitamura**
Positron Medical Center, Tokyo Metropolitan Institute of Gerontology,
*Waseda Univ., **Shimadzu Co.,

COMPARISON OF PARAMETRIC IMAGES RECONSTRUCTED BY FILTERED BACKPROJECTION AND OS-EM ALGORITHM IN ¹⁸F-FDG PET DYNAMIC STUDY

Filtered backprojection (FBP), which is universally used for reconstruction of emission tomography, tends to increase image noise and generate streak artifacts. Recently, ordered subset expectation maximization (OS-EM) algorithm was developed as a reconstruction algorithm free from streak artifacts and reasonably fast.

We have applied OS-EM to an ¹⁸F-FDG PET dynamic study to generate parametric images. A 45min dynamic scan was performed starting injection of 86-223MBq of FDG using a 2D PET scanner. The images were reconstructed using these two algorithms. OS-EM was performed with 3 iterations and 16 subsets. All images were smoothed by the Butterworth filter (cutoff 0.125cycle/mm and order 2). We calculated K1, k2 and k3 images using Marquardt method, and compared them between OS-EM and FBP.

When the images were reconstructed with OS-EM, as compared with FBP, the fitting error was equally affected by injected dose. The parametric images by OS-EM did not correlate well with those by FBP, possibly due to different noise characteristics. The result suggest that more work is required to use OS-EM images quantitatively for kinetic analysis.

PS-340

M.Tashiro¹, M. Itoh¹, H. Ota¹, T. Fujiwara¹, H. Nagasawa², Y. Takahashi³

¹Cyclotron Radioisotope Center, Tohoku University, Sendai, Japan

²Miyagi University, Miyagi, Japan. ³Tohoku-Gakuin University, Sendai, Japan

FDG-PET APPLICATION FOR SPORTS NEUROPHYSIOLOGY AND PSYCHOLOGY

PET with ¹⁸F-fluorodeoxyglucose (FDG) can be a powerful tool to analyze regional cerebral metabolism during exercise, because experiments can be carried out apart from a PET scanner due to metabolic trapping. The aim of this study is to see the regional changes in glucose uptake during running.

Subjects were right-handed 8 healthy male volunteers, aged from 19 to 40 years (24.3 ± 7.5 years) who consisted the running group and eight males (31.0 ± 12.1 years) as the controls. Subjects in the running group were asked to run outside on the road for 20 minutes after intravenous injection of FDG. Subjects were examined just after running for emission and transmission scans. The brain image data were realigned and normalized using Statistical Parametric Mapping Software Package 96 (SPM96), and comparison was performed between the running and control groups, using ANCOVA.

The results showed relative activation of certain brain regions including the supramarginal gyrus (Brodmann's areas 40), the supero-posterior parietal cortex (BA 5 and 7), the occipital visual cortex (BA 17, 18 and 19), and the premotor cortex (BA 6), and the cerebellar vermis. Relative deactivation was observed in the basal frontal cortex (BA 10/11), putamen, cerebellar hemisphere and the anterior and inferior temporal gyri (BA 20/21).

The supramarginal gyrus, the supero-posterior parietal cortex and the occipital visual cortex were relatively activated due to involvement in the "target recognition", including calibration of shifts in retinal images, execution of the body movement guided by the visual feedback, and multi-sensory integration of visual, auditory and proprioceptive inputs. The premotor area may be activated to be involved in "planning of actions" during running, where runner's center of gravity is continuously advancing and the legs must move at the right moment to support the body. Relative deactivation in the frontal cortex may explain euphoric state induced by running, and deactivation of the cerebellar vermis and putamen may be explained by adaptation to repetition of the same actions.

In summary, the higher sensory association cortex was more active than the motor cortex, and the premotor cortex was more active than the primary motor cortex. The present data may fit the previous understanding of neurophysiology on motor control and sports psychology. Our new technique will be useful in many researches in sports neurophysiology and psychology.

Neurology/Psychiatry: Dopamine + serotonin studies

PS-341

^{*}A.K. Borbely, ^{*}R.A. Brooks, ^{**}A. Gjedde, ^{**}D.F. Wong, ^{*}G. Di Chiro
^{*}National Institute of Neurosurgery, Department of Nuclear Medicine, Budapest, Hungary; ^{*}National Institutes of Health, Neuroimaging Branch, Bethesda, ^{**}Aarhus University Hospital, PET Center, Denmark, ^{**}Johns Hopkins Medical Institutions, Department of Radiology, Baltimore, USA

¹¹C-N-METHYL-SPIPERONE PET STUDY OF MPTP-INDUCED PARKINSONISM UNDER AND OFF L-DOPA THERAPY

¹¹C-N-Methyl-Spiperone (NMSP) is a radioligand which binds to serotonin HT_{2A} receptors with comparatively low affinity and to dopamine D_{2,4} receptors with comparatively high affinity.

PURPOSE: To determine if NMSP dynamics in Parkinsonism are altered by L-DOPA therapy.

MATERIALS AND METHODS: A case of MPTP-induced Parkinsonism was studied with Positron Emission Tomography (PET), using tracer NMSP as a dopamine receptor ligand. The first study was performed after L-DOPA medication had been suspended for three days, and the second was done seven days later, five days after restarting medication; the dose was 80 microgram NMSP (1.14 ug/kg). PET serial scanning began 1 minute after injection, with six 5 minute scans, two 10 minute scans, and one 30 minute scan. The time activity curves were analyzed to obtain estimates of k₃, the apparent binding rate constant of the irreversible NMSP binding to dopamine D_{2,4} receptors in the putamen, and p_B, the binding potential of the reversible binding of NMSP to serotonin HT_{2A} receptors. The time-activity curves were fitted by an operational equation of the reference region model of irreversible binding.

RESULTS: There was a slight clinical deterioration after the first study, and a marked but temporary clinical deterioration after the second study. The stronger clinical effect in the second study (on-medication) is consistent with the higher putamenal concentration of NMSP (12pmol/cc versus 8pmol/cc) and an increased (by 17%) rate constant k₃. However the dynamic analysis showed no sign of receptor saturation.

CONCLUSION: The absolute NMSP concentration in the basal ganglia is usually not reported. However, because of the clinical response, these values were very much of interest. The increased clinical effect is consistent with increased NMSP uptake and the larger k₃ value. Its duration suggests a binding lifetime of NMSP of at least one day. The results show that "tracer" NMSP doses should be kept well under 1 microgram/kg in subjects with impaired dopaminergic systems.

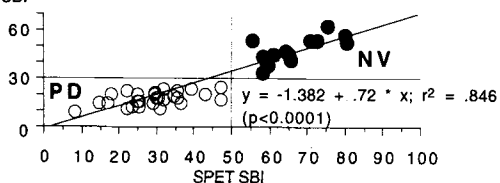
PS-342

D.C. Costa, Z. Walker, S. Dizdarevic, C. Ioannides, S. Gacinovic, R.W. Walker, A.G.M. Janssen, C.L.E. Katona.
 UCL Medical School, London, UK and Cygne bv, Eindhoven, The Netherlands.

STRIATAL BINDING INDEX OF FP-CIT: A SIMPLE METHOD TO SEPARATE PARKINSON'S DISEASE PATIENTS AND CONTROLS.

In this study we investigated the feasibility of a simple method to distinguish patients with Parkinson's disease (PD) from control subjects, in this case normal volunteers (NV). 14 drug naive PD patients (6 males, 8 females; age range 46-70; Hoehn and Yahr range 1-3) and 7 NV subjects (5 males, 2 females; age range 27-73) were investigated with [¹²³I]-2β-carbomethoxy-3β-(4-iodophenyl)-N-(3-fluoropropyl)nortropine (FP-CIT) and single photon emission tomography (SPET). A single detector gamma camera computer system (GE XCT) was used to acquire 36x40 seconds views on a 360 degree circular rotation, starting on an anterior projection. After reconstruction, a 3.3 cm transaxial brain section comprising the striatum (BG) was used to calculate the Striatal Binding Index (SBI)=[BG-Bk]x100/Bk on the right (R) and left (L) hemispheres. Background (Bk) was sampled from the occipital cortex. A similar index was calculated using the first (anterior) projection (planar image) and the fronto-parietal cortex above the BG as Bk. The results demonstrated good correlation between the tomographic (SPET) and planar SBI with clear-cut separation between PD and NV, as shown in the following plot:

Planar SBI



In conclusion, these preliminary data demonstrate the potential utility of a simple method to calculate SBI using planar imaging and FP-CIT to distinguish PD from NV. Further studies are necessary to confirm the validity of this method for wider clinical routine application.

PS-343

S. Dressel, M.-P. Kung, X.-F. Huang, K. Plössl, C. Hou, S. K. Meegalla, G. Patselas, M. Mu, J. Saffer, H. F. Kung

Department of Radiology, University of Pennsylvania, USA

SIMULTANEOUS SPECT STUDIES OF PRE- AND POSTSYNAPTIC DOPAMINE BINDING SITES IN BABOON'S BRAIN

The CNS dopamine transporters (DAT) and dopamine D₂/D₃ receptors are implicated in a variety of neurological disorders and are also targets for many drugs. With the development of [^{99m}Tc]TRODAT-1, imaging studies using this ligand for DAT imaging can be complemented by co-injection of a I-123 labelled D₂/D₃ receptor ligand to assess both pre- and postsynaptic sites of the dopaminergic system, simultaneously.

Striatal phantom studies were employed to determine optimal energy window settings and to measure cross-contamination between the two isotopes. Twelve SPECT scans were performed in two baboons after iv injection of 740 MBq [^{99m}Tc]TRODAT-1 and 185 MBq [I-123]IBZM or IBF using a triple-head gamma camera (Picker Prism 3000) equipped with UHR-fan beam collimators (scan time: 0 - 210 min.). Two sets of SPECT data were obtained by using energy windows of 15% centered on 140 keV for Tc-99m and 10% asymmetric starting at 159 keV for I-123. After coregistration with MRI, ROI analysis was performed using predefined templates from coregistered MRI. In blocking studies baboons were pre-treated with CFT (14 mg) or raclopride (14 mg).

In the phantom measurements, it was observed that 14.9% of I-123 counts measured in the I-123 window contributed to the counts in the Tc-99m window and 0.54% of the Tc-99m counts measured in the Tc-99m window contributed to the counts in the I-123 window. Image quality of dual-isotope baboon studies was similar to those obtained from single-isotope studies. When one site was blocked with CFT or raclopride, the binding of the respective ligand to the other site was not affected. Semi-quantitative analysis corrected for cross-contamination did not show any statistically significant differences compared to the uncorrected analysis.

This is the first example that clearly demonstrates the feasibility of simultaneous imaging of both pre- and postsynaptic sites of the dopaminergic system in baboons with dual-isotope SPECT studies. With or without corrections for cross-contamination of I-123 into the Tc-99m window, striatum/cerebellum ratios of dual-isotope experiments did not differ significantly from single-isotope experiments. This method may provide a valuable and cost effective tool to gain comprehensive information about the dopaminergic system in one session.

PS-344

J.W. Babich, A. Kozikowski*, G.L. Araldi*, D.R. Elmaleh, A.J. Fischman. Massachusetts General Hospital, Division of Nuclear Medicine and *Georgetown University.

INITIAL PHARMACOKINETIC EVALUATION OF POTENTIAL ANTI-COCAINE MEDICATIONS, PIPERIDINE-3-CARBOXYLIC ACID ESTERS, USING PET

Compounds which inhibit cocaine binding to the dopamine transporter without completely inhibiting dopamine transport may have value in the treatment of cocaine addiction. Piperidine-3-carboxylic acid esters with a phenyl group in position 4, have been shown to inhibit WIN 35,428 binding to the dopamine transporter (DAT) and [³H]dopamine uptake. These structures may be viewed as truncated versions of the WIN series compounds, i.e., they lack the two-carbon bridge of tropanes. To evaluate the DAT selectivity of these agents in vivo they were labeled with C-11 and imaged by PET in monkeys.

The cis and trans isomers of 2-[4-chlorophenyl]-3-carbomethoxy-N-methyl-piperidine were labeled via N-methylation. C-11 methyl iodide was bubbled into solutions of the nor-methyl isomer (1.5 mg free base in 0.3cc DMSO) and the mixtures were heated at 110°C for 7 min. The products were isolated by C-18 reverse phase HPLC and formulated in saline for injection. After passage through a 0.22µm filter, the sterile products were administered to three Rhesus monkeys and dynamic PET images were acquired over 90 minutes.

The C-11 labeled drug was produced in good radiochemical yield [-15%@EOS]. Radiochemical purities of the final products were >98% and specific activity were routinely >2,000 mCi/µmole [EOS]. Both isomers accumulated rapidly in the striatum with the cis isomer exhibiting greater nonspecific accumulation in the cortex. Studies with low specific activity tracer showed reduced striatal-to-cerebellar ratios compared with high specific activity preparations. When unlabeled CFT was administered 60 minutes after injection of the trans isomers, a selective decrease in the striatal activity was observed; consistent with the in vivo binding to the DAT.

These results establish that both the cis- and trans isomers of 2-[4-chlorophenyl]-3-carbomethoxy-N-methyl-piperidine have high levels of specific binding to striatal DAT sites; a characteristic that supports their investigation as agents for treating cocaine addiction.

Poster presentations

PS-345

J. Grétarsdóttir, H. Ekelund, B. Holmberg, S. Lindegren and C. Wikkelso.

Hospital: Sahlgrenska University Hospital, Göteborg, Sweden, Departments of Radiation Physics, Neurology and Pharmacy.

KINETICS OF D2-RECEPTOR LIGAND 123-I-NCQ298 IN HEALTHY VOLUNTEERS AND PATIENTS WITH PARKINSONIAN SYNDROMES.

The D2-receptor ligand 123-I-NCQ298 (123-I-iodo-5,6-dimethoxy-N-[(1-ethyl-2-pyrrolidiny)methyl]-salicylamide) is a radiofarmaceutical for visualizing the dopamine uptake sites in the brain. A quantitative evaluation of the uptake of 123-I-NCQ298 could contribute to the understanding of pathophysiology and differential diagnosis in parkinsonian disorders affecting the dopaminergic pathways in the brain. **Aim:** To study the kinetics of 123-I-NCQ298 in healthy volunteers and patients with parkinsonian syndromes such as Parkinson's disease (PD), progressive supranuclear palsy (PSP) and multiple system atrophy (MSA). **Method:** Six healthy volunteers (age 37 -56 y.), and 9 patients with different parkinsonian syndromes (2 PD, 3 PSP and 4 MSA, age 49-75 y.) were iv. injected with 50-140 MBq 123-I-NCQ298. Tomographic registrations (GE Neurocam) of the head were performed several times between 1.5 and 20 h. p.i. in the healthy volunteers and 4 h. p.i. in the patients. For the volunteers whole body scans (GE MAXXUS) were performed upto 20 hours p.i. **Results:** The uptake of 123-I-NCQ298 in the basal ganglia at 4 hours p.i., corrected for decay, injected amount and body weight, was 4.3 (2.3) c/MBq/kg (mean value (1 SD)) for the healthy volunteers and 4.4 (2.5) c/MBq/kg for all patients. The specific unspecific binding in a reference region was 0-1 count per pixel. The whole body retention of 123-I-NCQ298 was in average 63 % at 20 hours p.i. **Discussion:** The kinetics of 123-I-NCQ298 implies a possibility to estimate the density of the D2 receptors in the basal ganglia of healthy volunteers as well as patients. The specific/unspecific binding ratio was favorable with 123-I-NCQ298. Further studies are needed to investigate uptake values for the various parkinsonian syndromes.

PS-346

W.S. Huang, K.H. Ma, S.P. Wey, S.Z. Lin, G.Ting, R.S. Liu, and J.C. Liu
National Defense Medical Center, Institute of Nuclear Energy Research,
Departments of Nuclear Medicine, and Biology and Anatomy Taipei,
Taiwan, R.O.C..

IMAGING OF DOPAMINE TRANSPORTERS WITH ^{99m}Tc TRODAT-1 IN EXPERIMENTAL PARKINSON'S DISEASE

Parkinson's disease (PD) is a progressive neurodegenerative disorder characterized by a selective loss of dopamine in the basal ganglia and substantia nigra. This investigation was undertaken to evaluate the potential usefulness of ^{99m}Tc TRODAT-1 in evaluating PD. The experimental PD was recreated in a non-human primate (monkey) by injection of 6-hydroxy-dopamine into the medial forebrain bundle under MRI guide to eliminate the dopamine content of the striatum (ST). A healthy monkey served as the control. The expression of parkinsonian behaviour and ¹⁸F-6-fluoro-L-DOPA PET scan were used to evaluate the severity of the lesion. ^{99m}Tc TRODAT-1 was prepared from a lyophilized kit. After intravenous injection of the radiotracer (925 MBq), SPECT imagings were acquired over 4 hr using a Helix camera with fan-beam collimators. The preliminary results showed that a high radiouptake was found in the ST of the control. The radiouptake in the ST of the parkinsonian monkey was obviously decreased when compared with the control. The radiouptake ratios of ST/cerebrum and ST/cerebellum at 90-120 min postinjection were 1.7 and 2.1 in the diseased monkey, and 3.2 and 4.3 in the control. Notably, there was also a high radiouptake in the nasal area and parotid glands which suggested that dopamine transporters might exist in these areas. The ST/nasal area and ST/parotid gland ratios in the diseased and control monkeys at 90-120 min postinjection were 0.7, 0.9 and 1.2, 1.9 respectively. We, thus, considered ^{99m}Tc TRODAT-1 as a potential radiotracer in evaluating changes in dopamine transporters for patients with PD.

PS-347

Y. Nakabeppu, M. Nakajo, M. Mistuda*, S. Tsuchimochi, A. Tani, M. Osame*

Hospital: Kagoshima University, Departments of Radiology and*The Third Internal Medicine, Faculty of Medicine

IODINE-123-IODOBENZOFURAN(I-123-IBF) SPECT IN PATIENTS WITH PARKINSON'S SYNDROME(PS)

I-123-IBF is a dopaminergic antagonist which is suitable for SPECT imaging of D2 receptors. Purpose of this study is to evaluate the potential usefulness of quantitative parameters obtained from brain SPECT data of I-123-IBF for differential diagnosis in patients with PS.

Subjects were 10 patients with PS: 5 patients with Parkinson's disease (PD), 2 patients with striato-nigral degeneration (SND), 2 patients with progressive supranuclear palsy (PSP) and one patient with olivoponto-cerebellar atrophy (OPCA). The data were acquired with a triple-head gamma camera (Shimadzu, Prism3000, 128x128 matrix, high resolution fan-beam collimators, 1 projection/30 sec x90) at 2 hours after venous injection of 167 MBq of I-123-IBF. Transverse images were reconstructed using filtered backprojection and attenuation correction was performed using Chang's method ($\gamma=0.08$). Net binding index (NBI), the basal ganglio-to-frontal cortex ratio (GFR) and the basal ganglio-to-occipital ratio (GOR) were calculated from the data of the ROIs on the basal ganglia, the frontal cortex, the occipital cortex and background as quantitative parameters. The average and SD values of NBI, GFR and GOR in each disease group were as follows: 81.7 ± 13.0, 1.47 ± 0.18 and 1.57 ± 0.15 in PD, 36.5 ± 8.0, 0.62 ± 0.14 and 0.79 ± 0.10 in SND, 68.9 ± 11.6, 1.33 ± 0.37 and 1.60 ± 0.33 in PSP and 76.5, 1.51 and 1.91 in OPCA. Values of NBI, GFR and GOR were lower in SND than in the other disease groups. The quantitative parameters (NBI, GFR and GOR) obtained from brain SPECT data of I-123-IBF may be useful for differential diagnosis in patients with PS.

PS-348

J. Booij, R.J.J. Knol, L. Reneman, K. de Bruin, E.A. van Royen.

Graduate School of Neurosciences, Department of Nuclear Medicine, Academic Medical Center, University of Amsterdam, Amsterdam, The Netherlands.

[123I]NOR-β-CIT BINDS TO THE SEROTONIN TRANSPORTER IN VIVO AS ASSESSED BY BIODISTRIBUTION STUDIES IN RATS.

Because serotonergic function has been implicated in the pathophysiology of a number of diseases of the nervous system, efforts to image this system in vivo have received considerable attention recently. Promising preliminary results with the tracer 2β-carbomethoxy-3β-(4-iodophenyl)nortropane ([123I]nor-β-CIT), have prompted us to perform further studies. [123I]nor-β-CIT, a radioiodinated analogue of [123I]β-CIT with in vitro a tenfold higher affinity (IC₅₀=0.36 nM) to the serotonin (5-HT) transporter than [123I]β-CIT, was evaluated as an agent for the in vivo labelling of 5-HT transporters by biodistribution studies in rats. Intravenous injection of [123I]nor-β-CIT resulted in high accumulation of radioactivity in the 5-HT transporter-rich regions and striatum. Hypothalamus to cerebellum and striatum to cerebellum ratios were 4.5 and 6.8 at 240 min, respectively. While striatal uptake of radioactivity after injection of [123I]nor-β-CIT was blocked significantly by GBR12,909 (a selective dopamine transporter agent) but not by fluvoxamine (a selective serotonin transporter agent), the opposite was observed in brain areas known to be rich of serotonin transporters.

The results of this study indicate that [123I]nor-β-CIT, although not being a selective radioligand, binds specifically to the 5-HT transporter in vivo and thus suggest that [123I]nor-β-CIT promises to be a suitable radioligand for SPECT imaging of 5-HT transporters in humans.

Neurology/Psychiatry: Others

PS-349

D. Becerra García, M. Gómez Río**, R. Cabello*, B. Fernández Fernández, MA Hidalgo*, A. Rodríguez**, MC Bermúdez Morales, F. Casas*.
Hospital Universitario San Cecilio. Servicios de Medicina Nuclear y Neurología*.
Hospital Universitario Virgen de las Nieves. Servicio de Medicina Nuclear**.
Granada. SPAIN.

CEREBRAL PERFUSION CHANGES AND IMPAIRMENT OF COGNITIVE FUNCTIONS IN OBSTRUCTIVE SLEEP APNEA SYNDROME

Patients with Obstructive Sleep Apnea Syndrome (OSAS) are typically hypersomnolent during the daytime and impairment of cognitive executive functions has been suggested by some neuropsychological studies. Among typical symptoms of sleep apnea it is included snoring, restless sleep, excessive daytime somnolence, irritability, depression, memory deficits, inability to concentrate and decreased alertness. However, such functions have not been assessed directly. During apnea episodes has been described by magnetic resonance spectroscopy increased CBF and reduced arterial oxygen saturation with cerebral tissue hypoxia. Daytime sleepiness and impaired cognitive function can be a consequence of recurrent transient arousal from sleep and has been described associated with abrupt changes in the electroencephalogram (EEG) and evoked potentials (longer latencies frontally). Treatment of sleep apnea, primarily with continuous positive airway pressure (CPAV), reduces sleepiness and improves in cognitive function. The objective of the present study is to determine the association between chronic cerebral perfusion changes in OSAS patients with impairment of cognitive functions and posterior evolution after treatment with CPAV. We studied 35 OSAS patients suffering impairment of cognitive functions by ^{99m}Tc-HMPAO Brain SPECT in basal conditions. Qualitative analysis were performed by 4 nuclear medicine physicians. In case of presence of focal lesion a TC/MRI were made. The results shown the presence of a predominant pattern of heterogeneous distribution of radiotracer with multiple photopenic cortical lesions without predominant localization. Patients treated with CPAV showed improved cortical perfusion. These results suggest the presence of cortical perfusion alterations in OSAS patients with impairment of cognitive functions and the usefulness of ^{99m}Tc-HMPAO Brain SPECT to objective evolutive control after treatment.

PS-350

F. Chierichetti, P. Zanco, S. Cargnel, *A. Cagnin, *N. Freddi, *E. Sale, §P. Burra, §R. Naccarato, *M. Dam, *G. Pizzolato, G. Ferlin
Nuclear Medicine, Hospital of Castelfranco V. (TV), Italy,
*Dept. of Neurology and §Gastroenterology, University of Padua, Italy

CORTICAL METABOLIC DEFICITS IN PATIENTS WITH SUBCLINICAL HEPATIC ENCEPHALOPATHY (SHE) ARE REVERSED BY SUCCESSFUL LIVER TRANSPLANTATION: A [18F]FLUORODEOXYGLUCOSE (FDG) PET STUDY.

Objective: Brain functional alterations may be present in cirrhotic patients despite minor or absent neurological deficits. It is of utmost importance to detect such alterations in patients undergoing evaluation for liver transplantation. We used FDG PET to identify regional changes in brain glucose metabolism (rCMRglc) in patients with end-stage liver disease and with absent or minimal clinical symptoms of encephalopathy (SHE).

Methods: We studied 14 cirrhotic patients (mean age 50 ± 11 y) who were evaluated for liver transplantation and 8 age-matched control subjects using FDG PET (ECAT EXACT47). Five patients underwent a second PET study one year after successful liver transplantation. Cardiac input function was used for calculating rCMRglc in 19 cortical ROIs (identified by a semiautomated computer method taking as reference the Talairach stereotaxic co-ordinates), in the thalamus, caudate, putamen, and cerebellar hemispheres. Patients underwent a thorough neurologic, and neuropsychologic evaluation as well as EEG and CT/MRI scan of the brain.

Results: Neurologic examination and EEG were normal in all patients. CT/MRI showed mild atrophy in three patients with alcohol-related cirrhosis. rCMRglc was significantly reduced from control mean values in all the frontal and parietal ROIs assayed and in the supracalcarine region, whereas no significant changes were found in temporal ROIs, primary visual cortex, and subcortical regions. Mean values (μmol/100g/min) for all the assayed regions were 39.56 ± 0.95 in the control group and 21.48 ± 8.29 in the SHE patients group. Neuropsychologic evaluation showed prevalent impairment in visuospatial and frontal lobe-related abilities. In the group of patients who underwent liver transplantation rCMRglc values returned to near-control values in all examined regions. Mean values for all the examined regions in this group of transplanted patients was 39.59 ± 4.97.

Conclusions: PET shows that cortical functional alterations may be very common in patients with SHE. rCMRglc changes in frontal and parietal regions correlate with the pattern of prevalent neuropsychologic deficits. Cerebral metabolic deficits in SHE does not appear to be due to organic alterations since are completely reversed one year after successful liver transplantation.

PS-351

F. Chierichetti, U. Freo, *A. Cagnin, P. Zanco, S. Cargnel, *N. Freddi, D. Rubello, A. Fini, *G. Pizzolato, G. Ferlin
General Hospital: Neurology and Nuclear Medicine-PET Center, Castelfranco Veneto (TV), *Neurology Department, Padova Medical School, ITALY

The role of Positron Emission Tomography with 18F-fluoro-2-deoxy-D-glucose (FDG-PET) in the assessment of in Multiple Sclerosis (MS).

MS is a demyelinating inflammatory disease that causes brain tissue loss and motor and cognitive impairment. Measures of structure brain damage in MS, as assessed by MRI, do not correlate well with clinical measures of disability. We have used FDG PET to determine the regional cerebral metabolic rates for glucose (rCMRglc) in patients with MS; rCMRglc is an index of neuronal function that, hypothetically, could reflect accurately MS lesion impact on brain function.

Two groups (n = 7) of MS patients (Poser's criteria) with (MS+) or without (MS-) cognitive impairment but otherwise matched for demographic features, disability and depression severity, and one group of healthy controls were evaluated in regard to neuropsychiatric functioning, white matter hyperintensities (WMHI) and rCMRglc. Degree of disability and depression and neuropsychiatric performances were assessed by 21 tests and scales including EDSS, Ham-D, Full WAIS; WMHI were estimated by an arbitrary scoring method (0 = no abnormality; 4 = diffuse WMHI) on T₂ MRI sequences and rCMRglc by quantitative FDG PET scans (Siemens ECAT EXACT 47; 6.1 mm FWHM), obtained in a resting state. MS-patients were impaired in few tests and had diffuse rCMRglc reductions, significant (P < 0.05, Bonferroni correction) though only in frontotemporal neocortices (mean decline, 14%); MS+ patients performed poorly in most neuropsychological tests and presented marked rCMRglc reductions (mean decline, 36%) in 21 brain regions (80%). Mean WMHI score was significantly higher in MS+ than MS-patients (24±4 vs 12±3, P < 0.001).

Cognitive abnormalities are the major cause of disability in a substantial percentage of patients with MS. Whereas individual MS- patients present a variable degree of WMHI and frontotemporal rCMRglc decreases, MS+ have severe WMHI and marked, diffuse rCMRglc decreases. Cognitive deficits associated with MS may result from focal lesions specifically impacting diffuse networks that maintain attention. FDG PET appears as a sensitive tool to evaluate and follow-up brain dysfunction in MS, especially in patients with mild cognitive deficits.

PS-352

F. Chierichetti, P. Zanco, D. Rubello, S. Cargnel, A. Fini, B. Saitta, L. Vettorato, G. Ferlin.
General Hospital: Nuclear Medicine - PET Center, Castelfranco Veneto ITALY

18F-FLUORODEOXYGLUCOSE (18F-FDG) POSITRON EMISSION TOMOGRAPHY (PET) AFTER CLOSED HEAD INJURY.

AIM OF THE STUDY: to assess if 18F-FDG PET is a clinical tool in the evaluation of patients (pts) affected by sequences of closed head trauma complaining of cognitive impairments and/or psychiatric disorders.

PATIENTS AND METHODS: we performed 18F-FDG PET in 37 pts (33 males and 4 females, mean age 33.5 years) who suffered from closed head injury from 6 months to 7 years before. All pts were drug-free and studied by MRI, too. In 13 cases there was a previous coma lasting for less than 1 week and in 19 it lasted from 8 days to 2 months. 5 subjects did not experience coma. All pts presented cognitive impairments or psychiatric symptoms and, in 30 out of 37, there was permanent disability.

RESULTS: MRI showed stable vascular lesions in 23 cases, focal or diffuse atrophy in 8 and normal pattern in the other 6 subjects. PET study was abnormal in all pts, evidencing focal or diffuse brain hypometabolism involving in most cases association cortex, frontal lobes but also, in the majority, cerebellum (31) and thalamus (27). All these findings did not correlate to time from brain injury and presence or not of previous coma, even if cerebellum was affected more severely after previous prolonged coma, especially hypoxicemic. The cortical areas showing hypometabolism were greater in number and size in case of disability and agreed with cognitive and psychiatric impairments. For thalamus we did not find any explanation even if its hypometabolism was more evident in presence of memory loss and frontal lobes involvement.

CONCLUSIONS: from our preliminary data 18F-FDG PET is clinically useful in pts with sequences of closed brain injury, probably for legal purposes, too, when anatomical imaging is normal. Further follow up studies are needed especially to better understand if thalamus and cerebellum are a "target" in case of head trauma or if their lesion has a prognostic value.

PS-353

¹Nan-Tsing Chiu, ²Chao-Ching Huang, ³Bi-Fang Lee, ⁴Ying-Chao Chang, ¹Wei-Jen Yao. Depts of ¹Nuclear Medicine & ²Pediatrics, National Cheng-Kung University Hospital. ³Dept. of Nuclear Medicine, Kaohsiung Medical College. ⁴Dept. of Pediatrics, Chang-Gung Memorial Hospital, Taiwan.

Tc-99m HMPAO SPECT CEREBRAL BLOOD FLOW STUDY IN CHILDREN WITH TOURETTE'S SYNDROME

Tourette's syndrome (TS) is a chronic neuropsychiatric disorder of childhood onset, characterized by fluctuating involuntary motor and vocal tics. To date, the results of functional brain SPECT studies in TS patients are controversial, and few focus on children. Using HMPAO SPECT, we conducted this study to explore the incidence rate and location of cerebral perfusion abnormalities in children with TS.

Materials and Methods: High-resolution brain SPECT with Tc-99m HMPAO were performed on eighteen unmedicated children with TS (17 boys, 1 girl) at a mean age of 9.5 years (ranged from 5 to 14 years). To identify abnormalities, in addition to view all the slices on a color monitor, we generated regions of interest over cerebral cortex, basal ganglia and thalamus for semi-quantitative analysis.

Results: Fifteen of the eighteen (83.3%) TS children showed abnormally hypoperfused areas. The majority (22/25, 88%) of the abnormalities was on the left side. Left frontal cortex was most frequently (12/18, 66.7%) involved. Other involved areas included 5 in left temporal cortex, 5 in left basal ganglia, 2 in right basal ganglia and one in right temporal cortex.

Conclusions: Our findings suggest a high incidence rate of cerebral hypoperfusion in children with TS. Most of them involve left cerebral hemisphere, especially over left frontal cortex. The results are compatible with the current hypothesis of cortico-striatal circuit dysfunction in TS.

PS-354

Mirko Diksic

Department of Neurology and Neurosurgery, and Montreal Neurological Institute, McGill University, Montreal, Quebec, H3A 2B4, CANADA

MEASUREMENT OF BRAIN SEROTONIN SYNTHESIS IN LIVING BRAIN
Dysfunction of the brain serotonergic system has been implicated in many brain disorders. With advances in brain imaging methodologies, particularly with the study of different brain receptors, it becomes rather important to fully understand the biological bases of brain disorders in order to measure *in vivo* the rate at which neurotransmitter serotonin is synthesized in humans. We have developed a method which uses α -[11C] methyl-L-tryptophan [α -[11C]MTrp] as a tracer with positron emission tomography (PET) for imaging 5-HT synthesis in living brain. This methodology will be exemplified by the measurement of 5-HT synthesis in normal human and dog brains. A multivariate discriminate analysis was used to identify the brain structures contributing the most to the separation of the male (n=11) and female (n=14) subjects. This analysis was carried out on the log-transformed data, because the synthesis rate in some structures were not normally distributed. By entering selective brain structures into the calculation (frontal and occipital cortex, putamen, globus pallidus, hypothalamus, midbrain and amygdala) the difference between the two groups was significant (p<0.05).

The influence of MDMA (3,4-dimethylenedioxyamphetamine) on brain serotonin synthesis in dog brain was also studied. Since MDMA is a rather common drug, often misused at parties, and since there is some evidence to suggest it is neurotoxic in rat and non-human primate brains, we investigated its effects on brain serotonin synthesis immediately and several hours after injection. Serotonin synthesis was measured before MDMA injection (base line), 1 h after and 5 h after MDMA using α -[11C]MTrp and PET. It was found that 5-HT synthesis is increased about 9 times one hour, and reduced about 3 times 5 h after MDMA, when compared to the baseline. This result suggests that there is a large increase in 5-HT synthesis 1 h after MDMA, likely as a result of an attempt by serotonergic neurons to replenish MDMA released 5-HT. This increase in the 5-HT synthesis probably explains the euphoric effect reported by humans who use MDMA. Similarly, reduction in brain 5-HT synthesis 5 h after MDMA would explain the need for a "booster" dose several hours after the original ingestion. This reduction could also be related to reports of depressive feelings reported by users of MDMA. The method used, as well as its potential for the study of brain 5-HT synthesis, will be discussed. In addition, the use of stepwise multivariate discriminant analysis will be explained. The research presented has been supported in part by the US Public Health Service (R01-NS-29629) and the Medical Research Council of Canada (MT-13368).

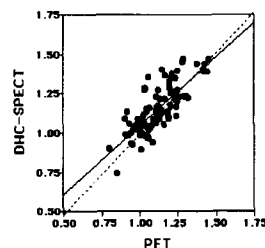
PS-355

K. Fukuchi, K Hayashida, T. Katafuchi, M. Sago, H. Oka, M. Toba, N. Kume, Y. Ishida, M. Takamiya.

Department of Radiology, National Cardiovascular Center, Osaka, Japan

BRAIN FDG-SPECT WITH DUAL HEAD COINCIDENCE DETECTION SYSTEM: COMPARISON WITH PET IN PERFORMANCE CHARACTERISTICS AND CLINICAL APPLICATION

The clinical utility of FDG-PET imaging for the evaluation of patients with neurological diseases is well documented, however, the disadvantages of PET have limited availability with expensive maintenance. Recently, SPECT with dual head coincidence detection system (DHC) have been proposed to offer an another alternative to FDG-PET. The purpose of this study including: (1) measurement the physical imaging characteristics of DHC-SPECT system and comparison with conventional FDG-PET; and (2) comparison the images of DHC-SPECT with those of PET directly and quantitatively in human brain F-18 FDG studies. **Methods:** (1)



Physical imaging characteristics, including system resolution and sensitivity, of DHC-SPECT (VERTEX PLUS MCD, ADAC Labo.) and PET (ECAT EXACT47, Siemens), were measured and compared. (2) Both brain DHC-SPECT and PET with F-18 FDG were performed in six patients with various cerebral disorders and three normal volunteers. Both DHC-SPECT and PET image were evaluated using the mean cortical-to-cerebellar ratio, semiquantitatively. **Results:** (1)

System resolution and system volume sensitivity of DHC-SPECT were comparable to those of PET, respectively. (2) In human FDG imaging, the mean cortical-to-cerebellar ratio of DHC-SPECT were correlated well with that of FDG ($Y = 0.87x + 0.18, r=0.79, p<0.001$). **Conclusions:** FDG-SPECT with DHC has a comparable performance as a dedicated PET camera. It enable us to visualized metabolic parameter of brain which will dedicate to clinical usefulness in terms of cost and availability.

PS-356

T.Ikegami, S.Koike, M.Saito, N.Takahashi and S.Matsubara
Hospital:Yokohama City University, Department of Radiology

INCREASED BRAIN PERFUSION BY GLYCEROL INFUSION IN ONE DAY PROTOCOL STUDY WITH ^{99m}TECHNETIUM-ECD

The purpose of this study was to examine whether glycerol increases brain perfusion and to develop a convenient and reliable method to measure both base line and drug-induced increase of brain perfusion in a sequential study (one day protocol). Basically CBF in the base line study was measured by the method of Matsuda with 370MBq of ^{99m}Tc ECD. A drip infusion of 500ml of 10% glycerol and the acquisition of first SPECT images was started at 10min after injection of ECD. After the end of infusion (about 60min later), the second dynamic images were achieved with 740MBq of ECD. After the background counts on the brain and aortic arch were subtracted from the second dynamic curve, the second study was also analyzed by the method of Matsuda. The second SPECT images were taken from 9min after the second ECD injection and reconstructed after subtraction of the first images. The stability of this method was verified by studies without glycerol infusion in 19 patients with no definite abnormality on CT or MRI and the average change in hemispheric CBF between the first and second CBF was 0.69% (n=38). However, the average change after glycerol infusion in the patients with metastatic brain tumor was +17% (n=18), which was statistically significant(p=0.0011). Average regional CBF in 16 ROIs defined semiautomatically in each patient on the cortex, basal ganglia, cerebellum, tumor core and peritumoral edema was significantly higher in glycerol treatment(44.87 and 53.05 ml/100g/min in base line and glycerol administration, respectively)(p<0.0001). These results suggest that glycerol can increase CBF.

PS-357

R. Junik, B. Steinborn, B. Galas-Zgorzalewicz, J. Sowiński, M. Gembicki
Depts. of Endocrinology and Developmental Neurology, University of Medical Sciences, Poznań, Poland

AN INTERICTAL STUDY OF BRAIN SPECT WITH ^{99m}Tc-HMPAO IN ADOLESCENTS WITH MIGRAINE

In migraine SPECT rCBF has been reported to change with the phase of the symptoms. The aim of our study was to evaluate the rCBF interictally in patients having attacks with and without aura using semiquantitated methods. We studied twenty three patients (9 boys, 14 girls) with migraine with aura (13 pts, MA+) or migraine without aura (10 pts, MA-), aged 10-16 yr (mean 12 yr) in free of symptoms intervals. SPECT scans were performed after the iv injection of a weight adjusted dose of ^{99m}Tc-HMPAO. Tomographic images were obtained using a rotating gamma camera equipped with a low-energy high-resolution collimator. Uptake of the tracer was determined in different regions of interest of the cortex. Differences of more than 10% between contralateral regions of the brain were considered significant.

Right to left asymmetries ranged within 11-23% in cortical regions and reduced rCBF were revealed in 11/13 (85%) patients MA+. The decreased perfusion and asymmetry ranged within 11-18% was observed in 4/10 (40%) patients with MA-. Eight patients (2 MA+, 6 MA-) showed homogeneous distribution over all cortical regions. Except foci of decreased perfusion, rCBF expressed as cerebral/cerebellar ratio was within normal ranges. In MA+ patients the foci of decreased rCBF were localized in parieto-occipital cortex in 10 cases (7 in right and 3 in left hemisphere), 3 foci in frontal lobe (1 right and 2 left, respectively), and 4 foci in temporal ones (3 right and 1 left, respectively). In MA- 3 patients had foci localized in right parieto-occipital cortex, 1 in left temporal, and 2 in left frontal lobe. In both groups the right hemisphere was more often affected than the left one (14 foci vs 9 foci). EEG and SPECT findings matched in 12 patients and in 11 mismatched.

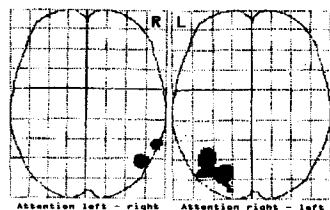
Conclusion: the interictal rCBF is both reduced and asymmetric in adolescents suffering from migraine.

PS-358

L. J. Kemna^{1,2}, B. J. Krause^{1,2}, H. Hinrichs³, M. Jacintha², H. Herzog², L. Tellmann², H. J. Heinze², H.-W. Müller-Gärtner¹
¹Department of Nuclear Medicine, Heinrich-Heine-University, Düsseldorf, Germany
²Institute of Medicine, Research Center Jülich, Germany
³Department of Clinical Neurophysiology Otto-von-Guericke University, Magdeburg, Germany

ACTIVATION OF THE CONTRALATERAL FUSIFORM GYRUS BY VISUAL ATTENTION

In a preceding study the contralateral fusiform gyrus was activated if attention was drawn to one visual hemifield in a pseudoletter comparison task. Event related potentials showed an influence of spatial attention on the electrophysiological activity at this site as early as 80 - 130 ms after stimulus onset. The present study was done to investigate if the attained activations were specific to the letter comparison task or due to a more general attention effect.



Blocks of vertical black and white stripes were shown for 100 ms on an isoluminant gray background randomly in the left and right visual hemifield. 12 healthy young male dexterous volunteers were asked to fixate a central cross and concentrate on one visual hemifield and to press a mouse button with their right index finger when they noticed a block that was 10 - 15% shorter than the others.

We used PET and O-15-butanol injection. Attention to the right hemifield compared to a control condition without attention or motor reaction revealed activation foci in the left thalamus and fusiform gyrus (Brodmann area (BA) 19/37). Attention to the left yielded activation in the right fusiform gyrus (BA19/37) and thalamus. The anterior cingulate cortex (BA24), the right prefrontal cortex (BA 9/46/45), and the cerebellum bilaterally and in the midline were activated in both tasks compared to control. The comparison attention to the right versus attention to the left hemifield and vice versa produced activation in the contralateral fusiform gyrus alone. We conclude that this activation is not specific to the letter comparison task but is an important target for the influence of attention on the processing of information at least in the ventral but probably also in the dorsal visual pathway.

Key words: visual attention, activation study, fusiform gyrus

PS-359

K. Kikukawa, H. Toyama, M. Katayama, T. Nishimura, K. Ejiri, N. Fujii, K. Senda, A. Takeuchi, K. Torikai, and S. Koga.
Departments of Radiology and Rheumatology, Fujita Health University, Toyoake, Japan.

EARLY AND DELAYED Tc-99m-ECD SPECT IN SLE PATIENTS WITH AND WITHOUT PSYCHIATRIC SYMPTOMS.

Psychiatric symptoms are not uncommon in clinical course of SLE. However, because psychiatric symptoms are not always parallel to disease activity, the accurate diagnosis is difficult. The purpose of this study is to evaluate the diagnostic utility of early and delayed ECD SPECT on SLE pts with and without psychiatric symptoms. Nineteen pts (31.4±11.6 yr, 3 M, 16F) were divided into 2 grps with psychiatric symptoms; CNS grp (CNS): 8 pts with definite psychiatric disorders (seizures, psychosis), non-CNS grp (non-CNS): 11 pts without definite psychiatric disorders. Pts with CVA were not included in this study. SPECT scans were performed 15 min (early scan)(ES) and 3 hrs (delayed scan)(DS) after the 600 MBq of ECD injection. We analyzed ES and DS by visual interpretation. SPECT findings were classified into 5 types as follows. Type 1a; ES, DS: normal, (CNS:1, non-CNS:4), Type 1b; ES: normal, DS: focal decreased uptake in medial frontal lobe (CNS:0, non-CNS:3), Type 2; ES: focal decreased uptake in frontal lobe, DS: focal decreased uptake in medial frontal lobe (CNS:0, non-CNS:1), Type 3; ES: diffuse uneven decreased uptake, DS: diffuse mottled decreased uptake (CNS: 7, non-CNS: 3). As a results, in CNS, ES and DS were abnormal in 7 pts (87.5%). In non-CNS, ES were abnormal in 4 pts (36.4%), and DS were abnormal in 7 pts (63.6%). High incidence and various ECD SPECT abnormality in CNS would provide useful objective diagnostic informations. Decreased uptake on ECD DS showing reduced retention in non-CNS, especially on medial frontal lobe could become useful early indicator of psychiatric symptoms.

PS-360

ZY Pan, DM Chen, SW Jia* and MJ Liu
Beijing Medical University, First Hospital, Beijing 100034, China and Shenzhen People Hospital*.

STUDY OF ACUPUNCTURE-INDUCED rCBF CHANGES IN CEREBRAL ISCHEMIC LESIONS

Aim: According to traditional Chinese medicine theory, acupuncture points of Yang Channels could cure stroke but Yin channels could not. The aim of this paper is to observe if it is true by using rCBF imaging.

Methods: 60 patients with cerebral ischemia diseases. 17 cases were acupuncture at Hegu and Chuchih points of Hand-Yangming channel, 21 cases at Tusanli and Shangchuhsu points of Foot-Yangming channel, 12 cases at Yiningchuan and Tichi points of Foot-Taiyin channel. ^{99m}Tc-ECD, GE Starcam SPECT, split-dose and image subtraction method were used to obtain pre-acupuncture and during-acupuncture images. Compared pre- and during acupuncture images, rCBF changes induced by acupuncture in cerebral ischemic lesions were divided into three categories. I significantly improve: ischemic lesions completely or almost completely disappeared. II improve: ischemic lesions diminished significantly. III no change: ischemic lesions diminished insignificantly or no any change. The first two mean effective.

Result:

Channel	No. of lesions	rCBF in ischemic lesions			efficacy
		I	II	III	
Hand-Yangming	17	7	8	2	88.2% [ⓐ]
Foot-Yangming	56	19	16	21	62.5% [ⓐ]
Foot-Taiyin	22	12	7	3	86.4% [ⓐ]

ⓐ to ⓑ P< 0.05, ① to ③ P>0.05, ② to ③ P<0.05

Conclusion: Acupuncture points of Yin channel (Foot-Taiyin) could improve rCBF in cerebral ischemic lesions as significantly as acupuncture points of Yang channels (Hand-Yangming and Foot-Yangming). This result seems to be inconsistent with traditional Chinese medicine theory. Further study of acupuncture all 6 Yang channels and 6 Yin channels are ready to be done.

Supported by IAEA CRP E1.30.09 and Chinese National Science Research Fund (38970800 and 39370825).

Poster presentations

PS-361

T. Sasaki, T. Amano, J. Hashimoto*, Y. Itoh, K. Muramatsu, A. Kubo* and Y. Fukuchi
Keio University School of Medicine, Department of Neurology, Department of Radiology*

"INVERTED TRIANGLE" PATTERN ON 3D SPECT IMAGES IS USEFUL TO DISTINGUISH ALZHEIMER'S DISEASE FROM VASCULAR DEMENTIA.

Some patients with Alzheimer's disease are reported to have ischemic lesions pathologically. Therefore, the differential diagnosis between Alzheimer's disease and vascular dementia is still problematic even when ischemic lesions are detected on CT scans and/or MRI. Patients with Alzheimer's disease are reported to show characteristic bilateral hypo-metabolism and hypoperfusion in the temporal and parietal cortex in PET and SPECT studies. However, the diagnostic accuracy of the hypoperfusion still varies widely. We have preliminary reported that three-dimensional imaging by SPECT (3D-SPECT) was able to detect the relatively mild hypoperfusion in the motor and sensory cortex in comparison with the rest of the cerebral cortex in the Alzheimer's disease. This pattern appeared in the form of an 'inverted triangle'. The 'inverted triangle' sign in the motor and sensory cortex detected by 3D-SPECT is thought to reflect the disproportionately mild atrophy of the primary motor and sensory strips observed by gross examination of the brain in Alzheimer's disease. The purpose of this study was to evaluate whether the 'inverted triangle sign' seen on 3D-SPECT images is useful for differentiating Alzheimer's disease from vascular dementia.

Method: Serial SPECT studies were performed on 14 patients with a diagnosis of probable Alzheimer's disease and 7 patients with a probable diagnosis of vascular dementia. The diagnosis of probable Alzheimer's disease was made on the basis of DSM IV, NINCDS-ADRDA criteria and the diagnosis of vascular dementia on the basis of NINDS-AIREN criteria, respectively. SPECT was performed using a triple-headed rotating gamma camera (Toshiba 9300 A/HG) with 99mTc-HMPAO or 99mTc-ECD as the tracer. The three-dimensional (3D) image was reconstructed by the maximum intensity projection method to show the cortical perfusion pattern.

Results: 1) The inverted triangle pattern appears in the relatively early stage of Alzheimer's disease. 2) This pattern was not seen in patients with vascular dementia. 3) Patients with vascular dementia exhibit a patchy decrease pattern on 3D-SPECT.

Conclusion: The inverted triangle pattern in the motor and sensory cortex on three dimensional SPECT images, which means relative maintenance of perfusion, is useful to distinguish Alzheimer's disease from vascular dementia.

PS-362

I. Uriarte, R. Quirce, A. Hernandez, A. Montero, NK. Vallina, C. Guede, I. Banzo, JM. Carril

Servicio de Medicina Nuclear. Hospital Universitario Marqués de Valdecilla. Santander. España.

CLINICAL IMPACT OF BRAIN BLOOD FLOW SPECT IN THE MANAGEMENT OF NEUROLOGICAL PATIENTS

The brain blood flow SPECT is available in many hospitals, but a little is known about its clinical impact. We performed a prospective study over the clinical history and the neuroimaging explorations (177 SPECT, 8 NRM, 11 CT). We analyzed 158 patients (P) in whom a final diagnosis was reached: 77 vascular disease (VD), 4 dementia (D), 7 infectious disease (ID), 3 epilepsy (E), 11 headaches (H), 4 psychiatric illness (PS), 2 head trauma (HD) and 6 other pathologies (OP). Pathology was ruled out in 2 P (NP).

Morpho-functional correlation was analyzed in 149P. SPECT and CT or NMR findings agreement in 30 P: in 8 both were normal and in 22 found the same lesion. There was no agreement in 119 P: in 31 P only the SPECT found alterations, in 1 only the CT did it and in 87 although both were abnormal the findings disagreement, in 52 of these 87 SPECT gave more information. In 83 of the 149 P (56%) SPECT was more relevant than CT or NMR. Considering the clinical repercussion in the 158 P, we can observe that only in 9 P (1D, 1ID, 2H, 1E, 4 OP) SPECT was not use. In 65 (41%) SPECT gives information about the functional aspect of the clinical picture (28 VP, 22D, 2 ID, 6 H, 1 HT, 4 PS, 2 OP). In 84 P (53%) SPECT was the main diagnostic tool (49 VD, 23 D, 4 ID, 3 H, 1 HT, 2 E, 2 NP). In 16 of these 84 (10% of the 158 P evaluated) SPECT was able to change the clinical approach (8 VD, 5 D, 1 E, 2 NP).

CONCLUSIONS: Brain blood flow SPECT is relevant in the clinical approach and management of patients, mainly in the vascular disease and in the dementia.

PS-363

Y. Ushijima, C. Okuyama, H. Sugihara, J. Narumoto, M. Kondo, M. Maeda
Department of Radiology, Neuropsychiatry, and Neurology, Kyoto Prefectural University of Medicine,

CROSSED CEREBELLAR DIASCHISIS IN ALZHEIMER TYPE DEMENTIA

Crossed cerebellar diaschisis (CCD) occurs in patients with contralateral supratentorial infarction or tumor. In Alzheimer type dementia (ATD) cerebral and cerebellar blood flow asymmetry sometimes are observed. We evaluated functional relationship between cerebrum and cerebellum in ATD. Regional cerebral blood flow (rCBF) was measured using I-123-IMP ARG method in 57 patients with ATD and 6 age matched control subjects. The lateralities of rCBF were calculated by asymmetry index (AI) of blood flow for matched left-right regions of interest in the cerebellum, thalamus, basal ganglia, and cerebral cortices. Cerebellar AIs correlated negatively with those of the frontal, parietal, and temporal cortices. The motor cortex showed no correlation with cerebellum. We classified ATD patients with two groups in each cerebral cortices: asymmetry (AI > 10) and symmetry (AI ≤ 10). Cerebellar asymmetry was demonstrated in 4 of 15 cases (27%) with frontal asymmetry, 6 of 20 cases (23%) with parietal asymmetry, and 4 of 23 cases (15%) with temporal asymmetry. These results suggest the existence of CCD in ATD. We suspect that frontal and parietal cortices especially influence function in the contralateral cerebellum.

PS-364

J.P. Wielepp^{1,5}, R. Noss², P. Bundeli³, J.A. Kinser¹, R. Hämmig⁴, R. Brenneisen³, T.E. Schläpfer²
Department of Nuclear Medicine¹, Psychiatric Neuroimaging Group², University of Berne/Inselspital; Pharmaceutical Institute³ and University Psychiatric Service⁴, University of Berne, Switzerland; Clinic for Nuclear Medicine⁵, MLU Halle, BRD

DIFFERENTIAL CEREBRAL BLOOD FLOW CHANGES ASSOCIATED WITH RUSH AND EUPHORIA AFTER i.v. HEROIN ADMINISTRATION

Opiates have a very high addiction potential, mainly because of the induced euphoria. Heroin is one of the most misused opiates. Up to now it has not been legal to perform neuroimaging studies using heroin. In this SPECT study the effect of acute i.v. heroin on the cerebral blood flow (CBF) of chronic heroin addicts is examined.

Methods: 9 male chronic heroin addicts (addiction period >5 years, average age 31.9 years [25-42]) were recruited for this study after receiving permission from the Ethic Commission of the University of Berne and after ruling out other psychiatric illnesses, cocaine abuse and HIV infection. The volunteers underwent 3 SPECT examinations 48 hours apart done at random: on 2 days they received heroin using a dose of 20 % more than the usual injected amount (range 100-160 mg) and on one day a placebo (NaCl) injected i.v. 45 sec. (A: subjective „flash“) or 15 min (B: subjective „euphoria“) after the heroin injection respectively 15 min (C: „placebo“) after injection of NaCl 750 MBq 99mTc-HMPAO were injected and after 60 min the acquisition on a 3-headed SPECT camera (Prism 3000, PICKER) was started. The analysis of the SPECT data followed using the statistical parametric mapping program and fitting of the data on the coordinate system of the stereotactic atlas of Talairach.

Results: The CBF after heroin (Phases A and B) shows a significant hyperperfusion in different brain regions in comparison to baseline CBF (Phase C).

Examination	Threshold	Significant brain regions
A - C	p=0.001 p=0.01	Precuneus Cerebellum
B - C	p=0.001	Cingulus anterior right
A - B	p=0.001	Cerebellum, precuneus Cingulus anterior inferior
B - A	p=0.001-0.05	none

Conclusions: The results show significant blood flow changes in different brain regions during the different subjective phases after heroin application as compared to the baseline CBF. The „high“ after heroin injection is associated with a hyperperfusion in the anterior cingulus, particularly during the early phase („flash“) after injection which reflects the functional involvement of the limbic system. In addition, there is activation in the precuneus and cerebellum.

PS-365

F. C. Wong, K. Jaeckle, E. E. Kim, S. Ilgan, D. A. Podoloff

**Hospital: The U of Texas M. D. Anderson Cancer Center
Departments of Nuclear Medicine and Neuro-Oncology**

WHOLE-BODY OMMAYOGRAM IN THE EVALUATION OF CSF FLOW IN PATIENTS WITH LEPTOMENINGEAL CARCINOMATOSIS (LC).

A traditional Ommayogram requires lengthy static images that evaluate the neural-axis in different scans. This study aims to evaluate the use of serial whole-body scans during an Ommayogram and to calculate the clearance of In-111 from the CSF pathways so as to correlate with clinical signs of obstruction in the patients with LC.

Thirty-three patients with LC, but no MRI evidence of spinal block, underwent injection of 0.5 mCi of In-111 DTPA into the Ommaya reservoir. Delayed anterior and posterior whole-body images and geometric-mean images were obtained with 247 keV peak at 1, 4, 20 and 24 h. Effective half-life (Te) of In-111 in CSF was correlated with signs of obstruction or elevated intracranial pressure. Four patients with suspected CSF leak were also studied in the same manner.

Only 28 patients had sufficient clinical data for evaluation of obstruction. The Te ranged from 7 to 50 h. Patients with clinical evidence of obstruction (11) had Te of 23.9± 11.7 h; patients with no clinical evidence of obstruction (14) had Te of 12.2± 3.9 h. Opening of VP shunt normalized the Te in 2/2 patients. Patients with CSF leak (2) had low Te, 7.5 and 8.5 h, respectively.

Serial whole-body scans provide a convenient method in the evaluation of patients requiring intrathecal therapy by displaying CSF flow in the entire neural axis. This preliminary study indicates that whole-body Ommayogram may also provide efficacious parameters (Te) to estimate CSF clearance which correlates with clinical symptoms of obstruction.

PS-366

**J. H. Zhao, X. T. Lin, Y. H. Guan, L. Q. Xu, G. M. Zhang, F. P. Xue
Dept. of Nucl. Med. Hua Shan Hospital, Shanghai Medical University,
Shanghai 200040, China**

RELATIONSHIP BETWEEN 99mTc-ECD SPECT IMAGES AND PERFORMANCE OF THE WISCONSIN CARD SORTING TEST IN HEALTHY HUMANS

PURPOSE To investigate relationship between 99mTc-ECD SPECT and performance of the Wisconsin Card Sorting Test (WCST) in normal young and aged volunteers through the semi-quantitative analysis of the baseline and cognitive activated rCBF images. **METHODS** 16 young and 14 aged volunteer were enrolled. The education of the two group is matched. All subjects were healthy and CT results of the aged volunteers were normal. The cognitive activated brain SPECT: The cognitive task is WCST. 1110MBq(30mci) 99mTc-ECD was administered by intravenous bolus injection 5 minutes after the onset of the WCST. The images were reconstructed and semi-quantitative analyzed. WCST were scored through 9 items: 1) period 2) categories 3) total corrects 4) conceptual level(%) 5) perseverative responses 6) total errors 7) perseverative errors 8) perseverative error(%) 9) non-perseverative errors. **RESULTS** 1)In aged subjects, the baseline rCBF values of frontal, temporal, parietal and anterior cingulate lobes were lower than that of youngs. But the values of occipital lobe and basal ganglia were slightly higher in aged subjects. 2)In aged subjects, the activated rCBF values of every cortical and sub-cortical regions were lower than that of young subjects. 3)WCST scores: The youngs had significantly better scores than that of the aged in 7 items. 4) The baseline and activated rCBF values of the frontal lobes and anterior cingulates were closely related to the scores of categories, perseverative responses, total errors and non-perseverative errors. **CONCLUSIONS** 1)The distribution of 99mTc-ECD have some difference in young and aged volunteers. 2) The mild hypoperfusion of the frontal lobe in aged group may be the cause of poor conceptual and thinking ability. 3)Significant correlations between anterior cingulates and performance of WCST have been observed.

Neurology/Psychiatry: Psychiatry

PS-367

**E. Ambrus, Gy. Szekeres, Sz. Kéri, L. Csernay, Z. Janka, L. Pávics;
Albert Szent-Györgyi Medical University, Szeged, Hungary**

RESTING AND ACTIVATED rCBF SPECT IN SCHIZOPHRENIC PATIENTS

Brain SPECT studies in schizophrenia revealed changes in regional cerebral blood flow (rCBF). The aim of this study was to assess the frontal and temporal rCBF changes under resting and frontal activation conditions. 11 chronic schizophrenic patients (average age: 46 years, 33-56 years) were studied in two HMPAO brain SPECT sessions, 48 h apart, both at rest and during a frontal activation task using the Raven test. All were receiving neuroleptic drugs. Resting and activated SPECT examinations were also performed on 5 normal control patients (average age: 45 years, 26-57 years). The images were evaluated visually and semiquantitatively. Under resting conditions the schizophrenic group had a significantly lower rCBF in the temporal region than that of the controls. Five patients displayed left, 3 right temporal and 2 diffuse hypoperfusion and 1 exhibited no rCBF abnormality. In the normal control group, there were no significant rCBF changes except in 1 person. In the Raven activation test, the control group showed a significantly higher blood flow in the left frontal region, as compared to the schizophrenic group. 4 normal persons had left frontal hyperperfusion (1 revealed no changes). In the schizophrenic group, 5 had left frontal hyperperfusion, while 6 patients no rCBF changes on activation.

Conclusion: In our sample, patients with chronic schizophrenia displayed significant temporal hypoperfusion. The Raven activation test significantly increased the rCBF in the frontal region in the normal control group. The chronic schizophrenic group exhibited a poor response to frontal activation.

PS-368

**G. Aras, N.Ö. Küçük, A. Aysev*, E. Ibiş, H. Erman*, E.A. Gençoğlu,
N. Çanakçı**, A. Akin.
Ankara University Medical School, Depts. of Nuclear Medicine,
Pediatric Psychiatry* and Anesthesiology**. Ankara/TÜRKIYE**

REGIONAL CEREBRAL PERFUSION IN CHILDHOOD AUTISM

Autism is a developmental syndrome defined by the presence of marked social deficits, specific language abnormalities and stereotyped repetitive behavior (DSM 3 R). A variety of imaging techniques have been used to study autism in an attempt to localise the responsible region of brain. In this study, we aimed to evaluate the cerebral blood flow with Tc 99m HMPAO SPECT in two groups of autistic pts with different severity symptoms.

11 pts with low symptoms (group 1) and 11 pts with severe symptoms (group 2), totally 22 pts (3 females, 19 males; mean age 7.34±2.89) were included in the study. EEG, CT and MRI were performed and found to be normal in all pts. Brain SPECT was performed on 20 of 22 pts under general anesthesia. The tracer was injected 15 minutes prior to anesthesia to reflect the rCBF. Qualitative and quantitative (side to side asymmetry indices, right-left asymmetry indices) analyses were done.

Hypoperfused areas were detected in 9 pts of group 1 and in 10 pts of group 2. Frontal hypoperfusion was observed in 6 pts (1 right, 5 left), parietal in 10 pts (6 right, 4 left), temporal in 3 pts (1 right, 2 left) and parietotemporal in one pt (left) and normal perfusion in 3 pts. All quantitative parameters in hypoperfused areas showed diminished uptake comparing with normal areas in both of group 1 and 2. But, frontal and parietal asymmetry indices in group 2 were found to be significantly lower than group 1 (p<0.05).

As conclusion: 1)The pts with severe symptoms (as group 2) have high hypoperfusion rate comparing with pts with low symptoms. 2)Frontal and parietal hypoperfusions are mostly seen findings. 3)Brain SPECT is usefull method for evaluation of brain functional status and severity of disease.

PS-369

M. Babar Imran, Kawashima R, Awata S, Sato K, Kinomura S, Sato M, Fukuda H.

Institute of Development Aging and Cancer,
Tohoku University, Sendai, Japan.

PARAMETRIC MAPPING OF CBF DEFICITS IN SDAT. A SPECT STUDY USING IMAGE STANDARDIZATION TECHNIQUE.

In this study, we assessed the accuracy and reliability of Automated Image Registration (AIR) for standardization of brain SPECT images of Alzheimer's patients. Standardized CBF images of patients with Alzheimer's disease (AD) and control subjects were then used for group comparison and covariance analyses. Twenty patients with Alzheimer's disease (age 71.1 ± 7.4 yrs, CDR 1-3, MMS 17.8 ± 5.3) and fifteen age matched normal subjects (age 70.2 ± 8.4 yrs) participated in this study. Tc-99m HMPAO brain SPECT and X-ray CT scans were acquired for each subject. SPECT images were transformed to a standard size and shape with the help of automated image registration (AIR). Accuracy of AIR was evaluated by overlap methodology (functional & anatomical). The group comparison was done with the help of SPM96. Significant differences were displayed on the respective voxel to generate three dimensional Z-maps.

X-ray CT scans of individual subjects were evaluated by computer program for brain atrophy. Voxel based covariance analysis was performed on standardized images taking age of patients, severity of disease (CDR, MMS, PSMS) and atrophy indices as independent variables. Z-maps showed significantly decreased rCBF in the frontal, parietal and temporal regions in patient group ($p < 0.001$), more marked in those patients having severe dementia. Covariance analysis revealed that aging and severity of disease have pronounced effect on rCBF especially that of left parietal region.

Conclusion: Cerebral blood flow in the left parietal region demonstrated a strong negative correlation with age of patients with Alzheimer's disease and severity of dementia.

PS-370

C.Decker, A.Korchounov*, K.Broich*, A.Mameros*, T.Mende

Dept. of Nuclear Medicine and Psychiatry*, Martin-Luther-University Halle-Wittenberg, Germany

STRIATAL DOPAMINE D2 RECEPTOR OCCUPANCY BY ATYPICAL NEUROLEPTICS IN PATIENTS WITH SCHIZOPHRENIA

The purpose of the study was the investigation of in vivo striatal dopamine D2 receptor binding in schizophrenic patients treated with atypical neuroleptics as olanzapine and clozapine in comparison to flupentixol and risperidone.

We performed a single photon emission tomography (SPET) with 123I-Jodobenzamide (IBZM) in 12 patients with schizophrenia and 4 age-matched controls. In each case 3 patients were treated with olanzapine, clozapine, risperidone and flupentixol. 90 minutes after intravenous injection of 185 MBq 123I-IBZM the acquisition was started using a CERASPECT camera (ADAC) followed by reconstruction of the raw data with filtered back projection and attenuation correction (Chang). The IBZM uptake of the basal ganglia (BG) was quantified as ratio to the frontal cortex.

There was a statistically significant difference of striatal IBZM binding between controls (1.84 ± 0.23) and all treatment groups (1.52 ± 0.12), $p < 0.01$. The patient group with atypical neuroleptic drugs and significant clinical improvement as a result of this therapy were characterized by higher mean BG/frontal cortex ratios of IBZM (clozapine 1.56 ± 0.20 , olanzapine 1.57 ± 0.29) than those medicated with flupentixol (1.49 ± 0.10) and risperidone (1.46 ± 0.21).

The results suggest, therapy with atypical neuroleptics as olanzapine and clozapine with sufficient antipsychotic effect is associated with lower degrees of in vivo striatal dopamine D2 occupancy.

PS-371

N.Ö.Küçük, E.Ö.Kılıç*, E.İbiş, A.Aysev*, E.A.Gençoğlu, G.Aras, G.Erbay.

Ankara University Medical School, Depts. of Nuclear Medicine and Pediatric Psychiatry*. Ankara/TÜRKIYE.

BRAIN SPECT FINDINGS IN LONG TERM INHALANT USERS

The study involves evaluation of brain perfusion in long term inhalant users like acetone, toluene, benzene and its derivatives.

Ten patients at ages 16-18 who have been inhalant dependent for a mean period of 48.3 months and have stopped using of inhalant before 1-11 months (mean 5.4 months) were included in the study. Psychiatric tests, biochemical tests and Tc-99m HMPAO brain SPECT was performed on all pts. Brain SPECT images were evaluated qualitatively and quantitatively.

The mean IQ level was found to be 84 (by psychiatric tests). Brain SPECT showed nonhomogenous HMPAO uptake and hypoperfusion areas on all pts (five left temporal, one right temporal, two left temporal + bilateral parietooccipital, one biparietal and one left temporoparietal). Seven pts had hyperperfused focuses (one unifocal area at 5 pts and two multifocal at 2 pts). Six of hyperperfused focuses were at parietal and one at temporoparietal localization. Mean perfusion ratio of abnormal to normal were found 0.75 ± 0.21 for hypoperfused areas and 1.41 ± 0.32 for hyperperfused areas.

This study suggests that inhalant dependents exhibit serious abnormalities in brain SPECT images like hypo and hyperperfusion focuses and nonhomogeneous uptake of the radiopharmaceutical. Further study with a larger number of pts and long term follow up may help to reach a more specific conclusion.

PS-372

J. Lavalaye¹, D.H.Linszen¹, E.A. van Royen², B.P.R. Gersons¹

Academic Medical Center, Amsterdam, The Netherlands,

¹Department of Psychiatry, ²Department of Nuclear Medicine

DOPAMINE TRANSPORTER IMAGING IN YOUNG PATIENTS WITH SCHIZOPHRENIA

Little is known about the role of the dopamine transporter (DAT) in schizophrenia. Even so, the effect of antipsychotic medication on the expression of the DAT in vivo has not been studied extensively. Olanzapine is a new antipsychotic drug with few extrapyramidal side effects. It is unknown if olanzapine influences the DAT.

15 patients (12 male, 3 female), mean age 20.4 years (17 to 25) were admitted to the adolescent clinic with first or second psychotic episode according to DSM IV criteria. Olanzapine dose was 13.7 mg (0 to 30 mg) for at least 4-6 weeks, 2 patients were drug free for two weeks. [123-I]-FP-CIT scans were performed 3h after injection of 110 MBq [123-I]-FP-CIT. Scans were made with a 12 headed dedicated brain SPECT camera (SME 810). Binding potential was calculated as described by Booij et al (*J Neurol Neurosurg Psych* 1997;62:133-40).

On visual inspection the images showed symmetrical striatal uptake with comparable uptake in the putamen and caudate nucleus. Striatal uptake: 2.48 (1.97-3.10), putamen: 2.50 (1.93-3.34), caudate: 2.60 (2.07-3.36). Ratio of striatum left/right: 1.06. Graphical analysis of striatal [123-I]-FP-CIT uptake versus milligram of olanzapine did not show a correlation. Spearman Rank Correlation $r = 0.04$, $p = 0.88$.

These data suggest that there is no significant influence of olanzapine on striatal [123-I]-FP-CIT binding.

PS-373

A. Fernández, J. Mora, A. Benitez, A. Muñoz, R. Puchal, MP Alonso, J. Vallejo and J. Martin-Comin
S. Medicina Nuclear. CSUB Hospital de Bellvitge. Hospitalet de Llobregat. Spain

Changes in regional brain blood flow (rCBF) in Obsessive-Compulsive (OCD) patients pre and post treatment. Comparison and normal population

The aim of the work was to analyse changes in rCBF in patients with OCD in comparison with normal population and following specific treatment.

17 patients with OCD DSM-III-R criteria (mean age 31 years, 15 f) and 17 volunteers (mean age 31 years, 5 f) were studied. In all cases a neuropsychiatric study and 99mTc-HMPAO SPECT were obtained using a single head gammacamera. Patient were restudied following 1 month of protocolized treatment. ROIs were drawn outlining cerebellum and right and left frontal, fronto-orbital, parietal, temporal and basal ganglia. An 50 % isocountour cortex ROI was also drawn. Activity ratio of brain areas versus cerebellum (I1) and isocountour (I2) were calculated.

Pre treatment activity in basal ganglia was significantly ($p < 0.05$) higher than in normal cases. Following treatment all patient improved clinically and normalised basal ganglia uptake. No differences were seen in other brain areas.

In summary basal ganglia uptake is increased in patients with OCD and seems to normalize in patients with positive response to treatment.

PS-374

D.Cifuentes, T.Massardo, J.Pallavicini, P.González, P.Arancibia, P.Padilla.
Clínica Psiquiátrica, Medicina Nuclear, Hosp. Universidad de Chile

BRAIN PERFUSION TOMOGRAPHY WITH 99mTc-ETHYL CYSTEINATE IN PATIENTS WITH DRUG DEPENDENCE.

We studied 43 patients (36±13 y.o.; 37 males) who met DSM IV drug dependence criteria, in their fourth week of detoxification therapy, with 740 MBq of 99mTc-ECD. All had minimal test (MMT) and neurological exam and a complete record of their drug habit. Fourteen cases presented monodrug dependence in 14 cases (8 alcohol, 5 cocaine derivative and 1 amphetamine) and 29 were polydrug consumer with a maximum of 6, including also tetrahydrocannabinol, nicotine, benzodiazepines and opioids, in different associations; alcohol was the most frequent (77%). Brain perfusion tomography was abnormal in 72% (31/43); 65% of them were polydrug consumers. Men had more perfusion abnormalities than women (78% vs 22% respectively, Fisher test: $p = 0.04$); mean length of consume and number of drugs were similar for both sexes. Monodrug had predominantly diffuse perfusion abnormalities (65%) and polydrug consumers predominantly focal (64%). Focal defects were bilateral in 88%, especially fronto or temporoparietal. All of normal perfusion patients had MMT ≥ 26 (maximum 30) vs 4 patients with abnormal perfusion with MMT < 25 ; there was no difference in the proportion of abnormal neurological exam 17% and 16%, respectively. Abnormal perfusion group had a trend to be older, with longer periods of dependence, and lower mean number of drugs than normal group, being these differences more intense in diffuse than focal pattern. Concluding, in patients with drug dependence 99mTc-ECD demonstrated an important presence of brain perfusion abnormalities, associated with sex and may be with consume length and number of drugs in a larger population.

PS-375

I. Mena, C.Sole, S. Neubauer, F. de la Barra, R. Garcia,C.Prado.

Clinica Las Condes, Department of Nuclear Medicine and Child Psychiatry Unit. Santiago. CHILE.

OBSESSIVE COMPULSIVE DISORDER IN CHILDREN: SPET OF 99mTc HMPAO FINDINGS.

In order to recognize the clinical continuity of Obsessive Compulsive Disorder (OCD) from childhood to adulthood, we demonstrate abnormalities of cerebral perfusion in 16 children (13.2±2.5 years) with OCD in comparison to 13 normal children (9.2±3.2 years). The normal children were studied with a protocol approved by the ethical committees of our Institutions and informed written consent was obtained. OCD data was analyzed retrospectively.

OCD was diagnosed according to International Classifications by two Pediatric Psychiatrist (F.B. and R.G.). 99mTc HMPAO SPET was performed after intravenous injection of 370-555 MBq using a single rectangular head Gammacamera (SOPHA Inc., Maryland, USA) with Ultrahigh Resolution Collimation. 3D reconstruction of the data was accomplished with normalization to the maximal activity in the brain and volume normalization of the studies was performed using the Tallairach technique. An average Brain Perfusion Distribution Image was constructed for the normal controls, with calculation of HMPAO uptake for each voxel were expressed as mean ± SD. A voxel by voxel comparison for each patient vs. the normal brain distribution was performed and the results for each patient's voxel, expressed as SD above or below the normal mean, using a calibrated color code. The criterion for abnormality was defined as 2SD above or below the normal mean. Finally a template of Brodmann Areas of Frontal Circuitry was projected on the patient's 3D color image. 83% of OCD children had increased frontal lobe perfusion mainly in the areas 8 and 9 of Brodmann, and less frequently in the area 46. 40% of OCD children had increased cingulate perfusion in comparison to normal controls similar to the findings reported by us in adult OCD patients.

PS-376

C. Baeken¹, K. Chavatte², P. Flamen², D. Terriere³, R. Boumon³, H. D'Haenen¹, A. Bossuyt², J. Mertens³.
AZ-VUB Psychiatric¹ and Nuclear Medicine², VUB-Cyclotron³, Brussels, Belgium.

PRECLINICAL EVALUATION OF A NEW 5HT2A TRACER FOR SPET.

123I-5-R91150 (4-amino-N-[1-[3-(4-fluoro-phenoxy)propyl]-4-methyl-4-piperidinyl]-5-iodo-2-methoxybenzamide) is actually evaluated as a new potential 5HT2A tracer for SPET. In normal subjects the amount of radioactivity bound in several cortical zones as well as the cortico-cerebellar ratios (Ri) reach an equilibrium value around 90 minutes which is maintained up to 240 minutes although the blood clearance curves show a sharp decrease down to 10-20% of the injected dose over the first 20-30 minutes p.i. This could fit a three-compartment (C) model with a reversible transfer between C1 and C2 and a non-reversible process between C2 and C3. Nevertheless inhibition of the specific binding of 123I-5-R91150 by risperidone proves that a reversible system is involved. As the tracer used in this study has a high specific binding, i.e. 370Bq/mmol, the radio ligand concentration in the brain is smaller than the amount of receptors and it can be proved the Ri is directly proportional to Bmax. The apparent non-reversibility is related to the pKa value of the ligand, i.e. 7.5-7.6, and the difference in pH value between the brain compartments (CSF 7.35, glia 7.2, neuron 6.9) and the blood (pH 7.4). The total process is reversible indeed but within the period of 3 hours the acquisition of the data by SPET is not sensitive enough to measure a slow equilibrium. The tracer has been used for the study of the dependence of 5HT2A receptor on age and gender. The mean Ri values for 5HT2A binding in every region of the cortex declined exponentially from 2 (23-30 years) to 1.4 (55-60 years) with age with a t1/2 of about 40 years. No gender nor left-right difference was observed.

Poster presentations

PS-377

Metka Milčinski, Marga Kocmur*, Nataša V Budihna**, Nucl. Med., University Medical Centre, *Psychiatry, **Nucl. Med., Oncology, 1525 LJUBLJANA, SLOVENIA

BRAIN PERFUSION BICISATE-SPET IN DEPRESSIVE PATIENTS BEFORE AND AFTER TREATMENT

Aim of our study was to evaluate brain perfusion (CBF) in depressive pts before therapy and after antidepressant drugs. **Methods:** severity of depression was assessed with Hamilton Depression Rating Scale (HAMD, 17 item) before every scintigraphic study. 99m-Tc-bicisate-SPET was performed in 10 pts before therapy, 3 weeks and 6 months after. Only pts with no change in antidepressant medication during the study were included. Semiquantitative visual analysis was used and CBF graded as normal (equal to cerebellum, 3), decreased (2), severely decreased (1).

Results:

	pts number	HAMD average range	CBF frontal average	CBF temporal average	CBF parieto-occipital average
before therapy	10	25.3 16-32	1.9	2.1	2.1
3 weeks	9	16 9-23	2.5	2.5	2.9
6 months	4	6.5 6-7	2.7	2.8	2.9

Conclusions: most prominent hypoperfusion was detected in frontal cortex. Clinical improvement, decrease in HAMD and visible amelioration of cortical perfusion reflected efficient drug treatment of depression after three weeks and even further at six months follow-up in our small group of depressed patients.

PS-378

F. Tamgac, E. Alper, M. Bakar, N. Konuk, A.T. Akbunar
Departments of Nuclear Medicine and Neurology, Uludag University Medical School, Bursa, Turkey

HEMISPHERIC LATERALISATION OF STUTTERING MEASURED BY Tc-99m HMPAO SPECT

To assess brain perfusion differences in stuttering, Tc-99m HMPAO SPECT was realized on 20 right-handed stutterers (5 F, 15 M). Mean age was 11±5yrs (limits 5-20 yrs). In 17/20 pts stuttering began after psychic trauma and in 3/20 pts the cause was unidentified. Mean beginning age of stuttering was 5±2yrs and it had lasted for 6±4 years. In visual analysis, brain perfusion of 15/20 pts was interpreted as normal, SPECT images showed regional perfusion defects in 5/20 pts (1 left parietal, 1 left fronto-parietal, 1 right temporal, 1 right temporal and right parietal, 1 right frontal and parietooccipital). For semi-quantitative analysis 5x5 pixels square ROIs were manually placed symmetrically on mesial (MF), superior lateral (SLF) and inferior lateral frontal (ILF); anterior (AP), middle (MP) and posterior parietal (PP); anterior (AT), middle (MT) and posterior temporal (PT); occipital (O) and basal ganglia (BG). Whole brain perfusion index (WBI) (one region/average of all regions) was calculated as counts per pixel in the ROIs. Mean WBI values were as shown:

WBI	MF	SLF	ILF	AP	MP (*)	PP
Right	1.01±0.05	1.02±0.04	0.98±0.04	0.97±0.04	1.00±0.04	1.02±0.04
Left	1.00±0.04	1.02±0.04	0.98±0.03	0.96±0.03	0.98±0.05	1.01±0.05
WBI	AT	MT (*)	PT (*)	O	BG	
Right	1.05±0.04	1.06±0.04	1.01±0.05	1.04±0.07	0.94±0.04	
Left	1.03±0.05	1.03±0.04	0.98±0.05	1.02±0.04	0.92±0.04	

(* difference between right-left hemisphere was significant at 0.05)

In conclusion, in our series, semiquantitative analysis showed lateralisation of the left hemisphere which was not supported by visual analysis findings.

PS-379

İ.Coskun, E.Varoğlu, M.Yıldırım, A.Çayköylü, H.Uslu

Depts. of Psychiatry and Nuclear Medicine, Atatürk University, School of Medicine, Erzurum - TURKEY

CEREBRAL BLOOD FLOW CHANGES IN OBSESSIVE COMPULSIVE DISORDER AND THEIR RELATIONSHIP WITH CLINICAL MEASURES

The aim of this study was to evaluate the diagnostic value of Tc-99m HMPAO Brain SPECT in Obsessive Compulsive Disorder (OCD) and the relationship between regional cerebral blood flow (rCBF) changes and clinical status. Twenty-three patients (13M, 10F, mean age: 33.2 ± 5.3) with OCD and 6 healthy volunteers (mean age: 31.5 ± 3.6) were included in the study. Fifteen minutes after i.v injection of 740 MBq Tc-99m HMPAO, SPECT study was performed, and transaxial, coronal, sagittal and orbitomeatal slices were reconstructed. Orbitomeatal slices were used for quantitative evaluation of SPECT images. Total 19 ROI were drawn on the 4 consecutive orbitomeatal slices. The ratio of mean counts / whole cerebellar counts of each ROI was used for quantitative analysis. Quantitative rCBF values were correlated to clinical criteria such as anxiety scores, Yale-Brown scores and Depression scores. The rCBF values of the right basal ganglia in patients with OCD were significantly higher than those of controls (p=0.02). The rCBF values of the right and the left basal ganglia, frontal cortex, and right parietal cortex were also higher in patients with severe OCD than in controls. There were significant positive correlations between the rCBF of right basal ganglia and Yale-Brown and depression scores, respectively (p=0.02, p=0.0006).

These results show that increased activity of the right basal ganglia may have an importance in OCD clinic and this increased activity has a positive correlation with severity of disorder and depression scores.

PS-380

A. Vella, D. Volterrani, L. Burrioni, G. Pacciani*, P. Bertelli, P. Castrogiovanni*, **A. Vattimo**. Departments of Nuclear Medicine and Psychiatry*, University of Siena, Siena, Italy.

CEREBRAL AND CEREBELLUM BLOOD FLOW CHANGES IN OBSESSIVE COMPULSIVE DISORDER PATIENTS

Obsessive-Compulsive Disorder (OCD) is characterized by recurrent, unwanted thoughts (obsessions) and conscious, ritualized acts (compulsions) usually attributed to attempts to deal with anxiety generated by the obsessions. Several SPET studies of patients with OCD have demonstrated an increased brain flow in the frontal lobes. PET studies have also described increased glucose metabolism in the frontal cortex of subjects with this disorder. Moreover, an involvement of the basal ganglia and thalamus has been described. Recently, an involvement of the cerebellum in the output cognitive function has been reported in literature. The aim of this study was to investigate differences of blood flow in the cerebral and cerebellum cortex, basal ganglia and thalamus in untreated and treated OCD pts matched with normal control subjects. Using SPET and 99mTc-ECD, we assessed brain perfusion in 30 pts affected by OCD (10 drug-free and 20 treated) and in 8 matched normal controls. Four transaxial slices were selected through the supraventricular, midventricular, midthalamic and the cerebellar level. A Perfusion Index (PI) was calculated as the ratio of the activity density for the ROI, divided by the activity for the whole brain. We observed in OCD drug-free pts a significant (p<.05) blood flow increase in both frontal, the right temporal, the left occipital cortex, in the left thalamus and in the cerebellum. On the contrary, treated pts did not show significant blood flow changes. Treated pts with more severe disorders showed a diffused hypoperfusion when compared with pts with slight disorders. The presence of AXIS I comorbidity (mood disorders) in OCD pts determined a pattern of lower perfusion compared with OCD pts without comorbidity. The disease duration significantly (p<.006) influenced PI only in the lenticular nuclei. In conclusion, our findings suggest that OCD is associated not only with a dysfunction of the neuronal circuits interconnecting limbic/paralimbic cerebral structures, but even with the cerebellum.

PS-381

Li Xian-Feng, Wang Jin, Hu Guang, Wang Jie, Zhang Cheng-Gang

Hospital 1st Hospital of Shan-Xi Medical University, Department of Nuclear Medicine

SEMIQUANTITATIVE ANALYSIS OF BRAIN SPECT IN DEPRESSION

PURPOSE The aim of this study was to observe the changes of the regional cerebral blood flow (rCBF) in Depression (DEP) patients (pts) with Technetium-99m-ECD SPECT. **METHOD** 11pts (male 5, female 6, mean age 43.2±13.6)and 13 normal subjects (male 6, female 7, mean age 46.2±12.3) were studied. Brain SPECT was performed 20-30 min after 1110 MBq 99mTc-ECD iv using Elscint SP-4HR SPECT. 11 pts were in hospital and met the Criteria for diagnosis of psychiatric disease whose physical and neurologic examinations were normal. Hamilton DEP Scale analysis were performed whose score is above 17 in pts group, under 6 in control group. 13 normal subjects had not any psychiatric disease history. Either in sex or age had no statistical significant between control and pts group. Regions of interest (ROI) were manually defined on the 7 transaxial tomograms, the ROIs included bilateral frontal, temporal, parietal, occipital, basal ganglia, cerebellum and cingula cortex ROI. rCBF ratio were calculated: every mean pixel counts of the regional cerebral ROIs / mean pixel counts of bilateral regional cerebellum ROIs. **RESULTS** The rCBF ratio were is as follow:

	control group	pts group
anterior frontal	93.5 ± 8.1	85.5 ± 6.3
posterior frontal	104.0 ± 8.3	96.8 ± 8.5
anterior temporal	85.9 ± 6.8	77.7 ± 7.1
posterior temporal	99.9 ± 8.5	96.3 ± 6.6
cingula	104.5 ± 8.6	93.4 ± 7.4
parietal	105.1 ± 9.9	96.7 ± 9.1
occipital	114.1 ± 12.1	102.1 ± 9.8
basal ganglia	98.0 ± 8.5	97.4 ± 7.9

Statistical analysis were performed by using Statistical Analysis System soft. The analysis showed significant rCBF reductions in the anterior frontal cortex and cingula cortex of DEP pts compared with control group, and P is under 0.01. In posterior frontal, anterior temporal and parietal cortex, the rCBF were decreased also, and P is under 0.05. **CONCLUSION** Brain SPECT can reflect the changes of the rCBF in DEP pts, and multi reduced rCBF is the main changes. Though the rCBF in posterior frontal, anterior temporal, parietal cortex were decreased, bilateral anterior frontal cortex and cingula were the obvious and sensitive area decreased.

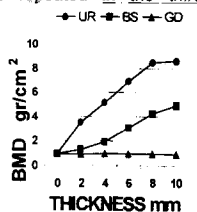
General nuclear medicine: Bone

PS-382

Tarik Basoğlu, Ayşegül Akar, Fevziye Canbaz, Irem Bernay, Murat Danacı, Kadriye Çakmak
Departments of Nuclear Medicine and Radiology, Ondokuz Mayıs University Hospital, Samsun, TURKEY

THE EFFECT OF CONTRAST-ENHANCING AGENTS ON DUAL ENERGY X-RAY ABSORPTIOMETRIC (DEXA) MEASUREMENTS

DEXA of the bone can be unreliable in patients with recently performed radiological examinations using contrast-enhancing agents (CEA). Our objective was (a) to determine the absorption rate of barium sulphate (BS), iodine (urografin) (UR) and gadolinium (GD) using a standard spine phantom, (b) to determine the influence of BS in patients with recently performed gastrointestinal X ray examinations (GIX). In the first part of the study, a plexiglass container was placed on the spine phantom and three repetitive measurements were performed for 2, 4, 6, 8 and 10 mm fluid thickness each, for all agents. Mean values were taken for the analysis. In the second part, 15 patients having had GIX with BS undergone a DEXA measurement approx. 2 hours after CEA application. All patients used laxatives the next day and the study was repeated in the third day. Phantom measurements with UR overlay showed 3.5, 5.2, 7.8, 5 and 8.6 fold; BR measurements showed 1.3, 2.3, 4.2 and 5 fold increment of the initial BMD value without CEA superimposition for 2, 4, 6, 8 and 10 mm fluid thickness respectively. GD showed no absorption up to 10 mm thickness. In patients with previous BR examinations 36.5% decrement in lateral lumbar spine (L1-L2) BMD values after laxative use was observed in the third day. In antero-posterior (AP) measurements the decrement was 52.7% with a range of 7-98%. In 7 of 15 patients, BMD values after laxative use were still excessively high. In lateral studies, increased values were observed even without visible CEA within the ROI. Mean BMD value in AP projections was higher than in lateral projections that was logical because of obligatory wide ROI definition. To conclude, DEXA studies should not be performed in the first 3 days following GIX. Although UR showed the highest experimental absorption rates, clinical studies are necessary to show the effects in vivo because of its higher clearance. Patients with previous GD enhanced MR studies can be presumably examined with DEXA during the same day, which should also be investigated clinically.



PS-383

V. Beauchat, D. Huglo, A. Delcourt, T. Prangère, U. Michon-Pasturel, M. Steinfeld
Regional and University Hospital, Department of Nuclear Medicine; Internal Medicine, Lille, France

UNILATERAL LOWER EXTREMITY HYPERTROPHIC OSTEOARTHROPATHY ASSOCIATED WITH AORTIC GRAFT INFECTION : ABOUT TWO CASES.

Radionuclide bone scanning is a sensitive examination for the detection of Hypertrophic OsteoArthropathy (HOA). In adults, which some of the aetiologies are known, there are uncommon causes. The aim of this study is to report two cases of unilateral HOA that reveal infected aortofemoral bypass grafts.

Patients : Two adults were studied. The first had previous history of vascular aortofemoral prosthesis in 1982, followed by a second graft in march 1994. The second had an aortobifemoral graft since 1986. In 1996, they presented a fever of unknown origin for several months. They equally suffered from pain or vasomotor troubles in one limb. All explorations were negative. They were sent for bone and gallium citrate or leucocytes scintigraphies to detect a deep sepsis.

Results : In these two cases, bone radionuclide imaging showed a monomelic HOA guiding the diagnostic. Gallium citrate imaging or/and white blood cell scintigraphies showed the infectious foci in the region of prosthetic vascular graft, confirmed by CT scan and surgery for the first and good evolution under antibiotherapy course for the second. Three months after treatment, new scintigraphies showed dramatically improved of OAH and abnormal abdominal gallium or labelled leucocytes uptake.

Discussion : Unilateral HOA is in fact an uncommon case described in infected aortic grafts with or without aortoenteric fistula. These two cases demonstrated the importance of nuclear medicine procedures. The knowledge of association between HAO and vascular graft infection could let to an early and efficient treatment.

PS-384

Z. BURAK, Z. ÖZCAN, K. KUMANLIOĞLU, A. MEMİŞ, D. SABAH, G. BAŞDEMİR, H. ÖZKILIÇ.
Departments Of Nuclear Medicine, Radiology, Orthopaedics and Pathology, Ege University, Izmir, Turkey.

ASSESSMENT OF PATHOLOGICAL VARIANTS OF OSTEOSARCOMA USING Tc-99m MDP THREE PHASE BONE SCINTIGRAPHY (TPBS).

Increasing experience with bone scan has suggested that different types of tumours tend to demonstrate particular alterations. In this study, we retrospectively evaluated the histological variants of osteosarcoma (OS) with respect to the characteristic patterns in Tc-99m MDP TPBS and also the role of bone scan in defining local tumour extent and detecting metastatic disease at initial diagnosis was revisited.

A total of 66 OS (34 M- 32 F, 7-39 ages) studied with TPBS were analysed. Tumours were located in femur (35), humerus (9), tibia (16) and other sites (6). All patients were evaluated with X-ray, CT and MRI. According to pathological diagnosis 28 of 66 OS were osteoblastic, 7 were chondroblastic, 7 were sclerotic, 5 were fibroblastic, 6 were malignant fibrous histiocytoma like, 4 were telangiectatic and 9 were para-periosteal OS. Scans were visually graded for (+) (++) and (+++) as (A) overall intensity of accumulation (B) the pattern of distribution and (C) the degree of cortical distortion and detection of scintigraphic margins of the lesion.

Results: (A): In all groups early images demonstrated high vascularity except para-periosteal OS showing lesser degree of accumulation. In delayed phase (DP), most remarkable uptake was observed in sclerotic OS while fibroblastic OS demonstrated less preferential uptake. (B): Most of the OS were visualised as patchy areas of decreased accumulation within high uptake while dough-nut pattern was also a common finding. Fibroblastic OS presented mostly as lobular cold lesions in TPBS. (C): All OS showed moderate distortion on bony out-line. Skip lesions were diagnosed in 6 OS while TPBS were positive in 16 of 22 patients with articular invasion.

In conclusion, no feature was unique to a particular variant and the grading for any type overlapped with another. Since fibroblastic and para-periosteal OS showed scan patterns overlapping with benign lesions, tumour seeking agents may be preferred for differential diagnosis.

Poster presentations

PS-385

C. De Sadeleer^{1,2}, J. Versijpt², Y. Van Belle², I. Dierckx³, M. De Meu¹, R.A. Dierckx²
O.L.V.-Hospital Geraardsbergen¹, University Hospital Gent², St.-Elisabeth Hospital Antwerp³, Belgium.

THE ROLE OF BONE SCINTIGRAPHY IN INDUSTRIAL OR INSURANCE MEDICINE: A RETROSPECTIVE STUDY

Patients with a suspicion of bone damage following an industrial or traffic accident are often referred for a bone scintigraphy as part of an insurance or industrial medicine investigation. In this patient population bone scintigraphy is mainly performed to exclude occult fractures of hand and feet, whiplash injuries, Sudeck's atrophy, avascular necrosis or to differentiate between an old or recent burst fracture.

Between 1996 and 1997, 70 consecutive patients (32 women and 38 men; mean age 39.3 years, range: 21-71 years) were referred by insurance or industrial physicians for a bone scintigraphy. Out of this group, in 53 patients, the preceding structural radiology (mean time between structural radiology and bone scintigraphy 2 days; range 0 to 8 days) was available.

In 30 out of these 53 patients (18 both positive and 12 both normal) bone scintigraphy findings concurred with structural imaging as to the number and location of abnormalities. In 17 patients, bone scintigraphy showed additional abnormal foci when compared to structural imaging, involving predominantly hands/wrists and feet/ankles. Most of these injuries were related to occult fractures (12) and to a lesser extent to periostitis (3) or Sudeck's atrophy (2). Of those 17 patients the scintigraphic diagnoses was subsequently confirmed in 10 cases by means of (computed) tomography. In 4 patients, the supplementary radiological investigations revealed no abnormalities and in 3 patients, no further investigations were required.

In the remaining patients, the structural image showed bone damage (burst fractures) while the corresponding bone scintigraphy was negative, thus excluding recent injury.

Conclusions: In this series of 53 patients the bone scintigraphy was decisive in 42% of the cases as part of the question raised by the insurance or industrial physician.

PS-386

Dierckx L., Everaert H., Momen A., Franken P., Bossuyt A.

Hospital: Free University of Brussels, Department of Nuclear Medicine

ADDITIONAL VALUE OF BONESPECT IN THE DORSAL SPINE AND THE RIBS

Aim of the study: comparison of planar and SPECT images for the detection and the localization of lesions in the dorsal spine and the ribs.

Methodology: 70 consecutive patients, who underwent both planar and SPECT images of the thorax, were selected retrospectively and independent of the clinical question. Imaging was acquired 2-3 hours after administration of 740 Mbq Tc^{99m}-MDP. Whole body images were performed using a 2-head bodyscan and displayed on XR-film (Gray scale). The SPECT images were performed using a 2-head camera. Reconstruction was done using a Butterworth filter adapted for count densities. The SPECT images were displayed on slices (transverse, coronal and sagittal) and volume rendered images. Planar and SPECT images were independently interpreted on the computerscreen.

Results: in 21 patients (30%) no lesions were seen on planar and SPECT images. For the dorsal spine a total of 39 lesions were seen on planar and 74 with SPECT. Of the lesions seen only with SPECT, the majority was localized on the anterior part of the vertebrae. For the ribs a total of 31 lesions was seen on planar and 64 with SPECT imaging. Of these lesions, a majority was found on the lateral arcs with an easier localization via the volume rendered images.

Conclusion: SPECT detects more scintigraphic abnormalities than planar images in the dorsal spine and the ribs. The majority of lesions only seen with SPECT were located in the anterior part of the corpus, hidden by the sternum, and the lateral arcs of the ribs.

PS-387

A. Dirlik, H. Akin, M. Taner, M. Esassolak, Z. Özcan, D. Sabah, Z. Burak
Department of Nuclear Medicine, Radiation Oncology and Orthopedic Ege University, İzmir, TURKEY

THE VALUE OF Tc^{99m}(V)DMSA SCINTIGRAPHY IN COMPARISON WITH THREE PHASE BONE SCINTIGRAPHY IN SOFT TISSUE SARCOMAS

Pentavalent form of DMSA (Tc^{99m}(V)DMSA) has been described as a tumour seeking agent. In this study, we aimed to investigate whether Tc^{99m}(V)DMSA scintigraphy had advantages over three phase bone scintigraphy (TPBS) in diagnosis and post-therapy follow-up of soft tissue sarcomas (STS). A total 19 patients (pts), 11 male, 8 female between 17-76 ages (mean=40.7±16.5 year) with soft tissue masses were studied. All pts were initially evaluated by TPBS. Within 5 days Tc^{99m}(V)DMSA scintigraphy was performed after injection of 370 MBq Tc^{99m}(V)DMSA and multiple projections of the body were obtained at 2 hr. All images were evaluated visually and quantitative analysis was performed by drawing regions of interest over the lesion and contra lateral normal tissue of Tc^{99m}(V)DMSA and TPBS. In 4 pts, both Tc^{99m}(V)DMSA scintigraphy and TPBS were applied during follow-up period in order to evaluate therapy response. Final diagnosis was determined by histopathological evaluation. 18 lesions were diagnosed as STS. Sarcomas with initial presentation, demonstrated similar uptake patterns both on Tc^{99m}MDP blood-pool (BP) phase and Tc^{99m}(V)DMSA scintigraphy. There was not a significant difference between mean uptake values of both tracers (1.82 ± 0.62 in BP MDP and 1.92 ± 0.35 in Tc^{99m}(V)DMSA scintigraphy $P > 0.05$). In 12 of 18 Tc^{99m}(V)DMSA avid sarcomas, increased Tc^{99m}MDP accumulation was observed on delayed phase. However, Tc^{99m}(V)DMSA uptake of STS was significantly higher than delayed phase Tc^{99m}MDP accumulation. In 4 pts evaluated at post-therapy period with a complete response to therapy, Tc^{99m}(V)DMSA scintigraphy was falsely positive in 3 out of 4 cases. Whereas, blood-pool activity of those lesions were significantly decreased concordant with good response to therapy. In conclusion, Tc^{99m}(V)DMSA scintigraphy seems to offer no advantage over TPBS in detection of STS. Tc^{99m}(V)DMSA scintigraphy appears to present poor results in the evaluation of post-therapeutic changes. Higher uptake ratios with Tc^{99m}(V)DMSA than delayed phase Tc^{99m}MDP accumulation suggests that further studies are indicated to lighten the Tc^{99m}(V)DMSA uptake mechanisms.

PS-388

N.Ö. Küçük, E. İbiş, Ş. Kutlay*, A. Kütükdeveci*, K.M. Kır, G. Aras, G. Tokuz.
Ankara University Medical School, Depts of Nuclear Medicine and Rehabilitation*. Ankara/TÜRKİYE

EVALUATION OF THE EFFECTIVENESS OF LOW DOSE US THERAPY WITH THREE PHASE BONE SCAN IN PTS WITH RSDS

Reflex sympathetic dystrophic syndrome (RSDS) is a complication presenting itself with burning pain, hyperesthesia, oedema, hyperhidrosis, trophic skin and bone changes in affected extremity. Its pathophysiology is not clear, but it is believed that increased activity of nervous system due to effect of autonomic reflex mediator may be responsible. There are recent reports about possible effects of low dose ultrasound (LDUS) therapy due to its property of increasing elimination of mediators and decreasing mediator effectivity on sympathetic ganglions. This study was planned to evaluate the effectiveness of LDUS therapy in pts with RSDS.

44 pts (24 female, 20 male, mean age 46.5±13.4) with RSDS were included in the study. All pts were treated with exercises, contrast bath and oral naproxen sodium. Additionally, LDUS (0.5 watt/cm²/day) therapy for 4 weeks was applied in 25 of 44 pts. Clinical (pain intensity, pain index of joint, extremity volume, activity) and scintigraphic (three phase Tc-99m MDP bone scanning) evaluations were performed on all pts at the beginning of therapy, first and third months. Radioactivity uptake of periarticular areas of the affected extremity were calculated and compared to that of healthy extremity on 2 hours images. Uptake ratio of RSDS/normal extremity were obtained.

The clinical parameters, except extremity volume, were found to be better in pts who had US therapy than pts without US therapy. Scintigraphic findings were similar in all pts as increased blood flow, blood pool activity and late phase uptake. But, there was no significant difference in scintigraphy and uptake ratio between pts with and without LDUS therapy. Decreased uptake ratio was found in pts in follow up period and it was 2.41±1.41 at the beginning, 1.82±0.3 at first month and 1.37±0.2 at third month in all RSDS pts.

As conclusion, RSDS pts with LDUS therapy has showed rapid recovery according to clinical findings and low dose US is an effective therapy. On the other hand, it is observed that quantitative three phase bone scan may be successfully used for the assessment of recovery.

PS-389

Y.Imai, Y.Nishimura, A.Ohkura, T.Imai, Y.Sasaki, T.Shinkai, Y.Nishimoto, H.Ohishi and H.Uchida. Dept.of Radiology, Nara Prefectural Mimuro Hospital Dept. of Oncoradiology and Radiology, Nara Medical University, Nara, Japan

CLINICAL EVALUATION OF BONE TUMOR WITH TL-201 SCINTIGRAPHY

The aim of this study is to evaluate the clinical usefulness of TL-201 scintigraphy in bone tumors. There were 10 subjects with osteosarcoma, 4 with chondrosarcoma, 2 with giant cell tumor, 2 with bone cyst, 2 with fibrous dysplasia, 1 with exostosis, 1 with nonossifying fibroma and other benign lesions. Tl-201 was intravenously injected at 111 MBq, and scintigrams were obtained 15 minutes and 3 hours after administration. The uptake was evaluated according to the criteria of L.R.Mendez et al. Grade 0 ; background activity, Grade 1 ; equivocal activity, Grade 2 ; definitive activity, less than in myocardium, Grade 3 ; definitive activity, equal to that in myocardium, Grade 4 ; activity greater than in myocardium. Tl-201 uptake was observed in the early phase and delayed phase in all cases with osteosarcoma, which is malignant. Moreover, the uptake grades improved after chemotherapy. Among benign tumors Tl-201 uptake was observed only in giant cell tumors and nonossifying fibroma. No Tl-201 uptake was observed in benign lesions such as infarction and osteophyte. These lesions showed radiographic images similar to those from bone tumors. This suggests that Tl-201 scintigraphy is useful for differentiation of benign and malignant bone tumors and for evaluation of therapeutic effects. However, Tl-201 uptake was observed also in benign tumors with rich blood flow, so their differentiation from malignant disease was difficult.

PS-390

SY Lee, JH Baek, SH Kim, YA Chung, YH Park, SK Chung, YW Bahk¹.

Catholic Univ. Medical College and Samsung Cheil Hospital¹, Seoul, KOREA

METABOLIC PROFILE STUDY OF FIBRO-OSSEOUS DYSPLASIA USING PINHOLE BONE SCAN.

We assessed metabolic profiles of fibrous dysplasia(FD) using pinhole bone scan(PBS) which can portray various FD lesions in great detail. PBS findings were retrospectively analyzed and correlated with radiographic findings of 51 foci in 20 lesions seen in 18 patients. Diagnosis based on either histology and/or radiography. The study subjects were 8 men and 10 women (age range: 16 -56 yr and mean: 41). The scan and radiography were taken at the same time or one day apart. The affected sites were the skull and face 4, rib 7, pelvis 4, clavicle 1, long bone 4. We used a single- head gamma camera (Siemens Orbiter Model 6601) and 4-mm pinhole collimator. Scan was performed 2 hr pi of ^{99m}Tc-HDP. Lesional tracer uptake was graded arbitrarily into 1+ (uptake same as normal bone), 2+ (moderate uptake), and 3+ (marked uptake). Topography and chemical profile were assessed with radiographic correlation.

The results were as shown in Table 1.

Tracer Uptake	X-ray				
	Radiolucent	GGO	Radiodense	Effaced cortex	LT
1+	5	1	0	0	0
2+	5	3	0	1	5
3+	0	1	5	18	7
Total (51)	10	5	5	19	12

GGO: Ground-glass opacity LT: Locular trabeculation

In conclusion, radiographically lucent lesions of fibrous FD accumulated less tracer whereas dense lesions of osseous FD accumulated more tracer, profiling metabolic activities of various radiographic types of FD. Pinhole scan was useful in the diagnosis and metabolic assessment of FD.

PS-391

G. Kuchta*, L. Wolska-Goszka*, G. Romanowicz**, P. Lass**, A. Hoppe***, S. Angielski***, J. M. Słomiński*.

*Dept. Pneumonology, **Dept. Nuclear Medicine, ***Dept. Clinical Biochemistry, Medical University of Gdańsk, Poland.

BONE COLLAGEN SYNTHESIS AND DEGRADATION MARKERS FOR DETECTING BONE METASTASES IN PATIENT WITH LUNG CANCER.

The presence of skeletal metastases in patient with lung cancer is a prognostic factor of major importance. Bone scintigraphy plays a major role in the diagnosis of bone metastases. The clinical utility of new biochemical markers of bone metabolism has recently been investigated in various bone diseases. The aim of the present study was to evaluate the role of some bone metabolism markers in comparison with bone scan in the follow-up of lung cancer patients. In a selected population of patients, possibly affected by metastases on the basis of scintigraphic examination, which is high sensitive but poorly specific, we assessed the efficiency of the markers. Serum bone alkaline phosphatase (BAP), the C-terminal propeptide of type I procollagen (PICP), the N-terminal propeptide of type I procollagen (PINP), the C-terminal cross-linked telopeptide of type I collagen (ICTP) were used to monitor bone formation and resorption, respectively. Using RIA method we evaluated this markers in serum in male patients (n=26) and healthy subjects (n=18). All values are expressed as means ± SE, p < 0.05).

The results of BGP, BAP, PICP, PINP, ICTP in both group in serum are below:

	BAP IU/L	PICP µg/L	PINP µg/L	ICTP µg/L
Healthy subjects	17,80±4,25	101,81±7,54	37,76±4,56	5,96±0,29
Lung cancer patient	45,28±10,55*	243,51±17,19*	84,10±13,76*	10,02±1,12*

*-p<0.05 vs. Healthy subjects values (unpaired t-Student test).

We conclude that the results of this preliminary study show that in patients with lung cancer the determination of bone metabolic markers could be suitable as a screening procedure for detecting bone metastases.

PS-392

X.D. Liu, X.T. Lin, F. Li, G.Deng.

Department of Nuclear Medicine, Sports Medicine, Radiology. Hua Shan Hospital, Shanghai Medical University, Shanghai 200040, China.

DIAGNOSIS AND MANAGEMENT OF PATIENTS WITH UNEXPLAINED BACK PAIN USING BONE SPECT

Purpose To investigate the value of SPECT, CT or MRI, X-ray in patients with chronic low back pain and to compare the results of SPECT with those of CT or MRI and X-ray. **Methods**: Bone SPECT, whole body planar image, X-ray, CT or MRI were performed in 31 cases with low back pain for more than 6 months and their results were compared and analyzed. **Results**: 28 patients had a positive SPECT, of whom 27 (96%) had an abnormal CT or MRI finding and 14 (50%) had an abnormal X-ray radiography. 29 patients showed a positive CT or MRI scan, of whom 27 (93%) had focus at SPECT. SPECT identified 98 foci, of which 88 (90%) were associated with CT or MRI foci. CT or MRI allowed identification of 90 lesions, of which 98% were associated with SPECT findings. **Conclusions**: SPECT is superior to planar image in diagnosis of patients with low back pain and is nearly the same sensitive as CT or MRI especially in patients with metastases which involve the lumbar vertebrae.

Poster presentations

PS-393

M Mitjavila, J Solis, *G Ocete.

Centro Diagnóstico Henares, Nuclear Medicine. * Centro Cánovas, Traumatology, Spain .

BONE SCINTIGRAPHY IN MILITARY PARACHUTISTS WITH LEG PAIN.

In the military literature, reported incidences of stress fractures varied between 2-31%. One possible explanation for this marked discrepancy is that not all authors perform a bone scan in every patient suspected of having stress fracture.

Patients and method: Fortytwo military parachutists have been referred to the Nuclear Medicine Department for bone scanning. All of them suffered from leg pain, with an average symptomatic period of 5 weeks, and with negative conventional radiography. Two-phase bone scintigraphy was performed and multi-view planar images were obtained. In patients with bone scintigraphic findings in the knee, MRI was obtained.

Results: All patients showed pathological bone scan. 59 lesions were detected. 39% (24/59) in the tibia (not including the tibial plateau); 66% (16/24) shin splint and 34% stress fracture. 6.7% in the femur (not including the femoral condyles). 49% in the knee (patella, condyles and tibial plateau) and only 3.3% in the feet. In 28% (12/42) patients asymptomatic sites of pathological uptake were visualized.

In 4/24 patients bone scintigraphy demonstrated additional more subtle bone injury than MRI.; 2 lateral femoral condyle, 1 medial femoral condyle and 1 lateral tibial plateau, but their location was appropriate for the type of sustained trauma.

Conclusion: 1- Bone scan contributes to accurate diagnostic evaluation in military parachutists. 2- Even asymptomatic lesions do, however, need to be treated. 3- MRI cannot reliably exclude the presence of an articular cartilage injury.

PS-394

MA Balsa, M Mitjavila, L Castillejos, P G^a Alonso, *JL Rodriguez, M Delgado, FJ Penin, C Pey. Hospital Universitario Getafe. Nuclear Medicine and Rheumatology departments. Spain.

BONE SCAN IN SYMPATHETIC MAINTAINED PAIN SYNDROME.

Patients and method: Twenty six patients (18M, 8F) suffering from reflex sympathetic dystrophy (RSD) have been referred to the nuclear medicine department for bone scanning. All patients met Doury criteria for RSD.

Bone scan was graded as : 1- normal; 2- diffusely increased juxta-articular tracer activity on delayed bone scan image and 3- focal abnormal uptake.

Results: In no patient normal bone scan was obtained. The 18 patients with the RSD variant showed on delayed bone scan images, diffuse increased tracer throughout the hand and wrist or the foot. Focal abnormal uptake in bone scan was obtained in 9 patients. 5/9 had focal pain without x-ray changes: 2 hips, 1 knee and 2 patients with only a single ray; and segmental or localized RSD variant was diagnosed.

Conclusion: Sympathetic maintained pain syndrome covers a broad grouping of clinical conditions in which pain and autonomic dysfunction are intimately related. Bone scan could provide an objective marker for the RSD variant and for segmental variety as well.

PS-395

P. Vansteenkiste*, J. Lammens**, M. De Roo*, M. Oostens*, G. Fabry**, L. Mortelmans*

Dept. of Nuclear Medicine and Orthopedics, University Hospital Gasthuisberg, Leuven, Belgium.

QUANTIFICATION OF GROWTHPLATE ACTIVITY OF THE KNEES BY Tc99m-MDP SPECT

Introduction: Children with genu valgum or genu varum are thought to have abnormal activity in the growth plates. In order to quantify these abnormalities, a normal database is needed. Therefore, we performed planar and SPECT images of the knees after injecting Tc99m-MDP in children with normal growth plates.

Methods: 3 hours after injecting Tc99m-MDP we performed a whole body scan and SPECT imaging (3-headed camera, 60 projections of 35 sec, matrix 128x128, high resolution collimator) of the knees in 33 children (age between 3 and 17 years) with no history of abnormalities of the legs. Each distal femoral and proximal tibial growth plate was divided into 4 quadrants and the following ratios were calculated using a thresholding algorithm applied on the iteratively reconstructed SPECT images: lateral to medial (lat/med), anterior to posterior (ant/post) and right to left (right/left).

Results: (Mean+/-SD):

	right femur	left femur	right tibia	left tibia
lat/med	1.12(0.10)*	1.10(0.09)*	1.02(0.09)	1.02(0.09)
ant/post	1.01(0.14)	0.99(0.08)	0.94(0.11)*	0.95(0.11)*
right/left	total	total planar	lateral	medial
distal femur	0.99(0.08)	1.00(0.09)	1.00(0.07)	0.99(0.11)
tibial plateau	0.98(0.08)	1.00(0.12)	0.99(0.09)	0.98(0.09)

*: p<0.05

Conclusion : the different activity ratios in the growthplates of the knees in normal children are approximately 1.00 with a S.D. of 0.10, with the exception of the lateral/medial ratio of the femoral growthplates (approximately 1.10+/-0.10) and the anterior/posterior ratio of the tibial growth plates (approximately 0.95+/-0.11).

PS-396

Zehra Özcan, Zeynep Burak, Kamil Kumanloğlu, Gülçin Başdemir, Dündar Sabah, Hayal Özkılıç. Ege University Medical Faculty, Nuclear Medicine, Pathology and Orthopedic Surgery Departments, İzmir, Turkey.

A SCINTIGRAPHIC PHENOMENON, "DOUGHNUT" APPEARANCE IN PRIMARY BONE TUMORS

Central hypoactivity surrounded by a hyperactive rim, namely "doughnut" sign is a well-known feature in bone scintigraphy. In this study it was aimed to examine the frequency of this finding and to test whether this phenomena is a specific pattern of a unique pathology. Tc-99m MDP three phase bone scintigraphies of 155 patients with primary bone tumors studied between 95 and 97 were retrospectively reviewed. Final diagnoses were osteogenic sarcoma (66), Ewing sarcoma (21), chondrosarcoma (17), giant cell tumor (11), aneurysmal bone cyst (8), primary lymphoma of bone (7), plasmacytoma (6), eosinophilic granuloma (6), soft tissue sarcoma (13). Appearance of doughnut like lesion was noted for each blood-pool phase and delayed images. On blood-pool phase images totally 45 lesions showed doughnut appearance most frequently in giant cell tumor (63.6%), aneurysmal bone cyst (62.5%), osteogenic sarcoma (37.8%) and plasmacytoma (33.3%). On osseous phase of bone scintigraphy this sign was mostly visualised in aneurysmal bone cyst (75%), giant cell tumor (72.7%), plasmacytoma (33.3%), eosinophilic granuloma (33.3%) with a total number of 26. Giant cell sarcoma, aneurysmal bone cyst, followed by plasmacytoma and osteogenic sarcoma were the most frequent tumors with doughnut sign on both early and delayed phases of the study with a total ratio of 15 out of 155. In conclusion, although mostly observed on giant cell tumor, doughnut sign may be observed in many other pathologic entities of bone and seems not to be a specific pattern attributable to a certain type of bone tumor. Moreover, mechanisms related to doughnut appearance may be different in this heterogeneous group of tumors including tissue necrosis, cystic degeneration, hemorrhage, absence of osteoblastic activity, and bony destruction.

PS-397

Aysun Özdemir¹, Hakan Özdemir², Fırat Güngör¹, Binnur Karayalçın¹, Metin Erkişiç¹, Akdeniz University Faculty of Medicine, Departments of Nuclear Medicine¹ and Orthopedic Surgery², Antalya, TURKEY.

THE DIAGNOSTIC ROLE OF BONE SCAN IN PATIENTS WITH TRAUMATIC WRIST PAIN

In most patients with distal radius fractures and related injuries, standart radiographic examination is satisfactory to solve clinical problems. However, in the evaluation of complex or occult fractures, in considering distal radioulnar and radiocarpal joints, as well as in the assessment of fracture healing and complications, bone scintigraphy may provide more information together with conventional radiography. The aim of this study was to identify the diagnostic role of bone scintigraphy in patients who sustained from wrist pain after distal radius fractures. Fifteen patients (aged between 28-87 years; 8 men, 7women) who had distal radius fractures with a mean period of 54 months ago (range between 48 to 63 months), were included in this study. All patients had been treated with closed reduction and plaster cast immobilization for 6 weeks. Arthrography had been performed in all patients after remove the cast. In arthrography, while 9 of 15 patients had triangular fibrocartilage complex (TFCC) or intercarpal ligament (ICL) lesions, 6 of 15 patients had not any abnormality. Although, radiological and functional findings of these 9 patients did not show any abnormality after the treatment, these patients had distal radioulnar pain. Bone scans were performed in all patients. Scintigraphies were found to be abnormal (increased uptake in radioulnar or radiocarpal compartment) on 8 of 9 patients (88 %)on the delayed images who had TFCC or TFCC+ICL lesions demonstrated by arthrography. Conversely, bone scans were normal on 6 patients (100 %) in whom having no demonstrable abnormality by arthrography. These results showed that bone scintigraphy has assumed an important role in the evaluation of TFCC lesions. It was thought that the responsible mechanism of increased uptake in these cases may be related to early degenerative disease due to ligamentous or cartilaginous abnormality.

We suggest that bone scintigraphy should performed after standart radiography in patients whose radiographies are normal but symptoms persist or in patients with suspected bone, cartiliginous or ligamentous abnormalities. Positive results warrant clinical correlation and further radiographic evaluation.

PS-398

F. Pons, R. Herranz, S. Vidal-Sicart, J. Pavía, L. Alvarez¹, P. Peris², N. Guañabens², A. Monegal², D. Fuster, J. Setoain. Departments of Nuclear Medicine, Clinical Biochemistry¹ and Rheumatology². Hospital Clinic, University of Barcelona, Spain.

QUANTITATIVE EVALUATION OF BONE SCINTIGRAPHY IN THE ASSESSMENT OF PAGET'S DISEASE ACTIVITY

Interest concerning the assessment of the degree of activity of Paget's disease has increased since the advent of effective therapies. The aim of this study was to develop a quantitative method for bone scintigraphic assessment of Paget's disease activity.

Methods: Twenty patients with Paget's disease (15 males, 5 females; mean age 65 years, range 35-83) were studied prospectively. Bone scintigraphy was performed after i.v. injection of 740 MBq of 99mTc-HMDP. A scintigraphic visual activity index as well as a quantitative activity index, which reflect both the extent and activity of the disease, were obtained for each patient. The quantitative activity index results from the sum of the activity (geometric mean measured from the anterior and posterior views) for all the affected bones divided by a reference obtained in a non affected bone. To evaluate the validity of the scintigraphic method, several biochemical markers of bone turnover were assessed: serum total alkaline phosphatase (TAP), serum propeptide aminoterminal of type I procollagen (PINP), urinary hydroxyproline (HYP) and urinary N-terminal cross-linked telopeptide of type I collagen (NTx).

Results: A high correlation was found between the visual and the quantitative indexes ($r = 0.78, p < 0.0001$). The highest correlations between the markers and the quantitative activity index were found for the PINP ($r = 0.69, p < 0.001$), which was the most sensitive marker of bone formation, and for urinary NTx ($r = 0.63, p < 0.005$), which was the most valuable marker of bone resorption.

In conclusion, quantitative evaluation of bone scintigraphy allows for easy and objective assessment of Paget's disease activity and it can be useful in evaluating the effectiveness of therapies.

PS-399

G. Ríos, F. Pérez¹, V. Llorens, V. Cosgaya, T. Rodriguez, J. Genollá, and JC. Fombellida

Nuclear and Reumatology¹ Services. Hospital de Cruces. Vizcaya. Spain.

SACRAL INSUFFICIENCY FRACTURES. SCINTIGRAPHIC VERSUS CLINICAL AND RADIOGRAPHIC DIAGNOSIS.

Sacral insufficiency fractures (SIF) are a sort of stress fractures. They are often difficult to diagnose, both by clinical and/or radiological means, so, they may be overlooked.

OBJETIVE

The aim of this study is to compare the bone scintigraphy with the clinical and radiological findings in the SIF diagnosis.

MATERIALS AND METHOD

From 1992 to 1996 thirteen patients were diagnosed of SIF by bone scintigraphy. 11/13 had fracture of the pubic rami associated.

The mean age was 72 years (61-88). 12/13 were females.

The next findings were taking into account in all scintigraphies: the uni or bilateral pattern of uptake, the location, and the agreement with clinical and radiological suspicion.

RESULTS

Clinical diagnosis of SIF was achieved in 8/13 cases (61.5%).

The pelvis radiography did not show sacral fracture in any case, however 5/13 (38.4%) showed pubic rami fracture.

Bone scan detected: 6 unilateral SIF (4 of them had associated pubic rami fractures), and 7 bilateral SIF (all of them with associated bilateral pubic rami fractures).

CONCLUSIONS

1) Bone scintigraphy is the best procedure for the diagnosis of SIF, and it is necessary to perform it, even when only pubic rami fracture is found by radiography. This fact is due to the high frequency of the SIF association which are not found in Rx examination.

2) Clinical suspicion is more useful than radiology in the diagnosis of SIF.

PS-400

L. Saidi, F. Archambaud, A. Ramadan, V. Gendreau, G. Grimon, I. Hallaj, E. Durand, A. Prigent. Hospital: Le Kremlin Bicêtre- Department of Nuclear Medicine- 78 Av Gal Leclerc Le Kremlin Bicêtre -AP-HP Paris. France

SPECT VERSUS PLANAR SCINTIGRAPHY (PS) IN BONE DISEASE.

The aim of this prospective study was to evaluate the contribution of bone SPECT to diagnosis and precise location of bone lesions. SPECT was performed in the presence of either a persistent bone pain with normal PS (PS- ; n = 21) or a moderate or imprecise hyperfixation on PS (PS+; n = 31).

Patients and Method: Fifty two patients (pts) with either neoplasia or only spinal pain were recruited for bone scintigraphy. Planar whole-body scan and SPECT of the spine, or hips or knees were performed after i.v. injection of 740 MBq of 99m Tc HMDP. Projections (30 sec) were acquired with a 6° step on 180° (spine) or 360° (hips or knees) in 64x64 matrix. Data were filtered and reconstructed to obtain transverse, sagittal and coronal slices. According to the clinical presentation, patients were classified into 2 categories : C1 : neoplasia with or without pain (n = 23) ; C2 : only spine pain (n = 29).

Results : When SPECT enabled to localize the bone lesions more precisely in order to evoke a benign or malign lesion, the patients were classified loc(+) and loc(-) otherwise.

PS(-)	SPECT(-)	SPECT(+)	n pts	PS(+)	Loc(-)	Loc(+)	n pts
C1	5	4	9	C1	7	8	15
C2	11	1	12	C2	12	4	16
n pts	16	5	21	n pts	19	12	31

In 3 out of 4 patients with neoplasia and a negative PS, SPECT evoked a metastatic lesion, while in the remaining patient a stress fracture was suspected, confirmed by MRI. In 12 pts with only spinal pain (C2), SPECT has shown a lesion in only one case. In 8 out of 15 pts with neoplasia and a positive PS, SPECT was helpful in suggesting either metastases (2pts) or benign lesions (6pts).

Conclusion : Although over a short series, SPECT has visualized hyperfixations not seen on PS in about half of the patients with a known neoplasia. Moreover, SPECT localizes more accurately hyperfixation in 37% of positive PS. SPECT may be recommended in patients with neoplasia and a persistent pain to evidence lesion not seen on PS and to precise the malign or benign nature of the localization.

Poster presentations

PS-401

D. Sandrock, G. Strey, B. Kettner, D.L. Munz

Clinic for Nuclear Medicine, Charité, Humboldt University Berlin, Germany

WHAT IS "NORMAL" IN THREE-PHASE BONE SCINTIGRAPHY OF HAND AND FINGER JOINTS ?

Three-phase bone scintigraphy is believed to be valuable for the detection of abnormalities in hand and finger joints for orthopedic and rheumatologic studies. However, only a few data are available about "abnormal" findings in normal persons.

Overall, 50 patients (28 women, 22 men) aged 19 to 77 years (mean +/- SD, 52 +/- 16 years) without pain, history of injuries or soft tissue or bone disease were studied. Three-phase bone scintigraphy of the hands was performed after i.v. injection of 600 MBq Tc-99m-MDP as follows: Phase I ("perfusion"): 12 x 5 s p.i.; phase II ("blood pool") between 1.5 and 5 min p.i.; phase III ("mineralisation") 3 h p.i. All scans of phase II and III were evaluated blinded by 2 experienced observers and the tracer intensity in joints was scored from 0 to 3.

Of 1800 joints studied overall, 80 (4.4 %) had increased tracer accumulation in phase II and 133 (7.4 %) in phase III. In phase II, 49 had a score of 1, 28 a score of 2, and 3 a score of 3. In phase III, 8 had a score of 1, 39 of 2, and 13 of 3. There was a prevalence of abnormal findings in phase II (in brackets phase III) of 4.0 % (9.0 %) for hand joints, of 3.8 % (11.2 %) for MCPs, and of 4.4 % (5.3 %) for PIP/DIPs. Careful follow-up investigations and intense questioning of the patients concerning their history could finally explain 20 % of the accumulations. There are still 80 % (170 joints) remaining with unexplained abnormal accumulations in phase II or III. 12 patients had at least 1 with a score \geq 2.

Conclusion: The prevalence of abnormal accumulations in hand and finger joints („false“ positive findings for orthopedic and rheumatologic studies) is at a clinically relevant level.

PS-402

A. Sankaya¹, A. C. Aygün², L. Candan², M. S. Ayhan², T. F. Çermik¹
Trakya University Faculty of Medicine Dpts. of Nuclear Medicine¹, Plastic and Reconstructive Surgery² Edirne, TURKEY

EVALUATION OF HYDROXYAPATITE, POROUS POLYETHYLENE AND SILICONE ELASTOMER IN A RABBIT CRANIAL DEFECT MODEL

Reconstruction of bone defect in the head region is difficult and often requires complex solutions to achieve functional and aesthetic results. In this study we investigated the tissue response and bone in growth, comparatively hydroxyapatite (HA), porous polyethylene (PP) and silicone elastomer (SE) as a bone graft substitute. 24 albino rabbit (8 rabbit for each implant) were used for this investigation. After frontal incision the periosteal elevated and bone cavities 1 cm wide was formed with a drill. HA 500 particles, SE rubber and high-density PP placed in the cavities. As a part of a prospective study the vascularization rate of all implant materials implanted was analysed 10 days and 2 months after surgery using Tc-99m MDP scintigraphy of the skull. Scintigraphic study were performed by means of a single head gamma camera with a pinhole collimator 2 h after intravenous injection of 148 MBq Tc-99m MDP. Tracer accumulation in the implantation area was visually rated as no vascularization (0), beginning vascularization(+), partial vascularization (++) , nearly complete vascularization (+++) and complete vascularization (++++). All tissue specimens were placed first in %10 nitric acid solution for decalcification. Hystological changes in the implantation areas were evaluated by macroscopic and microscopic specimens. The vascularization, connective tissue growth, foreign body reaction and bone regeneration around the implant evaluated. Scintigraphy results showed that increased tracer uptake at the HA subjects on tenth day was further increased at medium degree by second month. Increased tracer uptake at PP subjects on the tenth day found to be decreased but continued at the second month. Increase tracer uptake at SE subjects observed on the tenth day was lost by the second month. Results of this study suggested that HA and PP were stabilised in bone while silicone was mobile and HA implants has greater vascularization and biocompatibility comparing with PP.

PS-403

R.C. Smart, M.A. Pack, J.A. Rayner, T.H. Diamond†

Nuclear Medicine & Endocrinology† Departments, St. George Hospital, Kogarah, NSW, Australia

INTEROPERATOR AND INTRAOPERATOR VARIABILITY USING LUNAR EXPERT AND LUNAR DPXL BONE DENSITOMETERS

To assess the precision of the bone mineral density (BMD) measurement, the interoperator and intraoperator variability of the Lunar EXPERT and Lunar DPXL densitometers were assessed for the lumbar spine and femoral neck regions.

102 patients were studied over a 4 month period with each patient being scanned on both instruments on the same day. The patients ranged from normal to severely osteoporotic (L2-L4 BMD 0.7-1.7 g/cm³). Each of the patient scans was analysed twice by two experienced operators with a minimum period of one month between the analyses. The BMD values for the L2-L4 vertebrae on the AP spine and the BMD values for the femoral neck and Wards Triangle were recorded. The interoperator and intraoperator variability were assessed by calculation of the coefficient of variation (CV;%) and the standard error (SE; g/cm³) from linear regression analysis.

	Interoperator				Intraoperator			
	DPXL		EXPERT		DPXL		EXPERT	
	CV	SE	CV	SE	CV	SE	CV	SE
AP spine	0.74	.011	2.04	.024	0.75	.011	1.46	.022
Fem. neck	1.75	.018	1.83	.020	1.61	.019	1.25	.015
Wards Tri	2.65	.025	2.65	.020	2.40	.023	0.95	.008

The EXPERT densitometer gives a small improvement in precision for the femoral region but is less precise than the DPXL densitometer for the lumbar spine. This is most likely due to the less accurate edge detection on the AP spine scans, requiring more operator intervention.

PS-404

E. Urbanová, J. Vižďa, *K. Urban, P. Kafka.
Dpts. of Nuclear Medicine and *Orthopedic Surgery, University Hospital Hradec Králové, Czech Republic.

BONE SCINTIGRAPHY AND A REVISION HIP ARTHROPLASTY, WHERE BIOACTIVE GLASS-CERAMIC WAS USED.

The progress made in orthopedic reconstructive surgery using bone and joint prostheses and immobilization instruments has been supported by the development of biomaterials with good mechanical properties and biocompatibility. The ingrowth characteristic of bioactive glass-ceramics cannot be assessed by radiological methods such as standard X-rays or CT because they only visualize indirect phenomena. The aim of this study was to determine the utility of 99mTc-MDP after the revision operation for aseptic loosening of the total hip prosthesis. So far 11 patients were monitored during 22 months after surgery. Scintigraphy was made after i.v. injection of 555-740 MBq 99mTc-MDP as 3-phase bone scintigraphy and event. SPECT of pelvis by dual-head gamma camera. Scintigraphy showed highly increased osteoblastic activity in reconstructed acetabulum region in early phase (7 days to 1 months after). In the further follow-up 3,6,9,12 and 22 months the osteoblastic activity was gradually decreasing (9 pts.). Results of comparison region of interest - reconstructed acetabulum and os sacrum on transaxial slices, showed decrease in uptake of radioactivity. Delay in decrease of osteoblastic activity was done by slower healing and was followed longer immobilisation (2 pts.). Full weight bearing was allowed the sixth month after the operation. As a conclusion it is suggested that 3-phase bone scintigraphy and SPECT are valuable methods to follow up patients after hip revision operation, where bioactive glass-ceramic was used for the reconstruction.

PS-405

S.C. Tsai, S.P. Chang, L.H. Kao, W.Y. Lin, M.C. Lee and S.J. Wang.

Taichung Veterans General Hospital, and Chung-Shan Medical College Hospital, Taichung, Taiwan.

BONE MINERAL DENSITY IN YOUNG CHINESE FEMALE DANCERS.

For the evaluation of the effect of dancing on bone mineral density (BMD) of young girls, twenty-nine young Chinese girls (age: 16.3 ± 0.5 years) whom had regular dancing training for at least 6 years (dancing group) and twenty sex- and age-matched non-athletic controls (age: 16.6 ± 0.8 years) (control group) were included in this study. Body weight (BW), body height (BH) and body mass index (BMI, BW/BH²) were 50.6 ± 5.8 kg vs 56.6 ± 6.8 kg (p value < 0.01), 158.4 ± 3.9 cm vs 160.0 ± 3.7 cm (p value > 0.05) and 20.15 ± 2.20 kg/m² vs 22.08 ± 2.31 kg/cm² (p value < 0.01) in the dancing groups vs control groups, respectively. BMD was measured in all study subjects using a commercial dual-energy X-ray absorptiometer (DEXA) at the second to fourth lumbar spines (L2-4) and the right femoral neck (FN).

The results revealed the following: (1) there was no significant difference of BMD of L2-4 and FN between the dancing group (1.17 ± 0.14 g/cm²; 1.01 ± 0.14 g/cm²) and the control group (1.22 ± 0.07 g/cm²; 1.02 ± 0.09 g/cm²) (p value > 0.05); (2) there was no significant difference of BW- and BMI-corrected BMD of L2-4 between the dancing group (2.33 ± 0.24 *10⁻² g/cm²/kg; 5.84 ± 0.63 *10⁻² g/cm²/kg/m²) and the control group (2.19 ± 0.34 *10⁻² g/cm²/kg; 5.60 ± 0.77 *10⁻² g/cm²/kg/m²) (p value > 0.05); (3) there was significant difference of BW- and BMI-corrected BMD of FN between the dancing group (2.01 ± 0.28 *10⁻² g/cm²/kg; 5.06 ± 0.70 *10⁻² g/cm²/kg/m²) and the control group (1.82 ± 0.27 *10⁻² g/cm²/kg; 4.65 ± 0.59 *10⁻² g/cm²/kg/m²) (p value < 0.05).

The results revealed that the dancers were significantly thinner than controls and, for dancers, the negative effect of lower BW may neutralized the positive effect of dancing exercise on increasing BMD, especially on FN.

PS-406

Zhao Xinming, Yao Shukun, Wang Jiangfang, Wei Lanxiu, Xu Fang, Zang Zhijie, Sun Li

The Fourth Hospital of Hebei Medical University, China, Department of Nuclear Medicine.

COMPARATIVE STUDY OF ^{99m}Tc(V)-DMSA WITH ^{99m}Tc-MDP IN METASTATIC BONE TUMORS

Abstract: PURPOSE: To assess the clinical value of ^{99m}Tc(V)-DMSA imaging in the diagnose bone benign and malignant lesions. **METHODS:** ^{99m}Tc(V)-DMSA and ^{99m}Tc-MDP whole body bone scintigraphy were performed on 106 patients with suspected bone metastatic lesions. **RESULTS:** Seventy patients had positive ^{99m}Tc-MDP scans with multiple and solitary skeletal involvement, 68 out of 70 patients ^{99m}Tc(V)-DMSA scans showed some matched areas of increased radioactive tracer concentration in bony metastases. Two hundred and thirty-six bone metastatic lesions were demonstrated by ^{99m}Tc-MDP scintigraphy, while only 175 out of 236 bone metastatic lesions were displayed by ^{99m}Tc(V)-DMSA imaging. However, Twenty-four patients had positive ^{99m}Tc-MDP scans with bony benign lesions ^{99m}Tc(V)-DMSA none had concentration. Twelve patients had normal ^{99m}Tc-MDP and ^{99m}Tc(V)-DMSA scans and declared no bone metastatic disease. The sensitivity and specificity of ^{99m}Tc(V)-DMSA were 73.22% and 100%, respectively. **CONCLUSION:** Pentavalent ^{99m}Tc(V)-DMSA scanning shows a higher specificity for bone metastatic tumors than ^{99m}Tc-MDP scintigraphy, and is of clinical value in distinguishing benign and malignant bone tumors.

Key Words: radionuclide imaging; bone tumor; pentavalent technetium-99m- dimercaptosuccinic acid

General nuclear medicine: Gastroenterology

PS-407

Küçük NÖ., Aras G., Soylu A., Tolunay Ö., Örmeci N., Düzgün N., İbiş E., Akin A., Tokuz G.

Ankara University Medical School, Nuclear Medicine, Gastroenterology, Pathology and Immunology Depts. Ankara/Türkiye

EVALUATION OF GI INVOLVEMENT OF BEHÇET'S DISEASE WITH Tc99mHIG AND LEUKOCYTE SCINTIGRAPHY

Behçet's sendrome (BD) is a disease where immune mechanisms and/or infections are thought to be involved. 30 patients (pts) who were diagnosed with the major symptoms of BD according to ISG criteria and who were under long term colchicine therapy were imaged with two infection agents, Tc 99m HIG and Tc 99m HMPAO leukocytes (Tc-LC). 4 and 24 hour (hr) whole body scintigrams were taken and images were considered as positive if the 4 hr images showed abnormal activity. All the pts with gastrointestinal (GI) uptake of either radiopharmaceutical were sent to colonoscopy and biopsies were taken. 2 pts with positive Tc-HIG and Tc-LC uptake in the GI tract showed mucosal ulceration in colonoscopy. 11 pts with positive Tc-HIG and negative Tc-LC in the GI region did not show any abnormalities in the colonoscopy whereas immuno- and histopathologic findings were abnormal. These 11 pts didn't have any GI complaints. Tc-LC images and colonoscopy being negative is thought to reflect the fact that there is no acute or chronic infection in the mucosa. Positive Tc-HIG and pathology findings suggest that there is a submucosal involvement of the disease even in the intestinally symptom free period of BD. These findings are in agreement with the claims that incidence of GI involvement of BD is actually much higher than it has been reported.

This study may be an indication of the use of Tc-HIG for submucosal changes of the intestine.

PS-408

R. Bennink, M. Peeters, V. Van den Maegdenbergh, B. Geypens, M. De Roo, P. Rutgeerts, L. Mortelmans.

Dept. Nuclear Medicine UZ Leuven Belgium.

EVALUATION OF SMALL BOWEL TRANSIT TIME FOR SOLID AND LIQUID TEST MEAL IN HEALTHY MALE AND FEMALE VOLUNTEERS.

Evaluation of severe functional gastrointestinal motility disorders requires an investigation of the entire gastrointestinal tract. This should be possible with a single radionuclide imaging study. The purpose of this study was to define normal values of small bowel transit in men and women, and to assess if there is a difference between gender, since it has been shown that women have slower gastric emptying rates for solids. Iliocaecal transfer characteristics are observed in view of future combined gastric emptying, small bowel and colon transit studies. A standard gastric emptying test for a solid (Tc99m sulfur colloid, 230 Kcal) and liquid (In111 DTPA water) test meal was performed in 11 healthy male and 13 healthy female volunteers. After 135 min. the volunteer was placed in supine position for static imaging of the abdomen every 15 min. for 6 hours. Decay and cross-over corrected geometric mean gastric emptying data were fit to a modified power exponential function to determine the 10% stomach emptying time for solid and liquid test meal separately. A ROI was drawn around the caecum and colon ascendens to determine the arrival time of at least 10% of the solid and liquid test meal. 10% small bowel transit time (10%SBTT) and oro-caecal transit time (OCTT) were calculated. The results are shown below (mean ± SEM minutes).

	Male solid	Female solid	Male liquid	Female liquid
OCTT	281.8±15.0	288.8±20.4	281.8±15.2	288.8±20.4
10%SBTT	268.2±15.2	269.3±20.0	271.7±28.2	284.8±20.0

We observed a simultaneous transfer of solids and liquids from terminal ileum to caecum (correlation coefficient 0.93). There is no statistically significant difference in SBTT between gender or solids and liquids.

Conclusion: In contrary to the gastric emptying time, the SBTT of solids and liquids is not significantly different nor a difference between gender was found. Since iliocaecal transfer occurs as a bolus phenomenon, an In111 labeled test meal can also be used for the determination of colon transit in a single imaging study protocol.

Poster presentations

PS-409

C.M. Boivin¹, M.A. Toy¹, M.T. Hallissey², B. Hughes³

Departments of Nuclear Medicine¹ and Surgery², Queen Elizabeth Hospital and Clinical Investigations Unit³, University of Birmingham, Birmingham, UK

COMPARISON OF 14C AND 13C UREA BREATH TESTS FOR *H. PYLORI* INFECTION IN 248 PATIENTS

14C and 13C urea breath tests are both widely used, but most published comparisons have been on small numbers of patients. The selection of 13C protocol and normal cut-off appears to be backed by much larger clinical trials than the 14C test.

The aim of this study was to assess the degree of correspondence between the two tests in a large series with a view to standardising protocols and normal cut-offs for results.

248 consecutive clinic attendees (139M/109F), mean age 53 (13-84), mean weight 73kg (40-125) underwent simultaneous standard 13C (100mg urea) and 14C (100kBq) urea breath test protocols after an overnight fast and a test meal of pure orange juice. 232 had received previous *H. Pylori* eradication therapy finishing at least six weeks before attendance. Pre-, 20, 30 and 40-minute breath samples were taken for 14C and pre- and 30-minute samples for 13C.

The 30-minute samples showed excellent correlation ($r = 0.99$) and closely matched the theoretical conversion factor for this particular pair of tests of 14C %/mol = 0.63 x 13C excess parts/1000 over baseline (%), thus validating both methods. A 14C normal cut-off of 2.7%/mol best matched the standard 13C limit of 3.5%, giving 98.4% agreement (only 4/248 discordant results). The theoretical equivalent of 2.2%/mol gave 9/248 discordances. 2.7%/mol is equivalent to a weight-adjusted figure of 0.2%/mmol x kg, and is somewhat lower than the commonly used cut-off of 0.5%/mmol x kg which gave 22/248 discordances. There were 61 *H. Pylori* positive and 187 negative results by 13C. The 20, 30 and 40-minute 14C samples produced 15, 3 and 1 false positive and 1, 1 and 2 false negative results respectively compared to the 30 minute 13C sample. Weight-adjustment of the 14C result did not significantly reduce the degree of agreement (6/248 discordances).

The correspondence between the two tests was so high that they can be considered interchangeable. A single breath sample at 30 minutes is sufficient. Weight correction is not necessary, but might be considered in equivocal results for obese, underweight or paediatric patients. The 14C normal cut-off should be chosen to match that for 13C which is backed by large clinical trials. Both tests are very safe, and there is no evidence to suggest that the 14C radiation dose (7 μ Sv effective dose, corresponding to a 1 in 3 million excess chance of fatal cancer) is less safe than the amount of urea used in the 13C test (100mg compared to .003mg in the 14C test). Which test to use should be judged according to convenience and cost.

PS-410

L Rosa e Silva; LEA Troncon; RB Oliveira; FJHN Braga; L Gallo Jr; MC Foss. Faculdade de Medicina, Ribeirão Preto, USP, BRAZIL.

RAPID INTESTINAL TRANSIT (IT) IN CHRONIC PANCREATITIS (CP) IS ASSOCIATED WITH VAGAL AND SYMPATHETIC DENERVATION (D). In previous works we have shown that patients (pts) with CP and autonomic neuropathy (AN) have rapid IT of liquids. This work aimed to study the relationship between vagal and sympathetic D and transit rates through proximal and distal small bowel in CP. Subjects included 37 pts with CP and 18 healthy controls. Fasted subjects ingested a liquid meal (250ml, 437Kcal) labelled with 99mTc-phytate, 18 MBq. Abdominal scans were taken for 180 min with a gamma camera. Counts from ROIs over the small intestine yield measurement of the times of meal arrival to proximal (tPSB) and distal small bowel (tDSB) and to the cecum (tC). Subjects underwent 3 cardiovascular (CV) nerve function tests (respiratory arrhythmia, passive tilting, Valsalva manoeuvre), which yield 5 parameters related to CV autonomic control. Vagal activity was assessed by beat-to-beat variation during respiration (RV) and the initial heart rate variation after tilting (TV). Postural hypotension (PH) after tilting indicated sympathetic dysfunction (dysf). Based on abnormal results in any 2/5 CV parameters, 17 pts were regarded as having AN (groupCP-AN). CV tests were normal in the 20 other pts (groupCP). In controls tPSB was 13 min; 3-70 (median, range), tDSB was 30 min; (12-83); tC was 102 min; (50-180). In group CP, tPSB, (15 min, 2-34); tDSB (33 min; 5-64) and tC (97 min, 29->180) were similar to controls. In group CP-AN, tPSB (12 min; 1-45) did not differ ($p > 0.2$) from CP and controls; both tDSB (18 min, 4-60) and tC (40 min; 10-103) were lower ($p < 0.02$). In CP pts, tDSB correlated significantly with RV ($R_s = 0.38$, $p = 0.02$) and TV ($R_s = 0.4$, $p < 0.01$), but not with PH. The tC correlated significantly with RV ($R_s = 0.51$, $p < 0.01$), TV ($R_s = 0.38$, $p < 0.02$) and PH ($R_s = 0.54$, $p < 0.01$). In conclusion: pts with CP and AN rapid IT through PSB is associated with vagal dysf but accelerated DSB transit is associated with both vagal and sympathetic denervation.

PS-411

M. El-Desouki¹, M. Mohamadiyeh¹, R. Al-Rashed², S. Othman¹, I. Al-Mofleh².
¹ Nuclear Medicine Div., ² Gastroenterology Div., Dept. of Medicine, King Khalid University Hospital, King Saud University, Riyadh, Saudi Arabia.

Features Of Hepatic Cavernous Hemangioma On Planar And SPECT Tc-99m-Labeled Red Blood Cells Scintigraphy

Objective: To determine value and diagnostic accuracy of Tc-99m-labeled red blood cells scintigraphy, planar and SPECT, in the investigation of suspected hepatic cavernous hemangioma as found on ultrasound. **Patients and Methods:** One hundred patients, 89 females (89%) and 11 males (11%), with ages between 22 and 67 years (mean 38 years) were investigated for liver masses found on ultrasound of the abdomen. All the patients had undergone Tc-99m- red blood cells scintigraphy. The size of the lesions ranged between 1 and 9 cm. The final diagnosis was reached through cytology, biopsy and/or histopathology tests. **Results:** A total of 130 lesions were found. In regards to distribution of the lesions, 116 (89%) were single, 14 (3%) multiple, 118 (91%) in the right lobe and 12 (9%) in the left lobe, 83 (64%) posterior, and 47 (36%) anterior. In respect to the pattern of activity filling, 86 (66%) lesions were typical and 44 (34%) atypical. The results of Tc-99m- red blood cells scintigraphy showed sensitivity, specificity, positive and negative predictive and accuracy values of 97%, 83%, 98%, 77%, and 96% respectively. The use of SPECT improved the sensitivity value by 1% for lesions of 1 - 2 cm size. **Conclusions** Tc-99m-red blood cells scintigraphy is a noninvasive technique helpful for the diagnosis of hepatic hemangioma especially in those possessing the risk of hemodynamic changes. SPECT should be performed whenever planar imaging fails to show the lesion by 2h. The use of ultrasound should precede the scintigraphy for two important results; the size and the location of the lesion. Lesions of less than 1 cm in size are undetectable because they are beyond the limit of spatial resolution of gamma camera.

PS-412

M. Escribano, M.J. Tabuenca, J. de Haro, M. Santos (1), M. Fuentes (1), M. Alonso, I. Freile, V. Peiró, E. Mariño, M. P. Páramo, J. Ortiz Berrocal. Clínica Puerta de Hierro. Departments of Nuclear Medicine and Experimental Surgery (1). Madrid. Spain.

GAMMA SCINTIGRAPHY IN THE EVALUATION OF A NEW FLOATING DELIVERY RETAINING SYSTEM

Introduction: Gamma scintigraphy is being used routinely for the *in vivo* evaluation of new systems of oral sustained release which act as drug reservoirs from which active substances are released.

Objective: To assess a new galenic product that serves as a floating delivery system (FDS) by means of gastric emptying scintigraphy in an experimental animal model.

Material and methods: 1) *In vitro* assays. The product was labeled with 99mTc, and the radiochemical purity and stability of the galenic product, FDS, radiolabeled with 99mTc (99mTcGP-FDS) were determined.

2) *In vivo* assays. Landrace-Large-White pigs weighing between 20 and 30 kg were used for the experimental model. Each animal underwent a basal study with H₂O-99mTc-DTPA as a control, followed by the 99mTcGP-FDS study. Dynamic images were acquired over periods of 4 and 7 hours, respectively, at a rate of one image every 10 s in 64x64 matrix, using a dual-head gamma camera (Elsint, Helix model). We obtained activity/time curves, corrected for disintegration, and calculated the area below the curve. The groups were compared by analysis of variance (ANOVA), followed by Dunnet's test.

Results: Six pigs have been studied to date. The labeling efficiency was $\geq 80\%$. The mean percentage of activity remaining in the stomach was 33% at 1 hr and 15% at 4 hr in the controls and 72% at 1 hr, 67% at 4 hr and $\geq 50\%$ at 7 hr in the trials with 99mTcGP-FDS (with the exclusion of one case in which the product was biologically contaminated).

Conclusions: Gamma scintigraphy is a noninvasive technique that may play an important role in the development and evaluation of new drug-delivery systems since it provides *in vivo* information on their location and behavior in the gastrointestinal tract.

PS-413

J. Flores Rangel, N. Mendez Sanchez, A. Graef Sanchez, M. Uribe Esquivel.

Medica Sur Clinic Foundation and National Institute of Nutrition. Departments of Nuclear Medicine and Gastroenterology. Mexico City, Mexico.

DELAYED GASTRIC EMPTYING BUT NOT INTESTINAL TRANSIT TIME INFLUENCES THE ENTEROHEPATIC CYCLING OF UNCONJUGATED BILIRUBIN IN PATIENTS WITH GILBERT'S SYNDROME.

Recently was showed enterohepatic cycling (EHC) of unconjugated bilirubin (UCB) after distal small bowel resection in the rat (Gastroenterology 1996;110: 1945). Moreover we believe that both patients with Gilbert's syndrome and hamsters have an EHC of UCB because their bile contain principally bilirubin monoglucuronide (BMG) from reduced hepatic bilirubin UDP-glucuronyltransferase activity. Furthermore, a decreased intestinal motility has been found in fasting induced hyperbilirubinemic rats probably resulting in an increase in the EHC of UCB (Gastroenterology 1996; 111: 217).

Aim: The objective of the present report was evaluate the gastric emptying, intestinal transit time and serum UCB levels in patients with Gilbert's syndrome
Methods: Nine patients with Gilbert's syndrome (mean age 32.8 +/- 9.9 yr.) and five normal healthy volunteers acting as controls (mean age 25.4 +/- 1.5 yr.); were studied according to the following criteria: positive fasting unconjugated hyperbilirubinemia, no hemolysis, as well as absence of medications and gastrointestinal symptoms. Both groups were fasted 12 h. overnight; a standard meal mixed with 1 mCi of 99mTc-DTPA was administered; images were acquired every 10 min. for 110 min; gastric emptying was evaluated by geometric mean method. Intestinal transit time was considered complete when the radio-marker was seen in the ascending colon. Serum UCB levels were determined by HPLC. Statistics analysis was employed arithmetic mean, standard deviation y correlation of U-Mann Whitney.

	Gilbert's patients	Controls	p value
n	9	5	
Gastric Emptying (min)	134.1 +/- 42.8	90.0 +/- 6.5	0.05
Intestinal Transit Time (min)	138.1 +/- 62.8	183.8 +/- 11.2	NS

Conclusions: Gastric emptying is delayed significantly in Gilbert's syndrome and intestinal transit time differences between Gilbert's syndrome patients and controls were not significant. These observations suggest the possible role of gastrointestinal hormones in regulating bilirubin handling. Also these results support that EHC of bilirubin is facilitated by normal or rapid than decreased intestinal transit time.

PS-414

D. Fuster, F. Lomeña, M. Sans¹, FJ. Setoain, J. Llach², J. Panés¹, JM. Bordas², JM. Piqué¹, J. Setoain. Clinical Hospital of Barcelona, Departments of Nuclear Medicine and Gastroenterology¹ and Digestive Endoscopy Unit².

EARLY AND LATE SCANS WITH 99mTc-HMPAO-LEUKOCYTE TO EVALUATE ACTIVE INFLAMMATORY BOWEL DISEASE: WHICH IS MORE ACCURATE?

Purpose: To evaluate the accuracy of 99mTc-HMPAO-leukocyte scan (LS) in the assessment of extension and activity of inflammatory bowel disease (IBD) using early and late scan findings. **Methods:** 48 patients with active Crohn's disease (CD,n:24) or ulcerative colitis (UC,n:24) were included. All patients underwent clinical assessment, including Van Hees (CD) and Seo (UC) scores, colonoscopy and scintigraphy within 48 hours. LS was performed at 45' (early scan) and 3h (late scan) after labelled leukocyte reinjection. To evaluate the extension of IBD, colon was divided in 5 segments (rectum, sigmoid, descending, transvers and ascending) and LS results were compared to colonoscopy findings. To evaluate the IBD activity, labelled leukocyte uptake in LS was classified as 1)mild (<bone marrow), 2)moderate (>bone marrow, <liver) and 3)severe (>liver) and was compared to clinical scores and colonoscopy results.

Results: 1)IBD extension: LS sensitivity, specificity, predictive values and accuracy (202 colonic segments):
LS+ 45' LS+ 3h LS+ 45' or 3h LS+ 45' and 3h

Sens.	62.5%	72.6%	73.4%	61.7%
Spec.	78.3%	71.6%	71.6%	78.0%
PPV	83.3%	81.5%	81.7%	83.1%
NPV	54.7%	60.2%	60.9%	53.7%
Accuracy	68.3%	72.2%	72.7%	67.6%

2)IBD activity:

- a) Early scan vs clinical scores: r 0.36, p 0.01
- b) Late scan vs clinical scores: r 0.34, p 0.02
- c) Early scan vs colonoscopy: r 0.57, p 0.001
- d) Late scan vs colonoscopy: r 0.59, p 0.001

Conclusions: 1)LS may estimate the extension of IBD. Late scan is more accurate, but early scan is more specific. 2)The correlation between LS and colonoscopy was better than the correlation between LS and clinical scores.

PS-415

L. Galuska, M. Péter*, I. Garai, J. Varga, L. Bajnok, J. Tóth*, A. Szanyi

University Medical School, Nuclear Medical Centre and *Department of Radiology, Debrecen, Hungary

INVESTIGATION OF GALL-BLADDER CONTRACTILITY BY QUANTITATIVE CERULETIDE CHOLESTINTIGRAPHY AFTER RAPID GALL-STONE LITHOLYTIC THERAPY

The purpose of this study was to control the gall-bladder (GB) contractility of patients treated by methyl-terbutyl ether litholytic therapy (LT), and to investigate the prognostic value of the parameters calculated from a dynamic hepatobiliary gamma camera study concerning gall-stone (GS) recurrence.

From the 21 patients who had undergone litholytic therapy (through a transhepatic catheter, with 4-12 hours duration) of cholesterine GSs 2-6 (mean 3.5) years before, two groups were formed: 7 of them were without, while 14 with GS recurrence at the time of the gamma camera investigations. A third group consisted of 44 normal control persons. During the gamma camera study we acquired one min frames for 110 min after the intravenous administration of 150 MBq 99mTc-HIDA. At the final stage of GB filling (between 45-60 min) we started 1 ng/kg/min Ceruletide infusion for 45 min. Hepatic and hilar disappearance half time (T1/2) values did not show any significant difference between the hepatic and hilar transport of the radiopharmaceutical in the three groups (variance analysis, P>0.1). The gall-bladder ejection fraction (GB-EF) was calculated as the relative change between the maximum and minimum of the time-activity curves generated from the GB region. The normal limit of Ceruletide GB-EF calculated from the control group was 72 % without background subtraction. The disappearance half time of the radiopharmaceutical from the GB during the Ceruletide infusion was calculated, too.

As the distribution of neither the GB-EF, nor the GB T1/2 values is Gaussian in the treated groups, Kruskal-Wallis non-parametric test was used to compare the results, and showed that both parameters are significantly different (P<0.001) in the group with recurrent GSs. Parameter values of the treated patients without recurrence did not differ significantly (P>0.05) from those of the control group.

Based on these results we hope that CE cholescintigraphy before LT can have an important role in establishing the prognosis of GS recurrence of the GS patients. To prove whether there is a smaller probability of recurrent GSs in the case of patients with normal GB-EF requires further, prospective investigation.

PS-416

S. F. Grebe, D. Füllgraf, H. Müller, K. D. Müller, E. L. Sattler, S. K. G. Grebe, H. Lindemann, P. Bittner-Dersch.

Kerckhoff-Klinik (Max-Planck-Institute) Bad Nauheim, and Dept. of Nuclear-Medicine, Radiation-Center and Childrens-clinic of University Giessen, Germany.

EVIDENCE FOR BILE ACID MALABSORPTION IN CYSTIC FIBROSIS: ABSORPTION OF THE RADIOACTIVE BILE ACID ANALOGUE SELENIUM-75-HOMOTAUROCHOLIC ACID (75-Se-HCAT) IS IMPAIRED IN CYSTIC FIBROSIS PATIENTS.

Bile acid absorption can be measured using oral administration of Se-75-HCAT followed by total body radioactivity count. Using this method we have previously found evidence of bile acid malabsorption in 3 cases of patients with cystic fibrosis (CF). In the present study we extended our observations to a larger group of patients with CF. 18 subjects with CF (20f which were already investigated in the earlier study) and 39 control subjects took 1 mg of Se-75-HCAT (37KBq activity) and were examined using a whole body counter at 1 h, 24 h, 72 h, and 168 h. Study endpoint was the 168 h count expressed as percentage of the 1 h count. The mean 72 h and 168 h counts were significantly lower in CF patients than in controls (42,3 % and 15 % versus 73,3 % and 41 %; p < 0.00001). 15 subjects with CF had 168 h counts of less than 19 % (below the normal reference range), 7 of these had values of less than 12 % (severe malabsorption). Bile acid malabsorption may contribute to the gastrointestinal manifestation of CF. Mechanical barrier formation, caused by increased production of highly viscous mucous, hindering the transit of bile acid into enterocytes, may be the underlying mechanism. Further studies are needed to delineate the potential benefits of therapeutic interventions aimed at improving bile acid absorption in CF.

PS-417

Z. Janković, S. Marinković, S. Marković, R. Spaić, N. Stanković*, M. Petrović*

Military Medical Academy, Institute of Nuclear Medicine, Clinic for General and Vascular Surgery*, Belgrade, Yugoslavia

ASSESSMENT OF BILE FLOW AFTER CHOLECYSTECTOMY BY ^{99m}Tc-MEBROFENIN SCINTIGRAPHY

Cholecystectomy (CE) is the intervention that breaks the functional bond gallbladder - sphincter of Oddi and directs all secreted bile to papilla of Vater. We supposed that gallbladder removal had no significant influence on bile secretion and transit through bile ducts except common bile duct. The aim of our study was to assess the functional significance of CE on bile flow using cholescintigraphy and by analysis of the time activity curve recorded over confluence of the left and right hepatic ducts.

We used ^{99m}Tc-mebrofenin in the dose of 2.8 MBq/kg and examined 10 normal subjects (group A: 4 males and 6 females, mean age 46 years) and 10 asymptomatic patients (group B: 5 males and 5 females, mean age 52 years) who had been subjected to CE one to twelve months before scintigraphy. Time activity curves were generated over liver parenchyma and hepatic ducts. Normalized parenchymal curve was subtracted from biliary curve and final curve represented the true curve of hepatic ducts. That curve was processed by determination of characteristic points as time parameters: T1 the first point, T2 the point representing half of the maximal count rate and T3 the point of the maximal count rate. The descending part of the curve was not analysed because of influence of gallbladder radioactivity. The time of radioactivity appearance in small bowel was recorded.

The values of T1, T2 and T3 showed no significant statistical differences in both groups (t-test, p>0.05) and are presented in the following table (mean±s.d.):

group	T1 (min)	T2 (min)	T3 (min)
A	6.4±1.3	15.2±2.1	27.6±4.1
B	6.3±1.2	15.8±1.9	30.7±3.7

In four patients of group A radioactivity appeared in small bowel after more than 30 minutes of imaging time and in all patients of group B within 30 minutes after beginning of the study (Fisher's test, significant difference, p<0.05)

Our results indicate that in patients subjected previously to CE and without accompanying biliary disease the bile flow through hepatic ducts shows no difference in relation to normal subjects with intact gallbladder and that only the flow through common bile duct is changed significantly.

PS-418

Z. Janković, D. Pucar, S. Marković, S. Lukačević*, R. Doder*

Military Medical Academy, Institute of Nuclear Medicine, Clinic of Gastroenterology*, Belgrade, Yugoslavia

COMPARATIVE SCINTIGRAPHIC ASSESSMENT OF THERAPEUTIC RESPONSE AFTER BALLOON DILATATION AND BOTULINUM TOXIN APPLICATION IN PATIENTS WITH ACHALASIA

The aim of investigation was to assess the therapeutic effect of balloon dilatation (BD) and botulinum toxin injections (BTI) in patients with idiopathic achalasia.

The group of 11 patients (6 males and 5 females, age 18-72 years, mean 42 years) was examined by esophageal scintigraphy (ES) before and within three months after treatment (BD in six, BTI in two and both treatments in three patients). ES was performed in two phases and total acquisition time of 2.5 minutes (one frame / 4 seconds). In the first phase supine patients faced to gamma camera swallowed 18.5MBq ^{99m}Tc in 10 ml of aqueous solution and in the second they drank 100 ml of water in upright position. Last three frames of the study were used for count acquisition over stomach. The esophageal retention (ER) was calculated as percent of total swallowed radioactivity retained in esophagus after the second phase of data acquisition.

In 9 patients the images recorded before and after treatment in supine position showed no tracer elimination to stomach (it was seen in two patients after BD). In upright position partial spontaneous elimination happened in six patients after BD and in two patients after BTI (in one of them also before BTI). After drinking 100 ml of water significant ^{99m}Tc elimination to stomach and decrease of ER more than 50% of a baseline value occurred in six patients treated with BD (the same patients who demonstrated spontaneous elimination in upright position) and in only one patient subjected to BTI.

Our results show superiority of BD over BTI as therapeutic modality in patients with achalasia. Imaging with small diagnostic radionuclide volume in supine position is insufficiently sensitive for the changes of esophageal emptying after treatment of achalasia and therefore in most of patients not suitable for the evaluation of therapeutic response.

PS-419

Y. Kunjvasu, S. Hasebe, Y. Niio, K. Uchiyama, H. Shinohara, J. Nagashima, J. Kin*, K. Kumada*, K. Takizawa, M. Yamada, H. Shima, M. Honda, S. Matsuoka, and M. Obuchi. Showa University Fujioka Hospital, Departments of Radiology and Surgery* Fujioka 1-30, Aoba-ku, Yokohama, 227-8501, Japan.

PREOPERATIVE EVALUATION OF THE LIMITATION OF HEPATIC RESECTION USING ^{99m}Tc-GSA (GALACTOSYL HUMAN SERUM ALBUMIN) SCINTIGRAPHY.

This study aimed to evaluate the usefulness of the parameters obtained with ^{99m}Tc-GSA scintigraphy for preoperative indication on the limitation of hepatic resection to the patients with hepatic tumors.

Patients and Methods: Thirty-eight patients who underwent hepatic resection were studied on ^{99m}Tc-GSA scintigraphy before and after operation. These patients were divided into two groups. Group A had no postoperative complication (n=31). Group B had some postoperative complications (n=7). Preoperative parameters of ^{99m}Tc-GSA liver scintigraphy (HH15, LU15) were calculated from the activities of liver and cardiac ROIs at 5 and 15 minutes after injection. The resection ratio (RR) was obtained by comparing the liver volumes which were calculated from the pre- and postoperative SPECT studies. The resectability indices (Res) were calculated as follows: Res(LU15) = LU15 × (100 - RR(%)) / 100, Res(HH15) = (1/HH15) × (100 - RR(%)) / 100.

Results: The mean values of Res of patients who have had no postoperative complications, were 1.54(Res(HH15)) and 23.5(Res(LU15)). Otherwise, the mean values of Res of patients having some postoperative complications were 1.05(Res(HH15)) and 15.6(Res(LU15)). The threshold values of Res, of which half of patients had complication, were 1.10(Res(HH15)) and 16.4(Res(LU15)). There were statistically significant differences in the distribution of Res between A and B groups (p=0.002, Mann-Whitney test).

Conclusion: The resectability indices using ^{99m}Tc-GSA liver scintigraphy are useful for the preoperative evaluation of the limitation of hepatic resection.

PS-420

G. Marotta, L. Bonavina*, M. Castellani, E. Reschini, M. Pagani*, L. Antoniazzi*, A. Peracchia*, F. Voltini, A. Alberti, P. Gerundini Department of Nuclear Medicine and *Dept of General and Oncologic Surgery, IRCCS-Ospedale Maggiore, University of Milan, Italy

ESOPHAGEAL SCINTIGRAPHY BEFORE AND AFTER LAPAROSCOPIC MYOTOMY AND FUNDOPLICATION FOR ACHALASIA

Esophageal scintigraphy has been proven useful in the objective assessment of the results of Heller myotomy and Dor fundoplication in patients with esophageal achalasia. The purpose of this work was to evaluate the esophageal motility by means of radionuclide esophageal transit study before and after laparoscopic myotomy and anterior fundoplication in addition to clinical and manometric evaluation.

Twenty-one patients (7 males, mean age 39 yrs, range 21-66 yrs) were imaged in the upright position after a single swallow of 20 ml of water containing 37 MBq of ^{99m}Tc sulphur colloid. Sequential images were collected for 10 minutes (early phase: 0.5 sec/frame for 60 sec, late phase: 5 sec/frame for 9 minutes). Time-activity curves were generated by drawing ROIs on the proximal, middle and distal thirds of the esophagus. The percentage retention of radioactivity at 1 and 10 minutes were calculated from the curve analysis.

After a mean follow-up of 12 months the distal esophageal stasis at 1 and 10 minutes was improved by laparoscopic surgery, decreasing from 88.4±12.8% to 20.4±21.8% (p<0.001) and from 84.2±15.3% to 10.0±11.9% (p<0.001), respectively. The mean dysphagia score decreased from 2.1 to 0.3. Manometric evaluation showed a decrease of the lower esophageal sphincter pressure from 30.7 to 11.2 mmHg (p<0.001), and the residual pressure decreased from 14.7 to 2.8 mmHg (p<0.001).

In conclusion, laparoscopic myotomy combined with anterior fundoplication improves both symptoms and esophageal emptying and is a safe and effective procedure in patients with esophageal achalasia. Esophageal scintigraphy provides an easily performed and inexpensive test in the long-term follow-up of laparoscopic treatment of achalasia.

PS-421

A.Naito, K.Suzuki, H.Toyama, Y.Komori, A.Wakayama, A.Hasumi, M.Kuroda, K.Ejiri, T.Fujiwara, K.Ito, S.Koga.
Fujita Health University, Toyoake, Hokushin General Hospital, Nakano, Japan.

EVALUATION OF SEQUENTIAL CHANGES OF ASIALOGLYCOPROTEIN RECEPTOR BINDING WITH I-125-GSA ON ISCHEMIA/REPERFUSION INJURY IN RAT LIVER: HISTOPATHOLOGICAL VALIDATION.

We previously reported that asialoglycoprotein (ASGP) receptor binding may provide a valuable information of ischemia/reperfusion injury and recovery after hepatic lobectomy and transplantation. The purpose of this study is to validate the histopathological changes after hepatic ischemia/reperfusion as compared with the sequential changes of ASGP receptor binding with I-125-GSA. The hepatic artery, portal vein, and bile duct were cross-clamped for 90 min, then, reperfused. At 1, 3 hr, 1 and 2 wk after the reperfusion, I-125-GSA was injected. Five min after the injection, blood samples were obtained, and the liver was removed. Mean uptakes (% dose/g) of the liver and blood samples were calculated in each time point. Histology sections were stained with hematoxylin-eosin (HE) for assessment of ischemic damage and regeneration and triphenyl-tetrazolium chloride (TTC) for determination of regeneration. The liver uptakes of I-125-GSA were significantly decreased at 1 and 3 hr, and showed a significant increase at 1 wk. The blood uptakes were significantly higher at 1 and 3 hr. The histology section with HE stain demonstrated ischemic damage at 1 and 3 hr. The mitotic index and PCNA labeling index were highest at 1 wk showing liver regeneration. These results indicated that ASGP receptor binding correlated well with liver damage and regeneration and would be a useful marker to evaluate the ischemic liver damage and recovery.

PS-422

J B NEILLY, A WRAY, J EVANS, R MacKENZIE, J H McKILLOP, J GIBSON
Department of Nuclear Medicine Royal Infirmary Glasgow
Scotland United Kingdom

Technetium 99m-HMPAO leucocyte labelling in OFG and Crohn's disease

Orofacial granulomatosis (OFG) is a chronic non-caseating granulomatous disorder involving the tissues of the mouth and face. It may exist as a localised entity or represent the oral manifestations of Crohn's disease (CD) or sarcoidosis. Leucocyte labelling with 99Tc is an established way of identifying inflammatory bowel disease. The aim of this study was to ascertain the usefulness of leucocyte labelling in identifying patients with OFG who may also have gastrointestinal CD. Ten consecutive paediatric patients (9 male, 1 female; mean age 166 months, range 109-204 months) with OFG underwent 99Tc scanning. Seven patients (70%) showed no uptake in the gut one (10%) showed Grade 2 uptake in the nasopharynx only, two (20%) showed Grade 2 or 3 uptake in the gut and both were subsequently confirmed as CD histologically. Fifteen paediatric patients (8 male, 7 female; mean age 153 months range 93-202 months) with objective evidence of inflammatory bowel disease (radiological +/- histological) were used as positive controls. All fifteen patients (100%) showed Grade 2 or 3 uptake in the small or large intestine.

Given the results from this paediatric population with inflammatory bowel disorders, it is concluded that 99Tc HMPAO leucocyte labelling is a good screening test in identifying paediatric patients with OFG who have established CD of the gut. The non-invasive nature of this test makes it particularly useful in the paediatric population associated with OFG.

PS-423

V.Obradović, H.Chebib, V. Artiko, N. Petrović, M. Petrović.
Institute for Nuclear Medicine, CCS, Beograd - YU

DIAGNOSTIC VALUE OF DETECTION AND QUANTIFICATION OF ENTEROGASTRIC REFLUX BY DYNAMIC SCINTIGRAPHY

We investigated 162 patients with: duodenal (21) and gastric (15) ulcer, after Billroth I (12) and II (7) surgery, with gastroesophageal reflux (GER, 46), after cholecystectomy(28), with cholecystitis (20), with chronic duodenal diseases (13), as well as 10 controls. Dynamic acquisition was performed after i.v. application of 185 MBq 99m-Tc-EHIDA during 90 min (1f/min), anterior view, with test-meal stimulation in 30th minute. Gaster was labelled with 18 MBq 99mTc-S-colloid in 100 ml of water. According to the maximal and minimal activities of 99m-Tc-EHIDA in hepatobiliary system and gastric region, index of enterogastric reflux (EGR%) and reflux duration were calculated.

Reflux was registered in the controls in small quantity (EGR%=4.4+/-4.2%) exclusively postprandially, lasting shortly (4.3+/-2.0 min). The obtained values were significantly (p< 0.001) increased in patients after Billroth II resection(68.8+/-43.7%; 58.4+/-4.0min), with duodenal ulcer (36.6+/-33.0%; 40.3+/-22.2 min), cholecystitis (31.0+/-8.7%; 26.5+/-6.8 min), after Billroth I (28.2+/-22.7%; 34.1+/-12.4 min), postcholecystectomy (27.1+/-17.2%; 37.6+/-19.7 min), with gastric ulcer (24.5+/-13.6%; 21.9+/-10.2 min) with GER (24.5+/-14.9%; 29.6+/-19.5min) and chronic duodenal disease (17.2+/-5.6%; 27.3+/-8.0 min). Quantity of reflux was highly correlated (r=0.580, DF=75, p < 0.01) with its duration. Fasting reflux was detected in 28 out of 75 (37.3%) refluxers in average quantity of 41.0+/-29.7% which was significantly different (p < 0.01) from those postprandially detected (23.26+/-16%). Increased values of EGR index are found in 75 (46.3%) patients: 85.7% and 75% after BII and BI gastrectomy, 60% with gastric and 52.4% with duodenal ulcer, 46.1% with chronic duodenal disease, 41.3% with GER, 39.3% with cholecystectomized patients and 20% in those with cholecystitis.

The obtained results prove clinical value of dynamic scintigraphy, as a noninvasive physiological method, in EGR detection and estimation of its quantity and duration.

PS-424

N. Olesen, L. Astrup, L. Schlünzen, J. Mortensen

Aarhus University Hospital, Department of Nuclear Medicine and Department of Medicine V, Aarhus, Denmark

THE CLINICAL USE OF SOMATOSTATIN RECEPTOR SCINTIGRAPHY IN PATIENTS WITH SUSPECTED CARCINOID TUMORS

The clinical use of somatostatin receptor scintigraphy (SRS) in patients with suspected carcinoid tumors was evaluated in a prospective study of in total 16 patients. The diagnosis of carcinoid tumor required a positive histology or informations of carcinoid related signs and symptoms and an increased excretion of 5-HIAA. The final diagnosis of carcinoid tumor was negative in 4 patients (group A) and positive in 12 (group B). Two of 6 patients operated before SRS had a radical removal of their tumor and no metastases. Whole body scintigraphy and SPECT of abdomen were performed by a dual-headed Picker gammacamera 24 and 48 hrs after i.v. injection of 111 MBq In-111 pentetretotide. A positive SRS was a focus with increased activity as evaluated by a blinded visual inspection. Patients with a positive SRS were treated with Sandostatin. Tumor size measured ultrasonically and symptoms were evaluated before and after a treatment period of in median 12 months (1-24) in 9 patients. SRS was true negative in all four subjects in group A. Nine of 12 patients of group B showed true positive hepatic foci comprising 7 with metastases known before SRS and 2 with metastases recognized because of a positive SRS. Three primary tumors with unknown location were revealed by SRS, whereas 2 well-located primary tumors were not detected by SRS. The follow-up evaluation after treatment with Sandostatin showed that tumor size was unchanged in 6, possibly reduced in 2, and rapidly increased in one. Symptoms were improved in all 7 subjects with carcinoid syndrome. The results indicate that SRS is of value in the detection of carcinoid tumors and their hepatic metastases and in the prediction of a positive effect of treatment with Sandostatin on carcinoid signs and symptoms. The treatment was not found to lead to a significant reduction in tumor size but it may have prevented a growth of tumor.

PS-425

K.K.Bhargava, P. Rajvanshi*, S. Slehria*, C.J.Palestro and S. Gupta*
Div. of Nucl. Med., Long Island Jewish Med. Ctr., & Liver Res. Ctr.,
Albert Einstein Coll. Med*, NY.

Tc-99m-LABELED CELLS: APPLICATIONS IN OPTIMIZING LIVER
REPOPULATION WITH CELL TRANSPLANTATION

Hepatocyte transplantation is an effective method for repopulating the liver. We hypothesized that modulation of hepatic vascular tone could increase the distal deposition of transplanted cells into hepatic sinusoids, thereby increasing cell engraftment and liver repopulation. When genetically labeled hepatocytes isolated by collagenase perfusion were transplanted intrasplenically into dipeptidyl peptidase IV negative (DPPIV-) syngeneic rats, cells promptly entered liver sinusoids in periportal areas, although significant cell fractions were retained in portal spaces. While transplanted cells in hepatic sinusoids were integrated into the liver parenchyma, cells in portal areas were not integrated and were promptly cleared. To determine changes in the hepatic vascular tone, we used known splenic vasodilators, phentolamine (α -blocker), labetalol (α - and β -blocker), nifedipine (Ca^{++} channel-blocker), and nitroglycerine. Hepatic blood pools were measured by image analysis using Tc-99m-RBCs from syngeneic rats. Phentolamine and nitroglycerine most effectively abrogated phenylephrine-induced vasoconstriction of the rat hepatic blood pool. When 2×10^7 F344 rat hepatocytes were transplanted intrasplenically after priming of rats with phentolamine or nitroglycerine, more transplanted cells reached distal hepatic sinusoids at 2 hrs, along with greater cell engraftment at 2 wks ($p < 0.01$). To establish whether hepatic vasodilators would be safe in cell therapy settings, we determined portasystemic shunting of Tc-99m-labeled hepatocytes, which could potentially cause intrapulmonary embolizations. After administration of nitroglycerine, the Tc-99m-hepatocyte fraction in the host spleen was unchanged (10% vs. 10% control, $p = NS$), whereas due to vasodilation, the transplanted cell fraction in the liver increased (32% vs. 26%, $p < 0.01$). More cells were also shunted into the lungs (0.7% vs. 0.4%, $p < 0.03$), although the magnitude of this increase was inconsequential. Conclusions: Hepatic vasodilation resulted in increased deposition of transplanted cells into distal hepatic sinusoids with increased cell engraftment. Insights into mechanisms of liver repopulation using radionuclide methods will facilitate development of novel cell therapies.

PS-426

M. Piert*, H. Fischer*, G. Becker**, H.-J. Machulla**, P. Aldinger*, W. Lauchart*

Department of *General Surgery and **Nuclear Medicine, University of Tübingen, Germany

QUANTITATIVE MEASUREMENT OF REGIONAL LIVER BLOOD FLOW
BY $H_2^{15}O$ AND $C^{15}O$ POSITRON EMISSION TOMOGRAPHY (PET)

Purpose: Due to the dual blood supply of the liver, to date no satisfactory method has been available for the quantitative in vivo measurement of hepatic hemodynamics. This study was undertaken to evaluate $H_2^{15}O$ PET in the analysis of liver hemodynamics. In principle, the freely diffusible tracer $H_2^{15}O$ allows the determination of the arterial and portal venous blood flow. $C^{15}O$ labels red blood cells and in combination with PET allows the determination of the regional blood volume of the liver as well as the localization of large blood vessels.

Materials and Methods: Liver blood flow was investigated in 7 anesthetized pigs. To investigate the reliability of $H_2^{15}O$ PET measurements over a wide flow range, segmental arterial flow reductions were induced by occlusions of several branches of the hepatic artery of varying size and localization yielding different degrees of arterial flow impairment. The portal venous blood flow was not mechanically impaired. After bolus injection of $H_2^{15}O$, liver blood flow was measured by a 10-min. dynamic PET scan followed by a 10-min. $C^{15}O$ PET scan in 4 experiments. Kinetic parameters for arterial and portal venous blood flow were estimated from tissue, arterial and portal venous blood activity curves using an extended one tissue compartment model to account for the dual blood supply. The resulting flow estimates were then compared with microspheres reference blood flow measurements obtained from multiple liver tissue samples (post mortem).

Results: A highly significant positive correlation between regional arterial blood flow measurements using PET and microspheres was found ($y = 0.06 + 0.92x$, $r^2 = 0.70$, $p < 0.001$). As long as the shape of the portal venous blood activity curve was different from the tissue response curve, portal venous blood flow could be estimated with high accuracy ($y = 0.04 + 0.91x$, $r^2 = 0.77$, $p < 0.001$). In all other cases, $H_2^{15}O$ PET yielded inaccurate portal flow results. The portal vein was easily identified in $C^{15}O$ PET images, which allowed the definition of regions of interest within the portal vein in order to obtain the portal input function non-invasively.

Conclusion: The arterial liver blood flow can be estimated precisely with $H_2^{15}O$ PET. $H_2^{15}O$ PET can address portal venous blood flow, as long as the shape of the portal venous blood activity curve differs from the tissue response curve (which can easily be checked). Additional $C^{15}O$ PET eliminates the need to catheterize the portal vein for portal venous blood flow estimation, which is a precondition for clinical applications of the method.

PS-427

N.Prandini, P.Pazzi, R.Scagliarini, S.Gamberini, C.Rizzo,
L.Feggi, S.Gullini

Departments of Nuclear Medicine and Gastroenterology,
S.Anna Hospital, Ferrara, Italy

THE MEASUREMENT OF LIVER FUNCTION BY BOTH ^{99m}Tc -
BrHIDA AND ^{75}Se HCAAT IN CHRONIC LIVER DISEASES

The labeled bile acid ^{75}Se -homocholic acid taurine (^{75}Se HCAAT) provides a tool for the direct measurement of hepatic bile acid handling but is available only for oral administration. ^{99m}Tc -BrHIDA is used in the hepatobiliary scanning but there are only a few studies on liver kinetic. Therefore, the aim of the study was to compare the kinetics of ^{99m}Tc -BrHIDA and of ^{75}Se HCAAT, in 6 healthy controls (Ctr), in 6 patients with primary biliary cirrhosis stage I-II (PBC), and in 6 with chronic hepatitis C (CHC). An home-made saline solution of ^{75}Se HCAAT and ^{99m}Tc -BrHIDA were simultaneously iv injected. In all groups of patients uptake and excretion rates of the two compounds were similar: the plasma disappearance rates for ^{75}Se HCAAT were faster than for ^{99m}Tc -BrHIDA (K1 ns, K2 $p < 0.05$). Furthermore the hepatic transit time of ^{75}Se HCAAT was significantly shorter than ^{99m}Tc -BrHIDA ($p < 0.05$). We observed a significant correlation between K1 and hepatic uptake (^{99m}Tc -BrHIDA $r = 0.93$, $p = 0.016$; ^{75}Se HCAAT $r = 0.89$, $p = 0.033$), and K2 tended to correlate with excretion, but not with K1 and liver uptake. Uptake rates and K1 of the two compounds tended to be lower in CHC patients, but there was no significant difference between the three groups. Excretion rates were significantly lower in PBC ($p < 0.01$) and in CHC ($p < 0.05$) than in Ctr, and hepatic transit time was longer in PBC ($p < 0.05$) and in CHC ($p < 0.01$) than in Ctr. In conclusion, ^{99m}Tc -BrHIDA is efficiently handled by the liver, similarly to ^{75}Se HCAAT. The liver uptake and excretion are independent processes, whereas excretion is related to late plasma disappearance rate. CHC patients, as well as PBC, have an impaired excretion rate and a delayed intrahepatic transit time, suggesting retention of bile.

PS-428

D.O. Slosman, M. Allaoua, J. Gong, J. Belenger, J.P. Papazyan, J. Billet,
C. Becker, G. Mentha, F. Terrier.

Geneva University Hospital, CH.

DYNAMIC HEPATOBILIARY SPECT : A FEASIBILITY STUDY IN
ANIMALS AND HUMANS.

Purpose: To validate the dynamic hepatobiliary tomoscintigraphy (dynSPECT) technique in animals and to evaluate its feasibility in clinical setting. **Material and methods:** dynSPECT (i/v injection of $4mCi$ (150 MBq) BrHIDA-Tc99m using a 3-head camera (Toshiba GCA 9300HG; 20 rot. 120°/2min) was repeated twice (2-day interval) in 8 minipigs. Reproducibility (CV) of the BrHIDA Tmax, $T_{1/2}$ BrHIDA excretion, % residual BrHIDA activity (%ResA) were calculated. The glomerular filtration rate using Cr51-EDTA (GFR) and the BrHIDA blood clearance (BrBC) were determined. Forty-four dynSPECT (8mCi/300 MBq BrHIDA-Tc99m) were prospectively done in 31 patients (range: 17-79 yrs old) using similar protocol. Investigations were performed in patients with end-stage hepatic diseases prior to liver transplantation (n=6), post-transplantation follow-up (n=4), cirrhosis (n=4), traumatic liver rupture (n=1), liver tumors (n=3), pancreatic adenocarcinoma (n=4), miscellaneous (n=9). Laboratory data were recorded. Time-activity curve (TAC) were computed from dynSPECT and selected regional voxel. **Results:** As shown by the calculated CV of GFR (10.2%) and BrBC (24.8%), a wide physiological variability was observed due to the surgical procedure and the anesthesia. In comparison, the variability of the dynSPECT parameters were in the same range of values or smaller: the CV were for T-max (17.5%), $T_{1/2}$ (12.8%) and %ResA (10.5%). Clinical SPECT images, TAC and percutaneous cholangiography gave similar results to demonstrate biliary stasis and biliary tract obstruction. In addition, 1 stent obstruction and 1 partial obstruction were depicted first with SPECT. In the case of traumatic liver rupture, only SPECT enabled to demonstrate and localized the biliary leakage. TAC enabled proper identification of focal liver transplant rejection during the follow-up. **Conclusions:** dynSPECT appeared feasible and reproducible. The intra-animal CV was in the range of physiological variability. The parameters $T_{1/2}$ and %ResA showed the lowest variability. The preliminary results of our prospective study demonstrate that BrHIDA SPECT can be used for the follow-up of patient to monitor biliary excretion with regard to segmental anatomy.

PS-429

K.Suzuki, A.Naito, H.Toyama, Y.Komori, K.Torii, A.Hasumi, M.Kuroda, K.Ejiri, T.Fujiwara, K.Ito, S.Koga.
Fujita Health University, Toyoake, Hokushin General Hospital, Nakano, Japan.

EVALUATION OF SEQUENTIAL CHANGES OF ASIALOGLYCOPROTEIN RECEPTOR BINDING WITH I-125-DTPA-GALACTOSYL HUMAN SERUM ALBUMIN ON ISCHEMIA /REPERFUSION INJURY IN RAT LIVER.

Protection of hepatocyte from ischemia/reperfusion injury is an important issue in hepatic surgery and transplantation. Quantitative assessment of hepatic function and a patient's subsequent morbidity and mortality remain difficult. The purpose of this study is to evaluate the sequential changes of the acute liver damage and recovery following ischemia/reperfusion in rats using asialo-glycoprotein receptor (ASGP) ligand. The hepatic artery, portal vein, and bile duct were cross-clamped for 90 min, then, reperused. At 1, 3 hr, 1 and 2 wk after the reperfusion, I-125-GSA was injected. Five min after the injection, blood samples were obtained, and the liver was removed. Several lesions from each lobe were dissected, weighed and counted. Mean uptakes (% dose/g) of the liver and blood samples were calculated in each time point. The sham operated control rats were also analyzed with the same procedure. At 1 and 3 hr, GOT and GPT showed a significant increase. The liver uptakes of I-125-GSA were significantly decreased at 1 and 3 hr. The liver uptake showed a significant increase at 1 wk. The blood uptakes were significantly higher at 1 and 3 hr. The ASGP receptor binding may provide a valuable information of ischemia/reperfusion injury and recovery after hepatic lobectomy and transplantation.

PS-430

K.Uchiyama, Y.Kuniyasu, Y.Niio, S.Hasebe, H.Shinohara, S.Matsuoka, H.Shima, K.Doai, M.Yamada, M.Obuchi, K.Takizawa and M.Honda.
Showa University Fujigaoka Hospital, Department of Radiology. Fujigaoka 1-30, Aoba-ku, Yokohama, 227-8501, Japan.

EVALUATION OF THE TECHNETIUM-99m-GALACTOSYL HUMAN SERUM ALBUMIN (GSA) LIVER SCINTIGRAPHY FOR FULMINANT HEPATIC FAILURE.

In spite of improvements in intensive care such as plasma exchange and hemofiltration, the mortality rate of fulminant hepatic failure (FHF) remains high. In this paper, clinical usefulness of 99mTc-GSA scintigraphy in the diagnosis of FHF and prediction of the outcome has been evaluated.

Patients and methods: 37 patients who received 99mTc-GSA scintigraphy were studied. 13 patients were in FHF (PT≤40% and hepatic encephalopathy ≥ grade 2), 17 in severe acute hepatitis (SAH; PT≤40% without hepatic encephalopathy), 7 in acute hepatitis (AH; PT>40%). Eight in FHF were died during hospitalization. Parameters of 99mTc-GSA scintigraphy such as HH15, LHL15, LU15, Patlak Ku, Liver/Body uptake ratio (LB ratio), and Liver Volume Index (liver volume counts by SPECT/total injection counts;LVI) were compared among three hepatitis groups.

Results: HH15 in FHF was significant higher than those in other groups, and HH15 in hospital death patients (HD) was significant higher than that in AL. All other parameters of 99mTc-GSA scintigraphy in FHF were significantly lower than those in SAH, AH, and all parameters in HD were significantly lower than those in AL.

	FHF	SAH	AH	HD	AL
HH15	0.852±0.060	0.749±0.087	0.615±0.069	0.733±0.111	0.848±0.086
LHL15	0.717±0.076	0.813±0.086	0.918±0.025	0.704±0.073	0.840±0.089
LU15	9.37±4.58	17.98±7.24	22.47±4.50	8.28±2.76	17.82±7.22
Patlak Ku	0.053±0.041	0.113±0.067	0.169±0.090	0.052±0.051	0.112±0.074
LB ratio	0.191±0.122	0.392±0.130	0.535±0.073	0.150±0.080	0.401±0.154
LVI	2.05±0.88	3.26±1.07	4.08±0.81	2.06±0.57	3.23±1.12

Conclusion: Parameters of 99mTc-GSA scintigraphy are enough sensitive in the diagnosis of FHF and prediction of the outcome. 99mTc-GSA scintigraphy should be widely applied for acute severe hepatitis in order to select adequate therapy, and contribute to improve the prognosis of FHF.

General nuclear medicine: Hypertension

PS-431

A. Klissarova, K. Nedelchev,* G. Tranulov, D. Minchev,* E. Georgieva
Medical University, Varna, Departments of Nuclear Medicine and Neurology*

ASSESSMENT OF CEREBRAL VASOMOTOR REACTIVITY BY 99mTc-HMPAO SPECT AND EXERCISE TEST: A COMPARISON WITH DIAMOX AS VASODILATORY STIMULUS

Diamox HMPAO SPECT is a well established method of identification of reduced cerebral vasodilatory reserve capacity. Exercise testing induces changes in brain perfusion pressure and thus provides assessment of cerebral autoregulation. The aim of the study was to evaluate the clinical usefulness of exercise Tc-99m-HMPAO SPECT for detection of vasomotor reactivity.

Subjects of investigation were 10 patients, average age 35.11±8.21 years, with uncomplicated hypertension. Tc-99m-HMPAO SPECT was performed during bicycle ergometer exercise and after 1g i.v. Diamox as vasodilatory stimulus. We analysed the SPECT parameters that correlate best with CBF and that are most strongly influenced by blood flow resistance - the perfusion indices (PI), i.e., the right to left ratio of the activity rate. The PI for 10 symmetric sectorial areas in 3 OM-transversal slices and the interhemispheric index (PIi) were calculated by means of a brain quantification computer programme. A referent range within 0.95 - 1.05 was adopted.

Abnormal PI in 8 patients (80%) were detected during exercise testing mainly in parieto-occipital, temporo-occipital and temporo-parietal areas. Perfusion indices different from the referent values were established in 7 patients (70%) in the same areas when using Diamox as a vasodilatory stimulus. Positive correlation (r=0.43) was established between PI changes induced by both techniques applied.

Our results demonstrate that 99m-Tc-HMPAO SPECT during exercise test provides an adequate assessment of vasomotor reactivity. It is a well-tolerated procedure without side effects, useful for the clinical practice.

PS-432

K. Liepe¹, A. Seemann², P. Gross², J. Kropp¹, WG Franke¹,
University Hospital Dresden, ¹Dpts. of Nuclear Medicine, ²Medical III, Germany

INTERVENTIONAL RENOGRAPHY WITH LOSARTAN IN THE DIAGNOSIS OF RENOVASCULAR HYPERTENSION

Radionuclide renography (RNR) with ACE inhibition plays an important role in the diagnosis of renovascular hypertension (RVH). Our position hypothesis was, that the non-peptide angiotensin II receptor antagonist losartan has a higher sensitivity in comparison to captopril. In a first study we investigated 34 patients (pts) with suspected RVH. Tc-99m-DTPA-renography was performed before and one hour after Losartan (Los) (50 mg) and Captopril (Capt) (50 mg). The visual and quantitative evaluation of RNR was compared with the follow-up, results of angiography and the plasma renin activity. In addition, we calculated the glomerular filtration rate of 14 pts. The results of the RNR was positive for RVH in 7 pts during Los, 6 pts during Capt and 4 pts during Los/Capt. 13/18 pts with high grade renal artery stenosis were positive in RNR (5 pts during Los, 6 pts during Capt, 2 pt during Los/Capt). From 11 pts wit surgery and an improvement of hypertension 3 pts had a positive result in RNR during Los, 6 pts during Capt and 2 pts was negative. In addition, we investigated 3 pts. with RNR one and 5 hours after Los. One pt showed a decrease of renal function from one to five hours after Los. There fore we started a second study and performing the renography 5 hours after Los. After this time the active metabolite of Los has the peak maximum. RNR with Capt was started one hour after oral application. We investigated 5 pts, so far. The results of the RNR was positive for RVH in 3 cases, one during Los and two during Los/Capt. In comparison to angiography the two pts with positive results in RNR during Los/Capt had a high grade and one pt with positive results during Los an intermediate renal artery stenosis. Two pts were negative in RNR and angiography. One pt underwent surgery and showed a decrease of hypertension in the follow-up. The calculation of glomerular filtration rate and the plasma renin activity showed no additional information. **In conclusion:** In our preliminary study, RNR during 5 hours after Losartan showed a discret higher sensitivity in cases of RVH compared to RNR during Captopril.

Poster presentations

PS-433

A.Maini, B.K.Das, V. Kher, B.R.Mittal, D.R.Mukherjee
Hospital: Sanjay Gandhi P.G.I., Department of Nuclear
Medicine.

EXERCISE MEDIATED CHANGE IN GLOMERULAR FILTRATION RATE IN NORMOTENSIVE AND ESSENTIAL HYPERTENSIVE SUBJECTS.

Uncomplicated essential hypertension has been postulated to be due to abnormal afferent arteriolar vasoreactivity which can be studied using a physiological intervention like exercise to trigger the abnormal response. We used ^{99m}Tc -DTPA as a measure of global GFR by Gates' technique, which is easy to use, to measure this dysfunction on exercise in 15 essential hypertensive (EH) subjects and compared it with 15 normal volunteers and 15 patients of biopsy proven (FSGS) renal parenchymal hypertension (RPH). A baseline study with 185 MBq of ^{99m}Tc -DTPA was followed by exercise study on a separate day. The amount of exercise was sufficient to increase the heart rate at least by 25 BPM above the resting value. None of the normal volunteers had fall in global GFR. Renal dysfunction as seen by a significant fall in global GFR was noted in 33.0% of EH patients and 20.0% of RPH patients on exercise. The 95.0% disease frequency of EH and 2.3% frequency of RPH suggests that renal dysfunction would be present to a lower extent in RPH group also. In conclusion, our results support the hypothesis of EH being a disorder of abnormal afferent arteriolar vasoreactivity.

PS-434

C.G.Zhang, D.S.Zhao, H. Yang, J.H. Zhao, J.Z. Liu, G.Han and G. Hu.

1st Hospital, Shanxi Medical University, Department of Nuclear Medicine, Taiyuan, P.R.China.

CAPTOPRIL-EXERCISE SCINTIGRAPHY IN THE DIAGNOSIS OF BILATERAL RENOVASCULAR HYPERTENSION

The diagnosis of bilateral renovascular hypertension(BRVH) can be difficult.To improve the sensitivity of diagnosing BRVH we have developed a procedure by combining Captopril Scintigraphy with exercise(CAPEX).Using this technique, we have investigated more than 200 hypertensive patients. Four patients were positive and their bilateral renal vascular hypertension were confirmed by renal arteriography.

The 4 patients, 1 male(24 years) and 3 females(34,35 and 22 years) have normal serum creatinine and were off all medications for 1 week. Base-line upright DTPA Scintigraphy(BSL) with 5 mCi was acquired Q 3 sec x 8 min. and Q 30 sec x 22 min. The patients were then given 25 mg of Captopril orally. After 1 hour, the patients exercised for 20 minutes on an upright bicycle to achieve a heart rate of 60% x (220-age) and DTPA Scintigraphy(10 mCi) were recorded. Routine Captopril Scintigraphy(CAP) without exercise was performed 3-7 days after CAPEX. The results were:

Case No.	1	2	3	4
BSL	Normal	Normal	Small R*K*with slightly abnormal renogram Normal L* K	Non-functioning R K L K with slight delay in excretion
CAPEX	Abnormal renogram involving R&L K	Abnormal renogram involving R&L K	Abnormal renogram involving R&L K	Non-functioning R K L K with significant delay in excretion
CAP	Near normal renogram with abnormal L/R peak ratio	Abnormal renogram of LK RL with obvious excretion delay	Small RK with slightly abnormal renogram Normal LK	Non-functioning RK LK with slight delay in excretion

* R=right ; L=left ; K=kidney

The above observations show that the Captopril-Exercise Scintigraphy may be a valuable procedure for the detection of bilateral renal vascular hypertension.

PS-435

D.S.Zhao, C.G. Zhang and H. Yang.

1st Hospital , Shanxi Medical University, Department of Nuclear Medicine, Taiyuan, P.R. China.

A STUDY OF EXAMINING RENAL FUNCTION IN PATIENTS WITH MILD TO MODERATE ESSENTIAL HYPERTENSION USING EXERCISE AND CAPTOPRIL-EXERCISE DUAL RADIONUCLIDE SCINTIGRAPHY.

The purpose of the study was to observe the effect of exercise and captopril-exercise on the renal function of the patients with mild to moderate essential hypertension. 10 normal controls and 15 patients were studied. All subjects had normal BUN,creatinine,ECG ,no cardiovascular risk factors and off all medications for one week. Baseline upright scintigraphy was done with ^{99m}Tc -DTPA(3mCi) and ^{113m}In -OIH(300uCi) was acquired Q3sec x 8min.and Q30sec x 22 min.

Exercise(EX) study was done at 60% maximum predicted heart rate(220-age) for 20 min.on an upright bicycle. The patient was given 25mg of captopril orally during captopril-exercise. GFR and ERPF were measured simultaneously. GFR and ERPF were reduced significantly during EX and captopril-EX at the normals and the patients with mild to moderate essential hypertension. The baseline scintigraphy was normal in all subjects. 40% (6/15) of the patients with mild to moderate essential hypertension demonstrated the bilateral renal dysfunction during EX and 30% (5/15) of the patients had similar renal dysfunction during captopril-exercise. The renograms and images of the patients with the renal dysfunction showed the both kidneys with significant delay in excretion. The DTPA imaging was more obvious than that of OIH for showing the renal dysfunction.

Those results showed that EX or captopril-EX scintigraphy can induce the bilateral renal dysfunction in some of the patients with mild to moderate essential hypertension.The dual radionuclide scintigraphy not only can measure GFR and ERPF but also can show the glomerular and tubular function simultaneously.

General nuclear medicine: Lung

PS-436

Ü. Bilkay, Z. Burak, R. Erinc, E. Teber, G.Erenel, M. Argon and K. Kumanlioglu

Ege University, Medical School, Department of Nuclear Medicine,Izmir, Turkey

THE COMPARISON OF Ga-67 AND Tc99mMIBI IN THE EVALUATION OF PULMONARY SARCOIDOSIS

Ga-67 scintigraphy is widely used in the evaluation of pulmonary sarcoidosis for the confirmation of diagnosis, the detection of disease activity and monitorization of response to therapy. Being a myocardial perfusion agent ^{99m}Tc MIBI, is recently used for visualisation of malignant tumours. Accumulation of ^{99m}Tc MIBI is also tested in benign lesions and there is contradiction about the role of ^{99m}Tc MIBI as an alternative of Ga-67 scintigraphy.

The aim of our study was to test the value of ^{99m}Tc MIBI scintigraphy in the evaluation of sarcoidosis lesions in comparison with Ga-67. 15 pts. (8 female and 7 male, age range: 17-59) who had active sarcoidosis proven by clinical, radiological findings and lymph node biopsy or bronchoalveolar lavage were included in the study. None of the pts. had any therapeutic intervention. Planar images of cranium and thorax were performed 20 min. after the injection of 20 mCi ^{99m}Tc MIBI and 48hr. after injection of 5 mCi Ga-67 in the same week. Images were interpreted visually and 5 point semiquantitative analysis was also applied.

While all radiologically defined lesions demonstrated significant Ga-67 accumulation, only 6/15 pts. showed mildly increased (4 pts: 1+, 2 pts: 2+) ^{99m}Tc MIBI uptake. Additionally, 3 pts. who had panda sign (increased uptake at nasolacrimal and salivary glands) at Ga-67 scintigraphy, did not have this typical finding on ^{99m}Tc MIBI scan.

As a conclusion, our results indicate that, ^{99m}Tc MIBI cannot be an alternative to Ga-67 in sarcoidosis and when evaluating malignant potential of a thoracic mass, it must be kept in mind that sarcoidosis lesions can also be the cause of an increased ^{99m}Tc MIBI accumulation.

PS-437

M.F. Botelho, J.J.P. de Lima, C.M. Gomes, J.A.S. Rafael, M.A. Marques, M.F. Baganha. Serviço Biofísica/Biomatemática, Faculdade de Medicina, Coimbra, Portugal. Dep. Electrónica/Telecomunicações, Univ. de Aveiro, Portugal. Centro de Pneumologia, Univ. de Coimbra, Portugal

ALVEOLAR-CAPILLARY MEMBRANE PERMEABILITY TO ¹³³XE IN CIGARETTE SMOKERS

The alveolar-capillary membrane permeability of 20 volunteers, 14 non-smokers and 6 hard smokers (tabag charge of 8.0±2.4 packs year) was studied, using ¹³³Xe an inert radioactive gas normally required in Nuclear Medicine for ventilation studies.

To perform this study, the patients inhaled a mixture of O₂ and ¹³³Xe at maximum volume capacity and were requested to sustain an apnea period for a minimum of 15 - 20 sec. Acquisition of a sequence of (64x64) 0.2 sec images was carried out during this period. The mean transference times for each pixel were calculated from the time activity curves. These values were used to generate a pulmonary permeability parameter and a parametric image of the ¹³³Xe mean transference times. After the apnea period the patients continued to breath into a spirometer until equilibrium was attained to allow for the ventilation study. Washout period is then established and again a sequence of frames was acquired. Using the local mean washout times a parametric image of the mean washout times, which correlates with ventilation, was generated. A perfusion functional image was carried out in every patient after the ventilation study. This was obtained following the administration of an intravenous injection of ^{99m}Tc-HAM (148 MBq). The permeability results obtained in the two groups of patients, smokers and non-smokers, were compared with each other and with those obtained with the conventional CO test. The results obtained with the ¹³³Xe in the two groups are significantly different (t = 2.9 with p = 0.005). For the CO test, the statistical analysis of the results does not show a statistically significant difference between the two groups (t=0.26 with p = 0.39).

The possibility of a local evaluation and the better sensitivity of the scintigraphic method when compared with the CO test make the former a study with potential interest in nuclear pneumology.

PS-438

M.F. Botelho, J.N. Moreira, A.C. Santos, C.M. Gomes, I.C. Dormehl, J.J.P. de Lima Serviço de Biofísica, Faculdade de Medicina, Coimbra, Centro de Neurociências, Coimbra, Portugal, Institute for Life Sciences, Pretoria University, South Africa

USE OF LABELED LIPOSOMES IN LYMPHATIC VISUALIZATION BY PULMONARY DRAINAGE.

The aim of this work is to visualize the deep lung lymphatic drainage in baboons using liposomes labeled with ^{99m}Tc-HMPAO, administered by inhalation. The liposome double layer consisted of distearoylphosphatidylcholine (DSPC) phosphatidylcholine phosphatidylglycerol (EPG) and glutamine in concentrations 8:1:1. After ^{99m}Tc-HMPAO-liposomes administration a 30 min dynamic acquisition, at thorax level, 64x64 matrix, at one frame/minute, was carried out. Static images, 128x128, at 30, 60, 90 and 120 min. after inhalation, of thorax and pelvis, were subsequently acquired. To confirm the localization of the inguinal lymph nodes, in one baboon, rhenium sulfur labeled with ^{99m}Tc was injected in the first interdigital space of both feet. For ^{99m}Tc-ReS a 30 min dynamic acquisition, at pelvis level, 64x64 matrix, 1 frame/minute, was followed by a pelvis static image, 128x128, at 30 min after interdigital injection and after passive movements of both feet. In one baboon, to cross check, inhalation of native ^{99m}Tc-HMPAO aerosol was made, in order to compare those images with the ones of liposomes. For ^{99m}Tc-HMPAO aerosols, a 30 min dynamic acquisition was performed, at thorax level, 64x64 matrix; 1 frame/min, followed by static images, 128x128, at 30 and 60 min, of the thorax and pelvis, was performed. The last images were used as background for subtraction in the ^{99m}Tc-HMPAO-liposome images. For obtaining biokinetic information, activity-time curves of ROI's were obtained. The results obtained show that 30 min after inhalation the axilar lymphatic nodes are visualized, along side the lung activity. One hour after inhalation the axilar nodes become more evident, and abdominal aortic and inguinal lymph nodes are observed. Late images add no additional information. In all images activity in the abdominal organs was observed. When ^{99m}Tc-ReS was injected, 45 min after injection with passive movements of the feet, the left inguinal node was visualized, and corresponded to the area visualized with liposomes labeled with ^{99m}Tc-HMPAO. The distribution of the inhaled ^{99m}Tc-HMPAO showed no visualization of the lymph nodes. However abdominal activity, with visualization of the liver, gallbladder, spleen, kidneys and the ascendent and transverse colon, which masks the information on lymphatic abdominal chains, was detected. To conclude, we can say that the deep lymphatic chains of lung drainage and lymph nodes can be visualized with the proposed technique.

PS-439

JM Cordero, JM Castro, A Pacheco*, J Zapatero** and A Crespo.

Hospital Ramón y Cajal. Dpt. Nuclear Medicine, *Neumology and **Thoracic Surgery.

THE PREOPERATIVE LUNG PERFUSION SCINTIGRAPHY AS A EXCLUDING CRITERION FOR VOLUME REDUCTING SURGERY.

Purpose: The aim of this study is to evaluate the role of the lung perfusion scintigraphy in the protocol of multidisciplinary preoperative evaluation of the patients thought to be candidates for volume reducing surgery (VRS) (Washington University of San Luis, USA).

Metodology: Twentyseven patients were evaluated according to these inclusion parameters: dysnaea grade 2 or higher (MMCR), younger than 70 years old, adequate % of VEMS, Rx compatible with emphysema, PaCO₂ < 50 mmHg y systolic pulmonary pressure <30 mmHg, so as lung perfusion scintigraphy and thoracic computerized axial tomography (CT), these two latest looking for the presence of pulmonary reservation areas (RA) and target areas (TA). The departments of psychiatry and rehabilitation took part after the clinical evaluation and before the last decision

Results: Five patients were selected for VRS (18.5%), being the other 22 rejected because of the next reasons: 44.4 % showed inadequate TA according to the CT and the gammagraphic studies, 11.1 % had inappropriate RA (homogeneous emphysema) also according to these techniques, 31.8 % refused the surgery after a rehabilitation period between 4 to 6 weeks. Two patients were excluded because of being active smokers and one more due to irreversible alcoholism. One another was excluded because of showing pachypleuritis. There were no exclusions due to psychiatric disorders.

Conclusions: 1. The lung perfusion scintigraphy is, besides the CT, a fundamental diagnostic tool for the surgical decision in the patients candidates for VRS, which led to reject a 55.5% of them in our own serie. 2. The global clinical evaluation carried on by a multidisciplinary group must lead to a meticulous selection of the optimal patient candidates for VRS, in order to have the best functional outcomes and the least mortality.

PS-440

P. De Bondt, L. Carp, I. Tielieu ⁽¹⁾, P. Van Schil ⁽¹⁾, P. Blockx Nuclear Medicine Department and Department of Surgery ⁽¹⁾, Antwerp University Hospital, Belgium

VENTILATION SCINTIGRAPHY IN THE DIAGNOSIS OF BRONCHOPLEURAL FISTULA AFTER PNEUMONECTOMY.

Bronchopeural fistula (BPF) after pneumonectomy, although uncommon, is a serious and potentially lethal complication. Because of the clinical importance, the difficult recognition of BPF causes a major problem. Asymptomatic BPF can be treated with antibiotics, whereas advanced BPF, with symptoms of an empyema, can force drainage or even repeat thoracotomy.

The aim of this study is to assess the value of ^{99m}Tc-Technegas ventilation scintigraphy in the non-invasive, early diagnosis of BPF after pneumonectomy.

Methods: The prospective study protocol includes three consecutive ventilation scans on each patient undergoing pneumonectomy, about post-operative days 3, 7 and 31. Any tracer activity in the postpneumonectomy space is interpreted to be positive for the presence of a BPF.

Results: Up till now we studied 14 patients, with pneumonectomy [L (n = 8), R (n = 5)]. Thirteen patients had all normal scintigraphic examinations and the clinical and bronchoscopic follow-up confirmed the absence of a BPF. One patient with a right pneumonectomy showed a normal first ventilation scan, but still asymptomatic on day 10 postoperative, an air leak was found in the postpneumonectomy space on his second ventilation scintigraphy. On day 12 he developed serious breathlessness with productive cough. The presence of a BPF was confirmed by bronchoscopy on day 13. Several ventilation scans remained positive (n=6), whereas 2 of 11 bronchoscopies could not demonstrate any open BPF. Even 7 months postpneumonectomy, permanent drainage by thoracostomy is still needed.

Conclusion: These preliminary results suggest that ^{99m}Tc-Technegas ventilation scintigraphy is a useful tool in the non-invasive, early diagnosis and follow-up of BPF.

Poster presentations

PS-441

M. Bager, S. Muhassein, S. Al-Tailji, M. Khadada, E. Higazi, S. Heiba and A.H. Elgazzar, Depts of Nucl Med & Medicine, Kuwait Univ and Ministry of Health, Kuwait.

ROLE OF NUCLEAR PHYSICIANS IN ASSESSING POST-VENTILATION/PERFUSION (V/Q) SCAN PROBABILITY OF PULMONARY EMBOLISM (PE).

The decision making process in the management of patients with suspected PE using V/Q scans rely on post-scan or diagnostic probability considering the clinical prescan and the scan probabilities using Bayes' theorem. The role of nuclear medicine physicians (NMP) in determining the post scan in addition to the scan probability is controversial. The objective of this prospective study was to compare NMP and referring physicians (RP) assessment of pre and post scan probabilities of PE. Seventy nine patients routinely referred for V/Q scans were included (41 female and 38 males) with a mean age of 49 years. The pre and post-scan probabilities were determined independently by attending NMP and RP. The pre-scan probability was assessed by the physicians blind to scan findings. The disagreement was classified according to the degree of differences (0; no difference, minor; 1 grade and major; 2 grades difference).

The results show a disagreement between NMP and RP as follows :

	Pre-scan probability	Post-scan probability
Agreement	50/79 (63%)	70/79 (89%)
Minor disagreement	26/79 (33%)	8/79 (10%)
Major disagreement	3/79 (4%)	1/79 (1%)

There is a high degree of agreement between RP & NMP in the post scan probability since the disagreement in assessing the pre scan probability is predominantly minor. Accordingly, NMP can use their assessment of prescan clinical likelihood to determine the post scan probability of PE.

PS-442

A. Gezici, S. Otcu, H. Öztürk, A. İ. Dokucu, A. Kara, H. Öztürk, M. C. Tuncer, M. Z. Akkus, G. A. K. Heidendal
D.Ü. Medical Faculty Nuclear Medicine, Pediatric Surgery and Maastricht Academic Hospital Nuclear Medicine Departments, Diyarbakır/ Turkey

EVALUATION OF NITRIC OXIDE EFFECTS ON PULMONARY VASCULAR STATUS IN ACUTE PHASE OF TRAUMATIC DIAPHRAGM RUPTURE IN RATS WITH PULMONARY IMAGING

The aim of this study was to investigate the regulatory effects of nitric oxide on vascular status of left uninjured lung associated with left traumatic diaphragm rupture and to evaluate the effects by using 99mTc-MAA pulmonary imaging. **Methods:** Sixty Sprague-Dawley rats were divided into 6 groups. Group 1 (control group, n=10); pulmonary imaging was applied. Group 2 (sham group, n=10); after left traumatic diaphragm rupture animals were underwent pulmonary scintigraphy. Following left diaphragm rupture L-arginine (3mg/kg/min to group 3 n=10 and 10mg/kg/min to group 4 n=10) and L-NAME (30µg/kg/min to group 5 n=10 and 300µg/kg/min to group 6 n=10) were infused for 10 minutes and 99mTc-MAA pulmonary imaging was obtained. During the study hemodynamic parameters (mean blood pressure mm/Hg, heart rate/min and breathing count/min) were recorded. Left uninjured lung specimens were examined with light microscopy. **Results:** The L-arginine 3mg/kg/min infusion to group 3 and 10mg/kg/min infusion to group 4 decreased mean blood pressure mm/Hg but increased heart rate/min at 15min (versus to sham). However L-Arginine 3mg/kg/min infusion decreased but L-arginin 10mg/kg/min infuion increased breathing count/min at 15min in group 5 and in group 6 consequently (versus to sham group). 30µg/kg/min L-NAME infusion to group 5 increased mean blood pressure mm/Hg and breathing count/min rate but decreased heart/min at 15min as compared to sham group. 300µg/kg/min L-NAME infusion to group 6 increased mean blood pressure mm/Hg and breathing/ count/ min but decreased heart/min rate (compare to sham group). Pulmonary imaging results: Medians of uninjured lung activity uptake count in each group of rats were:

tm Group1 Group2 p* Group3 p* Group4 p* Group5 p* Group6 p*
15m 85763 61999 s 76956 s 96946 s 63275 n.s. 41842 s

Data are expressed as medians, p*= A p<0.05 was considered statistically significant
Histological result: Light microscopic examination revealed an intact vascular endothelial lining. **Conclusions:** Our results showed that by improving ventilation-perfusion matching while lowering pulmonary vascular resistance, nitric oxide may be beneficial in the treatment of acute respiratory distress syndrome associated with traumatic diaphragm rupture. In spite of these results additional measures to enhance cardiopulmonary perform may be desired.

PS-443

B. Günalp, N. Aslan, Y. Pabu'cu, S. Ilgan

Gülhane Military Medical Academy, Department of Nuclear Medicine and Department of Radiology, Ankara, Turkey

DETERMINATION OF VENTILATION PERFUSION (V/Q) SCAN CHARACTERISTICS OF SWYER-JAMES SYNDROME AND THE VALUE OF V/Q SCAN IN THE DIAGNOSTIC MANAGEMENT OF PATIENTS WITH UNILATERAL HYPERLUCENT LUNG

Swyer-James (Macleod's) syndrome (SJS) is a rare disease characterised by a hyperlucent lung or lobe, usually of normal or small size due to hypoplasia of a pulmonary artery and bronchiectasis of the affected lung. The aim of the study was to describe the V/Q scan findings in patients with SJS and compare these findings with those on plain radiographs, high resolution computed tomography (HRCT) and pulmonary angiography. We encountered six patients with SJS, documented by pulmer HRCT and angiography. All were men, and ranged in age from 20 to 66 years (mean, 28 years).

V/Q Scan: Patient was positioned with camera posterior. 740 MBq Xe-133 was injected into intake part as patient takes inspiration. Single breath, equilibrium and washout images obtained. After xenon had washed out the patient was injected 74 MBq Tc-99m MAA without changing his position. Functional images of lung ventilation and ventilation perfusion ratios were generated and regional clearance time analysis were performed.

Perfusion images showed markedly decreased perfusion of the affected lung or lobe without focal abnormalities. In all patients single breath images showed abnormal ventilation matched by abnormal perfusion. Washout images showed abnormal areas of Xe-133 retention that corresponds well to perfusion deficit and hyperlucent areas on HRCT and x-ray. Delayed clearance of xenon is a sign of air trapping, which are characteristics of this syndrome. Thus, Xe-133 inhalation scintigrams were useful to detect air trapping especially when mediastinal shift was not apparent on chest x-ray films. Bronchial damage is believed to cause this syndrome, and the present findings support this view.

V/Q scan is helpful in excluding other causes of hyperlucency by excluding pulmonary embolism, pulmonary artery agenesis, central airway obstruction, compensatory hyperinflation, it can spare some patients pulmonary angiography and bronchoscopy.

It is concluded that V/Q scan is a significant non-invasive means of diagnosis of SJS and a valuable tool for diagnostic management of patients with unilateral hyperlucent lung.

PS-444

E. İbis, E.A. Gençoğlu, E. Zeydan*, G. Aras, F. Berk, B. Çobanlı*, G. Erbay, A. Akin, A. Soyulu.
Ankara University Medical School, Depts of Nuclear Medicine and Chest Disease*. Ankara/TÜRKİYE

Tc 99m DTPA CLEARANCE AND Ga-67 SCINTIGRAPHY IN DIFFUSE INTERSTITIAL LUNG DISEASE

The aim of this study was to evaluate the pulmonary involvement and disease with activity Ga-67 scan, Tc 99m DTPA lung clearance in pts who have been diagnosed as diffuse interstitial lung disease (DILD), clinically and histopatologically.

Two group were included in study, as control and pts with DILD. The control group consisted of 13 healthy, nonsmoker volunteers without any pulmonary problems, so far. The DILD group have 25 pts (14 female and 11 male) with mean age 48.7±15.8 year, who were non smoker and did not get corticosteroid or immunosuppressive therapy, for the last 6 months. 11 pts had sarcoidosis, 8 had idiopathic pulmer fibrosis (IPF), 5 had fibrosing alveolitis (FA), 1 had histiocytosis X. Chest roentgenogram, pulmonary function tests, x-ray CT, Ga 67 scan and Tc 99m DTPA aerosol clearance study were performed on all of pts.

Ga 67 study showed diffuse lung uptake in 3 pts, mediastinal and hilar uptake in 8 pts, normal scan in 14 pts. 6/11 (55%) pts with sarcoidosis, 6/8 (75%) pts with IPF, 4/5 (80%) pts with FA and 1/1 pts with histiocytosis X and total of 17/25 (68%) pts showed a slow lung DTPA clearance as 2.1±0.5%.min⁻¹. Whereas this parameter was found as 0.8±0.1%.min⁻¹ in the control group.

It is concluded that Ga 67 has a low sensitivity in assessment of parenchymal involvement (12%) whereas Tc 99m DTPA lung clearance study was much more sensitive (55-80%). Thus, we think that, Tc 99 m DTPA clearance study may help early diagnosis and evaluation of disease activity in pts with diffuse interstitial lung disease.

PS-445

T.Imai, Y.Sasaki, T.Shinkai, Y.Nishimoto, Y.Imai, H.Ohishi and H.Uchida. Departments of Oncoradiology and Radiology, Nara Medical University, Kashihara, Japan

CLINICAL EVALUATION OF PULMONARY FUNCTION USING SCINTIGRAPHY IN CASES WITH TRACHEOBRONCHIAL STENTING.

The clinical usefulness of scintigraphy was evaluated in patients with stent insertion for tracheobronchial stenosis. There were 2 patients with lung cancer, 2 with tracheal cancer, 2 with tracheobronchial tuberculosis, and 1 with bronchial stenosis after resection of lung cancer. Ventilation scintigraphy was performed using 133-Xe gas, and ventilation (V %) and mean transit time (MTT sec) were evaluated. Following ventilation scintigraphy, perfusion scintigraphy was performed in the same position by intravenous injection of 99m-Tc-MAA, and perfusion (Q %) was evaluated.

Aerosol inhalation cine-scintigraphy (AICS) was performed using 99m-Tc-HSA aerosol. After inhalation, aerosol deposition in the airway and lung fields and the mucociliary clearance were evaluated. In patients in whom comparison of before and after stent insertion was possible, V, Q, and MTT were improved on the side of stent insertion accompanied by improvement in the clinical condition and the pulmonary function. In the aerosol deposition images, hot spots were seen at the site of stent insertion in all patients. Pulmonary deposition of aerosol was different according to the degree of airway patency. Therefore this method is sensitive to airway abnormalities and useful for follow-up. MCT was impaired at the site of stent insertion, but it improved in 1 patient in whom the stent was almost buried under the mucosa over a long course. Scintigraphy is considered to be useful for clinical evaluation of stent insertion in patients with tracheobronchial stenosis.

PS-446

T.Imai, Y.Sasaki, K.Nezu, T.Shinkai, Y.Nishimoto, K.Ide, Y.Imai, H.Ohishi and H.Uchida. Dept. of Oncoradiology, Radiology and 3rd Dept. of Surgery, Nara Medical University, Kashihara, Japan

CLINICAL EVALUATION OF 99m-Tc-TECHNEGAS SPECT IN THORACOSCOPIC LUNG VOLUME REDUCTION SURGERY IN PATIENTS WITH PULMONARY EMPHYSEMA.

99m-Tc-Technegas (TcGas) SPECT is useful for evaluating the patency of the airway and more sensitive in detecting regional ventilation impairment in Pulmonary emphysema (PE) than high resolution CT. The aim of this study is to evaluate regional ventilation impairment using this method before and after thoracoscopic lung volume reduction surgery (LVRS) in patients with PE. There were 11 patients with PE (6 patients had bullous emphysema). The mean patients' age was 64.1 years. All patients were males. LVRS was performed bilaterally in 8 patients and unilaterally in 3 patients. After inhalation of TcGas in the sitting position, the subjects were placed in the supine position and SPECT was performed by a triple head γ -camera (MULTISPECT3, Siemens). Distribution of TcGas on transverse images was classified into 4 grades, A:homogeneous, B:inhomogeneous, C:hot spot, D:defect. Three slices of transverse images, the upper, middle and lower fields were selected, and changes of deposition patterns after LVRS were scored (TcGas score). Simultaneously, changes after LVRS were also evaluated by volume rendered 3D imaging. After LVRS, dyspnea on exertion was improved in 9 patients and the FEV1.0 was improved in 8 patients. Before LVRS, inhomogeneous distribution, hot spots and defects were observed in all patients. After LVRS, improvement of distribution was obtained not only in the surgical field and other fields, but also in the contralateral lung of unilaterally operated patients. However in 4 patients some fields showed improvement while other fields showed deterioration. TcGas score correlated with improvements in DOE and FEV1.0, especially in the lower lung. Volume rendered 3D imaging precisely and visually evaluated regional ventilation impairment, and may be useful for objective evaluation of LVRS. TcGas SPECT is useful for evaluating changes in regional pulmonary function after LVRS.

PS-447

I.P.Koroluk, A.V.Kapichnikov Samara State Medical University, Department of Nuclear Medicine, Samara, Russia

EVALUATION OF ALVEOLAR PERMEABILITY, LUNG VENTILATION AND PERFUSION IN PNEUMOCONIOSIS

The aim of this study was to evaluate the potentiality of the aerosol technique in the determination of the ventilation-perfusion disorders and alveolar damage in pneumoconiosis (P). **Materials and methods:** Aerosol inhalation lung scintigraphy (radioaerosol MMAD = 0.9 μ , sigma g = 1.8) with ^{99m}Tc-DTPA or ^{99m}Tc-albumin, lung perfusion scintigraphy with ^{99m}Tc-MSA, chest X-ray (CXR) and pulmonary functional test (PFT) was performed in 65 patients (pts): 46 pts with 1st stage of P, 8 pts with 2nd stage of P and 11 pts with chronic obstructive pulmonary diseases (COPD). The computer methods was employed for quantitative analysis of the heterogeneity of perfusion (Q), ventilation (V) and the parametric image generation. Skew (S) and kurtosis (K) of the aerosol distribution was calculated by frequency histograms of the multiple views of inhalation images for the quantitation of the ventilation disorders. The ^{99m}Tc-DTPA pulmonary clearance rate (DTPA-PCR) as a parameter of the pulmonary alveolar-capillary membrane integrity was determined. The results were compared with those obtained from 17 healthy subjects. The influence of chronic tobacco exposure to DTPA-PCR was taken into consideration by division of surveyed subjects on smokers and non-smokers group.

Results: 1) Significant disorders of V and Q were revealed in all stages of P. In the majority of cases of this disease regional pattern of V and Q defects corresponded one another. In contrast, in COPD we more often observed an elevated Q/V ratio. An increased values of S, K and visible abnormalities of aerosol deposition was found in 17/28 (60,7%) pts with P with a normal PFT. 2) The mean level of DTPA-PCR in P was decreased (preferentially in the basal regions), but this change was not statistically significant due to very high individual variability of DTPA-PCR: from 84% to 412% and from 72% to 283% of the mean control value for smokers and non-smokers, respectively. On the other hand, the range of DTPA-PCR in COPD was similar to control. Lung alveolar permeability did not depend on CXR stages of P, but correlated positively with the unevenness of Q (r=+0.545; p<0.05) and negatively with the period without contact to a fibrogenic dust (r=-0.432; p<0.05).

Conclusions: Aerosol technique is more informative than PFT in recognition of the ventilatory impairment in pneumoconiosis. In some cases alveolar permeability can be helpful in the differential diagnosis between COPD and pneumoconiosis. It seems probable, that wide range of alveolar permeability in pneumoconiosis is stipulated by a different activity of alveolitis.

PS-448

M. Khadada, H.T. Mustafa, M. Mouro, A.M. Omar, A. Al-Bonny and A.H. Elgazzar. Depts. of Medicine and Nuclear Medicine, Mubarak Al-Kabeer and Ibn Sina Hospital and Faculty of Medicine Kuwait University, Kuwait.

ROLE OF Tc-99m-DTPA IN DETECTING EARLY EFFECTS OF DIABETES MELLITUS.

Diabetes mellitus affects multiple body organs leading to various complications if not well controlled. The objective of this prospective study was to evaluate the permeability of lung epithelial membranes in diabetic patients.

Twenty one patients (12 males and 9 females) with a mean age of 55 (42-70) were studied. All patients had no history of respiratory diseases and never smoked. Fifteen patients were non insulin dependent (NIDDM) and 6 had insulin requiring (IR) disease. Duration and control of diabetes were recorded for all patients. All patients had pulmonary function tests and Tc-99m DTPA aerosol ventilation scans performed. The results of Tc-99m DTPA aerosol clearance were compared to the established normal value in our laboratory of 61.5 \pm 3.95 for normal non smoker volunteers.

It was found that 8 patients had delayed Tc-99m DTPA aerosol clearance (6 NIDDM and 2 IR). All of the 8 patients except one had poor control of their diabetes and all but two had the disease for 10 years or more. The pulmonary function tests were normal in all patients. Carbon monoxide diffusion capacity was normal in all but two of the 8 patients with delayed aerosol clearance.

Our preliminary experience suggests that poorly controlled and long standing diabetes is associated with normal permeability of the lung epithelial membrane. Tc-99m DTPA appears more sensitive than pulmonary function tests and carbon monoxide diffusion capacity in detecting early diabetic changes in the lungs.

Poster presentations

PS-449

J. Kocsis, Z. Bártfai, I. Szilvási
3rd Dept. of Internal Medicine, Semmelweis Medical University
Dept. of Pulmonology, Semmelweis Medical University, Budapest
Dept. of Nuclear Medicine, Haynal University, Budapest

THE USE OF Tc-99m-MIBI SCINTIGRAPHY IN PATIENTS WITH LUNG CANCER

The aim of the study was to evaluate the role of Tc-99m-Sestamibi in the diagnosis and staging of lung cancer and in predicting the cytostatic responsiveness of the tumor. 24 patients were examined (12 small-cell and 12 non-small-cell lung cancer). Following intravenous administration of 600-800 MBq Tc-99m-MIBI planar (at 30 minutes and 3 hours) and SPECT imaging was performed. Scintigraphic results were compared to other radiologic findings (X-ray, CT) and histology. Results: The primary tumor was visualised in 18 cases. Among the negative cases 3 proved to be therapy resistant tumor and 1 was benign tumor. We had no false positive finding. Hilar and mediastinal metastases were detected in 8 cases agreeing X-ray and CT. Chemotherapy-sensitive tumors showed positive radionuclide uptake. Our results indicate that Tc-99m-Sestamibi scintigraphy is a specific method in lung cancer. SPECT overtakes planar scintigraphy in staging. At the case of small-cell lung cancer the method can help us detecting primary or acquired multi-drug resistance.

PS-450

H. Köhn, I. Neumann*, F.T. Meisl*

Department of Nuclear Medicine, III. Department of Medicine
Wilhelminenspital, Vienna, Austria

DETECTION OF PULMONARY AND EXTRAPULMONARY ANCA-ASSOCIATED VASCULITIS BY IN-111-OCTREOTIDE RECEPTOR SCINTIGRAPHY

Pulmo-renal vasculitis is characterized by involvement of small vessels and its association with antineutrophil cytoplasmic antibodies (ANCA) directed against intracellular antigens (PR3, MPO) of neutrophil granulocytes. Diagnosis of renal affection is relatively simple, but correct diagnosis of early manifestations in the respiratory tract or the lung, especially in case of relapse, where X-ray or other imaging modalities are often non-diagnostic, represents a clinical challenge. In 18 patients with histologically confirmed c- or p-ANCA-mediated vasculitis (12 Wegener's granulomatosis, 3 Churg-Strauss syndrome, 2 microscopic polyangiitis, 1 relapsing polychondritis), pulmonary and extrapulmonary (7 upper respiratory tract, 1 pericardium) granuloma localizations were visualized by In-111 Octreotide receptor scintigraphy (planar and 360° SPECT) due to its specific binding to receptors on granulomatous inflammatory cells in active disease, and became negative in 7 patients after successful therapy. 3 patients with Wegener's granulomatosis in remission had a negative scan, but 2 became positive in case of clinical relapse. Semi-quantitative data achieved by ROI technique (cpm/pixel ratios of lesion to background) were useful for objective assessment of therapy effects. In Wegener's granulomatosis uptake in lesions was significantly higher than in Churg-Strauss syndrome. Scans were negative in case of bacterial pneumonia, but were also positive in case of active sarcoidosis or tuberculosis, and surprisingly in a case of Goodpasture syndrome. Receptor scintigraphy with In-111 Octreotide seems to be a sensitive indicator of disease activity and to provide additional information for staging of patients with these rare disorders. Our data suggest that it is especially useful for early detection of disease relapse and assessment of the efficacy of immunosuppressive therapy.

PS-451

J. Kotzerke¹, R. Rodegro-Heinsen², T.O.F. Wagner³, A. Haverich⁴
¹Nuclear medicine, University of Ulm; ²Nuclear medicine, ³Dept. of Pneumology and ⁴Dept. of Heart-Thorax-Surgery, Hannover Medical School

ALVEOLAR PERMEABILITY AFTER LUNG TRANSPLANTATION - PERTECHNEGAS DETECTS EASILY INFLAMMATION AND REJECTION

Infection and rejection are important complications after lung transplantation (LuTx). In a single paper, Herve et al. (1991) reported an increased alveolar permeability in those circumstances which could be measured by means of Tc-99m-DTPA. The production of PTG aerosol is much easier and it can be delivered by a single breath. Therefore, we investigated whether PTG can be used instead of DTPA for detection of lung alterations.

Between 11/93 and 1/95, 30 patients after lung transplantation (13 single lung, 17 complete lungs) were investigated with a total of 84 scintigraphies. Time interval to LuTx ranged from 5 days to 5 years (mean: 234 days). Infections were diagnosed by bronchoalveolar lavage (BAL). An increased CRP was considered indicative of inflammation. Rejection was assumed by clinical parameters (e.g. fever combined with acute respiratory insufficiency) and treatment. Important changes in pulmonary function parameters were rated for rejection, too. For the lung clearance of PTG, a dynamic study of 15 mins was acquired followed by monoexponential analysis of the initial 5 mins. Reference values of 10.4 ± 2.1 mins were established from lung healthy persons. Changes of $\geq 15\%$ were considered significant.

In 49 uneventful episodes PTG clearance was 9.5 ± 3.0 mins, in 21 episodes of rejection the clearance was 7.1 ± 1.23 mins. During 10 episodes of infection clearance was 7.9 ± 2.2 mins, while the combination of infection and rejection ($n = 4$) resulted in clearance values of 6.5 ± 1.5 mins. Early after surgery (≤ 21 days postop), alveolar permeability was increased with clearance values of 6.0 ± 0.5 mins but normalized in follow-up (11.5 ± 2.3 mins). PTG and CRP could reveal a rejection in 64% and 71%, respectively. Combination of both methods improved sensitivity to 76.4%. For single patients with frequent investigations a good correlation of the alveolar permeability and the clinical course was found. In conclusion, the estimation of the alveolar permeability by means of PTG is an easy method to detect or to exclude alveolar alterations. An increased permeability indicates need of further investigations to explain the nature of the disturbance.

PS-452

J.T. Kuikka, E.L. Ansimies

Kuopio University Hospital, Department of Clinical Physiology, Kuopio, Finland

A FRACTAL MODEL FOR EVALUATION OF PULMONARY CIRCULATION IN MAN AT REST AND DURING EXERCISE

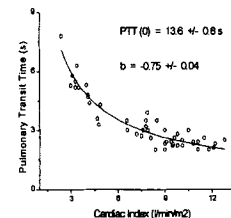
Changes in pulmonary circulation caused by muscular exercise and body position changes are very usual in daily life. Examination of these changes, however, requires methods which do not jeopardize the exercising subject during the investigation. In the present study the first-pass radiocardiography and a fractal model have been used to investigate pulmonary circulation at rest and during exercise.

The test series consisted of 16 healthy male volunteers (mean age of 32 years). The first-pass radiocardiography was recorded at rest. Bicycle exercise was started, and the second radiocardiography was performed after the heart rate had reached a level of 100-130 beat/min. The third examination was carried out at a heart rate of 2.5-3.0 times the initial rate (140-190 beat/min). Cardiac index, CI ($l/min/m^2$) and pulmonary transit time, PTT (s) were calculated. A fractal model characterized by an allometric scaling law of the form, $PTT = PTT(0) \cdot CI^b$, was fitted to data points where b is the scaling constant (West et al. 1997; Kuikka 1997).

Cardiac index increased on the average from 3.5 to 10.2 $l/min/m^2$. Pulmonary transit time obeyed an allometric function with the scaling constant of -3/4 which is the predicted value of the allometric exponent of the pulmonary resistance (cf. Figure). In addition, the relative spatial dispersion (i.e. standard deviation of the transit times divided by the mean transit time) decreased significantly when pulmonary blood flow increased being inversely proportional to the cubic root of the flow, i.e. $b = -1/3$.

The results suggest that the changes of pulmonary circulation in man at rest and during exercise obey the allometric scaling law probably due to the increased pulmonary resistance and due to the increased capillary volume during exercise.

West GB, Brown JH, Enquist BJ. *Science* 1997; 276: 122-126.
Kuikka JT. *Science* 1997; 278: 371-372 (letter).



PS-453

A. Montero, I. Uriarte, I. Banzo, R. Quirce, NK. Vallina, A. Hernández, C. Guede, JM. Carril
Hospital Universitario "Marqués de Valdecilla".
Servicio de Medicina Nuclear. Santander

LUNG TRANSPLANTATION FOLLOW-UP USING LUNG CLEARANCE OF RADIOAEROSOLS AND LUNG PERFUSION SCAN

Four lung transplantations (LT) (2 unipulmonary and 2 bipulmonary) were performed in 3 patients (PT) with pulmonary emphysema and 1 PT with pulmonary fibrosis, during the last year.

In all PT, follow-up studies included: measurement of lung alveolar permeability by determination of Tl/2 clearance of DTPA-Tc99m aerosol (DTPA-CL) expressed in minutes and lung perfusion scintigraphy (P). For the DTPA-CL, 50 frames of 30 seconds were obtained in posterior view of chest. We also analyzed visually the ventilation study (V). For the lung perfusion (P), 6 views were obtained after iv injection of 185 MBq of Tc99m-microspheres. The relative perfusion of each lung was calculated from the posterior view of P study. 20 studies were performed: 7 in the first month (3 in the first week), 4 in the second month, 7 between 3 and 6 months and 2 in the 9 month after LT. 6 acute rejection (AR) and 1 chronic rejection (CR) were diagnosed in 4 PT by biopsy or recovery after corticoid treatment. 2 of AR were associated to CMV infection.

RESULTS: DTPA-CL increased during the favourable clinical follow-up of PT. In 4 AR and 1 CR the DTPA-CL fall, in 1 AR was similar to the previous study corresponding to AR in resolution and in 1 AR the DTPA-CL increased. No abnormalities were observed in the RP of each lung during AR or CR or CMV infection. In unipulmonary LT, RP increased in transplanted lung and decreased in native lung. In bipulmonary LT, RP were similar. Changes in V and P were associated to chest X-ray abnormalities without relation to rejection.

CONCLUSIONS: DTPA-CL was the best diagnostic technique to predict rejects and CMN infection. V, P and RP studies were not useful for diagnosed of reject in LT.

PS-454

M. Nagao, K. Murase, Y. Yasuhara, T. Kikuchi, T. Mochizuki, J. Ikezoe

Department of Radiology, Ehime University Hospital, Ehime, JAPAN

QUANTITATIVE ANALYSIS OF PULMONARY EMPHYSEMA: THREE-DIMENSIONAL FRACTAL ANALYSIS OF TECHNEGAS SPECT IMAGES

Emphysema is a condition characterized by abnormal or permanent enlargement of the airspaces distal to the terminal bronchioles due to destruction of the airspace wall. The purpose of this study was to quantify the heterogeneous distribution of Tc-99m labeled ultrafine carbon aerosol (Technegas) in the lung in patients with pulmonary emphysema using SPECT and three-dimensional (3D) fractal analysis.

Technegas ventilation SPECT was performed on 19 patients (pts) with pulmonary emphysema (E), 7 pts with pulmonary emphysema suspect (ES) and 14 normal volunteers (N). We delineated the lungs using five cut-off levels (CL) (15, 20, 25, 30 and 35% of the maximal pixel count), and measured the total number of pixels in the areas surrounded by the contours obtained with each CL. We calculated 3D fractal dimensions (3D-FDs) from the slope of the linear regression equation between the total number of pixels and CLs transformed into logarithms.

The 3D-FD became greater according to the progress of emphysematous change. The 3D-FDs were 2.027 ± 0.611 , 0.768 ± 0.087 and 0.586 ± 0.055 (mean \pm SD) for E, ES and N, respectively. There was a significant difference between every two groups of these three groups. There was no significant difference between smokers (0.578 ± 0.071) and nonsmokers (0.593 ± 0.043) in the N group. The 3D-FD for E covered a wider range than those for ES and N. Eleven of the 19 pts with E had a 3D-FD over 2.0. In these pts, there were 3 pts who had oxygen therapy (OT) at home due to severe obstructive impairment and 5 pts had a forced expiratory volume rate in one second (FEV1.0%) of less than 40%. In the pts with a 3D-FD of less than 2.0, there were no pts who had OT at home and whose FEV1.0% was less than 40%. There were 4 pts who had no abnormal findings on chest CT in the ES group. Although their SPECT images showed homogeneous patterns, their 3D-FDs (0.786 ± 0.093) were significantly greater than those of N, indicating that 3D-FD is more sensitive to obstructive impairment than the visual assessment of CT or SPECT images.

In conclusion, our 3D fractal analysis appears to be clinically useful, since it allows us to simply and easily quantify the 3D heterogeneity of Technegas distribution in the lung and the severity of emphysematous changes in the lung.

PS-455

J.H. Risse, F. Grünwald, H. Bender, M. Bangard, Hj. Biersack

Dept. of Nuclear Medicine, University of Bonn, Germany

18-FDG-PET IN HEPATOCELLULAR CANCER AND SILICOSIS

Purpose: To present the data of a man with hepatocellular cancer (HCC) and high glucose metabolism rate in the lungs suggestive of pulmonary and mediastinal tumor spread, but due to an old silicosis.

Methods: A patient with HCC was referred to receive an internal liver radiation therapy by intraarterial application of I-131-Lipiodol. In the history a silicosis was known which disabled the patient to work more than 30 years ago but had been stable since then. An 18-FDG-PET as part of the staging showed the liver tumor as a region of elevated glucose metabolism. Additionally, both lungs showed regions of high glucose metabolism exceeding the liver cancer. Even considering the old silicosis, tumor spread had to be excluded. A present-day chest X-ray and CT of the thorax were performed and compared to previous chest X-ray examinations.

Results: The chest X-rays showed big perihilar masses in both lungs which had been unchanged for many years without evidence of new suspicious lesions. The CT of the thorax revealed calcifications in the perihilar tissue masses together with fibrosis throughout the lungs as typical signs of silicosis. No suspicious lesion or sign of malignancy could be detected. Last but not least, the PET SUV of the thoracic lesions exceeded the liver cancer by far. A diagnosis of HCC without evidence of tumor spread together with silicosis was made.

Conclusions: 1. Silicosis may be one reason for „hot lung lesions“ in PET of the thorax even in cases with an old history. 2. Silicosis may even in cases with an old history show a much higher glucose metabolism rate than a malign tumor such as HCC.

PS-456

A. Sargiotto, V Podio, M Mancuso, E Ruffini, S Peano, G Brusasco, M Petrarulo, G Bertuccio, C Carbonero, PG De Filippi, S Baldi, G Bisi

Nuclear Medicine Dpt, Ospedale Molinette, Turin and Nuclear Medicine Dpt., University of Turin (I)

Perfusion scintigraphy in postoperative assessment of lung transplanted patients

Lung transplantation has become the ultimate treatment for end-stage respiratory failure; transplanted lung (in most cases single) is generally better perfused, but can be involved in many complications (anastomotic, infections, acute or chronic rejection). Their early detection allows the optimal therapeutic option to be adopted, increasing treatment result.

37 transplanted patients (age 52 ± 11 years, mean \pm 1 SD) were studied with perfusion lung scintigraphy within three days after surgery and approximately at 3 weeks and at 3 and 9 months after administration of human albumin macroaggregates. In all patients we evaluated qualitatively and semiquantitatively images of vascular arrival and radiopharmaceutical distribution. Perfusion studies allowed the early identification of vascular anastomotic complications and led to reintervention in two subjects. Results of semiquantitative determination of perfusion to the transplanted lung showed a good prognostic value. The mean relative perfusion of transplanted lung compared to the contralateral was: 3.1 ± 4.2 , 3.5 ± 3.8 , 6.1 ± 7.7 and 4.1 ± 3.7 immediately, at 3 weeks and at 3 and 9 months after transplant in patients with a good outcome. No significant correlation was found with pO₂ and respiratory functionally tests. In the early phase post-surgery perfusion scintigraphy gave indication for more invasive procedure like pulmonary angiography.

PS-457

Y.Sasaki, T.Imai, T.Shinkai, H.Ohishi, Y.Nishimoto, Y.Imai, H.Uchida, T.Yoneda, M.Yoshikawa, N.Narita. Dept. of Oncoradiology, Radiology and 2nd Dept. of Internal Medicine, Nara Medical University, Japan

EVALUATION OF MUCOCILIARY TRANSPORT SYSTEM BY AEROSOL INHALATION CINE-SCINTIGRAPHY IN ATYPICAL PULMONARY MYCOBACTERIOSIS

Aerosol inhalation cine-scintigraphy (AICS) is a useful noninvasive method to evaluate the mucociliary transport system (MCT) as a pulmonary local defense function. The aim of this study is to assess the effects of MCT on the development and progression of atypical pulmonary mycobacteriosis (AM) by AICS. Thirty-eight AM patients, 27 with *M. avium* intracellulare complex (MAC) infection, 8 with *M. kansasii* (KAN), and 3 with other mycobacteria, participated in the study. They inhaled ^{99m}Tc -HSA aerosol generated from a nebulizer by tidal breathing in the sitting position. Subsequently, they assumed a supine position on the table, and posterior view images were obtained dynamically at 20 sec/frame for over 2 hr with a gamma camera. Then, serial frames were edited into a cinematographic presentation at 200 msec/frame. The bolus movement of radioactive aerosol (BRA) from the main bronchi on the affected side to the trachea was visually examined. The patterns of the BRA were classified into 4 types: I, rapid and smooth; II, slow; III, stagnation at halfway; and IV, complete stasis. Types II - IV represented increasing degrees of impaired MCT. Evaluation was done in the group with MAC infection and that with KAN & other infections. At the time of the initial examination, impaired MCT in the trachea was observed in 51.9% of the group with MAC infection and in 45.5% of the group with KAN & other infections. In the main bronchi on the affected side, the incidence of impaired MCT was 77.8% of the group with MAC. In the MAC group, 38% of the patients who were followed up showed improvement in MCT, while all patients showing no improvement in MCT relapsed. In the group with KAN & other infections, no patients showed improvement in MCT and none relapsed. These results suggest that MCT is an important factor associated with the development and progression of AM in particular with MAC infection.

PS-458

G. Scheuch, K. Sommerer, M. Kohlhaüfl, H. Lichte, A. Pohner, W. Hess, K. Häussinger and J. Heyder
Clinical Research Group 'Aerosols in Medicine' of the GSF-Institute for Inhalation Biology and the Clinic for Respiratory Medicine, Robert Koch Allee 6, D-82131 Gauting, Germany

CLEARANCE OF AEROSOL PARTICLES FROM BRONCHIAL AIRWAYS IN ASYMPTOMATIC SMOKERS AND NONSMOKERS

In 37 healthy subjects particle retention after shallow aerosol bolus inhalation was measured. Small volumes of aerosols were inhaled near endinspiration to deposit radiolabeled particles in conducting airways, exclusively. The efficiency of the clearance within 24 and 48 hours and the kinetics of the mucociliary clearance has been studied in nonsmokers and asymptomatic healthy smokers.

Method: Fourteen healthy asymptomatic smokers (S) and 23 nonsmokers (NS) inhaled aerosol boluses with a volumetric half width of 40ml into a lung depth of 40% of their individuals anatomic dead space (measured with mass spectrometry), according to 67 ml. The subjects inhaled monodisperse Fe_2O_3 (aerodynamic particle diameter = 3.5 μm) labeled with ^{99m}Tc during a tidal breath of 600ml starting from FRC. The flow rate was 250 ml/s. The inhalation was conducted with a respiratory aerosol probe (RAP, Pari Starnberg). An 8 s breathhold at end inhalation enhanced deposition of the particles in the airways. The subjects inhaled between 3 and 15 breaths to deposit 500kBq of activity in the lungs. With a gamma camera the particle distribution within the lungs was measured. Retention of the particles was measured during the following two days with a high sensitive collimated scintillation counter.

Results: Total particle deposition in the respiratory tract was found to be significantly higher in smokers than in nonsmokers: 53% NS; 67% S ($p < 0.01$). This was due to intrathoracic particle deposition, while extrathoracic deposition in both groups was not significantly different. After 24 hours we still found 54 % and after 48 h and 49% of the deposited particles still retained in the airways of both smokers and nonsmokers. The clearance kinetics could be described by using a double exponential function with a fast and slow phase. Within the first 10 hours clearance was significantly different between smokers and nonsmokers. While in nonsmokers the fast phase of the clearance function had a half time of 2.1 hours, in smokers it was 3.3 hours ($p < 0.005$).

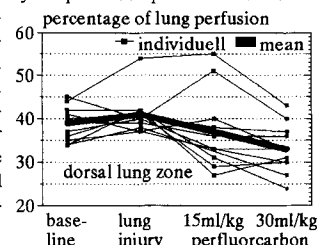
Conclusion: These results demonstrate that a significant fraction of particles which were deposited in airways are not cleared within 24 hours and that the clearance of smokers, even with normal lung function tests, showed a significant slower mucociliary clearance kinetics.

PS-459

G. Schulz, M. Max*, S.M. Reyle-Hahn*, B. Nowak, R. Rossaint*, U. Buell
Departments of Nuclear Medicine and *Anesthesiology, RWTH Aachen

LUNG PERFUSION DURING PARTIAL LIQUID VENTILATION IN ACUTE LUNG INJURY - MONITORED BY SERIAL SPECT WITH ^{99m}Tc -MAA

Partial liquid ventilation using perfluorocarbon can improve arterial oxygenation in acute lung injury. This effect may in part be due to a redistribution of pulmonary blood flow to ventilated lung segments. We investigated lung perfusion in ten anesthetized and ventilated pigs (30.5 \pm 2.8 kg body weight, supine position, positive endexpiratory pressure 5 mmHg) using ^{99m}Tc -labelled macroaggregates of human serum albumin (^{99m}Tc -MAA). After a baseline SPECT with 20 MBq ^{99m}Tc -MAA lung injury was induced in all animals by repeated lung lavage with saline until a $\text{P}_2\text{O}_2 < 100$ mmHg was achieved for one hour and a second SPECT was performed with 80 MBq ^{99m}Tc -MAA. Subsequently two doses of perfluorocarbon (15 ml/kg and 30 ml/kg body weight) were sequentially instilled through the endotracheal tube and pulmonary perfusion was studied with SPECT using 320 MBq ^{99m}Tc -MAA (15 ml/kg perfluorocarbon) and 1280 MBq ^{99m}Tc -MAA (30 ml/kg perfluorocarbon). All SPECT were performed using a three head gamma camera (Multispect 3, Siemens), 360° rotation in 120 steps (80, 40, 10 or 5 s resp. to radioactivity), 128² matrix, zoom 1.23, filtered backprojection Butterworth 3rd order, cutoff 0.5 cycles/pixel. Compressed transversal slices were analyzed by segmentation and standardized region of interest technique for ventral, medial and dorsal partial perfusion. Serial SPECT revealed a significant redistribution from dorsal to anterior partial perfusion between acute lung injury and during partial liquid ventilation with 30 ml/kg perfluorocarbon (41.4 \pm 4.7% vs. 33.1 \pm 5.9%).



Controversially to Gauger et al (Surgery 1997; 122: 313-23) SPECT with ^{99m}Tc -MAA detected relevant changes in lung perfusion during partial liquid ventilation with perfluorocarbon in pigs.

PS-460

A. Spanu, F. Ginesu, A. Farris, M.E. Solinas, P. Chiaramida, P. Pirina, G. Deiola, C. Bagella, G.C. Ginesu, S. Nuvoli, A. Masia and G. Madeddu.
Depts. of Nuclear Medicine, Respiratory Diseases and Oncology. University of Sassari. Italy.

THE ROLE OF ^{99m}Tc -TETROFOSMIN (T) SPECT IN LUNG CANCER (LC) DIAGNOSIS AND FOLLOW UP.

To evaluate the role of ^{99m}Tc -T-SPECT in LC pts, we studied 136 pts, 128 M and 8 F, aged 25 to 77 yrs: 122 pts (Group 1) had suspect malignant lung masses at conventional imaging procedures, while 14 (Group 2) had been previously operated for primary LC, 8 of whom had suspect local recurrence and 6 had no evidence of disease (NED). In all pts, after 740 MBq ^{99m}Tc -T injection, SPECT images of the chest were acquired using a rectangular dual head gamma camera. The images were analyzed both qualitatively and semiquantitatively, calculating, in the coronal slices, the Tumor/Background ratio (T/B). Scan data were compared to conventional imaging procedures (X-Ray, CT) and related to histopathological findings. T-SPECT was true positive in 105/105 Group 1 pts with histologically proven primary LC and true negative in 13/17 Group 1 pts in whom benign pulmonary lesions were ascertained at biopsy, sensitivity and specificity being 100% and 76.47%, respectively. False positive results were observed in 3 tuberculoma and in one sarcoidosis; however, T/B was higher in primary LC (2.30 \pm 0.88) in comparison with pulmonary benign lesions (1.42 \pm 0.24). T-SPECT was also positive for mediastinal lymph node involvement in 64/67 Group 1 lung cancer pts. Moreover, T-SPECT was true positive in 8/8 Group 2 pts with local recurrence and true negative in the remaining 6 NED pts. In 8 inoperable Group 1 LC pts, rechecked after radio and/or chemotherapy, disease regression (6 cases) or progression (2 cases) were determined by both T-SPECT and CT; however, in 1 progression patient, T-SPECT showed a more marked spread in mediastinum; moreover, additional information was obtained by T/B, since it decreased significantly ($p < 0.02$) or increased in regression or progression pts, respectively. Finally, T-SPECT was positive and T/B high in the only case with local residual tumor among those operated and who could be rechecked (4 cases) after the first observation. In this case CT was inconclusive. Our data seem to suggest that T-SPECT may be useful both in the diagnosis and follow up of lung cancer pts, T/B providing additional reliable information.

PS-461

K. Suzuki, K. Kamata, H. Terada, Y. Yokoyama, K. Abe, T. Ushimi, H. Koga, A. Tamura, S. Inokuma*
Hospital: Tokyo Metropolitan Komagome Hospital,
Department of Radiology and Internal Medicine*
CLINICAL SIGNIFICANCE OF VENTILATION/PERFUSION
SCAN IN THE PATIENTS WITH COLLAGEN DISEASE

The authors anticipated that ventilation/perfusion scan disclose the pulmonary disorders such as angitis in the patients with collagen lung diseases in the early stage.

One hundred and nine patients with various collagen diseases with or without pulmonary fibrosis were examined using Xe-133 gas and Tc-99m-MAA. Whole body scan was performed to evaluate shunt ratio in 65 patients.

V/Q increased areas were observed in 84 patients(77%), suggesting some impairment of pulmonary perfusion on the same site. These areas changed location and grade in the course of the disease, which may represent a deterioration. Eight patients(7.5%) showed a increased shunt ratio over 10%, indicating a formation of PA-PV shunt secondary to peripheral vascular impairment. Washout time is prolonged in 37 patients(33.9%), shortened in 18(16.5%), and is normal in 45(41.3%). Prolonged or normal washout time in the patients with pulmonary fibrosis may represent an obstructive changes in the peripheral air ways overlapping fibrosis.

Ventilation/perfusion scan is a very useful tool for evaluation of collagen lung disease in early stage, and contributes to decide treatment policy of the disease.

PS-463

P. Bonniaud, M. Toubeau, A. Berriolo, S. Roy, F. Branly, S. Schifano, C. Touzery, P. Foucher, N. Baudouin, F. Brunotte
Service de médecine nucléaire, Centre G.F. Leclerc, Dijon, France
Service de pneumologie, CHU, Dijon, France

USE OF HELIOX IN 99mTc-DTPA VENTILATION SCANS

In patients with severe chronic obstructive pulmonary disease (COPD), ventilation scintigraphy is particularly useful before surgery or for the diagnosis of pulmonary embolism. In these patients, the quality of 99mTc-DTPA aerosol scans is often very poor because of the important central deposition of particles due to turbulent flow.

To generate the aerosol, we tried to use Heliox, a mixture of helium (78%) and oxygen (22%). This gas, lighter than air or oxygen, is commonly used in critical care medicine units to treat acute or chronic upper airways obstructions.

Ten patients with a severe COPD who had a prior DTPA ventilation scan of poor quality were included in this study. After consent, a second DTPA scan, with Heliox instead of air or oxygen, was performed 48H later. For each patient, 6 views were recorded: ANT, POST, LAO, RAO, LPO, LRO, and compared to the first DTPA scan. The two scans were analyzed blindly by four experts for global quality, central deposits and peripheral activity.

Heliox scans were largely preferred by experts for global quality (80%), as for improvement of central deposits (72%) and peripheral activity (85%) with a very good agreement between experts.

This method is as simple as the conventional ventilation method and with no extra cost. The use of Heliox instead of air or oxygen seems to be particularly promising for patients with COPD whose scan interpretations are usually difficult due to aerosol central deposition.

PS-462

K. Tägil, E. Evander, J. Palmer, B. Jonson
Department of Clinical Physiology, Lund University Hospital

CLEARANCE OF 99mTc-DTPA AT ROUTINE PULMONARY SCINTIGRAPHY

Clearance of the water soluble substance diethylene triamine pentacetic acid (DTPA) deposited in the alveoli after inhalation is augmented in conditions with alveolar inflammation. Normally the clearance is monoexponential with a T½ of 70 min. In smokers and in states of alveolar inflammation, clearance is biexponential, with most of the tracer leaving the fast compartment with a short T½.

When 99mTc-DTPA is used for ventilation scan it should be possible to get an estimate of the clearance. The objective was to evaluate if it is feasible to do this during the short time course of a routine pulmonary scintigram.

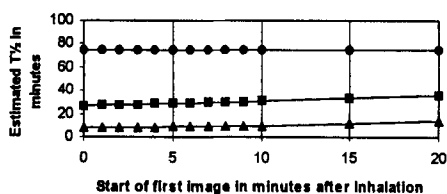
The ventilation scan precedes the perfusion scan and starts with a posterior image. An extra posterior image is collected at the end of the ventilation study. The time interval is registered. A region of interest is placed over both lung fields in the first and second posterior image. T½ is calculated, assuming an almost monoexponential clearance.

We found that the time interval neither between inhalation and the first image nor between first and last image was critical in determining a value for T½.

It is feasible, at routine pulmonary scintigraphy, to obtain a value for T½ to confirm increased alveolocapillary permeability of 99mTc-DTPA, representing alveolar inflammation.

Figure showing the T½ generated from 2 images 15 minutes apart at increasing time interval after inhalation to first image.

● = non-smoker, ■ = smoker and ▲ = patient with alveolitis



PS-464

A. Tutus, M. Kula, I. Gulmez.
Erciyes University, School of Medicine, Depts of Nuclear
Medicine and Internal Medicine, Kayseri, Turkey.

IMPAIRED LUNG EPITHELIAL PERMEABILITY IN HEPATITIS C VIRUS ANTIBODY POSITIVE PATIENTS DETECTED BY TC-99m DTPA AEROSOL SCINTIGRAPHY

Hepatitis C virus (HCV) infection has been shown to be associated with lymphoproliferative disorders and several autoimmune disorders have been related to HCV. It has recently incriminated as an etiologic agent in idiopathic pulmonary fibrosis. The present study was designed to determine the pulmonary clearance rate of Tc-99m-DTPA in asymptomatic patients with HCV antibody positive (HCV Ab+) patients and the role of Tc-99m DTPA aerosol scintigraphy in the early detection of lung involvement. Nineteen HCV Ab+ patients (45.52±10.60 years), no clinical pulmonary symptoms, and normal chest radiograms were studied. As a control group, 10 healthy non-smokers (44.80 ± 9.71 years) studied. Aerosol scintigraphy and pulmonary function tests were performed in all patients and in controls. On the basis of the scintigrams the percentage decline in activity per minute (Kep) was evaluated, which represented an accurate parameter of lung membrane permeability. The Kep values of healthy controls (0.719±0.133) were significantly lower than HCV Ab+ patients (1.146±0.349, p<0.05). In contrast, no significant change was observed in the pulmonary function tests (p>0.05). These findings indicate that in asymptomatic HCV Ab+ patients may frequently present with abnormal Tc-99m-DTPA clearance. We think that Tc-99m-DTPA aerosol scintigraphy may allow early detection of subclinical pulmonary involvement in HCV Ab+ patients.

PS-465

A. Van den Eeckhaut, G. Villeirs, Ch. Van de Wiele, F. De Baets, Ph. Duyck, R.A. Dierckx.
University Hospital Ghent, Belgium.

BRONCHIECTASES IN CHILDREN WITHOUT CYSTIC FIBROSIS: VALUE OF VENTILATION / PERFUSION SCINTIGRAPHY

Purpose: Evaluation of the additional value of ventilation-perfusion scintigraphy (V/Q) when compared to high resolution computed tomography (HRCT) for the detection of bronchiectases (BR) in children suffering from obstructive lungdisease (OL) and recurrent respiratory infections (RI).

Methods: V/Q and HRCT were performed in 48 patients (25 boys, 23 girls, mean age 5.9 years) within a mean time interval of 2.5 days. Twenty-nine patients (60%) had OL (asthma (n, number of patients = 20) and nonspecific bronchial hyperresponsiveness (n=9)) and 19 (40%) had RI (Ig-deficiencies (n=6) and tracheal malformations (n=2)). V/Q was performed using 7.4-74MBq (200µCi-2mCi) 99mTechnetium-MAA and 81mKryptongas. In 27 patients (mean age 7 years) HRCT was performed using 1-2mm slices with a 9mm interslice gap. In 21 restles children (mean age 4.6 years), 5-8mm scans were acquired when BR were suspected, additional 1mm HR-scans were obtained. Diagnosis of BR was based on HRCT-findings. The five pulmonary lobes were assessed separately.

Results: Sensitivity of V/Q was 11/17 (64.7%), specificity 212/223 (95.1%), positive predictive value 11/22 (50.0%) and negative predictive value 212/218 (97.2%). Eleven scintigraphic false negatives were attributed to parenchymal scarring (n=4), alveolar consolidation (n=2), localized cicatricial atelectasis (n=2), lobar atelectasis (n=1) and two unknown causes.

Conclusion: At present HRCT is considered state of the art for detection of BR. V/Q does not provide any additional information. Despite the high specificity V/Q fails to detect BR in 1/3 of cases.

PS-466

D. Mackey, J. S. Magnussen, P. Chicco, V. Bush, D. Johnson, M. Magee, G. Storey, G. Bautovich, H. Van der Wall

Concord Hospital, Sydney, Australia: Department of Nuclear Medicine.

ACCURACY OF THE PERCEPTION OF THE SIZE OF PERFUSION DEFECTS IN A SIMULATED MODEL OF TOMOGRAPHIC LUNG SCINTIGRAPHY IN COMPARISON TO PLANAR STUDIES.

Introduction. The PLOPED criteria for the detection of pulmonary embolism are predicated on the recognition of segmental anatomy of the lungs. Classification of perfusion abnormalities ranges from less than 25% of a segment to 100% of a segment. Previous work has shown that the accuracy of determination of defect size is poor in planar scintigraphy. We chose to study the accuracy of reported defect sizes in tomographic studies.

Methods. A model of the segmental anatomy of the lungs was developed from computed tomography, cadaveric human lungs and available anatomical texts. Counts were generated within the phantom by Monte Carlo simulation of photon emission. Eighteen single segmental lesions were interspersed with 47 subsegmental defects and displayed on an Icon reporting station. These were presented in the transaxial, sagittal and coronal planes to four experienced reporters to obtain assessment of defect size. Planar studies of the same defects were displayed to the same observers in the standard 8 views with a normal study for comparison.

Results. With planar studies, the accuracy of estimation of defect size was 51% compared with 97% using tomographic studies. Defects in the medial basal segment of the right lower lobe were not identified in planar studies but easily seen by all observers in the tomographic study.

Conclusion. There is marked improvement in the accuracy of determination of defect size for the tomographic studies over the planar equivalents. This is especially important in the lung bases, the most common reported site of pulmonary emboli. Tomography permits visualisation of defects in the medial basal segment of the right lung, which are not seen in planar studies.

PS-467

J. S. Magnussen, P. Chicco, V. Bush, D. Mackey, D. Johnson, M. Magee, G. Storey, G. Bautovich, H. Van der Wall

Concord Hospital, Sydney, Australia: Department of Nuclear Medicine.

PERCEPTION OF THE THRESHOLD OF DETECTABILITY OF SMALL PERFUSION DEFECTS IN A SIMULATED MODEL OF LUNG SCINTIGRAPHY: PLANAR VERSUS TOMOGRAPHY.

Introduction. Recognition of segmental anatomy of the lungs is the key aspect of the PLOPED criteria for the detection of pulmonary embolism. The classification of such perfusion abnormalities ranges from less than 25% of a segment to 100% of a segment. We therefore chose to study the threshold of detection of single defects varying from less than 35% to 100% of a segment. Thresholds were determined for planar and tomographic scintigraphy of the same defects.

Methods. A model of the segmental anatomy of the lungs was developed from computed tomography, cadaveric human lungs and available anatomical texts. Counts were generated within the phantom by Monte Carlo simulation of photon emission.

Of the 61 subsegments present in the phantom, 47 were 35% of a segment or less in size. A series of 47 simulations were performed, each with a single subsegmental defect. These were interspersed with 18 complete segmental defects. All studies were displayed on an Icon reporting station. These were presented in the transaxial, sagittal and coronal planes to four experienced readers who were asked to examine the studies for the presence of any defect. Planar studies of the same defects were displayed to the same observers in the standard 8 views, with a normal study for comparison.

Results. With planar studies, 76% of all defects were identified compared with 97% using tomographic studies. When only the lower lobe defects were considered, 72% were seen in the planar studies compared with 97% in the tomographic studies. Defects not detected in the lung bases in the planar studies were easily detected in the tomographic studies.

Conclusion. Tomography significantly adds to the sensitivity of detection of even small subsegmental defects. Defects that occur in the lung bases, the most common reported site of pulmonary emboli, are detected with greater frequency than in planar studies.

PS-468

V. Vondrak, P. Berzinec, N. Iliev, M. Letkovicova, D. Magula, V. Tinak, Z. Henzel

Regional Hospital Nitra/Dpt. of Nuclear Medicine, Institute of TB and Respiratory Diseases, Nitra-Zobor, Slovakia

COMBINATION OF GALLIUM SCAN, BRONCHOALVEOLAR LAVAGE (BAL) AND SERUM ANGIOTENSIN-CONVERTING ENZYME (SACE) IN THE DIAGNOSTICS OF PULMONARY SARCOIDOSIS

Aim of this study was to test the value of the combination of gallium scan, BAL -differential cell count - lymphocytosis, and SACE in the diagnostics of pulmonary sarcoidosis. The results of above mentioned tests were analyzed in 89 patients: 56 with recently diagnosed sarcoidosis, 33 with other respiratory diseases. The diagnosis of sarcoidosis was supported histologically, cytologically or with the presence of Löfgren's syndrome. For the statistical analysis were used: stepwise variable selection, multiple Kruskal-Wallis test and Bayesian theorem. Results - the probabilities of the correct diagnosis of pulmonary sarcoidosis according to the results of 3 tests are shown in the table:

Tests	Results	1. + = BAL LY > 10%	BAL LY > 10%	
1.	2.	3.	2. + = ⁶⁷ Ga positive	⁶⁷ Ga positive
			3. + = SACE > 130	SACE > 130
+ + +			0.95	0.96
+ + -			0.62	0.69
+ - +			0.58	0.66
+ - -			0.11	0.14
- + +			0.76	0.76
- + -			0.21	0.21
- - +			0.19	0.19
- - -			0.02	0.02

Conclusion: The probability of the correct diagnosis of pulmonary sarcoidosis is in our conditions 95-96% in case of positivity of all 3 tests. There remains only very small probability of the diagnosis (2%) in case of negativity of all 3 tests.

PS-469

M. Wartski, E. Fadel, E. Zerbib, Ph. Darteville, Ph. Herve

Departments of nuclear medicine, thoracic surgery and respiratory physiology- Marie Lannelongue Surgical Center-Le Plessis Robinson-France

99mTc-DTPA CLEARANCE IN PATIENTS WITH CHRONIC THROMBOEMBOLIC DISEASE : A FACTOR TO PREDICT BRONCHIAL BLOOD FLOW DEVELOPMENT ?

In experimental studies (Rizk, J Appl Physiol, 1984), values of ^{99m}Tc-DTPA clearance decrease after acute occlusion of pulmonary artery in dog. This decreased is greatly prolonged after an additional embolization of bronchial arteries. In patients with chronic thromboembolic pulmonary hypertension (CTEPH), several defects are present on lung perfusion scan. This disease is also associated with marked expansion of the collateral bronchial circulation and bronchopulmonary anastomoses. Therefore, we wanted to assess the hypothesis that the decrease in ^{99m}Tc-DTPA clearance in obstructed, not perfused lung areas could be attenuated in relationship with the development of bronchial collateral circulation. 30 CTEPH pts underwent a ^{99m}Tc-DTPA clearance and a lung perfusion scan before surgery of desobstruction. Lung spirometric volumes were normal in all the patients. The lung clearance of the radioactivity was followed over 20 min with a DST gamma camera (SMVI). Time activity curves were obtained from region of interest drawn on the total lungs (Global clearance), on lung regions not perfused (Regional clearance NP) and on lung regions normally perfused (Regional clearance P). The alveolar clearance expressed in %/min was assessed as a constant decay of the monoexponential function fitting these curves. Mean Regional clearances NP were not statistically different from Mean Regional clearances P (respectively 2.4%/min ranging from 0.25 to 5.9%/min and 1.95%/min ranging from 0.53 to 5.6%/min). Mean Global clearances were 2%/min, ranging from 0.25 to 5.9%/min. The most important result of this study is the presence of normal or accelerated clearance values in lung regions not perfused, reinforcing the hypothesis of a substantial collateral blood flow in these patients. The development of the collateral bronchial blood flow is of importance in these patients and may play a role in the prevention of the reperfusion pulmonary oedema, often present after surgery.

PS-470

Wen-hui Xie, Jun Zeng, Li-Hua Zhang, Zhi-Chang Yu
Department of Nuclear Medicine, Shanghai Chest Hospital, 241Huaihai West Road, Shanghai 200030, P.R. of China

THE EVALUATION OF CLINICAL ROLE OF TECHNETIUM-99M-HEXAKIS-2-METHOXYISOBUTYL ISONITRILE AND THALLIUM-201 CHLORIDE SPECT IMAGING IN PATIENTS WITH LUNG DISEASE

PURPOSE: A comparative study of Single Photon Emission Tomography (SPECT) of 201Tl and 99mTc-MIBI to evaluate the clinical role of 201Tl, 99mTc-MIBI and double isotopic SPECT imaging in detecting lung cancer.

METHODS: Our study was made up of 75 patients with lung disease, all patients had histological diagnosis. Double isotopic SPECT imaging was performed twice: 15min (early scan) and 120-180min (delay scan) after intravenous injection of 148MBq 201Tl and 555MBq 99mTc-MIBI. **RESULT:** Forty-three per cent of the patients who were mistakenly diagnosed with 99mTc-MIBI SPECT imaging were diagnosed correctly with 201Tl SPECT imaging, and twenty-five per cent of the patients who were mistakenly diagnosed with 201Tl SPECT imaging were diagnosed correctly with 99mTc-MIBI SPECT imaging. The sensitivity, negative predictive value and accuracy of double isotopic SPECT imaging were higher than that of 201Tl and 99mTc-MIBI single isotopic SPECT imaging, the specificity and positive predictive value of 201Tl and double isotopic SPECT imaging were no difference, but were higher than 99mTc-MIBI SPECT imaging in detecting lung cancer.

• Comparison of SPECT imaging with 99mTc-MIBI, 201Tl and double isotopic for evaluation of lung tumor positive imaging

	99mTc-MIBI	201Tl	double isotopic
• sensitivity	80%	85%	93%
• specificity	52%	64%	62%
• positive predictive value	73%	80%	80%
• negative predictive value	63%	72%	86%
• accuracy	69%	77%	81%

• **CONCLUSION:** These results indicate that double isotopic SPECT imaging with 201Tl and 99mTc-MIBI was superior to single isotopic SPECT imaging with 201Tl or 99mTc-MIBI and single isotopic SPECT imaging with 201Tl was superior to SPECT imaging with 99mTc-MIBI in detecting lung cancer.

PS-471

Y. Yamamoto, Y. Nishiyama, K. Fukunaga, Y. Kawasaki, M. Ohkawa, M. Tanabe
Kagawa Medical University, Asada Hospital, Department of Radiology

99mTc-MIBI AND 201Tl SPECT IN THE EVALUATION OF SOLITARY PULMONARY NODULES

99mTc-MIBI (MIBI) and 201Tl (Tl) are reported to be useful for lung cancer diagnosis. However, accumulation of these radionuclides in benign lesions has also been reported. The purpose of the present study was to assess the efficacy of dual-isotope SPECT imaging with MIBI and Tl for differentiating between malignant and benign solitary pulmonary nodules less than 3cm in diameter. Forty-three patients with diagnosis of solitary pulmonary nodule underwent dual-isotope imaging with MIBI and Tl. SPECT images were acquired 15 mins (early) and 2 hrs (delayed) after injection of 600 MBq MIBI and of 111 MBq Tl. Early ratio (ER), delayed ratio (DR) and retention index (RI = [(DR-ER) × 100] / ER) were calculated. There were 27 malignant lesions, all of which were lung cancer, and 16 benign lesions. Sensitivities of early and delayed MIBI and early and delayed Tl images in differentiating malignant and benign lesions were 44%, 48%, 56% and 52%, respectively. Corresponding specificities were 44%, 56%, 25% and 31%, respectively. Mean (± S.D.) values of ER, DR and RI using MIBI were: 1.4 ± 0.6, 1.3 ± 0.5 and -4.9 ± 10.2, respectively, in benign lesions; and 1.2 ± 0.3, 1.2 ± 0.3 and 1.8 ± 13.0, respectively, in malignant lesions. Corresponding values using Tl were: 1.7 ± 0.8, 1.5 ± 0.7 and -10.5 ± 11.7, respectively, in benign lesions; and 1.5 ± 0.5, 1.6 ± 0.7 and 4.1 ± 17.7, respectively, in malignant lesions. RI using Tl in malignant lesions was significantly higher (p < 0.01) than that in benign lesions. Thus, whereas MIBI appears to have little or no clinical value, RI using Tl seems to be a better parameter in differentiating between malignant and benign pulmonary nodules less than 3 cm in diameter.

PS-472

M. Yilmaz, H. Durak, G. An, E.S. Uçan, G. Çapa, R. Altın

Hospital: Dokuz Eylul University Hospital, Departments of Nuclear Medicine and Chest Diseases.

THE EFFECTS OF AMBROXOL, N-ACETYLCYSTEINE AND HYDRATION ON MUCOCILIARY CLEARANCE IN CHRONIC BRONCHITIS: EVALUATION WITH RADIOAEROSOL INHALATION SCINTIGRAPHY

Mucociliary clearance is an important pulmonary defence mechanism which is impaired in chronic bronchitis. Ambroxol and N-acetylcysteine (NAC) are mucolytic drugs which reduce the viscosity of mucus and improve mucociliary clearance. On the other hand, it is a common belief that intake of large amounts of fluid can facilitate removal of tracheobronchial hypersecretion. In this study, we investigated the effects of ambroxol, NAC and hydration on mucociliary clearance in patients with chronic bronchitis. Twenty three patients with chronic bronchitis (mean age: 62, 14M, 9F) were included in the study. Group A using ambroxol, Group B using NAC, and Group C, also as a control group, taking large amounts of fluid consisted of 8, 8 and 7 patients, respectively. Tc-99m MAA radioaerosol inhalation scintigraphy and pulmonary function tests were performed before and after therapy. Mucociliary clearance was evaluated visually and quantitatively by drawing ROIs on the central and peripheral airways. Retention index of inhaled radioaerosol and dyspnea score were calculated. Dyspnea score decreased in Group A, FEV₁ and FVC increased in Group B after therapy (p < 0.05). In hydration group, mucociliary clearance from the left and right total lungs was significantly slow (p < 0.05). Improvement of mucociliary clearance from both the left and right central airways and total lungs, and decrease in retention index after ambroxol therapy showed significant difference compared to those of hydration group (p < 0.05). Increase in FEV₁/FVC ratio after NAC therapy was significant compared to hydration group (p < 0.05). In conclusion, the most effective drug was ambroxol followed by NAC for the improvement of mucociliary clearance. A positive effect of hydration on mucociliary clearance was not observed. Radioaerosol inhalation scintigraphy is a useful technique to evaluate mucociliary function under physiologic conditions by providing both total and regional data.

Poster presentations

General nuclear medicine: Nephrology/urology

PS-473

A. Ahmed², J. Bomanji¹, E. Prvoulovich¹, M. Kellie¹, P. Ell¹

1- Inst. of Nuclear Medicine & Urology Dept., The Middlesex Hospital, London.
2- Institute of Nuclear Medicine & Molecular Biology, Gazda University, Sabin.

Evaluation of Qualitative and Quantitative Scintigraphic Parameters in Diagnosis of Renal Obstruction : A Proposed Holistic Approach.

The purpose of this retrospective study was to evaluate whether there is a complementary role for qualitative and quantitative scintigraphic parameters in improving the outcome of nuclear medicine in the clinical dilemma of equivocal renal obstruction. These measures were evaluated against pressure flow studies and/or clinical follow up (as gold standards) in all the cases of our series.

Between 1994 - 97, 22 patients (11-71 yrs) who underwent scintigraphy and pressure flow studies and in whom clinical follow up was available, were evaluated. Scintigraphy was carried out using Tc-99m MAG3 (100 MBq) or Tc-99m DTPA (300 MBq). Frusemide (0.5 mg/kg) was given at 15 min post-injection and pre & post-void images were obtained in all cases. Conventional visual analysis of the dynamic and static images in addition to the T/A curves, were carried out. Moreover, parenchymal transit time index (PTTI) and renal outflow efficiency (ROE) were calculated using Nuclear Diagnostics Ltd (NUD) software package. Pressure flow studies for all these patients were performed in the department of Urology. In patients where the latter was equivocal, clinical/surgical outcome was evaluated to reach a decision.

Of the 22 patients, 45% had severely impaired renal function as reflected in single kidney GFR (SKGFR = 16+ 5 ml/min). In one patient pressure flow study was non-diagnostic and clinical outcome excluded obstruction. Conventional visual interpretation and T/A curve analysis diagnosed renal obstruction with an accuracy of 68%. The accuracy for the PTTI and ROE was 82% and 68%, respectively. Combining qualitative and quantitative parameters, the accuracy was 96%. When this combined approach was applied to kidneys with severely impaired renal function, the accuracy was 90% (9 out of 10 pts) for detecting renal obstruction, and we were able to differentiate obstructive nephropathy from obstructing uropathy.

It is concluded that combining qualitative and quantitative renal Scintigraphic parameters (taking into account the limitations of each if taken separately) provides a simple non-invasive test to detect renal obstruction in patients with good and impaired renal functions with a high degree of accuracy. However, further assessment of the validity and reproducibility of this proposed holistic approach, a large multi-centre study, is recommended using a standardized protocol and particularly, considering inter/intra-operator variability in processing the quantitative parameters.

PS-474

A. Aktaş, A. Demirağ, M. Haberal

Başkent University Hospital, Ankara-TURKEY

COMPARISON OF SEVERAL SCINTIGRAPHIC PERFUSION PARAMETERS FOR DETECTING RENAL ALLOGRAFT REJECTION

Perfusion of the kidney is an important parameter to diagnose renal allograft dysfunction especially during the early postoperative period. The aim of this study was to compare the efficacy of several scintigraphic perfusion parameters in the diagnosis of acute renal allograft rejection.

Thirty-one patients with acute renal allograft rejection were included for this study. Serial imaging was performed in 22 of these patients when the baseline scintigraphy was abnormal or in the presence of a normal baseline scintigraphy when there is an increase in creatinine levels. For scintigraphic imaging, patients were administered 340 MBq of Tc-99m DTPA. Perfusion images were acquired at 1 sec frames during the first minute. As perfusion parameters, K/A (ratio of slopes of kidney and aorta), ΔP (time difference between the arterial and graft peaks), P/PL (ratio of peak to plateau counts) and cortical perfusion index (PI) were calculated. A value for the cortical perfusion index of more than 100 was regarded as pathologic.

Sensitivity of K/A, ΔP, P/PL and cortical perfusion index were 29%, 42%, 77% and 58%, respectively. On serial imaging, a value for the cortical perfusion index of more than 100 was only 50% sensitive to diagnose acute rejection episodes, while an increase in PI of more than 25 was 82% sensitive. The most sensitive parameter on serial scanning was a decrease in P/PL ratio of more than 25% (sensitivity 86%).

In conclusion, among the scintigraphic perfusion parameters, P/PL appeared to be the most sensitive parameter for detecting acute rejection episodes both at baseline and on serial scanning.

PS-475

K. Dilek, E. Alper, E. Selcoki, M. Gullulu, M. Yavuz, Y. Sadikoglu, M. Yurkuran

Departments of Nuclear and Internal Medicine, Uludag University Medical School, Bursa, TURKEY

TENOXCAM RENOGRAPHY USING TC-MAG 3: A NOVEL DIAGNOSTIC METHOD OF TRANSPLANT RENAL ARTERY STENOSIS

Prostaglandins (PG) act as vasodilator to maintain renal blood flow, especially in the setting of renal artery stenosis (RAS). We aimed to investigate whether the inhibition of renal PG synthesis with a nonsteroidal antiinflammatory agent, tenoxicam, would have a diagnostic potential in the detection of transplant (tx) RAS using Tc-99m-MAG 3 renal scanning. Six hypertensive patients (pt), 3 with and 3 without angiographic evidence of tx RAS (>50) underwent both baseline and tenoxicam renal scintigraphies (20 mg i.v., 20 minutes prior to imaging) with 111 MBq of Tc-99m-MAG 3. Evaluated criteria were time to peak (TTP), time to half clearance (T1/2) and residual cortical activity (RCA) at 20 minutes. In patients without tx RAS, no significant difference was observed between the parameters of baseline and tenoxicam scintigraphies. Patients with significant tx RAS, however, had increased TTP, T1/2 and RCA values from baseline to tenoxicam studies. The findings in the patients with stenotic renal artery are as follows:

	TTP (min)		T1/2 (min)		RCA (%)	
	B	T	B	T	B	T
Pt 1	3	8	8	12	33	48
Pt 2	2	6	7	11	29	40
Pt 3	6	7	8	12	45	65

B: Baseline Scintigraphy, T: Tenoxicam Scintigraphy

Following a successful angioplasty on pt 1, TTP, T1/2 and RCA values were 3, 8 and 33% in baseline, and 3, 8 and 30% in tenoxicam studies. Although a larger group of patients are needed to draw a conclusion, our preliminary results indicate that tenoxicam scintigraphy with MAG 3 could be used in the detection of tx RAS.

PS-476

Tarik Başoğlu, Halise Çıkman, Tuncay Onen, İrem Bernay

Departments of Nuclear Medicine and Pediatrics, Ondokuz Mayıs University Hospital, Samsun, TURKEY

CLINICAL EXPERIENCE IN 3-HOUR SINGLE PLASMA SAMPLE TC-99M-DTPA GLOMERULAR FILTRATION RATE MEASUREMENTS IN NORMAL AND DIABETIC CHILDREN

Overall reported experience with indirect Glomerular Filtration Rate (GFR) determination methods correlating activity of plasma samples in pediatric population is limited. By some of these methods, the results may be inaccurate if the subject's volume of tracer distribution is not in the adult normal range. Thus, for each proposed method, studies in pediatric populations are needed. Here we report our clinical experience with Russel's 180' single plasma sample (RSP) Tc-99m-DTPA GFR method in children realized as a common project with our department of pediatrics. The study was designed in two steps. First, 30 children (13 males / 17 females) within the age range of 6-18 yrs., without any evidence for renal disorder and with proven good renal function were prospectively examined. Dynamic renal scintigraphy (128x128 matrix, 1 sec/frame for 1 min. then 15 sec/frame for 29 min.) was performed after injection of 10 mCi Tc-99m-DTPA. Blood samples were obtained from the arm contralateral to the injection site exactly 180 min. following injection. GFR was calculated according to the following formula of Russel: $GFR \approx 82.42 \ln(Q_0 / P180) - 800.5$, where Q_0 represents the injected dose and P180 is the plasma activity. Split GFR was calculated using the 2-3 min. renogram data. In the second step, two groups of patients (1) 22 children (9 M/13F) having insulin dependent diabetes mellitus (IDDM) since 1-5 yrs., (2) 10 children (5M/5F) having IDDM since more than 5 yrs. were examined using the same protocol. Mean serum creatinine and GFR values in all groups were:

	NORMAL SUBJECTS	GROUP 1 - IDDM -	GROUP 2 - IDDM -
CREATININE (mg/dl)	0.5 ± 0.01	0.7 ± 0.02	0.7 ± 0.01
GFR (ml/min/1.73m ²)	112 ± 17	151 ± 11	142 ± 18

GFR values obtained in non-IDDM patients with normal renal function were in the acceptable range for the studied age group according to the literature. Increased GFR values were observed in 15 of 32 IDDM patients. This finding was presumably due to glomerular hyperfiltration which is observed in the early stages of diabetic nephropathy. In 5 of this 15 patients, microalbuminaemia was detected, which is known to be a consequence of glomerular hyperfiltration.

PS-477

Garcia, TMP; Braga, FJHN; Iazigi, N; Ferraz, AS. Unidade de Transplante Renal and Seção de Medicina Nuclear. Fac. Medicina de Ribeirão Preto, USP. BRAZIL.

CYCLOSPORIN A (CSA) NEPHROTOXICITY EVALUATED BY MEANS OF ^{99m}Tc-MAG3 DYNAMIC RENAL STUDY (DRS).

Kidney transplantation is one of the therapeutic choices for chronic renal failure and CSA is a well known immunosuppressive drug. Nevertheless, it has important side-effects, such as nephrotoxicity. Renal impairment evaluation is a big clinical challenge in such cases and the aim of our study was to eliminate all factors and changes induced by transplant itself. In the present work, 3 groups of 10 normal rats each were given 10 (Group 1, G1), 25 (G2) and 50 (G3) mg of CSA daily for one week. DRS (^{99m}Tc-MAG3, 30 MBq; initial phase: 10 frames of 1 sec; late phase: 120 frames of 15 sec) was performed before (B) and after (A) CSA administration in each animal. Time-activity curves were generated from ROIs over the left kidney and T 1/2 was determined. Creatinine (C) blood levels were also measured. G1 had T 1/2s of 16.62 min ± 4.27 B and 25.5 ± 15.21 A CSA (p = 0.007); G2 had mean T 1/2s of 17.85 min ± 4.48 B and 45.75 ± 21.6 A CSA (p = 0.001); G3 presented mean T 1/2s of 16.85 ± 2.54 B and 64 ± 18.75 A CSA (p = 0.0001). In addition, the arterial DRS peaks were reduced in all groups A CSA, but we were not able to quantify it due to the high cardiac frequency of rats. C levels after CSA increased in all groups but were significantly different only in G3, as compared to B levels. Prolonged T 1/2s are one of the main abnormalities seen in DRS in cases of acute tubular necrosis and reduced arterial peak indicates acute rejection. We conclude that CSA nephrotoxicity should be considered as a differential diagnosis in such situations. Moreover, DRS seems to be more sensitive than creatinine to evaluate CSA nephrotoxicity.

PS-478

¹S. Crnković, ¹D. Huić, ²Lj. Bubić-Filipi, ¹D. Grošev, ¹M. Poropat, ¹D. Dodig, ²Z. Purić
¹Clinical Department of Nuclear Medicine and Radiation Protection
²Center for Dialysis, Clinic of Urology
 University Hospital Rebro, Zagreb, Croatia

RENAL BLOOD FLOW IN FOLLOW-UP OF PATIENTS WITH RENAL TRANSPLANTS

Since the timing and selection of combined immunosuppressive therapy are of paramount importance, the aim of our study was to investigate the diagnostic usefulness of renal blood flow changes in follow-up of patients with renal transplants. During the four years period two hundred and thirty-three studies were performed in 60 patients (31 female, median age 37 years, range 11-62, cadaveric 42, 18 living related, median follow-up 21 months) using Tc-99m pertechnetate and I-131 OIH. Renal blood flow was calculated from the first-pass time activity curves generated over the kidney and aorta and expressed as a percentage of cardiac output (RBF/CO). In comparison with patients with normal graft function (11.4%±3.4%) the mean RBF/CO was significantly lower in patients with acute tubular necrosis (ATN, 6.5%±3.4%), as well as in patients with acute rejection (AR, 7.3%±3.4%). In patients affected with ATN the graft function improvement was followed with the mean rise in RBF/CO of 5.4%±3.4% (range -0.2% - 13.6%). The patients with previously diagnosed AR after successful treatment were also presented with the mean improvement in RBF/CO of 4.4%±3.7% (range -0.3% - 9.9%). Contrary, in the group of patients with previously normal graft function, AR was accompanied by deterioration in perfusion leading to the mean fall in RBF/CO of -3.2%±4.1% (range -3.1% - -13%). In conclusion, RBF/CO is a reliable indicator of graft function and could serve as a prognostic factor in the graft function recovery and evaluation of therapeutic effects, as well as in graft function deterioration.

PS-479

Y. Inoue, T. Ohtake, I. Yokoyama, K. Yoshikawa, J. Nishikawa
 Institute of Medical Science, University of Tokyo, Department of Radiology and University of Tokyo, Department of Radiology and Second Department of Internal Medicine

ESTIMATION OF Tc-99m MAG3 CLEARANCE BY A CAMERA-BASED METHOD

The aim of this study was to develop a camera-based method without blood sampling to estimate Tc-99m MAG3 clearance (CLmag). We performed renal scintigraphy with Tc-99m MAG3 in 21 adult patients. Eighty 3-sec frames were acquired after the bolus injection of 250 MBq of Tc-99m MAG3, followed by the collection of 52 frames at a rate of 30 sec/frame. Regions of interest were drawn for the kidneys and subrenal background areas, and background-subtracted renograms (cps/sec) were generated. Area under the curve was calculated at 0.5-1.5 min, 0.5-2 min, 1-2 min, 1-2.5 min, and 1.5-2.5 min after tracer arrival at the kidney, and percent renal uptake (RU) was obtained after attenuation correction assuming the attenuation coefficient at 0.12/cm. The slope of the background-subtracted renogram was determined at the same segments used in calculating area under the curve, and slope index (SI) was computed as slope after attenuation correction divided by injected dose (Kcpm) and multiplied by 1000. RUs and SIs were compared by linear regression analysis with CLmag determined by Bubeck's single plasma sample method. The CLmag measured by the single sample method had a wide range (17.5-320.0 ml/min/1.73m²). Correlation between RU and CLmag had mild dependence on the segments used for analysis, and the correlation coefficient ranged from 0.911-0.932. The RU at 1.5-2.5 min provided the best correlation with CLmag (CLmag = 10.417 x RU + 2.05, r = 0.932, SEE = 34.93). SI was better correlated with CLmag when an earlier segment was used. The correlation coefficient range from 0.887-0.972. The SI at 0.5-2 min was considered to be the most suitable for the estimation of CLmag (CLmag = 11.531 x SI + 6.24, r = 0.972, SEE = 22.80) among RUs and SIs. In conclusion, Tc-99m MAG3 clearance can be assessed by a camera-based method. A method based on the slope of the renogram may be more precise than that based on the area under the curve.

PS-480

K. Itoh, S. Tushima, Y. Tohma, M. Watanabe and Y. Hiraga
 HOSPITAL: JR Sapporo General Hospital, Departments of Radiology and Internal Medicine, Sapporo, Japan

DETERMINATION OF GLOMERULAR FILTRATION RATE BY MEANS OF A SINGLE -PLASMA -SAMPLE METHOD USING Tc-99m-DTPA

The purpose of this study identifies whether single-plasma-sample (SPS) method can be feasible in a determination of a glomerular filtration rate (GFR) using Tc-99m DTPA in Japanese, while most of the algorithms have been proposed from European institutions. We studied 50 patients (29 males and 21 females; age range being 25 to 91) who were admitted for treatment of diabetes mellitus. All patients gave informed consent. Tc-99m-DTPA was labeled in our hospital using commercially available instant kit (Daichi Radio-isotopes Co. Ltd., Tokyo, Japan). A solution containing 300 MBq of Tc-99m-DTPA per 2 ml was injected. Renal scintigraphy was carried out immediately for 20 minutes after the injection and 10 blood samples were entailed at 5, 15, 30, 45, 75, 120, 150, 180, 240 and 300 min following the injection. The plasma and standard solution were measured by a well-scintillation counter. Plasma concentration at each sampling time was calculated as percent injected dose per liter (%ID/L). GFR was determined by non-linear least squares fit of these plasma concentration (%ID) to 2 exponential curve. In addition, GFR in each patient was plotted to %ID normalized for body surface of 1.73 sqm (normalized %ID= V') at each sampling time. Plasma concentration (Ln(V')) of each sample correlated very well with GFR. Correlation coefficient between them was highest at 180 min postinjection. General formula for the determination of GFR within 120 from 300 min after injection was expressed as Y=A + BLn(V'), here A=463.12 - 3.4587t + 0.0121t² - 0.000015t³ (r²=0.998), and B=-212.6012 +1.4151t - 0.004834 + 0.0000062t³ (r²=0.994) sem=7.5734). We also examined 6 different SBS algorithms which have been proposed for simple determination of GFR so far. All algorithms gave the very correct value to the referred GFR.

SPS method can be feasible in the determination of GFR using Tc-99m-DTPA. Our algorithm obtained here may be feasible in a routine clinical practice as a conventional determination of GFR.

Poster presentations

PS-481

A. Jiménez-Heffernan, A. Ortega-Carpio*, AC Rebollo, J. Acosta**, C. Herrera, F. Picchi***
Hospitals Juan Ramón Jiménez and Infanta Elena***, Services of Nuclear Medicine, Critical Care and Emergency* and Pediatrics**, ***, HUELVA, SPAIN.

VARIABLES ASSOCIATED WITH RENAL DAMAGE ON Tc-DMSA SCINTIGRAPHY IN PATIENTS WITH URINARY TRACT INFECTION.

Tc-DMSA imaging is sensitive for renal scar screening in patients with urinary tract infection (UTI). We studied 173 patients (81♂ and 92♀) with mean age 4.1±0.64, range 1 month-16 years and related Tc-DMSA findings with age, sex, history of UTI and presence of vesico-ureteric reflux (VUR).

The age interval comprising more children was <1y age with 40%. The 1-6y and >6y age intervals comprised 33% and 26% of patients respectively. While girl's ages were evenly distributed among intervals, boys were typically concentrated in the youngest group 60%>1y age, 26% 1-6y and only 14% >6y age. A history of UTI was present in 139 children (80%), 83 (60) with recurrent UTI and 56 (40%) with first UTI. This difference was significant (p=0.0003). Nevertheless small boys were studied more frequently with first UTI (55%) than girls (27%) (RR=2.02, IC:1.3-3.1). MCU had been performed in 108 patients showing VUR in 75 (70%) and absence of VUR in 33 (31%). This difference was significant (p=0.0001).

Split renal function was within normal limits in 64% of patients. Scintigraphy was normal in 103 children (60%) and showed cortical defects/and or shrunken kidneys in 41 (34 unilateral and 7 bilateral). Abnormal studies were more frequent in girls 26 (34%) than in boys 14 (21%) p=n.s. Equivocal studies were obtained in 27 patients. Abnormality on Tc-DMSA was more frequent in older children since it was present in only 16% of those <1y age versus 36% and 38% of those in the 1-6y (RR=2.17, IC:1.1-4.3) and >6y (RR=2.27, IC:1.1-4.5) age intervals respectively. There was a nonsignificant tendency to present renal defects in patients with recurrent UTI (33%) versus first UTI (21%). VUR was associated with a higher proportion of abnormal studies (45% vs 13% without VUR) (RR=3.3, IC:1.2-8.5).

We confirm the tendency to preferentially study infant boys with first UTI, older girls with recurrent UTI and patients with VUR. On the other hand abnormality on DMSA imaging is higher in girls, increases with age and is associated with VUR.

PS-482

Levent Kabasakal, Metin Halaç, A. Fuat Yapar, Ebru Alkan, Bedii Kanmaz, Çetin Önsel, Kerim Sönmezoglu, Meltem Ayaz, Betül Kalender, Haluk B. Sayman, İlhami Uslu.,
Cerrahpaşa Medical Faculty, Department of Nuclear Medicine, Istanbul Turkey.

Prospective Validation of Single Plasma Sample Technetium-99m-Ethylenedicysteine Clearance in Adults

It has been shown that ^{99m}Tc-EC clearance shows strong correlation with OIH clearance and it is possible to estimate ERF from ^{99m}Tc-EC clearance. In routine clinical studies it is practical to use one or two plasma sample method instead of multiple plasma samples for clearance determination. A single sample technique was developed for ^{99m}Tc-EC and a regression formula was generated. In order to test the validity of this regression formula a prospective study is undertaken. **Methods:** Study population was composed of 26 patients with a wide range of renal function. Multiple plasma sample ^{99m}Tc-EC clearances were calculated from all patients using open two compartment model. Single plasma sample clearances were also determined from 54 min plasma sample using the regression formula published previously. **Results:** The multiple sample plasma clearance of ^{99m}Tc-EC ranged from 46 ml/min to 668 ml/min with a mean of 300.76±150.73 ml/min. The clearances obtained from 54 min plasma sample ranged from 49 ml/min to 699 ml/min, with a mean of 297.39±152.23 ml/min. There was an excellent correlation between the clearances obtained by two techniques (r=0.99, slope=0.9911). The standard error of estimation was found to be 25.9 ml/min. **Conclusion:** This study suggested that ^{99m}Tc-EC clearance can be estimated from 54 min plasma sample with an acceptable error of estimation for most routine clinical studies

PS-483

T. Kanazawa, M. Shimizu, H. Seto, M. Kageyama, K. Kameda, S. Toyoshima, G. Tomizawa, N. Watanabe and S. Inagaki*

Toyama Medical and Pharmaceutical University, Department of Radiology and *Division of Central Radiological Services, Japan.

Reproducibility of Tc-99m MAG3 Clearance in Normal Volunteers by Two Samples Method: Comparison with I-131 OIH

Reproducibility of Tc-99m MAG3 clearance has been controversial. Tc-99m MAG3 kit preparation is affected by various factors, therefore its radiochemical purity is not stable. The aim of this study was to evaluate the reproducibility of commercially available Tc-99m MAG3 (Dai-ichi Radioisotope Labs Ltd, Tokyo, Japan) clearance and to compare it with that of I-131 OIH, which has been used in many clinical situations and relied upon for a number of years in Japan. Twelve young healthy volunteers with a mean age of 23.4 years (range 19-28 yr) were enrolled in this study. Investigations were repeated at an interval of one month under similar physiological conditions. Each volunteer received a simultaneous injection of Tc-99m MAG3 and I-131 OIH commercially available in a form already labeled. Blood samples were obtained at 44 and 104 min post injection. Clearance values were calculated using the two samples method. For Tc-99m MAG3, the mean clearance value of the first measurements was 509.1 ml/min/1.73m² (399.4-566.9) and the mean value of the second series was 549.0 ml/min/1.73m² (455.2-649.8). For I-131 OIH, the mean clearance value of the first measurements was 723.6 ml/min/1.73m² (441.4-963.3) and the mean value of the second series was 703.5 ml/min/1.73m² (555.2-910.8). The mean change from the first to the second measurement was -7.1% ±11.1 (± s.d.) for Tc-99m MAG3, and was 1.7% ± 13.6 for I-131 OIH. There were no significant differences between the first and the second measurements for Tc-99m MAG3 and I-131 OIH clearance, respectively (A paired t-test, p > 0.01). The reproducibility of commercially available Tc-99m MAG3 clearance was demonstrated to be almost the same as that of I-131 OIH clearance and Tc-99m MAG3 clearance was found to be as useful as I-131 OIH clearance in healthy volunteers in our study.

PS-484

Y.A.Chung, S.H.Kim, H.G.Lee, Y.H.Park, H.S.Sohn, S.Y. Lee, S.K.Chung, K.S.Shinn.

Catholic University Medical College, Seoul, Korea

COMPARISON OF NORMAL FRACTIONAL MEAN TRANSIT TIME (MTT) BETWEEN LIVING DONOR KIDNEY (LDK), TRANSPLANTED LIVING DONOR KIDNEY (TLDK) AND TRANSPLANTED CADAVER DONOR KIDNEY (TCDK).

This study was undertaken to assess the differences in normal fractional MTT between pretransplanted living donor kidney (LDK) and the transplanted same kidney (TLDK), and transplanted cadaver donor kidney (TCDK). We examined 99 renograms of TLDK (43) and the corresponding LDK (43), and TCDK (13). All patients showed normal serum creatinine level on the day of renography and normal biopsy finding taken on the day of 14 posttransplantation. Tc-99m-DTPA renograms were obtained 2 to 4 weeks prior to donor nephrectomy and 1 week of transplantation. We measured MTT in renal outer and middle zone. The outer renal zone contained cortical nephron, and middle renal zone contained juxtamedullary nephron, calyces and the part of cortical nephron. Fractional MTT was determined by deconvolution analysis. The differences were determined by Student's t-test. The results (mean ± S.D.) were as follows;

	LDK	TLDK	TCDK
Outer zone MTT(sec)	110±22.6*	125.4±21.6*	130.7±19.8
Middle zone MTT(sec)	140.1±28.8	133.2±26.0	136.7±19.4

*P<0.01

In conclusion, the outer zone MTT was significantly prolonged in TLDK, compared with LDK. We expect that the measurement of fractional MTT before and after renal transplantation can be available in identifying posttransplantation complications.

PS-485

S.Komai, H.Toyama, H.Maeda, S.Kisohara, S.Minowa, M.Morooka, T.Sawai, K.Yokoyama, M.Yazaki, K.Senda, A.Takeuchi, S.Koga.
Fujita Health University, Toyoake, Japan.

EVALUATION OF RENAL PARENCHYMA AND TRANSFER FUNCTION WITH DYNAMIC Tc-99m-MAG3 SPECT IN CHILDREN.

Renal parenchymal scintigraphy with static Tc-99m-DMSA SPECT is carried out 1-2 hr after the injection, and requires 20-30 min imaging time. Also, renography or transfer function must be analyzed with Tc-99m-DTPA or Tc-99m-MAG3 later. The purpose of this study is to evaluate the feasibility of a rapid renal parenchymal SPECT image and the transfer function(TF) with Tc-99m-MAG3 in children with renal parenchymal diseases. Following intravenous bolus injection of 5-10 MBq/kg of Tc-99m-MAG3, serial SPECT of 30 sec intervals were performed for 20 min. Transaxial, coronal and sagittal SPECT images were reconstructed from initial 2 min acquisition sets. TF was calculated by the matrix algorithm from regional renogram (output) and time- activity curve over the heart (input). Minimum, mean, maximum transit time (TT), indices of excretory function, and initial height (IH), an index of relative ERPF, were determined from each TF. In 3 VUR pts who showed renal parenchymal scar with DMSA SPECT, MAG3 SPECT images were of somewhat inferior quality, but diagnostic. However, 1 focal defect in DMSA SPECT was not detectable in MAG3 SPECT. Mean TT averaged 4.0 ± 0.38 min in 2 remission state of nephrotic syndrome kidneys. In 1 rapid progressive glomerulonephritis pts, mean TT was prolonged (7.2 min). In conclusion, Tc-99m-MAG3 dynamic SPECT which is able to evaluate both renal parenchyma and TF at one short term examination might be clinically useful in children renal disorders.

PS-486

YZ Liu, XJ Liu, L Zhu*, F Guo, DY Wang, QW Wu, BG Zhou, HX Wei
Department of Nuclear Medicine, Cardiovascular Institute & Fu. Wai Hospital, CAMS & PUMC, Beijing, China
*National Research Center for CMS, S, Beijing, China

THE COMPARISON OF 99mTc-EC AND 99mTc-DTPA CAPTOPRIL TEST IN DETECTING UNILATERAL RENOVASCULAR HYPERTENSION

To compare the 99mTc-EC and 99mTc-DTPA Captopril test in detecting unilateral renovascular hypertension 40 cases were studied with both agents renal images before and after Captopril test.

Patients: 13 normal subject (M10, F3)

27 patients with unilateral renovascular hypertension

Results: Table. Unilateral renovascular hypertension group

		EC		DTPA	
		before CAPT	after CAPT	before CAPT	after CAPT
C20 (%)	IS	36.74±26.54	13.22± 20.79*	17.50±20.59	4.24± 4.96 *
	nor	61.71± 7.36	60.51±10.27(NS)	46.50±14.03	27.52±14.65*
PT(min)	IS	6.34±3.78	9.36± 6.63*	3.67± 2.84	9.55± 8.80*
	nor	4.81± 2.67	5.07±3.26(NS)	2.98± 2.47	5.80± 3.70**

*P,0.01 **P<0.05

Conclusion: The sensitivity of 99mTc-DTPA and 99mTc-EC for detecting ischemic Kidney may be comparable. However, The specificity for recognizing the normal Kidney, 99mTc-EC is much better than of 99mTc-DTPA.

PS-487

Y.Niio, K.Uchiyama, T.Yamamoto, T.Habu, Y.Kuniyasu, S.Hasebe, H.Shinohara, S.Matsuoka, H.Shima, K.Doai, M.Yamada, K.Takizawa, K.Hosoya*, and K.Yoshioka*
Showa University Fujioka Hospital, Department of Radiology, *GE Yokogawa Medical System. Fujioka 1-30, Aoba-ku, Yokohama, 227-8501, Japan

INFLUENCE FACTORS OF QUANTITATIVE MEASUREMENT OF RENAL UPTAKE RATE WITH TECHNETIUM-99m-MERCAPTOACETYL-TRIGLYCINE(MAG3) SCINTIGRAPHY

Recently, camera-based techniques to measure effective renal plasma flow(ERPF) using renal scintigraphy with technetium-99m-mercaptoacetyltriglycine(99mTc-MAG3) have become common. Because ERPF is calculated from renal uptake rate(RUR), accurate measurement of RUR is needed in this technique. However, camera-based techniques are necessary to some corrections such as renal depth, bed absorption, back ground, and linear attenuation coefficient of 99mTc of gamma camera systems (μ). In this study, we evaluated the influences of μ and renal depth in measuring RUR with 99mTc-MAG3 scintigraphy. **PATIENTS AND METHODS:** 1) The μ of STARCAM 3000XR/T was measured in phantom examinations. 2) Comparing our new proposal regression equations ($D_r=0.32xTa+0.87$, $DI=0.36xTa-0.08$, D_r : depth of the right kidney, DI : the left kidney, Ta : thickness of the abdomen) with conventional formulas, the influences of μ and renal depth correction in measuring RUR were studied for eight normal volunteers. **RESULTS:** 1) The μ of STARCAM 3000XR/T was determined 0.1385 based on phantom studies. The mean value of RUR calculated from the $\mu(0.1385)$ was underestimated 11.2% of that from Gate's formula ($\mu;0.153$) in volunteer group. If the value of μ was set at 0.110, the calculated RUR was underestimated 29.9% of that from Gate's formula. 2) Concerning the influence of renal depth correction, the value of RUR from Tønnesen's or Raynaud's formula showed 20-30% underestimation of that from the formula by accurate X-ray CT measurement of renal depth. While, the value of RUR from our proposal formula showed only 8% underestimation of that from the formula by X-ray CT. **CONCLUSION:** μ and renal depth correction have a lot of influences in measuring RUR with 99mTc-MAG3 scintigraphy. Accurate value of μ should be determined in each gamma-camera system in measuring RUR. It is considered that our new proposal regression equations is desirable for renal depth correction.

PS-488

H.Pena 1, 2, HR Ham 3, A.Piepsz 2, 3

Instituto de Medicina Nuclear-FML – Lisboa, Portugal 1, AZ VUB 2 and H. St. Pierre 3 – Brussels, Belgium

EFFECT OF THE LENGTH OF THE FRAME TIME ON THE Tc-99m MAG3 GAMMA CAMERA CLEARANCE

Many efforts have been put these last years into standardisation of the renographic procedure, particularly regarding the determination of renal clearance. In the present work, we have tried to evaluate the influence of the frame time on the clearance value.

Tc-99m MAG3 renograms were performed on 20 patients (40 kidneys), using acquisition frames of 1 second. The curves were then reframed using 5, 10, 15 and 20 second frames. Quadrangular regions of interest were drawn around the kidneys, the perirenal areas and the heart. A 3-point smoothing was applied on the renal curves, the background curves and the heart curve. A first background correction was applied, namely the subtraction from the rough renal curves of the surface normalised perirenal curve; the Rutland-Patlak plot was then constructed, the slope of the best fit representing the individual clearance. All the clearances were calculated within the interval of 60-160 sec post-injection.

The results showed that the differences observed when using different frame times were small and were comparable to the differences observed when using the same frame time but simply adding one frame for the calculation of the clearance.

Frame time (interval) vs	frame time (interval)	mean of differences	s.d. of differences
5 sec (61 - 155 sec) vs	5 sec (61 - 160 sec)	- 1.4 %	2.5 %
10 sec (61 - 150 sec) vs	10 sec (71 - 150 sec)	- 2.3 %	2.3 %
15 sec (61- 135 sec) vs	15 sec (61 - 150 sec)	- 2.9 %	2.4 %
20 sec (61 - 140 sec) vs	20 sec (61 - 160 sec)	- 2.9 %	2.4 %
5 sec (61 - 155 sec) vs	10 sec (61 - 150 sec)	+ 1.2 %	1.5 %
5 sec (61 - 155 sec) vs	15 sec (61 - 150 sec)	+ 1.5 %	4.0 %
5 sec (61 - 155 sec) vs	20 sec (61 - 160 sec)	+ 0.2 %	5.4 %
10 sec (61 - 150 sec) vs	15 sec (61 - 150 sec)	+ 0.2 %	3.0 %
10 sec (61 - 150 sec) vs	20 sec (61 - 160 sec)	- 1.0 %	4.5 %
15 sec (61 - 150 sec) vs	20 sec (61 - 160 sec)	- 1.3 %	3.5 %

In conclusion, the length of the frame time is unimportant as far as the calculation of the clearance is concerned.

Poster presentations

PS-489

D. Pucar, J. Butorajac*, B. Ajdinović, S. Marković

Military Medical Academy, Institute of nuclear medicine, Nephrology Clinic*, Belgrade, Yugoslavia

EVALUATION OF KIDNEY FUNCTION PRE / POST EXTRACORPOREAL SHOCK WAVE LITHOTRIPSY BY DYNAMIC RENAL SCINTIGRAPHY

Dynamic renal scintigraphy was performed in 28 adult patients (pts) before and after extracorporeal shock wave lithotripsy (ESWL). In twenty-two pts ^{99m}Tc-DTPA dynamic study was performed before and after ESWL; in 8 pts before, 7 days and 3 months after and in the other 14 pts before and after 7 days. Six pts were investigated using ^{131I}-OIH before and 7 days after ESWL and four of them 3 months after ESWL. Changes of separate clearances (SCI) and maximum times of time activity curves (T_{max}) were evaluated on the treated kidney.

There was no statistically significant differences of SCI before and after ESWL in pts who were investigated by DTPA. T_{max} were significantly shorter 3 months after ESWL than before and 7 days after ESWL (p<0.05). SCI obtained with ^{131I}-OIH 7 days after ESWL was significantly lower than before and 3 months after ESWL (p<0.05).

In conclusion, our results demonstrate improvement of kidney glomerular filtration three months after ESWL (decreasing T_{max}) and the temporary damage of tubular function (decreased SCI seven days after ESWL, improving three months after).

PS-491

PF Rambaldi, G Lama*, L Valentino*, D Capobianco, V Cuccurullo, L Mansi. Institute of Radiological Sciences, *Department of Paediatrics - II University, Naples

MAG3 DIURETIC RENOGRAM FOLLOW-UP TO DIAGNOSE SPONTANEOUS IMPROVEMENT IN CHILDREN WITH URINARY TRACT DILATION

Aim of the study was to analyse the role of MAG3 diuretic renogram in 2 year follow-up of newborns affected by hydronephrosis. 22 infants (12M, 8F, age:1-3 months) with urinary tract dilation at ultrasounds and without vesicoureteric reflux at cystography were retrospectively evaluated. A baseline diuretic MAG3 renogram during the first 4-12 weeks of life showed equivocal findings in 27 kidneys (T_{max}>20'). Follow-up studies were performed at 6-9 months and at 20-24 months. 8 kidneys with clear improvement at second MAG3 (T_{max}<20') were considered as dilated. 15 kidneys with mild improvement at the second study (T_{max}>20', 25-40% washout) furtherly improving at 2 yrs control (T_{max}<20', washout≤50%) were considered dilated but not obstructed. In 4 children without improvement at follow-up an increase of the washout was observed only after subsequent pyeloplasty. During follow-up split renal function was stable in all children.

In conclusion an antibiotic prophylaxis and the follow-up of individual renal function and washout using nuclear medicine studies are a correct management in children with urinary tract dilation allowing the evidence of spontaneous improvement to avoid unnecessary surgery.

PS-490

M.Rajić, M.Bogićević, S.Ilić, M.Avranić, B.Mitić

Clinical Center, Department of Nuclear Medicine, Niš, Yugoslavia

^{99m}Tc-DMSA RENAL UPTAKE IN GLOMERULAR KIDNEY DISEASES

The early phase of glomerular kidney diseases is commonly associated with tubular disorders.

This study was aimed to evaluate tubular function by determining the rate of ^{99m}Tc-DMSA renal uptake in glomerulonephritis and diabetic nephropathy patients.

Twelve primary glomerulonephritis patients (GN) and 19 insulin-dependent patients with overt diabetic nephropathy (DN) were included in the study. All patients had normal serum creatinine levels and reduced GFR (^{99m}Tc-DTPA clearance values were 76.1 ± 15.6 ml/min in GN patients, 82.0 ± 28.0 ml/min in DN patients and 121.0 ± 10.7 ml/min in 15 healthy volunteers). Renal uptake of ^{99m}Tc-DMSA up to 30 min was derived from renograms, while 120 min and 240 min uptake was determined from planar posterior images. Renal uptake and 240 min whole blood activity of DMSA values were expressed as percentage of injected net activity.

^{99m}Tc-DMSA renal uptake values at different time intervals (means ± SD)

Group	5 min	10 min	20 min	30 min	120 min	240 min
Control	14.1 ± 3.2	18.7 ± 3.0	25.7 ± 3.4	30.2 ± 3.6	46.4 ± 6.4	51.3 ± 7.3
GN	10.4 ± 3.7	11.7 ± 3.9 ^b	13.1 ± 4.8*	14.6 ± 6.0*	21.5 ± 6.8*	25.0 ± 8.1*
DN	10.6 ± 8.0	10.7 ± 4.9 ^c	11.8 ± 4.6*	12.6 ± 6.0*	17.8 ± 5.3*	21.4 ± 6.6*

vs. control : a - p < 0.001, b - p < 0.005, c - p < 0.01

Nonsignificant decrease of ^{99m}Tc-DMSA renal uptake at 5 min and more marked reduction at later time intervals was recorded in both patient groups. These results showed a greater contribution of tubular impairment than renal blood flow alteration to lower renal accumulation of ^{99m}Tc-DMSA. Decreased renal uptake induced slower blood clearance of ^{99m}Tc-DMSA which was manifested by higher blood activity in GN (27.5 ± 3.5%) and DN (27.7 ± 7.2%) patients, compared to control group (19.6 ± 3.4%) (p < 0.05). ^{99m}Tc-DMSA renal uptake was found reduced in GN and DN patients for 51 and 58%, while GFR was decreased only for 37 and 32%, respectively. These findings suggest more severe tubular than glomerular dysfunction in patients with both glomerulopathies with normal serum creatinine and impaired GFR.

PS-492

M Rutland, I. M Hassan, L. Que

Auckland Hospital [NZ]: Department Of Nuclear Medicine

RENAL DTPA UPTAKE RATE : NORMAL VALUES AND ASSESSMENT OF COMPENSATORY RENAL HYPERTROPHY.

Gamma camera renography studies were analysed to measure the fractional uptake rate of ^{99m}Tc-DTPA by the kidneys. Normal values were obtained from patients in different age groups, and these normal values then compared with results from patients with unilateral renal disease who had compensatory hypertrophy of the contralateral kidney

Results - Uptake rates of both kidneys [per million seconds].

AGE	2 NORMAL KIDNEYS			UNILATERAL DAMAGE		
	n	mean	sd	n	mean	sd
0-2 months	12	296	132	19	241	65
3-4 months	16	366	148	16	333	65
5-8 months	12	468	89	12	372	90
1-1.9 years	29	528	95	14	508	106
2-2.9 years	12	524	86	9	486	105
5-9 years	50	482	94	35	425	102
10-19 years	33	442	133	67	405	84
20-29 years	51	424	150	59	394	87
40-49 years	41	362	98	50	330	76
60-69 years	38	286	112	30	271	72
80-89 years	12	177	75	14	153	55

The results indicate that when renal function is expressed in terms of DTPA uptake rates, children reach adult levels of renal function between 4 and 8 months of age, and then exceed adult function until the age of 10 years. During adult life there is a decline in normal renal function, which is more evident after the age of 50 years.

In most age groups, patients with unilateral renal damage and compensatory hypertrophy are able to maintain a level of renal function which is approximately 90% that of patients with two normal kidneys.

PS-493

J.-P. Papazyan¹, J. Th. Locher², J. Darcourt³, Ph. Fernandez⁴, R. Jeandot⁴, D.O. Slosman¹. Nuclear Medicine Departments, Geneva University Hospital¹ (CH), Aarau Cantonal Hospital² (CH), Centre Antoine-Lacassagne Nice³ (F) & Bordeaux University Hospital⁴ (F).

^{99m}Tc-DMSA RENAL SCINTIGRAPHY IN CHILDREN: STUDY OF INTRA- AND INTER-OBSERVER AGREEMENT.

Aim : Acute pyelonephritis (APN) is a common infectious disorder in children. Technetium-99m DMSA renal scintigraphy is considered as "gold standard" for the diagnosis of APN and renal scarring. In this work, we evaluate the intra- and inter-observer agreement of DMSA scintigraphy interpretations. **Material & Methods:** We performed an analysis of 100 consecutive pediatric exams. All patients (mean age 2.6 years, range from 12 days to 14.4 years) with suspected APN (53%) or cortical scarring post-APN / combined with urological malformation were included and had a standard acquisition in 6 projections (3-heads Toshiba GCA-9300) 3 hours post-iv injection of 3.7 MBq / Kg of ^{99m}Tc-DMSA. Criteria of interpretation were defined prior the study and corresponded to codification that includes 4 choices. Six observers certified board in nuclear medicine from swiss et french university or affiliated hospitals have reviewed these exams blindly and independently. Two observers read twice all the scans for determining the intra-observer variability. **Results:** We obtain 61% of intra-observer reproducibility and a great inter-observer variability with an inter-reader correlation "kappa" index of 0.40 for the whole population and 0.38 for the patients with suspected APN. Interpretation criteria were reevaluated and after simplifying in 3 codes, the results were enhanced: "kappa" index respectively of 0.53 and 0.54 for the two groups. A correlation with clinical final diagnosis was done for the patients with suspected APN. Based on these results, 3 scintigraphic conclusions were defined with a likelihood ratio (LR): normal conclusive exam (LR 0.0), inconclusive exam (LR 2.3), pathological conclusive exam (LR 8.0). **Conclusions:** Based on these results and the application of Bayes' theorem, after determination of a clinical "a priori" probability, we can achieve a post-examination probability of APN similarly to the diagnostic approach in pulmonary embolism.

PS-494

Y. Tomaru, T. Inoue, N. Oriuchi, K. Takahashi, K. Endo

Department of Nuclear Medicine,
Gunma University School of Medicine; Gunma, JAPAN

SEMI-AUTOMATED RENAL REGION OF INTEREST SELECTION METHOD USING THE DOUBLE-THRESHOLD TECHNIQUE: INTER-OPERATOR VARIABILITY IN QUANTITATING Tc-99m-MAG3 RENAL UPTAKE

In calculating the relative and absolute renal uptake of technetium-99m mercaptoacetyltriglycine (MAG3), inter-operator variability in the assignment of the renal region of interest (ROI) is a critical factor. Our goal was to develop a semi-automated method of assigning the renal ROI and then to compare the inter-operator variability in calculating the percent injected dose (%ID) in the kidney at 1-2 min, using semi-automated versus manual ROIs. The manual ROIs were drawn independently by three operators (A, B and C). Operator A had about 20 years, experience in nuclear medicine, while operators B and C respectively had 3 years and 1 year of experience. In the semi-automated renal ROI selection method using the double-threshold technique, the operators only click around the centre of each kidney. The same three operators processed the ROIs using this double-threshold method on 1-2 min images. The semi-automated method failed in three kidneys with very markedly reduced function owing to superimposition by liver or spleen. Inter-operator reproducibility in the remaining 59 kidneys was estimated using manual and semi-automated ROIs. With manual ROIs, the %ID (mean ± standard error of mean) was 4.32±0.167 for A, 4.14±0.165 for B and 3.28±0.139 for C. Although there was good correlation among them, these values were significantly different (P<0.0001). Using semi-automated ROIs, the %ID was 4.38±0.160 for three operators. No significant difference was observed. Complete reproducibility was shown in 58 of 59 kidneys; the %ID difference of the remaining kidney was only 1.2%. The lowest %ID of all the kidneys successfully detected using the semi-automated method was 0.77%. The semi-automated renal ROI selection method using the double-threshold technique displays good detectability of the renal contour. The renal uptake calculated using this method is reproducible and acceptable in routine clinical practice.

PS-495

C. Van de Wiele, R. Vanholder, T. Verplancke, Y. D'Asseler, K. Casier, RA. Dierckx
University Hospital Gent, BELGIUM

CLINICAL USEFULNESS OF Tc-99m DTPA CAPTOPRIL SCINTIGRAPHY IN PATIENTS WITH A SOLITARY KIDNEY AND SUSPICION OF RENAL ARTERY STENOSIS

This retrospective study aimed to confirm Tc-99m DTPA captopril renal scintigraphy (CRS) reliability for diagnosing functionally significant renal artery stenosis (RAS) in hypertensive patients with solitary kidneys (SK) and reduced kidney function (RKF). From 1991-1996, 9 consecutive patients (6 women, mean age: 52.3 yrs, range : 35-74 yrs) with known RKF and SK, presenting with clinical signs suggesting RAS were included. Tc-99m DTPA renographies were performed under baseline condition and 1 h. after administration of 25 mg captopril within one week from each other. A repeat CRT was performed in two patients, resulting in a total of 11 evaluable examinations. CRT evaluation was performed using the Working Party on diagnostic criteria of renovascular hypertension. Final diagnosis was obtained by means of angiography (n, number of patients = 1), duplex ultrasound (n = 5), biopsy (n=2) and long term follow-up (≥ 2 years) available in all patients. All 9 patients referred for exclusion of RAS were accurately defined by CRT. In conclusion, the data presented suggest that also in patients with SK and RKF, Tc-99m qualitative Tc-99m DTPA CRT is a reliable tool for diagnosing RAS.

PS-496

SC Tsai, WY Lin, CH Kao, SJ Wang and JL Lan.

Department of Nuclear Medicine and Internal Medicine,
Taichung Veterans General Hospital, Taiwan.

LUPUS NEPHRITIS: A COMPARISON BETWEEN LABORATORY DATA, GALLIUM IMAGE, AND RENAL BIOPSY MEASUREMENT.

Lupus nephritis is a significant source of morbidity and mortality in patients with systemic lupus erythematosus (SLE). Many assays have been developed to aid both in the diagnosis and in the prediction of disease activity in SLE. The purpose of our study was to evaluate the relationship of various laboratory data, including anti-double-stranded DNA (anti-dsDNA), 24- hour urine protein, serum creatinine and gallium image, to changes in renal biopsy measures of activity index (AI), chronic index (CI) and World Health Organization (WHO) classification in lupus nephritis. Twenty-seven patients (mean age 31.9 ± 11.3 yrs.) with lupus nephritis were enrolled in this study. All of the patients underwent renal biopsy procedures, and laboratory examinations including anti-dsDNA, serum creatinine and 24-hour urine protein. 48-hour delayed gallium imaging was performed on all patients. A gallium uptake in the kidneys equal or greater to the uptake in the spine was considered to be positive. In addition, the cutoff values for serum creatinine and 24-hour urine protein were 2 mg/dl and 3 g/day respectively. For anti-dsDNA assay, the cutoff value was 50 U. Our data revealed: 1) Gallium scan showed the best correlation with AI (p value = 0.0015). 24-hour urine protein also showed good correlation with AI (p value = 0.0412). 2) Serum creatinine was the only parameter which showed good correlation with CI (p value= 0.0014). 3) No parameters showed good correlation with the WHO class in this study. We suggest that gallium scan or 24-hour urine protein may be a useful alternative to renal biopsy in the evaluation of disease activity and indicate an acute curable lesion, while serum creatinine may indicate a chronic lesion and be useful in the prediction of disease outcome.

Poster presentations

PS-497

E. Werner, S. Seybold, S. Muffert, J. Farahati, Chr. Reiners
Clinic for Nuclearmedizin, University of Würzburg, Germany

ACCURACY OF CALCULATION OF SPLIT RENAL FUNCTION WITH Tc-99mMAG3 USING THE PATLAKPLOT - A COMPARISON WITH STATIC RENAL 99mTc DMSA SCAN

Introduction and aim: The determination of split renal function is an important object of renal scanning. The aim of this study was the assessment of the accuracy of several methods for calculation split renal function.

Method: We retrospectively analysed 19 children and adolescents (age: 10±6 years) who had a Tc99m MAG3 and a Tc99m DMSA scan in our institution. Split renal function was calculated by the conventional (con) „Oberhausen“ method (integrals of background corrected time activity curves from 60th to 100th sec) and 3 Patlak methods. The Patlakplot was generated using time activity curves over the heart and the kidneys. This plot is linear between 40 and 120s. We also manually defined the period of linearity for each kidney because in some cases the period of linearity is longer than 120sec. The slopes of straight lines fitted for manual (man) and fixed period (fix) were used to calculate the split renal function. The Patlak procedure was also performed pixelwise and parametric images were produced using the slopes of straight lines fitted from 40-120sec. Then the noise of the image was measured by a ROI between the kidneys. The kidney ROIs were corrected for this noise and then split renal function was calculated (noise). The reference method was the split renal function derived from the posterior view of the background corrected static DMSA scan.

In order to assess the accuracy we determined the deviations of relative left kidney function calculated by the method of interest from function calculated by the reference method. The mean of these differences should be near by zero if there is no systematic deviation. The standard deviation (sd) of these differences corresponds to the accuracy of the methods. A large sd means a poor accuracy and vice versa.

Results: The mean values of the differences are near by zero indicating no systematic deviations from the reference method. The standard deviation of the differences is nearly twice as high in the conventional method compared to all patlak methods. This finding is significant (F-test for different variances). The standard deviation of the Patlak methods do not differ significantly.

	mean	sd	p (Patlak vs con)
con	0.30	4,1	
fix	-0,44	2,29	0,019
noise	-0,33	2,42	0,033
man	-0,11	2,47	0,041

Conclusions: The Patlak methods are more accurate in calculation of split renal function than the conventional („Oberhausen“) method.

PS-498

E. Werner, S.Seybold, C. Blasl, S. Muffert, J. Farahati, Chr. Reiners
Clinic for Nuclearmedizin, University of Würzburg, Germany

PARAMETRIC IMAGING BASED ON THE PATLAKPLOT - AN IMPROVEMENT IN RENAL SCANS WITH 99mTc MAG3 ?

Improvement of the quality of parenchymal imaging with 99mTc MAG3 using the Patlak plot may be useful in detection of local renal dysfunctions like scars. We evaluated the quality of parametric images based on Patlakplot (Gordon et al.) compared to simple sum images in this study.

Methods: We investigated 127 patients (247 kidneys) with 99mTc MAG3 and generated a Patlak plot using time activity curves over the heart and the kidneys. In the period after the perfusion phase (40.s) and the first escape of activity from the kidney (120. s) this plot is linear. In some cases the period of linearity is longer than this interval. Therefore we also defined the period of linearity for each kidney manually (man) and generated the patlakplot pixelwise. Straight lines were fitted for the fixed and the manually defined periods and parametric images were produced using the slopes of these straight lines. These parametric images were compared to the corresponding sum images by two observers with respect to loss of background (back), perceptibility of renal outline (line) and renal pelvis (pel).

Results: The table shows the percent of kidneys evaluated worse, equal or better in the Patlak image than in the corresponding sum image. The background of the Patlak images was lower in >99% of the kidneys compared to the sum images. The perceptibility of the renal outline and the renal pelvis was superior in 83% resp. 56% with fixed fit limits. In contrast to the perceptibility of the renal pelvis the perceptibility of the renal outline was further improved by manually defined fit limits.

N=247	back		line		pel	
	40-120s	man	40-120s	man	40-120s	man
worse [%]	0	0	2,4	2,4	0,8	2,8
equal [%]	0,4	0	7,7	8,1	34,8	44,9
better [%]	99,2	99,6	83,4	87,0	56,3	47,8
equivocal [%]	0,4	0,4	6,5	2,4	8,1	4,4

Conclusion: Parametric images based on the patlak plot improve the quality of parenchymal imaging with 99mTc-MAG3 and therefore they are helpful in the detection of local renal dysfunctions and renal scarring.

References: Gordon, I. Anderson, P.J., Lythgoe M.F., et al (1992): Can Technetium-99m-Mercaptoacetyltriglycin Replace Technetium-99m-Dimercaptosuccinic Acid in the Exclusion of a Focal Renal Defect? J Nucl Med,33:2090-2093

PS-499

I. Wouters, G. Martens, A. Sand, P. Wanet.

van Helmont Ziekenhuis, Departments of Urology and Nuclear Medicine, Vilvoorde, Belgium.

DIFFERENTIATION OF VENOGENIC AND ARTERIOGENIC IMPOTENCE BY RADIOISOTOPIC PENOGRAPHY.

The vascular mechanism of the erection can be either disturbed by arterial insufficiency or by an increased venous outflow. Most of the procedures used to assess the etiology of impotence are invasive. We have used an isotopic non-invasive method to determine the arterial or venous origin of impotence.

We have studied the penile blood flow during pharmacological (Caverject) induced erection in 120 patients. Two different methods have been used to differentiate arteriogenic from venogenic insufficiency :

Method 1 : Dynamic scintigraphy of the penile blood flow was performed using Tc99m labeled erythrocytes. A first study was performed in basal conditions and a second one after injection of 15 µg Caverject into the corpus cavernosum. In both cases several parameters have been calculated from the time activity curve. The half-time to reach the equilibrium (Teq) gives the best evaluation of the importance of the arterial insufficiency.

Method 2 : an injection of 4 Mbq (100 µCi) of pertechnetate into the corpus cavernosum has been performed 15 min. after intracorporeal injection of Caverject. The time activity curve allows the calculation of the wash-out index (Wi) which reflects the severity of the venous leakage.

Among the 120 examined patients, 57 were categorized by the clinician as arteriogenic, 26 as venogenic and 37 as psychogenic. Respective sensitivity and specificity were established by comparison with the other diagnostic modalities. For arterial studies the results show a specificity of 86% and a sensitivity of 74 %. For venous studies the results show a specificity of 86% and a sensitivity of 87 %.

We conclude that radioisotopic penography is a simple and non-invasive technique which allows to differentiate the arterial, venous or psychogenic origin of the impotence. It can also be used for follow-up under treatment. This technique is a good tool to obtain quantitative information concerning the vascularisation of the penis.

General nuclear medicine: Veterinary nuclear medicine

PS-500

L. Balogh, G. Andócs, J. Thuróczy, J. A. Mol, W. van den Brom, Gy. A. Jánoki
National "FJC" Research Institute for Radiobiology and Radiohygiene, Department of Applied Radioisotopes

EVALUATION OF VARIOUS RADIOPHARMACEUTICALS: BINDING PROPERTIES TO A CANINE MAMMARY CELL LINE

Purposes: In vitro assay were carried out to find the best radiopharmaceutical for oncological scintigraphy comparing the maximum cell binding capacity of 99mTc-pertechnetate, 99mTc-MDP, 99mTc-MIBI and 99mTc-DMSA(V) to a canine mammary tumor cell line. The biodistribution of the above radiopharmaceuticals was also studied.

Materials @ Methods: Canine mammary cell line (CMT-8) was incubated together in increasing concentrations of the above four radiopharmaceuticals in their original growing medium (mMEM) in 24-well plates. After 1 hour incubation (37 °C) the mediums were separated cells were washed out two times with sterile physiological saline and the cells were removed (SDS, 15 min.) from the plates. All the collected samples were measured using an automatic gamma counter (Cobra Auto-Gamma, Packard, Canberra Company) and results were evaluated with a dedicated softwer (Radling, McPherson 6.0). Tumor bearing Nude mice were injected by the radiopharmaceuticals and standard bioassay was carried out 2, 4, 6 and 12 hours after the applications. Biodistributions were also scintigraphically imagined and recorded at the same time.

Results: Four parallel incubations were carried out and evaluated in each concentrations of all the different radiopharmaceuticals. We were found very low maximum binding capacities in case of 99mTc-pertechnetate and 99mTc-MDP (Bmax=appr. 6,5 pmol/300 000 cells). In contrast of this 70-100 times higher maximum binding capacities were found in case of 99mTc-MIBI and 99mTc-DMSA(V) however maximum only 1 percent of the added doses were bound to the cell phases. In case of 99mTc-MIBI and 99mTc-DMSA(V) more than 5% of injected dose accumulated in the tumors of Nude mice and in the scintigraphic pictures target/background ratios were between 5-30.

Conclusion: On the base of more than 40 in vitro binding assays 99mTc-MIBI and 99mTc-DMSA(V) seem to be the best choice for oncological scintigraphy. Our in vivo examinations carried out in CMT-8 bearing Nude mice also underline the potential usefulness of these radiopharmaceuticals.

Keywords: 99mTc-MIBI, 99mTc-DMSA(V), CMT-8 bearing Nude mice xenograft

PS-501

R.J.Milner¹, I.C.Dormehl¹, W.K.A.Louw², F.Chaparro³, E.Kilian³

¹University of Pretoria, South Africa, ²Atomic Energy Corporation, Pelindaba, ³Pretoria Biomedical Research Centre

THE BIODISTRIBUTION, PHARMACOKINETICS, BONE LOCALIZATION AND THERAPEUTIC EFFECT OF RHENIUM-188-HEDP IN NORMAL DOGS AND DOGS WITH OSTEOSARCOMA OF THE APPENDICULAR SKELETON.
Rhenium-188(188Re) is a radioisotope derived from a 188Tungsten/188Rhenium generator ($t_{1/2}$ 16.9 hrs, β^- 2.1 MeV, γ 155 keV 15%), penetration in tissue max 11mm average 3.8mm. Rhenium's advantage is its availability as a generator and its strong beta particle in comparison to 153Sm. Elution of the generator provides carrier free 188Re-sodium perrhenate. Technetium labelling techniques can be applied with modification to 188Re-sodium perrhenate due its similar chemical properties. The purpose of the study was to evaluate the biodistribution, pharmacokinetics, bone localization and therapeutic effect of 188Re-HEDP in 4 normal dogs and dogs with osteosarcoma of the appendicular skeleton. General anaesthesia was used in all dogs and maintained by intravenous administration of pentobarbitone sodium. Scintigraphy was done using a Siemens Orbiter gamma camera with low energy collimator. An energy window set at 155keV(15%). Data acquisition was performed as a dynamic study of 60 x 1 min frames on a count down bolus injection of 148-259 MBq 188Re-HEDP with views of the thorax and abdomen. Statics images (64x64 word mode) of 2 min duration were done at 2, 3, 4 hours after tracer injection. Blood (heparin) and urine samples were collected. Four dogs with osteosarcomas underwent dynamic studies followed by therapeutic doses of 188Re-HEDP at 37 MBq/kg. Blood samples were collected at weekly intervals. Two dogs received repeated weekly therapeutic doses (37MBq/kg) of 188Re-HEDP for 4 weeks. Haematological parameters remained within the normal range for all dogs receiving a single therapeutic dose and for those receiving multiple doses. Dogs receiving multiple therapeutic doses showed significant slowing of tumour growth and pain control but relapsed within 2 months. The uptake ratio between tumour and normal bone (contra-lateral site) varied between 1.44:1 to 4.5:1, this is less than for 99mTc-MDP or 153Sm-EDTMP. Time activity curves for normal dogs show an average of 6% renal excretion within 4 hours and blood clearance $t_{1/2}$ <3 min. Between 9% and 13% retention of the diagnostic dose was present at 3 hours within the tumours. No differences in time activity curves were seen between abnormal and normal dogs except in dogs where reduced renal function was evident. In conclusion, while a single dose of 188Re-HEDP appears to have little effect, when given in repeated doses, 188Re-HEDP appears to have promise as a therapeutic bone targeting agent due to its effect on tumour growth, as well low bone marrow toxicity.

General nuclear medicine: Miscellaneous

PS-502

Z.Celen, E. Özbay, S. Zincirkeser, Y. Beyazıt, S. Mumcu

Hospital : University of Gaziantep, Department of Nuclear Medicine

SCINTIGRAPHIC EVALUATION OF THE EUSTACHIAN TUBE FUNCTIONS

Eustachian tube (ET) dysfunction is one of the most important factors in the etiology of middle ear disease. There are several methods such as Politzer, Tonybee, valsalva and inflation-deflation tests to assess the functions of ET. However, these methods evaluate only anatomic patency of tube but they do not evaluate one of the most important functions of the ET, drainage function. For this reason, we used a scintigraphic method on 42 patients 32 of whom had otitis media with effusion (study group) and 10 of whom had traumatic perforation of the ear drum (control group) respectively. After instilling 100 μ Ci (100 μ l) Technetium-99m-macroaggregated albumin (Tc-99m-MAA) into the middle ear, 60 images were taken at 15 second intervals. Both groups were investigated to see whether there was radioactivity passage through ET and, mean arrival time of the radioactivity to ET (RTE : reach time to ET) and to nasopharynx (RTN : reach time to nasopharynx) were calculated using a computer if the passage occurred. The mean RTE value was 1.55 \pm 0.88 min. in control group and 1.7 \pm 1.85 min. for passage occurred patients in the study group. The mean RTN was 2.17 \pm 0.94 min. in the control group and 2.45 \pm 2.55 minute in the study group. Radioactivity passage rates in the study and control groups were 5 (16 %) and 10 (100 %) , respectively. The difference between both groups was very significant (p<0.001).

In conclusion, we believe that the scintigraphic method is a safe, noninvasive, easy and fast method and, it can be used for the assessment of the ET function. Furthermore, this method in conjunction with the other conventional tests can be utilized for the follow up of patients with otitis media with effusion as well as for the selection of the patients who are candidate to tympanoplasty.

PS-503

T. Nikula¹, K. Väänänen², I. Jokinen², J. Riski³, T. Takala³, T. Parviainen⁴, R. Pakkanen⁵ and A. Mero³

¹ MAP Medical Technologies Oy, Tikkakoski, Finland; ² Department of Biological and Environmental Science, University of Jyväskylä, Finland; ³ Department of Biology of Physical Activity, University of Jyväskylä, Finland; ⁴ Department of Clinical Physiology, Central Hospital of Central Finland, Jyväskylä, Finland; ⁵ Nutricia Ltd, Turku, Finland

ABSORPTION OF ORALLY ADMINISTERED rhIGF-1 IN HUMAN SUBJECTS: A PILOT STUDY

The most prominent growth factors in bovine colostrum are insulin-like growth factors (IGF-1 and IGF-2). IGF-1 is the major growth factor in bovine colostrum. Six structurally related IGF binding proteins are known in humans. The biological activity of IGF-1 is supposed to be regulated by these binding proteins and mediated via IGF-receptor molecules, which have been found in bovine mammary tissues and epithelial cells. Orally administered IGF-1 is known to induce gut growth in test animals. However, little is known about the effects of orally administered colostrum fractions or purified growth factors on human subjects.

For in vivo experiments recombinant human IGF-1 was labelled with ¹²⁵I. Each batch of rhIGF-1 labelled with ¹²⁵I was tested for its biological functionality using a modified human placental receptor assay. Two volunteer human subjects took orally 50 MBq ¹²⁵I-IGF-1. Blood samples were taken at different time points (0-7h) to determine the radioactivity in plasma after ingestion.

The proteins were precipitated with TCA and the radioactivity of the total samples and TCA precipitates were measured in gamma counter. The result showed that 35-50% of the radioactivity precipitated with TCA. Plasma samples were fractionated in gel filtration columns to determine the molecular sizes of the radioactivity components. Only 5-6% of radioactivity was found in fractions containing proteins of molecular weight 40-100 kDa. Most of the radioactive material eluted with lower molecular weight components (MW<5 kDa).

As far as we know, our study is the first effort to investigate the absorption of orally administered IGF-1 in human subjects in more detail. A significant portion of IGF-1 was observed in jejunal part of the gut as shown on the gamma camera image, but label was also detected in the TCA-precipitates of blood plasma. Most of the labelled IGF-1 in blood was obviously fragmented, but a minor portion of it may be intact and associated with its binding proteins.

PS-504

C.G.Zhang, S.J.Han, J.Z.Liu, G.Hu, S.J.Li, X.F.Li, H.Gang and J. Wang.

¹ Hospital, Shanxi Medical University, Department of Nuclear Medicine, Taiyuan, P.R.China.

THE VALUE OF NUCLEAR MEDICINE IMAGING TO THE DEPARTMENT OF EMERGENCY

In the past 3 years the Department of Nuclear Medicine(NM) has provided urgent imaging to 105 patients(pts) from the Emergency Department(ED). This study is to evaluate the clinical value of NM procedures to this group of pts..The pts can be divided into 4 main groups. Group A(GA) consisted of pts admitted with chest pain and had myocardial perfusion imaging. There were 78pts, 66 male and 12 female, average age of 58 years ranging from 32 to 85. The standard static myocardial SPECT was performed with Tc-99m-sestamibi(925MBq) and images were acquired after a delay of 90-120 min. The results were made available to the treating physicians immediately. Group B(GB) was pts with signs and symptoms of cerebral vascular accident, but negative CT. There were 5 pts, 3 males and 2 females, with average age of 56 years ranging from 48 to 65. Brain SPECT was performed with Tc-99m-ECD(1110MBq) and images obtained after a delay of 30 min. Group C(GC) was pts with gastrointestinal bleeding(GIB) from unknown site. The 15 pts, 8males and 7 females, with average age of 47 years ranging from 7 to 79 had GI imaging. This was performed with in-vivo labeled Tc-99m-RBC(925 MBq). Group D(GD) were pts with acute peripheral vascular occlusive diseases. There were 7 pts , 3 males and 4 females with average age of 59 years ranging from 46 to 76 . Arterial imaging was performed with Tc-99m-RBC(370 MBq) and venous imaging with Tc-99m-MAA(370MBq) . The results were listed in the table below.

Group No.	Clinical Diagnosis.	Imaging Results.	Final Diagnosis.	Treatment
A 78	AMI	+(74) -(4)	AMI(74) Non-AMI(4)	Thrombolysis or other Discharged
B 5	CVA with(-)CT	+(5)	Brain infarct(5)	Thrombolysis or other
C 15	GI	+(6) -(9)	GI(6) GI(9)	Surgery or conservative Surgery or conservative
D 7	Peripheral vascular occlusive disease	+(7)	Arterial embolism(4) Deep vein thrombosis(3)	Surgery Conservative

The above study demonstrates that nuclear medicine procedures can play an important role in the management of some of the pts that come to the ED. Myocardial imaging identifies the non Q wave infarction and give the pts the benefit of thrombolytic therapy. A negative study in the right clinical situation would also give the clinician the confidence to discharge the pts. Brain scan is of great clinical value in identifying brain infarction with negative CT and assist clinician in deciding whether to use thrombolytic therapy. Bleeding from the lower GI tract can be difficult to identify the site. With GIB imaging the site of hemorrhage can usually be located during the active stage and the findings will assist the surgeon in.

Poster presentations

Endocrinology/Thyroid

PS-505

L. Adalet, P. Demirkale, S. Ünal, H. Oğuz, F. Alagöl, S. Cantez

University of Istanbul Faculty of Medicine Department of Nuclear Medicine, Istanbul Turkey

POOR RESULTS WITH Tc-99m TETROFOSMIN IN THE DETECTION OF MEDULLARY THYROID CARCINOMA METASTASES. COMPARISON WITH Tc-99m VDMISA

The aim of this prospective study was to assess the detectability of metastatic lesions by Tc-99m Tetrofosmin (Tetro) in medullary thyroid carcinoma (MTC) and to compare the results with Tc-99m VDMISA (VDMISA). We investigated 24 patients (10 M, 14 F, ages ranging from 23 to 76 yrs) with MTC following total thyroidectomy. Five of the cases were sporadic and 19 were familial. After the injection of 740 Mbq of Tetro and 740 Mbq VDMISA whole body scans and 5 minute static images of the head, neck, chest, abdomen and pelvis were obtained. All scintigraphic studies were compared to calcitonin levels, radiologic findings, histopathologic results and clinical follow up. 34 metastatic sites were detected in 12 patients. The results were as follows:

Metastatic sites	VDMISA		TETRO	
	Lesion	Sensitivity %	Lesion	Sensitivity %
LAP (16)	16/16	100	11/16	69
Soft tissue (4)	4/4	100	2/4	50
Lung (4)	4/4	100	4/4	100
Liver (3)	3/3	100	3/3	100
Bone (7)	3/7	43	2/7	29
Total (34)	30/4	88	22/34	65

Our results showed that VDMISA appears to be superior to Tetro in detecting MTC metastases.

PS-506

F. Alam, M.I. Hossain, F. Moslem, M.A. Karim.

Institute of Nuclear Medicine. BAEC. Block-A, IPGMR Hospital, Sahabag. Dhaka, Bangladesh.

EFFECT OF UNIVERSAL IODINATION OF COMMON SALT ON THE IODINE-131 UPTAKE OF THYROID GLAND IN BANGLADESH.

Bangladesh is a country of hyper-endemic goiter zone as well as iodine deficiency disorder. I-131 uptake test is still used here as one of the main investigation for evaluation of thyroid disorder. Iodination of common salt started for about 12 years. Before universal iodination of cooking and table salt (common salt) normal reference range of I-131 uptake was very high. The aim of this study is to evaluate present iodine-131 uptake status after iodination of common salt.

This was a prospective study started in December of 1995 and ended in August 1997. In this study 402 volunteers were selected, of them 228 (56.7%) were male and 174 (43.3%) were female. Volunteers were from both urban rural areas. The ages of the volunteers were between 10 to 45 years. All the volunteers were clinically and biochemically euthyroid. Volunteers having iodine containing drugs or iodine containing traditional medicines were excluded. About 5 micro curie to 15 micro curie I-131 was administered orally. After 2 and 24 hours of administration of I-131, uptake was taken with gamma counter in the thyroid and mid thigh region. Then uptake percentage was calculated in standard procedure. Serum T₃, T₄ were estimated by RI A and TSH were estimated by IRMA.

The 2 hour's uptake was found in the range between 1% to 14% with mean 4.08% and standard deviation $\pm 2.45\%$. The 24 hour's uptake was found in the range between 3% to 31% with mean 9.86% and standard deviation $\pm 5.37\%$. Before universal iodination of common salt normal reference range of I-131 uptake was 5% to 15% in 2 hours and 15% to 40% in 24 hours, which is much higher than present uptake percentage.

It is observed that the uptake percentage has certainly been reduced considerably after universal iodination of common salt, which may indicate that the iodination program is going nicely and mass people are using iodized salt satisfactorily.

PS-507

T. Athanasoulis, Ch. Kalliontzi, N. Sifakis, E. Papadaki, L. Karaloizos, S. Gerali

Dept of Nuclear Medicine, «Alexandra» University Hospital, Athens, Greece

ROLE OF TC99m-SESTAMIBI SCINTIGRAPHY IN THE INITIAL PRESURGICAL LOCALIZATION OF HYPERFUNCTIONAL PARATHYROID GLANDS

Initial pre-surgical imaging of pts with hyperparathyroidism (HPT) is considered to be unnecessary because of high probability of cure by the first surgery. However two of the most possible reasons of initial surgical failure are considered to be the small size of hyperfunctional parathyroid glands (HPG) or/and its ectopic position. In order to investigate the role of the Tc99m-sestamibi parathyroid scintigraphy (MIBI-SC) in detecting HPG before the initial surgery, two groups of patients with HPT were examined retrospectively selected from over than 100 MIBI-SCs. In the first group were included 14 pts whose initial interpretation of MIBI-SC was false negative in eight cases and false positive in six cases due to thyroid disorders. In the second group were included 10 pts whose the initial surgery failed without having any pre-surgical imaging exploration. The initial surgery was successful for all pts of the first group and revealed 9 cases with a single adenoma and 5 cases of hyperplasias all, except one, found in a normal position. All HPG of this group had a weight less than 300 mg. MIBI-SC was positive in 8/10 pts of the second group (6 in an ectopic cervical or cervico-mediastinal position) that was confirmed in a second surgery (8 adenomas). These results indicate that initial negative MIBI-SC due to small HPG which are found close to thyroid gland, do not predict surgical failure, while detection of HPG in an ectopic position, often large in size, should be very useful in some pts in order to avoid a second surgery. This implies that keeping a high specificity of MIBI-SC despite some loss of sensitivity, would be more helpful to an experimented surgeon resulting in a higher probability of treatment of HPT by the initial surgery.

PS-508

C S Bal, A K Padhy, P G Nair,

All India Institute of Medical Sciences, Department of Nuclear Medicine, New Delhi, India.

LONG-TERM FOLLOW-UP RESULTS OF I-131 TREATMENT OF RECURRENT HYPERTHYROIDISM PREVIOUSLY TREATED BY SUBTOTAL THYROIDECTOMY.

In patients with recurrent hyperthyroidism following previous subtotal thyroidectomy for Graves' disease or toxic MNG, radioiodine therapy is often recommended. However, our knowledge of the long-term effect of I-131 in this subset of patient is limited. We want to share our experience in this regard. 47 patients presented with post surgery recurrence at thyroid clinic of Nuclear Medicine Department from 1972 to 1996. Mean age of patients at presentation was 43 years (range 23-67 years), 10 were males and 28 had Graves' and rest toxic MNG. Time of recurrence following surgery varied widely from 6 months to 32 years, 21% recurrent within a year and 75% before tenth year. However, 15% recurred beyond 20 years. 11 patients (23.4%) were aged more than 50 years at the time of recurrence. 34 patients (72%) needed single dose of I-131 (mean dose 288 MBq and range 107-740 MBq) and remaining 13 patients multiple doses of I-131 to be free of thyrotoxicosis (7 patients: 2 doses, 3 patients: 3 doses, 2 patients: 4 doses and the last one 5 doses). 38 patients required ≤ 370 MBq for this purpose. One individual needed maximum of 1480 MBq in divided doses to be euthyroid. The maximum duration of follow-up was 26 years with mean follow-up of 10 years. 5 patients were lost to follow-up after their I-131 therapy. The end point considered as confirmed hypothyroidism or euthyroidism in the last visit. 26 patients (62%) were euthyroid and 16 were hypothyroid (38%) after 10 years of mean follow-up period. However, hypothyroidism at the end of 1 year was in 11 patients (26%). Comparing 88 age, sex, type of gland, time of I-131 treatment and RAIU matched non-operated thyrotoxic patients revealed hypothyroidism rate at first year was 9% and cumulative hypothyroidism after 9.8 years of follow-up (ranging 1-26 years) 36%. This study reveals 15% of patients recur even after 20 years, indicating life-long follow-up after thyroidectomy. The I-131 treatment in these patients shows high initial hypothyroidism rate (26% Vs 9%, $p < 0.01$), meaning close watch in first year. However, the cumulative hypothyroidism was same as non-operated patients, the long-term follow-up protocol may be as usual.

PS-509

T. Watanabe, C.A. Buchpiguel, M. Sapienza, P. Costa, M.I.C.C. Guimarães, F.H. Hironaka
Center of Nuclear Medicine São Paulo University Medical School (LIM-43), Brazil.

PRIMARY HYPERPARATHYROIDISM SCINTIGRAPHIC DIAGNOSIS - A COMPARATIVE STUDY BETWEEN THALLIUM-201 AND SESTAMIBI-TC-99M.

Scintigraphy has been established as an accurate method for localizing parathyroid adenomas. However, there are few studies comparing thallium-technetium subtraction with double-phase sestamibi techniques.

The purpose of this study was to evaluate retrospectively the preoperative ability of these two scintigraphic techniques in the detection and localization of hyperfunctioning parathyroids in patients with primary hyperparathyroidism who underwent to surgery. Twenty five patients were studied, 13 with double-phase sestamibi technique (group 1) and 12 with thallium-technetium subtraction technique (group 2). The scintigraphic results were compared to surgical findings.

The group 1 at surgery showed 14 abnormal and 37 normal glands (total = 51 glands). At scintigraphy, 13 out of 14 abnormal glands were found in this group (one double adenoma and 11 solitary adenomas). In the another group, surgery identified 45 glands, 13 abnormal and 32 normal glands, and only 9 out of 13 abnormal glands were correctly localized at scintigraphy (one carcinoma, one double adenoma and 6 solitary adenomas). The sensitivity, specificity, positive and negative predictive values of scintigraphy on group 1 and group 2 were respectively: 92.9%, 100.0%, 100%, 97.4%; 69.2%, 87.5%, 69.2%, 87.5%. Even though the difference in sensitivity was not statistically significant, the double-phase technique was more specific and provided better quality images with lower radiation exposure than thallium-technetium subtraction test and is more available at the most of nuclear medicine laboratories.

PS-510

J. Damilakis¹, N. Karkavitsas², K. Perisnakis¹, G. Kontakis³, E. Vagios⁴, N. Gourtsoyiannis⁴
Departments of ¹Medical Physics, ²Nuclear Medicine, ³Orthopaedics, and ⁴Radiology, University of Crete, 711 10 Greece

EFFECT OF LIFETIME OCCUPATIONAL PHYSICAL ACTIVITY ON SKELETAL STATUS

The purpose of this study was to examine the effect of lifetime occupational physical activity on skeletal status using dual energy X-ray absorptiometry (DXA) and two ultrasonic indices of bone. Seventy one healthy postmenopausal women aged 42-61 years who worked professionally at farms since the age of 18 or earlier were compared with 78 age matched sedentary female subjects (control group). Broadband ultrasound attenuation (BUA) and speed of sound (SOS) at the calcaneus were measured using an ultrasound transmission imaging system (Ubis 3000, DMS). Differences in BUA, SOS and bone mineral density (BMD) between farmers and controls were expressed relative to standard deviation (SD) of the farmers. Farmers had significantly higher BMD values than controls (difference = 1.3 SD in the spine and 1.5 SD in the femoral neck, p<0.0001 for both comparisons). Ultrasound variables were significantly higher in the farmers compared with the controls in calcaneus (difference = 1.1 SD for BUA and 0.7 SD for SOS, p<0.0001 for both comparisons). Postmenopausal status was associated with the same rate of bone loss for farmers and controls. These results suggest that lifetime physical activity has a positive effect on bone status of postmenopausal farmers.

PS-511

N. Erçakmak, E. Özalp, G. Vural, S. Aslan, B. Turgut

Ankara Oncology Hospital, Department of Nuclear Medicine, Ankara/TÜRKIYE

POST-THERAPY I-131 WHOLE BODY SCAN IN PATIENTS WITH WELL-DIFFERENTIATED THYROID CARCINOMA: A COMPARATIVE STUDY

The aim of this study was to evaluate the value of post-therapy scan in patients (pts) with well-differentiated thyroid carcinoma (DTC), who had suspicious pathologic findings. A group of 52 pts (38 F, 14 M, mean age 45.3, range: 16-48 yrs) consisting of 31 papillary, 15 follicular, 5 mixed papillary-follicular and 1 hurthle cell carcinoma, was included to this study. All pts had been assessed with clinical, radiological, I-131 whole body scan and laboratory (serum thyroglobulin-Tg, antithyroglobulin antibodies-TgAb) findings and finally compared with post-therapy scans (72 hours after therapy doses of 100 to 300 mCi). In comparison with diagnostic scans, new or additional sites (11 lung, 6 neck, 1 bone) of iodine accumulation were observed on post-therapy scans in 14 pts (27%), additional foci in the previously existing region were observed in 11 pts (21%), no difference was found in 27 pts (52%). Out of 11 pts with lung metastases diagnosed by post-therapy scan, 6 were radiologically positive, while 5 were negative. All, but two with high TgAb levels, had high Tg levels. No accumulation was observed on post-therapy scans in 5 pts with high Tg levels, who were radiologically interpreted as lung metastases. Our findings show that the post-therapy scan is of great value in detecting occult metastases especially in the lung. We concluded that post-therapy scan should be performed in follow up and therapy planning pts with suspected metastases of DTC.

PS-512

G. Förster, F. Krummenauer*, J. Andreas, G. Kahaly**
Departments of Nuclear Medicine, *Medical Statistics and **Endocrinology/Metabolism, Johannes Gutenberg-University Hospital, Mainz, Germany

INDIVIDUALLY DOSED LEVOTHYROXINE AND 150 µg IODIDE VERSUS 100 µg LEVOTHYROXINE COMBINED WITH 100 µg IODIDE: a randomised, double-blind study

Aim: The main pathomechanisms leading to goitre are intrathyroidal iodine deficiency and influence of TSH. Treatment with levothyroxine for suppression of pituitary TSH secretion and supplementary iodine have a synergistic effect in reducing goitre size. Aim of this study was to compare a fixed combination therapy of levothyroxine and iodide with an individually adjusted amount of levothyroxine with iodide.

Patients and Methods: In a double-blind study-design, 49 patients (24 female, aged 20 - 43 years) with an euthyroid diffuse goitre were randomly treated for 12 weeks either with an individually weight-adapted dosed levothyroxine (75, 100, or 125 µg) and 150 µg iodide (group A) or with a fixed combination of 100 µg levothyroxine and 100 µg iodide (group B). TSH levels, thyroid related hormones, urinary iodine excretion, thyroid volume, and hyperthyroid-score were registered.

Results: Baseline TSH decreased in both groups (p < 0.0001) without significant differences (median of relative difference: group A 78.1%; group B 52.8%). Thyroid volume decreased in both groups (p < 0.0001), independent of the treatment form (median of relative decrease: group A 37.6%; group B 30.9%; n. s.). Urinary iodine excretion increased in both groups (group A 107%; group B 49%). The hyperthyroidism-score did not change and side effects were not noted during therapy.

Conclusion: With respect to therapy of euthyroid endemic goitre, both concepts showed an equal efficacy and tolerance.

PS-513

G. Förster, F. Krummenauer*, S. Both, J. Andreas, G. Kahaly**

Departments of Nuclear Medicine,
*Medical Statistics and **Endocrinology/Metabolism,
Johannes Gutenberg-University Hospital, Mainz, Germany

REPRODUCIBILITY OF SOMATOSTATIN-RECEPTOR SCINTIGRAPHY IN PATIENTS WITH THYROID EYE DISEASE (TED)

Objective: Somatostatin-receptor scintigraphy using the single photon emission computed tomography (SPECT) technique allows the assessment of orbital inflammation in patients with TED. In this study, analysis of reproducibility in the evaluation of orbital SPECT images was done.

Material and Methods: SPECT data of 8 patients with TED were obtained 4 hr after intravenous injection of 110 MBq In-111 pentetreotide. Optimal transversal SPECT images were reconstructed (filtered back projection, post-best filter) and regions of interest for both orbits were defined 3 to 4 times by four independent observers. Results were expressed as counts/voxel and statistically analyzed as intra-observer, intra-class, and inter-observer reliability.

Results: The intra-observer reliability for both orbits was 87.5% (observer 1), 88.5% (observer 2), 97% (observer 3) and 97.5% (observer 4). For each observer, a mean value of 3 - 4 reconstruction for each patient was calculated. With respect to the patients scatter, reproducibility of the observers was 94%. Two replications were sufficient to reach an inter-class reliability of at least 90% (Spearman-Brown reliability). Furthermore, inter-observer reliability (comparison between one observer to the other three) was 84%.

Conclusions: With respect to the variable intra-observer reliability, an experienced and trained investigator, as routinely done in our department, is necessary for evaluation of orbital SPECT images, leading to representative and comparable data. The low inter-observer reliability is caused by a deviation in trend. High inter-class reproducibility with two replications only, allows an accurate differentiation of radionuclide activity in the orbits of patients with TED.

PS-514

Z.R. Gao, Y.X. Zhang, H. Zhan

Department of Nuclear Medicine, Union Hospital, Tongji Medical University, Wuhan, P.R. China

CLINICAL EVALUATION OF QUANTITATIVE ANALYSIS IN I-131 MIBG ADRENAL SCINTIGRAPHY

In order to define a quantitative diagnostic standard in I-131 MIBG adrenal scintigraphy, the adrenal uptakes in control group(group1), patients with pheochromocytoma(group2) and patients with adrenal medulla hyperplasia (group3) were analyzed quantitatively.

There were 25 patients in group1 (mean age 41yrs), 7 patients in group2 (37yrs) and 21 patients in group3 (38yrs) in this study. Whole body scintigraphys in anterior and posterior views were performed at 24, 48 and 72 hrs after i.v. injection of 74MBq I-131 MIBG in all patients. ROIs were drawn over the adrenal, heart, lung, liver, spleen and background, and the ratios of adrenal/ heart, lung, liver, spleen or background were calculated in different time, respectively.

The results suggested that the ratios, except the ratio of adrenal/spleen, can effectively make identification between group1 and group2 or group3 ($p < 0.05$). But the ratios of adrenal/heart and adrenal/background were more stable and sensitive than the ratios of adrenal/lung and adrenal/liver ($p < 0.01$). Furthermore, different background ROIs were of different identifying significances and the ROI beside left adrenal was the most satisfactory selection. The ratio of adrenal/heart was also an important identifying parameter between pheochromocytoma and adrenal medulla hyperplasia, and the cut-off levels of the ratio were 1.5(24hr), 1.5(48hr) and 1.8(72hr), respectively. Visualization of heart activity on MIBG scintigraphy, especially in delayed images (48, 72hrs), could be a useful clue to the exclusion of diagnosis of pheochromocytoma. There was no significant correlation between the ratios and age, sex, blood pressure, course of disease or catecholamine/ vanillylmandelic acid in blood/urine. We conclude that quantitative analysis of I-131 MIBG adrenal scintigraphy is an objective and sensitive method for diagnosing pheochromocytoma.

PS-515

P. González, M.J. Jofré, T. Massardo, A. Zavala

Nuclear Medicine Center, University of Chile Clinical Hospital

OPTIMAL IMAGING TIME FOR DELAYED IMAGES IN THE DIAGNOSIS OF ABNORMAL PARATHYROID TISSUE WITH SESTAMIBI Tc-99m

Double phase scintigraphy with Sestamibi Tc-99m is excellent for detecting hyperfunctioning parathyroid tissue. In order to assess the best time for delayed images (2 h versus 4 h) we studied 56 patients, 35 with primary hyperparathyroidism; mean age was 53±13 y.o. and 54% females. Cervical ultrasonography was performed on 29/56 (52%) patients and surgery in 16/56 (29%). The dose was 740 MBq i.v. and the acquisition was performed at 10 min, 2 h and 4 h using anterior views including mediastinum. There were 19/56 (34%) negative studies and 37/56 (66%) positive, 25 of them with 1 focus and 12 with ≥ 2 parathyroid foci. Positive studies were analyzed blindly by 2 independent observers, selecting the best definition for abnormal activity.

In the analysis we found 76% agreement between observers (the rest was classified by consensus). In 70% of the cases the best delayed image was at 2 h, in 16% was at 4 h ($p < 0.00001$) and in 14% both images were similar. In those cases with better images at 4 h, 2 h images also demonstrated the lesions. There were 2 cases whose lesions were seen only at 2 h. Our results could be explained by tracer decay and/or washout of parathyroid activity.

We conclude that the best protocol should include the early 10 min. image and the 2 h delayed one. Further controls do not appear necessary. This may be important for patient's throughput.

PS-516

R. Gorges^{1,2}, M. Engelbach³, S. Heerdt³, K. Diefenbach¹, W. Grimm¹, A. Bockisch²

Kliniken für ^{1,2}Nuklearmedizin und ³Endokrinologie.

Universitätskliniken ^{1,3}Mainz und ²Essen. Germany.

NEW ASPECTS IN THE FOLLOW-UP OF MEDULLARY THYROID CANCER PATIENTS BY SUPRASENSITIVE CALCITONIN MEASUREMENT.

Since suprasensitive assays for specific measurement of the monomeric form of calcitonin are available, occasionally measurable calcitonin levels are noticed in postoperative care although the patient has been classified as "cured" from medullary carcinoma. Until now, it is unknown whether this must be interpreted as relapse resp. persistence of the medullary carcinoma or as possibly physiological, extrathyroidal secretion (e.g., from neuroendocrine C-cells of the gastro-intestinal tract). We studied this issue by measuring calcitonin levels in healthy subjects as well as in thyroidectomized patients with and without medullary carcinoma with 2 suprasensitive assays (ILMA from Nichols Institute Diagnostics and IRMA from Medgenix; lower detection limit 0.35 resp. 2.4 pg/ml).

Patients. n = 208 patients undergoing thyroidectomy histologically classified as non-medullary (papillary, follicular, or Hürthle cell) thyroid cancer; n = 24 thyroidectomized patients having histologically proven medullary thyroid carcinoma; n = 95 subjects without thyroidal disease (non-thyroidectomized). **Results.** In the non-thyroidectomized healthy subjects, calcitonin levels ranged from <0.35 to 11.5 pg/ml (mean: 3.0 resp. 3.5 pg/ml in men resp. women). In 207/208 of the thyroidectomized patients with proven papillary, follicular, or Hürthle cell thyroid cancer, the calcitonin levels were below the detection limit. This only patient with demonstrable calcitonin values had been undergone repeated surgery because of a papillary thyroid cancer and a squamous cell carcinoma of the floor of the mouth, as well. By means of immunohistochemistry we were able to demonstrate that only the latter tumor was responsible for the calcitonin secretion. 11/24 of the thyroidectomized patients with medullary thyroid carcinoma showed demonstrable calcitonin levels. 3 of these had only values being slightly above the detection limit (within the normal range of non-thyroidectomized healthy subjects) and were formerly classified as "cured" (with the old, less sensitive assay).

Conclusions. In patients with medullary carcinoma undergoing thyroidectomy, calcitonin levels even just above the lower detection limit are highly suspicious for persistent or recurrent thyroidal C-cell tissue. A measurable, physiological calcitonin secretion from extrathyroidal origin is negligible. In seldom cases, other tumors can cause elevated calcitonin levels (e.g. squamous cell carcinoma of the floor of the mouth).

PS-517

L.J. Hahn, R. Kloiber, N. Veldhoen, F. Amoozegar
Foothills Hospital, Div. of Nuclear Medicine, Calgary, AB, Canada

A COMPARISON OF TWO METHODS USED FOR I-131 UPTAKE EVALUATION IN METASTASES IN THYROID CARCINOMA

Quantification of I-131 uptake in metastases from thyroid carcinomas is essential for appropriate patient selection and therapy dose calculations. Measurement of activity in opposing projections and tissue attenuation from a transmission scan has been considered the method of choice (M.J. Meyers et al., Br.J.Radiol., 1981, 54, p.1062). The technique is cumbersome because it uses external high activity flood source and needs regular gamma camera efficiency calibration. We have used the Co-57 sheet source. The second method which can be used is based on measurements of the reference standard under tissue equivalent absorbers to simulate soft tissue thicknesses measured from anatomical imaging studies. This method is convenient and safe to patients but requires additional measurements of the reference standard and knowledge of tissue thicknesses. To evaluate and to compare both methods the set of acrylic blocks 5cm, 10cm, 15cm, and 20cm thick and Rondo Humanoid Phantom with and without adipose overlay have been used. Different activity sources from 185 kBq up to 2.8MBq simulating the metastases have been used.

Results: Phantom studies have shown that both the transmission and reference source techniques are equivalent within the error limits and can be used interchangeably. The evaluated activities were within 11% of their assayed values for different simulated tissue thickness and for both methods. Preferred method used in our lab is reference standard as safer and more convenient for the patient.

PS-518

E. Hindié, P. Jeanguillaume, JM. Berthelot, V. Menoyo, D. Chiappini-Briffa, F. Chéhadé, H. Boulahdour, I. Hallaj, P. Galle, P. Urena

Mondor Hospital: University Paris XII, Department of Nuclear Medicine

SECONDARY HYPERPARATHYROIDISM: UTILITY OF SCANNING

Persistence or recurrence occur in 10 to 30% of uremic patients operated for secondary hyperparathyroidism. We investigated the possible usefulness of preoperative parathyroid 99m-Tc-Sestamibi / 123-I subtraction scintigraphy.

Eleven patients with severe secondary hyperparathyroidism were prospectively imaged and operated. Ten patients were undergoing hemodialysis therapy (mean duration 8.7 years) and one had benefited from a renal transplant. Parathyroid scanning was based on simultaneous double-window recording of 99m-Tc-Sestamibi and 123-I. Plasma intact PTH (iPTH) levels were available for all patients before and 6 months after subtotal parathyroidectomy.

Preoperative scanning pointed to 42 hot spots suggesting enlarged parathyroid glands. The intensity of 99m-Tc-Sestamibi uptake by parathyroid glands was arbitrarily defined as high, intermediate or low.

The parathyroidectomy was considered as successful in ten out of eleven patients. One of them, had a supernumerary parathyroid gland which was detected by scanning and resected from the left thymus. In another patient, the scan revealed a parathyroid gland in the upper mediastinum, which was excised through the neck incision. In one patient, the parathyroidectomy failed. Preoperative scanning was suggestive of the presence of five enlarged parathyroids. The surgeon disclosed only the 4 glands in normal position. Six months later, this patient showed a persistent hyperparathyroidism with plasma iPTH concentration of 527 ng/L, (normal value 10 - 58 ng/L). A second scan confirmed that a supernumerary parathyroid gland, at the middle of the right thyroid lobe, was missed by the surgery. No false positive images were documented in this series and, when limiting the analysis to parathyroid glands disclosed at surgery, the sensitivity of preoperative imaging was of 91% (41/45).

Subtraction scanning based on the simultaneous recording of 99m-Tc-Sestamibi and 123-I improves the imaging of enlarged parathyroid glands in secondary hyperparathyroidism. The technique was efficient in recognizing both ectopy and supernumerary parathyroid glands and should be, therefore, of critical assistance to the surgeon.

PS-519

D.M. Howarth, L. Lan, M. Epstein, L.W. Allen, P.A. Thomas.
Department of Nuclear Medicine John Hunter Hospital, Newcastle, NSW Australia.

OPTIMIZED TREATMENT STRATEGIES OF I-131 THERAPY IN GRAVES' DISEASE.

The use of empirical radioiodine therapy to treat Graves' disease may result in a high rate of hypothyroidism but may also achieve rapid and effective treatment of thyrotoxicosis. The aim of this study was to determine an optimal treatment regimen by comparing the clinical and biochemical outcome of patients with Graves' disease treated with empirical doses of radioiodine (Group A) to those treated with specified tissue doses (Group B). Patients were investigated by clinical assessment, biochemistry, immunology, technetium-99m thyroid scintigraphy and, in the case of Group B, by 24 hour I-131 uptake measurement and thyroid ultrasound. Group B patients (n=28) were randomized to receive either 60 Gy or 90 Gy thyroid tissue doses. Group A patients (n=28) received empirical treatment with I-131 doses ranging from 222MBq (6 mCi) to 2.2 GBq (60 mCi). All 56 patients were followed between 7 and 84 months (median = 16 months). Outcome was determined clinically and biochemically. Sixty one percent of Group A patients became hypothyroid in the follow-up period, compared to 13% from Group B. The median time to hypothyroidism was 28 weeks. Fourteen percent of Group A patients remained hyperthyroid six months after radioiodine compared to 47% from Group B. At six months after radioiodine therapy, a euthyroid state was achieved in 11 percent of Group A patients compared to 40 percent from Group B. In Group B significantly more patients who received a 90 Gy thyroid dose became hypothyroid compared to those who received 60 Gy (p<0.05), and significantly more patients who received 60 Gy remained hyperthyroid compared to those who received 90 Gy (p<0.05). It is concluded that better control of thyroid status can be achieved by specified tissue dose calculation but empirical radioiodine offers an effective treatment option where rapid control of hyperthyroidism is required and long term hypothyroidism is a recognized outcome trade-off.

PS-520

D. Huglo, V. Beauchat, A. Delcourt, F. Pattou, M. Lecomte-Houcke, B. Carnaille, C. Proye, X. Marchandise, M. Steinling
Nuclear Medicine, Anatomopathology and Endocrine Surgery Hospital C. Huriez - C.H.R.U. of Lille, 59037 Lille cedex - France

PARATHYROID SCINTIGRAPHY IN SECONDARY HYPERPARATHYROIDISM

The aim of this study was to evaluate the parathyroid scintigraphy in hyperparathyroidism secondary to chronic renal failure.

Methods and Patients : Images were obtained 20 minutes and 2 hours after intravenous injection of 550 MBq of Tc 99m-MIBI or Tc 99m-tetrofosmin and 2 hours after injection of 5.5 MBq of iodine 123. 50 chronic renal failure patients with secondary hyperparathyroidism underwent bilateral surgical neck exploration and the weight of each gland was notified. It was the first neck surgery for 40 patients and a reoperation for 10 patients. The threshold mass of scintigraphic detection was calculated, corresponding to the greatest number of positive glands above the threshold and negative glands below.

Results : At least one gland was seen on scintigraphy in 37 / 40 patients (92.5 %) surgically treated for the first time. 80 of 151 extirpated glands were positive on preoperative scan (the sensitivity was 53.0 %). In case of reoperation, at least one gland was positive in all patients and only 2 / 15 glands (80 and 260 mg) were negative. The mass of positive glands (69 - 4517 mg, 907 ± 943 mg) was significantly higher than the mass of negative glands (28 - 1050 mg, 259 ± 205 mg). The threshold mass was between 280 and 360 mg. The sensitivity of the scintigraphy was 83.5 % above 360 mg (71 / 85 glands), 50 % between 280 and 360 mg (6 / 12 glands) and 23.2 % below 280 mg (16 / 69 glands).

Conclusion : Before a first surgery in patients with secondary hyperparathyroidism, the sensitivity of the scintigraphy is still limited, mainly in relation with the small mass of the glands. The scan can only be justified to research ectopic glands. In patients reoperated, the scintigraphy is the procedure of choice.

PS-521

D. Huglo, V. Beauchat, A. Delcourt, B. Carnaille, F. Pattou, C. Proye, T. Prangere, M. Steinling
Department of Nuclear Medicine and Endocrine Surgery
Hospital C. Huriez - C.H.R.U. of Lille, 59037 Lille cedex - France

DETECTION OF PARATHYROID ABNORMAL GLANDS WITH Tc 99m-MIBI AND INTRAOPERATIVE PROBE

Intraoperative detection of Tc 99m-MIBI is proposed by some teams, sometimes instead of the preoperative scintigraphy. The aim of this preliminary study was to evaluate the usefulness of the intraoperative detection with and without the knowledge of the results of the scan.

Patients and Methods : 25 patients with primary hyperparathyroidism were studied before surgery. Images were obtained 20 min. and 2 h. after intravenous injection of 550 MBq of Tc 99m-MIBI and 2 h. after injection of 5.5 MBq of iodine 123. Before this injection, measurements were systematically performed during 15 sec. with a probe (CdTe detector) connected to a PC, on each side on upper and lower poles of the thyroid area and sub-maxillary glands, on mediastinum, heart and liver then freely anywhere. In 21 patients, these measurements were also performed by a second operator, without knowledge of the images. A cervical site was positive if the asymmetry was statistically significant.

Results : 24 patients were cured by exeresis of 30 pathologic glands. 19 of them (126 - 3350 mg) were seen on the scans. The negative glands (48 - 1024 mg, 5 < 100 mg) were associated with positive glands or thyroid abnormalities. With the knowledge of images, we obtained on cervical site 11 TP, 15 FP, 11 FN, 13 TN (and 13 TP, 5 FP, 7 FN if the side only was take in consideration). Without knowledge of images, we obtained 4 TP, 12 FP, 12 FN, 14 TN by site and 4 TP, 8 FP, 9 FN by side. Significant differences were observed in more than half other cases.

Conclusion : High background, sometimes thyroid uptake and differences of positioning of the probe can explain the poor results of the detection with the probe, lower than preoperative scintigraphy. The use of probe intraoperatively will be possible only in selected patients, with one clearly seen gland on the preoperative scintigraphy.

PS-522

R. Junik, K. Łacka, I. Kubik, J. Sowiński, M. Gembicki
Department of Endocrinology, K. Marcinkowski University of Medical Sciences, Poznań, Poland

COMPARISON OF BRAIN SPECT WITH 99mTc-HMPAO IN PATIENTS WITH CONGENITAL HYPOTHYROIDISM AND CONTROLS

Thyroid hormone is essential for the development of the nervous system and its deficiency in the infant impairs permanently the activity of the brain. The goal of this study was to compare SPECT rCBF in patients with congenital hypothyreosis and healthy normal volunteers. Twenty-nine patients with congenital hypothyreosis (14 males and 15 females, mean age 34,9 +/- 8,2 yr) and 26 controls were studied. None of the patients had received any medication except L-thyroxine prior to cerebral SPECT imaging. Tomographic images were obtained using a one-head rotating gamma camera equipped with a low-energy high-resolution collimator SPECT scans were performed after the iv injection of a 740 Mbq of 99mTc-HMPAO. Uptake of the tracer was determined in different regions of interest of the cortex. Differences of more than 10% between contralateral regions of the brain were considered significant.

Interhemispheric asymmetry ranged within 11-25% in cortical regions and reduced rCBF were observed in 24/29 (83%) patients with hypothyroidism. The regions showing the highest differences of rCBF between patients and controls were prefrontal and frontal (p<0,05) regions and the basal ganglia. In the left infero-frontal region and in the right basal ganglia the differences were even more pronounced (p<0,01).

Conclusion: the rCBF in patients with congenital hypothyroidism comparing to controls is both reduced and asymmetric.

PS-523

G.Kirsch, W. Meng, M. Kirsch, M. Trautmann, A. Zinke, U. Bohl

Greifswald University, Departments of Nuclear and Internal Medicine

SIZE-DEVELOPMENT OF THYROID AUTONOMY NODULES

There is little information about exact long time measurements of nodule-development in goitres with thyroid autonomy which is of interest in therapy planning.

Methods: Between 1991-97 448 follow-up-examinations of nodular goitres were selected (out of 5000) in which any thyroid therapy could be excluded. Follow up time varied from 2-60 month; mean 19 month. Size of thyroid and nodules were measured by ultrasound/doppler, correlated to hormone parameters and thyroid uptake and compared between different goitre-groups. In multifocal autonomy only the greatest nodules were considered. Paired comparisons were calculated. Size differences were related to starting values and corrected for time intervals. The examination methods did not change relevantly during this period .

Results: Starting values of goitre-volume (ml), nodule-diameter (mm) and hormones (SI-units); mean differences in size (%/year)

Goitre-Group	n	Goitre Vol. ml	Diff. %/y	Nodule mm	Diff. %/y	TSH	T3	TcTU %
All goitres	448	50	4,9	29	12	,96	3,0	2,9
cold nodules	194	51	2,8	32	13	,91	2,5	2,7
warm nodules	92	39	6,5	25	13	1,11	2,5	3,1
comp. Auton.	54	44	10,5	26	14	,53	2,7	2,5
dec. Auton.	15	49	15,0	39	19	,19	3,4	3,4
multifoc. Auton.	93	61	2,5	29	8	,36	2,7	2,9

Conclusion:

There are great differences in individual developments of goitres and nodules. Mean augmentation of goitre volume was about 5% per year. The mean augmentation of (long-axis) nodule diameter of 12% relates to a nodule volume change of about 50%. In goitres with warm autonomy nodules with "critical" size there are correlations between differences of nodular size and changes in thyroid hormon parameters.

PS-524

C.Körber, J. Farahati, S. Muffert, U.Mäder, M.Mörtl, Ch.Reiners
Clinic for Nuclear Medicine and Tumorcenter, University of Würzburg, Germany.

CHANGES IN INCIDENCE RATES OF THYROID CARCINOMA IN THE IODINE-DEFICIENT AREA LOWER FRANCONIA BETWEEN 1981 - 1995

BACKGROUND: Possible changes in incidence rate and prognosis of differentiated thyroid carcinoma (TC) were evaluated by this retrospective investigation.

METHODS: The study comprised 443 patients from Lower Franconia (1.3*10⁶ inhabitants) with TC treated and followed at the Clinic between 1981-1995. The incidence was evaluated with respect to histology, tumor stage, lymph node involvement, distant metastases and age in five-year intervals. **RESULTS:** Except of an increasing rate of papillary thyroid cancer (PTC) and a decreasing rate of follicular thyroid cancer (FTC) no significant changes in incidence rates were observed during the last 15 years. The 10-year survival of patients with TC (analysis carried out by Kaplan-Meier survival analysis) was significantly lower in group A than in group B and C, whereas recurrence rate was lower in former groups (A<B<C). However, the results concerning recurrent disease did not differ significantly.

	81-85	86-90	91-95	p*	p*	p*
(*y ² test: p<0.01 = significant)	A	B	C	A vs B	A vs C	B vs C
cases/100000/year (female)	2.92	3.04	3.40	0.14	0.15	1.00
cases/100000/year (male)	0.97	1.50	1.66	0.14	0.15	1.00
< 15 years of age	2%	4%	1%	0.4	0.2	0.04
15-45 "	30%	33%	24%	0.58	0.23	0.06
46-55 "	36%	40%	45%	0.48	0.14	0.44
>55 "	32%	23%	30%	0.08	1.00	0.08
papillary	55%	65%	75%	0.08	0.001	0.06
follicular	35%	28%	22%	0.2	0.01	0.18
T1	20%	29%	28%	0.07	0.08	1.00
T4	18%	17%	19%	1.00	0.75	0.58
N1	10%	12%	19%	0.58	0.04	0.10
M1	7%	7%	7%	1.00	1.00	0.75
10 year survival-rate	86%	94%	96%	0.001	0.001	0.02
recurrence free survival (10 yrs.)	94%	92%	90%	0.03	0.03	0.39

CONCLUSIONS: 1. Changes in incidence of TC could not be proved. 2. Analysis showed a redistribution in histologic types of differentiated TC with an increasing rate of PTC and simultaneous decreasing rate of FTC. 3. A redistribution concerning other prognostic factors, such as T4-, N- or M-stage and age has not been observed. 4. Additionally an improvement in outcome of patients with TC was observed.

PS-525

S.Kováčová, I.Makaiová, J.Podoba+, M.Srbecký++, P.Bánki, S.Skrášková, I.Belan+, Clinic of Nuclear Medicine St.Elisabeth Oncological Institute and Medical Faculty Comenius University, +Endocrinologic Department of Postgraduate Medical School, ++Radiodiagnostic Department of Postgraduate Medical School, BRATISLAVA, Slovak Republic

THE ATTEMPT OF QUANTIFICATION UPTAKE OF 111In-Pentetreotide IN THE PITUITARY GLAND

The variable physiological uptake of 111In-Pentetreotide in the pituitary gland may due some problems in interpretation of pituitary gland tumors and changes after somatostatin therapy.

In planar imaging the physiological uptake in the pituitary gland equals uptake in skull, evaluation of SPECT investigations showed, that the patients with assumption of physiological uptake in pituitary gland scan had greater difference between accumulation in the pituitary gland and in the skull.

This problem can be stressed in the interpretation of SPECT imaging. Therefore in 40 patients indicated for 111In-Octreoscan (Mallinckrodt) scintigraphy with variable diseases SPECT had been performed with DST Sophy Medical Vision dual heads camera and the volume (ccm) and volume activity (Bq/ccm) was specified by method based on an empirical threshold analysis, where threshold value was the value of 111In-Octreoscan uptake in the skull.

In „normal“ patients this rate varied between 1-2. Some patients had no the pituitary gland visualized at all. The rate uptake of pituitary/skull was estimated. In patients with adenoma was 4, after sufficient therapy 2. Despite of that, the volume (ccm) of pituitary gland was unchanged, the volume activity (Bq/ccm) was decreased, what correlated with the effectivity of therapy.

Conclusion: The visualization of 111In-Pentetreotide uptake in pituitary gland is more expressed in SPECT imaging. Therefore the physiologic range of uptake must be clearly specify. It is crucial especially in the estimation of the efficiency of the somatostatine therapy in pituitary adenomas.

PS-526

O.V.Kozak

Ukrainian Research Institute of Oncology and Radiology

The assessment of I-131 therapeutical activity distribution in children and adult patients with lung metastases of differential thyroid cancer

The patterns of I-131 therapeutical activity distribution on 34 patients (20 children and 14 adults) suffering from lung metastases of differentiated thyroid cancer upon radioiodine treatment have been studied according to scintigraphy data.

Several groups of values (T_{eff} in blood, T_{eff} in metastases, accumulation percent in lungs metastases) have been found. Correlation coefficients were calculated.

Coefficient k_1 (the ratio of T_{eff} in metastases to T_{eff} in blood), describing specific iodine excretion have been introduced on the basis of mathematical analysis of I-131 kinetics in lung metastases lesions.

Its value sharply increase upon the ablation of the significant thyroid remnants with following decrease after sequential radioiodine courses in the cases of advantageous outcome. In non-advantageous cases the dynamics of these values becomes inconsistent, even occasional increase may occur.

k_1 in children is significantly higher than in adults.

The mean absorbed doses in lungs have been calculated on the basis of the assumption of even isotope distribution

PS-527

E. Kresnik, H.J. Gallowitsch, P. Mikosch, M. Molnar, W. Pipam, I. Gomez, P. Lind.

Department of Nuclear Medicine and Endocrinology, Landeskrankenhaus Klagenfurt, Austria

EVALUATION of THYROID NODULES with TECHNETIUM-99m-TETROFOSMIN DUAL-PHASE SCINTIGRAPHY

^{99m}Tc Tetrofosmin, a lipophilic cationic complex molecule, was introduced for myocardial imaging. In some biodistribution studies it has also been reported to accumulate in the thyroid gland. Our objective was to determine which thyroid nodules retain Tetrofosmin and whether preoperative evaluation of malignancy is possible. **Methods:** Tetrofosmin scintigraphy was performed on 57 patients who had shown a cold thyroid nodule on previously performed pertechnetate scintigraphy. All patients had undergone ultrasonography and sonographically guided fine needle aspiration biopsy as well. The Tetrofosmin scintigrams were carried out 5 minutes (early image) and 1 hour (late image) after intravenous injection of 370 MBq. Only nodules that showed a clear tracer retention after 1 hour in comparison with those taken at 5 minutes were classified as TETRO positive. Nodules without late retention were classified as TETRO negative. All patients underwent surgery and the histological results were compared with the Tetrofosmin scintigraphy.

Results: Ten out of eleven patients with thyroid carcinoma (two pT1, three pT2, five pT4) were TETRO negative. One patient with papillary carcinoma (pT2) was TETRO positive. The mean nodular to thyroid tissue (N/T) ratio for the late performed scan was 1.02 +/- 0.20. There were 21 patients with thyroid adenomas (seven follicular, seven microfollicular and seven oxyphilic). Fifteen patients were TETRO positive and six TETRO negative. The mean N/T ratio for the late images was 1.34 +/- 0.41. All patients with degenerative goiter (24 cases) and the one with Hashimoto's disease were TETRO negative after one hour and the N/T ratio was about 0.92 +/- 0.12 on the late performed scan.

Conclusion:

Our results indicate that ^{99m}Tc-Tetrofosmin scanning is not specific for thyroid malignancy. Tetrofosmin rather indicates thyroid adenoma than a malignant tumor.

PS-528

Rakesh Kumar, AK Pandey, AK Gupta, AK Padhy, GS Pant, AC Amini

All India Institute of Medical Sciences, New Delhi-29, INDIA
Department of Nuclear Medicine, Radiology & Endocrinology.

INFLUENCE OF LITHIUM ON EFFECTIVE HALF LIFE OF RADIOIODINE IN PATIENTS OF GRAVES DISEASE.

Lithium carbonate is the drug of choice for bipolar psychiatric disorders and hypothyroidism is one of its major side effects. As to the etiology, a general consensus is that lithium inhibits the release of thyroid hormone. This study was undertaken to see the effect of lithium on the effective half life of radioactive iodine.

A total of 61 adult patients of grave's disease were studied under two groups of Lithium and No Lithium. The patients were assigned the groups randomly and their biochemical parameters (T3, T4 and TSH) as well as thyroid weights were approximately same. Effective half life was calculated from the exponential curve of counts taken over the thyroid at 24 hrs., 48 hrs., 72 hrs. and 96 hrs. after administering 20 mCi of I-131 orally.

Effective Half Life : Lithium group vs No-Lithium group

	Lithium	No Lithium
No. of patients	26	35
Mean EHL (days)	6.25	5.22
S.D.	1.35	1.59
p value	<0.001	

As per results of this study the effective half life of I-131 was significantly prolonged in patients who had received lithium as compare to those who had not.

In conclusion, lithium can be used in combination with I-131 therapy in patients of high uptake thyrotoxicosis and well differentiated carcinoma of thyroid.

PS-529

K. Kusakabe, N. Nishii, K. Kanaya, S. Kanaya, M. Momose, H. Kobayashi, M. Maki, and T. Obara.

Hospital: Tokyo Women's Medical College, Department of Radiology.

USEFULNESS OF LOW-DOSE IODOLECITHIN MEDICATION FOR HYPERTHYROIDISM FOLLOWING AFTER RADIOIODINE THERAPY OF GRAVES' DISEASE.

The persistent thyrotoxicosis after radioiodine therapy is difficult to control. It is known that the adjunctive potassium iodide after radioiodine therapy produce a transient decrease in serum thyroxine concentration. We evaluated the effect of low-dose of iodolecithin, 200 µg daily, to obtain the symptomatic control of hyperthyroidism after 131I treatment.

Fifty patients with Graves' hyperthyroidism who were medicated with iodolecithin following after a single dose of 131I for successful treatment of thyrotoxicosis between June 1987 and May 1996 were studied retrospectively. The clinical diagnosis of Graves' hyperthyroidism was supported in all instances by elevation of serum FT4, FT3, TRAb and inhibition of TSH. The method for dose calculation was performed by formulas involving estimated gland size, thyroidal uptake, and tracer retention in the gland aimed at bringing each patient to a normal metabolic state. Among 50 hyperthyroid patients after 131I therapy, 28 cases became euthyroid by medication of iodolecithin, requiring no further treatment for hyperthyroidism (Group 1) and other 22 cases were not controlled successfully by iodolecithin (Group 2). Medication of iodolecithin was started from one to thirteen months after 131I treatment (mean time in Group 1 and 2 was 6.2±3.6 and 3.0±1.4 months). The mean medication duration in Group 1 and 2 was 13.0±11.9 and 4.5±4.4 months respectively. Mean serum FT3(pg/ml) and FT4(ng/dl) concentrations one month after the medication of iodolecithin in Group 1 were 6.7±4.0 and 2.1±1.4, and those in Group 2 were 11.6±6.6 and 5.1±2.9. The significant difference of FT3 and FT4 levels on iodolecithin were observed between two groups, though there were no significant difference in age, gland size, 131I dose, pretreatment serum FT3, FT4 and TRAb concentration. The incidence of permanent hypothyroidism after iodolecithin medication was noted in three cases.

Low-dose of iodolecithin medication is possible to reduce thyroid hormone levels within one month, and thought to be useful in controlling symptomatic thyrotoxicosis following after radioiodine therapy.

PS-530

A. Lupi, *A. Brendolan, G. DeAntoni M., P. Orsolan, D. Cerisara, A. Vianello Dri.

Ospedale "S. Bortolo" - Vicenza - ITALY
Nuclear Medicine Service and *Nephrology Dept.

Double tracer scintigraphic evaluation of parathyroid abnormalities in dialyzed patients.

The relative risk of dialyzed pts. to require parathyroidectomy increases dramatically with the duration of the dialysis. The trend in surgical approach is to limit neck exploration, thus requiring more precise preoperative localization of parathyroid tissue. Aim of this paper is to evaluate the ability of dual-tracer scintigraphy in locating parathyroid abnormalities in these pts. and to compare it with ultrasound results.

Twenty-five chronic hemodialysis patients (17 M, 8F, overall mean age 54+14 ys., mean dialytic age 10+2 ys.) with clinical and biochemical signs of secondary hyperparathyroidism were studied with double tracer scintigraphy (99mTcO4-/99mTc sestamibi image subtraction technique + delayed imaging) and neck ultrasound (US) for parathyroid abnormalities. All of them presented increased PTH plasma levels (233-2406 pg/ml, n.r. 10-75) and X-rays signs of subperiosteal bone erosions, in spite of a long term therapy with oral VitD analogs and phosphate binders. Mean serum calcium was 9.6+2 mg/dl, mean serum phosphorus was 4.7+3 mg/dl.

The main positivity criterium for scintigraphic screening was the localization of hypercellular areas in subtraction images; an ancillary criterium was the presence of focal delay in sestamibi washout (WO). Fifteen patients (60%) were rated positive for adenoma or hyperplasia at subtraction imaging (11 of them were positive at WO too); 7 (28%) were negative, 3 (12%) uncertain. Only 5 pts (33%) out of the 15 scintigraphically positives were positive at US.

Eleven of the scintigraphic positives underwent parathyroidectomy; in two pts who died the parathyroid glands were studied at necropsy. In all of these 13 cases a complete correspondence between the scintigraphic picture and the surgical results was found, both for the identification and the location of abnormal parathyroid tissue. US was predictive for the presence of parathyroid abnormalities in 4 cases out of 13, but allowed proper localization of the finding only in 1.

We conclude that, while US role seems still complementary, double tracer scintigraphy is a valuable method for preoperative parathyroid abnormalities, even in complicated cases as hemodialyzed patients. Our results appear more satisfying than some recently reported data: a possible explanation for this may depend on the use of both subtraction and WO techniques in our series.

PS-531

M. Luster, M. Geling, U. Michalowski, B. Juchems, H. Timmermann*, Chr. Reiners

Department of Nuclear Medicine, University of Würzburg, Germany

* Department of Surgery, University of Würzburg, Germany

COMPARISON OF 3 IMAGING MODALITIES IN HYPERPARATHYROIDISM (HPT)

Objectives: 99m-Tc sestamibi (MIBI) -scintigraphy has been reported to significantly increase the reliability of localization of hyperfunctioning parathyroid tissue. We evaluated planar MIBI scintigraphy, MIBI-SPECT versus ultrasonography (US) in 16 patients with HPT documented by histology reports.

Methods: 16 consecutive patients (13 female, 3 male, mean age 59.3 (range 25-81) years) with HPT were investigated. 12 had primary hyperparathyroidism (pHPT) presenting as a solitary adenoma, 4 showed hyperplasia.

Before scanning all patients had an ultrasound of the neck region performed by an experienced physician using a 7.5 MHz transducer (SONOLINE Elegra, Siemens). After injection of 600-900 MBq 99m-Tc sestamibi planar spot images of the cervical/upper thorax region were acquired. MIBI-SPECT was performed with a double head camera (E.CAM, Siemens; high resolution low energy collimator, 128x128 word-mode matrix by using a 1.45 acquisition zoom).

Results:

Pat. No.	US	MIBI planar	MIBI-SPECT	Histology
1	FN	TP	TP	Adenoma left
2	TP	TP	TP	Adenoma left
3	TP	TP	TP	Adenoma left
4	TP	TP	TP	Adenoma right
5	FN	FN	TP	Adenoma left
6	FN	TP	TP	Adenoma mediastinal
7	TP	TP	TP	Adenoma left
8	TP	TP	TP	Adenoma left
9	TP	FN	TP	Adenoma left
10	TP	FN	TP	Adenoma right
11	FN	FN	FN	Adenoma left
12	TP	FN	TP*	Hyperplasia
13	FN	FN	FN	Recurrent Hyperpl.
14	FN	FN	TP*	Hyperplasia
15	FN	FN	FN	Hyperplasia
16	TP*	TP*	TP*	Hyperplasia

Table 1: Clinical features and imaging results in patients with HPT

FN = false negative; TP = true positive; TP* = only one out of four detected
In 10 of 11 cases with pHPT MIBI-SPECT was true-positive resulting in a sensitivity of 91% and a specificity of 100%.

Conclusion: In patients suffering from hyperparathyroidism ultrasonography and 99m-Tc sestamibi (MIBI)-scintigraphy provide helpful tools in the preoperative work-up. With regard to the high sensitivity and specificity MIBI-SPECT in primary HPT, a study evaluating the possibility of a unilateral surgical approach is underway.

PS-532

C. Mari, LL. Bernà, A. Flotats, JC. Martín, M. Estorch, A. Catafau, I. Carrió.

Hospital Sant Pau, Barcelona. Spain. Department of Nuclear Medicine.

111In-PENTETREOTIDE SCINTIGRAPHY SHOULD BE THE FIRST TEST IN THE ASSESSMENT OF GASTROENTEROPANCREATIC (GEP) TUMOURS

Aim: To assess the proper place of 111In-pentetreotide scintigraphy in the sequence of diagnostic tests in GEP tumours.

Methods: 24 patients were studied, 11 males and 13 females (mean age 51±16 years), all with GEP tumours histological and/or biochemically confirmed: 7 carcinoids, 5 gastrinomas, 3 glucagonomas, 1 vipoma, 1 insulinoma and 7 undifferentiated neuroendocrinologic carcinomas (UNC). All were studied by means the administration of 3 mCi of 111In-pentetreotide, obtaining images at 4 and 24 hours. In some cases SPECT was performed. TC/RM and abdominal ultrasound were also performed, their results were compared with those of scintigraphy.

Results: 111In-pentetreotide detected primary tumour in 8 of 15 patients who did not undergo surgery (S 53%): 2 carcinoids, 1 gastrinoma, 1 glucagonoma and 4 UNC; morphological tests in 7/15 (S 47%). In the 9 patients studied to assess recurrence/metastases, lesions were localized in 8/9 patients (S 88%) with 111In-pentetreotide and in 5/9 (S 55%) by means of morphological tests. We detected a grater number of localizations with 111In-pentetreotide. All the primary tumours and metastatic localizations detected by means of morphological tests were also detected with 111In-pentetreotide.

Conclusion: 111In-pentetreotide scintigraphy should be a diagnostic test of first choice in the diagnosis of GEP tumours. Morphological tests should be performed prior to surgical treatment.

PS-533

A. Masala, S. Alagna, D. Gallisai, C. Burrari, P.P. Rovasio, E. Lai, M.S. Taras, F. Satta, F. Fadda, S. Nuvoli, A. Falchi, A. Spanu and G. Madeddu. Depts. of Internal Medicine, Paediatrics and Nuclear Medicine. University of Sassari. Italy.

GONADOTROPIN SECRETION AND PUBERTAL DEVELOPMENT AFTER BONE MARROW TRANSPLANTATION (BMT) IN THALASSEMIA MAJOR (TM).

BMT represents nowadays the treatment of choice in TM. However, the occurrence of alterations in endocrine functioning have been reported in TM pts after BMT, presumably due to the effect of the cytotoxic agents used and to the immunosuppressive therapy with cyclosporine. In the present study, we examined gonadotropin secretion and gonadal development in 26 pts who underwent BMT to treat thalassemia. The pts, 10 males, and 16 females, aged 13-17 years, took part in a longitudinal study on endocrine abnormalities in thalassemia. All were studied 1 year after the end of cyclosporine therapy (2 years from BMT). Gonadotropin secretion in response to i.v. LRH (50µg), plasma testosterone and estradiol levels were measured in all pts by using specific IRMA methods. Only 5 of the 10 males and 6 of the 16 females studied had normal pubertal development (Group 1). In these pts baseline LH and FSH levels and their responses to LRH were in the normal range. All had normal levels of testosterone or estradiol. The other 5 M and 10 F pts exhibited severe gonadal failure as evidenced by absence of pubertal development (Group 2). In these pts baseline LH and FSH levels (M±SEM) were elevated (7.45±1.32 and 14.67±2.44 in males and 8.49±2.21 and 24.56±2.89 U/l in females for LH and FSH, respectively). Differences with respect to the values recorded in Group 1 pts were statistically significant (p<0.01). All Group 2 pts also had plasma testosterone (1.21±0.34 ng/ml in males) or estradiol levels (8.98±1.78 ng/ml in females) in the prepubertal range. Gonadotropin response to LRH was exaggerated. Data of the present study further indicate that BMT, though healing thalassemia, can induce severe endocrine alterations in TM patients.

PS-534

K. Milos, J. Kalk

Hospital: Departments of Nuclear Medicine and Endocrinology, Johannesburg Hospital, University of Witwatersrand, South Africa

RADIOIODINE TREATMENT OF GRAVES DISEASE: FIXED VS. ESTIMATED DOSE

OBJECTIVES: Since there are marked differences both in dose strategies and in outcome reported by different centres using I-131 as treatment of choice in hyperthyroidism, the intention in the present study was to define in our institution the results of radioiodine administered either by estimated or fixed dose regime.

DESIGN: A retrospective review of case records.

PATIENTS: The study included 126 patients who were divided into two subgroups according to the amount of I-131 administered: one (94 patients) received estimated dose of 4-10 mCi (mean 6.9 mCi) based on gland size assessment by palpation, and other (32 patients) received fixed dose of 10 mCi, with no account taken of size, iodine uptake or results of biochemistry. Age range was 14-78 yr, and female to male ratio 6:1. Most patients (119) were pretreated with antithyroid drugs. After a single administration of I-131 patients with persistent or recurrent disease were given an additional dose (mean total dose 19 mCi). The follow up ranged from 4 to 98 months (mean 4 yr).

RESULTS: The single dose of I-131 resulted in permanent cure of hyperthyroidism in 66 of 94 patients (70%) in the estimated dose group and 23 of 32 patients (72%) in the fixed dose group. The remaining 30% and 28%, respectively, required retreatment for permanent control of hyperthyroidism. They were more likely to have larger glands. Once retreated, the outcome was the same as in those cured with single I-131 dose. The average cumulative incidence of hypothyroidism at 6, 12 and 48 months was 45%, 77% and 91%, respectively. There was no significant difference in the rate of development of hypothyroidism in respect to the dose of I-131 given (p 0.94). When subgroups were created to compare patients who received relatively low (4-6 mCi), moderate (6-8 mCi) and high (8-10 mCi) doses, there was no significant difference in the therapeutic outcome with amounts higher than 6 mCi I-131 (p 0.78).

CONCLUSION: There was no significant difference in outcome between the two treatment regimes. High cure rate, with high and almost equal incidence of early hypothyroidism in patients treated with different doses might be viewed as secondary to use of a relatively large amounts of I-131. The absence of progressive increase in a single-dose cure rate with I-131 doses higher than 6 mCi suggests a possible threshold above which no additional thyroid ablative effect is to be anticipated. However, there is a need for further prospective studies to find the optimal treatment modality for this category of patients.

PS-535

MA Balsa, M Mitjavila, P G* Alonso, L Castillejos, *M Duran, R Soria, M Delgado, FJ Penin, C Pey. Hospital Universitario de Getafe. Nuclear Medicine and *Endocrinology departments. Spain.

TETROFOSMIN UPTAKE CAPABILITY AND HISTOPATHOLOGICAL TYPE OF THE RESECTED PERTECHNETATE THYROID COLD NODULES.

Objective: Determine which thyroid nodules retain tetrofosmin and whether preoperative evaluation of malignancy is possible.

Patients and method: tetrofosmin scintigraphy was performed in 30 patients (26F, 4M) with a cold thyroid nodule on previously performed pertechnetate scintigraphy. The tetrofosmin scintigrams were obtained 10 min (early image) and 150 min (late image) after intravenous injection of 555 MBq. All patients underwent surgery and the histological results were compared with the findings on tetrofosmin dual-phase scintigraphy. Radionuclide activities in each nodule were semiquantitatively assessed using the following 4 point score: 1- uptake greater than that of the normal thyroid tissue on early image and showed clear retention on late image; 2- uptake greater than that of the normal thyroid tissue and without retention on late image ; 3- uptake similar to that of surrounding thyroid tissue and without retention on late image and 4- no tetrofosmin uptake neither early nor late image.

Results: A total of 30 thyroid nodules were evaluated, of which 16 were goitre nodules, 4 adenomas and 10 malignant lesions.

Score	nodule goitre	adenomas	malignant
1	7	3	8
2	2	-	1
3	4	1	1
4	3	-	-

Conclusion: Our results indicate that 99mTc-tetrofosmin scanning is of little value preoperatively in distinguishing thyroid carcinoma from other thyroid nodules.

PS-536

A.M. Omar, E. Higazi, A. Khalaf, S. Baig, A.H. Elgazzar. Depts of Nucl Med, Ibn Sina and Amiri Hospital, Ministry of Public Health and Faculty of Medicine, Kuwait.

FINE NEEDLE ASPIRATION BIOPSY (FNAB) IN SINGLE VS MULTIPLE THYROID NODULES.

FNAB is useful in the management of nodular thyroid disease. The objective of this retrospective study was to evaluate the performance of FNAB in multinodular and uninodular thyroid disease.

We reviewed 864 thyroid scans routinely performed over 26 months using Tc-99m pertechnetate. 273 (31.5%) showed nodular disease; 156 (57%) had solitary nodules (SN) and 117 (43%) had multiple nodules (MN).

FNAB was obtained in 140 patients with nodular disease; 81 (58%) with SN and 59 (42%) with MN. FNAB results were correlated with tissue diagnosis in 48 patients who had surgery and showed the following results :

	# of patients	FNAB		Tissue Diagnosis	
		Benign	Malignant	Benign	Malignant
SN	29	25	4	28	1
MN	19	19	0	16	3

Three (10%) SN were falsely classified as malignant by FNAB. On the other hand FNAB was false negative in 3 (16%) of cases with MN. The performance of FNAB was better in SN (90% accuracy) than in MN in this group.

Although the number of our patients with final tissue diagnosis is relatively small, our results suggest potential shortcoming of FNAB in MN disease probably related to mis-representing sampling of multiple nodules.

Poster presentations

PS-537

E. Ozaalp, N. Ercakmak, G. Vural, S. Aslan, B. Turgut.

Ankara Oncology Hospital, Department of Nuclear Medicine, TÜRKİYE

PULMONARY METASTASES IN PATIENTS WITH WELL-DIFFERENTIATED THYROID CARCINOMA

The aim of this study was to evaluate pulmonary metastases in patients (pts) with well-differentiated thyroid carcinoma (DTC). We interpreted retrospectively 482 pts who received radioactive iodine (RAI) therapy for DTC in our department between 1985 and 1997. 59 pts who revealed lung metastases were included to this study. All pts had been assessed clinically, radiologically and with I-131 whole body (WB) scan and laboratory tests (serum thyroglobulin-Tg and antithyroglobulin antibodies-TgAb). 43 of them had pulmonary metastases at the time of diagnosis. Pulmonary metastases was associated with regional lymph node metastases in 29 (49%) pts, with other distant metastases in 9 (15%) pts and with both in 2 (3%) pts. Histological diagnosis was papillary carcinoma in 34 pts, follicular carcinoma in 18 pts, mixed papillary-follicular carcinoma in 6 pts and Hurthle cell carcinoma in 1 pts. The chest radiograph was normal in 17 of 41 pts with abnormal WB scans. There were 18 false-negative WB scans (14/34 papillary, 2/6 mixed, 2/18 follicular). All pts who had not concentrated radioactive iodine were older than 40 yrs. 5 pts revealed false-negative serum Tg levels. They all had high TgAb levels (3 of them were WB scan positive, 2 WB scan false negative). 7 pts were cured, 11 pts showed regression and 2 pts died of disease.

We observed that negative I-131 WB scans occurred more frequently in pts with papillary carcinoma and all of them were older than 40 yrs. We also observed that all pts with false-negative serum Tg levels had high TgAb levels. So, it should be underlined that a low Tg level is not of any value if the TgAb level is high.

PS-538

T. Özpaçacı, İ. Gözükara, N. Edis, T. Özüiker, E. Uyaruk.

Okmeydanı Educational Hospital, Istanbul, Turkey.

THE FOLLOW UP RESULTS OF THE PREGNANCIES AND THE CHILDREN OF THE PATIENTS TREATED WITH RADIOIODINE.

In order to assess the effect of radioiodine therapy (RIT) on the later pregnancies of the patients with thyroid Ca (TC) or hyperthyroidism (HT), this study was planned. Twenty seven patients with TC (16 papillary, 5 follicular and 6 papillofollicular) were given either 3700 or 7400 (in three cases) MBq of iodine 131(RI). Seven patients with HT(6 basedow, 1 plummer disease) were treated with 225-500(400±175)MBq of RI. Time between RIT and the first day of the pregnancy was 2 - 84 (22.5±23.0) months. The pregnant were 22 - 40 (29.7±5.2) year old. The pregnant were examined carefully and detailed laboratory and ultrasonography examination were done every months during the pregnancy period. After delivery, babies were controlled very carefully and they have been following up.

Three patients (2 TC and 1 HT) are now pregnant and no abnormality has been determined on their fetuses on the detailed investigations. Four patients (2 HT and 2 TC) showed normal grosses and fetal findings during whole pregnancy but delivered at the other hospitals and pediatric follow up could not be done. Twenty seven patients (4 HT and 23 TC) with 29 children (2 patients got pregnancy twice) showed normal pregnancy; and normal babies were born except one. A baby died during delivery and no important findings was seen at autopsy. Average birth weight and height of the babies was normal (3426±543 gr. and 51.3.0±2.0 cm). These babies are now 2 - 72 (35.2±24.0) months old. They have showed normal mental and motor maturation.

A patient, outside of the study group consisted of 34 patients above, known as infertile and given 3700 Mbq RI for TC (papillary type) learned her pregnancy 15 days after the RIT. She was at 3rd month of the grosses period on the time RIT. The rest of pregnancy lasted normally but a primary hypothyroid baby was born. This baby became euthyroid with proper therapy and developed normally, he is 6 years old now.

Our findings showed that RIT should not be a strict contraindication for new grosses; But, like in our one case, RIT given to pregnant may cause fetal hypothyroidism.

PS-539

T. Özpaçacı, E. Uyaruk, M. Mülazimoğlu, R. Şahin, İ. Gözükara

Okmeydanı Educational Hospital, İstanbul, Turkey.

THE BIOSTATISTICAL EVALUATION OF 1000 PATIENTS WITH THYROID CARCINOMA

In this study, the biostatistical evaluation results of 1000 thyroid carcinoma cases treated and followed up in our clinic in the last 15 years.

Eight hundred seventeen of these patients (81.7 %) were female, the other 183 patients (18.3 %) were male. The ratio of females to males was about 4.5.

Tumor types was as follows: Seven hundred thirty eight (73.8 %) papillary Ca (including 76 occult Ca), 91 (9.1 %) papillofollicular Ca, 106 (10.6 %) follicular Ca, 41 (4.1 %) medullar Ca and 24 (2.4 %) anaplastic Ca.

Metastasis frequencies and localizations were as follows: Four (0.4 %) metastatic thyroid Ca without primary focus in thyroid even in spite of total thyroidectomy, 21 patient (2.1 %) was inoperable at the time of diagnosis. Two hundred forty seven patient (24.7 %) showed lymph node metastasis; 37 patients showed pulmonary metastasis and 29 patients showed bony metastasis. In addition these metastasis 3 brain, 2 kidney and 3 liver metastasis were seen. Twenty (2.0 %) of the patients had a second malign tumor.

The surgical operations performed in our 1000 patients with Thyroid Ca was as follows: Total or near total thyroidectomy in 311 patients (31.1 %), one lob total - the other lob subtotal thyroidectomy in 116 patients (11.6 %), bilateral subtotal thyroidectomy in 469 patients (46.9 %), lobectomy in 31 patients (3.1), isthmectomy in 6 patients (0.6 %). Frozen section during the operation was applied in only 14 patients (1.4%), and FNAB was performed in only 12 patients (1.2 %).

Two hundred seventy eight of the patients (27.8) were reoperated. Multicentricity in tumor was seen in 138 patients (13.8 %). Neck dissection was performed in 103 patients (10.3 %); 59 of these (5.9 %) was radical type, the others (4.4 %) was modified type. Only lymphatic dissection was done in 134 patients (13.4 %).

The complications seen after these operations was as follows: shoulder ptosis in 69 patients (6.9 %), permanent hypoparathyroidism in 37 patient (3.7 %) permanent tracheostomy in 11 patients (1.1 %). Esophageal trauma was seen in 2 patients.

PS-540

S.D. Sarkar, E.Y. Manalili, C.J. Palestro.

Long Island Jewish Medical Center, New Hyde Park, N.Y.

OPTIMIZING RADIOIODINE SCANS BEFORE AND AFTER I-131 THERAPY IN DIFFERENTIATED THYROID CARCINOMA

We evaluated early & late I-131 imaging & three scintigraphic methods, both before & after radioiodine therapy, in previously thyroidectomized pts. referred for differentiated thyroid cancer over a 1 year period. Thirty-seven pre-therapy studies were performed 24 hours (early) & 72 hours (late) after administration of about 185 MBq (5 mCi) of I-131. Forty post-therapy studies were performed 2-3 days (early) & 7-8 days (late) after administration of 1.1-11.5 GBq (29-310 mCi) of I-131. Studies included a pinhole neck image & multiple static views (LFOV) & a whole-body scan using a high energy high resolution collimator. Early & late imaging are compared below:

	Early Better*		Late Better*		Early = Late		Total Studies
	PreRx	Post Rx	PreRx	PostRx	PreRx	PostRx	
Pinhole	0	0	7	5	30	35	77
LFOV Lungs	6	5	14	18	17	17	77
Whole-body	25	17	2	6	8	12	70

* Greater clarity and/or number of foci detected.

Results, including above table, were as follows. A) Late neck pinhole & lung LFOV images, both pre- & post-therapy, were better in 16% & 42% of studies respectively; furthermore, all lesions seen on early images were present on late images. B) 14% of late chest LFOV images were difficult to interpret because of 'star' artifacts caused by increased late uptake in large post-surgical thyroid remnants (average 24 hr pretherapy uptake = 4%, range =1.5%-10%). C) Star artifacts were more pronounced on late whole-body scans; consequently, early scans were generally better. However, for total body evaluation including the lungs, early & late whole-body scans were inferior to LFOV images in 71% of pre-therapy & 56% of post-therapy studies. D) Pinhole & LFOV images were complementary for assessing the number & location of cervical foci. In conclusion, a) pinhole views of the neck & LFOV images of the entire body obtained at 72 hrs for pre-therapy evaluation & at 7-8 days for post-therapy evaluation, are optimal in differentiated thyroid cancer; b) pulmonary evaluation is suboptimal in pts. with large thyroid remnants; these pts., in particular, merit additional workup including CT imaging.

PS-541

J. Paunkovic, N. Paunkovic

Medical Centre Zajecar, Nuclear Medicine

PREDICTIVE VALUE OF TSH RECEPTOR ANTIBODIES FOR RELAPSE IN PATIENTS WITH GRAVES' DISEASE TREATED BY ANTI-THYROID DRUGS

Positive findings of TSH receptor antibodies (TRAb) in patients with Graves' disease before treatment are indicative of autoimmunity, and change in their level marks the effect of anti-thyroid drugs. The aim of this study was to evaluate the predictive value of TRAb before anti thyroid drug treatment and after the therapy. Evaluation included data from 180 patients with Graves' disease for duration of 12 years. TRAb were performed by radioreceptor assay (TRAK – assay, BRAHMS), at the beginning of anti-thyroid drug treatment, multiple times during the treatment, and at the end of the therapy (18-20 months). The time of the first relapse was registered or duration of the remission up to 12 years. In Group 1 (TRAb negative at the beginning and at the end of the treatment) 22 of 38 patients relapsed; in Group 2 (TRAb positive before treatment and TRAb negative at the end of the treatment) 44 of 100 patients relapsed; and in Group 3 (TRAb positive before treatment and at the end of the treatment) 41 of 42 patients relapsed in less than six months. Our results support the significance of TRAb positive findings at the end of anti-thyroid drug treatment for the prediction of early relapse (97,6%). Predictive value of TRAb negative findings for the absence of relapse is lower (44-52%), but it improves for the prediction of the absence of early relapse (80%). TRAb findings before treatment had no predictive value for the relapse.

PS-542

Z.Petrovski, J.Gjorgievski, S.Mihajlovska

Department of Nuclear Medicine, Medical Center, Bitola, Macedonia

LATE FOLLOW UP RESULTS IN THE TREATMENT OF AUTONOMOUS THYROID ADENOMA

We studied 52 treated patients (43 female, 9 male, age range 18-74 years) with autonomous functioning thyroid adenoma for the period 1986-1997. 21 (40,3%) pts underwent surgery (enucleation), while 31 (59,7%) pts received 131-jodine therapy (740-1100 MBq). The results of the treatment were evaluated 6 months to 11 years after therapy. The standard diagnostic procedures were: clinical examination, determination of serum FT₄, FT₃ and TSH, scan and ultrasonography of the thyroid. Recurrent hyperthyroidism occurred in 3/21 (14,2%) pts, one to seven years after enucleation in comparison to none of the patients after radioiodine therapy. Hypothyroidism was observed in 2/31 (6,4%) pts treated by radioiodine. The mean serum concentrations of the thyroid hormones in the two study groups did not have significant difference. The pts after enucleation of autonomous nodule of the thyroid show increase incidence of late recurrent hyperthyroidism, while this was not observed following radioiodine treatment. These results are likely to be due to persistent functional autonomy in the parenchyma surrounding the autonomous adenoma. Apparently this persistent autonomy could be successfully removed by radioiodine. Extensive radioiodine therapy is an efficient treatment of autonomous adenoma and provides a safe protection in preventing late recurrent hyperthyroidism.

PS-543

D.Picard, M.Picard, J.Morais, R.Chartrand, M.Couturier, P.D'Amour

Centre Hospitalier Universitaire de Montréal, Campus Saint-Luc, Nuclear Medecine, Montreal, Canada.

PARATHYROID ADENOMA LOCALIZATION: COMPARED USEFULNESS OF 201TI/123I AND 99mTc MIBI IMMEDIATE, ONE AND FOUR HOURS SCINTIGRAPHY.

99mTc MIBI parathyroid scintigraphy appears promising and technically easier than dual isotope imaging (201TI/123I) which appears even better than 201TI/99mTc pertechnetate studies (phantom experiments). Is it worth pursuing the dual isotope technique and which images obtained with the 99mTc MIBI study are the most useful for the diagnosis of a parathyroid adenoma?

In this study, 30 patients had surgically proven parathyroid adenoma (PA). PA weight was 1.4 ± 1.9 g. All patients had both single and double isotope scintigraphy prior to surgery. For the 99mTc MIBI study, 740 MBq were injected and planar LFOV images (800 K) were obtained immediately, 1 and 4 hr post injection. Less than one week later, 24 hr post ingestion of 123I (26 MBq), immediately after injection of 201TI (81 MBq), ten 1 minute dynamic dual isotope images were obtained. Double blinded reading of the images was performed by 2 experienced readers. Easiness of adenoma detection was also assessed for both techniques (1: difficult; 2: easier; 3: obvious). The usefulness of the different phases of 99mTc MIBI study was also assessed, using the same parameters. Adequate parathyroid adenoma localization was:

	SIDE	SITE*	EASINESS
99mTc MIBI	29/30	25/30	2.0 ± 0.16(s.e.m.)
201TI/123I	25/30 [®]	19/30	1.5 ± 0.12(s.e.m.)

* SITE: superior vs inferior (in accordance with the vascular supply)

® SIDE: no visible abnormality in 3 cases

The 99mTc MIBI immediate scintigraphy demonstrated the PA 15 times out of 30, the 1 hour 27 times and the 4 hr 20 times. The combination of the immediate and the 1 hour scintigraphy permitted the diagnosis 27 times out of 30. The PA was easiest to detect in the 4 hr phase in 4 cases and in two cases, it was the only way to localize the adenoma. However, in all the other cases, the very late scintigraphy was less useful than the one hour scintigraphy.

In conclusion, 99mTc MIBI is both easier and more reliable in PA localization than 201TI/123I scintigraphy. The immediate and one hour delayed 99mTc MIBI scintigraphies are the most useful. The 4 hr 99mTc MIBI scintigraphy is useful only when the immediate and one hour delayed scintigraphies are not diagnostic.

PS-544

R.Pichler, C. Holzinger, M.Hatzl-Griessenhofer, H.Huber, W. Maschek

Depts. of Nucl. Med. and Ophthalmol., Gen.H.Linz

111In-Somatostatin-RECEPTOR SCINTIGRAPHY IN GRAVES' OPHTHALMOPATHY

Thyroid eye disease is a common finding in Graves' disease, therapeutic success by corticoid therapy is limited. Lanreotide, a long acting somatostatin analogue, was found to have benefic effect in patients with positive Octreoscan.

We prospectively evaluated 10 pts. with active GO (Graves' ophthalmopathy) from 11/97 - 3/98. Mean age was 41±13 yrs. (female:male = 4:1). All but one had received antithyroid agents, 3 corticoid treatment and 1 orbital radiation. The onset of thyrotoxicosis started 6 months before (median value). Thyrotropin receptor antibodies were elevated in 8/9 (♯62U/l).

Methods: SPECT was performed with a double headed rotating gamma camera 4h after application of 120 MBq 111In-Penetreotide. Semiquantitative evaluation was performed using SPECT slices with circular ROIs placed over the orbits and as references over the ipsilateral temporal cortex.

Results: Only one patient with moderate bilateral proptosis showed a marked uptake ratio greater than 2 (in both eyes). She was one of 4/10 pts. with diplopia and had previous received corticoids. In 5/20 eyes mildly elevated uptake (ratio about 1,5) was observed.

Conclusion: 1/10 pts. with GO had a positive octreoscan and therefore received treatment with lanreotide (30mg i.m. every 14d) which lead to clinical and sonographic remission. Beneficial effect of this therapy in case of modest orbital receptor density needs further investigation.

PS-545

R.Róka, M. Papós, E. Ambrus, M. Lázár, T. Séra, J. Julesz*, L. Pávics

Departments of Nuclear Medicine and Endocrinology*, Albert Szent-Györgyi Medical University, Szeged, Hungary

CLINICAL EXPERIENCE WITH OUTPATIENT RADIOIODINE THERAPY IN HYPERTHYROIDISM

Since 1993, outpatient radioiodine therapy has been available in our country.

AIM: The aim of this retrospective study was to investigate the efficacy of ambulant radioiodine treatment for subjects with hyperthyroidism.

PATIENTS AND METHODS: The data on 118 patients with Graves' disease and 36 patients with thyroid autonomy were analysed retrospectively. All patients were treated in the period 1994-1997 with individually calculated activities of I-131. The applied dose in Graves' disease was 150 Gy, and in thyroid autonomy was 300 Gy. 129 patients received a single dose of radioiodine, 25 patients underwent fractional therapy. The follow-up times were 3, 6 and 12 months after radioiodine therapy.

RESULTS: The radioiodine therapy was successful in 85% of the Graves' disease patients. The first 150 Gy I-131 treatment was effective in 70% of all patients, but only in 43% of the patients with an increased radioiodine turnover. In thyroid autonomy, the treatment was successful in 82% of the patients. The effectiveness of the first treatment was the same for single(53%) or for fractional(66%) administration. During the follow-up period, the radiation exposure of the surroundings remained below the prescribed limit.

CONCLUSION: Radioiodine therapy with a 150 Gy absorbed dose in Graves' disease and with a 300 Gy absorbed dose in thyroid autonomy proved successful. Outpatient radioiodine treatment is a valuable and cost-effective method for the therapy of hyperthyroidism by either single or fractional administration.

PS-546

D. Sandrock, B. Kettner, L. Geworski, U. Dopichaj-Menge, and D.L. Munz

Clinic for Nuclear Medicine, Charité, Humboldt University Berlin, Germany

DYNAMIC SUBTRACTION IMAGING FOR PARATHYROID SCINTIGRAPHY USING TETROFOSMIN

Aim of this study was to evaluate a subtraction protocol for parathyroid scintigraphy designed for the wash-in and wash-out kinetics of tetrofosmin.

In a double-sphere phantom simulating thyroid and parathyroid gland(s) we studied different subtraction procedures using tracer concentrations according to published wash-in and wash-out rates for tetrofosmin. The protocol established was studied on 24 patients (12 women, 12 men) aged 26 to 74 years (mean +/- sd: 52.5 +/- 13.9 years) with parathyroid adenomas (n = 10) or for exclusion of a parathyroid adenoma (n = 14). Dynamic scintigraphy for 60 min (12 frames of 5 min each) was performed after i.v. injection of 370 MBq Tc-99m tetrofosmin (+ 1 image 2 h p.i.). Finally, the summed frames acquired 5 to 10 min p.i. were subtracted from these between 50 and 60 min with normalisation for acquisition time and count rates in a thyroid region of equal shape and size, respectively.

In all patients without parathyroid adenoma, subtraction scintigraphy resulted in a (true negative) "empty" thyroid, i.e. without remaining abnormal tracer accumulation. Nine of these patients had a goiter, 7 of them nodules as well. A conventional thyroid scan demonstrated hot lesions in 3 and cold in 4. In 10 patients with parathyroid adenoma, subtraction yielded a (true) positive image with net counts in the adenoma at least two-fold above surrounding background. The use of the late image did not improve image quality or sensitivity. There was no significant correlation with age, sex or size of the adenoma.

Conclusion: The proposed procedure with just one dynamic scintigraphy and adequate subtraction is an appropriate technique for the use of tetrofosmin in parathyroid scintigraphy.

PS-547

A. Sargiotti¹, M. Baccega¹, M. Campana¹, G. Brusasco¹, M. Petrarolo¹, M. Taricco¹, G. Gaspari¹, PG De Filippi¹
A.O. San Giovanni Battista di Torino - Italy
¹ U.O. A. Medicina Nucleare, ² U.O.D.U. III Chirurgia Generale

HIGH SENSITIVE SCINTIGRAPHY IN LOCALIZATION OF ABNORMAL PARATHYROID. REVIEW OF EXPERIENCE

Patients (102) with biochemically confirmed hyperparathyroidism (HPT) prior to surgical neck exploration were included in our retrospective study. 76 patients had evidence of primary HPT (26 males, 50 females), average age 54.9 ± 15 years (group A), and 26 patients had secondary HPT (6 males, 20 females), average age 57.2 ± 11.5 years (group B). The two groups were evaluated by two imaging methods (double phase scintigraphy or subtraction scintigraphy) with a small field of view gamma camera acquiring dynamic anterior pinhole images. Subsequent static image of mediastinum with a parallel hole collimator was obtained to detection of ectopic glands. Double phase scintigraphy (DPS) was performed in each subject 5 and 120 minutes after injection of 555 MBq 99mTc Sestamibi. 99mTc-201Tl subtraction scintigraphy (SS) was performed 20 minutes after injection of 74 MBq 99mTc-pertechnetate and after administration of 74 MBq 201Tl.

Scans positive had focal hot spots indicating abnormal parathyroid tissue. In group A 24 patients were evaluated with DPS and 52 patients with SS. The sensitivity was 96% and 70% respectively. In group B 6 patients were studied with DPS and 20 with SS. The sensitivity was 98% and 85% respectively.

Mean weight of parathyroids in group A was 2241 mg (SD ± 3065) when SS was positive and 1462 mg (SD ± 1068) in DPS positive. In group B mean weight was 2103 mg (SD ± 1588) in SS positive and 1320 mg (SD ± 708) in DPS positive. There was no significant difference in size between detected and missed lesions in negative SS. DPS failed in identification of parathyroid adenoma weighting near 180 mg.

DPS technique and anterior pinhole image show high sensitivity in localization of abnormal parathyroid glands both in primitive and secondary hyperparathyroidism. DPS minimizes acquisition time and risk of patient movement, allowing to perform scintigraphy even in case of low tracer uptake by the thyroid in presence of iodine loading. DPS is now in routine clinical use.

PS-548

*M. M. Sathekge, J. Baetens, A. Maes, M. De Roo

*MEDUNSA (SOUTH AFRICA) and K.U. Leuven (Belgium),
DEPARTMENT OF NUCLEAR MEDICINE

THYROID/SALIVARY GLAND RATIO FOR IMPROVEMENT OF Tc-99m THYROID UPTAKE AS A TEST OF THYROID FUNCTION

Although the diagnosis of thyroid function is now primarily by assay of serum hormone levels, radionuclide uptake tests retain a confirmatory or clarifying role when other tests are ambiguous or contradictory and are useful in the interpretation of thyroid scans. To avoid the problem of significantly underestimating uptake measurement especially in nodular goitres, the thyroid/salivary gland ratio which is independent of background, nodularity (surface) of the thyroid, population or geographical area was evaluated in 34 patients. The diagnoses were determined by clinical and laboratory examinations, including serum T4, T3, and TSH. There were 22 euthyroid patients, while 12 hyperthyroid patients were included. Tc-99m was used as a tracer, followed by the 20 min Tc-99m uptake calculation and imaging. Acquisition for the thyroid/salivary gland ratio method was completed 25 min post injection. The field of view included both the submandibular gland and the thyroid. A profile was drawn from the submandibular gland to the hottest area of the thyroid in cases of nodular goitre. The ratio between the maximum activity in the thyroid and the maximum in the submandibular gland was determined from the profile. Ninety two percent of hyperthyroid cases were correctly identified by the thyroid/salivary gland ratio above 7:1 and all euthyroid cases by the ratio below 7:1. 20 min Tc-99m uptake identified 75% of hyperthyroid (i.e. above 6%) and 53% of euthyroid cases (i.e. between 2-6%), and wrongly classified 41% of euthyroid cases to be hypo thyroid (i.e. below 2%). The adequacy of the study was clearly supported by comparison with laboratory examination as well as by clinical evaluation. In conclusion, the thyroid/salivary gland ratio method is a simple, reliable and informative test of thyroid function and is preferable in many ways to the 20 min Tc-99m uptake studies in the diagnosis of hyperthyroidism, especially in cases of nodular goitre. The method is also suitable as a routine screening test as it combines a functional and visual display of the thyroid gland without any additional time to the patient.

PS-549

A. Soriano, R Alcázar, JC Alonso, M De la Torre, AG Vicente, R Alegre, G Caparrós, J Nieto, I Ferreras, C Molino.

Departments of Nuclear Medicine and Nephrology. Complejo Hospitalario Ciudad Real, Ciudad Real. Spain.

99mTc TETROFOSMIN FOR PARATHYROID LOCALIZATION IN PATIENTS WITH HISTOLOGICAL CONFIRMED HYPERPARATHYROIDISM

Preoperative localisation of parathyroid tissue is useful in patients with hyperparathyroidism undergoing parathyroidectomy. A large number of techniques for the detection of parathyroid gland abnormalities have been addressed. We report the value of double phase 99mTc Tetrofosmin scintigraphy (99mTc-TF) in the localisation of parathyroid tissue in patients with primary (PHP), secondary (SHP) or tertiary (THP) hyperparathyroidism

30 patients with biochemical proven hyperparathyroidism who were remitted for parathyroidectomy were assessed: 11 PHP, 16 SHP in patients in chronic hemodialysis, and 3 THP in kidney transplanted patients with normal renal function.

Neck and mediastinum planar anterior views were acquired at 10 minutes (thyroid phase), 30 and 60 minutes after the radiotracer administration (parathyroid phase). A persistent tracer uptake in the regions explored during the parathyroid phase was considered positive.

The results are shown in the following table

	n	PTH(pg/ml) mean±SE	glands with 99mTc-TF	glands at surgery	sensitivity
PHP	11	239±80.2	11	11	100 %
SHP	16	855±113	43	53	81 %
THP	3	247	3	3	100 %

The images acquired at 60 minutes did not improve the sensitivity achieved with the 30 minutes images.

The histology confirmed adenomas in the patients with PHP and THP. In SHP, all the adenomas and most of the hyperplasias were identified. Only the smallest, but hyperplastic glands removed at surgery were not identified with 99mTc-Tf scintigraphy (10 glands).

We conclude that double phase Tetrofosmin 99mTc is a simple and useful diagnostic test for preoperative localisation of parathyroid tissue. The high sensitivities observed minimize the usefulness of more laborious and expensive techniques as subtraction studies.

PS-550

M.B. Tomas, M.O. Afriyie, K.K. Bhargava, C.J. Palestro.

Long Island Jewish Medical Center, New Hyde Park, NY, USA.

THE EFFECT OF THYROID NODULES ON THE ACCURACY OF PARATHYROID SCINTIGRAPHY.

Preoperative parathyroid scintigraphy with Tc-99m sestamibi or Tc-99m tetrofosmin has an overall accuracy of about 85%-90%. Because thyroid nodules, as well as parathyroid lesions, can concentrate both of these tracers, we retrospectively reviewed the results of parathyroid scintigraphy, with Tc-99m tetrofosmin, in patients with thyroid nodules & compared these results to those obtained in patients with no thyroid disease. 40 pts with biochemical evidence of primary hyperparathyroidism are included in this review. After injection with 555 MBq of Tc-99m tetrofosmin pts underwent early pinhole neck imaging, followed by SPECT of the chest & neck, followed by late pinhole neck imaging, injection of 185 MBq of pertechnetate, & generation of a subtraction image. At surgery 43 parathyroid lesions were identified: 41 adenomas, 2 hyperplasia. 14 thyroid lesions were also identified at surgery: 2 malignant and 12 benign nodules. Of the thyroid lesions 4 were more intense on early images, 3 were equally intense on early & late images, & 7 were not identified on early or late images. No thyroid lesion was more intense on late than on early images. Comparing parathyroid imaging in pts with & pts without thyroid nodules, results were:

		Early	SPECT	Late	Subtraction
Nodule (+) (n=13)	Sensitivity	.78	.93	.57	.86
	Specificity	.38	.85	.62	.85
Nodule (-) (n=22)	Sensitivity	.66	.90	.69	.79
	Specificity	.92	1.00	.92	.96

These data demonstrate that thyroid nodules have an adverse effect primarily on the specificity of parathyroid scintigraphy. Single isotope dual phase planar imaging does not accurately differentiate parathyroid & thyroid nodules. While study specificity is marginally improved by the addition of subtraction imaging, the greatest increase in accuracy is with SPECT, which permits more precise localization of the abnormality.

PS-551

S. Afroz, V. Buachum, C. Chou, S. Kanaya, K. Kusakabe, M. Mohamed, A. Nursal, A. Padhy, A. Sin, Y. Tateno, J.F. Torres, D. Howarth, T. Yamasaki

International Atomic Energy Agency Coordinated Research Group, Asia

THE STANDARDIZATION OF I-131 TREATMENT FOR HYPERTHYROIDISM WITH AN INTENT TO OPTIMIZE RADIATION DOSE AND TREATMENT RESPONSE

Despite the high incidence of goiter and hyperthyroidism in Asia, the choice of methods using I-131 and evaluation of results have not been standardized. This coordinated research programme aims to prospectively obtain and analyze the Asia-wide statistics on remission rate and posttherapy hypothyroidism using two different dose approaches (conventional high dose vs low dose I-131); to determine effects of ethnic and geographic factors on response to I-131 therapy; to identify the most important factor(s), if any, affecting treatment response and to provide a standard protocol of I-131 treatment for Grave's disease. Included are 441 young adult hyperthyroid cases from 10 Asian countries namely: Bangladesh, China, India, Indonesia, Japan, Malaysia, Philippines, Singapore, Thailand and Australia. Clinical assessment and scoring were used to evaluate hyperthyroidism; radioimmunoassay of T3, T4 and TSH were the biochemical parameters. Thyroid volume and uptake were measured by ultrasound and/or nuclear scintigraphy. Thyroid antibody determination was done by countries Australia and China. Patients were randomized into two treatment dose groups according to the estimated absorbed dose: low dose, 50-60 Gy and high dose, 80-90 Gy. Patients from Bangladesh, India, Malaysia and Thailand were further grouped into subsets (with and without pre-treatment with Lithium). Clinical, biochemical and imaging parameters were assessed at the first, third and then every 6 months posttherapy (projected time, until 36 months posttherapy). In the 441 hyperthyroid Asian subjects, 228 (51.70 %) were given low dose radioactive iodine (50-60 Gy) while 213 (48.30 %) received high dose therapy (80-90 Gy). Results of the initial 3-month follow-up showed that of the 228 patients who received low dose therapy, 90 (39.47 %) remained hyperthyroid, 119 (52.19 %) became euthyroid and 19 (8.33 %) became hypothyroid. On the other hand, of the 213 patients treated with high dose radioactive iodine, 90 (42.25 %) remained hyperthyroid, 82 (38.49 %) became euthyroid and 41 (19.24 %) became hypothyroid. This is an ongoing study; participating countries will screen and treat more patients as well as continue follow-up of treated cases. This study will be carried on until 2000, possibly longer.

PS-552

J. Versijpt, K. Casier, B. Brans, C. Van de Wiele, A. Van den Eeckhaut, J.M. Kaufman, R.A. Dierckx
University Hospital of Gent.

EVALUATION OF RADIOACTIVE IODINE TREATMENT IN PATIENTS WITH GRAVES' THYROTOXICOSIS AND LONGSTANDING ANTITHYROID DRUG RESISTANCY

In Europe, antithyroid drugs remain the first treatment option in patients with Graves thyrotoxicosis (GTP). The aim of this study was to determine the percentage GTP with a previous history of long-standing resistancy to antithyroid drugs responding (euthyroid and hypothyroid) to secondary treatment with radioiodine. From 1980 till 1996, 50 patients (45 female, 5 male) resistant to longstanding (≥ 18 months) and/or multiple drug treatment regimens, were studied. Previous subtotal thyroidectomy was performed in 7 patients (14%). Mean age and average history of Graves' disease at the time of radioiodine treatment were respectively 48 yrs (range 27-81 yrs) and 7 yrs (range 1-16). Radioiodine dose calculation was performed according to the technique described by Silver S. et al., 1968. Overall 64% of patients recieved one radioiodine treatment, 32% two, 2% three and 2% four treatments . The median dose at first treatment was 8 mCi (=289 Mbq, range 4-25 mCi); for the second treatment this was 7 mCi (=259 Mbq, range 4-17 mCi).

Table 1 summarizes the % responders and non-responders after one year to one and two treatments.

	ONE TREATMENT	TWO TREATMENTS
EUTHYROID	28%	11%
HYPOTHYROID	28%	78%
HYPERTHYROID	44%	11%

In conclusion, this subpopulation of multi-drug resistant GTP prove difficult to treat with radioiodine . After their first treatment 44% (22/50) remained hyperthyroid. Following a second dose, calculated independently from the first, 78% (14/18) evolved to an early hypothyroid state.

PS-553

A. Voege, B. Meller, M. Baehre, E. Richter

Clinic of Radiotherapy and Nuclear Medicine, Medical University of Luebeck, Germany

RADIOIODINE THERAPY OF GRAVES' HYPERTHYROIDISM: VOLUME-MODIFIED TARGET-DOSE

Objective: Although radioiodine therapy (RITH) is effective in definitive treatment of graves' disease, there is still little known about factors influencing the therapeutic outcome after RITH.

Patients and methods: The study includes 102 patients treated by RITH between 1991-95, mostly suffering from relapsing hyperthyroidism after anti-thyroid drug withdrawal. RITH was performed after a radioiodine test, activity was calculated according to the formula of Marinelli, applying a volume-modified target dose in order to achieve small posttherapeutic thyroid volumes (PV). Thyroid metabolism and volume were evaluated before and 6 months after RITH.

Results: According to the thyroid volumes before therapy we divided the patients into three groups (group I < 15 ml, II 15-25 ml, III > 25 ml). Median effective target doses in these groups were 140, 190 and 230 MBq (p<0.05) respectively. The thyroid volumes before and after therapy were 11/6 ml, 20/7 ml and 38/18 ml (M) resp. The success rate (eu- or hypothyroidism) peaked in group II with 71 %. Success rates in group I were significantly (p<0.05) higher when a PV < 5 ml was achieved (85 %) compared to a PV > 5 ml (33 %). Similar effects were observed in group II for a PV < 10 ml (85 %) and > 10 ml (36 %) (p<0.05). Furthermore, differences in the PV, volume reduction and effective target dose, but not in the thyroid volumes before therapy, were observed in patients with therapeutic success as opposed to therapeutic failure 6 months after therapy.

Conclusion: We demonstrated the influence of effective target doses on posttherapeutic thyroid volumes and consequently on therapeutic outcome after radioiodine therapy. Due to our data target doses should be modified according to pretreatment thyroid volumes. Thus, we aim at improving the therapeutic outcome in patients with graves' disease after radioiodine therapy while administering lowest appropriate activity.

PS-554

C.G.Zhang, J.H.Jin, G.Hu and G.Han.

Department of Nuclear Medicine, 1st Hospital, Shanxi Medical University, Taiyuan, P.R. China.

99mTC-PERTECHNETATE AND 99mTC-SESTAMIBI IMAGING IN EVALUATION OF THYROID TUMORS.

We studied 37 patients with thyroid tumors using 99mTc-pertechnetate and 99mTc-sestamibi imaging. The study group includes 31 females and 6 males with a mean age of 49.4 years, ranging from 23-78 years. There were 5 papillary carcinoma, 1 undifferentiated carcinoma, 5 follicular adenoma, 23 adenoma with cyst and 3 toxic adenoma. All patients underwent both 99mTc-pertechnetate(370 MBq) and 99mTc-sestamibi(370MBq) imaging within 1 week before surgery or diagnostic procedures. Static images were obtained 30 min. after injection of 99mTc-pertechnetate or 99mTc-sestamibi. Imaging was performed with a gamma camera using a high resolution collimator. Activities in the thyroid tumors were classified and scored as follow: 1 = uptake in tumor lower than background outside of thyroid; 2 = uptake in tumor higher than background but lower than surrounding thyroid; 3 = uptake in tumor equal to thyroid tissue; 4 = uptake in tumor was higher than thyroid tissue. The results of the both images were divided into match and un-match groups and presented in the table below.

Group	Match		Un-match	
	99mTc/99mTc-sestamibi (mean ± sd)		99mTc/99mTc-sestamibi (mean ± sd)	
Thyroid cancer(6)			1.5 ± 0.54	3.3 ± 0.51*
Follicular adenoma(5)			1.6 ± 0.54	3.6 ± 0.54*
Adenoma with cyst (23)	1.3	1.3**		
Toxic adenoma(3)	4.0	4.0**		

*p> 0.05 ** p<0.05

These results suggest that 99mTc-pertechnetate and 99mTc-sestamibi imaging can not differentiate thyroid cancer from follicular adenoma but if the images of both imaging are match it is very likely to be a benign tumor with cyst or a toxic adenoma.

PS-555

Y.X.Zhang, Z.R.Gao, H.Zhan

Union Hospital, Tongji Medical University, Department of Nuclear Medicine, Wuhan, P.R. China

COMPARISON OF CLINICAL VALUE OF THYROID SCINTIGRAPHY AND FUNCTION STUDIES IN PATIENTS WITH SUBACUTE THYROIDITIS

To assess the clinical value of thyroid scintigraphy and function studies, 99mTc-pertechnetate thyroid imaging and assay of serum free thyroid hormones and anti-thyroid antibodies and TSH level were performed at the same period in the 99 patients with subacute thyroiditis. All patients were classified as diffuse and localized lesions according to radioactive distribution of thyroid. The diffuse lesions were again divided into grade 0 to II on the basis of thyroid 99mTc uptake ability (nonuptake and decreased and normal). The results show that 64.6% of patients were abnormal in thyroid imaging, 42.4% FT3 increased, 53.5% FT4 increased. Serum thyroid hormones levels were paralleled with thyroid 99mTc uptake grade. FT3 and FT4 were elevated in 92.3% patients with grade 0. But it's 59% and 79.4% with grade I and only 14.3% and 25.7% with grade II (euthyroid). Seventeen of all patients were presented one lobe or localized lesions on thyroid scintigrams. FT3 and FT4 levels were elevated in 29.4% and 41.2%. 13 of 17 patients, thyroid imaging demonstrated a localized "cool" or "cold" nodules. 10 of 13 patients were present a normal FT3 and FT4 levels.

The antithyroglobulin or antimicrosomal antibodies were positive in 20(20.2%) patients with generalized subacute thyroiditis during thyrotoxic phase(66.6%). Thyroid scintigraphy with relative quantification analysis were superior than serum FT3 and FT4 assay to established the diagnosis and determined extent of inflamed lesions, especially in some cases with localized lesions.

PS-556

C.G. Zhang, J.H. Jin and G. Hu

1st Hospital, Shanxi Medical University, Department of Nuclear Medicine, Taiyuan, P.R. China.

THE TREATMENT OF THYROTOXIC PERIODIC PARALYSIS WITH I-131

Of the 6280 hyperthyroidism patients who were treated with I-131, 90 patients or 1.4% also had thyrotoxic periodic paralysis. The purpose of this study was to evaluate the effect of I-131 therapy on the symptoms of periodic paralysis. There were 74 male and 16 female with a mean age of 39 years. They were divided into 3 groups based on their pulse rates. 3 patients were mild (pulse rate PR < 100/min.), 65 patients were moderate (PR > 100 < 120) and 22 patients were severe (PR > 120). The estimated weight of thyroid and therapeutic experience were the main factors for dose selection. The basic dose was 100 uCi I-131/per gram of thyroid. The peak time and rate of uptake, patients' symptoms, effective half time, therapeutic history and course of disease were also taken into consideration when deciding the doses. The mean dose was 6.59mCi of I-131. The mean dose for each gram of thyroid was 94.85uCi of I-131. 73 patients(81%) required 1 dose, 14 patients(16%) required a second dose, and a third dose was required by 3 patients(3%). The effect of I-131 therapy was listed at the table below.

Group	No.	Complete Remission	Partial Remission	No effect
Mild	3	3(100%)		
Moderate	65	53(81.5%)	12(18.5%)	
Severe	22	15(68.2%)	3(13.6%)	4(18.2%)

Following I-131 therapy, 18 patients(20%) developed hypothyroidism 6 months and later. The treatment of thyrotoxic periodic paralysis with I-131 has been shown to be effective, simple, safe and has a high rate of remission.

Infection/inflammation/hematology: Hematology

PS-557

C.Zachert, E. Conrad, G. Ender, G. Vogel*

Hospital: Klinikum Erfurt, Clinic of Nuclear Medicine,
*1. Medical Clinic

PATTERNS OF DEPOSITION OF LABELLED PLATELETS IN DEEP VEIN THROMBOSIS OF LOWER EXTREMITIES

The purpose of the study was to investigate the deposition patterns of labelled platelets in patients with proved venous thrombosis to determine the risk of pulmonary embolism.

Methods: The platelets were labelled with 10-15 mCi (400-600 MBq) lipophilic ^{99m}Tc-HMPAO. After reinjection we performed scintigrams of the whole body in pa- and ap-view 3h and 22h p.i. with a double head whole body scintillation camera and the ICON system (Siemens).

Patients: 45 patients were investigated to determine the activity and the deposition patterns in cases with angiographically proved thrombosis of the pelvis and/or the legs.

Results: 18 Patients showed no signs of pathological platelet deposition. This finding confirmed the diagnosis of an old venous thrombosis in these cases. In 27 patients we diagnosed a pathological deposition of platelets; 13 of them had the findings in the left leg, 7 in the right leg, 7 in both legs. 8 Patients had additional depositions in the pelvic veins. The total number of positive findings was 86, 3 of them were localized in the distal part of the Vena cava inferior. The pictures showed single hot spots, multiple hot spots and/or linear depositions.

Conclusion: The method allows the differentiation of active and non active thrombi. We used the results for the control of therapy, especially for the determination of risk for acute pulmonary embolism. This investigation we performed to compare newer thrombus-imaging agents with the classical platelet scintigraphy.

PS-558

¹D. Huić, ¹D. Dodig, ²B. Labar, ²D. Nemet, ³V. Ivančević, ³D.L. Munz
Clinical Departments of ¹Nuclear medicine and ²Haematology,
University Hospital Rebro, Zagreb, Croatia, ³Clinic for Nuclear
Medicine, University Hospital Charité, Humboldt University, Berlin,
Germany

VALIDATION OF BONE MARROW IMMUNOSCINTIGRAPHY IN HAEMATOLOGICAL PATIENTS WITH PANCYTOPENIA

Since recently normal values of bone marrow uptake in bone marrow immunoscintigraphy with the Tc-99m labelled anti-NCA 95 antigranulocyte antibodies (AGAb) have been established the aim of our study was to investigate the discriminative power of bone marrow immunoscintigraphy and bone marrow uptake ratio (UR) in haematological patients with pancytopenia.

Sixteen whole-body bone marrow scans were performed in 15 patients (8 women, 7 men; median age 50 years, range 17-74 years) 5 h after i.v. injection of 370 MBq of AGAb. UR was calculated from the posterior view drawing irregular regions of interest around the sacroiliac and background areas, respectively. The mean UR in patients with pancytopenia was 2.1±1.4 (range 0.4-4.9), this difference from the previously obtained control group of 50 patients (mean UR 7.3±2.3; range 4.4-12.6) being highly significant (p=0). The bone marrow appearance on scans seemed to be characteristic for particular haematological diseases. In myelofibrosis (N=5) bone marrow scans demonstrated diffusely decreased bone marrow activity and increased uptake in the spleen, probably related to extramedullary haematopoiesis. In aplastic anaemia (N=3) highly reduced patchy marrow uptake was observed that persisted even after blood cell counts had recovered to the near normal range. In myeloid leukaemia (N=6) bone marrow patterns were almost normal probably because the target antigen is often expressed on neoplastic myeloid cells. In conclusion, quantitative analysis of bone marrow uptake ratios and distinct patterns of AGAb distribution in bone marrow immunoscintigraphy for particular haematological diseases enhance diagnosis and follow-up of diseases with depression of the central haemopoietic activity.

This work was partially supported by IAEA 302-E1-CRO-9799 grant.

PS-559

V. Ivančević, A. Wolter, S. Sen Gupta, D. Huic, M. Voth, D.L. Munz
Clinics for Nuclear Medicine and Bone and Joint Surgery, Charité, Humboldt
University, Berlin, Germany, and Clinical Department of Nuclear Medicine,
University Hospital Rebro, Zagreb, Croatia

BONE MARROW IMAGING WITH Tc-99m LABELLED MONOCLONAL ANTI-NCA 90 Fab' FRAGMENT AND COMPARISON OF BONE MARROW UPTAKE WITH THE INTACT ANTI-NCA 95 GRANULOCYTE ANTIBODY

The aim of this prospective study was to investigate the accumulation of the Tc-99m labelled monoclonal anti-NCA 90 granulocyte antibody Fab' fragment (AGFab) in the haemopoietically active bone marrow in order to evaluate its usefulness as a bone marrow imaging agent and to compare bone marrow uptake with the well-known intact anti-NCA 95 granulocyte antibody.

Sixty-seven scans of 58 consecutive patients (age range, 12-85 years; median age, 56 years) referred for scintigraphy of inflammation, were included. One and 5 h after intravenous injection of up to 1.1 GBq of AGFab whole-body scans and 10-min planar images of the abdomen and pelvis were performed using a dual-head gamma camera. After 24 h additional planar 20-min images of the abdomen and pelvis were taken. All the scans were evaluated visually and bone marrow uptake was determined semiquantitatively as count density ratio from sacroiliac-minus-background to background area in posterior view. These uptake ratios were compared to ratios obtained from 50 age-matched normal bone marrow scans acquired with the Tc-99m-labelled intact anti-NCA 95 granulocyte antibody.

Sixty scans of 52 patients revealed a physiological activity distribution with activity accumulation in the central bone marrow and in the proximal one-thirds of the humeri and femora. Four patients had a moderate bone marrow extension and in 3 scans of 2 patients (metastasizing breast cancer and plasmacytoma) central bone marrow depression was observed. Bone marrow uptake amounted to 1.30±0.51, 0.87±0.36 and 0.78±0.44 (p<0.0001) after 1, 5 and 24 h, respectively, and was significantly lower than the mean uptake ratio of the intact anti-NCA 95 granulocyte antibody (7.17±0.29, p=0). In contrast to the results obtained with the intact anti-NCA 95 granulocyte antibody, AGFab bone marrow uptake was not dependent on patient age.

In conclusion, bone marrow uptake ratio of AGFab is significantly lower than that of the intact anti-NCA 95 granulocyte antibody and decreases with time. Due to the low uptake ratio reliable detection of bone marrow depression by semiquantitative means seems unlikely. The early AGFab scans can be useful in the visual evaluation of the central bone marrow of the spine and pelvis.

PS-560

Moechini T.O.; Nicoll P.; Messina S.; Palumbo B.; Palumbo I.;
Trottini M.*; Stivaktaki A.*; Romano R.*; Palumbo R.

University of Perugia; Department of Nuclear Medicine and
*Institute of Internal Medicine and Oncology Sciences.

67 GA SCAN CAN PREDICT DISEASE-FREE SURVIVAL AND OVERALL SURVIVAL AFTER THERAPY IN LYMPHOMA PATIENTS

In patients with malignant lymphoma localized above the diaphragm the capacity of 67Ga-scintigraphy to predict disease-free interval and survival after treatment with chemotherapy and/or radiotherapy was evaluated. METHODS: Seven of 42 pts were not evaluated: 4 had too short follow-up and 3 died from other causes. 35 pts, 20 males, 15 females (range 14-66yrs, mean 35 yrs) entered the study. 22 had Hodgkin's disease (HD) and 13 non-Hodgkin's lymphoma (NHL). The mean follow-up was 18 months (range 6-51). Diagnostic evaluation was routinely performed in the chest and head-neck regions by clinical examination, laboratory assessment, biopsy, histopathologic and immunophenotype analyses according to REAL classification and standard x-ray, CT, or MR. All patients were examined after the last therapy cycle. Planar scan and SPET were begun 48-72 hrs after i.v. injection of 222-296 Mbq 67Ga-Citrate. Patient clinical score was as follows: death, continuing disease, partial remission (disappearance of the disease in situ above the diaphragm) and complete remission. Correlation between Ga scan results, response to treatment and survival was evaluated.

RESULTS:

	67Ga	CT/RM
True-positive	12	12
True-negative	22	11
False-positive	1	12
False-negative	0	0
Sensitivity(%)	100	100
Specificity(%)	95	48

Of 13 positive 67Ga scan pts 6 are dead, 6 are in continuing disease and 1 in remission. Of 22 negative pts, 22 are in remission. The mean disease-free interval was calculated for 17 of 22 negatives as 22 months (range 7-51). 5 pts were not evaluated due to too short an interval (2,3,4,5,5 mths).
CONCLUSIONS: 67Ga scan is an accurate indicator to detect the presence of viable tumors and a reliable means for predicting good response to treatment in terms of disease-free and overall survival.

Poster presentations

PS-561

S. Kanayev, S. Novikov, L. Leenman, L. Jukova, K. Pozharisski. Research Institute of Oncology, Department of Radiation Oncology and Nuclear Medicine, 189646, Pesocny-2, St.-Petersburg, Russia.

SCINTIGRAPHY WITH ^{99m}Tc-COLLOIDS IN ASSESSMENT BONE MARROW HAEMATOPOIETIC ACTIVITY.

PURPOSE: To evaluate suggestion that bone marrow (BM) scintigraphy (BMS) with radiocolloids can be effectively used for semiquantitative estimation of BM haematopoietic activity.

METHODS: BMS and bone marrow biopsy (BMB) were performed in 88 patients with cancer. BM images of iliac bones were obtained in posterior projection 45-60 min after i/v injection of 8-10 MBq/kg of ^{99m}Tc-colloids. For BMS we used grading system that ranked intensity of BM tracer uptake (TU) from 1 to 4: 1 - absence of BM image (TU on the level of background), 2 - smooth image of iliac BM (markedly diminished TU), 3 - sharp borders of iliac BM with slightly reduced TU, 4 - normal BM scan. Results of BMB were classified in the following way: 1 - aplasia, 2 - severe hypoplasia (cellularity <10%), 3 - hypoplasia (cellularity 11-40%), 4 - normal BM cellularity (>40%).

RESULTS: Seven of eight patients with 1-2 BMS grades had aplasia or severe hypoplasia of BM on biopsy; in one case - BM hypoplasia was moderate (grade 3). Normal or slightly reduced TU associated with biopsy grades 3-4 in 74 patients and with biopsy grades 1-2 - in another 6 cases. Three of this six patients had normal peripheral blood counts at presentation and during follow-up and were considered as BMB sampling errors. Overall, BMS and BMB results agreed in 81 of 88 (92%) evaluated patients; BM activity was correctly estimated by BMS in 84 of 88 (95%) patients.

CONCLUSION: BMS with radiocolloids can be used for semiquantitative estimation of BM haematopoietic activity.

PS-562

RE O'Mara, VU Chengazi, DHP Streeten and DS Bell

University of Rochester, Division of Nuclear Medicine

RED CELL MASS AND PLASMA VOLUME IN CHRONIC FATIGUE SYNDROME

Purpose: Chronic fatigue syndrome (CFS) is an illness of unknown etiology characterized by orthostatic intolerance, profound exhaustion and numerous somatic complaints. The syndrome may occur in adults and children despite normal or minor abnormalities on physical exam and routine laboratory studies. The authors chose to evaluate the contribution of the determination of red cell mass and plasma volumes in these patients.

Methods: 19 patients, 15 female and 4 male, were studied after meeting the clinical criteria established by the Center for Disease Control for CFS and had a severity criteria of <5 hours of upright activity daily. RBC mass and plasma volume (PV) were determined with standard methods utilizing 40-50 uCi of Cr-51 labeled red blood cells and 5 uCi of I-125-RISA. The red cell mass was below the normal range in 14 of the 15 female patients and in 2 of the 4 males. In the 15 female patients, the RBC mass was below normal range and significantly lower than the 20 normal female subjects reported in the literature (p<0.001). The small number of males precluded any determination of statistical significance. PV was quite variable; being below the normal range in 10, normal in 3 and elevated in 2 of the female subjects. A similar spread was found in the male group.

Conclusion: The determination of normal peripheral hematocrit does not preclude CFS. The determination of a whole body hematocrit (the red cell mass/total blood volume) is necessary to relate to the diagnosis of CFS. The exact role that a sub-normal RBC mass and/or decrease circulating blood volume plays in this disease has yet to be determined conclusively and needs further study.

PS-563

KS Yoo, VU Chengazi, RE O'Mara

University of Rochester Division of Nuclear Medicine

DIAGNOSING AND FOLLOWING POLYCYTHEMIA IN POST RENAL TRANSPLANT PATIENTS UNDERGOING THERAPY WITH ENALAPRIL

Purpose: Polycythemia is a complication seen in renal transplant patients (4.3-15% incidence). Clinical suspicion and elevated peripheral hematocrit are not accurate enough alone to achieve a diagnosis. The use of combined red cell mass and plasma volume is necessary for the diagnosis of true polycythemia versus other causes of elevated hematocrit.

Methods: Twenty-two renal transplant patients with elevated hematocrit (>51%) were evaluated. Red cell mass was calculated utilizing approximately 50 uCi of Cr-51 sodium chromate to label red cells in a modified in vivo technique while the plasma volume was determined after the intravenous injection of 5-10 uCi of I-125 RISA.

Results: Eleven out of twenty-two patients demonstrated true polycythemia. All have undergone therapy with Enalapril 2.5-5 mg QD and followed by repeat studies which demonstrated reduction in RBC mass. The main cause of elevated hematocrit in the other post-transplant patients was reduced plasma volume. Post-treatment RBC masses were significantly lower than pre-treatment using a paired t-Test (p = 0.0001). Combined red cell mass and plasma volume determinations have demonstrated reduction of the red cell mass post therapy.

Conclusion: Simultaneous determination of red cell mass and plasma volume is an accurate, reliable and reproducible method of diagnosing and following polycythemia in post renal transplant patients who are candidates for therapy with Enalapril.

PS-564

D. Vassileva, *S. Sergieva, Y. Zhetchev, G. Arnaudov, *M. Beeva National Centre of Haematology and Transfusiology, *National Oncology Centre, Sofia, Bulgaria

SOMATOSTATIN RECEPTOR SCINTIGRAPHY, SERUM BETA-2 MICROGLOBULIN AND SERUM THYMIDINE KINASE IN PATIENTS WITH HODGKIN'S DISEASE

Precise staging is important in the treatment and prognosis of patients with Hodgkin's Disease (HD). The purpose of this study was to assess the value of Somatostatin Receptor Scintigraphy (SRS), serum beta-2-microglobulin and serum thymidine kinase in patients (pts) with HD and the correlation between them. 25 pts with HD were investigated. Planar images and/or SPECT were performed 24 and 48 hours after i.v. injection of 110-185 MBq ¹¹¹In labelled octreotide (Mallinckrodt, Petten) on the rotating gamma camera. SRS results were compared with the data of conventional methods (clinical examination, x-ray CT, bone marrow biopsy). Beta-2-microglobulin levels were measured by radioimmunoassay using the Immunotech international microtest. Thymidine kinase in serum was determined using Prolifigen radioenzyme assay (Sangtec, Sweden). In 21 of all 25 pts SRS was true positive. Fifty three lesions were identified, 14 of them were with extranodal localization. In 3 pts 4 additional unsuspected lesions were detected with SRS. Clinical stage of all these pts were changed according to Ann Arbor classification. Significant correlations were found in pts with true positive SRS and higher serum beta-2-microglobulin and serum thymidine kinase levels in pts with advanced disease as well as in patients with B-symptoms. In 1 pt a false positive results on the SRS was found. True negative scans were obtained in 3 pts. Increased value of beta-2-microglobulin and thymidine kinase were found in some pts with true negative SRS (clinical appearance of the disease was demonstrated in 1 pt two months later). In conclusion, SRS provides a sensitive non invasive diagnostic modality to localize tumour tissue of Hodgkin's Disease and the positive scintigraphy shows a good correlation with the data of serum beta-2-microglobulin and serum thymidine kinase in different stage of the disease.

Infection/inflammation/hematology: Infection/inflammation

PS-565

K.K. Akerman¹, K.A. Bergström¹, J.T. Kuikka¹, N. Çiftçioglu², J. Parkkinen³, A. Kukko¹, E.O. Kajander². ¹Department of Clinical Physiology, Kuopio University Hospital, ²Department of Biochemistry and Biotechnology, ³Department of Pathology, University of Kuopio, P.O.Box 1777, FIN-70211 Kuopio, Finland.

RADIOLABELLING AND IN VIVO DISTRIBUTION OF NANOBACTERIA IN RABBIT

Nanobacteria are minute bacteria recently isolated from mammalian blood having a property of producing apatite mineral around them, which distinguished them from other known contaminants present in animal sera after sterile filtration. Nanobacteria cause normal immune response, and could be immunostained with specific antibodies. Taxonomically they are placed into the alpha-2 subgroup of Proteobacteria. The structure of nanobacteria have been investigated with light and electron microscope. In light microscope they were seen as tiny coccoid particles, during culture they became more visible, optically opaque and bigger. In electron microscope the nonadherent nanobacteria were irregular-shaped, rough coccoid particles with a diameter of 200-500 nm. In older cultures the nanobacteria were surrounded with rough envelope showing fibrils and crystals resembling hydroxyapatite.

Nanobacteria was cultured in vitro and radiolabelled with ^{99m}Tc for studies of in vivo distribution with Single Photon Emission Computed Tomography (SPECT) imaging. A 25 µl wet pellet of nanobacteria from bovine origin was incubated for 20 minutes with SnCl₄*(H₂O) in water solution. The pellet was separated, washed and incubated with 30 mCi of ^{99m}TcO₄⁻ for 30 minutes. The labelling yield was over 30%. The previously prepared monoclonal antibody against the structures of nanobacteria was also labeled with radioiodide in order to develop future radiolabelling methods.

Two rabbits were studied with ^{99m}Tc-labelled nanobacteria. Dynamic planar imaging was performed in AP-position immediately after injection of tracer. Serial SPECT scans were further acquired up to 24 h and one planar image was taken at 45 h. A control study was performed administrating a similar dose of ^{99m}Tc-labelled albumin nanocolloids. Regional nanobacteria-to-nanocolloid ratios were calculated along with time.

After 45 h of injection rabbits were sacrificed tissues were removed, analyzed for radioactivity and stained for nanobacteria. The main finding was that radiolabelled nanobacteria remained intact and showed a tissue specific distribution with a high accumulation to the kidneys and urine. Spleen, stomach, heart and intestine had increased uptake of nanobacteria, too. Extraction into urine started 10-15 min after injection, and resulted in live nanobacteria in urine, which showed increased ability to penetrate into cells in vitro. Penetration in urine was via tubular cells because nanobacteria was found in the cytoplasm and on the tubular surface. The results suggest that nanobacteria use endocytic transport of tubular cells and might have a role in the pathogenesis of mineral formation in mammals, (kidney stones).

PS-566

K. Anzola, A.Llamas-Olier, M.Pabon, D.Paez.

Departments of Nuclear Medicine, Clinica Reina Sofia, SantaFe de Bogotá and Fundación Valle de Lili, Cali, Colombia.

DIAGNOSIS OF INFECTIOUS DISEASE USING Tc-99m-HUMAN POLYCLONAL IMMUNOGLOBULIN G.

Technetium-99m radiolabeled nonspecific human polyclonal immunoglobulin-G is one of the recently studied radiocompounds for inflammation imaging. In the present study, we assessed the diagnostic accuracy of radiolabeled IgG in routine clinical practice. **Methods:** Seventy-two patients with suspected inflammatory/infectious processes were injected with twenty millicuries of Tc-99m-IgG withdrawn from a reaction vial containing 1 mgr of the reagent linked to iminothioline (HIG, Mallinckrodt r). Studied sites included: bone and joint (n=48), pulmonary (n=6), abdominal (n=10) or elsewhere (n=8). Imaging was performed at 4,8 and 24 hours postinjection. A three-phase bone scan was undertaken on every patient with presumable bone or joint disease. **Results:** The normal biodistribution of Tc-99m-IgG occurs in highly vascularized organs. A good target-to-background ratio is obtained at the appendicular skeleton. Forty-eight patients with presumable bone or joint disease were assessed: 19 true positive, 21 true negatives, 5 false positives, 1 false negative and 2 unevaluable studies were obtained. The HIG-scan clearly identified infectious sites related to chronic osteomyelitis and was useful in patients who had not sustained trauma or surgery in the previous 8 months; on the other hand, it could not differentiate between aseptic or septic inflammation when it was performed shortly after trauma or surgery. The polyclonal IgG scan had a sensitivity of 95%, a specificity of 80% and a negative predictive value of 95%. Six patients with pulmonary infections were analyzed obtaining a low sensitivity (16%) for this purpose, probably explained by the biodistribution of the agent. Ten patients with abdominal disease were scanned obtaining 4 true positives, 1 true negative, 2 false positives, 1 false negative and 2 equivocal studies. Sensitivity was 80% with a 33% specificity. **Conclusions:** HIG-scan is a highly sensitive method for detecting inflammatory and infectious sites. It is attractive for bone and joint imaging, for assessing joint replacements, pseudoarthrosis longer than 8 months and chronic or low-virulence infections. However it is not recommended as a first line method to assess soft tissue inflammatory disease.

PS-567

M. Pourdehnad, A. Bhatnagar, A. Alavi, M. Rossman

Hospital of the University of Pennsylvania, Philadelphia, PA (USA)

18-FLUORODEOXYGLUCOSE POSITRON EMISSION TOMOGRAPHY IN THE MANAGEMENT OF PATIENTS WITH SARCOIDOSIS

Purpose: There is currently no accepted method for monitoring disease activity in patients with sarcoidosis. Lack of concordance between serum angiotensin converting enzyme (ACE) levels, Gallium-67 scanning and bronchoalveolar lavage findings has been well documented, and chest radiographs are not adequately sensitive. It is now well known that inflammatory cells take up increasing amounts of 18-FDG when stimulated but limited data exists for the use of FDG PET to stage disease and monitor activity in Sarcoidosis. Our aim was to evaluate the efficacy of FDG PET imaging in patients with Sarcoidosis.

Methods: Eight PET scans were obtained on 6 patients referred with a confirmed diagnosis of Sarcoidosis to define extent of disease and assist in their management. All PET studies were performed on a PENN PET 240H scanner after injection of 0.114mCi/kg 18-FDG intravenously. Attenuation correction was performed using a Cesium-137 single photon emitter source. Standardized uptake values (SUV) were obtained for abnormal areas.

Results: Five of the 6 initial studies performed were markedly abnormal showing active disease involving lymph nodes, lung parenchyma or intra-abdominal sites in more areas than suggested by other modalities. The SUVs ranged from 2.7 to 15.9 (mean 6.92). Decisions regarding treatment were based on a combination of clinical judgment, PET scan, and in some patients chest x-ray findings, serum ACE levels and pulmonary function tests (PFTs). Four patients were treated with varying doses of steroids. One with abnormalities limited to the hila was not treated as there was no parenchymal involvement, PFTs were normal and the patient was not symptomatic. One patient had a negative study except for prominence of the spleen and had an abnormal ACE level and chest x-ray. Based on the PET results, he was not treated. All patients have shown significant improvement based on clinical evaluation. In two cases, follow-up PET showed improvement with decreased number and intensity of lesions (decrease in SUV values by 40%). The patients are doing well on lower doses of steroids.

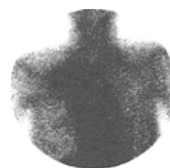
Conclusion: Based on our preliminary data, FDG PET as a single diagnostic study appears to provide comprehensive information regarding extent of disease and disease activity. Further prospective studies are needed to define the role of FDG PET for initial staging of patients and to monitor disease activity.

PS-568

BRAGA, FJHN; Arbex, MA; Haddad, J and Bonini, EH. CORA and, Hosp. Nestor Goulart Reis, Araraquara, Fis. Méd, FFCL and Centro de Ciências das Imagens e Física Médica, Fac. Med. Ribeirão Preto - USP. BRAZIL.

99mTc-GLUCO-HEPTONATE SCINTIGRAPHY (GH S) IN LUNG TUBERCULOSIS (tb) PATIENTS (pts): initial results.

The number of pts suffering from tb is increasing dramatically now-a-days. Lungs are far the most frequently affected organs. Conventional X-ray studies detect lung disease but it is not rare that this method is not able to gauge whether it is active or not. GH is a glucose analogue and it was expected that this radiopharmaceutical would be taken up by active tb lesions. We have studied 14 pts (31-72 y o) with highly suspected active tb as determined by the clinical and laboratorial-radiological findings, and 2 (45 and 58 y o) with proven pulmonary fibrosis caused by treated tb.



Each pt was injected with 750 MBq of 99mTc-GH and anterior, posterior and lateral images were acquired 3 h later (500,000 counts/image). GH S was abnormal in all cases in which clinical and radiological findings were positive but it was negative in the 2 other ones. We noted two scintigraphic patterns: a) focal, extensive, moderate-important uptake was detected in 12 pts (figure, abnormal uptake in the upper third of right lung.) and this was interpreted as focal active tb; b) diffuse and bilateral mild-moderate uptake and this was interpreted as active miliary tb. Comparison with chest X-rays showed that many radiologically abnormal areas were scintigraphically normal, meaning that these areas were probably free of disease. The two cases of miliary tb had radiological correspondance. Comparison with 67-Ga S and biopsies need to be performed in further studies but it seems that GH S is a good tool to differentiate active from inactive tb. The main advantages of GH S as compared to the 67-Ga one are the short time of diagnosis and its little cost.

PS-569

M. Larikka, A. Ahonen, J. Junila, H. Syrjälä

Oulu University Hospital, Oulu, Finland / Department of Clinical Chemistry, Department of Surgery and Department of Infection Control

DIAGNOSIS OF HIP PROSTHESIS INFECTION USING EXTENDED WHITE BLOOD CELL AND BONE GAMMA IMAGING

Combined ^{99m}Tc -white-blood-cell and ^{99m}Tc -MDP-imaging was done to 58 hip prosthesis patients of whom 20 had bilateral prosthesis. Indication was suspected prosthesis infection or loosening based on clinical and radiological examination. The imaging results were compared to intraoperative bacterial aspiration of the prosthesis site if available and otherwise to clinical follow-up of at least 1 year. ^{99m}Tc -white-blood-cell images were obtained between 2 to 4 hours and at about 24 hours post injection. Bone images were obtained in blood flow, early and bone metabolic phases. Intensity of uptake in different zones around the prosthesis was scored. If the ^{99m}Tc -white-blood-cell image score was higher than ^{99m}Tc -MDP bone image score the prosthesis was interpreted as infected. If the ^{99m}Tc -white-blood-cell image score was not higher than ^{99m}Tc -MDP bone image score the prosthesis was interpreted as non-infected and probably loose.

The number of intraoperatively confirmed infections was 5. The operations were done from 9 days to 4,5 months after the imaging. Dynamic bone images were positive in 16 of 57 studies. All the studies with bacteriologically confirmed infection were pathological, but the specificity was only 31 %. The comparison of the early leukocyte images with bone metabolic images gave a positive result in respect to infection criteria in 10 of 59 studies, but only two of these patients had bacteriologically confirmed infection. The same comparison with the late leukocyte images gave a positive result in 4 of 41 studies. These positive results included 3 confirmed infections and one false positive case. The confirmed infections had focally increased leukocyte uptake while the false positive case had diffusely increased uptake. Six false positive patients in the early images had also 24 hour imaging done and in all of them leukocyte uptake diminished in the late images.

It is concluded that dynamic bone imaging is sensitive but not specific in detecting hip prosthesis infection. We used a systematic scoring method for comparing leukocyte and bone images to get objective results in static imaging. The results of the early images were not satisfactory. The 24 hour leukocyte images facilitated observation of time trend and pattern of leukocyte uptake and improved clinical usefulness.

PS-570

K. Liewendahl, M. Löfberg, A. Lamminen, O. Korhola, H. Somer

Helsinki University Central Hospital, Division of Nuclear Medicine, Department of Neurology and Department of Radiology, 00290 Helsinki, Finland

DIAGNOSIS AND FOLLOW-UP OF INFLAMMATORY MYOPATHIES WITH ANTIMYOSIN SCINTIGRAPHY AND MAGNETIC RESONANCE IMAGING

Patients with polymyositis ($n = 16$) or dermatomyositis ($n = 1$), verified by biopsy, were examined with antimyosin immunoscintigraphy (IS) (In-111-labelled antibody from Centocor B.V.) and low-field MRI utilizing T1- and T2-weighted sequences. Both examinations were repeated 6 to 22 months after drug therapy. The diagnostic efficacy of these two methods was evaluated by comparison with clinical examination and creatine kinase (CK) levels. At diagnosis all patients had increased uptake of antibody in the lower extremities in at least one muscle group. In T2-MRI images increased signal intensity changes reflecting intramuscular edema and inflammation were found. After drug therapy the uptake of antibody and the signal intensities in T2-MRI had decreased, but there was no significant correlation between semiquantitative IS and MRI data. Uptake of antibody correlated with serum CK both at diagnosis ($R = 0.48$, $p = 0.05$) and follow-up ($R = 0.71$, $p = 0.004$). There was no correlation between the findings in T2-MRI and the CK levels. The kappa value for interobserver variation was 0.55 for IS and 0.71 for MRI. In T1-weighted MRI the signal intensity changes reflecting intramuscular fatty degeneration were more pronounced at follow-up than at diagnosis. Mean CK levels decreased from 1664 (SEM 564) U/l to 238 (59) U/l as the clinical condition improved.

Conclusions: IS and MRI are sensitive methods for detection of lesions caused by myositis. IS findings correlate with serum CK levels and therefore reflect disease activity better than MRI findings. IS may reduce the need for muscle biopsy at follow-up.

PS-571

H. Moustafa, K.H. Mohamed, Sh. Hantar and A. Abd El-Hakim

Dept. of Nuclear Medicine & Chest in Kasr El Aini Hosp. Cairo University, Egypt.

^{99m}Tc -INFECTON AND Tc-HIG IN EVALUATION OF DISEASE ACTIVITY IN PATIENTS WITH TUBERCULOSIS.

A prospective study of 29 patients with tuberculosis in chest (24 cases) and abdomen (5 cases) proved by bronchial lavage and septum analysis on biopsy from nodules in abdomen. ^{99m}Tc -infecton and ^{99m}Tc -HIG were given intravenous in a dose of 740 mBq (20mCi) with imaging at 1, 4 hours. Images were correlated with clinical radiologic and laboratory data for assessment of disease activity. ^{99m}Tc -Infecton and ^{99m}Tc -HIG showed true positive results in 26, 22 patients respectively and false negative study in 2,5 patients. A single case of true negative case proved to be lung cancer by bronchial biopsy. The sensitivity, specificity and accuracy of ^{99m}Tc -infecton were 92.8, 100% and 89.6% whereas Tc-HIG had 78.6%, 100%, 75.9% respectively. 10 patients were followed up for 6 months after therapy with anti-tuberculous therapy. Complete resolution of active lesions was seen in all patients with Tc-infecton, whereas ^{99m}Tc -HIG showed residual activity in 4 patients.

To conclude both ^{99m}Tc -infecton and Tc-HIG can be used in assessment of disease activity in tuberculous patients, however Tc-infecton had better results specially in follow up of treatment response.

PS-572

N. David, P.Olivier, B. Lehalle, N. Hassan, P.Y. Marie, G. Fieve, G. Karcher, A. Bertrand.

Nuclear Medicine and Vascular Surgery Departments. CHU Nancy, France

POTENTIAL DIAGNOSTIC CONTRIBUTION OF MDP-BONE SCAN IN SUSPECTED VASCULAR GRAFT INFECTION

Vascular graft infection is a critical situation, often subtle in presentation. Its diagnosis should be made early to avoid the associated major complications.

Several individual case reports of secondary hypertrophic osteoarthropathy (HOA) accompanying arterial prosthesis infection were published, some of whom depicted by bone scintigraphy. The aim of our study was to evaluate prospectively, using a bone scan, the frequency of the association between vascular graft infection and HOA, and thus to assess the potential diagnostic contribution of MDP bone scan in case of suspected vascular graft infection.

During a 18 months period, patients admitted in Vascular Surgery Department, for suspicion of arterial graft infection were prospectively considered. The following data were collected: clinical data, laboratory investigations and blood cultures, CT scan or sonography, and bone scintigraphy. Bone scintigraphy including whole body scan and static views centred on lower limbs was performed after injection of 740 MBq of ^{99m}Tc -MDP. Each scan was considered for the presence of signs associated with HOA on bones downstream from the considered vascular graft. These signs are represented by pericortical linear accumulation of tracer along the shafts of long bones and by increased periarticular uptake. All patients were surgically explored irrespective of bone scan results.

Study population included 17 patients (16 men), mean age: 65.8 ± 18 years (54 to 84 years). 12 patients presented with biological inflammatory signs, 11 with a local suppuration, 10 with a septic syndrome, 2 with an intestinal bleeding and 2 with septic distant metastasis. The interval from graft procedure to the hospital admission was 4.8 ± 8 years (1 month to 13 years). After surgical exploration, infection could be confirmed in 13 patients and excluded in the remaining 4 patients. Out of 13 infected patients, 8 had a pathologic bone scan whereas all 4 noninfected patients had a normal scan.

These preliminary results suggest bone scan should be considered in initial management of patients with suspicion of arterial graft infection. Scintigraphic abnormalities could represent an indirect additional argument for vascular graft infection and in our study, a pathologic bone scan seems to have a high specificity regarding this diagnosis.

PS-573

V.Soukhov, N.Fadeev, I.Tcherepanin, G.Khubulava
Central Reseach Institute of Roengenology and Radiology,
Military Medical Academy, St.Petersburg, Russia

PROSTHETIC VALVE ENDOCARDITIS: DIAGNOSIS WITH 99mTc-LABELED WBC AND SPECT.

The study was performed to assess the clinical value of SPECT with 99mTc-HMPAO (hexamethylpropilenaminooxime) labeled autoleucocytes in patients with intermittent fever of unknown origin. Twenty four patients (6 females and 18 males) aged 16-56 years with suspected prosthetic valve endocarditis (PVE) were evaluated. For the determining the source of fever each patient underwent CT, MRI and echocardiography, but because of the inadequacy of these diagnostic procedures whole-body scanning and SPECT of thorax were performed using 99mTc-leucocytes. In 1, 3 and 24 hours p.i. inflammatory foci were seen as the areas of pathogenic activity. In 7 patients the circumscribed activity seen in relation to heart valves convincingly demonstrated abscesses 8-15 mm in diameter. Two patients had the scintigraphic evidence of pancarditis. Considering these findings the diagnosis of PVE was settled and lately was proven by surgery. The rest patients showed a negative scan over the heart correlated with echocardiographic data, but whole body scanning revealed extracardiac infection (frontitis, sphenoiditis, ulcerative colitis, cholecystitis, empyema of pleura and mediastinitis). The data demonstrated that 99mTc-leucocytes imaging is a highly sensitive and specific (both 100%) for the detection of inflammatory heart diseases and also noncardiac infection.

PS-574

A. Tutus, M. Nardali, M. Öztürk, K. Unlühızarıcı, F. Bayram.
Erciyes University, School of Medicine, Depts of Nuclear
Medicine, Radiology and Endocrinology, Kayseri, Turkey.

TECHNETIUM-99M-NANOCOLLOID SCINTIGRAPHY IN DIABETIC FOOT INFECTIONS: A COMPARISON WITH MRI, THREE-PHASE BONE SCINTIGRAPHY AND PLAIN FILM RADIOGRAPHY.

Osteomyelitis of the foot is a well-known important complication of diabetes mellitus. The diagnosis of pedal osteomyelitis is often complicated by the presence of pre-existing bony abnormalities in diabetic patients. The aim of this study was to evaluate the diagnostic role of Tc-99m nanocolloid scintigraphy for the detection of complicated pedal osteomyelitis. The results were compared with MRI, three-phase bone scintigraphy, and plain film radiography. Forty patients (30 female, 10 male, mean age: 55±6.2) were included in this study. All patients underwent Tc-99m nanocolloid, Tc-99m MDP three-phase bone scintigraphy, MRI and plain film radiography. Total 54 foot lesions were detected. According to final diagnosis which was established by pathology or clinical follow-up, there were 24 osteomyelitis, 14 neuroarthropathy and 14 cellulitis. The diagnostic sensitivity, specificity and accuracy were %88, %89, and %88 for Tc-99m nanocolloid scintigraphy; %84, %92 and %88 for MRI; %96, %71 and %83 for three-phase bone scintigraphy; %65, %64 and %65 for plain film radiography, respectively. We conclude that Tc-99m Nanocolloid scintigraphy is a highly sensitive and specific test for the detection of pedal osteomyelitis as a safe and easily prepared technique. It has better diagnostic accuracy than three-phase bone scintigraphy, plain film radiography and more cost-effective than MRI.

Paediatrics

PS-575

A. Biggi*, L. Dardanelli, P. Cussino, R. Basta, O. Sernia, G.F. Camuzzini.
S.Croce Hospital:Nuclear Medicine* and Paediatrics -Cuneo;Division of Paediatrics -Savigliano - ITALY

REFLUX AND NON REFLUX PYELONEPHRITIS IN CHILDREN: THE FOLLOW UP OF THE AT "RISK KIDNEY".

Purpose of the study : we conducted a prospective clinical study in order to evaluate the degree of recovery of function of the "at risk" kidney in children with proven urinary tract infection (UTI) and the relationship among vesicoureteral reflux (VUR) and cortical scarring. Methods: 72 children (41 female, 31 male), 3 weeks - 8 years of age, with a proven UTI (positive urine culture, signs, symptoms and biological parameters of infection) underwent DMSA scan in acute phase and radionuclide cystography 1 month later. Treatment of children with a positive DMSA scan includes parenteral and oral therapy for one month. A follow-up scan was performed 6 months after the acute phase in children with a positive acute DMSA scan. Results: in the acute phase defects were observed in 61/144 kidney (42%), 22/61 (36%) with and 39/61 (64%) without VUR. In 11% of kidney, VUR without a positive scan was documented. Both in male and female the incidence of VUR in children less than 1 year old was found higher than in the older (67% vs. 33%); a positive DMSA scan was found in 83% of male and in 41% of female less than 1 year old. After six months a defect persists in 28/144 kidney (19%), 15/28 (54%) with and 13/28 (46%) without VUR. Conclusion: most of the children with a proven pyelonephritis (PNA) do not have VUR; rapid and prolonged treatment of PNA obtain a complete recovery of function in 54% of the "at risk kidneys"; recovery of function is unrelated to the sex and age of the children. The presence of VUR probably reduce the possibility of recovery of function after PNA.

PS-576

M.R.Castellani*,C.Colombo°, L. Maffioli*, S.Comi°, M.L. Melzi°, E.Bombardieri*.
* Nuc.Med. Division, Istituto dei Tumori of Milan;° Departments of Pediatrics, Universities of Milan and Sassari

Br-IDA SCAN IN CHILDREN WITH CYSTIC FIBROSIS (CF): A TEST TO PREDICT TREATMENT RESPONSE

During the last 8 years 36 patients with liver disease associated to CF, who were selected for the therapy with choleretic bile ursodeoxycholic acid (UDCA), has been systematically monitored with Br-IDA scintigraphy, repeated at 1-2 years intervals (in total 97 scans), with the aim to correlate the basal hepatobiliary findings with possible modifications induced by UDCA therapy. After i.v. injection of 37-148 MBq of 99mTc-Br-IDA, analogic and digital images were acquired for 60 min, using a large field of view gamma camera. Further images were collected in case of a delay in the visualization of the intestine or to study gallbladder emptying. Morphological abnormalities and functional parameters [time of intestine visualization (TIV); hepatic half-life time (HT), determined by the ROI method], were recorded for each examination. The results were compared with clinical, biochemical and ultrasonographic findings. On the baseline scan morphological abnormalities were present in 35 pts (97%), prolonged HT(>20 min) in 14 (40%) and prolonged TIV(>20 min) in 18(50%). TIV, which may provide information on the pattern of biliary drainage proved to be the most important predictor of treatment failure (22% in pts with abnormal TIV vs 61% in pts with normal TIV; Odds Ratio [95% CI] 5.50 [1.32-22.70]). In our opinion Br-IDA allows the selection of patients eligible for UDCA therapy, on the basis of the TIV results.

PS-577

B. Değirmenci, S. Miral, G. Çapa, H. Durak, L. İyilikçi, Z. Aydın, A. Baykara

Dokuz Eylül University, Medical School, Departments of Nuclear Medicine and Pediatric Psychiatry

TECHNETIUM- 99m HMPAO SPECT IN AUTISTIC CHILDREN AND THEIR FAMILIES

Autistic disorder is a severe developmental disorder characterized by deficits in verbal and nonverbal language, social skills, cognitive functioning and on abnormal repertoire of behaviours. Neurobiological mechanisms that underlie of this disorder is not well-understood. It has been reported that genetic factors play a role in autism.

The purpose of this study was to investigate the perfusion patterns in autistic children (AC) and their family, and to compare the perfusion alterations of AC and their families. Ten children (9 boy, 1 girl ; mean age 6.9±1.7) with autistic disorder defined by DSM-III-R criteria, age-matched 5 children (3 boy, 2 girl) as a control group and the volunteer family members of 8 AC were included in the study. Brain perfusion images were obtained with triple-head gamma camera equipped with high resolution collimators. In order to prevent motion artefacts, general anaesthesia was given all the AC. 370-444 MBq of Tc-99m HMPAO was injected at least 30 minutes prior to general anaesthesia. During the injection phase, the AC were in their usual state of behaviour. For adult study, 925 MBq Tc-99 HMPAO was used. A total of 128 frames were obtained in 64x64 matrix, 35s/frame and 360° Metz filter (FWHM:11mm) was used for filtering. Motion and attenuation corrections were made. The transaxial, sagittal and coronal slices were obtained parallel to orbito-meatal line. Visual and semiquantitative evaluations were performed. For semiquantitative evaluations, regions of interest (ROI's) were drawn first on right hemisphere and then mirrored ROI's were placed to the left hemisphere. Mean count values per pixel were obtained. ROI's / cerebellum ratios were calculated. All the AC and adults who have perfusion abnormality in brain SPECT had MRI-CT. Hypoperfusion was seen on right posterior parietal cortex in 3 AC, on bilateral parietal cortex in 1 AC, on bilateral frontal cortex in 2 AC, on left parietal and temporal cortex in 1 AC, on right parietal and temporal cortex in 1 AC. The asymmetric perfusion was observed on nucleus caudate in 4 AC. At semiquantitative evaluations, hypoperfusion on right temporal, right frontal, right parietal and left temporal cortices was statistically significant (Mann Withney U, p 0.05). In adult group hypoperfusion was observed on right posterior parietal in 4 parents, on bilateral frontal cortex in 2 parents and on right frontal and left parietal cortices in 2 brothers. The regional perfusion alterations of AC and their families showed similar localisation.

This study suggests that there are regional brain perfusion alterations in AC, especially frontal, parietal and temporal cortices, and their family, even the family members does not have autistic symptoms.

PS-578

RT Dhawan, A Jaffe, R Merwaha, R Buchdahl, J Bailey, M Rosenthal, SR Underwood, A Bush.
Departments of Paediatrics and Nuclear Medicine, Royal Brompton Hospital, London SW3 6NP, UK

DO KRYPTON VENTILATION SCANS ALTER THE CLINICAL MANAGEMENT OF CYSTIC FIBROSIS?

Introduction: Lung function tests are used routinely to monitor patients with cystic fibrosis (CF). Young children however are often unable to co-operate, making the procedure tedious, and one that usually requires sedation. We have routinely used Krypton (Kr-81m) ventilation scans in such children to supplement clinical and radiological assessment, a practice that to our knowledge is restricted to very few centres in the world.

Aim: To evaluate the impact of the ventilation scan (VS) on patient management.

Methods: 38 children (17 male, mean age 4.0 yrs, range 6 months to 6 years) were followed up prospectively between August 1996 and September 1997. Shwachman scores ranged from 65 to 100 (mean 88). Chest X-rays (CXR) were evaluated by Northern scores (evaluating the lungs in 4 quadrants). Clinical scores based on physical signs and VS scores were modelled on similar quadrants, and accorded severity values of 0-2. Blinded, independent observers performed all of the clinical, radiological, and scintigraphic assessments. Modifications to management, by way of microbiological investigations requested, addition of drugs (antibiotics, inhaled steroids), change in physiotherapy techniques, and bronchoscopy were assessed in all patients.

Results: CXR's were normal in 10% (4/38) of the children, and VS was normal in 68% (22/38). Clinical examination did not predict extent and severity of VS or CXR abnormalities. VS detected abnormalities not present on CXR in 18% (7/38) of children. Such additional information was used to guide management. Of the 22 children with normal VS, management was modified in 27% (6/22) whereas in the 16 children with abnormal VS, modifications were made in 75% (12/16).

Conclusion: Ventilation scans provide information additional to that available from CXR and clinical assessment. This information was used to stratify patients, and was frequently used to modify management when ventilation was abnormal. Krypton VS thus offers a simple, non-invasive technique to complement clinical and radiological assessment, and guide management in children with CF, who are unable to undergo conventional tests of lung function.

PS-579

M.Grmek, J. Fettich

Medical Centre Ljubljana, Department of Nuclear Medicine

FOLLOW UP INVESTIGATION AT REFLUXING UNITS (RU) WITH LOW GRADE VESICoureTERAL REFLUX (VUR)

The aim of the study was to evaluate the significance of low grade VUR, detected by cyclic radionuclide cystography (CRC).

In 643 children with 1286 RU, mean age 3 years 74 days (SD 2years 153 days), the CRC was performed for the following problems: urinary tract infection, previously detected VUR or sibling person with VUR. VUR was graded as grade I?-possible reflux into the ureter, grade I-reflux into the ureter, grade II?-possible reflux into the pylon, grade II-reflux into the pylon and grade III-reflux into dilated pylon. The CRC was repeated 1 year 88 days (SD 231 days) after the first investigation. A sequence of 5 sec. images from the beginning until the completion of the study is used for the first and final report.

Table: No. of RU with different grade of VUR at the time of the first investigation and at follow up investigation

First investigation		Follow up investigation					
Grade	No	0	I?	I	II?	II	III
0	315	188	26	35	22	36	8
I?	92	50	16	14	3	8	1
I	203	115	12	36	16	21	3
II?	214	108	15	27	30	29	5
II	352	139	31	42	30	91	19
III	110	18	11	16	15	30	20
No	1286	618	111	170	116	215	56

P values of Chi-square test between group without VUR at the time of first investigation and other groups of VUR are: 0:I? p=0,0787; 0:I p=0,3077; 0:II? p=0,0963; 0:II p=0,0000 and 0:III p=0,0000.

At follow up investigation RU with VUR I?, VUR I and VUR II? didn't statistically significantly differ from RU without VUR p>0,05; so the routine follow up of this groups of VUR is of questionable value.

PS-580

SL JOHNS, SC THOM, LM WILSON, PM KEMP, VJ LEWINGTON,
DEPARTMENT OF NUCLEAR MEDICINE
SOUTHAMPTON UNIVERSITY HOSPITALS NHS TRUST

PAEDIATRIC BONE SCANS- WHO NEEDS THEM?

Emergency paediatric bone imaging is labour intensive and demands expertise of the highest quality to deliver an accurate diagnosis. A retrospective survey was undertaken to establish whether the outcome of paediatric orthopaedic bone scans could be predicted by other investigations. 207 consecutive studies were performed in 1997. Haematology results, radiology reports and clinical notes were reviewed and correlated with the bone scan. 36 referrals for patients with known malignancy were excluded from the analysis, giving 171 orthopaedic studies for suspected infection, pain of unknown cause or trauma .

Results

- 60% (103/171) children had negative haematology ,radiographs and bone scans
- 22% (38/171) children had abnormal haematology and/or radiographs and a positive bone scan
- 15% (25/171) children had abnormal haematology and/or radiographs but a negative bone scan
- 3% (5/171) children had normal haematology and radiographs but a positive bone scan.

The bone scan was normal in 95% (103/108) of children who presented with normal haematology and radiographs. Discordant results (5 positive scans with normal haematology and radiographs) were obtained in two cases of unsuspected fracture, 1 case of Perthe's disease and two cases of non specific post viral synovitis.

Discussion

Bone scintigraphy adds little to the management of children who have normal haematology and radiographs and results in unnecessary radiation exposure. If other investigations are normal requests for bone scintigraphy should be considered jointly by orthopaedic and nuclear medicine staff, as bone imaging is unlikely to contribute to the clinical management in the majority of cases.

PS-581

N.Krivosogov, S.Ivanov, T.Kondrateva

Institute of Cardiology, Tomsk, Russia

POSSIBILITIES OF THE LUNGS CAPILLARY BLOOD FLOW RESERVE IN FALLOT'S TETRAD CHILDREN

The aim of this study was to evaluate the influence of ACE-inhibitors on the capillary blood flow in Fallot's tetrad (FT) children using lung scintigraphy.

Fourteen FT children aged 1 to 12 years with the signs of the I-IIA stages cardiovascular insufficiency were investigated. Lungs capillary blood flow was evaluated using ^{99m}Tc-TCK-8 lung scintigraphy. Bilateral lungs perfusion reduction was shown in all children, what was marked more in one of both lungs. Heterogeneous capillary blood flow was found in standard regions of interest. The mean parameters of pulmonary artery pressure were in norm. These changes were connected with the significant (40-60%) blood shunting to the greater circulation as well morofunctional changes of the pulmonary vessels. Positive dynamics of not functioned capillaries indicators was found in three weeks capoten treatment (1-1,5 mg/kg) in 8 pts because the volume of the blood shunting was not changed. The pulmonary artery pressure was not altered, but indices of the common and regional resistance diminished. Postoperative period in these pts was more favorable then in 6 pts without improvement of the capillary blood flow during the capoten treatment.

Thus, lung perfusion assessment before and after ACE-inhibitors therapy allows to define functional reserve of pulmonary microcirculation and can be used in surgical treatment prognosis in FT children.

PS-582

G.La Cava, ¹D.Seracini, ¹M.Materassi, M.Tommasi, A.Brocchi, C.Olianti

Nuclear Medicine, Dept of Clinical Physiopathology and ¹Dept of Paediatrics, University of Florence

EVALUATION OF ENDOTHELIN EXCRETION IN CHILDHOOD REFLUX NEPHROPATHY

To evaluate the role of endothelin in the glomerular damage progression because of the hyperfiltration due to the renal mass reduction we study the urinary endothelin (U-ET-1) excretion as index of renal production in a group of children with reflux nephropathy. We examined 30 pts (20 M and 10 F, mean age 9.8±4.2 ys) with GFR (Creatinine clearance) ranged from 18 to 120 mL/min/1.73 m² BSA and ERPF (Hippuran clearance) ranged from 114 to 640 mL/min/1.73 m² BSA. In 10 out of these the CRF was of various degree (GFR ranged from 65 to 18 mL/min/1.73 m² BSA); in 11 out of 30 pts we observed a prevalent side damage until anatomic or functional exclusion. As controls we evaluated 30 subjects of similar age. U-ET-1 was measured by RIA method on a urinary 24-hour-sample and it was expressed as daily excretion. The U-ET-1 levels were significantly higher in pts compared to controls (6.2±3.5 vs 3.9±1.4 ng/24 h, p<0.002); in particular, these values were higher in CRF group compared to those found in the other pts and in the controls (9.2±4.1 vs 4.8±1.9 and vs 3.9±1.4 ng/24 h respectively, p<0.0001). There was a significant correlation between the U-ET-1 levels and GFR (r=0.67, p<0.0001) in all groups (pts and controls); moreover in the pts group there was also a significant correlation with ERPF (r=0.57, p<0.001). The variance analysis, using as covariates GFR and ERPF, demonstrated a significant difference in U-ET-1 excretion (8.2±4.3 vs 5.1±2.4 ng/24 h, p<0.004) between pts with prevalent side damage and those with bilateral renal damage. The significant correlation observed between U-ET-1 and GFR and ERPF suggest that this local hormone may play a role in renal haemodynamic. In particular, the significant increase of this peptide excretion in the pts with prevalent side damage and/or in those with CRF postulate a role of U-ET-1 in the hyperfiltration in presence of renal mass reduction.

PS-583

M.Majd, E. Shalaby-Rana, M. Andrich, N. Movassaghi. Children's National Medical Center, Washington, D.C., USA

FUTILITY OF IODINE-131-MIBG SCINTIGRAPHY FOR THE DETECTION OF METASTATIC CENTRAL NERVOUS SYSTEM NEUROBLASTOMA

Objective: To report false negative I-131-MIBG scans in central nervous system (CNS) metastatic neuroblastoma.

Methods: From the database of 57 new patients with neuroblastoma seen in our institution from February 92 to March 98, four patients were identified to have CNS involvement documented by CT or MRI imaging. The whole-body I-131-MIBG scans of these 4 patients were retrospectively reviewed and compared to the CT/MRI studies. MIBG scans were obtained 2 days after intravenous injection of I-131-MIBG (1 mCi/ 1.73 sqm body surface area). The intervals between MIBG scans and CT/MRI studies were 4 days, 8 days, 7 weeks and 11 weeks. All patients were male, with ages ranging from 6 to 52 months (mean 26.3 months). All had stage IV disease at initial diagnosis. CNS involvement was detected at initial diagnosis in 1, and at 12, 13 and 17 months after initial diagnosis in the other 3 patients. Presenting signs and symptoms included vomiting, headache, neck pain and lethargy.

Results: CNS lesions included posterior fossa mass and diffuse intraspinal tumor in the first patient, anterior cranial fossa mass with extension into the frontal lobe in the second, multiple cerebral and cerebellar lesions in the third and a large intraventricular mass with invasion into adjacent parenchyma in the fourth. In all 4 patients, the MIBG scans showed no abnormal intracranial or intraspinal uptake.

Conclusion: I-131-MIBG is not a reliable imaging method to detect CNS metastases in patients with neuroblastoma.

PS-584

MD Mann, H Binns, F Gallie, H Zar, E Weinberg and S Wynchank. Institute of Child Health, University of Cape Town and Red Cross War Memorial Children's Hospital, RONDEBOSCH 7700, South Africa.

A METHOD FOR PERFORMING AEROSOL VENTILATION SCANS IN INFANTS AND YOUNG CHILDREN.

Ventilation scans provide valuable information in the diagnosis and management of pulmonary disorders in infants and children but are not widely used. Infants and young children are unable to co-operate by following specific instructions, and availability of radioactive gases is limited. Aerosol ventilation scans performed using a method based on the procedure for adult patients are often unsuccessful with more activity on the child's face, and in the mouth, oesophagus, and stomach than in the lungs. Some of the problems associated with the use of an aerosol can be overcome by collecting the aerosol in an anaesthetic bag and allowing the child to breathe from the bag through a close fitting mask, as described by O'Brodovich and Coates. A further reduction in contamination, increase in deposition in the lungs and improvement in image quality can be achieved by attaching a spacer device with one way valves to the anaesthetic bag. These spacer devices were developed to improve pulmonary deposition of bronchodilators given by metered dose aerosol inhalers.

We collect the aerosol in a 2l anaesthetic rebreathing bag, which can be sealed. A two-way tap (isolation valve) of the type used in medical gas lines is attached to the proximal end of the bag and a gas flow controller from a Baumanometer to the distal end. The bag is filled with Tc-99m DTPA aerosol by connecting it to a micro Cirrus nebuliser (Amersham Health Care Code N 1430, Amersham International plc, Amersham UK) with a 1m length of corrugated respirator tubing and passing oxygen vertically up through the nebuliser, corrugated tubing and bag at a flow rate of 6 l/min for a minimum of 10 minutes. A plastic tube on the flow valve on the distal end of the bag carries all aerosol passing through the bag to a trapping system. The bag is sealed by closing the Baumanometer flow valve and then the two way tap before being removed from the circuit and attached by the tap to a spacer device. We have used the Aerochamber (Boehringer Ingelheim Inhalation Therapy, Trudell Medical, London, Ontario, Canada) and the Babyhaler (Glaxo Wellcome). The spacers are supplied with a mask that can be replaced by a mouth piece if this is preferred by the patient. The patient breathes from the delivery system - spacer combination for 2 minutes. Activity in the lungs usually reaches plateau within the first 40 seconds, but it is sometimes a little longer in very small patients. In most studies at least 15% of the aerosol in the bag is deposited in the lungs with minimal contamination of the face, mouth, oesophagus and stomach.

PS-585

P.Orellana, P.Baquedano, F.Cavagnaro, C.García, E.Lagomarsino, L.Villarroel.
School of Medicine. Catholic University of Chile. Santiago, Chile

RISK FACTOR OF RENAL DAMAGE IN URINARY TRACT INFECTION

Urinary tract infection (UTI) may produce renal parenchymal damage (RPD) and the damage can subsequently lead to renal failure among others complications. In Chile, about 18% of children with chronic renal failure had chronic pielonephritis. In order to analyze risk factors related to the development of RPD, we retrospectively evaluated the relationship between the presence of RPD; at the static renal scintigraphy, with the age, gender, episode of UTI and presence of vesicoureteral reflux (VUR) in 337 children presenting non recent UTI and followed in our unit for 6 months at least. 237 females and 100 males, with a mean age of 4.2 years (71 < 1 year, 139 aged 1-5 years, 127 > 5 years). 103 were evaluated after the first known UTI. Children with obstructed kidneys and others anatomical anomalies of the urinary tract were excluded. RPD was observed in 161 out of 337 children (47.8%), 75.8% of them had VUR. 49.4% of females and 44% of males had RPD (p=ns). Among 122 children with VUR, 63.2% had RPD vs 27.1% of children without VUR (p<0.0001). In reference to episode of UTI, we found RPD in 35.9% of children with first known UTI vs. 47% in the group of recurrent (2 or more) infection (p=0.004). Related with age, RPD were found in 39.4% of children younger than 1 year, 43.2% of the group between 1-5 years and 57.5% in children older than 5 years (x², p<0.0037). We conclude that RPD are present in almost half of children studied for UTI, and the most important risk factor associated with the development of RPD in children with UTI were VUR, recurrent UTI and age older than 5 years. We suggest that all children with UTI should have a complete imaging study, including renal scintigraphy looking for RPD, irrespective of age, gender, number of infections and presence of VUR.

PS-586

Ş. Özkırlı, İ. Peksoy, B. Erbas, N. Kiper, A. Göçmen, U. Özçelik

Hacettepe University, Medical School. Dept. of Nuclear Medicine

99mTc-DTPA INHALATION SCINTIGRAPHY IN CHILDREN WITH PRIMARY CILIARY DYSKINESIA: CORRELATION WITH CT FINDINGS.

Primary ciliary dyskinesia (PCD), thought to be a genetic disorder, characterised by recurrent otitis media, sinusitis, bronchiectasis, atelectasis, and infertility.

In this study, 18 children with suppurative lung disease (12 F, 6 M) were included. The diagnosis of PCD was performed by the electron microscopic examination of nasal biopsy. Nine of those had ciliar ultrastructural and numerical abnormalities, such as dynein arms defects, transpositions of the microtubules and the ciliary aplasia or hypoplasia. Thorax-CT and 99mTc-DTPA inhalation studies were performed for each patients. Scintigraphic images were stored for 60 min. following inhalation of 25-30 mCi of 99mTc-DTPA. Images were evaluated visually and quantitatively. T1/2 of radioactivity from each lungs were calculated using exponential analysis of time-activity curves. The results were compared with 16 age-sex matched healthy children.

There was a significant difference between T1/2 values of patients with suppurative lung disease and controls (54.72 ± 1.83 min vs 45.19±2.43 min, p=0.005). However, no difference was observed between patients with and without ciliary pathology. In the 14 patients (78%), regional ventilation abnormalities were observed in the corresponding areas of abnormal thorax CT findings. Mostly, lower lobes were affected.

99mTc-DTPA inhalation scintigraphy may provide additional information in the clinical evaluation of patients with suppurative lung disease and primary ciliary dyskinesia.

PS-587

F. Arnello¹, HR Ham², M. Tondeur², A. Piepsz^{1,2,3}

Departments of Pediatrics ³ and Nuclear Medicine ¹, AZ VUB and Department of Nuclear Medicine, CHU St Pierre ², Brussels, Belgium

EVOLUTION OF OVERALL AND SINGLE KIDNEY CLEARANCE IN CHILDREN WITH URINARY TRACT INFECTION DURING AND AFTER THE ACUTE PHASE

The aim of this presentation was to evaluate the functional changes occurring during the acute phase of symptomatic urinary tract infection (UTI) and to compare them to what was observed some months later. Overall as well as single kidney glomerular filtration rate (SKGFR) were estimated using the combination of a left to right uptake ratio obtained from Tc-99m DMSA scintigraphy and a Cr-51 EDTA plasma clearance using a simplified algorithm adapted to the pediatric population. The material analyzed in this retrospective study was obtained from the data of 44 patients with obvious unilateral or bilateral DMSA abnormalities. In patients with unilateral lesions, both the overall clearance and the SKGFR were significantly higher during the acute phase of infection than at control, on the abnormal side as well as on the normal side. The relative percentage uptake was lower on the abnormal side than on the normal side, obviously due to loss of functional parenchyma. This percentage increased significantly at control examination, reflecting the total or partial healing of the renal lesions, despite the significant decrease of SGFR. During both the acute and the remission phase, the relative percentage uptake of the abnormal kidney was nevertheless in the normal range and often close to 50%, suggesting, despite the regional impairment, an intrarenal compensation in the normal parts of this kidney. In patients with bilateral lesions, the differences between acute phase and remission phase were not significant, although a marked decrease of clearance was observed in several patients.

PS-588

H.Pena 1, 2, F.Arnello Viveros 3, HR Ham 4, A.Piepsz 2, 4

Instituto de Medicina Nuclear-FML - Lisboa, Portugal 1, Hospital San Juan de Dios, Santiago, Chile 3, AZ VUB 2 and H. St. Pierre 4 - Brussels, Belgium

EFFECT OF EARLY FUROSEMIDE INJECTION ON THE RELATIVE Tc-99m MAG3 RELATIVE RENAL UPTAKE

Early furosemide injection (F-15=15 minutes before tracer injection; F0=together with the tracer) is sometimes used instead of the classical late injection (F20=20 min after the tracer). The advantages are a shortening in the procedure and, by using the F0 test, a simplified technique because of the simultaneous injection of tracer and furosemide. However, it is well known that the furosemide can considerably affect the tubular function and therefore any absolute measurement of the MAG3 clearance. Some investigators are even injecting furosemide 3 minutes after MAG3 injection (F3) in order to circumvent the problem.

It is not clear whether the relative function determined by MAG3 renography could also be affected, particularly when the function is asymmetrical and the sensitivity of the kidney to furosemide is not identical for both kidneys. The aim of the study was to compare, in children having had several successive MAG3 studies, the left and right relative uptake in both F0 and F20 conditions.

Only MAG3 studies performed after 2 months of age were included and no particular event occurred between two successive tests. In all patients, at least one F0 and one F20 were available, and often more than one. The variability of relative function between F0 and F20 could therefore be compared to the variability of the two control groups (F0 vs. F0 and F20 vs. F20) in the same patients. Relative uptake was measured using the integral method.

Results	F20 vs. F0	F20 vs. F20	F0 Vs F0
Number of cases	22	11	10
Mean of the differences (%)	-0,36	1,09	-0,9
SD of the differences (%)	3,08	4,5	3,1

The relative function using F0 was statistically not different from what was observed using F20 (Power=80%), suggesting that the early injection of furosemide (F0) does not affect the relative function and, as far as this parameter is concerned, can be used in clinical routine.

PS-589

M. Pruckmayer¹, S. Zacherl², U. Salzer-Muhar², M. Schlemmer², T. Leitha¹.

University Clin. of Nuclear Medicine¹ and Paediatrics², University of Vienna, Austria.

PULMONARY BLOOD FLOW PATTERNS AFTER THE PALLIATIVE BLALOCK-TAUSSIG-SHUNT FOR CONGENITAL HEART DISEASE ASSESSED BY LUNG PERFUSION SCINTIGRAPHY.

Introduction: Pulmonary artery architecture and symmetry after palliative operations for congenital heart disease may affect subsequent suitability for a definite surgery. Initial palliation - the so-called Blalock Taussig Shunt (BTS) consists of constructing an unobstructed pathway from the right ventricle to the systemic arterial circulation. The purpose of this study was to elucidate the regional lung perfusion changes in patients who had a palliative BTS prior to Glenn or Fontan procedure.

Patients and Methods: This study assessed the pulmonary and total body blood flow utilizing the microsphere technique by sequential injection of Tc-99m microspheres into an upper and lower limb vein and performing conventional lung imaging in 4 projections and anterior and posterior total body scans in 47 patients with congenital heart failure. All patients had either Glenn shunt alone or Fontan procedure. 24 of these patients had a palliative Blalock-Taussig-Shunt (BTS) prior to the definite surgery. 3 patients had a right BTS, 15 had a left BTS, and 6 patients had a BTS on both sides.

Results: 7/15 patients with a left BTS showed a hypoperfusion of the left upper lobe after injection into the arm vein, and 4 of these showed a corresponding hyperperfusion when injected into the foot vein, 5 showed a homogeneous perfusion into the left lung after injection into the foot vein.

4/6 patients with a BTS on both sides showed a hypoperfusion in both upper lobes over the superior vena cava, but normal perfusion over the inferior vena cava. 2/6 patients showed equal perfusion after both injections. 2/3 with a right BTS showed a hypoperfused right upper lobe after inj into the arm vein and a corresponding hyperperfusion after inj. into the foot vein, 1/3 showed no significant difference.

Conclusion: The above described image pattern seems to be indicative for arterial anastomoses which seem to occur due to arterial strictures at the site of the Blalock Taussig shunt. Lung perfusion scintigraphy is of great assistance to detect abnormal pulmonary blood flow patterns and may help to decide the suitable definite surgery after palliative procedures.

PS-590

Serrano, J.; Gómez, A.; Martínez, A.; Verdú, J.; Antón, M.A.; Griño, E. y Caballero, O. Hospital U. San Juan de Alicante. Nuclear Medicine Department. Spain

INFLAMMATORY BOWEL DISEASE (IBD) ACTIVITY ESTIMATED WITH 99m-Tc-HMPAO-LEUKOCYTE SCAN (T-LS).

Our aim was investigate the usefulness of scintigraphic indexes with T-LS for evaluating the activity of IBD.

Method: We studied 50 patients, 32 with Crohn's Disease (CD) and 18 with Ulcerative Colitis (CU). Abdominal scans were performed at 15, 30 and 120 minutes after the injection of 370 MBq of 99m-Tc-WBC. Previously, all patients were evaluated with clinical scales of activity (Harvey's for CD and Lichtberg's for UC). All cases were reported subjectively and, besides, we obtained ROIs over intestinal segments, if present, and were compared with background, bone marrow, liver and spleen. Growth indexes between early and late images were also estimated. All were compared with clinical indexes. Clinicians were asked for the usefulness of the technique in all cases.

Results: 1. In CD, all scintigraphic indexes showed a significative good correlation ($p < 0,001$) with clinical indexes. The best results were obtained with the indexes of gut/background ($r: 0,73$), gut/bone marrow ($r: 0,72$) and their respective growths ($r: 0,73$ and $r: 0,60$).

2. In UC, we obtain a lower correlation between clinical and scintigraphic indexes. Only moderate correlation ($p < 0,05$) were found with the indexes of growth of gut/background ($r: 0,52$) and gut/bone marrow ($r: 0,58$). The resting indexes showed no correlation.

All clinicians showed a complete agreement with the results of the technique. All disagreements were explained by previous treatments and particular circumstances.

CONCLUSIONS: Activity of IBD can be estimated with T-LS and scintigraphic indexes with moderate accuracy, specially in CD. Perhaps, activity of IBD could not be exactly measured with T-LS, but a good clinician could use this information as a very powerful tool in the management of these patients. The growths of activity in ROIs were the best indexes.

PS-591

Serrano, J.; Antón, M.A.; Martínez, A.; Verdú, J.; Serrano, S. y Caballero, O. Hospital U. San Juan de Alicante. Nuclear Medicine Department. Spain

ROLE OF BONE SCINTIGRAPHY IN THE PROGNOSIS OF LEGG-CALVE-PERTHES DISEASE (LCP)

LCP use to be initially asymptomatic. Radiological findings are insensitive and nonspecific. Our aim was evaluate the bone scintigraphy (BS) in the management and the prognosis of LCP Disease

Method: We studied 26 patients (7 females) with 7±3 years old with clinical suspicion of LCP. We performed two phase-BS using planar and Pin-Hole Collimator. The studies were reported using two scintigraphic patterns depending on the two proposed mechanisms occurred in the revascularization of femoral epiphysis: recanalization (RC) and neovascularization (NV)

Results: Of 26 patients, 5 of them developed bilateral ECP and the resting 21, unilateral. Of 31 pathologic hips, we estimated 18 scintigraphic patterns of NV and 13 of RV. 13 of the 18 hips with RV followed a bad evolution with collapse, fracture and extrusion of femoral head, only 5 followed good evolution without disruption of normal anatomy. 9 of the 13 hips with RC followed a good and rapid evolution. Only 4 followed a bad evolution with deformities of femoral head. Pin-Hole projection identified all LCP with an accuracy of 100%. Planar images showed only 80% of sensitivity. Besides, with planar images, is difficult to identify these two scintigraphic patterns.

CONCLUSIONS: In our study, the BS showed a very powerful tool in the management of LCP, allowing to made a prognosis with a great accuracy. Pin-Hole projections are essential for identifying all LCP and the RC and NV scintigraphic patterns.

PS-592

A. Staničić, R. Jakl*, D. Ivančević**, S. Popović**, Z. Milas***, V. Čapkun Departments of Nuclear Medicine and *Pediatrics, Clinical Hospital, Split, **Clinical Department of Nuclear Medicine and Radiation Protection, University Hospital, Zagreb, ***Faculty of Engineering, Split, CROATIA

QUANTIFICATION OF LEFT-TO-RIGHT CARDIAC SHUNTS BY TRANSIT TIME ADJUSTMENT OF THE SECOND GAMMA VARIATE FIT

Quantification of left-to-right cardiac shunts by the method of gamma variate fits is hampered by statistical fluctuations in the first shunt recirculation curve which is also affected by subsequent shunt and systemic recirculations. In this work, to reduce the errors of the standard procedure, second gamma variate fit with adjusted standard deviation of transit times was used to calculate the pulmonary to systemic flow ratio (Qp/Qs). Pulmonary time-activity curves obtained by radionuclide angiocardiology in 29 patients aged 1 week to 28 years (mean 14.5 years) were analyzed. The diagnosis of a simple left-to-right cardiac shunt was established by cardiac catheterization. We calculated the standard deviation of transit times of the first gamma variate fit (s1) as well as the standard deviation of transit times of the second gamma variate fit with area for the Qp/Qs ratio of oximetry (s2). Second gamma variate fit with area for the Qp/Qs ratio of oximetry was found in an iterative procedure, where slight changes in the peak time of the gamma variate, which was scaled to the peak of the initial segment of the difference curve, were done and best fit to the upslope of the initial segment was found in each step. The s2/s1 ratio was then investigated. In our patients an s2/s1 ratio of 1.06±0.18 was found. This finding was in accordance with expectation that the true first shunt recirculation curve should be wider than the first transit curve because of smearing of bolus in the central circulation. The variations in the ratio could mostly be explained by errors of oximetry, although some additional smearing of bolus in the central circulation might have contributed. Subsequently, the second gamma variate fit for the s2/s1 ratio of 1.06 was found and used to calculate the Qp/Qs ratio. There was a very good correlation with oximetry data ($r=0.90$, $SEE=0.26$, $p<0.0001$).

In conclusion, we believe that transit time adjusted second gamma variate fit can be used to calculate the Qp/Qs ratio in most cases of a simple left-to-right cardiac shunt, especially when the initial segment of the difference curve is not well delineated.

Poster presentations

PS-593

Verdú J, Juste M, Serrano J, Martínez A, Antón MA, Carratalá F, and Caballero O. Hospital U. San Juan de Alicante. Department of Nuclear Medicine. SPAIN

SEMISOLID ESOPHAGEAL TRANSIT SCINTIGRAPHY IN CHILDREN WITH GASTROESOPHAGEAL REFLUX

The aim of the study was to assess the utility of esophageal transit scintigraphy (ETS) with semisolid bolus in demonstrating esophageal motility abnormalities in children with gastroesophageal reflux (GER). We have studied 56 patients age 4.6±3.2 years. Group I: digestive symptoms (n=28); Group II: recurrent respiratory symptoms (n=15); Group III: digestive and respiratory symptoms (n=13); Control group: patients with mild transient digestive symptoms in whom gastroesophageal scintigraphy didn't demonstrate GER (n=12); their results were included retrospectively. Parameters of esophageal motility were obtained from the first swallow, calculating the 90% clearance time (CL90%). Threshold of pathology was obtained from the control group.

	CL90%	% ABNORMALS
Group I	39.0 ± 38.9*	53.8 %
Group II	22.8 ± 33.8*	28.6 %
Group III	26.4 ± 27.2	50.0 %
Control group	7.2 ± 2.1*	

Differences were significant between group I and control group, and groups I and II, with a p value of less than 0.05.

Conclusions: 1) Group I patients exhibit a significantly more prolonged semisolid clearance time than group II patients and controls. 2) The percent of abnormal results is clearly higher in the groups with digestive symptoms.

Radionuclide therapy

PS-594

Barry J Allen, Garry Goozee, Syed Rizvi, Samir Sarker*, Gerd Beyer+ Hospital: St George Cancer Care Centre, Gray St, Kogarah, NSW 2217 Australia, *University of Sydney, NSW, Australia, +University Hospital Geneva, Switzerland

THE ROLE OF ALPHA THERAPY FOR SYSTEMIC TREATMENT OF METASTATIC CANCER

The major problem in the management of cancer relates to our inability to control the development of metastases arising from malignant cancers such as melanoma, breast, prostate and other cancers.

Metastatic cancer proceeds through a number of quite separate stages in the development of lethal disease, ie cells in transit, preangiogenic lesions, subclinical and clinical lesions. Early stages offer the potential for control if targeted therapy is applied. However, the dose must be localised to the cancer cell and this requirement rules out beta emitting radionuclides, which are more suited for clinical lesions. Alpha emitting radionuclides are the most appropriate toxins, as their efficacy depends on the linear energy transfer (LET) and range of the alpha particles.

After matching the cancer stage, radiolabel and carrier, we find that ¹⁴⁹Tb is the radionuclide of choice for systemic targeted alpha therapy (TAT) in all aspects except production. The production of ¹⁴⁹Tb in µCi quantities has been achieved using the heavy ion reaction at the ANU tandem accelerator at Canberra and in multi-mCi quantities using the spallation reaction in combination with on-line isotope separation technology of ISOLDE at CERN. Tb is ideally suited for chelation to monoclonal antibodies to produce stable radio-immunoconjugates (RIC), and ¹⁵²Tb, a strong positron emitter, allows the development of benchmarks as well as PET kinetics.

²¹¹At is a halide and has potential for the elimination of early stage melanoma metastases as At-MTB. However, the availability of the alpha-generators ²²⁸Th-²¹²Bi and ²²⁵Ac-²¹³Bi facilitates the use of Bi-RIC in clinical trials, eg for acute myeloid leukaemia. We had achieved the first accelerator production of the Ac:Bi generator at CERN. Alpha therapy has the potential to control refractory cancers when treated at the minimum residual disease stage. Preclinical studies with ¹⁴⁹Tb, ²¹¹At and ²¹²Bi continue to demonstrate the efficacy of TAT, and the New York clinical trial with ²¹³Bi-RIC shows that TAT is safe and without complications for doses up to 50 mCi.

PS-595

M. gr. Darrelmann¹, M. Köhler², A. Heigl², H. Sörensen⁴, A.N. Savaser⁵, M. Andreiff¹, P. Nelz⁶, J. Kropp¹, W.-G. Franke¹ Depts. of Nucl. Med.¹ and Center for Animal Experiments⁶ Univ. Hosp. Dresden, Veterinary Hosp. Kalkreuth² and Wusterhausen³, Immanuel Hosp. Berlin⁴, Dept. of Nucl. Med. Hosp. Zehlendorf⁵; Germany

RADIOSYNOVECTOMY (RSO) IN HORSES: PRELIMINARY EXPERIENCE.

Aim: The therapeutic approach of RSO should be transferred and adapted to meet the therapeutical demands of veterinary medicine in horses with restrictions of movement due to activated arthrosis. Beyond this there is a therapeutical demand in animals suffering from bursitis and tenosynovitis. **Methods:** We performed RSO in horses in which the indication for a therapy of a joint with cortisone has been set after a standardized veterinary investigation which included: inspection/palpation, grading of the immobilization, provocative tests, grading of the restriction of movement, intra-articular anesthesia and nerve block, x-ray, and sonography. In addition to cortisone, we administered the therapeutic radiopharmaceutical into the synovial space. ¹⁸⁶Re-sulfur colloids and ⁹⁰Y-citrate were used in 32 horses used in sports, so far. There were 7 activated arthroses, 20 cases of bursitis, and 5 cases of tenosynovitis. The effect of the therapy was followed up three, six and nine months after the administration of the radioactive compound. Exactly the same criterias of the standardized investigation as for the indication was used in the follow up period and investigations. **Results:** The quote of success raised up to 80 % within nine months. In six cases a recurrence occurred due to a renewed trauma which had improved initially. In these cases a second RSO was performed and the results showed the same high degree of improvement.

Conclusions: Radiosynovectomy extends effectively the therapeutic spectrum in orthopedic diseases of horses with a high quote of success and with long term effects. But evaluation of indications, doses, and the radionuclide of choice have to be subjects of further investigations.

PS-596

Farahati J*, Lassmann M*, Dutschka K#, Sonnenschein W#, Alollio B#, Freystadt D*, Brandau W#, Bockisch A#, Reiners Chr*

Clinics for Nuclear medicine* and Internal Medicine§ University of Wuerzburg* and Clinic for Nuclear Medicine University of Essen#

EFFECT OF SPECIFIC ACTIVITY ON [¹³¹I]MIBG-UPTAKE IN PHEOCHROMOCYTOMA.

Background: In a recent study we observed a higher in vivo deiodination of no carrier added (n.c.a.) [¹²³I]mIBG than of commercial [¹²³I]mIBG in humans. However, the degradation could be due to extremely high specific activity of nca [¹²³I]mIBG (>7.4 TBq/µmol). In order to clarify the effect of specific activity (SA) on tumor uptake, a diagnostic scintigraphy with nca [¹³¹I]mIBG (46 GBq/µmol) was compared to com [¹³¹I]mIBG (0.3 GBq/µmol) with lower specific activity (LSA) in a patient with malignant pheochromocytoma and non-resectable liver metastasis (5x4x2.5 cm).

Methods: Following the administration of 70 MBq of [¹³¹I]mIBG with both SA (first study with nca- and 2 weeks later LSA mIBG) several whole body scans (WBS) were performed up to 10 d pi with a Siemens Body Scan gamma camera. The clearance of radioactivity from blood was determined by serial blood sampling up to 3 d pi. To assess the urinary loss of activity, urine collection were carried out at 2, 4 and 20 h after injection. The dosimetric study was carried out using quantitative conjugate view WBS.

Results: The tumor and organ uptake of radioiodinated mIBG did not remarkably differ between the two different specific activities. The retention of radioactivity in plasma was determined to be <1% with both SA up to 3 d after injection. A total of 33 MBq of nca mIBG and 35 MBq of com mIBG was excreted at 20 h pi. The dose to the tumor with both SA was estimated to be 8.5 Gy/GBq. Accordingly, the tumor/organ ratios at 6 d were comparable with both nca- and LSA mIBG (tumor/thigh: 112 vs. 108, tumor/lung: 56 vs. 55, tumor/liver: 7.5 vs. 7.2).

Conclusions: In contrast to nca [¹²³I]mIBG, distribution of nca [¹³¹I]mIBG in our patient does not seem to be affected by in vivo deiodination. The tumor and the organ uptake of nca [¹³¹I]mIBG was comparable to that of [¹³¹I]mIBG with lower specific activity. Due to a lower amount of pharmacologically effective mIBG, nca [¹³¹I]mIBG could be infused in a shorter period of time, and thus, may be of advantage in treatment of neuroendocrine tumors.

PS-597

N.Ö.Küçük, E.İbiş, G.Aras, S.Baltacı*, G.Özalp***, Y.Bedük*, N.Çanakçı**, A.Soylu
Ankara University Medical School, Depts. of Nuclear Medicine, Urology*, Anesthesiology** and Ankara Oncology Hospital***. Ankara/TÜRKİYE

PALLIATIVE EFFECT OF RE 186 HEDP IN DIFFERENT CANCER PATIENTS WITH BONE METASTASES

Re 186 hydroxyethylidene diphosphonate (Re 186 HEDP) is one of the radiopharmaceuticals suitable for palliative treatment of metastatic bone pain. The aim of this study was to investigate palliative and side effects of Re 186 HEDP in pts with different type of cancers and metastatic bone lesions.

Thirty one patients (10 pts with prostate Ca, 10 pts with breast Ca, 4 pts with rectum Ca, 5 pts with lung Ca, 2 pts with nasopharynx Ca) were included in the study. A total of 40 standard therapy doses of 1295 MBq were administered. The pain was assessed with ECOG and Karnofsky status index, and pain relief was evaluated weekly. The diary was marked daily for a maximum of 10 weeks.

Response was found as 87.5% in pts with breast and prostate cancer, 75% in pts with rectum cancer, 50% in pts with nasopharynx cancer and 20% in pts with lung cancer. Mean palliation period was 8-10 weeks. Maximal palliation effect was observed between 3 rd and 7 th weeks. Any serious side effects were not seen, excepts slight haematologic toxicity.

It is concluded that Re 186 HEDP is a highly effective agent in the palliation of metastatic bone pain in pts with prostate, breast or rectum cancer, mildly for nasopharynx cancer but not for lung cancer. On the other hand, Re 186 HEDP is a good alternative to Sr 89, because of its physical characteristics, (as short half life and gamma energy), low side effects and early response.

PS-598

Penttilä P¹, Mäkelä O², Hiltunen J¹, Haukka J¹, Kanckos S³ and Komulainen R⁴

¹MAP Medical Technologies Oy, Tikkakoski, ² Department of Clinical Studies, College of Veterinary Medicine, Helsinki University, ³ Vaasa Central Hospital, Vaasa and ⁴ Kotka Central Hospital, Kotka, Finland

ANIMAL BIODISTRIBUTION AND INITIAL HUMAN EXPERIENCE OF ¹⁶⁶Ho-FHMA FOR RADIOSYNOVIORTHESIS

Radiopharmaceuticals have been used for radiosynoviorthesis for more than 20 years. Y-90 most commonly, but the fairly rapid leakage from joints have compromised the merits. A newer colloid, Dy-165-FHMA has been used clinically and it does not show leakage from the injected joint within its very short half life (2.3 hrs). However it does prevent the wider use.

We report here the development of Ho-166-FHMA. Holmium has good physical properties for wide spread clinical use; T_{1/2} 26 hrs, γ 75 keV (6 %), β_{aver} 711 keV. Ho-166 delivers 90 % of the radiation dose within 2 mm. The production is almost equal to that of Dy-165-FHMA, with the difference that Ho-166-FHMA is sterilized by autoclaving. The particle size distribution is close to optimal; > 80 % of activity is bound to 3-8 μm particles and >99 % 1.2 - 25 μm particles.

The *in vivo* behaviour was studied in rabbits. Each rabbit received 60-80 MBq of Ho-166-FHMA into knee joint. The leakage from the injected joint was analyzed at 24, 48 and 72 hrs post injection by sacrificing the animal and counting relevant organs. Urine and faeces were also counted. No activity could be detected in faeces and minimal (< 0.03 % within 72 hrs) amounts in urine. The only elevated extra articular activity was detected (detection limit 0.5 kBq/sample) in kidneys, the other organs did not show increased activity (24 - 72 hrs pi). Thus the leakage is minimal in this animal model.

Five hemophilic patients were treated; one ankle, one elbow (370 MBq) and three knees (1.1 GBq). Blood analysis during different times showed no leakage (< 0.1 % of activity/blood volume) and < 0.05 % of activity/day was in urine. No side effects were detected. The treatment is painless and easy and all patients responded well for more than 4 months.. This very preliminary experience suggests Ho-166-FHMA being safe and efficient in therapy of inflammation in joints caused by f.ex. rheumatoid arthritis, other arthritis or hemophilia.

PS-599

R. Róka, T. Séra, F.F. Knapp*, J. Láng, L. Pajor, L. Thurzó, L. Dux, H. Palmedo**, H.J. Biersack**, L. Pávics
Albert Szent-Györgyi Medical University, Szeged, Hungary, Oak Ridge National Laboratory*, USA, University of Bonn**, Germany

FIRST CLINICAL RESULTS ON TWO-STEP RE-188 HEDP TREATMENT OF METASTATIC BONE PAIN

AIM: The aim of this study was to evaluate the efficacy of Re-188 HEDP for the treatment of metastatic bone pain.

METHODS: 7 patients (pts) with multiple painful bone metastases were treated. 5 pts with prostate cancer and 2 pts with breast cancer received a fixed activity of 3000 MBq of Re-188 HEDP intravenously in two steps. Complete blood counts were determined, blood chemistry examinations and urinalysis were performed before and 1, 2, 3, 4, 6, 8, 12 weeks following the treatment. A visual analogue score, a verbal rating scale, the Spitzer index and the Karnofsky score were used to assess pain and performance status. 3 hours after Re-188 HEDP administration gamma and beta-radiation dose measurements were made at 1 m from the anterior mid-trunk of the patients, together with urine dose measurements.

RESULTS: 1 pt become pain-free, 5 pts exhibited partial pain improvement and 1 pt gave no response to the Re-188 HEDP therapy. 3 of 7 pts, displaced a flare reaction within 1 week after the treatment. Transient decreases in platelet and white blood cell counts were observed. There were no significant changes in the liver and renal functions. Radiation dose rate values of 6.3±1.0 μSv/h for gamma, and of 183±40 s⁻¹ for beta-radiation were found. 25-32% of the administered dose was eliminated via the urinary tract.

CONCLUSION: Our observations suggest that Re-188 HEDP is an effective radiopharmaceutical in treatment for metastatic bone pain. An administered activity of 3000 MBq can bring about a pain reduction without causing any clinically significant bone marrow toxicity.

PS-600

S. J. Wang, W. Y. Lin, M. N. Chen, B. T. Hsieh, Z.T. Tsai, G. Ting, and *F. F. Knapp, Jr.

*Oak Ridge National Laboratory, TN, Taichung Veterans General Hospital and Institute of Nuclear Energy Research (INER), Taiwan.

DIRECT INTRATUMORAL INJECTION OF RHENIUM-188 MICROSPHERE CAN IMPROVE THE SURVIVAL TIME OF RATS WITH HEPATOMA.

Intratumoral injection of Y-90 microsphere is a potential alternative in the treatment of liver tumor. However, complicated preparation, lack of gamma ray for imaging is the shortages for the use of Y-90. In this study, we used Re-188, a generator-produced radioisotope with 155 keV gamma ray emission, to label microspheres. Biodistributions and survival times, following intratumoral injection of Re-188 microsphere into rats with hepatoma were analyzed.

Twelve rats with hepatoma were sacrificed for biodistribution study. Thirty rats bearing hepatoma were divided into two groups to evaluate survival time. Group 1 received intratumoral injection of 37 MBq Re-188 microsphere, while group 2 served as the control group, and received intratumoral injection of 0.1ml of normal saline only.

Our data showed that the radioactivity in the tumor was very high throughout this study. The biological half-time was 170.8 hours. Radioactivity in the lung was 1.78% inj. dose/g at 1h, but declined rapidly over time. The concentration in the urine was about 6.14% inj. dose/ml after the first hour, and rapidly declined thereafter. The concentrations of radioactivity in other organs such as normal liver, muscle, spleen, bone, testis and whole blood were quite low throughout the study. 12/15 (80%) of rats survived over 60 days after intratumoral injection of Re-188 microsphere, while only 4/15 (26.7%) survived over 60 days after injection of normal saline only (p < 0.05).

In conclusion, direct intratumoral injection of Re-188 microsphere can prolong the survival time of rats with hepatoma, and it can be used as a therapeutic alternative in hepatoma patients.

Poster presentations

Dosimetry and radiobiology: Biokinetics/dosimetry

PS-601

Ulrika Berndtsson, Peter Bernhardt, Ola Nilsson, Håkan Ahlman, Eva Forsell-Aronsson
University of Göteborg, Sahlgrenska University Hospital, Sweden,
Departments of Radiation Physics, Pathology and Surgery

REDUCTION OF RENAL UPTAKE OF ¹¹¹IN AFTER I.V. INJECTION OF ¹¹¹IN-DTPA-D-PHE1-OCTREOTIDE IN NUDE MICE

The results from scintigraphy, intraoperative localisation and therapy with ¹¹¹In-DTPA-D-Phe1-octreotide of neuroendocrine tumours are today limited by the uptake of ¹¹¹In in the normal tissues. The kidneys are one of the critical organs that receive the highest absorbed doses and will limit the amount of activity given for therapy. The aim of this study was to further investigate the mechanism of and methods for prevention of ¹¹¹In uptake in the kidneys, after injection of ¹¹¹In-DTPA-D-Phe1-octreotide.

Biodistribution studies were performed with male nude mice (BALB/c) receiving ¹¹¹In-DTPA-D-Phe1-octreotide, ¹¹¹In-chloride or ¹¹¹In-DTPA by i.v. injections. Some of the mice received octreotide s.c. prior to or DTPA-D-Phe1-octreotide i.v. at the same time as i.v. injection of ¹¹¹In-DTPA-D-Phe1-octreotide. Other groups of mice were i.p. injected with L-lysine in fractions prior and after injection of ¹¹¹In-DTPA-D-Phe1-octreotide, ¹¹¹In-chloride or ¹¹¹In-DTPA.

The uptake of ¹¹¹In in the kidneys after ¹¹¹In-DTPA-D-Phe1-octreotide injection was not influenced by s.c. injection of octreotide or i.v. injection of DTPA-D-Phe1-octreotide, but the uptake in the lungs decreased.

Additional injection of L-lysine reduced the ¹¹¹In uptake in the kidneys with up to 70% but also increased the concentration in the lungs and reduced the whole body content of ¹¹¹In. However L-lysine did not influence the kidney uptake of ¹¹¹In-chloride or ¹¹¹In-DTPA but increased the uptake in liver, lungs and spleen after ¹¹¹In-chloride administration.

If similar effects of L-lysine on the kidney uptake can be obtained also in man, therapeutic effects of ¹¹¹In-DTPA-D-Phe1-octreotide may be enhanced by permitting higher amounts of administered activity. The high uptake in the kidneys can not be explained by degradation of ¹¹¹In-DTPA-D-Phe1-octreotide to ¹¹¹In-DTPA, but may be by degradation to ¹¹¹In ion or ¹¹¹In-DTPA bound to one or more aminoacids.

PS-602

N. Iznaga-Escobar¹, J. González², T. Crombet¹, T. Herrera³, J. R. Martínez³, A. López¹, D. Morales¹ and R. Pérez¹.

Center of Molecular Immunology, Research Department, Havana, Cuba.

¹⁸⁸Re-LABELED ANTI-HUMAN EGF-R ANTIBODIES MURINE IOR *egf/r3* AND HUMANIZED R3: BIODISTRIBUTION AND PHARMACOKINETICS IN MONKEYS.

In the present paper we have evaluated the pharmacokinetics and biodistribution to normal organs of the ¹⁸⁸Re-labeled antibodies. Biodistribution studies were performed on two IRUS and three Baboon adult male monkeys. Planar anterior and posterior views were taken at 5 min, 1, 3, 6, 12, 24, 36 and 48 hr after injections. The geometric mean of anterior and posterior images corrected for decay was obtained using a computer program. Regions of Interest (ROIs) were drawn over the source organs heart, liver, kidneys, bladder and gastrointestinal tract to obtain the cpm for each organ in each time interval. Plasma disappearance curves of ¹⁸⁸Re-labeled anti-EGF-R murine ior *egf/r3* and humanized R3 antibodies were best fit by biexponential equations with a distribution half-life ($t_{1/2\alpha}$) of 6.60 ± 2.13 hr and 3.63 ± 2.93 hr and elimination half-life ($t_{1/2\beta}$) 25.4 ± 2.5 hr and 42.19 ± 7.54 hr for ¹⁸⁸Re-labeled anti-EGF-R murine ior *egf/r3* and humanized R3, respectively. Among the various organs, significant accumulation of the radiolabeled was found in liver (21.91 ± 9.56) % and (20.0 ± 0.9) % at 5 min post-administration and these values were reduced to (8.26 ± 1.73) % and (4.37 ± 0.90) % at 48 hr post-injection for ¹⁸⁸Re-labeled anti-EGF-R murine ior *egf/r3* and humanized R3, respectively. There was non-significant differences at ($p < 0.05$) level for the biodistribution to normal organs for both ¹⁸⁸Re-labeled antibodies.

PS-603

E.H. Kim, K.B. Park

Korea Cancer Center Hospital, Cyclotron Application Laboratory
Korea Atomic Energy Research Institute, Department of Radioisotope

DOSE ESTIMATION FOR USING A RADIOACTIVE STENT IN ESOPHAGEAL CARCINOMA TREATMENT

Objectives: A metal stent coated with beta-emitting radioisotope can be used to treat the esophageal carcinoma. The radioactive stent is inserted into the lesion of malignant esophageal obstruction and irradiates it. In this study, dose to the esophageal wall is estimated for a varying prescription of stent in terms of radioisotope, total activity, and the activity distribution pattern.

Methods: A geometrical model of the esophagus and its surrounding is developed to simulate the energy deposition to the esophageal wall. Dose estimation is performed for a cylindrical stent of a constant diameter of 2 cm and a varying height that is activated with various beta-emitting radioisotopes such as ⁹⁰Y, ¹⁸⁸Re, ¹⁶⁶Ho, ³²P, ¹⁸⁶Re, and ¹⁹²Ir. The Monte Carlo code EGS4 is used to simulate the radiation transport.

Results: With a stent of constant areal activity density, dose to the esophageal wall at the central height of the stent increases with an increasing stent height until reaching a saturation value. Dose is maximum at the esophageal wall surface and decreases as the target moves into the esophageal wall. The degree of dose decreasing varies among different radioisotopes. On the other hand, dose decreases by similar degree among different radioisotopes as the target moves from the stent central height toward the stent end. For a stent of 2 cm in diameter, more than 4 cm in height, and $2 \mu\text{Ci}/\text{cm}^2$ in areal activity density, dose at the esophageal wall surface and at the stent central height is ~ 15 Gy, ~ 12 Gy, ~ 10 Gy, ~ 5 Gy, and ~ 3 Gy for ⁹⁰Y, ¹⁸⁸Re, ¹⁶⁶Ho, ³²P, ¹⁸⁶Re, and ¹⁹²Ir, respectively.

Conclusion: Combined with the animal experiments, dose estimates provided in this study can be utilized in analyzing the relationship between the stent prescription and the therapeutic effect. The stent prescription of right choice helps completing the protocol of treating the esophageal carcinoma with a radioactive stent.

PS-604

M.Laßmann, H.Hänscheid, M.Luster, Chr.Reiners

Department of Nuclear Medicine, University of Würzburg, Germany

48H-WHOLE-BODY UPTAKE OF I-131 IN PATIENTS WITH DIFFERENTIATED THYROID CARCINOMA AFTER THE APPLICATION OF RECOMBINANT HUMAN TSH

Aim of the study: Aim of the study is to find out if there is a difference between the use of recombinant human TSH (rhTSH, Thyrogen™) and the withdrawal of thyroid hormones of the 48h hour whole-body uptake in patients with differentiated thyroid carcinoma (DTC) and a diagnostic activity of 150 MBq I-131.

Material und Methods: For 14 of 26 patients who were enrolled in a multicenter study of rhTSH („A Study on the Safety and Efficacy of Thyrogen in Detecting Well-Differentiated Thyroid Cancer by Radioiodine Whole Body Scanning and Thyroglobulin Testing“, see [1]) we determined the 48h retention of I-131 after withdrawal of thyroid hormones and after application of Thyrogen™. The 48h uptake values after oral administration of 150 MBq of I-131 were measured with a calibrated probe [2]. In the 48 hour gamma camera scans none of the scans showed thyroid remnants or metastases.

Results: The mean 48h whole body retention after the application of rhTSH was $2.6 \pm 2.9\%$ (Minimum 0.1%, Maximum 9%, Median 1.6%). Corresponding values after withdrawal of thyroid hormones were: mean value: $7.7 \pm 6.3\%$, minimum: 0.3%, maximum: 18%, median 7.2%.

Analysis of the data using the Wilcoxon-sign-rank-test for paired differences showed a statistically significant difference ($p: 0.0023$).

Conclusion: The remaining activity in the whole body 48h after administration of I-131 and, therefore, the radiation exposure is lower after the application of Thyrogen™ compared to the withdrawal of thyroid hormones. The main reason for that is the higher excretion of iodine in euthyrotic patients (Thyrogen™) compared to the hypothyroid state after withdrawal of thyroid hormones.

For the determination of necessary adjustment to the therapeutic activities of I-131 for radioiodine therapies after application of Thyrogen™ an international multicentric study on dosimetry is currently underway.

References:

1. Reiners, Ch. et al. (1997), Oral Presentation at the EANM'97 congress
2. Laßmann, M. et al. (1992). Nucl.-Med., 31, A 19.

PS-605

H. MERDAS

Radiation Protection & Safety Centre, Medical physics Department, P. O. Box 399 Alger-Gare, Algiers, ALGERIA

Radiation Absorbed Dose Calculation Based on SPECT Imaging and MIRD Scheme in ¹³¹I Therapy.

The dose delivered to tissues concentrating radioiodine depends upon the thyroid uptake, the effective half-life, the tumour mass and shape. Therapeutic radiation absorbed dose is calculated using simplified MIRD equations scheme. The source activity is assumed to be uniformly distribution and tumour has an ellipsoidal shape. In the present work the tissue absorbed dose has been determined using a source-target voxel's approach. Specific absorbed dose value ($S_{\text{target voxel} \leftarrow \text{source voxel}}$) of a couple of source-target voxels was calculated. The EGS4 radiation transport code was utilised to simulate the voxel specific absorbed dose of ¹³¹I for unit activity concentration in the source voxel. A three-dimensional absorbed dose kernel is generated and stored in a look up table (64 × 64 × 64 elements matrix). Absorbed dose at every specific target voxel is the total contribution of all source voxels. For this, SPECT tumour image (64 × 64 × 64 voxels and 6 mm voxel size) is convoluted with the generated look up table to produce 3-D tumour absorbed dose map. Tissue absorbed dose is directly the sum of each target voxel dose. Prescribed therapeutic activity is then the administered imaging activity scaled by a factor (f).

Our dose calculation method has been implemented and tested on Rando anthropomorphic phantom. Useful information such as isodose contours and dose volume histograms can be generated and may be used for radionuclide therapy monitoring in clinical routine. This dose planning approach is more accurate and patient specific.

PS-606

D. Moka, W. Schäfer, H. Brockmann, K. Schomäcker, H. Schicha
Department of Nuclear Medicine, University of Cologne, Germany

Biokinetic studies of myocardial perfusion marker using the isolated perfused Langendorff heart

Aim: It is known that there are difference in myocardial perfusion marker (Tc-99m-MIBI, Tc-99m-Tetrofosmin, Tc-99m-Furifosmin, TI-201-Cl) in extraction rate, retention in myocardial tissue as well as in tissue specific elimination velocity. It was the aim of this study to assess the biokinetics of these perfusion marker und to develop a specific compartment model for each radiopharmaceutical.

Methods: Depending of the rate-pressure-product, myocardial retention and elimination of the radiopharmaceutical were determined in 60 pressure- resp. flow-constant perfused isolated Langendorff-guinea pig hearts. Using the elimination kinetics and the simultaneous recorded hemodynamic parameter a specific 2 or 3 compartment model was develop for each radiopharmaceutical.

Results: TI-201-Cl and Tc-99m-MIBI showed a bi-exponential tissue elimination (2 compartment model); Tc-99m-Tetrofosmin and Tc-99m-Furifosmin showed a tri-exponential elimination (3 compartment model). Only TI-201-Cl and Tc-99m-MIBI showed an inverse correlation of the elimination velocity to the rate pressure product. Effective halflife in the last compartment: TI-201Cl: 150-275 sec, Tc-99m MIBI: 1325-1650 sec, Tc-99m-Tetroforsmin: 2000-4800 sec, Tc-99m-Furifosmin: >5000 sec. Ratio of myocardial retention in the last compartment: MIBI/Tetroforsmin: 1,97 ± 0,06; MIBI/Furifosmin: 4,00 ± 0,41; Tetroforsmin/Furifosmin: 2,03 ± 0,15.

Conclusion: Tc-99m-MIBI, Tc-99m-Tetrofosmin, Tc-99m-Furifosmin, TI-201-Cl showed completely different behavior in myocardial retention and elimination as well as in intracellularly distribution (2 resp. 3 different compartments). However, to what extend these results are caused by differences in cellular transport or accumulation mechanism remained uncertain and have to be solved in further investigations.

PS-607

A.M. Palmer, M. Saunders, and A.W. Preece.

Bristol Fetal Dosimetry Group, Radiopharmacy Unit, Bristol General Hospital, Bristol, BS1 6SY, United Kingdom.

PREFERENTIAL ACCUMULATION OF RADIONUCLIDES IN FETAL TISSUES

Background: Cancer incidence following environmental exposure to radioactive materials is frequently higher than predicted from calculation of the risk associated with the measured or estimated whole body radiation dose. Doses to the early embryo, when tissues are particularly radiosensitive, are often approximated to that received by the uterus. Dosimetry does not account for placental transfer or accumulation into specific fetal tissues. Far from acting as a barrier the placenta allows access to many elements and presumably has mechanisms for enhanced transport of elements particularly required for fetal development, many biochemically similar to those of interest as radioactive environmental pollutants and those used in medicine eg. iodine, strontium, caesium, cobalt, iron. The major risks to a live born child following *in utero* irradiation are severe mental retardation (SMR) and cancer. Risk of SMR would be increased by selective accumulation of activity in brain or tissues close to the brain such as skull or thyroid. Leukaemia risk will be enhanced by selective accumulation of activity in or near the sites of hematopoiesis which in the embryo include liver, spleen, thymus and at later gestational ages the bone marrow. **Materials & Methods:** We have measured maternal and fetal biodistribution of ¹³¹I-iodine, ⁵⁹Fe-iron, ⁸⁵Sr-strontium, ⁵⁷Co-cobalt, ¹³⁷Cs-caesium and ^{99m}Tc-technetium in pregnant guinea pigs at various times after bolus administration. ¹³¹I-iodine and ⁵⁹Fe-iron have also been administered to separate groups of animals by ingestion over three weeks in drinking water to simulate environmental contamination of food. **Results:** All the radionuclides readily cross the placenta and reach the fetus. All but caesium show preferential uptake into some key fetal tissues. Fetal:Maternal uptake ratios are frequently of the order to 3 to 4 and can be up to 11 in some tissues - not always the expected target organ for the particular radionuclides. Fetal liver, spleen, thyroid, thymus and bone marrow are frequently the high activity tissues with cobalt and strontium accumulating in fetal bone. **Conclusion:** Specific fetal accumulation of radionuclides found in the environment and used in medicine may result in higher than anticipated radiation doses to tissues involved in hematopoiesis during gestation.

PS-608

G.V.S.Rayudu, A. Ali, E.W. Fordham
Rush University Medical Center, Departments of Radiology, Nuclear Medicine and Medical Physics

TARGET ORGAN RADIATION DOSIMETRY OF NEW Tc-99m BRAIN AND HEART PERFUSION AGENTS

As the MIRD tables do not provide S values for myocardium and brain, calculations based on biodistribution, absorbed dose constant (Δ) and absorbed fraction ϕ for values of Tc-99m-ceretec, neuro-lite (ECD), sestamibi (SMIBI), furifosmin, cardiotec, tetrofosmin are presented. The standard weights of organ brain are 1400 gm and 300 gm for myocardium and the value for $\sum \Delta \phi = 0.082 \text{ gm-rad}/\mu\text{Ci-hr}$, average effective half life = 1.443 x 6hr which makes $\sum \Delta \phi \times 1.443 \times 6 = 0.71 \text{ gm rad}/\mu\text{Ci}$. The respective uptakes of the compounds are Tc-99m ceretec (2.5%), Tc-99m neuro-lite (2.5%) Tc-99m sestamibi (1.25%), Tc99m furifosmin (3.0%) Tc-99m cardiotec (1.25%) and Tc-99m tetrofosmin (1.2%). The estimated dosimetric values calculated using: Concentration/gm x average effective half life x $\sum \Delta \phi$, for 30 mCi (1110 MBq).

Tc-99m CERETEC = 30000 X 2.5% / 1400 X 0.71 = 0.38 rad (cGy)
Tc-99m ECD = 30000 X 2.5% / 1400 X 0.71 = 0.38 rad (cGy)
Tc-99m SMIBI = 30000 X 1.25% / 300 X 0.71 = 0.89 rad (cGy)
Tc-99m FURIFOSMIN = 30000 X 3.0% / 300 X 0.71 = 2.13 rad (cGy)
Tc-99m CARDIOTEC = 30000 X 1.25% / 300 X 0.71 = 0.89 rad (cGy)
Tc-99m TETROFOSMIN = 30000 X 1.2% / 300 X 0.71 = 0.85 rad (cGy)

Thus the radiation dosimetry values have been calculated based on tracer concentration, $\sum \Delta \phi$, average effective half life. The values for brain perfusion agents were estimated to be 0.38 rad (cGy) for the heart perfusion agents the values varied from 0.85 rad (cGy) for tetrofosmin with 1.2% uptake and the furifosmin with high uptake of 3.0% gave 2.13 rad (cGy). This method can be extended to organs such as gall bladder whose S values are not given. It is also possible to calculate penetrating and non-penetrating components separately by inserting 0.0449 and 0.0369 respectively in place of 0.082 gm-rad/ $\mu\text{Ci-hr}$.

PS-609

R Rossi Norrlund¹, A Ullén², P Sandström², D Holback³, L Johansson³, T Stigbrand², S-O Hietala¹, and K Riklund Åhlström¹.

Departments of Diagnostic Radiology¹, Immunology², and Radiation Physics³, University Hospital of Northern Sweden, S-901 85 Umeå, Sweden.

DOSIMETRY OF FRACTIONATED EXPERIMENTAL RADIOIMMUNOTARGETING WITH IDIOTYPIC AND ANTIIDIOTYPIC ANTICYTOKERATIN ANTIBODIES.

Repetitive injections of a ¹²⁵I-labeled tumor targeting anticytokeratin monoclonal antibody (TS1), and a non-labeled antiidiotypic monoclonal antibody against TS1 (α TS1), were compared to a single injection of the radiolabeled TS1 at experimental radioimmunotargeting. Anti-TS1 was used in order to remove nontargeting TS1. The animals in group A received a single injection of 13 MBq ¹²⁵I-labeled TS1. The animals in group B received four injections ¹²⁵I-labeled TS1 (8-13 MBq) followed by α TS1 24 hours later, in two weeks interval. The mean absorbed doses were calculated according to the Medical Internal Radiation Dose Committee formalism based on repetitive radioimmunoscinographies.

An mean dose of 11 Gy to the tumor and 2 Gy to the whole body was achieved in group A. Mean peak tumor uptake of 5% of the injected dose (ID), corresponding to 14 % ID/g was observed at day 17 after a single injection of the labeled MAb. A mean peak tumor uptake in the same order of magnitude was seen in group B. An absolute increase in the tumor uptake was observed in group B during the entire observation period. The mean absorbed dose to the tumors was 11 Gy at the end of the observation period, while the whole body dose was only 2.5 Gy in group B. Autoradiography of the tumors at the end of the observation period confirmed an intensive heterogeneous accumulation of activity in the entire tumor.

The fractionated strategy can contribute to a significant accumulation of radiolabeled TS1 in the tumors. Furthermore the use of α TS1 makes it possible to increase the tumor/nontumor dose ratio and to maintain a prolonged high activity accumulation in the tumor.

PS-610

P. Ryyänen^{1,2}, J. Benczik¹, M. Kulvik^{1,2}, J. Vähätalo¹, M. Snellman¹, S. Savolainen^{1,2}

¹University of Helsinki, FIN-00014 UNIVERSITY OF HELSINKI, Finland,

²Helsinki University Central Hospital, 00029 HYKS, Finland

BIODISTRIBUTION OF BORONOPHENYLALANINE (BPA) IN DOGS

BPA has been used in boron neutron capture therapy (BNCT) as a boron delivery agent. The aim of creating kinetic models of BPA is to be able to calculate accurately the delivered irradiation dose of the treatment. Biodistribution of BPA was investigated in 9 dogs. BPA-fructose was infused intravenously (approx. 250 mg/kg). Blood samples were taken during and after infusion, and urine was collected. Five dogs were sacrificed and tissue samples were collected.

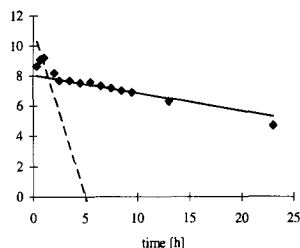


Fig 1. The plasma clearance of boron-10 for one dog in a relative logarithmic scale. The corresponding mean half-lives were 27 minutes for the fast and 8 hours for the slow component.

The boron-10 concentration was high in hypophysis, and especially high in urine. The plasma clearance curve was biexponential (Fig.1), with 19.5 ± 4.1 minutes and 10.4 ± 4.4 hours as mean half lives ($n=4$). The clearance of BPA from the plasma was 4.4 ± 1.5 mg/min. The starting point of an approx. 2 hour treatment will be one hour after the end of the infusion. The disappearance rate of BPA between the start of the treatment and two following hours was 0.003 ± 0.001 l/min ($n=4$). From the treatment viewpoint further studies are required to clarify the blood/brain ratio of boron-10 concentration as a function of time.

PS-611

T. Tolvonen, J. Hietala, M. Haaparanta, J. Bergman, V. Oikonen, U. Ruotsalainen
Turku PET Centre

BIODISTRIBUTION OF 18F-CFT IN HUMAN

Synthesis of F-18 labelled cocaine analogue CFT (2- β -carbomethoxy- β -(4-fluorophenyl)tropane, WIN 35,428) has made it possible to study the dopamine reuptake sites in human brain with PET. The aim of this study was to measure the biodistribution of 18F-CFT in humans for determination of patient dosimetry. In rats, the highest accumulation of 18F-CFT was found in the liver, urine, striatum and kidney by Haaparanta et al. (1996).

Radioactivity concentrations in urine were measured in twelve subjects 90 min after injection and in two subjects 200 min after injection. The maximum radioactivity concentrations in striatum and cerebellum were defined from dynamic PET acquisitions of 18 subjects. In addition, dynamic scans of abdominal region in two subjects were collected to define the maximum relative uptake of the tracer in liver, gall bladder and bone marrow. The relative amount of radioactivity in urine was $6 \pm 4\%$ 90 min after injection and $13.1 \pm 0.2\%$ 200 min after injection. The maximal uptake in the liver was 30% about 20 min after injection and in gall bladder 2%. The accumulation of 18F-CFT in the bone marrow was increasing with time and the relative uptake was 19% at the end of the dynamic study (90 min after injection). The accumulation of 18F-CFT reached a constant level about 200 min after the injection. At this time $0.29 \pm 0.04\%$ of the injected tracer had accumulated to the striatum and about $3.2 \pm 0.5\%$ to the whole brain.

These results show that 18F-CFT is excreted out of the body via liver, gall bladder and intestine rather than through kidneys with urine like for example FDOPA. The uptake of the tracer in bone marrow is important for radiation dosimetry.

Dosimetry and radiobiology: radiobiology/dosimetry

PS-612

I. Clairand¹, M. Ricard^{1,2}, M. Di Paola^{1,2}, B. Aubert^{1,2}

¹Institut Gustave-Roussy & ²INSERM U494, Villejuif, France.

INTERNAL DOSIMETRY: DEVELOPMENT OF A MONTE CARLO BASED SOFTWARE.

In nuclear medicine, several softwares have been developed to determine the absorbed dose at organ level. On the one hand, the MIRDOSE3 software developed by the University of Oak Ridge estimates the radiation dose per unit of administered activity for specific anatomic models. On the other hand, the most sophisticated methods dedicated to treatment planning use a three-dimensional set of images representing radionuclide distribution (SPECT/PET) and a corresponding set of images representing anatomy (CT/MRI).

As the first method is dedicated to fixed geometries and the second cannot be applied to every patient because very inconvenient we have developed an intermediate tool. Our program based on EGS4 Monte Carlo code calculates dosimetric parameters for a mathematical anthropomorphic phantom taking into account patient morphology. This phantom is defined by the combinatorial geometry MORSE-CG derived from the MORSE Monte Carlo code. This geometry confers flexibility to the phantom so that it may be easily adapted to the patient anatomy when it differs from the standard model. The validity of the main program as well as the description of geometry were verified by calculating S-factors in the case of the MIRD adult male phantom and comparing these results with S-factors provided by MIRDOSE3 for this phantom. The comparisons were performed for ¹³¹I and ^{99m}Tc and for different source organs.

The results show a good agreement between calculated data and MIRDOSE3 data. For the two studied radionuclides the S-values are within 25% of those published for most organs and within 4% when the source and target are the same. The largest differences correspond to small organs and hollow organs for which MIRDOSE3 uses analytical methods and simplifying assumptions.

The agreement between our results and those proposed for most organs in MIRDOSE3 confirms the validity of the description of the geometry and the program in general. Our program, therefore, may contribute to a more realistic patient dosimetry and radiation protection.

PS-613

S. Kojima*, O. Matsuki*, A. Kubodera**, Y. Honda***, S. Honda***

Department: *Research Institute for Biological Sciences and **Department of Pharmaceutical Sciences, Science University of Tokyo, Japan, and ***Tokyo Metropolitan Institute of Gerontology, Tokyo, Japan

INDUCTION OF mRNA EXPRESSION FOR THE REDUCED FORM OF GLUTATHIONE SYNTHESIS BY SMALL DOSES OF γ -RAY

In our previous study, changes in endogenous the reduced form of glutathione (GSH) levels in mice after small doses of γ -ray irradiation were examined, and GSH levels in some organs such as liver, brain and pancreas were significantly induced by a single irradiation with γ -ray at a dose of 50 cGy. In order to examine endogenous GSH synthesis after small doses of ionizing radiation, analysis of mRNA expression for GSH synthesis was conducted.

We examined mRNA induction for the reduced form of glutathione synthesis (GSH) in the liver of mice after small-dose γ -ray irradiation by using northern blotting. The mRNA of γ -glutamylcysteine synthetase (γ -GCS), a rate-limiting enzyme for *de novo* synthesis for GSH, was slightly induced quite long after γ -ray irradiation at a dose of 50 cGy. While mRNA for glutathione reductase (GR), an enzyme for the GSH regenerating cycle, was drastically induced soon after the radiation, and peaked much earlier than GR activity. Furthermore, mRNA for thioredoxin (TRX), which probably contributes to GSH biosynthesis via supplying cysteine to the *de novo* pathway, was also induced in similar fashion.

Next, the dose-dependent effects of γ -rays on the induction of mRNA expression of GR and TRX were investigated at 1 hr post irradiation. As a result, GR mRNA expression increased greatly in a dose-dependent manner at doses between 25 cGy and 100 cGy, with a maximum expression ratio of about 250% at 100 cGy. The same level of increase (250%) was observed at the highest dose of 200 cGy. For TRX mRNA, a transient increase was observed with a maximum peak at doses ranging from 25 cGy to 50 cGy. Between 100 and 200 cGy, mRNA expression decreased to about 50 % of the non-irradiated control (0 cGy). We are now investigating changes in GSH contents induced by small doses of γ -rays in connection with signaling transcriptional genes for GSH biosynthesis.

In this study, we have demonstrated that the elevation of GSH content in the liver of mice irradiated with small doses of γ -rays is followed by induction of mRNA transcripts coding for GR, one of the key enzymes in the regenerating cycle for GSH biosynthesis.

PS-614

A. Kubodera*, A. Yamamoto*, H. Fujishima**, S. Kojima**

Department: * Department of Pharmaceutical Sciences and **Research Institute of Biosciences, Science University of Tokyo, Tokyo, Japan

COMPARISON OF CYTOTOXICITY OF γ -RAY AND UV-A AGAINST TUMOR CELLS IN COMBINATION WITH CAMPTOTHECIN

Camptothecin (CAM) is a highly specific inhibitor of DNA topoisomerase I (topo I), and traps the covalent enzyme-DNA complex, the so-called cleavable complex. That is, CAM acts as a stabilizer of the cleavable complex, resulting in inhibition of DNA replication and repair. The ability of CAM to cause cell cycle arrest in the G2 phase leads to the accumulation of cells in the G2/M phase, which is the most radiation-sensitive phase of the cell cycle. In combination studies with CAM and X-ray, it has been found that CAM is an excellent radiosensitizer of an extremely radioresistant human melanoma (U1-Mel) as well as other tumor cell lines. Since the UV-A-sensitive phases of the cell cycle are considered to be similar to the X-ray-sensitive phases, CAM may be expected to enhance cell sensitivity to UV-A as well. Such a synergistic effect has been observed in the case of UV-A and caffeine, which is also an inhibitor of topo I. The purpose of this study was to examine whether CAM would enhance the cytotoxicity of UV-A to tumor cells *in vitro*, and also to compare the combination effect of CAM and UV-A with that of CAM and X-ray radiation.

The toxicity of UV-A to mouse melanoma (B-16) cells was assessed by measuring the incorporation of [³H] labelled thymidine into the cellular DNA. Exposure of cultured mouse melanoma (B-16) cells, to CAM after irradiation of the cells with UV-A synergistically enhanced the cytotoxicity. CAM treatment prior to irradiation had the same effect. Similar results were also obtained in the combination of γ -ray irradiation and CAM in this model.

The use of a combination treatment with CAM and UV-A, in place of CAM and X(γ)-ray irradiation, might have advantages such as easier control of the irradiation area and greater safety, etc. Further work seems justified to see whether this approach represents a potential clinical therapeutic procedure for the treatment of some cancers. *In vivo* trials of this combination treatment are in progress.

PS-615

J. Lee, D.S. Lee, J.M. Jeong, M.Y. Lee, Y.J. Kim, Y.S. Chang, S.A. Shin, M.M. Lee, J-K. Chung and M.C. Lee.

Seoul National University Hospital and Ewha Womans University, Seoul, Korea.

DOSIMETRY AND MIRD OF Re-188-DTPA FOR ENDOVASCULAR BALLOON BRACHYTHERAPY AGAINST RESTENOSIS AFTER CORONARY ANGIOPLASTY: COMPARISON WITH Re-188-PERRHENATE

Rhenium-188 (Re-188) could fill the balloon as liquid to yield homogeneous radiation around angioplasty balloon. If balloon ruptured, we need the liquid be excreted very rapidly. We calculated and adjusted doses of Re-188-DTPA and examined if it was more advantageous using Re-188-DTPA over Re-188-perrhenate for endovascular balloon brachytherapy.

We concentrated generator-eluted Re-188-perrhenate using ion column methods to more than 5550 MBq/ml. We labeled DTPA with Re-188 according to the method of M.A. Majali (J Radio Nucl Chem 1993). The labeling efficiency was 95% on average. Re-188-DTPA was stable *in vitro* (90% after 5 hours) and *in vivo* (88% at 60 minutes mixed with human plasma). Biodistribution after intravenous injection was similar to Tc-99m-DTPA in mice. Time-activity curves of kidneys in dogs showed that Re-188-DTPA was rapidly excreted via urine (Tmax= 1.1 minutes, T1/2=10.1 minutes). When we estimated radiation dose from an angioplasty balloon (20 mm length, 3 mm diameter cylinder) to the adjacent vessel wall using EGS4 Monte Carlo code, the radiation dose to the wall was 22.4 Gy at 0.5 mm with 37 MBq of Re-188 after 1 minute of exposure. Fifty percent of the energy deposited within 1 mm from the balloon surface. We needed 2627 MBq in one ml of solution to stay for 30 seconds to radiate 18 Gy to the surface of vessel wall. Using MIRDSE3 program we found that the estimated internal dose to the whole body (0.02 mGy/MBq) was less than the absorbed dose with Re-188-perrhenate (0.06 mGy/MBq). The dose to urinary bladder was 1.57 mGy/MBq and the whole body dose of 2627 MBq (single dose) was 5.2 mGy which is smaller than 15.6 mGy with Re-188-perrhenate.

We concluded that internal whole body dose of Re-188-DTPA was one third of Re-188-perrhenate and was better than Re-188-perrhenate regarding safety issues when the balloon ruptured. We suggest that Re-188-DTPA as an agent for endovascular balloon brachytherapy to inhibit coronary artery restenosis after angioplasty.

PS-616

M.Monsieurs, H. Thierens, L. De Ridder, C. Van de Wiele, A. Vral and RA. Dierckx.

University of Gent and University Hospital of Gent, Belgium.

IN-VIVO ADAPTIVE RESPONSE IN PATIENTS TREATED WITH ¹³¹I FOR MALIGNANT AND BENIGN THYROID DISEASE.

A prospective study was undertaken to assess the equivalent total body dose (ED) resulting from ¹³¹I therapy in 13 patients treated for thyrotoxicosis and thyroid carcinoma. The ED was determined by means of the cytokinesis block micronucleus assay. Using the same technique, the existence of an *in-vivo* adaptive response was investigated by *in-vitro* irradiation of blood samples taken before and one week after therapy.

This study comprises 10 thyrotoxicosis patients (μ activity 703 MBq, range 555 - 1110, μ age = 59, range 42 - 71) and 3 thyroid carcinoma patients (activity 3.7 GBq, μ age = 58, range 40 - 76).

For each patient, 2 blood samples were taken, one immediately before and one 7 days after therapy, and divided in 3 fractions. One fraction served as a non-irradiated control while the two others were irradiated with 0.5 Gy and 1 Gy by a ⁶⁰Co-beam. Micronuclei were scored on 1000 binucleated cells from each fraction and a calibration curve was calculated from the first blood sample. The micronucleus yield from the non-irradiated fraction of the second blood sample was fitted in this curve and the ED was calculated. The increase in micronucleus yield after *in-vitro* irradiation of both blood samples was compared. An adaptive response exists when the increase in micronucleus yield by *in-vitro* irradiation is significantly less in the blood sample after therapy than in the blood sample before therapy.

The mean ED found after ¹³¹I therapy was 0.32 Gy, which is more than 10 times lower than the ED found after large-field radiotherapy treatments for Hodgkin's disease or cervical cancer using the same methodology. The mean ED was somewhat lower for thyrotoxicosis patients (μ = 0.28 Gy (0.00 - 0.72)) than for thyroid carcinoma patients (μ = 0.44 Gy (0.20 - 0.70)). In the total patient population, the mean increase in micronucleus yield after *in-vitro* irradiation was significantly ($p = 0.04$) lower in blood samples taken after therapy than before therapy. For 8 out of 13 patients, a clear *in-vivo* adaptive response was found after ¹³¹I treatment.

PS-617

P. Oehr, J. Ruhlmann J., H. Rink*, B. Kozak, C. Menzel**,
P. Willkomm**, H.J. Biersack**.

PET-Zentrum, exp. Radiologie und Strahlenbiologie der Universität,**
Klinik für Nuklearmedizin Universität Bonn, Germany

18F-FDG UPTAKE IN VITRO: EFFEKT OF IRRADIATION DOSE.

Aim: The clinical role of FDG depends on the factors which are most related to its uptake. It is still a matter of discussion whether the uptake is more related to the cellularity or to the proliferative status. This investigation was undertaken to characterize the mechanism of in vitro uptake of F-18 FDG after irradiation with different doses in relation to the time after treatment.

Methods: HeLa cells, two strains of glioblastoma cells and embryonal mouse astrocytoma cells were seeded in separate petri-dishes. After addition of F-18 FDG its uptake was determined within 30 min. In other experiments the cells were irradiated with doses from 5 Gy to 100 Gy. The uptake of F-18 was determined within 30 min at different time intervals up to 168 hours.

Results: In tumor cells, increasing doses of irradiation caused an increased uptake (maximum 9-fold) of F-18 FDG within 48 hours. During the interval from 24 hours to 168 hours, the uptake decreased in cultures treated with high doses (50 Gy, 100 Gy). Mouse embryonal astrocytoma cells, however, did only show a slight increase of uptake after irradiation.

Conclusion: The dose dependent increase and/or decrease of F-18 FDG uptake shows that accumulation of FDG in cells can be highly increased even when proliferation is inhibited. This finding suggests that an interpretation of F-18 FDG uptake in irradiated patients should be related to the dose of treatment and to the time after treatment.

PS-618

L. Pasteur, N. Tronko, V. Markov, E. Klochko, N. Smirnova

Hospital: Institute of Endocrinology & Metabolism,
Department of Pathophysiology, Kyiv, Ukraine

RADIOIODINE-INDUCED PEROXIDATIVE PROCESSES IN THYROID (ABSORBED DOSE: 5 GY)

In the present study, the relation between radiation-induced promotion of lipid peroxidation in thyrocytes membrane and thyroid functions were examined. ¹³¹I-iodine was injected ip into the Wistar rats which were then fed an antioxidant-free diet. Thyroids (absorbed dose: 5 Gy) were surgically removed under ether anesthesia and cultured for 72 h at 37 °C in medium 199 with 10% bovine serum and thyrotropin, 10 mU/mL. For modelling processes of membrane peroxidation part of control's samples were incubated with hydroperoxide of oleic acid (HOA, 1 mM) or hydroperoxide of lecithine (HL, 1 mg/mL). The medium thyroid hormone levels were measured by radioimmunoassay. The lipid-protein cross-links (LPC) in the thyroid gland membranes were determined by fluorometric technique. The results obtained indicate that the medium thyroxine and triiodothyronine levels were 21.68±2.13 and 1.77±0.23 for the control (n=9), 12.34±1.38 and 0.99±0.17 for the ¹³¹I-iodine (n=4), 7.88±1.86 and 0.55±0.09 for the HOA (n=5), 4.24±0.80 nmol/L and 0.21±0.03 nmol/L for the HL group (n=5); the LPC coefficient were 23.2±2.4 (n=4), 62.7±8.2 (n=2), 36.4±4.3 (n=3) and 38.2±0.4 (n=2), respectively (Values are the mean±SD and statistically significant). Irradiation leads to an increase in malondialdehyde contents in thyroid tissue compared to the control (mean±SD; 2.25±0.45 vs. 1.15±0.15 nmol/mg lipid, p<0.05). We conclude that lipid peroxidation processes play a pathogenetic role in radiation injury of the rats thyroid gland exposed to radioiodine in a dose of 5 Gy under antioxidants depletion.

PS-619

C. Pirich, A. Pilger, D. Germadnik, U. Prüfert, E. Schwameis, A. Wanivenhaus, H. Sinzinger
Departments of Nuclear Medicine, Occupational Medicine and Orthopedics,
University of Vienna, Austria

EFFECTS OF INFLAMMATORY DISEASE ACTIVITY ON LEVELS OF BIOMARKERS OF CYTOGENETIC DAMAGE IN PATIENTS UNDERGOING RADIATION SYNOVECTOMY

Concerns persist about possible radiation-induced cytogenetic damage after radiation synovectomy (RS), but data are missing on the relation between radiation exposure, leakage, arthritis activity and the levels of biomarkers of cytogenetic damage.

Methods: Urinary excretion of 8-hydroxy-2'-deoxyguanosine and micronuclei formation in lymphocytes were measured in 16 patients undergoing 18 treatments of chronic synovitis of the knee with ¹⁶⁵Dysprosium Ferric-Hydroxide (median activity 9.7 GBq ¹⁶⁵Dy-FH). Local and systemic inflammatory activity were assessed clinically, by knee effusion analysis, measurements of the blood sedimentation rate and Tc-99m-HIG scintigraphy
Results: Levels of 8-OHdG (μmol/mol creatinine) and the frequency of micronuclei (micronuclei/500 binucleated cells) did not change after treatment. 4 patients only, showed a very moderate increase in biomarkers. Non-target organ leakage could be detected with a clinical whole body counter in 4 patients, too. Increased pre- and posttreatment biomarker levels were observed in 3 patients with high inflammatory activity. In summary, interindividual variations in biomarkers exceeded intraindividual variations due to the treatment.

Conclusion: Levels of biomarkers of cytogenetic damage might be influenced by the inflammatory activity of the underlying disease. Their levels do not significantly increase in the majority of patients after RS underlining the safety of this procedure.

Physics and instrumentation: PET

PS-620

D. Al-Azmi (1)*, J. Grootoank (2), T. Spinks (3) and N.M. Spyrou (1).

(1) Dept. of Physics, University of Surrey, (2) Wellcome Dept. of Cognitive Neurology, Institute of Neurology, (3) Cyclotron Unit, Hammersmith Hospital, London, England, UK. *Present address: Nuclear Medicine Dept., Ministry of Health, Kuwait.

THE EFFECT OF ENERGY SPECTRUM VARIATIONS DUE TO TEMPERATURE CHANGES ON TOMOGRAPHIC IMAGES.

Energy spectrum variations with temperature have been observed with a clinical PET scanner utilising BGO detectors. The temperature was monitored during the course of measurements over more than 12 hours in two energy windows, one centered on the full energy photopeak (380-850 keV) and the other in the Compton scattering range (200-380 keV). It was found that the relative number of acquired counts in the two energy windows correlated with the change in temperature, and that the photopeak shifted to higher energy at lower temperature. The ratio of the counts varied by up to 10% with a temperature change of 2 degrees C.

The effect of such spectral instability has been explored using a prototype PET scanner (with only one pair of coincident BGO detectors). Data were collected over a period of 63 hours in a scan-rotate motion using a collimated Ge-68 positron source in single photon counting mode for the transmission scan across a rat's head phantom for the attenuation correction method. In order to improve the quality of the data for calculation of attenuation correction factors, different fractions of the scattered data were subtracted from the photopeak. The quality of the resulting transmission scan data was assessed by reconstructing transmission images and comparing them using a fidelity test (with respect to the ideal image) to find the optimal scatter fraction which provides images of best quality. With increased scatter subtraction, the effect resulted in more degradation in the images. This may be due to an incorrect proportion of scattered counts subtracted from the corresponding photopeak counts because of temperature variations where in some cases the photopeak counts are reduced and the scattered counts are increased and in other cases the reverse occurs. The use of a wider energy window helps to reduce the effects of such a change in the energy spectrum.

PS-621

S.Cargnel, F.Chierichetti, B.Saitta, *G.Pizzolato, *A.C. Cagnin, G.Ferlin
Nuclear Medicine-PET Center, Castelfranco Veneto *Neurology Dpt., University of Padua

A SIMPLE NON-INVASIVE METHOD TO MEASURE REGIONAL CEREBRAL METABOLIC RATES FOR GLUCOSE (rCMRglc) IN A CLINICAL SET-UP

Fluorodeoxyglucose (FDG) method in positron emission tomography (PET) allows to measure regional cerebral metabolic rates of glucose (rCMRglc). The necessity to catheterize the patient is often an obstacle in a clinical set-up to evaluate the rCMRglc with FDG-PET, then only qualitative evaluation on the images is done. This protocol was designed to obtain quantitative measurement of regional cerebral glucose utilization (rCMRglc) using fixed rate constants for the population in a non invasive way to be applied in a disease state.

A dynamic cardiac scan is acquired before the emission scan on the brain and the input function is obtained employing six ¹⁸F-DG time-activity curves derived from regions of interest (ROIs) drawn on the left ventricular cavity, three time-activity curves from ROIs on myocardium and three venous samples at 25, 35 and 45 min from injection measured at a gamma counter. The venous samples and the myocardium curves are necessary to evaluate the spillover to left ventricular cavity. The method is validated on six patients measuring both the arterial input function and the dynamic scan input function.

The error on the input function integral obtained with the conventional and this new method is comprised between +7.6% and -9.6%. The regression line between rCMRglc obtained with the conventional method and rCMRglc derived by the dynamic cardiac scan is

$$y = 0.90x + 4.81 \quad (R^2 = 0.86)$$

The results confirm the possibility to use the dynamic cardiac acquisition and the venous samples to obtain the input function in a clinical environment.

PS-622

L. Geworski¹, B.O. Knoop², D.L. Munz¹

Clinic for Nuclear Medicine, ¹Charité, Humboldt University Berlin, ²Medical School Hannover, Germany

COMPARABILITY OF QUANTITATIVE RESULTS OF DIFFERENT PET SCANNERS

Frequently, results obtained with different PET scanners are presented in multicenter studies without prior evaluation of system comparability. Thus, the aim of this phantom study was to test the comparability of scanners from different PET centers.

The study was performed with two models of PET scanners (ECAT 951 [PET-1] and ECAT EXACT HR⁺ [PET-2]). The test phantom used consisted of a 20 cm Lucite cylinder with three sets of spheres. Each set contained four spheres (5, 10, 20, and 30 mm diameter). The sets were filled with different activity concentrations of F-18 solution to mimic cold, warm, and hot lesions. The background activity was modified in order to simulate different lesion to background ratios. The absolute concentration values were determined by normalising the measured values with data from a Ge-68 standard. The data were acquired in 2D and, if possible, in 3D mode. The concentrations in the lesions were determined using ROI technique (ROI size = lesion radius) and compared with the true values.

The mean difference between measured and true values of the Ge-68 standard was < 4.3 % PET-1 and < 2.5 % PET-2. The deviations of activity concentration values in the 30 mm spheres were 6.8 % PET-1 for the hot and 5 % for the warm lesion. For the 20 mm spheres the deviations were 14.7 % and 13.3 %, and for the 10 mm spheres 63.3 % and 65.6 %, respectively. The increasing deviations for decreasing lesion size are due to the recovery effect. PET-2 yielded similar results with slightly lower differences because of a better resolution. The sensitivity in the 3D mode for lesions in a cold background was 1.5fold higher as compared to the 2D mode and 6.5fold higher for lesions in a hot background due to increased solid angle covered by activity in the 3D mode.

Conclusion: The measurements performed allow a clinically relevant comparison of quantitative PET data from different institutions for multicenter studies.

PS-623

M. Ide, W. Takahashi, S. Yasuda, A. Shohtsu

Hospital: HIMEDIC Imaging Center at Lake Yamanaoka

CLINICAL FINDINGS FROM NORMAL SCREENING BY POSITRON EMISSION TOMOGRAPHY AT HIMEDIC IN JAPAN SINCE OCTOBER 1994.

HIMEDIC is a membership-based medical health club with clinical PET which was established in October 1994. We conducted medical health check-ups on our members using PET, MRI, spiral CT and other imaging modalities.

The purpose of this study is to report our clinical findings through 8,500 (will be exceed 10,000 cases until the end of this August) normal screening by PET at HIMEDIC in Japan since October 1994.

Results:

1. Brain Studies
We performed 2,156 brain FDG-PET studies, and found 32 cases of asymptomatic cerebral infarction, 10 cases of dementia of Alzheimer type, 6 cases of depressive state, 4 cases of intra-cranial hemorrhage etc. The rate of abnormal findings was 5.2%.
2. Heart studies
We conducted 1,190 stress ammonia PET studies since April 1996, and found 60(5.0%) cases of asymptomatic ischemia. In these ischemic cases, positive treadmill ECG test was found in 22(36.7%) cases, otherwise negative stress ECG test was found 38(63.3%).
3. Oncology Studies
We performed 3,681 FDG-PET studies for cancer screening, and found 7 cases of colon cancer, 5 cases of lung cancer, 3 cases of breast cancer, 3 cases of thyroid cancer, one case each of malignant lymphoma, renal cancer and gastric cancer. False negative cases of FDG-PET study were 4 cases of prostatic cancer, 3 cases of lung cancer, 3 cases of renal cancer, two cases of hepatoma, one case each of bladder, breast and colon cancer. But all of these false negative case of FDG-PET, were diagnosed by other imaging modalities or increase titer of tumor marker. False positive cases of FDG-PET study were sarcoidosis, lung tuberculosis, pneumonia, chronic thyroiditis, Wartin's tumor, rheumatoid arthritis etc.
Conclusion: Our results shows that the FDG-PET study is a powerful screening method for early detection of brain and malignant diseases, and stress NH3-PET for ischemic heart disease.

PS-624

P.J. Jolyan, J.L. Page and C.M. Boivin

Department of Nuclear Medicine, Queen Elizabeth Hospital, Birmingham, UK

THE NOISE EQUIVALENT COUNT RATE RESPONSE OF A GAMMA CAMERA COINCIDENCE PET SYSTEM AND EXTENSION TO MEASUREMENT FOR MORE REALISTIC COINCIDENCE FRACTIONS

The aim of this study was to measure the noise equivalent count rate (NEC) response for one of the new generation of dual-headed gamma camera PET systems (ADAC-MCD) to enable comparison with other similar systems and dedicated PET systems.

The NEC for our ADAC-MCD was measured in the standard NEMA way with a uniform cylinder of decaying activity and compared to published data for dedicated PET systems. NEC curves were also measured for a more realistic set-up where the cylinder is accompanied by a vial of activity outside the field-of-view. This produces additional singles and therefore random coincidences which are more representative of the clinical imaging situation, as shown by quantitative comparison to FDG patient studies. To validate the NEC measurements, all resulting images were analysed for uniformity.

When using the recommended mode of scanning with 30% photopeak-photopeak and 30% photopeak-Compton energy windows, the NEC shows a peak at ~6kcps for a phantom activity of ~30MBq (~4.7kBq/ml), giving the optimal activity with which to image this specific distribution. For a more realistic coincidence fraction (~2%) a peak NEC of ~3kcps was observed. This corresponds to an optimal administered activity for clinical imaging with FDG on this camera system of ~110MBq. The peak NEC was shown to coincide with the minimum integral non-uniformity within errors.

This work offers a useful comparison between gamma camera PET systems and dedicated scanners, and offers a method of comparing gamma camera PET systems as data becomes available. The measurement of NEC for realistic coincidence fractions gives a route to define optimal administered activities.

Poster presentations

PS-625

J B Cashmore, P J Julyan, M J Wilson and C M Boivin

Department of Nuclear Medicine, Queen Elizabeth Hospital, Birmingham, UK

OPTIMAL ENERGY WINDOW SETTING FOR A GAMMA CAMERA COINCIDENCE PET SYSTEM BY RETROSPECTIVE ANALYSIS OF LIST-MODE DATA

The manufacturer's recommended mode of scanning using our dual-headed gamma camera PET system (ADAC-MCD) is with symmetric 30% energy windows set over both the photopeak (511keV) and Compton (approximately 310keV) regions of the energy spectrum. Coincidences are then accepted between photopeak-photopeak or photopeak-Compton events.

We have investigated whether these settings are optimal for clinical FDG scanning for both the brain and the body.

Using the list-mode data that can be stored during acquisitions with the standard, or even wider, energy window settings we have developed a program to filter the data for alternative energy windows. The modified data files are then processed to form projections using the manufacturer's software which currently performs single-slice re-binning for subsequent 2-D reconstruction by an iterative algorithm.

Representative brain and body studies were filtered for a number of different settings.

Improvements in terms of resolution and contrast may be obtained in the brain and body by using photopeak-photopeak coincidences only although the number of events is reduced to approximately 58% and 54% respectively when compared to the standard mode. Further improvements are possible by increasing the lower threshold of the photopeak energy although eventually the loss of events results in domination of noise. Our initial analysis of a high-grade glioma shows a maximum in contrast when using only those events above 475keV corresponding to 38% of the originally acquired events. However, the choice of energy window is complex and generally will depend on the camera system used, the body region imaged and even potentially the quality of individual patient data.

We have shown that there is the potential for improvements to be made to FDG-PET scanning using a gamma camera by more considered use of energy window settings.

PS-626

W. T. Kranert, R. Aljazzar, P. Baldauff*, N. Zimny*, R. Standke*, A. Niesen, A. Hertel, G. Hör

Klinikum der Johann Wolfgang Goethe-Universität Frankfurt/M, Klinik für Nuklearmedizin; *SMV GmbH, Frankfurt

IMAGE QUALITY OF 511-KEV COINCIDENCE ACQUISITIONS WITH A HALF INCH CRYSTAL, DUAL-HEAD GAMMA CAMERA

The aim of the study was to measure resolution and contrast of 511 keV coincidence acquisitions with a dual-head gamma camera, which are the basic parameters for image quality.

Methods: Resolution was measured with a small point source (\varnothing 1,5 mm) placed in the center of the field of view and a line source (\varnothing 3,5 mm). For contrast evaluation point sources with different volumes and different inner to surrounding ratios of activity were placed in a cylindrical phantom (\varnothing 24 cm). By long lasting dynamic acquisitions the dependence of concentration on count rate and random counts is evaluated. Acquisitions are performed with a DST-XL (SMV) dual-head gamma camera equipped with a half inch crystal, mainly used in the routine for SPECT acquisitions including TI-201.

Results: For the point source without absorption medium a FWHM (full width of half maximum) of 6,2 mm could be found, rebinned with a zoom of two and a ramp-filter used for reconstruction. The rebinning of the same acquisition with different zooms shows, that resolution is limited by the pixel size. Measurement with the line source shows no change of the resolution over the whole length in the field of view, while pixel statistics decreases in the outer parts (zoom 1).

A dependence of contrast on ratio between the random and single was found with 27% randoms a point source of an activity concentration ratio of 3:1 to the surrounding medium can be visualized. This is not the case with higher randoms. 27% randoms yields in the highest number of true coincidences per second with a single count rate of 2,3 kcounts/s inside the 511 keV window. Activity in the phantom was 18 MBq. Higher activity in the phantom decreases the efficiency for the singles and for true coincidences. Smaller activities lead to loss of image quality due to smaller pixel statistics.

These data are compared to those measured with an ECAT EXACT PET which shows comparable results for the same activity ratio and geometry.

Conclusion: The dual-head gamma camera reaches image quality which allows to use it for patient acquisitions.

PS-627

W. D. Kunze, M. Baehre, E. Richter

Clinic of Radiotherapy and Nuclear Medicine, Medical University of Luebeck, Germany

SPET AND PET WITH A COINCIDENCE GAMMA CAMERA

Objective and Methods: A dual head gamma camera with coincidence option (Picker 2000XP PCD, 3/4" NaI(Tl)) was examined for its low energy single photon (99mTc) and high energy coincidence (18F) imaging performance using phantom and patient scintigrams. Comparisons are made to a dual head camera with a 3/8" NaI(Tl) crystal in the single photon and to conventional PET scanners in the coincidence acquisition mode of the camera.

Coincidence imaging is realized through two optional geometrical configurations. Mounting a lead scatter shielding with septa in axial orientation simulates a 2D PET while using an open frame scatter shielding is similar to a 3D PET acquisition. The image reconstruction algorithm performs a rebinning of detected coincidence events into virtual parallel projections with exact calculation of the transaxial and approximated calculation of the axial coordinate. The number of virtual parallel projections, photon energy width, zoom, matrix size and the used area of the total field of view are variable rebinning parameters. The relation between image quality and rebinning parameters was pronouncedly investigated.

Results: Regarding the 99mTc imaging, doubling the crystal thickness decreases the intrinsic spatial resolution and increases the photopeak sensitivity about 10 % each. A high resolution collimator nearly compensates for the intrinsic resolution loss.

Doing coincidence imaging, the spatial resolution in water is transaxially 6-7 mm (FWHM) for standard rebinning parameters, independent of the shielding configuration. The resolution can be improved to 4-5 mm when the transaxial length of the used field of view is limited to the central 100 mm. The axial resolution is dependent on the axial acceptance angle. The scatter fraction is roughly 25 % using the axial septa and nearly 40 % using the open frame shielding for standard rebinning parameters. It becomes smaller only if the energy width of valid coincidence events is narrowed. The sensitivity for 511 keV coincidence events is 6-7 times larger with the open frame as with axial septa shielding. Within a 30 % energy width and with the axial septa the sensitivity is 130 ct/(s MBq), within 100 % 300 ct/(s MBq) for a standard cylinder.

Conclusions: A comparison with conventional PET scanner shows that the resolution and scatter fraction are nearly similar while the count rate of true coincidences is considerably smaller using the coincidence gamma camera.

PS-628

P. Reinartz, M. Zimny, U. Cremerius, H. J. Kaiser, U. Buell

University Hospital, University of Technology Aachen, Germany, Department of Nuclear Medicine

REPOSITIONING IN WHOLE BODY PET STUDIES: QUANTIFICATION OF ERRORS IN SUPERIMPOSED TRANSMISSION AND EMISSION SCANS

Objective: To employ PET scanners economically, transmission (T) and emission (E) acquisitions have to be scheduled efficiently. This often results in a temporal separation of the examination where the T scan proceeds or follows the E scan by up to one day. The purpose of this study was to quantify repositioning errors introduced by such protocol. Repositioning errors are of special clinical interest since they may cause artifact induced misinterpretation of attenuation corrected PET studies or erroneous quantifications.

Methods: 30 whole body E and T scans have been performed with five bed-positions each. Repositioning of the patient was performed with the ECAT laser positioning system and body marks. Data was acquired with a Siemens ECAT Exact PET Scanner using 2D technique. Both T and E data were reconstructed using filtered backprojection and superimposed. The distance (in mm) between the outer boundaries of the superimposed T and E images were measured using a computerized distance measure tool. For analysis, scans were divided into four main body sections (cervical, thoracic, abdominal & pelvic). Within each section three planes, 14 mm apart, were evaluated.

Results: The Table shows the mean value \bar{x} , the standard error of the mean sem , and the standard deviation σ in mm obtained from the distance measured between the outer boundaries of the superimposed transmission and emission scans in the three orthogonal axes x, y, and z:

	$\bar{x} \pm sem$ [mm]			σ [mm]		
	x	y	z	x	y	z
cervical	11.83 ± 1.03	11.84 ± 0.85	12.04 ± 0.97	5.65	4.63	5.34
thoracic	12.60 ± 0.93	12.10 ± 0.76	9.59 ± 0.50	5.10	4.16	2.76
abdominal	13.14 ± 1.14	11.21 ± 0.70	8.87 ± 0.36	6.26	3.86	1.97
pelvic	14.55 ± 1.22	11.75 ± 0.69	9.93 ± 0.65	6.69	3.78	3.55

39 % of all measured differences were smaller than 10 mm, 54 % lie between 10 and 20 mm, and only 7 % exceed 20 mm.

Conclusions: The magnitude of the acquired data strongly indicates that repositioning errors are non negligible for the interpretation of PET studies. Therefore, a high precision standard in the repositioning of the patient is a prerequisite for employing attenuation corrected studies, especially for quantitative analyses and to prevent artifacts. However, the non-attenuation corrected emission scan should also be considered for the diagnosis of pathological findings. To minimize repositioning errors, hot transmission is the preferred solution.

PS-629

A.Schaefer, S. Schmidt, S. Kremp, D. Hellwig, C.-M. Kirsch

Department of Nuclear medicine, University clinics of the Saarland, Homburg, Germany

PERFORMANCE OF COINCIDENCE TRANSMISSION VERSUS SINGLE PHOTON-TRANSMISSION FOR PET

Purpose: Transmission measurements can be performed using either rotating coincidence sources such as $^{68}\text{Ge}/^{68}\text{Ga}$ rod sources or rotating single photon sources such as ^{137}Cs (662 keV) point sources. In this study we compared measured attenuation coefficients and count densities of both modes of transmission and the image quality of attenuation corrected emission data.

Method: An abdomen phantom with homogenously filled organs and simulated defects as well as patients with different carcinoma diseases were studied. An ECAT ART scanner (Siemens, CTT) was used, which was originally equipped with two $^{68}\text{Ge}/^{68}\text{Ga}$ rod sources. In January, the rod sources were exchanged by two collimated ^{137}Cs point sources. Measurements were performed pre- and post-injection of FDG.

Results: Transmission images acquired in singles mode differ significantly from those acquired in coincidence mode. The defects within the phantom ($\mu = 0.139 \pm 0.01$ 1/cm) are only resolved in the singles transmission images as well as the glassy bodies ($\mu = 0.1055 \pm 0.0034$ 1/cm) of the organs within the phantom. In patient studies the image contrast increases significantly with singles transmission correction of emission data: i.e. different organs can be exactly separated from each other and bone structures within arms or legs are resolved.

Conclusion: Collimated single photon transmission provides a better measurement of attenuation correction factors than coincidence transmission. Attenuation correction of PET emission data using single photon transmission provides a high degree of additional anatomical information.

PS-630

H.Zhang, S. Alyafei, T.Inoue, K.Matsubura, K.Tomiyoshi, K.Endo
Gunma University School of Medicine, Department of Nuclear Medicine, Gunma, Japan
T.Satou, K.Tanaka, Shimadzu Co, Kyoto, Japan

COMPARISON ON TWO-DIMENSIONAL AND THREE-DIMENSIONAL IMAGING CHARACTERISTICS OF A WHOLE-BODY PET SCANNER

To evaluate the clinical utility of three-dimensional imaging of a whole body PET scanner, the imaging characteristic of a new whole-body PET scanner (SET2400W, Shimadzu, Japan) in three-dimensional (3D) mode was investigated and compared to two-dimensional (2D) mode. Line-source measurements are performed to determine spatial resolution over the scanner FOV, and cylindrical phantom distributions are used to determine the sensitivity, scatter fraction and count rate performance of the system. Phantom and ^{18}F -FDG patient studies are used to evaluate image quality with 2D and 3D reconstruction algorithms. The system's transaxial spatial resolution varies from 4.26mm(4.51mm) full width at half-maximum(FWHM) at center to 5.37mm(6.36mm) FWHM tangentially and 6.45mm(8.08mm) FWHM radially at R=20cm in 2D mode and (3D mode). Average axial resolution changes from 4.27mm(6.61mm) FWHM at center to 7.85mm(10mm) FWHM at R=20cm in 2D mode and (3D mode) respectively. Total sensitivity for a 20cm cylinder phantom is 7.98kcps/kBq/ml in 2D at 350-800keV, and increases to 48.95kcps/kBq/ml in 3D mode at the same energy thresholds. In this energy window the noise equivalent count rate peaked at 73.9kcounts in 2D mode, compared to 86.1 kcounts in 3D mode. Scatter fraction varies in 2D from 9.2% to 14.9% for energy thresholds from 350-800keV for line sources in a 20cm diameter phantom. In 3D mode an increase of scatter of 20 is observed. The kinetic analyses of ^{18}F -FDG clinical brain and whole-body studies shows improvements in 3D over 2D. The results demonstrate that, with regard to sensitivity, there are significant gains in the physical performance of this tomography when operating in 3D compared to 2D mode and that the quantificant of PET studies using 3D data reflects this.

Physics and instrumentation: SPET

PS-631

W.Backfrieder¹, A.Gedrovics¹, T.Leitha², H.Bergmann^{1,3}, N.Gurker⁴
¹Dept. Biomedical Engineering & Physics, ²Clin. Nuclear Medicine, ³L.Boltzmann Institute Nuclear Medicine, University of Vienna, ⁴Dept. Technical & Applied Physics, Technical University, Vienna, Austria

SURFACE DETECTION FOR ATTENUATION CORRECTION IN SPECT

Filtered back-projection (FBP) is because of its effective computational implementation the method of choice in clinical SPECT. Application of several filter-families in the reconstruction process yields smoothing and/or preservation of edges in the images. Image artifacts from absorption within the body cannot be corrected by FBP. Among others, the inversion of the attenuated Radon-transform by exponential filtered back-projection (EXFBP), solves this problem in the case of uniform attenuation. Projection data have to be manipulated relative to the outer contour of the body. In this work the body contour is detected by a 3D magnetic tracking system (Polhemus 3SPACE ISOTRAK II) prior to SPECT examination. Sampled surface points are registered against the measured SPECT data using a set of ^{57}Co point sources. To calculate proper absorption lengths for normalization of projection data, the irregular surface point-set is transformed to a surface in 3D by Delaunay triangulation. EXFBP is performed presuming a Gaussian shaped point spread function (PSF) of variable width (FWHM).

The algorithm was tested using an Alderson phantom. The surface of the head and breast area was digitized. The phantom was filled with 1000 MBq $^{99\text{m}}\text{Tc}$. Data acquisition was done with a three headed Picker Prism3000 gamma camera, LEUHR parallel collimator, 120 projections/360°, 80s/projection, 128x128 matrix size and 3.6mm slice thickness. Transaxial slices were reconstructed by EXFBP using PSF of FWHM=1,2,3,5 pixel and compared to FBP using a generalized Hamming window with $\alpha=0.8$.

EXFBP shows proper correction of attenuation artifacts within the body. The use of a tracking system enables attenuation correction of non-spherical absorbers. Projection of laser grids could further improve surface detection for application in clinical SPECT.

PS-632

J.Billet, D.O. Slosman.

Nuclear Medicine Departments, Geneva University Hospital (CH).

IMPROVEMENT OF QUANTIFICATION IN SPECT USING TRANSMISSION COMPUTED TOMOGRAPHY: UTILISATION OF ^{153}Gd TRANSMISSION SOURCES.

Introduction: We have previously evaluated the use of $^{99\text{m}}\text{Tc}$ and ^{201}Tl isotopes for attenuation correction using transmission computed tomography (TCT). Our results had allow us to approach quantification analysis by using 3 rods sources of ^{201}Tl with a 3 heads gamma-camera. The aims of this present study were 1) to evaluate the utilisation of ^{153}Gd as a transmission isotope for quantitative analysis in reference to $^{99\text{m}}\text{Tc}$ and ^{201}Tl attenuation correction and to compare their accuracy, and 2) to investigate the possibility to perform the acquisition of a unique whole blank transmission scan for weekly clinical SPECT as a consequence of its 242 days physical half life.

Methods: Ten brain phantoms containing 3 externals sources, 3 internals sources and 1 central source with the same activity were scanned using a 3 heads gamma-camera Toshiba GCA 9300A/HG (30 steps of 4° (40s) covering 120° with fan beam collimation) and three ^{153}Gd rods sources. The difference between the external source activity and internal and central sources activity provides an index of the efficiency of the correction.

Results: Our results shows that the corrections methods improved significantly the image quality and the SPECT quantification. The difference between central and external activity is close to 10% for corrected images when it is about 30% for uncorrected images. TCT performed with the 3 different isotopes provided similar results, and in particular strong linear relationship between known and measured activities ($r^2=0.97$, $p<0.0001$). During a period of 3 weeks, analysis of the blank scans acquired did not significant change over time.

Conclusion: Therefore, we propose that TCT method with ^{153}Gd associated with the weekly acquisition of a whole blank scan can be apply to all clinical exams even so blank scan could not be performed (such as whole body acquisition).

Poster presentations

PS-633

G. Giorgetti, G. Sarti, S. Lazzari

Health and Medical Physics dpt, "M. Bufalini" Hospital Cesena - Italy

TRANSMISSIVE SPECT IMAGE CAN BE A STRONG SUPPORT TO CT/MR FOR TARGET DETERMINATION IN RADIOIMMUNOTHERAPY FOR BRAIN GLIOMAS

After a radioimmunotherapy cycle is performed, that means that Y90 labelled has been injected in the surgical cavity via catheters, to assess if the radioisotope has reached the target is a difficult and very important topic, either for the dosimetric calculations either for establishing the correctness of the therapy protocol. Difficulties are that Y90 is a pure beta emitter that gives therapeutical images which show only the spot and no anatomical reference point and the bremsstrahlung emission is masked by any other external marker and this could be avoided using transmissive SPECT techniques that give us rough anatomical information with a line source 153 Gd scan. Another problem is that this kind of procedure have never been used for the head, so the image files are not easily comparable with the ones coming from CT or MR scan. With the suitable software "hand-made" we reached the aim and, with the procedure errors estimated, we are now able to assess if a therapy has been successfully performed or not and we can estimate a more precise activity distribution in the head.

PS-634

C. Groiselle, J.-M. Rocchisani, J.-L. Moretti

UPRES 2360 - Université PARIS XIII – 93009 Bobigny FRANCE

ADAPTATIVE COMPTON SCATTERING CORRECTION FOR CODED APERTURE.

Image quantification in Nuclear Medicine requires to correct for Compton scattering artifacts. The global correction method of Pretorius is applicable for parallel projections. It uses two constants derived from an acquisition of a single point source with a parallel collimator and two energy windows. We have generalized this method to anisotropic projection and have corrected each pixel of the coded aperture acquisition.

Correction matrices have been computed with a 99mTc single point source in two contiguous energy windows: 126 keV to 140 keV and 140 keV to 154 keV. These matrices have been used to correct thyroid phantom images acquired in the same conditions. A reference view was obtained with the usual photopeak energy window. Projections were reconstructed with the ML-EM algorithm.

Noise decreased in $80\% \pm 17\%$ and the signal to noise ratio increased in $136\% \pm 12\%$.

The method provided a contrast enhancement and a better signal to noise ratio in the corrected images compared to the reference slices.

PS-635

M. Konno, E. Tsukamoto, T. Kohya, K. Morita, Y. Itoh, T. Shiga, A. Kitabatake and N. Tamaki

Hokkaido University School of Medicine

COMPARISON OF EJECTION FRACTION ESTIMATED FROM GATED MYOCARDIAL PERFUSION SPECT WITH 180 DEGREES AND 360 DEGREES RECONSTRUCTION

Myocardial perfusion SPECT with either the 180° or the entire 360° data collection is controversial. We have investigated whether this angular range may make any difference in estimating left ventricular ejection fraction (LVEF) using gated myocardial perfusion SPECT. ECG gated SPECT in 44 patients with various heart diseases were employed for the evaluation. One hour after injection of 600MBq of Tc-99m MIBI, 60 projections (60 seconds each) over 360° with 8 frames per cardiac cycle were acquired using three head rotating cameras. Gated SPECT images were reconstructed from cardiac anterior half 180° projection data and from full 360° projection data. We used commercially supplied QGS software based on Germano et al method (J Nucl Med 1995) for estimation of end-diastolic volume (EDV), end-systolic volume (ESV) and ejection fraction (EF).

	Mean±SD		correlation of 180° vs 360°			
	180°	360°	R	slope	intercept	SEE
EDV	125±12ml*	115±11ml*	0.998	1.059	2.164	5.0ml
ESV	74±13ml	67±11ml	0.992	1.208	-0.732	11.3ml
EF	50±2%	49±2%	0.983	1.030	-0.708	2.2%

(*P<0.01)

There was excellent agreement between EF values with 180° and 360° reconstructions, although EDV and ESV with 180° reconstruction were about 8-10% greater than those with 360° reconstruction.

Our results indicate that either 180° or 360° reconstruction makes no difference in estimating EF values from gated myocardial perfusion SPECT, despite some differences in actual volume calculation.

PS-636

P. Lahorte¹, S. Vandenberghe¹, Y. D'Asseler², M. Koole², K. Audenaert¹, I. Lemahieu², R. Dierckx¹

¹Department of Nuclear Medicine, University Hospital of Gent, Belgium;

²MEDISIP, Electronics and Information Systems Department, University of Gent, Belgium

STATISTICAL PARAMETRIC ANALYSIS OF ACTIVATION FOCI DETECTABILITY IN BRAIN SPECT IMAGING: IMAGE QUALITY VERSUS STATISTICAL POWER

Background and aim of the study: Recently it has been suggested that an increase in statistical power, gained by using a repeat-task design (replication paradigm), could outweigh the disadvantage of poorer image quality per scan for the detection of activation foci in SPECT neuroactivation studies. The present study was undertaken to investigate the main effects of a non-conventional SPECT replication paradigm framework, consisting of obtaining multiple datasets per activation task (simulation of clinical neuroactivation studies), on foci detectability in the brain, in relation to the varying size, position and activation of the foci.

Methods: Spherical activation foci of varying size and percentage of hyperactivity were created at clinically relevant positions in the digital three-dimensional Hoffman brain phantom. A repeat-task acquisition protocol was simulated for these phantoms on a triple-headed SPECT camera. This was performed using shareware sinogram simulation software. The acquisition images were subsequently reconstructed with filtered backprojection and analyzed using the Statistical Parametric Mapping software package (SPM96).

Results: Using the combined height and spatial extent threshold implemented in SPM96, study replication seems to result in slightly more significant activation foci at the cluster level. Also, at highly significant height thresholds the size of the detected activations seems to be closer to the true foci size in the case of study replication. However, exceptions to the general trends are observed related to foci position, activation and the maintained threshold level.

Conclusion: The presented results indicate that a very careful analysis has to be performed of the relative importance of study size, maintained threshold of the statistical tests and foci characteristics for determination of the trade-off between image quality and power of the statistical tests in SPECT neuroactivation studies.

PS-637

S. Lappi, S. Lazzari, G. Sarti, F. Del Dottore, G. Moscatelli, M. Agostini, P.L. Pieri
Hospital: Bufalini, Department of Health Physics and Nuclear Cardiology Unit, Cesena, Italy

RELIABILITY OF ACTIVITY DISTRIBUTION IN MYOCARDIAL SPECT IMAGES IMPROVES AFTER ATTENUATION CORRECTION. A PHANTOM STUDY.

AIM: The aim of this study was to assess the improvement in the reliability of activity distribution in myocardial SPECT images after attenuation correction. **METHODS:** An anthropomorphic phantom containing a Tc-99m filled cardiac insert was imaged by a dual headed camera (ADAC-Vertex), provided with two Gd-153 scanning sources. A female phantom was then obtained adding two water filled balloons as breast. Non-attenuation corrected (NC) and attenuation corrected (AC) images were reconstructed. The mean counts were calculated in 8 "myocardial" regions (4 apicals and 4 proximals) of the polar plots. **RESULTS:** In the NC images, the counts distribution showed a decrease in the proximal regions (especially in the inferior wall and, in the female phantom, in the anterior wall too), whereas in the AC images it was more uniform. The greatest differences between NC and AC images were observed in the proximal regions. The means & activities in the 8 regions were:

MALE PHANTOM	APICAL SEGMENTS			PROXIMAL SEGMENTS		
	NC	AC	p	NC	AC	p
ANTERIOR	85±7	86±5	n.s.	68±8	74±8	<.001
LATERAL	70±8	76±7	<.001	59±11	68±9	<.001
INFERIOR	68±4	77±6	<.001	54±6	70±6	<.001
SEPTAL	82±10	80±7	n.s.	67±9	76±8	<.001
FEMALE PHA.	NC	AC	p	NC	AC	p
ANTERIOR	75±10	81±7	<.001	59±16	76±11	<.001
LATERAL	84±6	77±8	<.001	73±6	73±5	n.s.
INFERIOR	74±9	81±1	<.001	54±5	72±5	<.001
SEPTAL	80±11	79±5	n.s.	62±11	74±7	<.001

CONCLUSIONS: Attenuation correction resulted in an increased reliability of the activity distribution in "myocardial" SPECT images, with a reduction of those artifacts that could lead to false-positives. No new defects or artifacts appeared in AC images.

PS-638

S. Lappi, S. Lazzari, G. Sarti, F. Del Dottore, G. Moscatelli, M. Agostini, P.L. Pieri
Hospital: Bufalini, Department of Health Physics and Nuclear Cardiology Unit, Cesena, Italy

TRUE MYOCARDIAL DEFECTS ARE NOT UNDERESTIMATED, AND APPEARS MORE DELINEATED, AFTER ATTENUATION CORRECTION. A PHANTOM STUDY. **AIM:** The aim of this study was to assess if attenuation correction improves the delineation of the perfusion defects extension in myocardial in SPECT images, and if it underestimates the defects severity. **METHODS:** In the mid-inferior wall of a Tc-99m filled cardiac insert placed in an anthropomorphic phantom, we simulated (by placing a fillable plastic segment) myocardial perfusion defects of different severity (0% and 45% activity). The phantom was imaged with a dual headed camera (ADAC-Vertex), equipped with two Gd-153 transmission scanning line sources that allow to obtain the morphological information (attenuation maps). To assess the effect of breast attenuation, the same defects were then simulated in the mid-anterior cardiac wall of a female phantom (obtained by adding two water filled balloons). Non-attenuation corrected (NC) and attenuation corrected (AC) images were reconstructed, respectively, with FBP and ML-EM algorithms. **RESULTS:** The defect severity (mean % activity in the defect area) and contrast (mean % change in counts between the defect area and the neighbouring area) are reported below:

SEVERITY (%)	0% DEFECT			45% DEFECT		
	NC	AC	p	NC	AC	p
MALE PHANTOM	32±3	35±7	0.3	46±2	47±3	0.4
FEMALE PHANTOM	24±9	25±5	0.8	57±7	52±5	0.1
CONTRAST (%)	0% DEFECT			45% DEFECT		
	NC	AC	p	NC	AC	p
MALE PHANTOM	29±6	50±5	<0.001	14±5	27±4	<0.001
FEMALE PHANTOM	23±18	49±7	0.001	19±5	31±1	<0.001

CONCLUSIONS: In both male and female phantoms, defects overcorrection does not occur, since not significant differences appears in defect severity between NC and AC images. The defect contrast increases in AC images, leading to a more accurate delineation of the defect extension.

PS-639

IR Lee, CW Choi, SM Lim, and SW Hong
Korea Cancer Center Hospital, Seoul, Korea

IMPROVED ACTIVITY ESTIMATION USING COMBINED SCATTER AND ATTENUATION CORRECTION IN SPECT.

Accurate estimation of the radioactivity on a region of interest in SPECT images can be practically accomplished by the compensation of scatter and attenuation effects. Tc-99m source simulating tumors (T) and normal brain tissue (B) was injected by varying the activity ratios T/B (2:1, 4:1) and the lesion depth (1cm, 8.5cm) in a 20.5cm diameter cylindrical phantom. We used a three-headed SPECT system (Trionix, Inc, Twinsburg, OH) equipped with low-energy, high resolution parallel-hole collimator. The projection data were acquired in a photopeak 126-154 keV and a lower-energy scatter 101-123 keV window. We implemented the scatter subtraction method (a factor of 0.4) proposed by Jaszczak et al. Then, the projections were reconstructed using the filtered backprojection method followed by fitting an ellipse to the object outline with an empirical attenuation coefficient, 0.10 cm⁻¹. We generated SPECT images using combined scatter and attenuation correction method (SC+AC), derived the activity quantification and compared with two cases that the only correction for attenuation (AC) and no correction (NONE). The system cross-calibration factors in three cases were determined using a 5 ml syringe of known Tc-99m activity.

We found that the estimated activity in SPECT images were similar to true values, especially in SC+AC method with errors of ±1% in two T/B ratios. AC and NONE cases gave larger estimate of errors, more than 45% and 2 to 9%, respectively. We observed that the bias from lesion depth was significantly decreased in SC+AC method (23%) than NONE (43%) at 8.5 cm position. Image contrast was also improved to 0.96 in SC+AC normalized with true value as 1 compared with 0.8(AC) and 0.87 (None). Based on this results of this study, the accurate activity quantification can be accomplished by compensation scatter and attenuation effects in SPECT imaging.

PS-640

Nikkinen P¹, Sipilä O^{1,2}, Savolainen S¹, Liewendahl K¹
¹Helsinki University Central Hospital and ²Helsinki University of Technology

Attenuation correction in brain basal ganglia phantom studies

With Chang attenuation correction automatic 1 per slice ellipse fitting is often difficult in basal ganglia receptor studies. We studied the effects of different attenuation correction methods on quantitation using a cylindrical phantom (d=21.5 cm, h=19 cm) containing Tc-99m 10-15 kBq/ml. Inside the cylinder two spheres with diameters of 4 cm were inserted. Six different sphere/cylinder activity ratios varying from 2.0 to 9.4 were used. Cold spheres were also studied. Transmission imaging of the phantom was performed with a triple head Picker Prism 3000XP gamma camera and a STEP transmission imaging device equipped with a Gd-153 source. Imaging without STEP was performed in dual window mode (108 keV and 140 keV) in order to subtract scatter in the standard SPET imaging.

STEP data were reconstructed using an iterative ML-EM algorithm and postfiltered with Wiener and LowPass filters. Filtered backprojection (FBP) algorithm was used for reconstruction of the second data set using the Tc-99m window with the same filters. Chang attenuation correction was done with μ=0.11 cm⁻¹. Dual window scatter correction was performed (k=0.5) and FBP+Chang attenuation correction was used in reconstruction. STEP+Wiener filter postfiltering overestimated the activity ratios. Dual window scatter correction did not significantly improve the results in FBP.

Conclusion: STEP+Low Pass postfiltering is the optimum protocol. However, it is too slow for clinical purposes: imaging time is ≥1 h and reconstruction time ≥40 min with the present computer system. FBP is more useful in clinical routine.

Poster presentations

PS-641

K. Perinakis¹, N. Karkavitsas², J. Damilakis¹ and N. Gourtsoyiannis³

Departments of ¹Medical Physics, ²Nuclear Medicine and ³Radiology, University of Crete, 711 10 Stavrakia, Iraklion, Crete, Greece

PLANAR AND SPECT HEPATIC IMAGING USING THE DUAL AND TRIPLE ENERGY WINDOW SCATTER CORRECTION METHODS

The effect of dual (DEW) and triple energy window (TEW) scatter correction methods on lesion detectability was investigated for both planar and tomographic hepatic imaging. All planar and tomographic acquisitions involved simultaneous collection of photons in the main photopeak window (126-154 keV) and three additional windows (94-116, 116-126 and 154-164 keV). Uncorrected and corrected for scatter images were obtained from the same acquisition data. The dual energy window (DEW) and the triple energy window (TEW) scatter compensation methods were used to obtain two sets of corrected images. The DEW method was implemented with main photopeak window 126-154 keV, Compton scatter window 94-126 keV and scatter multiplier $k=0.5$. A modified TEW method was also applied with main photopeak window 126-154 keV and scatter subwindows 116-126 keV and 154-164 keV. Phantoms were used to study the effect of scatter correction on contrast and signal-to-noise ratio. The observer's ability to identify lesions was studied on uncorrected and corrected patient images. In planar imaging, both scatter compensation methods yielded contrast enhancement with similar performance. However signal to noise ratio (SNR) was degraded by a factor of 0.63 and 0.67 when DEW and TEW were applied respectively. In SPECT images, contrast was increased by a factor of 2 and 1.7, while SNR was degraded by a factor of 0.60 and 0.64 when DEW and TEW methods were used respectively. Scatter correction using DEW and TEW methods may improve observer's ability to distinguish lesions in planar ($p<0.05$ for both methods) and SPECT ($p<0.05$ for both methods) liver studies.

PS-642

D.Ros¹, C.Falcón¹, I.Juvells², J.Pavía³

¹Lab. Biophysics and Bioengineering. Fac. Medicine, Univ. Barcelona,

²Lab. Optics. Fac. Physics, Nuclear Medicine Department. Hospital Clinic i Provincial of Barcelona. Spain

A CROSS-VALIDATION STOPPING RULE FOR ORDERED SUBSETS RECONSTRUCTION ALGORITHMS IN SPET

Introduction. The OS-EM algorithm is a useful method to speed up the ML-EM original algorithm. However, it is not clear when the iterative process must be stopped if corrections of attenuation, PSF and scattering are included. The aim of this work is to assess the usefulness in SPET of a stopping rule based on the maximum of a cross-validation function. This function is defined as the cross-likelihood of a data projections set B with respect to the image reconstructed from a data projections set A.

Materials and Methods. A cylindrical phantom 20 cm in diameter containing six solid cylinders 5, 4, 3, 2, 1.5 and 1 cm in diameter was used. Sixty projections of 64 bins and 200 kc were acquired. The reconstruction matrix was of 64x64 pixels. A projector-backprojector pair including a uniform attenuation map ($\mu=0.15 \text{ cm}^{-1}$) and the spatially variant PSF was employed. Subsets from 1 to 60 were used. Two figures of merit (FOM) were used to evaluate the quality of the images: RMS between the reconstructed image and the pattern, and the contrast (CON) of the cylinder 4 cm in diameter.

Results. The table shows the number of iterations derived from the stopping rule and the RMS and CON for these iterations. The values were obtained as the average over 10 acquisitions.

subset	1	2	3	4	5	10	15	20	30	60
iterat	51	26	17	13	10	5	3	2	1	2
RMS	0.180	0.181	0.181	0.182	0.180	0.181	0.179	0.176	0.176	0.252
CON	0.673	0.676	0.674	0.676	0.671	0.675	0.675	0.651	0.628	0.642

The table values show the robustness of the cross-validation stopping rule up to 20 subsets. In these cases, the images exhibit well-balanced values of noise and contrast. Our results demonstrate that for 30 and 60 subsets the values of all FOMs, deviate from those corresponding to one subset. Thus, the cross-validation stopping rule is an adequate criterion provided that the use of subsets leads only to an acceleration effect.

This work has been supported in part by the CICYT (SAF96/0062).

PS-643

T. Shiga, N.Kubo, Y. Itoh, T. Kaji, K.Kanegae, K. Morita, K. Nakada, E.Tsukamoto, M. Konno, T. Takayama, N. Motomura, T.Ichihara, N.Tamaki Hokkaido University School of Medicine, Sapporo, and Toshiba Medical Engeneering Laboratory, Tochigi, Japan

CLINICAL APPLICATION OF HIGH-SENSITIVITY,HIGH RESOLUTION COLIMATATOR SYSTEM

Gated myocardial SPECT has recently become popular, but it requires higher counts to acquire acceptable images. We have developed a new collimator system (H2 system) for a triple-head gamma camera comprising two long-focus (802.3 mm) fanbeam collimators and one parallel-hole collimator for myocardial SPECT. The purpose of this study is to evaluate the basic and clinical advantages of the new collimator system for gated myocardial SPECT by comparing the system against a conventional high-resolution parallel-hole collimator system (HR system).

The sensitivity and resolution of the HR and H2 systems were measured in phantom studies Tc-99m-sestamibi gated myocardial SPECT was performed in two cases using the H2 system with 360 degree rotation 80 min after resting injection of 600 MBq of Tc-99m-sestamibi immediately after routine gated SPECT with the HR system with 120 degree rotation. Gated Tl-201 SPECT was also performed in a normal volunteer after resting injection of 111 MBq of Tl. Acquisition time was similar in these systems.

The sensitivity of the H2 system was increased by 28 % compared with the HR system with similar resolution in phantom studies (FWHM: H2, 13.8 mm; HR, 14.3 mm). SPECT counts were increased by about 20 % in the H2 system compared to the HR system for both Tc-99m sestamibi and Tl-201 studies. Tl gated SPECT images acquired using the H2 system were more homogeneous and had sharper edges than those acquired using the HR system, based on visual assessment.

In conclusion, the H2 collimator system provides higher sensitivity with similar resolution compared to the HR system and is particularly useful for gated myocardial SPECT in the clinical setting.

PS-644

I. Szilvási, Z. Nagy, Zs. Varga, K. Buga

Haynal University of Health Sciences, Dept. of Nuclear Medicine, Budapest

DIAGNOSTIC IMPACT OF NON-UNIFORM ATTENUATION CORRECTION FOR MYOCARDIAL PERFUSION SPECT WITH Tl-201 IN PATIENTS AFTER ACUTE MYOCARDIAL INFARCTION.

Non-uniform attenuation correction (AC) in SPECT of myocardial perfusion is a useful technique to decrease the rate of false-positive findings caused by attenuation artifacts. Attenuation effect is more pronounced in case of Tl-201 than for Tc-99m-isonitriles. In patients after acute myocardial infarction (AMI) SPECT with Tl-201 is of prognostic and therapeutic importance, because reversible defects indicate more aggressive patient management. Aim of our study was to evaluate the diagnostic impact of non-uniform attenuation correction in Tl-201 myocardial perfusion SPECT of patients 2-4 months after an AMI. 54 patients (37 males, 17 females, mean age: 53 years) were prospectively examined. A conventional stress-rest Tl-201 myocardial perfusion scintigraphy was performed using a dual-head SPECT system with non-uniform AC capability. All studies were interpreted by three experienced NM physicians with and without using AC. As gold standard coronary angiography (in 36 patients) or non-invasive clinical data (ECG, Echo, RNV) were used. Segments were divided in two groups based on congruency of corrected and uncorrected SPECT images. Results: AC changed the scintigraphic interpretation in 14 out of 54 patients and in 13.5 per cent of segments. The next types of incongruencies were seen after AC: I.: extent or severity of perfusion defect is less: 6 patients, II.: defect is not fixed, but reversible: 3 patients, III.: perfusion defect is not detectable: 4 patients, IV.: inverse redistribution is not existing: 1 patients. No false-positive finding was created by using non-uniform AC. Incongruent interpretation occurred for all myocardial regions: 2 in anterior, 1 in septal, 10 in inferoposterior and 1 in lateral wall. In conclusion: using non-uniform AC in Tl-201 stress-rest myocardial perfusion SPECT in patients after AMI is a powerful technical tool to decrease false-positive rate, to more accurate grading of perfusion abnormalities and to detect reversible perfusion defects masked by attenuation.

PS-645

P. Wanet, A. Sand.

A.Z. Jan Palfijn, Nuclear Medicine, Gent, Belgium .

HIGH RESOLUTION TOMOGRAPHY - COMPARISON BETWEEN THREE METHODS : CIRCULAR PINHOLE SPECT, CIRCULAR AND ELLIPTICAL FAN BEAM SPECT.

Tomography of thyroid or cervical spine requires a very good resolution to obtain high quality images. The spatial resolution achievable with parallel collimators is too low in these two applications.

We have compared three different methods :

- 1- Pinhole tomography (P-SPECT) using a 4 mm pinhole, 180 degrees and a tilt of 15 degrees.
- 2- Fan-Beam tomography with a circular orbit of 20 cm.
- 3- Fan-Beam tomography with an elliptical acquisition with an ellipse of 10/20 cm.

The first method uses a tilt so that the distance between the pinhole aperture and the center of rotation is reduced. We used a modified cone-beam algorithm to reconstruct the P-SPECT images.

The fan beam algorithm is used in the 2 others methods, with a correction for the elliptical orbit.

P-SPECT gives for a distance of 10 cm a FWHM of 7.2 mm with a geometrical efficiency of $1.0 \cdot 10^{-4}$. Circular Fan Beam acquisitions allow to obtain a FWHM of 11.0 mm with an efficiency of $1.5 \cdot 10^{-4}$. Elliptical fan beam gives a FWHM of 8.5 mm with an efficiency of $1.3 \cdot 10^{-4}$.

Studies have been performed on phantoms and on 2 volunteers to compare the 3 methods. For thyroid studies, P-SPECT gives better results because of the higher resolution. For cervical spine studies, elliptical fan beam acquisition is better because of the larger field-of-view and the higher sensitivity.

PS-646

P. Wanet, A. Sand.

A.Z. Jan Palfijn, Nuclear Medicine, Gent, Belgium .

CORRECTION OF CENTER OF ROTATION IN PINHOLE TOMOGRAPHY

High resolution Pinhole SPECT (P-SPECT) can be used in routine for examining small organ like thyroid. Because of the high resolution, this method is extremely sensitive to variations of center of rotation (C.O.R.)

We have developed a method to correct this motion and to avoid severe artifacts generated during acquisition.

To measure the variation of the C.O.R. a point source is located exactly in the center of rotation. The position of the point source is adjusted with the camera located in anterior and in lateral positions. A P-SPECT study is performed with 60 projections, a matrix size of 128, an acquisition zoom 2 and a pinhole diameter of 1 mm. This pinhole diameter been chosen to increase the accuracy. The position of this small point source moves and is determined on every frame of the acquisition with an accuracy of 1/8 of pixel. The 60 values x and y of this position are recorded and produce a typical pattern which depends on the camera examined.

To correct an acquisition, each frame is then simply moved according to the values of x and y and the normalized acquisition is then used to generate the slices with the backprojection algorithm.

Ten cameras have been tested. Two of them have a sufficiently good stability to avoid the proposed correction in routine tomography. But on the other eight cameras, the variation of C.O.R. generates extremely severe artifacts visible with the thyroid phantom.

If a pinhole smaller than 4 mm is used, for example for studies on small animals, the C.O.R. correction must always be used.

We conclude that C.O.R. correction is very important in P-SPECT and that every system must be carefully checked before using it in clinical routine.

PS-647

N.Yui,K. Kinoshita,T.Togawa,Y.Tanaka, T.Kihara

Hospital:Chiba Cancer Center,Division of Nuclear Medicine
*Toshiba Medical System,Modality Engineering Department

A FRAMELESS REGISTRATION OF SPECT AND X-CT BY VOLUME MATCHING METHOD

In order to improve insufficient anatomical information of functional image by matching with morphological image, a method to register SPECT and X-CT was studied. We have developed a new frameless registration by volume matching method, which is able to combine the images with different modalities and unequal projection angles. Three-dimensional overlap of bone region was used for image matching. Transmission image(TCT)which was acquired simultaneously in SPECT examination for absorption correction was utilized to combine with X-CT. This method is based on the fact that TCT image has similar physical property to X-CT of the patient. The transformation matrix between two coordinate image systems was calculated and registered automatically by the optimization method. The coupling of TCT and X-CT lead to get accurate incorporation of SPECT and X-CT images of the patient. We verified the theory by phantom studies and got proper registration of the region within 2mm error between TCT and X-CT images. In clinical cases, we got accurate registered images of head and chest without any frame. We expect this method become an efficient tool to improve region identification in functional image and registered X-CT will provide much more accurate factors than TCT image by SPECT device for absorption correction.

Physics and instrumentation: Data analysis

PS-648

V. Beauchat, D. Huglo, A. Delcourt, T. Prangère, M. Steinling
Regional and University Hospital, Department of Nuclear Medicine,
Lille, France

MECKEL'S DIVERTICULUM AND FACTORIAL ANALYSIS : A PROMISING MARRIAGE ?

Aim : Evaluation of factorial analysis method of sequential images compared to standard method (Regions Of Interest and curves) for radionuclide imaging detection of Meckel's diverticulum.

Method : After antecubital injection of pertechnetate anion in fast patients, anterior abdominal dynamic acquisition was realized, with static (side or/and posterior views) and belated frames if necessary. First, visual analysis was performed. Then, activity curves was drawn in different Regions Of Interest to detect a similar evolution of gastric and suspect region uptake. Factorial analysis was realized with FAMIS software (three factors) (Sopha Medical Vision).

Results : 6 children were studied. In two of them, visual analysis revealed a focal abnormal abdominal uptake. Activity curves weren't contributory. On the other hand, factorial analysis clearly individualized vascularity, gastric and urinary activities. This method individualized the abnormal abdominal uptake in the gastric component. Surgery confirmed the diagnostic of ectopic gastric mucosa in these two cases. For the others children, scintigraphies were negative, whatever was imaging treatments.

Conclusion : In these six patients, there was no discordance between visual, factorial analysis and final diagnostic. In the positive children, factorial analysis was more performant than the ROIs method. This analysis, no time consuming, could be used in difficult cases to avoid the increased static acquisitions. A largest study is necessary, particularly to estimate utility in other cases of pathologic uptake : inflammation, some tumors, vascular malformations, ulcers and various urinary tract abnormalities.

Poster presentations

PS-649

M. J. Carroll, K. E. Britton

St Bartholomew's Hospital, Department of Nuclear Medicine

STATISTICAL DETECTION OF POINT SOURCE TUMOUR SIGNALS IN NUCLEAR MEDICINE

In this study we describe a statistical test for point source detection that is strictly valid for arbitrarily low image counts. In this test the source counts cs and background counts cb are compared where $cs(cb)$ arise from either a source region surrounded by an annular background region, or from homologous regions in images collected at different times. The p-value associated with the null hypothesis that the source and background count densities are the same is given by:

$p = I_f(cs, cb+1)$ where I_f is the incomplete beta function, and $f = As/(As+Ab)$ is the ratio of the area of the source region to the sum of the background and source regions. To process large numbers of probability values, a look up table is precomputed for a range of cs, cb value pairs allowing an accept/reject flag for a required significance level enabling rapid interactive analysis. Testing the statistic on a pixel by pixel basis generates a multiple hypothesis space and therefore a Bonferonni procedure is applied to determine a conservative overall significance level.

This technique is applicable to tumour detection in nuclear medicine and particularly to the detection of lymph node involvement in breast cancer. Imaging of involved lymph nodes provides the potential of imaging small, point sources of activity for which the proposed statistical test is ideally suited.

PS-650

J.Y. Kim, Y. Choi, W.H. Wu, C.K. Hoh, K.C. Im, S.E. Kim, J.H. Kim, Y.S. Choe, B.-T. Kim
Samsung Medical Center, Department of Nuclear Medicine
UCLA-School of Medicine, Department of Pharmacology

EXTRACTION OF INPUT FUNCTION FROM DYNAMIC FDG-PET STUDIES USING FACTOR ANALYSIS

We evaluated the feasibility of extracting pure arterial time-activity curves (TAC) from dynamic FDG-PET human brain and rat studies using factor analysis of dynamic structure (FADS). Seven Alzheimer's disease patients and four rats (weight of ~250g) with tumor mass were imaged over the brain and whole body, respectively, using a GE Advance tomograph (axial FOV: 15 cm). Dynamic images were acquired for 60 min and about 30 arterial blood samples were obtained. FADS was performed using the dynamic images of skull base containing carotid arteries in human studies and images of rat heart in animal studies. Area under the curves (AUC) and the FDG uptake constants for brain and tumor estimated using the three compartment model (K_{3cm}) were used to validate the accuracy of the FADS generated arterial TACs.

TACs derived using FADS matched well with those obtained by the blood samples in human studies (%difference of AUC: 3.4%). The %difference of AUC was larger in rat studies (13.3%). The FDG uptake constants for gray and white matter estimated using the input functions derived by blood samples and by FADS were linearly correlated ($Y=0.94X$, $r=0.98$) in human studies. In rat studies, the slope of regression line of FDG uptake constants for brain and tumor was 0.70 ($r=0.91$) in rat studies. The macroparameters, K_{3cm} [ml/min/g], are summarized below:

	Human Studies		Rat Studies	
	Gray matter	White matter	Brain	Tumor
Blood samples	0.034±0.008	0.012±0.003	0.031±0.011	0.041±0.016
FADS	0.033±0.007	0.034±0.008	0.040±0.008	0.049±0.010

The preliminary results of this study demonstrate that, although further improvement is required for the rat studies, the factor analysis of dynamic structure has the potential to extract the pure arterial TACs directly from dynamic FDG-PET studies of small structures without multiple blood sampling or ROI definition.

PS-651

J.Heikkinen¹, M.Kortesniemi², J.T.Kuikka³, A.Ahonen⁴, P.Rautio⁵, S.Savolainen⁶
¹Dept of Nucl Med, Mikkeli Central Hospital, ²Dept of Physics, University of Helsinki, ³Department of Clinical Physiology, Kuopio University Hospital, ⁴Department of Nuclear Medicine, Oulu University Hospital, ⁵Department of Clinical Physiology, North Karelia Central Hospital, ⁶Depts of Lab.Mod and Radiol, Helsinki University Central Hospital, Finland

COMPARISON OF ANALYSIS PROGRAMS IN DYNAMIC RADIONUCLIDE RENOGRAPHY: A PHANTOM STUDY

The aim of the study was to evaluate how much analysis programs may change the parameters of dynamic radionuclide renography. The simulation of three renography cases with the new phantom (Heikkinen) was made in 19 Finnish nuclear medicine laboratories. A routine clinical analysis was made by each laboratory. The time activity data from background subtracted areas of the kidneys and the heart were collected and reanalysed by independent physicist. In isotope renography the kidney transfer function (TF) is calculated by deconvolution analysis. In the method of biexponentials the blood time activity curve is replaced by its biexponential fit. The matrix method does not require mathematical modeling of convolution data. From three centers the raw kidneys and blood activity data of two simulated cases were available. The data was analyzed by calculating TF utilizing matrix algorithm. The mean transit time (MTT) and the relative clearance (RCL) were derived from TF. By applying the same algorithm to the data from three centers the changes in MTT were $26.7 \pm 16.5\%$ (range from 5.5 to 45.4%) and in RCL $7.4 \pm 8.1\%$ (from 0.3 to 19.8%). These preliminary results suggest that the numerical results of the renography are analysis program dependent. So, it is important that each laboratory produce their own normal values.

PS-652

G. Kontaxakis, L.G. Strauss, S. Pavlopoulos
German Cancer Research Center, Heidelberg, Germany.

ADVANCED PROCESSING OF MULTITRACER DYNAMIC ONCOLOGICAL STUDIES WITH PET ON DISTRIBUTED PENTIUM SYSTEMS

The processing and evaluation of the large data sets produced by multitracers dynamic positron emission tomography (mdPET) studies is a rigorous problem. A set of tools has been developed for the optimal management of mdPET data sets for oncological studies on distributed Pentium platforms. These include sinogram pre-processing (attenuation, normalization, etc., corrections), iterative image reconstruction techniques, image parameterization, quantification and ROI analysis.

Data from mdPET studies are obtained with a Siemens/CTI ECAT EXACT HR+ tomograph. Attenuation correction of the raw data is performed via μ -maps and OS-EM reconstruction of the attenuation factors, based on transmission and blank scans. The attenuation images are reprojected to the measured data space. Normalization is performed by the standard procedures provided by the ECAT7.03 software, adapted to the Windows NT 4.0 environment. The ML-EM, ISRA, WLS, and SAGE algorithms are available via a web-based interface for iterative image reconstruction (IIR). The user can select one of the methods or their accelerated ordered-subsets (OS) versions, the inclusion of the median root prior (MRP) bayesian method for the improvement of the signal-to-noise ratio and the application of pre- and post-reconstruction filtering. These data are transferred to a subnet server via SMTP and stored for further processing. The reconstruction program itself is running on distributed client systems of the subnet and each program is checking the reconstruction batch for new tasks. This structure provides "quasi-parallel" processing and is a simple but very efficient method for fast image reconstruction. Patlak, SUV, fractal and Fourier analysis, as well as kinetic analysis (with or without compartmental models) can be applied to the reconstructed images. A dedicated software has been developed for the viewing and the ROI analysis of the mdPET data. The viewer allows the display of slices via frames, the selection of multiple ROIs and their automatic propagation to all frames, or a range of slices in a frame for tumour-volume evaluation. The evaluation capabilities are significantly improved by the use of dedicated PC systems and software.

PS-653

J. Lampinen†*, K. Virtanen*, J. Pyykkönen* and S. Savolainen*
 †Dept of Physics, Helsinki University (POB 9, FIN-00014 Helsinki University),
 *Helsinki University Central Hospital

A METHOD FOR TL-201 MYOCARDIAL SPET QUANTIFICATION

The main method for evaluating SPET images of a thallium myocardial study is based on visual interpretation of the reconstructed images. This approach is limited by e.g. observer variability and inability to quantify the percentage of the myocardium that is involved with abnormality. An automated computer based method has also been suggested, but it uses a control group. Patients are, however, different in every respect and the use of a control group method is not generally accepted. We developed a new method for quantification of thallium distribution images. This method was developed to quantify images of a group of patients who are imaged several times, before and three months after a bypass operation and in a control imaging after six years. In this material, every patient is her/his own control. From the bypass operation, detailed information is available about each patient's coronary artery condition at the time of the first examination. The second examination gives the control image, since the coronary arteries with diseases have been previously bypassed. The quantification application was done using CLIP-language. The coronal slices are reconstructed from SPET images and arranged to a cylindrical form. This cylindrical presentation (a variation of a bullseye) is divided into four sectors. A reference level for each sector is given and the program calculates the portions of intensity below the reference. These are calculated for exercise, rest and washout images. The differences in the coronary blood flow distribution are then derived by comparing the values from the control and unknown images. Additional calibration coefficients of the quantification method are derived from the bypass operation information of 10 patients with well defined vessel status. So far, the best results are from washout images where the intensity levels of the control images are constant in each sector while the images with disease give variable values.

PS-654

J.S. Lee, D.S. Lee, S.K. Kim, S-K. Lee, K.S. Park, J-K. Chung, and M.C. Lee
 Seoul National University, Department of Nuclear Medicine, Neuropsychiatry, and Biomedical Engineering, Seoul, Korea.

APPLICATION OF ARTIFICIAL NEURAL NETWORK TO INTERPRET THE CEREBRAL METABOLIC PATTERN OF EPILEPSY.

For the objective interpretation of cerebral metabolic patterns in epilepsy patients, we developed computer-aided classifier using artificial neural network. We studied interictal brain FDG PET images of 257 epilepsy patients which were diagnosed as normal (n=64), LTLE (n=112), or RTLE (n=81) by visual interpretation. Automatically segmented volume of interest (VOI) was used to reliably extract the features representing patterns of cerebral metabolism. All images were spatially normalized to MNI standard PET template and smoothed with 16mm FWHM Gaussian kernel using SPM96. Mean count in cerebral region was normalized. The VOIs for 34 cerebral regions were previously defined on the standard template and 17 different counts of mirrored regions to hemispheric midline were extracted from the spatially normalized images. A three-layer feed-forward error back-propagation neural network classifier with 7 input nodes and 3 output nodes was used. The network was trained to interpret metabolic patterns and produce identical diagnoses with those of expert viewers. The performance of the neural network was optimized by testing with 5-40 nodes in hidden layer. Randomly selected 40 images from each group were used to train the network and the remaining 137 images were used to test the learned network.

The neural network gave concordance rates of 75-80% with 10 or 30 nodes in hidden layer. The optimized neural network gave a maximum concordance rate of 80.3% with expert viewers. It used 20 hidden nodes and was trained for 1508 epochs.

We conclude that artificial neural network performed as good as human experts and could be potentially useful supporting tool for the diagnosis of epilepsy.

PS-655

J.K. Wang, L.C. Wu, T. Kao*, R.S. Liu, and S.H. Yeh.

National PET/Cyclotron Center, Taipei Veterans General Hospital, and *National Yang-Ming University, Taipei, Taiwan.

REGISTRATION OF PET [F-18]FDG AND [F-18]FMISO BRAIN STUDIES.

PET studies with multi-tracer protocol can provide complementary and different diagnostic information for clinical purpose. However, the accuracy of images integrated interpretation is commonly limited by the movement of subject between scans. The purpose of this study was to develop a reliable and robust procedure to realign the PET [F-18]FDG and [F-18]FMISO brain studies.

All images were acquired with GE PC-4096WB PET scanner. A 30-min static scan was performed 45 minutes after the injection of 370 MBq [F-18]FDG. The [F-18]FMISO study was performed 2 hours after injection for 20 minutes. Our method utilized the similarity measure of masked gradient-value for registration. Firstly, FDG and FMISO emission images were reconstructed without attenuation correction (AC). Contour points of FDG emission images were derived and the mask area was created along the skull boundary with ten pixels width. The gradient-value dataset of FMISO was resliced with different displacement and rotation angle to match the FDG reference dataset and only the voxels inside the area of mask were calculated. The cross-correlation coefficients were calculated to indicate quantitatively the similarity of normalized gradient value. The spatial transformation parameters could be found when the maximum coefficient was achieved.

The major reason to apply registration algorithm on emission images without AC is that the misalignment between transmission and emission scan will seriously affect the accuracy of emission images registration. With the individual biochemical distribution, FDG images and FMISO images show markedly dissimilar uptake patterns. In our experiments, the gradient-value inside the skull has no contribution for the result of registration. Five brain studies with [F-18]FMISO and [F-18]FDG was applied for evaluation. Simulated mismatched FMISO images were reconstructed and rotated with the known parameters. The registration method could correct movements with an accuracy of 1 mm in translation and 1.5 degrees in rotation.

In summary, the method is capable of realigning the dataset of PET images obtained from the same subject with [F-18]FDG and [F-18]FMISO tracers.

PS-656

K. Murase, T. Inoue, H. Fujioka, A. Akamune, Y. Ishimaru, T. Kikuchi, T. Mochizuki, J. Ikezoe

Ehime University Hospital and Matsuyama Shimin Hospital, Ehime, JAPAN

ACCURACY OF A DOUBLE-INJECTION METHOD FOR SEQUENTIAL MEASUREMENT OF CEREBRAL BLOOD FLOW (CBF) WITH I-123 IMP: A SIMULATION STUDY BASED ON PATIENT DATA

A double-injection method for sequential measurements of CBF with N-isopropyl-[I-123] iodoamphetamine (IMP) is very useful to assess perfusion reserve. The purpose of this study was to investigate the accuracy of this method by simulation studies based on patient data obtained by dynamic SPECT in 16 patients with cerebrovascular diseases. The CBF values in the first session (CBF¹) were calculated using a microsphere model, i.e. $Cb(5)/Int_Ca'$, where $Cb(5)$ and Int_Ca' are the brain radioactivity at 5 min post first injection and the octanol-extracted radioactivity obtained by 5-min continuous arterial blood sampling, respectively. The CBF values in the second session (CBF²) were calculated using the following three methods based on a microsphere model. With Method 1, the CBF² value was calculated by $[Cb(tz+5)-Cb(tz)]/[Int_Ca^2 \cdot Ca(tz) \times 5]$, where $Cb(tz+5)$ and $Cb(tz)$ are the brain radioactivities at 5 min post second injection and at the time of the second injection (tz), respectively. Int_Ca^2 and $Ca(tz)$ are the radioactivity obtained by 5-min continuous arterial blood sampling after second injection and that obtained at tz, respectively. With Method 2, it was calculated by $[Cb(tz+5)-Cb(tz)]/[Int_Ca^2 \cdot R]$, where R is the injection dose ratio. With Method 3, it was calculated by $[Cb(tz+5)-Cb(tz) \times \exp(-CBF^2 \cdot 5/\lambda)]/Int_Ca^2$, where CBF² was obtained by Method 2, and λ is the distribution volume. In this study, λ was assumed to be 30 ml/g, the mean value in 16 patients (10 males and 6 females, 56 ± 11 years).

The percent changes in CBF between the first and second sessions $[(CBF^2-CBF^1)/CBF^1 \times 100]$ obtained by the above three methods are summarized in Tables for the cases when the true percent change is 0% (left) and 60% (right), with R and tz being taken as parameters. [Data represent the mean ± s.d. (%) in 16 patients.]

		R (=second dose/first dose)			R (=second dose/first dose)			
Method		1.0	2.0	3.0	Method	1.0	2.0	3.0
1		5.1 ± 4.0	2.6 ± 2.0	1.8 ± 1.3	1	64.7 ± 6.8	60.7 ± 3.6	59.4 ± 2.6
2		3.8 ± 3.5	1.6 ± 1.7	0.9 ± 1.1	2	62.7 ± 6.0	59.2 ± 3.2	58.0 ± 2.3
3		-0.1 ± 2.0	-0.1 ± 1.1	-0.1 ± 0.7	3	56.3 ± 3.5	56.3 ± 2.1	56.4 ± 1.7
		Time of 2nd injection, tz (min)			Time of 2nd injection, tz (min)			
Method		20	30	40	Method	20	30	40
1		7.5 ± 5.3	4.4 ± 3.2	2.6 ± 2.2	1	68.5 ± 8.6	63.5 ± 5.5	60.7 ± 3.9
2		6.0 ± 4.5	3.2 ± 2.8	1.6 ± 1.9	2	66.1 ± 7.5	61.8 ± 4.9	59.1 ± 3.5
3		0.1 ± 1.1	-0.1 ± 1.3	-0.2 ± 1.4	3	56.7 ± 2.3	56.4 ± 2.5	56.2 ± 2.7

In conclusion, these results suggest that Method 3 can estimate the change in CBF more stably than Method 1 or 2, without depending on R and tz.

PS-657

S. Oku, T. Ohtake, T. Momose, Y. Kumakura, S. Saegusa and Y. Sasaki.
Dept. of Radiology, University of Tokyo, Japan.

STANDARDIZED UPTAKE VALUE(SUV) CORRECTION FOR FDG-PET OF CANCER PATIENTS BY USE OF A CONVERSION TABLE BASED ON APPARENT TUMOR SIZE AND MEASURED ACTIVITY.

SUV has established its clinical utility as a semi-quantitative method in FDG-PET cancer studies, however, the accuracy of this value is still controversial, mainly because it is subject to many sources of variability such as patient size and plasma glucose level. Above all, the problem related to recovery coefficient and partial volume effects is hardly prevented. In the present study, a conversion table based on tumor size and measured activity was revised and SUV correction using this table was compared with conventional SUV determination.

Methods: A cylinder phantom containing spheres of different diameters was scanned with Headtome IV PET scanner (Shimadzu Medical, Kyoto, Japan). The spheres imitating tumor were each time filled with different known activity of FDG, i.e. SUV=8,6,4,3,2 and 1. The reconstructed data were transferred to the workstation and ROI's of various sizes relative to sphere sizes were placed in order to obtain a table to define diameter-contained activity-measured activity relationship. Eleven consecutive patients with rectal cancer underwent before and after pelvic radiotherapy of 50Gy. Changes in SUV for each slice were calculated based on 1) maximum count in the lesion 2) average count of ROI placed manually 3) automated ROI containing the pixels higher than 30% of maximum count. For 2) and 3), the above mentioned conversion table was applied for correction, thus 2c) and 3c) were calculated. To accomplish the two-dimensional conversion, a procedure was revised by the authors on MatLab(Math-Works, Chicago, USA).

Results: Changes by 3c) showed best correlation ($r=0.95$) with those by 1), which has been described as the relative choice in the literature. The lower SUV's in the lesions resulted the more influenced by methods to delineate ROI's. **Conclusion:** Taking errors regarding signal/noise into consideration, the present method appeared more stable and thus reliable in the clinical situation. Further estimation by animal model will reveal its validity.

PS-658

M.O. Afriyie, F. Leveque, M.B. Tomas, C.J. Palestro

Long Island Jewish Medical Center, New Hyde Park, NY 11040.

TISSUE/PIXEL SPECIFIC ATTENUATION CORRECTION ALGORITHM: AUTOMATIC METHOD OF ATTENUATION CORRECTION BASED ON ACQUISITION, CAMERA & TISSUE TYPE PARAMETERS

Existing methods for attenuation correction are based on tissue uniformity & scatter reduction without consideration for attenuation changes based on pixels as individual non uniform entities. Over/under attenuation estimation results in a hot rim artifact in corrected images. We have developed an automatic attenuation correction algorithm that takes into consideration the following parameters: acquisition pixel resolution, crystal size, locations of individual pixels & patient tissue type overlying each pixel. **Methods:** The absorption law: $I=I_0 \exp(-ux)$ defines the Activity detected by a camera-system at a distance x - cm. Correction for attenuation allows for the estimation of $I_0=I \exp(ux)$ for a pixel of average distance x cm from the image periphery. Following observations are also established: Pixels in a given image are defined as groups (n) having the same average distance S (equivalent of x) cm from image periphery=same attenuation effect; and $d(\Delta)$ as the average distance between two neighboring pixels. From these we derived the following equations: $n(i)=\text{number of groups}=1 \dots \text{pix res}/2=n(\text{max})$. Number of pixels in a group/having same attenuation effect= $P=4[2n(i)-1]$; $S(i)=d[(\text{pix res}/2) + 1] - d[n(i)]$; We concentrated all equations on n , making it easier to automatically compute the attenuation correction matrix $M(i)$ for pixel group $n(i)$; $M(i)=\exp[(u)S(i)]$; u =tissue type and radionuclide specific. The attenuation correction matrices $M(i)$ obtained from these equations are specific & engineered with parameters pertinent to a particular patient study. Multiplication of $M(i)$ & measured activity (I) at various pixels yields the original activity I_0 . A computer simulated non uniform attenuation was corrected by multiplication of the factors so derived. Pre and post attenuation correction profiles demonstrated the usual logarithmic form attenuation and the subsequent straight line. In summary, given accurate acquisition parameters & camera FOV, a computer may noninteractively estimate attenuation correction matrices & their application. By using average distances, artifacts are eliminated because the computer always estimates the peripheral pixel group to have a correction matrix of unity.

PS-659

P. Saxena *, D.G. Pavel, J.C. Quintana and K.Q. Lin

Dept. of Neurosurgery * and Nuclear Medicine, University of Illinois Medical Center, Chicago, IL.

DETERMINING THE EFFECTS OF SCALP/SKULL EDITING ON TALAIRACH NORMALIZATION OF SPECT IMAGES

Talairach normalization of PET/SPECT brain images is required for procedures such as Statistical Parametric Mapping (SPM). The Talairach space does not include the scalp and skull but Tc-HMPAO exhibits a significant concentration in those structures. In this study, we report about normalization errors in the SPM-based analysis of unedited SPECT images.

METHODS: Pairs of HMPAO-SPECT images from 11 patients were individually compared to 14 pairs of reference images using SPM analysis, with and without manual editing of the scalp and skull, in both normals and patients.

RESULTS: SPM failed to properly normalize any of the unedited images. In each case, SPM forced the normalization to contract the brain to a size smaller than the Talairach bounding box in order to accommodate the extracerebral tissue. In 3 cases, the unedited images showed areas of significant change, which disappeared when the images were edited to remove scalp and skull. The normalization images in these 3 cases showed the presence of extracerebral uptake. In 8 or 11 cases, there was a significant change in the position of the areas detected by SPM, and a 50% or greater change in the number of voxels involved. This difference was either higher or lower in the edited images compared to the unedited images. In the remaining 3 cases, there were no major differences between the SPM analysis of edited and unedited images. However, even in these cases, the normalized images showed a shrinkage of the cerebral cortex within the bounding box, and the SPM results are possibly due to a serendipitous matching of errors between these 3 cases and the control group.

CONCLUSION: Careful scalp and skull removal should be considered an essential preliminary to SPM-based normalization, when analyzing SPECT images obtained with Tc-HMPAO.

PS-660

K. Q. Lin, D. G. Pavel, P. Saxena, V. Ibanez*

University of Illinois Medical Center, Chicago, IL; Psychiatric Hospital, Belle-Idee, Geneva*

OPTIMIZATION OF THE IMAGE DISPLAY FOR SEQUENTIAL BRAIN SPECT STUDIES USING A PUBLIC DOMAIN SOFTWARE - AUTOMATED IMAGE REGISTRATION (AIR)

An accurate, efficient and operator-independent image registration method is essential for detailed qualitative and quantitative evaluations of sequential brain SPECT studies. As no such tool is presently available from gamma camera manufacturers, we have evaluated the use of AIR, a public domain registration utility widely used in PET and MRI studies.

Material and Method: Repeated brain SPECT studies of normal and abnormal brain as well as a Hoffman phantom were acquired in different positions on a triple head camera. Following transverse slice reconstruction, the following steps were carried out in batch mode: 1) Removing headers from data files. 2) Transferring data via FTP to a SUN workstation for image registration using AIR. 3) Transferring registered images back to the clinical computer and re-adding the headers. 4) Applying filtering and attenuation correction to the images. 5) Generating orthogonal slices. 6) Final display of the registered images side by side. 7) Subtracting paired studies from each other to produce differential images. 8) Statistical Parametric Mapping (SPM) was used to evaluate the significance of change. For registration error estimation, simulation of the malposition of studies was done by applying rigid-body transformation to an acquired reference study by rotating it up to 15 degrees in pitch, roll, and yaw.

Results: Visual comparison, quantitative subtraction, and SPM results all validated the effectiveness of AIR in correcting the spatial malpositioning between multiple studies. Subtraction results showed much smaller global differences after registration, and the maximal value of differences for simulated studies after registration was less than 2 percent of the average count rate per pixel. SPM reported no significant change in these studies. Even in clinical studies with marked abnormalities, the registration results were still very good.

Conclusion: Our procedure uses simple batch files with minimal manual interaction. AIR software is freely downloadable and fully automatic. The registered images have significantly improved the easiness and accuracy of clinical interpretations and the quality of registration meets the need of subsequent quantification processes.

PS-661

J.-M. Rocchisani¹, T. Delzescaux^{1,2}, C. Groiselle¹; I. Cohen³, R. Lengagne³, J.-L. Moretti¹
¹UPRES 2360 - Université PARIS XIII – 93009 Bobigny FRANCE
²ETIS URA 2235, INSERM U 494, ³INRIA Rocquencourt
 EDGE DETECTION OPTIMIZATION IN COMPUTERIZED TOMOGRAPHY

In tomography, edge detection is usually achieved on the reconstructed slices, additional filtering operations and reconstruction artifacts are therefore introduced, thus significantly modifying data acquisition. We present an edge detection method using active contours which allows one to work directly in the space of the projections.

Slice projections were acquired throughout 360° and gathered to generate the sinogram. Once the slice is reconstructed, the operator manually initializes the first snake whose transform is calculated in the projection space. In the sinogram, the searched region is enhanced. We used the image gradient to make the snake converge. The last step consists in calculating the inverse transform of the snake in slice (object space). An analytical, single, closed edge of a region was obtained with a subpixelic resolution and a better accuracy than direct detection could offer.

This method optimally uses data acquisition. In comparison with the first reference works, it allows one to extract the boundaries of concave internal region with a better localization and a lower resolution than a pixel.

PS-662

Nobuo Sugo, Yoshikatsu Seiki, Takao Kuroki, Hitoshi Ohishi, Toshiaki Mito and Iekado Shibata
 Department of Neurosurgery, Toho University School of Medicine, 6-11-1, Omori-Nishi, Ota-ku, Tokyo, Japan

Imaging of Infiltrative Growth of Glioma with Three-Dimensional ²⁰¹Tl SPECT - Using Integrative Three-Dimensional Imaging of SPECT and CT -

1. INTRODUCTION

Computed tomography(CT) does not provide an adequate quality of image to assess the infiltration of glioma. In this study, we investigated whether the degree of infiltration of glioma could be appropriately visualized by three-dimensional (3-D) imaging of ²⁰¹Tl SPECT. Meningioma, a compressive type of tumor, was selected for comparison.

2. MATERIAL & METHOD

Helical CT scan of 1 mm-thin-sliced projections and SPECT with two radionuclides of ²⁰¹Tl and ¹²³I-IMP were performed on glioma and meningioma. These raw data loaded into AVS-MV, a general-purpose medical imaging software, to be semiautomatically adjusted for creating integrative 3-D images of CT and SPECT. In each patient, thresholds of ²⁰¹Tl SPECT imaging were diversified to match ²⁰¹Tl-accumulated tumor images with a tumor region enhanced with a contrast medium.

3. RESULTS

In meningioma, contrast-enhanced tumor pictures were well fitted with ²⁰¹Tl-accumulated tumor by setting a specific value as a threshold of ²⁰¹Tl SPECT imaging. In glioma, however, ²⁰¹Tl-accumulated tissues were not matched with CT depicted tumor at any threshold of ²⁰¹Tl SPECT imaging.

4. CONCLUSION

Integrative 3-D imaging of CT and SPECT permitted us to examine in detail how differently tumors were displayed by the two types of tomography. Furthermore, it was suggested that the use of ²⁰¹Tl, reflecting the metabolism of tumors, creates an image of adequate quality to evaluate the degree of infiltration of glioma not attained CT.

PS-663

H. Toyama, T. Itou*, K. Uemura**, K. Oda, M. Senda.
 Positron Medical Center, Tokyo Metropolitan Inst. Gerontology, *Ochanomizu Univ. and **Waseda Univ., Tokyo, JAPAN

PARTIAL VOLUME EFFECT CORRECTION BY A DECONVOLUTION TECHNIQUE FOR THE QUANTITATIVE MYOCARDIAL POLAR MAP.

A deconvolution method was developed to correct for the partial volume effect (PVE) on the polar map created from myocardial short axis images. The principle of the method is based on the assumption that the area under the radial profile is equal to the product of the regional myocardial radioactivity concentration and the wall thickness regardless of the spatial resolution. This method was evaluated with a phantom made of two eccentric cylinders. The inner chamber was filled with water and the outer chamber, the width varying 6 mm to 16 mm, was filled with Ga-68 solution. Images were acquired by a PET camera and was reconstructed with resolution of 8 and 12 mm FWHM. The profile curves were calculated along 72 radial directions, and the wall thickness was determined by fitting to the convolution of a rectangle with the line spread function. The wall thickness was compared to the distance between the outer and inner edges obtained by the threshold method. The PVE corrected activity was obtained as the area under the profile curve divided by the wall thickness. Assuming that the activity distribution within the myocardium is uniform in the radial direction, the quantitative polar map was generated from the corrected activity. The results of the phantom study indicated that the recovery coefficient was nearly unity independent of the image resolution and wall thickness, whereas PVE uncorrected polar map had a recovery coefficient varying from 0.5 to 1.0. The polar map corrected by the deconvolution method presented uniform distribution with standard deviation of 9.1 and 8.3% at the resolution of 8 and 12 mm FWHM, respectively, in contrast to 15.6 and 17.4 % SD without correction. In conclusion, the partial volume effect on a short axial image was automatically corrected for by this method independent of the image resolution. This method may be useful for generating polar maps in gated human myocardial studies.

PS-664

K. Uemura*, H. Toyama, Y. Ikoma*, T. Yamada*, K. Oda, Y. Kimura**, M. Senda, A. Uchiyama*.
 Positron Medical Center, Tokyo Metropolitan Inst. Gerontology, *Waseda Univ. **Tokyo Medical and Dental Univ., Tokyo, JAPAN

EFFECTS OF HETEROGENEITY AND RESOLUTION ON RATE CONSTANT ESTIMATION IN COMPARTMENT MODEL ANALYSIS OF FDG PET

The estimation of rate constants in compartment model analysis is affected by the data noise and spatial resolution of PET due to partial volume effect. A digital brain phantom consisting of cortex, white matter, striatum and CSF space was created by means of MRI segmentation. The activity in each tissue was determined with a three parameter model for 18F-FDG. Noise was generated by Poisson process according to the collected count for each frame. Sinograms with various spatial resolutions were produced by forward projection, which were then back projected to reconstruct images with spatial resolution of 2 - 14 [mmFWHM]. Time activity curves were generated for circular ROIs with a diameter of 2 - 20 [mm], drawn over the striatum with size of 14 [mm] x 30 [mm] and were analyzed by Modified Marquardt method. The parameter estimates (K1, k2, k3, CMRGlc) were compared with the true values. In case of high resolution (2.0 [mmFWHM]), the estimates of k2 and k3 in small ROIs were higher than the true values because of noise. As the size of ROIs increased, the estimates of k2 and k3 became close to the true until the size of 16 [mm] ϕ , while k2 and k3 in larger than 16 [mm] ϕ and K1 became further lower due to mixture with white matter having lower rate constant. This method is useful for evaluating the effect of noise and spatial resolution on parameter estimates quantitatively and is much faster than the Monte Carlo approach.

Poster presentations

■ Physics and instrumentation: Mathematical models

Physics and instrumentation: Mathematical models

PS-665

L. Balkay, M. Emri, T. Márián, F. Németh, and L. Trón

PET Centre, University Medical School of Debrecen, Hungary

A RECURSIVE ARITHMETICAL FORM DERIVED FROM THE ONE-COMPARTMENTAL CEREBRAL BLOOD FLOW MODEL FOR FAST GENERATION OF PARAMETER MAPS

Cerebral blood flow conditions are routinely characterized by the perfusion (F) and the distribution volume (V) parameters. Numerical values of these variables can be obtained by nonlinear least squares optimization procedure using the general operation equation of the one-compartmental Kety-Schmidt model. In attempt to reduce the remarkable computational time involved we derived a simple recursive arithmetical form for the easy and fast construction of the time dependent tissue activity curve:

$$C(t_{i+1}) = A * C(t_i) + B * \int_{t_i}^{t_{i+1}} C_p(\tau) d\tau,$$

where C_p denotes plasma concentration of the tracer, A and B are simple algebraic functions of F and V and do not contain any integration or matrix calculation. This recursive form contains a simple integral only the computed values of which can be repeatedly reused during the regression analysis. Performance of the developed method was evaluated in comparison with that of conventional procedures using simulated tissue activity data with pseudo random noise added. Comparing analysis of more than 500 simulated data sets revealed calculation speed 20-50 times faster as compared to the conventional method based on the standard operation equation. Our procedure was superior to the weighted integration method yielding F and V values of 10-20% smaller SD using the same set of input data.

This study was supported by OTKA grants T 16149 and F16504 and ETT grant No. 362/96.

PS-666

I. Baltaoglu¹, B. Karayalçın¹, E. Güntekin², G. Karagözü³, S. Akman⁴, F. Güngör¹

Akdeniz University Medical School, Departments of Nuclear Medicine¹, Urology², Paediatric Surgery³ and Paediatrics⁴

Tc 99m EC PARENCHYMAL TRANSIT TIME INDEX WITH STANDARD (F+20) AND MODIFIED (F-15) DIURESIS RENOGRAPHY

Parenchymal transit time index (PTTI) reflects the effect of obstruction on the nephron, giving a noninvasive index of obstructive nephropathy. The aim of the study was to compare Tc-99m EC whole kidney transit time (WKTT), mean parenchymal transit time (MPTT) and PTTI with standard (F+20) and modified (F-15) diuresis renography protocols. Out of 17 children (range: 3 months-13years) with 19 suspected ureteropelvic junction obstruction, 10 underwent F+20 diuretic renography and 7 children studied with F-15 diuretic renography. After adequate hydration, 1mg/kg frusemide is injected either 20 min after or 15 min before 15-120 MBq of 99mTc-EC injection. The gamma camera is positioned to view the regions of the kidney and heart. Using deconvolution analyses MPTT, WKTT and PTTI are calculated. The results were compared with diuretic renography. Results of both diuretic renography protocols and deconvolution analyses are shown in the tables (NOD, OD: Nonobstructive and obstructive dilatation).

	TOTAL(Kidney)	NORMAL	NOD	OD
F+20diuretic ren.	20	7	9	4
F-15diuretic ren.	14	6	4	4

Results of deconvolution analyses

	NORMAL		NOD		OD	
	F+20	F-15	F+20	F-15	F+20	F-15
WKTT	5.68 ± 2.1	3.93 ± 0.5	9.80 ± 1.1	7.49 ± 1.3	12.9 ± 1.3	8.8 ± 1.3
MPTT	4.62 ± 1.2	3.92 ± 0.4	5.73 ± 0.4	5.19 ± 1.3	10.8 ± 1.9	7.29 ± 2.2
PTTI	1.21 ± 0.8	0.56 ± 0.4	3.42 ± 1.9	2.03 ± 1.1	7.01 ± 1.5	3.63 ± 1.8

WKTT, MPTT and PTTI values were found to be significantly higher in OD patients than in NOD patients ($p \leq 0.001$, $p \leq 0.001$, $p \leq 0.01$ respectively) but the difference between NOD and OD didn't reach statistical significance in F-15 protocol. Although WKTT, MPTT, and PTTI parameters are accelerated in all patients due to high urinary flow rates in the F-15 protocol, only acceleration in WKTT showed statistical significance ($p \leq 0.05$). Our results showed that deconvolution analyses with F-15 protocol may lead misinterpretations. We suggest that using F+20 protocol with deconvolution analyses is more reliable in the evaluation of obstructive uropathy.

PS-667

MIQUELIN, CA; Braga, FJHN; Dantas, RO; Oliveira, RB. Sec. Nuclear Medicine; Div. Gastroenterology. Faculdade de Medicina de Ribeirão Preto USP. BRAZIL.

THE VELOCITY (V) OF A RADIOACTIVE BOLUS (RB) IN THE OESOPHAGUS (O) EVALUATED BY MEANS OF AN IMAGE SEGMENTATION ALGORITHM (INITIAL RESULTS).

Classical scintigraphic evaluation of a RB through the O is based on ROIs and time/activity curves, which gives information only about the total time required for RB to cross the organ. Instantaneous parameters can be obtained if the exact position of RB (centroid, C) is known. For that, one needs to know the coordinates of the centre of mass of the bolus radioactivity distribution, which is given by:

$$\bar{x}(n) = \frac{\sum_{y=1}^{64} \sum_{x=1}^{64} [A(x,y,n) \cdot x]}{\sum_{y=1}^{64} \sum_{x=1}^{64} A(x,y,n)} \quad \bar{y}(n) = \frac{\sum_{y=1}^{64} \sum_{x=1}^{64} [A(x,y,n) \cdot y]}{\sum_{y=1}^{64} \sum_{x=1}^{64} A(x,y,n)}$$

From this, one can obtain V at each time. It is interesting to know this new parameter, to try to determine if the anatomical differences among the 3 thirds of O have a functional correspondence or not. We have studied of 8 normal volunteers (4 males, 33-68 yo; 40 MBq of 99mTc-phytate, 10 ml water; unique swallowing; 80 frames of 0.3 sec acquisition) in a scintillation camera. External marks were used to separate the pharynx from O. Images were transformed into bitmap by means of a Sophy Medical processing module and then analysed by means of the algorithm, which determines the co-ordinates of the bolus C for each frame and instant Vs of the RB throughout O. Different Vs were found in a typical evaluation. We conclude that V of a RB changes in the different parts of O.

PS-668

Y. Ikoma*, H. Toyama, T. Yamada*, K. Uemura*, Y. Kimura**, M. Senda, A. Uchiyama*.

Positron Medical Center, Tokyo Metropolitan Inst. Gerontology, *Waseda Univ. **Tokyo Medical and Dental Univ., Tokyo, JAPAN

ERROR IN RATE CONSTANT ESTIMATION ON COMPARTMENT MODEL ANALYSIS OF HUMAN PET DATA BY USING A NOISE-ADDED DYNAMIC DIGITAL PHANTOM.

In the PET kinetic analysis, the data noise affects precision in estimated parameters. A dynamic digital brain phantom was created from segmented MRI to estimate the noise and parameter estimation error in human data and to visually evaluate the quality of parametric images. This was applied to the flumazenil(FMZ) study with 2-parameter model and to the FDOPA study with 5-parameter model. Noise was generated and added to each frame according to the relative total count and the data acquisition schedule. The parameters were estimated by means of a modified Marquardt method. There was a good correlation between the noise level and the fitting error in parameter estimates and the mean absolute difference (MAD) between true and estimated values of rate constant increased as the fitting error increased. The data noise in human study was estimated from the fitting error. In a human FMZ study with administration dose of 710 MBq, the fitting error was 0.8 %, which corresponded to the data noise of 20 % at the last frame and MAD of 1.4 % for the distribution volume ($K_1/K_2 = DV$). In another study with administration dose of 170 MBq, the fitting error was 1.6 %, corresponding to the data noise of 40 % and MAD of 2.9 % for DV. The quality of human parametric images was comparable to that of the phantom for each case. In an FDOPA study with administration dose of 197 MBq, the fitting error was 3.6 %, corresponding to the data noise of 18 % and MAD of 15 % for K_1 . Thus, we can evaluate the error of the rate constant estimates based on the fitting error in parameter estimation in human data by using the dynamic digital phantom.

PS-669

L.C. Wu, R.S. Liu, J.K. Wang, P.F. Chiu, K.L. Chou, H.M. Lin, C.W. Chang, and S.H. Yeh.

National PET/Cyclotron Center, Taipei Veterans General Hospital, and National Yang-Ming University School of Medicine, Taipei, Taiwan.

MODEL ANALYSIS OF CARBON-11 ACETATE IN NASOPHARYNGEAL CARCINOMA.

[C-11]Acetate (ACE), an oxidative metabolic substrate, has been used to detect nasopharyngeal carcinoma (NPC) and has similar diagnostic efficiency. However, the mechanism of tumor uptake of ACE is unknown. This study was undertaken to analyze the model of ACE in NPC and compare the tumor uptake of FDG and hypoxic agent, [F-18]fluoromisonidazole (FMISO).

Data were acquired in a dynamic PET protocol after IV injection of 4.625 MBq/Kg body weight of ACE for 30 min. Twenty-seven frames were collected in the following sequence: 12x10-sec, 8x1-min, 5x2-min, and 2x5-min. Nineteen blood samples were drawn as follows: 6x20-sec, 8x1-min, 3x2-min, 1x4-min, 1x10-min. A time-activity curve (TAC) was generated from the ROI put in the nasopharynx and was fitted by the 4-k constants 3-compartment model proposed by Buck et al (J Nucl Med 1991; 32:1950-1957) for myocardial study. BLD programs were written and run in our Vaxstation to calculate the rate constants with the nonlinear least squares method. For comparison, tumor:background uptake ratio (TBR) and tumor:muscle retention ratio (TMR) were calculated for FDG and FMISO, respectively. $K = K_1 k_3 / (k_2 + k_3)$ was used to correlate with the above parameters.

Six patients (Pt) with NPC were studied and the results were as the following table:

	Pt#1	Pt#2	Pt#3	Pt#4	Pt#5	Pt#6
K	0.189	0.177	0.206	0.186	0.195	0.232
TBR	5.29	4.56	7.50	3.88	6.98	10.50
TMR	1.39	1.15	2.25	2.87	1.54	3.62

The correlation coefficient was 0.96 between K and TBR, while that between K and TMR was 0.77.

Our results indicate that the behavior of ACE in NPC is fairly closed to that of FDG instead of FMISO.

PS-670

G. Mariani, C. Augeri, E. Mereto, F. Pretolesi, G. Curti, A. Martelli, and R. Derchi.

Nuclear Medicine Service and Pharmacology Unit, DIMI, and Institute of Radiology, University of Genoa; Genoa (Italy).

AN EXPERIMENTAL STUDY FOR COMPARATIVE EVALUATION IN RABBITS OF EFFECTIVE RENAL PLASMA FLOW BY ¹²³I-HIPPURAN AND ¹²⁷I-o-iodoHIPPURATE

Radiolabeled hippuran (OIH) is commonly employed for evaluating effective renal plasma flow (ERPF) through either *in vivo* scintigraphy and/or plasma clearance curves. A new method for measuring levels of stable iodine (¹²⁷I) in biological samples has recently been described, based on the detection (by an NaI(Tl) crystal) of the X-ray fluorescence photons released by activation with an Americium-241 gamma source. The commercial RenalyzerTM system evaluates glomerular filtration rate in patients, based on a plasma sample taken after i.v. injection of the hydrosoluble contrast media commonly used for urography. We assessed the potential of such system for evaluating ERPF after i.v. injection of an iodinated contrast medium with total glomerular and tubular excretion (stable ¹²⁷I-o-iodo-hippurate, or ¹²⁷I-OIH). The results obtained were compared to the clearance values of ¹²³I-hippuran, which was considered as the reference standard.

The study was performed in five rabbits under general anesthesia, by double i.v. injection of ¹²³I-OIH (500 µCi) and ¹²⁷I-OIH (250-400 mg stable iodine). The corresponding plasma curves were evaluated from 4 to 60 minutes, to calculate ERPF as Dose/integral of plasma curve.

The initial distribution volumes of ¹²³I-OIH (148.5±12.5 ml/kg) and ¹²⁷I-OIH (149.2±12.3 ml/kg) were virtually superimposable, thus confirming the chemical identity of the two compounds. The plasma clearance values of ¹²⁷I-OIH (12.59±1.40 ml/min kg⁻¹) were systematically, although not significantly, higher than the ¹²³I-OIH values (11.24±1.77 ml/min kg⁻¹), due perhaps to a relative "mass" load effect of the iodinated medium (which was obviously absent with ¹²³I-OIH).

These results indicate that the new system based on the measurement of stable iodine content in biological samples by X-ray fluorescence activation can be utilized for evaluating ERPF, provided a correction equation derived from comparison with the ¹²³I-OIH reference values is employed.

PS-671

¹Y.Oikonen, ²P.Nuutila, ¹H.Sipilä, ¹T.Tolvanen, ²P.Peltoniemi,

¹U.Ruotsalainen

¹Turku PET Centre and ²Dept. of Medicine, University of Turku, Finland

QUANTIFICATION OF OXYGEN CONSUMPTION IN SKELETAL MUSCLE WITH PET AND OXYGEN-15 BOLUS

Glucose utilization and blood flow in skeletal muscle can be quantified with PET. Quantification of oxygen consumption during the same imaging session would be a valuable addition to these in metabolic studies.

High myoglobin content of muscle prevented us from applying traditional steady-state and bolus O-15 inhalation models developed for brain PET studies. Our model for single bolus inhalation studies consists of two tissue compartments: the first one is for free and myoglobin bound O-15, and the second compartment is for O-15 labeled water, formed in muscle itself or diffused from blood. Both arterial and venous radioactivity concentrations are included in the model. Extraction of oxygen and water is assumed to be 1. Non-linear fitting procedure provides us the blood flow (=K1) and oxygen extraction ratio (OER), calculated as $k_3/(k_2+k_3)$. The muscle metabolic rate MMRO2 is calculated as $\text{flow} \cdot \text{OER} \cdot [\text{O}_2]$ in arterial blood. The model was tested with femoral muscle data from 7-min bolus O-15 inhalation PET studies of six healthy persons. For comparison, A-V differences of whole leg and the blood flow in femoral regions (bolus of O-15 water) were measured.

The MMRO2s in femoral regions (2.9±2.0 ml/l*min) correlated well (r=0.98) with the values calculated using whole leg A-V differences (3.3±2.0 ml/l*min). Also blood flow values in all femoral muscle regions from O-15 and O-15 water studies correlated well (r=0.86). However, the separate values of blood flow and OER from O-15 bolus studies had considerable uncertainty, and the only useful parameter obtained is MMRO2, calculated as their product.

In conclusion, a single inhalation oxygen-15 study is suitable for determination of metabolic rate of oxygen in skeletal muscle.

PS-672

P. Välimäki¹, J. Lampinen^{1,3}, A. Kuronen², S. Savolainen³

¹ Dept. of Physics, Helsinki University, Finland, ² Lab. of Comp. Eng., Helsinki University of Technology, ³ Dept. of Radiology, Helsinki University Central Hospital

AN ANALYSIS OF THE CELL CLUSTER MODELS FOR MICRODOSIMETRY

The conventional way of modelling cell clusters for microdosimetry has been so called close-packed cubic geometry model in which cells form a symmetrical structure (Fig. 1b). In this study the conventional model was compared with the model constructed by CellPacker, the computer program developed for this study.

The central point of the first cell being located in the origin program examines all the reasonable points for the central point of the next cell in the system of spherical coordinates. Starting from the origin and increasing the coordinates in turn it thus systematically seeks a place for the cell as near to the origin as possible. In the exploration process the distances to the central points of the earlier located cells are calculated and compared with the sums of the radii and the possible intercellular distances of the respective cells. If the sum is smaller than the distance between the cells in every single case a sufficient room for the cell has been found. The coordinates of the corresponding point are then tabulated for the later use of determining distances.

The resulting cell cluster is asymmetrical in respect to all directions giving a sense of randomness (Fig. 1a). The most remarkable difference to the conventional close-packed cubic geometry model lies at the boundary of the tumour and normal tissue: The cluster constructed by the CellPacker lacks the large, unrealistic void at the boundary characterising the conventional model (Fig. 1).

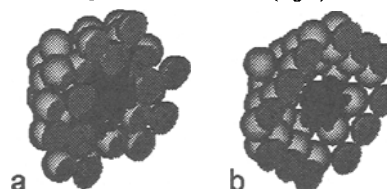


Fig. 1. Cross section of the CellPacker model (a) and the conventional model (b). The small balls portray tumour tissue and the big ones correspond to normal tissue.

Poster presentations

Physics and instrumentation: Quality assurance

PS-673

S. Z. Chen

Department of Nuclear Medicine, Cancer Hospital of Chinese Academy of Medical Sciences Beijing 100021, China

SET UP OF THE NATIONAL NETWORK FOR QUALITY CONTROL OF SPECT IN A DEVELOPING COUNTRY

The purpose of this study is to organize and standardize quality control of SPECT in developing country. In our country there are now more than 230 SPECT in operation, including 30 dual heads SPECT. The annual increasing rate is about 10% to 15%. In order to guarantee the good quality of SPECT in whole country the National Network for quality control was set up, supported by the National Society of Nuclear Medicine. The tasks of the Network include: 1) The national survey. A investigation form of the questionnaires of SPECT according to the IAEA recommendation was sent to each hospital and the feedback information was put into the national QC data base. The data base is upgraded annually. 2) Acceptance test. When a new SPECT machine was installed the Network sent specialists to the hospital to carry out acceptance test based on the NEMA standards. A certificate issued by the Society of Nuclear Medicine was given to the hospital as a professional authority if the acceptance was passed. 3) Training course on quality control. The national or regional training course was run regularly. The national training course is for the train-the trainers and the regional training course is for the technicians and junior doctors. 4) Comparison study. The performances comparison study was conducted using phantom simulation and black box survey in some big cities or regions. The results were evaluated by a group of specialists, and the suggestions and recommendations were sent to each hospital.

PS-674

M. L. de Cabrejas*, J. Paredes*, F. Ponce^{oo}, A.F. García*, R. Lillo**, J.G. Arashiro*, I. Alliende**, Y. Xie**
* CNEA, Argentina; ^o INAMEN, Bolivia; ^{oo} I. Card y Cir. Cardiovascular, Cuba; ^{*} Fac. Ciencias, Uruguay; ^{**} Univ. Chile, Chile; ^{oo} IAEA.

IMAGING CAPABILITY OF LATINAMERICA SPECT SYSTEMS

"Imaging Capability" has been evaluated in the Latinamerican region measuring performance parameters of Spect systems. Scores were assigned considering their relative importance according to the IAEA method. Fifty one Nuclear Medicine laboratories were visited, 53% of which had "new" instruments (installed after 1994). Instrument brands were: Picker (5), Elscint (12), Siemens (4), Toshiba (5), ADAC (7), General Electric (8), SMV (1), Technicare (1). Several parameters: Mechanical performance, Planar Uniformity (U), Planar Resolution (R), Center of Rotation (COR), Tomographic U and Tomographic R were measured. A survey was performed to state if Quality Control (QC) was carried out. Different performance categories were established for each test. Points, were assigned according to the importance of the parameter. For each of the 51 visited laboratories (28 in Argentina, 9 in Chile, 8 in Cuba, 5 in Uruguay and 1 in Bolivia) the brand, the age and the score obtained for each of the checked instruments adding the points assigned to each parameter (maximum 200 points) and the QC programme were evaluated. Instruments were considered Satisfactory (S) and adequate for clinical studies when the score ≥ 150 points while they were Non Satisfactory (NSat) when the score < 150 . Moreover if an instrument has some parameter with score = 0, it is considered NSat. Influence of the instrument's age and QC programme on the score were analysed. Results: a) The average score for "old" instruments is smaller than for "new" instruments (significant difference, $p < 0.05$): $X_{new} \pm \sigma_{new} = 184 \pm 15$, $n=19$; $X_{old} \pm \sigma_{old} = 159 \pm 41$, $n=9$. b) The average for Sat and NSat instruments was: $X_{Sat} \pm \sigma_{Sat} = 184 \pm 14$, $n=22$; $X_{NSat} \pm \sigma_{NSat} = 119 \pm 38$, $n=6$ ($p < 0.05$) c) The score can be high for "new" instruments even if the user does not carry out a QC programme, while for "old" Spect systems only those performing QC were Sat. d) only 4 % of the instruments have "bad" U (score = 0) and 6 % have "bad" R. The COR is OK for 98 % of the instruments and only 2 % of the instruments show severe Tomographic U imaging artifacts. Moreover 7 % of the instruments can not detect cylindrical cold or hot lesions, whose diameter is smaller than 18 mm; 17 % can detect lesions between 12 and 16 mm and 76 % can detect lesions of 11mm (most of the instruments can see small lesions). Total QC was performed in 47 % of the labs, partial QC (U and COR) in 39 % and no QC at all, in 14 %.

PS-675

S. Ekberg, M. Stenström

University Hospital Linköping Sweden, Department of Radiophysics.

TWO PEAK ENERGY CALIBRATION OF GAMMA CAMERA WITH ^{99m}Tc AND CHARACTERISTIC RADIATION FROM LEAD.

The radioactive sources used in energy calibration of gamma cameras today are not optimal and are often a compromise between different qualities. The most common sources for energy calibration are ⁶⁷Ga, ¹³³Ba, ²⁰¹Tl, ²⁴¹Am, ⁵⁷Co, ¹³¹I, ¹²³I and ^{99m}Tc. To make a correct energy calibration you should use at least two well separated energy peaks. This means that several of the mentioned isotopes has to be combined to meet this demand. Since most of nuclear medicine studies are using ^{99m}Tc it is important that one of the energy peaks is near ^{99m}Tc (140 keV). During energy calibration it is preferable that the different energy peaks are of similar intensity and the FWHM of the energy peaks should be as low as possible to get highest reproducibility. It is also important that the used isotopes are available at the department and not to be ordered specially for the energy calibration.

For low energy calibration it would be superior to have an isotope with one peak at 140 keV and another peak about half of this energy. This can be done by using characteristic radiation from lead combined with ^{99m}Tc. The K-alpha radiation from lead is 74.2 keV (78%). The peak is broaden somewhat from the K-beta radiation 85.4 keV (22%).

Different geometric set-ups of ^{99m}Tc and lead characteristic radiation source have been used to get similarly intensity from the two energy peaks simultaneously. The FWHM of the energy peaks was 14.7% (characteristic radiation) and 9.8% (^{99m}Tc).

Conclusion: With ^{99m}Tc and characteristic radiation from lead it is possible to get a two peak source to be used for energy calibration of gamma cameras in the low energy range.

PS-676

M. Fjälling, M. Suurkula, J. Grétarsdóttir, L. Jacobsson.

Hospital: Sahlgrenska University Hospital, Department of Nuclear Medicine, Göteborg, Sweden.

COUNT DENSITY AND DIAGNOSTIC ACCURACY IN BONE SCANS

The amount of administered activity for nuclear medicine investigations varies between different hospitals for the same type of investigation. Image quality depends not only on administered activity, but also on type of gamma camera (age of camera, collimator, uniformity, spatial resolution), mode of displaying images and length of acquisition time. The aim of the present study was to see the influence of count density on diagnostic accuracy in bone scans. **Method:** 65 consecutive patients, irrespective of age, sex and diagnose, were included in the study. Imaging was performed 3 h after iv injection of 500 MBq ^{99m}Tc MDP. Dynamic acquisition was done in a 256 x 256 matrix with 1 min/frame for 5 min. From the dynamic study static images were created with registration times of 1, 2, 3 and 5 min, thus creating images with four different count densities = image qualities for the same patient study. Totally 1 500 images were created. The study was performed on one gamma camera. **Image interpretation:** Images were interpreted and coded independently by two experienced physicians. The images were displayed on a black and white, and a colour screen. The images with the shortest acquisition time were viewed first, i.e. first the 1 min, then the 2 min and then the 3 min images. The last image to be interpreted and coded was the 5 min image simulating the highest administered activity and representing the final diagnosis. The images were displayed automatically and randomly on the screen one at a time and with neither patient identification nor clinical information. **Results:** In the 5 min images totally 168 findings were coded as pathological. With the 5 min images as the final result the number of false positive findings was roughly the same = 5 % for the 1, 2 and 3 min images and the number of true positive findings was 65 % for the 1 min images, increasing to 73 % for the 2 min and 78 % for the 3 min images. **Discussion:** The count density interval studied corresponds to 0.4 - 2 times the count density routinely used at our department and simulates an injected activity of 167 - 833 MBq for a registration time of 3 min. As there were 22% false negative findings for the 3 min images and 500 MBq it can be considered to increase the administered activity to 800 MBq or increase the registration time to 5 min.

PS-677

E.Gremillet, A.Champailler, S.Guillet

Centre d'Imagerie Nucléaire, Saint-Etienne, France

TWO-DIMENSIONAL KOLMOGOROV-SMIRNOV (2DKS) TEST AND GAMMA-CAMERA UNIFORMITY CONTROL: MONTE-CARLO SIMULATIONS.

The 2DKS test was introduced in astronomy to compare an observed 2D distribution with an expected one. Thus it could be used to compare a gamma camera flood image with a uniform distribution. Briefly the 2DKS test involves: i) scanning over all the observed points and, at each position, calculation of the absolute difference between the proportions of observed and theoretical points in each of the four natural image quadrants; ii) calculation of the probability level p using the KS probability law with, as argument, a function f of D (the maximum observed difference) and of the number N of points. A formula for f has been previously proposed, based on Monte-Carlo simulations with N up to 5000. For far larger N , such as the number of counts obtained in a flood image, validity of this formula is not established. We thus performed Monte-Carlo simulations of uniform images with increasing N : 100K, 200K, 400K, ..., 25600K. A frame size of 150x120 was used (ie roughly the CFOV of a rectangular camera sampled in 256x256). 1000 images were generated for each N . Design and management of random numbers generators (RNG) was critical because of the very large amount of numbers to generate: 2 RNG were used, based on Park-Miller algorithm with Bays-Durham shuffle and Schrage's anti-overflow method; RNG#1 was initialized once for each N and then produced 1000 seeds to initialize (once per image) RNG#2, who generated the x and y coordinates of each event. Then, for each of the nine N values, the D values corresponding to eight p levels from 0.20 to 0.001 were determined. Multiple regression was then used to determine the optimal function f , by fitting to theoretically expected values for each p level. The final best ($r=0.975$, $p=0.0001$) formula was $f(D, N) = 1.219D\sqrt{N} - 0.784$, ie a rather different result from Press et al formula ($-(D\sqrt{N})/1.25$). Conclusion: by Monte-Carlo simulations we obtained a formula allowing to use the 2DKS test for very large numbers of events, having comparison of gamma camera flood images with theoretical uniform images in view.

PS-678

J.Heikkinen

Dept of Nucl Med, Mikkeli Central Hospital, Finland

NEW PHANTOM FOR DYNAMIC RADIONUCLIDE RENOGRAPHY

The aim of the study was to develop and test a phantom simulating dynamic radionuclide renography. In 1993 bone scintigraphy and brain perfusion single photon emission tomography (SPET) were evaluated in 19 Finnish laboratories. After that Labquality Ltd (Helsinki) has organized four external quality assurance tests of nuclear medicine in Finland. In 1994 11 laboratories were studied with a new bone phantom. For brain perfusion SPET were bought a 3-D phantom which was imaged in 12 laboratories in 1995. In 1996 the quality of myocardial perfusion SPET between 19 Finnish laboratories were compared. Phantoms were commercially available for those studies. There were no commercially available renography phantom for external quality assurance purposes. Therefore I had to construct a new phantom. It consist five plastic containers simulating kidneys, heart, bladder and background. Dynamics is carried out with multiple movable steel plates between containers and gamma camera. Control of plates was performed manually with stopwatch. The simulation with the phantom was made in 19 Finnish nuclear medicine laboratories. Containers were filled with activities which produce count rates close to clinical situations and three patient cases were simulated in every laboratory. Gamma camera images from the phantom were close to a real patient and the time activity curves seemed similar between laboratories but calculated parameters varied. The average error in T_{max} (time to reach maximal activity) was $-3.2 \pm 8.4 \%$ (from -29.4 to $+17.8 \%$), in $T_{1/2}$ (time from maximal to half activity) $9.5 \pm 24.6 \%$ (-42.8 to $+66.2 \%$) and in 20-min/peak ratio $3.7 \pm 18.5 \%$ (-50.0 to $+81.7 \%$). The difference between laboratories is most probably due to variations in analysis protocols and programs. The phantom is suitable for interlaboratory comparison and calibration of analysis programs.

PS-679

R.Matheoud, F.Zito, C.Canzi, F.Voltini, L.Tsukerman*, P.Gerundini.

*ELGEMS Ltd, Haifa, Israel; Nuclear Medicine Dept. and Health Physics Service, I.R.C.C.S.-Ospedale Maggiore, Milan, Italy.

HIGH-FLUX IRRADIATION EFFECTS ON THE CARDIAL GAMMA CAMERA.

Exposure to high-count rates greatly affects performances of the gamma camera system; here the effect of a high flux irradiation (HFI) on the CardiaL system (Elscint) energy response is described. One detector of this dual-headed 90°-fixed gamma camera was accidentally left uncollimated when testing the system planar uniformity with a Co-57 flood source (7 mCi/259 MBq) on the other collimated head. The uncollimated crystal surface was exposed to a non-uniform γ flux of $0.6-2.0 \times 10^6$ cps for 30 min to which immediate PMT intrinsic-gain variations corresponded. Because of this effect, a drift of photopeak position and a loss of energy calibration was observed. To evaluate the importance of the damage and the intrinsic capability of PMTs to spontaneously recover original gains, the photopeak position was monitored using a 400 μ Ci (14.8MBq) Tc-99m point source for nearly 1 month after HFI. During this period the detector was not calibrated.

The HFI produced important and prolonged instabilities on the PMT intrinsic-gains as demonstrated by photopeak position which increased to 158 keV soon after the HFI, reached a value of 140 keV after 5 days and moved to a stable value of 130 keV after 15 days. The severity and the persistence of the damage was strictly related to the non-uniform distribution of the radiation flux on the detector and therefore it was greater for the more exposed PMTs. When PMT stabilities were reached, a new system calibration was performed to adjust electronic-gain offsets in order to recover the correct energy response.

This experience suggests that particular attention is required to avoid HFI on CardiaL system as it induces persistent PMT gain shifts and consequent loss of gamma camera energy calibration.

PS-680

Puchal R., Pavia J., Aguadé S., Castell J., Muxi A., Martin-Comin J., Nuño J.A., Garcia M.J., Casans Y., Martinez-Sampere J.J., Carrió, Y., Abós M.D., Castro J.M., Campos L., Freire J., Labanda P., Gómez C., Marín M.D. S.Medicina Nuclear. Hospital de Bellvitge. L'Hospitalet de Llobregat. Spain

GAMMACAMERA QUALITY CONTROL PROCEDURES IN THE SPANISH MULTICENTRE STUDY ON 99mTc-TETRAFOSMIN MYOCARDIAL PERFUSION

In a first phase of a nationwide multicentre study it is necessary to assure that the equipment that will be used fulfills some minimum requirements of quality. The aim of this work is to present the methodology used for the follow-up of the functional state of the tomocameras used to obtain 99mTc-Tetrafosmin myocardial perfusion scintigraphic patterns of normality in Spain.

It was decided to check the state of th cameras through the results of some well established patterns, once all the possible corrections have been applied to each camera. For this purpose three phantoms were designed: one to control the stability of the center of rotation, another one for the tomographic uniformity and a third one which simulated the left ventricle both in shape and orientation. These phantoms circulated between nineteen departments which correspond to 21 gammacameras. Very strict norms had to be followed in the acquisition and processing of these phantom studies. Cameras and/or centres were not allowed to participate in this study until they fulfilled the requeriments of quality.

Constancy of the center of rotation was quantified by means of the excentricity of a 360° orbit, having to be less than 10%. Tomographic uniformity was visually checked taking in account the number of slices with rings and their contrast and finally, no artifacts had to be present in the reconstructed study of the ventricle.

The center of rotation was within limits in all the cameras except one case (95.2%). Tomographic uniformity was correct, in a first round in 13 cases (65%) and in a second round in 20 (95.2%). One department retired from the study due to difficulties in repairing its camera on time.

Poster presentations

PS-681

Wen-kai Wu, Qinkun Zhang, Yingying Jia, Jiaxiu Li

Hospital: Chinese Academy of Medical Sciences, Peking Union Medical College Cancer Hospital, Department of Nuclear Medicine

SCORING METHOD FOR CERTIFICATION OF QUALITY CONTROL OF SPECT

Since 1994 we have worked on the regional project titled 'Certification of QC and preventive maintenance of SPECT in Asia', which is sponsored by IAEA. The goal of this project is giving assistance to participant countries to establish their effective system for certification of QC of SPECT. In study of the project we found that judging by the results of QC was very difficult to decide which system would be passed the certification test, or would stop the use to be repaired, or had to be scrapped. We have designed a scoring system of QC of SPECT on basis of QC standards and clinical requirements to remedy this inadequacy. According to the functions of SPECT the scoring system presented three parts: planar, tomography, and linear scan. The score of planar performance is the key parameter to assess the system condition and to judge whether the system has to be scrapped. The tomographic performance is on basis of the score of planar plus the score of tomography and the linear scan performance is on the score of planar plus the score of linear scan. Because of different systems may be produced by different vendors and they may be different models, the marks in the scoring system were given in accordance with normalized parameters of QC tests. The normalized parameters were values of QC test divided by the system technical specifications which were given by manufacturers. And also we set up values of the worst level. If any parameter of any system were worse than the worst level it would mean this system had to be stopped using. Ten SPECT systems of single head and ten systems of dual-head were chosen for rigorous comparison of QC test and results reported with scoring method. Same times we did tests of comprehensive performance and of organ phantoms also. Comparing the analysis reports, especially the images of organ phantoms, we modified scoring weights to reduce effects of improper factors and to improve adaptability of the scoring system. We analyzed the QC parameters of fifty two γ camera systems with the scoring system. According to the scoring levels forty-two of them passed test (81%), eight systems showed they ought to maintain (15%), two systems were recommended to be scrapped (4%). In random sampling we took clinical images of planar, topography and whole body scan from each of fifty-two systems. Two experienced doctors evaluated these films with 10 points system. The marks given by two doctors compared with QC scores with statistics analysis. The correlation coefficient for planar images is 0.76, for tomographic images is 0.78 and for whole body scan images is 0.83. The scoring system is not perfect yet, but it is practical and very useful for certification and inter-laboratory comparison of QC of SPECT.

Physics and instrumentation: Nuclear magnetic

PS-682

A.R. Formiconi, A. Passeri, S. Martini, A. Pupi, E. Loli Piccolomini, F. Zama, G. Zanghirati, Univ. of Florence, Dept. of Pathophysiology, Univ. of Bologna, Dept. of Mathematics

REGULARIZATION METHODS FOR THE QUANTIFICATION OF REGIONAL CEREBRAL FLOW WITH MRI

The fast transit of contrast agent in dynamic perfusion MRI studies requires special acquisition-reconstruction techniques such as the keyhole method. With this method a reduced number of phase-encoded samples are acquired so that reconstruction artifacts and loss of resolution may hamper the diagnostic potential of dynamic images. Since any attempt of quantitative derivation relies on the accuracy of the reconstructed images, several advanced reconstruction techniques were investigated and applied both on simulated and experimental data. The conventional keyhole (KH) method available in commercial systems was compared with the constrained reconstruction by the Tikhonov (T), truncated singular value decomposition (TSVD) and conjugate gradient (CG) methods. All the new methods gave slightly improved image quality with respect to KH. The regularization capabilities of the new methods were equivalent but CG was faster of a factor 10 and 100 than T and TSVD respectively. The results of this work showed that, in front of the inherent difficulty to extract reliable information from dynamic MRI for quantitative purposes, it is important to investigate reconstruction methods which make better use of the information available in the experimental data.

PS-683

F. Lethimonnier¹, A. Furber², P. Balzer¹, O. Morel¹, P. Pezard¹, P. Geslin², P. Jallet¹, JJ Le Jeune¹
Department of Nuclear Medicine¹, department of Cardiology², University hospital of Angers, France

Ejection Fraction Assessment by Magnetic Resonance Imaging: comparison with Radionuclide Angiography and Contrast Angiography.

Introduction: Cardiac MRI has been shown to be a robust and noninvasive method to assess the cardiac function. Measurement of left ventricular volumes and ejection fraction (EF) require to trace endo and epicardial contours. Recently, fast acquisition techniques and automated border detection methods provide a precise and quickly solution to estimate global and regional cardiac function. Purpose of this study was to compare EF measurements calculated with MRI and radionuclide angiography (RNA), reference exam, or contrast angiography (CA). End diastolic volume (EDV), end systolic volume (ESV), and mass were also assessed by MRI.

Materials and Methods: Thirty five patients with various diseases underwent MRI exam on the same period as RNA or CA in a GE 1.5T MR imager. Short-axis images were acquired with a fast gradient echo segmented sequence from apex to base. Each slice was acquired in breath-hold in multiphase mode with a temporal resolution of 81.6 ms. Epicardial and endocardial contours were drawn.

Results: Twenty six patients underwent MRI and RNA exams (group A), and 25 patients underwent MRI and CA exams (group B). Mean EF was 46±17% in MRI, 47±13% in RNA, 50±15% in CA. Mean EDV, ESV, mass measured in MRI were respectively 44±18 cc/m², 25±18 cc/m², 77±18 g/m². EF correlated well between modalities. For the group A: r=0.77 p<0.001, and for the group B: r=0.72 p<0.001. The acquisition time was between 20 to 30 minutes according to patient cooperation, and the average post-processing time was 10 minutes.

Conclusions: Using a breath-hold gradient echo acquisition and a automatic edge detection software, MRI can be useful in routine clinical application for a fast and accurate estimation of LV EF, EDV, ESV, and mass. MRI may prove to be the one imaging technique that can be used to evaluate global and regional myocardial function, and all aspects of coronary artery disease, including cardiac anatomy, regional myocardial perfusion, visualization of the major segments of coronary, and measurement of blood flow velocities in the coronary arteries.

PS-684

^aK. Raffelt, ^bD. Moka, ^aF. Süllentrop, ^aJ. Hahn, ^bH. Schicha

^aInstitute for Inorganic and Analytical Chemistry and ^bDepartment of Nuclear Medicine, University of Cologne, Germany.

31P MR Spectroscopy of Human Blood Plasma: A New Diagnostic Tool for Detection of Metastases/Tumorous Thyroid Tissue in the Aftercare of Thyroid Cancer ?

Introduction: Recently published studies proved the strong influence of tumour tissue on the lipid and phospholipid (PL) metabolism. 31P magnetic resonance spectroscopy (MRS) offers a new way to detect and quantify different phospholipid classes in blood plasma. The purpose of this study was to find out whether there are differences in the phospholipid metabolism in patients with metastases/residual thyroid tumour tissue in comparison to patients with thyroid carcinoma in remission after therapy. Furthermore we assessed the influence of thyroid dysfunction in phospholipid metabolism.

Methods: Blood of hypothyroid patients after thyroidectomy in preparation to a radioiodine therapy or whole body scintigraphy was examined by 31P-MRS. We detected and quantified six different phospholipids: phosphatidylethanolamine, sphingomyelin, 1- and 2-acyl-lyso-phosphatidylcholines, phosphatidylinositol and phosphatidylcholine. To assess the influence of thyroid hormones on phospholipids in human blood plasma we compared the plasma PL concentrations of 22 healthy volunteers (group A) with those of 17 hypothyroid patients (thyroid cancer in remission, group B) and those of 5 manifest hyperthyroid patients (group C), respectively. The next step was to examine whether the phospholipid concentrations of group B (hypothyroid in remission) differed significantly from those of 16 hypothyroid patients with metastatic thyroid cancer (group D). Finally we examined whether there are differences in plasma PL concentrations of euthyroid patients in remission (B*) in comparison to those of healthy volunteers (A).

Results: The comparison of healthy volunteers, hypo- and hyperthyroid patients showed a strong influence of thyroid hormones on the plasma PL content. The hypothyroid patients with metastatic thyroid cancer (D) show lower PL concentrations in blood plasma compared to those of the hypothyroid patients in remission (B). Thyroid cancer leads e.g. to significant lower concentrations of sphingomyelin and phosphatidylcholine. There was no difference in PL concentrations of euthyroid patients in remission (B*) and healthy volunteers (A).

Conclusion: 31P-MRS is suitable to assess changes of phospholipid metabolism in patients with thyroid cancer. Therefore, 31P-MRS could be develop to a potential diagnostic tool in the aftercare of thyroid cancer patients.

Physics and instrumentation: Telenuclear medicine

PS-685

J.W. Arndt, J.A.J. Camps, J.A.K. Blokland, F.J. Martens, F.P. Ottes, E.K.J. Pauwels

Leiden University Medical Centre, Division of Nuclear Medicine, Hiscom, Leiden, The Netherlands

REPORT AND REVIEW SYSTEM FOR NUCLEAR MEDICINE IMAGES II: Clinical experience.

We have developed a Picture Archival and Communication System (PACS) for nuclear medicine images, that is integrated with the Hospital Information System (HIS). The system consists of a central server, reporting stations at the department of nuclear medicine and several viewing stations at other locations in the hospital. Images and data analyses are sent from the acquisition and analysing systems to the reporting and reviewing system of the PACS.

This is the description of the daily use by the nuclear physician after a one year experience. The first step for the reporting physician is the approval of the acquired images, while the patient is still at the department. Images can also be accepted automatically.

The second step is the authorisation of the study: each study is displayed in a template configured to that particular kind of study. Changes in the sequence of images, colours, intensity and contrast can be performed, annotations can be added. While reporting and authorising, older studies and reports and laboratory data available through the HIS can be displayed on the same reporting screens. As soon as the study is authorised it can be viewed by the referring physician at remote places in the hospital on the viewing stations.

Advantages of the PACS for the reporting physician and department:

a) immediate availability of the studies (old and recent) for reporting and consultation; b) more diagnostic information through image manipulation and dynamic display; c) working from dedicated worklists; d) constant quality of studies, not influenced by the quality of a printer; e) no large archive and loss of old studies.

Advantages for referring physicians: a) immediate availability of studies at remote places in the hospital, same day directly after authorisation, older studies at all times.

Conclusion: although it takes some time from the reporting physician for authorisation of the studies the mentioned advantages outweighing this. The direct availability of studies and reports improves the consultation with the referring physicians.

PS-686

P.E. Christian, D.A. Baune

University of Utah School of Medicine, Salt Lake City, UT

INTEGRATING NUCLEAR MEDICINE IMAGING INTO ENTERPRISE WIDE RADIOLOGY PACS

Purpose: The aim of this project was to fully implement nuclear medicine images into enterprise wide radiology PACS. The goal was to allow nuclear medicine images to be archived and available through general PACS viewing stations, yet still be capable of retrieval and reprocessing any type of NM study. We also wanted to make CR, MR and CT available in nuclear medicine.

Methods: Full integration of NM imaging into radiology PACS required the evaluation and possible upgrade of the physical network (cabling, connectivity), storage systems, and file formats. We have cameras from three NM clinics with various manufacturers sharing digitally via Interfile format or a proprietary vendor format by network file system (nfs) mounting for several years. Centralized data storage requirements required consideration of storage capacity, data recovery capabilities, recovery time, redundancy, and reliability. Workflow management issues for patient studies and an appropriate search mechanism to provide realistic solution are required.

DICOM file format of NM images did not allow recovery of images for reprocessing for SPECT, gated or dynamic image sets. Viewing NM images through a general Radiology PACS viewer had problems with displaying color, appropriate cinematic display, evaluating gated SPECT and reprocessing NM files that have been converted into DICOM format. Additionally, images viewed with the radiology PACS viewer should show appropriate annotation, arrows, etc. These afore mentioned concerns all had to be addressed to provide usable and fully functional viewing of NM images.

Results: We were able to use existing 10baseT cabling but required an upgrade to switched hubs, along with fiber connections between imaging centers, as a result we have seen significantly improved network performance. A StorageTek RAID and tape jukebox system was implemented for archival storage. A software solution was effected for patient scheduling which activates pre-fetch retrieval and auto-routing of image files to workstations. Dual format storage utilization and dual databases have been implemented to allow storage, retrieval and reprocessing of NM image data from either radiology or NM viewing stations.

Conclusion: Nuclear medicine clinics at 3 separate locations have been incorporated into an enterprise wide PACS solution.

PS-687

L.C. Wu, J.H. Liu, S.C. Lee, L. Chang, J.K. Wang, P.F. Chiu, and R.S. Liu.

National PET/Cyclotron Center, Taipei Veterans General Hospital, and National Yang-Ming University School of Medicine, Taipei, Taiwan.

PUSHING PATIENTS' RESULTS TO PHYSICIAN'S DESKTOP.

As the web technology prevails today, a number of centers have implemented different web applications for teaching files, database access, PACS, and so on. However, users cannot see the web site's content unless they intentionally visit that site and wait for the transmission of the content. This study utilized the "push" concept and the active desktop environment to implement a medical information webcasting system (MIWS). The system can automatically deliver the patients' imaging results to the referring physician's active desktop so that the doctors can have immediate review of the patients' results.

MIWS is currently an intranet application. Its infrastructure can be divided into the server and client parts. In the server side, 3 Windows NT servers are utilized to work as the web, file, and SQL servers. The web server running the Internet Information Server and active server page (ASP) can communicate and control the SQL and file servers with the ASP-based applications. Using the channel definition format (CDF) file, clients running active desktop with Windows 95 can subscribe to the server. MIWS can then get the physician's ID from the cookie and all the patients that are referred or cared by the doctor can be queried from SQL server. The results are arranged into a CDF file with hyper link to the image files on the file server. The CDF file and the corresponding links are updated only if the doctor's new patient images have arrived in MIWS. With the scheduled refresh interval, the server can smartly deliver CDF and only changed content to the client. The client's active desktop will automatically change the patient list right on schedule. Users can point and click on the list to get patient's images displayed on the browser window. As the images are already pushed in the local cache, the physicians don't have to look for the patients and wait for the image transfer.

In summary, our MIWS utilizing the "push" concept in CDF and the technology of ASP can be incorporated into a web-based PACS. It is as simple as a cable TV channel for the physicians.

PS-688

J. Luo, Ph.D. and H.M. Abdel-Dayem, M.D.

St. Vincent's Hospital & Medical Center of NY, Department of Radiology, Nuclear Medicine Section, New York Medical College, Valhalla, NY.

REMOTE DATABASE SYSTEM FOR CLINICAL DATA TRANSFER AND MANAGEMENT USING A WINDOWS-NT-SQL SERVER

Purpose: Using Windows-NT-SQL server on PC to build a network database for nuclear medicine image and clinical data storage, management and exchange through conventional telephone line, modern local area network and Internet. **Method:** The network database server is on a general purpose personal computer under Windows NT 4.0 operating system to integrate different computer platforms, which is common in many clinical nuclear medicine departments, through TCP/IP standard. Another PC with Windows 95 operating system is used as front end console. One or more than one general purpose, non-dedicated PCS running Windows 95 or NT can be used as workstations locally and on remote sites. The network database uses client server technology. Windows NT and SQL server are employed to setup and manage patients' database to utilize database replication, file to file protection, multiple layer security, window based information query/retrieval and network accessibility. The dedicated server on local area network will control all data input/output, communication between the server and workstation both local and remote. User interface is built with Visual Basic scripts on a multi-level and multi-group format. Patient's record can be read into the database by conventional key board, cut/paste between networked computers, ftp or scanner for tables and hand writings. A Charge Coupled Device (CCD) camera is used to digitize X-ray, CT, MRI and NM films that are not stored on computer or not available to users. The image from the CCD camera is interfaced to workstation by a film grabber with variable field of view and pixel resolution upto 1024 X 1280. Clinical reports including image, table and plot can be generated and printed. **Result & Conclusion:** Typical NM image and record transfer takes less than one minute through 33.6 kps modem. Remote site can get a read only database with images and records either manually or automatically. Cut/paste on windows or CCD camera allows image input regardless format. Future development will include dynamic image display and DICOM standard.

Poster presentations

PS-689

F.P. Ottes, F.J. Martens (1), J.A.J. Camps, J.A.K. Blokland, J.W. Arndt (2)

(1) HISCOM, Leiden, The Netherlands and (2) Nuclear Medicine department of the Leiden University Medical Centre, Leiden, The Netherlands

REPORT AND REVIEW SYSTEM FOR NUCLEAR MEDICINE IMAGES I: Functionality and design.

A Picture Archival and Communication System (PACS) for nuclear medicine (NM) images has been realised, that is well integrated with the existing hospital information system.

The specification of the functionality has been carried out using the Joint Application Design method, whereas the development has been performed following the Software Development Methodology. The software has been developed for an Intel-based SCO UNIX server with an X-windows environment using the GNU C++ compiler and some Graphical User Interface tools.

The functionality of this NM PACS has been defined by a group comprising of professionals from 4 Dutch NM departments and an HIS vendor (HISCOM). The NM PACS provides facilities to capture, archive, display, manipulate, analyse, print and export nuclear medicine images. The NM PACS supports 1) the quality assessment of a study immediately after its execution, 2) the creation of the report using the newly created images of the on-hand study and clinical data of that patient, including images of previously performed NM studies, 3) the viewing of the images (by the referring physicians) on PC's throughout the entire hospital, together with the report and other parts of the electronic patient record, such as lab. results, discharge letters and medical reports.

The hardware architecture consists of a production and a backup UNIX server, some reporting stations (with two 21-inch monitors) and a number of review stations at the wards. The image stations are PC's.

This development has demonstrated that a NM PACS with the required functionality including HIS integration can be realised using general-purpose hardware, the hospital's network facilities and a one-layered storage architecture. This NM PACS is currently in operational use in a large general hospital and a university hospital in the Netherlands.

PS-690

D. R. R. White¹, J. R. Nixon² and A. S. Houston¹

¹Royal Hospital Haslar, Department of Nuclear Medicine

²PaxSys Ltd.

AN IMAGE AND DATA MANAGEMENT SYSTEM FOR NUCLEAR MEDICINE

A novel data management system has been developed for use by nuclear medicine departments.

The system includes data entry for all patient demographic, radiopharmacy and clinical report information. The generation of stock control, radiation protection and allied records are integral to the system.

Clinical reports utilise an automatic image archiving system, enabling images to be attached to an 'on-line' report screen for viewing and manipulation remotely over the network. The archiving system accepts images in most formats including Interfile, DICOM, bitmap and TIF. This allows the simultaneous display of clinical and diagrammatic images for information or training purposes.

The system has been developed using standard Microsoft Windows™ tools with industry standard communications protocols to facilitate customisation and ease of portability between departments. Networking is provided for communications throughout the Windows and UNIX environments enabling 'once only' input of patient data from any terminal.

Full security to C2 rating is implemented with graded access to different parts of the system, depending on the security level of the password used. As standard, security for entering information is limited to a local area network within the nuclear medicine department. A routine customisation allows full telemedicine capability, however, with the ability to send and receive images and reports over the Internet using the standard connect, browse and format tools (HTML) available to enable seamless distribution in this environment.

The system has been integrated successfully in the Nuclear Medicine Department and is used routinely by administrative and medical staff.

Physics and instrumentation: Others

PS-691

T. Korppi-Tommola¹, K. Malmivaara², S. Savolainen¹

¹Dept. of Radiology, Helsinki University Central Hospital, Finland

²Dept. of Physics, University of Helsinki

MULTIPLE WINDOWING SCATTER CORRECTION TECHNIQUE IN SIMULTANEOUS DUAL-ISOTOPE WHOLE BODY IMAGING

Aims: To develop a practical and fast scatter correction method for simultaneous dual isotope studies, especially, for whole body imaging.

Methods: Correction is based on the selection of isotope couples with separable main energy peaks and half-lives. A cross-talk correction technique was developed in which the scatter of the high energy isotope, received in the window of the lower energy isotope, was used to calculate the correction factor (i.e. matrix) to perform scatter free images. The imaging sessions were planned so that the faster and almost complete decay of the lower energy isotope could be benefited in order to obtain the image information of the high energy isotope only, in the last imaging session. Two identical rectangular water phantoms (27 L) with tilted capillary tubes (1 mL) were placed beside one another on an imaging table. In the tubes Tc-99m/In-111 and Tc-99m/I-131 isotope pairs were used with activities of 203/65 and 278/16 MBq, respectively. To simulate the body background the mixture of isotope pair (of the same activity) was stirred to the water of the other phantom. The used energy windows were: 20% for 140 keV and 247 keV and 15% for 364 keV energy peaks. Imaging was performed with Picker 2000 dual head gamma camera using the medium energy collimator and the whole body imaging protocol. The imaging was performed at 1,4,18,42 and 72h for Tc-99m/In-111, and 1,4,24,72 and 168h for Tc-99m/I-131. Images were processed using Odyssey VP image processing computer and it's image algebra routines. The correcting matrix was made by normalizing and dividing the low energy window image by the high energy window image from the last images of the session. The high energy images were then multiplied by this correcting matrix and subtracted from the original low energy images.

Results: Scatter free low energy images are achieved. Improvement can be seen in all images of the phantom studies. After the scatter correction the calculated scatter fractions in the original images for Tc-99m/In-111 images were: 1h 24%, 4h 29%, 18h 55%, 42h 78% and 72h 100%. The corresponding values for Tc-99m/I-131 images were: 1h 8%, 4h 10%, 24h 42%, 72h 65% and 168h 85%. The measured half-value widths of the capillary tubes at 200 mm depth of water improved for Tc-99m/In-111 3,8% and for Tc-99m/I-131 2,6%.

Conclusion: The scatter correction method is accurate and simple enough for clinical work.

PS-692

A. Larsson^{*}, L. Johansson^{*}, A. Rydh[†]

Hospital: Umeå University Hospital, ^{*}Department of Radiation Physics and

[†]Department of Diagnostic Radiology

A METHOD FOR ESTIMATING UPTAKE IN BONE METASTASES BASED ON PLANAR SCINTIGRAPHIC IMAGING

To quantify the activity in a tumour from a planar scintigraphic image, a correct subtraction of the background from over- and underlying tissue is essential. For bone scintigraphy this is especially complicated since the backgrounds originating from bone and normal tissue are different. The aim of this study was to develop a quantitative method, taking both the bone and normal tissue background into account in a tumour mass dependent background subtraction. The difference in attenuation characteristics between bone and normal tissue has also been cared for.

Eleven patients with prostate metastases in the skeleton were included in the study. They were injected with 550-660 MBq 99mTc SMDP and scintigraphic measurements from the anterior, posterior and a lateral side were made 3.5-4.5 hours later. The lateral image was needed to get a 3-dimensional location of the tumour. Regions of interest (ROIs) were drawn to cover the tumour, a small part of normal tissue and a part of the skeleton close to the tumour, on both the anterior and posterior images. For each patient the body and bone thicknesses at the site of the tumour were determined in the posterior - anterior direction, and the fraction of the bone in the "tumour-ROI" engaged by the tumour was estimated to be either 25%, 50%, 75% or 100% approximately. The corresponding part of bone and normal tissue in the "tumour ROI" was determined, and their count density, corrected for attenuation, was subtracted. The geometrical mean of the net tumour count rate, corrected for attenuation in the two types of tissue, was then calculated. A calibration factor in MBq/counts per second was assessed by performing scintigraphic images on a rectangular water phantom with a cylindrical bone substitute, containing a tumour-like hole filled with a 99mTc-solution of known activity concentration.

For most of the tumour ROIs in this study, the background originating from bone exceeded the background from normal tissue. Omitting the subtraction of the bone background would therefore lead to a considerable overestimation of tumour activity.

PS-693

M. Matović, M. Ravlić, Lj. Mijatović

Hospital: *University Clinical-Hospital Centre, Department of Nuclear Medicine, Kragujevac, Serbia, Yugoslavia*

OUR SOLUTION FOR INTERFACE BETWEEN GAMMA SCINTILLATION CAMERA (GSC) AND PERSONAL COMPUTER (PC)

In this paper we describe our original solution for interface between analog GSC and PC. Our low-cost and simple electronic interface supports data acquisition from gamma camera during both, static and dynamic studies. Emission computerized tomography and ECG gated studies are supported, too. Interface consist of analog-digital converters (ADC) block and TTL logic for connection with PC. Two 12 bit pipeline ADCs with maximum sampling rate of 30 MHz (Burr-Brown ADS821U), are used in ADC block. In term of needed speed, logical block between ADCs and PC is realized with classical TTL gates.

Our preliminary results during testing of this interface, linked with SIEMENS Rotta ZLC-37 Dual Head gamma camera and IBM PC Pentium /133, indicate that, this interface may be useful in practice with old models of analog GSC, which we want coupled with PC. Overall spatial resolution was under 6 mm, field nonuniformity was under 7% and maximum count rate was over 200000 cps. Figures 1, 2 and 3 show bar phantom study, static liver study and sequence of dynamic kidney study, respectively.



Figure 1

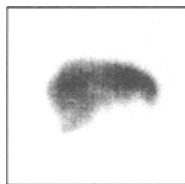


Figure 2

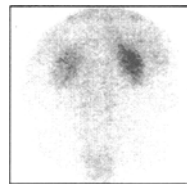


Figure 3

Radiopharmacy and radiochemistry: PET

PS-694

L. Aloj, E. Jagoda, L. Lang, C. Caraco', R. D. Neumann, R. L. Dedrick, C. Sung, W. C. Eckelman.

Nuclear Medicine, PET and BEIP, NIH, Bethesda MD, USA

TARGETING OF TRANSFERRIN RECEPTORS IN MICE BEARING A431 AND LS174T XENOGRAFTS WITH [F-18]HOLO-TRANSFERRIN: PERMEABILITY AND RECEPTOR DEPENDENCE

We are evaluating the use of a high molecular weight protein, transferrin (Tf), covalently labeled with F-18, to determine if specific binding can be obtained within 6 h in tumor xenografts and ultimately test its usefulness as a radiopharmaceutical to trace Tf receptors in tumors. We have previously shown that [F-18]holo-transferrin ([F-18]Tf) maintains all the properties of native transferrin *in vitro* and that it can specifically target liver Tf-receptor sites *in vivo*. The goal of this study was to determine if [F-18]Tf, with a molecular weight of 79 kDa, can specifically target Tf receptor sites in tumors within the time frame commensurate with the half life of F-18 (109.7 min). The distribution of [F-18]Tf, using [F-18]albumin (Alb) or [C-14]Alb as a control, was studied over a 6 h period in nude mice bearing LS174T and A431, a high- and a low-permeability tumor, respectively. Liver uptake values were higher for [F-18]Tf than for both [F-18]Alb and [C-14]Alb throughout the study indicating specific binding. The biodistribution of the three tracers in each xenograft was very similar. In each xenograft, the similar increase of tumor-to-blood ratios for all three tracers with time suggests that [F-18]Tf uptake is dominated by non-receptor mediated processes, even though Tf receptor concentration was higher in the xenografts than in the liver based upon measurements of tumor and liver extracts. Pharmacokinetic modeling of the data shows that the permeabilities of [C-14]Alb and [F-18]Tf in LS174T are 1.3 and 1.0 $\mu\text{L}/\text{min}/\text{g}$ respectively whereas the permeabilities of the two tracers in A431 are 0.79 and 0.44 $\mu\text{L}/\text{min}/\text{g}$. Given these low permeabilities, the high plasma and extracellular concentrations of endogenous Tf and the slow plasma clearance of the tracer, the observed uptake values in the two xenografts are consistent with a permeability controlled distribution. In the liver, the absence of a permeability barrier yields specific [F-18]Tf binding to receptors compared to the Alb control within 5 min after injection. We conclude that receptor-mediated accumulation in tumor xenografts of [F-18]Tf is impaired by rate determining permeability and cannot be achieved in a time frame of 6 h.

PS-695

G.J.Beyer, C.Morel, D.Slosman (1), S.Sakar(2), B.J.Allen (3), and the ISOLDE Collaboration. 1: Geneva University Hospital, (Switzerland), 2: University of Sydney, 3: St.George Cancer Care Centre, Gray St, Kogarah (Australia).

IS Tb-152 SUITABLE TO MONITOR TISSUE DOSES IN ALPHA THERAPY WITH Tb-149 USING PET ?

Introduction : Previously we proposed the alpha emitting lanthanide Tb-149 (17 % alpha decay, $T_{1/2} = 4.1$ h) for systemic radionuclide therapy when cancer cells in circulation are to be targeted [1]. We now propose to use the positron emitting Tb-152 (12 % positron decay) for in-vivo monitoring the biodistribution of Tb-149 in radionuclide therapy with PET, since the 4 % positron branching rate in the Tb-149 decay appears to be too low. The problem in PET imaging for both Tb-isotopes is the accompanied gamma radiation. We report here on the production technology of Tb-149 and Tb-152 and preliminary PET phantom studies.

Methods : Isotopically clean Tb-152 and Tb-149 have been produced via spallation reaction (1 GeV protons on 200 g/cm² Ta-target) in a combined process which includes the on-line isotope separation at the ISOLDE facility at CERN and a chemical (isobaric) separation using miniaturised cation exchange chromatography. Batches of 500 and 800 MBq have been obtained for Tb-152 and Tb-149, respectively, in a final volume of 100 μl 50 mMol HCl solution, suitable for labelling of modern chelated bioconjugates.

Results : A Jaszczak phantom was filled with 4 liters of a Tb-152 or Tb-149 solution. The PET studies were performed using the ECAT-ART PET scanner. The energy window was set narrow between 440 and 560 keV in order to reduce the disturbing effects of the 300 - 400 keV gamma radiation. The PET- images were acquired and reconstructed in 3-D mode showing significant better quality for Tb-152 compared to those images of Tb-149.

Conclusions : Our preliminary results justify to propose further studies with Tb-152 to monitor the biokinetics of Tb-149 radiotherapeutics with PET.

[1] Beyer,G.J., Allen, B.J., Morel,Ch.et al.(1996) The α - and β^+ -emitting Tb-149 - a suitable isotope for radionuclide therapy , Nucl.Med. 35, A100

PS-696

S.J. Oh, Y.S. Choe, D.Y. Chi, S.E. Kim, Y. Choi, H.J. Ha, and B.-T. Kim

Samsung Medical Center, Department of Nuclear Medicine; Hankuk University of Foreign Studies, Department of Chemistry; Inha University, Department of Chemistry; Sung Kyun Kwan University College of Medicine.

RE-EVALUATION OF 3-BROMOPROPYL-1-TRIFLATE AS THE PRECURSOR FOR THE PREPARATION OF 3-BROMO-1-[F-18]FLUOROPROPANE

For the preparation of F-18 labeled radiopharmaceuticals, nucleophilic substitution reaction is a very useful method to introduce F-18 into a precursor. 3-Bromo-1-[F-18]fluoropropane has been used as a [F-18]fluoropropylating agent of amines and amides, however the reaction conditions have not been optimized. We therefore re-evaluated 3-bromopropyl-1-triflate as the precursor for the preparation of 3-bromo-1-[F-18]fluoropropane including optimization of F-18 incorporation reaction conditions and development of an easy method to quench the unreacted triflate precursor. This would further increase the effective specific activity of the N-alkylated products. In this study, N-[F-18]fluoropropylspiperone (FPSP) was evaluated as an example. We synthesized 3-bromo-1-[F-18]fluoropropane by nucleophilic substitution of 3-bromopropyl-1-triflate with tetrabutylammonium [F-18]fluoride in THF. The amounts of the triflate (1, 5, or 10 μl) and reaction temperature (0, 25, 80, or 120 °C) were varied independently to optimize the reaction conditions. In order to increase the effective specific activity of the following N-alkylated product, various amounts of water (0, 10, 30, or 50 μl) were added to the reaction mixture prior to N-alkylation.

The radiochemical yield of 3-bromo-1-[F-18]fluoropropane ranged from 10 to 90% depending on the reaction temperature and the amounts of the precursor; the highest yield was obtained at 120 °C using the excess amount of the triflate (10 μl). However, 1 μl of the triflate was found to be the most optimal concentration considering the effective specific activity of the N-alkylated products even though the radiochemical yield was lowered to 70%. Addition of a small volume of water converts the triflate into the corresponding alcohol which would be readily separated from the fluorinated product on HPLC. As a result, 30 μl of water reduced the area of the mass peak close to or coeluted with [F-18]FPSP by a factor of 10-15.

In conclusion, the F-18 incorporation reaction into 3-bromopropyl-1-triflate at 120 °C was rapid, convenient and efficient, and did not need further purification step for the following N-alkylation reaction. Moreover, addition of water after the F-18 labeling resulted in reduction of the mass peak and thus increase of the effective specific activity of [F-18]FPSP.

PS-697

E. De Vos¹, F. Dumont¹, P. Santens², G. Slegers¹, R.A. Dierckx³ and J. De Reuck²
¹Department of Radiopharmacy, ²PET-centre, ³Department of Nuclear Medicine, University of Gent, Belgium

PHARMACOKINETIC PROFILE IN HUMANS AND METABOLISATION STUDIES IN MICE AND HUMANS OF 11C-PK11195.

11C-PK11195 has been reported as a useful PET ligand for in vivo studies of peripheral benzodiazepine binding sites. Absolute quantification of receptors is difficult due to lack of knowledge on the amount of metabolites in plasma and target organs.

Tow healthy controls and three stroke patients (50-75 year) were injected i.v. with 370 MBq 11C-PK11195 (s.a. GBq/μmol). At different time points arterial blood samples were taken in order to obtain a time-activity curve for blood and plasma. To 750 μl plasma obtained at 5, 20 and 35 min p.i. 750 μl of acetonitrile was added. After centrifugation the supernatant was analysed by HPLC for the detection of metabolites.

Three mice were injected i.v. by tail vein with 0.3 mCi 11C-PK11195. The animals were killed at 10 min p.i. Blood was collected and treated likewise. The heart and brain were removed and homogenized. 1.0 ml of acetonitrile was added to each tissue homogenate. The mixture was mixed and centrifuged. The supernatant was analysed by HPLC.

In all cases the extraction yield was higher than 90% and no degradation of 11C-PK11195 took place. All patients showed rapid metabolisation of 11C-PK11195. At 5, 20 and 35 min p.i. 5%, 22% and 32% respectively of the plasma activity consisted of two different polar metabolites. In mice at 10 min p.i. 28% of the activity in the plasma were metabolites. However, no metabolites could be detected in brain and heart.

PS-698

E. De Vos, F. Dumont, G. Slegers, J. Versypt and R.A. Dierckx
 Department of Nuclear Medicine, University Of Gent, Belgium

SYNTHESIS, BIODISTRIBUTION AND DISPLACEMENT STUDIES IN MICE OF 11C-2'-I-PK11195 FOR VISUALIZATION OF PERIPHERAL BENZODIAZEPINE RECEPTORS

To compare the pharmacological profile and behaviour of the inflammatory tracer 123I-2'-I-PK11195 with 11C-PK11195, we introduced a 11C labelling in 2'-I-PK11195 (11C-2'-I-PK11195). The availability of a tracer labelled both for PET and SPECT might hold promise for future validation of multiple emission tomography with hybrid cameras.

11C-2'-I-PK11195 has been synthesized by nucleophilic substitution with 11C-methyl iodide in the presence of a basic catalyst. A Radiochemical yield of 45% and a specific activity of 400 mCi/μmol at EOS were obtained.

For the biodistribution studies NMRI mice were injected with 100 μCi. At different time points p.i. animals were killed by decapitation. For the displacement studies animals were pretreated with PK11195 10 min before tracer administration (1mg/kg body weight).

The distribution studies showed a high uptake analogue to 11C-PK11195 by the lungs, heart, liver, kidneys and intestines (organ to blood ratios of 8, 4, 8, 12 and 4 respectively at 20 min p.i.). During the early period a moderate accumulation in the brain was also observed (up to 10 min p.i.). The uptake in lungs, heart and brain could be displaced by pretreatment with PK11195 (organ to blood ratio decreased to 3 and 1.5 respectively).

Further in vivo experiments studies including the effect of various drugs and metabolism are in progress.

PS-699

P. Goethals, M. van Eijkeren, A. Volkaert, R. Dams.

UZ-RUG PET-Centre Gent, Gent, Flanders, Belgium.

INFLUENCE OF THE METABOLITES OF [METHYL-11C]THYMIDINE ON THE PET-QUANTIFICATION DATA.

PET measures total activity, regardless of the chemical species with which the positron emitter is associated. To interpret the quantification data correctly, a detailed knowledge of the metabolic fate is required.

[Methyl-11C]TdR is presumed to be a suitable candidate for non-invasive studies on cell proliferation using PET. Previous studies have demonstrated that besides fast uptake in tissue with high cell proliferation rate, an important fraction of [methyl-11C]TdR (20-25%) is metabolised. Dynamic PET-experiments (0-40 min) in normal rats to study the time-dependent uptake in liver, heart, brain e.g. showed that the highest concentration of activity is blocked in the liver. To identify the accumulated activity, a fast radiochemical separation method, based on HPLC, was developed. Twenty min post injection of [methyl-11C]TdR, the animals were sacrificed, urine and blood samples were collected and liver, heart, brain, kidney were prelevated, homogenised by sonification and the supernatant prepared for HPLC-separation. All radio-chromatograms demonstrated that the main fraction of the activity was associated with metabolites, except for the urine.

The in vivo behaviour of 11CO₂, an important metabolite, was studied in normal rats by dynamic PET studies, showing that 11CO₂ is diffusely distributed with an important accumulation in the brain. Since [methyl-11C]TdR does not cross the blood-brain-barrier under normal circumstances, the main fraction of the activity consisted of metabolites.

PS-700

I. Guenther¹, C.-G. Swahn², M. Bottlaender¹, C. Loc'h¹, C. Halldin², L. Farde² and B. Mazière¹

¹CEA, SHFJ, DSV/DRM, Orsay, France; ²Karolinska Institutet, Department of Clinical Neuroscience, Stockholm, Sweden

SPECIES DEPENDENT DIFFERENCES IN METABOLISM OF THE DOPAMINE D2 PET LIGAND FLB 457

The substituted benzamide FLB 457 is a highly specific D2-dopamine receptor ligand which has been labelled with the PET radioisotopes C-11 and Br-76 for extrastriatal D2 receptor imaging. For the development of biomathematical models necessary to quantify the D2 receptor density, studies in 3 different monkey species (Baboons: *Papio papio* and *Papio anubis* and *Cynomolgus*: *Macaca fascicularis*) have been performed.

Unchanged tracer in deproteinised plasma has been measured using gradient radio HPLC and radio TLC. A good correlation (r=0.99) in the measurement of unchanged FLB 457 was found between HPLC and TLC methods.

In the three animal species the radiochromatographic profiles were similar but as shown in figure 1 the time courses of percent unchanged FLB 457 were different. One hour after tracer injection the unchanged radiotracer

accounted for 74, 49 and 31 % of total plasma activity for *P. anubis*, *M. fascicularis* and *P. papio*, respectively. For comparison the amount of unchanged FLB 457 in human plasma was 29% 1 h p.i. These results showed that only in two studied species (*P. papio*, *M. fascicularis*), the time course of FLB 457 in plasma was similar to human.

In conclusion caution should be exercised when extrapolating data to human studies.

This work has been performed within the BIOMED 2 (BMH4-CT-96-0220)

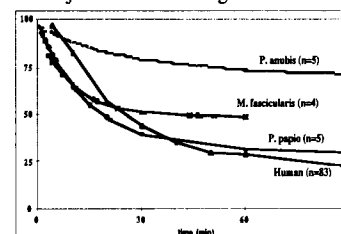


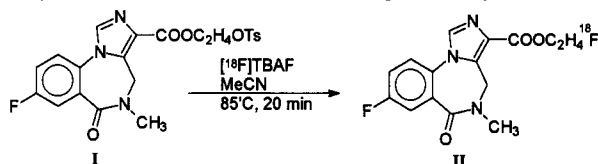
Fig. 1: Percentage of unchanged FLB 457 in plasma of different species

PS-701

S.H. Hong, J.M. Jeong, Y.S. Chang, D.S. Lee, J-K. Chung, M.C. Lee, C-S. Koh, J.H. Cho, S.J. Lee.
College of Medicine, Seoul National University, Korea Institute of Science and Technology, Hankuk University of Foreign Studies, Seoul, KOREA.

[F-18]3-(2-FLUORO) FLUMAZENIL FOR BENZODIAZEPINE RECEPTOR IMAGING AGENT.

Imaging benzodiazepine receptor is useful for diagnosis of various neurological diseases. [C-11]Flumazenil (Ro 15-1788) has been most widely used benzodiazepine receptor imaging agent for PET. We developed a new F-18 labeled flumazenil derivative, [F-18]fluoroflumazenil ((2-fluoroethyl) 8-fluoro-5-methyl-5,6-dihydro-6-oxo-4H-imidazo [1, 5-a] [1, 4]benzodiazepine-3-carboxylate).



Flumazenil was synthesized by modification of reported method. To synthesize a precursor for [F-18]fluoroflumazenil, we hydrolyzed flumazenil by tetrabutylammonium hydroxide. The precursor (I) was obtained by formation of ester between hydrolyzed flumazenil and ditosylethane (30-40%). The final product (II) was obtained by labeling I with F-18 with labeling efficiency higher than 80%. The reaction mixture was trapped by C18 cartridge, washed by 10% ethanol, and eluted by 40% ethanol. Decay corrected yield was 60 to 70% and total synthesis time was 40 min. Quality control by TLC (MeCN:water = 5:1) showed single peak (Rf = 0.6). Specific binding of [F-18]fluoroflumazenil to cerebral cortex of rat brain was found by *in vitro* autoradiography. According to biodistribution experiment in mice after tail vein injection at 10, 30, and 60 min, we found that 2.5 ± 0.4, 2.2 ± 0.3, and 2.1 ± 0.1 ID/g in the brain and 3.7 ± 0.4, 3.3 ± 0.1, and 3.3 ± 0.09% ID/g in the blood, respectively.

In conclusion, we succeeded in developing a new F-18 labeled flumazenil derivative with high labeling yield, simple labeling procedure, and benzodiazepine receptor binding activity.

PS-702

R.N.Krasikova¹, O.S.Fedorova¹, M.V.Korsakov¹, K.Nagren², B.Maziere³, C.Halldin⁴
¹Institute of the Human Brain, St. Petersburg, Russia; ²University of Turku, Finland; ³Service Hospitalier Frederic Joliot, Orsay, France; ⁴Karolinska Institutet, Stockholm, Sweden

THE ROBOTIC PREPARATION OF SOME COMMONLY USED 11C PET RADIOPHARMACEUTICALS AVOIDING HPLC PURIFICATION.

The large part of success in routine clinical application of PET can be attributed to the availability of simple, fast and reliable production methods for the commonly used radiotracers. Most of PET radiopharmaceuticals (RPs) preparations end up with semi-preparative HPLC purification which is associated with longer synthesis time, requires additional space and efforts of personal to handle HPLC system. A number of PET centres have been currently used a commercially available Anatech RB-86 robotic system equipped with a solid-phase extraction (SPE) work-station. Over the past years we have developed efficient production methods for several important 11C-labelled RPs: L-methyl-methionine, acetate and flumazenil, where recovery of the product from reaction mixture was performed by SPE technique instead of HPLC. With the use of robotics the conditions for SPE purification were optimized for each RPs to minimize the losses of the product during this step and provide high (more than 99%) radiochemical and good chemical purity of the final preparations. In the case of C11-flumazenil the main efforts were directed to remove the traces of nor-methylated precursor after hydrogen-bond-assisted methylation and achieve high specific activity which are of primary importance for application of receptor radioligands. As a result, using Neutral Alumina Sep-Pack and chloroform/methylene chloride as a solvent system, the content of precursor in the final preparation was reduced to similar levels as obtained by HPLC (0.2-0.6 micrograms in a volume of 4 ml). Specific activity of flumazenil was 600-1700 Ci/mmol (16-46 GBq/mmol), overall synthesis time 30 min, and radiochemical yield (EOB) 55%. This purification technique based on the use of commercially available cartridges is simple, fast and cost-efficient which is advantageous in production of routinely used PET RPs.

PS-703

B. Meller, M. Bæhre, E. Richter
Clinic of Radiotherapy and Nuclear Medicine, Medical University of Luebeck, Germany
SYNTHESIS OF [¹⁸F]FLUOROMISONIDAZOLE MEDIATED BY TETRABUTYLAMMONIUMHYDROGEN CARBONATE FOR CLINICAL PET.

Misonidazole is known as radiosensitizer for hypoxic cell in radiotherapy since several years. Recently, the correlation between hypoxia and therapy outcome in oncology became more important. In this context [¹⁸F]Fluoromisonidazole ([¹⁸F]FMISO) is a potential radiopharmaceutical for clinical PET and should therefore be available. Radiolabelling via Kryptofix and first in vivo applications are already reported.

Syntheses were carried out by a module for nucleophilic substitution (nuclear interface). After H₂¹⁸O recovery via a ion exchange column anion activation was carried out by tetrabutyl-ammoniumhydrogen carbonate. The radiofluorination of 10 mg of crystalline 1-(2'-Nitro-1'-imidazolyl)-2-O-tetrahydropyranyl-3-O-toluenesulfonylpropanediol (NITTP) was carried out in acetonitrile at 85 °C. The resulting solution was evaporated and the protecting group was splitted off by the addition of 2 ml 1 M HCl. The labelled product was purified by successive column technique using resin for ion retardation, C-18 and Al₂O₃ cartridges. Characterization and quality control were performed via radio-HPLC (CarboPac™/0.1 M NaOH and C-18 reverse phase/10 % CH₃CN/90 % H₂O) and GC. The solution became isotonic by the addition of NaCl and passed a sterilizing filter.

After optimization of the reaction and purification conditions we achieved a yield of 40-45 % (uncorrected) within 50 min. Radiochemical purity was 97-98 %. The product was identified by coapplications of characterized [¹⁸F]FMISO to different HPLCs and TLC. All quality controls (including microbiological) were passed without problems.

Conclusions: The tetrabutylammoniumhydrogen carbonate mediated synthesis of [¹⁸F]Fluoromisonidazole can be performed very easily without purification steps during reaction and hydrolysis. Therefore, [¹⁸F]FMISO can be produced without problems for clinical PET. Quality and yield are comparable to [¹⁸F]FDG synthesis using the similar technique.

PS-704

K. Nägren¹, C. Lundkvist², J. Sandell², C-G. Swahn² and C. Halldin².

¹Turku PET Centre, Radiopharmaceutical Chemistry Laboratory, Turku, Finland, ²Karolinska Institutet, Department of Clinical Neuroscience, Stockholm, Sweden.

[C-11]METHYL TRIFLATE AS THE LABELLED PRECURSOR IN THE SYNTHESIS OF THE DOPAMINE D2 PET RADIOLIGAND RACLOPRIDE

[C-11]Raclopride is the golden standard for PET examination of striatal dopamine D2 receptors. The product is obtained by [C-11]methyl iodide ([C-11]MI) alkylation of the phenolate of the O-desmethyl compound, generated in situ from its corresponding HBr salt (3.0 mg) using NaOH (6 µL, 5M, aq). Radiochemical yields and specific radioactivities are in most cases sufficiently high for PET-studies in human.

Occasionally this standard synthesis fails to give the desired product in normal yields, the quality of [C-11]MI in most cases being the major problem. The reaction mixture is also rather viscous and automation of the synthesis therefore cumbersome. The structural analogue [C-11]FLB 457, which is used for PET examination of extrastriatal D2 receptors, has successfully been prepared from [C-11]methyl triflate ([C-11]MT). We have thus investigated the use of [C-11]MT also in the synthesis of [C-11]-raclopride.

We have compared three methods: a) use of the commercially available precursor (HBr salt) b) precipitation of the bromide ion as silver bromide, and filtration before [C-11]-methylation, and c) use of the free base of norraclopride. The results obtained are summarized below:

Method	Precursor (mg)	Heating	NaOH	Rad.chem. yield (%)
HBr salt, [C-11]MT	1.0	A	6µL, 0.5M	<2
AgOAc, [C-11]MT	1.0	B	8µL, 1M	40-50
Free base, [C-11]MT	1.0	C	12µL, 0.5M	60

A: 3min, 80°C, DMSO, B: 1 min, 60°C, acetone, C: no heating, acetone. This work has been performed within the BIOMED 2 (BMH4-CT-96-0220)

Use of [C-11]MT and similar reaction conditions as for [C-11]MI using the HBr salt of the precursor results in almost quantitative formation of a volatile C-11-labelled byproduct, [C-11]methyl bromide. The removal of bromide ion from the precursor is thus essential for the successful use of [C-11]MT. As earlier shown for other radioligands, the precursor amount and reaction time can be considerably reduced by using [C-11]MT. The use of the free base of norraclopride, in analogy to the synthesis of [C-11]FLB 457, is the most convenient method which avoids the use of DMSO or pre-treatment of the precursor with silver bromide.

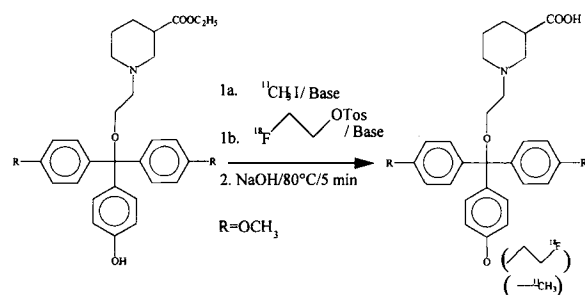
Poster presentations

PS-705

R. Schirmacher, W. Hamkens, M. Piel, J. Brockmann, F. Rösch
Department of Nuclear chemistry, University of Mainz, Mainz, Germany

SYNTHESIS OF ¹⁸F- AND ¹¹C-LABELED SUBSTITUTED TRIARYLNIPICOTIC ACID DERIVATIVES WITH HIGH AFFINITY FOR THE GABA TRANSPORTER GAT-3

GABA (γ -aminobutyric acid) is the major inhibitory neurotransmitter in the mammalian central nervous system. The level of GABA is determined by the rapid uptake of neurotransmitter via specific, high-affinity transporter located in the presynaptic terminal and/or surrounding glial cells. Up to now, there is no useful radioligand available to directly study GABAergic neurotransmission *in vivo* with PET. Recently, the triarylnipicotic acid derivative (S)-(-)-1-[2-tris(4-methoxyphenyl)-methoxy]ethyl-3-piperidincarboxylic acid was reported by Dhar to show high affinity for the GABA transporter subtype GAT-3. The aim of this work was to label the ligand with ¹¹C and ¹⁸F. The methoxy group of the trityl function was substituted to provide a precursor that comprises a phenolic hydroxy function in para position. Fluoroalkylation with [¹⁸F]fluoroethyltosylate by using bases like NaOH for the deprotonation of phenolic hydroxy function resulted in radiochemical yields of about 80%. Radiochemical yields of 40 to 60% could be detected by analogous labeling with [¹¹C]methyl iodide. Afterwards the ester function of the nipepicotic acid was cleaved quantitatively with 1.25 N NaOH within 5 minutes. The *in vitro* quantification of the binding affinity of the ¹⁸F-substituted GAT-3 ligand is in preparation.



Dhar, T.G.M., Borden, L.A., Tyagarajan, S. et al. (1994) *J Med Chem* 37: 2334-2342

PS-706

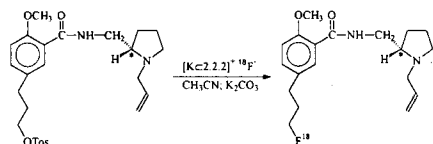
M. Piel, R. Schirmacher, W. Hamkens, J. Brockmann, F. Rösch
Institute of Nuclear chemistry, University of Mainz, D-55128 Mainz, Germany

IMPROVED PRECURSOR SYNTHESIS AND [¹⁸F]FLUORINATION OF [¹⁸F]DESMETHOXYFALLYPRIDE

The D₂-Antagonist [¹⁸F]Desmethoxyfallypride appears to be a promising candidate for the *in vivo*-quantification of the dopaminergic system by means of PET¹. However the precursor synthesis reported in the literature is complex and radio labeling yields are only 20-30%. In order to support the routine application of this tracer, both the chemical and radiochemical yields should be improved.

The precursor preparation started with a stereoconservative synthesis of (S)-N-Allyl-2-aminomethylpyrrolidine from L-proline². For this three-step process purification methods and reaction conditions were optimized. The subsequent reaction of (S)-N-Allyl-2-aminomethylpyrrolidine with 2-Methoxy-5-(3-hydroxypropyl)benzoic acid and the final tosylation of the hydroxypropyl-group leads to an fourfold overall yield compared to the literature.

Radiofluorination of this precursor under usual n.c.a. fluorination conditions resulted in radiochemical yields of 30%, comparable to literature¹. Attempts were made to improve the yield by systematic variation of the temperature, precursor concentration and others. However, only addition of potassium carbonate to the precursor succeeded in significant higher labeling yields of 70-90%. This effect correlates with a hypothesis that the use of protic solvents in the course of the precursor synthesis might protonate the tertiary nitrogen atom. Excess of carbonate is required in these cases, consequently.



Summary: In this study yields of the precursor synthesis as well as the [¹⁸F]fluorination of [¹⁸F]Desmethoxyfallypride were improved significantly. In particular molar ratios of 1:4 between precursor and potassium carbonate provided high labeling yields of 70-90%. This may facilitate the routine application of this D₂-Antagonist.

¹ J. Mukherjee, Z. Yang, T. Brown, M. Jiang, O. Kapp, C. Chen, M. Cooper, *Med. Chem. Res.*, 5, 174 (1994)
² T. Högberg, S. Rånby, P. Ström, *Acta chem. scand.*, 43, 660 (1989)

PS-707

S.W. Schwarz, T.J. McCarthy, G.G. Gaehele, N.T. King, W.H. Margenau, Jr., M.J. Welch
Division of Radiological Sciences, Mallinckrodt Institute of Radiology, Washington University Medical School.

PRODUCTION OF FLUORINE-18 USING THE GEMS HIGH PRESSURE TARGET ON A POSITIVE ION CYCLOTRON.

The General Electric Medical Systems (GEMS) PETTrace high pressure target, a silver target operated at pressures in excess of 400 psi, designed specifically for use on the GEMS PETTrace Cyclotron, produces an F-18 yield in excess of any other published yield. We have adapted the target for use on a positive ion cyclotron (TCC - CS15 Cyclotron). An automated control system for the target has been developed and built using AT-MIO-16DEX data acquisition board and a PC step OL3 motion controller board from National Instruments. The board operates the valves, pressure transducer, linear potentiometers and stepping motors that are part of the filling and loading system for the target. The boards are controlled using Labview version 4.0, a graphical programming language. This control system has allowed the automatic operation of the target system. The target which holds 1.5 mL O-18 water has been operated routinely for several months. Fluorine-18 has been produced at irradiation conditions up to an average beam current of 38 μ A and irradiation time up to 1.7 hrs. An average F-18 production of 62.4 \pm 5 mCi per μ A/hr has been obtained. This production rate is very close to the theoretical production yield and at 38 μ A beam current, a yield of 60 mCi per μ A/hr was achieved showing the linear production up to this high beam current. The fluoride from this target has been used in various F-18 syntheses carried out at our Institution and fluoride incorporations as high or higher than those obtained in our previously used titanium target were achieved. The F-18 has been used to produce F-18-2-fluoro-2-deoxyglucose (FDG) utilizing the GEMS FDG MicroLab system. In this system we have observed a decrease in synthesis yield with increasing activity. The dropoff is almost linear with yields of approximately 45% obtained when 500 mCi of starting activity were added dropping to approximately 20% when 2 Ci are added. In order to investigate the cause of this dropoff in yield, the radioactivity was allowed to decay for 2-3 hrs prior to addition. Yields equivalent to those obtained when the activity was not allowed to decay were obtained, suggesting that the reason for the decreased yield is not radiolysis but the presence of chemical impurities leached either from the target body or the target window. In this study we have shown that the GEMS high pressure target can be used on a positive ion cyclotron and theoretical yields of F-18 obtained up to a 40 μ A beam current. This allows the application of the high pressure technology to PET centers other than those possessing the PETTrace cyclotron.

PS-708

Jörg E. Spang, Gerrit Westera, Jörg T. Patt, Daniel Bertrand* and P. August Schubiger
Center for Radiopharmaceutical Science, Swiss Federal Institute of Technology Zürich, Paul Scherrer Institute Villigen and Clinic of Nuclear Medicine, University Hospital Zürich. *Department of Physiology, University of Geneva, Switzerland.

A NOVEL EPIBATIDINE ANALOGUE FOR PET STUDIES OF NICOTINIC ACETYLCHOLINE RECEPTOR SUBTYPES.

The neuronal nicotinic acetylcholine receptors (nAChRs) participate in a variety of physiological functions, such as learning, memory and cognitive performance. The nAChRs are ligand gated ion channels which are formed by five subunits which are essentially five membrane spanning helices. Presently a total of eleven neuronal subunits (α 2- α 9, β 2- β 4) are known. The nAChRs can be divided in two classes, those which bind α -bungarotoxin (α -Bgt) and those which are not α -Bgt sensitive. In this study the investigated receptor subtypes were the α 7 which belong to the first group and the α 4 β 2 and α 3 β 4 which are representatives of the second one.

We examined the influence of the intramolecular N-N-distance on the activation of the different nAChRs by using a new epibatidine analogue *exo*-2-(2-pyridyl)-7-azabicyclo[2.2.1]heptane (2PABH). As epibatidine is known to be a very potent and highly selective agonist for the α 4 β 2-nAChR subtypes we switched the pyridine nitrogen from the meta to the ortho position and eliminated the chlorine. The elimination of the halogen seems to have no impact on selectivity towards the α 4 β 2-subtype. Further *in vitro* studies with deschloroepibatidine are in progress.

The synthesis of 2PABH was performed by coupling the commercially available 2-bromopyridine with N-methoxycarbonyl-7-azabicyclo[2.2.1]-heptane via a Heck reaction followed by deprotection. The electrophysiological studies were carried out on neuronal NACHR subtypes (all cDNA vectors were cloned from rat) reconstituted in *Xenopus* oocytes using a two electrodes patch-clamp technique.

The experiments show that with decreasing N-N-distance and a changed spatial arrangement of the free electron pair of the pyridine nitrogen a loss of the high efficiency of epibatidine towards the α 4 β 2- and α 3 β 4-subtypes takes place.

The C-11 N-methylated and 18-F fluorinated derivatives will provide new tools to do PET studies on the various nAChR subtypes.

Radiopharmacy and radiochemistry: HALOGENS

PS-709

R. Boumon¹, K. Chavatte¹, D. Terriere¹, D. Tourwé², J. Mertens¹

VUB - Cyclotron¹, VUB - Organische Scheikunde², Brussels, Belgium

2-RADIOIODO-PHLORETINIC ACID: A NEW POTENTIAL TRACER FOR GLUCOSE TRANSPORTER COUPLED PATHOLOGIES

Earlier 3-radioiodo-phloretin was developed and evaluated in vitro and in vivo as a potential glucose transporter (GLUT)-tracer. Although this tracer was shown to bind to GLUT-proteins, its in vivo application was limited due to its rather high lipophilicity resulting in high binding to HSA and clearance through the liver and the intestinal tract, which is a major drawback for visualisation of tumours in those regions. Tracers with a charged group are supposed to mainly result in renal clearance. As at the pH of blood a carboxyl function is ionised, it was decided to develop phloretinic acid (4-(3-oxo-3-(2,4,6-trihydroxy-phenyl)propyl) benzoic acid) where the hydroxyl function in 4-position is replaced by a carboxyl function. 2-Bromo-phloretinic acid, the substrate for radioiodination, was obtained by a twelve-step synthesis, critical steps being formation of mono-bromo-amino intermediate by electrophilic substitution, formation of diazonium salt and the subsequent Pd/C catalysed reaction with CO for transformation to the acid function and coupling with 1,3,5-trihydroxybenzene. Radioiodination is performed using the CuI⁺ assisted non-isotopic nucleophilic exchange at 100°C. The actual labelling yield is about 60%. The lipophilicity of 2-iodo-phloretinic acid at pH 7.4, by means of reversed phase HPLC, is about 4 times lower than that of 3-iodo-phloretin. In in vitro conditions aspecific binding to cell tissue and HSA of the new tracer is about 10 times lower. In preliminary biodistribution experiments 2-radioiodo-phloretinic acid was intravenously injected in Hannover-Wistar rats. Clearance was observed mainly through the kidneys. Only a slight amount of the injected dose (I.D.) was cleared through the liver and the intestinal tract (less than 1 % I.D./g, 4 hours post injection). Further in vitro and in vivo experiments are currently in progress.

PS-710

F. Dumont¹, F. De Vos¹, J. Versypt², G. Slegers¹ and RA. Dierckx².

Department of ¹Radiopharmacy and ²Nuclear Medicine, University of Gent, Gent, Belgium.

SYNTHESIS, BIODISTRIBUTION AND DISPLACEMENT STUDIES IN MICE OF 123I-PK11195 FOR IN VIVO IMAGING OF THE PERIPHERAL BENZODIAZEPINE RECEPTORS

PK11195 is a peripheral benzodiazepine receptor antagonist that may be useful for the visualization of heart and brain inflammation. Thus, a 123I labelled analog might be useful for SPECT imaging. We used the solid-state isotopic exchange reaction for the synthesis of the 123I derivative and simplified the HPLC purification. The sterile and pyrogenfree solution was used for biodistribution as well as for displacement studies in mice. Approximately 2 µCi of the 123I tracer was injected into the tail vein of white mice (weight: 20-25 g). For the displacement studies, the mice were injected with cold PK11195 (1 mg/kg body-weight) 10 min before tracer injection. 20 and 40 sec, 1, 1.5, 2, 3, 5, 10, 20 and 40 min and 1, 2, 3, 6, 9, 15, 24 and 48 h after injection of the tracer, the mice were sacrificed. Three mice were studied per time-point. Blood samples were taken and intestines and other organs were excised, weighed and counted for radioactivity. The tissue uptake of radioactivity was measured as the % injected activity / g of tissue. Biodistribution studies showed penetration through the blood brain barrier and accumulation of the tracer in lungs, heart, kidneys and liver. Pretreatment with cold PK11195 resulted in a decrease of accumulation of radioactivity in heart and lungs, compared to controls.

PS-711

F. Dumont¹, F. De Vos¹, J. Versypt², G. Slegers¹ and RA. Dierckx².

Department of ¹Radiopharmacy and ²Nuclear Medicine, University of Gent, Gent, Belgium.

METABOLITES OF 123I-PK11195 IN BLOOD, HEART AND BRAIN OF MICE

PK11195 is a peripheral benzodiazepine receptor antagonist that may be useful for the visualization of heart and brain inflammation. From biodistribution and displacement studies it is known that 123I-PK11195 binds to myocardial benzodiazepine receptors and penetrates the blood brain barrier. We investigated metabolites in blood, heart and brain of mice to ensure the usefulness of the tracer in both target organs. Approximately 50 µCi 123I-PK11195 was injected into the tail vein of white mice (weight: 20-25 g). The animals were sacrificed 10 min after injection. Blood samples were centrifuged and 250 µL plasma was added to 750 µL acetonitrile. The supernatant, obtained after a second centrifugation, was injected into a HPLC system. Heart and brain were excised, 1000 µL acetonitrile was added and after mixing and centrifugation, the supernatant was also injected into the HPLC system. The HPLC eluent was collected in fractions and these were counted for radioactivity. For the determination of the recovery of the extracting method, blood, heart and brain of non-injected mice were spiked with ± 0.1 µCi 123I-PK11195 and treated the same way. For all samples, the extraction yield is > 90 %. In heart and brain of both groups, and in blood of the non-injected group none or few (< 10 %) metabolites were found. On the other hand, in the blood of the injected mice only 40 % original 123I-PK11195 was left. These studies show that although metabolites were present after 10 min in the blood of mice, there was no accumulation of metabolites in the two target organs. This implicates the usefulness for visualization of heart and brain inflammation.

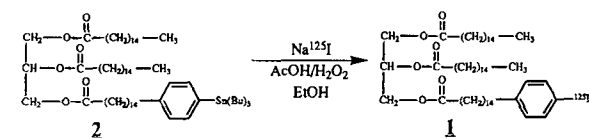
PS-712

D. W. McPherson¹, H. Luo¹, J. Kropp² and F. F. (Russ) Knapp, Jr¹.

¹Nuclear Medicine Group, Oak Ridge National Laboratory, Oak Ridge, TN
²Department of Nuclear Medicine, University of Dresden, Germany

IMPROVED RADIOIODINATION OF 1,2-DIPALMITOYL-3-IPPA VIA A TRIBUTYL TIN INTERMEDIATE.

1,2-Palmitoyl-3-(15-(4-iodophenyl)pentadecan-3-oyl)-rac-glycerol (1, "MIPAG"), is a ligand for the clinical evaluation of pancreatic lipase activity and has demonstrated promise in preliminary studies patients with pancreatic insufficiency. I-131-MIPAG was initially prepared via a thallium-iodide displacement. Because of the need for a simple method which is amendable for the routine clinical use of this agent, we have synthesized a tributyltin intermediate (2) which allows facile radioiodination. Methyl p-bromopentadecanate (3) was prepared from p-bromoacetophenone. The reaction of 3 with tributyltin in the presence of palladium afforded methyl p-(tributyltin)pentadecanate (4). Saponification of 4 followed by the subsequent esterification with 1,2-dipalmitoyl-rac-glycerol afforded the tributyltin compound (2). Electrophilic (NaI + CH₃CO₂H/H₂O₂) radioiodination of 2 afforded iodine-125-1 with a radiochemical yield of 65.9 % (±11.5) and a radiochemical purity of 94.3 % (±3.0) after sep-pak® purification in a time of less than 1 hour (n=6). The reaction time, labeling temperature, concentration of peracetic acid and mass of 2 were optimized. Iodine-125-labeled-1 co-chromatographed by TLC and HPLC analysis with the cold standard. This improved method now provides MIPAG for routine clinical evaluation.



ORNL is managed by Lockheed Martin Energy Research Corporation for the U.S. Department of Energy under contract DE-AC05-96OR22464.

Poster presentations

PS-713

J.Sartor, S.Guhlke, M.Tentler, E.Klemm, H.J.Biersack

Department of Nuclear Medicine, University of Bonn, Germany

A New High Yield KIT SYNTHESIS for IODINE-123 α -METHYL-L-TYROSINE (IMT)

IMT is an important SPECT tracer to visualize amino acid transport for example in the diagnosis of brain tumors.

The iodogen method seems to be the best to synthesize IMT due to the simplicity to separate the product from the oxidation reagent.

In older iodogen based procedures methyl tyrosine is reacted with radio iodide followed by purification via SepPak C-18. A disadvantage of the purification step was that up to 30% of the product (IMT) was sometimes lost by sticking effects to the SepPak C-18 column. The goal of this study was to avoid this loss of radioactivity and thus to obtain much higher yields (> 90%), thereby allowing injections without further purifications.

Our new method is based on a modified iodogen method at acidic conditions. In contrast to reaction at weak basic conditions the formation of a lipophilic side product can be decreased markedly (< 6%) and > 92% of radio iodide reacts to the desired product as shown by radio-HPLC. In the very rare case that iodide does not react quantitatively and purification from unreacted iodide is necessary, we have developed a new elution method using again SepPak C-18 columns but the elution of the purified product is carried out with 30% propanediol. Using this eluent 90-98% of the IMT is eluted through a sterile filter from the column and can be injected without further dilution.

In summary using our new method IMT is obtained with 92-97% RCY. In the rare case where purification via SepPak C-18 is necessary, elution with 30% propanediol leads to a product of >94% radiochemical purity.

We have used the kit method now for several patient syntheses with high quality SPECT images. We feel that this new kit procedure will be the method of choice for the preparation of this tracer.

Radiopharmacy and radiochemistry: Technetium

PS-714

M.L.Gomes^{1,2}, D.M.M. Mattos^{1,2}, R.S. Freitas¹, R.C.S. Conceição^{1,2} and M. Bernardo-Filho^{1,2}.

1- Instituto Nacional de Câncer, Serviço de Pesquisa Básica, 2- Universidade do Estado do Rio de Janeiro, Instituto de Biologia, Rio de Janeiro, RJ, Brasil, 20551-030. E.mail: bernardo@uerj.br

EFFECT OF MITOMYCIN-C AND VINCRISTINE ON THE BIODISTRIBUTION OF ^{99m}Tc-DTPA IN Balb/c MICE.

The biodistribution of radiotracers used in diagnostic imaging is grossly and recognizably altered by a wide variety of drugs and other treatment modalities, such as surgery and radiotherapy. Knowledge of such altered biodistribution is important both in making diagnostic inferences from scans and in dosimetric considerations. Mitomycin-C and vincristine are drugs those have been used as components of many chemotherapeutic regimens. Mitomycin-C becomes a bifunctional or trifunctional alkylating agent, after intracellular enzymatic or spontaneous chemical reduction of the quinone and loss of the methoxy group. This drug inhibits deoxyribonucleic acid (DNA) synthesis and cross-links DNA. In addition, single-strand breakage of DNA and chromosomal breaks are caused by mitomycin-C. Mitomycin-C is also a potent radiosensitizer and is teratogenic and carcinogenic in rodents. The biological activities of vincristine can be explained by its ability to bind specifically to tubulin and to block the ability of the protein to polymerize into microtubules. Through disruption of the microtubules of the mitotic apparatus, cell division is arrested in metaphase. In the absence of an intact mitotic spindle, the chromosomes may disperse throughout the cytoplasm or may clump in unusual groupings. The inability to segregate chromosomes correctly during mitosis presumably leads to cell death. We have studied the effect of vincristine and mitomycin-C on the biodistribution of the ^{99m}Tc-DTPA. Vincristine or mitomycin were administered by ocular plexus via into female isogenic Balb/c mice. One hour after the last dose, ^{99m}Tc-DTPA (7.4 MBq) was administered and after 0.5 hour the animals were sacrificed. The organs were isolated, the radioactivity determined in a well counter and the percentages of radioactivity (% rad) in the organs were calculated. Concerning to vincristine, the results have shown that the % rad has not been altered in pancreas, thyroid and brain and has been increased in thymus, ovary, uterus, spleen, kidney, heart, stomach, lung, liver and bone. Concerning to the mitomycin-C, the results have shown that the % rad has been decreased in pancreas, stomach, kidney, spleen, heart, lung and liver and has not been altered in ovary, uterus, thymus, thyroid, bone and brain. The effects of these chemotherapeutic drugs on the biodistribution of this radiopharmaceutical were statistically significant (Wilcoxon test, p<0.05) and they could be explained by the metabolization and/or therapeutic action of these drugs.

PS-715

G. Núñez¹, A. Morales¹, I. Caballero¹, N. Pérez¹, J. Ducongé², N. Iznaga-Escobar¹, A. de la Paz¹.

Center of Molecular Immunology, Research Department, Havana, Cuba.

BIOEQUIVALENCE STUDY OF A FREEZE-DRIED KIT ^{99m}Tc-LABELLED mAb ceal FOR IMMUNOSCINTIGRAPHIC STUDIES.

The aim of the present work is the performance of a bioequivalence study between the liquid formulation and the lyophilized kit (one step). The analytical methods comprised HPLC on Superose 12, electrophoresis (PAGE), Instant Thin Layer Chromatography (ITLC-SG), biological assessment of the radiolabeled molecule and pharmacokinetics and biodistribution studies. Two formulations were analyzed on Superose 12 HR and only one major peak was seen with a purity greater than 99 % without noticeable fragmentation of the molecule. These results were confirmed using native PAGE. Labeling efficiency was 98.8 % as a mean value for liquid formulation and 93.8 % for kit, both greater than 90 %. Radiocolloids were less than 5 % in both cases. The biological activity by immunohistochemical techniques using colonic tissue was similar for both preparations and the Lindmo assay showed an immunoreactivity fraction higher than 80 %. Also the inhibition curves for ELISA were very similar to the curve obtained using a native (non-reduced) antibody. The results of biodistribution indicated absence of any accumulation in the organs tested and the pharmacokinetic parameters were non-significant different for freeze-dried kit and mAb in solution. Considering the data collected in this study, we can conclude that the bioequivalence between the preparations was effectively proved and the method is extremely simple and efficient.

PS-716

A. Morales¹, I. Caballero¹, N. Pérez¹, G. Núñez¹, N. Iznaga-Escobar¹, J. Ducongé², J.C. Izquierdo¹, A. de la Paz¹ and F. Zayas³.

Center of Molecular Immunology, Research Department, Havana, Cuba.

A FREEZE-DRIED KIT FORMULATION FOR ^{99m}Tc-LABELLED mAb ior egf/r3. BIOEQUIVALENCE STUDY.

Monoclonal antibodies (mAb) have been useful for immunoscintigraphic applications in clinical diagnosis since they were introduced in the Nuclear Medicine practice. The purposes of these studies was to investigate if both formulations of freeze-dried kit formulation for mAb ior egf/r3 in solution and lyophilized are bioequivalents. No fragmentation was found during reduction step for both formulations. Both formulations were analyzed on Superose 12 HR 10/30 and only one peak was observed with a purity greater than 99.0 %. These results were confirmed using native PAGE. Labeling efficiency was 98.5 % using paper chromatography and saline 0.9 % and MEK as eluant and gel filtration chromatography on Superose 12 HR 10/30 on FPLC. Human Serum Albumin (HSA) impregnated ITLC-SG showed less than 1.5 % of radiocolloids. In radioreceptor assay, reduced antibody, reduced and lyophilized antibody and non-reduced control antibody, were able to compete in similar way with ¹²⁵I-labeled EGF for binding to the EGF-R, showing that the reduction using 2-ME and the lyophilization process do not affect the biological integrity and the immunoreactivity of the mAb ior egf/r3. Competition with DTPA and stability in HSA and human serum demonstrated no evidence of transcomplexation of ^{99m}Tc to DTPA, HSA or low molecular weight species in serum. Results of biodistribution in Balb/c mice and rats also demonstrated the equivalence of both formulations.

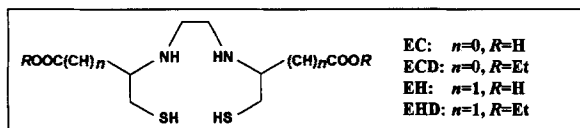
PS-717

K.O. Mang'era, C. Boonen, A.M. Verbruggen

Laboratory of Radiopharmaceutical Chemistry, F.F.W. K.U. Leuven, 3000 Leuven, Belgium

EFFECT OF SUBSTITUTION OF β-HOMOCYSTEINE FOR CYSTEINE ON CHARACTERISTICS OF 99mTc-L,L-EC AND 99mTc-L,L-ECD

99mTc-L,L-ethylene bis-cysteine diethylester (ECD) is in clinical use for brain perfusion studies. Its diacid derivative, 99mTc-EC, exhibits somewhat superior characteristics to those of 99mTc-MAG3 as a tracer for renal function studies. In pursuit of N2S2 bifunctional complexing agents with extended and therefore less sterically influenced side chains, we synthesised L,L-ethylene bis-β-homocysteine (EH). We then labelled EH and its diethylester derivative EHD with 99mTc and studied their electrophoretic characteristics and biological behaviour in mice. We compared them to 99mTc-EC and 99mTc-ECD.



As for Tc-ECD, Tc-EHD is neutral on electrophoresis at pH 6.0. However, Tc-EHD does not show significant brain uptake in mice (max. uptake = 0.1 % I.D. versus 1.2 % for Tc-ECD). Urinary excretion of Tc-EHD is much higher (42 % of I.D. after 30 min compared to 9 % for Tc-ECD). Blood clearance of the two complexes is similar.

During electrophoresis at pH 3.2 and 9.0, Tc-EH migrates to the same extent as Tc-EC, but migrates 25 % further at pH 6 and 12. Despite the apparently higher ionisation at approx. neutral pH, murine urine levels for Tc-EH are lower than those for Tc-EC (65 % and 85 % of I.D. for Tc-EH, and 74 % and 95 % for Tc-EC at 10 min and 30 min p.i., respectively). Tc-EH also shows slower blood disappearance and higher liver levels (7.3 % and 4.9 % at 10 min and 30 min p.i., versus 1.9 % and 1.0 % for Tc-EC, respectively).

The results show that although an extended side chain would be an advantage for bifunctional complexation, the biological behaviour of Tc-EH and Tc-EHD is substantially different, and in the case of Tc-EHD, the all-important uptake into and/or retention in brain is compromised.

PS-718

M. Neves, J. J. Pedroso de Lima, W. K. A. Louw and I. C. Dornhele

Instituto Tecnológico e Nuclear, Sacavém and IBILI, Serviço de Biofísica, Coimbra, Portugal; Atomic Energy Corp., Pelindaba and University of Pretoria, South Africa

BIOKINETICS OF 99mTc-BIG AS A RENAL SCANNING AGENT: COMPARISON TO 99mTc-DMSA

99mTc-DMSA is widely recognized as the best radiopharmaceutical for kidney imaging, in spite of some limitations, such as the long time to reach optimal renal uptake and the subsequent build-up of radiation dose. Biodistribution studies with the 99mTc complex of the biguanide H₂NC(=NH)NHC(=NH)NH₂ ligand, 99mTc-Big in mice and rats have shown significant values of kidney/liver %ID ratio at various time intervals p. i. as well as fast blood clearance and urinary excretion. Dynamic gamma-camera studies of 99mTc-Big and 99mTc-DMSA in rats and rabbits have shown an earlier visualization of the kidneys for 99mTc-Big than for 99mTc-DMSA. These investigations were continued in baboons (Papio ursinus) (n=5), under pentobarbitone anaesthesia. After an i. v. bolus injection of 99mTc-Big or 99mTc-DMSA (≈407MBq) dynamic acquisition for 1 hour (1fr/min) and static acquisition at 1 hour intervals for 4 hours were performed. At regular time intervals in the first hour and then every hour blood and urine samples were taken. The time-activity curves have shown that in the case of 99mTc-Big each kidney reached a maximum uptake of ≈20% ID within 5-10 min. p. i., which became 12% at 4 hours with T_{1/2} >4 hours. In the case of 99mTc-DMSA the kidney uptake is slow, with the maximum uptake of ≈35% achieved at 4 hours p. i. The time activity-curves for cardiac-blood pool, liver, spleen, lung and background have identical profiles, but in the case of Tc-Big, the T_{1/2} values are shorter when compared to 99mTc-DMSA for the same organs. The best comparison can be drawn from the ratio kidney/liver (%ID). At 30 min., 1, 2, 3 and 4 hours p.i., these ratios are, in the case of 99mTc-Big 1.98, 2.54, 3.71, 4.39 and 5.51, while in the case of 99mTc-DMSA at the same times, these ratios are 1.04, 1.96, 3.31, 4.04 and 4.93 respectively. At 1 hour p. i. of 99mTc-Big, 43.7% of the ID was excreted by the kidneys and 70% at 4 hours, while for 99mTc-DMSA at 1 hour p. i. the urinary excretion is less than 1% and at the 4th hour only 7.5%. As a consequence of the shorter residence times of 99mTc-Big in heart, kidneys, liver, lungs and spleen, the ratios "radiation dose due to 99mTc-DMSA/radiation dose due to 99mTc-Big" of some critical organs are: liver=1.83, kidneys=1.46, gallbladder=1.71, ovaries=1.40 and testes=1.61. In conclusion, 99mTc-Big offers the advantage of early acquisition of images and lower radiation doses.

PS-719

B. A. Nock, T. Maina, C. Tsoukalas, I. C. Pirmettis, M. S. Papadopoulos, D. Maindas* and E. Chiotellis

Institute of Radioisotopes - Radiodiagnostic Products, NCSR "Democritos", 15233 Ag. Paraskevi; *Institute of Isotopic Studies, 15125 Maroussi, Greece

PRELIMINARY IN VITRO STUDY ON BRAIN METABOLISM OF AN ESTER MODIFIED 99mTc(SNS/S) COMPLEX

The two major radiopharmaceuticals used today for SPECT imaging of the brain, 99mTcHM-PAO and 99mTcECD, are retained in brain tissue through different mechanisms. While 99mTcHM-PAO suffers nucleophilic attack by intracerebral glutathione (GSH), 99mTcECD is metabolized by brain esterases. Satisfactory brain retention is exhibited also by several 99mTc(SNS/S) mixed ligand complexes, as revealed during our recent studies. This retention is assigned to complex susceptibility against GSH attack on the complex metal center and formation of the hydrophilic 99mTc(SNS/GS) metabolite.

We report herein on the 99mTcO{[C₂H₅N(CH₂CH₂S)₂][p-C₆H₄OCO-C₆H₄S]} complex, 1, carrying a pendant ethyl ester group on the phenyl thiolate coligand. The introduction of this functional group allows complex 1 to follow, like 99mTcECD, the alternative metabolic pathway of brain esterases. As a result, the two mechanisms are expected to compete, or cooperate, *in vivo* to trap complex 1 in brain cells. Thus, complex 1 is incubated either with 1 mM GSH or 10 U esterase in phosphate buffered solution at 37°C, using 99mTcECD as a reference. Samples of 1, 10 and 45 min incubates are analyzed by RP-HPLC. This comparative *in vitro* study has shown, that complex 1 suffers both nucleophilic attack by GSH and enzymatic hydrolysis of its pendant ester group. However, the latter mechanism is much more rapid. In fact, the hydrolysis rate is found to be faster for complex 1, as for 99mTcECD. Further experiments in primates will demonstrate, if esterase induced hydrolysis is the prevailing mechanism of complex 1 metabolism also *in vivo*.

PS-720

B. A. Nock, T. Maina, D. Yannoukakos, I. C. Pirmettis, M. S. Papadopoulos and E. Chiotellis

Institute of Radioisotopes - Radiodiagnostic Products, NCSR "Democritos", 15233 Ag. Paraskevi, Athens, Greece

PROLONGED BRAIN RETENTION OF A 99mTc SNS/S MIXED LIGAND COMPLEX INDUCED BY GLUTATHIONE

As a part of our ongoing work on the design and evaluation of novel 99mTc brain perfusion agents based on the "3 + 1" mixed ligand system, the stability of several 99mTc(SNS/S) complexes under various conditions has been tested. Thus, the 99mTcO{[(C₂H₅)₂NCH₂-CH₂N(CH₂CH₂S)₂][p-O₂N-C₆H₄S]} complex, 1, turned out to be unstable in the presence of excess thiol or in alkaline aqueous medium. Given that intracerebral nonprotein thiol consists primarily of glutathione (GSH, ≈ 2 mM), we report herein on the effect of GSH nucleophilic attack on complex 1 - tested both *in vitro* and *in vivo* - on mouse brain retention.

Complex 1 is incubated with 1 mM GSH in phosphate buffered solution at 37°C. Aliquots thereof at 1, 10 and 45 min time intervals are analyzed by RP-HPLC. Similarly, incubates of complex 1 in mouse brain homogenates are analyzed by HPLC at the same time intervals. Eventually, tissue distribution of complex 1 is studied in mice, in order to test if *in vivo* behaviour and especially brain retention can be explained by data derived from *in vitro* experiments.

According to the results of *in vitro* tests, complex 1 suffers rapid nucleophilic attack on the complex metal center by the thiolate group of GSH. As a result, the monothiol coligand is substituted by GS⁻ with concomitant formation of the hydrophilic 99mTcO{[(C₂H₅)₂NCH₂-CH₂N(CH₂CH₂S)₂][GS]} complex, 2. The latter is isolated from mouse brain homogenates after incubation or injection of complex 1 in mice. Tissue distribution data in mice has revealed prolonged brain retention of 1. In conclusion, the retention of complex 1 in mouse brain can be attributed to its metabolism to the hydrophilic daughter complex 2, induced by intracerebral GSH.

Poster presentations

PS-721

S.A. Rao, V.S. ZaisteV, C.J. Cabahug, Z.H. Oster

SUNY at Stony Brook
Departments of Radiology and Chemistry

SIMPLE AND EASY PREPARATION METHOD OF ^{99m}Tc -SULFUR COLLOID FOR LYMPHOSCINTIGRAPHY

^{99m}Tc -antimony trisulfide colloid (^{99m}Tc -ATC) or ^{99m}Tc -micro colloids are not available commercially. Other alternatives are needed such as smaller particles < 30 nm., separated from ^{99m}Tc -sulfur colloid (^{99m}Tc -SC) preparations.

We are proposing a simple and accessible method suitable for all nuclear medicine facilities. We start with commercially available sulfur colloid kits (Mallinckrodt, Inc., or CIS-US, Inc.), by addition of 70-100 mCi of sodium pertechnetate in 1-2 ml. as per manufacturer's instructions. We differ from the procedure by heating the vial in rolling, boiling water bath for a shorter time of 2-3 min., rather than 5 min. The vial is allowed to cool, buffer is added, and the solution is filtered into 10 ml. syringe, using commercially available millipore filter 0.2 μm . The labelling efficiency was determined by ITC (SG) paper and 85% methanol. The labelling efficiencies of ^{99m}Tc -SC and filtered ^{99m}Tc -SC were $98.78 \pm 0.76\%$ ($n=12$), $93.62 \pm 4.69\%$ ($n=6$), respectively. The recovery of the filtrate was $20.42 \pm 6.28\%$ ($n=6$) from ^{99m}Tc -SC preparations. The concentration of 3-4 mCi/ml is adequate for this clinical application.

The colloid particle size was assayed using Laser Light Scattering Technology (set up argon laser ($\lambda=415.5$), LEXEL, Palo Alto, California). It appears from the distribution graph that the filtered sulfur colloid contained mostly particles of size < 21 nm. similar to the original ^{99m}Tc -ATC and is therefore in size suitable for lymphoscintigraphy studies. Human studies are planned after necessary approvals.

PS-722

P. Jackson, R. J. Baker[†], D. W. J. Mackey, H. Van der Wall, K. Allman

Concord Hospital, Sydney, Australia: Department of Nuclear Medicine.

[†]Prince of Wales Hospital, Sydney, Australia: Department of Nuclear Medicine.

TOWARDS CHARACTERISATION OF THE INTERMEDIATE COMPLEXES GENERATED DURING ^{99m}Tc -SESTAMIBI PREPARATION: MASS SPECTROMETRY AND DENSITY FUNCTIONAL THEORY RESULTS

$^{99m}\text{Tc}(\text{MIBI})_3^+$ (MIBI = 2-methoxyisobutylisonitrile, Cardiolite) is a widely used myocardial perfusion agent. Its preparation requires a heated reduction step for efficient radiolabelling, that is, greater than 90 % of the radiolabelled complex. The principle chemical impurities are dependent on the duration of the heating, the specific activity of $^{99m}\text{TcO}_4^-$ added and the age of the generator from which the $^{99m}\text{TcO}_4^-$ was eluted. Poor radiolabelling leads to a high percentage of $^{99m}\text{TcO}_4^-$, $^{99m}\text{TcO}_2 \cdot n\text{H}_2\text{O}$ together with some unidentified intermediate complexes [Hirsch JJ, Watson MA, *J Nucl Med Technol* 1996; 24:114-118].

Current economic considerations have precipitated studies of the feasibility of cold kit fractionation [Baker RJ, *J Nucl Med* 1996; 37 (suppl.):84p]. Such kits require augmentation with additional Sn(II) to support higher activities of added $^{99m}\text{TcO}_4^-$. To investigate the role of additional Sn(II) in the labelling process, electrospray ionisation mass spectrometry (ESI-MS) analysis of fractionated and unfractionated cold kits was undertaken. These studies identified ligand decomposition products of $\text{Cu}(\text{MIBI})_3^+$ (the starting material) present in both fractionated and unfractionated cold kits.

In order to understand the ligand decomposition process, *ab initio* density functional theory (DFT) calculations have been undertaken to determine the homolytic bond strengths (MNC-R[•]), where R = H, CH₃, CH(CH₃), C(CH₃), and C(CH₃)₂(OCH₃) and M = Cu, Tc. To ensure the results were reliable, the geometries for each model ion were first optimised within the (electron) spin-polarised local density approximation (LSDA) using a modest sized basis set of double-zeta quality. Single point binding energy calculations were then performed at the optimised LSDA geometry using a hybrid-DFT method (B3LYP) incorporating a Hay-Wadt relativistic effective core potential and more flexible basis sets for the metals that included higher angular momentum (f) functions. It is widely accepted that this method yields very accurate results for transition metal - ligand binding energies. The same level of theory has also been used to evaluate the heights of the transition barriers for: $\text{MCN}^{\cdot-} \rightarrow \text{MNC}^{\cdot}$, M = Cu, Tc. The intermediate complex formed during conversion to the nitrile complex may be implicated in the MIBI ligand decomposition process.

PS-723

S.-P. Wey, H.-Y. Tsai, J.-S. Jong, C.-H. Lin, L.-H. Shen, Z.-T. Tsai, G. Ting

Institute of Nuclear Energy Research, Atomic Energy Council, Taiwan, R.O.C.

FORMULATION OF AN LYOPHILIZED KIT FOR PREPARATION OF ^{99m}Tc -TRODAT-1

A novel tropane derivative, ^{99m}Tc -TRODAT-1, was reported showing high specific binding to dopamine transporters (DAT) in animal models, and was the first example of ^{99m}Tc -labelled tracer to image the CNS DAT in humans. Literature reported preparation of ^{99m}Tc -TRODAT-1 included multiple steps to individually prepare vials for TRODAT-1 free ligand, Sn(II)/glucoheptonate and EDTA sodium salt before labelling. Then the preparation was achieved by reacting ^{99m}Tc -pertechnetate with a fresh mixture of the ligand, the reducing agent and the chelating agent described above.

In order to simplify the multi-step procedure as mentioned above for routine clinical use, a stable kit formulation was developed for preparation of ^{99m}Tc -TRODAT-1. Our kit formulation contained TRODAT-1 ligand, 320 μg of sodium glucoheptonate, 930 μg of Na₂EDTA·2H₂O, 32 μg of SnCl₂·2H₂O, 20mg of mannitol, 4.1 mg of anhydrous Na₂HPO₄ and 460 μg of NaH₂PO₄·2H₂O. Here we used TRODAT-1·3HCl in place of labile TRODAT-1 free ligand. Systemic evaluation revealed that the optimal level of TRODAT-1·3HCl was 126 μg (equivalent to 100 μg of free ligand). Following reconstitution with approximately 1.11 GBq of ^{99m}Tc -pertechnetate in 5 mL saline, and autoclaving for 30 min to complete labelling, ^{99m}Tc -TRODAT-1 can be obtained in a neutral solution (pH = 7.0-7.5) with greater than 90% radiochemical purity over 6 hours, as determined by HPLC. The shelf life of the lyophilized kit lasts over two months when it was stored at room temperature. Further evaluation of the radiotracer prepared from our kit formulation was conducted on animal models. We conclude that a stable lyophilized kit formulation to prepare ^{99m}Tc -TRODAT-1 is feasible for clinical use of DAT imaging.

Radiopharmacy and radiochemistry: Proteins

PS-724

H. Sinzinger, Arsineh Arakil Aghajanian, L. Partyka, Aldona Dembinska-Kiec

Department of Nuclear Medicine, University of Vienna, Austria and
Department of Clinical Chemistry, University of Cracow, Poland

MODIFICATION OF FIBRINOGEN ALTERS FUNCTIONAL PROPERTIES AND INFLUENCES RADIOISOTOPIC IMAGING AND KINETIC RESULTS

Radiolabeled fibrinogen is used for determining kinetics, turnover and routine imaging of arterial/venous thrombosis with varying success. Free oxygen radicals are leading to oxidant stress inducing modification of proteins. Covalent oxidative modification could modify fibrinogen, thus showing a different functional and kinetic behaviour and altered imaging results. The relevance of this problem for radioisotopic studies has not been assessed yet. Fibrinogen was oxidized by Fenton reaction (iron/ascorbate; 5 min - 48 h) resulting in prothrombotic and promitogenic behaviour. Fibrinogen was purified before and after reaction with size exclusion and gel chromatography, the structure controlled with SDS-PAGE electrophoresis. Furthermore, glycosylation, malonylation, glycosylation and acetylation were induced and the biological characteristics (coagulation behaviour, platelet aggregation, smooth muscle cell proliferation, nitric oxide- and prostaglandin-production, among others) assessed. Commercially available (radiolabeled) fibrinogen from 4 different sources revealed extensive modification. Even autologous fibrinogen modified as a consequence of risk factors, diseases or drugs may not reflect typical behaviour. After radiolabeling, modified fibrinogen shows kinetics differing from the native one. Vascular entry is influenced as well. Activation induced by various types of modifications is partly (by various drugs) or almost completely (by acetylation) abolished. As a consequence, homologous radiolabeled fibrinogen is an unreliable test. Autologous protein has to be isolated, strictly avoiding modification for diagnostic use. Concomitant drug use may severely influence quality of results obtained.

These data indicate that modification of fibrinogen alters its functional properties significantly. Furthermore, a great number of drugs is either promoting or inhibiting the respective modification. The relevance for radioisotopic imaging is significant, may explain unsatisfactory results and needs further to be elaborated in detail.

PS-725

T.S.T. Wang, R.A. Fawwaz, C. DeRosa, R.L. Van Heertum

Columbia University, Dept. of Nuclear Medicine

MECHANISM OF LOCALIZATION OF STREPTAVIDIN IN BREAST TUMOR XENOGRAFTS IN MICE

Background: We have previously demonstrated that IV administered radiolabeled Streptavidin (SA) shows high concentration in breast tumor xenografts and postulated the mechanism to be due to high Biotin (B) content in tumors. This study was designed to test this hypothesis.

Methods: In one experiment In-111-SA was administered IV to nude mice (n=6) bearing the human MCF-7 breast tumor. In another experiment In-111-SA was saturated with B and the In-111-SA-B complex then injected IV into the tumor bearing mice (n=6). Tissues were obtained 2 hours, 6 hours, and 3 days later.

Results: The concentration of radioactivity in tumor following In-111-SA-B administration was half that observed with In-111-SA, while there was no significant difference in blood clearance or in concentration in normal tissues.

Conclusion: This study suggests that SA localization in breast tumor is related to B tumor content, a finding which may have important implications in the diagnosis and therapy of tumors.

Radiopharmacy and radiochemistry: Ria/Others

PS-726

F. Locchi, M. Tommasi, M.L. Brandi, F. Tonelli, U. Meldolesi.

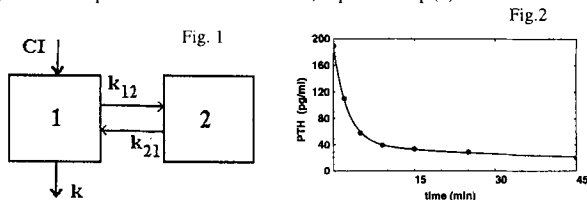
Dept. of Clinical Physiopathology, University of Florence, Italy.

MODEL OF iPTH CLEARANCE AFTER PARATHYROID ADENOMECTOMY

Primary hyperparathyroidism may be cured surgically by complete excision of abnormal parathyroid tissue, checked by the intraoperative monitoring of circulating intact parathormone (iPTH) molecule. The fast disappearance of the iPTH and the advent of rapid assays make this possible. However, it is necessary to obtain some reference values to confirm total extirpation of the affected gland(s). These values are easily determined from the clearance curve if its evolution is known, but, in reality, only a few points can be measured since the surgeon must be informed quickly. A possible two-step solution is: (i) develop an iPTH metabolism model to theoretically draw the clearance curve; (ii) develop a technique to reconstruct this curve for each patient, starting with the initial experimental points. For step (i) we developed a two-compartment model with continued infusion (CI, in pg/(ml.s)) (Fig.1) The first and second compartments represent the vascular and the extravascular space, respectively; k, k₁₂ and k₂₁ are the rate constants whereas CI simulates iPTH release from unsuppressed glands, the presence of which is our fundamental hypothesis. For the blood compartment, we have:

$$C(t) = A \cdot \exp(-\alpha t) + B \cdot \exp(-\beta t) + BV$$

where $A + B + BV = iPTH$ (pg/ml) at clamping ($t = 0$) with BV (basal value) = CI/k , α and $\beta =$ reciprocals of the time constants of the two exponentials. Model matching was achieved by performing the fitting of this function on the experimental data obtained by an IRMA method, collecting samples at 0,2,5,15,25,45,1440,2880 min. A very good example of fitting is shown in Fig.2, where only the initial points are reported. The α and β values are sensitive to BV which, in the intraoperative technique, cannot be determined by the fitting [few points]. At present our efforts are focused on "a priori" estimation of this value, to perform step (ii).



PS-727

P. Mikosch, H.J. Gallowitsch, E. Kresnik, M. Molnar, I. Gomez, P.Lind

Department of Nuclear Medicine and Special Endocrinology, Landeskrankenhaus Klagenfurt, Austria

Influence of Human Anti-Mouse-Antibodies (HAMA) on Thyrotropin In-Vitro Analysis: A Comparison of 6 Thyrotropin IRMA Kits

Objective: The aim of the study was to evaluate the influence of human anti-mouse antibodies (HAMA) on the measurement of thyrotropin (TSH).

Investigations: Samples from 11 patients with measurable HAMA titres (19µg/l-3880µg/l) after radioimmuno-scintigraphy were analysed with 6 different thyrotropin immuno-radiometric assay kits (IRMA). Each sample was analysed in the routine way (sample influenced by HAMA), as well as after incubation with murine immunoglobulin to precipitate HAMA (sample not influenced by HAMA).

Results: Two kits showed clear deviations of measured thyrotropin levels when the HAMA titres were higher than 1350µg/l. A third kit was influenced to a lesser extent by HAMA. Three of the 6 investigated thyrotropin IRMA kits presented no measurable deviations of thyrotropin due to elevated HAMA. In comparison with former studies after immunotherapy, the thyrotropin deviations were marginal. However, differences were found between the commercially available thyrotropin assays. According to the results of this study only three out of the six investigated kits were unaffected by human anti-mouse antibodies.

Conclusion: Since thyrotropin is one of the key parameters for the endocrinologist dealing with the thyroid gland, every laboratory should ensure high quality thyrotropin assays by critically analysing their thyrotropin assay for HAMA effects.

PS-728

M.C. Siqueira, F. Serejo, F. Ramalho, M. C. Moura

Center of Gastroenterology, Liver Unit, Faculty of Medicine, Lisbon, Portugal

PROSTAGLANDIN E2 (PGE2) IN CHRONIC HEPATITIS C TREATED WITH ALFA INTERFERON PLUS SULINDAC

Background/Aim: NSAID (Non Steroidal Anti-Inflammatory Drug) acts inhibiting the cyclooxygenase enzyme, reducing PGE2 and increasing 2,5 adenylate syntetase release. The aim of the study was to investigate whether PGE2 syntetase might be inhibited by Sulindac associated to Interferon therapy in chronic hepatitis C and if this association improves the response. **Patients:** twenty five patients (pts) were blindly studied and randomized in 2 Groups: Group 1 - 11 pts treated with interferon alone (6 MU, s.c., tiw, 6 months) and Group 2 - 14 pts treated with interferon (6 MU, s.c., tiw, 6 months) plus Sulindac (400 mg, tiw, 6 months). **Methods:** Plasmatic PGE2 was analysed before and at the end of therapy using RIA, after extraction and chromatography with 60-100% recovery (N.V. 388±73 pg/ml). HCV-RNA was quantified by PCR. **Results:** Values of PGE2, expressed as pg/ml, are shown in the table below:

	R		NR	
	Before	After	Before	After
Group 1	1356.3±144.9 pts=3	413.3±76.3	1451.25±443.6 pts=8	711.7±437.14
Group 2	1267.8±402.7 pts=10	390±101.9	1340±177.4 pts=4	726±409.4

R (patients with ALT normalization); NR (non responders).

There was a significant decrease of PGE2 after treatment in all the groups. Comparing with NR after treatment, only the R of Group 2 showed a significant decrease of PGE2 with normalization ($t=2.548$, $p=0.026$ Student's t test). HCV-RNA negativation was seen in 5/14 pts (35.5%) of Group 2, comparing with 3/11pts (27.2%) of Group 1. **Conclusions:** The association of Sulindac to the Interferon improves the response and the plasmatic PGE2 may be a useful marker for the follow up of the patients. These results must be confirmed with more data.

Poster presentations

PS-729

A. Brocchi, M. Tommasi, S. Raspanti, S. Spini, F. Tonelli, U. Meldolesi.

Department of Clinical Physiopathology, University of Florence.

METHODOLOGICAL EVALUATION OF A RAPID GASTRIN ASSAY.

Surgical exploration for gastrinoma has a high failure rate because of small primary tumours and occult metastasis. We have taken advantage of the short half-life of gastrin-17 in man (9.5 to 10.5) and the modification of a RIA that permits measurement of gastrin in 30 minutes to provide surgical guidance regarding the exploration and surgical removal of gastrinomas.

Serum gastrin concentrations were measured with the use of Clinical Assays Gammadab Gastrin 125I RIA kits (kindly supplied from Sorin Biomedica, Italy). Development of a "quick gastrin assay" involved changing some parameters such as time of incubation and temperature for antigen-antibody interaction.

We present three cases of gastrinoma who underwent exploratory laparotomy. In two cases gastrinomas were discovered and excised and the third case underwent a negative laparotomy.

The modified RIA was performed with 15-minute incubation at 37° C under agitation at 350 rpm. With this RIA the sensitivity was about 10 pg/ml and the precision profile indicated a coefficient of variation between 10.3% and 2.56% in the dose range from 40 to 500 pg/ml. The regression line between 43 gastrin values obtained by the standard method (x values) and the quick assay (y values) was $y = 50.779 + .83247 x$ with a correlation coefficient of .98401 ($p < .05$).

The changes in serum gastrin levels taken during surgery were related to the success of tumour removal in each of the three cases.

As in parathyroid surgery, the intraoperative measurement of declining serum gastrin levels by rapid assays would help in the early definition of surgical success of gastrinomas.

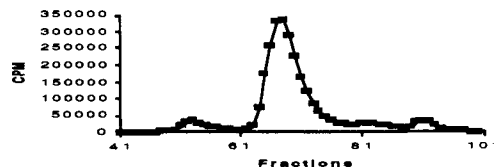
PS-731

C. Poiesi*, G. Maira, A. Caldinelli, G. Bettinoli

Nuclear Medicine Service, *III Analysis Service, Civic Hospital of Brescia, Italy

EVALUATION OF CIRCULATING 131I THYROGLOBULIN IN HUMAN SERA BY HIGH PERFORMANCE GEL PERMEATION CHROMATOGRAPHY (HPGPC)

We have developed a chromatographic blood test to detect endogenously 131I labeled thyroglobulin (Tg) in patients with differentiated thyroid carcinoma (DTC). Sera (2 ml) obtained from patients who had received a therapeutic dose of 131I 72h before, were centrifugated at 10,000 x g for 10 min. HPGPC was performed through two different columns used in series. Columns were equilibrated and eluted for 100 min with 0.05 M phosphate buffer pH 7.2 containing 0.15 M NaCl at a flow rate of 4 ml/min. Fractions were collected every 1 min and counted until reaching a counting error of 3% or for 15 min in an automatic gamma-counter [NaI (Th) detector, 3 inches, 131I efficiency 50%, Packard Instr.]. The elution volume of 131I-Tg had been previously determined by injecting a solution of molecular weight standards (BioRad) and testing fractions obtained from human sera for the presence of immunologically reactive hTg. Endogenously 131I Tg was positively identified if the radioactivity in the fractions containing Tg was at least three times the background activity. The figure shows an elution profile from a patient positive for endogenously radiolabeled 131I-Tg.



As shown in figure, 131I-Tg eluted from fractions 51 to 56 (confirmed by hTg immunological assays performed on these fractions). Fractions between 62 and 71 contained 131I albumin and 131I thyroid hormones bound to carrier proteins while free 131I thyroid hormones and free iodine 131 eluted in fractions 87-92.

This rapid chromatographic method could be used in addition to conventional procedures and to previously described chromatographic methods for the detection of 131I thyroid hormones in the follow up of patients with DTC.

Radiopharmacy and radiochemistry: Tumor markers

PS-730

H. Amthauer¹, S. Bolouri², E. Heißler², J. Ricke¹, C. Stroszczyński¹, B. Grünert¹, K.-T. Hoffmann¹, J. Bier¹, H. Eichstädt¹, R. Felix¹

Departments of Nuclear Medicine / Radiology¹ and Oro-Maxillo-Facial Surgery², Charité, Campus Virchow-Clinic, Humboldt-University Berlin, Germany

DIAGNOSIS OF RECURRENT DISEASE IN HEAD AND NECK CANCER USING THE TUMOR MARKER TATI AND CYFRA

Purpose. This study was designed to evaluate the diagnostic value of TATI (tumor associated trypsin inhibitor) and CYFRA (cytokeratin 19 fragment) serum levels for detection of recurrent disease in patients with squamous cell carcinoma (SCC) of head and neck.

Methods. In this study serum samples of 109 patients (30-89 years, mean age 58.7, 76 male, 33 female) with a histologically proven squamous cell carcinoma were analysed. Measurements were performed preoperatively, immediately after surgery and postoperatively every three months up to 18 months. Quantitative radioimmunoassays Spectria TATI® (Orion Diagnostica, Finland) and Centocor® CYFRA TM 21-1 (Centocor Diagnostics, USA) were used. For statistical test the analysis of variance and a Kruskal Wallis test were performed.

Results. Out of 109 patients 33 showed recurrent disease within 18 months after surgery. Those patients had a mean TATI serum level of 55.93 µg/l (range: 3.3-298 µg/l). In patients without tumor recurrence the mean TATI serum level was 21.03 µg/l (range: 2.8-71.3 µg/l). The analysis of CYFRA levels in patients without tumor recurrence demonstrated a mean value of 1.12 ng/ml (range: 0-4.8 ng/ml), in patients with tumor recurrence 3.89 ng/ml (range: 0.2-21.3 ng/ml). Sensitivity was 91% and the specificity 35% in detection of tumor recurrence by TATI. For CYFRA a sensitivity of 29% and a specificity of 97% were calculated.

Conclusions. We conclude that TATI improves screening of tumor recurrence in patients with SCC of head and neck. In combination with CYFRA patients with a high risk of tumour recurrence can be identified. Hence, the combination of CYFRA and TATI is helpful in deciding on adjuvant treatment modalities.

PS-732

S. Z. Deng, X. T. Lin, J. D. Song, L. P. Yang, W. Cheng

Dept. of Nucl. Med. Hua Shan Hospital, Shanghai Medical University, Shanghai 200040, China

THE CLINICAL APPLICATION VALUE OF THE SERUM FREE/TOTAL PSA RATIO

PURPOSE To evaluate the clinical application value of the serum free/total PSA ratio in prostatic disease patients. **METHODS** 154 prostatic disease patients which pathologically diagnosed were retrospectively reviewed. 128 were benign prostatic hyperplasia (BPH), 18 were untreated prostate cancer (Pca-untreated), 8 were treated prostate cancer (Pca-treated). Serum total PSA (T-PSA) and free PSA (F-PSA) were measured using immunoradiometric assay. Free/total PSA (F/T PSA ratio) ratios were calculated. **RESULTS:**

group	cases	T-PSA(ug/L)		F-PSA(ug/L)		F/T PSA ratio(%)	
		X ± SE	X ± SE	X ± SE	X ± SE		
BPH	128	70.76 ± 7.64	7.20 ± 3.80*	2.01 ± 1.73	27.40 ± 13.74*		
Pca-untreated	18	68.13 ± 10.92	11.31 ± 4.89*	0.88 ± 0.64	7.12 ± 3.65*		
Pca-treated	8	75.37 ± 8.88	9.06 ± 6.66	2.39 ± 1.10	26.20 ± 8.38		

(* P < 0.005)

using T-PSA 10ug/L and F/T PSA ratio mean value minus 1SE (14%) as diagnosis prostate cancer cutoff value, in BPH group, 21 cases T-PSA > 10ug/L, but 16/21 cases F/T PSA ratio > 14%. In prostatic cancer group, 7 cases T-PSA < 10ug/L, but F/T PSA ratio < 14%.

CONCLUSIONS 1) The study showed that the measurement of the serum T-PSA and F/T PSA ratio should be complemented each other for the diagnosis and differential diagnosis of prostate cancer and benign prostatic hyperplasia. 2) The sensitivity and specificity of F/T PSA ratio are 94.44% and 88.28% respectively; But there is no different between Pca-treated group and BPH group which may be related to metastatic.

PS-733

W. Louw¹, I. Dormehl², R. J. Milner², F. Schneeweiss³, F. Chaparro⁴, E. Kilian⁴, J. Wagener¹.

¹Atomic Energy Corp., Pelindaba, ²University of Pretoria, ³Institute for Medicine, Jülich, ⁴Pretoria Biomedical Research Centre.

BIODISTRIBUTION OF RADIOLABELLED POLYMIN-MP OF DIFFERENT MOLECULAR SIZES AS A SELECTIVE BONE SEEKER FOR THERAPY IN ANIMAL MODELS.

An ideal radiopharmaceutical for the treatment of neoplastic and inflammatory (benign) bone diseases would be a radiolabelled compound that predominately accumulates in bone lesions with limited access to normal bone and other organs. Neoplastic tissue's abnormal blood supply (increased permeability) and lack of lymphatics will selectively accumulate radiolabelled macromolecules. This enhanced permeability and retention effect forms the basis of the study, using various molecular sizes of the radiolabelled macromolecule polyethyleniminomethyl phosphonic acid (polymin-mp) for increased selectivity of the bone-seeking radiopharmaceutical. Polymin-mp was synthesized by condensation of polyethylenimin phosphonic acid and formaldehyde, followed by fractionation into different molecular sizes by membrane ultrafiltration. Labelling efficiency to ^{99m}Tc (as radiotracer) was ≈ 99% with complexes stable for 24 hours. The pharmacokinetics and biodistribution of various ^{99m}Tc-polymin-mp fractions was investigated using five experimental baboons per fraction and dogs with naturally (n=5) occurring appendicular osteosarcomas. All animals underwent general anaesthesia using pentobarbitone infusion. Scintigraphy was performed in the baboons after a bolus i.v. dose of ^{99m}Tc-polymin-mp (185 Mbq); both dynamic studies (30 x 1 min frames) and static studies (5 min acquisition every hour for four hours) were done. Blood and urine samples were also collected at 10 min intervals.

The dogs underwent static studies of the tumours at four hours post i.v. injection. From the results macromolecules with sizes ranging between 30 and 300 kDa were characterized by excessive liver (21-57% I.D.) and kidney (40% I.D.) uptake, and accompanying long residing times (T_{1/2} up to 24 hours). The percentage bone uptake averaged at 8% I.D., for these particles, excluding sizes 100-300 kDa where very little bone uptake was seen (<4%). In this case the blood clearance was also slow (T_{1/2} ≈ 75 ± 8 min). The fraction size 10-30 kDa had comparatively low accumulation and short residence times in the liver and kidneys (respectively 20%, T_{1/2} = 22 ± 4 min; 17.5%, T_{1/2} = 20 ± 3 min) and although the bone uptake of 18% in this case was high, it is still low for a bone-seeking agent. These particles cleared from the blood with T_{1/2} = 25 ± 2 min and seemed suitable for labelling with eg ¹⁵³Sm for therapy. Results for the dogs showed good uptake in the tumour with the 3-10 kDa fraction with reduced uptake with larger sizes (100-300 kDa).

PS-734

D.K. Hazra, P. Khanna, P.K. Gangwar, M.S. Agarwal, S.K. Juyal

Nuclear Medicine & RIA Unit, P.G. Dept of Medicine S.N. Medical College, AGRA, 282, INDIA

TWO STEP STRATEGY FOR USE OF PSA AS A TUMOUR MARKER

Prostate Specific Antigen (PSA) is an important tumour marker utilised in the diagnosis of Prostatic Carcinoma. In order to evaluate its diagnostic role, the IAEA had initiated a multicentre study, distributing an immunoradiometric PSA assay developed at NETRIA, London. Free PSA and free PSA/total ratio have been suggested as of greater discriminating value as compared to total PSA alone. However using both assays increases the cost of case finding. Using the IAEA assay, 205 subjects have been subjected to total PSA estimation. Out of the 45 controls all had total PSA levels below 4 ngm/ml and 90% below 2.5 ngm/ml. Among 136 cases of Benign Prostatic Hyperplasia (BPH) only very few (only 3) had levels more than 10 ngm/ml. Among 24 Prostate Carcinoma cases 90% have values over 10 ngm/ml and many over 100 ngm/ml. The number of cases requiring free PSA assay is thus very small justifying a two-step strategy (Total PSA for all cases and free PSA only for grey zone). However PSA estimation was not useful in differentiating BPH from control cases as a significant fraction. BPH cases have values below 4 ngm/ml.

PS-735

N. Iznaga-Escobar¹, I. Luis², J. C. Izquierdo¹, L. Suárez¹, R. Figueredo¹, D. Morales¹, J. A. Gómez¹ and R. Pérez¹.

Center of Molecular Immunology, Research Department, Havana, Cuba.

¹⁸⁸Re-DIRECT LABELING OF ANTI-HUMAN EPIDERMAL GROWTH FACTOR RECEPTOR ANTIBODIES MURINE IOR egf/r3 AND HUMANIZED R3.

In the present work we describe ¹⁸⁸Re-direct labeling of anti-human EGF+ receptor antibodies. The analytical methods comprised HPLC on TSK 3000, electrophoresis (PAGE), Instant Thin Layer Chromatography (ITLC-SG), biological assessment of the radiolabeled molecule using Lindmo method and Flow Cytometry and biodistribution studies in Balb/c mice. No fragmentation of the reduced molecules was found using 2-ME as a reducing agent. Labeling efficiency was greater than 99.0 % as a mean value for both antibodies. The radiolabeled product of two antibodies was analyzed on TSK 3000 and only one major peak was seen with a purity greater than 99 % without noticeable fragmentation of the molecule. These results were confirmed using native PAGE. Radiocolloids were less than 1.5 % in both cases. The biological activity measured by Flow Cytometry using H-125 lung adenocarcinoma cell line was similar for both antibodies preparations and the Lindmo assay showed an immunoreactivity fraction higher than 70 %. Challenge studies with DTPA, HSA 1 % and Cysteine demonstrated no evidence of transcomplexation of ¹⁸⁸Re to DTPA, HSA and only 20 % of the radiolabeled ¹⁸⁸Re was transcomplexed to 100 mM cysteine after 1 hr incubation at 37 C. Biodistribution studies indicated no accumulation of the radiolabeled antibodies in normal organs.

PS-736

J. Lemberger and E. Libman

General Hospital, Medical Centre, Depts of Nuclear Medicine and Gastroenterology, Subotica, Yugoslavia REACTIVITY OF FIVE ANTIBODIES TO DETECT TUMOR MARKERS IN THE BODY FLUIDS

The aim of this study was the comparison of reactivity of five monoclonal antibodies to tumor markers and to establish optimal combination in confirming malignancy. Simultaneous IRMA assay of CEA, CA 19-9, CA 50, CA 72-4 and CA 195 was done in serum and effusions (abdominal and pleural) in 47 cancerous patients: 25 with cancer of digestive tract and 22 with other cancer localizations. Each patient was tumor marker positive: one patient had only one and 12 patients had all 5 in serum and/or effusions. The mean positivity in serum and in effusions was 54%. However, the positivity in serum for digestive tract cancer (67%) was significantly higher than in other cancers (42%, $\chi^2=13$, 229;p<0,01). In effusions was no difference. The highest positivity in serum for digestive tract cancer was CEA (76%) and CA 50 (76%), and for other localizations CA 195 (59%). The most effective markers in serum of all patients were CA 195 and CA 50, and in effusions CA 72-4 and CA 19-9 with 65% positivity. This suggests that advanced cancers express several markers and their reaction pattern is distinct. No complementarity of markers was registered either in serum or in effusions. However, CA 195 in serum and CA 72-4 in effusions were complementary and by their simultaneous assay the positivity in digestive cancer expands to 100% and in other cancers to 86%. In conclusion, by simultaneous use of antibodies to CA 195 and CA 72-4 in body fluids, in 93% of patients it is possible to confirm malignancy.

PS-737

S. Nuvoli, A. Mocci, A. Scanu, A. Masia, A. Marrosu, C. Bagella, M.A. Foddai, A. Falchi, M.E. Solinas, F. Fadda, A. Spanu and G. Madeddu. Depts. of Nuclear Medicine and Urology. University and General Hospital of Sassari. Italy

BLADDER TUMOR ANTIGEN (BTA): A NEW BIOLOGICAL MARKER FOR BLADDER CANCER (BC) DETECTION.

To evaluate BTA effectiveness in the identification of primary BC, we investigated 44 BC affected pts, all diagnosed by histology, 15 pts with benign genitourinary diseases (BD), 10 of which benign prostatic hyperplasia (BPH) and 5 renal stone (RS), and 35 healthy subjects as controls (C). After trans-urethral resection (TUR), BC pts were subdivided for grading in G1 (12 cases), in G2 (12 cases), in G3 (13 cases) and in Gx (7 cases), while according to clinical stages, one case was classified as Ta, 17 as T1, 17 as T2, 5 as T3 and 4 as T4. In BC, BD and C, BTA was assayed in urine by IEMA and 2 different cut-off values were considered: 14 and 50 U/ml, respectively. In BC pts, BTA values were <14 U/ml in 14 cases (stages Ta, T1, T2), between 14 and 50 U/ml in one case (stage T2) and >50 U/ml in 29 cases (stages T2, T3, T4). According to the grading, BTA was <14 U/ml in 8 G1 and 6 G2, between 14 and 50 U/ml in one Gx, and >50 U/ml in 4 G1, 6 G2, 6 Gx and 13 G3. In BD, BTA levels were <14 U/ml in 7 cases (6 BPH, 1 RS), between 14 and 50 U/ml in 5 cases (1 BPH, 4 RS) and >50 U/ml in the remaining 3 BPH cases. Sensitivity and specificity were 68.2% and 47%, respectively, for a cut-off of 14 U/ml, and 65.9% and 80%, respectively, for a cut-off of 50 U/ml. Specificity was 100% considering C pts in whom BTA was <14 U/ml in all cases. Sensitivity in BC significantly increased with advancing disease stage and cancer progressive grading. Mean BTA levels were significantly higher in BC (1554 ± 3381.9 U/ml) in respect of BD (28.9 ± 29 U/ml) and C (7.1 ± 8 U/ml). According to the different stages, BTA levels were significantly higher in T2, T3 and T4 cases than in Ta and T1, while no statistical difference was found when T2, T3 and T4 were mutually compared. BTA values were besides more elevated in Gx and G3 cases compared to G1 and G2. These preliminary data suggest that BTA may be a useful marker to detect primary BC, also helping to discriminate between invasive and non invasive forms. Moreover, in our cases, by using a suitable cut-off, BTA could distinguish BC from BD with good specificity.

PS-738

Z. Petrovski, J. Gjorgievski, S. Mihajlovska

Department of Nuclear Medicine, Medical Center, Bitola, Republic of Macedonia

DIAGNOSTICAL VALUE OF SIMULTANEOUS DETERMINATION OF CYFRA 21-1 AND CEA IN LUNG CANCER

The aim of this study was to evaluate the usefulness of a common determination of tumour markers CYFRA 21-1 and CEA in lung cancer diagnosing. We examined 54 patients (M/F=39/15, mean age 56 ± 10 years) with lung cancer, which were histologically confirmed at bronchoscopy. Sensitivity, specificity and accuracy are analyzed individually for each histological type: non small cell lung cancer (NSCLC), adenocarcinoma, small cell lung cancer (SCLC) and also cancer stage in NSCLC (I, II, IIIa, IIIb and IV stage). The mean value of CYFRA 21-1 (normal to 3 ng/ml) and CEA (normal to 10 ng/ml) were: in NSCLC 6,71 and 8,18; in adenocarcinoma 3,45 and 15,04; in SCLC 3,92 and 12,76. There was statistically highly significant difference between the levels of CYFRA 21-1 in NSCLC and SCLC, ($p < 0,001$), and slightly difference of CEA serum concentrations between adenocarcinoma and SCLC ($p < 0,05$). CYFRA 21-1 has significantly higher sensitivity (72%), specificity (89%) and accuracy (82%) in the diagnosis of NSCLC which are in correlation with the stage of disease. Levels of CYFRA 21-1 was strongly associated to present of metastases and degree of histological differentiation. Consequently, CYFRA 21-1 was lower in patients who were operated upon when compared to unresectable ones. With simultaneous determination of the both tumour markers CYFRA 21-1 and CEA, the diagnostic sensitivity (74%) and specificity (92%) are increased for NSCLC and ensured the high percent of correctly diagnosed of lung cancer.

PS-739

J.E. Vasquez, G. Pimental*, A. Perera**, F. Freyre, J. Gavilondo, J. Olivia**, R. Baum***.

Center for Genetic Engineering, Div of Immunotechnology, *National Institute of Oncology, **Center for Clinical Research, La Habana, Cuba ***Central Clinic (PET Centre), Bad Berka, Germany

AN ANTI-CEA scFv ANTIBODY FRAGMENT: PRECLINICAL EVALUATION

A recombinant single chain (scFv) antibody directed against carcinoembryonic antigen (CEA) has been generated from hybridoma cells genetic material. This scFv has potential for radioimmolocalisation of human carcinomas, and could replace murine based or humanised whole anti-CEA IgG, already used for this application.

This scFv was expressed in methylotrophic yeast (*Pichia pastoris*) using 5 l fermentors (Biolaffite, France). Yields of 0.6 g/l of soluble and active protein was demonstrated by ELISA. Immunocytochemistry studies showed a positive recognition of LoVo cell line (a CEA expressing human carcinoma) by the scFv. The protein was purified at 90% or higher (under GMP conditions) by Metal affinity Chromatography employing a pH gradient. Labelling with Tc-99m at the C-terminus yielded 96% labelling efficiency without any major effects on biologic and *in vitro* stability.

Biodistribution studies were done in normal mice, compared simultaneously to non-recombinant Fab' fragments and the whole antibody. Results showed a normal organ distribution up to 24 hours with a very rapid blood clearance of the scFv, compared to the other molecules tested and similar molecules previously reported. *In vivo* targeting experiments using xeno-transplanted nu/nu mice are now running.

PS-740

B.C. Wang, J. Jin, P. Fang, Y.H. Tao, R.J. Zhang, L.F. Zhang

National Laboratory of Nuclear Medicine, P.R. China, Department of Biochemistry and Molecular Biology

RADIOIMMUNOASSAY OF HUMAN CARDIAC ACID ISOFERRITIN

Acid isoferritin (AIF), a ferritin isomer with a large proportion of H subunit, is different from basic isoferritin biochemically and immunologically. AIF was isolated and purified from human heart muscle. A RIA of AIF was established, on the equilibrium method, by raising the antiserum against AIF in rabbits and by preparing ^{125}I -AIF using the chloramine-T method. The data were processed using the automated smoothed spline function data processing program. The intra- and inter- CV of AIF RIA were 1.65% and 9.71%, respectively, the recovery rate, 102%. The antiserum provided a linear response from 7.0 to 369.6 $\mu\text{g/L}$ with ED₅₀ of 27.50 $\mu\text{g/L}$. The cross reactivity with AFP, CEA, lactoferrin and transferrin was negligible, and with ferritin, 1.74%. The serum AIF was measured in liver diseases including hepatic cancer, hepatic cirrhosis and acute and chronic hepatitis. Its sensitivity for diagnosis of hepatic cancer was 73.05%, independent of the severity of hepatic injury. A study for eight types of malignant tumors (Hepatoma, Esophagus carcinoma, Lung tumor, Stomach carcinoma, Rectal tumor, Breast carcinoma, Lymphosarcoma, Nasopharyngeal carcinoma) showed that AIF was most valuable in diagnosis of hepatic cancer, with its positive, negative, false-positive and false-negative rates being all ideal. Combine monitoring of AIF with AFP would increase the rate of detection of positive cases (89.94%) and improve the specificity of the method (95.46%) for the diagnosis of hepatic cancer. These results suggest that AIF may be a rather specific index of hepatic cancer.

Radiopharmacy and radiochemistry: Peptides

PS-741

WAP Breeman, M de Jong, LJ Hofland, DJ Kwekkeboom, TJ Visser, A Srinivasan, EP Krenning. Depts of Nuclear & Internal Med, University Hospital Rotterdam, The Netherlands, and Mallinckrodt Medical, St Louis, MO, USA

Radioiodinated [DOTA⁰,Tyr³]octreotide: studies in vitro and in rats

Peptide receptor scintigraphy with radiolabeled somatostatin analogs, such as [¹¹¹In-DTPA⁰]octreotide is a sensitive and specific technique to show in vivo the presence and abundance of somatostatin receptor on various tumors. There is also much attention to perform radiotherapy of these somatostatin receptor-expressing tumors by changing γ -emitters to particles-emitting radionuclides. Currently the β -emitting [⁹⁰Y-DOTA⁰,Tyr³]octreotide is under investigation to evaluate its antiproliferative effect on somatostatin receptor-positive tumors. Since [DOTA⁰,¹²⁵I-Tyr³]octreotide could also be an alternative, we investigated [DOTA⁰,¹²⁵I-Tyr³]octreotide (A) and found: high-affinity for the somatostatin receptor in the subnanomolar-range, and a 5-fold higher internalization rate in AtT20 cells in comparison with radioiodinated [Tyr³]octreotide (B) and [DTPA⁰,Tyr³]octreotide (C). In rats specific uptake in somatostatin receptor-positive tissues of A was also superior to B and C, see table. In addition, 1 h after the injection of A we found a ratio of 390 \pm 4 pancreas vs blood and 14 % ID per gram pancreas, but this rapidly declined to 8.8 at 4 h and 0.24 % ID/g at 24 h. This indicates a rapid cellular metabolism, resulting in a short residence time of radioactivity in the target and this may hamper its radiotherapeutic applications. Nevertheless, the combination of a high specific uptake, even with a short residence time makes this radioligand promising for radioguided surgery for intraoperative localization with a hand-held γ -detecting probe.

Tissue radioactivity in % ID/g at indicated h after the administration of [Tyr³]octreotide analogs A(=+DOTA), B and C(=+DTPA) in rats (n \geq 3);

	pancreas		adrenals		pituitary	
	4h	24h	4h	24h	4h	24h
A	8.8	.24	3.7	.016	4.4	.082
B	.37	.05	1.7	.14	.54	.20
C	.55	.027	1.7	.047	.29	.12

PS-742

Marion de Jong, Wout Breeman, Bert Bernard, Arthur van Gameren, Willem Bakker, Theo Visser, Ananth Srinivasan, Michelle Schmidt, Eric Krenning. Depts of Nucl Med and Intern Med III, Univ. Hosp. Dijkzigt, Rotterdam, The Netherlands; Mallinckrodt Medical, St. Louis, USA.

[DTPA,Tyr-3]OCTREOTIDE AND [DOTA,Tyr-3]OCTREOTIDE, RADIOLABELED WITH In-111 OR I-125.

Radiolabeled [DOTA,Tyr-3]octreotide (DOTATOC) was introduced for scintigraphy and radionuclide therapy of somatostatin receptor-positive tumors; it enables radioiodination (Tyr-3) and stable radiolabeling with e.g. Y-90 or In-111 (DOTA). Rat and human studies showed already favourable receptor binding and biodistribution of the radiometal compound. We compared rat biodistribution of DOTATOC and [DTPA,Tyr-3]octreotide (DTPATOC), labeled with In-111 or I-125. Also, the effect of labeling with excess stable In-115 (to change the charge of the DTPA/DOTA-group) after radioiodination of Tyr-3 was investigated. Results in %dose/g tissue, 1h, 4h and 24h p.i., n \geq 3. pit=pituitary; panc=pancreas.

peptide	DTPATOC				DOTATOC			
	blood	pit	panc	kidney	blood	pit	panc	kidney
In-111,1h	.16	2.06	9.75	2.35	.22	1.34	3.32	4.25
In-111,4h	.006	2.27	4.23	2.21	.021	1.03	3.46	4.84
In-111,24h	.002	1.75	1.70	2.04	.004	.94	1.74	4.51
I-125,1h	.26	1.91	6.50	3.68	.20	3.91	10.1	3.01
I-125,4h	.08	1.47	2.86	.97	.112	3.20	9.24	0.71
I-125,24h	.007	.58	.04	.19	.006	1.25	.34	0.08
I-125/In-115,1h	.26	2.22	6.16	2.71	.23	2.24	5.13	3.52
I-125/In-115,4h	.09	1.68	1.86	.94	.08	.84	2.49	.91
I-125/In-115,24h	.006	.80	.04	.20	.005	.59	.07	.10

All compounds showed high specific uptake (> that of OctreoScan) in receptor-positive organs like pancreas and pituitary. In these organs: 1) retention time of In-111 labeled compounds was longer than that of I-125-compounds; 2) uptake of In-111-DTPATOC in these organs exceeded that of In-111-DOTATOC; 3) for the I-125 labeled compounds the reverse was true; 4) In-115 complexation effect on uptake of I-125-DOTATOC exceeded that on uptake of I-125-DTPATOC. In vivo the DTPA-group of radioiodinated compounds will probably be "filled" with metal-ions. The DOTA-group, that requires heating for labeling, will be "empty" and more negatively charged, apparently favorable for receptor-mediated uptake (consistent with the In-115-experiment). We conclude: the radiometal compounds are very promising for scintigraphy and radionuclide therapy. Radioiodinated DOTATOC is very promising for radioguided surgery and possibly also for radionuclide therapy.

PS-743

M. T. Ercan, R. Senekowitsch-Schmidtke, S. Bernatz

Nuklearmedizinische Klinik und Poliklinik, Klinikum rechts der Isar der Technischen Universität München, Germany.

BIODISTRIBUTION OF Tc-99m-GLUTATHIONE IN MICE WITH OSTEOSARCOMA: EFFECT OF GAMMA IRRADIATION ON TUMOR UPTAKE

The aim of this study was to determine the efficacy of Tc-99m-glutathione (GSH) in scintigraphic demonstration of osteosarcoma tumor in mice and effect of gamma irradiation of tumor on tumor uptake of Tc-99m-GSH.

Thirty Balb C mice were implanted in their thighs with osteosarcoma tumor and 3 weeks later they were injected with 400 mCi Tc-99m-GSH in 0.1 ml through the tail vein. They were divided into 2 groups. The mice in the first group (control) were sacrificed at 1, 3, and 6 h post-injection. The tumors of mice in the second group were subjected to gamma irradiation for 10 min (20 mGy) immediately following injection and then sacrificed at the same time points. Planar scintigrams were obtained at each time point. The organs, the tumors, some muscle and some blood were removed, weighed and assayed for radioactivity against a standard.

The tumors were well visualized on scintigrams in both groups. In addition, the kidneys and the urinary bladder were also visualized. In biodistribution studies there was an increased uptake/g tissue values in all organs, blood and tumor except kidneys in irradiated group compared to control group. The tumor uptake values (mean \pm SD) were 3.27 \pm 0.80, 1.53 \pm 0.69 and 1.51 \pm 0.55 for control and 5.18 \pm 1.28, 0.399 \pm 0.120 and 1.67 \pm 1.05 %/g for irradiated groups at 1, 3, and 6 h, respectively. The increase at 1 h and decrease at 3 h in irradiated tumor uptake values were significant compared to control values (p<0.02). Tumor/muscle concentration ratios were 34.03 \pm 12.2, 21.4 \pm 11.3 and 18.7 \pm 11.4 for control and 18.8 \pm 7.2, 3.63 \pm 1.9, and 24.1 \pm 9.0 for irradiated groups at 1, 3, and 6 h, respectively. Gross autoradiography of tumor sections indicated focal sites of increased uptake within tumor tissue.

In conclusion, the advantages of Tc-99m-GSH as a radiopharmaceutical for tumor imaging are high target to non target ratios attained very early, low blood background, absence of uptake in organs other than kidneys, easy in-house preparation with a simple and rapid procedure and high labelling efficiency. More studies are needed for clarifying the localization mechanism(s) in tumor tissues.

PS-744

H. Kalamaz, M.S. Cooper*, J.R. Buscombe*, J.E. Agnew*.

University of Agriculture & Technology, Department of Animal Physiology, Faculty of Biology, Olsztyn; Poland.

Royal Free Hospital and School of Medicine*, Department of Medical Physics and Nuclear Medicine. London; UK.

A NEW ASPECTS IN BREAST CANCER DIAGNOSIS USING RADIOLIGAND FOR EPIDERMAL GROWTH FACTOR RECEPTOR.

The over exertion of the epidermal growth factor receptor (EGFR) has been demonstrated in many human cancers, especially in breast cancer. Patients who over-express EGFR in breast tumours tissue tend to have worse prognosis than patients with normal levels of EGFR, or those who over express steroids receptors. In practice, so far there is no sensitive, *in-vivo* diagnostic technique, which can distinguish patients who present these both types of receptors.

The aim of this initial study was to develop radiolabelled peptide which bind into EGFR, and then can be used to diagnose of breast cancer patients using nuclear medicine technique. The EGFR-2 peptide based on hTGF α which bind into EGFR have been synthesised. The peptide is base on B-loop β -sheet of the hTGF α . This region has been shown to be important determinant of EGF receptor binding affinity and biological activity.

EGFR-2 peptide was iodinated by two methods. In first radioiodinating EGFR-2 peptide procedure with using Iodogen and QAE Sephadex (modification of protein hormone method by M. Nett & T.E. Adams) has been employed with 1 μ g of peptide and 1mCi Na-I125. The major peak of radioactivity contained mono-iodinated peptide was observed. In second method radioiodinating EGF-R2 peptide procedure with using Iodogen and Resin (modification of the chloramine T method by Greenwood) has been applied with 5 μ g of peptide and 1mCi Na-I125 TCA/TCLC/. Resin test was complied for percent of binding peptide (>90%).

The preliminary study of Na-I125 EGFR-2 binding assay with using Scatchard analysis and SSD method suggests the presence of two classes of binding sites with high and low ability in MDA-468 cells. Both methods used iodinated EGFR-2 peptide will be able to apply as preliminary data to Tc-99m binding assay because this peptide contain residue which is used to bind Tc-99m.

Poster presentations

PS-745

V. Pallela, P.M. Consigny, R. Shi, M.L. Thakur, Thomas Jefferson University Hospital, Philadelphia, PA 19107

Tc-99m LABELED FIBRIN α -CHAIN PEPTIDE ANALOG FOR IMAGING VASCULAR THROMBOSIS

Scintigraphic imaging of vascular thrombosis continues to be challenging. Most of the recently evaluated antibodies or peptides are specific for IIb-IIIa glycoprotein receptors expressed on activated platelets. On aged venous thrombi (DVT), or pulmonary emboli (PE), where platelet accretion may be negligible, detection of clots by agents specific for activated platelets may be difficult. We hypothesize that a fibrinogen/fibrin binding peptide may facilitate detection of fresh or old clots.

N-terminal tripeptide of fibrin α -chain H-Gly-Pro-Arg-OH binds to fibrinogen and inhibits clotting (Kawasaki et al, Chem Pharm Bull 41, 975-977, 1993). An active analog of this peptide, H-Gly-Pro-Arg-Pro-NH₂ was modified at carboxy terminal by the addition of Gly-(D)Ala-Gly-Gly to provide amino groups for chelation of ^{99m}Tc and alpha aminobutyric acid (Aba) between the two moieties to minimize steric hindrance. This analog (Gly-Pro-Arg-Pro-Pro-Aba-Gly-Gly-(d)Ala-Gly) was then radiolabeled (^{99m}Tc-TP 850) via SnCl₂ reduction by an instant kit procedure.

The labeled peptide (specific activity 340 Ci/m mole) was evaluated for its ability to inhibit rabbit and dog platelets aggregation *in vitro* and to image experimental DVT and PE *in vivo*. DVT were induced in rabbits by passing 150 μ A current through an intravascular electrode. PE were induced by injecting into the lungs via the right jugular vein 3 mm x 5 mm tantalum impregnated autologous blood clots formed *in vitro*. ^{99m}Tc-TP 850 (2 mCi/ μ g) was injected i.v. and serial images were obtained for 4 hrs. Animals were then sacrificed, the excised lungs were x-rayed, and radioactivity associated with dissected DVT, PE, other tissues, and blood was quantified.

TP 850 facilitated quantitative incorporation of ^{99m}Tc and inhibited ADP induced rabbit (IC₅₀=167 μ M) and dog (IC₅₀=336 μ M) platelet aggregation. DVT and PE were detectable with clot to blood radioactivity ratios of 1.8-14.8. Scintiphotos of PE conformed with x-ray images. These data suggest that the modified analog of fibrinogen binding peptide H-Gly-Pro-Arg-OH can be labeled with ^{99m}Tc and is worthy of further studies in imaging DVT and PE.

PS-746

RF Wang, JAM Tafani, JM Zajac, R Guiraud

The First Hospital, BMU, Department of Nuclear Medicine; Hopital Purpan, CHU, Service de Medecine Nucleaire; CNRS 205, LPTF IN VIVO BINDING ASSAY AND QUANTITATIVE AUTORADIOGRAPHIC LOCALIZATION OF [I-125]7 α -O-IA-DPN IN MOUSE BRAIN

To localize and characterize binding sites for opioid receptors in specific anatomical regions of mouse, we reported the studies of [I-125]7 α -O-IA-DPN, for future *in vivo* visualization of the opioid receptors by autoradiographic localization of high-affinity binding sites. Mice were sacrificed by decapitation at 20 min following intravenous (i.v.) administration of 200 μ Ci (100 pmol) of [I-125]7 α -O-IA-DPN, and their brains were quickly removed and isolated carefully into two complete moieties (one for binding assay, another for autoradiography). The blocking study was carried out co-injection with tracer and 2000 pmol naloxone (μ -selective antagonist). *In vivo* opioid receptor binding assay, close to 72% of the total radioactivity coeluted in HPLC with intact [I-127]7 α -O-IA-DPN at the first 30-60 min; 20 min postinjection, near to 35.3% of the cerebral radioactivity was bound, with 63.4% of its specific binding to opioid receptors. There existed more constant level (40%-50%) of specific binding and good degradation-resistant of this agent at the first 60 min after i.v. injection. *Ex vivo* autoradiography future conformed the high uptake and retention of this new compound in area rich in opioid receptors, such as striatum, thalamus, hypothalamus, hippocampus, superior and inferior colliculus, cortex, and displayed a remarkably high *in vivo* target-(basal ganglion)-to-non target (cerebellum) ratio in mice. The findings in our current research suggested that this new iodinated DPN tracer appears to be as a potential radioprobe for *in vivo* binding assay or visualization CNS opioid receptors in human with SPECT.

Radiopharmacy and radiochemistry: Molecular biology/peptides

PS-747

O.K.Hjelstuen¹, B.By¹, H.H.Tønnesen¹, E.S.Dugstad², P.O.Bremer³, B.Cleynhens⁴, A.Verbruggen⁴

¹University of Oslo, ²Institute for energy technology, ³Isopharma AS, Kjeller, Norway, ⁴Catholic University of Leuven, Belgium

PHOSPHODIESTER AND PHOSPHOROTHIOATE OLIGODEOXYNUCLEOTIDES CONJUGATED TO MAG2 AND LABELED WITH ^{99m}Tc

In the search for a bifunctional chelating agent that can be conjugated to oligonucleotides to give yields sufficient for a kit formulation, the N-hydroxysuccinimide (NHS) ester of S-benzyl-mercaptoacetyldiglycine (MAG2) was studied. Two different 20-mer oligodeoxynucleotide (ODN) sequences with phosphodiester (PO) and with phosphorothioate (PS) backbones were used. All ODNs were synthesised with an aminoethyl linker on the 3'-end where the free amino terminal is conjugated to S-benzyl-MAG2 with the formation of a new tetraligand.

Conjugation: To 50 nmol ODN in 100 μ l 0.05 M phosphate buffer (PB) pH 7.5 was added 0.4 mg NHS-S-benzyl-MAG2 in 10 μ l DMF. The mixture was left to react for 2 h and then purified using a Sep-Pak C18 Light column conditioned with ethanol and 0.05 M PB pH 7.5. After application of the sample, the column was eluted successively with 1 ml 0.05 M PB pH 7.5, 1 ml water and 400 μ l acetonitrile. The S-benzyl-MAG2-ODN eluted with the acetonitrile, which was evaporated under a stream of nitrogen. Labelling: To a solution of the conjugate in a mixture of 100 μ l 1 M carbonate buffer pH 8.5 and 20 μ l acetonitrile were added 5 mg potassium sodium tartrate tetrahydrate, 50 μ g stannous and 0.5-1 GBq ^{99m}TcO₄⁻ and the solution was heated in a boiling waterbath for 10 min. The labelling mixtures were analysed by reversed phase HPLC.

In the HPLC analysis, all four radiolabelled ODNs elute as single peaks 1.5 min after the unconjugated ODNs and are well separated from unconjugated ^{99m}Tc-MAG2. Labelling yields: ODN1 (PO) 80.3%, ODN1 (PS) 84.1%, ODN2 (PO) 74.9% and ODN2 (PS) 70.0%.

Conclusions: MAG2 can be conjugated to 20-mer ODNs. The conjugates can be purified and labelled with ^{99m}Tc to give complexes of high yields apparently without influence of the ODN backbone modification. With optimisation of the purification method, the conjugates could potentially be useful for kit formulations of ODNs for ^{99m}Tc-labelling

PS-748

J. Kropp¹, M. Eisenhut², W.D. Lehmann³, F.F. Knapp, Jr.⁴, W.G. Franke¹ Dep. of Nucl. Med. Univ. of ¹Dresden and ²Heidelberg, ³German Cancer Research Center Heidelberg, Germany; ⁴Nucl. Med. Group Oak Ridge, USA.

FURTHER EVALUATION OF THE METABOLITES OF THE FATTY ACID 15-(p-IODOPHENYL)-3-R,S-METHYLPENTADECANOIC ACID (BMIPP)

This study further characterize the major metabolite(s) [M(s)] of 15-(p-iodophenyl)-3-R,S-methylpentadecanoic acid (BMIPP). **Methods:** Radioactive Ms of [I-131]BMIPP were evaluated from isolated rat hearts as well as of [I-123]BMIPP from blood samples of 20 patients (pts). Rat hearts were perfused with Krebs-Henseleit buffer with or without 0.4 mM BSA or 0.4 mM palmitate (PAL). Lipids were extracted and hydrolyzed from the outflow as well as from homogenized hearts. Radioactive Ms were analyzed by thin layer (TLC) and high performance liquid chromatography (HPLC). Ms were then further characterized by electron spray mass spectrometry. **Results:** The perfusate showed one major M (TLC; R_f= 0.35; solvent=benzene-dioxane-acetic acid 80:18:2) and adding of BSA/PAL increased significantly backdiffusion of BMIPP as well reduced BMIPP uptake and metabolism (p<0.05). In mass spectrometry the major M was identified as (p-iodophenyl)acetic acid (IPAA). In the TLC and HPLC analysis of the serum lipids of the pts the same M was found increasing over time (0%, 5.2%, 11.8% i.d.; 3 min, 30 min, 3 h p.i., respectively). In the heart lipids hydrolysate BMIPP, α -methyl-14(p-iodophenyl)tetradecanoic acid, (p-iodophenyl)dodecanoic, -hexanoic, and IPAA were found in 53.9%, 20.8%, 17.1%, 5.2%, and 1.1%, respectively. **Conclusion:** The animal results demonstrate the complexity of uptake, metabolism and release of BMIPP from which a part is metabolized via α - and subsequent β -oxidation to the final metabolite IPAA which could be further characterized by this study whereas the results in man suggest that the slow wash-out observed *in vivo* may represent a similar process.

PS-749

S. Samnick, S. Siebert, J. Bader, A. Schäfer, C.-M. Kirsch

Department of Nuclear Medicine, D-66421 Homburg/Saar

COMPARATIVE UPTAKE STUDY OF RADIOIODINATED AMINO ACID DERIVATIVES BY HUMAN GLIOMA CELLS IN VITRO

The synthetic amino acid L-3-[¹²⁵I]iodo- α -methyl-tyrosine (IMT) is currently under clinical evaluation as SPET tracer for imaging brain tumors. In our effort to develop radioiodinated analogs suitable for a widespread clinical application with SPET, p-[¹²⁵I]iodo-dl-phenylalanine (DL-IPA), p-[¹²⁵I]iodo-l-phenylalanine (L-IPA), L-[¹²⁵I]iodo-tetrahydroisoquinoline-3-carboxylic acid (ITIQC) and IMT were prepared either by direct electrophilic iodination or by exchange labelling, followed by a reversed-phase HPLC purification. The radiopharmaceuticals were investigated and compared in terms of their uptake in human glioma cells. The radioiodinated amino acids, including IMT showed a rapid cell uptake ($t_{1/2} = 2 - 7$ min), which appeared temperature and pH dependent. The radioactivity accumulation in gut washed cells after a 60 min incubation varied from 6 to 18% at 37°C (ITIQC < DL-IPA < IMT \leq L-IPA). Coincubation of the radioiodinated amino acids with a mixture of naturally-occurring L-amino acids resulted in lowering the cell uptake, whereas variations in the plasma membrane potential (K^+ buffer concentration) and alteration of the mitochondrial membrane potential with valinomycin or nigericin induces, respectively, a significant increase or decrease of iodinated amino acids uptakes in different manners, suggesting that protein concentration, plasma and mitochondrial membrane potentials play an important role in the cell uptake. In addition, the radioactivity uptakes measured in normal rat brain after biodistribution studies were low (0.45 ± 0.2 % i.d./g, 30 min p.i.) and comparable with the reported IMT data (0.3 i.d./g, 15 min p.i.), however with higher retention (IMT < ITIQC < L-IPA). These data suggest that the investigated radioiodinated amino acids exhibit interesting characteristics with promise for further *in vivo* brain tumor investigations.

Radiopharmacy and radiochemistry: Ria/Others

PS-750

A. Ando, I. Ando, N. Tonami, S. Kinuya, K. Kazuma, A. Kataiwa, M. Nakagawa, N. Fujita
Faculty of Medicine, Kanazawa University, Kanazawa, Japan

Lu-177-EDTMP : A POTENTIAL THERAPEUTIC BONE AGENT

This study was undertaken to synthesize and evaluate Lu-177-EDTMP (ethylenediaminetetramethylene phosphonic acid) as a therapeutic radiopharmaceutical for the pain palliation of bone metastases.

Lutetium-177 has 176 (12.2 %), 384 (9.1 %) and 497 (78.6%) keV beta particle emissions which are suitable for tissue irradiation. Gamma emissions of 113 (6.4 %) and 208 (11.0 %) keV allow gamma imaging. Its physical half-life (6.75 days) is reasonable in terms of shelf life compared to the relatively short-lived Re-186 or Sm-153. Lutetium-177 can be produced in high specific activity because of high cross section for the Lu-176 (n, γ) Lu-177 reaction.

Lutetium-177 chloride in 1 N HCl solution was purchased from Japan Atomic Energy Research Institute (Tokyo, Japan). EDTMP was commercially available from Dojin Laboratories (Kumamoto, Japan).

Chelation of Lu-177 to EDTMP was simply obtained by heating for 30 min in boiling water at pH 8.8, resulting in the radiochemical yield over 99%. The compound was stable for 20 days without any appreciable dissociation. Biodistribution studies in normal rats indicated selective bone accumulation, showing faster blood clearance, higher bone uptake and higher bone-to-soft tissue ratios than Tc-99m-MDP.

In conclusions, Lu-177-EDTMP would have favorable biological and physical characteristics for the palliative treatment of painful bone metastases.

PS-751

R.Casati, F.R.Colombo, M.Gasparini, A.Fulgenzi, M.M.Corsi, M.E.Ferrero, P.Gerundini.

Nuclear Medicine Department, IRCCS-Ospedale Maggiore, Institute of General Pathology, University of Milan, Milan, Italy.

Tc-99m NAIVE AND MEMORY RAT LYMPHOCYTE LABELING AND IN VIVO BIODISTRIBUTION.

The aim of this study was to evaluate the *in vivo* migration of naive and memory T cells and to define their exact preferential homing. The data clarify the preferential homing of each lymphocyte subset following intravenous injection and appear potentially useful to ameliorate therapy in humans. Lymphocytes are known to selectively migrate into lymphoid organs when displaying a naive phenotype and into non-lymphoid organs when they are memory T cells. This concept has been verified by examining the homing of CD4 and CD8 naive (CD45RC-hi) and memory (CD45RC-lo) cells obtained from the thoracic duct of Fischer rats (inbred). Following intrafemoral injection of each lymphocyte subset labeled with Tc-99m HM-PAO, naive lymphocytes preferred homing to the heart, lung and liver, whereas memory lymphocytes preferentially migrated to the spleen. The data, as revealed by using a gamma camera until 12 hrs and confirmed measuring the radiolabeling distribution by autopsy (as % of injected dose per gram of tissue, table) may be useful for develop a therapy with lymphocyte targeting to selected organs. The results contradict the concept of selective organ-specific migration of naive and memory lymphocytes: the data indicate that, whereas naive lymphocytes migrate first to the heart, lungs, liver and kidneys, memory lymphocytes initially reach the spleen in very large numbers. This finding is useful to accurately predict the location of a subset of lymphocytes immediately after injection or subsequently. The possibility to reach an organ by previously selected lymphocytes from the same patient could permit to study new therapeutic strategies useful in correcting the perturbation of the homeostasis of the lymphocyte population in HIV patients, in cases of transplant rejection, to enhance tumor immunotherapy and also in gene therapy.

TABLE	Heart	Lung	Liver	Kidneys	Spleen	Thymus
Blood lymphocyte(24 hrs)	0.07	0.09	0.31	6.43	1.41	1.36
Lymph lymphocyte	0.18	0.55	0.44	4.95	9.18	0.03
Lymph CD4 naive	0.17	0.39	1.08	5.75	10.11	0.08
Lymph CD4 memory	0.12	0.49	1.59	5.19	16.71	0.15
Lymph CD8 naive	0.13	0.56	1.14	5.86	0.76	0.09
Lymph CD8 memory	0.45	1.37	0.73	5.18	1.53	0.25

PS-752

P. Garnuszek, I. Licińska, J.S. Skierski, M. Koronkiewicz, A.P. Mazurek

Drug Institute, 30/34 Chełmska St, 00 725 Warsaw, Poland.

I-131 LABELLED MIXED LIGAND PLATINUM(II) COMPLEX: RADIOCHEMICAL SYNTHESIS AND *IN VITRO* EVALUATION OF CYTOSTATIC ACTIVITY.

Application of some biological response modifiers (BRMs), equally as adjunctive radiotherapy for potentiation of antineoplastic activity of platinum chemotherapy have been proved effective. Aim of our study is a development of the new generation of platinum based anticancer drugs containing the potential synergistically acting moieties *i.e.* I-131 and biological active ligand. At present stage we have chosen L-methionine molecule (one of the responsible for deactivation of cisplatin *in vivo*) for coordinating to Pt(II)-iodohistamine complex, both for testing mixed ligand platinum complex formation, and for establishing the reference in means of biodistribution and cytostatic activity. **Methods:** The radiochemical synthesis of Pt(II)-[¹³¹I]-iodohistamine complex followed by attaching of methionine molecule has been investigated with chromatographic methods. Biodistribution of the radioiodinated platinum complex in healthy Wistar rats has been compared with that of ¹³¹I-histamine. Based on radiosynthesis scheme, the cold platinum complex has been synthesised and *in vitro* cytostatic activity was tested. Cytostatic/cytotoxic effects of different doses of the platinum complex were investigated using L-1210, HL-60, COLO-205, MOLT-4 and VERO cell lines and flow cytometry method. **Results:** Biodistribution of the HPLC-purified (L-Met;S,N)Pt(131-I-iodohistamine;N⁺)₂ complex resulted in different excretion and activity uptake in the organs compared to ¹³¹I-histamine (*e.g.* with urine: 6.7 and 50.6, in liver: 33.6 and 1.7, in 1 ml of blood: 1.5 and 0.6 %ID at 2h p.i. respectively). The cytometric study showed moderately cytostatic activity of the complex mainly toward COLO-205 and HL-60 cell lines. **Conclusion:** Our results indicate simplicity of the Pt(II) complex formation with iodohistamine (carrier of isotope) and biological ligand - L-methionine, which is stable both *in vitro* and *in vivo*. The mixed ligand platinum complex possess moderately cytostatic activity, and this observation is promising for further studies with application of BRMs, as well as for testing antineoplastic activity on animal tumour models *in vivo*.

PS-753

C. Chebli, S. Buczkowski, L. Cartilier and N.G. Hartman

Faculty of Pharmacy, University of Montreal, Montreal (Quebec) CANADA

CONTROLLED RELEASE STUDY OF RE-186 RHENIUM (VII) OXIDE FROM SUBSTITUTED AMYLOSE TABLETS

Substituted Amylose (SA) polymers were prepared by reacting amylose chains with a suitable substituent, such as glycidol and 1,2-epoxydodecane, in a basic medium. SA polymers were investigated as excipients for matrices obtained by direct compression for drug controlled release of bioactive materials. Using acetaminophen as a model drug, SA matrices released it in a time range of 5 to 20 hours in a phosphate buffer solution (PBS) pH 7.35, depending on the degree of substitution (DS) and the nature of the substituent attached. SA matrices control the drug release by swelling, and the formation of a gel layer. Since these matrices are amylose-based polymers, they are subject to degradation by α -amylase enzymes present in the gastro-intestinal tract. In a classical tablet dissolution study, turbidity of the medium and the interference of present enzymes complicated standard analytical operations, such as spectrophotometry, giving non-valuable results. Seeking an accurate analytical method, gamma spectrometry was used. The idea was also to develop a simple procedure to test our different SA polymers' resistance to enzymatic degradation. For this reason, tablets containing 10% of natural abundant rhenium (VII) oxide as a model drug were prepared, and the PBS pH 7.35 medium was replaced by a PBS pH 6.80 (containing 100,000 units of α -amylase per litre medium). Rhenium (VII) oxide was chosen for its apt properties, having a high neutron irradiation cross-section and being soluble in water. Subsequently, tablets were neutron-activated in a Slowpoke™ reactor at the École Polytechnique using the (n, γ) reaction in a flux of approximately 1×10^{12} neutrons / (cm².sec.). Since natural abundance rhenium was used, we allowed sufficient time for decay of the Re-188 after the neutron activation, before commencing with the investigation. Volumes of 1 ml were taken from each tablet's dissolution bath at various time intervals, and subsequently counted in a Ge(Li) detector system, and all spectrograms were corrected for decay (using the Re-186 energy peaks). During the 21 hour experiment, SA tablets studied maintained their structure and released the Re-186 in a time range of 10 to 15 hours depending on the DS and the nature of the substituent attached, showing no significant degradation of tablets by α -amylase for standard matrix tablets.

Substituted amylose polymers are interesting excipients for the preparation of drug controlled release tablets. In addition to the easy manufacturing of tablets by direct compression, results show that SA polymers can resist α -amylase. In conclusion, this study clearly indicates that SA polymer matrices can be designed to facilitate colonic drug delivery.

PS-754

S.R. Hesslewood, A.P. Mills

Radiopharmacy Department, City Hospital NHS Trust, Birmingham UK

DISPENSING ⁹⁹Tc^m RADIOPHARMACEUTICALS - THE HANDS-OFF APPROACH

Preparation and dispensing of ⁹⁹Tc^m radiopharmaceuticals constitutes the major workload of radiopharmacy departments. Since many procedures are repetitive, automation is desirable, thereby reducing radiation of exposure of personnel.

An automated syringe filling station (SFS Amcare) installed within a laminar flow cabinet has been evaluated. It has the advantage of using disposable syringes and needles which can be filled with solution and subsequently emptied in variable aliquots. It is controlled remotely, thus reducing contact between fingers and radioactive solutions when dispensing. It accurately filled and emptied 2, 5 and 10ml syringes and the timing of such operations is comparable with that achievable manually.

Syringe Size (mL)	% of expected fill (SD)	% retained after emptying(SD)	Time to fill (s)	Time to empty (s)
2	100.0 (2.2)	2.5 (1.4)	78	70
5	98.8 (2.0)	2.5 (1.4)	65	50
10	96.8 (1.8)	1.9 (1.6)	72	47

By adapting working practices to enable several aliquots to be dispensed from a single syringe fill, the time taken has been reduced without loss of accuracy.

Syringe (mL)	Aliquot vol(mL)	% obtained
5	1	102.0 (4.5)
10	1	97.8 (4.8)
10	2	94.8 (3.0)

Monitoring within the laminar flow cabinet has demonstrated that operation of the syringe filling station did not generate either microbial or particulate contamination. The SFS has proved accurate and reliable. It has enabled more efficient throughput and scheduling of work and offers the possibility of large reductions in finger dosage of radiopharmacy staff.

PS-755

Preparation, Quality control and Animal test of ¹⁵³Sm-OEDTMP.

Bai Hongsheng, Jin X.H., Cheng Zh., Du J., Fan H.Q., Zhang J.M., Chen D. M. Wang F., Wang Y.M. Department of Isotope, China Institute of Atomic Energy, P. O. Box 275 (58), 102413, Beijing, China.

Bone metastases often causes serious pain of patient and affects life quality. The aim of my research group was that we tried to design some new seeking-bone agent and labeled with radionuclide (such as ¹⁵³Sm, ¹⁸⁶/¹⁸⁸Re, ⁹⁰Y) in order to relief pain of patients with bone cancer. The synthesis of OEDTMP, labeling condition, establishment of quality control and animal test of ¹⁵³Sm-OEDTMP were introduced in this paper. The labeling efficiency was more than 97% under condition that OEDTMP reacted with ¹⁵³SmCl₃ for 60 minutes at room temperature, pH =7.0-9.0 and mole ratio of OEDTMP / Sm = 60:1. ¹⁵³Sm-OEDTMP was incubated in the 0.9% NaCl solution and 1% HAS solution for seven days, no dissociation was found. The radiochemical purity was determined with column chromatography (cation exchange resin Bio-Rex 70, elution agent : 0.9% NaCl solution) and paper chromatography (Whatman No 1 paper, developing agent : NH₄OH : H₂O=2:40 + 2g NH₄Cl, R_f of ¹⁵³SmCl₃=0.0, R_f of ¹⁵³Sm-OEDTMP=0.9-1.0). The distribution of ¹⁵³Sm-OEDTMP with time in rats were listed in the Table 1. The data of animal test showed that bone uptake reached to maximum at 3hr post-injection (33.37% I.D./g) and liver uptake was 0.315 % I.D./g. The liver and bone uptake of ¹⁵³Sm-OEDTMP were connected closely with injected quantity of OEDTMP. The research results indicated that liver uptake decreased with injected quality of OEDTMP increasing, when injected quantity is at range of 40-100 ug, liver uptake did not decrease. When injected quantity of OEDTMP was more than 200 ug, bone uptake decreased apparently with injected quantity increasing. ¹⁵³Sm-OEDTMP is excreted in original form.

Table 1. Distribution of ¹⁵³Sm-OEDTMP with time in rats (% I. D./g)

Time	blood	liver	bone	muscle	heart	kidney
0.5h	0.775	1.045	10.450	0.556	0.311	1.098
3.0h	0.215	0.315	33.370	0.112	0.102	2.100
24.0h	0.098	0.289	28.910	0.056	0.034	0.890

PS-756

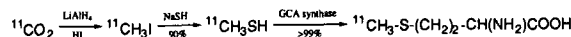
S. Kaneko, K. Ishiwata, S. Ishii, H. Omura, M. Senda.

Positron Medical Center, Tokyo Metropolitan Institute of Gerontology and Ikeda Food Research Co., Ltd.

AN ENZYMATIC APPROACH TO [¹¹C]-L-METHIONINE SYNTHESIS

[¹¹C]-L-Methionine ([¹¹C]MET) is very useful for clinical PET as a tumor imaging agent. We developed a new synthesis method for [¹¹C]MET by the immobilized γ -cyano- α -aminobutylic acid (GCA) synthase.

Method: GCA synthase from *Bacillus stearothermophilus* was prepared from the cell free extract of recombinant *E. coli*. [¹¹C]Methyl iodide obtained from [¹¹C]CO₂ was converted to [¹¹C]methanethiol instantaneously. Mixture of [¹¹C]methanethiol and *O*-acetyl-L-homoserine was passed through the immobilized GCA synthase column at room temperature within 30 sec. After dryness in vacuo, the residue was dissolved in physiological saline and the solution was passed through a membrane filter.



Results: The radiochemical yield and radiochemical purity of [¹¹C]methanethiol was approximately 90 % and >99 %, respectively. Within 15 minutes from EOB, radiochemically and enantiomerically pure [¹¹C]MET was prepared with the radiochemical yield of approximately 70 % based on [¹¹C]methyl iodide.

Conclusion: This method provides a useful and practical new approach to obtain radiochemically and enantiomerically pure [¹¹C]MET with the high radiochemical yield.

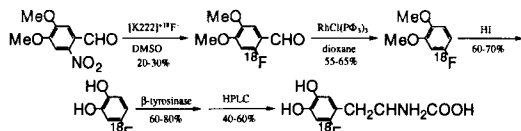
PS-757

S. Kaneko, K. Ishiwata, K. Hatano, M. Honda, K. Ito, H. Omura, M. Senda
Positron Medical Center, Tokyo Metropolitan Institute of Gerontology.; Ikeda Food Research Co., Ltd.; Department of Biofunctional Research, National Institute for Longevity Sciences.

AN ENZYMATIC APPROACH TO N.C.A. 6-[18F]FDOPA SYNTHESIS

6-[18F]FDOPA is widely used for studying the presynaptic dopaminergic function by PET. We have developed a new approach for production of 6-[18F]FDOPA with β -tyrosinase.

Methods: The method consists of chemical synthesis of 4-[18F]fluorocatechol followed by enzymatic reaction with pyruvate and ammonia. β -Tyrosinase from *Citrobacter intermedius* was prepared from the cell free extract of recombinant *E. coli*.



Results: 4-[18F]Fluorocatechol, which was very unstable, was isolated only in acidic ethanol with the radiochemical yield of 9.2%. By enzyme reaction, 4-[18F]fluorocatechol was effectively converted to 6-[18F]FDOPA (60-80%) within five min under 5% ethanol solution. By preparative HPLC, radiochemically and enantiomerically pure 6-[18F]FDOPA was isolated with the radiochemical yield of 2.0%. Total synthesis time was about 150 min from EOB.
Conclusion: N.c.a. 6-[18F]FDOPA was enzymatically synthesized from 4-[18F]fluorocatechol with a high conversion yield.

PS-758

T. Nikula¹, E. Havas², A. Savonen¹, J. Toivanen³, V. Viikko³, J. Hiltunen¹

¹ MAP Medical Technologies Oy, Tikkakoski, Finland, ²LIKES-Research Center, Jyväskylä, Finland ³Central Hospital of Central Finland, Jyväskylä, Finland

CLEARANCE OF 99mTc-HSA AFTER INTRAMUSCULAR INJECTION

The purpose of this study was to compare different commercial 99mTc-HSA kits for the use in studies on the lymph flow dynamics in skeletal muscle. three commercial hsa kits were labeled with 99mTc according to manufactures' procedure and native HSA was labeled using ascorbic-acid method. Quality control of the labeled 99mTc-HSA preparations were performed using FPLC with Superdex 200 HR 10/30 column and ITLC strips.

100-150 μ l injection of 99mTc-HSA (20-60 MBq) was injected into biceps brachialis muscles of 11 health volunteers. During the first 45 min after injection the muscles were at rest, then 10 min bouts of submaximal elbow flexions were performed with 30 min intervals. LFWO gamma-images were obtained from the injection site every 15 min for a four hour period.

The labeling efficiencies of the commercial kits were over 98% measured by ITLC. The results of quality control with FPLC-Superdex 200 HR 10/30 column are collected on the following table. The percentages represent the activity:

	< 20000 Da	Monomer	Dimer	Tetramer	Macromolec.
HSA KIT-1	2.0	44.7	46.9	4.6	1.8
HSA KIT-2	21.7	83.7	10.1	1.7	2.8
HSA KIT-3	19.7	55.7	17.9	5.1	1.7
Ascorbic acid		56.7	4.4		38.9
Purified HSA		100			

Clearance of different preparations are shown on the table below. The four hour total clearance was 31% for macromolecular-HSA, whereas that of monomer HSA was 54% and that of the dimer-monomer-HSA 56% (in three hours).

Time and treatment	Macromolecular	Monomer-dimer	Monomer
0-45 min, rest	0.18	0.71	0.74
45-90 rest+exercise	0.18	0.27	0.18
90-180 rest+exercise	0.12	0.12	0.10
180-240 rest+exercise	0.08	-	0.06

The markedly different behaviour of the preparations must be taken into account when intramuscular fluid dynamics and lymph flow are to be studied.

PS-759

AC PERKINS, M FRIER, JM HEBDEN, PE BLACKSHAW, PJ GILCHRIST, CG WILSON
Depts. of Medical Physics, University Hospital, Nottingham and Pharmaceutical Sciences, Strathclyde University.

VALIDATION OF SCINTIGRAPHY FOR MONITORING THE INVIVO RELEASE OF ORAL PHARMACEUTICAL FORMULATIONS

Introduction: Scintigraphic studies are gaining importance as a method for monitoring the time and site of *invivo* release of orally administered drugs. These place stringent requirements on both good manufacturing practice (GMP) and good clinical practice (GCP). We have validated the accuracy of our scintigraphic method by performing both *invitro* and *invivo* studies of formulation release.

Methods: Immediate release tablets containing Tc-99m-lactose were placed in an *Erweka* dissolution apparatus and dynamic images recorded. Visual time of release was compared with data from activity time curve data. *Invivo* studies were undertaken on 65 occasions in volunteers taking delayed release gelatin capsules containing 1MBq In-111-amberlite resin and 50mg quinine dihydrochloride (a rapidly absorbed plasma marker). Correlation of site and time of formulation release was assessed from images and measurements of quinine in blood measured by reversed phase HPLC.

Results: Dynamic images showed *invitro* dispersion of the tablets within 2 minutes, this being no different to that of the control tablets. Scintigraphic measurements of the onset of capsule release *invivo*, up to 12 hours after oral administration correlated well with the appearance of plasma quinine ($r = 0.836$), thus justifying the experimental technique.

Conclusion: These data confirm the accuracy of gamma scintigraphy for monitoring formulation release. Validation of the radiolabelling and scintigraphic techniques are an essential feature of studies of this nature.

PS-760

M.Roca, F. Armero, V. Garcia, F. Iglesias, A. Muñoz, A. Fernández, A. Benítez, V. Gomes and J. Martín-Corin.
S. Medicina Nuclear. Hospital de Bellvitge. L'Hospitalet de Llobregat. Spain.

STABILIZATION OF Tc-99m-d,l-HM-PAO USING TOUIDIN BLUE AND ITS USEFULNESS IN THE LABELLING OF LEUKOCYTES. FIRST RESULTS.

Background: Toluidin blue (TB) has been mainly used as anti-metahaemoglobinemia drug in nitrate, nitrite, or aromatic amine poisoning. TB has a structural formulae similar to methylene blue, and like it, it is able to stabilize Tc-99m-d,l-HM-PAO (TcHMPAO).

Purpose: Improve the stability of the TcHMPAO using TB and test the usefulness of the stabilized TcHMPAO in the labelling of leukocytes.

Material and Methods: TB concentrations from 0.01 to 2% were tested. In order to stabilize the TcHMPAO, a volume of TB solution equal to the 10% of the radiopharmaceutical was added. 20 leukocyte concentrations were labelled according to our standard labelling method using both : 2 h stabilized TcHMPAO, and unstabilized just prepared TcHMPAO.

Results: TB at concentrations between 0.05% and 2%, with a final pH comprised between 6 and 7, stabilized the radiopharmaceutical in the same degree, obtaining a radiochemical purity at 6 h greater than 90%. Using 0.1% TB in 0.001N HCl, we obtained the following radiochemical purity (RP):

	10 min.	2 hours	4 hours	6 hours
%RP (m \pm sd)	96.5 \pm 1.23	96.4 \pm 0.95	95.9 \pm 1.02	95.1 \pm 1.50
N $^{\circ}$ samples	84	80	44	49

Leukocyte labelling efficiencies were 70.9 \pm 5.2% and 71.9 \pm 4.3% using 2 h stabilized and unstabilized TcHMPAO respectively and they didn't show statistical differences. In 8 of them, we measured the TcHMPAO bound to the cells at 2 h and at 4 h after labelling. The percents of activity were 93.4 \pm 0.7% and 93.2 \pm 0.8% at 2 h and 87.6 \pm 2.3% and 87.3 \pm 1.8% at 4 h, using stabilized TcHMPAO and non-stabilized TcHMPAO respectively. No statistical difference was found. The Eosin Y test in all leukocyte samples showed always an *invitro* viability greater than 98%.

Conclusions: 1) TcHMPAO can be efficiently stabilized with Toluidin Blue. 2) The 2 h stabilized TcHMPAO can label leukocytes with the same labelling efficiency and quality as unstabilized TcHMPAO.

Poster presentations

PS-761

F. Szelecsényi, S. Takács, F. Tárkányi, M. Sonck*, A. Hermanne*
 Institute of Nuclear Research of the Hungarian Academy of Sciences, Debrecen,
 P.O.Box 51, Hungary, H-4001 and *Cyclotron Department, Vrije Universiteit Brussel
 (VUB), Laarbeeklaan 103, 1090 Brussels, Belgium

STUDY OF PRODUCTION POSSIBILITY OF ¹⁸⁶Re VIA THE ¹⁸⁶W(d,n)¹⁸⁶Re NUCLEAR REACTION FOR USE IN RADIOTHERAPY

Rhenium-186 has been regarded as an ideal radionuclide for radioimmunotherapy because of its decay properties. For its routine production the ¹⁸⁶W(p,n)¹⁸⁶Re reaction was recently proposed by Shigettha *et al.* [1]. However, the available physical yield of this reaction is rather low (~5 MBq/μAh). The aim of the present work was to investigate the W+d processes as an alternative route for routine production of ¹⁸⁶Re. In our present study we have (1) investigated the excitation function of the ¹⁸⁶W(d,n)¹⁸⁶Re nuclear reaction from the threshold up to 21 MeV (to clear the contradictions found among the previously presented results), and (2) optimized the production of ¹⁸⁶Re via the above reaction.

For the cross section measurements natural tungsten foils of 25 μm (14 pcs) were activated in the form of a stack at the CGR-560 cyclotron (VUB, Brussels) with an incident deuteron energy of 21.12 MeV. The activity of the irradiated foils were measured without chemical separation using HPGe detector coupled to PC-based multichannel analyzer.

Cross sections were calculated from the measured activities for the natW(d,n)¹⁸⁶Re reaction as well as for some processes that resulted in other longer lived Re isotopes (i.e. natW(d,x)¹⁸²Re, natW(d,x)¹⁸³Re and natW(d,x)¹⁸⁴Re). The excitation function of the ¹⁸⁶W(d,n)¹⁸⁶Re reaction seems to reach its maximum of ~430 mb at about 12.5 MeV. (The ¹⁸⁶W(p,n) reaction has a maximum value of only ~100 mb at about 10 MeV.) Comparing our experimental values with the available results of Pement *et al.* [2] and Nassif *et al.* [3] it can be concluded that our values are in good agreement with the early values of Pement *et al.* [2] over the investigated energy region and make questionable the work of Nassif *et al.* [3].

Taking into account of the present cross section measurements the available yield is higher than the yields via the W(p,n) reaction. The optimum energy range for the production of ¹⁸⁶Re was found to be 18→10 MeV. For production purposes, however, it is suggested to use highly enriched ¹⁸⁶W both to increase the available yield (max. ~350%) and to decrease the yields of the undesirable contaminants.

- [1] Shigettha N. *et al.* *J. Radioanal. Nuclear Chemistry, Articles* 205(1996)85
- [2] Pement F. W. *et al.* *Nucl. Phys.* 86(1966)429
- [3] Nassif S. J. *et al.* *Radiochim. Acta* 19(1973)97

General topics: Radiation protection/quality control/others

PS-762

L. Johansson⁽¹⁾, S. Mattsson⁽²⁾, B. Nossli⁽²⁾, T. Smith⁽³⁾, D. Taylor⁽⁴⁾

⁽¹⁾Umeå Univ. Hospital Dept. of Radiation Physics, ⁽²⁾Malmö Univ. Hospital Dept. of Radiation Physics, ⁽³⁾Great Ormond Street Hospital for Children, Dept. of Radiology, ⁽⁴⁾University of Wales Cardiff, Department of Chemistry.

DOSE TO PATIENTS FROM RADIOPHARMACEUTICALS - RECENT ACTIVITIES OF AN ICRP TASK GROUP

A Task Group of the International Commission on Radiological Protection (ICRP) on Dose to Patients from Radiopharmaceuticals has recently prepared a second supplement to the ICRP Publication 53, "Dose to the Patient from Radiopharmaceuticals." The first Addendum, which included a table of effective doses from radiopharmaceuticals calculated with the new weighting factors of ICRP Publication 60 was published in 1993 as an inclusion in ICRP Publication 62.

New radiopharmaceuticals that the Task Group has included in Addendum 2 are shown in the table below, which also includes the effective dose per unit activity administered for adults. The coming report will also contain results from recalculations for a number of common radiopharmaceuticals. This comprises organ doses as well as the effective dose. The absorbed dose has been calculated applying the biokinetic data in ICRP Publication 53 completed with the new age-dependent bladder-voiding model presented in Addendum 1.

Radiopharmaceutical	E (mSv MBq ⁻¹)	Radiopharmaceutical	E (mSv MBq ⁻¹)
In-111 Octreotide	0.054	Tc-99m Perthechnegas	0.0012
In-111 labelled HIG	0.16	O-15 Water	0.0010
Tc-99m labelled HIG	0.0065	Methyl C-11 thymidine	0.0033
Tc-99m Tetrofosmin, rest	0.0076	2-C-11 thymidine	0.0026
Tc-99m Tetrofosmin, stress	0.0070	C-14 urea, helicobacter negative	0.025
Tc-99m Technegas	0.015	C-14 urea, helicobacter positive	0.071

PS-763

K.Ejiri, K.Minami, M.Kato, S.Maeda, T.Nishimura, K.Suzuki, H.Toyama, T.Orito, and S.Koga
 Departments of Health Physics and Radiology, Fujita Health University, Toyoake, Japan

RADIATION DOSE RATE FROM PATIENTS UNDERGOING Tc-99m-GSA STUDY

To estimate the radiation dose of a person who may come into close contact to the Tc-99m-GSA (administration dose of 185 MBq) patients, dose rates around 15 adult patients were measured with three ionization surveymeters (Aloka ICS-301). These surveymeters were set up to the first cervical vertebrae (Level I), xiphoid process (Level II) and anterior superior iliac spine (Level III) of the patients. Dose rate measurements were carried out at 0.7 h, 3 h, 6 h and 24 h after injections of Tc-99m-GSA solutions. Distances between the detectors and patients were 0.05 (surface), 0.5, 1.0 and 1.5 m. The maximum dose rate of 4.26 mR/h was recorded at 0.05 m in the first detection (0.7 h). Dose rates at 0.5, 1.0 and 1.5 m from the patients were one-fifth, one-tenth and one-twentieth of the surface rates, respectively. The effective half life of the Tc-99m-GSA in human body was 5.8 h. Total doses around the patients was calculated from the initial dose rates and the effective half life as shown in table 1.

Table 1. Total equivalent dose (H_{1cm}) and effective dose (E) around Tc-99m-GSA patients.

Dose evaluation tissue	μSv/°h/185MBq (n=15)			
	Distance from ^{99m} Tc-GSA patient			
	0.05m	0.5m	1.0m	1.5m
Head and neck (H _{1cm, Level I})	106	45	20	11
Thorax and brachium (H _{1cm, Level II})	367	70	25	14
Abdomen and femur (H _{1cm, Level III})	264	62	24	13
Effective dose (E)	289	64	24	13

$E = 0.06H_{Level I} + 0.28H_{Level II} + 0.61H_{Level III} + 0.05H_{MAX}$

Tc-99m-GSA patients might provide only a small risk to persons around them, but to their family it would be necessary to recommend avoiding a long contact with them at a short distance for one day after a administration of a Tc-99m-GSA solution.

PS-764

M. Medvedec, D. Grošev, D. Dodig, Ž. Pavlinović

University Hospital Rebro, Department of Nuclear Medicine and Radiation Protection, Zagreb, Croatia

EXTERNAL RADIATION DOSIMETRY ASPECTS OF PATIENTS RECEIVING ABLATION RADIOIODINE FOR THYROID CANCER

The purpose of this work was to consider thyroid cancer patients as an external sources of radiation following administration of radioactive iodine (I-131), in regard to the recommended radiation precautions usually taken into account (retained bodily activity < 1110 MBq, instantaneous absorbed dose rate < 50 μGy/h, effective absorbed dose < 1 mSv). Thirty patients were investigated after ablation I-131 activity was administered because of residual thyroid tissue after surgery. Collimated whole-body counter was used to determine whole body retention by means of net full energy spectrum supine and prone counts, in order to minimize effects of activity distribution, body size and statistical counting uncertainties. Absorbed dose rates were measured at one meter distance from the patient by calibrated beta-gamma survey meter. A correction for deadtime was made if it was necessary. The fitting of the curve of activity and dose rate against time was performed for each patient using typically six points data set. Biexponential effective radiation decay was found; whole body activity as $A(t)/A_0 = 0.86 \exp(-0.0863t) + 0.14 \exp(-0.0224t)$ and absorbed dose rate as $DR(t)/DR_0 = 0.89 \exp(-0.0888t) + 0.11 \exp(-0.0224t)$, where $A_0 = 2533 \pm 874$ MBq and $DR_0 = 137.0 \pm 47.1$ μSv/h were initial mean ± SD whole body activity and absorbed dose rate, and numerical parameters were mean relative intensity and decay constant for each exponential component. Mean effective half-times of short and long lived components were 9.1 ± 2.5 and 44.7 ± 29.7 h for retained whole body activity, and 9.1 ± 2.8 and 44.9 ± 31.9 h for absorbed dose rate. Mean absorbed dose rate per unit retained activity was 0.055 ± 0.022 μSv/h/MBq during the first 168 hours after radioiodine administration. Because of the rapid effective radiation decay observed, thyroid cancer patients receiving standard ablation activity of 1.1 GBq and 4.4 GBq I-131 may generally be discharged from the hospital on the day 0 and 1 following treatment respectively, keeping the effective absorbed dose of constantly exposed hypothetical individual at one meter from the patient below 1 mSv. Our data, therefore, suggest more liberal policy in regard to the radiation safety precautions during ablation procedure.

PS-765

J.H. Risse, C. Ponath, F. Grünwald, Hj. Biersack
Department of Nuclear Medicine, University of Bonn, Germany

NEW DEVELOPMENTS IN RADIATION PROTECTION IN INTRAARTERIAL I-131-LIPIODOL LIVER THERAPY

Purpose: Assessment of radiation doses to the medical staff in intraarterial application of I-131-Lipiodol in liver malignancies and amelioration of the radiation protection system.

Methods: 11 patients were treated by 17 intraarterial applications of I-131-Lipiodol (1110 - 1924 MBq) during hepatic angiography. Radiation doses (RD) to the fingers, eyes, and whole body during injection and post-angiography patient care were determined. A lead container with two outlet canals was developed to be filled with a tube containing the nuclide, thus allowing transport and application of highly radioactive material from a great distance without risk to the staff under usual angiography conditions. Additionally, a lead cover put on the patient's abdomen after angiography was introduced.

Results: The lead container (a) allowed application from a long distance and (b) reduced the risk of contamination. Finger RD during application could be reduced from initially 20,000 µSv to < 10 µSv and eye RD from 90 to < 5 µSv. During post-angiographic patient care, the abdominal lead cover reduced the radiation load by 30 %. The finger RD during femoral artery compression is unavoidably about 120 µSv, but the whole body dose was reduced from 120 to 15-25 µSv.

Conclusions: A significant reduction of radiation dose to the medical staff during and after angiography-guided radionuclide application was achieved by the new radiation protection system. This equipment will work for all liquid radionuclides including those with high viscosity and high activity and might improve the compliance for such procedures.

PS-766

JC Alonso, A Soriano, A.G. Vicente, C. Rubio *, C Encinas **, C Molino.
Nuclear Medicine Unit, Department of Rheumatology*, Department of Pharmacology**
C. Hospitalario de Ciudad Real, Plaza de Pio XII s/n 13002 Ciudad Real, Spain.

QUALITY CONTROL OF Tc-99m HMPAO LABELED LEUKOCYTES

The quality control of Tc-99m HMPAO labeled leukocytes is a critical step of image evaluation. The quality control may be affected by several factors: labeling efficiency, quality control of Tc-99m HMPAO, leukocytes viability, etc. Few studies have reported the factors that influence the labeling efficiency of Tc-99m HMPAO labeled leukocytes. **Purpose:** 1. - To evaluate the factors influencing the labeling efficiency 2. - To determine the correlation between labeling efficiency and images quality. **Methods:** we have studied 35 consecutive patients (13 men and 22 women and age 43.21±15.74 yr). The previous diagnoses were: 15 to detect intestinal involvement in patients with seronegative spondyloarthropaties, 10 bowel inflammatory disease and 10 to confirm infectious disease. The labeling efficiency was determined = (Resuspended Tc-leukocyte activity) / (resuspended Tc-leukocyte activity)+(supernatant activity). The following parameters were assessed: quality of the HMPAO, medication and hematology values (erythrocytes, leukocytes and platelets). The quality of the images was evaluated in two ways: A) Assigning a visual scale of 1 (bad), 2 (regular) or 3 (good) B) Assessing the uptake percentage between bone marrow and background in a semiquantitative scale. **Results:** The means percentages of labeling efficiency were 52.14 (± 3.36, 44.50 lowest, 59.80 highest), while the quality of Tc-99m HMPAO were higher than 90% (92.85% ± 6.9).

VARIABLE: Labeling efficiency of leukocytes and:	Correlation Coefficients	P	Significance
Quality Tc-99m HMPAO	0.206	0.339	NO
Leukocytes	0.061	0.78	NO
Hematocrite	-0.514	0.014	YES
Hemoglobin	-0.563	0.006	YES
Medications		0.429	NO
Quality of the images	-0.14	0.618	NO

Conclusion: 1. - The quality control of Tc-99m HMPAO labeled leukocytes is not influenced by just one parameter but probably by a combination of several factors. 2. - The percentage of labeling efficiency doesn't influence in the quality the images.

PS-767

J Davidson, F W Poon, J H McKillop, H W Gray
Department of Nuclear Medicine Royal Infirmary Glasgow
Scotland United Kingdom

PETHIDINE AUGMENTED HMPAO WHITE CELL STUDY (PRELIMINARY RESULTS)

The purpose of this study is to assess whether we can increase our confidence of reading the HMPAO white blood cell scans in our institution by reducing the gastrointestinal excretion of the tracer with the use of a small dose of iv pethidine.

All patients with suspected inflammatory bowel disease are fasted overnight and for the duration of the study. Intra venous pethidine at a dose of 0.3mg/kg body weight is administered at the same time as re-injection of the labelled white blood cell. Standard images are acquired at one hour and 2.5 hours after injection. The scans are graded by two observers. Grade 0 is considered negative and Grade 1-3 are less, equal and more intense uptake than bone marrow. Grade 4 uptake is equal to splenic uptake.

46 patients were recruited in this preliminary trial, with 23 patients in the control (ie fasted but without pethidine) and 23 patients in the pethidine group. In the control group, there were four normal and 12 abnormal scans. In the pethidine group, there were 13 normal and eight abnormal studies. 7 (30.5%) studies in the control group and 2 (8.7%) in the pethidine group were deemed non-diagnostic because of the presence of Grade 1 small bowel uptake at one hour and Grade 1 or 2 uptake at 2.5 hours. This is just outside the significance level (p=0.06) but we hope that a larger patient sample will clarify the situation further.

Conclusion

The gastrointestinal excretion of tracers is known to cause difficulties in interpreting HMPAO white blood cell scans. The use of low dose intravenous pethidine may reduce this and therefore decrease the number of non-diagnostic studies.

PS-768

E.Delcourt, Ch.Henuzet, W.Kostucki, R.Amir, P.Tran, K.Zouaoui, M Vanhaeverbeek
C.H.U. VESALE 6110 Montigny le Tilleul BELGIUM

VARIABILITY OF LEFT VENTRICULAR EJECTION FRACTION ESTIMATED FROM DIFFERENT TECHNIQUES

This study assessed the range of agreement of left ventricular ejection fraction (EF) obtained from four different methods in a sample of 46 patients.

Method: After injection of 700 Mbq of 99mTc HSA, patients underwent an equilibrium nuclear angiographic study (N) in the LAO projection. N study was processed either with a fixed (Nf) or a variable (Nv) ROI method. EF was also calculated from biplane echography (Ec) and from monoplane contrast angiography (An). Agreement of the 4 methods was evaluated from ANOVA and Bonferroni tests. The test of Bland and Altman was applied thereafter, determining the bias or mean difference (MD) and the standard deviation (SD) of the measurements obtained with each pair of methods.

Results: ANOVA showed a significant difference between the 4 techniques (p < 0.05), due to a lack of agreement of An with the other methods (Bonferroni test p < 0.05). There was no significant difference between the other 3 methods. Agreement of each pair of methods was as follows:

	An-Nf	An-Nv	An-Ec	Ec-Nf	Nv-Nf	Ec-Nv
MD	5.6	5.0	7.5	-1.9	0.6	-2.5
SD	15.0	12.8	13.9	11.6	6.8	9.7

Conclusion: An gives a systematic overestimation of the EF and the lowest agreement with any of the other methods. While there is no significant difference in the EF measured from Nf, Nv or Ec in the population sample as a whole, EF should however be interpreted with some caution in clinical practice, owing to the fairly weak agreement of different methods in individual patients, in the range of that reported in other studies.

Poster presentations

PS-769

G. Sobal, H. Sinzinger

Department of Nuclear Medicine, University of Vienna, Austria.

HOW TO ENHANCE THE STABILITY OF (^{99m}Tc) HMPAO AND HOW TO SIMPLIFY THE QUALITY CONTROL PROCEDURE-A COMPARATIVE STUDY.

Technetium-99m d,l-hexamethyl propyleneamine oxime (^{99m}Tc) HMPAO is a radiopharmaceutical that is being used for SPECT imaging of regional cerebral perfusion and for labeling of blood cell elements. The use of this radiopharmaceutical is often limited because the technetium labeling of freeze-dried HMPAO kit produces a lot of impurities (pertechnetate, reduced-hydrolysed technetium and secondary complex) changing with time. We have found that the stabilisation with methylene blue enhances the stability of lipophilic (^{99m}Tc)HMPAO complex up to 3 hours after reconstitution. (82.4%±3.4 versus 55.4%±4.9, n=12 p<0.0001 for not stabilised) and is persistent over the time (87.0%±2.0 after 15 min versus 82.4%±3.4 after 3 hours, n=12 n.s.). The method used for radiochemical purity estimation was a standard chromatographic procedure which needs paper and instant thin-layer strips in three different solvents and is quite time-consuming taking about 30 min. Using the more rapid and simple solvent extraction method with octanol which needs only about 10 min to complete we could obtain a good correlation with a chromatographic method (85.5%±3.7 versus 87.0%±2.0 n=12 n.s.). Using ethyl acetate as solvent instead of octanol we found a higher extraction-rate of the lipophilic complex of about 10% (94.9%±6.3 versus 85.5%±3.7 n=12 p<0.001). We therefore conclude, that the stability of the lipophilic (^{99m}Tc)HMPAO complex can be enhanced with methylene blue and the ethyl acetate extraction method is the most rapid and efficient method to perform the quality control for (^{99m}Tc)HMPAO in clinical routine.

PS-770

B. E. Zimmerman, J. T. Cessna, B.M. Coursey, and D. B. Golas*

Physics Laboratory, National Institute of Standards and Technology, Gaithersburg, MD, USA; Nuclear Energy Institute, Washington, DC, USA.

THE ROLE OF THE NATIONAL INSTITUTE OF STANDARDS AND TECHNOLOGY IN MEASUREMENT AND QUALITY ASSURANCE FOR THE RADIOPHARMACEUTICAL INDUSTRY IN THE UNITED STATES.

The National Institute of Standards and Technology (NIST) is the primary standardization body for radionuclides used in nuclear medicine in the United States. As part of a Cooperative Research and Development Agreement (CRADA) with the Nuclear Energy Institute (NEI), NIST supervises and administers an expanding measurement assurance program for the radiopharmaceutical industry. This provides traceability for the suppliers of radiochemicals and radiopharmaceuticals, dose calibrators, and nuclear pharmacy services. The United States Food and Drug Administration (FDA) also participates as part of a separate CRADA. During a yearly cycle, 10 samples prepared at NIST of known, but undisclosed, activity are distributed to each of the participants to be assayed. The radionuclides, chosen by the participants, are those of interest to the industry, such as strontium-89 and phosphorus-32. There are also two "open months" for participants to send samples to NIST to be calibrated. In addition to the measurement assurance program, NIST also maintains one of the most active research programs in the world for developing radioassay techniques and calibrations for new radionuclides being investigated for use in nuclear medicine. The existence of a radioassay protocol that is traceable to NIST is generally a prerequisite for approval by FDA for the marketing of new radiopharmaceuticals in the United States. The radionuclides to be standardized are decided through the Medical Subcommittee of the Council for Ionizing Radiation Measurements and Standards (CIRMS) or by direct request from laboratories and companies researching new radiopharmaceuticals. NIST has already standardized and maintains standards for a long list of radionuclides used in nuclear medicine. This paper details the recent activities of the Radiopharmaceutical Standards Program at NIST and will discuss how new standards are produced, citing examples from some of the more recently standardized nuclides, which include fluorine-18, tin-117m, and holmium-166.

PS-771

L. Burroni, G. Ciofetta, P.F. Rambaldi, G. Boni, A. Lupi, A. Signore, L. Feggi, D. De Palma, F. Dalla Pozza, G. Bonelli* and N. Magnani*, The Italian Group of Pediatric Nuclear Medicine and Institute of Psychiatry*, University of Siena, Siena, Italy.

SCINTIGRAPHIC EXAMINATIONS IN CHILDHOOD: THE PSYCHOLOGICAL IMPACT ON PARENTS.

The burden of radiation for children is a well known hazard in nuclear medicine and it is sometimes difficult to explain to the parents procedures and risks involved in examination since clinicians give insufficient explanation or frighten the children's parents. The aim of our study is to evaluate the psychological impact of scintigraphic examination on parents, their knowledge of the exam and positive or negative aspects revealed. 261 multiple-answers questionnaires were collected over 2 months from 9 Italian departments of Nuclear Medicine. It was filled in by 376 parents (M: 36.7±8.0 yrs.; F: 34.5±5.8 yrs.) accompanying their children (aged 5.9±4.4 yrs.) to scan examinations. 78.6% of the parents reported being fairly informed about the illness of the child; only 61.5% of them had received adequate explanation of the scintigraphic examination. The parents evaluated their child's examination as indispensable (45.8%), very useful (40.9%), somewhat useful (12.8%), useless (0.04%) or noxious (0.006%). 85.2% of the parents were satisfied with the service offered during examinations, 0.03% were unsatisfied and the others did not comment. 26.0% of the parents desired further information concerning the examination, 11.2% found the nuclear medicine departments unfit for children and 21.0% felt scintigraphy to present risks. The positive factors most frequently mentioned were kindness and knowledge of the health staff, while the negative aspects were the long wait for examination and small waiting-rooms. Preliminary results show that scintigraphic examinations are well accepted by parents and considered very useful for correct diagnosis. However, further information regarding examination could reduce the anxiety of parents probably related to radiation burden. Nuclear medicine personnel appears capable of dealing with young patients, although a more suitable atmosphere for children would be desirable.

PS-772

A. Kubo, N. Tamaki.

Subcommittee for Surveillance of Nuclear Medicine Practice, Medical and Pharmacological Committee, Japan Radioisotope Association, Japan

NUCLEAR MEDICINE PRACTICE IN JAPAN: A REPORT OF THE 4TH NATION-WIDE SURVEILLANCE IN 1997.

Nation-wide surveillance of in-vivo and in-vitro nuclear medicine practice is performed every 5 years in Japan by the Subcommittee for Surveillance of Nuclear Medicine Practice. Our subcommittee mailed to 1241 institutes and 1195 of them (96.3%) answered the questionnaires about the number of radionuclide studies over one month to estimate annual number of total tests and specific tests. The in-vivo study results in 1997 were compared to the previous results.

Years	1982	1987	1992	1997
Estimated No. of tests	1,500,000	1,560,000	1,645,000	1,860,000
Bone imaging	11.1%	19.1%	24.5%	27.1%
Cardiac study	5.6%	10.4%	13.5%	26.8%
Brain study	2.3%	2.5%	10.0%	13.6%
Tumor imaging	7.9%	12.1%	14.1%	12.9%
Renal study	3.0%	5.2%	3.6%	6.7%
Thyroid study	14.5%	13.0%	8.2%	4.8%
Pulmonary study	3.5%	3.5%	3.4%	3.5%
Liver study	23.8%	9.1%	3.6%	2.4%

A total estimated number of in-vivo tests significantly increased by 13% in 5 years. A great increase in cardiac (79%) and brain (44%) studies is noted, mainly due to new radiopharmaceutical development, such as I-123 BMIPP and I-123 MIBG for cardiac studies, and I-123 IMP, Tc-99m HMPAO and Tc-99m ECD for brain studies. A constant increase in bone imaging is also noted over 20 years. A great change also in in-vitro nuclear medicine practice was seen for 5 years. This report should be useful for understanding the current trends in in-vivo and in-vitro nuclear medicine procedures in Japan.

PS-773

J.M. Martí-Climent, I. Peñuelas, R. Calvo, MJ García-Velloso, J.A. Richter
PET-CUN Center. University Hospital. School of Medicine. University of
Navarra. Pamplona. Spain

**REGIONAL DISTRIBUTION OF ^{18}F -FDG FOR POSITRON
EMISSION TOMOGRAPHY**

The increasing interest on positron emission tomography and costs optimization suggest the possibility of 'regional' distribution of ^{18}F -FDG to nearby centres.

The Cyclone 18/9 cyclotron is used to produce ^{18}F bombarding H_2^{18}O with 18 MeV protons. The saturation yield is 9.25 GBq/ μA (250 mCi/ μA), thus allowing the production of 111 GBq (3 Ci) after 2 hours of bombardment.

^{18}F -FDG is produced by an automated synthesis module with a yield higher than 50 % (uncorrected), in a 28 minutes synthesis. An aliquot is submitted to the laboratory for the radiopharmaceutical quality control procedures to ensure final product and safety.

^{18}F -FDG is shipped in a 25 cm³ vial included in a package meeting the national transportation regulations for radioactive materials. The package consist of: a first 3 cm lead container, a second 3 cm lead container (concentric), foam, and a stainless steel can (54 cm x Φ 38 cm), with a total weight of 44 kg. For a package containing 3.7 GBq (100 mCi), the exposure rate at the container surface is 10 $\mu\text{Sv/h}$, and 1 $\mu\text{Sv/h}$ at a distance of 1 m (Transportation Index = 0.1).

Considering a total transportation time of 120 minutes, utilising private air and ground couriers, it is possible to distribute 22.2 GBq (600 mCi) of ^{18}F -FDG and perform 7 PET explorations, with the arrival activity and allowing 1 hour between administrations of 370 MBq (10 mCi) per patient.

The regional distribution of ^{18}F -FDG is feasible, providing the availability of this product on sites where no cyclotron is available, and due to the combination of a high production cyclotron and an efficiency synthesis module, the distribution do not set constrains to the onsite overall work load with ^{18}F -FDG and other radiopharmaceuticals.

PS-774

G. De Laet, J. Naudts, J. Vandevivere
Universiteit Antwerpen UIA and
AZ Middelheim, Department of Nuclear Medicine

PROCESS AUTOMATION IN A NUCLEAR MEDICINE DEPARTMENT

State of the art information systems in a department of nuclear medicine consist of a Picture and Archiving Communication System (PACS) integrated with a local administrative system (Radiology Information System RIS), acquisition modalities, the Hospital Information System (HIS), and other external systems. The present paper studies the incorporation of a Workflow Management System (WFMS) into the departmental information system. The WFMS anticipates the next step in the workflow, provides the necessary information, and triggers execution. The activity of the department is controlled via workflow management tools.

The central part of the WFMS is the workflow engine. It is a generic piece of software, driven by a script, which describes the process logic and which can be easily adapted to the local situation. The components of the information system are coordinated by the exchange of messages which adhere to standards (HL7, DICOM 3.0, HTTP). It is easy to add plug-ins for communication with legacy equipment. The WFMS accepts orders from the RIS and prepares worklists for radio-pharmacy, for the camera's, and for the workstations of the physicians. Results, when produced, are transferred automatically to the next stage by the WFMS. Validated studies are archived and distributed, may be printed, and are kept on-line for consultation purposes. The servers of the hospital are notified about the availability of new results.

A prototype of WFMS has been introduced in a department of nuclear medicine which extends over 4 hospitals. Most of the existing equipment had to be adapted to fit into the workflow context. Benefits of the WFMS are increased efficiency, more complete documentation of all studies, reduction of human made errors, increased accessibility, and improved accuracy. The reading physician has access to all parameters of the study, increasing the quality of his/her work. The WFMS allows also for a better integration of the departmental information system into that of the hospital.

This work is part of the IT-project "Adding images to an Integrated Multimedia Patient Record" funded by the Flemish Government.

Radiochemistry and radiopharmaceuticals

OT-1

E.R. Hamer^{1,2}, L.C.S. Porto¹, J.J. Carvalho¹ and M. Bernardo-Filho^{1,2}.

1- Instituto de Biologia Roberto Alcântara Gomes, Universidade do Estado do Rio de Janeiro, 2- Instituto Nacional de Câncer, Centro de Pesquisa Básica, Rio de Janeiro, RJ, Brasil, 20230-130. E.mail: bernardo@uerj.br

EVALUATION OF THE RADIOPHARMACEUTICAL DISTRIBUTION TO BLOOD COMPARTMENTS USING AUTORADIOGRAPHY AND CENTRIFUGATION

^{99m}Tc labels a variety of radiopharmaceuticals used in nuclear medicine. When a radiopharmaceutical is administered, a part of it is bound to blood compartments. As drugs can alter this binding, we decided to evaluate the cyclofosfamide influence on the distribution of the radiopharmaceuticals Na^{99m}TcO₄, ^{99m}Tc-MDP and ^{99m}Tc-GHA to blood elements. Blood was incubated (0, 1, 2, 3, 4, 6 and 24 h) with the radiopharmaceuticals. Samples were centrifuged and plasma (P) and cells were separated (C). Other aliquots were precipitated and soluble (SF) and insoluble (IF) fractions of P and C were isolated. Blood samples (0 and 24h) were also dried, fixed and treated with autoradiographic emulsion. In order to study the cyclofosfamide effect, blood was incubated with this drug 1h before the addition of the radiopharmaceutical. The percentage of radioactivity (% rad) in P, C, P-SF, P-IF, C-SF and C-IF were determined. The analysis of our results showed that (i) Na^{99m}TcO₄ distribution during the early periods of incubation on P was higher than on blood cells until 6h, and cyclofosfamide did not interfere with this distribution; (ii) Na^{99m}TcO₄ binding to P-IF was low and the drug did not interfere with this binding to plasma proteins until 6h; (iii) ^{99m}Tc-MDP distribution in cellular compartment was low and hence, the %rad in P was high, the drug was not capable to alter the radiopharmacokinetic behavior of the ^{99m}Tc-MDP distribution in P and C compartments; (iv) ^{99m}Tc-MDP radioactivity in C-IF increased with the passing of time, the drug blocked this binding, in P-IF can be observed a similar increasing effect of the drug and the % rad bound to P-IF was decreased at 24h; (v) ^{99m}Tc-GHA distribution in P was increased and diminished with the passing of time, the %rad in blood cells increased with the period of incubation time and the drug increased radioactivity on P until 6h; (vi) ^{99m}Tc-GHA was slightly higher in C-IF than in P-IF. In P-IF the drug inhibited the radiopharmaceutical binding until 6h and (vii) the comparison of the results obtained with the autoradiographic process and with the separation of P and C by centrifugation showed that %rad bound on P and cells was qualitatively in accordance with both techniques.

OT-2

S. Arndt, F.-J. Gildehaus, K. Tatsch, K. Hahn

Department of Nuclear Medicine, Ludwig-Maximilians-University of Munich, Munich, Germany

QUALITY CONTROL OF Tc-99m-MAG3 IN CLINICAL ROUTINE-A COMPARISON OF ALTERNATIVE METHODS

Sometimes labeling of radiopharmaceuticals with Tc-99m does not result in the high quality expected. Compromised radiochemical purity is a rare finding, however, if it occurs, it may degrade image quality and cause problems with diagnostic interpretation. Therefore, we routinely perform quality controls (QC) to rule out radiochemical impurities.

The goal of the present study was to compare various chromatographical procedures for estimation of the radiochemical purity of Tc-99m-MAG3. We describe advantages and disadvantages of 4 methods with respect to handling, time consumption, accuracy, reproducibility, and cost.

Paper (PC), Instant Thin Layer (ITLC), Sep-Pak Cartridge (Sep-Pak), and High Pressure Liquid Chromatography (HPLC) are widely used quality control methods, which work in principal as outlined below:

PC/ITLC: The separation is based on the solid phase extraction by a mobile solvent. The solid phase is attached to a carrier which is moved upwards by the mobile phase due to capillary force. **Sep-Pak:** This is a special variation of column chromatography. The elution flows mediated by gravity or weak external pressure through a cartridge which is filled with the solid phase. **HPLC:** In contrast to Sep-Pak in this case the mobile phase is pumped with high pressure through a separation column.

In this study we investigated 25 MAG3 kits labeled according to the instructions and compared the data to those of 12 kits, which have been intentionally prepared to result in a high level of radiochemical purity.

With HPLC the most accurate results were achieved. The method, however, is very expensive with respect to initial investment and continuing cost (separation columns, detector, pump). PC is a very cheap method, however, it seems to be extremely sensitive for faults and hence does not provide reproducible results. Furthermore it takes about 45 min, which is a comparatively long time. For evaluating ITLC a linear analyzer or scanner is recommended. The time consumption is rather low (20 min). Sep-Pak has shown to be a fast (10 min) and easy to handle method associated with low cost. In addition the results achieved were highly reproducible.

Taking the criteria mentioned above into account, Sep-Pak has shown to be the most appropriate method for quality control of Tc-99m-MAG3 in the clinical routine setting. The method combines low cost and easy handling with reproducible, highly precise results.

OT-3

U. Dopichaj-Menge, Ch. Reim, D. Sandrock, D.L. Munz

Clinic for Nuclear Medicine, Charité, Humboldt University Berlin, Germany

HOW MUCH LABELING TIME IS NECESSARY FOR LUNG PERFUSION SCINTIGRAPHY ? IN VITRO AND IN VIVO RESULTS

In the labeling instructions for a commercially available lung perfusion scintigraphy kit (CIS bio international) varying labeling times are recommended in different European countries. Hence, it was the aim of this study to evaluate the effect of labeling time by using thin layer chromatography (TLC). Furthermore, the image quality of 30 lung scans performed after different time intervals between start of labeling and injection of the radiopharmaceutical was rated visually paying attention to accumulation in the thyroid.

The labeling yield was determined at one minute intervals up to 10 minutes and at 5 minute intervals up to 30 min, respectively. The TLC (stationary phase: Silica gel; mobile phase: Ethyl-methyl-ketone) was performed from aliquots of the „complete“ suspension and also from aliquots of the supernatant. Some kits were shaken manually, others were mixed with a roller mixer.

Results:

i) As early as 5 min after start of labeling, TLC revealed less than 2 % free pertechnetate.

ii) All lung scans had standard quality independent of the time interval between preparation and injection.

iii) There was no tracer accumulation in the thyroid.

Conclusion:

The commercially available kit for lung perfusion scintigraphy tested in this study can be used safely with a preparation time of 5 min.

OT-4

Sabine Marton, M. Jonas, L. Heuser

Department of Radiology and Nuclear Medicine University Bochum, Germany

RED BLOOD CELL LABELLING WITH Tc-99m: A QUANTITATIVE EVALUATION OF LABELLING YIELDS

Tc-99m labelled red blood cells (RBC) are used for blood pool scintigraphy (radionuclide-ventriculography, detection of gastrointestinal bleeding and haemangioma studies). The labelling yields (LY) are often very different and are influenced by many factors (chemotherapy, heparin load, decreased haematocrit and poor clinical condition of the patient). Furthermore generator ingrowth time (GIT) has been described to influence the labelling yield.

In our study the LY using eluates from GIT ≤ 24 h and ≥ 72 h were compared in the same volunteers (14f, 19m, 23-57 y, mean age 33,7 y). After an i.v. injection of 0,25mg SnCl₂ / 20,6 mg DTPA and erythrocyte pre-tinning time of 25 min, 15 ml blood was withdrawn into a heparinized syringe. In vitro the blood was mixed with 500-700 MBq Tc-99m O₄⁻ and rotated for 30 min. For quality control activity in 0,5 ml blood and 0,5 ml plasma were determined using a dose calibrator. The percentage of labelling was calculated as follows.

$$LY \% = 100 \% - \frac{(100 \% - HK) \times \text{activity plasma (MBq)}}{\text{activity blood (MBq)}}$$

The SnCl₂ / DTPA labelling technique presents great variation of LY (range: 31% - 96%). There is no statistically significant difference using GIT ≤ 24h (80,7% ± 13,8) and ≥ 72h (75,5% ± 14,7). In 38 of 66 labelling studies (57%) good LY > 80% were obtained. 16 of 66 studies (24%) revealed insufficient LY < 70%. In these cases labelling was repeated with the UltraTag RBC™ kit. In contrast to the SnCl₂ / DTPA labelling technique excellent LY (range: 99,4-99,6%) were achieved.

We conclude that RBC labelling with the UltraTag RBC™ kit is a safe and rapid but the more expensive method. Because of the excellent LY UltraTag RBC™ kit should be preferred in the diagnosis of GI bleeding. If the SnCl₂ / DTPA method is used, i.e. for radionuclide-ventriculography, quality control should be performed before reinjection of Tc-99m labelled RBC. In our study poor LY are unexplainable. An influence of drugs, bad clinical condition and GIT can be excluded.

OT-5

K. Waterstram-Rich

Rochester Institute of Technology

BLOOD CONTAMINATION IN THE NUCLEAR MEDICINE LABORATORY

Blood contamination in the nuclear medicine laboratory can be a serious problem if not properly addressed. Universal precautions decrease the opportunity for blood exposures among technologists, health care workers in general, and patients. This talk reviews universal precautions, various decontamination techniques, the standard of care for infection control, and the possible consequences for not following accepted standards. In addition, methods for prevention of exposure and possible sites of blood contamination will be discussed. One commonly overlooked site of blood contamination is the lead pigs which carry doses and used syringes. Lead pigs were surveyed in different areas of the United States and it was discovered that many of them were contaminated with blood. However, those pigs which properly used plastic inserts were not contaminated. Finally, we show that with proper controls and handling techniques blood contamination in the nuclear medicine laboratory can be controlled.

OT-6

Y Lu, S.Z. Deng, X.T. Lin,

Huashan Hospital, Shanghai Medical University, Shanghai 200040
China

STUDY OF RELATIONSHIP BETWEEN SLE AND THE RELATED SERUM HORMONES

Purpose: The study aims at investigating the diagnostic values of PRL, GH and GH-receptor (GH-R) serum levels in patients with systemic lupus erythematosus (SLE) and their hormone changes in different phases of the disease. **Materials & Methods:** 28 SLE patients (16 in active phase, 12 in inactive phase) were involved in the study as well as 20 normal subjects were for control. PRL, GH and anti-ds-DNA-antibody were detected with respective radioimmunoassay (RIA) kits while GH-R were by radioreceptor assay (RRA). Anti-ds-DNA-antibody serum levels, combined with other clinical indices, were used to divide the phases of SLE. **Results:** PRL serum levels were significantly higher in SLE patients in active phase than those of patients in inactive phase ($P < 0.05$) and also those of normal subjects ($P < 0.01$). GH serum levels in patients with SLE were significantly higher than those in normal subjects ($P < 0.01$) while significant difference was also found between SLE patients in active phase and those in inactive phase ($P < 0.05$). However, GH serum levels were poorly related with GH-R serum levels from which there was no significant difference found between SLE patients and control group ($r = 0.23$, $p > 0.05$). Both PRL and GH serum levels were well correlated with the anti-ds-DNA-antibody serum levels ($r_1 = 0.54$, $p < 0.05$; $r_2 = 0.67$, $p < 0.01$). **Conclusion:** High serum levels of pituitary hormones as PRL, GH may indicate that SLE is in active phase although these hormones may not exert relevant biological effects. The mechanism that results in the increment of these pituitary hormones in patients with SLE is still under our investigation.

Oncology

OT-7

Limin Cao, Jiahe Tian, Jinming Zhang, Luxiao Jiao, Yiali Li

The PLA General Hospital, Department of Nuclear Medicine & Gynecology

CLINICAL VALUE OF TC-99M-MIBI IN DIFFERENTIAL DIAGNOSIS OF PELVIC MASS IN FEMALES.

^{99m}Tc -MIBI has long been reported useful in diagnosing malignant tumors. 26 females, age 29 ~ 77, with pelvic mass were studied using ^{99m}Tc -MIBI, and the findings compared with pathologic ones. Each patient was fasted for 6 h to slow down movement of tracer in digest tract. After an intravenous injection of 740 ~ 925 MBq ^{99m}Tc -MIBI, planar images of pelvic and lower abdomen was taken at 5, 15, 45, and 120m after injection. Tomography was employed only in those with equivocal results. Exploitative surgery was performed within 1 week after scan. It was found that in 11 cases of malignancies, 9 had fixed abnormal uptake of ^{99m}Tc -MIBI at the mass, the shape and location was in accordance with surgical findings if the mass is bigger than ϕ 3cm. One case had diffused uptake was found to have wide spread lesions. The only false negative was a huge serious papillary cystadenocarcinoma in a 64yr lady. While 13/15 benign lesions showed no fixed uptake, especially at later images. Two false positives were found in cases with cellular leiomyoma of uterus. The PPV was 83.3%, NPV 92.8%, and Accuracy 88.4% in our group of patients. In 8 cases, all under age of 57, persistent radioactivity was found in uterus, which was on top of and moved with bladder, thus was easy to distinguish from tumors. In no case did the activity in intestine interfere with interpretation of pelvic images. In conclusion, ^{99m}Tc -MIBI is useful in differentiating benign and malignant pelvic masses in gynecologic patients.

OT-8

Ningyi Jiang, Xianping Lu, Lu bin.

Memorial Hospital SunYat-Sen University of Medical Sciences
Guangzhou, 510120 P.R. China

THE USE OF TUMOR IMAGING WITH ^{99m}Tc LABELED ANT-CEA MONOCLONAL ANTIBODIES C50

To study the clinical usefulness of tumor radioimmunoimaging (RII) using ^{99m}Tc labeled anti-CEA monoclonal antibody (McAb) C50. 152 tumor patients were studied, including the ovarian neoplasms 115, intestinal neoplasms 26 and lung neoplasms 11. C50 was labeled with ^{99m}Tc using 2-mercaptoethanol reducing agent and MDP complex compound. The mean labeling efficiency of the labeled antibody was over 90%. The McAb dosage was $1.2 \pm 0.3\text{mg}$ every one. The ^{99m}Tc -C50 was injected after dexamethasone 5mg IV 30 min. Inject 740~925 MBq of ^{99m}Tc -C50 4 to 6 hours before imaging, the planar or SPECT imaging was obtained by SOPHY DSX SPECT. It was positive diagnosis that the radioactivity has been accumulated in tumor site and the ratio of T/NT was over 1. 2. All were pathologically proved after operation. At the same term the ovarian neoplasms was examined with B-ultrasonic. A comparative study has been made among the result of RII with the blood CEA level, the size of the tumor, the CEA content and the distribution in the tumor tissue by immunohistochemical examination. The sensitivity of ^{99m}Tc -C50 RII for tumor was 96.2%, the specificity was 81.2%, the accuracy was 83.7%, the metastasis point detective rate was 84.1%. The sensitivity and accuracy was higher than B-ultrasonic. The quality of the RII had no relationship with the blood CEA level, but was significantly correlated with the main diameter of tumor, the CEA content and the positive CEA reaction distribution in the tumor tissue. The result show that ^{99m}Tc -C50 RII is a reliable method for detecting the tumor and metastasis point. The method is simple, effective and accurate for differentiating the malignant tumors from benign ones noninvasively.

OT-9

M. Núñez, O. Alonso, J. Cánepa, F. Mut

Nuclear Medicine Centre and School of Medical Technology, University of Uruguay, Montevideo, Uruguay.

PROPOSED TECHNICAL PROTOCOL FOR Tc-99m MIBI IMAGING IN MELANOMA PATIENTS.

Tc-99m MIBI scanning has been proposed as an accurate technique for the detection of active disease in patients (pts) with melanoma (ML). However, the nuclear medicine technologist should be aware of the clinical condition of the patient in order to obtain useful information. Based on our experience with 150 pts studied so far, we recommend the following protocol: Image acquisition starts 10 minutes post i.v. injection of 740 MBq of Tc-99m MIBI. The injection site has to be carefully chosen depending on the topography of the primary lesion in order to avoid nonspecific accumulation of the tracer in regional lymph nodes (RLN) due to accidental extravasation. Imaging conditions should be adapted to the clinical status of the patient. *Pts with primary ML:* We perform planar imaging of RLN followed by a whole-body scan immediately after. *Disease-free pts* after surgical resection of primary lesion: Planar RLN images and whole-body scan. *Pts with known recurrent disease:* whole body scan. Previous voiding is mandatory for evaluation of inguinal lymph nodes. If abnormal MIBI accumulation is shown in the whole-body scan, additional planar images or SPECT are indicated. We use a LFOV gamma camera fitted with a LEHR collimator. For planar imaging, a 256 x 256 matrix is recommended, using an acquisition time of 10 minutes. In the whole-body study, a scan speed of 16 cm/minute is used. We perform the SPECT study acquiring data over 360° in 64 angular steps for 20 seconds per view. For reconstruction of cross-sectional images by filtered back-projection, we use a fourth-order Butterworth filter with a cutoff at 0.35 of the Nyquist frequency. Employing this protocol, we have demonstrated a sensitivity of 92% and a specificity of 96% in the diagnosis of recurrent ML with Tc-99m MIBI.

OT-10

S. Boutsali, G Panoutsopoulos, P Liotsou, A Diona, D Parmenidou, C Batsakis, J Christacopoulou

Dept of Nuclear Medicine, "SOTIRIA" Chest Hospital, Athens

GALLIUM SCINTIGRAPHIC PROTOCOLS IN LYMPHOMA.

Background. CT and MRI are widely used imaging modalities in staging, evaluation of therapeutic effects, estimation of residual mass and detection of recurrences of lymphoma. However, the main used criterion, the size of lymph node, is not always reliable. Thus, recently Gallium-67 citrate imaging has been the method of choice in the evaluation of patients with lymphoma, especially in the detection of residual mass, the estimation of the prognosis and the relapse of the disease. Although many protocols are used (early or delayed), the 48 or 72 h. post injection whole body imaging protocols are the more convenient and most common used. In the early protocols several times the increased bowel activity obscures the area of the abdomen.

The aim of the study was to evaluate the practical value of an early (2 d. p. i.) and two delayed protocols (5 and 9 d. p. i.).

Patients and method. Forty one patients (47 examinations), 22 males and 19 females (mean age 47 y, range 9-76 y), suffering from lymphoma and being at the middle point or at the end of their therapy underwent whole body gallium imaging in anterior and posterior views 48 hours after IV injection of 185-296 MBq Ga-67-citrate. In case of the first set of data was non diagnostic, because of increased bowel activity, reimaging was done on the 5th day. Furthermore, a third set of data was obtained on the 9th day in the cases that even the second set was non diagnostic.

Results. In 14 scans the 48-h-images were diagnostic and further investigation was not necessary. In the majority of the patients of this group the disease was limited above the diaphragm. In 24 examinations a second scan was necessary on the 5th day. Only in 9 cases a third scan was needed on the 9th day. In the majority of the patients of the last two groups the disease was below the diaphragm.

Conclusions. The 48-h- protocol is adequate and quite convenient in case that the disease is limited above the diaphragm, otherwise, the 5th-day-protocol is the second choice. In a small percentage of patients a scan on the 9th day is needed.

OT-11

S.A. Barrow, J.W. Babich, D.R. Elmaleh, P. Meltzer, B.K. Madras, A.J. Fischman.

Massachusetts General Hospital, Division of Nuclear Medicine

COMPARISON OF F-18 FDG-SPECT WITH PET IN CLINICAL ONCOLOGY.

PET with F-18 FDG has become an important imaging procedure for diagnosis, staging and therapeutic monitoring of patients with a variety of tumors. However, because of the cost and complexity of the necessary equipment, clinical application of PET has been limited to large medical centers. Over the past several years, most gamma camera manufacturers have developed ultra high energy (UHE) collimators for imaging 511 Kev photons with conventional gamma cameras. In this report we describe our experience with this technique.

A series of patients with tumors of lung, esophagus, pancreas, breast or lymphoma were imaged with F-18 FDG PET and SPECT. After discontinuing all glucose containing I.V. fluids and fasting for at least 6 hrs, 10-15 mCi of F-18 FDG were injected and 45 min. later images were acquired with a GE-PC 4096 PET camera. Each patient was then positioned in the gantry of dual detector SPECT camera equipped with UHE collimators (Siemens, MS2) and peaked for 511 Kev photons (15% window). SPECT acquisition was performed over 360°; 96 - 14 sec frames.

For all patients, diagnostic quality images of the main site(s) of tumor involvement were obtained with both PET and SPECT. However, in several cases, small lesions (<1.5 cm) and lesions with low intensity FDG accumulation that were detected by PET were not identified by SPECT. Furthermore, as expected, tumor borders, margins and contours were considerably less well defined by SPECT compared with PET. However, due to the larger field of view provided by the SPECT camera, some lesions were detected only by SPECT.

These results indicate that FDG SPECT has several important characteristics. Most large lesions are easily detected. The large field of view provided by SPECT cameras improves anatomic coverage. Dual photon imaging can be performed with FDG and a variety of single-photon radiopharmaceuticals; Tc-99m-MIBI, Ga-67, radiolabeled antibodies, etc. Most importantly, FDG SPECT makes metabolic imaging of tumors possible at almost every Nuclear Medicine facility around the world.

OT-12

Yang Z., Mou A.P., Lin B.H., Zhao Ch.Y., Xu X.B., Ma Y.X., Han Y., Zhang M.Y., Xu G.W.

Beijing Cancer Hospital, Department of Nuclear Medicine

STUDY OF 188RE RADIOLABELLING ANTI-GASTRIC CANCER MONOCLONAL ANTIBODY 3H11

To search a good RAIT pharmacy, the use of 188Re from 188W/188Re generator has been studied for antibody radiolabelling. The direct labelling of anti-gastric Cancer McAb 3H11 with 188Re has been described. Prior to radiolabelling, 3H11 was reduced by 2-mercaptoethanol. Then, stannous ion in 0.05mM ABS was added into the reduced antibody, together with a stabilizer to keep the tin(II) from oxidation in solution. And then the solution was immediately treated with freshly eluted Na188ReO₄ solution and reacted 2h at room temperature. Under the labelling condition, 1mg reduced 3H11 can be conjugated 550MBq 188Re and the labelling yield was from 90% to 95%. The incorporation rate was depended upon reaction time and the volume of reaction solution. The biodistribution results in rats demonstrated that 188Re-3H11 was cleared from the blood faster than 131I-3H11 and given rise to good tumor to nontumor ratios at 24 to 96h postinjection. The tumor uptake appeared to reach a peak at 24h postinjection and fell slowly thereafter. The i.d.%/g of tumor was 8.55 ± 1.78 and 3.92±0.98 at 24h and 96h postinjection respectively. The tumor/nontumor ratios was increased from 24h to 96h postinjection. The RAIT results in nude mice bearing 823 gastric cancer xenografts suggested that the 188 Re-3H11 can kill tumor cell effectively and prolong survival time significantly. In conclusion, the direct method makes 188Re-radiolabelled monoclonal antibody a simple and convenient method of cancer radioimmunotherapy with a beta-emitting radionuclide.

■ General topics

General topics

OT-13

A.M. Bosma, A. van Lingen, R. Pijpers, S. Meijer, G.J.J. Teule.
Free University Hospital, Departments of Nuclear Medicine and
Surgical Oncology, Amsterdam, The Netherlands.

GAMMA PROBES: THE TRANSITION FROM RESEARCH TO ROUTINE PROCEDURE.

After scientific evaluation, gamma probes are introduced for sentinel node biopsy in the routine of Nuclear Medicine. This study focusses on the identification and management of issues forming an important role in the transition from research to routine. Of major importance are the setup and documentation of equipment use, quality control (QC) and the evaluation of occupational radiation exposure of personnel. For the latter, measurements on phantoms and patients have been conducted.

For routine QC, we found sensitivity and spectrum measurements together with a battery and settings check to be sufficient. Precise sensitivity measurements were obtained using a special source holder, containing a 1 MBq ⁵⁷Co-source. In case of more than 10% deviation in sensitivity an energy spectrum is obtained from 40 to 200 keV in steps of 5 keV. Absorbed dose rates were measured at several distances of ^{99m}Tc- sources (syringe, spheres) under 0, 2 and 4 cm of water. These measurements were compared with in vivo measurements on 10 patients referred for sentinel node procedure. Absorbed dose rates due to transport of labelled lymph nodes were obtained from measurements on sources in small containers.

Over a 8 weeks period, 2 of 3 probes remained constant; one probe showed decreased sensitivity due to a shifted photopeak in the energy spectrum. Maximum dose rate at 10 cm distance (surgeon's hands) amounts to 8-12 μSv/h/10MBq. At distances over 50 cm (nurses and Nuclear Medicine technologists) dose rates are ≤0.7 μSv/h/10MBq. Transport of lymph node biopsies requires simple packaging of the tissue. We conclude that the sentinel node procedure is easily implementable in Nuclear Medicine routine. Procedures for equipment use, QC and dosimetry are readily documented.

OT-14

S. Sengupta, M. Osterloh, A. Niesen, R.P. Baum, G. Hör

University Hospital of Frankfurt/M, Germany
Clinic for Nuclear Medicine, PET Center

AIM AND PROCEDURE OF IMAGE FUSION OF F-18-FDG-PET AND CT OR MRI IN ONCOLOGICAL PATIENTS

The aim of image fusion is to define the exact anatomical localization of metabolic lesions. The anatomical orientation of F-18-FDG-PET in many cases is not sufficient for example before surgery. To overcome this problem we superimpose the functional images of PET with morphological informations of CT or MRI.

The PET, CT or MRI studies are aquired and reconstructed in different formats. The main preparation for superimposition is the correlation of parameters like scaling and pixel size. In our hospital we leave the parameters of PET images and change the CT and MRI.

An experienced physician decides the exact anatomical superimposition with the help of anatomic structures (e.g. skin, bone) visuable in both imaging modalities.

In our group we have some experiences in bronchial lesions, esophagus cancer, liver lesions and little in other cancer entities.

Conclusion: Even if the technique of image fusion is quite complicated and time consuming, a technician can load and correlate the different studies and do a first superimposition of the studies. This is a very interesting work and eases the exact image fusion by the physician.

OT-15

M.Göransson, B.Jansson and S. Richter

Department of Nuclear Medicine, Huddinge University Hospital,
Huddinge, Sweden.

FLOW-CHART FOR TROUBLE-SHOOTING IN SITUATIONS OF LESS-THAN-OPTIMUM IMAGING OUTCOMES

There are many factors involved in obtaining high quality scans in nuclear medicine procedures. Even in a well-organized set-up with qualified personnel and high resolution gamma camera systems, high quality images do not always come easy.

In this presentation we will review some methodological points related to trouble-shooting in order to evaluate possible sources of low quality scans.

Our nuclear medicine team consists of physicians, technologists, physicists and pharmacists and a cohesive, interactive cooperation has resulted in a QA program in order to assure optimal conditions for imaging and patient care management. As part of this we designed a flow-chart to use in trouble-shooting situations of less-than-optimum imaging outcomes.

The protocol covers patient- and radiopharmaceutical related parameters, e.g. drug-radiopharmaceutical interactions, as well as apparatus related parameters like energy and collimator adjustment.

The flow-chart also proved very useful for ascertaining optimal conditions for each imaging procedure in order to avoid undesirable interactions.

OT-16

P. Prananto, H. De Winter

O.L. V-Ziekenhuis Aalst, Department of Nuclear Medicine
Moorselbaan 164, B 9300 Aalst Belgium

DO WE NEED MANAGEMENT ?

The word management sounds for many of us (nuclear medicine technologists = NMT) rather strange.

Nevertheless, this is an attempt to persuade NMT that managing the patient focused-care also belongs to our task.

On the other hand, such concept will be condemned to failure when the physician does not give any support.

NMT are the go-between among patient and physician, we keep the boss happy and the patient as well.

Except of producing pictures, investigating myocard viability, localising hotspot ...etc we also must take account the needs of the patient as a human being (often who are in discomfort and distress). Some examples : friendly welcome, no irrelevant questions, acceptable waiting time, sufficient information, privacy, correct examination...etc.

It is wrong to think that improving those issues would cost more money.
Poor service is not cost effective.

How can we improve the quality of care without rising cost ?

- First of all we must be able to let go our traditional operating concept and willingness to recognize problems.
- Instilling a broader sense of ownership would benefit to patients
- Job rotation, cross-training would decrease the structural idle time, leading to an increased efficiency.
- Due to the higher degree of the schedulability and predictability of the outpatients, a clear planning could be made.

The implementation of such restructuring needs a minimum leadership.

The preliminary results show a significant decline of the waiting time : 9 to 10 percent. Patient satisfaction is tending upwards.

What is done ? How is it done ? How well is it done ? are the three questions which we have to ask to ourself all the times.

In conclusion, this paradigm shift might liberate us from declining performance without rising cost.

It might be interesting if this talk would initiate us to further act.

OT-17

J.L.M.M. Bemelmans, R.J.M. Baert

Spaarne Hospital, department of Nuclear Medicine

EXPERIENCES WITH A DIGITAL HOTLAB MANAGEMENT SYSTEM

Radiopharmacy is an essential part in Nuclear Medicine. Every investigation starts with the application of a radiopharmakon to the patient.

Handling of radioactive drugs is strictly ruled by national and international laws.

The responsibility for the quality of the preparations is in the hands of pharmacists.

Very tight requirements in pharmacopees demand that preparations are carried out conforming to Good Manufacturing Practice and Good Radiopharmacy Practice.

The total preparation procedure should therefore be protocolled in standardised in-proces control, starting with ordering, and finally recording of usage. There are a lot of steps in between that require perfect recording and administration.

Normally this requires a lot of paperwork, so we looked for a software package that might support us in this complex proces.

The Hotlab Management system gives us this opportunity in the daily procedure and has a huge possibility of making hard-copy abstracts of stocks, radioactive wastes, patient-doses a.s.o. in a well considered way and according to law requirements.

OT-18

H.E.Patterson, B.F.Hutton

Departments Medical Physics, Nuclear Medicine and Ultrasound, Westmead Hospital, Sydney. Australia.

THE NEED FOR A 2-TIER STRUCTURE FOR TECHNOLOGIST ACCREDITATION

The aims of accreditation are to establish standards for practicing technologists, provide recognition for trained technologists and encourage further development through continuing education programmes. Many countries with well established nuclear medicine have mechanisms for technologist accreditation and reciprocity between countries, whereas technologists in many developing countries have few opportunities to have formal training or gain accreditation. It has taken many years to formulate the present standards for accreditation but these may be inappropriate for immediate involvement of developing countries. It may be relevant to introduce a structure which is achievable for most technologists in the field where their work practice and standards are assessed. By providing an entry point for basic accreditation technologists would be encouraged to progress to the more advanced and globally accepted accreditation level.

One method of assessment of technologist work practice could be through a Distance Assisted Training Programme, such as that sponsored by the Australian government, currently being conducted under the auspices of the IAEA. It provides learning in the workplace with emphasis on practical skills, safety and quality assurance. Student assessment and course evaluation are an important component of the programme. The material has been translated to Chinese, with translation to French, Spanish and Arabic also being considered and the material will form the basis for a project soon to be conducted in Africa. This programme encourages a common basic standard which could form the basis for the entry level accreditation.

The mechanism to establish this structure needs to be addressed by those bodies which are establishing accreditation and competency based standards. This proposal should be given serious consideration before advancing technology further widens the gap between regions and acceptable levels of competency.

Distance Assisted Training material developed at Westmead Hospital, Sydney is freely available through the IAEA

Oncology

OT-19

N.Arslan, E. Öztürk, S.İlgan, Ö.Karaçaloğlu and H.Bayhan

Gülhane Military Medical Academy and Medical Faculty, Department of Nuclear Medicine, Etik/ANKARA/TURKEY

EVALUATION OF ^{99m}Tc-MIBI BREAST TUMOR UPTAKE IN INFILTRATING DUCTAL CARCINOMA (IDC) AS A PROGNOSTIC SIGN: COMPARISON WITH MICROSCOPIC GRADING

IDC is the most widely type of breast cancer affecting women. Tumor cells of IDC are graded according to the degree of nuclear pleomorfism, mitotic activity and tubular formation by histologic examination. Especially, in the early stages of breast cancer, microscopic grading greatly effects therapeutic management as a prognostic factor. The aim of this study was to investigate whether ^{99m}Tc-MIBI Scintimammography can be used as a prognostic sign or not in IDC patients. Therefore, we compared the microscopic grades of 20 patients with early (5th minute) and late (1st hour) MIBI uptake levels. Tumor to normal breast tissue (T/BG) mean uptake ratios were determined by drawing regions of interest manually over areas of increased uptake and over corresponding regions of normal breast tissue. T/BG Counts of early and late prone lateral scintimammographic images were compared with microscopic grades separately. The results are presented as follows:

	MIBI T/ BG Uptake Levels	
	5 th minute	1 st hour
Grade I (3 Case)	1.61 ± 0.30	1.76 ± 0.39
Grade II (10 Case)	2.51 ± 0.89	2.60 ± 0.96
Grade III (7 Case)	2.89 ± 0.93	2.96 ± 1.14

Early MIBI uptake levels of Grade I patients were statistically different from Grade II and Grade III patient's (p<0.05). However, no correlation was found between the early MIBI uptakes of grade II-III and late MIBI uptakes of all patient group's (p>0.05). In conclusion, our findings confirmed that low degree early MIBI uptake level may be used as an indicator of well-differentiated IDC tumor and prediction of prognosis. As our data based on a limited group, further investigations are required to fully address this issue.

OT-20

E.A. Clarke, A. Notghi and L.K. Harding.

Department Of Physics And Nuclear Medicine, City Hospital NHS Trust, Birmingham, UK

REVIEWING AND IMPROVING YOUR SKILL IN SCINTIMAMMOGRAPHY

We began scintimammography in 1997 investigating the extent of disease in the breast and lymph node involvement using ^{99m}Tc^m Tetrofosmin. Two protocols for these studies have been compared following a change in camera system and output, breast mattress and imaging times. Nineteen studies (protocol 1) were performed on an analogue camera using a "homemade" imaging cushion; the standard procedure of 10 minute lateral and anterior views and nipple markers was employed. Images were reported from film. Following installation of a digital system, purchase of a commercially available breast mattress and reduction in protocol to 5 minute images, twenty three studies (protocol 2) were performed. These images were reported directly from the screen output.

All patients had known breast lesions confirmed by surgery and pathology. In total, thirty seven of the 42 lesions were identified on scintimammography: 15/19 protocol 1, 22/23 protocol 2. Lymph node (LN) status was correct in 26/42 cases (see table).

LN Status	Protocol 1	Protocol 2
True Positive	2	8
False Positive	1	2
True Negative	10	6
False Negative	6	7

Protocol 1 showed a sensitivity of 79% for breast lesions and 25% for lymph nodes; protocol 2, 96% and 53% respectively.

The improved technique has increased sensitivity for both breast lesions and lymph nodes and is now our routine procedure. Reducing the acquisition times has also made the study more acceptable for the patient.

OT-21

M. Núñez, R. Vila, O. Alonso, M. Beretta, F. Mut.

Nuclear Medicine Service, Asociación Española 1a. de Socorros Mutuos. Montevideo, Uruguay.

VALIDATION OF A SPECIAL TABLE FOR SCINTIMAMMOGRAPHY WITH A DUAL-HEAD CAMERA: A PHANTOM STUDY.

Tc-99m MIBI scintimammography with a dual-head camera can potentially reduce acquisition time significantly. We designed a table for simultaneous prone imaging of both breasts, which can be placed over the conventional imaging table. A wooden insert lined with 0.5 mm lead sheet separates the breasts, avoiding contribution of activity from the opposite side. To evaluate the effectiveness of the shielding, we used a cardiac phantom with "hot" inserts filled with water and Tc-99m, yielding a lesion-to-normal tissue ratio of about 2:1. Interposition of the shielding device between the phantom and the camera resulted in a count rate at the background level. We also developed a thoracic phantom with two breasts, placing a 9 mm and a 22 mm lesion in each breast respectively. We imaged the phantom in the prone position using both detectors simultaneously for a total time of 10 min. A SPECT study was then performed with the phantom in the same position, using a 180° orbit and 30 steps of 20 sec each. SPECT was repeated in similar conditions but without the table. Regions of interest were drawn around the lesions and over the "normal tissue" using the planar images and the transverse, coronal and sagittal SPECT slices. Lesion-to-normal ratios (LNR) were then calculated. Using the special imaging table, SPECT images resulted in significant reconstruction artifacts, whereas without the table, the study was of very good quality, with higher LNRs (3.10 vs 2.18 for the larger lesion, 2.64 vs 1.87 for the smaller one) and better diagnostic reliability. While both lesions could be seen on the planar and SPECT images, LNRs were higher with SPECT (3.10 vs 1.33 for the larger, 2.64 vs 1.13 for the smaller lesion). In conclusion, the new table allows for simultaneous imaging of both breasts. For SPECT imaging, however, the table must be removed because it generates serious reconstruction artifacts.

OT-22

D.S.Thakrar, J.B.Cwikla*, J.R.Buscombe, A.J.W.Hilson.
Royal Free Hospital and School of Medicine; Department of Nuclear Medicine.
London; UK

*PSK 2; Department of Radiology and Nuclear Medicine. Otwock; Poland

PRONE SPECT SCINTIMAMMOGRAPHY: A NEW TECHNIQUE FOR IMAGING BREAST CANCER.

Single photon emission tomography (SPECT) normally provides more accurate localisation of pathology than planar imaging. An exception to this rule appears to be the use of prone lateral dependent scintimammography where results have shown a higher accuracy than supine SPECT studies. This is probably because there is better separation of the breast tissue from underlying chest activity when the patient is prone and the breasts dependent. A new couch has been developed which allows for SPECT imaging in this position and the aim of this study was to compare prone planar and prone SPECT scintimammography.

Standard prone lateral and anterior supinar planar scintimammography was performed in 17 patients with suspected breast cancer 5 minutes after 740mbq Tc-99m MIBI. After this a 20 minute prone SPECT image was performed on a dual headed gamma camera. This initial study was performed in 17 patients with suspicious of breast cancer. The SPECT data was reconstructed using a ramp back projection filter and a Metz smoothing filter. Images were displayed as transaxial, coronal and sagittal slices and planar imaging. All studies were read blind and then compared with the final histology from samples taken from the breast and axillae.

SPECT correctly diagnosed 8/9 patients with cancer within the breast, planar identified 7 breast cancers. However there were 4 false positive studies on SPECT and 2 on planar imaging. On review of the images it was found that the false positive uptake on the SPECT scan related to backprojection artifacts in the left breast from heart activity. One patient had negative study. Planar imaging was correct in 7 cases, and false in 2. Six patients had proven axillary node involvement. SPECT identified 5 of these patients and planar 3 patients. However there were 2 false positive studies in the axilla with SPECT but none with planar imaging.

At present prone SPECT is more sensitive than planar imaging in finding cancer in the breast and lymph nodes. However the specificity is worse. The main cause being SPECT reconstruction artifacts. The combination of interactive reconstruction (thus avoiding back-projection artifacts) and prone SPECT scintimammography may prove to be more reliable than planar imaging.

OT-23

G. Prisco, M. Fiorenza, M. Chinol, M. Cremonesi, C. De Cicco, A. Luini*, and G. Paganelli.

Division of Nuclear Medicine and Senology*, European Institute of Oncology, Milan, Italy.

TECHNICAL ASPECTS OF LYMPHOSCINTIGRAPHY IN BREAST CANCER.

Lymphoscintigraphy (LS) has recently advanced for its applications in the study of sentinel-node (SN) in breast cancer. The aim of this study was to optimize a simple scintigraphic procedure in SN localization to facilitate the SN removal during surgery.

Patients and methods: 300 patients with operable breast carcinoma were injected in order to detect the first axillary lymph-node (LN). Microcolloidal particles of human serum albumin labelled with ^{99m}Tc were used. Particle size within range of 0.2-1.0 µm was chosen for the characteristic to be drained by lymphatic vessels and stopped to the nearest LN. The volume was established in 0.4 ml and the activity in 8-10 MBq. Early and late (15 min, 30 min, 3 h p.i.) scintigraphic images were obtained in anterior-oblique (A-O) 40° and anterior (A) projections of the involved breast and axillary area, with the pts supine and the arm laterally extended at 90°. In case of overlapping between the injection area and the axillary region, the breast was shifted medially to the thorax. For better drainage, the injected area was massaged for some minutes. Finally, the skin was marked in correspondence with the SN visualized in A-O view, using a pen point marker ⁵⁷Co placed on top of the hot spot. The A view was useful to visualize non-axillary SN. The skin mark was helpful to the surgeon to find and remove the SN guided by a gamma detecting probe (GDP); the LS images were available in the operating room to assist the surgeon in locating the SN.

Results: LS was successful in 98% of pts and clearly revealed the SN which appeared to be the hottest node when more than one were visualized.

Conclusions: The LS technique we adopted was efficient and easy to apply. We found that the A-O projection was the best to visualize the SN. The size of the radiolabeled albumin particles we used were the most effective. In all cases the LS revealed the SN, which could also be identified by the GDP the next day.

OT-24

J. de Swart, YAM Kaandorp, WW de Herder, AEM Reijs, EP Krenning, DJ Kwekkeboom.
Departments of Nuclear Medicine and Internal Medicine III,
University Hospital Rotterdam.

A COMPARISON OF 123I-EPIDEPRIDE SPECT AND 123I-IBZM SPECT IN THE SAME PATIENTS WITH PITUITARY ADENOMAS.

123I-IBZM can demonstrate dopamine D2-receptors in vivo using SPECT. Recently, the substituted benzamide 123I-epidepride has become available for clinical use. The affinity for dopamine D2-receptors is in the pM range, compared to an affinity in the nM range for 123I-IBZM.

The aim of the study was to compare pituitary SPECT after 123I-epidepride and 123I-IBZM for the imaging of D2-receptors in clinically nonfunctioning pituitary adenomas (NFPA) and in macroprolactinomas in the same patients. Fifteen patients with a NFPA and four with a prolactinoma were studied.

185 MBq 123I-IBZM was administered as an intravenous bolus and acquisition was started after 75 min. Acquisition parameters were: 10 scans, 12s/frame, 60 projections, 360 degrees, 64x64 matrix. Before reconstruction, the scans were summated and prefiltered with a Metz filter. Three hours after the administration of 111-185 MBq 123I-epidepride acquisition started with parameters: 1 scan, 36s/frame, 120 projections, 360 degrees, 64x64 matrix.

All 4 macroprolactinomas showed specific binding of 123I-epidepride, and only 1/4 after 123I-IBZM. Nine of 15 NFPA were visualized after 123I-epidepride (60%), and 6/15 after 123I-IBZM (40%). All these 6 were also visualized after 123I-epidepride. In the visualized macroadenomas the tumor/cerebellar ratio ranged from 3.9-38.0 after 123I-epidepride and from 0.7-1.7 after 123I-IBZM.

Conclusions: 123I-epidepride SPECT is more sensitive than 123I-IBZM SPECT to demonstrate D2-receptors on pituitary tumors. 123I-Epidepride SPECT could serve to predict the response of NFPA to dopamine agonist therapy.

Heart/SPET

OT-25

L. Sanders and A. S. Houston

Royal Hospital Haslar, Department of Nuclear Medicine

THALLIUM SPECT IMAGE PATTERNS IN NORMAL PATIENTS

The aim of this study is to explain the apparent differences in biodistribution of ²⁰¹Tl observed in patients with normal stress myocardial perfusion SPECT studies.

Fifty-six patients (26 male and 30 female) with no history of myocardial infarction and normal SPECT images were selected. These patients underwent pharmacological stress with adenosine. After injection at peak stress, each patient was scanned on a SOPHA DSX gamma camera, acquiring 32 projections of 30 seconds, and the data reconstructed using a Hann filter. Regions of 67 pixels were used to determine counts from the heart and lungs in the anterior (ANT) and left anterior oblique (LAO); and heart, lung and left kidney in the left lateral view (LLAT). These values were analysed using the SPSS statistical package. A neural network was trained to predict heart/lung and kidney/lung ratios in the LLAT view given the patient's sex, age and weight.

For males and females, differences between the heart to lung ratio were probably significant in the ANT view (<0.05), significant in the LAO (<0.01) and highly significant in the LLAT view (<0.001), in all cases lower in females. These differences were greatest in the LLAT and LAO views for patients over 55 and in the LLAT and ANT views for patients under 55. The kidney to lung ratios show probable difference (<0.05) between male and female with the greatest difference being for patients over 55. The neural network was trained on 39 patients and produced good results on a test set of the remaining 17 patients suggesting that sex, age and weight are good predictors of the observed distribution patterns.

The differences shown between male and female patients can, in general, be explained by breast attenuation, however this study suggests attenuation is more lateral in older female patients and more anterior in younger patients. It has been suggested that changes in breast tissue density with age cause a change in attenuation, however the answer may be due to changes in female shape when in the prone position as breast tissue becomes less firm. Similarly the decrease in kidney/lung ratio in males may be due to increased attenuation around the abdomen with increasing age.

OT-26

SF-Yang, ZC-Yu, HP-Zhu, JD-Ye, DW-Guo

Hospital: Shanghai Chest Hospital, Department of Nuclear Medicine

HOW ACCURATE IS ^{99m}Tc-MIBI PLANAR PERFUSION IMAGING AT REST FOR DETECTION OF CORONARY ARTERY DISEASE ? (100 COMPARISONS WITH CORONARY ARTERIOGRAPHY)

PURPOSE: In order to evaluate the role of rest ^{99m}Tc-MIBI planar myocardial perfusion in patient with coronary artery disease (CAD) and to compare its accuracy with coronary arteriography. **METHODS:** From 1992 to Aug. 1996, ^{99m}Tc-MIBI planar perfusion imaging at rest had been performed in 857 subjects who receiving therapy in a university teaching hospital setting. of 857 patients, 100 (85 men, 15 women, mean age 57 years;) with significant CAD (at least 1 vessel with greater than or equal to 50% diameter narrowing) were revealed by coronary arteriography. there were anginal pain in 51 cases, previous myocardial infarction 31 (associated with aneurysm 10 cases), acute myocardial infarction 3, associated with rheumatic heart disease 2 and other disease 5; Single vessel disease was observed in 32 patients. double-vessel disease in 24, triple-vessel disease in 44. The situation of coronary artery stenosis can be summarized as follows: I° (50%≤ stenosis ≤79%), II°(80%≤ stenosis ≤95%) and III°(96%≤ stenosis ≤100%). According to the patient's heart conditions: normal or clockwise or counterclockwise, the positions of acquisition were careful to adjust. In general, images were acquired in 5 positions: anterior view, the 40° left anterior oblique (LAO), the LAO60°, the LAO75° and left lateral for adding significantly to left circumflex (LCX). Tracer uptake was visual and quantitative analyzed in 7 segments for each patient (anterior wall, apex, inferior wall, septal wall, lateral wall, posterior wall and anterolateral wall). All patients were 700 segments. As a "gold standard", the result of coronary arteriography must be recorded in detail so that we might analyze with tracer distribution. **RESULTS:** The overall sensitivity and specificity for planar imaging at rest were 76.4% and 95.4%, respectively. The sensitivity for detecting CAD in the LAD,LCX and RCA was 80.1%,72.1% and 79%, respectively, and the specificity was 97.9%,90.4% and 98.4%, respectively. Sensitivity and specificity in identifying one-vessel, two-vessel and three-vessel of coronary artery stenosis were 80.7%/92.2%; 79.4%/96% and 73.2%/98.2%, respectively. The sensitivity and specificity for detecting the degree of stenosis in I°, II° and III° were 82.5%/92.8%; 75.6%/97% and 73.6%/97%, respectively. The positive predictive rate and negative predictive rate were 91.1% and 86.8%. **CONCLUSIONS:** ^{99m}Tc-MIBI planar perfusion imaging at rest is still a good method to accurately CAD by analyzing carefully and more positions, particularly the elderly and MI patients.

OT-27

P. Dibbets, J.A.K. Blokland, B.L.F. van Eck – Smit, E.K.J. Pauwels

Leiden University Medical Centre, Division of Nuclear Medicine, Leiden, The Netherlands

RECONSTRUCTION FILTERS AFFECT EJECTION FRACTION MEASUREMENTS FROM GATED SPECT MYOCARDIUM PERFUSION STUDIES.

Gated SPECT studies of the myocardial perfusion will enable visualisation of the perfusion as well as the wall motion. Also the ejection fraction can be calculated from the gated data.

SPECT reconstruction filters may affect the results of subsequent quantitative analysis. The transaxial slices may become too smooth or too noisy. In this study we investigated the influence of the filter on the left ventricular ejection fraction (LVEF).

We analysed 35 consecutive patient studies, acquired after injection of either 500 MBq (S1) or 750 MBq (S2) ^{99m}Tc-tetrofosmin. Data were acquired using a step (4°, 90 projections) and shoot method in a 64²-matrix (16 frames/RR cycle). Transaxial slices were reconstructed with cut-off frequencies (COFs) ranging from 0.18 cycles/pixel (cpp) to 0.36 cpp for S1 studies and from 0.24 cpp to 0.40 cpp for S2 studies. The LVEF was calculated using a standard software package (Germano, et al). For each patient study the relative LVEFs were calculated by normalisation to the average LVEF calculated over the values obtained with the five highest COFs. At each COF the mean and the standard deviation of these normalised LVEFs were calculated.

All studies showed a decreasing LVEF with increasing COF. The mean normalised LVEF ranged from 1.12 to 0.99. The standard deviation decreased from 0.14 at low cut-off frequencies to 0.01 at higher COFs. The normalised LVEFs did not change much (< 2%) when the COF was equal to 0.28 cpp, or higher. However, the image quality was very poor with COFs above 0.32 cpp and 0.38 cpp for S1 respectively S2 studies.

We conclude that the COF must be chosen above 0.26 cpp, but it should not be too high to prevent poor image quality. The injected dose will also affect the choice.

OT-28

E. Wandke, U. Dopichaj-Menge, W.S. Richter, D.L. Munz

Clinic for Nuclear Medicine, Charité, Humboldt University Berlin, Germany

HOW MUCH WAITING TIME IS NECESSARY AFTER IN VIVO LABELING OF RED BLOOD CELLS FOR RADIONUCLIDE VENTRICULOGRAPHY ?

Usually, the acquisition of a radionuclide ventriculography starts 20 min after in vitro labeling of red blood cells with Tc-99m. However, the validity of this time interval has been questioned. Hence, it was the aim of this prospective study to evaluate the accuracy of calculation of the cardiac ejection fraction (EF) at different time intervals between labeling and acquisition.

Overall, 50 consecutive patients (11 male, 39 female, aged 53 +/- 14 years) were studied. Special care was taken to position the patients in an appropriate manner (modified left anterior oblique 30° position). After i.v. injection of 10 MBq/kg body weight up to 6 ECG-triggered gated studies were acquired at 4 min intervals. Data processing was performed using standard software („automatic“, RNV-Frankfurt, Germany) as well as manually drawn cardiac regions of interest („manual“).

There was a fairly good correlation between „automatic“ and „manual“ EF (mean difference 8.05 % +/- 7.50). Intraindividually, there were considerable mean differences (mean +/- SD) of the EF-values at different time points (expressed as % difference from the „standard-EF“ after 20 min) as listed below (without significant change with time):

Time (min p.i.)	„automatic“	„manual“
4	12.1+/-9.5	11.9+/-9.5
7	16.2+/-11.5	11.9+/-9.7
10	14.1+/-9.8	11.5+/-8.6
13	12.6+/-10.0	14.1+/-10.6
16	12.1+/-9.5	12.7+/-11.3
20	0	0

Conclusion: There is no significant difference in the mean „error“ of the calculation of the EF at different time intervals between labeling and data acquisition.

OT-29

N. Mijnders, J. Akkermans

Ignatius Hospital, Dept. of Nuclear Medicine, Breda, The Netherlands

IS A DUAL HEAD 90° CAMERASYSTEM A 'MUST' IN MYOCARDIAL PERFUSION IMAGING?

If a camera is mainly used for myocardial perfusion imaging, a variable angle gammacamera is obvious. But many minor and major factors play a part. Two variable angle gammacameras are compared with a 180°-fixed detectors gammacamera.

Using an antropomorphic torsophantom filled with 99mTc, the biodistribution of a 99mTc-labelled myocardial perfusion agent is simulated. A 'defect' is placed in the inferal wall of the cardiac insert. SPECT-acquisitions were made on three dual head gamma-cameras of different manufactures. The acquisitions were made with the detectors in the 90°- and the 180°-geometry (except the 180°-system). Normalised acquisition parameters were: total acquisition time, matrix, pixelsize, step/angle, LEHR-collimator. Normalised processingparameters: Filtered back projection, Butterworth pre-proces filter, ramp processing filter, 1 pixel thickness reconstruction in all projections, no 'inter'-slicing adjustment. The short axes slices were used to calculate the contrast and FWHM. The results were also visually interpreted.

Systems with the detectors in a 90°-geometry should compensate the dead angle by increasing the distance to the patient. If that's not the case and they follow the contours of the patient ideally, reconstruction errors could appear, specially in the apical region. Cameras with a 180°-geometry and with automated patientcontourmechanismes have no dead angle and will follow the patient contours ideally. One variable angle camera leads to better results in a 180°-geometry than in a 90°-position! The results of the other variable angle gammacamera in the 180°-geometry could not be evaluated due to software-limitations. Nevertheless the results in the 90°-geometry of this system were the best. The results of the fixed 180°-geometry system were better in comparison with one variable angle-system, but not as good as the other one.

In conclusion: Prefatory concluding that a 90°-geometry is superior to a 180°-geometry is false. More important: the contrary is demonstrated in one variable angle system. When different camera systems are compared, the detector geometry is of minor importance. So a 90°-geometry is no 'must' in myocardial perfusion imaging.

OT-30

U. Dopichaj-Menge, L. Geworski, V. Ivancevic, D.L. Munz

Clinic for Nuclear Medicine, Charité, Humboldt University, Berlin, Germany

MEASURED ATTENUATION COEFFICIENTS IMPROVE SPET RECONSTRUCTION

Attenuation correction of SPET data is usually performed by Chang's method on the basis of the mathematically derived attenuation coefficient (μ) of the respective radionuclide. Although approximative, this procedure generally enhances image quality in comparison to uncorrected SPET data. However, applying calculated absorption coefficients yields overcorrected images, if no prior scatter correction was performed. Since measured attenuation coefficients result from both absorption and scatter, they should represent a means of absorption correction, also using the scatter fraction present in the SPET data. Thus, attenuation coefficients of the radionuclides applied in SPET imaging most frequently were measured using a cylinder phantom and a dual-head large-field-of-view gamma camera. The cylinder phantom was filled with a homogeneous solution of the respective radionuclide and high-count SPET studies were acquired with acquisition parameters (matrix size, number of projections, reconstruction filter) being the same as in in-vivo studies of the respective radionuclide. SPET data was reconstructed by filtered backprojection without attenuation correction. The resulting transaxial slices were summed up and a line count profile was put across the centre. Due to attenuation these count profiles showed higher count rates along the phantom margin as compared to those in the central area. Systematically varying attenuation coefficients were then implemented into Chang's attenuation correction algorithm which was run over the reconstructed data. The attenuation coefficient which yielded a straight count profile with homogeneous count rates at the margin and in the central area of the phantom was considered best. For Tc-99m the most favourable measured attenuation coefficient was $\mu=0.12 \text{ cm}^{-1}$ as opposed to the calculated value of $\mu=0.15 \text{ cm}^{-1}$. With I-123 the measured coefficient amounted to $\mu=0.11 \text{ cm}^{-1}$ and with In-111 to $\mu=0.09 \text{ cm}^{-1}$. Calculated absorption coefficients for the latter radionuclides are not easily available. The measured attenuation coefficients were employed in patient studies and yielded a significant improvement in visual quality of the images, most notably in the abdomen, where the well-known rim artefact in the liver, i.e. rising count rates towards the periphery of the organ, was abolished.

In conclusion, attenuation correction using measured attenuation coefficients represents an effective method of absorption correction of SPET data. Measured attenuation coefficients are easily implemented into most of the existing attenuation correction software.

Therapy/brain

OT-31

Jiahe Tian, Jinming Zhang, Qiantian Hou, Q. H Oyang, Jianmin Wang

The PLA General Hospital, Department of Nuclear Medicine

MULTICENTRAL TRIAL ON EFFICACY AND TOXICITY OF SM-153-EDTMP AS PALLIATION FOR PAINFUL BONE METASTASES IN CHINA

As part of an international cooperated research project(CRP) sponsored by IAEA, 6 clinics located at north China were jointly organized to investigate the efficacy and toxicity of 153Sm-EDTMP in palliating bone pain caused by metastases. 127 patients were studied following standard CRP protocol. All patients had pathologically confirmed primaries at lungs, breast, digest-tract, urogenital system, etc. with X-ray and scintigraphic evidence of bony involvement. After intravenous injection of 153Sm-EDTMP at two dosages(18.5MBq/Kg, n=49; and 37MBq/Kg, n=78), the treaties were followed on regular basis. The follow-up included physical evaluation, blood counts, organ function tests, with records of daily consumption of analgesics and symptoms from treaties. Sum of effect product (SEP) was used to quantitatively analyses the effect based on pain score and duration of response after the treatment. No other tumor-oriented treatment was allowed during the study. It was proved that in 85.5% patients positive palliation occurred which started at 2 ~ 24d(8.7 ± 5.4d), lasted for an average of 8.7 ± 4.7w, with no significant difference between the two dosage-groups(SEP in 18.5MBq group 20.1 ± 13.9, vs 37MBq group 22.3 ± 14.5). 18 cases had no response (SEP<2). No serious side-effect was noticed, but WBC and platelet drop were noticed in 52/127 and 49/127 cases. There were also a trend of liver function change, but only 10 cases showed abnormal ALT titer. In conclusion, 153Sm-EDTMP is a safe, effective treatment for painful bony metastases with no serious side-effect; both efficacy and side-effect seemed dosage-independent at current dosage range.

OT-32

Basmanov V., Skoblov Yu., Pavlovich V., Soulim E.
Ministry of Russian Federation for Atomic Energy, Institute of Physics and Power Engineering, Obninsk, Russia

32-P AND 89-Sr BASED RADIOPHARMACEUTICALS FOR THERAPEUTIC PURPOSES

Radionuclide therapy using β -emitters is a perspective alternative to chemotherapy, immunotherapy and external beam radiotherapy methods. The aim of this study was to develop the production technologies of radiopharmaceuticals on the basis of sodium [32-P]phosphate and [89-Sr]strontium chloride which are effective palliation agents for patients with myeloproliferative diseases and skeletal metastases. It was used (n,p) nuclear reaction for 32-P and 89-Sr carrier-free radionuclides production (specific activity is 17000 Ci/g Sr and 160 Ci/g P); precipitation, sublimation, solvent extraction methods and ion-exchange chromatography for their isolation from irradiated targets; preparation of the radiopharmaceuticals using phosphate buffer isotonic solution and isotonic aqueous mixture of strontium and sodium chlorides with normal, medium and high specific and concentration activity of resulting products. The radionuclide purity both [89-Sr]strontium chloride and [32-P]orthophosphoric acid are not less than 98% and sufficient for radiopharmaceuticals production. The medium available concentration activity of prepared "Sodium [32-P]phosphate" is 30 mCi/ml and "[89-Sr]Strontium chloride" is 10 mCi/ml. The content of 90-Sr impurity in "[89-Sr]Strontium chloride" is limited and it is not more than 2,3·10⁻⁸% at expire. These radiopharmaceuticals meet completely medical requirements for parenteral injections. Animal and clinical tests of these radiopharmaceuticals are planned.

OT-33

Jinming Zhang, Jiaye Tian, Zhi Yang, Hongsheng Bai

The PLA General Hospital, Department of Nuclear Medicine

IMPROVEMENT OF BONY UPTAKE OF 188RE-HEDP BY MODIFYING PREPARATION TECHNOLOGY.

Rhenium-188 -HEDP is an attractive radiopharmaceutical for the treatment of bone metastases. But the biodistribution of 188Re-HEDP prepared from 188W^o/188Re generator in bone is fairly lower(about 2.0%ID/g at 4h) . We added a appendage agent during process of labelling to improve the bone uptake of radioactivity.

188Re-HEDP was prepared with 188Re eluted from 188W^o/188 Re generator. A appendage agent was added to 188Re-HEDP in the process of labeling. The labelling yield is over 95%. The in vitro stability of 188Re-HEDP labeled that way is good for 12h . The in-vivo distribution in mice was studied with two kinds of 188Re-HEDP, one was normally labeled 188Re-HEDP(group I), the other with appendage agent (group II).

The distribution of two kinds of 188Re-HEDP in mice at 4h.

%ID/g	heart	liver	spleen	lung	kidney	femur
group I	0.42	0.83	0.28	1.44	1.77	1.92 ± 0.61
group II	0.28	0.41	0.20	1.71	1.72	7.86 ± 1.62*

The uptake of femur bone in group I was lower than groups II (P<0.001). There was no difference on the concentration of radioactivity in other organs at same time .

In conclusion, 188Re-HEDP is a potential agent for treatment of bone metastases. The bone uptake of it can be improved evidently when appendage agent was added in labeling 188Re-HEDP.

OT-34

Jiaye Tian, Yong Ding, Jinming Zhang, Limin Cao

The PLA General Hospital, Department of Nuclear Medicine

EXPERIMENTAL PROPHYLACTIC RADIOTHERAPY USING I-131-MONOCLONAL ANTIBODY IN TUMOR-BEARING MOUSE

The therapeutic effect of radio-labeled monoclonal antibody (MoAb) had been reported not good in big tumor, because of low ID%/g and uneven distribution of radiation. We tried to treat/prevent metastases by RIT using 131I-MoAb in tumor-bearing mouse. A animal model was established on inbreeding mouse T739(n=120), seeding to hind-leg a malignant mouse adenocarcinoma cell, LA795, which had a very high potential of metastases(100% metastases in lung 2 weeks after seeding). 28 animal died during before start of study. The rest 92 mice were set into 6 test groups(G), all had amputation at 1 week after tumor implant, when tumor mass became about φ 1.5cm in size. G1(n=19) had no additional treatment. G2(n=14) was given 0.8mg Ara-C daily; G3(n=13) was given cold MoAb(C50), 1.0mg every 3 days; G4(n=15), 25uCi 131I-C50 every 3d; G5(n=13), 300uCi 131I-C50 given twice at 9d interval; and G6(n=18), 100uCi 131I-C50 3d. An autopsy was undertaken once a mouse died or killed at 60d. It was found that G1 survived 11 ~ 38d, all being cachexia before death; G2 lost appetite and weight, surviving 12 ~ 52d; G3 had short life(10 ~ 35d); G4 survived 18 ~ 45d; G5, 18 ~ 43d; the longest survive was in G6(35 ~ 60+d). All animals, but 4 of G6, had massive lung metastases found postmortemly. In conclusion, the preliminary results strongly suggested the prophylactic use of radiolabeled MoAb at proper dosage early after surgery had positive effect on metastases.

OT-35

S.A. Barrow, J.W. Babich, D.R. Elmaleh, P. Meltzer, B.K. Madras, A.J. Fischman.

Massachusetts General Hospital, Division of Nuclear Medicine

SPECT IMAGING OF PARKINSONS DISEASE WITH I-123 ALTROPANE.

Parkinson's disease (PD) is a progressive neurodegenerative disease that is associated with depletion of pre-synaptic dopamine (DA) transporter sites in the striatum. Thus, radioligands that bind to these sites are useful for monitoring disease progression. In this investigation, we used [I-123] 2b-carbomethoxy-3 beta-(4-fluorophenyl)-N-(1-iodoprop-1-en-3-yl)nortropine ([I-123]-Altoprane) for imaging MPTP treated monkeys, healthy human volunteers and patients with PD.

Three male rhesus monkeys (before and after MPTP induced PD), 7 healthy volunteers and 8 male PD patients were studied. The animals were injected with approximately 5 mCi of [I-123] Altoprane and SPECT was performed 30 min. later. Regions of interest were drawn over the striatum and cerebellum and accumulation ratios were calculated. The human subjects were injected with 5-10 mCi of I-123 Altoprane and dynamic SPECT / arterial blood sampling was performed over 1.5-2 hrs. Striatal (Str) binding potential (BP, B' max / KD) was calculated from Str TAC's using occipital cortex as reference.

Prior to MPTP treatment, the striatal to cerebellar ratio at 30 min. after injection of [I-123] Altoprane was ~6:1 and striatal accumulation was completely displaced by the DA transporter ligand, CFT (1 mg/kg), but was unaffected by a similar dose of the selective serotonin (5-HT) transporter ligand, citalopram. After MPTP treatment, striatal accumulation of Altoprane was completely abolished; striatum/ cerebellum ratio ~1:1. In the healthy volunteers, Altoprane accumulated rapidly in the striatum and excellent quality images were obtained within 1 hr after injection. Tracer selectivity was supported by lack of accumulation in serotonin rich regions of the brain. Average BP was 1.77±0.18. In the patients with PD, striatal accumulation was significantly reduced. This reduction was most pronounced in the posterior putamen and the caudate nuclei were relatively spared. In the PD patients, BP was reduced to 0.92 ± 0.05 (p<0.001).

These results establish that I-123 Altoprane has the favorable characteristics of: 1. High accumulation in normal striatum. 2. Reduced accumulation in striatum of PD patients and MPTP treated monkeys. 3. Selectivity for dopamine vs. serotonin binding sites. 4. Pharmacokinetics that are well matched to the physical half-life of I-123. In the future, this radiopharmaceutical could be of great value in the diagnosis and therapeutic monitoring of patients with PD and for evaluating new therapeutic agents in animal models.

OT-36

P.Steifer, R.Junik, J.Sowiński

Department of Endocrinology, University of Medical Sciences Poznań, Poland

AN OPTIMIZATION PROCESS OF SEMI-QUANTITATIVE ANALYSIS rCBF 99mTc-HMPAO BRAIN SPECT

A critical analysis of rCBF ^{99m}Tc-HMPAO SPECT has been a standard procedure independent of an image quality (reconstruction with permanent parameters). The aim of this work was the optimization of parameters for semi-quantitative analysis with regard to maximum counts for pixel in tomographic projections. The acquisitions were obtained using one-headed gammacamera Diacam (Siemens). The studies were realized in technique step-and-shoot with a rotation angle 360°, matrix 64x64, collimator HIREs and number of projection 64. The analysed studies were divided on three groups proportionally to maximum counts for pixel. The first group consisted of studies with low number of counts 0-70, the second 70-140 and the third above 140. The data set contained from 9 studies, 3 in each group. The optimization process of semi-quantitative analysis manage from the point of view of fast selection the cut-off frequency f_c , the low-pass filter Butterworth (order $n=7$) according to kind of group, and attenuation correction coefficient c and matrix size of interpolation filter. The following cut-off frequencies were taken into account: for the first group $f_c=\{0,35; 0,40; 0,45\}f_n$, for the second one $f_c=\{0,40; 0,45; 0,50\}f_n$, for the third one $f_c=\{0,45; 0,50; 0,55; 0,65\}f_n$ (f_n -Nyquist frequency). In all studies were applied the attenuation correction with coefficient $c=\{0,09; 0,12; 0,15\}$ 1/cm and interpolation with the size of the matrix $\{3x3; 7x7; 11x11\}$. As a criterion of image usability assumed a difference in contrast for loss between standard tomographic image (Butterworth filter $f_c=0,45$ $n=7$; attenuation correction $c=0,12$ 1/cm with interpolation $11x11$) and analysed one. The statistical analysis of results proved a dependence $P<0,05$ between average geometric contrast of images with maximum counts for pixel higher than 140, reconstructed with the cut-off frequency $f_c=0,55$ f_n , and the standard image. Also it was found the same dependence between the first group and the standard image at the cut-off frequency $f_c=0,40$ f_n . The analysis of attenuation coefficient c showed important differences. For further studies was accepted attenuation coefficient $c=0,12$ 1/cm, consistent with common standard. Optimization of the matrix order of interpolation filter proved increasing of contrast with decreasing size of the matrix. Conclusion: According to maximum counts for pixel in projection it should change parameters of image reconstruction, particularly the cut-off frequency f_c of Butterworth filter. One should apply attenuation correction with coefficient $c=0,12$ 1/cm, and interpolation with matrix size equal $3x3$.

Miscellaneous

PT-1

M.Soto, I.Mendo, D.Rodriguez, D.Fuster, F.J.Setoain.
Clinic Hospital. Department Nuclear Medicine. Barcelona.

IS HYDRATION APPROPRIATE IN BONE SCAN ?

The aim of our study was to assess whether hydration before bone scan improves the quality of the images; with regard to: bone/soft tissue uptake and the visualization of pelvic structures with filled bladder.

Methods: 100 patients (pats): 50 breast cancer (B.C) and 50 prostatic cancer (P.C) were studied, according to the following protocol: 50 patients (25 P.C and 25 B.C) were encouraged to drink between 1 and 1.5 liters of water p.i. and the remaining 50 patients (25 P.C and 25 B.C) did not drink anything. All patients were requested to void before the beginning of the scintigraphic procedure. Whole body scintigraphy was performed 1.5-3 hours after i.v. injection 25 mCi of ^{99m}Tc HMDP. Images acquisition was performed using a dual-head gammacamera Helix, Elscint, with a matrix size of 512x512 and speed of 15 cm/min. Visual scoring of the bladder size was evaluated using a qualitative scale: I=small size, II=medium size and III=large size. Semiquantitative scoring of the bone/soft tissue activity (B/S.T) was evaluated by means of ROIs and the ratio was corrected by decay and the injected dose.

Results: Bladder visual scoring in the P.C. hydration group showed: I=5 pat, II=13 pat, III=7 pat, and in the P.C. group without hydration: I=16 pat, II=7 pat, III=0 pat. Bladder visual scoring in the B.C. hydration group showed: I=3 pat, II=12 pat, III=10 pat and in the B.C. group without hydration: I=18 pat, II=7 pat, and III=0 pat. In the hydration B.C. group semiquantitative scoring showed a B/S.T ratio of 0.0975. In the without hydration B.C. group the B/S.T ratio was 0.1244 (t-test: P<0.05).

Conclusions: In P.C patients, the use of bone scan without hydration could be a better means of obtaining clearer visualization of pelvic structures. Furthermore, bone scan without hydration could also improve the quality of images in B.C patients, given that the B/S.T ratio increased without hydration.

PT-2

J.Katzwinkel, K. Wilhelmi, K. P. Kaiser, B. Klemenz, H. Wieler

Central Military Hospital of Germany, Dept. of Nuclear Medicine, P.O. Box 7460, 56064 Koblenz, Germany

DOES THE LEVEL OF HYDRATION EFFECT IMAGE QUALITY IN BONE SCINTIGRAPHY ?

This study was to test whether and in what way different levels of hydration influence the image quality of bone scans carried out with Tc-99m-MDP.

Materials and methods: 160 patients that have no renal disease were divided into 3 groups according to the fluid-amounts (I: 0.25 l; II: 1.0 l; and III: 1.5 l fluid intake) they drank between the injection and the subsequent image. Routine acquisition started 180 minutes after the injection of 555 MBq Tc 99m-MDP on a SOPHA DSX one-head-camera (LEAP-Collimator, scan speed 20cm/min.). B/S.T ratio was calculated using an ROI over the whole femoral diaphysis compared to a contralateral adductor area (mean of ventral and dorsal projections). Image quality was assessed independently on a semiquantitative score by different observers. There were no differences regarding thigh circumference, fluid intake prior to injection and the start of bone scan p.i.

Results and Discussion: No significant differences in B/S.T ratio or image quality were demonstrated with different amounts of fluid intake. The median values of B/S.T ratios were 1.90 (I), 1.93 (II), and 1.84 (III). Obviously there is no connection between drinking amounts and image quality so that there is no need to drink a lot during the break.

Conclusion: Large drinking amounts are not necessary for patients' preparation as they neither increase B/S.T ratios nor improve image quality in bone scintigraphy. Nonetheless patients should drink a lot after the completing of the examination to reduce the effects of radiation.

PT-3

Marchi G., Cimatti G., Dalmonte A., Frontali B., Zampagna C.

Nuclear Medicine Dpt, Ospedale per gli Infermi, Faenza AUSL Ravenna (Italy)

ROLE OF ^{99m}Tc-HMPAO-LEUKOCYTE SCAN (WBS) AND ^{99m}Tc-MDP BONE SCINTIGRAPHY (BS) IN DIABETIC FOOT.

Early and accurate diagnosis of osteomyelitis (OM) in diabetic patients (pts) represents the main key to successful management but it's difficult because the clinical likelihood of OM often does not appear through radiographic imaging.

Aim of the study was to evaluate the diagnostic efficacy of WBS and BS in diabetic foot.

We have studied 35 pts, (14 male and 21 female) with mean-age 59 (range 22-74 yr.) with insulin dependent-diabetes, foot ulceration and suspicion of OM; all patients were submitted to clinical examination, radiography, ultrasonography and bacterial culture. All pts underwent BS with 740 MBq Tc-99m-MDP while injected, five minutes and three hours after being injected; a week later they were submitted to WBS. Leukocyte separation was performed with multiple density-gradient centrifugation of a 50ml blood venous sample added with ACD; for labeling we have used a HMPAO vial for each pt and fresh eluted Tc-99m (dose between 370 and 1110 MBq) in a maximum volume of 5 ml. The labeling rate resulted of 56% (range 31-84%). The acquisitions were performed 30 minutes after the administration to verify the bone marrow distribution and 4 and 24 hours post injection.

OM was confirmed in 18 cases with WBS and BS; in 9 patients WBS and BS were negative for OM, confirmed by clinical follow-up; in 3 patients who resulted affected by OM, BS was negative while WBS was positive. In 3 patients giving negative results, BS showed a false-positive pattern, while in 2 patient with OM and BS positives, WBS was false negative.

Calculated sensitivity, specificity and accuracy of the two methods resulted of 91, 100 e 94% for WBS, and 87, 75 e 83% for BS respectively.

Our data show the relevance of Nuclear medicine procedures in the diagnosis of OM in diabetic foot; compared with BS, WBS proved to be more sensitive, specific and accurate.

PT-4

Özden ÜLKER, Gamze ÇAPA, Ender ELLİDOKUZ, Hale AKPINAR, Hatice DURAK, İlkay ŞİMŞEK

Dokuz Eylül University, Faculty of Medicine, Departments of Nuclear Medicine and Gastroenterology, İzmir, TURKEY

THE VALUE OF Tc. 99m HMPAO LABELED LEUCOCYTE AND Tc. 99m HIG SCINTIGRAPHY IN THE DIAGNOSIS OF INFLAMMATORY BOWEL DISEASES

The diagnosis of ulcerative colitis and Crohn's disease are made by endoscopy and biopsy. The clinicians need some other diagnostic methods than colonoscopy and colon-grahy with contrast media which are contraindicated during the acute phases to determine the spread and severity of the inflammatory bowel disease. In this study we investigated the value of Tc. 99m HMPAO labeled leucocyte and Tc. 99m Hig scintigraphy in the diagnosis of inflammatory bowel diseases. We included 9 patients (mean age= 46±14) with the diagnosis of ulcerative colitis and Crohn's disease. After giving 4 mCi of Tc-99m HMPAO labeled leucocytes intravenously, the imaging was performed at 4th and 24th hours. The images of the abdomen were taken from the anterior and both lateral projections with a gamma camera (GE, XR/T). Two days later Hig scintigraphy with 20 m Ci Tc 99m performed under the same conditions. Tc-99m HMPAO labeled leucocyte scitigraphy showed the exact localization with the colonoscopy in all the patients while showing additional uptake sites in 5 patients. Activity uptake at the ileocecal region was seen in 2 patients and 1 patient had the diagnosis of Crohn's disease after total colectomy. In the remaining 3 patients colonoscopy ad colon-grahy could not be performed because of the severe clinical symptoms. Tc. 99m Hig scintigraphy has shown the true localization in 5 patients. The amount of activity uptake was lower than the amount of leucocyte scintigraphy. However the 2 patients whose pathologic diagnosis were severe chronic active colitis showed increased uptake than the others.

It can be concluded that the Tc. 99m HMPAO labeled leucocyte scintigraphy can be used for the determination of the spread, whereas the Tc. 99m Hig scintigraphy can be used in the determination of the severity of the inflammatory bowel disease.

PT-5

Ayten GÖZÜCİ, Ahmet Kara, Ersoy Kekilli, M.Cudi Tuncer
Dicle University, Medical Faculty, Nuclear Medicine and
Anatomy Departments, Diyarbakir

**EXPERIMENTAL STUDY: LOCATION OF THE NEW AGENT
Tc-99m INFECTON IN BACTERIAL INFECTION AND
STERIL INFLAMMATION IN RATS**

Conventional radionuclide agents such Ga67 and radiolabeled leucocytes can identify general inflammation but can not distinguish bacterial and non-bacterial inflammatory processes. The aim of this experimental study was to compare accumulation of the new agent Tc-99m Infecton (based on the ciprofloxacin) in bacterial infection and with steril inflammation. White albino rats left thigh muscle were infected with *S.aureus*(group 1) and steril inflammation was created by chemical irritant left thigh muscle (group 2). Images were obtain at 1,4 and 24 hours after administration of 1mCi Tc-99m Infecton. For quantification "Relative Uptake (RU)" = [lesion count-background count / background count] and "Residual Activity (RA%)" = [lesion count - pixel corrected background count/ total body count] were calculated. Following Tc-99m infecton administration, accumulation of activity continuously increased during 24 h in bacterial infected side(group1). In group 2 RU and RA% were significantly higher than in group2 at 4 hrs (p<0.005) and at 24 hrs (p<0.001) but no significant differences were found at 1hr (p>0.05). In this in vivo study showed bacterial inflamed area accumulated Tc-99m Infecton more than steril inflammatory area. Further research is necessary to determine how to relate these findings to true human clinical situation.

PT-6

J.L.RIU, J.L.FILIPPI, I. DRAPIER, C. CELTON, C. BILLOTEY.
Hospital Saint-Louis : Department of Nuclear Medicine, Paris, France.

ADVANTAGES OF PARATHYROID SCINTIGRAPHY USING ^{99m}Tc - MIBI, FADS AND SPECT.

Aim :
Emphasize interest of using ^{99m}Tc - MIBI, Factor Analysis of Dynamic Structure (FADS) and Single-Photon Emission Computed Tomography (SPECT) to detect abnormal parathyroid glands.

Technical conditions :

Patient is 4h fasting.

1 - **Dynamic acquisition** is started at the time IV bolus injection of 660 to 740 MBq of ^{99m}Tc -Mibi and performed with a pin-hole collimator centered on the thyroid area (30 one minute-images matrix 128 x 128, zoom factor 1,33 to 1,6).

2 - **Planar static views** (all-purpose collimator) ,

- a- lateral views of necks (600 kcts, matrix 128 x 128, zoom factors 1,6 to 2)
- b- Thorax anterior view (1000 kcts, matrix 128 x 128, zoom factor 1 to 1,33)
- c- 2 or 3 radiomarkers of ¹³³Ba are placed on sternum and clavicle. Dual isotope acquisition of thorax is performed with the same technical criteria.

3 - **SPECT** of thorax and neck (dual isotope acquisition -360°-64 steps of 55 sec - elliptical mode - matrix 128 x 128)

Discussion :

Because of Mibi is trapped inside mitochondria as ²⁰¹Tl and because of oxyphilic cells of parathyroid tissue have a large content of mitochondria, ²⁰¹Tl could be replaced by Mibi-^{99m}Tc, with better physical qualities. Because of FADS applied to the initial dynamic acquisition allows to detect abnormal parathyroid gland in the thyroid uptake area, FADS replace a subtraction technic. So we have single tracer method with high background and scattering allowing a high quality SPECT. Permanent availability of Mibi ^{99m}Tc and more favorable dosimetry constitute additional advantages.

Conclusion :

This new method allows to detect more 85% abnormal parathyroid glands including hyperplastic glands even in cases of posterior and small glands.

PT-7

A. Onodera, A. Arima

Hospital: Funabashi Municipal Medical Center, Department of Radiology

EVALUATION OF SEQUENTIAL Tl-201 THYROID SPECT WITH FAN BEAM COLLIMATOR.

The aim of this study is to evaluate sequential SPECT imaging of the thyroid gland, by a double-headed system with continuous repetitive rotating acquisition mode and a fan beam collimator on the purpose of establishment of an objective examination method for Tl-201 labeled thyroid gland. We examined 45 patients with nodular goiter(1994.4-1998.2). SPECT was conducted from 15 min after intravenous injection of Tl-201 for a total of 30 min over 6phases (5min/phase)and the transverse and coronal images were constructed.

These images were subjected to 2-dimensional polar coordinate expression and the estimation of retention index. Thus, parametrical expression of Tl-201 retention was attempted. The cases of which retention levels were varied, including benign and malignant goiters could be visually discriminated based on these sequential SPECT images and the differences were significant. In addition, the semi-quantitative expression was possible by the use of circumference map. Since the imaging sensitivity was improved by the utilization of sequential SPECT with fan beam collimator, it became possible to magnify the images. These results suggest that sequential SPECT with fan beam collimator is available for local qualitative diagnosis of a small organ such as thyroid gland, from which Tl-201 is rapidly washed out.

PT-8

P. Cook, B. Bedford, A. Bell, P. Lang, C.Leiper, A. Prouse.

Bankstown - Lidcombe Hospital, NSW, Australia.

EVALUATION OF A POSITIVE VENTILATION DELIVERY SYSTEM (PVDS) IN ADMINISTERING TECHNEGAS TO THE NONCOMPLIANT PATIENT.

Certain groups of patients have been excluded from ventilation lung scanning due to their inability to comply with instruction. Tetley Manufacturing have recently developed a Positive Ventilation Delivery System (PVDS) which assists in delivering Technegas to patients who are unable to cooperate fully. The aim of this study is to evaluate the PVDS in the clinical setting.

Twenty seven frail aged and psychogeriatric patients, mean age 78 years, were ventilated with Technegas using the PVDS. The decision to ventilate the patient with the PVDS was based on an initial assessment of the patients ability to comply with instructions, or failure of the conventional ventilation method to produce an adequate count rate. Technegas was prepared in the usual manner and then delivered to the patients lungs by squeezing a black anaesthetic bag synchronously with the patients breathing, until a count rate of approximately 1000 counts/second was obtained.

All patients achieved a satisfactory count rate, mean 1344 counts/second (range 600 to 2200), allowing adequate ventilation images to be obtained. Time to reach this count rate varied between patients, mean 127 seconds (range 40 to 300). The number of assisted breaths also varied, mean 9 (range 3-15). In addition, seven patients who required a switch from the conventional method to the PVDS, increased their initial count rate from a mean 157 counts/second to a mean of 1300 counts/second. This was statistically significant at p = 0.003.

Our initial results demonstrate the ability of the PVDS to facilitate ventilation imaging in noncompliant patients such as the frail aged and psychogeriatric. Ventilation times and amounts of radioisotope used were acceptable, economical and practical within a busy department.

PT-9

G. Larsson, I. Nikadon, E. Svensson, B. Bake, J. Grétarsdóttir.
Hospital: Sahlgrenska University Hospital, Göteborg, Sweden,
Departments of Clinical Physiology and Radiation Physics.

99mTc - CONTAMINATION OF TECHNOLOGISTS DURING TECHNEGAS VENTILATION

Ventilation scintigraphy using Technegas is widely used. In our department, the presumed 99mTc-contamination caused by these investigations has been of concern to the staff performing the studies.

Aim: To investigate whether the performance of Technegas ventilation scintigraphy causes a substantial 99mTc-contamination of the technologist in our Nuclear Medicine Department. **Method:** The study was performed according to the table below. WBC = whole body counting in a scanning bed geometry with two NaI(Tl) detectors.

During inhalation the technologist wore an extra robe, a disposable

Nr. of studies	Applied activity	Step 1	Step 2	Step 3	Step 4	Step 5
5	900 MBq	WBC	Other work in the department	WBC	Ventilating the patient	WBC
5	500 MBq			WBC	Ventilating the patient	WBC

hat and mask and double pair of gloves. The activity contaminating these clothes was later measured on an uncollimated gamma camera. Prior to all measurements in the whole body counter the technologist changed all working clothes to a clean robe. **Results:** The contamination of the technologists from 99mTc-Technegas was 10 - 50 kBq in nine out of ten cases. For the tenth case the value was 160 kBq. The contamination from other work in the department showed similar distribution, below 1 kBq for four cases and almost 400 kBq for one. The amount of 99mTc remaining on the disposed clothes was 30 - 300 kBq. **Conclusion:** A substantial amount of the 99mTc, contaminating the technologist during inhaling the patient, was found on the protection clothes. A yearly performance of 100 ventilation scintigraphies with the highest level of contamination measured in this study, would result in a yearly intake below 1 % of ALI (3000 MBq).

PT-10

L.Loufi, G Al-Mutairi

Faculty of Medicine and Faculty of Allied Health Sciences & Nursing, Departments of Nuclear Medicine and Radiological Sciences, Kuwait University, Kuwait

POSITIONING GUIDELINES FOR DYNAMIC RENAL SCINTIGRAPHY. A STUDY OF RENAL AND SKELETAL LANDMARK RELATIONSHIP IN 99mTc MDP BONE SCAN

Correct patient positioning for dynamic renal scanning cannot be predicted due to lack of external renal landmarks. A fixed landmark of the human body is needed to help in positioning the patient for optimal performance of these studies.

To address this issue, we reviewed 10 whole body bone scans, where both kidneys and skeletal structures are readily visualized, to find a bony marker that could be useful for positioning the patient in a renogram study. The main indication for the bone scan was evaluation for metastatic disease of the skeleton. The age range of the patients studied was 16-60 yr. Whole body bone scans were performed 2-3 hours after intravenous injection of 740 MBq (20 mCi) 99mTc MDP using a dual head scintillation camera (Multispect, Siemens). The camera was used in scanning mode with a speed of 7-8 cm/min without zoom. Images were recorded on nuclear medicine transparency film with no image manipulation.

we identified the iliac crests to be the most suitable bony structures amenable to external identification by simple palpation for the purpose of patient positioning. For each scan, the following measurements were obtained: top of kidney to iliac crest (TK-IC), bottom of kidney to iliac crest (BK-IC), top of kidney to bladder (TK-BL). Measurements on film were calibrated to actual distance.

The maximum distance TK-IC was identified to be 21 cm, which resulted in a recommendation for placing top of the field of view of the scintillation camera not less than 21 cm above the iliac crest. Using large field of view cameras and the above recommendation both kidneys and the bladder (maximum distance TK-BL: 40 cm) would be included in the imaging field.

PT-11

A. Lindh, M. Malmgren, S. Ekberg, M. Stenström, G. Granerus

University Hospital, Section of Nuclear Medicine, Linköping, Sweden

ANALYSIS OF THE DIURETIC RESPONSE TO 7 ml/kg HYDRATION PRIOR TO CAPTOPRIL RENOGRAPHY

According to the international consensus on ACE inhibitor renography detecting renovascular hypertension (JNM 1996; 37, 1876-82) a hydration protocol with 7 ml water per kilogram of body weight 30 to 60 min prior to the test is suggested. Too low urine flow rate will invalidate the criteria used for interpreting the test and must be recognised and should be avoided.

A consecutive material of 146 patients following a strictly standardised protocol was studied. The patients received 25 mg captopril one hour before the injection of the indicator, 75 MBq 99mTc-MAG3, and simultaneously hydration with water was started. The patients were asked to empty the bladder just before acquisition and immediately afterwards, the volume and time interval were recorded and used for calculation of the urine flow rate. The following parameters were recorded as well: Age, diagnosis, blood pressure before and in 15 min intervals after captopril to detect possible hypotensive response, indications of residual urine, renal function and actual medical treatment with diuretics and ACE inhibitors. Low urine flow rate was defined as less than 2 ml/min.

The mean flow rate in the whole material was 4.8 ml/min (SD 3.8 ml/min). A low urine flow rate was found in 35/146 (24%). An analysis of variance (ANOVA) in the group of patients with a low urine flow rate revealed no significant correlation between the recorded parameters. The number of parameters needed to be extended in a final analysis, including all medical antihypertensive treatment, in order to examine a course relationship to low urine flow rate.

In conclusion there were no single or combination of parameters which could predict a low diuretic response in this material. Therefore, measurement of urine production when performing the Captopril renographic test is highly recommended.

PT-12

İ. Evren, H. Durak, B. Değirmenci, E. Derebek, E. Özbilek, G. Çapa

Dokuz Eylül University School of Medicine, Departments of Nuclear Medicine

THE USEFULNESS OF CARDIOFOCAL COLLIMATOR IN STATIC RENAL IMAGING

The purpose of this study was to investigate the usefulness of the cardio-focal collimator used for myocardial perfusion imaging in static renal scintigraphy.

Fifteen children (age range:4 to 8) referred to nuclear medicine department in order to investigate cortical renal lesions. Four hours after Tc99m DMSA injection, static views from posterior projection were obtained low energy general purpose (LEGP) in 256x256 matrix and 5 minutes duration (General Electric XR/T gamma camera). Then additional three more static views from posterior projection were obtained with low energy high resolution (LEHR), cardio-focal (Siemens Multispect-2 gamma camera) and pinhole collimators (General Electric XR/T gamma camera). The total counts for each collimator were the same. Images were evaluated visually. The visual interpretations were made by four nuclear medicine physicians as follows: Very good:4, good:3, moderate:2, and bad:1. The mean values were 3.4±0.9 for pinhole collimator, 2.7±0.3 for cardio-focal collimator, 2.6±0.4 for LEHR and 2.4±0.5 for LEAP. Cardio-focal collimator took the second highest point from nuclear medicine physicians at the point of image quality.

This study suggests that pinhole collimator may be best collimator for static renal scintigraphy and cardio-focal collimator might be used for static renal imaging.

PT-13

G. Bern, M. Finnbogason, H. Jacobsson, S.A. Larsson and P.O. Schnell
Karolinska Hospital, Department of Nuclear Medicine, Stockholm, Sweden

MEASUREMENTS AND ANALYSES OF PATIENT MOTION DURING 99m Tc-DMSA -SPECT OF CHILDREN

Introduction. Long exposure times may introduce artefacts and image blurring due to patient motion. This is one of the reasons why the value of 99mTc-DMSA renal SPECT in pediatric nuclear medicine has been questioned in relation to planar imaging. The common indications for these examinations are pyelonephritis or assessments of relative kidney functions. We routinely perform SPECT examinations in addition to a posterior view. The purpose of this study was to assess the extent of kidney motion during SPECT.

Method. Twenty children with a mean age of 22 months and ranging from 3 to 54 months were examined. All children were fixed in the vacuum bag and only three required mild sedation. The children were given 2 MBq/kg of 99mTc-DMSA and SPECT examination was performed after four hours on a three headed gamma camera equipped with low energy ultra high resolution collimators. The acquisition parameters were 90 views over 360° for total time of 30 min. The reconstructed spatial resolution was about 12 mm (FWHM). Since each projection is acquired three times during the examination, patient movements could be assessed by comparing the kidney positions at these occasions, 10 min. apart. The difference in renal position was determined at four views: anterior, posterior, right and left laterals by subtracting the three different images from each other. A profile was positioned over the subtracted images and the magnitude of deviations appearing at the kidney borders were compared to those of a phantom study with controlled axial and transverse displacements. The smallest level of displacement detection was <5 mm in all directions.

Results. Motion artefacts could be observed in 5 of the 20 cases. In one case, there was an axial motion 44 mm which made findings inconclusive. In the other four cases, motion artefacts were between 6 and 13 mm but conclusive findings could still be made. In 3 of these 4 cases, the motion seemed to be restricted to one kidney only and only during the first 10 minutes. This indicates an internal displacement of the kidney rather than a movement of the body.

Conclusions. With our immobilisation devices and our paediatric routines we conclude that 99mTc-DMSA-SPECT is a reliable technique that can be performed on most children. The movement of a single kidney indicates internal repositionings which suggests 10 min rest in supine position before examination.

PT-14

C. de Haan, M. Versteeg, A. van Lingen, G.J.J. Teule.
Free University Hospital, Department of Nuclear Medicine, Amsterdam, The Netherlands.

FIXATION BY VACUME CUSHION: ARE THERE EFFECTS ON IMAGE QUALITY IN SMALL CHILDREN ?

Fixation cushions are often used to restrain small children during e.g. renography. However, it is not clear whether this tool hampers the image quality, such as uniformity or spatial resolution. We studied these effects by means of static phantom images using 99mTc. Spatial resolution was obtained from a line source (3 MBq) at distances of 2 cm (without cushion) and 4.5 cm (with and without) from the camera. Spheres (diameters: 3, 5, 7 cm) were imaged (0.1 Mcnts, zoom factor 2) at the same distances both with and without cushion. FWHM and FWTM were measured from the line source images. The spheres were visually analysed to see whether the effects were noticeable. Scatter contribution was determined from the FWTM. Image uniformity was assessed by acquiring 25 Mcnts images of a (350 MBq) 57Co flood source with and without the cushion. The cushion was applied by folding it such that one half was less than 1 cm thick and the other half had a thickness of 10 cm. The effect on uniformity was assessed from a profile over both halves.

At 2 cm FWHM and FWTM were 6 and 12 mm, respectively. At 4.5 cm these numbers were 8 and 16 mm, respectively. The cushion had no effect on the spatial resolution. The images of the spheres did not show any visual change in diameters nor in image contrast. The uniformity image profiles, however, showed a 2% decrease in contrast due to attenuation in the cushion. This 2% was visually noticeable, due to the sharp delineation between the two halves. Hence, we conclude that use of a fixation cushion does not impair image quality in terms of spatial resolution and contrast.

PT-15

Y. Katagiri, Y. Odawara, M. Kuroda, Y. Fujiwara, H. Oomoto, T. Nakata, S. Shimoshige, K. Shimamoto, K. Fujimori, K. Morita.
Sapporo Medical University, Division of Radiology and Nuclear Medicine.

REGIONAL AND GLOBAL ASSESSMENT OF LEFT VENTRICULAR FUNCTION AND PERFUSION BY AUTOMATED MYOCARDIAL GATED SPECT

Simultaneous assessment of myocardial perfusion and function can provide not only diagnostic but also prognostic information and might contribute to cardiac patient management. However, the data processing technique has not been established. We newly developed automated data analysis using myocardial gated SPECT data with technetium-99m labeled sestamibi or tetrofosmin to regionally and globally evaluate left ventricular perfusion and function. In addition to serial display of tomographic images and 2-dimensional displays by polar map and unfolded surface map, 3-dimensional perfusion display is possible. The software can provide left ventricular ejection fraction (LVEF) by using a new edge-detection technique with a maximum-count based circumferential analysis. The LVEF closely correlated with that obtained from radionuclide ventriculography with a regression line of $y=0.918x+6.0$, $r=0.88$, in 49 patients with known and suspected coronary artery disease. Regional perfusion was quantified as a percent peak count at end-systole and end-diastole and regional wall thickening was quantified as normalized percent thickening using the following formula:

$$\text{Normalized percent thickening (\%)} = \frac{(\text{End-systolic count} - \text{End-diastolic count}) \times 100}{\text{Max} (\text{End-systolic count} - \text{End-diastolic count})}$$

The regional wall motion assessed by this technique was well related to that by 2-dimensional echocardiograms in 43 acute myocardial infarct patients. In this software, manual operation is limited to the selections of cardiac long axis for reconstruction of SPECT images and short axis slices for 2- and 3-dimensional displays. The inter-observer error of LVEF was 5.2%. Thus, automated gated SPECT analysis can provide a highly reliable information of myocardial perfusion and function and might be useful for quantitative regional assessment of perfusion and contraction in routine clinical practice.

PT-16

L. Evren, E. Özbilek, H. Durak, E. Derebek, B. Değirmenci

Dokuz Eylül University School of Medicine, Departments of Nuclear Medicine

THE EFFECT OF LOW OR HIGH DOSE Tc-99m MIBI ON CALCULATING LEFT VENTRICLE EJECTION FRACTION

The purpose of this study was to investigate the effect of low or high dose Tc-99m MIBI on calculating left ventricle ejection-fraction (LVEF) in both low dose rest and high dose stress gated myocardial perfusion spect (GMPSPECT).

Thirty-five patients (12 female, 23 male, mean age:57±0.5) were included in this study. The GMPSPECT images were acquired with Simens Multispect-2 gamma camera equipped with low energy high resolution parallel hole collimator and were recorded in 64x64 matrix. A same day rest-stress GMPSPECT imaging protocol was used in all patients, with 7mCi of Tc-99m mibi injected at rest and 25mCi of Tc-99m mibi at stress. Thirty-two images were acquired using the step-and-shoot method with 30 seconds and 40 seconds each for rest and stress respectively, beginning from 45° RAO to 135° LPO projection. Rest and stress images were gated at 8 frames per cardiac cycle. A butterworth filter (cut off frequency:0.5 and power factor:5) was applied during reconstruction. End systolic and end diastolic spect images were obtained as short and vertical and horizontal long axis slices. The LVEF was calculated from both rest and stress study using both manuel and automatic programs. Student t test was used for statistical evaluation. The results are summarized in the table.

LVEF	Low dose (REST) (%)	High dose (STRESS) (%)
Manuel	54±16	55±16
Automatic	63±24	63±17

There was no statistically significant difference between the LVEF values obtained from low and higy dose Tc99-m mibi by manuel and automatic programs.

This study indicates that the amount of sestamibi dose given to patient and type of protocol used do not affect the LVEF values significantly.

PT-17

K.Mori, H.Maruno, K.Saito, A.Okazaki, M.Onoguchi*

Hospital: Toranomon Hospital, Division of Nuclear Medicine
*School of Health Sciences, Faculty of Medicine, Kanazawa University

CARDIAC FUNCTION ANALYSIS WITH FUNCTIONAL G-MAP METHOD IN NORMAL SUBJECTS

We evaluated regional cardiac function with a new analysis method (Functional G-map method) in 10 normal subjects using ECG gated SPECT. Methods: ECG gated SPECT data were acquired 1 hour after the intravenous injection of 1110 MBq ^{99m}Tc-tetrofosmin dividing a cardiac cycle into 12 frames. Firstly every short-axis images were reconstructed using 11 of 12 frames. These short-axis images were repeated performing slice thickness correction to make 10 slices with same thickness, and each short-axis series of subsequent images was divided by 40 radii into 40 segments. The time-activity curve was generated from the total counts included in each segment plus both neighboring segments. Afterward the curve fitting was performed using Fourier expansion. We calculated the following parameters and generated maps; MAX (End-systolic count), MIN (End-diastolic count), %CI (Percent count increase), PCR (Peak contraction rate), PDR (Peak distention rate), CT (Contraction time). Each Functional G-map was divided into 5 regions. Results: In normal subjects, %CI was greater in anterior and septal region than lateral region. %PCR and %PDR was lower in lateral regions than anterior region. Conclusion: This method is useful for the estimation of cardiac function in addition to myocardial perfusion. It is necessary to make the normal file for clinical use because the significant difference among some regions is shown in some parameters.

PT-18

A.Lorotte, S. Fayolle, D. Langlet, C. Lupon, F. Mabire, M. Pelletier, A. Prigent.

Department of nuclear medicine, hôpital Antoine Bécclère, AP-HP, 92141 Clamart, FRANCE.

A SIMPLE METHOD TO REDUCE ²⁰¹Tl WASTE.

In our department, we use about 4 500 MBq of ²⁰¹Tl a week for myocardial perfusion imaging (stress and reinjection studies). The purpose of our study is to evaluate the relation between the residual ²⁰¹Tl activity and the corresponding injected volume.

Method : two different injected doses of either 111 (± 10) MBq for stress in both 0.8 and 1.5 mL or 56 (± 5) MBq for reinjection in the range 0.4 to 1.5 mL has been used to assess the respective effect of the injected activity (IA) on the volumic activity (MBq/mL). Injected activities have been determined by the difference between pre- and post-injection syringe counts. Residual activities were expressed in % of the pre-injection syringe count (m ± SD).

Results : n = number of syringes.

n	IA = 111 MBq		IA = 56 MBq			
	28	28	16	16	16	16
mL	0,8	1,5	0,4	0,8	1	1,5
MBq/mL	138.5	74	140	73.5	56	37.3
m	5,9 %	3,7 %	6 %	4,6 %	3,9 %	2,9 %
(± SD)	(1,6)	(0,9)	(1,4)	(1,4)	(1,7)	(1,1)

Although the benefit for imaging appears marginal, the reduction of the residual activity by about 40 to 50 % when using a final injected volume of 1.5 mL enables us to decrease the weekly radioactive waste from about 220 MBq to 135 MBq.

Conclusion : the use of injected volume of at least 1.5 mL for the recommended ²⁰¹Tl activities for stress and rest myocardial perfusion studies allows the reduction of our department radioactive waste to about 50 %. This simple measure may be recommended to improve radioprotection and optimizes the use of ²⁰¹Tl.

PT-19

S.Yanagimoto, T.Sone, K.Nagai, N.Otsuka, H.Mimura, T.Tomomitsu, M.Fukunaga

Kawasaki Medical School, Department of Radiology

COMPARTMENT ANALYSIS OF ¹²³I-IOMAZENIL ACCUMULATION IN THE BRAIN ON EARLY AND DELAYED SPECT.

We investigated the intracerebral behavior of ¹²³I-Iomazenil (IMZ) on SPECT images in 12 adults (6 males and 6 females, with a mean age of 56.1 years). The washout rate of ¹²³I-IMZ from the brain was estimated from two SPECTs done at 15 min and 3 hr after injection. Although the washout was relatively slow, the rates differed in each intracerebral region, suggesting that the distribution of ¹²³I-IMZ was changing with time. In addition, when ¹²³I-IMZ kinetics in the brain was assumed as the three-compartment, two-parameter model, the transition rate constant (K₁) from the blood to the brain and the binding potentials (BP) of benzodiazepine to the receptor were calculated. BP and K₁ values were compared with ¹²³I-IMZ SPECT counts and CBF values by ¹²³I-IMP. The BP values correlated more closely with the counts on the delayed SPECT than those on the early SPECT. It was confirmed that delayed SPECT images reflect better the distribution of the benzodiazepine receptor than early images. On the other hand, the K₁ values correlated highly with CBF obtained by ¹²³I-IMP, and this finding suggested that super-early SPECT images might be remarkably influenced by the distribution of CBF.

PT-20

K.Saito, H.Maruno, K.Mori, A.Okazaki

Hospital: Toranomon Hospital, Division of Nuclear Medicine

THE ERROR IN REGIONAL CEREBRAL BLOOD FLOW VALUES BY VARIATION IN CONTOUR THRESHOLD OF AUTO-DRAWING ATTENUATION CORRECTION MAP

The error in regional cerebral blood flow (rCBF) values caused by variation in the contour threshold of an auto-drawing attenuation correction map was evaluated. Images were reconstructed without scatter correction but with attenuation correction using $\mu=0.07/cm$ with an auto-drawing attenuation correction map by the Sorenson method, and with both scatter correction using the triple-energy window method and attenuation correction using $\mu=0.146/cm$. The rCBF values were obtained by the Iodine-123-IMP Autoradiography method. The variation in the contour threshold levels of the auto-drawing attenuation correction map was 2~4%. Thus, differences in the diameter of the attenuation map were 5~6 mm in the whole brain when scatter correction was not done. Consequently, errors in rCBF values were 1 ml/100ml/min (within 3 % error for rCBF). However, when both scatter correction and attenuation correction were done, the map of attenuation correction at the cerebellum level had an irregular shape and larger diameter difference than those at the basal ganglia and thalamus level in some cases. Thus, errors in rCBF values in the cerebellum were 3 ml/100ml/min (about 5% error for rCBF). Measurement of rCBF values with both scatter correction and attenuation correction must be done carefully when fixing contour threshold levels of an auto-drawing attenuation correction map.

PT-21

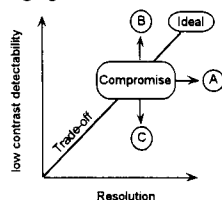
J.A. Pires Jorge¹, F.R. Verdun², E. Chevalier³, A. Bischof Delaloye³

1. Ecole TRM - Bugnon 21 - CH 1005 Lausanne
2. Institut Radiophysique Appliquée - CH 1015 Lausanne
3. Service de Médecine nucléaire - CHUV - CH 1011 Lausanne

CHOICE OF THE OPTIMUM FILTER IN SPECT IMAGING

SPECT filters greatly affect the quality of clinical images by their degree of smoothing. Thus, the determination of optimum filters is an important task in nuclear medicine. This subject has been extensively described, however, the optimum filter depends also on factors which are camera dependent such as the detector response.

In this study, a SPECT acquisition of a Jaszczak phantom acquired on a triple head camera (Trionix) has been reconstructed with all the available filters to evaluate the low contrast detectability and resolution parameters. The results are schematized on the following figure.



Filters of the "Compromise", "A", "B" and "C" domains have been tested in two clinical situations, the detection of discrete perfusion abnormalities in myocardial SPECT and of small thyroid remnants after surgery and ablative I-131 therapy, both performed after injection of Tc-99m MIBI. The clinical observer was blinded to the results of the phantom studies. For the myocardial perfusion study the filter with the highest detection coefficient in the phantom study (B) was chosen as giving the best compromise between image quality (smoothness) and discrimination of abnormal and normal tracer distribution, whereas the filter chosen for the search of occult thyroid remnants was the filter which showed the best resolution in the phantom study (A).

This study confirms that filtering of SPECT has to be adapted to the particularities of any clinical study in order to give the appropriate results.

PT-22

Th. Berthold, A. Buck

PET center, Nuclear Medicine, University Hospital, Zurich, Switzerland.

Beer Bottle Calibration of a PET Scanner

Quantitative PET imaging requires the exact calibration of PET scanner and counting devices such as well counter and blood sampling devices. This is usually done by counting a specified amount of radioactivity in the well counter and subsequent measurement of a phantom in the PET scanner. The manufacturers usually require that the PET measurement be done in a standard phantom. However, the handling of these phantoms is often cumbersome. It would be more convenient to use a smaller container for the PET measurement. The aim of this study was to test, whether calibration using a 1 liter beer bottle would be a feasible alternative. The bottle was 8 cm in diameter and the old-fashioned snap lid allowed easy handling. **Methods:** 20 MBq F-18 were put into the standard phantom of 20 cm diameter and measured for 10 minutes in the PET scanner (GE Advance, 3D mode). Then the bottle was filled with fluid from the phantom and measured again in the scanner. Attenuation correction was performed with a 10 minute transmission scan. **Results:** the difference between the measured activity in the phantom (A_{ph}) and the bottle (A_b), expressed in percent difference from A_{ph} ($(A_{ph}-A_b)/A_{ph} * 100$) was $3.4 \pm 0.4\%$ (mean \pm std of 5 experiments).

Conclusion: The difference between the measurements in the phantom and the bottle is minimal. Therefore calibration of a PET scanner to other counting devices can be performed with a commercially available glass bottle. This facilitates the calibration procedure and saves time. It should be noted that this conclusion does not hold for uniformity measurements which require the use of the standard phantom.

PT-23

F. Kinoshita, N. Yui, T. Togawa, M. Morisada, S. Maru, H. Ichihara.

Hospital: Chiba Cancer Center, Division of Nuclear Medicine,

AN ATTEMPT TO IMPROVE QUALITY OF GALLIUM-67 IMAGE BY APPLYING TRIPLE ENERGY WINDOW METHOD USING LOW-ENERGY COLLIMATORS

To improve resolution of Ga-67 image, we attempted to apply the triple energy window (TEW) method which has been recently developed for scatter correction of SPECT image. We used low energy general-purpose collimator for this study, not measuring high-energy photo peak of Ga-67 (300keV), because gamma-ray signals passing through the collimator septa could be eliminated by TEW technic, resulting more accurate localization of the lesion. One of the disadvantages of this method is that reduction of count value, reaching to approximately 40% lower than conventional method obtained by 3 photo peaks using medium energy general-purpose (MEGP) collimator. Therefore, we tried to take images with this new method within 6 hours after the administration of Ga-67 for the purpose of collecting sufficient amount of counts.

By applying TEW method and low energy collimator, we achieved to get early image with excellent quality comparable to 72 hours image taken by conventional method. This method enable the patient to finish the examination in one day and make the physicians to interpret the image without interface from bowel activities of the patient. The experimental studies and clinical cases will be presented.

PT-24

M. Takano, J. Yamazaki, H. Yamashina, T. Morishita, H. Takahashi, K. Kosakai, H. Kojima, J. Sugita, M. Takahashi

Toho University Ohmori Hospital, Tokyo, JAPAN

INTEGRATION DISPLAY OF MIBI 3D-MULTIGATED MYOCARDIAL IMAGE WITH 3D-MULTIGATED MYOCARDIAL MRI

In this study, integration of MIBI 3D-Multigated (G) myocardial image with 3D-G myocardial MRI was performed. The PRISM-3000 was used for data acquisition by MIBI G-SPECT. G-gate collected in a 64×64 matrix using 50 msec intervals. Also G-MRI data was collected using same condition. After masking of short axis images of ventricle for elimination of the background, which provided the basic for 3D-G images were constructed using a newly developed system (AVS·MV). Software modules were incorporated in such a way that two different kinds of data could be imposed on the same viewer for the AVS·MV images. Integration of MIBI 3D-G images with 3D-G MRI was attempted, which would allow simultaneous assessment of myo-cardial perfusion and structure. It was suggested that 3D display may permit integration of myocardial of morphological images such as MRI with nuclear images.

PT-25

A. van der Ree, A. Spijkerboer, J. Habraken, L. Roolker, E. Busemann-Sokole, B. de Vries*, M. van der Zee*, E. van Royen

Academic Medical Centre, Dept of Nuclear Medicine and *ICT-services Software Engineering; Amsterdam, the Netherlands

DISTRIBUTION OF NUCLEAR MEDICINE IMAGES VIA THE HOSPITAL INTRANET.

In a hospital there are many sources of patient information. Many departments insist on storing their information local. Storing all the data on a central Hospital Information System (HIS) is expensive and undesirable. This poses a problem for physicians who wish to efficiently access all the relevant data for a particular patient. An intranet project, Zouga, has been developed in our hospital that tackles this problem. Its basic philosophy is that all the patient information is stored locally in a digital format but can be collected for review by any authorized user. For the past few years the department of Nuclear Medicine (NM) has participated in this project.

The Zouga application, programmed in Java, combines the patient information of several systems and presents it to the user. Each department can supply the system with data that are desirable to share, and put authorizations on them that may be different from the HIS authorizations. Currently, Zouga can present the data of the HIS, the Radiology and the NM department, and medical literature systems. In order to reduce the amount of data, the NM department shares only the final study images with Zouga. To be able to connect with the HIS-report, each image has a patient identification number and a study number. The relevant images of a study are reformatted from the NM application by the technologist and authorized by the NM physician. A NM-image can only be viewed together with the NM-report and only if the user is authorized to read the NM-report.

We have made an intranet-application that can present data from different sources to the user at low cost. It provides physicians with the full status and progress of a particular patient. In the future it will also include the diagnosis and treatment therapy. The system can be used all over the hospital, since the user only needs to have a computer with an internet browser capable of running Java Applets. The system will reduce costs in the future, since fewer expensive hard copies will have to be made. The system is quality improving since it makes patient information more accessible and presents it in a logical manner.

PT-26

Özden ÜLKER, Meral KÜÇÜKGÜVEN, Hatice DURAK, Nuran YULUĞ

Dokuz Eylül University, Faculty of Medicine, Departments of Nuclear Medicine and Microbiology, İzmir, TURKEY

EVALUATION OF THE USEFULNESS OF THE KITS AFTER RECONSTITUTION WITH SERUM PHYSIOLOGIC

The pharmaceutical kits used for diagnosis are labeled with Tc. 99m pertechnetate to achieve radiopharmaceuticals and then are given to the patients intravenously. As it is known, once a kit is labeled with radioactivity, it has to be used within first 6 hours depending on the features of the radioactive element and the pharmaceuticals that are used. But in some situations a kit has to be used even in the presence of very few patients. This sometimes can cause economical problems.

In this study we investigated that if a cold kit could be used after reconstitution with 0.09% serum physiologic by taking the required amounts of aliquots from the kit and labeling it with Tc. 99m pertechnetate. HDP, DMSA, Tin colloid, DTPA, MAA, MAG3 and Tetrafosmin kits were included in the study. First the kits were reconstituted with 0.09% serum physiologic according to the manufacturer's descriptions. After that, small amounts of aliquots were taken from the reconstituted kits and they were labeled with suitable amounts of Tc 99m pertechnetate immediately, at 6th, 24th, 48th and 72nd hours. The labeling efficiencies were calculated using ITLC Silica Gel thin layer chromatography method. Small amounts of aliquots were also taken from the reconstituted kits under aseptic conditions and they were placed in to the suitable medias to check the sterility of the reconstituted kits in the department of microbiology. All the samples were found to be sterile at the end of the week. The percentage of the labeling efficiencies were found as in the table below:

%Labeling Efficiency	HDP	DMSA	Tin colloid	DTPA	MAA	Tetrafosmin	MAG3
Immediately	>99%	98%	>99%	>99%	>99%	94%	48%
6 th hour	>99%	82%	>99%	>99%	>99%	92%	25%
24 th hour	>99%	20%	>99%	>99%	>99%	92%	24%
48 th hour	>99%	0%	>99%	>99%	>99%	88%	24%
72 nd hour	>99%	-	>99%	>99%	>99%	85%	18%

In conclusion DMSA and MAG3 kits were found unsuitable for using after reconstitution with 0.09% serum physiologic. It's seen that Tetrafosmin kit should be carefully used after 48th hour and the remaining kits could be used after reconstitution and it may be helpful in reducing the costs in the nuclear medicine departments.

PT-27

K. Masuda,*T. Suzuki, S. Matuo, H. Ohnishi, T. Kida, M. Hamazu, M. Yoshimura, K. Noma, I. Yamamoto, R. Morita,*M. Mochizuki, and *S. Itoh
Hospital: Shiga University of Medical Science, Department of Radiology and *Shizuoka General Hospital

ESTIMATION OF MINIMUM AND OPTIMUM NUMBER OF 99mTc MAA PARTICLES IN LUNG PERFUSION IMAGING WITH WIENER SPECTRUM IMAGE ANALYSIS

A routine lung perfusion scanning by the injected dose of MAA particles safety for adults, may cause fatality in the patients with severe pulmonary hypertension or emphysema, because the constriction in the small arteries in these diseases, produces the blockage of the more peripheral arterioles and capillary segments by MAA particles. Therefore, when studying these patient, it is, very important to give careful consideration to limiting the number of injected particles necessary for a good-quality lung perfusion images. We labeled the MAA particles of the commercial kit with 99mTc pertechnetate. Immediately after thoroughly mixing and sonicating the labeled MAA particles in gelatin solution in the beaker, so as to prevent the movement of MAA particles in the liquid, we poured the 99mTc MAA gelatin solution into four same-size square phantoms different MAA particle number with the same radioactivity: 8 particles/cm³, 33 particles/cm³, 166 particles/cm³ and 333 particles/cm³ by the dilution of the MAA kit containing 1,600,000 particles with the diameter of 10-60 μm (the mean diameter = 35 μm)/vial. We collected 300k counts from the 99mTc-MAA phantoms with the lead bar (10mm wide) on it, with the scintillation camera with the high resolution collimator and analyzed the image data of phantoms by Wiener-spectrum analysis. The Wiener spectrum value of 8 particles/cm³, under the frequency area of 0.1 cycle/cm, was close to 10⁻⁴, but that of other particles numbers/cm³ were about 10⁻⁵. And also it was difficult to recognize the lead bar over the phantom of 8 particles/cm³. From these data, the minimum MAA particles number/cm³ was 33 particles/cm³ and the optimum number/cm³ enough to get a good quality lung perfusion image, was 100 particles/cm³.

PT-28

Fengqing Lin

The No 211 Hospital, Department of Nuclear Medicine

THE CLINICAL SIGNIFICANCE OF A DYNAMIC OBSERVATION ON URINE PGE₂ AND PGF₂α TITERS IN HEPATITIS-A USING RADIOIMMUNOASSAY.

Prostaglandin(PG) E₂ and F₂α were considered a "local" biological factor because it was produced and metabolized *in-situ* around tissues. The titers of PGE₂ and PGF₂α in 24-hour urine were detected using domestic RIA kits at various stages of 43 cases of Hepatitis-A(M 23, F20, age 19-52), and the results were compared with 43 controls, sex and age matched. At early stage(2-5 days) after onset of jaundice, slight increase of PGE₂ (2951.1± 510.6 pmol/L vs 1809.5± 497.2 pmol/L) and PGF₂α(2279.1±509.2 pmol/L vs 1376.2±481.5 pmol/L) were found in patients. Repeated studies showed the titers declined at 12-17days(2393.2± 478.5 pmol/L for PGE₂, and 1876.2±480.1 pmol/L for PGF₂α), and dropped back to normal (1769.2±505.4 pmol/L and 1401.4±491.2 pmol/L) at 3-4 weeks. Both PGs correlated well with other parameters of liver function, e.g. icteric index, bilirubin and ALT. The results suggested liver might be an important site for metabolism of those biological factors. The dynamic change of urinary PGE₂ or PGF₂α reflected clinical process of hepatitis-A, indicating those immune and inflammation related biological factors should not be viewed "local" anymore. In conclusion: (1)urine PGE₂ and PGF₂α were found arise in icteral period of hepatitis A; (2)their titers in urine kept in pace with, thus reflected the pathological process of the liver disease; (3)liver might play an important role in the *in-vivo* handling of the particular PGs.

PT-29

Fengying Lin

No.211 Hospital, Department of Nuclear Medicine

A SIMPLE, FAST, QUANTITATIVE RIA METHOD FOR DETERMINATION OF SERUM α -FP.

The RIA method using paper-carrier for assessing serum α -FP had been introduced before, but simply dropping blood on a thin-layer filter-paper made quantitation difficult. With several years efforts, a modified paper-method was innovated, by using micro-liquid-sampler, 50 μ l blood was drawn from ear-lobe, then dropped onto the filter-paper. The entire blood stain on the paper-carrier was then resolved and utilised for RIA in a central Lab to which many sample-papers were sent by mail from many remote, smaller medical facilities. Being completely resolved, the blood sample suspension went through all process as routine RIA. Results using this method was compared with that using classical method in 443 subjects, an excellent correlation was proven ($r=0.97$, $y=6.047+0.924x$). The sensitivity of the paper method was 9.2ng/ml, with good recovery (97.3%), and fairly low variation (intra-group ABCV 6.8%; and 11.9 % inter-group). The paper-method was reliable and stable, with accurate results reproducible from the air-dried samples stored for 12 weeks at room temperature, or for 4 weeks at 45-50 °C. The method enabled sample collection from some wide-spread or isolated rural areas, and made possible a more and easier α -FP RIA, which resulted in assistance in screening 14 cases of liver cancer from 5,215 surveyed subjects, and in finding 4 fetal abnormalities in 6,783 pregnant women over 3.5 years. All those positive results were confirmed by later clinical data. In conclusion: the quantitative, thin layer paper method was simple, accurate, and easy-to-use RIA technique for α -FP determination.

PT-30

M.Göransson and B.Jansson

Department of Nuclear Medicine, Huddinge University Hospital, Huddinge, Sweden.

RAPID MINIATURIZED CHROMATOGRAPHY FOR 99m Tc-RADIOPHARMACEUTICALS.

The purpose of this work was to develop rapid, miniaturized chromatography systems to accurately assess the radiochemical purity of 99m Tc radiopharmaceuticals without the problems and time requirements associated with some of the procedures recommended by the manufacturers.

Methods: The systems, consisting of different types of Bond Elut® extraction cartridges eluted with appropriate solvents, were developed for the radiochemical purity assessment of different 99m Tc preparations, e.g. tetrofosmin, HM PAO, bicisate, DMSA and MIBI.

The appropriate extraction mechanisms (non-polar, polar or ion-exchange) were selected, and to evaluate the systems radiochemical purity assessments were performed simultaneously on the 99m Tc preparations using both the methods recommended by the manufacturers and the miniaturized systems.

General procedure:

1. the Bond Elut® cartridge was conditioned by rinsing with one cartridge volume of solvent
2. 100-200 μ l of the preparation was applied to the sorbent bed
3. the cartridge was eluted with 1-3 ml of solvent
4. the eluted radioactivity and the one retained in the cartridge was measured in a radioisotope calibrator and the labeling efficiency was calculated.

Results: Radiochemical purity results for the different 99m Tc radiopharmaceuticals were similar with both recommended and miniaturized chromatography systems, with a mean difference of 1.8 ± 1.4 %.

It takes 3 minutes to perform our radiochemical purity tests. This enables us to supply the result before the preparation is administered to the patient.

Conclusion: Our results demonstrate that the miniaturized chromatography systems, based on sorbent extraction procedures are effective in evaluating the radiochemical purity of different 99m Tc radiopharmaceuticals. The method is easy to use and the time to perform radiochemical purity assessments is substantially reduced.

PT-31

Pia Bostroem, C. Liljedahl, E. Nilsson, T. Wennbom, A. Pettersson, JE Westlin, S. Nilsson
Department of Oncology, Section of Nuclear Medicine, University Hospital, S- 751 85 Uppsala, Sweden

SAFETY ROUTINES, DEVELOPED FOR SYSTEMIC RADIOTHERAPY WITH 111 IN-DTPA-D-(PHE³)-OCTREOTIDE

Introduction: The number of patients who require radioactive isotope therapy has increased in recent years. Therefore it is necessary to improve safety routines to minimise irradiation to the staff.

Method: To carry out therapy as problem free as possible, the patient needs either a central venous access or a cannula, in both arms, the arms should then be wrapped in "under pads" forming a cradle under each arm. If the patient has a central venous access, the "underpad" should be placed under the 3-way-stopcock. Prior to beginning the therapy, Methyleneblue is mixed with 111 In, and the infusion set is flushed with Albumin and Sodium-Chloride. A special lead holder is used for the therapy. This lead holder is a simplified alternative to the infusions pump routinely used.

Result/conclusion: The afore mentioned measures have improved staff protection at our Department. With cannulas in both arms, one cannula functions as a reserve, if for some reason the one in use fails during therapy. Thus the therapy can proceed quickly, and the radiation dose to the staff is kept to a minimum. Radioactive leakage is readily apparent due to the mixing of Methylene blue with 111 In and the "under pad" prevents radioactive leakage from contaminating the bed. The Methylene blue colouring also facilitates the supervision of the patient from a greater distance, which in turn decreases the radiation dose to the staff.

The leadholder simplifies administration of the therapy. Flushing the infusion tubing with Albumin prior to the administration of 111 In, decreases the amount of activity which fastens inside the tubing. With the addition of Sodium-Chloride the remaining radioactivity detected inside the tubing is practically zero. Rinsing of the infusion system after therapy is easily monitored due to the Methylene blue.

PT-32

A. Pettersson, C. Liljedahl, E. Nilsson, P. Bostroem, T. Wennbom, S. Nilsson, JE. Westlin.

Department of Oncology, Section of Nuclear Medicine, University Hospital, S-751 85 Uppsala Sweden

DEVELOPMENT OF A NEW APPARATUS FOR ADMINISTRATION OF SYSTEMIC RADIOTHERAPY

Introduction: With the increasing number of patients requiring systemic radiotherapy, radiation to the staff needs to be minimized.

Therefore our department has developed an apparatus which simplifies the administration of systemic radiotherapy and reduces the exposure of the staff to radiation.

Method: This apparatus consists of a specially constructed iv stand with a cylindrical container. This container is constructed to hold a 100 ml standard iv glass bottle within a 3 cm thick lead shielding. The cover, made of 3 cm thick lead, is fastened with two screws. The cover has a cone shaped hole in the center to facilitate insertion of the tubing into the radioactive tracer bottle and to avoid pinching the connecting tubing to the sodium chloride solution used for flushing after treatment. The bottle containing the radioactive tracer is placed in the container, and the cover locked in place in the Hot Lab. Prior to administration, the tubing is inserted, the container is fastened to a framework on the iv stand, a pawl is unfastened and the holder is rotated "upside down", and the treatment is initiated. In the event of radioactive leakage, an absorbing pad is placed under the holder. A moveable lead glass frame is placed between the container and the personal. When the radiotherapy is finished, the tubing is then thoroughly flushed with a 100 ml sodium chloride.

Result/conclusion: This apparatus simplifies the administration of systemic radiotherapy and reduces exposure of the staff to radiation. The lead glass placed between the infusion container and the staff further reduces radiation exposure. Flushing the system with sodium chloride has a two fold effect. Firstly, the patient receives a dose as close as possible to that prescribed. Secondly the amount of radioactive tracer in the tubing is negligible, thereby minimizing radioactive waste.

PT-33

Limin Cao, Jiahe Tian, Jinming Zhang

The PLA General Hospital, Department of Nuclear Medicine

INTRABURSAL INJECTION OF GOLD-198-COLLOID AS AN EFFECTIVE TREATMENT OF STUBBORN VILLONODULAR SYNOVITIS

Villonodular synovitis sometimes might be painful, causing hydrothrosis dysfunction of the joints, yet hard to treat with ordinary modalities. 19 patients, age 20 ~ 32, having swollen knee(s) for 1 ~ 3.5 yr were referred to us for failing other treatments. 12 were male, 7 females. Puncture of bursa of the sick joint was performed with a long, fine needle, at either side junction of patellar ligament to lower edge of patella and 185 ~ 259MBq/2 ~ 4ml 198Au-colloid was injected for each joint. In case of high intracapsular-pressure, light brown liquid from bursa was drained out before 198Au administration. The patients were asked to move their knees and kept under observation for a while before discharge. Monitor of the in-vivo distribution of 198Au was carried out with a LFOV camera in both spot and whole-body modes at 5m, 1, 2, 24, 48 and 72h post-injection. If needed the treatment was repeated at 2 month interval. In our group, 5 had 1 injection, 9 received 2, and 5 underwent 3 sessions of treatment. The number of session seemed related to the length and severity of illness. As the result, all cases were benefited from the therapy, 13 painfree. No radioactivity could detected outside knee. No blood cell count, nor liver and renal function tests showed any abnormal change. Followed for 16 ~ 29 months, no symptom recurred. The only contraindication is in those under age of 20, for fear of influencing epiphysis. In conclusion, intrabursal administration of 198Au-colloid is an effective treatment for villonodular synovitis incurable by other therapeutic modalities.

PT-34

R.Th. VERSTEEGH, M.A.B.D. PLAIZIER, A.A. GELDOF, J. v.d. BERG, G.J.J. TEULE.

Department of Nuclear Medicine, Free University Hospital, Amsterdam, The Netherlands.

PLATING DENSITY AND CLONOGENIC CAPACITY OF PC-3 PROSTATE CANCER CELLS DURING RADIONUCLIDE THERAPY IN VITRO.

Palliation of bone metastases can be performed with radionuclides. This treatment can be combined with radio- or chemotherapy. To investigate the effects of these three treatments in vitro, we have established a model using the PC-3 human prostate cancer cell line. The radiation effects of 186-Re-HEDP were evaluated by a clonogenic tumor cell assay in RPMI 1640 medium containing 0, 0.74 and 1.48 MBq 186-Re/ml in 6 wells-cluster plates. We validated this approach by varying the amount of medium and the cell plating density. After 8-10 days of culturing, the colonies (>50 cells) were fixed with 95% ethanol, stained with Giemsa and counted. The experiments showed a linear relationship between number of plated cells and number of formed colonies. The 186-Re treated cells with 0.74 MBq/ml showed a linearity until the maximum number of 1600 plated cells, while the 1.48 MBq/ml resulted in hardly any colony. The non-treated cells showed a linearity until 800 plated cells and moreover there is a statistical significance (at p=0.05) between the 0.74 and 1.48 MBq/ml treated and non-treated cells. There was also no significant difference (at p=0.05) between applying 5 or 10 ml of total volume per well, for the 0.74 MBq/ml treated as well as for the non-treated cells.

The average number of colonies is tabulated as follows :

186-Re (MBq/ml)	number of plated PC-3 cells per well in 6-wells-cluster plates				
	100	200	400	800	1600
0	29.2	64.2	130.6	217.2	300
0.74	8.2	14	36	79	178.2
1.48	0.25	0.25	0.25	0	4.5

Conclusions : We have shown a linearity between cell plating densities and clonogenic growth for 186-Re treated and non-treated cells. So this model is suitable for measuring clonogenic capacity without underestimating the number of colonies within the range not exceeding 800 and 1600 plated cells for 0 and 0.74 MBq/ml respectively. For studies with radionuclides like 186-Re a total volume of 5 ml per well yields results comparable with those from (radiotherapy) studies employing a volume of 10 ml per well.

PT-35

Jinming Zhang, Jiahe Tian, Hongsheng Bai, Xiaohai Jin

The PLA General Hospital, Department of Nuclear Medicine

YTTRIUM-90-CHARCOAL AS A NEW AGENT FOR INTERNAL RADIOTHERAPY

Yttrium-90 glass therapy microsphere (90Y-GTMS) has been used in internal radiotherapy of the hepatic tumor. But it has a few shortages: (1) it has to be produced in reactor, (2) it is difficult to use because GTMS can not be steadily suspended in saline for reason of specific gravity. Yttrium-90-Charcoal(90Y-C) could be directly labeled with elution from 90Sr/90Y generator and could be suspended easily in saline.

90Y-EDTA eluted from 90Sr/90Y generator was mixed with charcoal for 30 min. The upper liquid was removed by centrifugation. After rinsed with saline for three times, the adsorption of 90Y-EDTA on charcoal remained more than 90%. There is no desorption of 90Y from charcoal in flushing saline. After injected to mice by i.m and i.p, about 99% radioactivity were retained in point of injection. The in-vivo distribution of 90Y-C is favorable in terms of potential use internally.

The distribution of 90Y-C in mice in different injection way at 72h (n=5)

organs	heart	liver	spleen	lung	kidney	femur
i.m	BG	BG	BG	BG	0.017 ± 0.004	0.0017 ± 0.0008
i.p	BG	0.003	0.068	BG	0.056 ± 0.001	0.035 ± 0.007

The activity in all organs are close to background except for bone and kidney in i.m group. But there are more radioactivity in liver and spleen in i.P groups. It was suggested that the biokinetic of 90Y-C might be relate to injection way.

In conclusion, 90Y-C is stable in vitro and doesn't degraded in vivo. It might be a potential agent for internally therapeutic use for solid tumor.